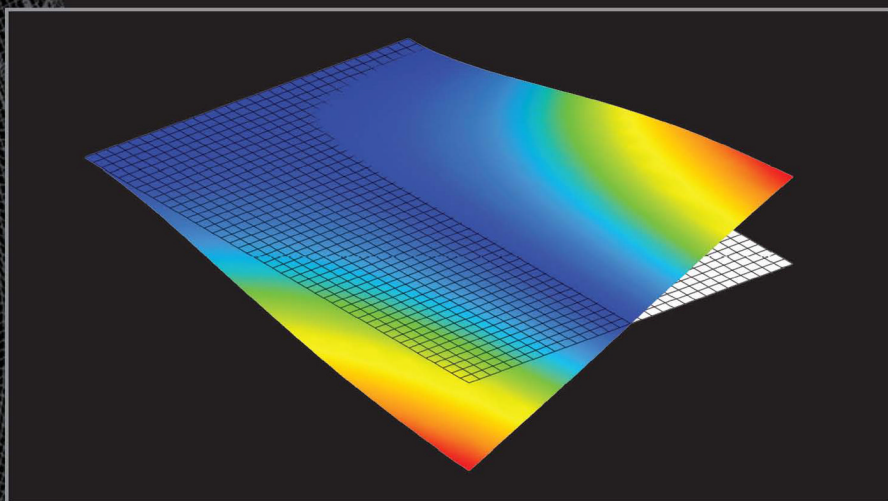


Mechanical Vibrations

Theory and Application
to Structural Dynamics

Third Edition



Michel Géradin
Daniel J. Rixen

WILEY

$\delta \int_{t_1}^{t_2} (T - V) dt = 0$

MECHANICAL VIBRATIONS

MECHANICAL VIBRATIONS

THEORY AND APPLICATION TO STRUCTURAL DYNAMICS

Third Edition

Michel Géradin

University of Liège, Belgium

Daniel J. Rixen

Technische Universität München, Germany

WILEY

This edition first published 2015
© 2015 John Wiley & Sons, Ltd

Second Edition published in 1997
© 1997 John Wiley & Sons, Ltd

Registered office

John Wiley & Sons Ltd, The Atrium, Southern Gate, Chichester, West Sussex, PO19 8SQ, United Kingdom

For details of our global editorial offices, for customer services and for information about how to apply for permission to reuse the copyright material in this book please see our website at www.wiley.com.

The right of the author to be identified as the author of this work has been asserted in accordance with the Copyright, Designs and Patents Act 1988.

All rights reserved. No part of this publication may be reproduced, stored in a retrieval system, or transmitted, in any form or by any means, electronic, mechanical, photocopying, recording or otherwise, except as permitted by the UK Copyright, Designs and Patents Act 1988, without the prior permission of the publisher.

Wiley also publishes its books in a variety of electronic formats. Some content that appears in print may not be available in electronic books.

Designations used by companies to distinguish their products are often claimed as trademarks. All brand names and product names used in this book are trade names, service marks, trademarks or registered trademarks of their respective owners. The publisher is not associated with any product or vendor mentioned in this book

Limit of Liability/Disclaimer of Warranty: While the publisher and author have used their best efforts in preparing this book, they make no representations or warranties with respect to the accuracy or completeness of the contents of this book and specifically disclaim any implied warranties of merchantability or fitness for a particular purpose. It is sold on the understanding that the publisher is not engaged in rendering professional services and neither the publisher nor the author shall be liable for damages arising herefrom. If professional advice or other expert assistance is required, the services of a competent professional should be sought.

Library of Congress Cataloging-in-Publication Data

Géradin, Michel, 1945 –

Mechanical vibrations : theory and application to structural dynamics / Michel Gérardin,
Daniel J. Rixen. – Third edition.

pages cm

Includes bibliographical references and index.

ISBN 978-1-118-90020-8 (hardback)

1. Structural dynamics. I. Rixen, Daniel. II. Title.

TA654.G45 2014

624.1'76–dc23

2014014588

A catalogue record for this book is available from the British Library.

ISBN: 978-1-118-90020-8

Typeset in 10/12pt Times by Laserwords Private Limited, Chennai, India

Contents

Foreword	xiii
Preface	xv
Introduction	1
Suggested Bibliography	7
List of main symbols and definitions	9
1 Analytical Dynamics of Discrete Systems	13
Definitions	14
1.1 Principle of virtual work for a particle	14
1.1.1 <i>Nonconstrained particle</i>	14
1.1.2 <i>Constrained particle</i>	15
1.2 Extension to a system of particles	17
1.2.1 <i>Virtual work principle for N particles</i>	17
1.2.2 <i>The kinematic constraints</i>	18
1.2.3 <i>Concept of generalized displacements</i>	20
1.3 Hamilton's principle for conservative systems and Lagrange equations	23
1.3.1 <i>Structure of kinetic energy and classification of inertia forces</i>	27
1.3.2 <i>Energy conservation in a system with scleronomic constraints</i>	29
1.3.3 <i>Classification of generalized forces</i>	32
1.4 Lagrange equations in the general case	36
1.5 Lagrange equations for impulsive loading	39
1.5.1 <i>Impulsive loading of a mass particle</i>	39
1.5.2 <i>Impulsive loading for a system of particles</i>	42
1.6 Dynamics of constrained systems	44
1.7 Exercises	46
1.7.1 <i>Solved exercises</i>	46
1.7.2 <i>Selected exercises</i>	53
References	54
2 Undamped Vibrations of n-Degree-of-Freedom Systems	57
Definitions	58
2.1 Linear vibrations about an equilibrium configuration	59

2.1.1	<i>Vibrations about a stable equilibrium position</i>	59
2.1.2	<i>Free vibrations about an equilibrium configuration corresponding to steady motion</i>	63
2.1.3	<i>Vibrations about a neutrally stable equilibrium position</i>	66
2.2	Normal modes of vibration	67
2.2.1	<i>Systems with a stable equilibrium configuration</i>	68
2.2.2	<i>Systems with a neutrally stable equilibrium position</i>	69
2.3	Orthogonality of vibration eigenmodes	70
2.3.1	<i>Orthogonality of elastic modes with distinct frequencies</i>	70
2.3.2	<i>Degeneracy theorem and generalized orthogonality relationships</i>	72
2.3.3	<i>Orthogonality relationships including rigid-body modes</i>	75
2.4	Vector and matrix spectral expansions using eigenmodes	76
2.5	Free vibrations induced by nonzero initial conditions	77
2.5.1	<i>Systems with a stable equilibrium position</i>	77
2.5.2	<i>Systems with neutrally stable equilibrium position</i>	82
2.6	Response to applied forces: forced harmonic response	83
2.6.1	<i>Harmonic response, impedance and admittance matrices</i>	84
2.6.2	<i>Mode superposition and spectral expansion of the admittance matrix</i>	84
2.6.3	<i>Statically exact expansion of the admittance matrix</i>	88
2.6.4	<i>Pseudo-resonance and resonance</i>	89
2.6.5	<i>Normal excitation modes</i>	90
2.7	Response to applied forces: response in the time domain	91
2.7.1	<i>Mode superposition and normal equations</i>	91
2.7.2	<i>Impulse response and time integration of the normal equations</i>	92
2.7.3	<i>Step response and time integration of the normal equations</i>	94
2.7.4	<i>Direct integration of the transient response</i>	95
2.8	Modal approximations of dynamic responses	95
2.8.1	<i>Response truncation and mode displacement method</i>	96
2.8.2	<i>Mode acceleration method</i>	97
2.8.3	<i>Mode acceleration and model reduction on selected coordinates</i>	98
2.9	Response to support motion	101
2.9.1	<i>Motion imposed to a subset of degrees of freedom</i>	101
2.9.2	<i>Transformation to normal coordinates</i>	103
2.9.3	<i>Mechanical impedance on supports and its statically exact expansion</i>	105
2.9.4	<i>System submitted to global support acceleration</i>	108
2.9.5	<i>Effective modal masses</i>	109
2.9.6	<i>Method of additional masses</i>	110
2.10	Variational methods for eigenvalue characterization	111
2.10.1	<i>Rayleigh quotient</i>	111
2.10.2	<i>Principle of best approximation to a given eigenvalue</i>	112
2.10.3	<i>Recurrent variational procedure for eigenvalue analysis</i>	113
2.10.4	<i>Eigensolutions of constrained systems: general comparison principle or monotonicity principle</i>	114
2.10.5	<i>Courant's minimax principle to evaluate eigenvalues independently of each other</i>	116

2.10.6	<i>Rayleigh's theorem on constraints (eigenvalue bracketing)</i>	117
2.11	Conservative rotating systems	119
2.11.1	<i>Energy conservation in the absence of external force</i>	119
2.11.2	<i>Properties of the eigensolutions of the conservative rotating system</i>	119
2.11.3	<i>State-space form of equations of motion</i>	121
2.11.4	<i>Eigenvalue problem in symmetrical form</i>	124
2.11.5	<i>Orthogonality relationships</i>	126
2.11.6	<i>Response to nonzero initial conditions</i>	128
2.11.7	<i>Response to external excitation</i>	130
2.12	Exercises	130
2.12.1	<i>Solved exercises</i>	130
2.12.2	<i>Selected exercises</i>	143
	References	148
3	Damped Vibrations of n-Degree-of-Freedom Systems	149
	Definitions	150
3.1	Damped oscillations in terms of normal eigensolutions of the undamped system	151
3.1.1	<i>Normal equations for a damped system</i>	152
3.1.2	<i>Modal damping assumption for lightly damped structures</i>	153
3.1.3	<i>Constructing the damping matrix through modal expansion</i>	158
3.2	Forced harmonic response	160
3.2.1	<i>The case of light viscous damping</i>	160
3.2.2	<i>Hysteretic damping</i>	162
3.2.3	<i>Force appropriation testing</i>	164
3.2.4	<i>The characteristic phase lag theory</i>	170
3.3	State-space formulation of damped systems	174
3.3.1	<i>Eigenvalue problem and solution of the homogeneous case</i>	175
3.3.2	<i>General solution for the nonhomogeneous case</i>	178
3.3.3	<i>Harmonic response</i>	179
3.4	Experimental methods of modal identification	180
3.4.1	<i>The least-squares complex exponential method</i>	182
3.4.2	<i>Discrete Fourier transform</i>	187
3.4.3	<i>The rational fraction polynomial method</i>	190
3.4.4	<i>Estimating the modes of the associated undamped system</i>	195
3.4.5	<i>Example: experimental modal analysis of a bellmouth</i>	196
3.5	Exercises	199
3.5.1	<i>Solved exercises</i>	199
3.6	Proposed exercises	207
	References	208
4	Continuous Systems	211
	Definitions	212
4.1	Kinematic description of the dynamic behaviour of continuous systems: Hamilton's principle	213
4.1.1	<i>Definitions</i>	213

4.1.2	<i>Strain evaluation: Green's measure</i>	214
4.1.3	<i>Stress–strain relationships</i>	219
4.1.4	<i>Displacement variational principle</i>	221
4.1.5	<i>Derivation of equations of motion</i>	221
4.1.6	<i>The linear case and nonlinear effects</i>	223
4.2	Free vibrations of linear continuous systems and response to external excitation	231
4.2.1	<i>Eigenvalue problem</i>	231
4.2.2	<i>Orthogonality of eigensolutions</i>	233
4.2.3	<i>Response to external excitation: mode superposition (homogeneous spatial boundary conditions)</i>	234
4.2.4	<i>Response to external excitation: mode superposition (nonhomogeneous spatial boundary conditions)</i>	237
4.2.5	<i>Reciprocity principle for harmonic motion</i>	241
4.3	One-dimensional continuous systems	243
4.3.1	<i>The bar in extension</i>	244
4.3.2	<i>Transverse vibrations of a taut string</i>	258
4.3.3	<i>Transverse vibration of beams with no shear deflection</i>	263
4.3.4	<i>Transverse vibration of beams including shear deflection</i>	277
4.3.5	<i>Travelling waves in beams</i>	285
4.4	Bending vibrations of thin plates	290
4.4.1	<i>Kinematic assumptions</i>	290
4.4.2	<i>Strain expressions</i>	291
4.4.3	<i>Stress–strain relationships</i>	292
4.4.4	<i>Definition of curvatures</i>	293
4.4.5	<i>Moment–curvature relationships</i>	293
4.4.6	<i>Frame transformation for bending moments</i>	295
4.4.7	<i>Computation of strain energy</i>	295
4.4.8	<i>Expression of Hamilton's principle</i>	296
4.4.9	<i>Plate equations of motion derived from Hamilton's principle</i>	298
4.4.10	<i>Influence of in-plane initial stresses on plate vibration</i>	303
4.4.11	<i>Free vibrations of the rectangular plate</i>	305
4.4.12	<i>Vibrations of circular plates</i>	308
4.4.13	<i>An application of plate vibration: the ultrasonic wave motor</i>	311
4.5	Wave propagation in a homogeneous elastic medium	316
4.5.1	<i>The Navier equations in linear dynamic analysis</i>	316
4.5.2	<i>Plane elastic waves</i>	318
4.5.3	<i>Surface waves</i>	320
4.6	Solved exercises	327
4.7	Proposed exercises	328
	References	333
5	Approximation of Continuous Systems by Displacement Methods	335
	Definitions	337
5.1	The Rayleigh–Ritz method	339
5.1.1	<i>Choice of approximation functions</i>	339

5.1.2	<i>Discretization of the displacement variational principle</i>	340
5.1.3	<i>Computation of eigensolutions by the Rayleigh–Ritz method</i>	342
5.1.4	<i>Computation of the response to external loading by the Rayleigh–Ritz method</i>	345
5.1.5	<i>The case of prestressed structures</i>	345
5.2	Applications of the Rayleigh–Ritz method to continuous systems	346
5.2.1	<i>The clamped–free uniform bar</i>	347
5.2.2	<i>The clamped–free uniform beam</i>	350
5.2.3	<i>The uniform rectangular plate</i>	357
5.3	The finite element method	363
5.3.1	<i>The bar in extension</i>	364
5.3.2	<i>Truss frames</i>	371
5.3.3	<i>Beams in bending without shear deflection</i>	376
5.3.4	<i>Three-dimensional beam element without shear deflection</i>	386
5.3.5	<i>Beams in bending with shear deformation</i>	392
5.4	Exercises	399
5.4.1	<i>Solved exercises</i>	399
5.4.2	<i>Selected exercises</i>	406
	References	412
6	Solution Methods for the Eigenvalue Problem	415
	Definitions	417
6.1	General considerations	419
6.1.1	<i>Classification of solution methods</i>	420
6.1.2	<i>Criteria for selecting the solution method</i>	420
6.1.3	<i>Accuracy of eigensolutions and stopping criteria</i>	423
6.2	Dynamical and symmetric iteration matrices	425
6.3	Computing the determinant: Sturm sequences	426
6.4	Matrix transformation methods	430
6.4.1	<i>Reduction to a diagonal form: Jacobi’s method</i>	430
6.4.2	<i>Reduction to a tridiagonal form: Householder’s method</i>	434
6.5	Iteration on eigenvectors: the power algorithm	436
6.5.1	<i>Computing the fundamental eigensolution</i>	437
6.5.2	<i>Determining higher modes: orthogonal deflation</i>	441
6.5.3	<i>Inverse iteration form of the power method</i>	443
6.6	Solution methods for a linear set of equations	444
6.6.1	<i>Nonsingular linear systems</i>	445
6.6.2	<i>Singular systems: nullspace, solutions and generalized inverse</i>	453
6.6.3	<i>Singular matrix and nullspace</i>	453
6.6.4	<i>Solution of singular systems</i>	454
6.6.5	<i>A family of generalized inverses</i>	456
6.6.6	<i>Solution by generalized inverses and finding the nullspace N</i>	457
6.6.7	<i>Taking into account linear constraints</i>	459
6.7	Practical aspects of inverse iteration methods	460
6.7.1	<i>Inverse iteration in presence of rigid body modes</i>	460
6.7.2	<i>Spectral shifting</i>	463

6.8	Subspace construction methods	464
6.8.1	<i>The subspace iteration method</i>	464
6.8.2	<i>The Lanczos method</i>	468
6.9	Dynamic reduction and substructuring	479
6.9.1	<i>Static condensation (Guyan–Irons reduction)</i>	481
6.9.2	<i>Craig and Bampton’s substructuring method</i>	484
6.9.3	<i>McNeal’s hybrid synthesis method</i>	487
6.9.4	<i>Rubin’s substructuring method</i>	488
6.10	Error bounds to eigenvalues	488
6.10.1	<i>Rayleigh and Schwarz quotients</i>	489
6.10.2	<i>Eigenvalue bracketing</i>	491
6.10.3	<i>Temple–Kato bounds</i>	492
6.11	Sensitivity of eigensolutions, model updating and dynamic optimization	498
6.11.1	<i>Sensitivity of the structural model to physical parameters</i>	501
6.11.2	<i>Sensitivity of eigenfrequencies</i>	502
6.11.3	<i>Sensitivity of free vibration modes</i>	502
6.11.4	<i>Modal representation of eigenmode sensitivity</i>	504
6.12	Exercises	504
6.12.1	<i>Solved exercises</i>	504
6.12.2	<i>Selected exercises</i>	505
	References	508
7	Direct Time-Integration Methods	511
	Definitions	513
7.1	Linear multistep integration methods	513
7.1.1	<i>Development of linear multistep integration formulas</i>	514
7.1.2	<i>One-step methods</i>	515
7.1.3	<i>Two-step second-order methods</i>	516
7.1.4	<i>Several-step methods</i>	517
7.1.5	<i>Numerical observation of stability and accuracy properties of simple time integration formulas</i>	517
7.1.6	<i>Stability analysis of multistep methods</i>	518
7.2	One-step formulas for second-order systems: Newmark’s family	522
7.2.1	<i>The Newmark method</i>	522
7.2.2	<i>Consistency of Newmark’s method</i>	525
7.2.3	<i>First-order form of Newmark’s operator – amplification matrix</i>	525
7.2.4	<i>Matrix norm and spectral radius</i>	527
7.2.5	<i>Stability of an integration method – spectral stability</i>	528
7.2.6	<i>Spectral stability of the Newmark method</i>	530
7.2.7	<i>Oscillatory behaviour of the Newmark response</i>	533
7.2.8	<i>Measures of accuracy: numerical dissipation and dispersion</i>	535
7.3	Equilibrium averaging methods	539
7.3.1	<i>Amplification matrix</i>	540
7.3.2	<i>Finite difference form of the time-marching formula</i>	541
7.3.3	<i>Accuracy analysis of equilibrium averaging methods</i>	542
7.3.4	<i>Stability domain of equilibrium averaging methods</i>	543

7.3.5	<i>Oscillatory behaviour of the solution</i>	544
7.3.6	<i>Particular forms of equilibrium averaging</i>	544
7.4	Energy conservation	550
7.4.1	<i>Application: the clamped–free bar excited by an end force</i>	552
7.5	Explicit time integration using the central difference algorithm	556
7.5.1	<i>Algorithm in terms of velocities</i>	556
7.5.2	<i>Application example: the clamped–free bar excited by an end load</i>	559
7.5.3	<i>Restitution of the exact solution by the central difference method</i>	561
7.6	The nonlinear case	564
7.6.1	<i>The explicit case</i>	564
7.6.2	<i>The implicit case</i>	565
7.6.3	<i>Time step size control</i>	571
7.7	Exercises	573
	References	575
Author Index		577
Subject Index		581

Foreword

The first two editions of this book had seven skillfully written chapters, organized in my mind in three parts. Collectively, they aimed at giving the reader a coherent presentation of the theory of vibrations and associated computational methods, in the context of structural analysis. The first part covered the analytical dynamics of discrete systems, and both undamped and damped vibrations of multiple-degree-of-freedom systems. It also served as a good introduction to the second part, which consisted of two chapters. The first one focused on the dynamics of continuous systems and covered the subject of wave propagation in elastic media. It was followed by a chapter which bridged this topic with the first part of the book, by introducing the novice to the concept of displacement methods for semi-discretizing continuous systems. It also culminated with a brief and yet well-executed initiation to the finite element method. All this led to the third part of the book, which indulged into a concise and effective treatment of classical numerical methods for the solution of vibration problems in both frequency and time domains. Covering all of these topics in a unified approach, making them interesting to both students and practitioners, including occasional references to experimental settings wherever appropriate, and delivering all this in less than 400 pages, was a daunting challenge that the authors had brilliantly met. For this reason, the previous editions of this book have been my favourite educational publication on this subject matter. I have used them to teach this topic at the MS level, first at the University of Colorado at Boulder, then at Stanford University.

So what can one expect from a third edition of this book?

In its third edition, the overall organization of this book and that of its chapters has remained mostly unchanged. However, several enhancements have been made to its technical content. The notion of the response of a system to a given input has been refined throughout the text, and its connections to the concepts of dynamic reduction and substructuring (which remain timely) have been made easier to observe, follow, and understand. Chapter 3 has gained a new section on experimental methods for modal analysis and some associated essentials in signal processing and system identification. The mathematical content of Chapter 6 has been somehow refreshed, and its scope has been enhanced by two welcome enrichments. The first one is a new section on linear equation solvers with particular emphasis on singular systems. Such systems arise not only in many mechanical and aerospace engineering problems where the structure of interest is only partially restrained or even unrestrained, but also as artifacts of many modern computational methods for structural analysis and structural dynamics. The second enrichment

brought to Chapter 6 is an updated section on the analysis of the sensitivity of frequencies and mode shapes to parameters of interest, and its association with model updating. Most importantly, the third edition comes now with carefully designed problem sets (and occasionally some solutions) that will certainly enhance both processes of teaching and learning. Overall, the third edition has added about 150 pages of technical content that make it a better textbook for students and teachers, a useful reference for practitioners, and a source of inspiration for researchers.

*Charbel Farhat
Stanford University
1 January 2014*

Preface

This monograph results from a complete recasting of a book on Mechanical Vibrations, initially written in French and published by Masson Éditions in 1992 under the title *Théorie des vibrations, Application à la dynamique des structures*. The first edition in English was issued shortly after, thanks to the support of DIST (French Ministry of Scientific Research and Space) and published by John Wiley & Sons in 1994. The book was indubitably felt to fill a gap since both editions were a success in France as well as internationally, so that both versions were almost immediately followed by a second edition by the same publishers: in French in 1996, and in 1997 for the English version. Due to the short delay between editions, only minor changes – essentially corrections – took place between the first and second versions of the manuscript.

The numerous constructive comments received from readers – university colleagues, students and practising engineers – during the following decade convinced both of us that a deep revision of the original manuscript was definitely needed to meet their expectations. Of course there were still remaining errors to be corrected – and the very last one will never be discovered, error-making being a common trait of human beings – and more rigor and accuracy had to be brought here and there in the presentation and discussion of the concepts. But the subject of mechanical vibration has also rapidly evolved, rendering the necessity of the addition of some new important topics. Proposed exercises to help, on the one hand, teachers explain the quintessence of dynamics and, on the other hand, students to assimilate the concepts through examples were also missing.

We were already planning to produce this third edition in French in the early 2000s, but the project could never be achieved due to overwhelming professional duties for both of us. The necessary time could finally be secured from 2010 (partly due to the retirement of the first author). However, priority has now been given to the English language for the writing of this third, entirely new edition since our perception was that the demand for a new, enhanced version comes essentially from the international market. We are indebted to Éditions Dunod for having agreed to release the rights accordingly.

We are thus pleased to present to our former readers a new edition which we hope will meet most of their expectations, and to offer our new readers a book that allows them to discover or improve their knowledge of the fascinating world of mechanical vibration and structural dynamics.

Without naming them explicitly, we express our gratitude to all those who have helped us to make this book a reality. Indeed, we received from many colleagues, friends and relatives much support, which could take various forms, such as a careful and critical reading of some parts, the provision of some examples and figures, appropriate advice whenever needed, personal support and, not the least, the understanding of our loved ones when stealing from them precious time to lead such a project to its very end.

Michel Gérardin and Daniel J. Rixen
München
24 January 2014

Introduction

We owe to Lord Rayleigh the formulation of the principles relative to the theory of vibration such as they are applied and taught nowadays. In his remarkable treatise entitled *Theory of Sound* and published in 1877 he introduced the fundamental concept of oscillation of a linear system about an equilibrium configuration and showed the existence of vibration eigenmodes and eigenfrequencies for discrete as well as for continuous systems. His work remains valuable in many ways, even though he was concerned with acoustics rather than with structural mechanics.

Because of their constant aim to minimize the weight of flying structures, the pioneers of aeronautics were the first structural designers who needed to get vibration and structural dynamic problems under control. From the twenties onwards, aeronautical engineers had to admit the importance of the mechanics of vibration for predicting the aeroelastic behaviour of aircraft. Since then, the theory of vibration has become a significant subject in aeronautical studies. During the next forty years, they had to limit the scope of their analysis and apply methods that could be handled by the available computational means: the structural models used were either analytical or resulted from a description of the structure in terms of a small number of degrees of freedom by application of transfer or Rayleigh-Ritz techniques.

The appearance and the progressive popularization of computing hardware since 1960 have led to a reconsideration of the entire field of analysis methods for structural dynamics: the traditional methods have been replaced by matrix ones arising from the discretization of variational expressions. In particular, the tremendous advances in the finite element method for setting up structural models gave rise to the development of new computational methods to allow design engineers to cope with always increasing problem sizes.

Today, the elaboration of efficient computational models for the analysis of the dynamic behaviour of structures has become a routine task. To give an example, Figure 1 illustrates the computational prediction of the vibration modes of a stator section of an aircraft engine. The fineness of the finite element model has been adapted in this case for the needs of the associated stress analysis, the latter requiring a level of detail that is not really needed for a modal analysis. The eigenmode represented is a 3-diameter mode exhibiting a global deformation of the structure. What makes the modal analysis of such a structure very difficult is the high level



Figure 1 Finite element model of a stator section of aircraft engine. Source: Reproduced with permission from Techspace Aero – SAFRAN Group.

of cyclic symmetry (resulting from the number of stator blades) which is responsible for the appearance of a high number of nearly equal eigenvalues.

Development of computing, acquisition and sensing hardware has led to a similar revolution in the field of experimental techniques for identification of vibrational characteristics of structures. For more than thirty years, experimental modal analysis techniques have been developed which are based either on force appropriation or on arbitrary excitation.

The methods for dynamic analysis, whether they are numerical or experimental, have now taken an important place everywhere in engineering. If they were rapidly accepted in disciplines such as civil engineering, mechanical design, nuclear engineering and automotive production where they are obviously needed, they have now become equally important in the design of any manufactured good, from the micro-electromechanical device to the large wind turbine.

From its origin in the early sixties, the aerospace department of the University of Liège (Belgium) has specialized mainly in structural mechanics in its education programme. This book results from more than twenty years of lecturing on the theory of vibration to the students of this branch. It is also based on experience gathered within the University of Liège's Laboratory for Aerospace Techniques in the development of computational algorithms designed for the dynamic analysis of structures by the finite element method and implemented in the structural analysis code the team of the laboratory has developed since 1965, the SAMCEF™ software.¹

The content of the book is based on the lecture notes developed over the years by the first author and later formatted and augmented by one of his former students (the second author). This work reflects the teaching and research experience of both authors. In addition to his academic activity at the University of Liège, the first author has also spent several years as head of the European Laboratory for Safety Assessment at the Joint Research Centre in Ispra (Italy). The second author has accumulated until 2012 lecturing and research experience at

¹ From 1986, SAMCEF™ has been industrialized, maintained and distributed by SAMTECH SA, a spin-off company of the University of Liège.

the Delft Technical University (The Netherlands) and is currently pursuing his career at the Technische Universität München (Germany). The book has been adopted internationally as course reference in several universities.

Due to its very objective, the book has a slightly hybrid character: the concepts of vibration theory are presented mainly with the intention of applying them to dynamic analysis of structures and significant attention is paid to the corresponding methods. Even though the foundations of analytical mechanics are reviewed, a preliminary acquaintance with this subject is necessary. A good knowledge of matrix algebra and theory of complex numbers, calculus, structural mechanics and numerical analysis for linear systems is required. It is also assumed that the reader is familiar with the theory of the single-degree-of-freedom oscillator. However, the presentation of the finite element method is deliberately made simple since its study requires a course of its own. Finally, the very important fields of nonlinear vibration and random vibration have been intentionally omitted in the present text since they are highly specialized subjects.

What is new in this third edition?

Although the overall structure of the book, its organization into individual chapters and the main topics addressed, remain unchanged, this new version is the result of important revision work to achieve major improvements.

Regarding the theoretical content itself, the main changes with respect to the previous edition are the following:

- The response of an either discrete or continuous system has been the object of deep rethinking and turned out to be a thread towards the important concepts of dynamic reduction and substructuring. The latter are explained and developed, starting from the observation that the response of a part from the overall system is the result either from an excitation of its support, or from the application of a set of loads at selected points of the structure. Such duality can be exploited in at least two ways. On the one hand, it allows a system description in terms of the classical concepts of mechanical impedance or admittance. On the other hand, it naturally leads to the concept of dynamic substructuring based on an expansion of the response in terms of the spectral content of the impedance and admittance relationships.
- Experimental modal analysis is an essential ingredient in structural dynamics since it allows to confirm by experiment the structural properties predicted through numerical modelling. Therefore it was felt necessary to include in this new version of the book the essentials of signal processing and identification techniques that allow us to extract the spectral properties of a linear structure from measured dynamic responses.
- In the same spirit, the concept of eigensolution sensitivity to physical parameters has been further detailed since it is the basis for the development of appropriate numerical tools for improving the numerical model of a real dynamic system.
- The considerable evolution of the size of the structural systems to be considered for eigenvalue extraction and transient dynamic analysis in the context of large engineering projects had to be reflected and addressed properly. Models reaching the size of several millions of degrees of freedom (such as the one displayed on Figure 1) are now common practice. The efficiency of the eigenvalue solvers (such as the Lanczos method) and implicit

time integrators (based on the Newmark family) depends for one part on the tuning of the algorithms themselves, but perhaps even more on the performance of the linear solvers that are used at each solution step. Therefore it was felt necessary to cover in a deeper manner the topic of linear solvers, introducing not only the principle of the algorithms but also their implementation taking into account the sparse character of the large sets of equations generated by finite element discretization. Much attention is also brought to the case of singular systems since they frequently occur in the context of structural dynamics.

- The link that was made in the previous edition between vibration and wave propagation did not allow the reader to easily grasp the physical nature of the wave propagation phenomena that can occur in a continuous medium. The discussion of the fundamental cases of wave propagation in solids (both in one-dimensional and three-dimensional media) has thus been reviewed and better illustrated in order to improve the didactics of the presentation.
- The presentation of the finite element method has still been limited to one-dimensional structures (bars, beams) since the main objective of the book is not to go deeply into finite element technology. The chapter devoted to it has, however, been complemented with the development of a beam element including the shear deformation. The motivation behind the presentation was to show that, as is often the case, remaining within the strict context of the variational principle of displacements leads to shortcomings which can easily be removed through the use of mixed variational formulations.
- The stability and accuracy properties of the Newmark family of time integration algorithms have been revisited, their rigorous discussion being achieved in terms of the invariants of the amplification matrix. Also, it is shown that dissociating displacement interpolation and expression of equilibrium allows us to imbed most integration schemes of the Newmark family in the same formalism.

As a result, the original manuscript has been almost completely rewritten. The opportunity has been taken to improve or clarify the presentation whenever necessary, including the quality of the figures.

A great effort has been achieved to adopt throughout the manuscript notations that are as coherent and uniform as possible. Therefore a general list of notations and symbols is provided after this introduction. However it was still necessary in many cases to depart locally from these general conventions, and therefore to introduce in each chapter an additional list of local definitions that complements the general one.

Among the many constructive comments received regarding the previous editions, a major deficiency felt and reported by the users was the absence of exercises proposed to the reader. A few solved exercises are now detailed at the end of each chapter, and both teachers and students will certainly appreciate the fact that a number of selected problems are also suggested. The numerical solution of some of them requires the use of a numerical toolbox, in which case softwares such as MATLAB[®] or the Open Source ones OCTAVE[®] and SCILAB[®] are appropriate. Some others involve cumbersome analytical developments that are greatly facilitated by symbolic computation using software tools such as MAPLE[®] or MATHEMATICA[®].

The content

The content of the book is organized as follows:

Chapter 1 is dedicated to analytical dynamics of discrete systems. Hamilton's principle is taken as a starting point: first the equations of motion are found for one particle and then those for a system of particles under kinematic constraints are derived. Considering the equations of motion in the Lagrangian form, the structure of the inertia terms and the classification of the forces are established. In the last two sections of the chapter, the less common case of impulsive loading of systems is dealt with and the method of Lagrange multipliers is introduced.

Chapter 2 discusses the undamped vibrations of n -degree-of-freedom systems and begins by introducing the concepts of equilibrium position and of equilibrium configuration corresponding to steady motion. After a review of the classical concepts of eigenmodes and eigenfrequencies, some more specific aspects are considered: the forced harmonic response is developed and is shown to lead to the concepts of dynamic influence coefficient and mechanical impedance. The modal expansion technique is applied for calculating the dynamic response to transient external loading. It is shown that limiting the points of load application leads to the concept of reduced mechanical admittance. The case of systems excited through support motion is discussed in depth and also examined from the point of view of dynamic substructuring. Variational methods for characterizing the eigenvalues of a vibrating system are then discussed. The solution of the motion equations of rotating systems is considered in a specific section at the end of the chapter, with the main objective to show the existence of instability zones linked to the existence of gyroscopic forces.

Chapter 3 deals with the damped oscillations of n -degree-of-freedom systems. First, the concept of lightly-damped systems and its equivalence to the modal damping assumption are discussed. Then the principles of modal identification through appropriate excitation and the characteristic phase-lag theory are outlined. The formulation of damped system equations in state-space form is developed in order to provide a suitable mathematical model for describing systems with arbitrarily large damping. In the last section, a basic presentation is made of the signal processing and identification techniques that are commonly used to best fit the parameters of the mathematical model from experimental measurements.

In Chapter 4, the theory of vibration is extended to the analysis of continuous systems, taking as a starting point the variational principle operating on displacements. The chapter begins by considering the case of three-dimensional continuous media: strain measure, stress-strain relationships, variational formulation and equations of motion. The effects of the second-order terms arising from the presence of an initial stress field are investigated in detail. Then the concepts of eigenmodes, eigenfrequencies and modal expansion are generalized to the continuous case. It is also shown that the principle of reciprocity commonly described for structures under steady loading can be generalized to dynamics. In a major part of the chapter, a quite extensive study is made of some one-dimensional or two-dimensional continuous systems: the bar in extension, the vibrating string, the bending of a beam without and with shear deflection and finally the bending vibration of thin plates. Numerous examples of closed-form solutions are given and particular attention is devoted to the effects resulting from the rotation of beams and,

for systems in bending, from initial extension. Their respective properties as one-dimensional wave guides are discussed. The last section provides an elementary presentation of wave propagation phenomena in an elastic medium, with a derivation of the fundamental solutions and a discussion of their physical meaning.

In Chapter 5, the approximation problem for continuous systems is investigated by means of displacement methods. First, the Rayleigh–Ritz method is reviewed and then applied to some classical problems such as the bar in extension, and the bending of a beam and of a thin plate. The case of prestressed structures is once more considered. The second part of the chapter is dedicated to an introduction to the finite element method, the principles of which are illustrated by several simple examples. The chapter ends with the more complex but instructive case of finite element modelling of the beam with shear deformation.

Chapter 6 deals with solution methods for the eigenvalue problem. After an introduction where a classification of the existing methods is suggested, a successive survey of the most classical methods is made and their related numerical aspects are discussed. The methods efficiently implemented in structural computation codes are pointed out, namely the subspace method and the Lanczos algorithm. A significant part of the chapter is devoted to the efficient solution of large, sparse linear systems since they form in fact the kernel of eigenvolvers based on inverse iteration such as Lanczos and subspace iteration. The particular case of singular structures is discussed in depth since frequently occurring in the context of structural dynamics. The methods of dynamic reduction and substructuring already introduced in Chapter 2 are discussed again, with three objectives in mind: to review the principle of dynamic reduction in a more general manner, to show that dual points of view can be adopted, depending upon the physical nature (displacement or force) of the primary variables and to propose dynamic reduction and substructuring as a practical approach for the solution of large problems of structural dynamics. A section is also devoted to the computation of error bounds to eigenvalues. The last section deals with the concept of eigensolution sensitivity to structural modifications.

Chapter 7 outlines some aspects of direct methods for integrating the transient dynamic response. After having introduced the concepts of stability and accuracy for an integration operator, it discusses the one-step formulas of Newmark's family. Their properties are analyzed as well as those of variants commonly used in structural analysis: the Hilber-Hugues-Taylor α -method and the Generalized- α variant which provides a neat way to introduce numerical damping in the model and the central difference integration scheme especially well adapted to impact problems. Eventually, there is a short discussion of the time integration of nonlinear systems.

The scope

The book has been devised to be used by senior undergraduate and graduate students. Therefore, the associated concepts are revealed by numerous simple examples. Nevertheless, although the text is primarily aimed at students, it is also dedicated to research and design engineers who wish to improve their understanding and knowledge of the dynamic analysis of structures. Solved exercises are also proposed to readers at the end of each chapter, and a number of selected problems are provided to allow them to practice the concepts and assess their assimilation. In order to simplify the presentation, most examples and solved exercises are presented in a nondimensional manner.

Finally, the authors do not claim to cover within the following text the field of vibration theory and dynamic analysis in an exhaustive way. Neither have they made explicit reference to all the bibliographic work they have consulted throughout their writing. Therefore the following list of references is suggested for further details on the various aspects of structural dynamics.

Suggested bibliography

Reference works on linear and nonlinear vibration theory (phenomenological aspects and analytical methods):

- Biezeno CB and Grammel R 1939 *Technische Dynamik*. Springer Berlin.
- Crede CE and Harris CM 1977 *Shock and Vibration Handbook* (2nd edition). McGraw-Hill, New York.
- Del Pedro M and Pahud P 1997 *Mécanique vibratoire: systèmes discrets linéaires*. Presses Polytechniques Romandes, Lausanne.
- Den Hartog J 1947 *Mechanical Vibrations*. McGraw-Hill, New York.
- Genta G 2009 *Vibration Dynamics and Control*. Springer.
- Gérardin M 1990 *Dynamique des constructions mécaniques*. Course lecture notes, University of Liège.
- Hagedorn P 1981 *Non-linear Oscillations*. Clarendon Press, Oxford.
- Hussey M 1983 *Fundamentals of Mechanical Vibrations*. Macmillan.
- Lalanne M, Berthier P and Der Hagopian J 1980 *Mécanique des vibrations linéaires*. Masson, Paris.
- Lord Rayleigh BJWS 1894 *Theory of Sound* (2 volumes) 2nd edn. Macmillan and Co., London and New York (first edition in 1877).
- Magnus K 1961 *Schwingungen; eine Einführung in die theoretische Behandlung von Schwingungsproblemen*. Teubner, Stuttgart.
- Mazet R 1966 *Mécanique vibratoire*. Dunod, Paris.
- Meirovitch L 1967 *Analytical Methods in Vibrations*. The Macmillan Company, New York.
- Meirovitch L 1975 *Elements of vibration analysis*. McGraw-Hill.
- Müller PC and Schiehlen WO 1985 *Linear Vibrations: A Theoretical Treatment of Multi-Degree-of-Freedom Vibrating Systems*. Martinus Nijhoff Publishers, Dordrecht.
- Nayfeh AH and Mook DT 1979 *Nonlinear Oscillations*. John Wiley & Sons, Inc., New York.
- Rao S 1986 *Mechanical Vibrations*. Addison-Wesley, Reading, MA.
- Rocard Y 1960 *Dynamique générale des vibrations*. Masson, Paris.
- Roseau M 1984 *Vibrations des systèmes mécaniques: méthodes analytiques et applications*. Masson, Paris.
- Timoshenko S 1937 *Vibration Problems in Engineering* 2nd. edn. D. Van Nostrand.
- Tong KN 1960 *Theory of Mechanical Vibration*. John Wiley & Sons, Inc., New York.

Reference works on random vibration:

- Crandall SH and Mark WD 1963 *Random Vibration in Mechanical Systems*. Academic Press, New York.
- Preumont A 1994 *Random Vibrations and Spectral Analysis*. Kluwer Academic.

Reference works on structural dynamics:

- Argyris J and Mlejnek H 1991 *Dynamics of Structures*. Elsevier, Amsterdam.
- Clough RW and Penzien J 1975 *Dynamics of Structures*. McGraw-Hill, New York.
- Craig R and Kurdila A 2006 *Fundamentals of Structural Dynamics*. John Wiley & Sons, Inc., New York.
- Fraeijs de Veubeke B, Gérardin M and Huck A 1972 *Structural Dynamics*. number 126 in *CISM Lecture Notes (Udine, Italy)*. Springer.
- Hurty WC and Rubinstein MF n.d. *Dynamics of Structures*. Prentice-Hall New Jersey.
- Meirovitch L 1980 *Computational Methods in Structural Dynamics*. Sijthoff & Noordhoff.
- Preumont A 2013 *Twelve Lectures on Structural Dynamics*. Springer.

Reference works dedicated to the finite element method:

- Bathe K 1996 *Finite Element Procedures in Engineering Analysis*. Prentice Hall, Englewood Cliffs NJ.
- Batoz JL and Dhett G 1990 *Modélisation des structures par éléments finis* vol. 1, 2 and 3. Presses Université Laval.
- Craveur JC 1996 *Modélisation des structures, calcul par éléments finis*. Masson, Paris.
- Dhatt G and Touzot G 1984 *Une présentation de la méthode des éléments finis*. Collection de l'Université de Compiègne, edited by Maloine.
- Hughes T 1987 *The Finite Element Method – Linear Static and Dynamic Finite Element Analysis*. Prentice Hall Inc., New Jersey.
- Imbert J n.d. *Analyse des structures par éléments finis*. Cepadues Editions, Toulouse.
- Kardestuncer H and Norrie DH 1987 *Finite Element Handbook*. McGraw-Hill, Inc.
- Zienkiewicz O and Taylor R 1989 *The Finite Element Method* 4th edn. McGraw-Hill. 2 volumes.

Reference works on aeroelasticity:

- Bisplinghoff RL and Ashley H 1975 *Principles of Aeroelasticity*. Dover Publications, New York.
- Bisplinghoff RL, Ashley H and Halfman R 1955 *Aeroelasticity*. Addison-Wesley, Cambridge, Mass.
- Dowell E, Clark R, Cox D, Curtiss H, Edwards J, Hall K, Peters D, Scanlan R, Simiu E and Sisto F 2004 *A Modern Course in Aeroelasticity (Fourth Revised and Enlarged Edition)*. Kluwer Academic Publishers.
- Försching HW 1974 *Grundlagen der Aeroelastik*. Springer-Verlag, Berlin.
- Fung Y 1955 *An Introduction to the Theory of Aeroelasticity*. John Wiley & Sons, Ltd, Chichester.

Reference works on fluid-structure interaction and acoustics:

- Morand-Fahy FJ and Gardonio P 2007 *Sound and structural vibration: radiation, transmission and response*. Academic press.
- Morand HJP and Ohayon R 1992 *Interactions fluides-structures*. Masson, Paris.
- Ohayon R and Soize C 1997 *Structural Acoustics and Vibration: Mechanical Models, Variational Formulations and Discretization*. Elsevier.

Reference works on classical mechanics:

- Goldstein H 1986 *Classical Mechanics*. Addison-Wesley, Reading, MA.
- Komzisk L 2014 *Applied Calculus of Variations for Engineers*. 2nd edn. CRC Press.
- Lanczos C 1949 *The Variational Principles of Mechanics* Mathematical Expositions, No. 4. University of Toronto Press, Toronto, Canada.
- Meirovitch L 1970 *Methods of Analytical Dynamics*. McGraw Hill, New York.
- Whittaker ET 1952 *Analytical Dynamics of Particles and Rigid Bodies*. Cambridge University Press, New York.

Reference works on solid mechanics:

- Fraeijns de Veubeke B 1979 *A Course in Elasticity* vol. 29 of *Applied Mathematical Sciences* Springer.
- Fung Y 1965 *Foundations of Solid Mechanics*. Prentice Hall, New Jersey.

Reference works on dynamics of mechanical systems:

- Bauchau OA 2011 *Flexible Multibody Dynamics*. vol. 176. Springer Science.
- Gérardin M and Cardona A 2001 *Flexible Multibody Dynamics: The Finite Element Method Approach*. John Wiley & Sons, Ltd, Chichester.
- Pfeiffer F 2005 *Mechanical System Dynamics* vol. 40. Springer.
- Shabana AA 2005 *Dynamics of Multibody Systems*. Cambridge University Press.

Reference works on experimental methods in vibration:

- Brandt A 2011 *Noise and Vibration Analysis: Signal Analysis and Experimental Procedures*. John Wiley & Sons, Ltd, Chichester.

- Brincker R 2013 *Introduction to Operational Modal Analysis*. John Wiley & Sons, Ltd, Chichester.
- Ewins DJ 2000 *Modal Testing: Theory, Practice and Application*. Research Studies Press, Baldock.
- Heylen W, Lammens S and Sas P 1997 *Modal Analysis Theory and Testing*. Katholieke Universiteit Leuven, Department Werktuigkunde, Heverlee.
- McConnell KG and Varoto PS 2008 *Vibration Testing: Theory and Practice* second edn. John Wiley & Sons, Ltd, Chichester.
- Silva JM and Maia NM 1999 *Modal analysis and testing NATO Science Series E* vol. 363 Springer.
- Zaveri K 1984 *Modal Analysis of Large Structures – Multiple Exciter Systems*. Brüel & Kjær, BT 0001-11.

Reference works on vibration control:

- Preumont A 2006 *Mechatronics: Dynamics of Electromechanical and Piezoelectric Systems* vol. 136. Springer.
- Preumont A 2011 *Vibration Control of Active Structures: An Introduction* vol. 179. Springer.

Reference works on rotor dynamics:

- Friswell MI, Penny JE, Garvey SD and Lees AWi 2010 *Dynamics of Rotating Machines*. Cambridge University Press.
- Genta G 2005 *Dynamics of Rotating Systems*. Springer, New York.
- Lalanne M, Ferraris G and Der Hagopian J 1998 *Rotordynamics Prediction in Engineering* (2nd edition). John Wiley & Sons, Inc., New York.

Reference works on numerical methods for linear and eigenvalue solutions:

- Golub GH and Van Loan CF 1989 *Matrix Computations*. John Hopkins University Press.
- Householder AS 1964 *The Theory of Matrices in Numerical Analysis*. Blaisdell.
- Komzsik L 2003 *The Lanczos Method: Evolution and Application*. SIAM.
- Wilkinson J 1965 *The Algebraic Eigenvalue Problem*. Clarendon Press, Oxford.

Reference works on numerical methods for time integration:

- Belytschko T and Hughes T 1983 *Computational Methods for Transient Analysis*. North-Holland.
- Gear C 1971 *Numerical Initial Value Problems in Ordinary Differential Equations*. Prentice Hall, Englewood Cliffs, NJ.

List of main symbols and definitions

The list below provides the definitions of variables and quantities that are common to all book chapters. A separate list is provided at the beginning of each chapter with definitions that remain local to the chapter.²

In the text, we will use bold characters to denote matrices. Lower case bold symbols will represent uni-column matrices whereas upper case ones denote multi-column matrices. For instance,

$$\mathbf{a} = \begin{bmatrix} a_1 \\ a_2 \\ \vdots \end{bmatrix}$$

² Multiple use of same symbol has been avoided as much as possible, but may still occur locally.

and

$$\mathbf{A} = \begin{bmatrix} a_{11} & a_{12} & a_{13} & \cdots \\ a_{21} & a_{22} & \cdots & \\ a_{31} & \vdots & \ddots & \\ \vdots & & & \end{bmatrix} = [\mathbf{a}_1 \ \mathbf{a}_2 \ \cdots] .$$

Nonbold symbols represent scalars. A subscript like a_{rs} typically denotes the coefficient rs of a matrix \mathbf{A} .

Subscripts in parentheses (e.g. $\mathbf{a}_{(s)}$) indicate that the quantity is associated to mode s .

\mathbb{E}	n -dimensional space.
\mathbb{E}^p	subspace of first p eigenmodes.
dof	degree-of-freedom.
\mathbf{B}_{rig}	rigid mobility matrix.
\mathbf{C}	damping matrix.
\mathbf{D}	strain differential operator.
\mathbf{F}	flexibility matrix.
\mathbf{G}	gyroscopic matrix.
$\mathbf{H}(\omega^2)$	admittance (dynamic flexibility) matrix of undamped system.
\mathbf{I}	identity matrix.
\mathbf{K}	stiffness matrix.
\mathbf{K}_g	geometric stiffness matrix.
\mathbf{K}^*	modified stiffness matrix (rotating system).
\mathbf{M}	mass matrix.
\mathbf{R}	modal reduction matrix.
\mathbf{U}	matrix of rigid body modes.
\mathbf{X}	matrix of elastic eigenmodes.
$\bar{\mathbf{X}}$	imposed load per unit of volume.
$\mathbf{Z}(\omega^2)$	impedance (dynamic stiffness) matrix of undamped system.
\mathbf{e}_i	i -th unit vector.
$\mathbf{p}(t)$	vector of external loads.
$\mathbf{q}(t)$	vector of generalized coordinates.
\mathbf{q}_0	generalized coordinates at $t = 0$.
$\dot{\mathbf{q}}$	vector of generalized velocities.
$\dot{\mathbf{q}}_0$	generalized velocities at $t = 0$.
$\ddot{\mathbf{q}}$	vector of generalized accelerations.
\mathbf{t}	vector of surface tractions.
$\bar{\mathbf{t}}$	vector of imposed surface tractions.
$\mathbf{u}_{(i)}$	i -th rigid body mode.
$\mathbf{x}_{(r)}$	eigenvector of conservative system associated to ω_r .
\mathcal{D}	dissipation function.
EA	bar extensional stiffness.
EI	beam bending stiffness.
\mathcal{E}	total energy.

$\mathcal{F}[\dots]$	Fourier transform.
$\Im m$	imaginary part of a complex number.
$k'AG$	beam shear stiffness.
$\mathcal{L}[\dots]$	Laplace transform.
Q_s	s -th generalized force conjugated to q_s .
$\Re e$	real part of a complex number.
S	external surface of continuous body.
S_σ	part of external surface with imposed surface tractions.
S_u	part of external surface with imposed displacements.
\mathcal{T}	kinetic energy.
\mathcal{T}_0	transport kinetic energy.
\mathcal{T}_2	relative kinetic energy.
\mathcal{T}_1	complementary kinetic energy.
V	volume of continuous body.
\mathcal{V}	potential energy.
V_0	volume of reference configuration.
\mathcal{V}_{ext}	external potential energy.
\mathcal{V}_{ext}^*	complementary external potential energy.
\mathcal{V}_g	geometric part of internal potential energy.
\mathcal{V}_{int}	internal potential energy.
\mathcal{V}_{int}^*	complementary internal potential energy.
\mathcal{V}^*	$= \mathcal{V} - \mathcal{T}_0$ modified potential.
g	gravity constant.
$g(t)$	step response function.
$h(t)$	impulse response function.
i	imaginary number.
ℓ	length.
n	number of generalized coordinates.
n	number of degrees of freedom.
q_s	s -th generalized coordinate.
t	time.
Ω^2	diagonal matrix of eigenvalues ω_r^2 .
λ	vector of Lagrange multipliers.
ϵ	strain matrix, collecting the strain components ϵ_{ij} .
$\eta(t)$	vector of normal coordinates of elastic modes $\eta_r(t)$.
μ	diagonal matrix of generalized masses μ_r .
σ	stress matrix, collecting the strain components σ_{ij} .
$\xi(t)$	vector of normal coordinates of rigid body modes $\xi_i(t)$.
∇^2	Laplacian operator.
Ω	rotation velocity.
δ	variation symbol.
δ_{rs}	Kronecker symbol.
$\delta(t)$	Dirac function.
ϵ_{ij}	strain tensor.
$\epsilon_{ij}^{(1)}$	linear part of strain tensor.

$\varepsilon_{ij}^{(2)}$	quadratic part of strain tensor.
$\eta_r(t)$	normal coordinate of elastic mode r .
γ_r	generalized stiffness of mode r .
μ_r	generalized mass of mode r .
ν	$= \frac{\omega}{2\pi}$ frequency (in Hz).
ω	circular frequency (in rad/s).
ω_r^2	r -th eigenvalue of second order system.
ω_r	circular frequency of mode r (in rad/s).
$\phi_r(t)$	load participation factor of mode r .
ρ	volumic mass.
ρ_0	volumic mass in reference configuration.
σ_{ij}	stress tensor.
σ_{ij}^0	tensor of initial stresses.

1

Analytical Dynamics of Discrete Systems

The *variational approach* to mechanics is based on the concepts of energy and work and therefore provides a better understanding of mechanical phenomena. In some sense one can say that variational principles consider the system in a global sense, disregarding the specificities of the forces associated to kinematic constraints imposed on the system. It provides at the same time a very powerful tool for two main reasons:

- It considerably simplifies the analytical formulation of the motion equations for a complex mechanical system.
- It gives rise to approximate numerical methods for the solution of both discrete and continuous systems in the most natural manner, as will be later explained in Chapters 5 and 6.

The objective of this chapter is to recall to the reader, how the fundamental Newton's equations for dynamics can be effectively applied to general systems on which kinematic constraints are imposed. First we recall the concept of virtual displacements and the principle of virtual work for a single mass point (Section 1.1), then for a system of particles (Section 1.2), explaining how it leads to a global dynamic description of a system where unknown reaction forces associated to kinematic constraints do not appear. The intimately related concepts of kinematic constraints and generalized coordinates (or degrees of freedom) are also discussed in those sections. Note that in this book we will not discuss the dynamics of rigid bodies. Although a rigid body can be seen as a collection of constrained point masses and therefore a special case of the systems treated here, analyzing the dynamics of a rigid body and building models of multiple rigid components is a topic in itself that will not be handled here since the main scope of the book is vibrational behaviour of flexible systems.¹

In Section 1.3 the dynamics of systems is described in an even more abstract way, using the energy concepts to show that the virtual work principle can be written as a variational principle, namely Hamilton's principle. It is then shown that the equations of motion can be

¹ For a thorough discussion of analytical dynamics for systems of rigid bodies, the reader is referred to (Lur'ë 1968, Meirovitch 1970, Meirovitch 1980, Whittaker 1965, Goldstein 1986, Géradin and Cardona 2001).

derived from the energy description of the system: the Lagrange equations. Those equations are outlined for the general case of nonconservative systems in Section 1.4.²

Section 1.5 deals with the generalization of the Lagrange equations to systems undergoing impulsive loading (i.e. shocks, impact). Finally, Section 1.6 provides an introduction to the dynamics of constrained systems. It is shown that the method of Lagrange multipliers provides an efficient way to extend Lagrange's equations to systems described by coordinates for which constraints need to be explicitly accounted for.

Definitions

The list below complements the general definitions given in the book introduction, but remains local to Chapter 1.

F_s	gyroscopic forces.
N	number of particles.
P_s	s -th generalized impulse.
R	number of constraints.
$U_{ik}(q_s, t)$	i -th displacement component of k -th particle in terms of generalized coordinates.
\mathcal{V}_d	dislocation potential.
X_i, X_{ik}	i -th component of force on (k -th) particle.
m, m_k	mass of (k -th) particle.
u_i, u_{ik}	i -th displacement component of (k -th) particle.
x_{ik}	reference configuration of k -th particle.
λ_r	Lagrange multiplier.
ξ_{ik}	i -th instantaneous configuration of k -th particle.

1.1 Principle of virtual work for a particle

1.1.1 Nonconstrained particle

Let us consider a particle of mass m , submitted to a force field X of components X_i . The dynamic equilibrium of the particle can be expressed in d'Alembert's form:

$$m\ddot{u}_i - X_i = 0 \quad i = 1, 2, 3 \quad (1.1)$$

where u_i represents the displacement of the particle.

Let us next imagine that the particle follows during the time interval $[t_1, t_2]$ a motion trajectory u_i^* distinct from the real one u_i . This allows us to define the virtual displacement of the

² The point of view adopted in this chapter is far from being the only possible one. It would also be possible to apply Kane's method (Kane and Levinson 1980) which implements the concept of generalized speeds (quasi-velocity coordinates) as a way to represent motion, similar to what the concept of generalized coordinates does for the configuration. Kane's implementation focuses on the motion aspects of dynamic systems rather than only on the system configuration. It therefore provides a suitable framework for treating nonholonomic constraints of differential type (see Section 1.2.2).

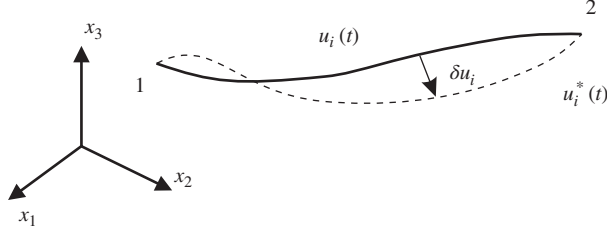


Figure 1.1 Virtual displacement of a particle.

particle by the relationship (Figure 1.1):

$$\delta u_i = u_i^* - u_i \quad (1.2)$$

By its very definition, the virtual displacement δu_i is arbitrary for $t_1 < t < t_2$. However, let us suppose that the varied trajectory and the real one both pass through the same points at the ends of the time interval. The end conditions then take the form:

$$\delta u_i(t_1) = \delta u_i(t_2) = 0 \quad (1.3)$$

An immediate consequence of definition (1.2) is that the variation operator δ commutes with the time-derivative operator d/dt since

$$\frac{d}{dt}(\delta u_i) = \frac{d}{dt}(u_i^* - u_i) = \dot{u}_i^* - \dot{u}_i = \delta \dot{u}_i \quad (1.4)$$

Let us next multiply the dynamic equilibrium equations (1.1) by the associated virtual displacement and sum over the components. The virtual work expression results:

$$\sum_{i=1}^3 (m\ddot{u}_i - X_i) \delta u_i = 0 \quad (1.5)$$

which shows that

The virtual work produced by the forces acting on the particle during a virtual displacement δu_i is equal to zero.

1.1.2 Constrained particle

Equation (1.5) represents the scalar product between the forces acting on the particle and the virtual displacement $\vec{\delta u}$. It thus represents the *projection of the equilibrium along the direction $\vec{\delta u}$* . If (1.5) is satisfied for all variations δu_i , then the trajectory $u_i(t)$ satisfies the dynamic equilibrium in all directions.

If no kinematical constraint is imposed onto the particle, namely if no restriction is imposed on its displacement, the trajectory of the material point is determined by the equilibrium in all directions. But when kinematic constraints are specified for the particle, there exist reaction forces in addition to the applied forces. These reaction forces are inherent to the constraining

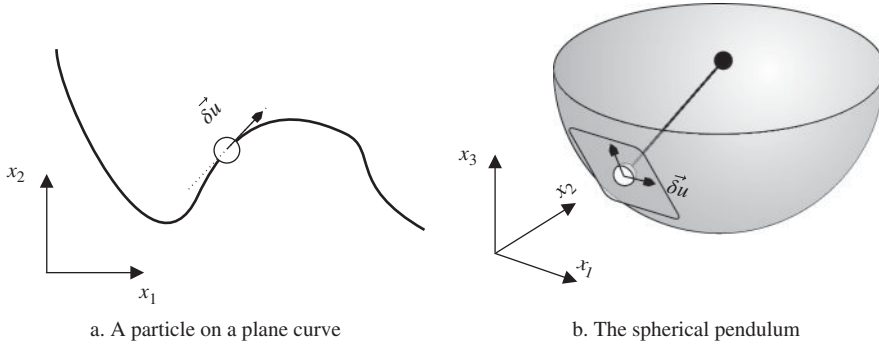


Figure 1.2 Kinematically admissible virtual displacements.

mechanism and ensure that the imposed kinematical constraints are satisfied. Those reaction forces are not known in advance since they depend on the motion itself.

Figure 1.2 describes a particle constrained to move along a curve and a spherical pendulum where a particle is constrained to have a constant distance with respect to a fixed point. On one hand, the presence of reaction forces acting in the direction of the constraint generally renders the equilibrium description more complex since those unknown forces must be determined along the entire trajectory such that kinematical constraints are satisfied. On the other hand, solving the equilibrium equations in the direction constrained by the kinematical conditions is not useful since, in that direction, the trajectory is prescribed by the constraint and thus known.

In the system described in Figure 1.2.a only the motion along the direction tangent to the curve needs to be determined. In doing so, the reaction forces, which act in the direction normal to the curve, do not participate to the motion and thus need not be determined: the position of the particle in the direction normal to the curve is obviously imposed by the constraint and does not require solving the equilibrium equation in that direction. In the same way, if the equilibrium of the particle of the spherical pendulum is expressed in the plane tangent to the sphere (Figure 1.2.b), only the forces actually applied participate in the determination of the trajectory.

Let us therefore decide that, in the presence of kinematical constraints, we consider only virtual displacements δu_i compatible with the constraints or, in other words, *kinematically admissible*. Equation (1.5) then describes the projection of the dynamic equilibrium in the space compatible with the constraints, namely in directions orthogonal to unknown reaction forces. The form (1.5) thus involves only effectively applied forces and stipulates that

*The virtual work produced by the **effective** forces acting on the particle during a virtual displacement δu_i compatible with the constraints is equal to zero.*

This is the *virtual work principle* for a constrained particle. Conversely, Equation (1.5) indicates that

*If the trajectory u_i of the particle is such that the **effectively applied** forces produce no virtual work for any virtual displacement **compatible with the constraints**, the equilibrium is then satisfied.*

The usefulness of the virtual work principle comes from the fact that it allows us to express the dynamic equilibrium in a simple manner along the directions compatible with the constraints. This will be explained next in more detail for a system of several particles.

1.2 Extension to a system of particles

1.2.1 Virtual work principle for N particles

Every particle k of a system of N particles with mass m_k satisfies the dynamic equilibrium:

$$m_k \ddot{u}_{ik} - X_{ik} = 0 \quad \begin{array}{l} i = 1, 2, 3 \\ k = 1, \dots, N \end{array} \quad (1.6)$$

where X_{ik} are the force components representing the known external forces and where R_{ik} are the unknown reactions resulting from the kinematic constraints imposed on the system.

For every particle k , one considers virtual displacements δu_{ik} such as:

$$\delta u_{ik} = u_{ik}^* - u_{ik} \quad i = 1, 2, 3 \quad (1.7)$$

$$\delta u_{ik}(t_1) = \delta u_{ik}(t_2) = 0 \quad k = 1, \dots, N \quad (1.8)$$

The virtual work principle is obtained by projecting the dynamic equilibrium equations on the virtual displacements and by summing up over the particles:

$$\sum_{k=1}^N \sum_{i=1}^3 (m_k \ddot{u}_{ik} - X_{ik} - R_{ik}) \delta u_{ik} = 0 \quad (1.9)$$

As for the case of one particle, we decide to consider only virtual displacement *compatible with the constraints*. Hence, the virtual displacements must satisfy constraints imposed on one particle as well as constraints imposed between particles. The situation where two points are rigidly linked to one another is an important example of such constraints. In that case, the reaction forces linking the particles are equal and opposite (Figure 1.3):

$$\vec{R}_1 + \vec{R}_2 = 0$$

and the virtual work associated to a virtual displacement $(\vec{\delta u}_1, \vec{\delta u}_2)$ is:

$$\delta \tau = \sum_{i=1}^3 (R_{i1} \delta u_{i1} + R_{i2} \delta u_{i2}) = \vec{R}_1 \cdot \vec{\delta u}_1 + \vec{R}_2 \cdot \vec{\delta u}_2 = \vec{R}_1 \cdot (\vec{\delta u}_1 - \vec{\delta u}_2) = 0$$

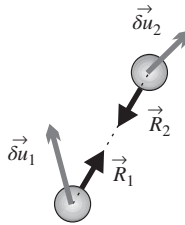


Figure 1.3 Virtual work of constraints between particles.

since the compatible virtual displacements must be equal in the direction of the rigid link. Projecting the equations onto the kinematically admissible displacements thus consists in summing up the equilibrium equations in the constrained direction such that the unknown linking forces vanish.

Since the reaction forces do vanish when projecting the equations of motion onto kinematically admissible displacement directions, the virtual work principle (1.9) is written as

$$\sum_{k=1}^N \sum_{i=1}^3 (m_k \ddot{u}_{ik} - X_{ik}) \delta u_{ik} = 0 \quad (1.10)$$

So as for a single particle (Section 1.1.2), it can be stated that

*The virtual work of the forces effectively applied onto a system of particles is zero with respect to any kinematically compatible virtual displacement **if and only if** the system is in dynamic equilibrium.*

Again, the principle of virtual work corresponds to the projection of the equilibrium equations in the directions compatible with the kinematical constraints. The resulting equations are then easier to solve since the constraining forces are no longer unknowns for the problem.

1.2.2 The kinematic constraints

Without kinematic constraints, the state of the system would be completely defined by the $3N$ displacement components u_{ik} since, starting from a reference configuration x_{ik} , they represent the instantaneous configuration:

$$\xi_{ik}(t) = x_{ik} + u_{ik}(x_{jk}, t) \quad \begin{array}{l} i, j = 1, 2, 3 \\ k = 1, \dots, N \end{array} \quad (1.11)$$

The system is then said to possess $3N$ degrees of freedom.

In most mechanical systems, however, the particles are submitted to kinematic constraints, which restrain their motion and define dependency relationships between particles.

Holonomic constraints

The *holonomic* constraints are defined by implicit relationships of type:

$$f(\xi_{ik}, t) = 0 \quad (1.12)$$

If there is no explicit dependence with respect to time, the constraints are said to be *scleronomic*. They are *rheonomic* otherwise.

A holonomic constraint reduces by one the number of degrees of freedom of the system.

Example 1.1

Let us consider the case of two mass particles connected by a rigid link of length ℓ . Their instantaneous positions ξ_{i1} and ξ_{i2} verify the relationship:

$$f(\xi_{ik}, t) = \sum_{i=1}^3 (\xi_{i2} - \xi_{i1})^2 - \ell^2 = 0$$

The variation of the constraint with respect to virtual displacements can be expressed by:

$$\delta f = \sum_{i=1}^3 ((\xi_{i1} - \xi_{i2})\delta u_{i1} - (\xi_{i1} - \xi_{i2})\delta u_{i2}) = 0$$

indicating that virtual displacements must satisfy (see also Figure 1.3):

$$(\vec{\xi}_1 - \vec{\xi}_2) \cdot \vec{\delta u}_1 = (\vec{\xi}_1 - \vec{\xi}_2) \cdot \vec{\delta u}_2$$

Hence virtual displacements must be equal in the direction of the link, and a system of two particles that are rigidly linked has $6 - 1 = 5$ degrees of freedom.

Nonholonomic constraints

A constraint is said *nonholonomic* if it cannot be put in the form (1.12). In particular, non-holonomic constraints often take the form of differential relationships:

$$f(\dot{\xi}_{ik}, \xi_{ik}, t) = 0 \quad (1.1)$$

Such relationships are generally not integrable, and therefore they do not allow reduction of the number of degrees of freedom of the system.

Example 1.2

Let us consider the case of the centre of a rigid wheel with radius r constrained to roll without sliding on a plane (Figure 1.4).

It is also assumed that the rotation axis remains parallel to the plane. The second material point considered in the description is a reference point located on the circumference of the

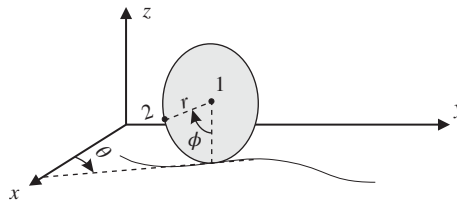


Figure 1.4 Nonholonomic constraint.

wheel. The rolling-without-sliding condition can be expressed by the constraints:

$$\dot{x}_1 + r\dot{\phi} \cos \theta = 0 \quad (\text{E1.2.a})$$

$$\dot{y}_1 - r\dot{\phi} \sin \theta = 0 \quad (\text{E1.2.b})$$

where the angles ϕ and θ are such as:

$$x_2 - x_1 = r \sin \phi \cos \theta \quad (\text{E1.2.c})$$

$$y_2 - y_1 = -r \sin \phi \sin \theta \quad (\text{E1.2.d})$$

The four relationships above yield two implicit nonholonomic constraints between x_i and y_i . Finally, the wheel kinematics imposes the constraint:

$$z_2 - z_1 = -r \cos \phi \quad (\text{E1.2.e})$$

$$z_1 = r. \quad (\text{E1.2.f})$$

The system is thus described in terms of the eight variables:

$$x_1, y_1, z_1, x_2, y_2, z_2, \phi, \theta$$

and is submitted to:

- the two nonholonomic constraints (E1.2.a) and (E1.2.b)
- the four holonomic constraints (E1.2.c), (E1.2.d), (E1.2.e) and (E1.2.f).

The wheel degrees of freedom are restrained only by the holonomic constraints and therefore four independent variables are left: two translations in the rolling plane and two rotations. The non-holonomic constraints act as behaviour constraints: they do not restrict the possible configurations of the system but simply the way to reach them.

If we introduce the additional holonomic constraint that the orientation θ is fixed to a constant θ_{fixed} , namely $\theta = \theta_{\text{fixed}}$ one observes that the nonholonomic constraints (E1.2.a) and (E1.2.b) now become integrable and one can write:

$$x_1 + r\phi \cos \theta_{\text{fixed}} = x_1(\phi = 0)$$

$$y_1 - r\phi \sin \theta_{\text{fixed}} = y_1(\phi = 0)$$

In this case all constraints are holonomic and the system has only one degree of freedom: it can for instance be seen that ϕ describes the configuration in a unique way.

1.2.3 Concept of generalized displacements

If R holonomic kinematic constraints exist between the $3N$ displacement components of the system, the number of degrees of freedom is then reduced to $3N - R$. It is then necessary to define $n = 3N - R$ configuration parameters, or *generalized coordinates*, denoted (q_1, \dots, q_n) in terms of which the displacements of the system particles are expressed in the form:

$$u_{ik}(x_{jk}, t) = U_{ik}(q_1, \dots, q_n, t) \quad (1.14)$$

When only holonomic constraints are applied to the system, the generalized coordinates q_s remain independent and may be varied in an arbitrary manner without violating the kinematic constraints. The virtual displacements δu_{ik} compatible with the holonomic constraints may be expressed in the form:

$$\delta u_{ik} = \sum_{s=1}^n \frac{\partial U_{ik}}{\partial q_s} \delta q_s \quad (1.15)$$

The virtual work equation becomes:

$$\sum_{s=1}^n \left[\sum_{k=1}^N \sum_{i=1}^3 (m_k \ddot{u}_{ik} - X_{ik}) \frac{\partial U_{ik}}{\partial q_s} \right] \delta q_s = 0 \quad (1.16)$$

The coefficients $\frac{\partial U_{ik}}{\partial q_s}$ define the displacement directions of mass k when the generalized coordinate q_s is varied. The variations δq_s are totally independent by definition, meaning that they can be chosen arbitrarily without violating any kinematic constraint. The identity (1.16) being satisfied for any virtual displacement, it follows that each associated term in the virtual work (1.16) principle must be zero. These terms correspond to the equilibrium projected onto the direction of the generalized coordinate q_s and written as:

$$\sum_{k=1}^N \sum_{i=1}^3 \left(m_k \frac{d^2 U_{ik}(q_1, \dots, q_n, t)}{dt^2} - X_{ik} \right) \frac{\partial U_{ik}}{\partial q_s} = 0 \quad s = 1, \dots, n \quad (1.17)$$

The second term in this equation corresponds to the *generalized force* conjugate to the degree of freedom q_s :

$$Q_s = \sum_{k=1}^N \sum_{i=1}^3 X_{ik} \frac{\partial U_{ik}}{\partial q_s} \quad (1.18)$$

The first term in (1.17) has the meaning of a generalized inertia force; its structure is obtained in the next section in terms of generalized coordinates.

Example 1.3

Figure 1.5 depicts a simple two-dimensional pendulum. The system has $2 - 1 = 1$ degree of freedom and we choose θ as generalized coordinate so that Equation (1.14) for the

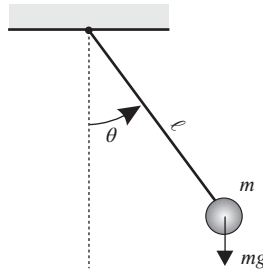


Figure 1.5 The simple pendulum.

pendulum is:

$$u_1 = \ell \cos \theta - \ell$$

$$u_2 = \ell \sin \theta$$

and the compatible virtual displacements are:

$$\delta u_1 = (-\ell \sin \theta) \delta \theta$$

$$\delta u_2 = (\ell \cos \theta) \delta \theta$$

which defines the direction orthogonal to the rigid link. The virtual work equation is then written as:

$$(m\ddot{u}_1 - mg)(-\ell \sin \theta) + (m\ddot{u}_2)(\ell \cos \theta) = 0 \quad (\text{E1.3.a})$$

The accelerations can be expressed as:

$$\ddot{u}_1 = -\ell\ddot{\theta} \sin \theta - \ell\dot{\theta}^2 \cos \theta$$

$$\ddot{u}_2 = \ell\ddot{\theta} \cos \theta - \ell\dot{\theta}^2 \sin \theta$$

and replacing in (E1.3.a), one finds the equation of motion:

$$m\ell^2\ddot{\theta} + mg\ell \sin \theta = 0 \quad (\text{E1.3.b})$$

Example 1.4

Let us consider the double pendulum of Figure 1.6. The system is made of two mass particles. The motion is restricted to 2-D motion, so that its kinematics is described by the four instantaneous position components ξ_{ik} . The two holonomic constraints applied to the system express the length invariance of the members:

$$\xi_{11}^2 + \xi_{21}^2 = \ell_1^2$$

$$(\xi_{12} - \xi_{11})^2 + (\xi_{22} - \xi_{21})^2 = \ell_2^2$$

The system kinematics may thus be described in terms of $4 - 2 = 2$ generalized coordinates. As a straightforward choice one may adopt the two rotation angles of the pendulum θ_1 and θ_2

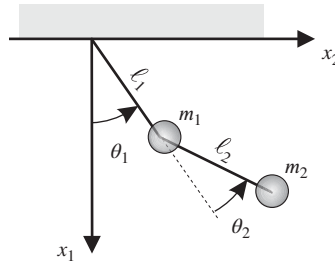


Figure 1.6 The double pendulum.

(the second angle being measured relatively to the first):

$$\xi_{11} = \ell_1 \cos \theta_1 \quad (\text{E1.4.a})$$

$$\xi_{21} = \ell_1 \sin \theta_1 \quad (\text{E1.4.b})$$

$$\xi_{12} = \xi_{11} + \ell_2 \cos(\theta_1 + \theta_2) = \ell_1 \cos \theta_1 + \ell_2 \cos(\theta_1 + \theta_2) \quad (\text{E1.4.c})$$

$$\xi_{22} = \xi_{21} + \ell_2 \sin(\theta_1 + \theta_2) = \ell_1 \sin \theta_1 + \ell_2 \sin(\theta_1 + \theta_2) \quad (\text{E1.4.d})$$

The equations of motion can then be written using the virtual work principle. This will not be done here (see Section 1.7.1).

1.3 Hamilton's principle for conservative systems and Lagrange equations

Hamilton's principle (Hamilton 1834) is no more than a time-integrated form of the virtual work principle obtained by transforming the expression:

$$\int_{t_1}^{t_2} \left[\sum_{k=1}^N \sum_{i=1}^3 (-m_k \ddot{u}_{ik} + X_{ik}) \delta u_{ik} \right] dt = 0 \quad (1.19)$$

where δu_{ik} are arbitrary but compatible virtual displacements which verify the end conditions (1.8).

First, let us assume that the applied forces X_{ik} can be derived from a potential \mathcal{V} . By definition the potential is such that:

$$X_{ik} = -\frac{\partial \mathcal{V}}{\partial u_{ik}} \quad (1.20)$$

So the virtual work of the forces can be expressed in the form:

$$\begin{aligned} \sum_{k=1}^N \sum_{i=1}^3 X_{ik} \delta u_{ik} &= - \sum_{k=1}^N \sum_{i=1}^3 \frac{\partial \mathcal{V}}{\partial u_{ik}} \sum_{s=1}^n \frac{\partial U_{ik}}{\partial q_s} \delta q_s \\ &= - \sum_{s=1}^n \frac{\partial \mathcal{V}}{\partial q_s} \delta q_s = \sum_{s=1}^n Q_s \delta q_s = -\delta \mathcal{V} \end{aligned}$$

It is thus seen that the generalized forces are derived from the potential \mathcal{V} by the relationship:

$$Q_s = \sum_{k=1}^N \sum_{i=1}^3 X_{ik} \frac{\partial U_{ik}}{\partial q_s} = -\frac{\partial \mathcal{V}}{\partial q_s} \quad (1.21)$$

Next the term associated with inertia forces is transformed by noting that:

$$\begin{aligned} \frac{d}{dt} (m_k \dot{u}_{ik} \delta u_{ik}) &= m_k \ddot{u}_{ik} \delta u_{ik} + m_k \dot{u}_{ik} \delta \dot{u}_{ik} \\ &= m_k \ddot{u}_{ik} \delta u_{ik} + \delta \left(\frac{1}{2} m_k \dot{u}_{ik} \dot{u}_{ik} \right) \end{aligned}$$

Owing to the definition of the kinetic energy \mathcal{T} of the system:

$$\mathcal{T} = \frac{1}{2} \sum_{k=1}^N \sum_{i=1}^3 m_k \dot{u}_{ik} \dot{u}_{ik} \quad (1.22)$$

(1.19) may be rewritten in the form:

$$\left[- \sum_{k=1}^N \sum_{i=1}^3 m_k \dot{u}_{ik} \delta u_{ik} \right]_{t_1}^{t_2} + \delta \int_{t_1}^{t_2} (\mathcal{T} - \mathcal{V}) dt = 0 \quad (1.23)$$

in which the time boundary term can be eliminated by taking account of the end conditions (1.8).

The functional (1.23) can be expressed in terms of the generalized coordinates q_s by noticing that:

$$\dot{u}_{ik} = \frac{\partial U_{ik}}{\partial t} + \sum_{s=1}^n \frac{\partial U_{ik}}{\partial q_s} \dot{q}_s \quad (1.24)$$

and therefore, that \mathcal{T} and \mathcal{V} respectively take the forms:

$$\mathcal{T} = \mathcal{T}(q, \dot{q}, t) \quad \mathcal{V} = \mathcal{V}(q, t) \quad (1.25)$$

By making use of Equations (1.8) and (1.15), the boundary conditions may also be written:

$$\delta q_s(t_1) = \delta q_s(t_2) = 0 \quad (1.26)$$

Hamilton's principle for a conservative system may thus be stated in the following form:

The real trajectory of the system is such that the integral

$$\int_{t_1}^{t_2} (\mathcal{T} - \mathcal{V}) dt$$

remains stationary with respect to any compatible virtual displacement, arbitrary between both instants t_1 and t_2 but vanishing at the ends of the interval.

$$\boxed{\begin{aligned} \delta \int_{t_1}^{t_2} (\mathcal{T} - \mathcal{V}) dt &= 0 \\ \delta q(t_1) &= \delta q(t_2) = 0 \end{aligned}} \quad (1.27)$$

Starting from expression (1.27) of Hamilton's principle, the system equations of motion are easily obtained in terms of generalized coordinates: owing to (1.25) one may write:

$$\delta \mathcal{T} = \sum_{s=1}^n \left(\frac{\partial \mathcal{T}}{\partial q_s} \delta q_s + \frac{\partial \mathcal{T}}{\partial \dot{q}_s} \delta \dot{q}_s \right)$$

giving the more explicit form of (1.27):

$$\int_{t_1}^{t_2} \sum_{s=1}^n \left[\left(\frac{\partial \mathcal{T}}{\partial q_s} + Q_s \right) \delta q_s + \frac{\partial \mathcal{T}}{\partial \dot{q}_s} \delta \dot{q}_s \right] dt = 0$$

in which the second term can be integrated by parts:

$$\int_{t_1}^{t_2} \frac{\partial \mathcal{T}}{\partial \dot{q}_s} \delta \dot{q}_s dt = \left[\frac{\partial \mathcal{T}}{\partial \dot{q}_s} \delta q_s \right]_{t_1}^{t_2} - \int_{t_1}^{t_2} \frac{d}{dt} \left(\frac{\partial \mathcal{T}}{\partial \dot{q}_s} \right) \delta q_s dt$$

Taking into account the boundary conditions, the following expression equivalent to Hamilton's principle results:

$$\int_{t_1}^{t_2} \sum_{s=1}^n \left[-\frac{d}{dt} \left(\frac{\partial \mathcal{T}}{\partial \dot{q}_s} \right) + \frac{\partial \mathcal{T}}{\partial q_s} + Q_s \right] \delta q_s dt = 0 \quad (1.28)$$

The variation δq_s being arbitrary on the whole time interval, the motion equations result in the form obtained by *Lagrange* (Lagrange 1788):

$$\boxed{-\frac{d}{dt} \left(\frac{\partial \mathcal{T}}{\partial \dot{q}_s} \right) + \frac{\partial \mathcal{T}}{\partial q_s} + Q_s = 0 \quad s = 1, \dots, n} \quad (1.29)$$

The Lagrange equations (1.29) are a set of n equations for the n unknown degrees of freedom q_s and are equivalent to the equations obtained from the virtual work principle (1.17). The advantage of the Lagrange form is however that, once the kinetic energy \mathcal{T} has been expressed in terms of the degrees of freedom q_s , the inertia terms are directly obtained in terms of q_s and their derivatives, whereas the virtual work Equations (1.17) contain \ddot{u}_{ik} that still needs to be expressed in terms q_s (see for instance the last step in Example 1.3).

The first two terms in (1.29) represent the generalized inertia forces associated with the generalized coordinates q_s . Their structure will be detailed in the next paragraph after taking account of the kinematic constraints.

Although here the discussion was made assuming that the effective applied forces derive from a potential, the Lagrange equations (1.29) are also valid if the applied forces do not derive from a potential. For forces deriving from a potential the generalized forces Q_s can be computed by (1.21), otherwise one has to use the fundamental definition (1.18). Their classification will be given in a later section.

Example 1.5

Consider the simple two-dimensional pendulum described in Figure 1.7.a. As found before (see Example 1.3) we can choose the angle θ as degree of freedom so that:

$$\begin{aligned} u_1 &= \ell \cos \theta - \ell & \text{and} & & \dot{u}_1 &= (-\ell \sin \theta) \dot{\theta} \\ u_2 &= \ell \sin \theta & & & \dot{u}_2 &= (\ell \cos \theta) \dot{\theta} \end{aligned}$$

The kinetic and potential energy of the system are then written for θ :

$$\mathcal{T} = \frac{1}{2}m(\dot{u}_1^2 + \dot{u}_2^2) = \frac{1}{2}m\ell^2\dot{\theta}^2$$

$$\mathcal{V} = -mgu_1 = mg\ell(1 - \cos \theta)$$

Observe that, by definition, the potential energy is such that $-\partial\mathcal{V}/\partial u_1$ yields the applied force in direction of u_1 . One computes:

$$\frac{d}{dt} \frac{\partial \mathcal{T}}{\partial \dot{\theta}} = \frac{d}{dt} (m\ell^2 \dot{\theta}) = m\ell^2 \ddot{\theta}$$

$$\frac{\partial \mathcal{T}}{\partial \theta} = 0$$

$$Q = -\frac{\partial \mathcal{V}}{\partial \theta} = -mg\ell \sin \theta$$

The Lagrange equation thus yields the expected pendulum equation:

$$m\ell^2 \ddot{\theta} + mg\ell \sin \theta = 0$$

Example 1.6

Consider now the pendulum in Figure 1.7.b, where a constant acceleration is given to the attachment point so that $u_{2,att} = \frac{a}{2}t^2$, where a is a given constant. With this rheonomic/holonomic constraint the system has one degree of freedom and we again choose θ to describe the system so that:

$$\begin{aligned} u_1 &= \ell \cos \theta - \ell & \text{and} & & \dot{u}_1 &= (-\ell \sin \theta) \dot{\theta} \\ u_2 &= \ell \sin \theta + \frac{a}{2}t^2 & & & \dot{u}_2 &= (\ell \cos \theta) \dot{\theta} + at \end{aligned}$$

and the energies are computed as:

$$\mathcal{T} = \frac{1}{2}m(\dot{u}_1^2 + \dot{u}_2^2) = \frac{1}{2}m\ell^2\dot{\theta}^2 + \frac{1}{2}m(at)^2 + mat(\ell \cos \theta) \dot{\theta}$$

$$\mathcal{V} = -mgu_1 = mg\ell(1 - \cos \theta)$$

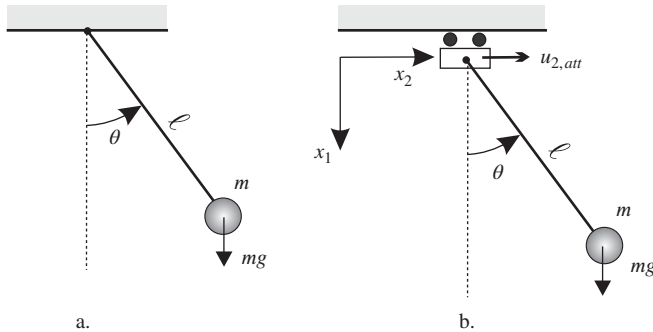


Figure 1.7 The simple pendulum with scleronomic (a) and with rheonomic constraint (b).

The terms in the Lagrange equations are obtained as:

$$\begin{aligned}\frac{d}{dt} \frac{\partial \mathcal{T}}{\partial \dot{\theta}} &= \frac{d}{dt} (m\ell^2 \ddot{\theta} + a\ell \cos \theta) = m\ell^2 \ddot{\theta} + m a \ell \cos \theta - m a \ell \dot{\theta} \sin \theta \\ \frac{\partial \mathcal{T}}{\partial \theta} &= -m a \ell (\ell \sin \theta) \dot{\theta} \\ Q &= -\frac{\partial \mathcal{V}}{\partial \theta} = -m g \ell \sin \theta\end{aligned}$$

The Lagrange equation yields:

$$m\ell^2 \ddot{\theta} + m a \ell \cos \theta + m g \ell \sin \theta = 0$$

Note that this equation can also be written as:

$$m\ell^2 \ddot{\theta} + m\ell \sqrt{g^2 + a^2} \sin(\theta + \alpha) = 0 \quad \text{where } \alpha = \arctan \frac{a}{g}$$

indicating that the problem can be considered as a pendulum in a combined acceleration field of the gravity and the imposed acceleration on the support. It also shows that motion of the support at constant velocity does not affect the system behaviour.

1.3.1 Structure of kinetic energy and classification of inertia forces

Let us substitute in the general kinetic energy expression (1.22) the velocities expressed in terms of generalized coordinates (1.24). The kinetic energy is then split naturally in three contributions:

$$\mathcal{T}(q, \dot{q}, t) = \mathcal{T}_0 + \mathcal{T}_1 + \mathcal{T}_2 \quad (1.30)$$

where \mathcal{T}_0 , \mathcal{T}_1 and \mathcal{T}_2 are respectively homogeneous forms of degree 0, 1 or 2 in the generalized velocities \dot{q}_s .

– The first term:

$$\mathcal{T}_0 = \frac{1}{2} \sum_{k=1}^N \sum_{i=1}^3 m_k \left(\frac{\partial U_{ik}}{\partial t} \right)^2 = \mathcal{T}_0(q, t) \quad (1.31)$$

is obviously the *transport kinetic energy* of the system since it corresponds to the situation where the degrees of freedom q_1, \dots, q_n are frozen.

– The second term:

$$\mathcal{T}_1 = \sum_{s=1}^n \sum_{k=1}^N \sum_{i=1}^3 \frac{\partial U_{ik}}{\partial t} m_k \frac{\partial U_{ik}}{\partial q_s} \dot{q}_s \quad (1.32)$$

is the *mutual kinetic energy*.

– The third term:

$$\mathcal{T}_2 = \frac{1}{2} \sum_{s=1}^n \sum_{r=1}^n \sum_{k=1}^N \sum_{i=1}^3 m_k \frac{\partial U_{ik}}{\partial q_s} \frac{\partial U_{ik}}{\partial q_r} \dot{q}_s \dot{q}_r \quad (1.33)$$

is the *relative kinetic energy* since it corresponds to what is left when the explicit dependence of velocities \dot{U}_{ik} with respect to time is suppressed.

Let us note that frequent use will be made of the following expressions for \mathcal{T}_1 and \mathcal{T}_2 :

$$\mathcal{T}_1 = \sum_{s=1}^n \dot{q}_s \frac{\partial \mathcal{T}_1}{\partial \dot{q}_s} \quad \mathcal{T}_2 = \frac{1}{2} \sum_{s=1}^n \dot{q}_s \frac{\partial \mathcal{T}_2}{\partial \dot{q}_s} \quad (1.34)$$

which result immediately from Euler's theorem on homogeneous functions.

Euler's theorem on homogeneous functions

If $f(x_1, \dots, x_n)$ is homogeneous of degree m in the variables (x_1, \dots, x_n) the following equality is satisfied:

$$\sum_{i=1}^n x_i \frac{\partial f}{\partial x_i} = mf \quad (1.35)$$

The proof holds by observing that if f is homogeneous of degree m , it may be written in the form:

$$f(x_1, \dots, x_n) = x_1^m g\left(1, \frac{x_2}{x_1}, \dots, \frac{x_n}{x_1}\right)$$

Noting $y_i = x_i/x_1$, one obtains:

$$\begin{aligned} x_1 \frac{\partial f}{\partial x_1} &= mx_1^m g - x_1^{m+1} \sum_{i=2}^n \frac{x_i}{x_1^2} \frac{\partial g}{\partial y_i} \\ x_i \frac{\partial f}{\partial x_i} &= x_i x_1^{m-1} \frac{\partial g}{\partial y_i} \quad i \neq 1 \end{aligned}$$

The proof of Euler's theorem holds by summing up all the above relations.

Let us make use of the decomposition (1.30) to interpret the term describing the generalized inertia forces in Lagrange's equations (1.29):

$$\begin{aligned} -\frac{d}{dt} \left(\frac{\partial \mathcal{T}}{\partial \dot{q}_s} \right) + \frac{\partial \mathcal{T}}{\partial q_s} &= -\frac{d}{dt} \left(\frac{\partial \mathcal{T}_1}{\partial \dot{q}_s} + \frac{\partial \mathcal{T}_2}{\partial \dot{q}_s} \right) + \frac{(\partial \mathcal{T}_0 + \mathcal{T}_1 + \mathcal{T}_2)}{\partial q_s} \\ &= -\frac{\partial}{\partial t} \left(\frac{\partial \mathcal{T}_1}{\partial \dot{q}_s} \right) - \sum_{r=1}^n \left[\frac{\partial^2 \mathcal{T}_1}{\partial \dot{q}_s \partial q_r} \dot{q}_r \right] - \frac{d}{dt} \left(\frac{\partial \mathcal{T}_2}{\partial \dot{q}_s} \right) \\ &\quad + \frac{\partial(\mathcal{T}_0 + \mathcal{T}_1 + \mathcal{T}_2)}{\partial q_s} \end{aligned} \quad (1.36)$$

– The *transport inertia forces* are those obtained by setting $\dot{q}_s = 0$. One obtains:

$$-\frac{\partial}{\partial t} \left(\frac{\partial \mathcal{T}_1}{\partial \dot{q}_s} \right) + \frac{\partial \mathcal{T}_0}{\partial q_s} \quad (1.37)$$

– The *relative inertia forces* are those obtained by assuming that the constraints do not depend explicitly on time ($\partial U_{ik}/\partial t = 0$). The remaining terms are the \mathcal{T}_2 terms:

$$-\frac{d}{dt} \left(\frac{\partial \mathcal{T}_2}{\partial \dot{q}_s} \right) + \frac{\partial \mathcal{T}_2}{\partial q_s} \quad (1.38)$$

– The *complementary inertia forces* contain the missing terms:

$$F_s = - \sum_{r=1}^n \frac{\partial^2 \mathcal{T}_1}{\partial \dot{q}_s \partial q_r} \dot{q}_r + \frac{\partial \mathcal{T}_1}{\partial q_s}$$

Making use of (1.34) they can be put in the equivalent form:

$$F_s = \sum_{r=1}^n \dot{q}_r \left[\frac{\partial^2 \mathcal{T}_1}{\partial q_s \partial \dot{q}_r} - \frac{\partial^2 \mathcal{T}_1}{\partial q_r \partial \dot{q}_s} \right] = \sum_{r=1}^n \dot{q}_r g_{rs} \quad (1.39)$$

where the coefficients:

$$g_{rs} = \frac{\partial^2 \mathcal{T}_1}{\partial q_s \partial \dot{q}_r} - \frac{\partial^2 \mathcal{T}_1}{\partial q_r \partial \dot{q}_s} = -g_{sr} \quad (1.40)$$

do not depend on the velocities \dot{q}_s , but only on the generalized displacements and time. The complementary inertia forces have the nature of *Coriolis* or *gyroscopic forces*. As a consequence of the skew symmetry of the coefficients (1.40), the associated instantaneous power is equal to zero:

$$\sum_{s=1}^n F_s \dot{q}_s = 0 \quad (1.41)$$

1.3.2 Energy conservation in a system with scleronomic constraints

When the kinematic constraints are independent of time, the kinetic energy (1.30) reduces to the sole term \mathcal{T}_2 and therefore becomes a homogeneous quadratic form of the generalized velocities. Owing to (1.34) one may write:

$$2\mathcal{T} = \sum_{s=1}^n \dot{q}_s \frac{\partial \mathcal{T}}{\partial \dot{q}_s}$$

or, after differentiation:

$$2 \frac{d\mathcal{T}}{dt} = \sum_{s=1}^n \ddot{q}_s \frac{\partial \mathcal{T}}{\partial \dot{q}_s} + \sum_{s=1}^n \dot{q}_s \frac{d}{dt} \left(\frac{\partial \mathcal{T}}{\partial \dot{q}_s} \right) \quad (1.42)$$

On the other hand, since $\mathcal{T} = \mathcal{T}(q, \dot{q})$, one may also write

$$\frac{d\mathcal{T}}{dt} = \sum_{s=1}^n \ddot{q}_s \frac{\partial \mathcal{T}}{\partial \dot{q}_s} + \sum_{s=1}^n \dot{q}_s \frac{\partial \mathcal{T}}{\partial q_s} \quad (1.43)$$

Therefore, by subtracting (1.43) from (1.42) and making use of Lagrange equations (1.29),

$$\frac{d\mathcal{T}}{dt} = \sum_{s=1}^n \dot{q}_s \left[\frac{d}{dt} \left(\frac{\partial \mathcal{T}}{\partial \dot{q}_s} \right) - \frac{\partial \mathcal{T}}{\partial q_s} \right] = \sum_{s=1}^n \dot{q}_s Q_s \quad (1.44)$$

Since in the conservative case the forces Q_s depend also on a potential,

$$\sum_{s=1}^n \dot{q}_s Q_s = \sum_{s=1}^n \dot{q}_s \left(-\frac{\partial \mathcal{V}}{\partial q_s} \right) = -\frac{d\mathcal{V}}{dt}$$

one obtains

$$\boxed{\frac{d}{dt}(\mathcal{T} + \mathcal{V}) = 0} \quad (1.45)$$

The corresponding energy integral:

$$\mathcal{T} + \mathcal{V} = \mathcal{E} \quad (1.46)$$

plays a fundamental role in the theory governing the linear oscillations of a stable system about its equilibrium position.

Example 1.7

The vibrational behaviour of a pendulum (Figure 1.5) can easily be described in terms of total energy conservation.

The kinetic and potential energies corresponding to an angular displacement θ are:

$$\mathcal{T} = \frac{1}{2}m\ell^2\dot{\theta}^2 \quad \mathcal{V} = mg\ell(1 - \cos \theta) \quad (\text{E1.7.a})$$

The total energy conservation law yields:

$$\mathcal{E} = \mathcal{T} + \mathcal{V} \quad (\text{E1.7.b})$$

where \mathcal{E} is the energy input into the system.

Figure 1.8.a shows the potential energy of the system as a function of the angular displacement. The horizontal lines represent various initial energy levels \mathcal{E}_i and we call \mathcal{E}_3 the maximum possible potential energy, namely $\mathcal{V} = 2mg\ell$.

If the total energy level of the system is lower than \mathcal{E}_3 , the system can reach a state where $\mathcal{E}_3 = \mathcal{V}$ and where the kinetic energy is null. In that configuration the system has zero velocity and has reached its maximum angular displacement θ_{\max} , solution of:

$$\mathcal{E} = mg\ell(1 - \cos \theta_{\max}) \quad (\text{E1.7.c})$$

The kinetic energy is obtained by subtracting from \mathcal{E} the potential energy:

$$\mathcal{T} = \mathcal{E} - \mathcal{V}$$

and in the case $\mathcal{E} < \mathcal{E}_3$ we can use (E1.7.c) together with (E1.7.a) to obtain:

$$\dot{\theta} = \pm \sqrt{\frac{2g}{\ell}(\cos \theta - \cos \theta_{\max})} \quad (\text{E1.7.d})$$

In a phase-space representation $(\theta, \dot{\theta})$ this relation yields closed trajectories as represented by the dotted curves in Figure 1.8.b.

If the total energy level is $\mathcal{T} > \mathcal{E}_3$, the system can reach its maximum potential position with a non-zero velocity since $\mathcal{E} - \mathcal{V} = \mathcal{T} > 0$ for the entire motion. The velocity is then found from the energy conservation as:

$$\mathcal{T} = \mathcal{E} - \mathcal{V}$$

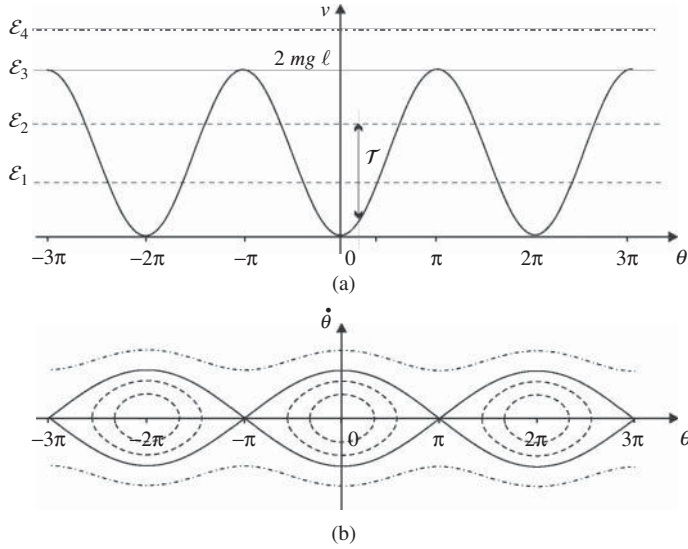


Figure 1.8 The nonlinear pendulum: (a) potential energy, (b) phase space diagram $\dot{\theta} = f(\theta)$.

and in the case $\mathcal{E} < \mathcal{E}_3$ we can use (E1.7.c) together with (E1.7.a) to obtain:

$$\dot{\theta} = \pm \sqrt{\frac{2g}{\ell} \left(\cos \theta - 1 + \frac{\mathcal{E}}{mg\ell} \right)} \quad (\text{E1.7.e})$$

This leads to nonclosed trajectories in the phase-space as indicated by the dash-dotted line in Figure 1.8.b.

To summarize, three regions can be distinguished:

- For $\mathcal{E} < \mathcal{E}_3$, the motion is oscillatory and the corresponding trajectories in the phase space are closed regular curves (of the ellipse type if $\cos \theta \simeq 1 - \frac{\theta^2}{2}$).
- For $\mathcal{E} = \mathcal{E}_3$, the positions $\theta = \pm(2n+1)\pi$, ($n = 0, 1, \dots$) are bifurcation points of the solution.
- For $\mathcal{E} > \mathcal{E}_3$, the motion is no longer oscillatory but the pendulum undergoes complete rotation with variable rotation speed.

In the case $\mathcal{E} < \mathcal{E}_3$, making use of Equation (E1.7.d), the oscillation period can be computed if we notice that from the definition of velocity:

$$\dot{\theta} = \frac{d\theta}{dt}$$

the time required to undergo a displacement $d\theta$ is:

$$dt = \frac{d\theta}{\dot{\theta}} = \pm \sqrt{\frac{\ell}{2g(\cos \theta - \cos \theta_{\max})}} d\theta$$

Due to symmetry of the phase-plane trajectory, the period – which is the time corresponding to the path of one closed trajectory – is given by:

$$T = 4\sqrt{\frac{\ell}{2g}} \int_0^{\theta_{\max}} \frac{d\theta}{\sqrt{\cos \theta - \cos \theta_{\max}}} \quad (\text{E1.7.f})$$

This last integral can be transformed into a known elliptic integral via the following change of variable:

$$\sin \frac{\theta}{2} = \sin \frac{\theta_{\max}}{2} \sin \phi$$

where $[0, \theta_{\max}] \rightarrow [0, \frac{\pi}{2}]$. We find successively:

$$d\theta = \frac{2 \sin \frac{\theta_{\max}}{2} \cos \phi}{\sqrt{1 - \sin^2 \frac{\theta_{\max}}{2} \sin^2 \phi}} d\phi$$

and

$$\sqrt{\cos \theta - \cos \theta_{\max}} = \sqrt{2} \sin \frac{\theta_{\max}}{2} \cos \phi$$

From the results above, the expression of the period becomes:

$$T = 4\sqrt{\frac{\ell}{g}} \int_0^{\pi/2} \frac{d\phi}{\sqrt{1 - \sin^2 \frac{\theta_{\max}}{2} \sin^2 \phi}} \quad (\text{E1.7.g})$$

Expanding the integral (Abramowitz and Stegun 1970) into:

$$\int_0^{\pi/2} \frac{d\phi}{\sqrt{1 - k^2 \sin^2 \phi}} = \frac{\pi}{2} \left[1 + \frac{k^2}{4} + \dots \right]$$

allows us to write the period as a function of the angular displacement amplitude:

$$T = 2\pi\sqrt{\frac{\ell}{g}} \left[1 + \frac{\theta_{\max}^2}{16} + \dots \right] \quad (\text{E1.7.h})$$

This shows that the period is a quadratic increasing function of the amplitude.

1.3.3 Classification of generalized forces

A distinction can be made between *internal* and *external* forces to the system. In both cases they are said to be *conservative* if the associated virtual work is recoverable.

Internal forces

Among the internal forces, the distinction can be made between the linking forces, those associated with elastic deformation and those resulting from a dissipation mechanism.

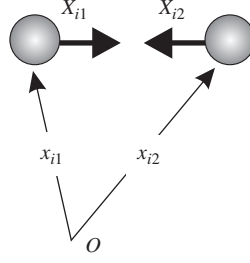


Figure 1.9 Linking forces.

Linking forces

The linking forces appear in a rigid connection between two particles. As already discussed in Section 1.2.1 they are such as the system of forces is in equilibrium (Figure 1.9):

$$X_{i1} + X_{i2} = 0 \quad (1.47)$$

The virtual work associated with the virtual displacement $(\delta u_{i1}, \delta u_{i2})$ is:

$$\begin{aligned} \delta \tau &= \sum_{i=1}^3 (X_{i1} \delta u_{i1} + X_{i2} \delta u_{i2}) \\ &= \sum_{i=1}^3 [X_{i1} (\delta u_{i1} - \delta u_{i2})] \\ &= 0 \end{aligned}$$

since the nonzero relative virtual displacements are not compatible with the constraints. Hence it can be deduced that *the linking forces do not contribute to the generalized forces* acting on the global system. Their absence from the evaluation of the generalized forces is one of the attractive aspects of Lagrangian mechanics.

Elastic forces

An elastic body can be defined as a body for which any produced work is stored in a recoverable form, thus giving rise to a variation of internal energy:

$$\delta \mathcal{V}_{int} = \sum_{i=1}^3 \sum_{k=1}^N \frac{\partial \mathcal{V}_{int}}{\partial u_{ik}} \delta u_{ik} = -\delta \tau$$

where τ is the virtual work of internal forces. It can be expressed in terms of generalized displacements:

$$\begin{aligned} \mathcal{V}_{int} &= \mathcal{V}_{int}(q, t) \\ \delta \tau &= \sum_{s=1}^n Q_s \delta q_s = -\delta \mathcal{V}_{int} \end{aligned}$$

with the generalized forces of elastic origin

$$Q_s = -\frac{\partial \mathcal{V}_{int}}{\partial q_s} \quad (1.48)$$

Dissipation forces

A dissipation (or dissipative) force may be characterized by the fact that it remains parallel and in opposite direction to the velocity vector and is a function of its modulus. Therefore, a dissipation force acting on a mass particle k may be expressed in the form:

$$\mathbf{X}_k = -C_k f_k(v_k) \frac{\mathbf{v}_k}{v_k}$$

or, in terms of components:

$$X_{ik} = -C_k f_k(v_k) \frac{v_{ik}}{v_k} \quad (1.49)$$

where

- C_k is a constant
- $f_k(v_k)$ is the function expressing velocity dependence
- v_k is the absolute velocity of particle k :

$$v_k = |\mathbf{v}_k| = \sqrt{\sum_{i=1}^3 v_{ik}^2} = \sqrt{\sum_{i=1}^3 \dot{u}_{ik}^2}$$

The virtual work of the dissipation forces acting on the system is:

$$\begin{aligned} \sum_{s=1}^n Q_s \delta q_s &= \sum_{i=1}^3 \sum_{k=1}^N X_{ik} \delta u_{ik} \\ &= \sum_{i=1}^3 \sum_{k=1}^N \sum_{s=1}^n X_{ik} \frac{\partial u_{ik}}{\partial q_s} \delta q_s \end{aligned}$$

yielding:

$$Q_s = - \sum_{i=1}^3 \sum_{k=1}^N C_k f_k(v_k) \frac{v_{ik}}{v_k} \frac{\partial u_{ik}}{\partial q_s} \quad (1.50)$$

By noticing that:

$$\begin{aligned} v_{ik} &= \frac{du_{ik}}{dt} = \frac{\partial u_{ik}}{\partial t} + \sum_{r=1}^n \frac{\partial u_{ik}}{\partial q_r} \dot{q}_r \\ \frac{\partial v_{ik}}{\partial \dot{q}_s} &= \frac{\partial u_{ik}}{\partial q_s} \end{aligned} \quad (1.51)$$

one may write:

$$Q_s = - \sum_{i=1}^3 \sum_{k=1}^N C_k f_k(v_k) \frac{v_{ik}}{v_k} \frac{\partial v_{ik}}{\partial \dot{q}_s}$$

$$\begin{aligned}
&= - \sum_{k=1}^N C_k \frac{f_k(v_k)}{v_k} \frac{\partial}{\partial \dot{q}_s} \left[\frac{1}{2} \sum_{i=1}^3 v_{ik}^2 \right] \\
&= - \sum_{k=1}^N C_k f_k(v_k) \frac{\partial v_k}{\partial \dot{q}_s}
\end{aligned} \tag{1.52}$$

Let us next introduce the dissipation function D as:

$$D = \sum_{k=1}^N \int_0^{v_k} C_k f_k(\gamma) d\gamma \tag{1.53}$$

and thus:

$$Q_s = - \frac{\partial D}{\partial \dot{q}_s} \tag{1.54}$$

The dissipated power takes the form:

$$P = \sum_{s=1}^n Q_s \dot{q}_s = - \sum_{s=1}^n \dot{q}_s \frac{\partial D}{\partial \dot{q}_s}$$

By assuming that the dissipation function D is homogeneous of order m in the generalized velocities, one gets from (1.53) the energy dissipation equation

$$\boxed{\frac{d}{dt}(\mathcal{T} + \mathcal{V}) = -mD} \tag{1.55}$$

The order m of the dissipation function and thus the order $m - 1$ of the generalized dissipation forces Q_s describes the physical dissipation mode:

$m = 1$	\leftrightarrow	dry friction
$m = 2$	\leftrightarrow	viscous damping
$m = 3$	\leftrightarrow	aerodynamic drag

Let us finally note that the dissipation forces, although classified here as internal forces, may have external origins too.

External forces

Conservative forces

When the external forces are conservative, their virtual work remains zero during a cycle:

$$\delta \tau = \oint Q_s \delta q_s = 0$$

and a potential of external forces $\mathcal{V}_{ext}(q, t)$ can be introduced such as:

$$Q_s = - \frac{\partial \mathcal{V}_{ext}}{\partial q_s} \tag{1.56}$$

Nonconservative forces

When the external forces are of the nonconservative type, the evaluation of the corresponding generalized forces is achieved by making use of a virtual work equation:

$$\begin{aligned}\delta\tau &= \sum_{s=1}^n Q_s \delta q_s = \sum_{i=1}^3 \sum_{k=1}^N X_{ik} \delta u_{ik} \\ &= \sum_{i=1}^3 \sum_{k=1}^N \sum_{s=1}^n X_{ik} \frac{\partial u_{ik}}{\partial q_s} \delta q_s\end{aligned}$$

and thus:

$$Q_s = \sum_{i=1}^3 \sum_{k=1}^N X_{ik} \frac{\partial u_{ik}}{\partial q_s} \quad (1.57)$$

Taking into account the nonconservative external forces, the power balance of a system can be written in the more general form:

$$\boxed{\frac{d}{dt}(\mathcal{T} + \mathcal{V}) = -mD + \sum_{s=1}^n Q_s \dot{q}_s} \quad (1.58)$$

1.4 Lagrange equations in the general case

In the general case of a nonconservative system with rheonomic constraints, the Lagrange equations of motion may be explicitly expressed in the form:

$$\boxed{-\frac{d}{dt} \left(\frac{\partial \mathcal{T}}{\partial \dot{q}_s} \right) + \frac{\partial \mathcal{T}}{\partial q_s} - \frac{\partial \mathcal{V}}{\partial q_s} - \frac{\partial D}{\partial \dot{q}_s} + Q_s(t) = 0 \quad s = 1, \dots, n} \quad (1.59)$$

or, by explicitly introducing the relative inertia forces:

$$\boxed{\frac{d}{dt} \left(\frac{\partial \mathcal{T}_2}{\partial \dot{q}_s} \right) - \frac{\partial \mathcal{T}_2}{\partial q_s} = Q_s(t) - \frac{\partial \mathcal{V}^*}{\partial q_s} - \frac{\partial D}{\partial \dot{q}_s} + F_s - \frac{\partial}{\partial t} \left(\frac{\partial \mathcal{T}_1}{\partial \dot{q}_s} \right) \quad s = 1, \dots, n} \quad (1.60)$$

where

- $Q_s(t)$ nonconservative external generalized forces
 $\mathcal{V} = \mathcal{V}_{ext} + \mathcal{V}_{int}$ total potential
 $\mathcal{V}^* = \mathcal{V} - \mathcal{T}_0$ potential modified by the transport kinetic energy
 $F_s = \sum_{r=1}^n \dot{q}_r G_{rs}$ generalized gyroscopic forces
 D dissipation function

Example 1.8

Let us derive the equations of motion for the system of Figure 1.10 made of a wheel of rotating inertia I inside which a mass m is attached through a system of springs and a viscous damper.

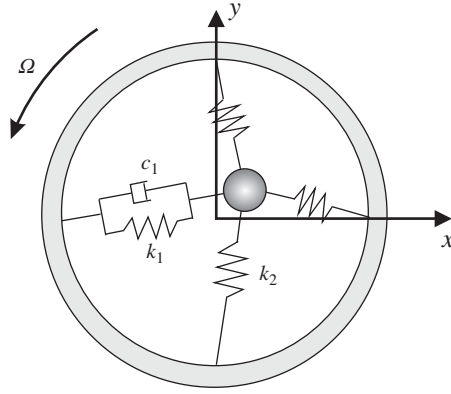


Figure 1.10 Rotating system.

Assuming a coordinate system (x, y) rotating at a constant rotation speed Ω and attached to the wheel, mass m has the following absolute velocity components:

$$\mathbf{v} = [\dot{x} - \Omega y, \dot{y} + \Omega x]$$

Hence the kinetic energy is given by:

$$\mathcal{T} = \frac{1}{2}m [(\dot{x} - \Omega y)^2 + (\dot{y} + \Omega x)^2] + \frac{1}{2}I\Omega^2$$

Assuming that displacements x and y remain small, the potential energy of the springs is equal to

$$\mathcal{V} = \frac{1}{2}k_1x^2 + \frac{1}{2}k_2y^2$$

while the dissipation function of the damper takes the form:

$$\mathcal{D} = \frac{1}{2}c_1\dot{x}^2$$

By applying the Lagrange equations (1.59), the equations of motion are obtained in the form:

$$m\ddot{x} - 2m\Omega\dot{y} - m\Omega^2x + c_1\dot{x} + k_1x = 0$$

$$m\ddot{y} + 2m\Omega\dot{x} - m\Omega^2y + k_2y = 0$$

They can also be put in the matrix form:

$$\mathbf{M}\ddot{\mathbf{q}} + (\mathbf{C} + \mathbf{G})\dot{\mathbf{q}} + (\mathbf{K} - \Omega^2\mathbf{M})\mathbf{q} = 0 \quad (\text{E1.8.a})$$

where the vector of generalized displacements $\mathbf{q}^T = [x \ y]$ and the mass, damping, stiffness and gyroscopic coupling matrices are defined below:

$$\mathbf{M} = \begin{bmatrix} m & 0 \\ 0 & m \end{bmatrix} \quad \mathbf{C} = \begin{bmatrix} c_1 & 0 \\ 0 & 0 \end{bmatrix}$$

$$\mathbf{K}^* = \begin{bmatrix} k_1 & 0 \\ 0 & k_2 \end{bmatrix} \quad \mathbf{G} = \begin{bmatrix} 0 & -2m\Omega \\ 2m\Omega & 0 \end{bmatrix}$$

The meaning of the different terms is more apparent when using the Lagrange equations in the form (1.60):

$$\mathcal{T}_0 = \frac{1}{2}m\Omega^2(x^2 + y^2) = \frac{1}{2} \begin{bmatrix} x & y \end{bmatrix} \begin{bmatrix} m\Omega^2 & 0 \\ 0 & m\Omega^2 \end{bmatrix} \begin{bmatrix} x \\ y \end{bmatrix} = \frac{\Omega^2}{2} \mathbf{q}^T \mathbf{M} \mathbf{q} \quad (\text{E1.8.b})$$

$$\mathcal{T}_1 = m\Omega(x\dot{y} - \dot{x}y) = \begin{bmatrix} \dot{x} & \dot{y} \end{bmatrix} \begin{bmatrix} 0 & -m\Omega \\ m\Omega & 0 \end{bmatrix} \begin{bmatrix} x \\ y \end{bmatrix} = \frac{1}{2} \dot{\mathbf{q}}^T \mathbf{G} \mathbf{q} \quad (\text{E1.8.c})$$

$$\mathcal{T}_2 = \frac{1}{2}m(\dot{x}^2 + \dot{y}^2) = \frac{1}{2} \begin{bmatrix} \dot{x} & \dot{y} \end{bmatrix} \begin{bmatrix} m & 0 \\ 0 & m \end{bmatrix} \begin{bmatrix} \dot{x} \\ \dot{y} \end{bmatrix} = \frac{1}{2} \dot{\mathbf{q}}^T \mathbf{M} \dot{\mathbf{q}} \quad (\text{E1.8.d})$$

$$\mathcal{V} = \frac{1}{2}(k_1x^2 + k_2y^2) = \frac{1}{2} \begin{bmatrix} x & y \end{bmatrix} \begin{bmatrix} k_1 & 0 \\ 0 & k_2 \end{bmatrix} \begin{bmatrix} x \\ y \end{bmatrix} = \frac{1}{2} \mathbf{q}^T \mathbf{K} \mathbf{q} \quad (\text{E1.8.e})$$

$$\mathcal{D} = \frac{1}{2}c_1\dot{x}^2 = \frac{1}{2} \begin{bmatrix} \dot{x} & \dot{y} \end{bmatrix} \begin{bmatrix} c_1 & 0 \\ 0 & 0 \end{bmatrix} \begin{bmatrix} \dot{x} \\ \dot{y} \end{bmatrix} = \frac{1}{2} \dot{\mathbf{q}}^T \mathbf{C} \dot{\mathbf{q}} \quad (\text{E1.8.f})$$

By subtracting (E1.8.b) from (E1.8.e), the modified potential takes the form:

$$\mathcal{V}^* = \mathcal{V} - \mathcal{T}_0 = \frac{1}{2} \mathbf{q}^T (\mathbf{K} - \Omega^2 \mathbf{M}) \mathbf{q} = \frac{1}{2} \mathbf{q}^T \mathbf{K}^* \mathbf{q}$$

The mass and damping matrices of the system are clearly positive definite. The effective stiffness matrix \mathbf{K}^* , however, loses its positive definite character when $\Omega^2 > \min(k_1/m, k_2/m)$. The stability behaviour of the system is thus controlled by its rotating speed, as will be shown in Section 2.11.

Remark 1.1 Although the physical meaning of centrifugal forces $-\Omega^2 \mathbf{M} \mathbf{q}$ in Equation (E1.8.a) is usually easily understood, this is not the case of gyroscopic forces $\mathbf{G} \dot{\mathbf{q}}$ (also called Coriolis forces) which are more difficult to explain. The gyroscopic forces are in fact fictitious forces in the sense that they appear in the equation of motion of the system when they are expressed with respect to a moving frame as it is the case here.

In order to have a physical insight, let us assume that in the inertia wheel system, the mass m remains on the rotating axis x and moves with a varying velocity \dot{x} as described in Figure 1.11. We will graphically show that such a motion in fact corresponds to absolute accelerations given to mass m which will prove the presence of centrifugal and gyroscopic forces.

Figure 1.11.a shows the configuration and absolute velocities of the system at a given time and at a small time interval Δt later. Let the time interval the axis has rotated be an amount $\Delta\phi = \Omega\Delta t$. The velocity along the x axis has changed because of the relative acceleration \ddot{x} along x and the velocity along y has changed because its position on the x axis has changed by $\Delta x = \dot{x}\Delta t$. Also, observe that in that time interval the direction of the axes x and y has changed.

If we now analyze the variation of the absolute velocity (Figure 1.11.b), we observe that:

- the velocity change along x results in the absolute acceleration components:
 - i. $\frac{\Delta \dot{x}}{\Delta t} = \ddot{x}$ along x due to the relative velocity variation,
 - ii. $\frac{\dot{x}\Delta\phi}{\Delta t} = \dot{x}\Omega$ along y due to the change of direction of the x axis,

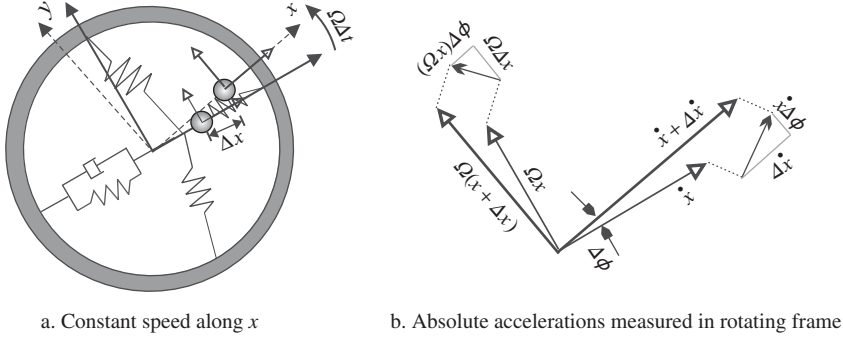


Figure 1.11 Physical interpretation of gyroscopic forces.

- the velocity change along y results in the absolute acceleration components:
 - i. $-\frac{(x\Omega)\Delta\phi}{\Delta t} = -x\Omega^2$ along x due to the change of direction of the y axis,
 - ii. $\frac{\Delta x\Omega}{\Delta t} = \dot{x}\Omega$ along y due to the change of position of the mass along x in the time interval.

Clearly, (i.) is the relative acceleration generating the relative inertia forces, (ii. + iii.) are the Coriolis accelerations generating the gyroscopic forces and (iv.) is the centripetal acceleration generating the centrifugal forces.

1.5 Lagrange equations for impulsive loading

1.5.1 Impulsive loading of a mass particle

Let us consider a particle undergoing a displacement u_i . Hamilton's principle takes the form:

$$\delta I = \int_{t_1}^{t_2} \sum_{i=1}^3 \left[\delta \left(\frac{1}{2} m \dot{u}_i \dot{u}_i \right) + X_i \delta u_i \right] dt = 0 \quad (1.61)$$

$$\text{with } \delta u_i(t_1) = \delta u_i(t_2) = 0$$

and it is assumed that \dot{u}_i and $\delta \dot{u}_i$ are piecewise continuous.

In representing the momentum of the particle, the possible discontinuity of the velocity field \dot{u}_i for certain t values does not allow performing the time derivative of the momentum $m\dot{u}_i$. Therefore, let us integrate by parts the second term of principle (1.61), in order to let the force integral over the time interval appear:

$$\begin{aligned} \delta I &= \left[\sum_{i=1}^3 \delta u_i \int_{t_1}^t X_i(t') dt' \right]_{t_1}^{t_2} + \int_{t_1}^{t_2} \sum_{i=1}^3 \left[m \dot{u}_i - \int_{t_1}^t X_i(t') dt' \right] \delta \dot{u}_i dt \\ &= \int_{t_1}^{t_2} \sum_{i=1}^3 M_i \delta \dot{u}_i dt = 0 \end{aligned} \quad (1.62)$$

For the sake of conciseness let us define:

$$M_i = m\ddot{u}_i - \int_{t_1}^t X_i(t') dt' \quad (1.63)$$

and in order to obtain the variational derivatives of this modified form of Hamilton's principle let us demonstrate first *du Bois-Reymond's theorem* (Courant and Hilbert 1953):

$$\begin{aligned} & \int_{t_1}^{t_2} \sum_{i=1}^3 M_i \delta \dot{u}_i dt = 0 \\ & \text{for piecewise continuous } \delta \dot{u}_i \text{ and } \delta u_i(t_1) = \delta u_i(t_2) = 0 \\ & \iff \\ & M_i = C_i \\ & \text{where } C_i \text{ are constants} \end{aligned} \quad (1.64)$$

The proof goes as follows:

Sufficient condition: if $M_i = C_i$, then

$$\begin{aligned} \int_{t_1}^{t_2} \sum_{i=1}^3 M_i \delta \dot{u}_i dt &= \sum_{i=1}^3 C_i \int_{t_1}^{t_2} \delta \dot{u}_i dt \\ &= \left[\sum_{i=1}^3 C_i \delta u_i \right]_{t_1}^{t_2} = 0 \end{aligned}$$

Necessary condition: since

$$\int_{t_1}^{t_2} \sum_{i=1}^3 M_i \delta \dot{u}_i dt = 0$$

for any virtual velocity $\delta \dot{u}_i$ piecewise continuous verifying $\delta u_i(t_1) = \delta u_i(t_2) = 0$, let us take:

$$\delta u_i = \int_{t_1}^t (M_i - C_i) dt' = \int_{t_1}^t M_i(t') dt' - C_i(t - t_1)$$

with

$$C_i = \frac{1}{t_2 - t_1} \int_{t_1}^{t_2} M_i(t') dt'$$

The corresponding virtual velocity is:

$$\delta \dot{u}_i = M_i - C_i$$

and one may write:

$$\begin{aligned}
 \int_{t_1}^{t_2} \sum_{i=1}^3 M_i \delta \dot{u}_i dt &= \int_{t_1}^{t_2} \sum_{i=1}^3 M_i \delta \dot{u}_i dt - \int_{t_1}^{t_2} \sum_{i=1}^3 C_i \delta \dot{u}_i dt \\
 &= \int_{t_1}^{t_2} \sum_{i=1}^3 (M_i - C_i) \delta \dot{u}_i dt \\
 &= \int_{t_1}^{t_2} \sum_{i=1}^3 (M_i - C_i)^2 dt \\
 &= 0
 \end{aligned}$$

Therefore $M_i = C_i$ which concludes the proof.

By making use of du Bois-Reymond's theorem, Hamilton's principle in the form (1.62) provides the equations of motion:

$$m \dot{u}_i(t) - \int_{t_1}^t X_i(t') dt' = C_i \quad i = 1, 2, 3 \quad (1.65)$$

where $C_i = m \dot{u}_i(t_1)$ are the components of the momentum at time t_1 , hence:

$$m(\dot{u}_i(t) - \dot{u}_i(t_1)) = \int_{t_1}^t X_i(t') dt' \quad i = 1, 2, 3 \quad (1.66)$$

This last form expresses that *the variation of the momentum of the particle over the time interval $[t_1, t]$ is equal to the impulse of the external forces impressed on the particle during the same time interval.*

In many shock and impact problems, the application time of the loading compared to the time scale at which phenomena are observed is so small that it is valid to consider that the external force is of impulse type, i.e. applied during an infinitesimal time interval but impressing on the system a finite impulse:

$$P_i = \int_{t_-}^{t_+} X_i(t) dt \quad (1.67)$$

In the impulsive case, Equation (1.66) becomes:

$$\boxed{m \dot{u}_i(t_+) - m \dot{u}_i(t_-) = P_i \quad i = 1, 2, 3} \quad (1.68)$$

showing that a velocity discontinuity such as represented by Figure 1.12 results from an impulsive loading equal to P_i/m .

Equations (1.68) are the only applicable ones in the impulsive case since the instantaneous force X_i becomes infinite during the shock. Alternatively this result is classically derived from the time-integration of Newton's equation, taking the limit for an infinite force on a zero time interval. In the next section we show that the same mathematical reasoning as presented here for a particle can be followed in order to find the impulse equations in terms of generalized coordinates.

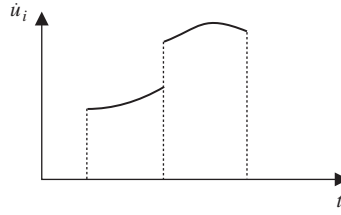


Figure 1.12 Velocity discontinuity.

1.5.2 Impulsive loading for a system of particles

For a system of N mass particles described by n generalized coordinates q_s , Hamilton's principle takes the form:

$$\delta I = \int_{t_1}^{t_2} \sum_{s=1}^n \left[\frac{\partial \mathcal{T}}{\partial \dot{q}_s} \delta \dot{q}_s + \left(\frac{\partial(\mathcal{T} - \mathcal{V})}{\partial q_s} + Q_s - \frac{\partial D}{\partial \dot{q}_s} \right) \delta q_s \right] dt = 0 \quad (1.69)$$

with

$$\delta q_s(t_1) = \delta q_s(t_2) = 0 \quad (1.70)$$

Let us integrate the second term by parts in order to let the time integral of the forces appear:

$$\begin{aligned} \delta I = & \left[\sum_{s=1}^n \delta q_s \int_{t_1}^t \left(\frac{\partial(\mathcal{T} - \mathcal{V})}{\partial q_s} + Q_s - \frac{\partial D}{\partial \dot{q}_s} \right) dt' \right]_{t_1}^{t_2} \\ & + \int_{t_1}^{t_2} \sum_{s=1}^n \left[\frac{\partial \mathcal{T}}{\partial \dot{q}_s} - \int_{t_1}^t \left(\frac{\partial(\mathcal{T} - \mathcal{V})}{\partial q_s} + Q_s - \frac{\partial D}{\partial \dot{q}_s} \right) dt' \right] \delta \dot{q}_s dt \end{aligned}$$

Hence, by setting:

$$M_s = \frac{\partial \mathcal{T}}{\partial \dot{q}_s} - \int_{t_1}^t \left(\frac{\partial(\mathcal{T} - \mathcal{V})}{\partial q_s} + Q_s - \frac{\partial D}{\partial \dot{q}_s} \right) dt' \quad (1.71)$$

one obtains:

$$\delta I = \int_{t_1}^{t_2} \sum_{s=1}^n M_s \delta \dot{q}_s dt = 0$$

As previously, du Bois-Reymond's theorem (Courant and Hilbert 1953) can be stated in the form:

$$\int_{t_1}^{t_2} \sum_{s=1}^n M_s \delta \dot{q}_s dt = 0$$

with $\delta q_s(t_1) = \delta q_s(t_2) = 0$ and $\delta \dot{q}_s$ piecewise continuous

$$\iff$$

$$M_s = C_s$$

with C_s constants

(1.72)

The demonstration is similar to the case of one mass particle. Hence, the generalization of Equations (1.65) to (1.68) is written:

$$\frac{\partial \mathcal{T}}{\partial \dot{q}_s} - \int_{t_1}^t \left(\frac{\partial(\mathcal{T} - \mathcal{V})}{\partial q_s} + Q_s - \frac{\partial D}{\partial \dot{q}_s} \right) dt' = C_s \quad s = 1, \dots, n \quad (1.73)$$

$$\frac{\partial \mathcal{T}}{\partial \dot{q}_s} - \left[\frac{\partial \mathcal{T}}{\partial \dot{q}_s} \right]_{t_1} = \int_{t_1}^t \left(\frac{\partial(\mathcal{T} - \mathcal{V})}{\partial q_s} + Q_s - \frac{\partial D}{\partial \dot{q}_s} \right) dt' \quad s = 1, \dots, n \quad (1.74)$$

In the case of impulsive loading, one may write:

$$P_s = \int_{t_-}^{t_+} Q_s dt' \quad (1.75)$$

and

$$\left[\frac{\partial \mathcal{T}}{\partial \dot{q}_s} \right]_{t_+} - \left[\frac{\partial \mathcal{T}}{\partial \dot{q}_s} \right]_{t_-} = P_s \quad s = 1, \dots, n \quad (1.76)$$

since $\frac{\partial(\mathcal{T} - \mathcal{V})}{\partial q_s} - \frac{\partial D}{\partial \dot{q}_s}$ remains finite between t_- and t_+ .

This result is the generalization of (1.68) to a system of particles. Let us finally note that the equality relationships (1.74) to (1.76) between the change of momentum and the impulse impressed on the system could also be deduced from a time integration of the Lagrange equations (1.29), taking the limit for an infinite force on a zero time interval.

Example 1.9

Let us consider the system of Figure 1.13 made of two masses m_1 and m_2 lying on a horizontal plane. m_2 is initially at rest, while m_1 moves with constant velocity $v_1 = V$ and hits mass m_2 at time $t = t^-$. We are interested in v_1^+ and v_2^+ , the velocities after the shock (at time $t = t^+$).

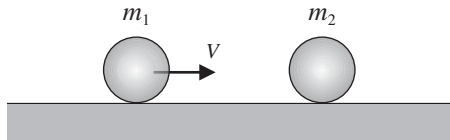


Figure 1.13 Collision of two masses.

A first relation is obtained by expressing conservation of the total energy of the system, which in this case reduces to the kinetic energy:

$$\mathcal{T} = \frac{1}{2}m_1(v_1^-)^2 + \frac{1}{2}m_2(v_2^-)^2 = \frac{1}{2}m_1V^2 = \frac{1}{2}m_1(v_1^+)^2 + \frac{1}{2}m_2(v_2^+)^2 \quad (\text{E1.9.a})$$

The second relation results from the computation of the jump in velocities through the shock. The latter are obtained from the Lagrange equations (1.76) which read in this case:

$$\left[\frac{\partial \mathcal{T}}{\partial v_i} \right]_{t_+} - \left[\frac{\partial \mathcal{T}}{\partial v_i} \right]_{t_-} = P_i \quad i = 1, 2$$

and yield:

$$\begin{aligned} m_1 v_1^+ - m_1 v_1^- &= P_1 \\ m_2 v_2^+ - m_2 v_2^- &= P_2 \end{aligned}$$

P_1 and P_2 being the internal impulses generated by the shock, they are in equilibrium:

$$P_1 + P_2 = 0$$

and therefore we get the equation of momentum conservation:

$$m_1 v_1^+ + m_2 v_2^+ = m_1 V \quad (\text{E1.9.b})$$

This leads to:

$$v_2^+ = \frac{m_1}{m_2} (V - v_1^+) \quad (\text{E1.9.c})$$

and substituting into Equation (E1.9.a) yields after simplification:

$$V^2(m_1 - m_2) + (v_1^+)^2(m_1 + m_2) - 2m_1 V v_1^+ = 0$$

Solving for v_1^+ and substituting into (E1.9.c) provides the only feasible solution:

$$v_1^+ = \frac{m_1 - m_2}{m_1 + m_2} V \quad v_2^+ = \frac{2m_1}{m_1 + m_2} V \quad (\text{E1.9.d})$$

It can be observed from (E1.9.d) that after the shock:

- if $m_1 > m_2$, both masses move in the same direction as initial velocity V .
- if $m_1 = m_2$, there is exchange of velocities between masses ($v_1^+ = 0$, $v_2^+ = V$).
- If $m_2 > m_1$, the masses move in opposite directions.

1.6 Dynamics of constrained systems

In the way they have been formulated in Section 1.3 Lagrange equations involve only the forces effectively applied onto the systems thanks to the choice of kinematically admissible coordinates q_s . They thus express the equilibrium in a subspace orthogonal to the constraints so that reaction forces do not appear in the equations of motion. In some cases it is nevertheless useful or easier to make the reaction forces appear explicitly in the expression of the equilibrium and to choose generalized coordinates that do not satisfy some of the kinematic constraints. The only constraints considered here are the holonomic ones. A discussion on the treatment of nonholonomic constraints can be found for instance in (Géradin and Cardona 2001, Lanczos 1949).

Let us suppose that a subset of m kinematic constraints (1.12) is not explicitly satisfied by the choice of the generalized coordinates q_s . Substitution of (1.11) and (1.14) into the holonomic constraints (1.12) allows expressing the constraints for the generalized coordinates:

$$f_r(x_{ik} + U_{ik}(q_s, t)) = f_r(q_s, t) = 0 \quad r = 1, \dots, m \quad (1.77)$$

Their variation:

$$\delta f_r = \sum_{s=1}^n \frac{\partial f_r}{\partial q_s} \delta q_s = 0 \quad r = 1, \dots, m \quad (1.78)$$

indicates that the constraints are still verified if the δq_s define a motion orthogonal to the direction determined by $\frac{\partial f_r}{\partial q_s}$ in the space of the generalized coordinates. Thus, the derivatives determine the directions of the reaction forces and can be expressed by:

$$R_{rs} = \lambda_r \frac{\partial f_r}{\partial q_s} \quad (1.79)$$

where λ_r denotes the intensity of the reaction associated to constraint f_r . It is called a *Lagrange multiplier*.

Using (1.78) and (1.79), the virtual work of the reaction forces is:

$$\sum_{r=1}^m \sum_{s=1}^n R_{rs} \delta q_s = \sum_{r=1}^m \lambda_r \sum_{s=1}^n \frac{\partial f_r}{\partial q_s} \delta q_s = \sum_{r=1}^m \lambda_r \delta f_r \quad (1.80)$$

The latter can be added to the virtual work expression (1.28) obtained from Hamilton's principle:

$$\int_{t_1}^{t_2} \sum_{s=1}^n \left[-\frac{d}{dt} \left(\frac{\partial \mathcal{T}}{\partial \dot{q}_s} \right) + \frac{\partial \mathcal{T}}{\partial q_s} + Q_s + \sum_{r=1}^m \lambda_r \frac{\partial f_r}{\partial q_s} \right] \delta q_s dt = 0 \quad (1.81)$$

It provides the Lagrange equations of motion in terms of generalized coordinates q_s which do not satisfy the constraints:

$$\frac{d}{dt} \left(\frac{\partial \mathcal{T}}{\partial \dot{q}_s} \right) - \frac{\partial \mathcal{T}}{\partial q_s} = Q_s + \sum_{r=1}^m \lambda_r \frac{\partial f_r}{\partial q_s}$$

where the Lagrange multipliers λ_r (i.e. the reaction force intensities) are determined to satisfy the conditions (1.77). The Lagrange equations together with the complementary conditions form a system of $n + m$ equations with $n + m$ unknowns:

$$\left\{ \begin{array}{ll} \frac{d}{dt} \left(\frac{\partial \mathcal{T}}{\partial \dot{q}_s} \right) - \frac{\partial \mathcal{T}}{\partial q_s} - Q_s - \sum_{r=1}^m \lambda_r \frac{\partial f_r}{\partial q_s} = 0 & s = 1, \dots, n \\ f_r(q_s, t) = 0 & r = 1, \dots, m \end{array} \right. \quad (1.82)$$

These Lagrange equations can also be deduced from Hamilton's principle if one introduces an additional potential representing the work produced by the constraining forces, i.e. the dislocation potential \mathcal{V}_d :

$$\mathcal{V}_d = - \sum_{r=1}^m \lambda_r f_r(q_s, t) \quad (1.83)$$

This potential is then added to the potential of the system and it can be verified that Hamilton's principle (1.27) yields the equilibrium and compatibility equations (1.82) when stating the stationarity with respect to q_s and λ_r respectively.

Example 1.10

Let us reconsider the simple pendulum described in Figure 1.5, but now let us try to write the constrained equations of motion using the Cartesian displacements as unknowns. The constraint on the system can be written as:

$$f = \sqrt{(\ell + u_1)^2 + u_2^2} - \ell = 0 \quad (\text{E1.10.a})$$

Taking the derivatives of the constrain with respect to u_1 and u_2 , one finds the direction of the reaction forces, namely

$$\vec{R} = \lambda \begin{bmatrix} \frac{\partial f}{\partial u_1} \\ \frac{\partial f}{\partial u_2} \end{bmatrix} = \lambda \begin{bmatrix} \frac{(\ell + u_1)}{\sqrt{(\ell + u_1)^2 + u_2^2}} \\ \frac{u_2}{\sqrt{(\ell + u_1)^2 + u_2^2}} \end{bmatrix} = \lambda \begin{bmatrix} \frac{(\ell + u_1)}{\ell} \\ \frac{u_2}{\ell} \end{bmatrix}$$

The constrained equations can thus be written as:

$$\begin{cases} \ddot{m}u_1 - mg - \lambda \frac{(\ell + u_1)}{\ell} = 0 \\ \ddot{m}u_2 - \lambda \frac{u_2}{\ell} = 0 \\ \sqrt{(\ell + u_1)^2 + u_2^2} - \ell = 0 \end{cases}$$

If we choose the degree of freedom θ such that:

$$\begin{aligned} u_1 &= \ell \cos \theta - \ell \\ u_2 &= \ell \sin \theta \end{aligned}$$

the constraint (E1.10.a) is always satisfied. Using these relations the reaction forces can be expressed as:

$$\vec{R} = \lambda \begin{bmatrix} \frac{(\ell + u_1)}{\ell} \\ \frac{u_2}{\ell} \end{bmatrix} = \lambda \begin{bmatrix} \frac{\ell \cos \theta}{\ell} \\ \frac{\ell \sin \theta}{\ell} \end{bmatrix} = \lambda \begin{bmatrix} \cos \theta \\ \sin \theta \end{bmatrix}$$

and as discussed in Example 1.3, projecting this force in the direction compatible with the constraint leads to the unconstrained equation of motion for the pendulum.

1.7 Exercises**1.7.1 Solved exercises**

Problem 1.1 Prove that a system of N particles that are rigidly linked to one another (thus forming a rigid body in space) can be described by 6 degrees of freedom when $N > 2$.

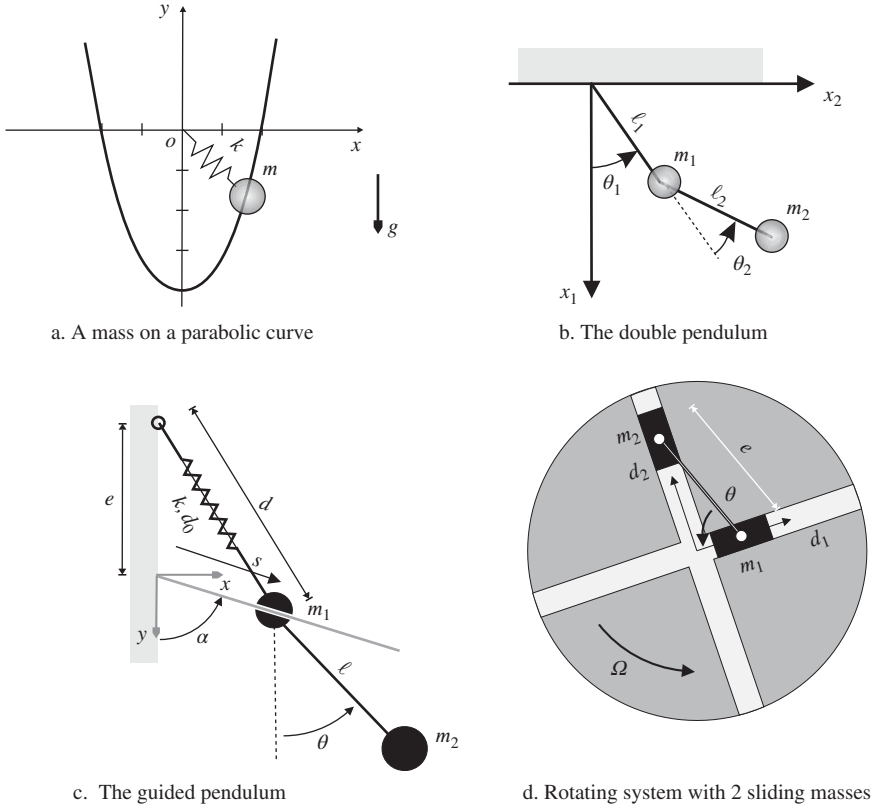


Figure 1.14 Solved exercises.

Solution

Every individual particle has 3 degrees of freedom if it is not rigidly linked. Since the particles form a rigid body, the distance between any pair of particles is constant. If the system is made of 2 particles ($N = 2$), one constraint can be defined. If a particle is then added to the system of 2 particles, 2 additional constraints must be defined in order to ensure that the third particle has a constant distance with respect to the 2 previous ones. For any additional particle in the system, 3 additional nonredundant constraints must be defined in order to ensure that the particle is rigidly connected to the system. Hence, for a system of N particles rigidly linked, $1 + 2 + 3(N - 3)$ nonredundant holonomic constraints can be defined so that the system has $3N - (1 + 2 + 3(N - 3)) = 6$ degrees of freedom.

Problem 1.2 In the system described in Figure 1.14.a a mass moves on a parabolic curve described by the equation:

$$y(x) = \frac{x^2}{\ell} - 4\ell$$

where ℓ is a given length. A linear spring with stiffness k is attached to the mass and fixed to the point $(0, 0)$. The spring has a zero natural length. The gravity acts in the direction $-y$.

Choose x as the degree of freedom of the system. Write the potential and kinetic energies of the system and derive the Lagrange equations.

Solution

Calling u the deformation of the spring we find:

$$\mathcal{V} = \frac{1}{2}ku^2 + mgy = \frac{1}{2}k(x^2 + y(x)^2) + mgy(x) \quad (\text{P1.2.a})$$

$$\mathcal{T} = \frac{1}{2}m(\dot{x}^2 + \dot{y}^2) = \frac{1}{2}m\left(\dot{x}^2 + 4\frac{x^2}{\ell^2}\dot{x}^2\right) = \frac{1}{2}m\dot{x}^2\left(1 + 4\frac{x^2}{\ell^2}\right) \quad (\text{P1.2.b})$$

The terms of the Lagrange equation (1.59) then write:

$$\frac{d}{dt}\left(\frac{\partial\mathcal{T}}{\partial\dot{x}}\right) = \frac{d}{dt}\left(m\dot{x}\left(1 + 4\frac{x^2}{\ell^2}\right)\right) = m\ddot{x}\left(1 + 4\frac{x^2}{\ell^2}\right) + \frac{8mx}{\ell^2}\dot{x}^2 \quad (\text{P1.2.c})$$

$$\frac{\partial\mathcal{T}}{\partial x} = \frac{4mx\dot{x}^2}{\ell^2} \quad (\text{P1.2.d})$$

$$\frac{\partial\mathcal{V}}{\partial x} = k\left(x + y\frac{\partial y}{\partial x}\right) + mg\frac{\partial y}{\partial x} = kx\left(2\frac{x^2}{\ell^2} - 7\right) + 2mg\frac{x}{\ell} \quad (\text{P1.2.e})$$

and there are no nonconservative forces in this system. The equation of motion is thus:

$$m\left(1 + 4\frac{x^2}{\ell^2}\right)\ddot{x} + \frac{4mx}{\ell^2}\dot{x}^2 + kx\left(2\frac{x^2}{\ell^2} - 7\right) + 2mg\frac{x}{\ell} = 0 \quad (\text{P1.2.f})$$

Problem 1.3 Let us consider the double pendulum undergoing 2-D motion in a gravity field g as already introduced in Example 1.4. Using as generalized coordinates the relative angular displacements as shown on Figure 1.14.b, you are asked:

- To express the position coordinates ξ_{ik} of both masses in terms of the generalized coordinates θ_1 and θ_2 as displayed on Figure 1.14.b.
- To express the Cartesian velocities of both masses.
- To express the potential and kinetic energies of the system.
- To develop the system equations of motion in Lagrange form.

Solution

The positions of the masses were given in the Example 1.4, Equations (E1.4.a–E1.4.d) and the absolute velocities are computed as we compute the velocities:

$$\dot{u}_{11} = -\ell_1\dot{\theta}_1 \sin \theta_1$$

$$\dot{u}_{21} = \ell_1\dot{\theta}_1 \cos \theta_1$$

$$\dot{u}_{12} = -\ell_1\dot{\theta}_1 \sin \theta_1 - \ell_2(\dot{\theta}_1 + \dot{\theta}_2) \sin(\theta_1 + \theta_2)$$

$$\dot{u}_{22} = \ell_1\dot{\theta}_1 \cos \theta_1 + \ell_2(\dot{\theta}_1 + \dot{\theta}_2) \cos(\theta_1 + \theta_2)$$

The kinetic energy is then expressed as:

$$\begin{aligned}\mathcal{T} &= \frac{1}{2}(m_1(\dot{u}_{11}^2 + \dot{u}_{21}^2) + m_2(\dot{u}_{12}^2 + \dot{u}_{22}^2)) \\ &= \frac{1}{2}(m_1\ell_1^2\dot{\theta}_1^2 + m_2(\ell_1^2\dot{\theta}_1^2 + \ell_2^2(\dot{\theta}_1 + \dot{\theta}_2)^2 + 2\ell_1\ell_2\dot{\theta}_1(\dot{\theta}_1 + \dot{\theta}_2)\cos\theta_2))\end{aligned}\quad (\text{P1.3.a})$$

The potential energy of the system due to gravity forces is:

$$\mathcal{V} = -m_1gu_{11} - m_2gu_{12}$$

which, in terms of the generalized coordinates is:

$$\mathcal{V} = m_1g\ell_1(1 - \cos\theta_1) + m_2g(\ell_1(1 - \cos\theta_1) + \ell_2(1 - \cos(\theta_1 + \theta_2)))\quad (\text{P1.3.b})$$

Let us then compute the different terms of the Lagrange equations (1.59), noting that no non-conservative forces are present:

For $s = 1$, namely $q_s = \theta_1$,

$$\begin{aligned}\frac{d}{dt}\frac{\partial\mathcal{T}}{\partial\dot{\theta}_1} &= \frac{d}{dt}(m_1\ell_1^2\dot{\theta}_1 + m_2(\ell_1^2\dot{\theta}_1 + \ell_2^2(\dot{\theta}_1 + \dot{\theta}_2) + \ell_1\ell_2(2\dot{\theta}_1 + \dot{\theta}_2)\cos\theta_2)) \\ &= m_1\ell_1^2\ddot{\theta}_1 + m_2(\ell_1^2\ddot{\theta}_1 + \ell_2^2(\ddot{\theta}_1 + \ddot{\theta}_2) + \ell_1\ell_2(2\ddot{\theta}_1 + \ddot{\theta}_2)\cos\theta_2 - \ell_1\ell_2(2\dot{\theta}_1 + \dot{\theta}_2)\dot{\theta}_2\sin\theta_2) \\ \frac{\partial\mathcal{T}}{\partial\theta_1} &= 0 \\ \frac{\partial\mathcal{V}}{\partial\theta_1} &= m_1g\ell_1\sin\theta_1 + m_2g(\ell_1\sin\theta_1 + \ell_2\sin(\theta_1 + \theta_2))\end{aligned}$$

For $s = 2$, namely $q_s = \theta_2$,

$$\begin{aligned}\frac{d}{dt}\frac{\partial\mathcal{T}}{\partial\dot{\theta}_2} &= \frac{d}{dt}(m_2(\ell_2^2(\dot{\theta}_1 + \dot{\theta}_2) + \ell_1\ell_2\dot{\theta}_1\cos\theta_2)) \\ &= m_2(\ell_2^2(\ddot{\theta}_1 + \ddot{\theta}_2) + \ell_1\ell_2\ddot{\theta}_1\cos\theta_2 - \ell_1\ell_2\dot{\theta}_1\dot{\theta}_2\sin\theta_2) \\ \frac{\partial\mathcal{T}}{\partial\theta_2} &= -m_2\ell_1\ell_2\dot{\theta}_1(\dot{\theta}_1 + \dot{\theta}_2)\sin\theta_2 \\ \frac{\partial\mathcal{V}}{\partial\theta_2} &= m_2g\ell_2\sin(\theta_1 + \theta_2)\end{aligned}$$

Substituting these results in the Lagrange equations:

$$\frac{d}{dt}\frac{\partial\mathcal{T}}{\partial\dot{\theta}_1} - \frac{\partial\mathcal{T}}{\partial\theta_1} + \frac{\partial\mathcal{V}}{\partial\theta_1} = 0\quad (\text{P1.3.c})$$

$$\frac{d}{dt}\frac{\partial\mathcal{T}}{\partial\dot{\theta}_2} - \frac{\partial\mathcal{T}}{\partial\theta_2} + \frac{\partial\mathcal{V}}{\partial\theta_2} = 0\quad (\text{P1.3.d})$$

then yields the equations of motion.

Problem 1.4 Let us consider the guided double pendulum of Figure 1.14.c where a mass m_1 is prescribed to move without friction on a bar making an angle α with respect to the vertical direction. The spring of stiffness k is attached to a fixed point and its undeformed length is d_0 . Gravity g is acting along y . Using the degrees of freedom s and θ , write the energies of the system and find its equations of motion.

Solution

The positions of mass m_1 and m_2 are given by:

$$\begin{aligned} x_1 &= s \sin \alpha & x_2 &= x_1 + \ell \sin \theta \\ y_1 &= s \cos \alpha & y_2 &= y_1 + \ell \cos \theta \end{aligned}$$

and the absolute velocities are then:

$$\begin{aligned} \dot{u}_{x1} &= \dot{s} \sin \alpha & \dot{u}_{x2} &= \dot{u}_{x1} + \ell \dot{\theta} \cos \theta \\ \dot{u}_{y1} &= \dot{s} \cos \alpha & \dot{u}_{y2} &= \dot{u}_{y1} - \ell \dot{\theta} \sin \theta \end{aligned}$$

The kinetic and potential energies are then computed, yielding:

$$\mathcal{T} = \frac{1}{2} m_1 \dot{s}^2 + \frac{1}{2} m_2 (\dot{s}^2 + \ell^2 \dot{\theta}^2 + 2\ell \dot{s} \dot{\theta} \sin(\alpha - \theta)) \quad (\text{P1.4.a})$$

$$\mathcal{V} = -m_1 g s \cos \alpha - m_2 g (s \cos \alpha + \ell \cos \theta) + \frac{1}{2} k (d - d_0)^2 \quad (\text{P1.4.b})$$

where

$$\begin{aligned} d^2 &= (e + s \cos \alpha)^2 + (s \sin \alpha)^2 \\ &= e^2 + s^2 + 2se \cos \alpha \end{aligned} \quad (\text{P1.4.c})$$

The terms in the Lagrange equations (1.59) (all forces being conservative) are obtained as follows:

$$\begin{aligned} \frac{d}{dt} \frac{\partial \mathcal{T}}{\partial \dot{s}} &= (m_1 + m_2) \ddot{s} + m_2 \ell \ddot{\theta} \sin(\alpha - \theta) & \frac{d}{dt} \frac{\partial \mathcal{T}}{\partial \dot{\theta}} &= m_2 \ell^2 \ddot{\theta} + m_2 \ell \sin(\alpha - \theta) \ddot{s} \\ &- m_2 \ell \dot{\theta}^2 \cos(\alpha - \theta) & &- m_2 \ell \dot{s} \cos(\alpha - \theta) \dot{\theta} \\ \frac{\partial \mathcal{T}}{\partial s} &= 0 & \frac{\partial \mathcal{T}}{\partial \theta} &= -m_2 \ell \dot{s} \dot{\theta} \cos(\alpha - \theta) \\ \frac{\partial \mathcal{V}}{\partial s} &= -m_1 g \cos \alpha - m_2 g \cos \alpha + k(d - d_0) \frac{\partial d}{\partial s} & \frac{\partial \mathcal{V}}{\partial \theta} &= m_2 g \ell \sin \theta \end{aligned} \quad (\text{P1.4.d})$$

Finally the Lagrange equations are written:

$$\begin{cases} (m_1 + m_2) \ddot{s} + m_2 \ell \ddot{\theta} \sin(\alpha - \theta) - m_2 \ell \dot{\theta}^2 \cos(\alpha - \theta) \\ - (m_1 + m_2) g \cos \alpha + k(d - d_0) \frac{s + e \cos \alpha}{d} = 0 \\ m_2 \ell^2 \ddot{\theta} + m_2 \ell \sin(\alpha - \theta) \ddot{s} + m_2 g \ell \sin \theta = 0 \end{cases} \quad (\text{P1.4.e})$$

Problem 1.5 Consider the rotating system of Figure 1.14.d. A wheel is rotating with constant angular velocity Ω imposed to the system. Two masses m_1 and m_2 slide without friction into the orthogonal grooves. The mass points are linked through a rigid bar of length e . The inertia of the rigid bar is neglected.

- Find the equations of motion in terms of the displacements d_1 and d_2 of the masses along the grooves.
- If $m_1 = m_2 = m$ and if no force is applied to the system, show that
 1. the reaction force in the rigid link is also constant and the bar is always under traction;
 2. the velocity $\dot{\theta}$, namely the angular velocity of the bar relative to the wheel remains constant.

Solution

Let us define the angular position of the disk:

$$\phi(t) = \Omega t$$

with respect to an inertial frame centred on the rotation axis of the system. In that system, the masses have the instantaneous coordinates:

$$\begin{aligned} x_1 &= d_1 \cos \phi & x_2 &= -d_2 \sin \phi \\ y_1 &= d_1 \sin \phi & y_2 &= d_2 \cos \phi \end{aligned} \quad (\text{P1.5.a})$$

and absolute velocities:

$$\begin{aligned} \dot{x}_1 &= \dot{d}_1 \cos \phi - d_1 \Omega \sin \phi & \dot{x}_2 &= -\dot{d}_2 \sin \phi - d_2 \Omega \cos \phi \\ \dot{y}_1 &= \dot{d}_1 \sin \phi + d_1 \Omega \cos \phi & \dot{y}_2 &= \dot{d}_2 \cos \phi - d_2 \Omega \sin \phi \end{aligned} \quad (\text{P1.5.b})$$

The local displacements d_1 and d_2 are constrained by the fixed length e requiring that:

$$\sqrt{d_1^2 + d_2^2} = e \quad (\text{P1.5.c})$$

This condition could be satisfied by choosing a single generalized coordinate. If one would choose for instance θ , the angle of the rod relative to the wheel, one would write:

$$d_1 = e \cos \theta \quad d_2 = e \sin \theta \quad (\text{P1.5.d})$$

and substitute these equations in (P1.5.b). However in this exercise we consider the two degrees of freedom d_1 and d_2 , and impose the condition (P1.5.c) explicitly on the system using a Lagrange multiplier (Section 1.6).

Let us compute the kinetic energy:

$$\mathcal{T} = \frac{1}{2} m_1 (\dot{x}_1^2 + \dot{y}_1^2) + \frac{1}{2} m_2 (\dot{x}_2^2 + \dot{y}_2^2) \quad (\text{P1.5.e})$$

or, after substitution of (P1.5.b),

$$\mathcal{T} = \frac{1}{2} m_1 (\dot{d}_1^2 + d_1^2 \Omega^2) + \frac{1}{2} m_2 (\dot{d}_2^2 + d_2^2 \Omega^2) \quad (\text{P1.5.f})$$

In the absence of external force, the dynamics of the system is governed by the Lagrangian obtained from the addition to (P1.5.f) of the inextensibility constraint (P1.5.c) with a Lagrangian multiplier λ :

$$\mathcal{L}(d_1, d_2, \phi, \lambda) = \frac{1}{2}m_1(\dot{d}_1^2 + d_1^2\Omega^2) + \frac{1}{2}m_2(\dot{d}_2^2 + d_2^2\Omega^2) + \lambda(\sqrt{d_1^2 + d_2^2} - e) \quad (\text{P1.5.g})$$

Taking the variations with respect to δd_1 , δd_2 , and $\delta \lambda$ one obtains the equations of the system (the constrained Lagrange equations (1.82)):

$$-m_1\ddot{d}_1 + \left(m_1\Omega^2 + \frac{\lambda}{e}\right)d_1 = 0 \quad (\text{P1.5.h})$$

$$-m_2\ddot{d}_2 + \left(m_2\Omega^2 + \frac{\lambda}{e}\right)d_2 = 0 \quad (\text{P1.5.i})$$

$$\sqrt{d_1^2 + d_2^2} - e = 0 \quad (\text{P1.5.j})$$

the last equation being obviously equivalent to the constraint (P1.5.c).

In case the masses are equal, namely $m_1 = m_2 = m$, an elegant way to compute the Lagrange multipliers is obtained by multiplying Equations (P1.5.h) and (P1.5.i) by d_1 and d_2 respectively and summing up

$$-m(d_1\ddot{d}_1 + d_2\ddot{d}_2) + \left(m\Omega^2 + \frac{\lambda}{e}\right)(d_1^2 + d_2^2) = 0$$

Accounting for the constraint (P1.5.j) one finds:

$$\lambda = me(d_1\ddot{d}_1 + d_2\ddot{d}_2 - \Omega^2) \quad (\text{P1.5.k})$$

Writing the constraint (P1.5.j):

$$d_1^2 + d_2^2 = e^2$$

and taking the time derivative twice we get:

$$\dot{d}_1 d_1 + \dot{d}_2 d_2 = 0 \quad \text{and} \quad \ddot{d}_1 d_1 + \ddot{d}_2 d_2 = -(\dot{d}_1^2 + \dot{d}_2^2) = -e^2 \dot{\theta}^2 \quad (\text{P1.5.l})$$

where the last equality was obtained using the time derivatives of (P1.5.d). Thus, from Equation (P1.5.k), the multiplier is obtained as:

$$\lambda = -me(\Omega^2 + \dot{\theta}^2) \quad (\text{P1.5.m})$$

It is always negative, thus according to (P1.5.h–P1.5.i) always in the direction opposite to the centrifugal force, showing that the connecting bar is always in traction.

Let us now find the Lagrange equation corresponding to the minimum coordinate θ and first write the expression (P1.5.f) of the kinetic energy using (P1.5.d),

$$\mathcal{T} = \frac{1}{2}me^2(\dot{\theta}^2 + \Omega^2) \quad (\text{P1.5.n})$$

and writing the Lagrange equation in this case yields:

$$me^2\ddot{\theta} = 0 \quad (\text{P1.5.o})$$

showing that when masses are equal the angular velocity is constant, and therefore also the constraining force λ according to (P1.5.m).

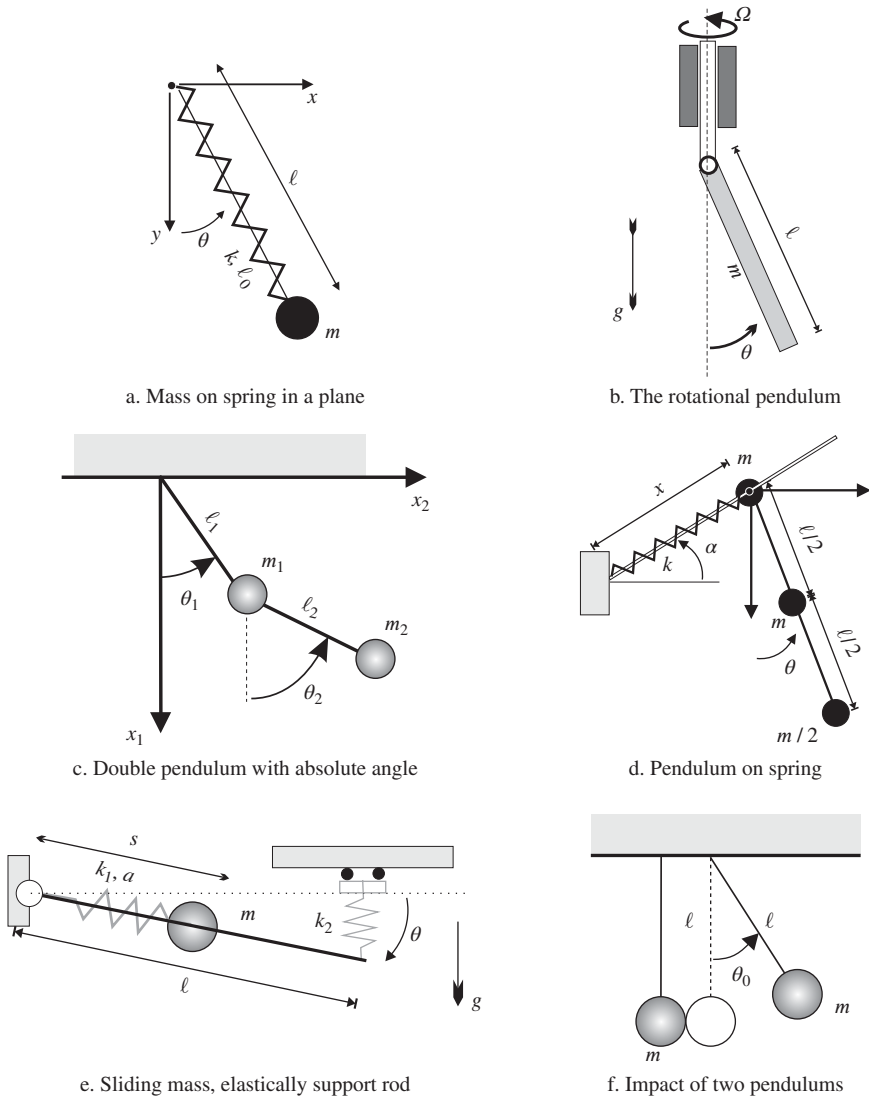


Figure 1.15 Selected exercises.

1.7.2 Selected exercises

Problem 1.6 For the mass on a linear spring depicted in Figure 1.15.a write the potential and kinetic energies using the angle θ and the length ℓ of the spring as generalized coordinates. Gravity is acting along direction y . The spring has a natural length equal to ℓ_0 and the system is assumed to move in the plane (x, y) . Find the equations of motions using the Lagrange equations.

Problem 1.7 Let us consider a bar hinged on a vertical rotating shaft as described in Figure 1.15.b. The bar behaves like a pendulum in the gravity field g . The rotation speed Ω is constant and given. The bar has a uniform mass per unit length of m and a length ℓ . You are asked to

1. Using the angle θ as degree of freedom, determine the absolute velocity of a point on the bar as a function of the rotation speed Ω .
2. Compute the kinetic and potential energy of the entire bar.
3. Find the equation of motion using the Lagrange formalism.

Problem 1.8 Repeat the exercise of the double pendulum described in Problem 1.3 but now using absolute coordinates as displayed on Figure 1.15.c. Compare the equations of motion obtained with both sets of generalized coordinates.

Problem 1.9 A mass m slides without friction on a rod positioned at a fixed angle α with respect to the horizontal direction (Figure 1.15.d). The mass is fixed to a nonlinear spring developing a force kx^3 where x is its extension. The spring is aligned with the rod. To the sliding mass a single pendulum is attached. The pendulum consists of a massless rod and two masses attached to it: a mass m at a distance $\ell/2$ and a mass $m/2$ at a distance ℓ . Gravity acts in the vertical direction.

Write the kinetic and potential energy of the system using x and θ as degrees of freedom, then find the equations of motion of the system.

Problem 1.10 The mass m shown in Figure 1.15.e slides without friction on a massless rod of length ℓ . The mass is attached to a linear spring k_1 aligned with the rod (natural length a). A second linear spring k_2 is attached to the end of the rod (zero natural length). This spring is attached to a massless slider so that it remains vertical. Gravity acts in the vertical direction.

Using the generalized coordinates s and θ , respectively the position of the mass on the rod and the angle between the horizontal direction and the rod, write the kinetic and potential energies and derive the equations of motion. What would the equations of motion be if, in parallel to spring k_2 , a viscous damper d would be present?

Problem 1.11 Let us consider the system of Figure 1.15.f made of 2 identical pendulums of mass m , length ℓ and moving in a gravity field g .

They are aligned so that there is no reaction force in the equilibrium position $\theta_1 = \theta_2 = 0$. Assuming that one of the pendulums is displaced from its equilibrium position and released from an initial angle θ_0 , you are asked to:

- Determine the collision time t^- and the angular velocity of the moving pendulum just before the shock.
- Determine the angular velocities of both pendulums just after the shock.
- Sketch the trajectories of both pendulums in the phase plane $(\theta, \dot{\theta})$.

References

- Abramowitz M and Stegun I 1970 *Handbook of Mathematical Functions*. Dover Publications, New York.
 Courant R and Hilbert D 1953 *Methods of Mathematical Physics* vol. 1. Interscience Publishers, New York.

- Gérardin M and Cardona A 2001 *Flexible Multibody Dynamics: The Finite Element Method Approach*. John Wiley & Sons, Ltd, Chichester.
- Goldstein H 1986 *Classical Mechanics*. Addison-Wesley, Reading, MA.
- Hamilton WR 1834 On a general method in dynamics; by which the study of the motions of all free systems of attracting or repelling points is reduced to the search and differentiation of one central relation, or characteristic function. *Philosophical Transactions of the Royal Society of London* **124**, 247–308.
- Kane TR and Levinson DA 1980 Formulation of equations of motion for complex spacecraft. *Journal of Guidance and Control*, vol. 3, Mar.–Apr. 1980, pp. 99–112. *Research supported by the Lockheed Missiles and Space Independent Research Program* **3**, 99–112.
- Lagrange JL 1788 *Mécanique analytique*. Chez la Veuve Desaint, Libraire, rue du Foin S. Jacques, Paris.
- Lanczos C 1949 *The Variational Principles of Mechanics* Mathematical Expositions, No. 4. University of Toronto Press, Toronto, Canada.
- Lur' é L 1968 *Mécanique analytique (tomes 1 et 2)*. Librairie Universitaire, Louvain (translated from Russian).
- Meirovitch L 1970 *Methods of Analytical Dynamics*. McGraw Hill, New York.
- Meirovitch L 1980 *Computational Methods in Structural Dynamics*. Sijthoff & Noordhoff.
- Whittaker E 1965 *A Treatise on the Analytical Dynamics of Particles and Rigid Bodies*. Cambridge University Press. (4th edition).

2

Undamped Vibrations of n-Degree-of-Freedom Systems

From the theory and examples discussed in Chapter 1 one should remember that the description of the dynamics of a mechanical system as obtained from Hamilton's principle, from the Lagrange equations or from the principle of virtual work generally leads to a set of nonlinear equations. Solving such nonlinear equations usually requires applying time-integration techniques as those described later in Chapter 7. Nevertheless, for many practical applications, dynamical behaviour manifests itself only as time-varying perturbation around a static solution. Indeed systems can often be described as being in an statical equilibrium configuration, around which they undergo only small dynamic motion, namely *vibrations*.

In that case, the description of the system can be significantly simplified and a linearization around an equilibrium position of the generally nonlinear dynamic equations is possible. Although such a linear description is valid only for small perturbations, it is an essential step in grasping fundamental concepts in mechanical vibrations such as stability, eigenfrequencies and eigenmodes. The mathematical tools available to theoretically investigate the vibration of systems is rich and versatile, allowing scientists and engineers to build fundamental understanding of dynamical problems.

In this chapter only systems without dissipative forces are considered (dissipative systems will be the subject of Chapter 3). We will first define the concept of equilibrium position and vibration, discussing both the cases when the equilibrium position corresponds to a truly static configuration and when it has to be understood as an overall steady motion (Section 2.1). In particular we outline how the linear form can be obtained from the energy description underlying the Lagrange equations, allowing us to express the vibration behaviour in a matrix form exhibiting symmetry for the stiffness and mass contributions, and skew-symmetry for the gyroscopic part resulting from overall transport motion.

In Sections 2.2 through 2.4 the matrix description is exploited to investigate the free vibration of systems, leading to the fundamental concepts of eigenfrequencies and eigenmodes which essentially describe the intrinsic dynamics of a system and which exhibit important orthogonality properties. In Sections 2.5 through 2.9 the framework provided by the modal description of mechanical vibrations is used to study the dynamic response to initial conditions and to external excitation (both for applied loads and imposed displacements).

In Section 2.10 the eigenfrequencies of a system are further characterized by showing that they are related to minimum energy ratios (i.e. the Rayleigh quotient) and to variations of dynamical behaviour when constraints are added to the system. This theoretical discussion reveals basic thoughts that underly many of the approximation methods and solution algorithms used in engineering dynamics and discussed later in Chapters 5 and 6.

The last topic treated in this chapter relates to rotating systems, the vibrations of which exhibit specific aspects due to the presence of gyroscopic effects. In Section 2.11 we outline how the modal analysis can be extended to such systems.

Definitions

The list below complements the general definitions given in the book introduction, but remains local to Chapter 2.

A	$2n \times 2n$ system matrix (rotating system in state space form).
B	$2n \times 2n$ system matrix (rotating system in state space form).
F'	residual flexibility matrix.
$H(x)$	Hessian matrix.
K_{22}^*	condensed stiffness matrix on interface.
K_{ij}	submatrix of stiffness matrix K .
L_i	Boolean operator for extraction of degrees of freedom q_i .
M_{22}^0	additional mass matrix on the support.
M_{22}^*	condensed mass matrix on interface.
M_{ij}	submatrix of mass matrix M .
P	projection operator.
Q	$(2n \times 2n)$ matrix of eigenmodes of rotating system.
T	static condensation matrix.
\bar{X}	reduced set of eigenmodes.
\tilde{X}	matrix of eigenmodes of fixed interface system.
$\bar{q}_2(t)$	imposed acceleration to the support.
$r(t)$	$2n$ state vector (system in rotation).
r_0	initial condition associated to $2n$ state vector $r(t)$.
$r_2(t)$	reaction forces on interface degrees of freedom q_2 .
$u_{2(i)}$	i -th rigid body mode on the support.
$w_{(r)}$	real part of complex eigenvector of rotating system (dimension $2n$).
$\tilde{x}_{(r)}$	r -th eigenmode of fixed interface system.
$y_1(t)$	motion of degrees of freedom q_1 relative to support.
y	$2n$ amplitude vector (system in rotation).
$y_{(r)}$	$= w_{(r)} + z_{(r)}$ complex eigenvector of rotating system (dimension $2n$).
$z_{(r)}$	imaginary part of complex eigenvector of rotating system (dimension $2n$).
$H(t)$	step (Heaviside) function.
g_r	step response of modal coordinate r .
h_r	impulse response of modal coordinate r .
k	spring stiffness.

m	lumped mass.
m_S	mass of the structure attached to the support.
m_T	total mass of the structure.
Γ	modal participation matrix (support excitation).
Ω	matrix of circular frequencies ω_r (not diagonal for rotating system).
$\bar{\Omega}^2$	reduced set of eigenvalues.
$\tilde{\Omega}^2$	matrix of eigenvalues of fixed interface system.
Ω^*	matrix of circular frequencies ω_r (rotating system).
$\Sigma(t)$	$(2n \times 2n)$ impulse response matrix for rotating system).
$\chi(t)$	$2n$ vector of normal coordinates of rotating system.
$\bar{\eta}(t)$	reduced set of normal coordinates.
ϕ	phase lag.
$\Delta(\lambda)$	characteristic equation (system in rotation).
α	real part of eigenvalue (system in rotation).
$\gamma_{(r)}$	modal participation of eigenmode r (support excitation).
ϵ	infinitesimal quantity.
λ	$= \alpha \pm i\omega$ eigenvalue of system in rotation.
$\tilde{\omega}_r^2$	r -th eigenvalue of fixed interface system.

2.1 Linear vibrations about an equilibrium configuration

Let us call the equilibrium configuration of a system a time-independent configuration,

$$q_s(t) = q_s(0) \quad \dot{q}_s(t) = 0 \quad s = 1, \dots, n$$

Going back to Lagrange equations in the form (1.60), such a configuration is found to exist if and only if the modified potential $\mathcal{V}^* = \mathcal{V} - \mathcal{T}_0$ and the non conservative generalized forces are only functions of the chosen generalized displacements q_s and not explicitly dependent on time, namely if $\mathcal{V}^* = \mathcal{V}^*(\mathbf{q})$ and $Q_s(t) = 0$. Let us further assume that the nonconservative forces acting on the system are zero when $\dot{q}_s(t) = 0$ and that, if rheonomic constraints are applied, the imposed transport corresponds to a steady motion, namely a uniform rotation or translation.¹ In that case an equilibrium position is solution of:

$$\frac{\partial \mathcal{V}^*}{\partial q_s} = \frac{\partial (\mathcal{V} - \mathcal{T}_0)}{\partial q_s} = 0 \quad s = 1, \dots, n \quad (2.1)$$

The following cases have to be considered, depending on whether or not the transport kinetic energy term \mathcal{T}_0 exists.

2.1.1 Vibrations about a stable equilibrium position

The restriction is made here to a system which does not undergo overall motion so that its kinetic energy is reduced to the only quadratic term $\mathcal{T} = \mathcal{T}_2(\dot{q})$ in the generalized velocities.

¹ Equilibrium positions of systems undergoing uniformly accelerated translation are the subject of Exercise 2.1.

The equilibrium position is then the solution of:

$$\frac{\partial \mathcal{V}}{\partial q_s} = 0 \quad s = 1, \dots, n \quad (2.2)$$

Concept of equilibrium stability

In order to investigate the stability of the equilibrium position, let us consider the case of a conservative system for which $\mathcal{T} + \mathcal{V}$ remains constant.

To simplify the discussion, we will move the origin of generalized coordinates so that, at equilibrium,

$$q_s = 0 \quad s = 1, \dots, n \quad (2.3)$$

the q_s representing the deviations from equilibrium. Further, since the potential energy is defined only up to a constant, we choose it to be zero at equilibrium so that:

$$\mathcal{V}(q_s = 0) = 0$$

as schematically illustrated in Figure 2.1.

If an initial energy \mathcal{E} is given to the system at $t = 0$, energy conservation at any later instant implies:

$$\mathcal{T} + \mathcal{V} = \mathcal{E} \quad (2.4)$$

We then define the local stability of an equilibrium position as follows:

The equilibrium position (2.3) is stable when an energy bound \mathcal{E}^ exists such that, for any energy $\mathcal{E} < \mathcal{E}^*$ given to the system, one has $\mathcal{T} \leq \mathcal{E}$ at any later instant, equality occurring only at equilibrium.*

This definition is illustrated in Figure 2.1 (comparable to the potential of single pendulum depicted in Figure 1.8). It implies that in the vicinity of a stable equilibrium:

$$\mathcal{V} \geq 0 \quad (2.5)$$

showing that a stable equilibrium position corresponds to a *relative minimum* of the potential energy. Moreover, since kinetic energy is a positive definite quantity, the energy conservation

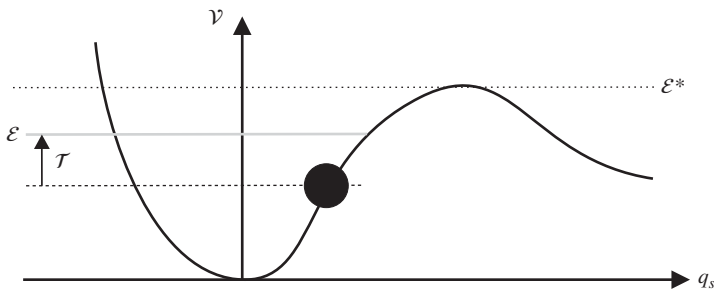


Figure 2.1 Potential of a locally stable system.

(2.4) implies that at any instant:

$$0 \leq \mathcal{V} \leq \mathcal{E}$$

so that if the initial energy \mathcal{E} is small enough, the deviations from the equilibrium position will themselves remain small.

Linearization of potential and kinetic energies

By *linearized form of energy* we mean a quadratic expression in terms of generalized displacements or their derivatives, so that the corresponding generalized forces are linear.

Since the generalized displacements q_s represent deviations from equilibrium, the potential energy could be expanded in the form of a Taylor series in the neighbourhood of the equilibrium position:

$$\mathcal{V}(\mathbf{q}) = \mathcal{V}(\mathbf{0}) + \sum_{s=1}^n \left(\frac{\partial \mathcal{V}}{\partial q_s} \right)_{q=0} q_s + \frac{1}{2} \sum_{s=1}^n \sum_{r=1}^n \left(\frac{\partial^2 \mathcal{V}}{\partial q_s \partial q_r} \right)_{q=0} q_s q_r + O(q^3)$$

by assuming that \mathcal{V} has C_1 continuity at $q_s = 0$.

Since the potential energy is defined only to a constant, we have made earlier the assumption that $\mathcal{V}(\mathbf{0}) = 0$. Furthermore, all forces being in equilibrium at $\mathbf{q} = \mathbf{0}$, (2.2) holds and one obtains the second-order approximation:

$$\mathcal{V}(\mathbf{q}) = \frac{1}{2} \sum_{s=1}^n \sum_{r=1}^n k_{sr} q_s q_r > 0 \quad \text{for } \mathbf{q} \neq \mathbf{0} \quad (2.6)$$

with the *stiffness coefficients*:

$$k_{sr} = k_{rs} = \left(\frac{\partial^2 \mathcal{V}}{\partial q_s \partial q_r} \right)_{q=0} \quad (2.7)$$

Expression (2.6) may also be put in the matrix positive definite quadratic form:

$$\mathcal{V}(\mathbf{q}) = \frac{1}{2} \mathbf{q}^T \mathbf{K} \mathbf{q} > 0 \quad \text{for } \mathbf{q} \neq \mathbf{0} \quad (2.8)$$

where \mathbf{K} , the *linear stiffness matrix* of the system, of general term (2.7), is *symmetric and positive definite*.

The kinetic energy reduces here to the sole term \mathcal{T}_2 . Since \mathcal{T}_2 is homogeneous and quadratic in velocities, the linearized expression is obtained by expanding the coefficients of the quadratic form in the neighbourhood of $q_s = 0$:

$$\begin{aligned} \mathcal{T}_2(\dot{\mathbf{q}}, \mathbf{q}) &= \frac{1}{2} \sum_{s=1}^n \sum_{r=1}^n \left(\frac{\partial^2 \mathcal{T}_2}{\partial \dot{q}_s \partial \dot{q}_r} \right) \dot{q}_s \dot{q}_r \\ &= \frac{1}{2} \sum_{s=1}^n \sum_{r=1}^n \left(\frac{\partial^2 \mathcal{T}_2}{\partial \dot{q}_s \partial \dot{q}_r} \right)_{q=0} \dot{q}_s \dot{q}_r + O(\dot{\mathbf{q}}^2, \mathbf{q}) \end{aligned}$$

We thus adopt the second-order approximation:

$$\mathcal{T}_2(\dot{\mathbf{q}}) = \frac{1}{2} \sum_{s=1}^n \sum_{r=1}^n m_{sr} \dot{q}_s \dot{q}_r \quad (2.9)$$

where owing to relation (1.33) the *inertia coefficients* are:

$$\begin{aligned} m_{sr} = m_{rs} &= \left(\frac{\partial^2 \mathcal{T}_2}{\partial \dot{q}_s \partial \dot{q}_r} \right)_{q=0} \\ &= \sum_{k=1}^N m_k \sum_{i=1}^3 \left(\frac{\partial U_{ik}}{\partial q_s} \right)_{q=0} \left(\frac{\partial U_{ik}}{\partial q_r} \right)_{q=0} \end{aligned} \quad (2.10)$$

Thus, in matrix form, kinetic energy is a positive definite quadratic form of velocities:

$$\mathcal{T}_2(\dot{\mathbf{q}}) = \frac{1}{2} \dot{\mathbf{q}}^T \mathbf{M} \dot{\mathbf{q}} > 0 \quad \text{for } \dot{\mathbf{q}} \neq \mathbf{0} \quad (2.11)$$

where \mathbf{M} , the *linear mass matrix* of the system, is also *symmetric and positive definite*.²

Equations for free vibrations about a stable equilibrium position

Making use of the definitions (2.6) and (2.9) for potential and kinetic energies, the Lagrange equations provide the system of equations of motion governing the free vibrations about a stable equilibrium position:

$$\sum_{r=1}^n (m_{sr} \ddot{q}_r + k_{sr} q_r) = 0 \quad s = 1, \dots, n$$

or, in matrix form:

$$\mathbf{M} \ddot{\mathbf{q}} + \mathbf{K} \mathbf{q} = \mathbf{0} \quad (2.12)$$

This equation is the fundamental equation describing the free vibration of a conservative system around an equilibrium position.

Example 2.1

Let us consider two pendulums coupled by a spring (Figure 2.2).

In terms of the angles θ_1 and θ_2 adopted as generalized coordinates, the system energies take the form:

$$\begin{aligned} \mathcal{T} &= \frac{1}{2} m \ell^2 (\dot{\theta}_1^2 + \dot{\theta}_2^2) \\ \mathcal{V} &= mg\ell(1 - \cos \theta_1) + mg\ell(1 - \cos \theta_2) + \frac{1}{2} k \zeta^2 \end{aligned}$$

where:

$$\begin{aligned} \zeta(\theta_1, \theta_2) &= L - D \\ L(\theta_1, \theta_2) &= \sqrt{a^2(\cos \theta_2 - \cos \theta_1)^2 + (a \sin \theta_2 - a \sin \theta_1 + D)^2} \end{aligned}$$

² In some special cases degrees of freedom are defined to help describing the kinematic of the system without being related to an inertia. In such pathological cases the mass matrix is only semi-definite positive, which has consequences from a numerical standpoint.

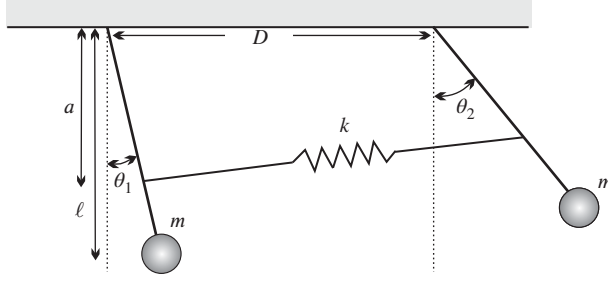


Figure 2.2 Coupled pendulums.

Let us notice that the potential energy expression satisfies $\mathcal{V}(\theta_1 = 0, \theta_2 = 0) = 0$. Moreover, verifying that the configuration $(\theta_1 = 0, \theta_2 = 0)$ corresponds to a stable equilibrium position is straightforward:

$$\frac{\partial \mathcal{V}}{\partial \theta_s} = mg\ell \sin \theta_s + k\zeta \frac{\partial L}{\partial \theta_s} = 0, \quad s = 1, 2 \quad \text{at} \quad \theta_1 = \theta_2 = 0$$

and $\mathcal{V}(\theta_s) \geq 0$. Indeed, the computation of the second-order derivatives yields:

$$\left(\frac{\partial^2 \mathcal{V}}{\partial \theta_s \partial \theta_r} \right)_{0,0} = mg\ell \delta_{rs} + k \left(\frac{\partial L}{\partial \theta_s} \right)_{0,0} \left(\frac{\partial L}{\partial \theta_r} \right)_{0,0}$$

where

$$\left(\frac{\partial L}{\partial \theta_1} \right)_{0,0} = -a \quad \text{and} \quad \left(\frac{\partial L}{\partial \theta_2} \right)_{0,0} = a$$

and the linearized potential energy thus takes the form:

$$\mathcal{V} \simeq \frac{1}{2} \sum_{s=1}^2 \sum_{r=1}^2 \left(\frac{\partial^2 \mathcal{V}}{\partial \theta_s \partial \theta_r} \right)_{\theta=0} \theta_s \theta_r = \frac{1}{2} mg\ell [\theta_1^2 + \theta_2^2] + \frac{1}{2} k[a(\theta_2 - \theta_1)]^2$$

The linearized stiffness and mass matrices are:

$$\mathbf{K} = \begin{bmatrix} mg\ell + ka^2 & -ka^2 \\ -ka^2 & mg\ell + ka^2 \end{bmatrix} \quad \mathbf{M} = \begin{bmatrix} m\ell^2 & 0 \\ 0 & m\ell^2 \end{bmatrix}$$

2.1.2 Free vibrations about an equilibrium configuration corresponding to steady motion

Linearization of energy expressions

Let us now consider the more general case of a system undergoing steady motion (uniform rotational or translational transport motion). Its equilibrium configuration defined by (2.1) corresponds to equilibrium between restoring forces of potential origin ($\partial \mathcal{V} / \partial q_s$ term) and

centrifugal forces ($\partial\mathcal{T}_0/\partial q_s$ term). It is an equilibrium configuration in the sense that the \dot{q}_s , which represent the relative velocities with respect to the transport motion, vanish although the system itself is not at rest.

The following results will be useful for analyzing the stability of systems in steady motion such as rotating systems.

Let us perform successively the linearization of the following terms:

- The effective potential energy $\mathcal{V}^* = \mathcal{V} - \mathcal{T}_0$ for which the second-order approximation is:

$$\mathcal{V}^*(q) = \frac{1}{2} \sum_{s=1}^n \sum_{r=1}^n k_{sr}^* q_s q_r \quad (2.13)$$

with the *effective stiffness coefficients*:

$$k_{sr}^* = k_{sr} - \left(\frac{\partial^2 \mathcal{T}_0}{\partial q_s \partial q_r} \right)_{q=0} \quad (2.14)$$

- The relative kinetic energy which keeps its previous expression:

$$\mathcal{T}_2(\dot{q}) = \frac{1}{2} \sum_{s=1}^n \sum_{r=1}^n m_{sr} \dot{q}_s \dot{q}_r \quad (2.15)$$

- The coupling kinetic energy, linear in the generalized velocities, can also be linearized with respect to generalized displacements in the form:

$$\mathcal{T}_1 = \sum_{s=1}^n \dot{q}_s \frac{\partial \mathcal{T}_1}{\partial \dot{q}_s} \simeq \sum_{s=1}^n c_s \dot{q}_s + \sum_{s=1}^n \sum_{r=1}^n f_{sr} \dot{q}_s q_r \quad (2.16)$$

with the coefficients:

$$c_s = \left(\frac{\partial \mathcal{T}_1}{\partial \dot{q}_s} \right)_{q=0} \quad f_{sr} = \left(\frac{\partial^2 \mathcal{T}_1}{\partial \dot{q}_s \partial q_r} \right)_{q=0} \quad (2.17)$$

We deduce from Equation (1.32) that c_s and f_{sr} remain constant in a transport motion with uniform speed and, in that case, the contribution of the coupling kinetic energy to inertia forces is:

$$\frac{d}{dt} \left(\frac{\partial \mathcal{T}_1}{\partial \dot{q}_s} \right) - \frac{\partial \mathcal{T}_1}{\partial q_s} = \sum_{r=1}^n (f_{sr} - f_{rs}) \dot{q}_r$$

It is interesting noting that the same result can be obtained from Equation (1.39), observing that the definition (1.40) for g_{rs} allows writing $(g_{rs})_{q=0} = f_{rs} - f_{sr}$ at equilibrium.

Equations for free vibrations about an equilibrium configuration

The equilibrium configuration generated by steady motion remains stable as long as the condition $\mathcal{V}^* \geq 0$ is verified, corresponding to the fact that the effective stiffness matrix remains positive definite.

In the neighbourhood of such a configuration, the linearized equations of motion take the form:

$$\sum_{r=1}^n [m_{sr}\ddot{q}_r + (f_{sr} - f_{rs})\dot{q}_r + k_{sr}^*q_r] = 0 \quad s = 1, \dots, n$$

or, in matrix form:

$$\mathbf{M}\ddot{\mathbf{q}} + \mathbf{G}\dot{\mathbf{q}} + \mathbf{K}^*\mathbf{q} = \mathbf{0} \quad (2.18)$$

with the matrix of gyroscopic coupling \mathbf{G} of general term:

$$g_{sr} = f_{sr} - f_{rs} = -g_{rs}$$

which is equivalent to expression (1.40).

It is possible to show that absence of a stable equilibrium configuration – which means that the positive definite character of the effective stiffness is lost – does not necessarily imply the instability of the system in a dynamic sense. Indeed, for sufficiently large transport velocity, the gyroscopic terms may generate stable trajectories about an unstable equilibrium configuration (see Section 2.11.2 and Example 2.9 for a discussion of the stability of rotating systems). The system stability then results from the specific form of the temporal solution of Equations (2.18).

The structure of Equations (2.18) renders the analysis of systems undergoing overall motion more difficult. In many cases, however, it is effectively observed that there is complete uncoupling between transport and relative motions in the kinetic energy expression (absence of \mathcal{T}_1 term). The motion equations then reduce to the form:

$$\mathbf{M}\ddot{\mathbf{q}} + \mathbf{K}^*\mathbf{q} = \mathbf{0} \quad (2.19)$$

where the stiffness matrix is simply modified by the presence of the centrifugal inertia term. Such systems may be treated in a manner similar to systems having a stable equilibrium position as long as their effective stiffness matrix remains positive definite, the only difference being that the stable equilibrium position still exists but now concerns the relative motion.

Example 2.2

Let us consider a system made of a mass m rotating about a fixed direction axis with angular velocity Ω . A spring of initial length a connects the mass to the rotation axis (Figure 2.3). The

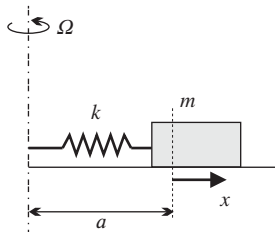


Figure 2.3 Spring-mass system under rotation.

absolute velocity of the mass is calculated as follows: calling X and Y the fixed coordinates and x the relative coordinate about the rotating axis,

$$X = (a + x) \cos \Omega t \quad Y = (a + x) \sin \Omega t$$

and thus

$$\begin{aligned} v^2 &= \dot{X}^2 + \dot{Y}^2 = [-(a + x)\Omega \sin \Omega t + \dot{x} \cos \Omega t]^2 + [(a + x)\Omega \cos \Omega t + \dot{x} \sin \Omega t]^2 \\ &= (a + x)^2 \Omega^2 + \dot{x}^2 \end{aligned}$$

where x is the only generalized coordinate of the system. The kinetic and potential energies are expressed by:

$$\begin{aligned} \mathcal{V} &= \frac{1}{2} k x^2 \\ \mathcal{T} &= \mathcal{T}_0 + \mathcal{T}_2 \\ \mathcal{T}_0 &= \frac{\Omega^2}{2} m (x + a)^2 \quad \mathcal{T}_2 = \frac{1}{2} m \dot{x}^2 \end{aligned}$$

The equilibrium configuration is obtained as the solution of:

$$\left. \frac{\partial \mathcal{V}^*}{\partial x} \right|_{eq} = k x_{eq} - \Omega^2 m (x_{eq} + a) = 0$$

hence

$$x_{eq} = \frac{\Omega^2 m a}{k - \Omega^2 m}$$

This result shows that the system becomes unstable for $\Omega^2 = k/m$. When $\Omega^2 > k/m$, x_{eq} becomes negative and corresponds to an unstable position since the stiffness coefficient $\frac{\partial^2 \mathcal{V}^*}{\partial x^2}$ is negative. In that case a small perturbation around the equilibrium position results in a change of centrifugal force higher than the change in spring force, pushing the mass away from its equilibrium.

2.1.3 Vibrations about a neutrally stable equilibrium position

Another case which deserves attention is that of systems that can exhibit a behaviour corresponding to a global motion but where either the global velocity is negligible or the additional kinetic energy generated by the global motion remains constant. The determination of global motion and the analysis of relative motion are then uncoupled problems, the relative motion occurring about a neutrally stable (and thus nonunique) equilibrium position as suggested by Figure 2.4. Examples of such systems are

- a shaft in torsion and simply supported on its bearings,
- an airplane in rectilinear flight,
- any structure supported on springs which are very soft compared to its stiffness.

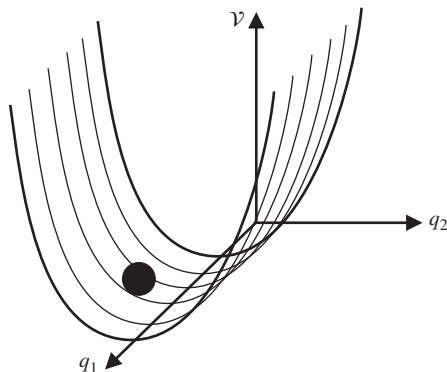


Figure 2.4 Neutrally stable equilibrium position.

In all cases, particular nonzero displacement modes exist such that the associated potential energy vanishes:

$$\mathcal{V}(\mathbf{q}) = \frac{1}{2} \mathbf{q}^T \mathbf{K} \mathbf{q} = 0 \quad \text{for } \mathbf{q} \neq \mathbf{0} \quad (2.20)$$

It is easy to verify that the necessary and sufficient condition for the existence of such solutions is that the homogeneous system:

$$\mathbf{K} \mathbf{q} = \mathbf{0} \quad (2.21)$$

possesses nontrivial solutions. These solutions, denoted \mathbf{u} , represent rigid-body displacements of the system and are called *rigid-body modes*. They correspond either to global rigid motion or to the existence of a mechanism where parts of a system move rigidly relative to one another.

The equations of motion of a system with rigid-body modes do not differ from those of a system with a stable equilibrium position (2.12). *They differ only through the existence of nonzero solutions \mathbf{u} for the associated homogeneous static system (2.21).*

2.2 Normal modes of vibration

In order to solve the free vibration linear Equations (2.12):

$$\mathbf{M} \ddot{\mathbf{q}} + \mathbf{K} \mathbf{q} = \mathbf{0}$$

let us seek a particular solution such that the generalized coordinates are governed to a common factor by the same temporal law:

$$\mathbf{q} = \mathbf{x} \phi(t) \quad (2.22)$$

\mathbf{x} is a vector of constants, known only to a common scale factor, which governs the *shape* of the motion. Motions described by (2.22) are called *synchronous* since all degrees of freedom follow the same time function. Substituting a solution of this type yields:

$$\ddot{\phi}(t) \mathbf{M} \mathbf{x} + \phi(t) \mathbf{K} \mathbf{x} = \mathbf{0} \quad (2.23)$$

Two cases have to be considered at this point.

2.2.1 Systems with a stable equilibrium configuration

The matrix \mathbf{K} is then nonsingular (and \mathbf{M} is per definition nonsingular). Equation (2.23) can be put in the form:

$$\mathbf{K}\mathbf{x} = -\frac{\ddot{\phi}(t)}{\phi(t)}\mathbf{M}\mathbf{x} \quad (2.24)$$

where $\mathbf{K}\mathbf{x}$ and $\mathbf{M}\mathbf{x}$ do not vanish if one excepts the trivial solution $\mathbf{x} = \mathbf{0}$. Therefore,

$$-\frac{\ddot{\phi}(t)}{\phi(t)} = \lambda \text{ and } \mathbf{K}\mathbf{x} = \lambda\mathbf{M}\mathbf{x} \quad (2.25)$$

where λ is a constant with respect to time. Relation (2.25) defines an eigenvalue problem, where the eigenvector \mathbf{x} represents a synchronous free vibration shape of the system and is called an *eigenmode*, and where λ is the associated eigenvalue. Let us show that λ is a real and positive quantity.

To this purpose let us consider the most general case where the eigenmode is complex, $\mathbf{x} = \mathbf{a} + i\mathbf{b}$, yielding:

$$\mathbf{K}(\mathbf{a} + i\mathbf{b}) = \lambda\mathbf{M}(\mathbf{a} + i\mathbf{b}) \quad (2.26)$$

Let us multiply this relationship to the left by $(\mathbf{a} - i\mathbf{b})^T$. Owing to the symmetry of \mathbf{K} and \mathbf{M} we obtain:

$$\begin{aligned} \mathbf{a}^T \mathbf{K} \mathbf{b} &= (\mathbf{a}^T \mathbf{K} \mathbf{b})^T = \mathbf{b}^T \mathbf{K} \mathbf{a} \\ \mathbf{a}^T \mathbf{M} \mathbf{b} &= (\mathbf{a}^T \mathbf{M} \mathbf{b})^T = \mathbf{b}^T \mathbf{M} \mathbf{a} \end{aligned}$$

where each term is a positive definite quadratic form, and thus we get:

$$\lambda = \frac{\mathbf{a}^T \mathbf{K} \mathbf{a} + \mathbf{b}^T \mathbf{K} \mathbf{b}}{\mathbf{a}^T \mathbf{M} \mathbf{a} + \mathbf{b}^T \mathbf{M} \mathbf{b}} > 0 \quad (2.27)$$

λ may thus be renamed ω^2 with ω real. Equations (2.24) become:

$$-\frac{\ddot{\phi}(t)}{\phi(t)} = \omega^2 \quad (2.28)$$

$$(\mathbf{K} - \omega^2 \mathbf{M})\mathbf{x} = \mathbf{0} \quad (2.29)$$

This last system of n linear and homogeneous equations admits a nontrivial solution $\mathbf{x}_{(r)}$ such that:

$$\boxed{(\mathbf{K} - \omega_r^2 \mathbf{M})\mathbf{x}_{(r)} = \mathbf{0}} \quad (2.30)$$

if ω_r^2 is a root of the algebraic equation:

$$\det(\mathbf{K} - \omega^2 \mathbf{M}) = 0 \quad (2.31)$$

The eigenvalue Equation (2.29) is of degree n in ω^2 and possesses thus n roots ω_r^2 which have been shown to be real and positive.

To each root ω_r^2 there corresponds a real solution $\mathbf{x}_{(r)}$ given by (2.30) – the *eigenmode* associated with the eigenvalue ω_r^2 .

Owing to (2.28), the temporal solution ϕ_r associated with the mode $\mathbf{x}_{(r)}$ is governed by:

$$\ddot{\phi}_r(t) + \omega_r^2 \phi_r(t) = 0 \quad (2.32)$$

and is of harmonic type:

$$\phi_r(t) = \alpha_r \cos \omega_r t + \beta_r \sin \omega_r t \quad (2.33)$$

The eigenvalue ω_r can thus be interpreted as the *circular frequency* of mode r . We will also call it frequency although strictly speaking frequency ν (in *hertz*) and circular frequency ω (in *radians per second*) are related by $\nu = \omega/2\pi$.

It is interesting to observe that the stability property of solution (2.33) is an immediate consequence of the positive definite character of \mathbf{M} and \mathbf{K} . Indeed, if they were not positive definite, λ could no longer be positive, in which case the solution of (2.25) would be an exponentially growing function of time.

Finally let us stress that the eigenmodes defined here are special solutions for the free vibration problem in the sense that they represent synchronous vibrations and therefore are governed by the fundamental eigenvalue problem (2.30). Obviously any combination $\sum_r \alpha_r \mathbf{x}_{(r)} \phi_r(t)$ of those motions is also solution of the homogeneous free vibration equation (2.12), but the result is in general not synchronous.

2.2.2 Systems with a neutrally stable equilibrium position

In the case where the system admits rigid-body displacement modes, we have seen that these modes, denoted \mathbf{u} , are solutions of

$$\mathbf{K}\mathbf{u} = \mathbf{0} \quad (2.34)$$

Comparing Equation (2.34) to Equation (2.30) governing the free vibration around a stable equilibrium position, it appears that the rigid-body modes can be considered as eigenmodes with zero frequency.

Owing to Equation (2.34), the displacements:

$$\mathbf{q} = \eta(t)\mathbf{u} \quad (2.35)$$

verify the equations of motion (2.12) if:

$$\ddot{\eta}(t)\mathbf{M}\mathbf{u} = \mathbf{0} \quad (2.36)$$

and thus, since \mathbf{M} is positive definite,

$$\ddot{\eta}(t) = 0 \quad (2.37)$$

The time-dependent part of the solution corresponds to a uniformly accelerated motion:

$$\eta(t) = \gamma + \delta t \quad (2.38)$$

Hence it may be said that when a system possesses a neutrally stable equilibrium position, its linearized vibration analysis provides two types of solutions:

- Rigid-body modes $\mathbf{u}_{(i)}$, in equal number to the degree of singularity of the stiffness matrix, which may be regarded as eigenmodes with zero eigenfrequency. To each rigid-body mode corresponds a modal solution describing a contribution to overall motion:

$$(\gamma_i + \delta_i t)\mathbf{u}_{(i)}$$

- Eigenmodes $\mathbf{x}_{(r)}$ associated with nonzero eigenfrequencies ω_r by Equation (2.30). For each of them there is a corresponding modal solution representing a vibration about the overall motion:

$$(\alpha_r \cos \omega_r t + \beta_r \sin \omega_r t)\mathbf{x}_{(r)}$$

Since these modes, in contrast to rigid-body modes, imply an elastic deformation of the system, they may also be called *elastic eigenmodes*.

2.3 Orthogonality of vibration eigenmodes

2.3.1 Orthogonality of elastic modes with distinct frequencies

Let us examine the case of two eigenmodes with distinct eigenfrequencies, denoted $\mathbf{x}_{(r)}$ and $\mathbf{x}_{(s)}$, and associated with distinct frequencies ω_r and ω_s , namely $\omega_r \neq \omega_s$. Premultiplication by $\mathbf{x}_{(s)}^T$ of Equation (2.30) verified by eigenmode $\mathbf{x}_{(r)}$ yields:

$$\mathbf{x}_{(s)}^T \mathbf{K} \mathbf{x}_{(r)} = \omega_r^2 \mathbf{x}_{(s)}^T \mathbf{M} \mathbf{x}_{(r)} \quad (2.39)$$

Similarly, starting from the equation verified by eigenmode $\mathbf{x}_{(s)}$, we obtain:

$$\mathbf{x}_{(r)}^T \mathbf{K} \mathbf{x}_{(s)} = \omega_s^2 \mathbf{x}_{(r)}^T \mathbf{M} \mathbf{x}_{(s)} \quad (2.40)$$

Subtracting (2.40) from (2.39) while taking into account the symmetry of the mass and stiffness matrices provides the result:

$$(\omega_r^2 - \omega_s^2) \mathbf{x}_{(s)}^T \mathbf{M} \mathbf{x}_{(r)} = 0$$

and thus, for distinct eigenfrequencies:

$$\mathbf{x}_{(s)}^T \mathbf{M} \mathbf{x}_{(r)} = 0 \quad (2.41)$$

Moreover, the substitution of this result into (2.39) also yields:

$$\mathbf{x}_{(s)}^T \mathbf{K} \mathbf{x}_{(r)} = 0 \quad (2.42)$$

Equations (2.41) and (2.42) are the *orthogonality relationships* between eigenmodes of distinct eigenfrequencies. They play an essential role when expressing the general solution of the equations of motion for an n -degree-of-freedom vibrating system.

In order to obtain the physical meaning of these relationships, let us interpret (2.41) as the product of the inertia forces $\mathbf{M} \mathbf{x}_{(r)}$ of eigenmode r by the eigenmode $\mathbf{x}_{(s)}$. Equation (2.41) thus expresses that:

The virtual work produced by the inertia forces of mode r in a virtual displacement described by mode s is zero.

Similarly, Equation (2.42) expresses that:

The virtual work produced by the elastic forces of mode r in a virtual displacement described by mode s is zero.

The quadratic forms:

$$\begin{aligned}\mathbf{x}_{(r)}^T \mathbf{K} \mathbf{x}_{(r)} &= \gamma_r \\ \mathbf{x}_{(r)}^T \mathbf{M} \mathbf{x}_{(r)} &= \mu_r\end{aligned}$$

measure respectively the contribution of mode r to the deformation energy and to the kinetic energy. They are respectively called the *generalized stiffness* and the *generalized mass* of mode r . Indeed, both quantities are known only to a constant factor since the amplitude of eigenmode $\mathbf{x}_{(r)}$ is undetermined. This indeterminacy may be removed by calculating their quotient, since by setting $r = s$ into Equation (2.39):³

$$\frac{\mathbf{x}_{(r)}^T \mathbf{K} \mathbf{x}_{(r)}}{\mathbf{x}_{(r)}^T \mathbf{M} \mathbf{x}_{(r)}} = \frac{\gamma_r}{\mu_r} = \omega_r^2 \quad (2.43)$$

The indeterminacy in the norm of eigenmode $\mathbf{x}_{(r)}$ allows one when necessary to choose its most appropriate form, the most usual choices being:

- setting the largest component to unity,
- setting the generalized mass to unity.

When the latter choice is adopted, the orthogonality relationships may be rewritten in the simpler form:

$$\boxed{\begin{aligned}\mathbf{x}_{(s)}^T \mathbf{K} \mathbf{x}_{(r)} &= \omega_r^2 \delta_{rs} \\ \mathbf{x}_{(s)}^T \mathbf{M} \mathbf{x}_{(r)} &= \delta_{rs}\end{aligned}} \quad (2.44)$$

where δ is Kronecker's symbol defined by:

$$\delta_{rs} = \begin{cases} 1 & \text{if } r = s \\ 0 & \text{if } r \neq s \end{cases}$$

Example 2.3

In order to illustrate the concept of modes and orthogonality, let us consider again the coupled pendulums as described in Figure 2.2 for which the linearized mass and stiffness matrices were constructed in Example 2.1. Let us compute the associate eigensolutions by solving the

³ The quotient $\frac{\mathbf{x}^T \mathbf{K} \mathbf{x}}{\mathbf{x}^T \mathbf{M} \mathbf{x}} = \omega^2$ for any vector \mathbf{x} is called the *Rayleigh quotient*. Its noteworthy properties will be discussed separately in Section 2.10.

eigenvalue problem (2.30) which, for the coupled pendulum, is written as:

$$\begin{aligned}
 (\mathbf{K} - \omega_r^2 \mathbf{M})\mathbf{x}_{(r)} &= \left(\begin{bmatrix} mgl + ka^2 & -ka^2 \\ -ka^2 & mgl + ka^2 \end{bmatrix} - \omega_r^2 \begin{bmatrix} ml^2 & 0 \\ 0 & ml^2 \end{bmatrix} \right) \mathbf{x}_{(r)} \\
 &= \begin{bmatrix} mgl + ka^2 - \omega_r^2 ml^2 & -ka^2 \\ -ka^2 & mgl + ka^2 - \omega_r^2 ml^2 \end{bmatrix} \begin{bmatrix} \theta_1 \\ \theta_2 \end{bmatrix}_{(r)} = \mathbf{0}
 \end{aligned} \tag{E2.3.a}$$

Expressing the characteristic equation, i.e. setting the determinant of the matrix to zero, yields:

$$mgl + ka^2 - \omega_r^2 ml^2 \pm ka^2 = 0$$

and thus the eigenfrequencies:

$$\omega_1 = \sqrt{\frac{g}{\ell}} \quad \omega_2 = \sqrt{\frac{g}{\ell} + 2\frac{ka^2}{ml^2}} \tag{E2.3.b}$$

The corresponding modes are obtained through substitution of (E2.3.b) into the eigenvalue Equation (E2.3.a). Choosing a unit amplitude for the first degree of freedom one finds:

$$\mathbf{x}_{(1)} = \begin{bmatrix} 1 \\ 1 \end{bmatrix} \quad \mathbf{x}_{(2)} = \begin{bmatrix} 1 \\ -1 \end{bmatrix} \tag{E2.3.c}$$

In the first mode both pendulums move in phase, thus without compression of the connecting spring so that the frequency is identical to the frequency of a single pendulum. In the second mode the pendulums move in opposite direction and at a higher frequency due to the spring deformation.

It can be easily checked that the modes are \mathbf{M} - and \mathbf{K} -orthogonal since:

$$\begin{bmatrix} 1 & 1 \end{bmatrix} \begin{bmatrix} ml^2 & 0 \\ 0 & ml^2 \end{bmatrix} \begin{bmatrix} 1 \\ -1 \end{bmatrix} = 0 \quad \text{and} \quad \begin{bmatrix} 1 & 1 \end{bmatrix} \begin{bmatrix} mgl + ka^2 & -ka^2 \\ -ka^2 & mgl + ka^2 \end{bmatrix} \begin{bmatrix} 1 \\ -1 \end{bmatrix} = 0$$

The modal mass of the modes are:

$$\begin{bmatrix} 1 & 1 \end{bmatrix} \begin{bmatrix} ml^2 & 0 \\ 0 & ml^2 \end{bmatrix} \begin{bmatrix} 1 \\ 1 \end{bmatrix} = 2ml^2 \quad \text{and} \quad \begin{bmatrix} 1 & -1 \end{bmatrix} \begin{bmatrix} ml^2 & 0 \\ 0 & ml^2 \end{bmatrix} \begin{bmatrix} 1 \\ -1 \end{bmatrix} = 2ml^2$$

We can scale the modes to unit modal mass and redefine:

$$\mathbf{x}_{(1)} = \frac{1}{\ell\sqrt{2m}} \begin{bmatrix} 1 \\ 1 \end{bmatrix} \quad \mathbf{x}_{(2)} = \frac{1}{\ell\sqrt{2m}} \begin{bmatrix} 1 \\ -1 \end{bmatrix}$$

One can easily verify that the modal stiffness of these modes is equal to the associated eigenfrequency squared as indicated in (2.44).

2.3.2 Degeneracy theorem and generalized orthogonality relationships

The purpose of the degeneracy theorem is to generalize the orthogonality concept between eigenmodes to the case where several eigensolutions degenerate and give rise to a multiple eigenvalue.

Degeneracy theorem *To a multiple root ω_p^2 of system:*

$$\mathbf{K}\mathbf{x} - \omega_p^2 \mathbf{M}\mathbf{x} = \mathbf{0}$$

corresponds a number of linearly independent eigenvectors equal to the root multiplicity.

In other words, the m eigenvectors corresponding to an eigenvalue with multiplicity m are linearly independent and may be combined in order to give an orthogonal basis spanning a subspace of dimension m . Any vector \mathbf{x} contained in this subspace, namely any linear combination of the eigenmodes associated with ω_p^2 , is also solution of the algebraic system:

$$(\mathbf{K} - \omega_p^2 \mathbf{M}) \mathbf{x} = \mathbf{0} \quad (2.45)$$

The proof of the degeneracy theorem is obtained as follows.

Proof. Let us consider an eigenmode $\mathbf{y} = \mathbf{x}_{(p)}$ normalized with respect to \mathbf{M} and associated with an eigenvalue ω_p^2 with multiplicity m such that:

$$\mathbf{K}\mathbf{y} = \omega_p^2 \mathbf{M}\mathbf{y} \quad (2.46a)$$

and

$$\mathbf{y}^T \mathbf{M}\mathbf{y} = 1 \quad \mathbf{y}^T \mathbf{K}\mathbf{y} = \omega_p^2 \quad (2.46b)$$

The proof of the theorem holds by projecting the eigenvalue problem in a subspace orthogonal to \mathbf{y} with respect to \mathbf{M} and then observing that this subspace contains $m - 1$ eigenmodes associated with ω_p .

Let n denote the number of degrees of freedom of the system, i.e. the dimension of matrices \mathbf{K} and \mathbf{M} . It is always possible to construct $n - 1$ vectors $\mathbf{z}_{(i)}$ linearly independent and orthogonal to $\mathbf{M}\mathbf{y}$, i.e. \mathbf{M} -orthogonal to \mathbf{y} . These vectors are stored in columns in the matrix: \mathbf{Z}

$$\mathbf{Z} = [\mathbf{z}_{(2)} \quad \dots \quad \mathbf{z}_{(n)}] \quad (2.46c)$$

such that:

$$\mathbf{y}^T \mathbf{M}\mathbf{Z} = \mathbf{0} \quad (2.46d)$$

and, by taking account of (2.46a),

$$\mathbf{y}^T \mathbf{K}\mathbf{Z} = \mathbf{0} \quad (2.46e)$$

The mass matrix being positive definite, Equation (2.46d) implies that the vectors $\mathbf{z}_{(i)}$ are linearly independent of \mathbf{y} .

Indeed, let us suppose that the vectors $\mathbf{z}_{(i)}$ are linearly dependent on \mathbf{y} . This would imply:

$$\mathbf{y} + \sum_{i=2}^n c_i \mathbf{z}_{(i)} = \mathbf{0}$$

and premultiplying by $\mathbf{y}^T \mathbf{M}$ would yield:

$$\mathbf{y}^T \mathbf{M}\mathbf{y} + 0 = 0$$

which is impossible since \mathbf{M} is positive definite.

Since any vector \mathbf{x} can be expressed as a linear combination of the n linearly independent vectors \mathbf{y} and $\mathbf{z}_{(i)}$, let us perform the change of generalized coordinates:

$$\mathbf{x} = \alpha \mathbf{y} + \sum_{i=2}^n b_i \mathbf{z}_{(i)} = \alpha \mathbf{y} + \mathbf{Z} \mathbf{b}$$

This change of variable can be written in the following matrix form:

$$\mathbf{x} = [\mathbf{y} \ \mathbf{Z}] \begin{bmatrix} \alpha \\ \mathbf{b} \end{bmatrix} \quad (2.46f)$$

For this new set of generalized coordinates the eigenvalue problem can be put in the form:

$$\left\{ \begin{bmatrix} \mathbf{y}^T \\ \mathbf{Z}^T \end{bmatrix} (\mathbf{K} - \omega^2 \mathbf{M}) [\mathbf{y} \ \mathbf{Z}] \right\} \begin{bmatrix} \alpha \\ \mathbf{b} \end{bmatrix} = \mathbf{0} \quad (2.46g)$$

Taking account of the orthogonality relationships (2.46d) and (2.46e), the transformed eigenvalue problem (2.46g) may be written as:

$$\left\{ \begin{bmatrix} \omega_p^2 & \mathbf{0} \\ \mathbf{0} & \mathbf{Z}^T \mathbf{K} \mathbf{Z} \end{bmatrix} - \omega^2 \begin{bmatrix} 1 & \mathbf{0} \\ \mathbf{0} & \mathbf{Z}^T \mathbf{M} \mathbf{Z} \end{bmatrix} \right\} \begin{bmatrix} \alpha \\ \mathbf{b} \end{bmatrix} = \mathbf{0}$$

and the eigenvalue equation associated with (2.46g) thus becomes:

$$(\omega_p^2 - \omega^2) \det(\mathbf{Z}^T \mathbf{K} \mathbf{Z} - \omega^2 \mathbf{Z}^T \mathbf{M} \mathbf{Z}) = 0 \quad (2.46h)$$

Since (2.46h) is equivalent to the initial eigenvalue equation, ω_p^2 is still a root with multiplicity $m - 1$ to the system:

$$(\mathbf{Z}^T \mathbf{K} \mathbf{Z} - \omega_p^2 \mathbf{Z}^T \mathbf{M} \mathbf{Z}) \mathbf{b} = \mathbf{0} \quad (2.46i)$$

of dimension $(n - 1)$. A second eigenvector associated with ω_p^2 and linearly independent of \mathbf{y} exists, since we may write:

$$\mathbf{x}_{(p+1)} = \mathbf{Z} \mathbf{b}$$

It will be possible to extract in a similar manner m linearly independent solutions $\mathbf{x}_{(p)}, \mathbf{x}_{(p+1)}, \dots, \mathbf{x}_{(p+m-1)}$ associated with the root ω_p^2 of multiplicity m .

The degeneracy theorem is essential not only to allow the *generalization of the orthogonality relationships* (2.44) to the case of multiple eigenvalues, but also to *guarantee the stability of the free vibration solution*.

Indeed, if a root ω_p^2 of multiplicity m had a single associated eigenvector $\mathbf{x}_{(p)}$, one could show that the contribution of this eigenmode to the general free vibration solution would be of type:

$$\sum_{k=0}^{m-1} \{ (\alpha_k t^k) \cos(\omega_p t) + (\beta_k t^k) \sin(\omega_p t) \} \mathbf{x}_{(p)}$$

which would be unstable in time.

Thanks to the degeneracy theorem, it is always possible to imagine that the m linearly independent solutions associated with ω_p^2 have been made orthonormal through the *Gram–Schmidt* orthogonalization process. The orthogonality relationships (2.44) may thus be accepted in all generality.

Example 2.4

Consider the coupled pendulums described in Figure 2.2 for which the modes and frequencies were computed in Example 2.3. Setting the spring stiffness k to zero so that the pendulums are now uncoupled, the free vibration equation is written as:

$$\left(\begin{bmatrix} mg\ell & 0 \\ 0 & mg\ell \end{bmatrix} - \omega_r^2 \begin{bmatrix} m\ell^2 & 0 \\ 0 & m\ell^2 \end{bmatrix} \right) \mathbf{x}_{(r)} = \mathbf{0}$$

yielding the double eigenfrequency (multiplicity 2):

$$\omega_1 = \omega_2 = \sqrt{\frac{g}{\ell}}$$

The associated modes can be chosen to be, for instance,

$$\mathbf{x}_{(1)} = \begin{bmatrix} 1 \\ 0 \end{bmatrix} \quad \mathbf{x}_{(2)} = \begin{bmatrix} 0 \\ 1 \end{bmatrix}$$

corresponding to the vibration of one pendulum only. But another licit choice of \mathbf{M} - and \mathbf{K} -orthogonal modes would be the modes found when the pendulums are coupled by the spring (see Example 2.3):

$$\mathbf{x}_{(1)} = \begin{bmatrix} 1 \\ 1 \end{bmatrix} \quad \mathbf{x}_{(2)} = \begin{bmatrix} 1 \\ -1 \end{bmatrix}$$

Note that when the masses of the pendulums are not equal, the frequencies are no longer multiple and the modes are uniquely defined.

2.3.3 Orthogonality relationships including rigid-body modes

The existence of rigid-body modes represents a particular application of the degeneracy theorem, in the sense that they give rise to a multiple zero eigenvalue. Let m be the number of rigid-body modes of the system. They can always be assumed to be \mathbf{M} -orthogonal:

$$\mathbf{u}_{(i)}^T \mathbf{M} \mathbf{u}_{(j)} = \mu_i \delta_{ij} \quad (2.47)$$

Owing to the relationship (2.34), the rigid-body modes are likewise \mathbf{K} -orthogonal:

$$\mathbf{u}_{(i)}^T \mathbf{K} \mathbf{u}_{(j)} = 0 \quad (2.48)$$

The elastic eigenmodes of the system are also orthogonal to each other and verify the orthogonality relationships:

$$\mathbf{x}_{(r)}^T \mathbf{M} \mathbf{x}_{(s)} = \mu_r \delta_{rs} \quad \mathbf{x}_{(r)}^T \mathbf{K} \mathbf{x}_{(s)} = \gamma_r \delta_{rs} \quad (2.49)$$

Finally, rigid-body modes and elastic modes are associated with distinct eigenvalues and are necessarily orthogonal:

$$\mathbf{u}_{(i)}^T \mathbf{K} \mathbf{x}_{(s)} = 0 \quad \mathbf{u}_{(i)}^T \mathbf{M} \mathbf{x}_{(s)} = 0 \quad (2.50)$$

2.4 Vector and matrix spectral expansions using eigenmodes

Because the eigenmodes $\mathbf{x}_{(r)}$ (including the rigid-body modes, if present) are independent and orthogonal with respect to the mass matrix \mathbf{M} , they form a vector basis spanning the n -dimensional space in which an arbitrary vector such as the displacement vector admits a unique expansion:

$$\mathbf{x} = \sum_{s=1}^n \alpha_s \mathbf{x}_{(s)} \quad (2.51)$$

This expansion of a vector will be used extensively in vibration analysis for instance to compute the solution of the linearized dynamic equations and will be referred to as *mode superposition*. The projection coefficients α_r , i.e. the generalized coordinates describing \mathbf{x} in the eigenmode basis, are evaluated by \mathbf{M} -orthogonal projection of \mathbf{x} on the eigenmodes $\mathbf{x}_{(r)}$. To this purpose, let us premultiply \mathbf{x} by $\mathbf{x}_{(r)}^T \mathbf{M}$ and make use of the orthogonality relationships. One obtains:

$$\alpha_r = \frac{\mathbf{x}_{(r)}^T \mathbf{M} \mathbf{x}}{\mu_r} \quad (2.52)$$

and the modal expansion of \mathbf{x} :

$$\mathbf{x} = \sum_{s=1}^n \left\{ \frac{\mathbf{x}_{(s)}^T \mathbf{M} \mathbf{x}}{\mu_s} \right\} \mathbf{x}_{(s)} \quad (2.53)$$

The products in (2.53) may be rearranged in a different manner⁴ to provide matrix expression:

$$\mathbf{x} = \sum_{s=1}^n \frac{\mathbf{x}_{(s)} \mathbf{x}_{(s)}^T \mathbf{M}}{\mu_s} \mathbf{x} \quad (2.54)$$

valid for arbitrary \mathbf{x} . From this result one deduces the spectral expansion of the unit matrix:

$$\mathbf{I} = \sum_{s=1}^n \frac{\mathbf{x}_{(s)} \mathbf{x}_{(s)}^T \mathbf{M}}{\mu_s} \quad (2.55)$$

Let us also consider the case where the vector to be expanded in the modal basis is related to a force distribution. It will be seen later that it is more appropriate in this case to perform the expansion in terms of the inertia forces $\mathbf{M} \mathbf{x}_{(r)}$ generated by the eigenmodes:

$$\mathbf{p} = \sum_{s=1}^n \beta_s \mathbf{M} \mathbf{x}_{(s)} \quad (2.56)$$

⁴ Looking at the last two factors of (2.53), $\mathbf{x} \mathbf{x}_{(s)}$, a dimensional incongruity in terms of matrix operation is observed. This originates from the mode superposition expression (2.51) where the product $\alpha_s \mathbf{x}_{(s)}$ is, strictly speaking, not admissible since it is a product of matrices of dimension 1×1 and $n \times 1$. Although such expressions are commonly used, one should write $\mathbf{x}_{(s)} \alpha_s$ to be dimensionally correct, which then leads to the expansion form (2.54).

in which case the coefficients are obtained in the form:

$$\beta_r = \frac{\mathbf{x}_{(r)}^T \mathbf{p}}{\mu_r} \quad (2.57)$$

The β_r coefficients of expansion (2.56) are called *modal participation factors* to the loading \mathbf{p} .

Let us next make use of the spectral expansion of the unit matrix. By either pre- or post-multiplication by an arbitrary $n \times n$ matrix \mathbf{A} , it is possible to build two equivalent expressions for the spectral expansion of \mathbf{A} :

$$\mathbf{A} = \sum_{s=1}^n \frac{\mathbf{A} \mathbf{x}_{(s)} \mathbf{x}_{(s)}^T \mathbf{M}}{\mu_s} = \sum_{s=1}^n \frac{\mathbf{x}_{(s)} \mathbf{x}_{(s)}^T \mathbf{M} \mathbf{A}}{\mu_s} \quad (2.58)$$

Some spectral expansions of interest can be deduced from (2.58) by taking into account the orthogonality relationships with respect to mass and stiffness:

$$\mathbf{M} = \sum_{s=1}^n \frac{\mathbf{M} \mathbf{x}_{(s)} \mathbf{x}_{(s)}^T \mathbf{M}}{\mu_s} \quad (2.59)$$

$$\mathbf{K} = \sum_{s=1}^n \frac{\omega_s^2}{\mu_s} \mathbf{M} \mathbf{x}_{(s)} \mathbf{x}_{(s)}^T \mathbf{M} \quad (2.60)$$

$$\mathbf{M}^{-1} = \sum_{s=1}^n \frac{\mathbf{x}_{(s)} \mathbf{x}_{(s)}^T}{\mu_s} \quad (2.61)$$

$$\mathbf{K}^{-1} = \sum_{s=1}^n \frac{\mathbf{x}_{(s)} \mathbf{x}_{(s)}^T}{\omega_s^2 \mu_s} \quad (2.62)$$

the last one being valid only if \mathbf{K} is nonsingular and thus, if ω_s^2 is nonzero.

2.5 Free vibrations induced by nonzero initial conditions

In the absence of external loading, let us express the general solution of the system resulting from nonhomogeneous initial conditions

$$\mathbf{M} \ddot{\mathbf{q}} + \mathbf{K} \mathbf{q} = \mathbf{0}$$

given $\mathbf{q}(0) = \mathbf{q}_0, \quad \dot{\mathbf{q}}(0) = \dot{\mathbf{q}}_0$

(2.63)

by eigenmode superposition.

2.5.1 Systems with a stable equilibrium position

Let us solve system (2.63) by making the change of generalized coordinates:

$$\mathbf{q}(t) = \sum_{s=1}^n \mathbf{x}_{(s)} \eta_s(t) = \mathbf{X} \boldsymbol{\eta}(t) \quad (2.64)$$

where

X is the matrix of eigenmodes:

$$X = [x_{(1)} \quad \dots \quad x_{(n)}]$$

η is the vector of *modal coordinates* (also called *normal coordinates*):

$$\eta^T(t) = [\eta_1(t) \quad \dots \quad \eta_n(t)]$$

The equations of motion become:

$$MX\ddot{\eta} + KX\eta = 0 \quad (2.65)$$

Next, we project the dynamic equilibrium equations on the eigenmodes: premultiplying (2.65) by X^T and taking account of the orthogonality relationships between eigenmodes:

$$X^T MX = \mu \quad X^T KX = \gamma \quad (2.66)$$

with

$$\mu = \text{diag}(\mu_1 \quad \dots \quad \mu_n) \quad \gamma = \text{diag}(\gamma_1 \quad \dots \quad \gamma_n)$$

one obtains the system of n uncoupled equations:

$$\mu\ddot{\eta} + \gamma\eta = 0 \quad \text{or} \quad \ddot{\eta} + \Omega^2\eta = 0 \quad (2.67)$$

where

$$\Omega^2 = \gamma\mu^{-1} = \text{diag}(\omega_1^2 \quad \dots \quad \omega_n^2)$$

or, in terms of components, the *normal equations*:

$$\ddot{\eta}_r + \omega_r^2 \eta_r = 0 \quad r = 1, \dots, n \quad (2.68)$$

showing that the system vibrates as if it were made of n independent oscillators corresponding to its eigenmodes:

$$\eta_r = \alpha_r \cos \omega_r t + \beta_r \sin \omega_r t \quad r = 1, \dots, n$$

Thus the general solution is expressed in the form:

$$q(t) = \sum_{s=1}^n (\alpha_s \cos \omega_s t + \beta_s \sin \omega_s t) x_{(s)} \quad (2.69)$$

where the $2n$ constants are obtained by imposing the initial conditions:

$$q_0 = \sum_{s=1}^n \alpha_s x_{(s)} \quad \dot{q}_0 = \sum_{s=1}^n \beta_s \omega_s x_{(s)} \quad (2.70)$$

which shows that α_s and $\beta_s\omega_s$ are the modal coordinates of \mathbf{q}_0 and $\dot{\mathbf{q}}_0$ respectively. They are obtained through premultiplication of (2.70) by $\mathbf{x}_{(r)}^T \mathbf{M}$ and by making use of the orthogonality relationships:

$$\alpha_r = \frac{\mathbf{x}_{(r)}^T \mathbf{M} \mathbf{q}_0}{\mu_r} \quad \beta_r = \frac{\mathbf{x}_{(r)}^T \mathbf{M} \dot{\mathbf{q}}_0}{\mu_r \omega_r}$$

Summarizing, the linear vibration solution about a stable equilibrium position takes the form:

$$\mathbf{q}(t) = \left(\sum_{s=1}^n \frac{\mathbf{x}_{(s)} \mathbf{x}_{(s)}^T \mathbf{M}}{\mu_s} \cos \omega_s t \right) \mathbf{q}_0 + \left(\sum_{s=1}^n \frac{\mathbf{x}_{(s)} \mathbf{x}_{(s)}^T \mathbf{M}}{\mu_s \omega_s} \sin \omega_s t \right) \dot{\mathbf{q}}_0 \quad (2.71)$$

where the generalized masses μ_s are most often set equal to 1. It should be observed that the modal contribution:

$$\frac{\mathbf{x}_{(r)} \mathbf{x}_{(r)}^T \mathbf{M}}{\mu_r}$$

does not depend on the scale factor of $\mathbf{x}_{(r)}$.

It is worthwhile noticing that transformation (2.64) allows one to express the potential and kinetic energies of the system in the form:

$$\mathcal{V} = \frac{1}{2} \mathbf{q}^T \mathbf{K} \mathbf{q} = \frac{1}{2} \sum_{s=1}^n \gamma_s \eta_s^2(t) = \frac{1}{2} \sum_{s=1}^n \omega_s^2 \mu_s \eta_s^2(t) \quad (2.72)$$

$$\mathcal{T} = \frac{1}{2} \dot{\mathbf{q}}^T \mathbf{M} \dot{\mathbf{q}} = \frac{1}{2} \sum_{s=1}^n \mu_s \dot{\eta}_s^2(t) \quad (2.73)$$

It shows that the coupling of either inertial or elastic nature is not a physical property of the system but simply depends on the choice of generalized coordinates.

Example 2.5

Let us consider again the example of two coupled pendulums displayed on Figure 2.2 for which the motion equations have been developed in Example 2.1 and for which the eigensolutions were computed in Example 2.3:

$$\omega_1 = \sqrt{\frac{g}{\ell}} \quad \omega_2 = \sqrt{\frac{g}{\ell} + 2 \frac{ka^2}{m\ell^2}} \quad (\text{E2.5.a})$$

$$\mathbf{x}_{(1)} = \begin{bmatrix} 1 \\ 1 \end{bmatrix} \quad \mathbf{x}_{(2)} = \begin{bmatrix} 1 \\ -1 \end{bmatrix} \quad (\text{E2.5.b})$$

According to (2.69) the free motion of the system is described by the general solution:

$$\begin{aligned} \theta_1(t) &= \alpha_1 \cos \omega_1 t + \beta_1 \sin \omega_1 t + \alpha_2 \cos \omega_2 t + \beta_2 \sin \omega_2 t \\ \theta_2(t) &= \alpha_1 \cos \omega_1 t + \beta_1 \sin \omega_1 t - \alpha_2 \cos \omega_2 t - \beta_2 \sin \omega_2 t \end{aligned} \quad (\text{E2.5.c})$$

Let us compute the coefficients (α_i, β_i) for the initial conditions obtained by moving the first pendulum away from the equilibrium position:

$$\theta_1(0) = \theta_0, \theta_2(0) = 0, \dot{\theta}_1(0) = \dot{\theta}_2(0) = 0$$

Equations (E2.5.c) become:

$$\begin{aligned} \theta_1(t) &= \frac{1}{2}\theta_0(\cos \omega_1 t + \cos \omega_2 t) = \theta_0 \cos \frac{\Delta\omega t}{2} \cos \omega_m t \\ \theta_2(t) &= \frac{1}{2}\theta_0(\cos \omega_1 t - \cos \omega_2 t) = \theta_0 \sin \frac{\Delta\omega t}{2} \sin \omega_m t \end{aligned} \quad (\text{E2.5.d})$$

where we defined the mean frequency ω_m and the frequency spread $\Delta\omega$:

$$\omega_m = \frac{\omega_1 + \omega_2}{2} \quad \Delta\omega = \omega_2 - \omega_1 \quad (\text{E2.5.e})$$

In the particular case of a weak spring coupling, the frequencies (E2.5.a) can be written as:

$$\omega_2 = \omega_1 \sqrt{1 + 2\epsilon} \simeq \omega_1(1 + \epsilon) \quad \text{where} \quad \epsilon = \frac{ka^2}{m\ell g} \ll 1$$

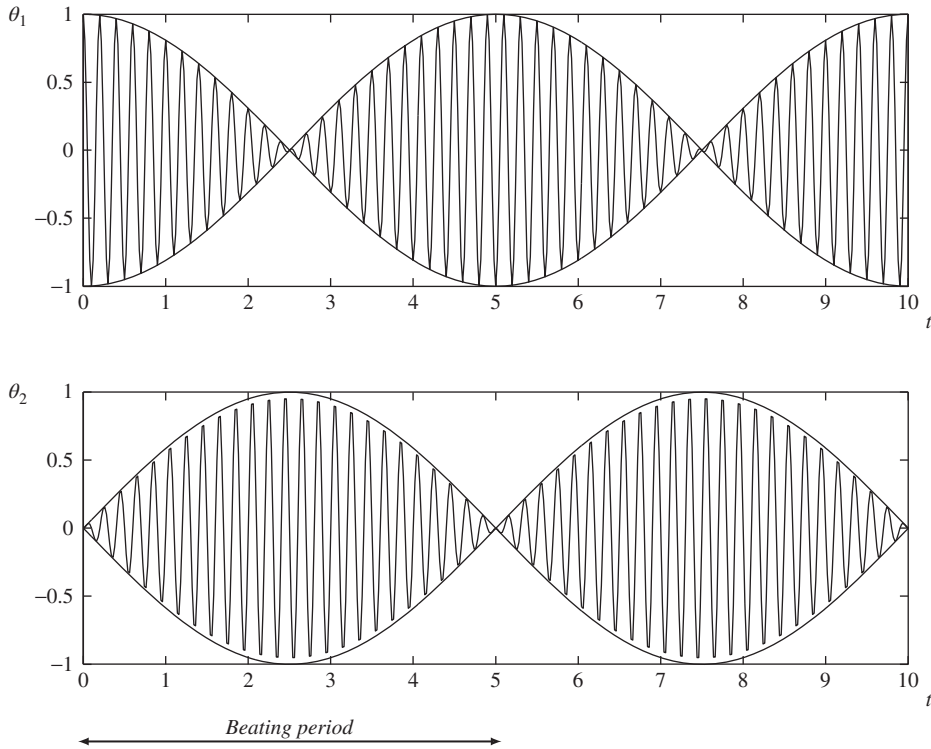


Figure 2.5 Beating phenomenon in a coupled pendulum system: exchange of energy between degrees of freedom ($\Delta\omega = \omega_m/50$).

The mean frequency and the frequency spread can then be found as:

$$\begin{aligned}\omega_m &= \frac{\omega_1 + \omega_2}{2} \simeq \omega_1 \left(1 + \frac{\epsilon}{2}\right) \\ \Delta\omega &= \omega_2 - \omega_1 \simeq \omega_1 \epsilon\end{aligned}\tag{E2.5.f}$$

For the case of weak coupling, Equations (E2.5.d) and (E2.5.f) show that the motion consists of a motion at frequency ω_m whose amplitude is slowly modulated by a harmonic function of frequency $\frac{\Delta\omega}{2}$. As displayed on Figure 2.5, $\Delta\omega$ is the beating frequency. The beating phenomenon put in evidence on this example results from a periodic energy exchange between both degrees of freedom, since the displacement amplitude of one is maximum while the other one is close to zero. Note that beating can also occur for a single degree of freedom under harmonic loading (see Exercise 2.6).

Example 2.6

As an application of the mode superposition and matrix spectral expansion concept, let us compute the total energy of a conservative system undergoing linear vibrations generated by non-homogeneous initial conditions. The general form of the system response has been obtained in Section 2.5. Restricting the problem to a system with stable equilibrium position, the normal coordinates and their time derivatives are given by:

$$\begin{aligned}\eta_r &= \frac{\mathbf{x}_{(r)}^T \mathbf{M} \mathbf{q}_0}{\mu_r} \cos \omega_r t + \frac{\mathbf{x}_{(r)}^T \mathbf{M} \dot{\mathbf{q}}_0}{\mu_r \omega_r} \sin \omega_r t \\ \dot{\eta}_r &= -\frac{\mathbf{x}_{(r)}^T \mathbf{M} \mathbf{q}_0}{\mu_r} \omega_r \sin \omega_r t + \frac{\mathbf{x}_{(r)}^T \mathbf{M} \dot{\mathbf{q}}_0}{\mu_r} \cos \omega_r t\end{aligned}$$

The energy expressions (2.72) and (2.73) may thus be put in the form:

$$\begin{aligned}\mathcal{V} &= \frac{1}{2} \sum_{s=1}^n \gamma_s \eta_s^2 = \frac{1}{2} \sum_{s=1}^n \gamma_s \left\{ \frac{\mathbf{x}_{(s)}^T \mathbf{M} \mathbf{q}_0}{\mu_s} \cos \omega_s t + \frac{\mathbf{x}_{(s)}^T \mathbf{M} \dot{\mathbf{q}}_0}{\mu_s \omega_s} \sin \omega_s t \right\}^2 \\ \mathcal{T} &= \frac{1}{2} \sum_{s=1}^n \mu_s \dot{\eta}_s^2 = \frac{1}{2} \sum_{s=1}^n \mu_s \omega_s^2 \left\{ -\frac{\mathbf{x}_{(s)}^T \mathbf{M} \mathbf{q}_0}{\mu_s} \sin \omega_s t + \frac{\mathbf{x}_{(s)}^T \mathbf{M} \dot{\mathbf{q}}_0}{\mu_s \omega_s} \cos \omega_s t \right\}^2\end{aligned}$$

The total energy takes the form:

$$\mathcal{T} + \mathcal{V} = \frac{1}{2} \sum_{s=1}^n \left\{ \frac{\omega_s^2}{\mu_s} (\mathbf{x}_{(s)}^T \mathbf{M} \mathbf{q}_0)^2 + \frac{1}{\mu_s} (\mathbf{x}_{(s)}^T \mathbf{M} \dot{\mathbf{q}}_0)^2 \right\}$$

or, by rearranging the terms,

$$\mathcal{T} + \mathcal{V} = \frac{1}{2} \mathbf{q}_0^T \left\{ \sum_{s=1}^n \frac{\omega_s^2}{\mu_s} \mathbf{M} \mathbf{x}_{(s)} \mathbf{x}_{(s)}^T \mathbf{M} \right\} \mathbf{q}_0 + \frac{1}{2} \dot{\mathbf{q}}_0^T \left\{ \sum_{s=1}^n \frac{1}{\mu_s} \mathbf{M} \mathbf{x}_{(s)} \mathbf{x}_{(s)}^T \mathbf{M} \right\} \dot{\mathbf{q}}_0$$

Recognizing that the expressions under brackets are the modal expansions of \mathbf{K} and \mathbf{M} given by (2.59) and (2.60) yields the final result:

$$\mathcal{T} + \mathcal{V} = \frac{1}{2} \mathbf{q}_0^T \mathbf{K} \mathbf{q}_0 + \frac{1}{2} \dot{\mathbf{q}}_0^T \mathbf{M} \dot{\mathbf{q}}_0$$

which shows that the total energy of the system remains constant and is equal to the initial energy communicated to the system. A similar reasoning could also be made in the case of a system with a neutrally stable equilibrium position discussed in the next section.

2.5.2 Systems with neutrally stable equilibrium position

When the system possesses m rigid-body modes, the solution found in (2.71) for the response to initial conditions is not applicable, some of the frequencies being zero. However a similar reasoning based on modal superposition can be followed provided that the contributions of rigid-body and elastic modes are handled separately. So we express the solution as:

$$\mathbf{q} = \sum_{i=1}^m \mathbf{u}_{(i)} \xi_i(t) + \sum_{s=1}^{n-m} \mathbf{x}_{(s)} \eta_s(t) = \mathbf{U} \boldsymbol{\xi}(t) + \mathbf{X} \boldsymbol{\eta}(t) \quad (2.74)$$

where

\mathbf{X} and $\boldsymbol{\eta}$ keep the meanings of elastic mode matrix and vector of normal coordinates
 \mathbf{U} is the rigid-body mode matrix:

$$\mathbf{U} = [\mathbf{u}_{(1)} \quad \dots \quad \mathbf{u}_{(m)}]$$

$\boldsymbol{\xi}$ is the vector of normal coordinates associated with rigid-body modes:

$$\boldsymbol{\xi}^T = [\xi_1(t) \quad \dots \quad \xi_m(t)]$$

The linear vibration equations become:

$$\mathbf{M} \mathbf{U} \ddot{\boldsymbol{\xi}} + \mathbf{M} \mathbf{X} \ddot{\boldsymbol{\eta}} + \mathbf{K} \mathbf{X} \boldsymbol{\eta} = \mathbf{0}$$

Premultiplying by \mathbf{U}^T and \mathbf{X}^T successively and taking account of the orthogonality relationships, they can be split into two systems of uncoupled equations:

$$\ddot{\boldsymbol{\xi}} = \mathbf{0} \quad \ddot{\boldsymbol{\eta}} + \boldsymbol{\Omega}^2 \boldsymbol{\eta} = \mathbf{0}$$

The normal equations for the elastic modes remain unchanged, while a given rigid-body normal equation:

$$\ddot{\xi}_i = 0$$

has the solution:

$$\xi_i(t) = \gamma_i + \delta_i t$$

The general solution may thus be expressed by the eigenmode expansion:

$$\mathbf{q}(t) = \sum_{i=1}^m (\gamma_i + \delta_i t) \mathbf{u}_{(i)} + \sum_{s=1}^{n-m} (\alpha_s \cos \omega_s t + \beta_s \sin \omega_s t) \mathbf{x}_{(s)}$$

the $2n$ coefficients being determined by the initial conditions:

$$\mathbf{q}_0 = \sum_{i=1}^m \gamma_i \mathbf{u}_{(i)} + \sum_{s=1}^{n-m} \alpha_s \mathbf{x}_{(s)} \quad \dot{\mathbf{q}}_0 = \sum_{i=1}^m \delta_i \mathbf{u}_{(i)} + \sum_{s=1}^{n-m} \beta_s \omega_s \mathbf{x}_{(s)}$$

Those coefficients are thus modal coordinates of the initial conditions that can be obtained as before by projection on the modes (premultiplication by $\mathbf{u}_{(i)}^T \mathbf{M}$ and $\mathbf{x}_{(s)}^T \mathbf{M}$). The general solution finally takes the form:

$$\begin{aligned} \mathbf{q}(t) = & \left(\sum_{i=1}^m \frac{\mathbf{u}_{(i)} \mathbf{u}_{(i)}^T \mathbf{M}}{\mu_i} + \sum_{s=1}^{n-m} \frac{\mathbf{x}_{(s)} \mathbf{x}_{(s)}^T \mathbf{M}}{\mu_s} \cos \omega_s t \right) \mathbf{q}_0 \\ & + \left(\sum_{i=1}^m \frac{\mathbf{u}_{(i)} \mathbf{u}_{(i)}^T \mathbf{M}}{\mu_i} t + \sum_{s=1}^{n-m} \frac{\mathbf{x}_{(s)} \mathbf{x}_{(s)}^T \mathbf{M}}{\mu_s \omega_s} \sin \omega_s t \right) \dot{\mathbf{q}}_0 \end{aligned} \quad (2.75)$$

where the modes are usually scaled so that the modal masses are equal to one. The stable character of the response is destroyed by the presence of the rigid-body terms. The latter will eventually generate overall motion of such amplitude that it might become necessary to re-examine the validity of the linearity assumption for kinetic and potential energies.

In the presence of rigid-body modes, the energy quadratic forms become:

$$\mathcal{V} = \frac{1}{2} \mathbf{q}^T \mathbf{K} \mathbf{q} = \frac{1}{2} \sum_{s=1}^{n-m} \omega_s^2 \mu_s \eta_s^2 \quad (2.76)$$

$$\mathcal{T} = \frac{1}{2} \dot{\mathbf{q}}^T \mathbf{M} \dot{\mathbf{q}} = \frac{1}{2} \left(\sum_{i=1}^m \mu_i \dot{\xi}_i^2 + \sum_{s=1}^{n-m} \mu_s \dot{\eta}_s^2 \right) \quad (2.77)$$

The relationship (2.77) shows that the small vibration assumption guarantees complete uncoupling between overall rigid motion and elastic deformation in the evaluation of kinetic energy.

2.6 Response to applied forces: forced harmonic response

Motion in a mechanical system originates either from initial conditions (as discussed in Section 2.5), from imposed motion on some degrees of freedom or from applied loads. Those excitations can be combined, in which case, for a linear(ized) system, the total response is the sum of the responses to each individual excitation. Imposed degrees of freedom, namely when exciting a system through its support, will be discussed later in Section 2.9.

In the following two sections we will discuss how the response to applied loads, i.e. external forces, can be computed making use of the modal basis and its associated orthogonality properties. The case of general time varying excitation will be treated in the next section since here, we first investigate the case where a system is assumed to be excited through external harmonic loads, namely loads that have a harmonic time variation. We will assume that the harmonic force has been applied for long enough so that all transients have vanished and the only remaining response is a forced motion that has, for linear system, the same harmonic signature as the excitation.

The case of the forced harmonic response of an n -degree-of-freedom oscillator is important mainly for two reasons:

- On one hand, the system response in the frequency domain is often used for experimental identification of a dynamic system (see Section 3.4). As a matter of fact any excitation can be seen as a superposition of harmonic excitations when considering its Fourier series expansion.
- On the other hand, the harmonic regime is representative of many excitation cases encountered in engineering practice, such as vibration induced by unbalance, and torsional vibration in engines.

2.6.1 Harmonic response, impedance and admittance matrices

Forced vibration of an n -degree-of-freedom oscillator is defined as the motion resulting from the application of a harmonic force with constant amplitude:

$$\mathbf{M}\ddot{\mathbf{q}} + \mathbf{K}\mathbf{q} = \mathbf{s} \cos \omega t \quad (2.78)$$

where ω is the excitation frequency and \mathbf{s} describes the spatial distribution of the excitation amplitude. The forced response is then the part of the response synchronous to the excitation:

$$\mathbf{q} = \mathbf{x} \cos \omega t \quad (2.79)$$

Substituting the solution form (2.79) into the equations of motion yields the algebraic system governing the amplitude of the response:

$$(\mathbf{K} - \omega^2 \mathbf{M})\mathbf{x} = \mathbf{s} \quad (2.80)$$

and, by assuming that $(\mathbf{K} - \omega^2 \mathbf{M})$ is nonsingular, namely that the excitation frequency is not an eigenfrequency,

$$\mathbf{x} = (\mathbf{K} - \omega^2 \mathbf{M})^{-1} \mathbf{s} \quad (2.81)$$

The matrix:

$$\mathbf{Z}(\omega^2) = (\mathbf{K} - \omega^2 \mathbf{M}) \quad (2.82)$$

is generally known as the mechanical *impedance matrix* of the system and sometimes also called the *dynamic stiffness matrix*. Its inverse:

$$\mathbf{H}(\omega^2) = (\mathbf{K} - \omega^2 \mathbf{M})^{-1} \quad (2.83)$$

is called the *admittance matrix*, *dynamic flexibility* or *dynamic influence coefficient matrix* of the system. Its general element $h_{kl}(\omega^2)$ represents the forced vibration amplitude of the degree of freedom q_k for a harmonic loading of unit amplitude applied on degree of freedom q_l at frequency ω .

From its very definition, the dynamic influence coefficient matrix extends to harmonic motion the concept of the static influence coefficient as classically used for the description of a structural system under steady load.

2.6.2 Mode superposition and spectral expansion of the admittance matrix

Let us solve the algebraic relationship (2.80) by an eigenmode series expansion including the possible presence of m rigid-body modes:

$$\mathbf{x} = \sum_{i=1}^m \alpha_i \mathbf{u}_{(i)} + \sum_{s=1}^{n-m} \beta_s \mathbf{x}_{(s)}$$

Substituting in Equation (2.80) the development above and taking account of eigenmode orthogonality provides the n spectral coordinates of the amplitude vector \mathbf{x} :

$$\alpha_i = -\frac{\mathbf{u}_{(i)}^T \mathbf{s}}{\omega^2 \mu_i} \quad \beta_s = \frac{\mathbf{x}_{(s)}^T \mathbf{s}}{(\omega_s^2 - \omega^2) \mu_s}$$

A factorization to the right gives the forced response amplitude expression:

$$\mathbf{x} = \left\{ -\frac{1}{\omega^2} \sum_{i=1}^m \frac{\mathbf{u}_{(i)} \mathbf{u}_{(i)}^T}{\mu_i} + \sum_{s=1}^{n-m} \frac{\mathbf{x}_{(s)} \mathbf{x}_{(s)}^T}{(\omega_s^2 - \omega^2) \mu_s} \right\} \mathbf{s} \quad (2.84)$$

showing that the dynamic influence coefficient matrix can be spectrally expanded as:⁵

$$(\mathbf{K} - \omega^2 \mathbf{M})^{-1} = -\frac{1}{\omega^2} \sum_{i=1}^m \frac{\mathbf{u}_{(i)} \mathbf{u}_{(i)}^T}{\mu_i} + \sum_{s=1}^{n-m} \frac{\mathbf{x}_{(s)} \mathbf{x}_{(s)}^T}{(\omega_s^2 - \omega^2) \mu_s} \quad (2.85)$$

In order to establish the properties of the dynamic influence coefficients, let us extract from (2.85) a given coefficient $h_{kl}(\omega^2)$ by keeping in each outer product the term corresponding to components k and l :

$$h_{kl}(\omega^2) = -\frac{1}{\omega^2} \sum_{i=1}^m \frac{u_{k(i)} u_{l(i)}}{\mu_i} + \sum_{s=1}^{n-m} \frac{x_{k(s)} x_{l(s)}}{(\omega_s^2 - \omega^2) \mu_s} \quad (2.86)$$

Let us then consider both of the following cases.

System without rigid-body modes

When the excitation frequency tends to zero ($\omega^2 \rightarrow 0$), the matrix $(\mathbf{K} - \omega^2 \mathbf{M})^{-1}$ converges to the static influence coefficient matrix \mathbf{K}^{-1} of spectral expansion given by (2.62):

$$g_{kl} = \sum_{s=1}^n \frac{x_{k(s)} x_{l(s)}}{\omega_s^2 \mu_s} \quad (2.87)$$

It is thus observed that the dynamic coefficient $h_{kl}(\omega^2)$ may be deduced from the static one g_{kl} by applying to each term of the spectral expansion of g_{kl} the *dynamic amplification factor*:

$$\left(1 - \frac{\omega^2}{\omega_s^2} \right)^{-1}$$

A principal coefficient $h_{kk}(\omega^2)$ (also called driving-point admittance) possesses the fundamental property:

$$\frac{dh_{kk}}{d\omega^2} = \sum_{s=1}^n \frac{x_{k(s)}^2}{(\omega_s^2 - \omega^2)^2 \mu_s} > 0 \quad (2.88)$$

i.e. the principal coefficients of the dynamic influence matrix are always increasing with excitation frequency. This implies that two resonance eigenfrequencies ω_r and ω_{r+1} are separated by an *antiresonance frequency* noted ω_r^k (Figure 2.6):

$$\omega_r < \omega_r^k < \omega_{r+1}$$

⁵ In (2.85) one observes that the admittance matrix has only single poles in the sense that the poles ω_s^2 appear as a first order form in the denominator. This is typical of mechanical systems. It would not be the case for defective dynamic systems where the modes do not form a complete basis.

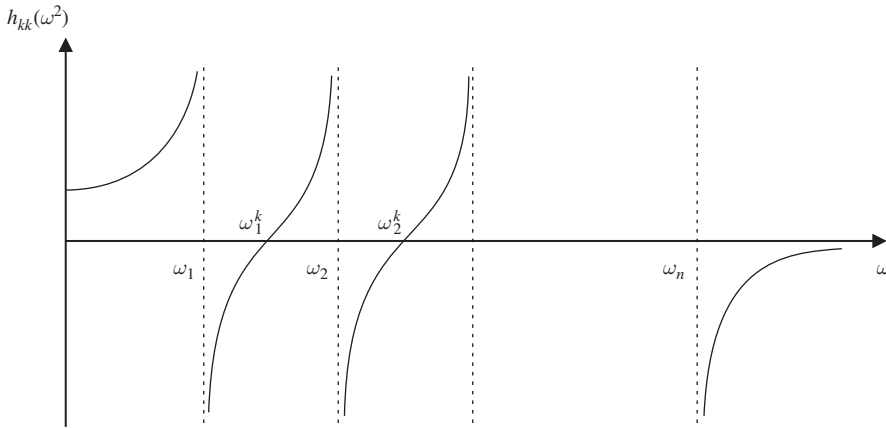


Figure 2.6 Principal dynamic influence coefficient for a system with no rigid-body mode.

By contrast with the resonance eigenfrequencies, the antiresonance frequencies are specific to the degree of freedom k associated with h_{kk} . From a physical point of view, they may be regarded as the resonance eigenfrequencies of the modified system obtained by fixing degree of freedom q_k .

Example 2.7

To illustrate the concept of antiresonance, let us consider a simple system of two masses and springs attached on one side (Figure 2.7). If one considers the force response of the middle mass when it is excited harmonically, according to Figure 2.6 the mass will move in phase with the force ($h_{11} > 0$) as long as $\omega < \omega_1$. Above the first resonance ω_1 , the forced response is out-of-phase ($h_{11} < 0$) until ω becomes equal to the antiresonance frequency $\omega_1^{k=1}$. At that frequency mass 1 is excited by the harmonic load but has zero displacement. This seems peculiar but can be understood as follows: for that frequency the second mass is vibrating with an amplitude such that the deformation of the spring between the two masses generates a force exactly compensating the applied load. So the applied load can also be interpreted as a reaction force to fix the first mass (see Figure 2.7).

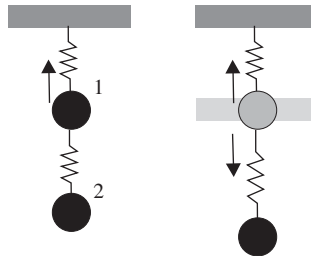


Figure 2.7 Interpretation of the antiresonance $\omega_1^{k=1}$ for a simple 2 dof system.

It seems now paradoxical that mass 2 is vibrating as a fixed spring-mass system while no external load acts on it. Clearly such a free vibration can exist only at the eigenfrequency of the fixed system. Therefore one can say that the antiresonance frequency $\omega_1^{k=1}$ is equal to the frequency of the system when dof $k = 1$ is fixed, the applied harmonic force being equal to the reaction force associated to the fixed boundary condition. A similar reasoning can be used to interpret $\omega_1^{k=2}$.

The antiresonance phenomenon is exploited in so-called *dynamic dampers* where the vibration at one degree of freedom is cancelled out by connecting to it a spring-mass system tuned so that one of the antiresonance frequencies ω_r^k of degree of freedom number k coincides with the excitation frequency.

Writing the diagonal element $h_{kk}(\omega^2)$ from (2.86) under a common denominator would result in a ratio of two polynomials in ω^2 of order n for the denominator and of order $n - 1$ for the numerator,

$$h_{kk}(\omega^2) = g_{kk} \frac{\prod_{s=1}^{n-1} \left(1 - \left(\frac{\omega}{\omega_s^k} \right)^2 \right)}{\prod_{s=1}^n \left(1 - \left(\frac{\omega}{\omega_s} \right)^2 \right)} \quad (2.89)$$

The poles (roots of the denominator) are the eigenfrequencies of the system, whereas its zeros (roots of the numerator) are antiresonance frequencies associated with degree of freedom k .

System with m rigid-body modes

In this case, at least one eigensolution corresponds to $\omega^2 = 0$ and the static influence coefficients g_{kl} become infinite. The properties of a principal influence coefficient $h_{kk}(\omega^2)$ may, however, be determined as follows.

Let us deduce from (2.86) the expression of the principal coefficients:

$$h_{kk}(\omega^2) = -\frac{1}{\omega^2} \sum_{i=1}^m \frac{u_{k(i)}^2}{\mu_i} + \sum_{s=1}^{n-m} \frac{x_{k(s)}^2}{(\omega_s^2 - \omega^2)\mu_s} \quad (2.90)$$

Differentiation with respect to ω^2 yields:

$$\frac{dh_{kk}}{d\omega^2} = \frac{1}{(\omega^2)^2} \sum_{i=1}^m \frac{u_{k(i)}^2}{\mu_i} + \sum_{s=1}^{n-m} \frac{x_{k(s)}^2}{(\omega_s^2 - \omega^2)^2 \mu_s} > 0 \quad (2.91)$$

the only difference with the previous case (Equation (2.88)) being that when $\omega^2 \rightarrow 0$ the slope of the principal influence coefficient tends to infinity (Figure 2.8).

The number of antiresonance frequencies is then equal to the number of resonance frequencies (excluding $\omega_r = 0$) where:

$$\omega_{r-1} < \omega_r^k < \omega_r \quad r = 1, \dots, n - m$$

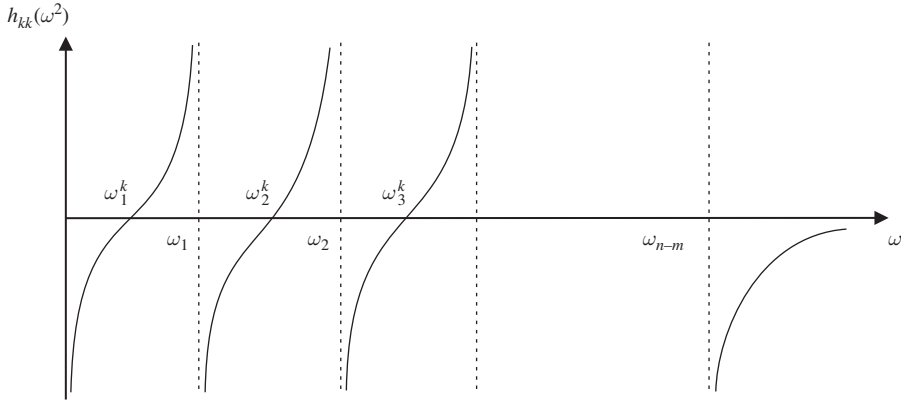


Figure 2.8 Principal dynamic influence coefficient for a system with rigid-body modes.

Taking the limit of expression (2.90) when $\omega^2 \rightarrow 0$ yields the result:

$$\lim_{\omega^2 \rightarrow 0} \omega^2 h_{kk}(\omega^2) = - \sum_{i=1}^m \frac{u_{k(i)}^2}{\mu_i} = - \frac{1}{I_{kk}} < 0$$

where I_{kk} has the meaning of an inertia coefficient. This coefficient provides a measure of the apparent inertia of the system along degree of freedom q_k under sufficiently low excitation frequency to obtain purely inertial behaviour. One can thus write a driving-point admittance coefficients $h_{kk}(\omega^2)$ as a rational function similar to (2.89),

$$h_{kk}(\omega^2) = - \frac{1}{\omega^2 I_{kk}} \frac{\prod_{s=1}^{n-m} \left(1 - \left(\frac{\omega}{\omega_s^k} \right)^2 \right)}{\prod_{s=1}^{n-m} \left(1 - \left(\frac{\omega}{\omega_s} \right)^2 \right)} \quad (2.92)$$

Due to its specific physical meaning, the equivalent inertia I_{kk} may be measured experimentally from a low frequency test.

2.6.3 Statically exact expansion of the admittance matrix

The matrix of influence coefficients $\mathbf{H}(\omega^2)$ defined by (2.83) is often referred to as mobility matrix or *mechanical admittance* matrix. An alternate form can be given to it which, as will be seen later, is more appropriate from a computational point of view.

Let us start from the matrix form of Equation (2.86):

$$\mathbf{H}(\omega^2) = - \frac{1}{\omega^2} \sum_{i=1}^m \frac{\mathbf{u}_{(i)} \mathbf{u}_{(i)}^T}{\mu_i} + \sum_{s=1}^{n-m} \frac{\mathbf{x}_{(s)} \mathbf{x}_{(s)}^T}{(\omega_s^2 - \omega^2) \mu_s} \quad (2.93)$$

Making use of the identity:

$$\frac{1}{\omega_s^2 - \omega^2} = \frac{1}{\omega_s^2} + \frac{\omega^2}{(\omega_s^2 - \omega^2)\omega_s^2} \quad (2.94)$$

we will rewrite the second term of (2.93) to isolate the static contribution:

$$\mathbf{H}(\omega^2) = \sum_{s=1}^{n-m} \frac{\mathbf{x}_{(s)}\mathbf{x}_{(s)}^T}{\omega_s^2\mu_s} - \frac{1}{\omega^2} \sum_{i=1}^m \frac{\mathbf{u}_{(i)}\mathbf{u}_{(i)}^T}{\mu_i} + \omega^2 \sum_{s=1}^{n-m} \frac{\mathbf{x}_{(s)}\mathbf{x}_{(s)}^T}{(\omega_s^2 - \omega^2)\omega_s^2\mu_s} \quad (2.95)$$

or, in more synthetic form:

$$\mathbf{H}(\omega^2) = \mathbf{F} - \frac{1}{\omega^2} \mathbf{B}_{rig} + \omega^2 \sum_{s=1}^{n-m} \frac{\mathbf{x}_{(s)}\mathbf{x}_{(s)}^T}{(\omega_s^2 - \omega^2)\omega_s^2\mu_s} \quad (2.96)$$

Equation (2.96) can be interpreted as follows:

- The first term represents the static contribution.

$$\mathbf{F} = \sum_{s=1}^{n-m} \frac{\mathbf{x}_{(s)}\mathbf{x}_{(s)}^T}{\omega_s^2\mu_s} \quad (2.97)$$

It can be regarded as a *generalized flexibility matrix* since it coincides with \mathbf{K}^{-1} (Equation (2.62)) in the absence of rigid body modes. Mathematically speaking it is a *pseudo-inverse* to the stiffness matrix, a concept that will be discussed in length in Chapter 6, Section 6.6.2.

- The second one represents the inertia contribution of the rigid body modes. It is described in terms of the *rigid mobility matrix*:

$$\mathbf{B}_{rig} = \sum_{i=1}^m \frac{\mathbf{u}_{(i)}\mathbf{u}_{(i)}^T}{\mu_i} \quad (2.98)$$

- The third one corresponds to the dynamic contribution from the vibration modes.

The form (2.96) of the admittance matrix is useful when not all modes are known. Indeed, the form (2.93) yields a poor approximation of the harmonic response when only a few modes are used in the expansion, whereas (2.96) (assuming that the flexibility matrix \mathbf{F} is obtained as the (pseudo-)inverse of \mathbf{K} and not through modal synthesis) guarantees at least that the static response is correct. This reasoning will also form the basis for the mode acceleration method explained in Section 2.8.2.

2.6.4 Pseudo-resonance and resonance

It is possible to obtain a response of harmonic type – and thus of finite amplitude – even when the excitation frequency becomes equal to an eigenfrequency ω_i of the system under the condition that the external loading obeys the *pseudo-resonance condition*:

$$\mathbf{x}_{(i)}^T \mathbf{s} = 0 \quad (2.99)$$

expressing that the loading produces no work on eigenmode $\mathbf{x}_{(l)}$. This result is obtained from (2.84) or by noticing that the singular linear system $(\mathbf{K} - \omega_l^2 \mathbf{M})\mathbf{x} = \mathbf{s}$ admits a solution if and only if \mathbf{s} is orthogonal to the solutions of the associated homogeneous linear system (see Section 6.6.4 for the detailed discussion of solutions for singular systems).

Example 2.8

In order to be convinced that a linear system may vibrate harmonically at an eigenfrequency ω_l , let us develop both the excitation amplitude \mathbf{s} and the response \mathbf{x} in terms of eigenmodes:

$$(\mathbf{K} - \omega_l^2 \mathbf{M}) \left\{ \sum_{s=1}^n c_s \mathbf{x}_{(s)} \right\} = \sum_{s=1}^n d_s \mathbf{M} \mathbf{x}_{(s)}$$

and, since $\mathbf{x}_{(l)}$ is the solution of the homogeneous problem,

$$(\mathbf{K} - \omega_l^2 \mathbf{M}) \left\{ \sum_{\substack{s=1 \\ s \neq l}}^n c_s \mathbf{x}_{(s)} \right\} = \sum_{s=1}^n d_s \mathbf{M} \mathbf{x}_{(s)}$$

The equation above has a nontrivial solution if and only if $d_l = 0$, which means that \mathbf{s} is orthogonal to $\mathbf{x}_{(l)}$. In that case c_l (the contribution of mode s in the harmonic response) is undetermined.

When condition (2.99) is not verified, it is possible to show that the contribution of eigenmode $\mathbf{x}_{(l)}$ to the motion is a harmonic term of timewise linearly increasing amplitude, and resonance then occurs in the ordinary sense (see also Exercise 2.6).

2.6.5 Normal excitation modes

In the previous sections, the problem was formulated as determining the response of a system to an arbitrary harmonic excitation. Let us now consider the problem in a reverse manner by addressing the question of determining which harmonic excitation has to be applied to the system in order to generate a vibration $\mathbf{q} = \mathbf{x} \cos \omega t$ with prescribed amplitude and frequency.

In particular, let us determine which excitation $\mathbf{s}_{(r)}$ will generate a harmonic response with an amplitude corresponding to eigenmode $\mathbf{x}_{(r)}$:

$$\mathbf{s}_{(r)} = (\mathbf{K} - \omega^2 \mathbf{M})\mathbf{x}_{(r)}$$

Since $\mathbf{x}_{(r)}$ is an eigenmode, $\mathbf{K}\mathbf{x}_{(r)} = \omega_r^2 \mathbf{M}\mathbf{x}_{(r)}$ and the following expression of the normal excitation mode is obtained:

$$\mathbf{s}_{(r)} = (\omega_r^2 - \omega^2) \mathbf{M}\mathbf{x}_{(r)} \quad (2.100)$$

It shows that the forces required to sustain a vibration of amplitude $\mathbf{x}_{(r)}$ must be distributed proportionally to the modal inertia forces, irrespective of the excitation frequency.

The amplitude of the normal excitation mode is a frequency dependent quantity and it vanishes at resonance, thus expressing the fact that *no external force is needed in the absence of damping to maintain the eigenmode at its eigenfrequency*.

For a rigid-body mode, Equation (2.100) takes the form:

$$\mathbf{t}_{(i)} = -\omega^2 \mathbf{M} \mathbf{u}_{(i)} \quad (2.101)$$

showing that the excitation mode is nothing else than the modal inertia force distribution.

The orthogonality relationships of the system may then be expressed in terms of normal eigenmodes and normal excitation modes:

$$\begin{aligned} \mathbf{s}_{(r)}^T \mathbf{x}_{(s)} &= 0 & r &\neq s \\ \mathbf{t}_{(i)}^T \mathbf{u}_{(j)} &= 0 & i &\neq j \\ \mathbf{s}_{(r)}^T \mathbf{u}_{(j)} &= 0 \\ \mathbf{t}_{(i)}^T \mathbf{x}_{(r)} &= 0 \end{aligned} \quad (2.102)$$

expressing the property that *a normal excitation mode produces no work under a displacement corresponding to another eigenmode*.

The specific properties of normal excitation modes may be exploited experimentally to identify the vibration behaviour of structures through the so-called *force appropriation methods* (Section 3.2.3).

2.7 Response to applied forces: response in the time domain

When an n -degree-of-freedom system is submitted to external forces $\mathbf{p}(t)$ known as a function of time, its transient response is governed by:

$$\begin{aligned} \mathbf{M} \ddot{\mathbf{q}} + \mathbf{K} \mathbf{q} &= \mathbf{p}(t) \\ \text{given } \mathbf{q}(0) &= \mathbf{q}_0, \quad \dot{\mathbf{q}}(0) = \dot{\mathbf{q}}_0 \end{aligned}$$

(2.103)

2.7.1 Mode superposition and normal equations

Let us restrict ourselves to the most frequent case of a system without rigid-body modes. Since the normal vibration modes provide a complete set for the expansion of an arbitrary vector, the system response may be expressed through modal expansion:

$$\mathbf{q}(t) = \sum_{s=1}^n \eta_s(t) \mathbf{x}_{(s)} \quad (2.104)$$

Owing to orthogonality between eigenmodes, the substitution of (2.104) into (2.103) and the premultiplication by each eigenmode $\mathbf{x}_{(r)}$ successively yields:

$$\mathbf{x}_{(r)}^T \mathbf{M} \mathbf{x}_{(r)} \ddot{\eta}_r(t) + \mathbf{x}_{(r)}^T \mathbf{K} \mathbf{x}_{(r)} \eta_r(t) = \mathbf{x}_{(r)}^T \mathbf{p}(t)$$

Hence the n normal equations are:

$$\ddot{\eta}_r(t) + \omega_r^2 \eta_r(t) = \phi_r(t) \quad r = 1, \dots, n \quad (2.105)$$

with the *modal participation factor* of mode r to the loading:

$$\phi_r(t) = \frac{\mathbf{x}_{(r)}^T \mathbf{p}(t)}{\mu_r} \quad (2.106)$$

which represents the amplitude associated with mode r in the expansion of \mathbf{p} with respect to the inertia forces (2.56).

The normal Equations (2.105) show that, in the absence of damping, calculating the response of an n -degree-of-freedom system reduces to the solution of n uncoupled single-degree-of-freedom systems excited by the external forces (2.106).

The initial conditions on η_r at $t = 0$ for the normal Equations (2.105) are found by projecting the initial conditions on \mathbf{q} on the modal basis:

$$\mathbf{q}_0 = \sum_{s=1}^n \eta_s(0) \mathbf{x}_{(s)} \quad \text{and} \quad \dot{\mathbf{q}}_0 = \sum_{s=1}^n \dot{\eta}_s(0) \mathbf{x}_{(s)}$$

After premultiplication by $\mathbf{x}_{(r)}^T \mathbf{M}$ we get:

$$\eta_s(0) = \frac{\mathbf{x}_{(r)}^T \mathbf{M} \mathbf{q}_0}{\mu_r} \quad \text{and} \quad \dot{\eta}_s(0) = \frac{\mathbf{x}_{(r)}^T \mathbf{M} \dot{\mathbf{q}}_0}{\mu_r} \quad (2.107)$$

2.7.2 Impulse response and time integration of the normal equations

General formulation

Each of the normal equations may be integrated in the form of a convolution product by making use of the step response and impulse response concepts.

Each of the normal Equations (2.105) may be integrated in the form of a convolution product. To that purpose, let us define the Laplace transforms $\bar{\eta}_r(s)$ and $\bar{\phi}_r(s)$:

$$\bar{\phi}_r(s) = \mathcal{L}[\phi_r(t)] = \int_0^{+\infty} e^{-st} \phi_r(t) dt \quad (2.108)$$

$$\bar{\eta}_r(s) = \mathcal{L}[\eta_r(t)] = \int_0^{+\infty} e^{-st} \eta_r(t) dt \quad (2.109)$$

The Laplace transform of a normal Equation (2.105) is then:

$$s^2 \bar{\eta}_r(s) - s \eta_r(0) - \dot{\eta}_r(0) + \omega_r^2 \bar{\eta}_r(s) = \bar{\phi}_r(s)$$

Hence,

$$\bar{\eta}_r(s) = \frac{s \eta_r(0) + \dot{\eta}_r(0) + \bar{\phi}_r(s)}{s^2 + \omega_r^2} \quad (2.110)$$

Assuming $\omega_r \neq 0$ (no rigid body mode), the inverse Laplace transform of (2.110) is found by defining the Laplace transform of the response $h_r(t)$ to initial velocity:

$$h_r(t) = \mathcal{L}^{-1} \left[\frac{1}{s^2 + \omega_r^2} \right] = \frac{\sin \omega_r t}{\omega_r} \quad (2.111)$$

Observing that

$$\mathcal{L} \left[\frac{dh_r}{dt} \right] = \frac{s}{s^2 + \omega_r^2} - h(0) = \frac{s}{s^2 + \omega_r^2}$$

we get

$$\frac{dh_r}{dt} = \mathcal{L}^{-1} \left[\frac{s}{s^2 + \omega_r^2} \right] = \cos \omega_r t \quad (2.112)$$

The solution $\eta_r(t)$ is then found from (2.110) as:

$$\eta_r(t) = \eta_r(0) \frac{dh_r}{dt} + \dot{\eta}_r(0) h_r(t) + \int_0^t \phi_r(\tau) h_r(t - \tau) d\tau \quad (2.113)$$

The first two terms of this solution represent the response to the initial conditions. The last term is a convolution product known as *Duhamel's integral* and represents the forced response to the external loads $p(t)$.

Physical meaning

Physically, Equation (2.113) can be interpreted with the concept of the impulse response: when an impulse $\phi_r(\tau) \Delta \tau$ is applied at time τ to a one-degree-of-freedom system described by the normal Equations (2.105), the response is a jump in the velocity such that:

$$\Delta \dot{\eta}(\tau) = \phi(\tau) \Delta \tau \quad (2.114)$$

Observing then from the second term in (2.113) that $h_r(t)$ is the time response to initial velocity $\dot{\eta}_r(0) = 1$, it is understood that $h_r(t - \tau)$ is the dynamic response of the system at time t to a unit change of velocity at time τ . Since a step in velocity is equivalent to a load impulse, as indicted by (2.114), $h_r(t)$ is also known as the *impulse response function*. Therefore, if we now assume that any force can be decomposed in a series of impulses such as described in Figure 2.9.a, the convolution product in (2.113) is understood as the sum of the responses to impulses at times $\tau \in [0, t]$. It keeps track of the system history from $t = 0$ and shows thus that the system response verifies the *causality principle*.⁶

Recurrence formulation

The convolution product describing the forced response in Equation (2.113) can be integrated in closed form if a piecewise linear variation of the excitation is assumed. Equation (2.113) may then be exploited in order to perform the time integration in a recurrent manner.

For an undamped oscillator over a time interval $[t_n, t_{n+1}]$ we consider $\eta_{r,n}$ and $\dot{\eta}_{r,n}$ as initial conditions at time t_n . The displacement and velocity $\eta_{r,n+1}$ and $\dot{\eta}_{r,n+1}$ at time $t_{n+1} = t_n + \Delta t$ are

⁶ In Classical Mechanics, the principle of causality states that a cause must always precede its effect.

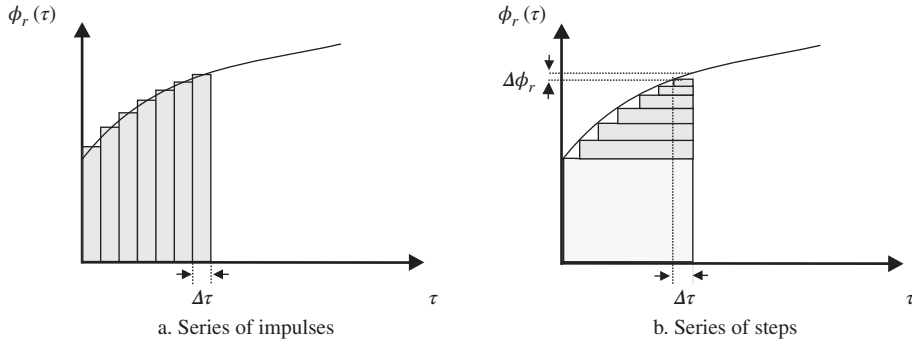


Figure 2.9 Interpreting a force as a series of impulses or steps.

then computed from (2.113) as:

$$\eta_{r,n+1} = \eta_{r,n} \cos \omega_r \Delta t + \dot{\eta}_{r,n} \frac{\sin \omega_r \Delta t}{\omega_r} + \frac{1}{\omega_r} \int_{t_n}^{t_{n+1}} \phi_r(\tau) \sin(\omega_r(t_{n+1} - \tau)) d\tau$$

Similarly, the velocity is obtained by computing the time derivative of (2.113):⁷

$$\dot{\eta}_{r,n+1} = -\omega_r \eta_{r,n} \sin \omega_r \Delta t + \dot{\eta}_{r,n} \cos \omega_r \Delta t + \int_{t_n}^{t_{n+1}} \phi_r(\tau) \cos(\omega_r(t_{n+1} - \tau)) d\tau$$

Next, let us introduce the linearity assumption for the excitation on the time interval:

$$\phi_r(t) = \phi_{r,n} \frac{t_{n+1} - t}{\Delta t} + \phi_{r,n+1} \frac{t - t_n}{\Delta t} \quad t_n < t < t_{n+1}$$

and define the frequency parameter $\alpha = \omega_r \Delta t$. The recurrence relationships are then obtained in the form:

$$\begin{aligned} \begin{bmatrix} \eta_{r,n+1} \\ \Delta t \dot{\eta}_{r,n+1} \end{bmatrix} &= \begin{bmatrix} \cos \alpha & \frac{\sin \alpha}{\alpha} \\ -\alpha \sin \alpha & \cos \alpha \end{bmatrix} \begin{bmatrix} \eta_{r,n} \\ \Delta t \dot{\eta}_{r,n} \end{bmatrix} \\ &+ \frac{(\Delta t)^2}{\alpha^2} \begin{bmatrix} \frac{\sin \alpha}{\alpha} - \cos \alpha & 1 - \frac{\sin \alpha}{\alpha} \\ \alpha \sin \alpha + \cos \alpha - 1 & 1 - \cos \alpha \end{bmatrix} \begin{bmatrix} \phi_{r,n} \\ \phi_{r,n+1} \end{bmatrix} \end{aligned} \quad (2.115)$$

which is exact if the excitation is linear within a time step.

2.7.3 Step response and time integration of the normal equations

Instead of an interpretation in terms of impulse responses as in Section 2.7.2, the system response could be developed using the concept of step response as well, in which case the loading would be interpreted as an initial jump $\phi_r(0)$ followed by a sum of infinitesimal steps $\Delta\phi_r(\tau) = \frac{d\phi_r}{d\tau} \Delta\tau$ (see Figure 2.9.b).

⁷ Since the upper bounds of the convolution integral in (2.113) is a function of time, Leibniz's rule (see e.g. Wazwaz 2011) should be used, although in the present case the boundary terms vanish.

We call $g_r(t)$ the *step response function* for mode r and define it as the solution of:

$$\ddot{g}_r(t) + \omega_s^2 g_r(t) = H(t) \quad (2.116)$$

where $H(t)$ is the step function (also called *Heaviside* function), defined as being zero for $t < 0$ and unity for $t > 0$. Taking the time-derivative of this equation and noting that the derivative of the step function is the impulse Dirac function $\delta(t)$, one finds:

$$\ddot{\dot{g}}_r(t) + \omega_s^2 \dot{g}_r(t) = \delta(t) \quad (2.117)$$

showing that $\dot{g}_r(t)$ is the dynamic response to an impulse and thus:

$$\dot{g}_r(t) = h_r(t) \quad (2.118)$$

Substituting this result in the dynamic response expression (2.113):

$$\eta_r(t) = \eta_r(0)\ddot{g}_r(t) + \dot{\eta}_r(0)\dot{g}_r(t) + \int_0^t \phi_r(\tau)\dot{g}_r(t-\tau)d\tau$$

and integrating by part the convolution product term:

$$\eta_r(t) = \eta_r(0)\ddot{g}_r(t) + \dot{\eta}_r(0)\dot{g}_r(t) + \phi_r(0)g_r(t) + \int_0^t \frac{d\phi_r}{d\tau}g_r(t-\tau)d\tau \quad (2.119)$$

where we accounted for the fact that $g_r(0) = 0$.

We observe in (2.119) that the response to the load can now be interpreted as the step response to the initial load plus the sum of the responses to all subsequent load steps $\Delta\phi(\tau) = \frac{d\phi}{d\tau}\Delta\tau$. Note that in practice the impulsive response form (2.113) is applied more frequently since applying the step response approach (2.119) involves the time-derivative of the load, which is often not readily available.

2.7.4 Direct integration of the transient response

In Chapter 6.5 we will explain that computing eigensolutions of engineering models is computationally expensive. In practice, it is not possible to compute all of them. Modal approximations can be found when only a limited number of modes are known (see Section 2.8). However when a broad modal spectrum is needed to obtain sufficient accuracy mode superposition methods may be unattractive. This is particularly the case under shock loading where the frequency content of the excitation is such that a very large number of modes contribute to the response. The limitations of mode superposition have favoured the development of numerical methods based on the direct integration of the motion equations (2.103) by time-stepping algorithms. Chapter 7 is devoted entirely to their description.

2.8 Modal approximations of dynamic responses

In the previous sections we have seen that the behaviour of linear (or linearized) dynamic systems can be conveniently computed in the space of its eigenmodes. Since not all modes can be computed in practice (Chapter 6.5) the full modal superposition can very often not be applied. In this section we will discuss how an approximation of the dynamic response can be built when only a limited number of modes are known.

2.8.1 Response truncation and mode displacement method

When expressing the system response to external loading through mode superposition, it generally occurs that the number of degrees of freedom is so large that the modal expansion has to be restricted to a subset of k modes:

$$\mathbf{q}(t) = \sum_{s=1}^k \eta_s(t) \mathbf{x}_{(s)} \quad k < n \quad (2.120)$$

Let us suppose for simplicity's sake that the external load is of type:

$$\mathbf{p}(t) = \mathbf{g}\varphi(t)$$

where \mathbf{g} designates a static load distribution applied with the time-variation law $\varphi(t)$. For a system initially at rest, the transient response is calculated by the truncated series (2.120) with the normal coordinates obtained from (2.113) as:

$$\eta_s(t) = \frac{\mathbf{x}_{(s)}^T \mathbf{g}}{\omega_s \mu_s} \int_0^t \sin(\omega_s(t - \tau)) \varphi(\tau) d\tau \quad (2.121)$$

The global convergence of (2.120) determines the quality of the displacement solution. It can be measured using the \mathbf{M} -norm:

$$\begin{aligned} \|\mathbf{q}\|_M &= (\mathbf{q}^T \mathbf{M} \mathbf{q})^{\frac{1}{2}} = \left(\sum_{s=1}^k \mu_s \eta_s^2(t) \right)^{\frac{1}{2}} \\ &= \left(\sum_{s=1}^k \frac{(\mathbf{x}_{(s)}^T \mathbf{g})^2}{\mu_s} \left(\frac{1}{\omega_s} \int_0^t \sin(\omega_s(t - \tau)) \varphi(\tau) d\tau \right)^2 \right)^{\frac{1}{2}} \end{aligned} \quad (2.122)$$

Each term of the series is expressed as the product of a spatial and a temporal contribution. Its convergence is thus governed by:

- A spatial factor whose amplitude:

$$\frac{|\mathbf{x}_{(s)}^T \mathbf{g}|}{\sqrt{\mu_s}}$$

depends only on the projection of the load on the mode under consideration.

- A temporal factor:

$$\theta_s(t) = \left| \frac{1}{\omega_s} \int_0^t \sin(\omega_s(t - \tau)) \varphi(\tau) d\tau \right| \quad (2.123)$$

which depends simultaneously on the system eigenspectrum and on the time variation of the system excitation.

The convergence of the modal expansion (2.121) is thus governed by two types of convergence:

- A *convergence of quasi-static type*, occurring if the applied load \mathbf{g} admits a sufficiently accurate spatial representation on the basis of the $k < n$ retained eigenmodes. This is equivalent to assuming that the load distribution \mathbf{g} must be nearly orthogonal to the $(n - k)$ omitted eigenmodes which therefore will not be excited or will be only slightly excited.
- A *convergence of spectral type*, conditioned by the convergence to zero of the convolution products (2.123) when progressing in the eigenspectrum of the system. It thus depends both on the frequency content of the excitation and on the system eigenspectrum. For example:
 - for a Heaviside step load:

$$\varphi(t) = H(t) \quad \text{we get} \quad \theta_s(t) = \left| \frac{1 - \cos \omega_s t}{\omega_s^2} \right| \leq \frac{2}{\omega_s^2} \quad (2.124a)$$

- for an impulse loading:

$$\varphi(t) = \delta(t) \quad \text{we get} \quad \theta_s(t) = \left| \frac{\sin \omega_s t}{\omega_s} \right| \leq \frac{1}{\omega_s} \quad (2.124b)$$

- in the case of a harmonic load⁸ starting at $t = 0$:

$$\varphi(t) = H(t) \cos \omega t, \quad \text{we get} \quad \theta_s(t) = \left| \frac{\cos \omega_s t - \cos \omega t}{\omega^2 - \omega_s^2} \right| \leq \frac{2}{|\omega^2 - \omega_s^2|} \quad (2.124c)$$

The global convergence of development (2.121) results from the combination of both convergence types described, and it thus remains difficult to measure quantitatively since it depends on the vibration modes which have not been computed during the eigenvalue analysis and hence have been neglected. Error estimates can however be found using bounds such as (2.124a–2.124c) and further knowing that ω_k , the last frequency included in the superposition, is a lower bound for the eigenfrequencies of all neglected modes.

Experience shows that this mode superposition method, known as the *mode displacement method*, should be applied with care. It would be valuable to control at least the quasi-static convergence by representing correctly the load $\mathbf{p}(t)$ in the eigenmode basis. And for this reason a variant of mode displacement was developed, which is presented in Section 2.8.2.

2.8.2 Mode acceleration method

The method of mode accelerations, although presented in a different manner, was already proposed by Lord Rayleigh in his famous work (Lord Rayleigh 1894). It is based upon the observation that a statically exact response to the problem is available in the form:

$$\mathbf{K}\mathbf{q} = \mathbf{p}(t) - \mathbf{M}\ddot{\mathbf{q}}$$

by applying the truncated modal representation to only the inertia forces:

$$\mathbf{K}\mathbf{q} = \mathbf{p}(t) - \sum_{s=1}^k \ddot{\eta}_s(t) \mathbf{M}\mathbf{x}_{(s)} \quad (2.125)$$

⁸ This result can be obtained through the convolution (2.123) or derived as in Exercise 2.6. In the purely harmonic case (Section 2.6), the response to initial conditions should be removed from the response, so that Equation (2.124c) becomes $\theta_s(t) = \left| \frac{\cos \omega t}{\omega^2 - \omega_s^2} \right| \leq \frac{1}{|\omega^2 - \omega_s^2|}$.

The solution of the equation of motion expressed in this form is:

$$\mathbf{q}(t) = \mathbf{K}^{-1}\mathbf{p}(t) - \sum_{s=1}^k \frac{\ddot{\eta}_s(t)}{\omega_s^2} \mathbf{x}_{(s)} \quad (2.126)$$

where $\eta_s(t)$ verifies the normal equations (2.105) and therefore:

$$\ddot{\eta}_s = \frac{\mathbf{x}_{(s)}^T \mathbf{p}(t)}{\mu_s} - \omega_s^2 \eta_s$$

The result (2.126) may then be put in the final form:

$$\mathbf{q}(t) = \sum_{s=1}^k \mathbf{x}_{(s)} \eta_s(t) + \left\{ \mathbf{K}^{-1} - \sum_{s=1}^k \frac{\mathbf{x}_{(s)} \mathbf{x}_{(s)}^T}{\omega_s^2 \mu_s} \right\} \mathbf{p}(t) \quad (2.127)$$

the last term being the static correction computed from the known modes and the static response. By expressing \mathbf{K}^{-1} in the spectral form (2.62), it may also understood as:

$$\mathbf{q}(t) = \sum_{s=1}^k \mathbf{x}_{(s)} \eta_s(t) + \left\{ \sum_{s=k+1}^n \frac{\mathbf{x}_{(s)} \mathbf{x}_{(s)}^T}{\omega_s^2 \mu_s} \right\} \mathbf{p}(t) \quad (2.128)$$

It shows that *the mode acceleration method* consists in complementing the mode displacement solution with the missing terms from the modal expansion of the static response. There are numerous applications where the mode acceleration method provides a significant improvement in the numerical quality of the response with hardly any extra computational cost.⁹

Considering the special case of the forced harmonic response as in (2.78), the normal Equations (2.105) yield $\eta_s = \mathbf{x}_{(s)}^T \mathbf{s} / (\mu_s(-\omega^2 + \omega_s^2))$ so that the mode acceleration expression (2.127) results in:

$$\begin{aligned} \mathbf{x} &= \sum_{s=1}^k \frac{\mathbf{x}_{(s)} \mathbf{x}_{(s)}^T}{\mu_s(-\omega^2 + \omega_s^2)} \mathbf{s} + \left\{ \mathbf{K}^{-1} - \sum_{s=1}^k \frac{\mathbf{x}_{(s)} \mathbf{x}_{(s)}^T}{\omega_s^2 \mu_s} \right\} \mathbf{s} \\ &= \left\{ \mathbf{K}^{-1} + \omega^2 \sum_{s=1}^k \frac{\mathbf{x}_{(s)} \mathbf{x}_{(s)}^T}{(\omega_s^2 - \omega^2) \omega_s^2 \mu_s} \right\} \mathbf{s} \end{aligned} \quad (2.129)$$

which corresponds to the solution obtained with the statically correct admittance matrix (2.96) (when no rigid modes are present).

2.8.3 Mode acceleration and model reduction on selected coordinates

According to the mode acceleration method (2.127) the dynamics of a system can often be well described by a small number k of modes and by the residual static corrections pertaining to the external loads. If the loads are applied only on a few degrees of freedom (called \mathbf{q}_2 in

⁹ The static correction can also be used to estimate the error associated to the spatial convergence discussed in Section 2.8.1.

this section), the system can be considered as having a reduced number of degrees of freedom, namely the coordinates of the modes included in the superposition and the loaded degrees of freedom. The mass and stiffness matrices of the full system can then be reduced in the approximation space as will be shown hereafter.

Let us first rewrite Equation (2.127) in the condensed matrix form:

$$\mathbf{q}(t) = \mathbf{F}'\mathbf{p}(t) + \bar{\mathbf{X}}\bar{\boldsymbol{\eta}}(t) \quad (2.130)$$

with the following definitions:

- The reduced set of modes included in the response:

$$\bar{\mathbf{X}} = [\mathbf{x}_{(1)} \quad \dots \quad \mathbf{x}_{(k)}]$$

and the associated set of normal coordinates $\bar{\boldsymbol{\eta}}(t)$

- The residual flexibility matrix:

$$\mathbf{F}' = \mathbf{F} - \bar{\mathbf{X}}(\bar{\boldsymbol{\Omega}}^2\bar{\boldsymbol{\mu}})^{-1}\bar{\mathbf{X}}^T \quad (2.131)$$

where $\bar{\boldsymbol{\Omega}}^2$ and $\bar{\boldsymbol{\mu}}$ are the diagonal matrices of eigenvalues and generalized masses associated with the reduced set of modes and with the flexibility matrix:

$$\mathbf{F} = \mathbf{K}^{-1} \quad (2.132)$$

Let us reorganize the generalized coordinates in two separate sets:

$$\begin{bmatrix} \mathbf{q}_1(t) \\ \mathbf{q}_2(t) \end{bmatrix} = \begin{bmatrix} \mathbf{L}_1 \\ \mathbf{L}_2 \end{bmatrix} \mathbf{q}(t) \quad (2.133)$$

where \mathbf{L}_1 and \mathbf{L}_2 are appropriate Boolean operators of dimensions $n_1 \times n$ and $n_2 \times n$ respectively. Their transposes allow to reconstruct the generalized forces:

$$\mathbf{p}(t) = \begin{bmatrix} \mathbf{L}_1^T & \mathbf{L}_2^T \end{bmatrix} \begin{bmatrix} \mathbf{p}_1(t) \\ \mathbf{p}_2(t) \end{bmatrix} \quad (2.134)$$

Let us now assume that the load $\mathbf{p}(t)$ is applied to the set \mathbf{q}_2 only, and thus:

$$\mathbf{p}(t) = \mathbf{L}_2^T \mathbf{p}_2(t) \quad (2.135)$$

Substituting (2.135) into (2.130) yields:

$$\mathbf{q}(t) = \mathbf{F}'\mathbf{L}_2^T \mathbf{p}_2(t) + \bar{\mathbf{X}}\bar{\boldsymbol{\eta}}(t) \quad (2.136)$$

and partitioning this result according to (2.133) we get:

$$\mathbf{q}_1(t) = \mathbf{F}'_{12} \mathbf{p}_2(t) + \bar{\mathbf{X}}_1 \bar{\boldsymbol{\eta}}(t) \quad (2.137a)$$

$$\mathbf{q}_2(t) = \mathbf{F}'_{22} \mathbf{p}_2(t) + \bar{\mathbf{X}}_2 \bar{\boldsymbol{\eta}}(t) \quad (2.137b)$$

with the residual flexibility submatrices:

$$\mathbf{F}'_{12} = \mathbf{L}_1 \mathbf{F}' \mathbf{L}_2^T \quad \text{and} \quad \mathbf{F}'_{22} = \mathbf{L}_2 \mathbf{F}' \mathbf{L}_2^T \quad (2.138)$$

and the subsets of eigenvectors:

$$\bar{X}_i = L_i \bar{X} \quad i = 1, 2$$

The interesting aspect of this partitioning is that Equation (2.137b) can be inverted in the form:

$$p_2(t) = [F'_{22}]^{-1}(q_2(t) - \bar{X}_2 \bar{\eta}(t)) \quad (2.139)$$

Let us now recall that the normal coordinates $\bar{\eta}(t)$ are solutions of the normal equations:

$$\bar{\mu} \ddot{\bar{\eta}} + \bar{\mu} \bar{\Omega}^2 \bar{\eta} = \bar{X}^T p(t) = \bar{X}_2^T p_2(t) \quad (2.140)$$

and let us substitute (2.139) into (2.140) to write:

$$\bar{\mu} \ddot{\bar{\eta}} + (\bar{\mu} \bar{\Omega}^2 + \bar{X}_2^T [F'_{22}]^{-1} \bar{X}_2) \bar{\eta} - \bar{X}_2^T [F'_{22}]^{-1} q_2 = 0 \quad (2.141)$$

Finally, Equations (2.139) and (2.141) can be collected in a single matrix equation involving generalized stiffness and mass matrices:

$$\underbrace{\begin{bmatrix} [F'_{22}]^{-1} & -[F'_{22}]^{-1} \bar{X}_2 \\ -\bar{X}_2^T [F'_{22}]^{-1} & (\bar{\mu} \bar{\Omega}^2 + \bar{X}_2^T [F'_{22}]^{-1} \bar{X}_2) \end{bmatrix}}_{\text{stiffness matrix}} \underbrace{\begin{bmatrix} q_2 \\ \bar{\eta} \end{bmatrix}}_{\text{mass matrix}} + \underbrace{\begin{bmatrix} 0 & 0 \\ 0 & \bar{\mu} \end{bmatrix}}_{\text{mass matrix}} \begin{bmatrix} \ddot{q}_2 \\ \ddot{\bar{\eta}} \end{bmatrix} = \begin{bmatrix} p_2(t) \\ 0 \end{bmatrix} \quad (2.142)$$

The stiffness matrix is obtained from the knowledge of the static influence coefficients $G_{22} = L_2 F L_2^T$ and the modal shapes \bar{X}_2 on the q_2 . The mass matrix is remarkably simple since it consists only of the generalized masses of the eigensolutions included in the superposition.

Equation (2.142) forms in fact the basis of the well-known and widely used MacNeal reduction method (MacNeal 1971), in which the solution is described in terms of two sets of information:

- the eigenshapes \bar{X} of the initial system and the associated eigenvalues and generalized masses;
- the so-called attachment modes: they are computed in terms of the influence coefficients obtained from unit loading of the degrees of freedom q_2 (Equation 2.144) and collected in the matrix:

$$X_{\text{attachment modes}} = \begin{bmatrix} F_{12} \\ F_{22} \end{bmatrix} \quad (2.143)$$

After solving Equation (2.142), the generalized displacements q_1 can be recuperated from Equation (2.137a).

The method was referred to as a hybrid method by R.H. MacNeal himself (MacNeal 1971) since its starts from the flexibility relationship (2.137b), thus with nodal forces and normal coordinates as unknowns. The reconstruction of the stiffness matrix in (2.142) results from an artifice. A drawback of the method is that there is a mass deficiency due to the fact that the mass attached to the missing modes is neglected. This deficiency is in fact inherent to the mode acceleration method from which Equation (2.142) is derived. The topic of model reduction will be further discussed in Section 6.9.

Remark 2.1 Let us note that to find the residual flexibility matrix \mathbf{F}' defined in (2.131) the inverse of the stiffness matrix is needed. However for the reduced form (2.142) and for the retrieval of the generalized displacements \mathbf{q}_1 in (2.137a), only the submatrices \mathbf{F}_{12} and \mathbf{F}_{22} are needed. Hence one does not need to compute the full inverse of \mathbf{K} , but it is sufficient to solve n_2 linear systems of the form:

$$\mathbf{K}\mathbf{F}_2 = \mathbf{L}_2^T \quad (2.144)$$

and extract $\mathbf{F}_{12} = \mathbf{L}_1\mathbf{F}_2$ and $\mathbf{F}_{22} = \mathbf{L}_2\mathbf{F}_2$.

Remark 2.2 Note that (2.142) represents a reduced model of the original system only if the number k of modes retained in $\bar{\mathbf{X}}$ is such that $k < (n - n_2)$. One should observe that the residual flexibility \mathbf{F}' defined by (2.131) has a rank of $n - k$. Therefore \mathbf{F}'_{22} will be singular if $k > (n - n_2)$ and the reduced stiffness in (2.142) cannot be built.

2.9 Response to support motion

A relatively common excitation mode in structural mechanics is the case of imposed ground motion (response of a building to an earthquake, vibration of equipment carried by a vehicle, etc.).

In what follows it will be shown first how, in the most general case of differential support motion, the response may be decomposed into a quasi-static deformation induced by the motion of the supports and a vibration of the structure clamped onto the supports. It will be seen next that in the case where the imposed motion is a global one, only the acceleration associated with the rigid motion is involved.

The relatively common but approximate technique which consists of expressing the differential motion of the supports by the application of a set of equivalent forces to the system modified through the addition of support masses will also be justified.

Finally, the important concept of effective modal mass will be introduced in order to help the selection of the system eigenmodes which have dominant participation in the support motion response.

2.9.1 Motion imposed to a subset of degrees of freedom

Let us consider the system of Figure 2.10, for which we consider that the only excitation source is the motion induced by the supports. Let us partition its degrees of freedom in two sets:

- the n_1 displacements \mathbf{q}_1 remaining completely free;
- the n_2 displacements \mathbf{q}_2 imposed at support level.

The equations of motion take the partitioned form:

$$\begin{bmatrix} \mathbf{M}_{11} & \mathbf{M}_{12} \\ \mathbf{M}_{21} & \mathbf{M}_{22} \end{bmatrix} \begin{bmatrix} \ddot{\mathbf{q}}_1 \\ \ddot{\mathbf{q}}_2 \end{bmatrix} + \begin{bmatrix} \mathbf{K}_{11} & \mathbf{K}_{12} \\ \mathbf{K}_{21} & \mathbf{K}_{22} \end{bmatrix} \begin{bmatrix} \mathbf{q}_1 \\ \mathbf{q}_2 \end{bmatrix} = \begin{bmatrix} \mathbf{0} \\ \mathbf{r}_2(t) \end{bmatrix} \quad (2.145)$$

The first set of equations extracted from (2.145):

$$\mathbf{M}_{11}\ddot{\mathbf{q}}_1 + \mathbf{K}_{11}\mathbf{q}_1 = -\mathbf{K}_{12}\mathbf{q}_2 - \mathbf{M}_{12}\ddot{\mathbf{q}}_2 \quad (2.146)$$

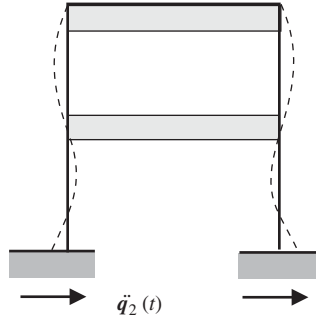


Figure 2.10 System undergoing differential support motion.

allows us to compute the response of the unrestrained degrees of freedom (the right-hand side being determined by the imposed displacements), while the second one:

$$\mathbf{r}_2(t) = \mathbf{K}_{21}\mathbf{q}_1 + \mathbf{M}_{21}\ddot{\mathbf{q}}_1 + \mathbf{K}_{22}\mathbf{q}_2 + \mathbf{M}_{22}\ddot{\mathbf{q}}_2 \quad (2.147)$$

will allow us to compute the reaction forces $\mathbf{r}_2(t)$ between the structure and its supports.

The governing equation (2.146) can be handled as a common dynamic equation. However, since the excitation is originating from imposed displacements, its right-hand side is a special forcing term and specific approaches can be considered as outlined next.

Let us first compute the quasi-static response of the unrestrained part of the structure. If one neglects the inertia force terms of (2.146), one obtains:

$$\mathbf{q}_1^{qs}(t) = -\mathbf{K}_{11}^{-1}\mathbf{K}_{12}\mathbf{q}_2 = \mathbf{T}\mathbf{q}_2 \quad (2.148)$$

where \mathbf{T} is the static condensation matrix at foundation level describing the static deformations on \mathbf{q}_1 for unit displacements on \mathbf{q}_2 . This allows one to write the complete response to (2.146) in the form:

$$\mathbf{q}(t) = \begin{bmatrix} \mathbf{I} & \mathbf{T} \\ \mathbf{0} & \mathbf{I} \end{bmatrix} \begin{bmatrix} \mathbf{y}_1 \\ \mathbf{q}_2 \end{bmatrix} \quad (2.149)$$

where $\mathbf{y}_1(t)$ represents the sole dynamic part of the response, i.e. the perturbations relative to the quasi-static response describing the vibration of the structure on its support.

Through substitution of the solution decomposition (2.149) into (2.145), the equation governing the motion of the unrestrained degrees of freedom takes the form:

$$\mathbf{M}_{11}\ddot{\mathbf{y}}_1 + \mathbf{K}_{11}\mathbf{y}_1 = \mathbf{g}_1(t) \quad (2.150)$$

where

$$\mathbf{g}_1(t) = -\mathbf{M}_{11}\ddot{\mathbf{q}}_1^{qs}(t) - \mathbf{M}_{12}\ddot{\mathbf{q}}_2(t) = -(\mathbf{M}_{11}\mathbf{T} + \mathbf{M}_{12})\ddot{\mathbf{q}}_2(t) \quad (2.151)$$

is the equivalent load computed in terms of the acceleration of the supports and the static modes that their motion generates.

The solution to Equation (2.150) governing the relative displacements \mathbf{y}_1 can be expanded in terms of eigenmodes pertaining to the matrices \mathbf{M}_{11} and \mathbf{K}_{11} , namely the modes of the system

fixed to the ground, solutions of the internal eigenproblem:

$$\mathbf{K}_{11}\tilde{\mathbf{x}} = \tilde{\omega}^2\mathbf{M}_{11}\tilde{\mathbf{x}} \quad (2.152)$$

The fixed interface modes and associated eigenfrequencies are denoted by:

$$\begin{cases} \tilde{\omega}_1^2 \leq \tilde{\omega}_2^2 \leq \dots \leq \tilde{\omega}_{n_1}^2 \\ \tilde{\mathbf{x}}_1, \tilde{\mathbf{x}}_2, \dots, \tilde{\mathbf{x}}_{(n_1)} \end{cases} \quad (2.153)$$

The modes are collected in matrix $\tilde{\mathbf{X}}$ and normalized so that $\tilde{\mathbf{X}}^T\mathbf{M}_{11}\tilde{\mathbf{X}} = \mathbf{I}$. The solution to Equation (2.150) is then computed as a mode superposition in the form:

$$\mathbf{y}_1(t) = \sum_{r=1}^{n_1} \tilde{\mathbf{x}}_{(r)}\eta_r(t) = \tilde{\mathbf{X}}\boldsymbol{\eta}(t) \quad (2.154)$$

Once the response of the unrestrained part of the structure is known, the reactions to the ground may be obtained from the application of relationship (2.147).

2.9.2 Transformation to normal coordinates

Combining Equations (2.149) and (2.154) allows writing the absolute response of the system in the form:

$$\mathbf{q}(t) = \begin{bmatrix} \tilde{\mathbf{X}} & \mathbf{T} \\ \mathbf{0} & \mathbf{I} \end{bmatrix} \begin{bmatrix} \boldsymbol{\eta} \\ \mathbf{q}_2 \end{bmatrix} = \mathbf{R} \begin{bmatrix} \boldsymbol{\eta} \\ \mathbf{q}_2 \end{bmatrix} \quad (2.155)$$

The internal modes $\tilde{\mathbf{X}}$ are supposed orthonormal and their eigenvalues collected in the diagonal matrix:

$$\tilde{\boldsymbol{\Omega}}^2 = \tilde{\mathbf{X}}^T\mathbf{K}_{11}\tilde{\mathbf{X}}$$

Substituting (2.155) into (2.145) and multiplying by \mathbf{R}^T yields:

$$\mathbf{R}^T\mathbf{M}\mathbf{R} \begin{bmatrix} \ddot{\boldsymbol{\eta}} \\ \ddot{\mathbf{q}}_2 \end{bmatrix} + \mathbf{R}^T\mathbf{K}\mathbf{R} \begin{bmatrix} \boldsymbol{\eta} \\ \mathbf{q}_2 \end{bmatrix} = \mathbf{R}^T \begin{bmatrix} \mathbf{0} \\ \mathbf{r}_2(t) \end{bmatrix} \quad (2.156)$$

We compute successively:

$$\mathbf{R}^T\mathbf{K}\mathbf{R} = \mathbf{R}^T \begin{bmatrix} \mathbf{K}_{11} & \mathbf{K}_{12} \\ \mathbf{K}_{21} & \mathbf{K}_{22} \end{bmatrix} \mathbf{R} = \begin{bmatrix} \tilde{\boldsymbol{\Omega}}^2 & \mathbf{0} \\ \mathbf{0} & \mathbf{K}_{22}^* \end{bmatrix} \quad (2.157a)$$

$$\mathbf{R}^T\mathbf{M}\mathbf{R} = \mathbf{R}^T \begin{bmatrix} \mathbf{M}_{11} & \mathbf{M}_{12} \\ \mathbf{M}_{21} & \mathbf{M}_{22} \end{bmatrix} \mathbf{R} = \begin{bmatrix} \mathbf{I} & \boldsymbol{\Gamma} \\ \boldsymbol{\Gamma}^T & \mathbf{M}_{22}^* \end{bmatrix} \quad (2.157b)$$

with

$$\mathbf{K}_{22}^* = \mathbf{K}_{22} + \mathbf{K}_{21}\mathbf{T} \quad (2.158a)$$

$$\mathbf{M}_{22}^* = \mathbf{M}_{22} + \mathbf{M}_{21}\mathbf{T} + \mathbf{T}^T\mathbf{M}_{12} + \mathbf{T}^T\mathbf{M}_{11}\mathbf{T} \quad (2.158b)$$

$$\mathbf{M}_{12}^* = \mathbf{M}_{11}\mathbf{T} + \mathbf{M}_{12} = \mathbf{M}_{21}^{*T} \quad (2.158c)$$

$$\boldsymbol{\Gamma} = \tilde{\mathbf{X}}^T\mathbf{M}_{12}^* \quad (2.158d)$$

\mathbf{M}_{22}^* and \mathbf{K}_{22}^* are the condensed mass and stiffness matrices of the support. \mathbf{M}_{12}^* is a mass coupling term expressing the mass transfer from the internal system to its support. When the mass matrix is diagonal, it reduces to $\mathbf{M}_{12}^* = \mathbf{M}_{11}\mathbf{T}$.

$\mathbf{\Gamma}$ results from the projection of \mathbf{M}_{12}^* on the modal basis $\tilde{\mathbf{X}}$, and is referred to as the *modal participation matrix*. It can be split into individual modal contributions in the form:

$$\mathbf{\Gamma}^T = [\gamma_{(1)} \quad \dots \quad \gamma_{(n_1)}] \quad \text{with} \quad \gamma_{(r)} = \mathbf{M}_{21}^* \tilde{\mathbf{x}}_{(r)} \quad (2.159)$$

Assuming an arbitrary acceleration $\ddot{\mathbf{q}}_2$ of the support, the relative motion to the foundation is determined by solving the first set of equations in (2.156),

$$\ddot{\boldsymbol{\eta}} + \tilde{\boldsymbol{\Omega}}^2 \boldsymbol{\eta} = -\mathbf{\Gamma} \ddot{\mathbf{q}}_2 \quad (2.160)$$

which are in fact the normal equations associated to (2.150). The reaction on the supports are computed next from the second set of equations in (2.156):

$$\mathbf{r}_2(t) = \mathbf{K}_{22}^* \mathbf{q}_2 + \mathbf{M}_{22}^* \ddot{\mathbf{q}}_2 + \mathbf{\Gamma}^T \ddot{\boldsymbol{\eta}} \quad (2.161)$$

Finally, let consider the case of forced harmonic response at excitation frequency ω by assuming:

$$\begin{bmatrix} \boldsymbol{\eta}(t) \\ \mathbf{q}_2(t) \\ \mathbf{r}_2(t) \end{bmatrix} = \begin{bmatrix} \boldsymbol{\eta} \\ \mathbf{q}_2 \\ \mathbf{r}_2 \end{bmatrix} e^{i\omega t}$$

In the frequency domain Equations (2.160) and (2.161) become:

$$-\omega^2 \boldsymbol{\eta} + \tilde{\boldsymbol{\Omega}}^2 \boldsymbol{\eta} = \omega^2 \mathbf{\Gamma} \mathbf{q}_2 \quad (2.162a)$$

$$\mathbf{r}_2 = \mathbf{K}_{22}^* \mathbf{q}_2 - \omega^2 \mathbf{M}_{22}^* \mathbf{q}_2 - \omega^2 \mathbf{\Gamma}^T \boldsymbol{\eta} \quad (2.162b)$$

$\boldsymbol{\eta}$ can be extracted from (2.162a):

$$\boldsymbol{\eta} = \omega^2 (\tilde{\boldsymbol{\Omega}}^2 - \omega^2 \mathbf{I})^{-1} \mathbf{\Gamma} \mathbf{q}_2$$

which provides the relationship between support motion and reactions:

$$\mathbf{r}_2 = \mathbf{Z}_{22}^*(\omega^2) \mathbf{q}_2 \quad (2.163)$$

with the matrix:

$$\begin{aligned} \mathbf{Z}_{22}^*(\omega^2) &= \mathbf{K}_{22}^* - \omega^2 \mathbf{M}_{22}^* - \omega^4 \mathbf{\Gamma}^T (\tilde{\boldsymbol{\Omega}}^2 - \omega^2 \mathbf{I})^{-1} \mathbf{\Gamma} \\ &= \mathbf{K}_{22}^* - \omega^2 \mathbf{M}_{22}^* - \omega^4 \sum_{r=1}^{n_1} \frac{1}{\tilde{\omega}_r^2 - \omega^2} \boldsymbol{\gamma}_{(r)} \boldsymbol{\gamma}_{(r)}^T \end{aligned} \quad (2.164)$$

Expression (2.164) is nothing else than the impedance matrix of the boundary, a concept which will be discussed in Section 2.9.3 from a different perspective.

It is worthwhile investigating the expression of the dynamic impedance (2.164) at the limit of the excitation frequency range.

- If $\omega \ll \tilde{\omega}_1$ – i.e. the excitation frequency is well below the fundamental frequency of the internal structure – then the internal mass is transferred statically to the foundation:

$$\mathbf{Z}_{22}^*(\omega^2) \simeq \mathbf{K}_{22}^* - \omega^2 \mathbf{M}_{22}^* \quad (2.165)$$

- If $\omega \gg \tilde{\omega}_{n_1}$ – i.e. the excitation frequency is well above the fundamental frequency of the internal structure – only a fraction of the structural mass contributes to inertia forces since:

$$\mathbf{Z}_{22}^*(\omega^2) \simeq \mathbf{K}_{22}^* - \omega^2 \mathbf{M}_{22}^* + \omega^2 \mathbf{F}^T \mathbf{F} \quad (2.166)$$

- In the intermediate range, a criterion is needed to determine which eigensolutions effectively provide a significant contribution to the reaction forces \mathbf{r}_2 .

The meaning of the mass operator $\mathbf{F}^T \mathbf{F}$ appearing in Equation (2.166) will be discussed in Section 2.9.5.

2.9.3 Mechanical impedance on supports and its statically exact expansion

When the number of degrees of freedom in a system is very large, dynamic analysis may become unfeasible in practice. So the system is broken down into several substructures whose dynamical behaviour is described by their harmonic response when forces are applied onto their interface boundaries. In doing so, we can define a reduced set of variables for approximating the dynamics of each substructure and hence of the entire system.

Let us consider the case of a mechanical subsystem such as that represented by Figure 2.11, which is described by its stiffness and mass matrices \mathbf{K} and \mathbf{M} . It is connected to the rest of the system by the boundary degrees of freedom \mathbf{q}_2 , and its n_1 internal degrees of freedom \mathbf{q}_1 are considered as free.

The *impedance matrix* was defined in Section 2.6.1 as the frequency dependent matrix which relates the applied force amplitudes \mathbf{s} to the displacement amplitudes \mathbf{q} of the forced harmonic

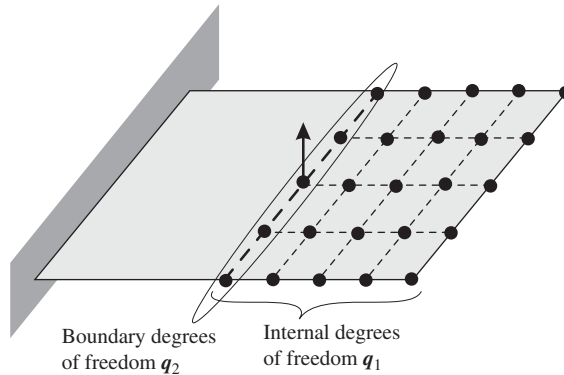


Figure 2.11 The mechanical impedance concept.

response:

$$\mathbf{s} = \mathbf{Z}(\omega^2)\mathbf{q} \quad (2.167)$$

with

$$\mathbf{Z}(\omega^2) = \mathbf{K} - \omega^2\mathbf{M} \quad (2.168)$$

the inverse of which is the dynamic influence coefficient matrix (Section 2.6.1).

Since the internal degrees of freedom \mathbf{q}_1 are not externally loaded, one may write:

$$\begin{bmatrix} \mathbf{Z}_{11}(\omega^2) & \mathbf{Z}_{12}(\omega^2) \\ \mathbf{Z}_{21}(\omega^2) & \mathbf{Z}_{22}(\omega^2) \end{bmatrix} \begin{bmatrix} \mathbf{q}_1 \\ \mathbf{q}_2 \end{bmatrix} = \begin{bmatrix} \mathbf{0} \\ \mathbf{s}_2 \end{bmatrix} \quad (2.169)$$

with $\mathbf{Z}_{ij}(\omega^2) = \mathbf{K}_{ij} - \omega^2\mathbf{M}_{ij}$ and the force amplitudes \mathbf{s}_2 representing the external loads and/or the boundary reactions. The first Equation (2.169) may be used to eliminate the internal degrees of freedom:

$$\mathbf{q}_1 = -\mathbf{Z}_{11}^{-1}\mathbf{Z}_{12}\mathbf{q}_2 \quad (2.170)$$

yielding the relationship:

$$\mathbf{Z}_{22}^*(\omega^2)\mathbf{q}_2 = \mathbf{s}_2 \quad (2.171)$$

with the *reduced impedance matrix*:

$$\mathbf{Z}_{22}^* = \mathbf{Z}_{22} - \mathbf{Z}_{21}\mathbf{Z}_{11}^{-1}\mathbf{Z}_{12} \quad (2.172)$$

One notes immediately that \mathbf{Z}_{22}^* admits as poles the zeros of:

$$\det(\mathbf{Z}_{11}) = \det(\mathbf{K}_{11} - \omega^2\mathbf{M}_{11})$$

which correspond to the eigenfrequencies of the subsystem with its boundary degrees of freedom \mathbf{q}_2 fixed. Therefore matrix:

$$\mathbf{Z}_{11}^{-1} = (\mathbf{K}_{11} - \omega^2\mathbf{M}_{11})^{-1}$$

is expanded in terms of the eigensolutions associated to \mathbf{M}_{11} and \mathbf{K}_{11} , namely those of the subsystem clamped on its boundary. Those eigensolutions are called $\tilde{\omega}_r$ and $\tilde{\mathbf{x}}_{(r)}$ and were defined earlier in Section 2.9.2, Equations (2.152) and (2.153). We also assume the modes to be \mathbf{M}_{11} -normalized. To find the spectral expansion of \mathbf{Z}_{11}^{-1} we follow the steps perform in Section 2.6.2 to obtain the modal expression (2.85) for the complete dynamic influence matrix, but now considering only the internal dynamics and assuming that no rigid mode exists when the interface is fixed. One finds:

$$\mathbf{Z}_{11}^{-1}(\omega^2) = \sum_{s=1}^{n_1} \frac{\tilde{\mathbf{x}}_{(s)}\tilde{\mathbf{x}}_{(s)}^T}{\tilde{\omega}_s^2 - \omega^2} \quad (2.173)$$

In particular one deduces:

$$\mathbf{K}_{11}^{-1} = \sum_{s=1}^{n_1} \frac{\tilde{\mathbf{x}}_{(s)}\tilde{\mathbf{x}}_{(s)}^T}{\tilde{\omega}_s^2} \quad (2.174)$$

Applying twice the relation:

$$\frac{1}{\tilde{\omega}_s^2 - \omega^2} = \frac{1}{\tilde{\omega}_s^2} + \frac{\omega^2}{\tilde{\omega}_s^2(\tilde{\omega}_s^2 - \omega^2)}$$

Equation (2.173) can be put in the form:

$$\begin{aligned} \mathbf{Z}_{11}^{-1}(\omega^2) &= \mathbf{K}_{11}^{-1} + \omega^2 \sum_{s=1}^{n_1} \frac{\tilde{\mathbf{x}}_{(s)} \tilde{\mathbf{x}}_{(s)}^T}{\tilde{\omega}_s^2(\tilde{\omega}_s^2 - \omega^2)} \\ &= \mathbf{K}_{11}^{-1} + \omega^2 \sum_{s=1}^{n_1} \frac{\tilde{\mathbf{x}}_{(s)} \tilde{\mathbf{x}}_{(s)}^T}{\tilde{\omega}_s^4} + \omega^4 \sum_{s=1}^{n_1} \frac{\tilde{\mathbf{x}}_{(s)} \tilde{\mathbf{x}}_{(s)}^T}{\tilde{\omega}_s^4(\tilde{\omega}_s^2 - \omega^2)} \end{aligned} \quad (2.175)$$

Owing to the \mathbf{M}_{11} -orthonormality of the modes and to expansion (2.174) one can verify that this expression can further be written as:

$$\mathbf{Z}_{11}^{-1}(\omega^2) = \mathbf{K}_{11}^{-1} + \omega^2 \mathbf{K}_{11}^{-1} \mathbf{M}_{11} \mathbf{K}_{11}^{-1} + \omega^4 \sum_{s=1}^{n_1} \frac{\tilde{\mathbf{x}}_{(s)} \tilde{\mathbf{x}}_{(s)}^T}{\tilde{\omega}_s^4(\tilde{\omega}_s^2 - \omega^2)} \quad (2.176)$$

Next, let us write the reduced impedance (2.172) in terms of system matrices:

$$\begin{aligned} \mathbf{Z}_{22}^* &= \mathbf{K}_{22} - \omega^2 \mathbf{M}_{22} - (\mathbf{K}_{21} - \omega^2 \mathbf{M}_{21}) \mathbf{Z}_{11}^{-1} (\mathbf{K}_{12} - \omega^2 \mathbf{M}_{12}) \\ &= \mathbf{K}_{22} - \omega^2 \mathbf{M}_{22} \\ &\quad - \mathbf{K}_{21} \mathbf{Z}_{11}^{-1} \mathbf{K}_{12} + \omega^2 (\mathbf{M}_{21} \mathbf{Z}_{11}^{-1} \mathbf{K}_{12} + \mathbf{K}_{21} \mathbf{Z}_{11}^{-1} \mathbf{M}_{12}) - \omega^4 \mathbf{M}_{21} \mathbf{Z}_{11}^{-1} \mathbf{M}_{12} \end{aligned} \quad (2.177)$$

To obtain an expansion in terms of maximum order 4 in ω we will make use of Equations (2.176, 2.175, 2.173) respectively in the last three terms of (2.177). Finally we obtain:

$$\begin{aligned} \mathbf{Z}_{22}^* &= \mathbf{K}_{22} - \mathbf{K}_{21} \mathbf{K}_{11}^{-1} \mathbf{K}_{12} \\ &\quad - \omega^2 [\mathbf{M}_{22} - \mathbf{M}_{21} \mathbf{K}_{11}^{-1} \mathbf{K}_{12} - \mathbf{K}_{21} \mathbf{K}_{11}^{-1} \mathbf{M}_{12} + \mathbf{K}_{21} \mathbf{K}_{11}^{-1} \mathbf{M}_{11} \mathbf{K}_{11}^{-1} \mathbf{K}_{12}] \\ &\quad - \omega^4 \sum_{s=1}^{n_1} \frac{(\mathbf{K}_{21} - \tilde{\omega}_s^2 \mathbf{M}_{21}) \tilde{\mathbf{x}}_{(s)} \tilde{\mathbf{x}}_{(s)}^T (\mathbf{K}_{21} - \tilde{\omega}_s^2 \mathbf{M}_{21})^T}{\tilde{\omega}_s^4(\tilde{\omega}_s^2 - \omega^2)} \end{aligned} \quad (2.178)$$

It is left to the reader to verify that this expression is equivalent to (2.164), which was obtained using the representation (2.155) that allows describing the dynamics of the substructure in terms of static modes associated to the interface (or support) displacements and in terms of modes of the fixed interface (internal) modes. The expansion (2.178) or (2.155) indicates that those static and vibration modes of a substructure form a relevant basis to describe its dynamics. In case not all internal modes are considered, the representation leads to an approximate but reduced description of the substructure. This forms the main idea underlying the Craig-Bampton method discussed later in Chapter 6, Section 6.9. The last term in (2.178) reveals that the importance of an internal mode in the description of the interface dynamics of a substructure and thus for the global dynamics of the system is related to the reaction force $(\mathbf{K}_{21} - \tilde{\omega}_s^2 \mathbf{M}_{21}) \tilde{\mathbf{x}}_{(s)}$ it produces on the interface.

2.9.4 System submitted to global support acceleration

Let us now consider the particular case where a system is excited through a global motion of its support as illustrated in Figure 2.12. The imposed acceleration on degrees of freedom \mathbf{q}_2 can then be written as:

$$\ddot{\mathbf{q}}_2 = \mathbf{u}_2 \ddot{\varphi}(t) \quad (2.179)$$

where $\ddot{\varphi}(t)$ is a collective acceleration function and \mathbf{u}_2 is part of a rigid body motion such that there exists an associated displacement \mathbf{u}_1 for the internal displacements and

$$\begin{bmatrix} \mathbf{K}_{11} & \mathbf{K}_{12} \\ \mathbf{K}_{21} & \mathbf{K}_{22} \end{bmatrix} \begin{bmatrix} \mathbf{u}_1 \\ \mathbf{u}_2 \end{bmatrix} = \mathbf{0} \quad (2.180)$$

From this last relation it is clear that that quasi-static response of the internal degrees of freedom, as defined earlier in the general by (2.148), is simply:

$$\mathbf{q}_1^{qs}(t) = -\mathbf{K}_{11}^{-1} \mathbf{K}_{12} \mathbf{q}_2 = \mathbf{T} \mathbf{u}_2 \varphi(t) = \mathbf{u}_1 \varphi(t) \quad (2.181)$$

Separating the solution in quasi-static and vibrational parts now is simply written as:

$$\ddot{\mathbf{q}} = \begin{bmatrix} \ddot{\mathbf{q}}_1 \\ \ddot{\mathbf{q}}_2 \end{bmatrix} = \begin{bmatrix} \ddot{\mathbf{y}}_1 \\ \mathbf{0} \end{bmatrix} + \begin{bmatrix} \mathbf{u}_1 \\ \mathbf{u}_2 \end{bmatrix} \ddot{\varphi}(t) \quad (2.182)$$

the second term of which is known.

Substituting the representation (2.182) in the dynamic equation (2.146) for the internal displacements the displacements with respect to the foundation can be computed as before from (2.150) but now the load associated to \mathbf{y}_1 take a form which involves only the global acceleration and the inertia forces associated with the rigid-body modes of the system:

$$\mathbf{g}_1(t) = -(\mathbf{M}_{11} \mathbf{u}_1 + \mathbf{M}_{12} \mathbf{u}_2) \ddot{\varphi}(t) \quad (2.183)$$

The reaction forces on the support are given by Equation (2.161), which in case of global support motion simplifies to:

$$\mathbf{r}_2(t) = \mathbf{M}_{22}^* \mathbf{u}_2 \varphi(t) + \mathbf{\Gamma}^T \ddot{\boldsymbol{\eta}} \quad (2.184)$$

since the condensed stiffness $\mathbf{K}_{22}^* \mathbf{q}_2 = (\mathbf{K}_{22} - \mathbf{K}_{21} \mathbf{K}_{11}^{-1} \mathbf{K}_{12}) \mathbf{u}_2 \ddot{\varphi}$ is null according to (2.180).

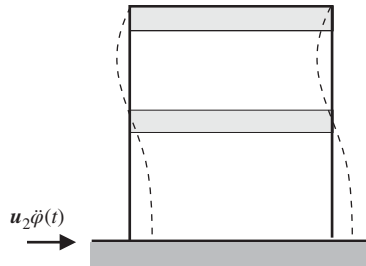


Figure 2.12 System submitted to global support acceleration.

2.9.5 Effective modal masses

Let us assume that the the boundary of the structure undergoes a rigid body motion $\mathbf{u}_{2(i)}$ of unit intensity in direction (i). A measure of the energy exchanged in harmonic motion between the structure and its boundary under imposed motion $\mathbf{q}_2 = \mathbf{u}_{2(i)}$ can be computed from Equations (2.163–2.164), reminding that $\mathbf{K}_{22}^* \mathbf{u}_2$,

$$-\mathbf{r}_2^T \mathbf{q}_2 = \omega^2 \mathbf{u}_{2(i)}^T \mathbf{M}_{22}^* \mathbf{u}_{2(i)} + \omega^4 \mathbf{u}_{2(i)}^T \mathbf{\Gamma}^T (\tilde{\mathbf{\Omega}}^2 - \omega^2 \mathbf{I})^{-1} \mathbf{\Gamma} \mathbf{u}_{2(i)} \quad (2.185)$$

The first term represents the rigid body inertia of the structure in mode $\mathbf{u}_{2(i)}$. The second one, which represents the dynamic effect due to the deformation of the internal structure, is governed by two factors:

– the modal participation factors to the response, computed as:

$$\mathbf{u}_{2(i)}^T \boldsymbol{\gamma}_{(r)} = \mathbf{u}_{2(i)}^T (\mathbf{M}_{21} + \mathbf{T}^T \mathbf{M}_{11}) \tilde{\mathbf{x}}_{(r)} \quad (2.186)$$

– The dynamic amplification factors:

$$\frac{\omega^2}{\omega_r^2 - \omega^2}$$

resulting from the flexibility of the internal structure.

The relative importance of the modal participation factors can be assessed by using the concept of *effective modal mass* (Imbert 1984, Preumont 1994).

Let us compute the expression:

$$\mathbf{u}_{2(i)}^T \mathbf{\Gamma}^T \mathbf{\Gamma} \mathbf{u}_{2(i)} = \sum_{r=1}^{n_1} (\mathbf{u}_{2(i)}^T \boldsymbol{\gamma}_{(r)})^2 \quad (2.187)$$

and develop the matrix $\mathbf{\Gamma}^T \mathbf{\Gamma}$ appearing in the left-hand side. Owing to (2.61), which gives rise to the identity (the eigenmodes being supposed orthonormal):

$$\tilde{\mathbf{X}} \tilde{\mathbf{X}}^T = \mathbf{M}_{11}^{-1} \quad (2.188)$$

one obtains:

$$\begin{aligned} \mathbf{\Gamma}^T \mathbf{\Gamma} &= \mathbf{M}_{21}^* \tilde{\mathbf{X}} \tilde{\mathbf{X}}^T \mathbf{M}_{12}^* = (\mathbf{T}^T \mathbf{M}_{11} + \mathbf{M}_{21}) \mathbf{M}_{11}^{-1} (\mathbf{M}_{11} \mathbf{T} + \mathbf{M}_{12}) \\ &= \mathbf{T}^T \mathbf{M}_{11} \mathbf{T} + \mathbf{T}^T \mathbf{M}_{12} + \mathbf{M}_{12}^T \mathbf{T} + \mathbf{M}_{12}^T \mathbf{M}_{11}^{-1} \mathbf{M}_{12} \\ &= \mathbf{M}_{22}^* - \mathbf{M}_{22} + \mathbf{M}_{12}^T \mathbf{M}_{11}^{-1} \mathbf{M}_{12} \end{aligned} \quad (2.189)$$

The last term in (2.189) vanishes for a lumped mass matrix. More generally, it is of second order in the coupling term \mathbf{M}_{12} and may thus be neglected anyway, so that one obtains the expression:

$$\mathbf{\Gamma}^T \mathbf{\Gamma} \simeq \mathbf{M}_{22}^* - \mathbf{M}_{22} \quad (2.190)$$

Removing also the restriction on the orthonormality of the eigenmodes, Equation (2.187) may thus be rewritten:

$$m_T = m_S + \sum_{r=1}^{n_1} \frac{(\mathbf{u}_{2(i)}^T \boldsymbol{\gamma}_{(r)})^2}{\mu_r} \quad (2.191)$$

where

- m_T represents the total mass of the structure, computed from the mass matrix condensed on the boundary:

$$m_T = \mathbf{u}_{2(i)}^T \mathbf{M}_{22}^* \mathbf{u}_{2(i)} \quad (2.192)$$

- m_S represents the part of the structural mass attached to the support:

$$m_S = \mathbf{u}_{2(i)}^T \mathbf{M}_{22} \mathbf{u}_{2(i)} \quad (2.193)$$

Equation (2.191) is verified provided that all the eigenmodes are included in the series of the right-hand side. In practice, however, the series will be truncated, so that the equality is no longer verified and the corresponding residue then represents the missing mass.

It provides a useful criterion for selecting the number $k < n_1$ modes in the mode superposition. Calling $P_{(i)}$ the percentage of the total mass needed to represent properly the structure excited by its support in direction (i) , the model basis will be selected so that the condition:

$$\sum_{r=1}^{n_1} \frac{(\mathbf{u}_{2(i)}^T \boldsymbol{\gamma}_{(r)})^2}{\mu_r} \geq P_{(i)}(m_T - m_S) \quad (2.194)$$

is fulfilled. Typically one chooses $P_{(i)}$ to be in the range 90–95%.

The global support excitation $\mathbf{u}_{2(i)}$ can be a translation or a rotation. The effective modal participation of a given mode $\mathbf{x}_{(r)}$ to the series in Equation (2.191) depends on the direction of excitation and it can be significant in one direction while being negligible in other ones. For a structure likely to be excited in different directions, the choice of the modal basis will result from the application of criterion (2.194) to all relevant directions.

2.9.6 Method of additional masses

The method of additional masses is an approximate technique that allows one to treat the response to ground acceleration excitation as a response to external forces, which are easily determined from the sole knowledge of the support motion.

One way to present it consist of regarding the imposed motion to the support as a set of kinematic constraints to be fulfilled by the system. It has been seen in Chapter 1, Section 1.6 that constraints can be solved exactly using the Lagrange multipliers method. They can also be treated in an approximate manner as done here using the concept of penalty. It is classical to use the penalty method to impose constraints on displacements, it is not usual to apply it to introduce constraints on accelerations.

In order to develop the method of additional masses, let us consider the following equation of virtual work:

$$\delta \mathbf{q}^T (\mathbf{K} \mathbf{q} + \mathbf{M} \ddot{\mathbf{q}}) + \delta \mathbf{q}_2^T \mathbf{M}_{22}^0 (\ddot{\mathbf{q}}_2 - \ddot{\bar{\mathbf{q}}}_2) = 0 \quad (2.195)$$

The second term in (2.195) has been introduced to impose equality between the externally imposed accelerations $\ddot{\bar{\mathbf{q}}}_2$ and the computed ones $\ddot{\mathbf{q}}_2$. \mathbf{M}_{22}^0 is a symmetric and positive definite matrix of penalty coefficients. It has the physical meaning of additional masses attached to the support. The higher they are, the better are fulfilled the constraints.

The displacements \mathbf{q}_2 attached to the support can be extracted from the full set through a localization operation described by a Boolean matrix \mathbf{L}_2 :

$$\mathbf{q}_2 = \mathbf{L}_2 \mathbf{q}$$

and Equation (2.195) can be rewritten as:

$$\delta \mathbf{q}^T [\mathbf{K} \mathbf{q} + (\mathbf{M} + \mathbf{L}^T \mathbf{M}_{22}^0 \mathbf{L}) \ddot{\mathbf{q}} - \mathbf{L}^T \mathbf{M}_{22}^0 \ddot{\mathbf{q}}_2] = 0$$

yielding the modified equation of equilibrium:

$$\mathbf{K} \mathbf{q} + (\mathbf{M} + \mathbf{L}^T \mathbf{M}_{22}^0 \mathbf{L}) \ddot{\mathbf{q}} = \mathbf{L}^T \mathbf{M}_{22}^0 \ddot{\mathbf{q}}_2 \quad (2.196)$$

If the \mathbf{q} are ordered as:

$$\mathbf{q} = \begin{bmatrix} q_1 \\ q_2 \end{bmatrix} \quad \text{then} \quad \mathbf{L} = \begin{bmatrix} 0 & \mathbf{I} \end{bmatrix}$$

and the system (2.196) can be split in the form:

$$\begin{bmatrix} \mathbf{M}_{11} & \mathbf{M}_{12} \\ \mathbf{M}_{21} & \mathbf{M}_{22} + \mathbf{M}_{22}^0 \end{bmatrix} \begin{bmatrix} \ddot{\mathbf{q}}_1 \\ \ddot{\mathbf{q}}_2 \end{bmatrix} + \begin{bmatrix} \mathbf{K}_{11} & \mathbf{K}_{12} \\ \mathbf{K}_{21} & \mathbf{K}_{22} \end{bmatrix} \begin{bmatrix} \mathbf{q}_1 \\ \mathbf{q}_2 \end{bmatrix} = \begin{bmatrix} \mathbf{0} \\ \mathbf{M}_{22}^0 \ddot{\mathbf{q}}_2 \end{bmatrix} \quad (2.197)$$

The initial problem of response to ground acceleration is thus replaced by an equivalent problem with external forces on the support equal to the additional mass matrix multiplied by the imposed accelerations. The numerical solution of (2.196) does not require matrix partitioning as needed when developing the exact solution as done in Section 2.9.1.

The magnitude of the additional mass matrix is chosen large enough to keep the modelling error small. In practice, however, $\|\mathbf{M}_{22}^0\|$ should be kept between 10^2 and 10^4 times $\|\mathbf{M}_{11}\|$ in order to preserve the numerical conditioning of the mass matrix.

2.10 Variational methods for eigenvalue characterization

2.10.1 Rayleigh quotient

Let us start from the expression (1.27) of Hamilton's principle for a conservative system:

$$\delta \int_{t_1}^{t_2} (\mathcal{T} - \mathcal{V}) dt = 0$$

with the kinetic and potential energy quadratic forms:

$$\mathcal{T} = \frac{1}{2} \dot{\mathbf{q}}^T \mathbf{M} \dot{\mathbf{q}} \quad \text{and} \quad \mathcal{V} = \frac{1}{2} \mathbf{q}^T \mathbf{K} \mathbf{q}$$

If one assumes that, in a free vibration, the generalized coordinates vibrate in phase:

$$\mathbf{q} = \mathbf{x} \cos(\omega t + \phi) \quad (2.198)$$

the kinetic and potential energies take the form:

$$\mathcal{T} = \mathcal{T}_{\max} \sin^2(\omega t + \phi) \quad \text{and} \quad \mathcal{V} = \mathcal{V}_{\max} \cos^2(\omega t + \phi)$$

where $2\mathcal{T}_{max} = \omega^2 \mathbf{x}^T \mathbf{M} \mathbf{x}$ and $2\mathcal{V}_{max} = \mathbf{x}^T \mathbf{K} \mathbf{x}$. Hamilton's principle is then applied while varying the components of the spatial part of the solution, \mathbf{x} .

Because the variations of solution (2.198) must vanish at the limits t_1 and t_2 , one takes:

$$\omega t_1 + \phi = -\frac{\pi}{2} \quad \omega t_2 + \phi = \frac{\pi}{2}$$

since this choice implies that:

$$\delta \mathbf{q} = \delta \mathbf{x} \cos(\omega t + \phi)$$

is equal to zero at times $t = t_1$ and $t = t_2$ for arbitrary \mathbf{x} . Hamilton's principle then leads to the well-known *Rayleigh principle* (Lord Rayleigh 1894, Meirovitch 1967):

$$\delta_{\mathbf{x}} \mathcal{T}_{max} = \delta_{\mathbf{x}} \mathcal{V}_{max}$$

and the equations of motion take the form:

$$(\mathbf{K} - \omega^2 \mathbf{M}) \mathbf{x} = \mathbf{0} \quad (2.199)$$

which is the eigenvalue Equation (2.29) governing the motion amplitude of a free vibration mode.

Finally, let us note that if \mathbf{x} is an eigenmode, the following equality holds:

$$\omega^2 = \frac{\mathbf{x}^T \mathbf{K} \mathbf{x}}{\mathbf{x}^T \mathbf{M} \mathbf{x}} \quad (2.200)$$

The quotient so introduced is the *Rayleigh quotient*. It plays a fundamental role in the variational approach to the eigenvalue problem.

2.10.2 Principle of best approximation to a given eigenvalue

The principle of best approximation to an eigenvalue stipulates that:

When the Rayleigh quotient (2.200) is computed with a first-order error on the eigenmode $\mathbf{x}_{(r)}$, namely

$$\mathbf{x} = \mathbf{x}_{(r)} + \epsilon \mathbf{y} \quad (2.201)$$

it yields an approximation of the associated eigenvalue ω_r^2 with an error of second-order.

In other words, the quotient (2.200) remains *stationary* in the vicinity of an eigenvalue of the system.

Let us suppose that vector \mathbf{x} is an estimation of eigenvector $\mathbf{x}_{(r)}$ obtained from an iterative procedure. In order to measure the discrepancy with respect to mode $\mathbf{x}_{(r)}$, one may assume that the generalized mass is kept constant:

$$\mathbf{x}^T \mathbf{M} \mathbf{x} = \mathbf{x}_{(r)}^T \mathbf{M} \mathbf{x}_{(r)} \quad (2.202)$$

since, if one recalls the homogeneous form of the Rayleigh quotient, the eigenmodes are defined only to an arbitrary scale factor. The assumptions (2.201) and (2.202) give the

relationship:

$$\mathbf{y}^T \mathbf{M} \mathbf{x}_{(r)} = -\frac{\epsilon}{2} \mathbf{y}^T \mathbf{M} \mathbf{y} \quad (2.203)$$

which shows that the error vector \mathbf{y} is orthogonal to eigenmode $\mathbf{x}_{(r)}$ to the first order.

Let us next explicitly define the Rayleigh quotient:

$$\begin{aligned} \omega^2 &= \frac{\mathbf{x}^T \mathbf{K} \mathbf{x}}{\mathbf{x}^T \mathbf{M} \mathbf{x}} = \frac{\mathbf{x}_{(r)}^T \mathbf{K} \mathbf{x}_{(r)} + 2\epsilon \mathbf{x}_{(r)}^T \mathbf{K} \mathbf{y} + \epsilon^2 \mathbf{y}^T \mathbf{K} \mathbf{y}}{\mathbf{x}_{(r)}^T \mathbf{M} \mathbf{x}_{(r)}} \\ &= \omega_r^2 + 2\epsilon \frac{\mathbf{x}_{(r)}^T \mathbf{K} \mathbf{y}}{\mathbf{x}_{(r)}^T \mathbf{M} \mathbf{x}_{(r)}} + \epsilon^2 \frac{\mathbf{y}^T \mathbf{K} \mathbf{y}}{\mathbf{x}_{(r)}^T \mathbf{M} \mathbf{x}_{(r)}} \end{aligned}$$

By noticing that

$$\mathbf{K} \mathbf{x}_{(r)} = \omega_r^2 \mathbf{M} \mathbf{x}_{(r)}$$

and owing to the relationship (2.203), the following expression of the eigenvalue error is finally obtained:

$$\delta\omega^2 = \omega^2 - \omega_r^2 = \epsilon^2 \frac{\mathbf{y}^T (\mathbf{K} - \omega_r^2 \mathbf{M}) \mathbf{y}}{\mathbf{x}_{(r)}^T \mathbf{M} \mathbf{x}_{(r)}} \quad (2.204)$$

This expression is effectively of second order and the Rayleigh quotient is thus stationary in the vicinity of an eigenmode. It is, however, not possible to characterize this extremum as a maximum or minimum without restricting the space of comparison vectors, since the matrix $(\mathbf{K} - \omega_r^2 \mathbf{M})$ is not positive definite.

It is noteworthy that (2.204) immediately provides the second derivative matrix (*Hessian matrix*) of the Rayleigh quotient at a stationary point:

$$\begin{aligned} H_{(\mathbf{x}=\mathbf{x}_{(r)})} &= \left(\frac{\partial^2}{\partial x_i \partial x_j} \left(\frac{\mathbf{x}^T \mathbf{K} \mathbf{x}}{\mathbf{x}^T \mathbf{M} \mathbf{x}} \right) \right)_{\mathbf{x}=\mathbf{x}_{(r)}} \\ &= \frac{(\mathbf{K} - \omega_r^2 \mathbf{M})}{\mathbf{x}_{(r)}^T \mathbf{M} \mathbf{x}_{(r)}} \end{aligned} \quad (2.205)$$

It is of rank $(n - 1)$, indicating from a geometric point of view the existence of a line of zero curvature, issuing from the origin, which is the locus of the points \mathbf{x} such that $\omega^2 = \omega_r^2$.

2.10.3 Recurrent variational procedure for eigenvalue analysis

Let us go back to result (2.204) of the previous section and expand the eigenmode error in terms of the system eigenmodes $\mathbf{x}_{(k)}$:

$$\mathbf{y} = \sum_{k=1}^n \alpha_k \mathbf{x}_{(k)}$$

One finally obtains:

$$\delta\omega^2 = \omega^2 - \omega_r^2 = \epsilon^2 \sum_{k=1}^n \sum_{\ell=1}^n \alpha_k \alpha_\ell \frac{\mathbf{x}_{(k)}^T (\mathbf{K} - \omega_r^2 \mathbf{M}) \mathbf{x}_{(\ell)}}{\mathbf{x}_{(r)}^T \mathbf{M} \mathbf{x}_{(r)}} \quad (2.206)$$

Owing to the orthogonality relationships:

$$\mathbf{x}_{(k)}^T \mathbf{M} \mathbf{x}_{(\ell)} = \mu_k \delta_{k\ell}$$

and equality:

$$\mathbf{K} \mathbf{x}_{(k)} = \omega_k^2 \mathbf{M} \mathbf{x}_{(k)}$$

one obtains:

$$\delta\omega^2 = \omega^2 - \omega_r^2 = \epsilon^2 \sum_{\substack{k=1 \\ k \neq r}}^n \alpha_k^2 (\omega_k^2 - \omega_r^2) \frac{\mu_k}{\mu_r} \quad (2.207)$$

Let us next restrict the search for the stationary points of quotient (2.200) in the subspace orthogonal to the previously computed $r - 1$ eigenmodes (as is typically done in iterative eigensolvers, see for instance Section 6.5.2):

$$\mathbf{x}^T \mathbf{M} \mathbf{x}_{(j)} = 0 \quad j = 1, \dots, r - 1 \quad (2.208)$$

In that case, $\alpha_k = 0$ for $k < r$ so that one obtains:

$$\delta\omega^2 = \omega^2 - \omega_r^2 = \epsilon^2 \sum_{k=r+1}^n \alpha_k^2 (\omega_k^2 - \omega_r^2) \frac{\mu_k}{\mu_r} \geq 0 \quad (2.209)$$

Hence the *recursive* method to compute eigenvalues:

The r th eigenvalue ω_r^2 of the linear system (2.199) and the associated eigenmode $\mathbf{x}_{(r)}$ are the minimum value and the corresponding minimum point of the functional:

$$\omega^2 = \frac{\mathbf{x}^T \mathbf{K} \mathbf{x}}{\mathbf{x}^T \mathbf{M} \mathbf{x}} \quad (2.210)$$

in the subspace orthogonal to the $(r - 1)$ first eigenvectors:

$$\mathbf{x} : \{\mathbf{x}^T \mathbf{M} \mathbf{x}_{(j)} = 0, \quad \forall j = 1, \dots, r - 1\} \quad (2.211)$$

2.10.4 Eigensolutions of constrained systems: general comparison principle or monotonicity principle

Introducing the Rayleigh quotient becomes particularly useful when considering the problem of computing the eigensolutions in the presence of constraints. A constraint imposed on the system takes the algebraic form:

$$f(x_1, \dots, x_n) = 0 \quad (2.212)$$

and must be compatible with the equilibrium position, hence:

$$f(0, \dots, 0) = 0$$

Under the linear vibration assumption, the constraint can be linearized in the neighbourhood of the equilibrium position:

$$f(x_1, \dots, x_n) \simeq \left(\frac{\partial f}{\partial x_1} \right)_0 x_1 + \dots + \left(\frac{\partial f}{\partial x_n} \right)_0 x_n$$

giving the linear form:

$$c_1 x_1 + \dots + c_n x_n = 0$$

which can be put in the more concise form:

$$\mathbf{c}^T \mathbf{x} = 0 \quad (2.213)$$

The new system now has $(n - 1)$ degrees of freedom and thus $(n - 1)$ eigensolutions, which can be denoted:

$$\begin{cases} \tilde{\omega}_1^2 \leq \tilde{\omega}_2^2 \leq \dots \leq \tilde{\omega}_{n-1}^2 \\ \tilde{\mathbf{x}}_{(1)}, \tilde{\mathbf{x}}_{(2)}, \dots, \tilde{\mathbf{x}}_{(n-1)} \end{cases}$$

It is also possible to introduce the projection operator concept: let an arbitrary vector \mathbf{x} be defined in the initial space \mathbb{E}_n . It is possible to construct a projection operator \mathbf{P} so that vector $\mathbf{P}\mathbf{x}$ is orthogonal to the plane of the constraint (2.213):

$$\mathbf{P} = \mathbf{I} - \frac{\mathbf{c}\mathbf{c}^T}{\mathbf{c}^T\mathbf{c}} \quad (2.214)$$

Indeed its application to \mathbf{z} yields:

$$\mathbf{P}\mathbf{z} = \mathbf{z} - \mathbf{c} \frac{\mathbf{c}^T\mathbf{z}}{\mathbf{c}^T\mathbf{c}}$$

and

$$\mathbf{c}^T\mathbf{P}\mathbf{z} = \mathbf{c}^T\mathbf{z} - \mathbf{c}^T\mathbf{z} = 0$$

More generally, the system may be submitted to a number $m < n$ of linear constraints which reduce to $(n - m)$ its number of degrees of freedom and eigensolutions:

$$\mathbf{c}_j^T \mathbf{x} = 0 \quad j = 1, \dots, m \quad (2.215)$$

The projection operator:

$$\mathbf{P} = \mathbf{I} - \sum_{j=1}^m \frac{\mathbf{c}_j\mathbf{c}_j^T}{\mathbf{c}_j^T\mathbf{c}_j} \quad (2.216)$$

projects an arbitrary vector \mathbf{z} orthogonally to the planes of constraints (2.213). It is intuitively obvious that:

If the admissible solutions of a minimization problem are constrained to verify a certain number of additional constraints, the problem so modified admits an absolute minimum which is certainly not lower than the minimum of the initial problem.

This general statement results simply from the fact that all the admissible solutions of the modified system are also admissible solutions of the initial system. It is known as the *general comparison principle*, or *monotonicity principle*.

2.10.5 Courant's minimax principle to evaluate eigenvalues independently of each other

Courant's principle (Courant and Hilbert 1953, Fraeijs de Veubeke *et al.* 1972) states that

The r th eigenvalue of a vibrating system is the maximum value that the minimum of the Rayleigh quotient can take when subjected to $(r - 1)$ additional constraints:

$$\omega_r^2 = \max_{\substack{\mathbf{c}_i \\ i < r}} \left\{ \min_{\mathbf{x} : \mathbf{c}_i^T \mathbf{x} = 0} \left\{ \frac{\mathbf{x}^T \mathbf{K} \mathbf{x}}{\mathbf{x}^T \mathbf{M} \mathbf{x}} \right\} \right\} \quad (2.217)$$

The proof holds as follows. Let the functional:

$$\omega^2 = \frac{\mathbf{x}^T \mathbf{K} \mathbf{x}}{\mathbf{x}^T \mathbf{M} \mathbf{x}} \quad (2.218)$$

be minimized with respect to \mathbf{x} under the $(r - 1)$ linear constraints:

$$\mathbf{c}_i^T \mathbf{x} = 0 \quad i = 1, \dots, r - 1 \quad (2.219)$$

Let us first note that this functional ω^2 has a minimum equal to eigenvalue ω_r^2 when submitted to the $(r - 1)$ constraints:

$$\mathbf{c}_i = \mathbf{M} \mathbf{x}_{(i)} \quad i = 1, \dots, r - 1 \quad (2.220)$$

since the recurrent calculation of the eigenvalues (Section 2.10.3) states that:

$$\left\{ \begin{array}{l} \min_{\mathbf{x}} \frac{\mathbf{x}^T \mathbf{K} \mathbf{x}}{\mathbf{x}^T \mathbf{M} \mathbf{x}} = \omega_r^2 \\ \mathbf{x} : \{ \mathbf{c}_i^T \mathbf{x} = \mathbf{x}_{(i)}^T \mathbf{M} \mathbf{x} = 0 \} \end{array} \right\} \quad (2.221)$$

It remains thus to show that any other set of $(r - 1)$ constraints \mathbf{c}_i results in a minimum for the functional ω^2 that is lower than ω_r^2 .

Let us therefor expand the trial solution \mathbf{x} in terms of eigenmodes of the nonconstrained system (assumed mass-normalized):

$$\mathbf{x} = a_1 \mathbf{x}_{(1)} + \dots + a_n \mathbf{x}_{(n)} \quad (2.222)$$

Since the functional ω^2 is invariable with the norm of \mathbf{x} , we impose as before that:

$$\mathbf{x}^T \mathbf{M} \mathbf{x} = \sum_{j=1}^n a_j^2 = 1 \quad (2.223)$$

and the functional is written as:

$$\omega^2 = \mathbf{x}^T \mathbf{K} \mathbf{x} = \sum_{j=1}^n \omega_j^2 a_j^2 \quad (2.224)$$

Substituting (2.222) in the constraints (2.219), one finds the constraint equations for the modal coordinates a_j :

$$\sum_{j=1}^n (\mathbf{c}_i^T \mathbf{x}_{(j)}) a_j = \bar{\mathbf{c}}_i^T \mathbf{a} = 0 \quad i = 1, \dots, r - 1 \quad (2.225)$$

It is permissible to choose:

$$a_{r+1} = \dots = a_n = 0 \quad (2.226)$$

since it leaves r coordinates a_j , $j \leq r$, to satisfy the r conditions expressed by (2.223) and (2.225). Let us call such a choice \mathbf{a}^* . The functional (2.224) for this selection is:

$$\omega^2(\mathbf{a}^*) = \sum_{j=1}^r \omega_j^2 a_j^{*2} \quad (2.227)$$

This result can be bounded by:

$$\omega^2(\mathbf{a}^*) \leq \omega_r^2 \sum_{j=1}^r a_j^{*2} = \omega_r^2 \quad (2.228)$$

and since this is only a particular choice for a_j we also have that:

$$\min_{\mathbf{x}: \mathbf{c}_i^T \mathbf{x} = 0} \omega^2 = \min_{\mathbf{a}: \tilde{\mathbf{c}}_i^T \mathbf{a} = 0} \omega^2(\mathbf{a}) \leq \omega^2(\mathbf{a}^*) \leq \omega_r^2 \quad (2.229)$$

This result was obtained for an arbitrary set of $(r - 1)$ constraints \mathbf{c}_i and thus we can conclude that no $(r - 1)$ constraints will yield a minimum for ω^2 higher than ω_r^2 , which concludes the proof.

In theory, Courant's principle (Courant and Hilbert 1953) allows the determination of a given eigenvalue without prior knowledge on other eigenvalues. It is, however, of no practical use to compute the eigenvalues directly. On the other hand, it makes it possible to get results of considerable practical importance such as Rayleigh's theorem on constraints.

2.10.6 Rayleigh's theorem on constraints (eigenvalue bracketing)

Courant's principle allows prediction of the direction in which the eigenspectrum alteration will occur when the system is modified by the addition of m constraints:

$$\mathbf{g}_j^T \mathbf{x} = 0 \quad j = 1, \dots, m \quad (2.230)$$

on the admissible displacement modes \mathbf{x} .

The constraints (2.230) may be written in the form:

$$\begin{bmatrix} \mathbf{g}_1^T \\ \vdots \\ \mathbf{g}_m^T \end{bmatrix} \mathbf{x} = [\mathbf{G}_m \quad \mathbf{G}_{n-m}] \mathbf{x} = [\mathbf{G}_m \quad \mathbf{G}_{n-m}] \begin{bmatrix} x_1 \\ \vdots \\ x_m \\ \mathbf{v} \end{bmatrix} = \mathbf{0} \quad (2.231)$$

where \mathbf{G}_m is a square matrix of full rank and where \mathbf{v} collects the $(n - m)$ independent degrees of freedom. The expression of \mathbf{x} as a function of \mathbf{v} takes the form:

$$\mathbf{x} = \begin{bmatrix} -\mathbf{G}_m^{-1} \mathbf{G}_{n-m} \\ \mathbf{I} \end{bmatrix} \mathbf{v} \quad (2.232)$$

or

$$\mathbf{x} = \mathbf{A}\mathbf{v}$$

The minimum of Rayleigh quotient in the subspace orthogonal to the constraint planes is also the minimum of:

$$\tilde{\omega}^2 = \frac{\mathbf{v}^T(\mathbf{A}^T\mathbf{K}\mathbf{A})\mathbf{v}}{\mathbf{v}^T(\mathbf{A}^T\mathbf{M}\mathbf{A})\mathbf{v}} = \frac{\mathbf{v}^T\tilde{\mathbf{K}}\mathbf{v}}{\mathbf{v}^T\tilde{\mathbf{M}}\mathbf{v}} \quad (2.233)$$

The matrices:

$$\tilde{\mathbf{K}} = \mathbf{A}^T\mathbf{K}\mathbf{A} \quad (2.234a)$$

$$\tilde{\mathbf{M}} = \mathbf{A}^T\mathbf{M}\mathbf{A} \quad (2.234b)$$

are the reduced stiffness and mass matrices of the system.

According to Courant's minimax property (Section 2.10.5), the r th eigenvalue, $\tilde{\omega}_r^2$, corresponds to the largest value that the minimum of Rayleigh quotient (2.233) can take when submitted to $(r-1)$ additional constraints $\mathbf{c}_i^T\mathbf{x} = \mathbf{c}_i^T\mathbf{A}\mathbf{v} = 0$, $i = 1, \dots, r-1$:

$$\begin{aligned} \tilde{\omega}_r^2 &= \max_{\substack{\mathbf{c}_i \\ i < r}} \left\{ \min_{\mathbf{v}: \mathbf{c}_i^T\mathbf{A}\mathbf{v}=0} \left\{ \frac{\mathbf{v}^T\tilde{\mathbf{K}}\mathbf{v}}{\mathbf{v}^T\tilde{\mathbf{M}}\mathbf{v}} \right\} \right\} \\ &= \max_{\mathbf{c}} \tilde{m}(\mathbf{c}_1, \dots, \mathbf{c}_{r-1}) \end{aligned} \quad (2.235)$$

This result may also be written:

$$\begin{aligned} \tilde{\omega}_r^2 &= \max_{\substack{\mathbf{c}_i \\ i < r}} \left\{ \min_{\mathbf{x}: \begin{cases} \mathbf{x}^T\mathbf{c}_i=0 \\ \mathbf{x}^T\mathbf{g}_j=0 \end{cases}} \left\{ \frac{\mathbf{x}^T\mathbf{K}\mathbf{x}}{\mathbf{x}^T\mathbf{M}\mathbf{x}} \right\} \right\} \\ &= \max_{\mathbf{c}} m(\mathbf{c}_1, \dots, \mathbf{c}_{r-1}; \mathbf{g}_1, \dots, \mathbf{g}_m) \end{aligned} \quad (2.236)$$

by allowing only the constraints \mathbf{c} to be varied. Courant's theorem also allows one to compute the eigenvalues ω_r^2 and ω_{r+m}^2 of the initial problem in the following manner:

$$\omega_r^2 = \max_{\mathbf{c}} m(\mathbf{c}_1, \dots, \mathbf{c}_{r-1}) \quad (2.237)$$

and

$$\omega_{r+m}^2 = \max_{\mathbf{c}, \mathbf{g}} m(\mathbf{c}_1, \dots, \mathbf{c}_{r-1}; \mathbf{g}_1, \dots, \mathbf{g}_m) \quad (2.238)$$

– On one hand, by applying the monotonicity principle one obtains:

$$\omega_r^2 \leq \tilde{\omega}_r^2 \quad (2.239)$$

since $\tilde{\omega}_r^2$ is computed from the minimum problem in which the class of admissible solutions \mathbf{x} is reduced to the subspace orthogonal to the constraints (2.230).

– On the other hand:

$$\tilde{\omega}_r^2 \leq \omega_{r+m}^2 \quad (2.240)$$

since the eigenvalue ω_{r+m}^2 of the initial problem is obtained from Courant's principle by varying all the constraints simultaneously in the minimax problem (2.238).

Hence the statement of Rayleigh's theorem:

If m arbitrary constraints (2.230) are imposed on an eigenvalue problem, the eigenvalues $\tilde{\omega}^2$ of the modified problem are bracketed by those of the initial problem according to the inequality

$$\omega_r^2 \leq \tilde{\omega}_r^2 \leq \omega_{r+m}^2 \quad (2.241)$$

2.11 Conservative rotating systems

The small free vibrations of a conservative rotating system are governed by the general Equations (2.18):

$$\mathbf{M}\ddot{\mathbf{q}} + \mathbf{G}\dot{\mathbf{q}} + \mathbf{K}^*\mathbf{q} = \mathbf{0} \quad (2.242)$$

where \mathbf{K}^* is the stiffness matrix modified by the presence of centrifugal forces, and \mathbf{G} is the skew-symmetric gyroscopic matrix. In this section we will study the properties of these particular dynamic systems.

2.11.1 Energy conservation in the absence of external force

Premultiplying Equations (2.242) by $\dot{\mathbf{q}}^T$ yields:

$$\dot{\mathbf{q}}^T \mathbf{M} \ddot{\mathbf{q}} + \dot{\mathbf{q}}^T \mathbf{G} \dot{\mathbf{q}} + \dot{\mathbf{q}}^T \mathbf{K}^* \mathbf{q} = 0$$

By invoking next the skew-symmetry of \mathbf{G} :

$$\dot{\mathbf{q}}^T \mathbf{G} \dot{\mathbf{q}} = 0$$

indicating that gyroscopic (apparent) forces, unlike damping forces, do not dissipate energy nor do they introduce energy to in the system. They only transfer energy from one generalized coordinate to another. The energy conservation can then be written in the form:

$$\frac{d}{dt}(\mathcal{T}_2 + \mathcal{V} - \mathcal{T}_0) = 0 \quad (2.243)$$

and may further be rewritten as:

$$\frac{d}{dt}(\mathcal{T}_2 + \mathcal{V}) = \frac{d}{dt}\mathcal{T}_0$$

expressing that the variation rate of the relative energy is equilibrated by the power required to drive the system.

2.11.2 Properties of the eigensolutions of the conservative rotating system

Let us express the general solution of Equations (2.242) in the form:

$$\mathbf{q}(t) = \mathbf{x}e^{\lambda t}$$

where \mathbf{x} is a vector of amplitudes and where λ is the inverse of a time constant.

\mathbf{x} and λ are solutions of the eigenvalue problem:

$$(\mathbf{K}^* + \lambda \mathbf{G} + \lambda^2 \mathbf{M}) \mathbf{x} = \mathbf{0} \quad (2.244)$$

Owing to the skew-symmetry of \mathbf{G} , the determinant of (2.244):

$$\Delta(\lambda) = \det(\mathbf{K}^* + \lambda \mathbf{G} + \lambda^2 \mathbf{M}) \quad (2.245)$$

is such that

$$\begin{aligned} \Delta(\lambda) &= \det(\mathbf{K}^* + \lambda \mathbf{G} + \lambda^2 \mathbf{M}) = \det(\mathbf{K}^* + \lambda \mathbf{G} + \lambda^2 \mathbf{M})^T \\ &= \det(\mathbf{K}^* - \lambda \mathbf{G} + \lambda^2 \mathbf{M}) = \Delta(-\lambda) \end{aligned} \quad (2.246)$$

Since the eigenvalues λ , root of the polynomial (2.245), come in real or complex conjugate pairs, and since they must have opposite signs according to (2.246), they must be either real or imaginary. They are thus necessarily of the following types:

- i. pairs of real eigenvalues $\lambda = \pm\alpha$. In this case, the positive one is generating an instability of the solution.

Substituting a real eigenvalue α into (2.244) shows that the corresponding eigenvector \mathbf{x} can be put in real form:

$$(\mathbf{K}^* + \alpha \mathbf{G} + \alpha^2 \mathbf{M}) \mathbf{x} = \mathbf{0}$$

and premultiplying by \mathbf{x}^T provides the result:

$$\alpha^2 = -\frac{\mathbf{x}^T \mathbf{K}^* \mathbf{x}}{\mathbf{x}^T \mathbf{M} \mathbf{x}} \quad (2.247)$$

which shows that the existence of a real eigenvalue α is possible only if the effective stiffness matrix is not positive-definite. The existence of real eigenvalues can in fact be linked to the sign of $\det(\mathbf{K}^*)$. Indeed from (2.245) it can be observed that $\Delta(0) = \det(\mathbf{K}^*)$ and, for λ real, $\lim_{\lambda \rightarrow \infty} \Delta(\lambda) = \infty$, so that at least one real positive eigenvalue will always occur if $\det(\mathbf{K}^*) < 0$.

Furthermore, considering the eigenvalues $\sigma_j(\mathbf{K}^*)$ of the modified stiffness matrix and observing that $\det(\mathbf{K}^*) = \prod_j \sigma_j(\mathbf{K}^*)$, the sign of $\det(\mathbf{K}^*)$ will clearly be negative (and the system unstable) under the condition that \mathbf{K}^* has an odd number of negative eigenvalues σ_j .

- ii. Pairs of imaginary eigenvalues $\lambda = \pm i\omega$.

When there is no real eigenvector \mathbf{x} such that $\mathbf{x}^T \mathbf{K}^* \mathbf{x} < 0$, there is no real eigenvalue to the system. All the eigenvalues consist of pairs of imaginary eigenvalues $\pm i\omega$ that generate oscillatory contributions to the response at vibration frequency ω (thus positive), and the system remains stable.

Substituting an imaginary eigenvalue $i\omega$ into (2.244) shows that the corresponding eigenvector must now be complex:

$$(\mathbf{K}^* + i\omega \mathbf{G} - \omega^2 \mathbf{M}) (\mathbf{y} + i\mathbf{z}) = \mathbf{0} \quad (2.248)$$

It is straightforward to show that mode associated to the conjugate eigenvalue $-i\omega$ is the conjugate mode $(\mathbf{y} - i\mathbf{z})$. Indeed if (2.248) holds then:

$$(\mathbf{K}^* - i\omega \mathbf{G} - \omega^2 \mathbf{M}) (\mathbf{y} - i\mathbf{z}) = \mathbf{0}$$

which can be verified by comparing the real and imaginary parts of this relation and of (2.248).

2.11.3 State-space form of equations of motion

The aim of this section is to solve (2.242) through mode superposition. However, modal analysis in the form discussed for nonrotating systems is no longer applicable here, since a projection upon the space of the eigenmodes of $(\mathbf{K} - \omega^2 \mathbf{M})$ does not allow one to uncouple the equations of the system. It will be seen that uncoupling is made possible here through projection on the eigenmodes calculated in the state-space.

In order to transform the system (2.242) of n second-order differential equations into a system of $2n$ first-order equations, let us define the state vector:

$$\mathbf{r}^T = [\dot{\mathbf{q}}^T \ \mathbf{q}^T] \quad (2.249)$$

and the system matrices:

$$\mathbf{A} = \begin{bmatrix} \mathbf{M} & \mathbf{0} \\ \mathbf{0} & \mathbf{K}^* \end{bmatrix} \quad \mathbf{B} = \begin{bmatrix} \mathbf{G} & \mathbf{K}^* \\ -\mathbf{K}^* & \mathbf{0} \end{bmatrix} \quad (2.250)$$

The original second-order system (2.242) is equivalent to the first-order system of dimension $2n$:

$$\mathbf{A}\dot{\mathbf{r}} + \mathbf{B}\mathbf{r} = \mathbf{0} \quad (2.251)$$

where \mathbf{A} is symmetric while \mathbf{B} is skew-symmetric. \mathbf{A} is also positive definite if \mathbf{K}^* is so.

The general solution of Equation (2.251) can be expressed in the form:

$$\mathbf{r} = \mathbf{y}e^{\lambda t}$$

where \mathbf{y} is now a vector of amplitudes of dimension $2n$.

\mathbf{y} and λ are solutions of the eigenvalue problem:

$$(\mathbf{B} + \lambda \mathbf{A})\mathbf{y} = \mathbf{0} \quad (2.252)$$

which admits $2n$ eigenvectors $\mathbf{y}_{(r)}$ associated with the eigenvalues λ_r obtained by solving the characteristic equation:

$$\det(\mathbf{B} + \lambda \mathbf{A}) = 0$$

Example 2.9

Let us consider again the system of Figure 1.10 where a mass is linked through springs to an inertia wheel rotating at a constant and imposed speed. In order to investigate the stability of the system in the absence of damping, we have to solve the eigenvalue problem (2.244) for λ , considering the linearized mass, gyroscopic and effective stiffness matrices obtained for the

motion around the equilibrium position at the center of the wheel:

$$\mathbf{M} = \begin{bmatrix} m & 0 \\ 0 & m \end{bmatrix} \quad \mathbf{G} = \begin{bmatrix} 0 & -2m\Omega \\ 2m\Omega & 0 \end{bmatrix} \quad \mathbf{K}^* = \begin{bmatrix} k_1 - \Omega^2 m & 0 \\ 0 & k_2 - \Omega^2 m \end{bmatrix}$$

Let us assume that $m = 1$, $k_1 = 50$ and $k_2 = 98$. The natural frequencies of the nonrotating system are:

$$\omega_1 = \sqrt{2k_1/m} = 10 \quad \text{in the } x \text{ direction}$$

$$\omega_2 = \sqrt{2k_2/m} = 14 \quad \text{in the } y \text{ direction.}$$

We observe that

- when $\Omega < \omega_1$, $\sigma(\mathbf{K}^*)$ contains 2 strictly positive eigenvalues so that $\det(\mathbf{K}^*) > 0$ and \mathbf{K}^* is positive definite;
- when $\omega_1 < \Omega < \omega_2$, $\sigma(\mathbf{K}^*)$ contains one strictly negative eigenvalue so that $\det(\mathbf{K}^*) < 0$;
- when $\Omega > \omega_2$, $\sigma(\mathbf{K}^*)$ contains 2 strictly negative eigenvalues and therefore $\det(\mathbf{K}^*) > 0$ (\mathbf{K}^* being negative definite).

Setting up the state-space form (2.251), one can solve the standard eigenvalue problem (2.252) for λ (e.g. using Matlab®). In Figure 2.13.a we have plotted the real and imaginary part of all eigenvalues λ when the rotation speed is varied from 0 to 25.

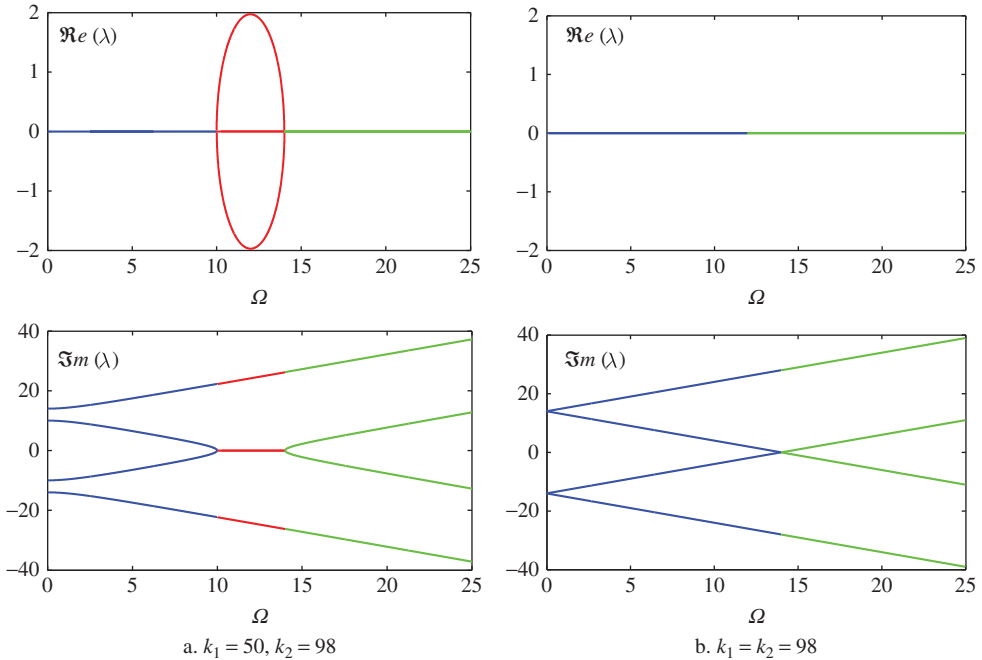


Figure 2.13 Real and imaginary parts of λ vs. rotation speed Ω for the inertia wheel problem.

It is seen that

- for $\Omega < \omega_1$, all λ are purely imaginary. One of the conjugate pair tends towards zero (oscillation with decreasing frequency) while the other conjugate pair corresponds to an increasing frequency. The system is stable.
- for $\omega_1 < \Omega < \omega_2$, two eigenvalues λ become purely real, one positive, one negative. The system is unstable. The two other λ are the purely imaginary ones corresponding to an increasing frequency.
- for $\omega_2 < \Omega$, all eigenvalues λ are again purely imaginary. The system is stable.

These results are in agreement with the theory. The re-stabilization of the system for $\Omega > \omega_2$ (negative definite \mathbf{K}^*) is clearly due to the presence of the gyroscopic forces. If we now take $k_1 = k_2 = k$, $\omega_1 = \omega_2$, $\det(\mathbf{K}^*)$ is always positive except for the critical speed $\Omega_{cr} = \sqrt{k/m}$. The values of λ are plotted in Figure 2.13.b. Clearly the equilibrium position is now stable for any $\Omega \neq \Omega_{cr}$.

Let us note that the stability we investigate here corresponds to the stability of the equilibrium when the system is in free motion (no external force). However, in practice, rotating systems are very often submitted to external forces due for instance to bearing supports, unbalanced masses or fluctuating forces such as aerodynamic forces on the blades of turbines. Hence, in nearly every practical application, rotation systems are submitted to external excitations that have a frequency equal to N times the rotation speed (N being called the order of the excitation or engine order). For instance,

- gravity will introduce a harmonic excitation in the rotating frame with a frequency equal to the rotation speed;
- for a disk equipped with M blades mounted on a turbine shaft, the aerodynamic loads being generated by a nonuniform flow will introduce a disturbance of frequency $M\Omega$ and possibly secondary harmonics at frequencies multiple of $M\Omega$.

Hence, in rotating systems, one should check if the relevant engine orders coincide with system eigenvalues since instabilities related to resonance would then appear.

To that purpose, let us consider the graph of the imaginary part of λ (i.e. frequencies) as function of the rotation speed in Figure 2.13.a. (known as Campbell diagrams). In dynamic analysis

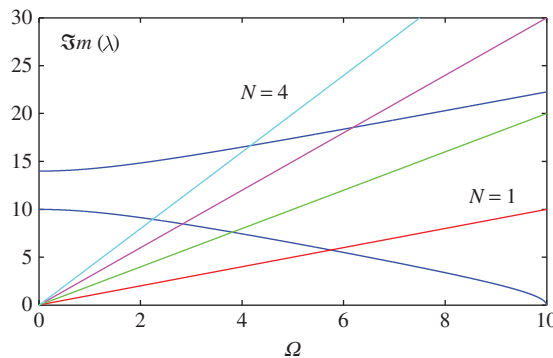


Figure 2.14 Campbell diagram: engine orders and resonance of rotating systems.

of rotating systems it is then customary to plot lines $\omega = N\Omega$ corresponding to relevant engine orders (see Figure 2.14): the intersection between the engine order lines and the eigenfrequency curves indicate resonance points and therefore rotation speeds that must be avoided when operating the system.

The study of these phenomena is beyond this text, but one should be aware that, in rotating systems, the stability of the equilibrium in free motion is not always the most dangerous phenomenon since resonance with engine orders can happen for much lower Ω .

2.11.4 Eigenvalue problem in symmetrical form

The eigenvalue problem (2.252) involves the skew-symmetric matrix \mathbf{B} . Its solution may, however, be obtained from the solution of an associated symmetric eigenproblem obtained as follows.

Let us transform the original eigenproblem (2.252) by writing successively:

$$\begin{aligned}\mathbf{A}\mathbf{y} &= -\lambda^{-1}\mathbf{B}\mathbf{y} \\ \mathbf{y} &= -\lambda^{-1}\mathbf{A}^{-1}\mathbf{B}\mathbf{y} \\ \mathbf{B}\mathbf{y} &= -\lambda^{-1}\mathbf{B}\mathbf{A}^{-1}\mathbf{B}\mathbf{y} = +\lambda^{-1}\mathbf{B}^T\mathbf{A}^{-1}\mathbf{B}\mathbf{y}\end{aligned}$$

and thus

$$\mathbf{B}^T\mathbf{A}^{-1}\mathbf{B}\mathbf{y} = -\lambda^2\mathbf{A}\mathbf{y} = +\mu\mathbf{A}\mathbf{y} \quad (2.253)$$

where the system matrix $\mathbf{S} = \mathbf{B}^T\mathbf{A}^{-1}\mathbf{B}$ of the left-hand side is now symmetric. It follows from the results of Section 2.11.2 that Equation (2.253) admits pairs of equal eigenvalues:

- i. Pairs of positive eigenvalues μ associated to the imaginary eigenvalues of the original problem:

$$\sqrt{\mu} = \pm\omega \quad (2.254)$$

The corresponding eigenvectors are real and linearly independent. As shown hereafter, they correspond to the real and imaginary parts of the complex eigenmodes of the eigenvalue problem (2.252).

- ii. Pairs of negative eigenvalues μ associated to the real eigenvalues of the original problem:

$$\sqrt{-\mu} = \pm\alpha \quad (2.255)$$

The corresponding eigenvectors are also real and linearly independent. They necessarily correspond to linear combinations of the real eigenmodes of the eigenvalue problem (2.252).

Remark 2.3 Let us show that real and imaginary parts of the complex eigenmodes of the original eigenvalue problem (2.244) are in fact linearly independent solutions of the symmetric eigenproblem (2.253).

To that purpose, let us split the nonsymmetric state-space eigenproblem verified by one eigenpair $[i\omega_r, \mathbf{w}_{(r)} + i\mathbf{z}_{(r)}]$ into real and imaginary parts:

$$\mathbf{B}(\mathbf{w}_{(r)} + i\mathbf{z}_{(r)}) + i\omega_r\mathbf{A}(\mathbf{w}_{(r)} + i\mathbf{z}_{(r)}) = \mathbf{0}$$

or

$$\mathbf{B}\mathbf{w}_{(r)} = \omega_r\mathbf{A}\mathbf{z}_{(r)} \quad (2.256a)$$

$$\mathbf{B}\mathbf{z}_{(r)} = -\omega_r\mathbf{A}\mathbf{w}_{(r)} \quad (2.256b)$$

Solving Equation (2.256b) for the real part $\mathbf{w}_{(r)}$:

$$\mathbf{w}_{(r)} = -\frac{1}{\omega_r}\mathbf{A}^{-1}\mathbf{B}\mathbf{z}_{(r)}$$

substituting into Equation (2.256a) and taking into account the skew-symmetry of \mathbf{B} yields the eigenvalue equation verified by the imaginary part $\mathbf{z}_{(r)}$:

$$\mathbf{B}^T\mathbf{A}^{-1}\mathbf{B}\mathbf{z}_{(r)} - \omega_r^2\mathbf{A}\mathbf{z}_{(r)} = \mathbf{0} \quad (2.257)$$

Similarly, eliminating the imaginary part from Equations (2.256a) and (2.256b) yields a similar relationship for the real part $\mathbf{w}_{(r)}$:

$$\mathbf{B}^T\mathbf{A}^{-1}\mathbf{B}\mathbf{w}_{(r)} - \omega_r^2\mathbf{A}\mathbf{w}_{(r)} = \mathbf{0}$$

which shows that both real and imaginary parts of the eigenmodes are solutions of the same symmetric eigenproblem:

$$\mathbf{B}^T\mathbf{A}^{-1}\mathbf{B}\mathbf{y} - \omega^2\mathbf{A}\mathbf{y} = \mathbf{0} \quad (2.258)$$

The corresponding eigenvalues ω_r^2 are positive and have multiplicity 2. According to the degeneracy theorem (Section 2.3.2), $\mathbf{w}_{(r)}$ and $\mathbf{z}_{(r)}$ are linearly independent eigenvectors.

Remark 2.4 Let us show in the same way that the eigenvalues of the symmetric eigenproblem (2.253) associated to the real eigensolutions of (2.252) are negative and correspond respectively to sum and difference of the eigenmodes of the original eigenvalue problem.

To that purpose, let us denote by $(-\alpha_s, \mathbf{y}_{(s)})$ and $(+\alpha_s, \mathbf{y}_{(s+1)})$ the corresponding real eigenpair. They verify the eigenvalue equations:

$$\mathbf{B}\mathbf{y}_{(s)} = \alpha_s\mathbf{A}\mathbf{y}_{(s)} \quad (2.259a)$$

$$\mathbf{B}\mathbf{y}_{(s+1)} = -\alpha_s\mathbf{A}\mathbf{y}_{(s+1)} \quad (2.259b)$$

which provide the linear combinations:

$$\mathbf{B}(\gamma\mathbf{y}_{(s)} - \delta\mathbf{y}_{(s+1)}) = \alpha_s\mathbf{A}(\gamma\mathbf{y}_{(s)} + \delta\mathbf{y}_{(s+1)}) \quad (2.260a)$$

$$\mathbf{B}(\gamma\mathbf{y}_{(s)} + \delta\mathbf{y}_{(s+1)}) = \alpha_s\mathbf{A}(\gamma\mathbf{y}_{(s)} - \delta\mathbf{y}_{(s+1)}) \quad (2.260b)$$

Through inversion of matrix \mathbf{A} and premultiplication by \mathbf{B} we get:

$$\mathbf{B}\mathbf{A}^{-1}\mathbf{B}(\gamma\mathbf{y}_{(s)} - \delta\mathbf{y}_{(s+1)}) = \alpha_s\mathbf{B}(\gamma\mathbf{y}_{(s)} + \delta\mathbf{y}_{(s+1)})$$

$$\mathbf{B}\mathbf{A}^{-1}\mathbf{B}(\gamma\mathbf{y}_{(s)} + \delta\mathbf{y}_{(s+1)}) = \alpha_s\mathbf{B}(\gamma\mathbf{y}_{(s)} - \delta\mathbf{y}_{(s+1)})$$

By making use of Equations (2.260a–2.260b) and invoking the skew-symmetry of \mathbf{B} we get:

$$\mathbf{B}^T \mathbf{A}^{-1} \mathbf{B}(\gamma \mathbf{y}_{(s)} - \delta \mathbf{y}_{(s+1)}) = -\alpha_s^2 \mathbf{A}(\gamma \mathbf{y}_{(s)} - \delta \mathbf{y}_{(s+1)})$$

$$\mathbf{B}^T \mathbf{A}^{-1} \mathbf{B}(\gamma \mathbf{y}_{(s)} + \delta \mathbf{y}_{(s+1)}) = -\alpha_s^2 \mathbf{A}(\gamma \mathbf{y}_{(s)} + \delta \mathbf{y}_{(s+1)})$$

Therefore, associated to the real eigenpair $(\alpha_s, \mathbf{y}_{(s)})$ and $(-\alpha_s, \mathbf{y}_{(s+1)})$ of the original problem (2.252), there exists a negative eigenvalue $-\alpha^2$ of multiplicity 2 for the symmetric eigenproblem. The original eigenmodes are obtained through linearly independent combinations of the corresponding eigenmodes solutions of:

$$\mathbf{B}^T \mathbf{A}^{-1} \mathbf{B} \mathbf{y} = -\alpha^2 \mathbf{A} \mathbf{y}$$

2.11.5 Orthogonality relationships

The only case of interest from a practical standpoint is when the system is stable, in which case all eigenvalues of the original eigenvalue problem (2.252) are imaginary. The $2n$ eigensolutions of the corresponding symmetric eigenproblem (2.258) may be collected in columns of a real matrix \mathbf{Q} of dimension $2n$:

$$\mathbf{Q} = [\mathbf{w}_{(1)} \ \mathbf{z}_{(1)} \ \mathbf{w}_{(2)} \ \mathbf{z}_{(2)} \ \dots \ \mathbf{w}_{(n)} \ \mathbf{z}_{(n)}] \quad (2.261)$$

Owing to its structure, matrix \mathbf{A} is not positive definite but is nonsingular, so that the eigenvalue problem (2.258) is not degenerated and therefore the eigenmodes (2.261) are linearly independent.

The eigenmodes (2.261) verify the orthogonality relationships of the symmetric eigenproblem. To write the latter explicitly, we proceed as follows. Let us consider the eigenmodes $\mathbf{w}_{(s)}, \mathbf{z}_{(s)}, \mathbf{w}_{(r)}$ and $\mathbf{z}_{(r)}$ which verify the relationships:

$$\mathbf{B}^T \mathbf{A}^{-1} \mathbf{B} \mathbf{w}_{(s)} = \omega_s^2 \mathbf{A} \mathbf{w}_{(s)} \quad (2.262a)$$

$$\mathbf{B}^T \mathbf{A}^{-1} \mathbf{B} \mathbf{z}_{(s)} = \omega_s^2 \mathbf{A} \mathbf{z}_{(s)} \quad (2.262b)$$

$$\mathbf{B}^T \mathbf{A}^{-1} \mathbf{B} \mathbf{w}_{(r)} = \omega_r^2 \mathbf{A} \mathbf{w}_{(r)} \quad (2.262c)$$

$$\mathbf{B}^T \mathbf{A}^{-1} \mathbf{B} \mathbf{z}_{(r)} = \omega_r^2 \mathbf{A} \mathbf{z}_{(r)} \quad (2.262d)$$

Next, let us premultiply (2.262a) by $\mathbf{w}_{(r)}^T$ and (2.262c) by $\mathbf{w}_{(s)}^T$ and subtract them. Likewise we premultiply (2.262b) by $\mathbf{z}_{(r)}^T$ and (2.262d) by $\mathbf{z}_{(s)}^T$ and subtract the result. Owing to the symmetry of matrices $\mathbf{B}^T \mathbf{A}^{-1} \mathbf{B}$ and \mathbf{A} , one obtains:

$$(\omega_s^2 - \omega_r^2) \mathbf{w}_{(s)}^T \mathbf{A} \mathbf{w}_{(r)} = 0 \quad (\omega_s^2 - \omega_r^2) \mathbf{z}_{(s)}^T \mathbf{A} \mathbf{z}_{(r)} = 0,$$

providing thus the results:

$$\mathbf{w}_{(s)}^T \mathbf{A} \mathbf{w}_{(r)} = 0 \quad \mathbf{z}_{(s)}^T \mathbf{A} \mathbf{z}_{(r)} = 0 \quad r \neq s$$

and also

$$\mathbf{w}_{(s)}^T \mathbf{B}^T \mathbf{A}^{-1} \mathbf{B} \mathbf{w}_{(r)} = 0 \quad \mathbf{z}_{(s)}^T \mathbf{B}^T \mathbf{A}^{-1} \mathbf{B} \mathbf{z}_{(r)} = 0 \quad r \neq s \quad (2.263)$$

Let us next premultiply (2.262a) by $\mathbf{z}_{(r)}^T$, (2.262d) by $\mathbf{w}_{(s)}^T$ and subtract them. We get:

$$\mathbf{w}_{(s)}^T \mathbf{A} \mathbf{z}_{(r)} = 0 \quad r \neq s \quad (2.264)$$

and

$$\mathbf{w}_{(s)}^T \mathbf{B}^T \mathbf{A}^{-1} \mathbf{B} \mathbf{z}_{(r)} = 0 \quad r \neq s \quad (2.265)$$

Finally, let us premultiply (2.256a) by $\mathbf{w}_{(r)}^T$. Owing to the skew-symmetry of \mathbf{B} we get:

$$\mathbf{w}_{(r)}^T \mathbf{A} \mathbf{z}_{(r)} = 0 \quad \forall r \quad (2.266)$$

and thus

$$\mathbf{w}_{(r)}^T \mathbf{B}^T \mathbf{A}^{-1} \mathbf{B} \mathbf{z}_{(r)} = 0 \quad \forall r \quad (2.267)$$

showing that real and imaginary parts are linearly independent.

For $r = s$, we get the eigenvalues ω_r^2 in the form of Rayleigh quotients of both real and imaginary parts:

$$\omega_r^2 = \frac{\mathbf{w}_{(r)}^T \mathbf{B}^T \mathbf{A}^{-1} \mathbf{B} \mathbf{w}_{(r)}}{\mathbf{w}_{(r)}^T \mathbf{A} \mathbf{w}_{(r)}} = \frac{\mathbf{z}_{(r)}^T \mathbf{B}^T \mathbf{A}^{-1} \mathbf{B} \mathbf{z}_{(r)}}{\mathbf{z}_{(r)}^T \mathbf{A} \mathbf{z}_{(r)}} \quad (2.268)$$

Let us try to orthonormalize the eigenmodes with respect to \mathbf{A} . \mathbf{A} being not positive definite¹⁰, we must write:

$$\mathbf{w}_{(r)} \leftarrow \frac{\mathbf{w}_{(r)}}{|\mathbf{w}_{(r)}^T \mathbf{A} \mathbf{w}_{(s)}|^{\frac{1}{2}}} \quad (2.269a)$$

$$\mathbf{z}_{(r)} \leftarrow \frac{\mathbf{z}_{(r)}}{|\mathbf{z}_{(r)}^T \mathbf{A} \mathbf{z}_{(s)}|^{\frac{1}{2}}} \quad (2.269b)$$

providing the orthonormality relationships in the form:

$$\mathbf{w}_{(r)}^T \mathbf{A} \mathbf{w}_{(s)} = \pm \delta_{rs} \quad (2.270a)$$

$$\mathbf{z}_{(r)}^T \mathbf{A} \mathbf{z}_{(s)} = \pm \delta_{rs} \quad (2.270b)$$

All these orthogonality relationships may be gathered under the single matrix form:

$$\mathbf{Q}^T \mathbf{A} \mathbf{Q} = \mathbf{J} \quad (2.271)$$

where \mathbf{J} is a diagonal matrix of the form:¹¹

$$\mathbf{J} = \text{diag} (\pm 1 \pm 1 \dots \pm 1 \pm 1) = \mathbf{J}^{-1}$$

If one now returns to the original eigenvalue problem (2.252), through appropriate premultiplication of the relationships (2.256a) and (2.256b) and making use of the orthonormality relationships (2.264, 2.266, 2.270a–2.270b) we get:

$$\mathbf{w}_{(r)}^T \mathbf{B} \mathbf{w}_{(s)} = \omega_s \mathbf{w}_{(r)}^T \mathbf{A} \mathbf{z}_{(s)} = 0 \quad \forall s, r \quad (2.272a)$$

¹⁰ \mathbf{K}^* (and thus \mathbf{A}) is positive definite for a rotating speed Ω under the first critical speed (see Example 2.9).

¹¹ \mathbf{J} becomes the identity matrix in the case when \mathbf{A} is positive definite.

$$\mathbf{z}_{(r)}^T \mathbf{B} \mathbf{w}_{(s)} = \omega_s \mathbf{z}_{(r)}^T \mathbf{A} \mathbf{z}_{(s)} = \pm \delta_{rs} \omega_s \quad (2.272b)$$

$$\mathbf{z}_{(r)}^T \mathbf{B} \mathbf{z}_{(s)} = -\omega_s \mathbf{z}_{(r)}^T \mathbf{A} \mathbf{w}_{(s)} = 0 \quad \forall \quad s, r \quad (2.272c)$$

$$\mathbf{w}_{(r)}^T \mathbf{B} \mathbf{z}_{(s)} = -\omega_s \mathbf{w}_{(r)}^T \mathbf{A} \mathbf{w}_{(s)} = \mp \delta_{rs} \omega_s \quad (2.272d)$$

which may be summarized in matrix form:

$$\mathbf{\Omega} = \mathbf{Q}^T \mathbf{B} \mathbf{Q} = \begin{bmatrix} 0 & \mp \omega_1 & \dots & 0 & 0 \\ \pm \omega_1 & 0 & \dots & 0 & 0 \\ \vdots & \vdots & \ddots & \vdots & \vdots \\ 0 & 0 & \dots & 0 & \mp \omega_n \\ 0 & 0 & \dots & \pm \omega_n & 0 \end{bmatrix} = \text{diag} \left(\begin{bmatrix} 0 & \mp \omega_r \\ \pm \omega_r & 0 \end{bmatrix} \right) \quad (2.273)$$

\mathbf{J} and $\mathbf{\Omega}$ being such that:

$$\mathbf{\Omega}^* = \mathbf{J} \mathbf{\Omega} = \text{diag} \left(\begin{bmatrix} 0 & -\omega_r \\ +\omega_r & 0 \end{bmatrix} \right) \quad (2.274)$$

2.11.6 Response to nonzero initial conditions

In order to express the response of a stable system (2.242) to initial conditions $\mathbf{q}(0) = \mathbf{q}_0$ and $\dot{\mathbf{q}}(0) = \dot{\mathbf{q}}_0$, let us construct the state vector at time $t = 0$:

$$\mathbf{r}_0^T = [\dot{\mathbf{q}}_0^T \quad \mathbf{q}_0^T]$$

and solve the equivalent first-order problem:

$$\begin{cases} \mathbf{A} \dot{\mathbf{r}} + \mathbf{B} \mathbf{r} = \mathbf{0} \\ \mathbf{r}(0) = \mathbf{r}_0 \end{cases} \quad (2.275)$$

Since the eigenmodes $\mathbf{w}_{(s)}$ and $\mathbf{z}_{(s)}$ form a complete basis in the state space, the solution may be expanded in the form:

$$\mathbf{r} = \sum_{s=1}^n (\xi_s(t) \mathbf{w}_{(s)} + \eta_s(t) \mathbf{z}_{(s)}) = \mathbf{Q} \boldsymbol{\chi}(t) \quad (2.276)$$

with the vector of time-varying functions:

$$\boldsymbol{\chi}^T(t) = [\xi_1(t) \quad \eta_1(t) \quad \dots \quad \xi_n(t) \quad \eta_n(t)]$$

Substituting (2.276) into (2.275) yields:

$$\mathbf{A} \mathbf{Q} \dot{\boldsymbol{\chi}}(t) + \mathbf{B} \mathbf{Q} \boldsymbol{\chi}(t) = \mathbf{0} \quad (2.277)$$

Let us next premultiply by \mathbf{Q}^T and make use of the orthogonality relationships (2.271) and (2.273) to get:

$$\dot{\boldsymbol{\chi}}(t) + \mathbf{J} \mathbf{\Omega} \boldsymbol{\chi}(t) = \mathbf{0} \quad (2.278)$$

One observes that Equations (2.278) uncouple partially and that each pair of time-varying functions $[\xi_r(t), \eta_r(t)]$ is governed by a system of equations of the form:

$$\begin{bmatrix} \dot{\xi}_r(t) \\ \dot{\eta}_r(t) \end{bmatrix} + \begin{bmatrix} 0 & -\omega_r \\ +\omega_r & 0 \end{bmatrix} \begin{bmatrix} \xi_r(t) \\ \eta_r(t) \end{bmatrix} = \mathbf{0} \quad r = 1, \dots, n \quad (2.279)$$

The solution to (2.278) is conveniently obtained by taking its Laplace transform, which we put in the form:

$$\mathcal{L}[\dot{\chi}(t) + \mathbf{\Omega}^* \chi(t)] = [s\mathbf{I} + \mathbf{\Omega}^*] \bar{\chi}(s) = \chi(0)$$

or

$$\bar{\chi}(s) = [s\mathbf{I} + \mathbf{\Omega}^*]^{-1} \chi(0)$$

Matrix $[s\mathbf{I} + \mathbf{\Omega}^*]^{-1}$ is block-diagonal, with as elementary contribution:

$$\begin{bmatrix} s & -\omega_r \\ \omega_r & s \end{bmatrix}^{-1} = \frac{1}{s^2 + \omega_r^2} \begin{bmatrix} s & +\omega_r \\ -\omega_r & s \end{bmatrix}$$

and thus

$$[s\mathbf{I} + \mathbf{\Omega}^*]^{-1} = \text{diag} \left(\frac{1}{s^2 + \omega_r^2} \begin{bmatrix} s & +\omega_r \\ -\omega_r & s \end{bmatrix} \right) \quad (2.280)$$

We then compute its Laplace inverse, defining the impulse response matrix of the system $\Sigma(t)$ as:

$$\mathcal{L}^{-1}([s\mathbf{I} + \mathbf{\Omega}^*]^{-1}) = \text{diag} \left(\begin{bmatrix} \cos \omega_r t & \sin \omega_r t \\ -\sin \omega_r t & \cos \omega_r t \end{bmatrix} \right) = \Sigma(t) \quad \Sigma(0) = \mathbf{I} \quad (2.281)$$

which takes the form of a block-diagonal matrix with as elementary contribution an orthogonal matrix of harmonic functions. We may thus put the response in the form:

$$\mathbf{r}(t) = \mathbf{Q} \Sigma(t) \chi(0) \quad (2.282)$$

Let us finally express $\chi(0)$ in terms of the vector of initial conditions in state-space. Starting from:

$$\mathbf{r}_0 = \mathbf{Q} \chi(0)$$

and invoking orthonormality with respect to \mathbf{A} we get:

$$\chi(0) = \mathbf{J} \mathbf{Q}^T \mathbf{A} \mathbf{r}_0 \quad (2.283)$$

By combining (2.282) and (2.283) we finally get:

$$\mathbf{r}(t) = \mathbf{Q} \Sigma(t) \mathbf{J} \mathbf{Q}^T \mathbf{A} \mathbf{r}_0 \quad (2.284)$$

which represents the response to initial conditions of an undamped linear gyroscopic system within its stability domain.

2.11.7 Response to external excitation

The same path may be followed to compute the response of a rotating conservative system to an external excitation within the stability domain. It is governed by equation:

$$\begin{cases} M\ddot{q} + G\dot{q} + K^*q = p(t) \\ q_0, \quad \dot{q}_0 \text{ initial conditions,} \end{cases} \quad (2.285)$$

which can be put in the first-order equivalent form:

$$\begin{cases} A\dot{r} + Br = s(t) \\ r_0^T = [\dot{q}_0^T \ q_0^T] \text{ initial conditions} \end{cases} \quad (2.286)$$

with the excitation vector $s(t) = [p^T(t) \ 0]$.

Equation (2.276) is again used to transform the system equation (2.286) into modal coordinates:

$$A\mathbf{Q}\dot{\chi}(t) + B\mathbf{Q}\chi(t) = s(t) \quad (2.287)$$

Let us next premultiply by \mathbf{Q}^T and make use of the orthonormality relationships (2.271) and (2.273) to get:

$$\dot{\chi}(t) + \mathbf{J}\mathbf{\Omega}\chi(t) = \mathbf{J}\mathbf{Q}^T s(t) = \phi(t) \quad (2.288)$$

Taking the Laplace transform of (2.288) yields:

$$[s\mathbf{I} + \mathbf{\Omega}^*]\bar{\chi}(s) = \chi(0) + \bar{\phi}(s)$$

and thus

$$\chi(t) = \mathcal{L}^{-1}([s\mathbf{I} + \mathbf{\Omega}^*]^{-1}(\chi(0) + \bar{\phi}(s)))$$

or

$$\chi(t) = \mathcal{L}^{-1}\left(\text{diag}\left(\frac{1}{s^2 + \omega_r^2}\begin{bmatrix} s & +\omega_r \\ -\omega_r & s \end{bmatrix}\right)(\chi(0) + \bar{\phi}(s))\right) \quad (2.289)$$

Recalling the impulse response matrix defined earlier in (2.281) and using the fact that to an ordinary product in the Laplace domain corresponds a convolution product in the time domain we can write:

$$r(t) = \mathbf{Q}\Sigma(t)\mathbf{J}\mathbf{Q}^T A r_0 + \mathbf{Q} \int_0^t \Sigma(t - \tau)\mathbf{J}\mathbf{Q}^T s(\tau)d\tau \quad (2.290)$$

which is the response to external excitation of the undamped linear gyroscopic system within its stability domain. The first term of (2.290) represents the response to initial conditions already obtained in Section 2.11.6. The second one represents the forced response under external loads, expressed in the form of a Duhamel integral.

2.12 Exercises

2.12.1 Solved exercises

Problem 2.1 The equilibrium condition (2.1) is valid only for uniform rotational or translational transport motion. Let us now consider a system undergoing a uniformly accelerated

translational transport, with no nonconservative forces present. Explain why in that case the equilibrium position is given by:

$$\left(\frac{d}{dt} \frac{\partial \mathcal{T}_1}{\partial \dot{q}} \right)_{\dot{q}=0} + \frac{\partial \mathcal{V}^*}{\partial q} = 0 \quad (\text{P2.1.a})$$

Apply this result to a one-dimensional system consisting of a spring k having an imposed displacement with a uniform acceleration (denoted by a) on one side and a mass m attached on the other.

Solution

Considering the Lagrange equation (1.59) in the absence of nonconservative forces:

$$\begin{aligned} \frac{d}{dt} \frac{\partial \mathcal{T}(\dot{q}, q)}{\partial \dot{q}} - \frac{\partial \mathcal{T}(\dot{q}, q)}{\partial q} + \frac{\partial \mathcal{V}(q)}{\partial q} = \\ \frac{d}{dt} \frac{\partial (\mathcal{T}_2 + \mathcal{T}_1)}{\partial \dot{q}} - \frac{\partial (\mathcal{T}_2 + \mathcal{T}_1 + \mathcal{T}_0)}{\partial q} + \frac{\partial \mathcal{V}(q)}{\partial q} = 0 \end{aligned}$$

and evaluating the terms for an equilibrium position (i.e. when $\ddot{q} = 0$ and $\dot{q} = 0$), one finds:

$$\left(\frac{d}{dt} \frac{\partial (\mathcal{T}_2 + \mathcal{T}_1)}{\partial \dot{q}} - \frac{\partial (\mathcal{T}_2 + \mathcal{T}_1 + \mathcal{T}_0)}{\partial q} \right)_{\substack{\dot{q}=0 \\ \ddot{q}=0}} + \frac{\partial \mathcal{V}}{\partial q} = \left(\frac{d}{dt} \frac{\partial \mathcal{T}_1}{\partial \dot{q}} \right)_{\dot{q}=0} - \frac{\partial \mathcal{T}_0}{\partial q} + \frac{\partial \mathcal{V}}{\partial q} = 0$$

where we accounted for the fact that \mathcal{T}_2 and \mathcal{T}_1 are homogeneous of order 2 and 1 in \dot{q} respectively. This leads directly to the result (P2.1.a). Note that when the transport motion is uniform, $\partial \mathcal{T}_1 / \partial \dot{q}$ is not explicitly a function of the time, but only of q , possibly. Hence the first term of (P2.1.a) vanishes and the condition for an equilibrium position is then given by (2.1).

Considering now a spring-mass system with a uniformly accelerated basis, the absolute position and velocity of the mass can be written as:

$$u = a \frac{t^2}{2} + q \quad \dot{u} = at + \dot{q}$$

where q represents the displacement relative to the transport motion. The kinetic energy and potential energies are:

$$\mathcal{T} = \frac{1}{2} m (\dot{q}^2 + 2at\dot{q} + a^2 t^2) = \mathcal{T}_2 + \mathcal{T}_1 + \mathcal{T}_0 \quad \mathcal{V} = \frac{1}{2} k q^2$$

The first term in (P2.1.a) is thus:

$$\frac{d}{dt} \frac{\partial (\mathcal{T}_1)}{\partial \dot{q}} = ma$$

whereas

$$\frac{\partial \mathcal{T}_0}{\partial q} = 0$$

Hence, for the case of linearly accelerated systems with constant imposed acceleration, the apparent force must be considered for finding the equilibrium position in terms of degrees of freedom relative to the overall motion. The equilibrium equation finally is written as

$$ma + kq = 0$$

Problem 2.2 Let us consider a mass m moving on a parabolic curve $y(x) = x^2 - 4$ (solved problem in Chapter 1, Problem 1.2, Figure 1.14.a). The spring k has a zero natural length and the Lagrange equation of motion was found in (P1.2.f) when taking x as generalized coordinate. Depending on the value of m and k , find the equilibrium positions of the mass and discuss their stability. For each stable equilibrium compute the associated eigenfrequency.

Solution

The Lagrange equation was found in (P1.2.f) as:

$$m \left(1 + 4 \frac{x^2}{\ell^2} \right) \ddot{x} + \frac{4mx}{\ell^2} \dot{x}^2 + kx \left(2 \frac{x^2}{\ell^2} - 7 \right) + 2mg \frac{x}{\ell} = 0 \quad (\text{P2.2.a})$$

and the equilibrium positions must satisfy this equation when $\dot{x} = 0$ and $\ddot{x} = 0$, namely:

$$kx \left(2 \frac{x^2}{\ell^2} - 7 \right) + 2mg \frac{x}{\ell} = 0 \quad (\text{P2.2.b})$$

This condition could also be found from the equilibrium condition (2.1). The roots of this equation yield the three equilibrium positions:

$$x_{eq1} = 0 \quad x_{eq2} = \ell \sqrt{\frac{7}{2} - \frac{mg}{k\ell}} \quad x_{eq3} = -\ell \sqrt{\frac{7}{2} - \frac{mg}{k\ell}} \quad (\text{P2.2.c})$$

Equilibrium positions x_{eq2} and x_{eq3} exist only if $m < \frac{7k\ell}{2g}$.

Around an equilibrium position the Lagrange equation (P2.2.a) can be linearized by setting:

$$x = x_{eq} + q \quad \dot{x} = \dot{q} \quad \ddot{x} = \ddot{q}$$

where q are small perturbations. Neglecting all higher orders (P2.2.a) becomes:

$$m_{x_{eq}} \ddot{q} + k_{x_{eq}} q = 0 \quad (\text{P2.2.d})$$

where the inertia and stiffness coefficients are:

$$m_{x_{eq}} = \frac{\partial^2 \mathcal{T}}{\partial \dot{x}^2} = m \left(1 + 4 \frac{x_{eq}^2}{\ell^2} \right) \quad k_{x_{eq}} = \frac{\partial^2 \mathcal{V}}{\partial x^2} = k \left(6 \frac{x_{eq}^2}{\ell^2} - 7 \right) + 2 \frac{mg}{\ell} \quad (\text{P2.2.e})$$

As indicated above, those coefficients can also be found following the theory of Section 2.1.1, Equations (2.7) and (2.10), considering the energy expressions (P1.2.a) and (P1.2.b) for this system.

For the discussion of the stability frequencies associated to the equilibria, let us distinguish the cases where one or three equilibrium position exists according to (P2.2.c).

Case $m > \frac{7k\ell}{2g}$: only one equilibrium position exists, namely $x_{eq1} = 0$, and the inertia and stiffness coefficients (P2.2.c) are then:

$$m_{x_{eq1}} = m \quad k_{x_{eq1}} = -7k + 2 \frac{mg}{\ell} \quad (\text{P2.2.f})$$

The linear stiffness $k_{x_{eq1}}$ being always positive in this case, the equilibrium position is stable. The eigenfrequency is:

$$\omega_{x_{eq1}}^2 = \frac{k_{x_{eq1}}}{m_{x_{eq1}}} = -7\frac{k}{m} + 2\frac{g}{\ell} \quad (\text{P2.2.g})$$

Case $m < \frac{7k\ell}{2g}$: three equilibria exists and the linearized coefficients are:

$$m_{x_{eq1}} = m \quad k_{x_{eq1}} = -7k + 2\frac{mg}{\ell} \quad (\text{P2.2.h})$$

$$m_{x_{eq2,3}} = m \left(15 - \frac{mg}{k\ell} \right) \quad k_{x_{eq2,3}} = 14k - 4\frac{mg}{\ell} \quad (\text{P2.2.i})$$

In this case the first equilibrium is unstable since $k_{x_{eq1}} < 0$, the two other equilibria being stable and having an eigenfrequency given by $\omega_{x_{eq2,3}}^2 = k_{x_{eq2,3}}/m_{x_{eq2,3}}$.

Problem 2.3 Consider the double pendulum studied in Problem 1.3, using the relative angles as generalized coordinates (Figure 1.14.b). Find the equilibrium positions and discuss their stability. Compute the eigenfrequencies and eigenmodes around the stable configuration assuming $m_1 = m_2 = m$ and $\ell_1 = \ell_2 = \ell$.

Solution

The kinetic and potential energies of the double pendulum were found in Problem 1.3 as being:

$$\mathcal{T} = \frac{1}{2}(m_1\ell_1^2\dot{\theta}_1^2 + m_2(\ell_1^2\dot{\theta}_1^2 + \ell_2^2(\dot{\theta}_1 + \dot{\theta}_2)^2 + 2\ell_1\ell_2\dot{\theta}_1(\dot{\theta}_1 + \dot{\theta}_2)\cos\theta_2)) \quad (\text{P2.3.a})$$

$$\mathcal{V} = m_1g\ell_1(1 - \cos\theta_1) + m_2g(\ell_1(1 - \cos\theta_1) + \ell_2(1 - \cos(\theta_1 + \theta_2))) \quad (\text{P2.3.b})$$

Equilibrium positions of the double pendulum are defined by (2.1). For the double pendulum, it means that equilibrium positions are the solution to:

$$\begin{cases} (m_1g + m_2g)\ell_1 \sin\theta_1 + m_2g\ell_2 \sin(\theta_1 + \theta_2) = 0 \\ m_2g\ell_2 \sin(\theta_1 + \theta_2) = 0 \end{cases} \quad (\text{P2.3.c})$$

These equation could also have been obtained by setting to zero all velocities and accelerations in the equations of motion (P1.3.c–P1.3.d). Clearly, equilibrium positions are found for:

$$\theta_1 = 0 \quad \text{or} \quad \pi$$

$$\theta_2 = 0 \quad \text{or} \quad \pi$$

indicating that there are four equilibrium configurations for the system.

Let us then find the linearized equations of motion around the equilibrium position corresponding to $\theta_1 = \theta_2 = 0$. We compute the stiffness and inertia coefficients as defined by (2.7) and (2.10):

$$k_{11} = \left(\frac{\partial^2 \mathcal{V}}{\partial \theta_1 \partial \theta_1} \right)_{\theta_1=\theta_2=0} = (m_1 + m_2)g\ell_1 + m_2g\ell_2$$

$$\begin{aligned}
k_{12} = k_{21} &= \left(\frac{\partial^2 \mathcal{V}}{\partial \theta_1 \partial \theta_2} \right)_{\theta_1=\theta_2=0} = m_2 g \ell_2 \\
k_{22} &= \left(\frac{\partial^2 \mathcal{V}}{\partial \theta_2 \partial \theta_2} \right)_{\theta_1=\theta_2=0} = m_2 g \ell_2 \\
m_{11} &= \left(\frac{\partial^2 \mathcal{T}}{\partial \dot{\theta}_1 \partial \dot{\theta}_1} \right)_{\theta_1=\theta_2=0} = m_1 \ell_1^2 + m_2 (\ell_1 + \ell_2)^2 \\
m_{12} = m_{21} &= \left(\frac{\partial^2 \mathcal{T}}{\partial \dot{\theta}_1 \partial \dot{\theta}_2} \right)_{\theta_1=\theta_2=0} = m_2 (\ell_2^2 + \ell_1 \ell_2) \\
m_{22} &= \left(\frac{\partial^2 \mathcal{T}}{\partial \dot{\theta}_2 \partial \dot{\theta}_2} \right)_{\theta_1=\theta_2=0} = m_2 \ell_2^2
\end{aligned}$$

Hence the linearized equations of motion of the double pendulum around $\theta_1 = \theta_2 = 0$ are:

$$\begin{bmatrix} m_1 \ell_1^2 + m_2 (\ell_1 + \ell_2)^2 & m_2 (\ell_2^2 + \ell_1 \ell_2) \\ m_2 (\ell_2^2 + \ell_1 \ell_2) & m_2 \ell_2^2 \end{bmatrix} \begin{bmatrix} \ddot{\tilde{\theta}}_1 \\ \ddot{\tilde{\theta}}_2 \end{bmatrix} + \begin{bmatrix} (m_1 + m_2) g \ell_1 + m_2 g \ell_2 & m_2 g \ell_2 \\ m_2 g \ell_2 & m_2 g \ell_2 \end{bmatrix} \begin{bmatrix} \tilde{\theta}_1 \\ \tilde{\theta}_2 \end{bmatrix} = \mathbf{0} \quad (\text{P2.3.d})$$

where $\tilde{\theta}_1, \tilde{\theta}_2$ are the perturbations around the equilibrium position. To analyze the stability of the system, we compute the eigenvalues ν of the linearized stiffness matrix in order to verify if the matrix is positive definite. Solving $\det(\mathbf{K} - \nu \mathbf{I}) = 0$ the reader can verify that the eigenvalues are:

$$\nu = g \frac{(m_1 + m_2) \ell_1 + 2 m_2 \ell_2 \pm \sqrt{(m_1 + m_2)^2 \ell_1^2 + 4 m_2^2 \ell_2^2}}{2}$$

Since those eigenvalues are always positive, the linearized stiffness is always positive definite and thus the system is stable around the equilibrium $\theta_1 = \theta_2 = 0$. When $m_1 = m_2 = m$ and $\ell_1 = \ell_2 = \ell$ the linearized system (P2.3.d) has eigensolutions satisfying:

$$\left(\begin{bmatrix} 3mg\ell & mg\ell \\ mg\ell & mg\ell \end{bmatrix} - \omega^2 \begin{bmatrix} 5m\ell^2 & 2m\ell^2 \\ 2m\ell^2 & m\ell^2 \end{bmatrix} \right) \begin{bmatrix} \tilde{\theta}_1 \\ \tilde{\theta}_2 \end{bmatrix} = \mathbf{0} \quad (\text{P2.3.e})$$

Solving the eigenvalue problem yields the eigensolutions:

$$\omega_1^2 = \frac{g}{\ell} (2 - \sqrt{2}) \quad \mathbf{x}_{(1)} = \frac{1}{\sqrt{m\ell^2}} \begin{bmatrix} 0.3827 \\ 0.1585 \end{bmatrix} \quad (\text{P2.3.f})$$

$$\omega_2^2 = \frac{g}{\ell} (2 + \sqrt{2}) \quad \mathbf{x}_{(2)} = \frac{1}{\sqrt{m\ell^2}} \begin{bmatrix} 0.9239 \\ -2.2304 \end{bmatrix} \quad (\text{P2.3.g})$$

where the modes have been mass-normalized. In the first modes the two masses of the pendulum are in phase, while in the second they vibrate out of phase.

Let us now write the linearized equations of motion for the equilibrium configuration corresponding to $\theta_1 = \pi, \theta_2 = 0$. Computing then the stiffness and inertia coefficients around this

equilibrium yields the linearized equations of motion:

$$\begin{bmatrix} m_1 \ell_1^2 + m_2(\ell_1 + \ell_2)^2 & m_2(\ell_2^2 + \ell_1 \ell_2) \\ m_2(\ell_2^2 + \ell_1 \ell_2) & m_2 \ell_2^2 \end{bmatrix} \begin{bmatrix} \ddot{\theta}_1 \\ \ddot{\theta}_2 \end{bmatrix} - \begin{bmatrix} (m_1 + m_2)g\ell_1 m_2 g \ell_2 & m_2 g \ell_2 \\ m_2 g \ell_2 & m_2 g \ell_2 \end{bmatrix} \begin{bmatrix} \tilde{\theta}_1 \\ \tilde{\theta}_2 \end{bmatrix} = \mathbf{0} \quad (\text{P2.3.h})$$

One can verify that this stiffness matrix has two negative eigenvalues and the system is thus unstable.

Finally, if we consider the equilibrium position corresponding to $\theta_1 = \theta_2 = \pi$, the linearized equations of motion are:

$$\begin{bmatrix} m_1 \ell_1^2 + m_2(\ell_1 - \ell_2)^2 & m_2(\ell_2^2 - \ell_1 \ell_2) \\ m_2(\ell_2^2 - \ell_1 \ell_2) & m_2 \ell_2^2 \end{bmatrix} \begin{bmatrix} \ddot{\theta}_1 \\ \ddot{\theta}_2 \end{bmatrix} + \begin{bmatrix} -(m_1 + m_2)g\ell_1 + m_2 g \ell_2 & m_2 g \ell_2 \\ m_2 g \ell_2 & m_2 g \ell_2 \end{bmatrix} \begin{bmatrix} \tilde{\theta}_1 \\ \tilde{\theta}_2 \end{bmatrix} = \mathbf{0} \quad (\text{P2.3.i})$$

for which the linearized stiffness has one negative and one positive eigenvalue, thus the system is unstable around this configuration.

Problem 2.4 The Lagrange equations of the guided pendulum described in Figure 1.14.c were found in Problem 1.4. Consider again s and θ as the generalized coordinates and assume $\alpha = \pi/2$.

- Find the equilibrium positions of the system and determine if the equilibrium positions are stable or not.
- When the natural length of the spring is such that $d_0 = 2e$, consider the stable positions and compute the associated eigenfrequencies, assuming also that $m_1 = 2m_2 = 2m$ and $k = mg/\ell$.

Solution

Since the system does not undergo any transport motion (no scleronomic constraints) and implies only conservative forces the equilibrium condition is given by the derivatives of the potential, namely (2.1), which was already evaluated in (P1.4.d). Using the assumption $\alpha = \pi/2$ the equilibrium conditions write:

$$\begin{cases} \frac{\partial \mathcal{V}}{\partial s} = k(d - d_0) \frac{s}{d} = 0 \\ \frac{\partial \mathcal{V}}{\partial \theta} = m_2 g \ell \sin \theta = 0 \end{cases} \quad (\text{P2.4.a})$$

where

$$d^2 = e^2 + s^2 \quad (\text{P2.4.b})$$

So the equilibrium positions are clearly given by:

$$s_{eq1} = 0 \quad s_{eq2,3} = \pm \sqrt{d_0^2 - e^2} \quad (\text{P2.4.c})$$

which can be combined with any of the solutions:

$$\theta_{eq1} = 0 \quad \theta_{eq2} = \pi \quad (\text{P2.4.d})$$

Obviously the equilibria $s_{eq2,3}$ exist only if $d_0^2 > e^2$.

The stability can be checked through the positiveness of the linearized stiffness matrix. The stiffness coefficients (2.7) are:

$$k_{ss} = \frac{\partial^2 \mathcal{V}}{\partial s^2} = \frac{\partial}{\partial s} \left(k \left(1 - \frac{d_0}{d} \right) s \right) = k \left(1 - \frac{d_0}{d} + \frac{d_0 s^2}{d^3} \right) \quad (\text{P2.4.e})$$

$$k_{s\theta} = k_{\theta s} = \frac{\partial^2 \mathcal{V}}{\partial s \partial \theta} = 0 \quad (\text{P2.4.f})$$

$$k_{\theta\theta} = \frac{\partial^2 \mathcal{V}}{\partial \theta^2} = m_2 g \ell \cos \theta \quad (\text{P2.4.g})$$

The stiffness matrix is thus diagonal and its positiveness is determined by the diagonal terms. For the configurations where $\theta_{eq2} = \pi$, $k_{\theta\theta} < 0$ and the system is unstable. When $\theta_{eq2} = 0$, we have to check the positiveness of k_{ss} and we consider two cases:

Case $d_0 < e$: only the equilibrium position $s_{eq1} = 0$ exists. From (P2.4.b) we find $d_{eq1} = e$ and thus:

$$k_{ss}(s = s_{eq1} = 0) = k \left(1 - \frac{d_0}{e} \right) > 0 \quad (\text{P2.4.h})$$

Hence the system is stable.

Case $d_0 > e$: here the three equilibrium positions (P2.4.c) exist. Noting that from (P2.4.b) we can write that $d_{eq2,3} = d_0$,

$$k_{ss}(s = s_{eq1}) = k \left(1 - \frac{d_0}{e} \right) < 0 \quad (\text{P2.4.i})$$

$$k_{ss}(s = s_{eq2,3}) = k \left(1 - \frac{e^2}{d_0^2} \right) > 0 \quad (\text{P2.4.j})$$

Let us then compute the eigenfrequencies, the inertia coefficients being found according to (2.10) and (P1.4.a) as:

$$m_{ss} = \frac{\partial^2 \mathcal{T}}{\partial s^2} = m_1 + m_2 \quad (\text{P2.4.k})$$

$$m_{s\theta} = \frac{\partial^2 \mathcal{T}}{\partial s \partial \theta} = m_2 \ell \sin(\pi/2 - \theta) = m_2 \ell \cos \theta \quad (\text{P2.4.l})$$

$$m_{\theta\theta} = \frac{\partial^2 \mathcal{T}}{\partial \theta^2} = m_2 \ell^2 \quad (\text{P2.4.m})$$

Taking $d_0 = 2e$, we found that there are two equilibrium positions, namely $(s_{eq2,3}, \theta_{eq1})$. The linearized free vibration equations for the perturbations are obtained from (P2.4.g, P2.4.j) and (P2.4.k–P2.4.m). Taking $m_1 = 2m_2 = 2m$ and $k = mg/\ell$, we find for both stable equilibrium positions:

$$\begin{bmatrix} 3m & m\ell \\ m\ell & m\ell^2 \end{bmatrix} \begin{bmatrix} \ddot{s} \\ \ddot{\theta} \end{bmatrix} + \begin{bmatrix} \frac{3}{4}mg/\ell & 0 \\ 0 & mg\ell \end{bmatrix} \begin{bmatrix} \tilde{s} \\ \tilde{\theta} \end{bmatrix} = \mathbf{0} \quad (\text{P2.4.n})$$

We observe that there is a coupling in the mass matrix but not in the stiffness one. The eigen-solutions can be found by solving:

$$\left(\begin{bmatrix} \frac{3}{4} & 0 \\ 0 & 1 \end{bmatrix} - \omega^2 \frac{\ell}{g} \begin{bmatrix} 3 & 1 \\ 1 & 1 \end{bmatrix} \right) \begin{bmatrix} \tilde{s} \\ \tilde{\theta} \end{bmatrix} = \mathbf{0} \quad (\text{P2.4.o})$$

The solutions are:

$$\omega_1^2 = 0.2276 \frac{g}{\ell} \quad \mathbf{x}_{(1)} = \frac{1}{\sqrt{m\ell^2}} \begin{bmatrix} 0.5215\ell \\ 0.1537 \end{bmatrix} \quad (\text{P2.4.p})$$

$$\omega_2^2 = 1.6474 \frac{g}{\ell} \quad \mathbf{x}_{(2)} = \frac{1}{\sqrt{m\ell^2}} \begin{bmatrix} 0.4775\ell \\ -1.2151 \end{bmatrix} \quad (\text{P2.4.q})$$

Problem 2.5 Let us develop a discrete model of an elastic beam in bending by assimilating it to a system of N rigid links connected by equal torsional springs of stiffness k as displayed on Figure 2.15.

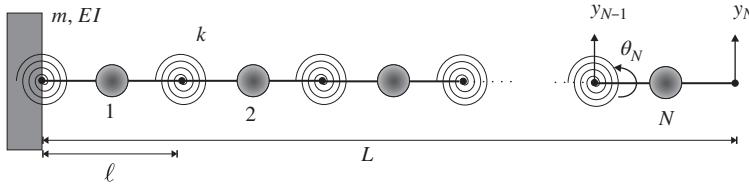


Figure 2.15 Discrete model of a beam.

The beam has bending stiffness EI (see Section 4.3.3), length L and mass per unit length m . The spring stiffness is such that

$$C = k\theta$$

C being the applied torque and θ the resulting rotation. It can be shown (based on the Bernoulli beam model developed in Section 4.3.3) that the end rotation of a cantilever beam of length ℓ submitted to a unit moment is equal to ℓ/EI . Hence the stiffness of the torsional springs of our beam model can be approximated by:

$$k = \frac{EI}{\ell} = \frac{N EI}{L}$$

where $\ell = \frac{L}{N}$ is the length of the elementary rigid link. Each rigid link has as individual mass $M = \frac{mL}{N} = m\ell$, m being the mass per unit length.

The kinematics of the system can be described in terms of 2 kinds of kinematic variables:

- The rotations θ_i ($i = 1, N$) which can be regarded as internal variables and are collected in the column vector θ :

$$\theta = [\theta_1 \quad \theta_2 \quad \dots \quad \theta_N]$$

- The vertical displacements y_i ($i = 1, N$) at the right-end of the rigid links. Those displacements y_i are chosen as the set of generalized coordinates \mathbf{q} :

$$\mathbf{q} = [y_1 \quad y_2 \quad \dots \quad y_N]$$

The rotations are kinematically related to the displacement degrees of freedom through the relationships:

$$\begin{cases} \theta_1 &= \frac{1}{\ell} y_1 \\ \theta_i &= \frac{1}{\ell} (y_i - y_{i-1}) \quad i = 2, N \end{cases}$$

In matrix form we get:

$$\theta = Cq \quad (\text{P2.5.a})$$

with the connection matrix:

$$C = \frac{1}{\ell} \begin{bmatrix} +1 & 0 & 0 & \dots & 0 \\ -1 & +1 & 0 & & \\ 0 & \ddots & \ddots & \ddots & \vdots \\ \vdots & & -1 & +1 & 0 \\ 0 & \dots & 0 & -1 & +1 \end{bmatrix} \quad (\text{P2.5.b})$$

The potential energy of the system results from the summation of the strain energies accumulated in the torsional springs. It may be written as:

$$\mathcal{V} = \frac{k}{2} (\theta_1^2 + (\theta_2 - \theta_1)^2 + \dots + (\theta_N - \theta_{N-1})^2)$$

In matrix form we get:

$$\mathcal{V} = \frac{1}{2} \theta^T J \theta \quad (\text{P2.5.c})$$

where J is the (banded) stiffness kernel matrix of the system:

$$J = k \begin{bmatrix} +2 & -1 & 0 & \dots & 0 \\ -1 & +2 & & & \\ 0 & \ddots & \ddots & \ddots & \vdots \\ \vdots & & & +2 & -1 \\ 0 & \dots & 0 & -1 & +1 \end{bmatrix}$$

Substituting the connection relationship (P2.5.a) into (P2.5.c) provides the expression of the potential energy in terms of the displacement generalized coordinates:

$$\mathcal{V} = \frac{1}{2} q^T K q \quad (\text{P2.5.d})$$

with the stiffness matrix:

$$K = C^T J C \quad (\text{P2.5.e})$$

The kinetic energy of the system can be approximated by assuming that the mass of each individual link is concentrated at its mid-point. We get thus:

$$\mathcal{T} = \frac{1}{2} m \ell \left(\frac{\dot{y}_1}{2}^2 + \left(\frac{\dot{y}_1 + \dot{y}_2}{2} \right)^2 + \dots + \left(\frac{\dot{y}_{N-1} + \dot{y}_N}{2} \right)^2 \right)$$

or, in matrix form:

$$\mathcal{T} = \frac{1}{2} \dot{q}^T M \dot{q} \quad (\text{P2.5.f})$$

Table 2.1 Nondimensional eigenvalues $\frac{\omega_r^2 mL^4}{EI}$ of the discretized beam

r	$N = 10$	error	$N = 100$	error	$N = 200$	error	exact
1	1,025E+01	17,1%	1,212E+01	1,9%	1,224E+01	1,0%	1,236E+01
2	4,157E+02	14,4%	4,761E+02	1,9%	4,807E+02	1,0%	4,855E+02
3	3,418E+03	10,2%	3,735E+03	1,9%	3,770E+03	1,0%	3,807E+03
4	1,411E+04	3,5%	1,435E+04	1,8%	1,448E+04	1,0%	1,462E+04
5	4,282E+04	7,2%	3,925E+04	1,7%	3,957E+04	0,9%	3,994E+04

with the mass matrix:

$$\mathbf{M} = m\ell \begin{bmatrix} 1/2 & 1/4 & 0 & \dots & 0 \\ 1/4 & 1/2 & & & \\ 0 & \ddots & \ddots & \ddots & \vdots \\ & & & & 0 \\ \vdots & & & 1/2 & 1/4 \\ 0 & \dots & 0 & -1/4 & 1/4 \end{bmatrix} \quad (\text{P2.5.g})$$

The resulting eigenvalue problem $\mathbf{K}\mathbf{x} = \omega^2 \mathbf{M}\mathbf{x}$ can then easily be solved using MATLAB® or similar numerical software, for arbitrary number N of elements used in the discretization of the system.

Table 2.1 displays the first 5 eigenvalues put in the nondimensional form $\frac{\omega^2 mL^4}{EI}$ obtained for increasing values of N . They are compared to the analytical eigensolutions obtained for the continuous Bernoulli beam model that will be described in Section 4.3.3.

Problem 2.6 The forced response to a harmonic excitation is given in (2.84). As discussed in Section 2.6.4 the forced response becomes infinite when the excitation frequency is equal to an eigenfrequency, unless the applied force is orthogonal to the corresponding eigenmode (pseudo-resonance). The fact that the forced response becomes infinite in case of resonance indicates that the response must be understood as a time response. Consider therefore a linear undamped system (no rigid mode present), initially at rest and excited by a harmonic load of frequency ω applied for $t > 0$.

1. Express the general response of the system using mode superposition.
2. Show that when the excitation frequency ω is close to the first eigenfrequency ω_1 , the contribution of the first mode to the response exhibits beating, namely a harmonic behaviour of frequency ω_m with an amplitude slowly varying at frequency $\Delta\omega/2$, where:

$$\omega_m = \frac{\omega + \omega_1}{2} \quad \Delta\omega = \omega - \omega_1$$

3. From the previous result, deduce the dynamic transient response when ω is equal to the first eigenfrequency ω_1 .

Solution

The dynamic equilibrium for a linear system excited by a harmonic force starting at time $t = 0$ is written as:

$$\mathbf{M}\ddot{\mathbf{q}} + \mathbf{K}\mathbf{q} = s \cos \omega t \quad t > 0 \quad (\text{P2.6.a})$$

where ω is a given excitation frequency. This equation is identical to the one written for the forced harmonic response (2.78), but whereas in Section 2.6.1 we computed only the forced response and assumed the form (2.79), here we will search for the time response (transient and forced) to a harmonic force applied at time $t = 0$ using mode superposition written in its matrix form:

$$\mathbf{q}(t) = \mathbf{X}\boldsymbol{\eta}(t) \quad (\text{P2.6.b})$$

Substituting this in (P2.6.a), projecting on the eigenmodes and using orthogonality as usual (assuming that the modes are mass-normalized), we obtain the normal equations:

$$\ddot{\boldsymbol{\eta}} + \boldsymbol{\Omega}^2 \boldsymbol{\eta} = \mathbf{X}^T s \cos \omega t \quad (\text{P2.6.c})$$

where $\boldsymbol{\Omega}^2$ is the diagonal matrix of squared eigenfrequencies. The general solution of this uncoupled normal equation is the sum of the solution of the homogeneous solution and the particular solution, namely:

$$\boldsymbol{\eta} = \cos \boldsymbol{\Omega} t \boldsymbol{\alpha} + \sin \boldsymbol{\Omega} t \boldsymbol{\beta} + (-\omega^2 \mathbf{I} + \boldsymbol{\Omega}^2)^{-1} \mathbf{X}^T s \cos \omega t \quad (\text{P2.6.d})$$

where we use the notation $\cos \boldsymbol{\Omega} t$ as the diagonal matrix of elements $\cos \omega_s t$. The vectors of coefficients $\boldsymbol{\alpha}$ and $\boldsymbol{\beta}$ are determined by the zero initial conditions, so the time response is finally written as

$$\mathbf{q}(t) = \mathbf{X}(\omega^2 \mathbf{I} - \boldsymbol{\Omega}^2)^{-1} \mathbf{X}^T s (\cos \boldsymbol{\Omega} t - \cos \omega t \mathbf{I}) \quad (\text{P2.6.e})$$

showing that the response is a combination of a forced term at frequency ω and a transient response involving all eigenfrequencies.

The time response for mode s in (P2.6.e) can also be written as:

$$\eta_s = \mathbf{x}_{(s)}^T s \frac{\cos \omega_s t - \cos \omega t}{\omega^2 - \omega_s^2} = \frac{2\mathbf{x}_{(s)}^T s}{\omega^2 - \omega_s^2} \sin \frac{(\omega - \omega_s)t}{2} \sin \frac{(\omega + \omega_s)t}{2} \quad (\text{P2.6.f})$$

and if ω is close to ω_1 , this expression shows that η_1 exhibits beating with a slow amplitude modulation at a frequency $\Delta\omega/2$. This can be seen as a single dof beating in comparison to the beating described in Example 2.5 where the beating originated from the combination of two modal responses of close eigenfrequencies in free vibration.

If the excitation frequency ω becomes equal to the first eigenfrequency ω_1 , the modal coordinate of the first mode becomes undetermined. This can be resolved by applying l'Hôpital's rule, yielding:

$$\eta_1 = \mathbf{x}_{(1)}^T s \lim_{\omega \rightarrow \omega_1} \frac{\cos \omega_1 t - \cos \omega t}{\omega^2 - \omega_1^2} = \mathbf{x}_{(1)}^T s \frac{\partial(\cos \omega_1 t - \cos \omega t)/\partial \omega}{\partial(\omega^2 - \omega_1^2)/\partial \omega} \Big|_{\omega=\omega_1} = \mathbf{x}_{(1)}^T s \frac{t \sin \omega_1 t}{2\omega_1}$$

which is a resonance characterized by an oscillation with linear increasing amplitude.

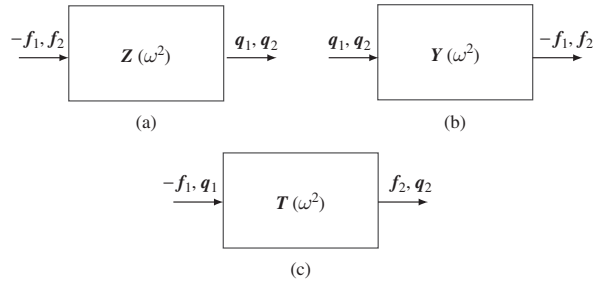


Figure 2.16 Impedance (a) admittance (b) and transfer (c) relationships.

Problem 2.7 A one-dimensional element (e.g. spring, mass, bar, beam) can be regarded as a dipole in which the input/output variables in 2 nodes noted 1 and 2 are the forces \mathbf{f} and the conjugated displacements \mathbf{q} . It can be represented either by its impedance matrix $\mathbf{Z}(\omega^2)$ (a) or its admittance matrix $\mathbf{Y}(\omega^2)$ (b) as displayed by Figure 2.16. The minus sign on the input force f_1 indicates that one considers the reaction force to the input and not the input f_1 itself. The reason for this convention will appear later on. It can also be described by a *transfer matrix* $\mathbf{T}(\omega^2)$ (Figure 2.16.c) allowing to compute forces and moments at node 2 from the knowledge of the same conjugated variables at node 1. Starting from the impedance matrix split in the form:

$$\mathbf{Z}(\omega^2) = \begin{bmatrix} Z_{11}(\omega^2) & Z_{12}(\omega^2) \\ Z_{21}(\omega^2) & Z_{22}(\omega^2) \end{bmatrix} \quad (\text{P2.7.a})$$

you are asked:

1. to develop the corresponding expression of $\mathbf{T}(\omega^2)$ in the form:

$$\mathbf{T}(\omega^2) = \begin{bmatrix} \mathbf{T}^{ff}(\omega^2) & \mathbf{T}^{fq}(\omega^2) \\ \mathbf{T}^{qf}(\omega^2) & \mathbf{T}^{qq}(\omega^2) \end{bmatrix} \quad (\text{P2.7.b})$$

such that:

$$\begin{bmatrix} f_2 \\ q_2 \end{bmatrix} = \mathbf{T}(\omega^2) \begin{bmatrix} f_1 \\ q_1 \end{bmatrix} \quad (\text{P2.7.c})$$

2. to demonstrate that the transfer matrix is such that:

$$\det(\mathbf{T}(\omega^2)) = 1 \quad (\text{P2.7.d})$$

a mathematical property that results from the symmetry of the impedance matrix.

3. to show how transfer matrices can be used recursively to express the transfer matrix of a simply-connected system of dipoles.
4. to show that cancelling each block of the transfer matrix corresponds to the eigenvalue equation of the system with specific boundary conditions.

Solution

1. With the sign convention adopted, forces and displacements obey to the impedance relationship:

$$\begin{bmatrix} f_1 \\ f_2 \end{bmatrix} = \begin{bmatrix} -Z_{11} & -Z_{12} \\ Z_{21} & Z_{22} \end{bmatrix} \begin{bmatrix} q_1 \\ q_2 \end{bmatrix} \quad (\text{P2.7.e})$$

Solving the first equation in (P2.7.e) for q_2 yields:

$$q_2 = -Z_{12}^{-1}(f_1 + Z_{11}q_1) \quad (\text{P2.7.f})$$

and through substitution into the second equation in (P2.7.e) we get:

$$f_2 = -Z_{22}Z_{12}^{-1}f_1 + (Z_{21} - Z_{22}Z_{12}^{-1}Z_{11})q_1 \quad (\text{P2.7.g})$$

so that the transfer matrix (P2.7.b) has for explicit expression:

$$T = \begin{bmatrix} T^{ff} & T^{fq} \\ T^{qf} & T^{qq} \end{bmatrix} = \begin{bmatrix} -Z_{22}Z_{12}^{-1} & Z_{21} - Z_{22}Z_{12}^{-1}Z_{11} \\ -Z_{12}^{-1} & -Z_{12}^{-1}Z_{11} \end{bmatrix} \quad (\text{P2.7.h})$$

2. The determinant of the transfer matrix (P2.7.h) can be computed by recalling that:

$$\det \begin{bmatrix} A & B \\ C & D \end{bmatrix} = \det(A) \cdot \det(D - CA^{-1}B) \quad (\text{P2.7.i})$$

We compute first:

$$\begin{aligned} T^{qq} - T^{qf}(T^{ff})^{-1}T^{fq} &= -Z_{12}^{-1}Z_{11} - Z_{12}^{-1}(Z_{22}Z_{12}^{-1})^{-1}(Z_{21} - Z_{22}Z_{12}^{-1}Z_{11}) \\ &= -Z_{22}^{-1}Z_{21} \end{aligned} \quad (\text{P2.7.j})$$

and by substituting (P2.7.h) into Equation (P2.7.i), *owing to the symmetry of the impedance matrix* we get:

$$\det(T) = \det(Z_{22}Z_{12}^{-1}) \det(Z_{22}^{-1}Z_{21}) = 1 \quad (\text{P2.7.k})$$

3. Let us consider 2 dipoles operating on similar conjugate variables (f , q) characterized by their transfer matrices T_{10} and T_{21} as displayed in Figure 2.17.

We may write:

$$\begin{bmatrix} f_2 \\ q_2 \end{bmatrix} = T_{21} \begin{bmatrix} f_1 \\ q_1 \end{bmatrix} = T_{21}T_{10} \begin{bmatrix} f_0 \\ q_0 \end{bmatrix} = T_{20} \begin{bmatrix} f_0 \\ q_0 \end{bmatrix} \quad (\text{P2.7.l})$$

More generally, for a chain of n dipoles, we get:

$$\begin{bmatrix} f_n \\ q_n \end{bmatrix} = T_{n,n-1} \dots T_{21}T_{10} \begin{bmatrix} f_0 \\ q_0 \end{bmatrix} = T(\omega^2) \begin{bmatrix} f_0 \\ q_0 \end{bmatrix} \quad (\text{P2.7.m})$$

with the system transfer matrix:

$$T(\omega^2) = T_{n,n-1} \dots T_{21}T_{10} \quad (\text{P2.7.n})$$

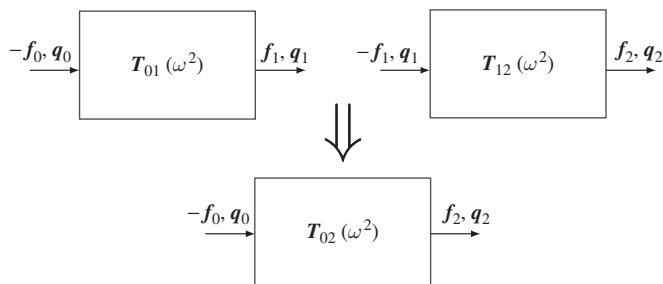


Figure 2.17 Principle of the transfer method.

Table 2.2 Eigenvalue equations of 1-D systems obtained from transfer matrix for different boundary conditions

	0 fixed end	0 free end
n fixed end	$\det(\mathbf{T}^{ff}(\omega^2)) = 0$	$\det(\mathbf{T}^{qq}(\omega^2)) = 0$
n free end	$\det(\mathbf{T}^{ff}(\omega^2)) = 0$	$\det(\mathbf{T}^{fq}(\omega^2)) = 0$

4. The transfer relationship of the assembled system is split in the form given by Equation (P2.7.h):

$$\begin{bmatrix} f_n \\ q_n \end{bmatrix} = \begin{bmatrix} \mathbf{T}^{ff}(\omega^2) & \mathbf{T}^{fq}(\omega^2) \\ \mathbf{T}^{qf}(\omega^2) & \mathbf{T}^{qq}(\omega^2) \end{bmatrix} \begin{bmatrix} f_0 \\ q_0 \end{bmatrix} \quad (\text{P2.7.o})$$

The eigenvalue equation corresponding to specific boundary conditions can be extracted from Equation (P2.7.o) by remembering that the condition $\mathbf{f} = 0$ is fulfilled by a free end, while a fixed end is characterized by $\mathbf{q} = 0$. Therefore, one gets in the different cases the eigenvalue equations as given by Table 2.2. It is straightforward to observe that the transfer matrix can also be used to compute responses of 1-D systems under harmonic force or displacement inputs.

The transfer matrix was introduced by (Holzer 1921) to solve torsional vibration problems and was later on extended by Myklestad to bending vibration problems (Myklestad 1945). The success encountered by the transfer matrix method was due to its ability to provide a rather easy numerical solution to simply-connected (or even branched) systems without using a large matrix formalism (Meirovitch 1997). It has now lost much of its interest with the considerable development of numerical matrix methods.

In Chapter 4 it will be shown that closed-form solutions can be used to develop rather simple transfer matrix expressions for elements of 1-D systems such as bars and beams.

2.12.2 Selected exercises

Problem 2.8 Consider the one-dimensional system made of two masses and two linear springs depicted in Figure 2.18.a. As degree of freedom we choose the displacement of the upper mass and the *relative* displacement of the lower one. Write the free vibration matrix equation of the system and compute the eigenfrequencies and eigenmodes.

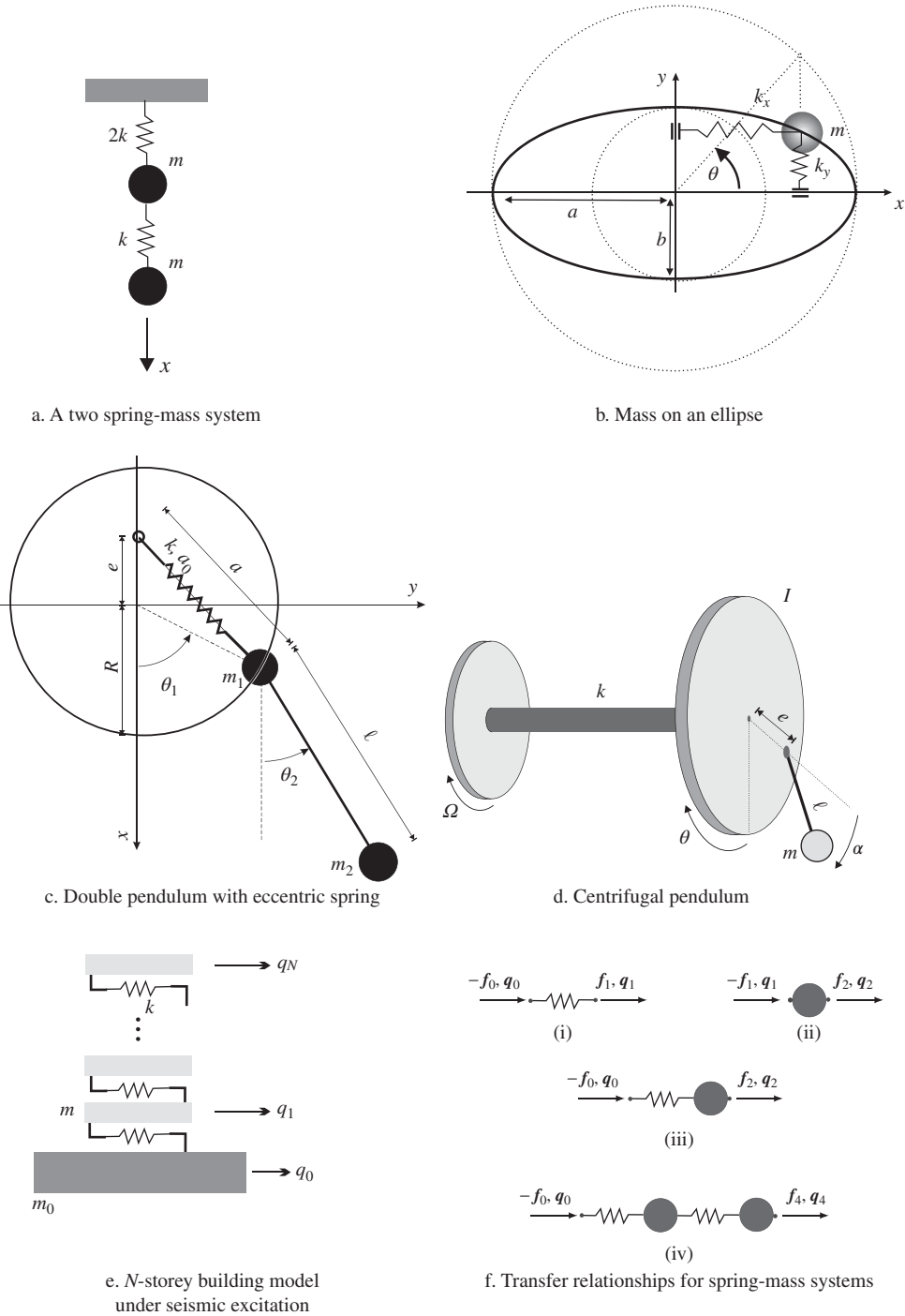


Figure 2.18 Selected exercises.

Problem 2.9 A mass m is constrained to move on an ellipse (see Figure 2.18.b). The ellipse is described by:

$$\frac{x^2}{a^2} + \frac{y^2}{b^2} = 1$$

and is in a horizontal plane (no gravity is acting on the mass). The mass is connected to 2 springs (k_x and k_y). The springs can slide freely on the y (respectively x) axis. The natural length of the springs is null. Choosing θ as the degree of freedom for the system (see Figure 2.18.b) so that:

$$\begin{cases} x = a \cos \theta \\ y = b \sin \theta \end{cases}$$

you are asked to analyze the system according to the following steps:

1. Consider the free body diagram of the mass and write the Newton equations describing the dynamics in the x and y directions. Apply then the virtual work principle, namely project the dynamic equilibrium equations in direction $\delta_\theta \mathbf{u}$ (see Equation (1.17)).
2. Find the kinetic and potential energies of the system and obtain the equations of motion using the Lagrange equations.
3. Find the static equilibrium positions of the mass.
4. Analyze the linear static stability of the system around the equilibrium positions (when $a^2 k_x > b^2 k_y$ and when $a^2 k_x < b^2 k_y$).
5. Find the eigenfrequency of the system around the stable equilibrium positions.

Problem 2.10 Consider the double pendulum where the first mass is connected to an eccentric spring as depicted in Figure 2.18.c. The spring has a stiffness k and is attached at a distance e above the origin of the pendulum. The spring has a natural length equal to a_0 and a is its deformed length. Gravity acts in the direction of the x axis. Taking the absolute angles θ_1 and θ_2 as degrees of freedom,

1. write the kinetic and potential energies of the system,
2. show that if:

$$a_0 = R \quad e = \frac{R}{2} \quad \ell = R \quad m_1 = m_2 = m \quad mg = \frac{kR}{16}$$

there exist two unstable and one stable equilibrium positions,

3. compute, for those values, the eigenfrequencies and eigenmodes around the stable equilibrium.

Problem 2.11 In the system shown in Figure 2.18.d a rotation speed Ω is imposed on the left disk which is connected through a shaft to a second disk of rotational inertia I around its centre. The shaft has a torsional stiffness k and its inertia is neglected. The rotation angle of the second disk measured with respect to an reference rotating with Ω is θ . On the second disk, at a distance e from its center, a pendulum is attached (point mass m and length ℓ). The relative angle between the radial direction of the disk and the pendulum is called α . We consider θ and α as the generalized coordinates of the system. Gravity is not considered.

1. Write the kinetic and potential energies of the system

2. Find the linearized equations of motion of the system.
3. Find the equilibrium positions of the system and determine their stability
4. Assuming from now on that:

$$m = \frac{I}{4\ell^2} \quad e = \frac{\ell}{2}$$

For the stable equilibrium position(s) of the system, compute the eigenfrequencies and eigenmodes.

Problem 2.12 A N -storey building is modelled as a series of masses interconnected by springs as displayed on Figure 2.18.e. All masses and springs are equal except for the foundation which has a mass equal to M . The system undergoes seismic motion described as imposed horizontal acceleration \ddot{u} . The degrees-of-freedom are noted as (q_0, q_1, \dots, q_N) , q_0 being the displacement of the foundation. You are asked:

1. To express the equations of motion of the system in matrix form.
2. To determine the static condensation matrix S at foundation level (hint: matrix S can be obtained by simple inspection in this case).
3. To compute the stiffness and mass matrices condensed on the boundary.
4. To formulate the internal eigenvalue problem.
5. To write in explicit form the equilibrium equation for mass j in the middle of the structure.
6. To verify that it obeys to a general solution of the form:

$$q_j = A \sin(j\mu + \phi) \quad j = 0, \dots, N$$

7. To express the boundary conditions, and show that this provides the analytical solution to the internal eigenvalue problem.
8. To verify that the eigenvalues are:

$$\omega_k = 2\sqrt{\frac{k}{m} \sin\left(\frac{2k-1}{2N+1} \cdot \frac{\pi}{2}\right)}$$

and to provide the explicit expression of the eigenmodes.

9. To express the reaction force at the foundation.
10. Assuming that the building has 5 storeys, to compute numerically the effective modal masses in order to determine which modes contribute to 85% to the effective mass.

Problem 2.13 The eigenvalue equation of simply connected systems made of springs and masses can easily be obtained using the concept of transfer matrix as developed in Exercise 2.7. As an application, you are asked to:

1. Express the transfer matrix of a spring (Figure 2.18.f.i).
2. Express the transfer matrix of a vibrating mass (Figure 2.18.f.ii).
3. Making use of the results from steps 1 and 2, construct the transfer matrix of a spring-mass system (Figure 2.18.f.iii).
4. Use the transfer matrix obtained at step 3 to express the transfer matrix of the system of Figure 2.18.f.iv.

5. Determine the eigenvalues of the system for all possible boundary conditions. Validate your results.
6. Using the results at intermediate steps, determine the eigenmodes for the case $f_0 = f_4 = 0$.

Problem 2.14 For the model approximating a beam as constructed in the solved Problem 2.5, consider that $N = 2$, namely that the model is consisting of only two segments. Calculate by hand the eigenfrequencies and the eigenmodes of that model, and verify that the eigenmodes satisfy the orthogonality properties with respect to the mass and the stiffness matrix.

Problem 2.15 Consider the double pendulum when taking the *absolute* angles as degrees of freedom (see Problem 1.8 and Figure 1.15.c.).

1. Find the equilibrium positions and discuss their stability.
2. Write the linearized free vibration equations and show that, for the stable equilibrium position, they are equivalent to Equations (P2.3.d) obtained for the relative angles.
3. Compute the eigenfrequencies and eigenmodes around the stable configuration assuming $m_1 = m_2 = m$ and $\ell_1 = \ell_2 = \ell$.

Problem 2.16 In Problem 1.6 of a sliding mass on a massless rod is considered in a gravity field (Figure 1.15.a). The generalized coordinates are taken as θ and ℓ . Find the equilibrium positions and determine their stability. Then compute the eigenfrequencies and eigenmodes around the stable equilibrium position.

Problem 2.17 For the rotational pendulum of Figure 1.15.b described in Problem 1.7, compute the equilibrium positions and determine their stability. Then compute the eigenfrequencies and eigenmodes around the stable equilibrium position.

Problem 2.18 The pendulum on a nonlinear spring depicted in Figure 1.15.d was analyzed in Problem 1.9. Find the equilibrium position and determine their stability. Then, taking $\alpha = \pi/2$ and $mg = k\ell$, compute the eigenfrequencies and eigenmodes around the stable equilibrium position.

Problem 2.19 Consider the mass sliding on an elastically supported rod depicted in Figure 1.15.e as discussed in Problem 1.10. Take:

$$k_1 = k_2 = k \quad mg = ka \quad \ell = 2a$$

Find the equilibrium position and determine their stability. Compute the eigenfrequencies and eigenmodes around the stable equilibrium position(s).

Problem 2.20 Generalize the formula (2.115) to integrate a normal equation (2.105) when it corresponds to a rigid body mode (hint: apply l'Hôpital's rule and take the limit for $\alpha \rightarrow 0$).

Problem 2.21 Consider the rotating system of Example 2.9, page (145), with the same numerical values. Following the theory and notations introduced in Section 2.11, solve the associated symmetric eigenproblem (Section 2.11.4):

$$\mathbf{B}^T \mathbf{A}^{-1} \mathbf{B} \mathbf{w} = \mathbf{S} \mathbf{w} = \mu \mathbf{A} \mathbf{w}$$

using Matlab® or equivalent numerical software to get the matrices of eigenvalues and eigenvectors μ and W .

1. Observe that all eigenvalues μ_r have multiplicity 2 and are all positive for rotating speeds $\Omega < \omega_1$ and $\Omega > \omega_2$, while a negative eigenpair appears for $\omega_1 < \Omega < \omega_2$.
2. Concentrate next your analysis to the stability zone $\Omega > \omega_2$ by assuming a sufficiently large value of Ω . Compute the projection of the system matrices on the eigenmodes by forming the matrix products $W^T A W$, $W^T S W$, and $W^T B W$. Observe their structure and sign properties.
3. Normalize the eigenmodes in the form:

$$P = W \text{diag} \left(\frac{1}{\sqrt{|w_{(r)}^T A w_{(s)}|}} \right)$$

to compute the normalized matrices $J = P^T A P$ and $\Omega = P^T B P$.

References

- Courant R and Hilbert D 1953 *Methods of Mathematical Physics* vol. 1. Interscience Publishers, New York.
- Fraeijs de Veubeke B, G radin M and Huck A 1972 *Structural Dynamics*. number 126 in *CISM Lecture Notes (Udine, Italy)*. Springer.
- Holzer H 1921 *Analysis of Torsional Vibration*. Springer, Berlin.
- Imbert J 1984 *Analyse des structures par  l ments finis*. Cepadues Editions, Toulouse.
- Lord Rayleigh BJWS 1894 *Theory of Sound, Vol. I* 2nd edn. Macmillan and Co., London and New York (first edition, 1877).
- MacNeal RH 1971 A hybrid method of component mode synthesis. *Computers and Structures* **1**(4), 581–601.
- Meirovitch L 1967 *Analytical Methods in Vibrations*. The Macmillan Company, New York.
- Meirovitch L 1997 *Principles and Techniques of Vibrations*. Prentice Hall New Jersey.
- Myklestad N 1945 New method of calculating natural modes of coupled bending-torsion vibration of beams. *Trans. ASME* **67**(1), 61–67.
- Preumont A 1994 *Random Vibrations and Spectral Analysis*. Kluwer Academic.
- Wazwaz AM 2011 *Linear and Nonlinear Integral Equations*. Springer.

3

Damped Vibrations of n-Degree-of-Freedom Systems

Damping forces have already been introduced briefly in Chapter 1 to underline their non-conservative character.

Damping is one of the most important aspects to model and predict in structural analysis, as it determines for a major part the performance of a structural system or the amplitude of its vibrations. It is probably also one of the most uncertain and difficult ones to address in vibration analysis and structural dynamics, due to the variety and complexity of its physical origin. Indeed damping can arise from many different sources, such as (Mead 1998):

- intrinsic damping of the structural material;
- Coulomb friction and partial-impact energy loss at structural interfaces;
- energy lost into surrounding air, water or ground and into contained fluids;
- friction between the structure and mounted equipment, furnishings, payload and people;
- viscous damping between sliding and lubricated machines surfaces.

In all generality, the damping forces can be expressed as functions of the structural velocities $\dot{\mathbf{q}}$, the strain rates $\dot{\epsilon}_{ij}$ in the material and the system configuration \mathbf{q} . The strains ϵ_{ij} being themselves expressed as spatial derivatives of \mathbf{q} (see Chapter 4, Section 4.1), we may write in all generality:

$$\mathbf{f}_d = \mathbf{f}_d(\dot{\mathbf{q}}, \mathbf{q}) \quad (3.1)$$

and this function can be dependent on the history of the behaviour of the system. In this chapter, we will make the approximation that the damping is linear in the velocities (viscous damping) and independent of \mathbf{q} unless otherwise stated. It can thus be described by a dissipation function quadratic in velocities as introduced in Chapter 1, Section 1.3.3.

Structural damping in itself is a huge subject which could not be covered in a single book chapter. The presentation will focus on the following aspects.

In Section 3.1 the linear damping model will be described and its essential mathematical properties will be outlined. The classical assumption of modal damping which consists of

neglecting the coupling of eigenmodes through damping will be introduced and its validity range discussed. A general method based on modal expansion to construct a proportional damping matrix matching experimentally measured modal damping ratios will be presented.

Section 3.2 is devoted to the harmonic response of damped systems. The essential features of the response of the damped system in the frequency domain, together with its graphical representation (Nyquist plot, amplitude and phase diagram), will be recalled. The hysteretic damping model, which has the interesting property of keeping the linear character of the response in the frequency domain while fitting better the structural damping observed in practice, will be presented. Finally, the principles of force appropriation testing – a widely used modal testing method in the aeronautical community – will be described. The specificity of force appropriation testing is its ability to identify one by one the normal modes of vibration of the associated undamped system through cancelation of the damping forces by the excitation system.

Section 3.3 addresses the case of linear systems subject to arbitrarily large viscous damping. The original dynamic model is cast in an equivalent first-order canonical form (the state-space representation) so that the formal analysis in terms of complex eigensolutions of the damped system can be defined. This more general formulation opens the way to experimental testing techniques that allow identifying the modal parameters (complex eigenfrequencies and eigenmodes) of the damped structural systems.

These experimental techniques are discussed in Section 3.4. They can be developed either in the time domain or in the frequency domain. The principle of both approaches will be presented using classical identification techniques (the Least-Squares Complex Exponential method in the time domain and the Rational Fraction Polynomial identification in the frequency domain) and illustrated through simple examples.

Definitions

The list below complements the general definitions given in the book introduction, but remains local to Chapter 3.

\bar{z}	complex conjugate of a complex number z .
A	system matrix in state space (zeroth order term).
B	system matrix in state space (first order term).
K', K''	real, imaginary part of K (hysteretic damping).
f	amplitudes of harmonic excitation (complex).
$f_{(k)}$	excitation amplitudes associated to r_k .
r	dynamic response in state space (state vector).
$r_{(k)}$	response normal modes k associated to ϕ_k .
s	excitation in state space.
s_0	amplitudes of harmonic excitation in state space (complex).
$y_{(r)}$	eigenvector r in state space.
z	amplitude of harmonic response (complex).
$z_{(r)}$	eigenmode of damped system (complex).
H_j^{exp}	experimentally measured FRF at frequency ω_j .

$H_{rs}(\omega)$	dynamic influence coefficient, coefficient of the transfer function $\mathbf{H}(\omega)$.
\mathcal{P}	complex power.
\mathcal{P}_R	real part of complex power (active power).
\mathcal{P}_I	imaginary part of complex power (reactive power).
E', E''	storage and loss modulus (hysteretic damping).
h_{kl}	dynamic influence, coefficient of \mathbf{H} .
$h_{rs}(t)$	impulse response of dof r to impulse on s .
β_r	diagonal damping coefficients of mode $\mathbf{x}_{(r)}$ (β_{rr}).
β_{rs}	damping coefficients (undamped modal space).
ε_r	modal damping ratio of mode $\mathbf{x}_{(r)}$.
γ	loss factor (hysteretic damping).
λ_r	r -th eigenvalue of damped system (complex).
ω_{0r}	r -th frequency (associated conservative system).
$\phi_{0j}(t)$	amplitude of an harmonic modal participation $\phi_j(t)$.
$\phi_j(t)$	modal participation of damped or undamped mode j .
ϕ_k	characteristic phase lag k associated to $\mathbf{r}_{(k)}$.
ψ_s	phase lag of modal contribution s .
$\rho_{rs(k)}$	residue of mode k , input s , output r .
\tilde{y}_r	generalized stiffness of state space mode \mathbf{y}_r .
$\tilde{\mu}_r$	generalized mass of of state space mode \mathbf{y}_r .
<hr/>	
DFT	Discrete Fourier Transform.
FFT	Fast Fourier Transform.
FRF	Frequency Response Function.
LCSE	Least Square Complex Exponential.
RFP	Rational Fraction Polynomial.

3.1 Damped oscillations in terms of normal eigensolutions of the undamped system

In Section 2.1 we discussed the linearization of forces deriving from the potential energy and in particular showed in (2.7) that the stiffness matrix can be computed as the second derivative of \mathcal{V} with respect to \mathbf{q} . Similarly one can linearize the dissipation forces (1.54) in the neighbourhood of an equilibrium position $\mathbf{q} = \mathbf{0}$, $\dot{\mathbf{q}} = \mathbf{0}$ by developing the generalized dissipation forces as:

$$-Q_s = \frac{\partial D}{\partial \dot{q}_s} \simeq -Q_s \Big|_{\substack{\mathbf{q}=\mathbf{0} \\ \dot{\mathbf{q}}=\mathbf{0}}} + \sum_{r=1}^n \dot{q}_r \frac{\partial^2 D}{\partial \dot{q}_s \partial \dot{q}_r} \Big|_{\substack{\mathbf{q}=\mathbf{0} \\ \dot{\mathbf{q}}=\mathbf{0}}} + \sum_{r=1}^n q_r \frac{\partial^2 D}{\partial \dot{q}_s \partial q_r} \Big|_{\substack{\mathbf{q}=\mathbf{0} \\ \dot{\mathbf{q}}=\mathbf{0}}}$$

Assuming that no dissipation force is present when the velocity is zero (this could be the case for Coulomb friction), we find that:

$$-Q_s \simeq \sum_{r=1}^n \dot{q}_r \frac{\partial^2 D}{\partial \dot{q}_s \partial \dot{q}_r} \Big|_{\substack{\mathbf{q}=\mathbf{0} \\ \dot{\mathbf{q}}=\mathbf{0}}}$$

and thus that the linear damping coefficients can be computed from:

$$c_{sr} = \frac{\partial^2 \mathcal{D}}{\partial \dot{q}_s \partial \dot{q}_r} \bigg|_{\substack{q=0 \\ \dot{q}=0}} \quad (3.2)$$

Note the strong similarity between this result and (2.7). The damping matrix \mathbf{C} is thus symmetric and usually nonnegative for passive structures.¹

Including in the Lagrange equations of the system a dissipation mechanism described by linearized viscous-like dissipation forces (3.2), the damped vibration problem is then governed by equation:

$$\mathbf{M}\ddot{\mathbf{q}} + \mathbf{C}\dot{\mathbf{q}} + \mathbf{K}\mathbf{q} = \mathbf{p}(t) \quad (3.3)$$

As will be seen later on, the presence of the damping term complicates considerably the solution of the problem and makes it more difficult to understand the behaviour of the dynamic system. Taking it into account is, however, most essential in the elaboration of methods allowing the experimental determination of modal characteristics such as eigenmodes, eigenfrequencies and generalized masses. We are thus considering the behaviour of the damped system to a certain extent for computational reasons but mainly for experimental purposes.

Let us consider the conservative system associated with the real system: it is governed by equations $\mathbf{M}\ddot{\mathbf{q}} + \mathbf{K}\mathbf{q} = \mathbf{0}$ and its eigenmodes and eigenfrequencies will be noted respectively $\mathbf{x}_{(r)}$ and ω_{0r}^2 .

Since the modes $\mathbf{x}_{(r)}$ of the associated conservative system form a complete basis one can, as in the undamped case, solve the system of Equations (3.3) through the modal expansion

$$\mathbf{q} = \sum_{s=1}^n \eta_s(t) \mathbf{x}_{(s)} \quad (3.4)$$

3.1.1 Normal equations for a damped system

The presence of the damping term causes a coupling of the resulting equations. Indeed, by substituting (3.4) into (3.3) and making use of the eigenmode orthogonality relationships with respect to \mathbf{M} and \mathbf{K} , one obtains:

$$\ddot{\eta}_r + \sum_{s=1}^n \frac{\beta_{rs}}{\mu_r} \dot{\eta}_s + \omega_{0r}^2 \eta_r = \phi_r(t) \quad r = 1, \dots, n \quad (3.5)$$

with the *modal damping coefficients*:

$$\beta_{rs} = \mathbf{x}_{(r)}^T \mathbf{C} \mathbf{x}_{(s)}$$

which do not vanish in general, even for $k \neq s$, since the damping may have a very different distribution from stiffness and inertia. The modal participation factors in the excitation are

¹ This result is straightforward in the case of pure viscous damping since in that case (Lord Rayleigh 1894):

$$\mathcal{D} = \frac{1}{2} \dot{\mathbf{q}}^T \mathbf{C} \dot{\mathbf{q}} \geq 0$$

which is quadratic in the generalized velocities (see Section 1.3.3).

still defined by Equation (2.106). The form (3.5) of the resulting equations shows that, unless restrictive assumptions are made with respect to the damping distribution, the modal approach is not interesting for obtaining a numerical solution to the equations of motion. Indeed, the normal equations remain coupled by the damping coefficients β_{rs} .

Nevertheless, even when the relative importance of the damping terms prevents any simplifying assumptions, the modal approach is of interest when the displacement representation is limited to a small number of modes, since the system size to be integrated is then reduced to the number of modes retained in the spectral expansion of the solution.

When one applies the *mode displacement method* (see Section 2.8.1), the solution is simply reconstructed using (3.4) after one has solved system (3.5) reduced to the dimension $k < n$, neglecting the contribution of the unknown modes.

The *mode acceleration method* (Section 2.8.2) may be generalized to the damped case by computing the response in the form:

$$\mathbf{q}(t) = \sum_{s=1}^{k < n} \mathbf{x}_{(s)} \eta_s + \left(\mathbf{K}^{-1} - \sum_{s=1}^{k < n} \frac{\mathbf{x}_{(s)} \mathbf{x}_{(s)}^T}{\omega_{0s}^2 \mu_s} \right) \mathbf{p}(t) \quad (3.6)$$

the modal amplitudes η_s of the retained modes being obtained from (3.5). From a numerical point of view, an interesting alternative to the modal superposition of the damped system consists of performing, as suggested earlier for the undamped system, a direct integration of the equations of motion under the form (3.3). The direct integration methods will be discussed in detail in Chapter 7. In opposition to modal methods, they do not suffer from limitation due to the presence of arbitrary damping.

3.1.2 Modal damping assumption for lightly damped structures

Equation (3.5) shows that the computation of the damped response would be considerably simplified if the coupling through damping did not exist ($\beta_{kl} = 0, k \neq l$). In order for this to be the case, the dissipation forces should have the same distribution forces as inertia and elastic forces, but there is no reason for this to be so. However, the damping distribution is almost always ill-defined and thus it is generally necessary to make an assumption regarding its repartition. The simplest assumption consists then in assuming that the matrix $[\beta_{rs}]$ is diagonal. This assumption has no real physical background but it will be shown to be consistent with the assumption that the structure is *lightly damped*.

To show it, let us analyze the free vibrations of the damped system starting from the homogeneous system of equations:

$$\mathbf{M}\ddot{\mathbf{q}} + \mathbf{C}\dot{\mathbf{q}} + \mathbf{K}\mathbf{q} = \mathbf{0} \quad (3.7)$$

and let us introduce the assumption that the damping terms are of an order of magnitude lower than the stiffness and mass terms.

Equation (3.7) admits solutions of general form:

$$\mathbf{q} = \mathbf{z} e^{\lambda t} \quad (3.8)$$

with roots λ_k and vibration eigenmodes $\mathbf{z}_{(k)}$ solutions of:

$$(\lambda_k^2 \mathbf{M} + \lambda_k \mathbf{C} + \mathbf{K}) \mathbf{z}_{(k)} = \mathbf{0} \quad (3.9)$$

Without damping one would have $\lambda_k = \pm i\omega_{0k}$ and $\mathbf{z}_{(k)} = \mathbf{x}_{(k)}$, ω_{0k} and $\mathbf{x}_{(k)}$ being the eigenmodes and eigenfrequencies of the associated conservative system:

$$(\mathbf{K} - \omega_{0k}^2 \mathbf{M}) \mathbf{x}_{(k)} = \mathbf{0} \quad (3.10)$$

If the system is assumed to be lightly damped, it can be supposed that λ_k and $\mathbf{z}_{(k)}$ differ only slightly from $i\omega_{0k}$ and $\mathbf{x}_{(k)}$ respectively (Fraeijs de Veubeke *et al.* 1972, Huck 1976):

$$\begin{aligned} \lambda &= i\omega_{0k} + \Delta\lambda \\ \mathbf{z}_{(k)} &= \mathbf{x}_{(k)} + \Delta\mathbf{z} \end{aligned} \quad (3.11)$$

Substituting (3.11) into Equation (3.9) yields:

$$\{(-\omega_{0k}^2 + 2i\omega_{0k}\Delta\lambda + (\Delta\lambda)^2) \mathbf{M} + (i\omega_{0k} + \Delta\lambda) \mathbf{C} + \mathbf{K}\} (\mathbf{x}_{(k)} + \Delta\mathbf{z}) = \mathbf{0}$$

Neglecting next the second-order terms and taking account of the fundamental relationship: (3.10) verified by eigenmode $\mathbf{x}_{(k)}$, one obtains:

$$(\mathbf{K} - \omega_{0k}^2 \mathbf{M}) \Delta\mathbf{z} + (2i\omega_{0k} \mathbf{M} + \mathbf{C}) \mathbf{x}_{(k)} \Delta\lambda + i\omega_{0k} \mathbf{C} (\mathbf{x}_{(k)} + \Delta\mathbf{z}) \simeq \mathbf{0}$$

The light-damping assumption allows one to neglect the terms in $\mathbf{C}\Delta\lambda$ and $\mathbf{C}\Delta\mathbf{z}$. One then obtains the first-order relationship:

$$(\mathbf{K} - \omega_{0k}^2 \mathbf{M}) \Delta\mathbf{z} + i\omega_{0k} (\mathbf{C} + 2\Delta\lambda \mathbf{M}) \mathbf{x}_{(k)} \simeq \mathbf{0} \quad (3.12)$$

from which, after multiplication by $\mathbf{x}_{(k)}^T$, the correction to the eigenvalue may be extracted:

$$\mathbf{x}_{(k)}^T (\mathbf{C} + 2\Delta\lambda \mathbf{M}) \mathbf{x}_{(k)} \simeq 0$$

and

$$\Delta\lambda \simeq -\frac{\beta_{kk}}{2\mu_k}$$

providing the approximate expression:

$$\lambda_k \simeq -\frac{\beta_{kk}}{2\mu_k} + i\omega_{0k} \quad (3.13)$$

Result (3.13) has two important consequences:

- Each eigenvalue correction takes the form of a real negative part and thus transforms each term of the fundamental solution into a damped oscillatory motion.
- This first-order correction involves only the diagonal damping terms:

$$\beta_{kk} = \mathbf{x}_{(k)}^T \mathbf{C} \mathbf{x}_{(k)} \quad (3.14)$$

and thus the influence of the nondiagonal terms is only of second order.

Therefore one is authorized to neglect the nondiagonal damping terms without significant alteration of the eigenspectrum of the lightly damped system.

It is also possible to obtain from Equation (3.12) the eigenmode correction through a modal expansion in terms of the undamped system eigenmodes:

$$\Delta \mathbf{z} = \sum_{\substack{s=1 \\ s \neq k}}^n \alpha_s \mathbf{x}_{(s)}$$

After substitution and premultiplication by $\mathbf{x}_{(l)}^T$ for $l \neq k$ one obtains:

$$\mathbf{x}_{(l)}^T (\mathbf{K} - \omega_{0k}^2 \mathbf{M}) \sum_{\substack{s=1 \\ s \neq k}}^n \alpha_s \mathbf{x}_{(s)} + i\omega_{0k} \mathbf{x}_{(l)}^T (\mathbf{C} + 2\Delta\lambda \mathbf{M}) \mathbf{x}_{(k)} \simeq 0$$

and, taking account the orthogonality relationships,

$$\alpha_l = \frac{i\omega_{0k} \beta_{kl}}{\mu_l (\omega_{0k}^2 - \omega_{0l}^2)}$$

and the resulting eigenmode expression:

$$\mathbf{z}_{(k)} = \mathbf{x}_{(k)} + \sum_{\substack{s=1 \\ s \neq k}}^n i\omega_{0k} \frac{\beta_{ks}}{\mu_s (\omega_{0k}^2 - \omega_{0s}^2)} \mathbf{x}_{(s)} \quad (3.15)$$

Formula (3.15) is valid only if the β_{kl} are first-order quantities and if $(\omega_{0k}^2 - \omega_{0s}^2)$ remains finite. It shows that, *as long as the eigenfrequencies of the associated conservative system are well-separate*, it may be considered that *the influence on the eigenmodes of the coupling through damping is of the same order of magnitude as the damping coefficients β_{ks}* .

It also shows that the eigenmode correction is an imaginary term, having as its consequence the fact that *a free vibration of the damped system is no longer a synchronous motion of the whole system*. Indeed,

$$\mathbf{q} = \mathbf{z} e^{\lambda t} = [\mathbf{x}_{(k)} + i \Im m(\Delta \mathbf{z})] e^{(i\omega_{0k} + \Delta\lambda)t}$$

and degree of freedom q_i is no longer in phase with another degree of freedom q_j . For lightly damped systems with well-separate eigenvalues, the eigenmode expression (3.15) can be approximated by $\mathbf{z}_{(k)} \simeq \mathbf{x}_{(k)}$ and the general solution of the free vibration system takes the form

$$\mathbf{q} \simeq \mathbf{x}_{(k)} e^{(i\omega_{0k} + \Delta\lambda)t}$$

which is consistent with the approximation:

$$\mathbf{x}_{(k)}^T \mathbf{C} \mathbf{x}_{(s)} = \beta_{kk} \delta_{ks}$$

The discussion above shows that the modal damping assumption is in most cases physically consistent with the low-damping assumption: when a system is weakly damped and when its eigenfrequencies are well-separate, the effect of the cross-damping terms β_{ks} , $k \neq s$ on the eigenspectrum can be neglected according to (3.13) and (3.15). This assumption was proposed

by *Lord Rayleigh* in Lord Rayleigh (1894).² It allows simplifying the normal Equations (3.5) in the form:

$$\ddot{\eta}_r + \frac{\beta_r}{\mu_r} \dot{\eta}_r + \omega_{0r}^2 \eta_r = \phi_r(t) \quad r = 1, \dots, n \quad (3.16)$$

where β_r now represents the diagonal damping term (3.5). By analogy with the single-degree-of-freedom system, one may define a nondimensional *modal damping ratio*:

$$\varepsilon_r = \frac{\beta_r}{2\omega_{0r}\mu_r} \quad (3.17)$$

such that the contribution of eigenmode r to the solution becomes aperiodic when $\varepsilon_r \geq 1$. The normal equations are then rewritten in the form:

$$\ddot{\eta}_r + 2\varepsilon_r\omega_{0r}\dot{\eta}_r + \omega_{0r}^2\eta_r = \phi_r(t) \quad r = 1, \dots, n \quad (3.18)$$

A simple way to construct a damping matrix \mathbf{C} that guarantees diagonal modal damping consists of making a weighted sum of the mass and stiffness matrices:

$$\mathbf{C} = a\mathbf{K} + b\mathbf{M} \quad (3.19)$$

This matrix is commonly known as a *proportional damping* (or *Rayleigh damping*) matrix and results in a diagonal modal damping matrix with coefficients:

$$\beta_r = a\gamma_r + b\mu_r$$

and the associated modal damping ratios are:

$$\varepsilon_r = \frac{1}{2} \left(a\omega_{0r} + \frac{b}{\omega_{0r}} \right) \quad (3.20)$$

Hence, if the damping ratios are known from experimental vibration testing (see Section 3.4) for two eigenfrequencies, the coefficients a and b for the proportional damping matrix can be determined, as shown in Example 3.1.

Example 3.1

Let us consider the 2-DOF damped system of Figure 3.1. The stiffness, mass and damping matrices are:

$$\mathbf{K} = \begin{bmatrix} 4 & -2 \\ -2 & 6 \end{bmatrix} \quad \mathbf{M} = \begin{bmatrix} 5 & 0 \\ 0 & 10 \end{bmatrix} \quad \mathbf{C} = \begin{bmatrix} 5c & -1c \\ -1c & 8c \end{bmatrix} \quad (\text{E3.1.a})$$

In the absence of damping ($c = 0$), its eigensolutions are easily obtained as:

$$\begin{aligned} \omega_{01} &= 0.6325 & \mathbf{x}_{(1)}^T &= \begin{bmatrix} 1 & 1 \end{bmatrix} \\ \omega_{02} &= 1.0 & \mathbf{x}_{(2)}^T &= \begin{bmatrix} 1 & -0.5 \end{bmatrix} \end{aligned} \quad (\text{E3.1.b})$$

² The assumption that modes can be assumed uncoupled through the damping contributions is sometimes named *Basile's assumption* (from a French engineer), in particular in the context of experimental modal analysis.

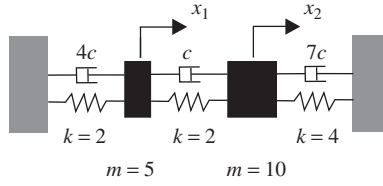


Figure 3.1 A two-degree-of-freedom system with viscous damping.

The generalized masses and diagonal modal damping coefficients are:

$$\begin{aligned} \mu_1 &= 15.0 & \beta_{11} &= 11c \\ \mu_2 &= 7.50 & \beta_{22} &= 8c \end{aligned} \quad (\text{E3.1.c})$$

For $c = 0.1$ (which corresponds to relatively light damping), we get the approximate eigenvalues (Equation (3.13)) and modal damping coefficients (Equation (3.17)):

$$\begin{aligned} \lambda_1 &= -0.0367 \pm i0.6335 & \varepsilon_1 &= 0.0580 \\ \lambda_2 &= -0.0533 \pm i1.0 & \varepsilon_2 &= 0.0533 \end{aligned} \quad (\text{E3.1.d})$$

Finally, a proportional damping matrix can be reconstructed using Equation (3.19). The coefficients a and b are solutions of:

$$\begin{bmatrix} \omega_{01}^2 & 1 \\ \omega_{02}^2 & 1 \end{bmatrix} \begin{bmatrix} a \\ b \end{bmatrix} = \begin{bmatrix} \frac{\beta_{11}}{\mu_1} \\ \frac{\beta_{22}}{\mu_2} \end{bmatrix} \quad \rightarrow \quad \begin{bmatrix} a \\ b \end{bmatrix} = \begin{bmatrix} 0.0556 \\ 0.0511 \end{bmatrix}$$

leading to a proportional damping matrix that gives rise to a slight redistribution of damping into the system:

$$\mathbf{C}' = \begin{bmatrix} 0.4778 & -0.1111 \\ -0.1111 & 0.8444 \end{bmatrix} \quad \text{such that} \quad \mathbf{X}^T \mathbf{C}' \mathbf{X} = \begin{bmatrix} 1.1 & 0 \\ 0 & 0.8 \end{bmatrix}$$

The proportional damping matrix is slightly different from the physical one (Equation (E3.1.a) with $c = 0.1$).

The proportional damping matrix (3.19) can be tuned with the two parameters a and b , but (3.20) indicates that such damping matrix will generate higher damping ratios in the lower and higher frequency ranges, and lower ones in the intermediate range (Figure 3.2). This is usually far from reality and therefore the proportional damping approach is not satisfactory when the damping needs to be modelled properly for a broad frequency range. If modal damping ratios are known for many modes from experimental tests or are prescribed by industrial standards, other approaches need to be followed to build a damping matrix \mathbf{C} as explained next.

Remark 3.1 It is worthwhile noticing that the form (3.19) of the modal damping matrix is a particular case of a more general formula introduced in (Caughey 1960). It consists of

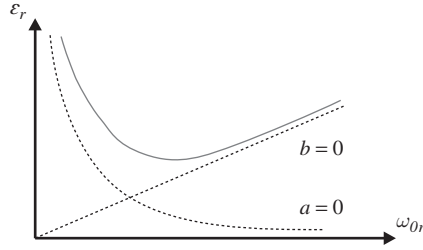


Figure 3.2 Proportional damping matrix: weighted sum of mass and stiffness matrices.

expressing the damping matrix \mathbf{C} in the form:

$$\mathbf{C} = \sum_{i=1}^n a_i \mathbf{M} (\mathbf{M}^{-1} \mathbf{K})^{i-1}$$

It can be shown that the coefficients a_k of the development are linearly related to the damping coefficients ϵ_s through:

$$\mathbf{W} \mathbf{a} = \boldsymbol{\epsilon}$$

where \mathbf{a} and $\boldsymbol{\epsilon}$ are the uni-column matrices of the coefficients a_i and ϵ_s respectively, and where \mathbf{W} is a matrix built from successive powers of the system eigenfrequencies (Géradin and Rixen 1997). The method suffers from several drawbacks:

- The power expansion of the damping matrix leads to full matrix and the numerical cost to get its explicit expression is prohibitive even for moderately large systems.
- The matrix \mathbf{W} becomes ill-conditioned for increasing number of eigenfrequencies and becomes singular for multiple eigenfrequencies.
- In addition, it leads to a frequency-dependent model that does not take into account the spatial distribution of damping in the physical system.

The proportional damping model (3.19) did not have these drawbacks but had only two parameters to fit the structural damping. In Section 3.1.3 we present a method combining proportional damping for the part of the spectrum for which the damping is not well-known and a spectral expansion built on modes for which the damping is known.

3.1.3 Constructing the damping matrix through modal expansion

The objective of the structural analyst is always to develop a dynamic model which fits well the real one. An information generally available either from dynamic testing or from engineering practice is the percentage of critical damping, i.e. the modal damping ratio, for individual vibration modes, generally the lower frequency ones.

Assuming first that all eigenmodes are available and their damping characterized by the damping coefficients ϵ_s , building on the basis of such information a damping matrix \mathbf{C} satisfying the diagonal modal damping assumption can be achieved through expansion in terms of

either inertia or elastic force modal contributions as follows:

$$\mathbf{C} = \sum_{s=1}^n \mathbf{M} \mathbf{x}_{(s)} \frac{2\varepsilon_s \omega_{0s}}{\mu_s} \mathbf{x}_{(s)}^T \mathbf{M} = \sum_{s=1}^n \mathbf{K} \mathbf{x}_{(s)} \frac{2\varepsilon_s}{\omega_{0s}^3 \mu_s} \mathbf{x}_{(s)}^T \mathbf{K} \quad (3.21)$$

Both assumptions (3.21) generate a diagonal modal damping matrix with coefficients:

$$\beta_{rr} = \mathbf{x}_{(r)}^T \mathbf{C} \mathbf{x}_{(r)} = 2\varepsilon_r \omega_{0r} \mu_r \quad (3.22)$$

An interesting consequence of the building procedure is that it automatically avoids associating damping to the rigid body modes, which was a major drawback of the Rayleigh model (Equation (3.19)). However,

- In practice, the resulting matrix is full. This damping model does not take into account the topology of the discretized model and thus, cannot be related to the spatial distribution of damping into the system. This can be penalizing when using such a damping model in a finite element context.
- In practice, when measured data are used and/or when only a small number of modes are included in the expansion, the damping model remains incomplete since it will automatically generate zero damping for the missing modes:

$$\mathbf{C} \simeq \sum_{s=1}^{m < n} \mathbf{K} \mathbf{x}_{(s)} \frac{2\varepsilon_s}{\omega_{0s}^3 \mu_s} \mathbf{x}_{(s)}^T \mathbf{K} \rightarrow \begin{cases} \beta_{rr} = 2\varepsilon_r \omega_{0r} \mu_r & r \leq m \\ \beta_{rr} = 0 & r > m \end{cases} \quad (3.23)$$

The truncated modal expansion (3.23) can however be corrected by assuming for the higher modes a linearly increasing damping coefficient with frequency as obtained through damping proportional to stiffness. To that purpose, suppose that the damping of the higher modes is governed by:

$$\mathbf{C} = a\mathbf{K} \quad (3.24)$$

So we set:

$$\varepsilon_r = \frac{\beta_{rr}}{2\omega_{0r} \mu_r} = \frac{a\omega_{0r}}{2} \quad r > m \quad (3.25)$$

and aim at constructing a spectral expansion of the damping matrix that fits the following data:

$$\begin{cases} \beta_{rr} = 2\varepsilon_r \omega_{0r} \mu_r & r \leq m \\ \beta_{rr} = a\omega_{0r}^2 \mu_r & r > m \end{cases} \quad (3.26)$$

It is built by adding to (3.23) the contribution (3.24) proportional to stiffness, and then subtracting from the latter the spectral contribution of the modes already present in the model:

$$\mathbf{C} = a\mathbf{K} + \sum_{s=1}^{m < n} \mathbf{K} \mathbf{x}_{(s)} \left(\frac{2\varepsilon_s}{\omega_{0s}^3 \mu_s} - \frac{a}{\omega_{0s}^2 \mu_s} \right) \mathbf{x}_{(s)}^T \mathbf{K} \quad (3.27)$$

The damping model (3.27) gives to the analyst full control of the amount of damping present in the model over the whole frequency range. It does not allow us, however, to take into account information that could be available on its spatial distribution.

3.2 Forced harmonic response

3.2.1 The case of light viscous damping

Let us assume harmonic motion with excitation frequency ω :

$$\mathbf{K}\mathbf{q} + \mathbf{C}\dot{\mathbf{q}} + \mathbf{M}\ddot{\mathbf{q}} = \mathbf{f}e^{i\omega t}$$

and assume that the response is limited to the forced term $\mathbf{q} = \mathbf{z}e^{i\omega t}$, so that the excitation and response amplitudes verify the complex equation:

$$(\mathbf{K} - \omega^2\mathbf{M} + i\omega\mathbf{C})\mathbf{z} = \mathbf{f} \quad (3.28)$$

The modal damping assumption allows us to construct the modal expansion of the dynamic influence coefficient matrix in terms of undamped eigenmodes. Indeed, if the response amplitude is developed in terms of eigenmodes:

$$\mathbf{z} = \sum_{s=1}^n \alpha_s \mathbf{x}_{(s)}$$

the orthogonality relationships together with the modal damping assumption provide the coefficients:

$$\alpha_r = \frac{\mathbf{x}_{(r)}^T \mathbf{f}}{\mu_r (\omega_{0r}^2 - \omega^2 + 2i\varepsilon_r \omega \omega_{0r})}$$

Hence the spectral expansion of the *dynamic influence coefficient matrix*:

$$(\mathbf{K} - \omega^2\mathbf{M} + i\omega\mathbf{C})^{-1} = \sum_{s=1}^n \frac{1}{(\omega_{0s}^2 - \omega^2 + 2i\varepsilon_s \omega \omega_{0s})} \frac{\mathbf{x}_{(s)} \mathbf{x}_{(s)}^T}{\mu_s} \quad (3.29)$$

and the dynamic influence coefficients can be written as:

$$h_{kl}(i\omega) = \sum_{s=1}^n \frac{1}{(\omega_{0s}^2 - \omega^2 + 2i\varepsilon_s \omega \omega_{0s})} \frac{x_{k(s)} x_{l(s)}}{\mu_s} \quad (3.30)$$

Obviously, when the excitation frequency ω tends towards 0, the dynamic influence coefficients converge to the static influence coefficients g_{kl} given by (2.87), as long as the system does not contain rigid-body modes.

Example 3.2

Consider a lightly damped system with three degrees of freedom and with no rigid-body mode, the principal dynamic influence coefficients of which are represented on a Nyquist diagram in Figure 3.3.

It is observed that, if the system eigenfrequencies are sufficiently separate from each other, only one term at a time can contribute significantly to the development (3.30) for a given ω .

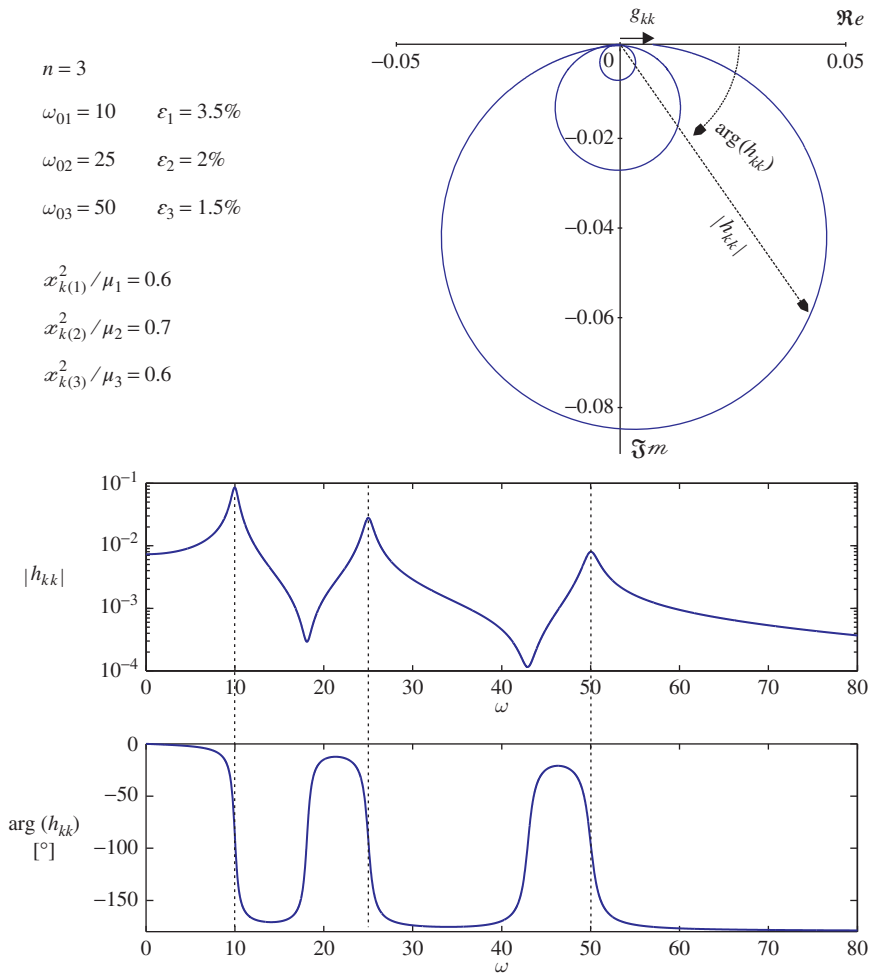


Figure 3.3 Nyquist diagram, amplitude and phase lag of a principal dynamic influence coefficient for a lightly damped system.

This produces a Nyquist diagram formed by concentric circles, the ‘circle’ being characteristic of the harmonic response of a damped single-degree-of-freedom system. In the opposite case of clustered eigenfrequencies and of stronger damping, the Nyquist diagram is more intricate, since several modes contribute simultaneously in a significant manner to the influence coefficients (3.30) for a given excitation frequency ω (Figure 3.4). The Nyquist diagram is then characterized by loops. Note that in practice, when the damping is strong or when the frequencies are clustered, neglecting the coupling of the mode through the damping, as done to derive (3.30), might be a crude assumption (see Section 3.1.2).

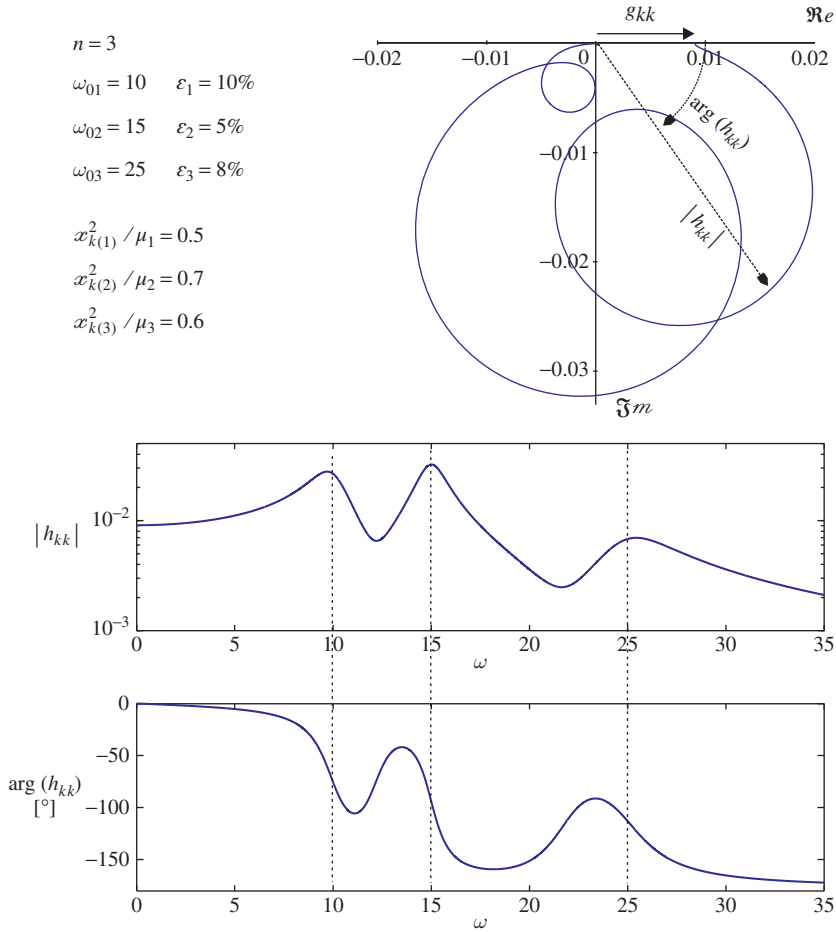


Figure 3.4 Nyquist diagram, amplitude and phase lag of a principal for a system with higher damping dynamic influence coefficient.

3.2.2 Hysteretic damping

A convenient assumption often made to model linear damping is to assume that the damping forces in the frequency domain (that is when the system is forced to move in a harmonic motion) are independent of the frequency but proportional to the motion amplitude and in phase with the velocity.

Let us assume, like in Section 3.2.1, that the applied force is harmonic and that we look at the forced response in the form $\mathbf{q} = \mathbf{z}e^{i\omega t}$.

The assumption of hysteretic damping consists of writing the harmonic dynamic equation as:

$$(-\omega^2 \mathbf{M} + \mathbf{K}' + i\mathbf{K}'')\mathbf{z} = \mathbf{f} \quad (3.31)$$

indicating that there is a dissipation force (i.e. in phase with the velocities) but which amplitude is independent of the frequency.³ The matrix $\mathbf{K}' + i\mathbf{K}''$ is usually obtained by assuming that the material in the structure has a complex Young's modulus:⁴

$$E_{\text{hysteretic}} = E' + iE'' \quad (3.32)$$

where E' and E'' are constants called the *storage modulus* and the *loss modulus* respectively. This assumption is also sometimes called *structural damping*. One can write:

$$E_{\text{hysteretic}} = E'(1 + i\gamma) \quad (3.33)$$

where $\frac{E''}{E'}$ is called the *loss factor*. The dynamic problem (3.31) can obviously be solved in the frequency domain, meaning that one can compute the complex harmonic response \mathbf{z} for a range of excitation frequency ω . One can also compute eigenmodes and eigenfrequencies by solving the eigenvalue problem, similarly to (3.9),

$$(\lambda^2 \mathbf{M} + (\mathbf{K}' + i\mathbf{K}''))\mathbf{z}_{(r)} = \mathbf{0} \quad (3.34)$$

which is not a common eigenproblem since one matrix is complex. If however one wants to solve a transient problem where a time response is computed for an arbitrary applied force in time, the system (3.34) needs to be transformed into the time domain. As mentioned before (see footnote on page 163) this can not be done, but an approximate problem can still be constructed in the time domain provided that the damping is small so that, as explained next, one can define quantitatively equivalent viscous damping ratios by analyzing the system in the basis of the modes $\mathbf{x}_{(r)}$ of the associated conservative system, defined by:

$$(\mathbf{K}' - \omega_{0r}^2 \mathbf{M}) \mathbf{x}_{(r)} = \mathbf{0}$$

In the general case, the imaginary part of the stiffness \mathbf{K}'' is not proportional to the real one \mathbf{K}' , so that it does not become diagonal when projected onto the eigenmodes $\mathbf{x}_{(r)}$ of the undamped system.

One can however now define a modal damping ratio ε_r per eigenfrequency if one assumes that the light damping assumption as formulated in Section 3.1.2 is applicable (small damping and well-separated eigenfrequencies).

Developing the solution \mathbf{z} of Equation (3.31) in terms of the normal modes $\mathbf{x}_{(r)}$, and projecting the problem on that modal space, yields the normal equations:

$$\left(-\omega^2 \mu_r + i \sum_{s=1}^n \mathbf{x}_{(s)}^T \mathbf{K}' \mathbf{x}_{(r)} + \omega_{0r}^2 \mu_r \right) \eta_r = \mathbf{x}_{(r)}^T \mathbf{f} \quad (3.35)$$

³ It can be shown that the hysteretic damping model is not physically correct because it violates the principle of causality (see Chapter 2, Section 2.7.2) and therefore, cannot be transposed to the time domain. One observes for instance that with such a model, damping forces will exist even for a static excitation, which is unexpected. The reason for using such a damping model is that, in a limited frequency range, it represents quantitatively representative of a large class of real structures such as assembled structures where the mechanical joints generate dry friction forces. The latter are nonlinear, and generate in harmonic motion dissipation forces that do not increase linearly with excitation frequency.

⁴ The concept of Young's modulus E is introduced in Chapter 4, Section 4.1.3. For a structure made of a single material and behaving linearly, its stiffness matrix is proportional to it.

Using the small damping assumption Equation, (3.35) can be approximated as:

$$(-\omega^2 \mu_r + i \mathbf{x}_{(r)}^T \mathbf{K}' \mathbf{x}_{(r)} + \omega_{0r}^2 \mu_r) \eta_r = \mathbf{x}_{(r)}^T \mathbf{f} \quad (3.36)$$

Comparison of Equation (3.36) with the normal equation of a linear viscously damped system:

$$(-\omega^2 \mu_r + i \omega \beta_{rr} + \omega_{0r}^2 \mu_r) \eta_r = \mathbf{x}_{(r)}^T \mathbf{f}$$

provides the equivalence:

$$\omega \beta_{rr} = \mathbf{x}_{(r)}^T \mathbf{K}' \mathbf{x}_{(r)} \quad (3.37)$$

Around the eigenfrequency ω_{0r} one can thus define an equivalent viscous damping for mode r by:

$$\varepsilon_r = \frac{\beta_{rr}}{2\mu_r\omega_{0r}} = \frac{\mathbf{x}_{(r)}^T \mathbf{K}' \mathbf{x}_{(r)}}{2\mu_r\omega_{0r}^2} \quad (3.38)$$

Using these equivalent viscous damping ratios per mode, one can then construct a viscous damping matrix \mathbf{C} as discussed in Sections 3.1.2 and 3.1.3.

The situation is greatly simplified when $\mathbf{K}'' = \gamma \mathbf{K}'$ (for instance when the entire structure is a monolithic construction made of a single material) since in that case, damping remains proportional, and (3.38) is written as

$$\varepsilon_r = \frac{\gamma}{2} \quad (3.39)$$

3.2.3 Force appropriation testing

The most frequent objective of a vibration test is to determine the modal characteristics (eigenmodes and eigenfrequencies) of the associated conservative system. A natural procedure consists of forcing the vibration of the structure in each of its eigenmodes successively, requiring proper tuning of the frequency and force amplitudes in order to reach the appropriate excitation for each mode.

There is no direct method to determine the appropriate excitation of a given vibration mode. It must be obtained through successive approximations from criteria such as the *phase lag quadrature* or the *stationary nature of reactive power* to verify that the mode appropriation is effectively achieved.

Phase lag quadrature criterion

When a harmonic vibration test is performed on a damped system, the amplitudes of applied forces and the response amplitudes at the different points verify the complex relationship (3.28):

$$(\mathbf{K} - \omega^2 \mathbf{M} + i\omega \mathbf{C}) \mathbf{z} = \mathbf{f} \quad (3.40)$$

Extracting a given eigenmode of the associated conservative system through appropriate excitation is equivalent to assuming that:

$$\mathbf{z} = \mathbf{x}_{(k)} \quad \text{and} \quad \omega = \omega_{0k}$$

Equation (3.40) then becomes:

$$(\mathbf{K} - \omega_{0k}^2 \mathbf{M} + i\omega_{0k} \mathbf{C}) \mathbf{x}_{(k)} = \mathbf{f}_{(k)} \quad (3.41)$$

where $\mathbf{f}_{(k)}$ is the excitation mode which allows one to achieve the appropriate excitation. Because ω_{0k}^2 and $\mathbf{x}_{(k)}$ are eigensolutions of the associated conservative system, one has:

$$(\mathbf{K} - \omega_{0k}^2 \mathbf{M}) \mathbf{x}_{(k)} = \mathbf{0}$$

and the expression of the excitation which makes it possible to excite eigenmode $\mathbf{x}_{(k)}$ at its resonance frequency results from Equation (3.41):

$$\mathbf{f}_{(k)} = i\omega_{0k} \mathbf{C} \mathbf{x}_{(k)} \quad (3.42)$$

This shows that the excitation, when appropriate, is in phase with the dissipation forces and thus has a phase lag of 90° with respect to the response.

The reciprocal is always true: if it is supposed that all excitation forces are synchronous and that the response at every point of the structure is in phase quadrature with the excitation, the phase relationship between response and excitation may be expressed by assuming that \mathbf{z} is a real vector and \mathbf{f} an imaginary one. The real and imaginary parts may then be separated in Equation (3.40), namely:

$$(\mathbf{K} - \omega^2 \mathbf{M}) \mathbf{z} = \mathbf{0}$$

$$\mathbf{f} = i\omega \mathbf{C} \mathbf{z}$$

showing that the only admissible solutions for ω and \mathbf{z} are the eigensolutions of the associated conservative system.

In order to understand the concept of phase quadrature, let us consider the representation of the equation of motion in the complex plane. When the excitation is appropriate, all degrees of freedom are in phase and dynamic equilibrium is expressed in the form:

$$(\mathbf{K} - \omega_{0k}^2 \mathbf{M} + i\omega_{0k} \mathbf{C}) \mathbf{x}_{(k)} - \mathbf{f}_{(k)} = \mathbf{0} \quad (3.43)$$

the complex plane representation of which is given by Figure 3.5.

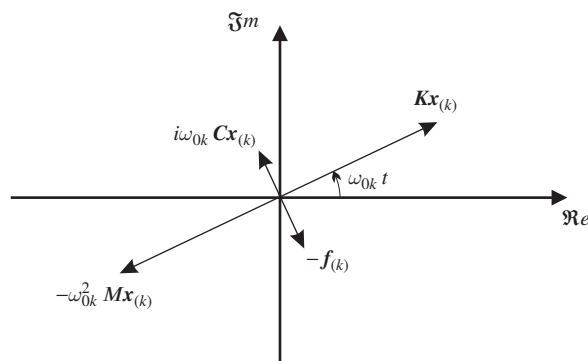


Figure 3.5 Representation of phase quadrature in the complex plane under appropriate excitation.

This shows that, when the excitation is appropriate, the elastic forces $\mathbf{K}\mathbf{x}_{(k)}$ and the inertia forces $\omega_{0k}^2 \mathbf{M}\mathbf{x}_{(k)}$ cancel each other as if the system were vibrating in an undamped fashion, while the excitation force $\mathbf{f}_{(k)}$ equilibrates the damping forces which are proportional to velocity and thus have a phase advance of $\pi/2$.

The *phase quadrature criterion* may thus be formulated as follows:

The structure vibrates according to one of the eigenmodes of the associated conservative system if and only if all degrees of freedom vibrate synchronously and have a phase lag of $\pi/2$ with respect to the excitation.

Once the phase quadrature criterion is verified during the experimental test, one may take note of ω_{0k} and measure the corresponding eigenshape $\mathbf{x}_{(k)}$.

Stationary reactive power criterion

Although beyond the scope of this text, a complete discussion of the stationary reactive power criterion is given in the literature (Fraeijs de Veubeke 1965). Let us simply mention that it is equivalent to the phase quadrature criterion applied to all degrees of freedom simultaneously, but has the advantage that it is able to provide *a global measure of the accuracy with which the phase quadrature criterion is verified*.

In order to get a better insight into the forces acting on a damped system, let us return to the dynamic equilibrium for a harmonic excitation expressed in the complex space:

$$\mathbf{K}\mathbf{q} + \mathbf{C}\dot{\mathbf{q}} + \mathbf{M}\ddot{\mathbf{q}} - \mathbf{p} = 0$$

where $\mathbf{q} = \mathbf{z}e^{i\omega t}$ and $\mathbf{p} = \mathbf{f}e^{i\omega t}$, yielding:

$$(\mathbf{K} - \omega^2 \mathbf{M} + i\omega \mathbf{C}) \mathbf{z} - \mathbf{f} = 0$$

Let us note that, for appropriate excitation testing, the applied forces are synchronous, i.e. they all have the same phase lag. We can thus assume that the vector \mathbf{f} of excitation amplitudes is real. By expanding the complex amplitudes \mathbf{z} in terms of the modes of the associated conservative system:

$$\mathbf{z} = \sum_{s=1}^n \eta_s \mathbf{x}_{(s)} e^{-i\psi_s}$$

the dynamic equilibrium becomes:

$$\gamma_s \eta_s - \omega^2 \mu_s \eta_s + i\omega \sum_{r=1}^n \beta_{rs} \eta_r e^{i(\psi_s - \psi_r)} - \phi_s e^{i\psi_s} = 0 \quad s = 1, \dots, n \quad (3.44)$$

where η_s are the modal amplitudes and ψ_s their phase lag with respect to the modal participation factor $\phi_s = \mathbf{x}_{(s)}^T \mathbf{f}$. The equilibrium can then be studied by considering the projection of the complex vectors on the real axis in Figure 3.6 where we assume $\gamma_s / \mu_s = \omega_{0s}^2 < \omega^2$ and, for the sake of clarity, $\beta_{rs} = 0$, $r \neq s$.

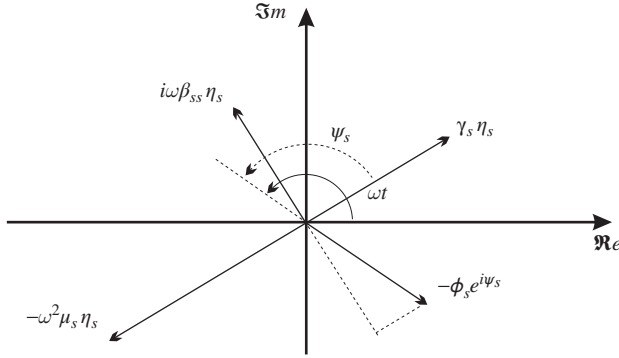


Figure 3.6 Dynamic equilibrium of a damped system under harmonic excitation.

The instantaneous power of the damping forces is given by:

$$\begin{aligned} \Re e(\dot{\mathbf{q}})^T \Re e(\mathbf{C}\dot{\mathbf{q}}) &= \sum_{s=1}^n \sum_{r=1}^n \omega^2 \eta_s \eta_r (\mathbf{x}_{(s)}^T \mathbf{C} \mathbf{x}_{(r)}) \sin(\omega t - \psi_s) \sin(\omega t - \psi_r) \\ &= \frac{\omega^2}{2} \sum_{s=1}^n \sum_{r=1}^n \eta_s \eta_r \beta_{rs} (\cos(\psi_s - \psi_r) - \sin(2\omega t - \psi_s - \psi_r)) \end{aligned} \quad (3.45)$$

The resulting forces arising from the elastic and inertia forces have as instantaneous power:

$$\Re e(\dot{\mathbf{q}})^T \Re e((\mathbf{K} - \omega^2 \mathbf{M})\mathbf{q}) = -\omega \sum_{s=1}^n \eta_s^2 (\gamma_s - \omega^2 \mu_s) \frac{\sin(2(\omega t - \psi_s))}{2} \quad (3.46)$$

Let us note that in the particular case of appropriate excitation, we have $\omega^2 = \omega_{0k}^2 = \gamma_k / \mu_k$ and $\eta_s = 0$ for $s \neq k$: the inertia and elastic forces equilibrate each other at every instant, and at every instant the applied forces equilibrate the dissipation forces. The phase lag is then $\psi_k = \pi/2$, which corresponds to phase lag quadrature. In the case of a general harmonic excitation, the power (3.46) developed by the elastic and inertia forces changes its sign four times in the interval $(\omega t - \psi_s) \in [0, 2\pi]$ so that it balances to zero over one cycle. The energy input during one cycle due to the external forces is thus equal to the energy dissipated through damping:

$$\begin{aligned} \int_0^{\frac{2\pi}{\omega}} \Re e(\dot{\mathbf{q}})^T \Re e(\mathbf{p}) dt &= \int_0^{\frac{2\pi}{\omega}} \Re e(\dot{\mathbf{q}})^T \Re e(\mathbf{C}\dot{\mathbf{q}}) dt \\ &= \pi\omega \sum_{s=1}^n \sum_{r=1}^n \eta_s \eta_r \beta_{rs} \cos(\psi_s - \psi_r) = \pi\omega \mathbf{z}^T \mathbf{C} \bar{\mathbf{z}} \end{aligned} \quad (3.47)$$

where

$$\bar{\mathbf{z}} = \sum_{s=1}^n \eta_s \mathbf{x}_{(s)} e^{i\psi_s}$$

is the complex conjugate of \mathbf{z} .

In a general way we will define the *complex power* \mathcal{P} associated with a force \mathbf{p} and a complex displacement \mathbf{q} by:

$$\begin{aligned}\mathcal{P} &= \mathbf{p}^T(t) \dot{\mathbf{q}}(t) \\ &= (e^{i\omega t} \mathbf{f}^T) (-i\omega e^{-i\omega t} \bar{\mathbf{z}}) \\ &= -i\omega \mathbf{z}^T (\mathbf{K} - \omega^2 \mathbf{M} + i\omega \mathbf{C}) \bar{\mathbf{z}}\end{aligned}\quad (3.48)$$

and its real part yields the *active power*:

$$\mathcal{P}_R = \Re \{ \mathcal{P} \} = \omega^2 \mathbf{z}^T \mathbf{C} \bar{\mathbf{z}} \quad (3.49)$$

It corresponds to the amplitude of the instantaneous power of the damping forces (3.45) and is equal to the energy input over one cycle to a factor π/ω . The imaginary part of the complex power yields the *reactive power*:

$$\mathcal{P}_I = \Im \{ \mathcal{P} \} = -\omega \mathbf{z}^T (\mathbf{K} - \omega^2 \mathbf{M}) \bar{\mathbf{z}} \quad (3.50)$$

corresponding to the amplitude of the power (3.46) exchanged between the elastic and inertia forces, and the excitation at every instant.

The stationary reactive power criterion is based on the definition of the complex power delivered to the system, which can be measured during a vibration test with simultaneous excitation on several degrees of freedom.

Let us determine under which condition the reactive power \mathcal{P}_I becomes stationary with respect to a modification, at constant frequency, of the excitation amplitude or, equivalently since they are uniquely linked to each other, to a modification of the response amplitude. The following result is obtained:

$$\begin{aligned}\delta \mathcal{P}_I &= -\omega \delta \mathbf{z}^T (\mathbf{K} - \omega^2 \mathbf{M}) \bar{\mathbf{z}} - \omega \mathbf{z}^T (\mathbf{K} - \omega^2 \mathbf{M}) \delta \bar{\mathbf{z}} \\ &= 0 \quad \text{for every } \delta \mathbf{z} \text{ if and only if } \omega = \omega_{0k} \quad \text{and} \quad \mathbf{z} = \mathbf{x}_{(k)}\end{aligned}\quad (3.51)$$

which shows that the reactive power becomes insensitive to slight excitation changes when the system is vibrating according to one of the undamped eigenmodes $\mathbf{x}_{(k)}$ at the corresponding frequency ω_{0k} . In that case, we also observe that, owing to relation (3.50), the reactive power at any instant is zero, meaning that inertia and elastic forces compensate one another without needing any power transfer from the excitation.

When the stationary reactive power criterion is verified, measuring the reactive power allows evaluation of the corresponding modal damping, since we then have:

$$\mathcal{P}_R = \omega_{0k}^2 \mathbf{x}_{(k)}^T \mathbf{C} \mathbf{x}_{(k)} = \omega_{0k}^2 \beta_{kk} \quad (3.52)$$

Conversely, when the frequency is modified while the excitation amplitude is maintained constant, the variation of reactive power with frequency is given by:

$$\begin{aligned}\frac{\partial \mathcal{P}_I}{\partial \omega} &= -\mathbf{z}^T (\mathbf{K} - \omega^2 \mathbf{M}) \bar{\mathbf{z}} - \omega \frac{\partial \mathbf{z}^T}{\partial \omega} (\mathbf{K} - \omega^2 \mathbf{M}) \bar{\mathbf{z}} \\ &\quad - \omega \mathbf{z}^T (\mathbf{K} - \omega^2 \mathbf{M}) \frac{\partial \bar{\mathbf{z}}}{\partial \omega} + 2\omega^2 \mathbf{z}^T \mathbf{M} \bar{\mathbf{z}}\end{aligned}$$

or, when the excitation is appropriate:

$$\frac{\partial P_I}{\partial \omega} = 2\omega_{0k}^2 \mathbf{x}_{(k)}^T \mathbf{M} \mathbf{x}_{(k)} = 2\omega_{0k}^2 \mu_k \quad (3.53)$$

Therefore, varying reactive power with frequency allows measurement of the generalized mass of the mode.

The methods based on excitation appropriation are by far the most reliable ones to determine the modal characteristics of structures (eigenfrequencies and mode shapes, generalized masses, modal damping coefficients). They allow visualization of the real modes of the structure. Moreover, in the case of appropriate excitation, the eigenmodes and the frequencies of the structure are measured directly, which also allows observation of the non-linear behaviour.

These methods are, however, long and delicate to implement, since they require a simultaneous excitation of several degrees of freedom and lead to trial-and-error procedures to reach the appropriate excitation conditions (phase quadrature between excitation and response at all shakers, or reactive power stationarity). Moreover, this experimental technique requires a lot of equipment, as suggested by the sketch of the testing setup in Figure 3.7.

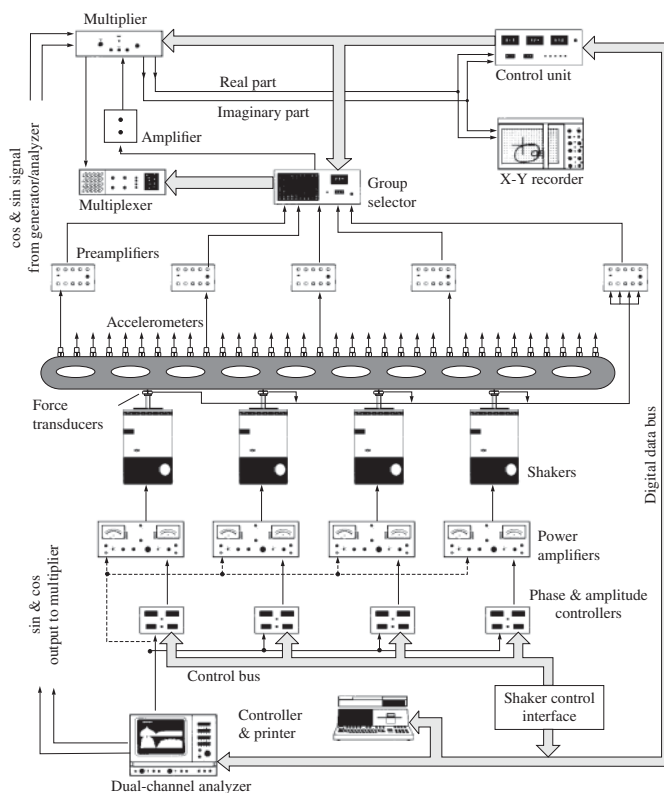


Figure 3.7 Experimental setup for modal analysis of a large structure using appropriate excitation (Zaveri 1984). Source: Reproduced with permission. Copyright © Brüel & Kjær Sound & Vibration Measurement A/S.

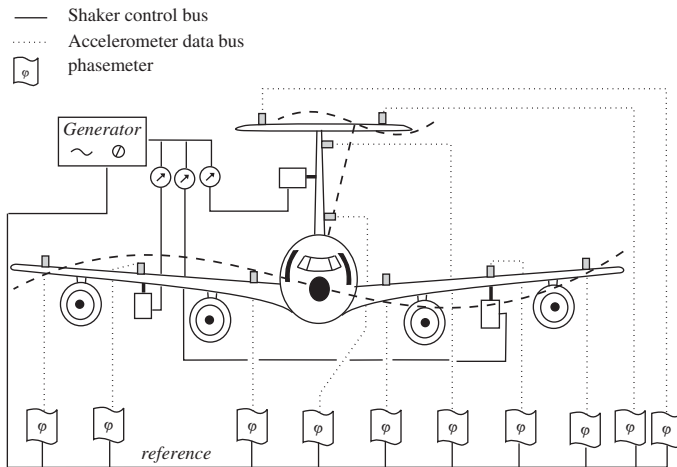


Figure 3.8 Modal analysis of an airplane through appropriate excitation.

Use of these methods is therefore limited to the testing of structures for which it is necessary to have very accurate knowledge of modal properties – airplanes (Figure 3.8) and spacecraft in particular – and for which testing techniques based on the measurement of transfer functions (see below) are often less suitable.

As seen above, in force appropriation testing, the phase lag criterion or the stationarity of the reactive power (with respect to the amplitudes) can be used to assert that a mode and eigenfrequency of the undamped system have been found. When appropriation is achieved, the observed active power yields the corresponding modal damping and the modal mass is obtained through variation of the reactive power with the frequency. Finding such an appropriate force distribution during testing is however a difficult iterative task. An iterative strategy to converge to it can be devised using the concept of characteristic phase lags as explained in Section 3.2.4.

3.2.4 The characteristic phase lag theory

The phase lag criterion (see previous section) states that during an appropriation test, the amplitude and frequency of the excitation must be tuned such that all degrees of freedom respond synchronously and with a (single) phase lag of $\pi/2$. Reaching such a state requires iteratively varying the frequency and amplitude of the excitation. One way to guide the experimentalist in this task is explained next.

Let us imagine that during an appropriation testing, several steps in excitation frequencies are performed. For each of these steps, the excitation frequency ω is fixed and the shakers are driven such that the forces they produce on each degree of freedom have a unique phase. The amplitudes of the force applied at each degree of freedom are then adjusted until all the responses are synchronous (see a schematic representation of the test setup in Figure 3.8). As will be outlined in this section, such synchronous responses for a given excitation frequency ω are specific solutions called *response normal modes*, and the phases between those synchronous responses and synchronous excitations are characteristics of the system. If these

response normal modes are obtained for each frequency step ω , the undamped eigenmodes will be the response normal modes when their characteristic phase lag is equal to $\pi/2$.

Characteristic phase lags and normal modes (Fraeijs de Veubeke 1965)

Let us assume that the harmonic excitation is such that all forces have the same phase (taken as reference). The forced response is then governed by equation:

$$\mathbf{M}\ddot{\mathbf{q}} + \mathbf{C}\dot{\mathbf{q}} + \mathbf{K}\mathbf{q} = \mathbf{f} \sin \omega t \quad (3.54)$$

Generally speaking the forced harmonic response would not be synchronous (see Section 3.2), i.e. all degrees of freedom would respond with a different phase due to the damping forces. Let us however seek for special single phase responses $\mathbf{q}_{(k)}$:

$$\mathbf{q}_{(k)} = \mathbf{r}_{(k)} \sin(\omega t - \phi_k) \quad (3.55)$$

that, when the excitation frequency ω is given, can exist only under specific excitation amplitudes $\mathbf{f}_{(k)}$ and for specific phase lags ϕ_k . The response amplitudes $\mathbf{r}_{(k)}$ will be called *response normal modes*.

Substituting (3.55) into (3.54) leads to the temporal equation:

$$(\mathbf{K} - \omega^2 \mathbf{M}) \mathbf{r}_{(k)} \sin(\omega t - \phi_k) + \omega \mathbf{C} \mathbf{r}_{(k)} \cos(\omega t - \phi_k) = \mathbf{f}_{(k)} \sin \omega t \quad (3.56)$$

One may develop the $(\omega t - \phi)$ terms and separate the terms in $\sin \omega t$ and $\cos \omega t$, which yields the system of equations:

$$\cos \phi_k (\mathbf{K} - \omega^2 \mathbf{M}) \mathbf{r}_{(k)} + \omega \sin \phi_k \mathbf{C} \mathbf{r}_{(k)} = \mathbf{f}_{(k)} \quad (3.57)$$

$$\sin \phi_k (\mathbf{K} - \omega^2 \mathbf{M}) \mathbf{r}_{(k)} - \omega \cos \phi_k \mathbf{C} \mathbf{r}_{(k)} = \mathbf{0} \quad (3.58)$$

The excitation frequency ω being given, both equations contain the unknowns $\mathbf{r}_{(k)}$, $\mathbf{f}_{(k)}$ and ϕ_k corresponding to a synchronous solution. If $\phi_k \neq \pi/2$, one may divide (3.58) by $\cos \phi_k$, which gives:

$$\tan \phi_k (\mathbf{K} - \omega^2 \mathbf{M}) \mathbf{r}_{(k)} = \omega \mathbf{C} \mathbf{r}_{(k)} \quad (3.59)$$

Equation (3.59) may be interpreted as an eigenvalue problem of dimension n for eigenvalues $\tan \phi_k$, and eigenvectors $\mathbf{r}_{(k)}$. It shows that, at a given excitation frequency ω , the structural response is characterized by:

- the *response normal modes* $\mathbf{r}_{(k)}$ and their *characteristic phase lag* ϕ_k verifying (3.59),
- the corresponding force distribution $\mathbf{f}_{(k)}$ computed from (3.57).

Let us note that the eigenvalues $\tan \phi_k$ are effectively real since:

$$\tan \phi_k = \frac{\omega \mathbf{r}_{(k)}^T \mathbf{C} \mathbf{r}_{(k)}}{\mathbf{r}_{(k)}^T (\mathbf{K} - \omega^2 \mathbf{M}) \mathbf{r}_{(k)}} \quad (3.60)$$

Once $\tan \phi_k$ is known, the phase lags ϕ_k are uniquely determined owing to the condition:

$$0 \leq \phi_k \leq \pi$$

Moreover,

1. When $\omega \rightarrow 0$, $\tan \phi_k \rightarrow 0^+$: all the phase lags tend to 0 and the response remains necessarily in phase with the excitation.
2. When $\omega \rightarrow \infty$, $\tan \phi_k \rightarrow 0^-$: all the phase lags tend to π and the response is in phase opposition to the excitation.
3. The most important case is when the excitation frequency ω equals one of the eigenfrequencies ω_{0s} of the associated undamped system. In that case, let us rewrite the characteristic phase lag equation in the form:

$$(\mathbf{K} - \omega^2 \mathbf{M}) \mathbf{r}_{(k)} = \frac{\omega \mathbf{C} \mathbf{r}_{(k)}}{\tan \phi_k}$$

One can immediately verify that when:

$$\phi_k = \frac{\pi}{2}$$

the associate normal response mode $\mathbf{r}_{(k)}$ is an undamped normal mode of the system and the frequency for which this occurs is the associated eigenfrequency:

$$\mathbf{r}_{(k)} = \mathbf{x}_{(s)} \quad \text{and} \quad \omega = \omega_{0s}$$

To summarize,

When the excitation frequency is equal to one of the natural eigenfrequencies, one of the normal response modes coincides with the associated eigenmode of the undamped system, and its characteristic phase lag is equal to 90° .

Energy dissipated per cycle

The energy \mathcal{E}_k dissipated per cycle in the response mode $\mathbf{r}_{(k)}$ is written:

$$\mathcal{E}_k = \int_0^{2\pi/\omega} \dot{\mathbf{q}}^T \mathbf{f}_{(k)} \sin \omega t \, dt = \omega \mathbf{r}_{(k)}^T \mathbf{f}_{(k)} \int_0^{2\pi/\omega} \sin \omega t \cos(\omega t - \phi_k) \, dt$$

or

$$\mathcal{E}_k = \mathbf{r}_{(k)}^T \mathbf{f}_{(k)} \pi \sin \phi_k \quad (3.61)$$

Returning to relationships (3.57, 3.58) and multiplying them by $\sin \phi_k$ and $\cos \phi_k$ yields:

$$\begin{cases} \sin \phi_k \cos \phi_k (\mathbf{K} - \omega^2 \mathbf{M}) \mathbf{r}_{(k)} + \omega \sin^2 \phi_k \mathbf{C} \mathbf{r}_{(k)} = \mathbf{f}_{(k)} \sin \phi_k \\ \cos \phi_k \sin \phi_k (\mathbf{K} - \omega^2 \mathbf{M}) \mathbf{r}_{(k)} - \omega \cos^2 \phi_k \mathbf{C} \mathbf{r}_{(k)} = \mathbf{0} \end{cases}$$

and subtracting one expression from the other yields:

$$\mathbf{f}_{(k)} \sin \phi_k = \omega \mathbf{C} \mathbf{r}_{(k)}$$

By taking into account the relationship above, the energy \mathcal{E}_k may still be written in the form:

$$\begin{aligned} \mathcal{E}_k &= \pi \omega \mathbf{r}_{(k)}^T \mathbf{C} \mathbf{r}_{(k)} \\ &= \int_0^{2\pi/\omega} \dot{\mathbf{q}}^T \mathbf{C} \dot{\mathbf{q}} \, dt \end{aligned} \quad (3.62)$$

One notes then that only dissipative forces contribute to the dissipated energy. Therefore, measuring \mathcal{E}_k enables us to evaluate the damping coefficients β_k when $\mathbf{r}_{(k)} = \mathbf{x}_{(k)}$, as already indicated in (3.52).

Orthogonality of normal response modes

Let us express the characteristic equation for the normal response modes k and l :

$$\tan \phi_k (\mathbf{K} - \omega^2 \mathbf{M}) \mathbf{r}_{(k)} = \omega \mathbf{C} \mathbf{r}_{(k)}$$

$$\tan \phi_l (\mathbf{K} - \omega^2 \mathbf{M}) \mathbf{r}_{(l)} = \omega \mathbf{C} \mathbf{r}_{(l)}$$

Premultiplying the first expression by the normal response mode l and the second one by mode k yields:

$$\tan \phi_k \mathbf{r}_{(l)}^T (\mathbf{K} - \omega^2 \mathbf{M}) \mathbf{r}_{(k)} = \omega \mathbf{r}_{(l)}^T \mathbf{C} \mathbf{r}_{(k)}$$

$$\tan \phi_l \mathbf{r}_{(k)}^T (\mathbf{K} - \omega^2 \mathbf{M}) \mathbf{r}_{(l)} = \omega \mathbf{r}_{(k)}^T \mathbf{C} \mathbf{r}_{(l)}$$

By subtracting and taking account of the symmetry of \mathbf{C} and $(\mathbf{K} - \omega^2 \mathbf{M})$ one obtains the orthogonality relationships, if $\phi_k \neq \phi_l$,

$$\begin{aligned} \mathbf{r}_{(l)}^T (\mathbf{K} - \omega^2 \mathbf{M}) \mathbf{r}_{(k)} &= 0 \\ \mathbf{r}_{(l)}^T \mathbf{C} \mathbf{r}_{(k)} &= 0 \end{aligned} \quad l \neq k \quad (3.63)$$

Application of the degeneracy theorem introduced in Section 2.3.2 shows that the relationships above remain valid if $\phi_l = \phi_k$, since the normal response modes associated with multiple characteristic phase lags are linearly independent and can thus be orthogonalized. Let us note that the very specific case $\phi_l = \phi_k = \frac{\pi}{2}$ is not considered: it would require further discussion.

Furthermore, let us observe that if relationship (3.58) is multiplied to the left by $\mathbf{r}_{(l)}^T$, the orthogonality relationships become:

$$\mathbf{r}_{(l)}^T \mathbf{f}_{(k)} = 0 \quad l \neq k \quad (3.64)$$

which establishes the important property:

The energy introduced by a given excitation is distributed only on the associated normal response modes.

Example 3.3

In order to illustrate the concept presented above, let us consider again the two-degree-of-freedom system of Figure 3.1. The eigenvalues of the undamped system were already computed in Example 3.1.

For a given excitation frequency ω , the eigenvalue problem obtained from Equation (3.59):

$$(\mathbf{K} - \omega^2 \mathbf{M}) \mathbf{r} = \lambda \mathbf{C} \mathbf{r}$$

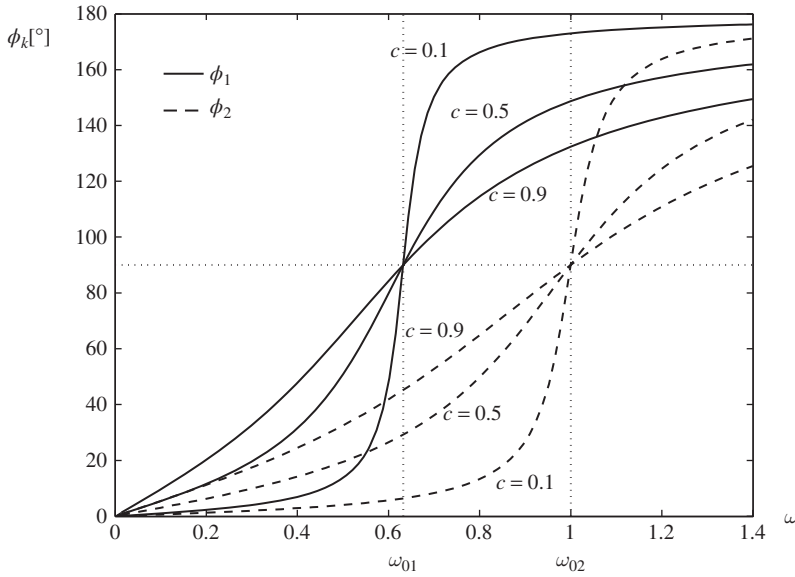


Figure 3.9 Characteristic phase lags of the 2-DOF system for different damping values.

can be solved the using a numerical toolbox and the phase lags are computed from its eigenvalues as:

$$\phi_i(\omega) = \arctan\left(\frac{\omega}{\lambda_i}\right) \quad i = 1, 2$$

Figure 3.9 displays the evolution of both phase lags $\phi_i(\omega)$ over the frequency range $[0-1.4]$ rad/s for different values of the damping coefficient c . It shows that the crossing points of both series of curves occur at $\phi = \frac{\pi}{2}$ for an excitation frequency equal to the resonance frequency ω_{0i} . The response modes $\mathbf{r}_{(i)}$ being known only to a constant, they have been scaled so that $\mathbf{r}_{(i)}^T = [1 \ r_{(i),2}]$. Both of them are displayed on Figure 3.10 for $c = 0.1$. It is easily verified from Figure 3.10 that they coincide with the normal vibration mode when the excitation frequency equals the corresponding eigenfrequency of the undamped system.

3.3 State-space formulation of damped systems

The knowledge of the general structure of the solution to Equations (3.3) governing the behaviour of a damped system is especially useful for the development of experimental methods in structural identification.

In order to solve (3.3), let us transform it into a system of $2n$ first-order equations by considering the velocities $\dot{\mathbf{q}}$ as independent unknowns. Adding the equality $\mathbf{M}\dot{\mathbf{q}} - \mathbf{M}d\mathbf{q}/dt = \mathbf{0}$ the extended dynamic equilibrium equation is obtained:

$$\begin{bmatrix} \mathbf{C} & \mathbf{M} \\ \mathbf{M} & \mathbf{0} \end{bmatrix} \frac{d}{dt} \begin{bmatrix} \mathbf{q} \\ \dot{\mathbf{q}} \end{bmatrix} + \begin{bmatrix} \mathbf{K} & \mathbf{0} \\ \mathbf{0} & -\mathbf{M} \end{bmatrix} \begin{bmatrix} \mathbf{q} \\ \dot{\mathbf{q}} \end{bmatrix} = \begin{bmatrix} \mathbf{p} \\ \mathbf{0} \end{bmatrix} \quad (3.65)$$

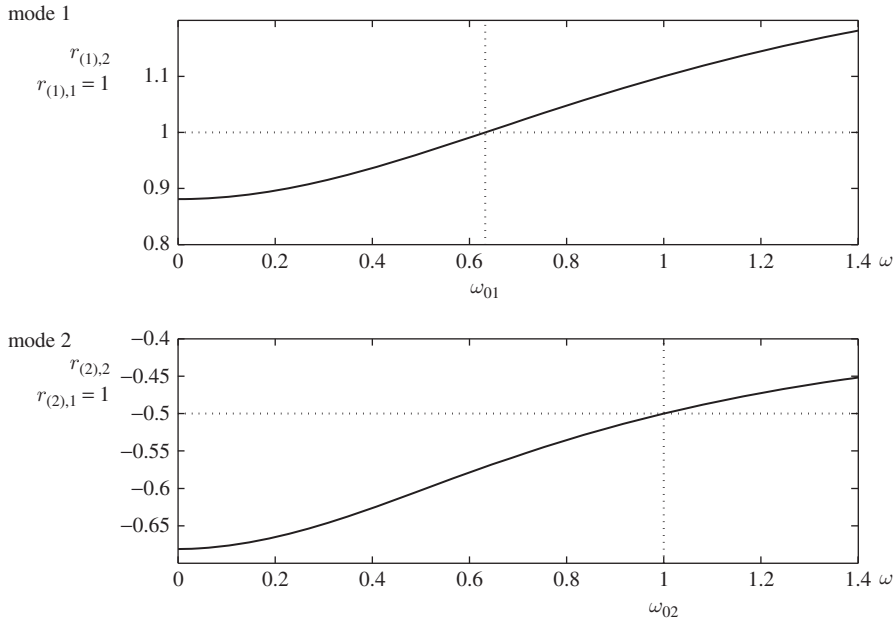


Figure 3.10 Response normal modes of the 2-DOF system for $c = 0.1$.

thus takes the canonical form:

$$A\mathbf{r} + B\dot{\mathbf{r}} = \mathbf{s} \quad (3.66)$$

with the symmetric matrices:

$$A = \begin{bmatrix} K & 0 \\ 0 & -M \end{bmatrix} \quad B = \begin{bmatrix} C & M \\ M & 0 \end{bmatrix} \quad (3.67)$$

and the state and excitation vectors:

$$\mathbf{r} = \begin{bmatrix} q \\ \dot{q} \end{bmatrix} \quad \mathbf{s}(t) = \begin{bmatrix} p(t) \\ 0 \end{bmatrix} \quad (3.68)$$

Note that this state-space form is not unique. The choice proposed here results in a symmetric form, making the analysis more convenient.

3.3.1 Eigenvalue problem and solution of the homogeneous case

In the absence of external excitation applied to the system, one obtains the homogeneous problem:

$$A\mathbf{r} + B\dot{\mathbf{r}} = \mathbf{0} \quad (3.69)$$

and substitution of a solution of the form:

$$\mathbf{r} = \mathbf{y}e^{\lambda t}$$

gives the eigenvalue problem:

$$\mathbf{A}\mathbf{y} + \lambda\mathbf{B}\mathbf{y} = \mathbf{0} \quad (3.70)$$

having $2n$ eigensolutions called $(\lambda_k, \mathbf{y}_{(k)})$.

Orthogonality relationships

Let us consider the relationships verified by two eigensolutions k and j , and premultiply each of them by the other eigenvector:

$$\mathbf{y}_{(j)}^T \mathbf{A} \mathbf{y}_{(k)} + \lambda_k \mathbf{y}_{(j)}^T \mathbf{B} \mathbf{y}_{(k)} = 0$$

$$\mathbf{y}_{(k)}^T \mathbf{A} \mathbf{y}_{(j)} + \lambda_j \mathbf{y}_{(k)}^T \mathbf{B} \mathbf{y}_{(j)} = 0$$

By taking into account the symmetry of the matrices \mathbf{A} and \mathbf{B} one obtains:

$$(\lambda_k - \lambda_j) \mathbf{y}_{(j)}^T \mathbf{B} \mathbf{y}_{(k)} = 0$$

Hence, provided that $\lambda_k \neq \lambda_j$ for $k \neq j$, the orthogonality relationships take the form:

$$\begin{aligned} \mathbf{y}_{(j)}^T \mathbf{B} \mathbf{y}_{(k)} &= \tilde{\mu}_k \delta_{kj} \\ \mathbf{y}_{(j)}^T \mathbf{A} \mathbf{y}_{(k)} &= \tilde{\gamma}_k \delta_{kj} \end{aligned} \quad (3.71)$$

where we use the notations $\tilde{\gamma}_k$ and $\tilde{\mu}_k$ by analogy with the modal mass and stiffness of undamped modes. Note that in general $\tilde{\gamma}_k$ and $\tilde{\mu}_k$ are complex. Taking $k = j$ it becomes apparent that the eigenvalues may also be obtained by forming the Rayleigh quotient:

$$\lambda_k = -\frac{\tilde{\gamma}_k}{\tilde{\mu}_k} = -\frac{\mathbf{y}_{(k)}^T \mathbf{A} \mathbf{y}_{(k)}}{\mathbf{y}_{(k)}^T \mathbf{B} \mathbf{y}_{(k)}} \quad (3.72)$$

Conjugate eigensolutions

If $(\lambda_k, \mathbf{y}_{(k)})$ is an eigensolution, its conjugate $(\bar{\lambda}_k, \bar{\mathbf{y}}_{(k)})$ is also a solution, because the matrices \mathbf{A} and \mathbf{B} are real. Indeed, by setting:

$$\mathbf{y}_{(k)} = \mathbf{u} + i\mathbf{v} \quad \lambda_k = \sigma + i\nu$$

then

$$\mathbf{A}(\mathbf{u} + i\mathbf{v}) + (\sigma + i\nu)\mathbf{B}(\mathbf{u} + i\mathbf{v}) = \mathbf{0}$$

and by separating the real and imaginary parts:

$$\mathbf{A}\mathbf{u} + \sigma\mathbf{B}\mathbf{u} - \nu\mathbf{B}\mathbf{v} = \mathbf{0} \quad \mathbf{A}\mathbf{v} + \nu\mathbf{B}\mathbf{u} + \sigma\mathbf{B}\mathbf{v} = \mathbf{0}$$

To verify the announced property, one may simply observe that equation:

$$\mathbf{A}(\mathbf{u} - i\mathbf{v}) + (\sigma - i\nu)\mathbf{B}(\mathbf{u} - i\mathbf{v}) = \mathbf{0}$$

leads to the same relationships.

Example 3.4

The exact eigenvalues of the system of Figure 3.1 can easily be computed by solving the eigenvalue problem (3.70) with the standard eigenvalue extraction algorithm available in several numerical toolboxes.

The eigenvalues and associated damping coefficients are:

$$\lambda_k^{exact} = \begin{cases} -0.0367 \pm 0.6314i \\ -0.0533 \pm 0.9986i \end{cases} \quad \varepsilon_k^{exact} = \begin{cases} 0.0581 \\ 0.0533 \end{cases} \quad (\text{E3.4.a})$$

It is a case where the damping is sufficiently small and eigenvalues well separated, so that the comparison with Example 3.1 shows that the modal damping assumption made in Section 3.1.2 was fully justified.

The complex eigenmodes appear to be also very close to those of the associated undamped system

$$\mathbf{Z}^{exact} = \begin{bmatrix} 1.0000 & 1.0000 \\ -0.4999 \pm 0.0083i & 0.9997 \pm 0.0105i \end{bmatrix} \quad (\text{E3.4.b})$$

Stability of the general solution

The general solution of Equation (3.3) remains stable if the damping matrix \mathbf{C} is positive definite. By making use of definition (3.68) of the state vector \mathbf{r} , one may write an eigenvector of system (3.69) in the form:

$$\mathbf{y}_{(r)} = \begin{bmatrix} \mathbf{z}_{(r)} \\ \lambda_r \mathbf{z}_{(r)} \end{bmatrix} \quad (3.73)$$

where $\mathbf{z}_{(r)}$ is a complex mode of the initial homogeneous system (3.7). At this point, it is important to understand that $\mathbf{z}_{(r)}$ is a complex eigenmode of the damped system, unlike $\mathbf{x}_{(r)}$ previously defined as a real eigenmode of the associated undamped system.

One obtains in this case the quadratic matrix pencil (Lancaster 1966):

$$(\lambda_r^2 \mathbf{M} + \lambda_r \mathbf{C} + \mathbf{K}) \mathbf{z}_{(r)} = \mathbf{0}$$

and through premultiplication by its conjugate $\bar{\mathbf{z}}_{(r)}^T$:

$$\lambda_r^2 m_r + \lambda_r c_r + k_r = 0$$

with the real constants (the system being stable and thus \mathbf{C} positive definite)

$$\begin{aligned} m_r &= \bar{\mathbf{z}}_{(r)}^T \mathbf{M} \mathbf{z}_{(r)} && \text{positive definite} \\ c_r &= \bar{\mathbf{z}}_{(r)}^T \mathbf{C} \mathbf{z}_{(r)} && \text{positive definite} \\ k_r &= \bar{\mathbf{z}}_{(r)}^T \mathbf{K} \mathbf{z}_{(r)} && \text{positive semi-definite} \end{aligned}$$

Hence, the eigenvalues are written as:

$$\lambda_r = \frac{-c_r \pm \sqrt{c_r^2 - 4k_r m_r}}{2m_r}$$

and they can be put in the complex form:

$$\lambda_r = -\alpha_r \pm i\omega_r \quad (3.74)$$

with

$$\alpha_r = \frac{c_r}{2m_r} \quad \text{and} \quad \omega_r = \sqrt{\left(\frac{k_r}{m_r}\right) - \left(\frac{c_r}{2m_r}\right)^2} \quad (3.75)$$

We note that $\alpha_r > 0$. Further, when $c_r < 2\sqrt{k_r m_r}$, ω_r is real and can be interpreted as the eigenfrequency of the damped mode $z_{(r)}$, sometimes called the *damped eigenfrequency*. For damping values equal or greater than the critical value, namely $c_r \geq 2\sqrt{k_r m_r}$, the eigenvalues λ_r become real negative and the response of the damped system corresponding to $z_{(r)}$ is no longer an oscillation but is monotonically decaying in time. In both cases, the eigensolutions are stable as expected.

In what follows, damping will always be assumed to be subcritical so that ω_r remains real and λ_r is complex. In other words, we are no longer tied by the too restrictive light damping hypothesis made in Section 3.1.2, but still we assume that damping is small enough for the motion to remain oscillatory.

3.3.2 General solution for the nonhomogeneous case

In order to construct the solution of the nonhomogeneous problem (3.65), let us decompose the state vector \mathbf{r} in a series of eigenmodes $\mathbf{y}_{(k)}$:

$$\mathbf{r} = \sum_{k=1}^{2n} \eta_k(t) \mathbf{y}_{(k)} \quad (3.76)$$

By substituting (3.76) into the canonical Equation (3.66) and premultiplying by $\mathbf{y}_{(j)}^T$ one obtains:

$$\mathbf{y}_{(j)}^T \mathbf{A} \mathbf{y}_{(j)} \eta_j + \mathbf{y}_{(j)}^T \mathbf{B} \mathbf{y}_{(j)} \dot{\eta}_j = \mathbf{y}_{(j)}^T \mathbf{s}$$

Thus the problem consists of solving $2n$ first-order equations:

$$-\lambda_j \eta_j + \dot{\eta}_j = \phi_j(t) \quad (3.77)$$

with the eigenvalues and modal participation factor associated to the $\mathbf{y}_{(j)}$:

$$\lambda_j = -\frac{\mathbf{y}_{(j)}^T \mathbf{A} \mathbf{y}_{(j)}}{\mathbf{y}_{(j)}^T \mathbf{B} \mathbf{y}_{(j)}} = -\frac{\tilde{\gamma}_j}{\tilde{\mu}_j} \quad \text{and} \quad \phi_j(t) = \frac{\mathbf{y}_{(j)}^T \mathbf{s}(t)}{\mathbf{y}_{(j)}^T \mathbf{B} \mathbf{y}_{(j)}}$$

Equation (3.77) is solved by multiplying it by $e^{-\lambda_j t}$:

$$\frac{d}{dt}(e^{-\lambda_j t} \eta_j) = e^{-\lambda_j t} \phi_j(t)$$

and integrating to find:

$$\eta_j(t) = e^{\lambda_j t} \left\{ \int_0^t \phi_j(\tau) e^{-\lambda_j \tau} d\tau + \eta_j(0) \right\} \quad (3.78)$$

It is easy to deduce from Equations (3.76) and (3.78) that, in case of free vibration, the response of a degree of freedom r can be expanded in the form (see Exercise 3.4):

$$q_r(t) = \sum_{k=1}^{2n} c_{rk} e^{\lambda_k t} \quad (3.79)$$

with coefficients c_{rk} depending on the initial conditions $(\mathbf{q}_0, \dot{\mathbf{q}}_0)$.

3.3.3 Harmonic response

Under harmonic excitation:

$$s(t) = s_0 e^{i\omega t}$$

in particular, the participation factors to the excitation take the form:

$$\phi_j(t) = \phi_{0j} e^{i\omega t} \quad \text{with} \quad \phi_{0j} = \frac{\mathbf{y}_{(j)}^T \mathbf{s}_0}{\mathbf{y}_{(j)}^T \mathbf{B} \mathbf{y}_{(j)}}$$

Cancelling the transient part of the solution (3.78) provides the expression of the forced response:

$$\eta_j(t) = e^{\lambda_j t} \int_0^t \phi_{0j} e^{(i\omega - \lambda_j)\tau} d\tau = \frac{\phi_{0j} e^{i\omega t}}{i\omega - \lambda_j}$$

This result could also have been deduced from the normal Equations (3.77) by considering a harmonic excitation and response. Remembering that the eigenmodes appear in complex conjugate pairs and that the eigenvalues can be written as $\lambda_j = -\alpha_j \pm i\omega_j$ (Section 3.3.1), the forced harmonic response of a subcritically damped system thus takes the form:

$$\mathbf{r} = \sum_{j=1}^n \left\{ \frac{1}{\mathbf{y}_{(j)}^T \mathbf{B} \mathbf{y}_{(j)}} \frac{\mathbf{y}_{(j)} \mathbf{y}_{(j)}^T}{\alpha_j + i(\omega + \omega_j)} + \frac{1}{\bar{\mathbf{y}}_{(j)}^T \mathbf{B} \bar{\mathbf{y}}_{(j)}} \frac{\bar{\mathbf{y}}_{(j)} \bar{\mathbf{y}}_{(j)}^T}{\alpha_j + i(\omega - \omega_j)} \right\} s_0 e^{i\omega t} \quad (3.80)$$

If, by returning to the expression of the state vector, one notes that the quadratic form:

$$\begin{aligned} \tilde{\mu}_j &= \mathbf{y}_{(j)}^T \mathbf{B} \mathbf{y}_{(j)} = \begin{bmatrix} \mathbf{z}_{(j)}^T & \lambda_j \mathbf{z}_{(j)}^T \end{bmatrix} \begin{bmatrix} \mathbf{C} & \mathbf{M} \\ \mathbf{M} & \mathbf{0} \end{bmatrix} \begin{bmatrix} \mathbf{z}_{(j)} \\ \lambda_j \mathbf{z}_{(j)} \end{bmatrix} \\ &= \mathbf{z}_{(j)}^T \mathbf{C} \mathbf{z}_{(j)} + 2\lambda_j \mathbf{z}_{(j)}^T \mathbf{M} \mathbf{z}_{(j)} \end{aligned} \quad (3.81)$$

may be adopted as the squared norm of eigenvector \mathbf{z}_j , the expansion of the harmonic response (3.80) leads to the following spectral expansion of the dynamic influence coefficient matrix in terms of complex eigenmodes:

$$\begin{aligned} \mathbf{H}(\omega) &= (\mathbf{K} - \omega^2 \mathbf{M} + i\omega \mathbf{C})^{-1} \\ &= \sum_{k=1}^n \left\{ \frac{1}{\alpha_k + i(\omega + \omega_k)} \frac{\mathbf{z}_{(k)} \mathbf{z}_{(k)}^T}{\tilde{\mu}_k} + \frac{1}{\alpha_k + i(\omega - \omega_k)} \frac{\bar{\mathbf{z}}_{(k)} \bar{\mathbf{z}}_{(k)}^T}{\bar{\tilde{\mu}}_k} \right\} \end{aligned} \quad (3.82)$$

3.4 Experimental methods of modal identification

It is not intended in this section to cover in full detail the very important topic of experimental identification of the frequency and modal properties of a linearly damped system. The purpose is rather to introduce the most common methods and describe their very principle. The well-known difficulties linked to practical aspects such as occurrence of noise measurement, limitation of the sampling period and of the sampling frequency will not be addressed here. For the reader interested in getting deeper into the subject, the reader is referred to (Brandt 2011, Ewins 2000, Heylen *et al.* 1997, McConnell and Varoto 2008, Silva and Maia 1999).

Let us recall first that a given time-varying signal x can equivalently be observed and/or described in the time and frequency domains:

$$x(t) \leftrightarrow X(\omega)$$

$X(\omega)$ being the Fourier transform of $x(t)$. They are linked together by the direct and inverse relationships:

$$X(\omega) = \mathcal{F}[x(t)] = \int_{-\infty}^{\infty} x(t)e^{-i\omega t} dt \quad (3.83a)$$

\downarrow

$$x(t) = \mathcal{F}^{-1}[X(\omega)] = \frac{1}{2\pi} \int_{-\infty}^{\infty} X(\omega)e^{i\omega t} d\omega \quad (3.83b)$$

The same signal can thus be equivalently identified in the time or frequency domain. If its description is available in the time domain, the frequency description can be obtained through application of the direct Fourier transform (3.83a). Conversely, if it has been identified in the frequency domain, its time description results from the application of the inverse Fourier transform (3.83b).

Experimental identification of the frequency and modal properties of a system is based on the a priori knowledge of an appropriate analytical model, the parameters of which are adapted to fit at best the experimental data. The most common methods of system identification are based on the following models and related experiments:

- *In the time domain*, the system can be released from nonhomogeneous initial conditions (initial displacement, initial velocity or impulse), generating on an individual degree of freedom r a response of type (see Exercise 3.4):

$$q_r(t) = \sum_{k=1}^{2n} c_{rk} e^{\lambda_k t} \quad (3.84)$$

System identification in the time domain consists in recording the free response over a certain time period, and determining the $2n$ eigenvalues λ_k and the coefficients c_{rk} from a fitting process. The latter represent the amplitudes of the modal contributions at node r . As the eigensolutions arise as conjugate pairs, Equation (3.84) may equivalently be written in the form:

$$q_r(t) = \sum_{k=1}^n \left(c_{rk} e^{\lambda_k t} + \bar{c}_{rk} e^{\bar{\lambda}_k t} \right) \quad (3.85)$$

The least-squares complex exponential method (LSCE) described in Section 3.4.1 is one of the most widely used for system identification in the time domain.

- In the frequency domain, the objective consists in measuring a dynamic influence coefficient (3.82) which can be put in the so-called *Pole-Residue* form:⁵

$$H_{rs}(\omega) = \sum_{k=1}^n \left(\frac{\rho_{rs(k)}}{i\omega - \lambda_k} + \frac{\bar{\rho}_{rs(k)}}{i\omega - \bar{\lambda}_k} \right) \quad (3.86)$$

with the so-called residues:

$$\rho_{rs(k)} = \frac{z_{r(k)} z_{s(k)}^T}{\tilde{\mu}_k} \quad (3.87)$$

Although it is possible to directly record it in the frequency domain through a sine sweep on the excitation, it is more practical to obtain it from the simultaneous knowledge of any system response $q_r(t)$ of DOF r and of the external excitation $p_s(t)$ on DOF s to which it corresponds. In the time domain, they are related by the convolution product (see Section 2.7.2):

$$q_r(t) = \int_0^t h_{rs}(t - \tau) p_s(\tau) d\tau \quad (3.88)$$

Performing a Fourier transform of Equation (3.88) yields the relationship:

$$Q_r(\omega) = H_{rs}(\omega) P_s(\omega) \quad (3.89)$$

since a convolution product in the time domain corresponds to an ordinary product in the frequency domain.

The dynamic influence coefficient $H_{rs}(\omega)$, also referred to as *transfer function* or *frequency response function* (FRF), can thus be obtained from signals recorded in the time domain in the form:

$$H_{rs}(\omega) = \frac{Q_r(\omega)}{P_s(\omega)} = \frac{\mathcal{F}[q_r(t)]}{\mathcal{F}[p_s(t)]} \quad (3.90)$$

In practice, in order to experimentally measure $H_{rs}(\omega)$, the time signals $q_r(t)$ and $p_s(t)$ are recorded over a finite period of time T with a sampling frequency Δt and transformed to the frequency domain. The Fourier transform \mathcal{F} has thus to be replaced by its discrete approximation, the so-called Discrete Fourier Transform (DFT), which will be described in Section 3.4.2.⁶

⁵ The dynamic influence coefficients are the Fourier transforms of the impulse responses of the system. Indeed for an impulse excitation $\delta(t)$ on dof s the response is a solution of:

$$\mathbf{M}\ddot{\mathbf{q}} + \mathbf{C}\dot{\mathbf{q}} + \mathbf{K}\mathbf{q} = \delta(t)\mathbf{e}_s \quad \rightarrow \quad q_r(t) = h_{rs}(t)$$

where \mathbf{e}_s is zero for all dofs but 1 for dof s , and where $h_{rs}(t)$ is defined as the impulse response at dof r for an impulse at s . The Fourier transform of this problem results in:

$$(-\omega^2 \mathbf{M} + i\omega \mathbf{C} + \mathbf{K}) \mathbf{Q}(\omega) = \mathbf{e}_s \quad \rightarrow \quad Q_r(\omega) = H_{rs}(\omega)$$

where H_{rs} is by definition a dynamic influence coefficient and is clearly the Fourier transform of the corresponding impulse response $h_{rs}(t)$. Note that we use here the notation $\mathbf{Q}(\omega)$ instead of \mathbf{z} used previously to conform to the convention introduced in (3.83b). For the same reason we use the notation $H_{rs}(\omega)$ (and not $h_{rs}(\omega)$ as in the rest of the book) in order to clearly discriminate between time functions $h_{rs}(t)$ and their Fourier transforms.

⁶ Note that usually transfer functions are not directly computed from the ratio (3.90) but rather from the cross- and auto-spectra of the inputs and outputs in order to improve the quality of the estimate for H_{rs} and evaluate its coherence (see for instance Ewins 2000).

Finally, system identification in the frequency domain consists in determining the eigenvalues λ_k and the residues $\rho_{rs(k)}$ through a fitting process of Equation (3.86). A widely used fitting method is the Rational Fraction Polynomial method (RFP) which will be described in Section 3.4.3.

Let us note that the LSCE fitting method advised for identification in the time domain is also applicable for system identification from the measurement of transfer functions as well. Indeed the impulse response $h_{rs}(t)$ can be obtained from the transfer function $H_{rs}(\omega)$ (Equation (3.90)) as

$$h_{rs}(t) = \mathcal{F}^{-1} [H_{rs}(\omega)] \quad (3.91)$$

through inverse DFT. In signal processing, this way of extracting the impulse response $h_{rs}(t)$ from the convolution product (3.88) is referred to as *deconvolution*. It is a mixed approach since the processing of the measured signals in the frequency domain is followed by a fitting in the time domain.

3.4.1 The least-squares complex exponential method

To develop the Least-Squares Complex Exponential method (LSCE) proposed in (Brown *et al.* 1979), let us suppose the system has n degrees of freedom and that its free response has been sampled at a single DOF q_r (subscript r being dropped from now on for sake of simplicity) in the time domain at $N + 1 + 2n$ ($N + 1 \geq 2n$) equidistant points providing the discrete series:

$$[q_0, q_1, q_2, \dots, q_{N+2n-1}, q_{N+2n}] \quad (3.92)$$

At a given time $t_m = m\Delta t$, we may thus rewrite Equation (3.84) in the form (c_k and λ_k being complex in general):

$$\begin{aligned} q(t_m) = q_m &= \sum_{k=1}^{2n} c_k e^{m\lambda_k \Delta t} \\ &= \sum_{k=1}^{2n} c_k v_k^m \end{aligned} \quad (3.93)$$

with

$$v_k = e^{\lambda_k \Delta t} \quad k = 1, \dots, 2n \quad (3.94)$$

characteristic values expressing the amplitude and phase variation for the modal contribution k during a time interval Δt , λ_k being the complex eigenvalues of the discretized system.

Forming the following product:

$$\begin{aligned} \prod_{k=1}^{2n} (v - v_k) &= a_0 + a_1 v + a_2 v^2 + \dots + a_{2n-1} v^{2n-1} + v^{2n} \\ &= \sum_{\ell=0}^{2n-1} a_\ell v^\ell + v^{2n} = 0 \end{aligned} \quad (3.95)$$

one obtains a polynomial of order $2n$ in v where the coefficients a_ℓ are real since v_k come in conjugate pairs. Hence the characteristic values v_k can be regarded as the roots of a polynomial like (3.95) with unknown coefficients a_ℓ .

Let us now compute the linear combination of $2n$ successive time responses (3.93) using the same coefficients:

$$S = a_0 q_0 + a_1 q_1 + a_2 q_2 + \dots + a_{2n-1} q_{2n-1} + q_{2n} \quad (3.96)$$

We get:

$$\begin{aligned} S &= a_0 \sum_{k=1}^{2n} c_k + a_1 \sum_{k=1}^{2n} c_k v_k + a_2 \sum_{k=1}^{2n} c_k v_k^2 + \dots + a_{2n-1} \sum_{k=1}^{2n} c_k v_k^{2n-1} + \sum_{k=1}^{2n} c_k v_k^{2n} \\ &= \sum_{k=1}^{2n} c_k (a_0 + a_1 v_k + a_2 v_k^2 + \dots + a_{2n-1} v_k^{2n-1} + v_k^{2n}) = 0 \end{aligned} \quad (3.97)$$

and therefore (3.96) provides the following equation between the coefficients a_i :

$$a_0 q_0 + a_1 q_1 + a_2 q_2 + \dots + a_{2n-1} q_{2n-1} = -q_{2n} \quad (3.98)$$

More generally, for any $m > 0$ one can write:

$$a_0 q_m + a_1 q_{m+1} + a_2 q_{m+2} + \dots + a_{2n-1} q_{m+2n-1} = -q_{m+2n} \quad (3.99)$$

We may thus build on the sampling interval a recursive linear system of dimension $(N + 1 \times 2n)$ whose unknowns are the coefficients a_ℓ of the polynomial (3.95)⁷:

$$\begin{bmatrix} q_0 & q_1 & q_2 & \dots & q_{2n-1} \\ q_1 & q_2 & q_3 & \dots & q_{2n} \\ q_2 & q_3 & q_4 & \dots & q_{2n+1} \\ \vdots & \vdots & \vdots & & \vdots \\ q_N & q_{N+1} & q_{N+2} & \dots & q_{N+2n-1} \end{bmatrix} \begin{bmatrix} a_0 \\ a_1 \\ a_2 \\ \vdots \\ a_{2n-1} \end{bmatrix} = - \begin{bmatrix} q_{2n} \\ q_{2n+1} \\ q_{2n+2} \\ \vdots \\ q_{N+2n} \end{bmatrix} \quad (3.100)$$

or, in symbolic form:

$$Qa = r \quad (3.101)$$

Equation (3.101) has to be solved in a least-squares sense:

$$\min_a \frac{1}{2} (Qa - r)^T (Qa - r)$$

providing thus the solution in the form:

$$a = (Q^T Q)^{-1} Q^T r \quad (3.102)$$

The characteristic values v_k are next obtained by computing the roots of the polynomial equation:

$$P(v) = \sum_{\ell=0}^{2n-1} a_\ell v^\ell + v^{2n} = 0 \quad (3.103)$$

⁷ Here we outline the simplest version of the LCSE. A set of equations similar to (3.100) can be built for every input and output, and solved simultaneously in a least-squares sense to compute a global estimate of the poles. In that case the method is known as the polyreference LCSE.

According to Equation (3.94), from the values of the roots v_k we can compute the eigenvalues of the original differential system:

$$\lambda_k = \alpha_k \pm i\omega_k = \frac{\ln(v_k)}{\Delta t} \quad (3.104)$$

The coefficients c_k representing the modal amplitudes can be computed next by expressing Equation (3.93) on the sampling interval:

$$\begin{bmatrix} 1 & 1 & 1 & \dots & 1 \\ v_0 & v_1 & v_2 & \dots & v_{2n} \\ v_0^2 & v_1^2 & v_2^2 & \dots & v_{2n}^2 \\ \vdots & \vdots & \vdots & & \vdots \\ v_0^N & v_1^N & v_2^N & \dots & v_{2n}^N \end{bmatrix} \begin{bmatrix} c_1 \\ c_2 \\ c_3 \\ \vdots \\ c_{2n} \end{bmatrix} = \begin{bmatrix} q_0 \\ q_1 \\ q_2 \\ \vdots \\ q_N \end{bmatrix} \quad (3.105)$$

We notice that this linear system can be formally written as:

$$\mathbf{L}\mathbf{c} = \mathbf{q} \quad (3.106)$$

The system matrix \mathbf{L} has dimension $N + 1 \times 2n$ ($N + 1 \geq 2n$) and is complex. The vectors \mathbf{c} and \mathbf{q} collect respectively the modal amplitudes and the time samples of the response.

Equation (3.106) also has to be solved in a least-squares sense. A convenient way to do this is to simply multiply it by the conjugate transpose of \mathbf{L} , yielding thus the result:

$$\bar{\mathbf{L}}^T \mathbf{L} \mathbf{c} = \bar{\mathbf{L}}^T \mathbf{q} \quad \rightarrow \quad \mathbf{c} = (\bar{\mathbf{L}}^T \mathbf{L})^{-1} \bar{\mathbf{L}}^T \mathbf{q} \quad (3.107)$$

Example 3.5

Modal identification of a 2-DOF system using the LSCE method.

Demonstrating the effectiveness of the Least-Squares Complex Exponential method for modal identification requires the availability of experimental data corresponding to a free response of a damped linear system in the time domain. This can be achieved artificially by developing a numerical time response which will simulate the experimental data. It is of course an ideal situation since the data will not be affected by the noise and measurement errors that affect experimental data. The results presented hereafter can easily be reproduced using any numerical toolbox.

For that purpose, let us consider again the 2-DOF system of Example 3.1 displayed on Figure 3.1, using the damping value $c = 0.1$. The time response of the system can be generated using the simple time-marching scheme developed in Exercise 3.11. In Exercise 3.12, it is then proposed to compute the response with the following input data and integration parameters:

- As initial conditions, the system is released from the initial equilibrium position corresponding to the application of a unit load on DOF q_1 .

$$\mathbf{f}^T = [1 \quad 0] \quad \rightarrow \quad \mathbf{q}_0 = \mathbf{K}^{-1} \mathbf{f}_0, \quad \dot{\mathbf{q}}_0 = 0$$

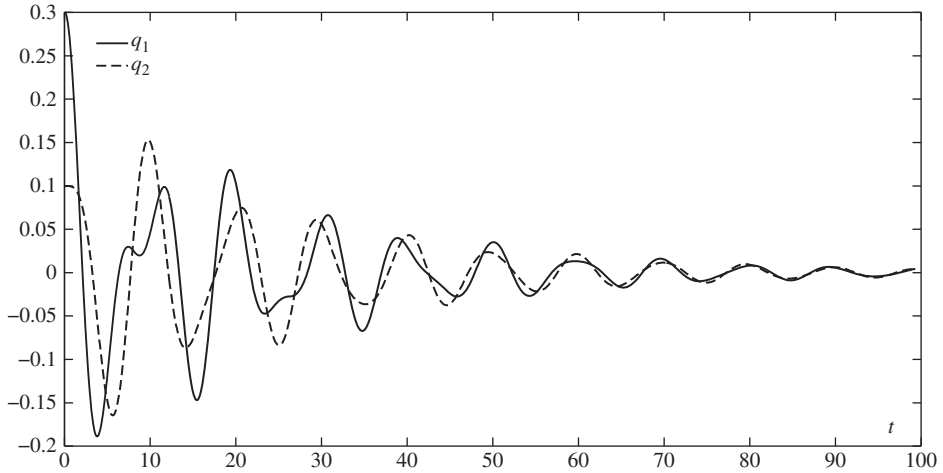


Figure 3.11 Time response of a 2 DOF system under initial conditions.

- The time window is chosen to cover a few periods of the lower frequency:

$$T_{max} = 10 T_1 = 10 \frac{2\pi}{\omega_1}$$

- We consider 2^{10} discrete times, corresponding to a sampling time (equal to the step size in the time integration) of:

$$\Delta t = T_{max}/(2^{10} - 1)$$

With these data, the time marching scheme will provide a response very close to the exact one. The corresponding response at both DOF is displayed on Figure 3.11. Considering the entire signal length (namely $N + 1 + 2n = 2^{10}$ and $n = 2$), the linear system of Equation (3.101) is built for each DOF of the system:

$$\mathbf{Q}_k \mathbf{a}_k = \mathbf{r}_k \quad k = 1, 2$$

and is solved according to Equation (3.102):

$$\mathbf{a}_k = (\mathbf{Q}^T \mathbf{Q})_k^{-1} \mathbf{Q}_k^T \mathbf{r}_k \quad k = 1, 2$$

The following matrices and right-hand sides are obtained:

$$(\mathbf{Q}^T \mathbf{Q})_1 = \begin{bmatrix} 2.9973 & 2.9444 & 2.8760 & 2.7927 \\ 2.9444 & 2.9076 & 2.8553 & 2.7879 \\ 2.8760 & 2.8553 & 2.8190 & 2.7678 \\ 2.7927 & 2.7879 & 2.7678 & 2.7326 \end{bmatrix} \quad (\mathbf{Q}^T \mathbf{Q})_2 = \begin{bmatrix} 2.1097 & 2.1002 & 2.0818 & 2.0545 \\ 2.1002 & 2.0997 & 2.0902 & 2.0718 \\ 2.0818 & 2.0902 & 2.0897 & 2.0802 \\ 2.0545 & 2.0718 & 2.0802 & 2.0797 \end{bmatrix}$$

$$(\mathbf{r}^T \mathbf{Q})_{1,2} = \begin{cases} \begin{bmatrix} -2.6954 & -2.7063 & -2.7021 & -2.6830 \end{bmatrix} \\ \begin{bmatrix} -2.0185 & -2.0446 & -2.0618 & -2.0703 \end{bmatrix} \end{cases}$$

Due to the absence of measurement errors in this ideal case, both systems provide the same solution:

$$\mathbf{a}^T = [0.9827 \quad -3.9350 \quad 5.9219 \quad -3.9695]$$

from which we deduce the polynomial Equation (3.103):

$$v^4 - 3.9695v^3 + 5.9219bv^2 - 3.9350v + 0.9827 = 0$$

Its roots v_k ($k = 1, \dots, 4$) are complex conjugate:

$$v_k = [0.9902 \pm 0.0962i \quad 0.9946 \pm 0.0610i]$$

The roots λ_k ($k = 1, \dots, 4$) of the original differential system are computed from Equation (3.104). We obtain the eigenvalues:

$$\lambda_k = [-0.0532 \pm 0.9978i \quad -0.0366 \pm 0.6312i]$$

that match extremely well the exact ones (see Example 3.4).

The next step consists in computing the eigenmodes by expressing and solving the linear system (3.106) for both DOFs. The roots v_k being the same, the system matrix \mathbf{L} is unique. The system (3.107) has to be solved for two different right-hand sides:

$$\mathbf{c}_k = (\bar{\mathbf{L}}^T \mathbf{L})^{-1} \bar{\mathbf{L}}^T \mathbf{q}_k \quad k = 1, 2$$

The matrix resulting from the least-squares process is complex:

$$\bar{\mathbf{L}}^T \mathbf{L} = 10^2 \begin{bmatrix} 0.9727 & 0.0078 - 0.0513i & 0.0699 - 0.2650i & 0.0085 - 0.0629i \\ 0.0078 + 0.0513i & 0.9727 & 0.0085 + 0.0629i & 0.0699 + 0.2650i \\ 0.0699 + 0.2650i & 0.0085 - 0.0629i & 1.4096 & 0.0097 - 0.0812i \\ 0.0085 + 0.0629i & 0.0699 - 0.2650i & 0.0097 + 0.0812i & 1.4096 \end{bmatrix}$$

and the right-hand sides are:

$$(\bar{\mathbf{L}}^T \mathbf{q})_1 = \begin{bmatrix} 7.0387 - 3.7063i \\ 7.0387 + 3.7063i \\ 12.5952 - 0.5677i \\ 12.5952 + 0.5677i \end{bmatrix} \quad (\bar{\mathbf{L}}^T \mathbf{q})_2 = \begin{bmatrix} -2.7798 - 2.2598i \\ -2.7798 + 2.2598i \\ 11.4967 - 2.4031i \\ 11.4967 + 2.4031i \end{bmatrix}$$

We get thus for each DOF the set of coefficients:

$$\mathbf{c}_{1,2}^T = \begin{cases} [0.0666 + 0.0061i & 0.0666 - 0.0061i & 0.0832 + 0.0086i & 0.0832 - 0.0086i] \\ [-0.0332 - 0.0036i & -0.0332 + 0.0036i & 0.0832 + 0.0077i & 0.0832 - 0.0077i] \end{cases}$$

Finally, after normalization we get the eigenmodes:

$$\mathbf{Z} = \begin{bmatrix} 1.0000 & 1.0000 \\ -0.5000 \pm 0.0084i & 0.9997 \pm 0.0105i \end{bmatrix}$$

Again, there is very small deviation from the exact solution (see Example 3.4).

As a final remark let us note that, in practice, the number of degrees of freedom of a system is not known. In other words, one does not know in advance the order n of the model that needs to be considered to fit the measured data. Therefore the analyst will identify eigenfrequencies, dampings and modes for an increasing order n and will estimate the appropriate order based on the variation of the results with the chosen order n . If the results are changing significantly with n , the order is probably too low (the model is not capable to fit well the data) or too high (erroneous identified values are found due to overfit and numerical errors). For the LCSE method the quality of the fit can also be checked a posteriori by evaluating the fitting residue, namely the error in (3.93). The issue of order determination is similar in all identification methods.

3.4.2 Discrete Fourier transform

The implementation of the frequency approach is based on the use of the Discrete Fourier Transform (DFT) to translate time signals in the frequency domain. Therefore it is worthwhile introducing briefly the concept, algorithm and fundamental properties of the DFT.

Let us consider a function $x(t)$ defined in the time domain $t \in [0, \infty[$. Its Fourier transform:

$$X(\omega) = \int_0^{\infty} x(t)e^{-i\omega t} dt$$

can be approximated as:

$$X(\omega) \simeq \int_0^T x(t)e^{-i\omega t} dt \quad (3.108)$$

where T is a sufficiently large sampling interval in time. Equation (3.108) can be discretized in the form:

$$X(\omega) \simeq \sum_{m=0}^N x(t_m)e^{-i\omega t_m} \Delta t \quad (3.109)$$

$N + 1$ being the number of sampling points. The sampling interval and the sampling times are thus given by:

$$\Delta t = \frac{T}{N} \quad \text{and} \quad t_m = \frac{mT}{N} \quad (m = 0, \dots, N) \quad (3.110)$$

Substituting (3.110) into (3.109) yields the result:

$$X(\omega) \simeq \frac{T}{N} \sum_{m=0}^N x_m e^{\frac{-im\omega T}{N}} \quad (3.111)$$

Let us now evaluate (3.111) at $N + 1$ sampling points in the frequency domain:

$$\omega_k = \frac{2\pi k}{T} \quad k = 0, \dots, N \quad (3.112)$$

The system of $N + 1$ equations results:

$$\boxed{X_k = \frac{T}{N} \sum_{m=0}^N x_m e^{\frac{-2im\pi k}{N}}} \quad k = 0, \dots, N \quad (3.113)$$

which provides a discrete representation of $X(\omega)$ over the interval $[0, \omega_{max}]$ with:

$$\omega_{max} = \frac{2N\pi}{T} \quad (3.114)$$

In order to get the inverse relationship to (3.113), let us compute the expression:

$$I_\ell = \sum_{k=0}^N X_k e^{\frac{2i\ell k\pi}{N}} \quad (3.115)$$

Through substitution of (3.113) into (3.115) we get:

$$\begin{aligned} I_\ell &= \frac{T}{N} \sum_{k=0}^N \sum_{m=0}^N x_m e^{\frac{-2imk\pi}{N}} e^{\frac{2i\ell k\pi}{N}} \\ &= \frac{T}{N} \left\{ x_\ell + \sum_{\substack{m=0 \\ m \neq \ell}}^N \sum_{k=0}^N x_m e^{\frac{2i(\ell-m)\pi k}{N}} \right\} \end{aligned} \quad (3.116)$$

We next note that the second part of Equation (3.116) vanishes since the integral:

$$\int_0^T e^{\frac{2i(\ell-m)\pi t}{T}} dt$$

vanishes for $\ell \neq m$ (ℓ and m being integers) and can be discretized in the form:

$$\sum_{k=0}^N e^{\frac{2i(\ell-m)\pi k}{N}} = 0$$

We thus get the final result providing the inverse relationship to (3.113):

$$x_m = \frac{N}{T} \sum_{k=0}^N X_k e^{\frac{2imk\pi}{N}} \quad m = 0, \dots, N \quad (3.117)$$

It can be observed that sampling time Δt and maximum frequency contained into the model are directly linked to one another since by combining Equations (3.110) and (3.114) we get the fundamental relationship:

$$\omega_{max} \Delta t = 2\pi \quad (3.118)$$

which shows that the maximum frequency that can be extracted is directly related to the sampling time Δt . The frequency resolution, namely the difference between two frequencies that can be found, is related to the total measurement time T as seen from (3.112).

In practice, the DFT is always computed using the FFT (Fast Fourier Transform) algorithm originally proposed in (Cooley and Tukey 1965). The FFT algorithm is nothing else than a specific implementation of the DFT in which 2^N time samples are considered, the time window T being divided in $(2^N - 1)$ sampling intervals, thanks to which the computational cost can be reduced from $O(N^2)$ to $O(N \log N)$.

It is important being aware that, even in the absence of measurement errors, two different spurious effects may result from the discretization of the Fourier transform.

- The so-called *aliasing effect* results from the finite size of the sampling time Δt . It can be shown that the sampling of sine functions with frequency $\omega > \omega_{\max}/2 = 2\pi/\Delta t$ will generate spurious low frequencies in the spectrum. The aliasing effect can be prevented through filtering of the original signal by a low-pass filter.
- The so-called *leakage effect* results from the finite size of the time observation window $[0, T]$. The discretization process transforms thus a nonperiodic signal into a periodic one, which introduces amplitude and frequency errors. The leakage effect can be minimized through pre-multiplication of the original time signal by an appropriate time window.

Example 3.6

Frequency response function and impulse function of a 1-DOF system.

Let us consider a spring-mass-dashpot with the following data: stiffness $k = 1000 \text{ N/m}$, mass $m = 10 \text{ kg}$, damping $c = 25 \text{ N/m/s}$. A triangular pulse of maximum intensity equal to 20 N is applied during 1 s as shown on Figure 3.12. The vibration frequency and period of the undamped system are $\omega_0 = 10 \text{ rad/s}$, $T = 0.628 \text{ s}$.

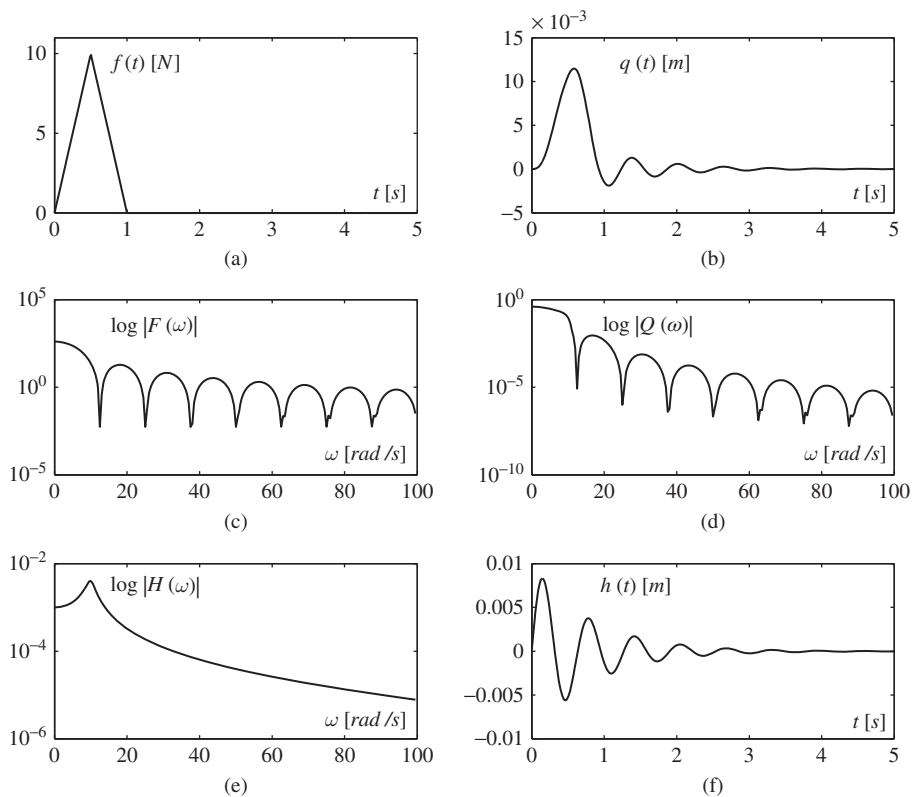


Figure 3.12 1-DOF system: Computation of the transfer function $H(\omega)$ and of the impulse response $h(t)$ through application of DFT on input/output data in the time domain.

The FRF and the impulse response of the system are determined as follows (using a numerical toolbox):

- The response is computed using the time marching scheme described in Exercise 3.11. sampled on a time window $[0, 10 T]$ with $10 T/(2^N - 1)$ sampled times, $N = 10$.
- The FFT algorithm is applied to compute the Fourier transforms $F(\omega)$ and $Q(\omega)$ of the excitation and of the response.
- The FRF is computed next as $H(\omega) = \frac{Q(\omega)}{F(\omega)}$.
- Finally, the impulse response is obtained through deconvolution as $h(t) = \mathcal{F}^{-1} [H(\omega)]$ using the inverse FFT algorithm.

Figure 3.12 displays successively:

- The applied force (a) and the displacement response (b) in the time domain;
- The absolute values of the applied force (c) and the displacement response (d) in the frequency domain (on the range $0 - 100 \text{ rad/s}$);
- The absolute value of the FRF (e), for which it can be verified that it matches very well the analytical transfer function:

$$H_{\text{exact}}(\omega) = \frac{1}{k} \frac{1}{1 - \left(\frac{\omega}{\omega_0}\right)^2 + \frac{2i\varepsilon\omega}{\omega_0}}$$

- The impulse response (f), which also matches very well the analytical form developed in Exercise 3.3.

3.4.3 The rational fraction polynomial method

The Rational Fraction Polynomial (RFP) method (Richardson and Formenti 1982) is frequently used for fitting of frequency response functions (FRF). The method is based on a viscously damped system of which the FRFs are expressed as a ratio of two polynomials. Let us concentrate on one single influence coefficient of the FRF (3.82), written in the Pole-Residue form (3.86, 3.87). Dropping subscripts r, s to simplify the notations,

$$H(\omega) = \sum_{k=1}^n \left(\frac{\rho_{(k)}}{i\omega - \lambda_k} + \frac{\bar{\rho}_{(k)}}{i\omega - \bar{\lambda}_k} \right) \quad (3.119)$$

which can be written in the equivalent rational fraction:

$$H(\omega) = \frac{\sum_{k=0}^{2n-1} a_k (i\omega)^k}{\sum_{k=0}^{2n-1} b_k (i\omega)^k + (i\omega)^{2n}} \quad (3.120)$$

with real coefficients a_k and b_k , owing to the complex conjugate terms in the FRF. The method to evaluate the real coefficients a_k and b_k of the polynomials is based on a minimization of the

error between the model and the measured values on some frequency interval. This error at circular frequency ω_j is thus described as:

$$e_j = \sum_{k=0}^{2n-1} a_k (i\omega_j)^k - H_j^{exp} \left(\sum_{k=0}^{2n-1} b_k (i\omega_j)^k + (i\omega_j)^{2n} \right) \quad (3.121)$$

where H_j^{exp} is the measured FRF at frequency ω_j . In matrix form one is written as:

$$e_j = \mathbf{p}_j^T \mathbf{a} - H_j^{exp} \mathbf{p}_j^T \mathbf{b} - H_j^{exp} (i\omega_j)^{2n} \quad (3.122)$$

where we used the notations:

$$\begin{aligned} \mathbf{p}_j^T &= [1 \quad i\omega_j \quad \cdots \quad (i\omega_j)^{2n-1}] \\ \mathbf{a}^T &= [a_0 \quad a_1 \quad \cdots \quad a_{2n-1}] \\ \mathbf{b}^T &= [b_0 \quad b_1 \quad \cdots \quad b_{2n-1}] \end{aligned} \quad (3.123)$$

Assuming that the FRF is measured at m frequency points ($m \geq 4n$), m errors like (3.123) can be written to build a set of linear equations:

$$\begin{aligned} \mathbf{E} &= \mathbf{P}\mathbf{a} - \text{diag} \left(H_j^{exp} \right) \mathbf{P}\mathbf{b} - \mathbf{h} \\ &= \mathbf{T}\mathbf{y} - \mathbf{h} \end{aligned} \quad (3.124)$$

with

$$\begin{aligned} \mathbf{P}^T &= [\mathbf{p}_1 \quad \mathbf{p}_2 \quad \cdots \quad \mathbf{p}_m] & (2n \times m) \\ \mathbf{h}^T &= [(i\omega_1)^{2n} H_1^{exp} \quad (i\omega_2)^{2n} H_2^{exp} \quad \cdots \quad (i\omega_m)^{2n} H_m^{exp}] & (1 \times m) \\ \mathbf{T} &= [\mathbf{P} \quad -\text{diag} \left(H_j^{exp} \right) \mathbf{P}] & (m \times 4n) \\ \mathbf{y}^T &= [\mathbf{a}^T \quad \mathbf{b}^T] & (1 \times 4n) \end{aligned} \quad (3.125)$$

The global error is now defined by the real quadratic form:

$$J = \bar{\mathbf{E}}^T \mathbf{E} = (\bar{\mathbf{T}}\mathbf{y} - \bar{\mathbf{h}})^T (\mathbf{T}\mathbf{y} - \mathbf{h}) \quad (3.126)$$

where we used the fact that \mathbf{y} , the polynomial coefficients, are real. Minimizing Equation (3.126) yields:

$$\frac{\partial J}{\partial \mathbf{y}} = (\bar{\mathbf{T}}^T \mathbf{T} + \mathbf{T}^T \bar{\mathbf{T}}) \mathbf{y} - (\mathbf{T} + \bar{\mathbf{T}})^T \mathbf{h} = 0 \quad (3.127)$$

It is a linear system of the form:

$$\mathbf{S}\mathbf{y} = \mathbf{w} \quad (3.128)$$

with the real system matrix and right-hand side:

$$\begin{aligned} \mathbf{S} &= \bar{\mathbf{T}}^T \mathbf{T} + \mathbf{T}^T \bar{\mathbf{T}} & (4n \times 4n) \\ \mathbf{w} &= (\mathbf{T} + \bar{\mathbf{T}})^T \mathbf{h} & (4n \times 1), \end{aligned} \quad (3.129)$$

matrix \mathbf{S} being nonsingular for a number of sampling points $m \geq 2n$.

Once the system (3.128) has been solved:

- computing the roots $\lambda_k = \alpha_k \pm i\omega_k$ of the polynomial:

$$b_0 + b_1\lambda + \dots + b_{2n}\lambda^{2n} = 0 \quad (3.130)$$

will provide the eigenfrequencies ω_k and associated damping coefficients α_k ;

- the \mathbf{a} values can be used to compute the residues and thus obtain the modal shapes. A straightforward method to do it consists in looking at the FRF expression (3.119) in the form:

$$H(\omega) = \sum_{k=1}^{2n} \frac{\rho_{(k)}}{i\omega - \lambda_k} \quad (3.131)$$

where, for sake of notation simplicity, we do not consider the complex conjugate character of the eigensolutions. Comparing now the FRF (3.131) with the rational fraction form (3.120) one can write:

$$\sum_{k=1}^{2n} \rho_k \prod_{\substack{\ell=1 \\ \ell \neq k}}^{2n} (i\omega - \lambda_\ell) = \sum_{k=0}^{2n-1} a_k (i\omega)^k \quad (3.132)$$

Equation (3.132) can be rewritten in the matrix form:

$$\mathbf{r}^T \boldsymbol{\rho} = \mathbf{p}^T \mathbf{a} \quad (3.133)$$

where \mathbf{p} is as defined earlier in (3.123), $\boldsymbol{\rho}$ is the vector of components ρ_k and \mathbf{r} a vector of components:

$$r_k(i\omega) = \prod_{\substack{\ell=1 \\ \ell \neq k}}^{2n} (i\omega - \lambda_\ell)$$

Equation (3.133) can be expressed at discrete frequencies ω_j to give:

$$\mathbf{r}_j^T \boldsymbol{\rho} = \mathbf{p}_j^T \mathbf{a} \quad j = 1, \dots, m \geq 2n \quad (3.134)$$

allowing thus to build with the row vectors \mathbf{r}_j^T and \mathbf{p}_j^T a new linear system with complex coefficients:

$$\mathbf{R}\boldsymbol{\rho} = \mathbf{P}\mathbf{a} \quad \mathbf{R}, \mathbf{P} \in (m \times 2n)$$

It may be solved in a least-squares manner to get the residues:

$$\bar{\mathbf{R}}^T \mathbf{R}\boldsymbol{\rho} = \bar{\mathbf{R}}^T \mathbf{P}\mathbf{a} \quad \rightarrow \quad \boldsymbol{\rho} = (\bar{\mathbf{R}}^T \mathbf{R})^{-1} \bar{\mathbf{R}}^T \mathbf{P}\mathbf{a} \quad (3.135)$$

The eigenmodes are directly obtained from the knowledge of the residues according to Equation (3.87). As shown by Equation (3.87), each component of the residual vector $\boldsymbol{\rho}$ is proportional to the contribution of the corresponding DOF to the different eigenmodes. The modal amplitudes being arbitrary, the matrix of complex eigenmodes can thus be built as:

$$\mathbf{Z} = [\mathbf{z}_{(1)} \quad \dots \quad \mathbf{z}_{(2n)}] = \begin{bmatrix} \rho_1 \\ \vdots \\ \rho_m \end{bmatrix} \quad (3.136)$$

m being the number of DOF effectively taken into account in the identification process. Let us note that:

- To identify eigenfrequencies and associated dampings, it is sufficient to apply the Rational Fraction Polynomial (RFP) method to one row or one column of the matrix of dynamic influence coefficients $\mathbf{H}(\omega)$. In theory, one would get the same eigenvalues λ_k from any line or column of \mathbf{H} since eigenvalues are global properties of the system. In practice, however, due to the various errors in the measurement and computational processes, this will never be the case: when applying the method to a multi-degree of freedom system, slightly different eigenfrequencies and damping will be obtained for the same system if all FRFs are identified separately. Therefore, a global method named Global Rational Fraction Polynomial (GRFP) method has been proposed (Richardson and Formenti 1985) in which multiple FRFs are taken into account simultaneously.
- The numerical conditioning of matrix \mathbf{S} is strongly affected by the increasing number of poles included in the identification process. For that reason, it is recommended to use a set of orthonormal polynomials instead of the regular polynomials defined in Equation (3.120).
- A more recent method, similar to the RFP but considering simultaneously all the measured coefficients of \mathbf{H} , computationally efficient and numerically robust is the PolyMAX method proposed in (Guillaume *et al.* 2003).

Example 3.7

Modal identification of 2-DOF system using the RFP method.

Let us consider one last time the simple 2-DOF system of Example 3.1, Figure 3.1, using again the damping value $c = 0.1$. To simulate the experimental measurement, a triangular pulse of 5 N amplitude is applied on DOF 1 during 1 s (Figure 3.13.a). The system response has been computed (using a numerical toolbox) over a time interval $T_{\max} = 119.2$ s corresponding to 12 fundamental periods, using a time step size $\Delta t = T_{\max}/(2^{16} - 1) = 0.0018$ s. The displacement responses obtained on both DOFs are also displayed on Figure 3.13.b for the time interval $[0, T_{\max}/4]$.

With the sampling rate adopted, the frequency response can be obtained on the frequency interval $[0, 3.454 \text{ e3}]$ rad/s with a resolution of $\Delta\omega = 0.0527$ rad/s. The FFT algorithm is first applied to both displacement responses and to the excitation using an appropriate numerical toolbox, and the transfer functions are then computed from Equation (3.90). Figures 3.13.c–f display the results obtained in amplitude and phase for both dynamic influence coefficients $H_{11}(i\omega)$ and $H_{21}(i\omega)$ over the frequency interval $[0, 50\Delta\omega] = [0, 2.64]$ rad/s.

The RFP method of identification is then applied to the dynamic influence coefficients $H_{11}(i\omega)$ and $H_{21}(i\omega)$ over the frequency interval $[0, 2.64]$ rad/s with a sampling of 51 frequency points.

The first step consists in computing the sets \mathbf{a} and \mathbf{b} of polynomial coefficients as described by Equations (3.121–3.128). The following results are obtained:

$$\text{for } H_{11} : \begin{cases} \mathbf{a} &= [0.1182 \quad 0.0155 \quad 0.1979 \quad -0.0001] \\ \mathbf{b} &= [0.3997 \quad 0.1156 \quad 1.4080 \quad 0.1797 \quad 1.0000] \end{cases}$$

$$\text{for } H_{12} : \begin{cases} \mathbf{a} &= [0.0386 \quad 0.0017 \quad -0.0014 \quad -0.0001] \\ \mathbf{b} &= [0.3991 \quad 0.1155 \quad 1.4062 \quad 0.1796 \quad 1.0000] \end{cases}$$

One would expect exactly the same values for the \mathbf{b} coefficients. The slight differences possibly result from numerical round-offs and the FFT of the time signal. As a result, resolving the polynomial Equation (3.130) gives two slightly different sets of eigenvalues as displayed in Table 3.1. They are compared to the exact ones and to the values computed from the LSCE method. The complex eigenmodes result from the application of Equations (3.134 – 3.136). After normalization of Equation (3.136), one gets:

$$\mathbf{Z} = \begin{bmatrix} 1.0000 & 1.0000 \\ -0.5035 \pm 0.0099i & 1.0035 \pm 0.0125i \end{bmatrix}$$

The results obtained from both LSCE and RFP methods are excellent for these simulated measurements: the discrepancy is less than 1% on eigenmodes and still lower on eigenvalues.

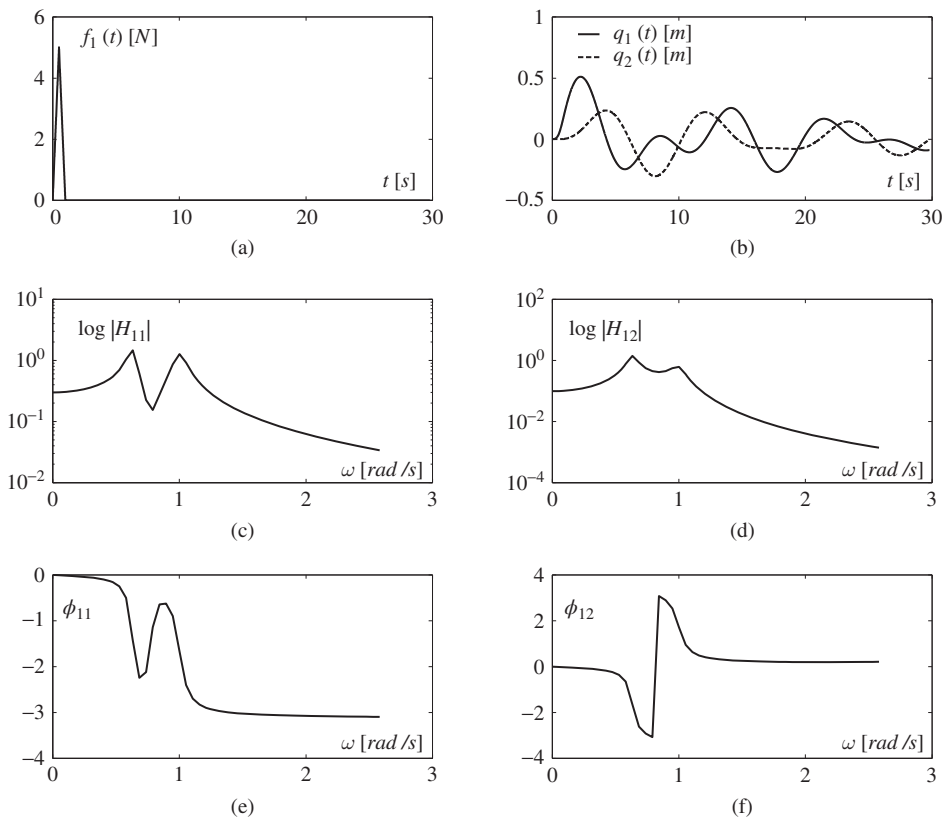


Figure 3.13 2-DOF system: Determination of the FRF through application of DFT on input/output data in the time domain.

Table 3.1 Eigenvalues computed from RFP fitting of h_{11} and h_{12}

	RFP - h_{11}	RFP - h_{12}	exact	LSCE method
ω_1	$-0.0532 \pm 0.9980i$	$-0.0534 \pm 0.9990i$	$0.0533 \pm 0.9986i$	$-0.0532 \pm 0.9978i$
ω_2	$-0.0365 \pm 0.6311i$	$-0.0365 \pm 0.6308i$	$0.0367 \pm 0.6314i$	$-0.0366 \pm 0.6312i$

3.4.4 Estimating the modes of the associated undamped system

Several vibration analyzers and software packages are on the market which allow measurement of the modal characteristics of a structure using the transfer function technique briefly described above. The principle of experimental setups for arbitrary excitation modal analysis is illustrated by Figure 3.14.

Such techniques are very fast since, in contrast to force appropriation approaches (Section 3.2.3), they do not require simultaneous excitation of several degrees of freedom. However, when applied to large structures, they do not exhibit the same reliability as appropriate excitation methods. Another difference is that nonappropriation experimental techniques as presented in the previous sections extract from the measured responses the complex modes $z_{(k)}$ and poles λ_k of the damped system, whereas the appropriation techniques aim at finding the modes $x_{(k)}$ and eigenfrequencies ω_{ok} of the associated conservative system. It is interesting to note that in case of light damping one can estimate one from the other as explained next.

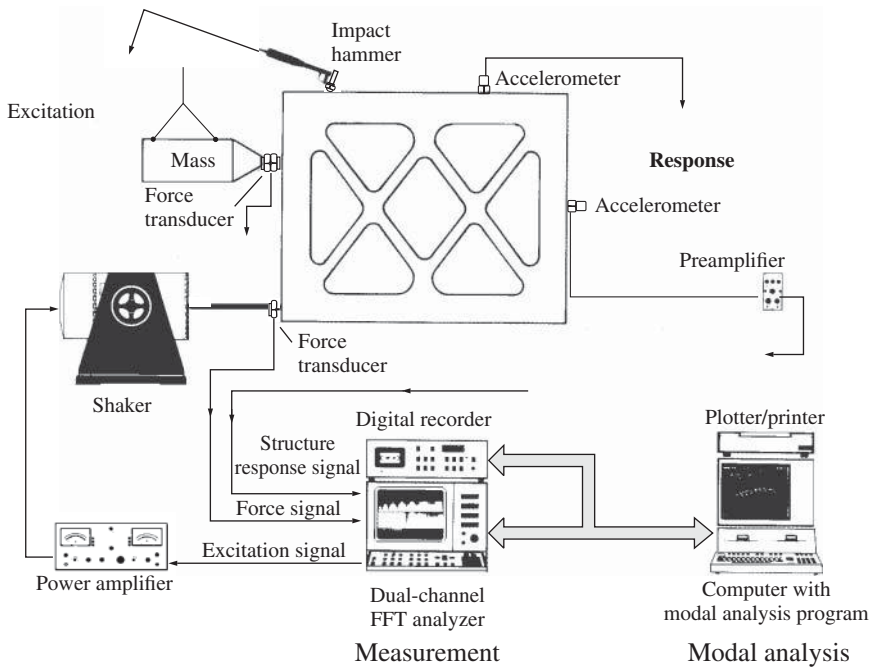


Figure 3.14 Experimental modal analysis through arbitrary excitation (Brüel & Kjær 1984). Source: Reproduced with permission. Copyright © Brüel & Kjær Sound & Vibration Measurement A/S.

In order to reconstruct the eigenshapes of the associated undamped system, the first-order approximations (3.13) and (3.15) may be used in case of light damping. These give rise to the following approximate relationships in terms of the modal characteristics of the undamped system (Dat 1978):

$$\mathbf{z}_{(k)} \mathbf{z}_{(k)}^T \simeq \mathbf{x}_{(k)} \mathbf{x}_{(k)}^T + i\omega_{0k} \sum_{\substack{l=1 \\ l \neq k}}^n \frac{\beta_{kl}}{\mu_l(\omega_{0k}^2 - \omega_{0l}^2)} (\mathbf{x}_{(k)} \mathbf{x}_{(l)}^T + \mathbf{x}_{(l)} \mathbf{x}_{(k)}^T)$$

$$\tilde{\mu}_k \simeq \mathbf{x}_{(k)}^T \mathbf{C} \mathbf{x}_{(k)} + 2 \left(\frac{-\beta_k}{2\mu_k} + i\omega_{0k} \right) (\mu_k + O(\beta_{ks}^2)) + O(\beta_{ks}^3) \simeq 2i\omega_{0k} \mu_k$$

The residues (3.87) can thus be approximated as:

$$\rho_{rs(k)} = \frac{\mathbf{z}_{r(k)} \mathbf{z}_{s(k)}^T}{\tilde{\mu}_k} \simeq \frac{\mathbf{x}_{r(k)} \mathbf{x}_{s(k)}}{2i\omega_{0k} \mu_k} + \frac{1}{2} \sum_{\substack{l=1 \\ l \neq k}}^n \frac{\beta_{kl}}{\mu_k \mu_l (\omega_{0k}^2 - \omega_{0l}^2)} (\mathbf{x}_{r(k)} \mathbf{x}_{s(l)} + \mathbf{x}_{r(l)} \mathbf{x}_{s(k)})$$

3.4.5 Example: experimental modal analysis of a bellmouth

A representative example of modal analysis is the identification of the eigenfrequencies and mode shapes of the so-called bellmouth displayed on Figure 3.15. It is an air inlet duct made of composite material constructed to perform ground testing of a small civil aircraft turbofan engine on the motor testing bench of Techspace Aero (Safran). The experimental modal analysis is described in (Marin 2012). The bellmouth is suspended for the test by means of its four hoisting eyes, leading to nearly free-free boundary conditions. The test procedure consists in impacting the specimen at a defined and constant point while measuring the response at a sufficient number of points to describe accurately its geometry. The final grid is presented

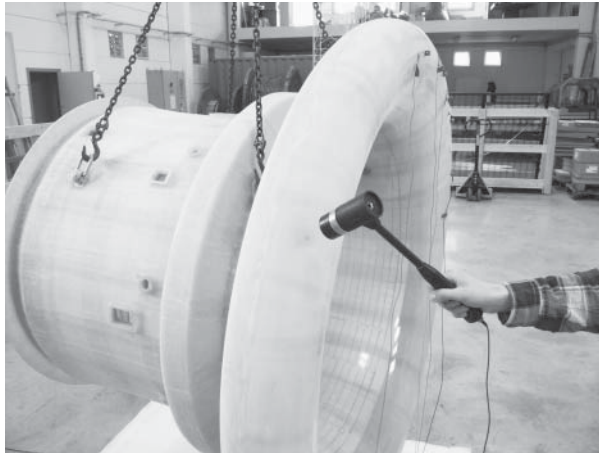


Figure 3.15 Measurement of bellmouth frequency response functions through hammer excitation. Source: Reproduced with permission from Techspace Aero – SAFRAN Group & V2i SA.

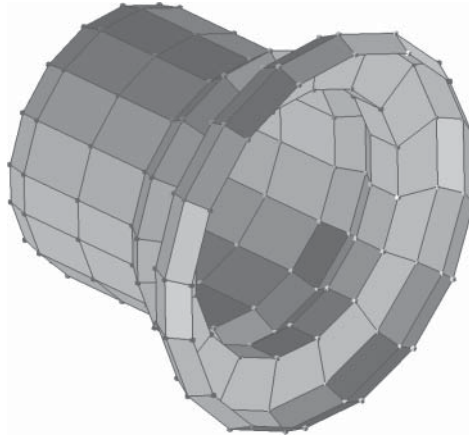


Figure 3.16 Grid of measurement points. Source: Reproduced with permission from V2i SA.

in Figure 3.16 and is constituted of 160 measurement points. A triaxial accelerometer being glued on each measurement point, the total number of measured frequency response functions is equal to 480. The acquisition parameters were defined as follows:

- Bandwidth: 1024 Hz
- Number of spectral lines: 4096
- Resolution: 0.25 Hz

Figure 3.17 displays a set of measured FRFs on the frequency interval 0–500 Hz. The LSCE method was applied to identify the eigenfrequencies, modal damping ratios and mode shapes

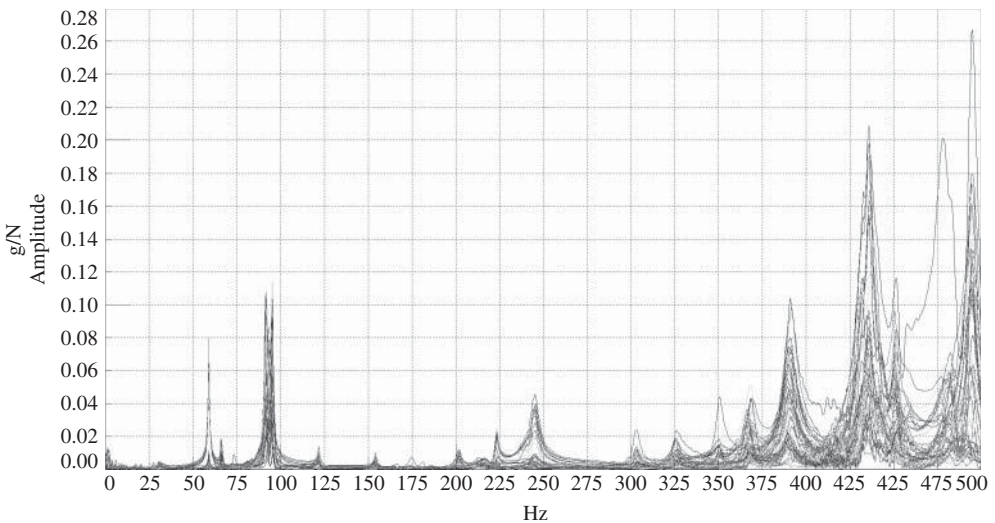


Figure 3.17 Set of FRFs over the frequency interval 0–500 Hz. Source: Reproduced with permission from V2i SA.

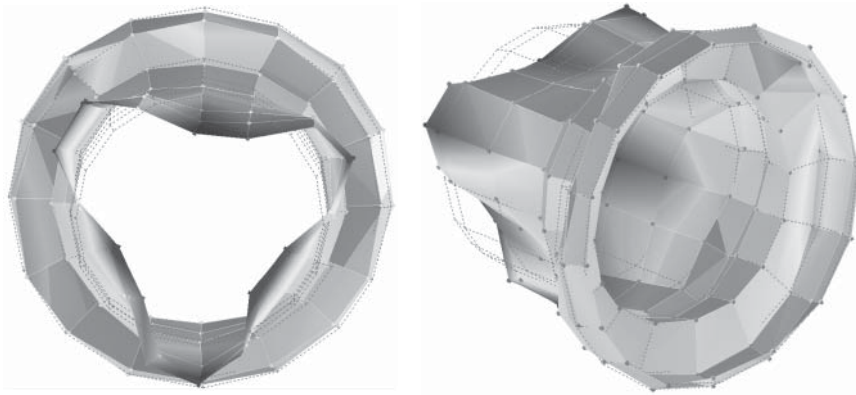


Figure 3.18 Experimental identification of the first global mode eigenmode with 3θ symmetry. Source: Reproduced with permission from V2i SA.

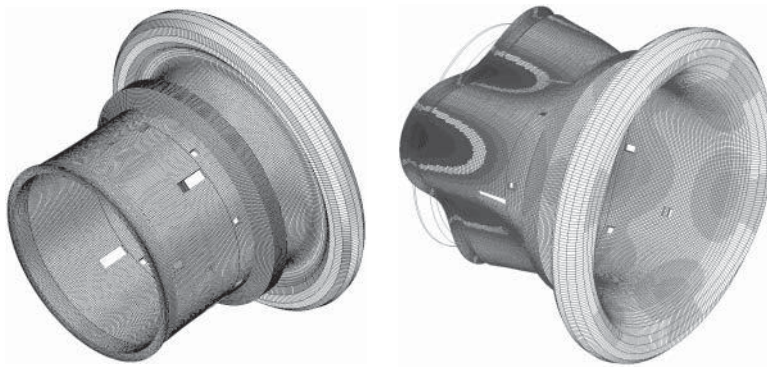


Figure 3.19 Bellmouth: finite element mesh and computed eigenmode with 3θ symmetry. Source: Reproduced with permission from Techspace Aero – SAFRAN Group.

in the frequency range 0–400 Hz. For confidentiality reasons, detailed quantitative results are not reported here.

Figure 3.18 displays two different perspective views of one experimentally identified eigenshape: it is the global mode exhibiting deformation pattern with 3θ symmetry in the (r, θ) plane, a characteristic mode of structures with revolution symmetry. The same structure has been modelled by the finite element method using the Samcef™ software. The finite element mesh and the same eigenmode with 3θ symmetry obtained numerically are displayed by Figure 3.19. One can observe excellent agreement between the experimentally measured and computed eigenshapes.

Remark 3.2 *When performing experimental modal analysis in practice, major difficulty often results from the existence of possible nonlinearities. Nonlinear behaviour of a structural system always arises at sufficiently large excitation amplitude. There are however systems in which*

it arises even at small amplitude, due to specific phenomena such as backlash, contact, dry friction, etc. In which case, the methodology established for experimental analysis rapidly fails. It is beyond the scope of this presentation to address the case of such nonlinear structures; let us simply say that one way to detect the occurrence of significant nonlinearities is to observe the dependence of measured transfer functions with the excitation amplitude.

Remark 3.3 Another source of discrepancy is the uncertainty on the boundary conditions since the latter are never perfect as generally assumed in the mathematical description of structural systems. They have always finite stiffness properties, and may also be source of local nonlinearities. They are generally very difficult to characterize both qualitatively and quantitatively. As a result, the eigenfrequencies and modal shapes identified from experiment may significantly differ from those predicted through numerical simulation. A possible way to minimize the effect of the boundary conditions in experimental modal analysis is to test the structure in free-free condition, which can be done using an elastic suspension as done on the example described in Section 3.4.5. The setup has then to be designed in such a way that the eigenfrequencies of all rigid body modes remain very small compared to those of the elastic modes.

Remark 3.4 Operational modal analysis (Brincker 2014) consists in estimating the modal parameters (frequencies, mode shapes and modal damping coefficients) of structural systems in operation (e.g. vehicles, buildings, offshore platforms), thus submitted to unknown external forces inherent to operation (e.g. road roughness, air turbulence, water waves) rather than excited in laboratory conditions. It can be shown that experimental analysis of such structures that cannot be isolated from their environment is still feasible under the assumption that the force input, although not measurable, can be described as a white noise stationary process. In which case the modal parameters can be identified from input-output data resulting from a correlation analysis between responses at different degrees of freedom of the system.

3.5 Exercises

3.5.1 Solved exercises

Problem 3.1 Consider the one-dimensional problem with two degrees of freedom depicted in Figure 3.20.a.

- Write the system matrices of the system and determine the undamped modes and frequencies. Compute the associate modal damping ratios assuming that $c = 0.06\sqrt{km}$.
- Compute (using a numerical software) the complex eigenvalues and the complex eigenmodes of the damped system. Compare the results with the approximation one would obtain using the assumption of light damping.

Solution

The system matrices can easily be found to be:

$$\mathbf{M} = \begin{bmatrix} m & 0 \\ 0 & 2m \end{bmatrix} \quad \mathbf{C} = \begin{bmatrix} 2c & -c \\ -c & c \end{bmatrix} \quad \mathbf{K} = \begin{bmatrix} 2k & -k \\ -k & 3k \end{bmatrix}$$

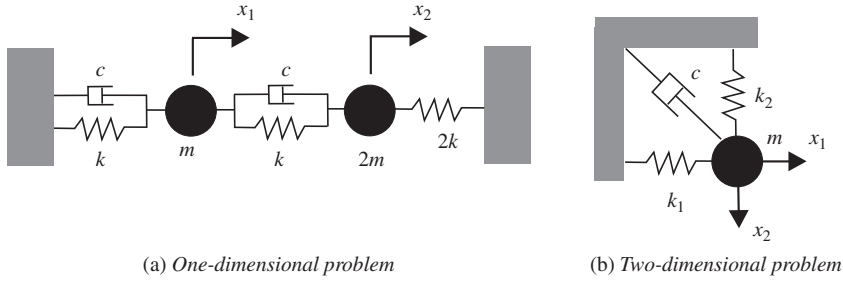


Figure 3.20 Example of damped systems.

The eigensolutions of the associated conservative system are found by solving:

$$\det \left(\begin{bmatrix} 2 & -1 \\ -1 & 3 \end{bmatrix} - \omega^2 \frac{m}{k} \begin{bmatrix} 1 & 0 \\ 0 & 2 \end{bmatrix} \right) = 0$$

Defining $v^2 = \omega^2 \frac{m}{k}$ the nondimensional frequency, the characteristic polynomial is written as

$$(2 - v^2)(3 - 2v^2) - 1 = 0$$

whose roots yield:

$$\begin{aligned} v_1^2 &= 1 & \text{and} & & \omega_{01}^2 &= \frac{k}{m} \\ v_2^2 &= \frac{5}{2} & \text{and} & & \omega_{02}^2 &= \frac{5k}{2m} \end{aligned}$$

and the eigenmodes are found to be:

$$\mathbf{x}_{(1)} = \begin{bmatrix} 1 \\ 1 \end{bmatrix} \quad \text{and} \quad \mathbf{x}_{(2)} = \begin{bmatrix} 1 \\ -1/2 \end{bmatrix}$$

with modal masses of $\mu_1 = 3m$ and $\mu_2 = 1.5m$. The modal damping matrix is:

$$\beta = \begin{bmatrix} \mathbf{x}_{(1)}^T \\ \mathbf{x}_{(2)}^T \end{bmatrix} \begin{bmatrix} 2c & -c \\ -c & c \end{bmatrix} [\mathbf{x}_{(1)} \quad \mathbf{x}_{(2)}] = c \begin{bmatrix} 1 & 1 \\ 1 & 13/4 \end{bmatrix}$$

Assuming that $c = 0.06\sqrt{km}$ so that the diagonal modal damping ratios are:

$$\begin{aligned} \epsilon_1 &= \frac{\beta_{11}}{2\omega_{01}\mu_1} = 0.0100 \\ \epsilon_2 &= \frac{\beta_{22}}{2\omega_{02}\mu_2} = 0.0411 \end{aligned}$$

Note that the second modal damping is higher since, in the first mode, the damper between the two masses is not active.

Let us now compute the complex modes and eigenvalues of the system by computing the eigensolutions of the state space form (3.70), namely solving the eigenproblem:

$$\left(\lambda \begin{bmatrix} \mathbf{0} & \mathbf{M} \\ \mathbf{M} & \mathbf{C} \end{bmatrix} + \begin{bmatrix} -\mathbf{M} & \mathbf{0} \\ \mathbf{0} & \mathbf{K} \end{bmatrix} \right) \begin{bmatrix} \lambda \mathbf{z} \\ \mathbf{z} \end{bmatrix} = \mathbf{0}$$

This eigenvalue problem can be solved using a numerical software:

$$\begin{aligned} \lambda_1 &= (-0.009986 + i1.0002) \sqrt{\frac{k}{m}} & \mathbf{z}_{(1)} &= \begin{bmatrix} 0.5246 + i0.4715 \\ 0.5065 + i0.4932 \end{bmatrix} \\ \lambda_2 &= (-0.065014 + i1.5794) \sqrt{\frac{k}{m}} & \mathbf{z}_{(2)} &= \begin{bmatrix} 0.2482 - i0.3796 \\ -0.1114 + i0.1964 \end{bmatrix} \end{aligned}$$

Applying the approximation derived in (3.13) for small damping, one finds:

$$\begin{aligned} \lambda_1 &= -\frac{\beta_{11}}{2\mu_1} \pm i\omega_{01} = (-0.01 + i) \sqrt{\frac{k}{m}} \\ \lambda_2 &= -\frac{\beta_{22}}{2\mu_2} + i\omega_{02} = (-0.065 + i1.5811) \sqrt{\frac{k}{m}} \end{aligned}$$

which is clearly a good approximation of the complex eigenvalue. Hence the small damping assumption is valid in this case. Let us also note that the complex eigenmodes of the damped system as found by Matlab[®] (see above) are defined at a complex constant. So, in order to compare them to the non-damped eigenmodes $\mathbf{x}_{(s)}$, we can also write:

$$\begin{aligned} \mathbf{z}_{(1)} &= \begin{bmatrix} 0.5246 + i0.4715 \\ 0.5065 + i0.4932 \end{bmatrix} / (0.5246 + i0.4715) = \begin{bmatrix} 1 \\ 1.0015 + i0.03997 \end{bmatrix} \\ \mathbf{z}_{(2)} &= \begin{bmatrix} 0.2482 - i0.3796 \\ -0.1114 + i0.1964 \end{bmatrix} / (0.2482 - i0.3796) = \begin{bmatrix} 1 \\ -0.4970 + i0.03138 \end{bmatrix} \end{aligned}$$

showing that the complex mode are very close to the modes of the associated conservative system, thanks to the fact that the damping is small and that the eigenfrequencies are well separate.

Problem 3.2 Let us consider now the mass suspended in the horizontal and vertical directions by springs of stiffness k_1 and k_2 respectively (Figure 3.20.b). A damper is attached to the mass at an angle of 45 degrees.

- For the undamped system, compute the eigenfrequencies and eigenmodes when $k_1 \neq k_2$ and when $k_1 = k_2 = k$.
- For the damped system, find the damped modes and associated eigenvalues in the case $k_1 = k_2 = k$.

Solution

$$\mathbf{M} = \begin{bmatrix} m & 0 \\ 0 & m \end{bmatrix} \quad \mathbf{K} = \begin{bmatrix} k_1 & 0 \\ 0 & k_2 \end{bmatrix}$$

$$\omega_1^2 = \frac{k_1}{m} \quad \omega_2^2 = \frac{k_2}{m}$$

$$\mathbf{x}_{(1)} = \begin{bmatrix} 1 \\ 0 \end{bmatrix} \quad \mathbf{x}_{(2)} = \begin{bmatrix} 0 \\ 1 \end{bmatrix}$$

If $k_1 = k_2 = k$, then the undamped modes are not uniquely defined since then the eigenfrequencies are equal (multiplicity 2) and one can also choose the \mathbf{M} -orthogonal set:

$$\mathbf{x}_{(1)} = \begin{bmatrix} 1 \\ 1 \end{bmatrix} \quad \mathbf{x}_{(2)} = \begin{bmatrix} 1 \\ -1 \end{bmatrix}$$

Let us now consider the damped system. Calling v the local velocity in the direction of the damper, the dissipation function (1.53) of the viscous damper is:

$$D = \frac{1}{2}cv^2 = \frac{1}{2}c\left(\dot{x}_1 \cos \frac{\pi}{4} + \dot{x}_2 \cos \frac{\pi}{4}\right)^2$$

The damping matrix is obtained according to (3.2), namely:

$$\mathbf{C} = \frac{\partial^2 D}{\partial \dot{q} \partial \dot{q}} = \frac{1}{2} \begin{bmatrix} c & c \\ c & c \end{bmatrix}$$

So to compute the modes of the damped system one needs to solve the eigenvalue problem:

$$\left(\lambda^2 \begin{bmatrix} m & 0 \\ 0 & m \end{bmatrix} + \lambda \frac{1}{2} \begin{bmatrix} c & c \\ c & c \end{bmatrix} + \begin{bmatrix} k_1 & 0 \\ 0 & k_2 \end{bmatrix} \right) \begin{bmatrix} z_1 \\ z_2 \end{bmatrix} = \mathbf{0}$$

One could solve this eigenvalue problem by putting it in the a state-space form and using a symbolic computation software or a numerical software (if values are given for the spring, damper and mass). If however the stiffnesses are equal, namely $k_1 = k_2 = k$, the symmetry of the system gives us good reasons to believe that the modes are:

$$\mathbf{z}_{(1)} = \begin{bmatrix} 1 \\ -1 \end{bmatrix} \quad \mathbf{z}_{(2)} = \begin{bmatrix} 1 \\ 1 \end{bmatrix}$$

which, in this particular case are purely real. One indeed can verify that these modes satisfy the eigenvalue problem for the associated eigenvalues:

$$\lambda_1 = \pm i\omega_0 \quad \text{and} \quad \lambda_2 = -\varepsilon\omega_0 \pm i\omega_0\sqrt{1 - \varepsilon^2}$$

where ω_0 is the undamped frequency $\sqrt{k/m}$ and $\varepsilon = c/(2m\omega_0)$. So whereas the nondamped modes are not uniquely defined when $k_1 = k_2 = k$, the presence of damping combines the possible modes of identical frequency in such a way that the damped modes are unique. We observe that in the first mode, the mass moves orthogonally to the damper which explains why λ_1 is purely imaginary.

Problem 3.3 Obtain through Laplace transformation the response to the normal equation:

$$\begin{cases} \ddot{\eta} + 2\varepsilon\omega_0\dot{\eta} + \omega_0^2\eta = \phi(t) \\ \eta(0) = \eta_0, \dot{\eta}(0) = \dot{\eta}_0 \end{cases} \quad (\text{P3.3.a})$$

in the form:

$$\eta(t) = \eta_0 d(t) + \dot{\eta}_0 h(t) + \int_0^t \phi(\tau) h(t - \tau) d\tau$$

To that purpose, it is advised to make use of the following identities:

- Laplace transform of an exponential with negative real part:

$$\mathcal{L}[e^{\lambda t}] = \frac{1}{s - \lambda} \quad \Re(\lambda) < 0$$

- To an ordinary product in the Laplace domain corresponds a convolution product in the time domain:

$$\mathcal{L}^{-1} [F_1(s)F_2(s)] = \int_0^t f_1(\tau)f_2(t - \tau)d\tau$$

Solution

The Laplace transformation of the equilibrium equations (P3.3.a) with nonhomogeneous initial conditions yields:

$$\eta(s) = \frac{s\eta(0) + \dot{\eta}(0) + \Phi(s)}{s^2 + 2\varepsilon\omega_0 s + \omega_0^2} = \frac{s\eta(0) + \dot{\eta}(0) + \Phi(s)}{(s - \lambda_1)(s - \lambda_2)} \quad (\text{P3.3.b})$$

with $\lambda_i = -\alpha \pm i\omega$.

$$H(s) = \frac{1}{(s - \lambda_1)(s - \lambda_2)}$$

is the Laplace transform of the response to unit initial velocity, or impulse response. Let us write it in the form:

$$H(s) = F_1(s)F_2(s) \quad \text{with} \quad F_i(s) = \frac{1}{s - \lambda_i} \quad \rightarrow \quad f_i(t) = e^{\lambda_i t}$$

Therefore we get:

$$\begin{aligned} h(t) &= \int_0^t f_1(\tau)f_2(t - \tau)d\tau \\ &= \int_0^t e^{\lambda_1 \tau} e^{\lambda_2(t - \tau)} d\tau = \frac{e^{\lambda_1 t} - e^{\lambda_2 t}}{(\lambda_1 - \lambda_2)} = e^{-\alpha t} \frac{\sin \omega t}{\omega} \end{aligned}$$

Let us note next that:

$$\mathcal{L} \left[\frac{dh}{dt} \right] = sH(s) - h(0) = sH(s)$$

and therefore, looking at (P3.3.b), we get the response to a unit initial displacement in the form:

$$\begin{aligned} d(t) &= \mathcal{L}^{-1} [sH(s)] \\ &= \frac{dh}{dt} = e^{-\alpha t} \left(\cos \omega t - \frac{\alpha}{\omega} \sin \omega t \right) \end{aligned}$$

The response is finally expressed in the form:

$$\eta(t) = \eta_0 d(t) + \dot{\eta}_0 h(t) + \int_0^t \phi(\tau) h(t - \tau) d\tau \quad \text{with} \quad \begin{cases} h(t) = e^{-\alpha t} \frac{\sin \omega t}{\omega} \\ d(t) = e^{-\alpha t} \left(\cos \omega t - \frac{\alpha}{\omega} \sin \omega t \right) \end{cases}$$

Problem 3.4 Develop the spectral expression of response to initial conditions $(\mathbf{q}_0, \dot{\mathbf{q}}_0)$ of a damped system recast in first-order form $\mathbf{A}\mathbf{r} + \mathbf{B}\dot{\mathbf{r}} = \mathbf{0}$. Show that the response at a single DOF can be put in the form:

$$q_r(t) = \sum_{k=1}^{2n} c_{kr} e^{\lambda_k t}$$

Provide the explicit expression of the coefficients c_{kr} . Demonstrate that their knowledge allows determining the system eigenmodes.

Solution

The response is expanded in the form:

$$\mathbf{r}(t) = \sum_{k=1}^{2n} \eta_k(t) \mathbf{y}_{(k)} \quad (\text{P3.4.a})$$

and in particular:

$$\mathbf{r}_0 = \begin{bmatrix} \mathbf{q}_0 \\ \dot{\mathbf{q}}_0 \end{bmatrix} = \sum_{k=1}^{2n} \eta_k(0) \mathbf{y}_{(k)}$$

Owing to orthogonality we get:

$$\mathbf{y}_{(k)}^T \mathbf{A} \mathbf{r}_0 = \mathbf{y}_{(k)}^T \mathbf{A} \mathbf{y}_{(k)} \eta_k(0) = \lambda_k \mathbf{y}_{(k)}^T \mathbf{B} \mathbf{y}_{(k)} \eta_k(0)$$

and thus:

$$\eta_k(0) = \frac{1}{\lambda_k \tilde{\mu}_k} (\mathbf{z}_{(k)}^T \mathbf{K} \mathbf{q}_0 - \lambda_k \mathbf{z}_{(k)}^T \mathbf{M} \dot{\mathbf{q}}_0)$$

with

$$\tilde{\mu}_k = \mathbf{y}_{(k)}^T \mathbf{B} \mathbf{y}_{(k)}$$

The time evolution of the normal coordinates takes thus the form (using (3.78)):

$$\eta_k(t) = \frac{e^{\lambda_k t}}{\lambda_k \tilde{\mu}_k} (\mathbf{z}_{(k)}^T \mathbf{K} \mathbf{q}_0 - \lambda_k \mathbf{z}_{(k)}^T \mathbf{M} \dot{\mathbf{q}}_0) \quad (\text{P3.4.b})$$

Substituting (P3.4.b) into (P3.4.a) and keeping the first n components of the state vector provides the spectral development of the free displacement response in the form:

$$\mathbf{q}(t) = \sum_{k=1}^{2n} \frac{e^{\lambda_k t}}{\lambda_k \tilde{\mu}_k} \mathbf{z}_{(k)} \mathbf{z}_{(k)}^T (\mathbf{K} \mathbf{q}_0 - \lambda_k \mathbf{M} \dot{\mathbf{q}}_0)$$

The response at a single DOF can formally be written in the form:

$$q_r(t) = \sum_{k=1}^{2n} c_{kr} e^{\lambda_k t}$$

with the coefficients:

$$c_{kr} = \frac{\mathbf{z}_{(k)}^T (\mathbf{K} \mathbf{q}_0 - \lambda_k \mathbf{M} \dot{\mathbf{q}}_0)}{\lambda_k \tilde{\mu}_k} z_{r(k)}$$

They are such that

$$\frac{c_{kr}}{c_{ks}} = \frac{z_{r(k)}}{z_{s(k)}}$$

Therefore, since eigenmodes are determined only to a constant, identifying the coefficients c_{kr} results in the eigenmode k expressed in the dofs r .

Problem 3.5 Consider the dynamic influence matrix (or FRF) $\mathbf{H}(\omega)$ as given in (3.82):

$$\mathbf{H}(\omega) = \sum_{s=1}^n \left\{ \frac{1}{(i\omega - \lambda_s)} \frac{\mathbf{z}_{(s)} \mathbf{z}_{(s)}^T}{\tilde{\mu}_s} + \frac{1}{(i\omega - \bar{\lambda}_s)} \frac{\bar{\mathbf{z}}_{(s)} \bar{\mathbf{z}}_{(s)}^T}{\bar{\mu}_s} \right\} \quad (\text{P3.5.a})$$

with $\tilde{\mu}_s$ defined as in (3.80). This expansion results from a decomposition in the basis of the complex conjugate modes $\mathbf{z}_{(s)}$ of the damped system, with the associated eigenvalues λ_s .

Show that, in case of light damping and well separate eigenfrequencies, the form (a) can be approximated by the expression (3.29):

$$\mathbf{H}(\omega) = \sum_{s=1}^n \frac{1}{(\omega_{0s}^2 - \omega^2 + 2i\varepsilon_s \omega \omega_{0s})} \frac{\mathbf{x}_{(s)} \mathbf{x}_{(s)}^T}{\mu_s} \quad (\text{P3.5.b})$$

where the dynamic admittance matrix is now written as an expansion in terms of modal damping ratios ε_s , and modes and frequencies of the associated conservative system.

Solution

If the damping is light and the eigenfrequencies are well separate, we have seen in Section 3.1.2 that a first order approximate is given by:

$$\lambda_s \simeq -\frac{\beta_{ss}}{2\mu_s} + i\omega_{0s} = -\varepsilon_s \omega_{0s} + i\omega_{0s} \quad \bar{\lambda}_s = -\varepsilon_s \omega_{0s} - i\omega_{0s} \quad (\text{P3.5.c})$$

$$\mathbf{z}_{(s)} \simeq \alpha \mathbf{x}_{(s)} \quad (\text{P3.5.d})$$

where α_s is an arbitrary complex amplitude of the mode.

The coefficients $\tilde{\mu}_s$ can be computed by using (P3.5.c) and (P3.5.d) in (3.80), yielding:

$$\begin{cases} \tilde{\mu}_s = (\beta_{ss} + 2\lambda_s \mu_s) \alpha^2 \\ \bar{\mu}_s = (\beta_{ss} + 2\bar{\lambda}_s \mu_s) \bar{\alpha}^2 \end{cases}$$

and substituting the result (P3.5.c) in the above expressions one finds:

$$\begin{cases} \tilde{\mu}_s = i2\mu_s \alpha^2 \omega_{0s} \\ \bar{\mu}_s = -i2\mu_s \bar{\alpha}^2 \omega_{0s} \end{cases} \quad (\text{P3.5.e})$$

Substituting (P3.5.c), (P3.5.d) and (P3.5.e) in the Pole-Residue expression (P3.5.a) of the FRF, one finds:

$$\mathbf{H}(\omega) = \sum_{s=1}^n \frac{\mathbf{x}_{(s)} \mathbf{x}_{(s)}^T}{i2\mu_s \omega_{0s}} \left\{ \frac{1}{(i\omega - \lambda_s)} + \frac{-1}{(i\omega - \bar{\lambda}_s)} \right\}$$

$$\begin{aligned}
&= \sum_{s=1}^n \frac{\mathbf{x}_{(s)} \mathbf{x}_{(s)}^T}{i2\mu_s \omega_{0s}} \frac{-\bar{\lambda}_s + \lambda_s}{(i\omega - \lambda_s)(i\omega - \bar{\lambda}_s)} \\
&= \sum_{s=1}^n \frac{\mathbf{x}_{(s)} \mathbf{x}_{(s)}^T}{i2\mu_s \omega_{0s}} \frac{i2\omega_{0s}}{(-\omega^2 - i\omega(\bar{\lambda}_s + \lambda_s) + \bar{\lambda}_s \lambda_s)}
\end{aligned}$$

Finally from (P3.5.c) we deduce that $\bar{\lambda}_s + \lambda_s = -2\varepsilon_s \omega_{0s}$ and that $\bar{\lambda}_s \lambda_s \simeq \omega_{0s}^2 (\varepsilon_s^2 + 1) \simeq \omega_{0s}^2$ for light damping, yielding the final result (P3.5.b).

Problem 3.6 Let us assume that the viscous damping matrix of a model is given by the modal expansion (3.21). As explained in Section 3.1.3 such a damping model is a good approximation of damping in practice when the assumption of diagonal modal damping can be done (light damping and well separate frequencies).

Show that if such a damping model is used even for large modal damping ratios (which then might not be an accurate representation of reality), the modes of the undamped system are still equal to the modes of the damped one, but that the eigenvalues of the damped system are related to the nondamped frequencies by:

$$\lambda_s = -\varepsilon_s \omega_{0s} \pm i\omega_{0s} \sqrt{1 - \varepsilon_s^2} \quad (\text{P3.6.a})$$

Solution

To simplify the notation we will use the matrix \mathbf{X} which columns contain the undamped modes $\mathbf{x}_{(r)}$. The eigenvalue problem corresponding to the damped system, with a viscous damping in the form (3.21), is written as:

$$\left[\lambda_s^2 \mathbf{M} + \lambda_s \mathbf{M} \mathbf{X} \text{diag} \left(\frac{2\varepsilon_k \omega_{0k}}{\mu_k} \right) \mathbf{X}^T \mathbf{M} + \mathbf{K} \right] \mathbf{z}_{(s)} = \mathbf{0} \quad (\text{P3.6.b})$$

Let us express the damped mode $\mathbf{z}_{(s)}$ as a modal superposition of the undamped modes:

$$\mathbf{z}_{(s)} = \mathbf{X} \mathbf{a}_s \quad (\text{P3.6.c})$$

where \mathbf{a}_s contains participations of the undamped modes in the damped mode $\mathbf{z}_{(s)}$. Substituting (P3.6.c) in (P3.6.b), premultiplying by \mathbf{X}^T and using the \mathbf{K} - and \mathbf{M} -orthogonality properties of \mathbf{X} , one finds:

$$\text{diag} \left(\lambda_s^2 + \lambda_s 2\varepsilon_k \omega_{0k} + \omega_{0k}^2 \right) \mathbf{a}_s = \mathbf{0}$$

Hence, when projected in the modal basis \mathbf{X} , the damped eigenvalue problem becomes trivial and the eigensolutions of the damped problem (P3.6.b) can thus be written as:

$$\lambda_s = -\varepsilon_s \omega_{0s} \pm i\omega_{0s} \sqrt{1 - \varepsilon_s^2} \quad \text{and} \quad \mathbf{z}_{(s)} = \mathbf{x}_{(s)} \quad (\text{P3.6.d})$$

Notes:

- This expression for the eigenvalues is in agreement with (3.74) for the damped eigenvalues, in case $\mathbf{z}_{(s)} = \mathbf{x}_{(s)}$.
- If we make the further assumption that damping ratios are small, hence $\sqrt{1 - \varepsilon_s^2} = 1$ in a first order approximation, one retrieves the approximation (3.13).

3.6 Proposed exercises

Problem 3.7 Let us consider the free-free system of Figure 3.7, which could be representative of the fundamental behaviour of bending vibration for an airplane in flight. Take $M = 8m$ as the fuselage mass, m the wing lumped mass (including engines) and k as the stiffness between the vertical displacements of the fuselage and the vertical displacement of the wing lumped mass (a simplified representation of the bending stiffness of the wing). The system possesses a rigid body mode for which the damping is assumed to be zero. You are asked to:

- For a wing eigenfrequency $\sqrt{\frac{k}{m}} = 2$ Hz, determine the eigenfrequencies and mode shapes of the system (hint: this can be done most easily by simple reasoning if taking advantage of the system symmetry, making use of orthogonality to get the mode shapes and of the Rayleigh quotient to compute the eigenfrequencies).
- Assuming that the elastic eigenfrequencies match quite well the experimentally measured ones and that their damping coefficients have been measured to be $\varepsilon_1 = 2\%$, $\varepsilon_2 = 5\%$, build a damping matrix that matches these values.
- Draw a Nyquist plot of the transfer functions $\frac{q_1}{f_2}$ and $\frac{q_2}{f_2}$ over the frequency range $[0.5-10]$ Hz.

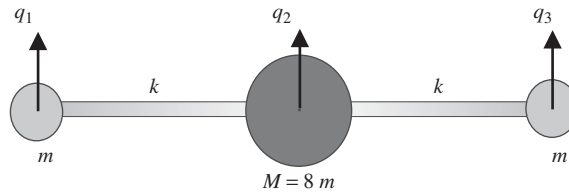


Figure 3.21 A schematic representation of a wing-fuselage assembly (3-dof free-free system).

Problem 3.8 Consider the normal Equation (3.18), which is also the equilibrium equation of a single DOF system. Develop its solution expressing the response to a nonzero initial displacement

$$\begin{cases} \ddot{\eta} + 2\varepsilon\omega_0\dot{\eta} + \omega_0^2\eta = 0 \\ \eta(0) = \eta_0 \end{cases}$$

To do so:

- Assume a general solution of the form $\sum_i A_i e^{\lambda_i t}$.
- Solve the associate eigenvalue equation to compute the λ_i . Observe that they are of the form $\lambda_{1,2} = -\alpha \pm i\omega$.
- Compute the coefficients A_i in order to match the initial condition.
- Develop the final expression (in real form) of the response in terms of α and ω .

Problem 3.9 Repeat Exercise 3.8 to get the response to a nonzero initial velocity:

$$\begin{cases} \ddot{\eta} + 2\varepsilon\omega_0\dot{\eta} + \omega_0^2\eta = 0 \\ \dot{\eta}(0) = \dot{\eta}_0 \end{cases}$$

Deduce from it the impulse response h of the system, defined as the solution of:

$$\ddot{h} + 2\varepsilon\omega_0\dot{h} + \omega_0^2 h = \delta(t)$$

where $\delta(t)$ represents the Dirac function.

Problem 3.10 Using the results of Exercises 3.8 and 3.9, develop the expression of the response under arbitrary excitation as described by Equation (P3.3.a) in Exercise 3.3.

Problem 3.11 It will be shown in Chapter 7 that the simplest integration scheme with adequate stability and accuracy properties to time integrate a first-order differential equation $\dot{x} = f(x, t)$ is the trapezoidal rule:

$$\frac{\dot{x}_{n+1} + \dot{x}_n}{2} = \frac{x_{n+1} - x_n}{\Delta t} \quad (\text{P3.11.a})$$

where Δt is the time step size.

You are asked to apply (P3.11.a) to Equation (3.3) recast in the first-order form:

$$\begin{aligned} M\dot{\mathbf{v}} + C\mathbf{v} + K\mathbf{q} &= \mathbf{p}(t) \\ \dot{\mathbf{x}} &= \mathbf{v} \end{aligned} \quad (\text{P3.11.b})$$

and show that it leads to a time-marching scheme described by the following equations:

$$\begin{cases} \left(K + \frac{2}{\Delta t}C + \frac{4}{\Delta t^2}M \right) \mathbf{q}_{n+1} = \mathbf{g}_{n+1} \\ \mathbf{v}_{n+1} = \frac{2}{\Delta t}(\mathbf{q}_{n+1} - \mathbf{q}_n) - \mathbf{v}_n \\ \mathbf{a}_{n+1} = \frac{2}{\Delta t}(\mathbf{v}_{n+1} - \mathbf{v}_n) - \mathbf{a}_n \end{cases} \quad (\text{P3.11.c})$$

with the right-hand side:

$$\mathbf{g}_{n+1} = \mathbf{p}_{n+1} + C \left(\mathbf{v}_n + \frac{2}{\Delta t} \mathbf{x}_n \right) + M \left(\mathbf{a}_n + \frac{4}{\Delta t} \mathbf{v}_n + \frac{4}{\Delta t^2} \mathbf{x}_n \right) \quad (\text{P3.11.d})$$

Problem 3.12 Apply the time-marching scheme developed in Exercise 3.11 to the system of Figure 3.1 (with $c = 0.1$) released from an initial position corresponding to the application of a static load $\mathbf{f}^T = [1 \ 0]$. The numerical solution will be developed in a numerical toolbox with the following data:

- Time window of the response: $[0, T_{\max}]$ with $T_{\max} = \frac{2\pi}{\omega_1}$
- Time step size: $\Delta t = T_{\max}/(2^{10} - 1)$.

References

- Brandt A 2011 *Noise and Vibration Analysis: Signal Analysis and Experimental Procedures*. John Wiley & Sons, Ltd, Chichester.
- Brincker R 2014 *Introduction to Operational Modal Analysis*. John Wiley & Sons, Ltd, Chichester.
- Brown D, Allemang R, Zimmerman R and Mergeay M 1979 Parameter estimation techniques for modal analysis. *SAE Transactions, SAE Paper Number 790221* **88**, 828–846.

- Brüel & Kjær 1984 Structural testing using modal analysis. BG 0112-11.
- Caughey T 1960 Classical normal modes in damped linear dynamic systems. *Journal of Applied Mechanics, Trans. ASME* **27**, 269–271.
- Cooley JW and Tukey JW 1965 An algorithm for the machine calculation of complex fourier series. *Math. Comput.* **19**, 297–301.
- Dat R 1978 *Vibrations Aéroélastiques* ENSAE, Toulouse.
- Ewins DJ 2000 *Modal Testing: Theory, Practice and Application*. Research Studies Press, Baldock.
- Fræijs de Veubeke B 1965 Analyse de la réponse forcée des systèmes amortis par la méthode des déphasages caractéristiques. *Revue Française de Mécanique* (13), 49–58.
- Fræijs de Veubeke B, Géradin M and Huck A 1972 *Structural Dynamics*. number 126 in *CISM Lecture Notes (Udine, Italy)*. Springer.
- Géradin M and Rixen D 1997 *Mechanical Vibrations – Theory and Application to Structural Dynamics*, second edn. John Wiley & Sons, Inc. New York.
- Guillaume P, Verboven P, Vanlanduit S, der Auweraer HV and Peeters B 2003 A poly-reference implementation of the least-squares complex frequency domain-estimator *Proceedings of the 21th International Modal Analysis Conference*, pp. 390–397, Kissimmee (FL), USA.
- Heylen W, Lammens S and Sas P 1997 *Modal Analysis Theory and Testing*. Katholieke Universiteit Leuven Department Werktuigkunde, Heverlee.
- Huck A 1976 Méthodes numériques en réponse dynamique avec amortissement structural. PhD thesis, Report LTAS VF-30, University of Liège, Belgium.
- Lancaster P 1966 *Lambda-Matrices and Vibrating Systems*. Pergamon Press, Oxford.
- Lord Rayleigh BJWS 1894 *Theory of Sound, Vol. 1* 2nd edn. Macmillan and Co., London and New York (first edition in 1877).
- Marin F 2012 Vibration measurement report–tested item: Silvercrest Bellmouth (confidential). Technical report, V2i, Liège, Belgium.
- McConnell KG and Varoto PS 2008 *Vibration Testing: Theory and Practice*, second edn. John Wiley & Sons, Ltd, Chichester.
- Mead D 1998 *Passive Vibration Control*. John Wiley & Sons, Inc. New York.
- Richardson MH and Formenti DL 1982 Parameter estimation from frequency response measurements using rational fraction polynomials *Proceedings of the First International Modal Analysis Conference*, vol. 1, pp. 167–181.
- Richardson MH and Formenti DL 1985 Global curve fitting of frequency response measurements using the rational fraction polynomial method *Proceedings of the Third International Modal Analysis Conference*, pp. 390–397.
- Silva JM and Maia NM 1999 Modal analysis and testing *Nato Science Series E* vol. 363 Springer.
- Zaveri K 1984 Modal analysis of large structures – multiple exciter systems. Brüel & Kjær, BT 0001-11.

4

Continuous Systems

So far, vibrating systems have been regarded as an assembly of discretized elements, namely rigid elements with inertia as their only physical property, linked together by springs and/or dissipative elements, characterized by their stiffness and their damping coefficient but with no inertia. The number of degrees of freedom of a discrete system is determined by its number of masses N and the associated constraints, and its mathematical model consists of a set of n coupled ordinary differential equations as explained in Chapter 1.

In practice, the representation of a physical system by a discrete model is usually an idealized view. In most cases, the main bodies which compose a mechanical system are deformable and the elastic elements (springs) which connect the main bodies also have their own inertia. Therefore, each constituent of a system possesses simultaneously inertia, stiffness and damping properties: the mathematical model of a continuous system undergoing time-dependent deformation used in *elastodynamics* is then relevant.

In order to formulate the governing equations of a continuous system, we will resort to the theory of continuum mechanics where the equations of motion are expressed in terms of the displacement field:

$$u(x, y, z, t)$$

$$v(x, y, z, t)$$

$$w(x, y, z, t)$$

together with the boundary conditions to be satisfied. The space variables x , y and z being continuous, the system so described possesses an infinity of degrees of freedom.

The continuous systems may be considered as limiting cases of discrete systems. To be convinced of this, one can consider the example of a system of masses and springs whose limiting case is the elastic bar (see Section 4.1). It is thus not surprising that most of the concepts encountered during the study of discrete systems can be generalized to continuous systems. For instance, the concept of eigenvalues associated with vibration frequencies will reappear for continuous systems, this time with an infinity of solutions, countable or not according to whether the continuum is finite or infinite. Similarly, the fundamental orthogonality property of vibration eigenmodes remains valid. In the discrete case, symmetry of the stiffness matrix

expressed the reciprocity of action and effect between two degrees of freedom. The same property is translated for the continuum by the Betti-Maxwell's reciprocity principle which can be generalized to dynamics. The concept of boundary conditions in space, which appears only indirectly for the discrete case, becomes of primary importance for a continuous medium, since it describes how the medium interacts with the external world. Generally, the formulation of the boundary conditions of a given problem is the result of a thorough and delicate analysis.

In many cases, the specific geometry of the continuous bodies under investigation allows a simplified formulation of the equations of motion in terms of one or two displacement components, themselves functions of one or two space variables and time. Such situations, which are often encountered in practice and lead to common concepts such as bars, strings, beams and plates, will be treated case by case after a general presentation of the dynamics of continuous media. Membranes and shells will not be discussed here.

Due to the need to take into account the boundary conditions in space, Lagrange equations lose much of their interest in the context of continuous media. They could still be generalized to 1-dimensional systems (as was done in G  radin and Rixen 1997) but cannot be generalized to 2-D and 3-D continua. Therefore, in this chapter the motion equations will be systematically derived from the application of Hamilton's principle. Such an approach has the main advantage to lead to a rigorous expression of the boundary conditions applicable to the problem under consideration.

A physical phenomenon intimately linked to free vibration of an elastic continuum is wave propagation. In fact, free vibration according to an eigenmode at its own frequency can be regarded as a standing wave resulting from the superposition of two travelling waves propagating in opposite directions. The wave propagation phenomenon is relatively simple to describe in systems such as bars, taut strings and membranes. Its complexity rapidly increases when taking into account the specific geometry and boundary conditions of the medium and, eventually, the material inhomogeneity.

Let us finally note that the concept of structural damping, although it has not been envisaged throughout this chapter, could be introduced and developed in a manner similar to the discrete case.

Definitions

The list below complements the general definitions given in the book introduction, but remains local to Chapter 4.

\bar{a}	a imposed on the system (load or displacement).
A	area of beam or bar cross-section.
D	bending stiffness of a plate.
E	Young's modulus of a material.
G	shear modulus of material (2nd Lam�� constant).
$H(t)$	step (Heaviside) function.
K_n	Kirchhoff's shear force in plates.
\mathcal{L}_g	$= \mathcal{T} - \mathcal{V}$ Lagrangian of the system.
M	moment of beam cross-section.
M_n, M_s	bending moments on plate cross-section.

M_{ns}	twisting moment on plate cross-section.
N_0	axial prestress force on a string or beam.
N_{xy0}	membrane shear prestress in a plate.
N_{x0}, N_{y0}	membrane axial prestress in a plate.
N	axial force in a bar.
Q_n	shear force along an edge of normal \vec{n} in a plate.
T	transverse shear force of beam cross-section.
Z_n	Kirchhoff's corner load in plates.
c	propagation speed of a wave.
c_L	propagation speed of a longitudinal wave.
c_R	propagation speed of a Rayleigh surface wave.
c_{SH}	propagation speed of a Love surface wave.
c_T	propagation speed of a transverse wave.
e	divergence of displacement field.
k'	cross-sectional reduction factor for shear in beam.
ℓ	length of a bar, a string or a beam.
m	mass per unit length.
\bar{p}	distributed transverse load applied on a beam.
\bar{q}	distributed moment applied on a beam.
r	gyration radius of beam cross-section.
$\delta(S_\sigma)$	Static correction for surface tractions.
ϕ_r	modal participation to mode r for boundary loads.
α	the rotatory inertia parameter of a beam.
χ	curvatures of the plate.
ϵ	vector containing the components of the strain tensor.
ϵ_{ij}	components of the strain tensor.
η	the shear parameter of a beam.
λ	Lamé constant for volumetric dilatation.
ν	Poisson's ratio of a material.
$\tilde{\omega}$	nondimensional frequency.
ψ	rotation of cross-section in a beam.
σ	vector containing the components of the stress tensor.
σ_{ij}	components of the stress tensor.

4.1 Kinematic description of the dynamic behaviour of continuous systems: Hamilton's principle

The Hamilton principle stated in Chapter 1 to represent the dynamic behaviour of discrete systems is in fact a *displacement variational principle* (a more global formulation of the virtual work principle) that may easily be generalized to continuous systems as explained next.

4.1.1 Definitions

Let us consider an elastic body undergoing in time a certain motion measured from the undeformed configuration. The latter is supposed to be time-invariant, and corresponds to the

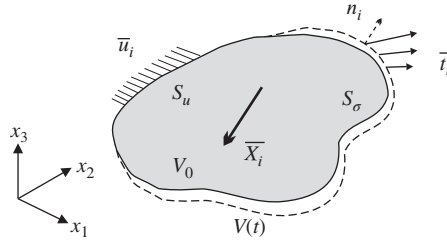


Figure 4.1 Continuous systems: definitions.

equilibrium position of the system in the absence of external forces (Figure 4.1). Let us define the following variables:

$V(t)$	the volume occupied by the elastic body in the deformed configuration and its associated mass density ρ
V_0	the volume in the undeformed configuration and its associated mass density ρ_0 ; V_0 is supposed to be time-invariant and is adopted as a reference configuration (<i>Lagrangian</i> description of motion)
$x_i = [x_1, x_2, x_3]$	the Cartesian coordinates of a given point of the undeformed body; we will also use the more explicit notation (x, y, z) whenever possible
$S = S_u + S_\sigma$	the total surface of the body in undeformed configuration can be split into: S_u , the portion of surface on which the displacements are imposed:
	$u_i = \bar{u}_i$
	S_σ , the complementary part of the surface on which surface tractions are imposed:
	$t_i = \bar{t}_i$
\bar{X}_i	the applied body forces
\bar{t}_i	the surface tractions imposed on S_σ
n_i	the direction cosines of the outward normal to the surface S
\bar{u}_i	the displacements imposed on S_u

For the explicit expression of Hamilton's principle it is first necessary, in order to compute the strain energy, to choose an appropriate measure of strain.

4.1.2 Strain evaluation: Green's measure

Let us agree to compute the deformation at every point of the volume with respect to the reference configuration, i.e. to express the deformation at a point A of coordinates x_i before

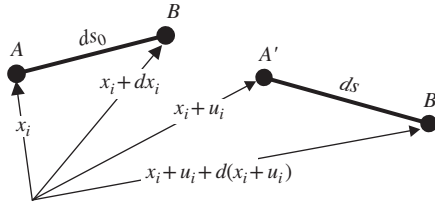


Figure 4.2 Strain measure of a segment.

deformation (*Lagrangian* point of view, by contrast to the *Eulerian*, where the deformed configuration would be adopted as reference). Let B be a second point in the neighbourhood of A and occupying the position $x_i + dx_i$ in the undeformed state. After deformation, the points A and B occupy the new positions $x_i + u_i$ and $x_i + u_i + d(x_i + u_i)$, respectively (see Figure 4.2).

Let us denote ds_0 and ds as the lengths of segment AB before and after deformation:¹

$$ds_0^2 = dx_i dx_i$$

$$ds^2 = d(x_i + u_i) d(x_i + u_i)$$

By taking account of:

$$du_i = \frac{\partial u_i}{\partial x_j} dx_j \quad i = 1, 2, 3 \quad (4.1)$$

one may write:

$$\begin{aligned} ds^2 &= \left(dx_i + \frac{\partial u_i}{\partial x_j} dx_j \right) \left(dx_i + \frac{\partial u_i}{\partial x_m} dx_m \right) \\ &= dx_i dx_i + \frac{\partial u_i}{\partial x_j} dx_j dx_i + \frac{\partial u_i}{\partial x_m} dx_m dx_i + \frac{\partial u_i}{\partial x_j} \frac{\partial u_i}{\partial x_m} dx_j dx_m \\ &= dx_i dx_i + \left(\frac{\partial u_i}{\partial x_j} + \frac{\partial u_j}{\partial x_i} + \frac{\partial u_m}{\partial x_j} \frac{\partial u_m}{\partial x_i} \right) dx_j dx_i \end{aligned}$$

Let us next define the components of *Green's symmetric strain tensor* ε_{ij} in such a way that the length increment of segment \overline{AB} is expressed as:

$$ds^2 - ds_0^2 = 2\varepsilon_{ij} dx_i dx_j \quad (4.2)$$

Hence, according to the previous expressions, the strain components may be written:

$$\boxed{\varepsilon_{ij} = \frac{1}{2} \left(\frac{\partial u_i}{\partial x_j} + \frac{\partial u_j}{\partial x_i} + \frac{\partial u_m}{\partial x_j} \frac{\partial u_m}{\partial x_i} \right)} \quad (4.3)$$

It is a symmetric second-order tensor, quadratic in the displacements u_i . Relations (4.2) and (4.3) directly imply the following:

¹ For simplicity's sake, from now on *Einstein's* notation will be used, according to which the repetition of one suffix inside a product implies summation on this suffix: $dx_i dx_i = \sum_{i=1}^3 dx_i^2$.

The necessary and sufficient condition for the motion of an elastic body to be rigid, i.e. to consist of global rotations and translations preserving the distance between particles, is that the strain tensor vanishes.

A particular case: linear deformation

The *geometric linearity* assumption may be split into two parts:

1. The extension strains remain infinitesimal:

$$\frac{\partial u_i}{\partial x_i} \ll 1 \quad i = 1, 2, 3 \quad (4.4)$$

2. The rotations have small amplitudes:

$$\frac{\partial u_i}{\partial x_j} \ll 1 \quad i \neq j \quad (4.5)$$

This leads to the linear expression of the infinitesimal strain tensor

$$\boxed{\varepsilon_{ij} = \frac{1}{2} \left(\frac{\partial u_i}{\partial x_j} + \frac{\partial u_j}{\partial x_i} \right)} \quad (4.6)$$

The definition (4.2) of strain seems arbitrary at first, but it corresponds effectively to the concept of relative-length variation. Indeed, let us consider an infinitesimal segment collinear to axis x_1 and deformed in the direction parallel to it:

$$\begin{aligned} ds^2 - ds_0^2 &= (ds - ds_0)(ds + ds_0) = 2\varepsilon_{11} dx_1^2 \\ &= 2\varepsilon_{11} ds_0^2 \end{aligned}$$

hence:

$$\varepsilon_{11} = \frac{ds - ds_0}{ds_0} \frac{1}{2} \left(1 + \frac{ds}{ds_0} \right)$$

and in the case of infinitesimal strain:

$$\varepsilon_{11} = \frac{ds - ds_0}{ds_0}$$

Example 4.1

In order to fully understand the meaning of each term in the Green strain tensor expression, let us consider the following simple example.

A straight bar is subjected to a deformation resulting from a planar displacement field (u, v) function of the only Lagrangian coordinate x of the system (Figure 4.3). Its extension strain

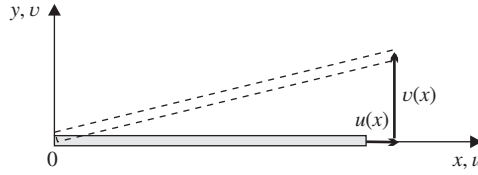


Figure 4.3 Strains: the straight bar example.

has as its general expression:

$$\epsilon_{xx} = \frac{du}{dx} + \frac{1}{2} \left(\frac{du}{dx} \right)^2 + \frac{1}{2} \left(\frac{dv}{dx} \right)^2 \quad (\text{E4.1.a})$$

Let us analyze the different possible cases and the resulting simplifications.

The case of large strains

In the case where the rotation term dv/dx and the extension deformation term du/dx are important, no simplification can be made in (E4.1.a). Indeed, let us for example imagine that the bar rotates about its end without being stretched (Figure 4.4).

One may write:

$$u(x) = -2x \sin \frac{\alpha}{2} \sin \frac{\alpha}{2} \quad v(x) = 2x \sin \frac{\alpha}{2} \cos \frac{\alpha}{2}$$

The computation of the axial strain provides the result:

$$\begin{aligned} \epsilon_{xx} &= \frac{du}{dx} + \frac{1}{2} \left(\frac{du}{dx} \right)^2 + \frac{1}{2} \left(\frac{dv}{dx} \right)^2 \\ &= -2\sin^2 \frac{\alpha}{2} + 2\sin^4 \frac{\alpha}{2} + 2\sin^2 \frac{\alpha}{2} \cos^2 \frac{\alpha}{2} \\ &= -2\sin^2 \frac{\alpha}{2} + 2\sin^2 \frac{\alpha}{2} \left(\sin^2 \frac{\alpha}{2} + \cos^2 \frac{\alpha}{2} \right) \\ &= 0 \end{aligned} \quad (\text{E4.1.b})$$

which shows the importance of each term for a correct evaluation of the strains.

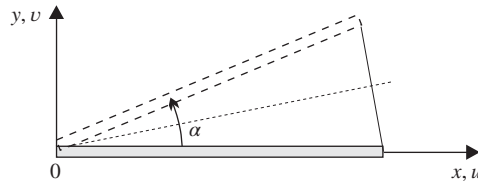


Figure 4.4 Rotation without strain.

The large displacement approximation

When the axial deformation remains small one has (Figure 4.5):

$$\frac{du}{dx} < \frac{dv}{dx} \quad \frac{du}{dx} \ll 1$$

and the strain admits the approximate expression:

$$\epsilon_{xx} \simeq \frac{du}{dx} + \frac{1}{2} \left(\frac{dv}{dx} \right)^2 \quad (\text{E4.1.c})$$

This case is very frequent in the nonlinear analysis of structures subjected to bending, since it consists of taking into account the large displacements generated by the rotation of the system, while keeping the small strain assumption. This is the so-called large displacement approach.

When the axial displacement vanishes, it is possible to verify Green's formula and compute the corresponding extension (Figure 4.5):

$$u = 0 \quad v = x \tan \alpha$$

and thus:

$$\epsilon_{xx} = \frac{1}{2} \tan^2 \alpha$$

Applying then the definition (4.2) of the Green tensor one obtains the result:

$$\begin{aligned} ds^2 - ds_0^2 &= 2\epsilon_{xx} dx^2 \\ &= \tan^2 \alpha dx^2 \\ &= \left(\frac{dx}{\cos \alpha} \right)^2 - dx^2 \end{aligned}$$

which is consistent with the geometric relationships $ds_0 = dx$ and $ds = \frac{dx}{\cos \alpha}$ observed in Figure 4.5.

The infinitesimal case

When both rotations and displacements are small,

$$\frac{du}{dx} \ll 1 \quad \frac{dv}{dx} \ll 1$$

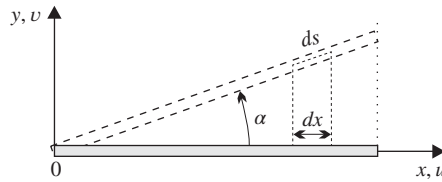


Figure 4.5 Large displacements and rotation at small strain.

and by neglecting the quadratic terms in the strain expression, one finds the classical linear form (4.6) for the straight bar:

$$\varepsilon_{xx} = \frac{du}{dx}$$

4.1.3 Stress–strain relationships

We will limit ourselves to the case of *hyperelastic* material, which can be characterized by the fact that the work of the mechanical stresses is stored in the form of internal energy and is thus recoverable.

The stress–strain relationship of a hyperelastic material takes the form of a one-to-one relationship:

$$\sigma_{ij} = f(\varepsilon_{kl}) \quad (4.7)$$

where σ_{ij} denote the components of the stress tensor. This relation is illustrated in the one-dimensional case by Figure 4.6.

Strain energy density

To a strain increment $d\varepsilon_{ij}$ in the stress state σ_{ij} corresponds a strain energy increment per unit of volume:

$$dW = \sigma_{ij} d\varepsilon_{ij} \quad (4.8)$$

The *strain energy density* may thus be defined by:

$$W(\varepsilon_{ij}) = \int_0^{\varepsilon_{ij}} \sigma_{ij} d\varepsilon_{ij} \quad (4.9)$$

The latter depends only on the deformation state, and the associated stresses may be obtained through differentiation:

$$\sigma_{ij} = \frac{\partial W}{\partial \varepsilon_{ij}} \quad (4.10)$$

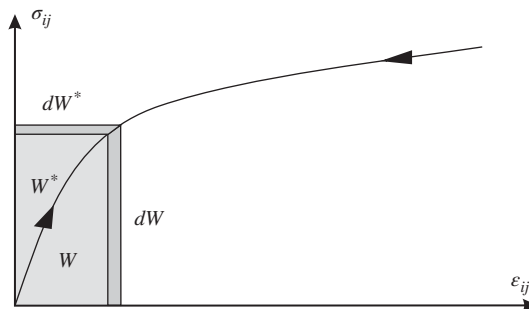


Figure 4.6 Stress–strain relationship.

The symmetric stress tensor σ_{ij} thus defined is *energetically conjugate* to the Green strains ϵ_{ij} . It is called the *second Piola–Kirchhoff* stress tensor (also known as the *Kirchhoff–Trefftz* stress tensor (Fung 1965)). Recall that the second Piola–Kirchhoff stress tensor does not represent the true stresses (i.e. the Cauchy stresses) inside a structure with respect to the initial reference frame. Rather, it describes the stress field in a reference frame attached to the body (and thus subjected to its deformation) and it is related to the elementary area of the undeformed structure.

In the one-dimensional case, the strain energy density is measured by the surface between the stress–strain curve and the strain axis.

The *complementary energy density* W^* of the material is similarly defined as the surface between the stress–strain curve and the stress axis. It is such that:

$$W^* = \sigma_{ij}\epsilon_{ij} - W \quad (4.11)$$

and is thus obtained from a *Legendre* transformation between the conjugate variables σ_{ij} and ϵ_{ij} . It is a function of the stress state only:

$$W^*(\sigma_{ij}) = \int_0^{\sigma_{ij}} \epsilon_{ij} d\sigma_{ij} \quad (4.12)$$

From definitions (4.11) and (4.12), one obtains the relationship:

$$\epsilon_{ij} = \frac{\partial W^*}{\partial \sigma_{ij}} \quad (4.13)$$

which exhibits the reciprocal roles played by stresses and strains on the one hand, and the strain and complementary energy densities on the other hand.

Linear material

A material has linear elastic properties when the stress state remains strictly proportional to the strain state. Owing to the symmetry of the tensors σ_{ij} and ϵ_{kl} , such a material is characterized in the general case by 21 distinct coefficients C_{ijkl} so that:

$$\sigma_{ij} = C_{ijkl} \epsilon_{kl} \quad (4.14)$$

in terms of which the strain energy is expressed:

$$W = \frac{1}{2} C_{ijkl} \epsilon_{ij} \epsilon_{kl} \quad (4.15)$$

When the material has isotropic properties, it is characterized by the simpler *Hooke* law, which may be put in the form:

$$\sigma_{ij} = \lambda (\epsilon_{11} + \epsilon_{22} + \epsilon_{33}) \delta_{ij} + 2G \epsilon_{ij} \quad (4.16)$$

where

$$\lambda = \frac{E\nu}{(1+\nu)(1-2\nu)} \quad \text{and} \quad G = \frac{E}{2(1+\nu)} \quad (4.17)$$

are the Lamé constants. The first term generates the principal stresses due to the volumetric dilatation, while the second one is linked to shear deformation and is known as the shear modulus. The coefficients E and ν are the commonly used Young's modulus and Poisson's ratio, respectively.

4.1.4 Displacement variational principle

The displacement variational principle is Hamilton's principle expressed for a continuous system. Let us recall that it states that:

Among the feasible trajectories of the system subjected to the restrictive conditions:

$$\delta u(t_1) = \delta u(t_2) = 0 \quad (4.18)$$

at the end of the considered time interval $[t_1, t_2]$, the real trajectory of the system is the stationary point of the mechanical action in Lagrange's and Hamilton's sense:

$$\delta \int_{t_1}^{t_2} \mathcal{L}_g[u] dt = \delta \int_{t_1}^{t_2} (\mathcal{T} - \mathcal{V}) dt = 0 \quad (4.19)$$

The kinetic energy of the continuous system of Figure 4.1 may be evaluated from an integration over the reference volume: by making use of Einstein's notation it takes the form:

$$\mathcal{T}(u) = \frac{1}{2} \int_{V_0} \rho_0 \dot{u}_i \dot{u}_i dV \quad (4.20)$$

The total potential energy \mathcal{V} results from the summation of the strain energy of the body and the potential energy of the external forces, supposed conservative:

$$\mathcal{V} = \mathcal{V}_{int} + \mathcal{V}_{ext} \quad (4.21)$$

The strain energy can be expressed by:

$$\mathcal{V}_{int} = \int_{V_0} W(\epsilon_{ij}) dV \quad (4.22)$$

and the external potential energy is computed by assuming the existence of body forces: \bar{X}_i and external surface tractions \bar{t}_i on the portion S_σ of the surface:

$$\mathcal{V}_{ext} = - \int_{V_0} \bar{X}_i(t) u_i dV - \int_{S_\sigma} \bar{t}_i(t) u_i dS \quad (4.23)$$

The displacement field must verify a priori the kinematic conditions:

$$u_i = \bar{u}_i(t) \quad \text{on } S_u, \forall t \quad (4.24)$$

Conditions (4.18) and (4.24) are *essential* conditions to the applicability of the principle, whereas the conditions resulting from the application of principle (4.19) are said to be *natural*.

4.1.5 Derivation of equations of motion

By applying Hamilton's principle to the continuous system we will derive the general equations of motion with the assumption that the forces applied to the system do not depend on the displacement field u_i .

In the case where displacement dependent loads $P_i(u_j)$ exist, it is easy to generalize the formulation by adding to the principle their virtual work:

$$\delta \int_{t_1}^{t_2} (\mathcal{T} - \mathcal{V}) dt + \int_{t_1}^{t_2} \delta \mathcal{W} dt = 0 \quad (4.25)$$

with

$$\delta \mathcal{W} = \int_{V_0} P_i \delta u_i dV \quad (4.26)$$

By substituting (4.20) and (4.21) in (4.25) and performing the variation one obtains the expression:

$$\delta \int_{t_1}^{t_2} \mathcal{L}_g[u] dt = \int_{t_1}^{t_2} \left\{ \int_{V_0} \left[\rho_0 \dot{u}_i \delta \dot{u}_i - \frac{\partial W}{\partial \varepsilon_{ij}} \delta \varepsilon_{ij} + \bar{X}_i \delta u_i \right] dV + \int_{S_\sigma} \bar{t}_i \delta u_i dS \right\} dt \quad (4.27)$$

This expression must then be integrated by parts both in time and space in order to reveal the virtual displacements δu_i and deduce in this manner the equations of motion. One has on one hand:

$$\int_{t_1}^{t_2} \rho_0 \dot{u}_i \delta \dot{u}_i dt = [\rho_0 \dot{u}_i \delta u_i]_{t_1}^{t_2} - \int_{t_1}^{t_2} \rho_0 \ddot{u}_i \delta u_i dt \quad (4.28)$$

where the boundary term vanishes in view of the essential conditions (4.18). On the other hand, in view of expressions (4.10) of the stresses and (4.3) of the strains, the term corresponding to the variation of the strain energy can be expressed in the form:

$$\int_{V_0} \frac{\partial W}{\partial \varepsilon_{ij}} \delta \varepsilon_{ij} dV = \frac{1}{2} \int_{V_0} \sigma_{ij} \left(\delta \frac{\partial u_j}{\partial x_i} + \delta \frac{\partial u_i}{\partial x_j} + \frac{\partial u_m}{\partial x_i} \delta \frac{\partial u_m}{\partial x_j} + \frac{\partial u_m}{\partial x_j} \delta \frac{\partial u_m}{\partial x_i} \right) dV \quad (4.29)$$

Its space-integration by parts (Gauss' formula) yields:

$$\begin{aligned} \int_{V_0} \frac{\partial W}{\partial \varepsilon_{ij}} \delta \varepsilon_{ij} dV = & \frac{1}{2} \int_S \left[n_i \sigma_{ij} \left(\delta u_j + \delta u_m \frac{\partial u_m}{\partial x_j} \right) + n_j \sigma_{ij} \left(\delta u_i + \delta u_m \frac{\partial u_m}{\partial x_i} \right) \right] dS \\ & - \frac{1}{2} \int_{V_0} \left[\frac{\partial \sigma_{ij}}{\partial x_i} \delta u_j + \frac{\partial \sigma_{ij}}{\partial x_j} \delta u_i \right. \\ & \left. + \frac{\partial}{\partial x_j} \left(\sigma_{ij} \frac{\partial u_m}{\partial x_i} \right) \delta u_m + \frac{\partial}{\partial x_i} \left(\sigma_{ij} \frac{\partial u_m}{\partial x_j} \right) \delta u_m \right] dV \end{aligned}$$

or, by taking into account the symmetry of the stress tensor σ_{ij} and the essential kinematic condition (4.24),

$$\begin{aligned} \int_{V_0} \frac{\partial W}{\partial \varepsilon_{ij}} \delta \varepsilon_{ij} dV = & \int_{S_\sigma} n_i \left(\sigma_{ij} + \sigma_{im} \frac{\partial u_j}{\partial x_m} \right) \delta u_j dS \\ & - \int_{V_0} \frac{\partial}{\partial x_i} \left(\sigma_{ij} + \sigma_{im} \frac{\partial u_j}{\partial x_m} \right) \delta u_j dV \end{aligned} \quad (4.30)$$

The substitution of (4.28) and (4.30) into the variational expression (4.27) finally yields:

$$\delta \int_{t_1}^{t_2} \mathcal{L}_g[u] dt = \int_{t_1}^{t_2} \left\{ \int_{S_\sigma} \left[\bar{t}_j - n_i \left(\sigma_{ij} + \sigma_{im} \frac{\partial u_j}{\partial x_m} \right) \right] \delta u_j dS + \int_{V_0} \left[\frac{\partial}{\partial x_i} \left(\sigma_{ij} + \sigma_{im} \frac{\partial u_j}{\partial x_m} \right) - \rho_0 \ddot{u}_j + \bar{X}_j \right] \delta u_j dV \right\} dt = 0 \quad (4.31)$$

The displacement variation δu_j being arbitrary inside V_0 and on S_σ , one obtains the natural conditions expressing the dynamic equilibrium of the body in the volume and on the surface:

$$\boxed{\begin{aligned} \frac{\partial}{\partial x_i} \left(\sigma_{ij} + \sigma_{im} \frac{\partial u_j}{\partial x_m} \right) + \bar{X}_j - \rho_0 \ddot{u}_j &= 0 && \text{in } V_0 \\ t_j &= n_i \left(\sigma_{ij} + \sigma_{im} \frac{\partial u_j}{\partial x_m} \right) = \bar{t}_j && \text{on } S_\sigma \end{aligned}} \quad (4.32)$$

These expressions are equivalent to the dynamic equilibrium equations of a deformable body in terms of the Kirchhoff–Trefftz stresses and thus justify the formulation above of Hamilton's principle for continuous systems. Let us note that equations (4.32) express the equilibrium of the *deformed* body and thus take into account the geometric nonlinearity (Fung 1965).

The equilibrium conditions are *natural* conditions to the principle in the sense that the principle takes care of their best possible enforcement by the trial functions adopted for u . The latter must themselves verify a priori the *essential* compatibility conditions:

$$\varepsilon_{ij} = \frac{1}{2} \left(\frac{\partial u_j}{\partial x_i} + \frac{\partial u_i}{\partial x_j} + \frac{\partial u_m}{\partial x_i} \frac{\partial u_m}{\partial x_j} \right) \quad \text{in } V_0 \quad (4.33)$$

$$u_j = \bar{u}_j \quad \text{on } S_u \quad (4.34)$$

4.1.6 The linear case and nonlinear effects

When applying Hamilton's principle as a variational principle operating on displacements, in the general case the strains are computed from the Green relationships (4.3). However, as already mentioned in Section 4.1.2, important simplifications can be made in the common case of small rotations and small displacements: the system energies and the equilibrium equations may then be reduced to simple forms both in the linear case and in the initial stress case.

Starting from expression (4.3) of the Green strain tensor, one may write:

$$\begin{aligned} \varepsilon_{ij} &= \frac{1}{2} \left(\frac{\partial u_i}{\partial x_j} + \frac{\partial u_j}{\partial x_i} + \frac{\partial u_m}{\partial x_i} \frac{\partial u_m}{\partial x_j} \right) \\ &= \varepsilon_{ij}^{(1)} + \varepsilon_{ij}^{(2)} \end{aligned} \quad (4.35)$$

by defining:

$$\begin{aligned} \varepsilon_{ij}^{(1)} &= \frac{1}{2} \left(\frac{\partial u_i}{\partial x_j} + \frac{\partial u_j}{\partial x_i} \right) \dots\dots\dots \text{the terms linear in the displacements which correspond to the strain measure in the infinitesimal case;} \\ \varepsilon_{ij}^{(2)} &= \frac{1}{2} \frac{\partial u_m}{\partial x_i} \frac{\partial u_m}{\partial x_j} \dots\dots\dots \text{the terms quadratic in the displacements.} \end{aligned}$$

The pure linear case

When both rotations and displacements maintain a small amplitude (case of *geometric linearity*), the quadratic terms can be neglected, so:

$$\epsilon_{ij} \simeq \epsilon_{ij}^{(1)} = \frac{1}{2} \left(\frac{\partial u_i}{\partial x_j} + \frac{\partial u_j}{\partial x_i} \right)$$

Applying Hamilton's principle and following the same steps as in Section 4.1.5 yields the natural conditions:

$$\boxed{\begin{aligned} \frac{\partial \sigma_{ij}}{\partial x_i} + \bar{X}_j - \rho_0 \ddot{u}_j &= 0 & \text{in } V \\ t_j = n_i \sigma_{ij} &= \bar{t}_j & \text{on } S_\sigma \end{aligned}} \quad (4.36)$$

The equations above are the linearized equations of motion for an elastic body undergoing infinitesimal displacements and rotations. They express equilibrium in the undeformed state $V_0 \simeq V$.

Nonlinear effects

In the case where geometric nonlinear effects are taken into account, it is necessary to consider the complete expression of the Green tensor, and the equilibrium equations are then the relationships (4.32). For a linear material, the strain energy density may be put in the form:

$$\begin{aligned} W &= \frac{1}{2} C_{ijkl} \epsilon_{ij} \epsilon_{kl} \\ &= \frac{1}{2} C_{ijkl} \left(\epsilon_{ij}^{(1)} + \epsilon_{ij}^{(2)} \right) \left(\epsilon_{kl}^{(1)} + \epsilon_{kl}^{(2)} \right) \\ &= \frac{1}{2} C_{ijkl} \epsilon_{ij}^{(1)} \epsilon_{kl}^{(1)} + C_{ijkl} \epsilon_{ij}^{(1)} \epsilon_{kl}^{(2)} + \frac{1}{2} C_{ijkl} \epsilon_{ij}^{(2)} \epsilon_{kl}^{(2)} \end{aligned} \quad (4.37)$$

The first term of this expression corresponds to elastic forces varying linearly with displacements, and the following two terms generate the elastic forces arising from nonlinear effects.

Example 4.2

To illustrate the concept of nonlinear effects, let us consider the one-dimensional system consisting of a central mass particle fixed to a cable (Figure 4.7). If the cable is not stretched, we will see that the transverse motion is conditioned only by nonlinear effects.

To analyze the transverse motion of the mass particle M in the (x, y) plane, let us assume that the cable is massless so that it remains straight on both sides of the mass. The cable is subjected to no initial stress and the diameter of the mass is negligible compared to the cable length ℓ . We may thus write:

$$\begin{aligned} \frac{\partial v}{\partial x} &= \frac{2v_M}{\ell} & \text{when } 0 < x < \frac{\ell}{2} \\ \frac{\partial v}{\partial x} &= \frac{-2v_M}{\ell} & \text{when } \frac{\ell}{2} < x < \ell \end{aligned} \quad (\text{E4.2.a})$$

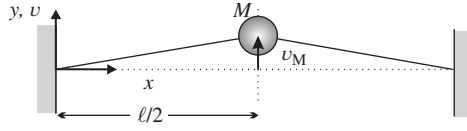


Figure 4.7 Cable with central mass particle.

where v_M , the transverse displacement of mass M , is the only independent variable of the problem. If the analysis is limited to the transverse motion, the axial strain can be expressed by:

$$\epsilon_x = \frac{1}{2} \left(\frac{\partial v}{\partial x} \right)^2 \quad (\text{E4.2.b})$$

The kinetic and potential energies take the form:

$$\begin{aligned} \mathcal{T} &= \frac{1}{2} M \dot{v}_M^2 \\ \mathcal{V}_{int} &= \frac{1}{2} \int_0^\ell EA \epsilon_x^2 dx \end{aligned} \quad (\text{E4.2.c})$$

Let us now apply Hamilton's principle to obtain the equation of motion in the absence of external forces:

$$\int_{t_1}^{t_2} \left\{ M \dot{v}_M \delta \dot{v}_M + \int_0^\ell EA \epsilon_x \delta \epsilon_x dx \right\} dt = 0$$

and next, by making use of Equation (E4.2.b),

$$\int_{t_1}^{t_2} \left\{ M \dot{v}_M \delta \dot{v}_M + \int_0^\ell \frac{EA}{2} \left(\frac{\partial v}{\partial x} \right)^3 \delta \frac{\partial v}{\partial x} dx \right\} dt = 0$$

Taking account of the application rules of the principle, integrating by parts the first term and making use of relationships (E4.2.a) yields:

$$M \ddot{v}_M \delta v_M + \int_0^{\ell/2} \frac{EA}{2} \left(\frac{2v_M}{\ell} \right)^3 \frac{2}{\ell} \delta v_M dx + \int_{\ell/2}^\ell \frac{EA}{2} \left(\frac{2v_M}{\ell} \right)^3 \frac{2}{\ell} \delta v_M dx = 0$$

and thus:

$$\left\{ M \ddot{v}_M + \ell \frac{EA}{\ell} \left(\frac{2v_M}{\ell} \right)^3 \right\} \delta v_M = 0$$

Since δv_M is arbitrary, the equation governing the free transverse motion takes the final form:

$$M \ddot{v}_M + EA \left(\frac{2v_M}{\ell} \right)^3 = 0 \quad (\text{E4.2.d})$$

The relationship above expresses equilibrium of mass M when the restoring force is due to non-linear effects only. In other words, when the mass particle M moves in the perpendicular

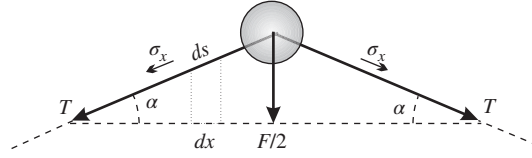


Figure 4.8 Free body diagram of the central mass.

direction to x , the cable is stretched. This is commonly called the cable effect. Let us notice the nonlinear form of the restoring force versus v_M .

To understand the physical meaning of equation (E4.2.d), let us consider Figure 4.8.

Let $N = A\sigma_x = EA\epsilon_x$ be the axial force in the cable computed from the Green measure of strain and from the conjugate Kirchhoff stress. The true force T is such that its virtual work is equivalent to that produced by N :

$$EA\epsilon_x\delta\epsilon_x = T\delta\left(\frac{ds}{dx}\right)$$

Since the Green measure is such that:

$$\epsilon_x = \frac{1}{2} \frac{ds^2 - dx^2}{dx^2}$$

one has:

$$\delta\epsilon_x = \frac{ds}{dx} \delta\frac{ds}{dx}$$

from which it can be deduced that:

$$T = N \frac{ds}{dx} = \frac{N}{\cos \alpha}$$

The last relationship is a direct consequence of the fact that the Kirchhoff–Trefftz stresses are expressed with respect to the deformed frame but are measured relative to the surface of the undeformed structure. The force F acting vertically on the mass particle is thus equal to:

$$\begin{aligned} F &= 2T \sin \alpha \\ &= 2N \tan \alpha \\ &= 2AE\epsilon_x \frac{2v_M}{\ell} \end{aligned}$$

By noting also that:

$$\epsilon_x = \frac{1}{2} \left(\frac{\partial v}{\partial x} \right)^2 = \frac{1}{2} \left(\frac{2v_M}{\ell} \right)^2$$

one finally obtains:

$$F = EA \left(\frac{2v_M}{\ell} \right)^3$$

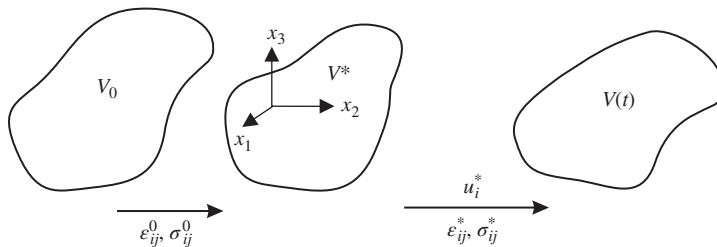


Figure 4.9 Undeformed, prestressed and deformed states.

The case of initial stresses

Initial stress is a particular case of nonlinear effects often encountered in practice. A structure is said to be *prestressed* when it is submitted to a prescribed field of initial stresses σ_{ij}^0 and to the associated field of initial strains ϵ_{ij}^0 , both being independent of time. The analysis of such a structure consists thus in determining the fields σ_{ij}^* and u_i^* which are added to this initial state (Debondie 1991). The notations adopted are summarized by Figure 4.9, and the relationships

$$\epsilon_{ij} = \epsilon_{ij}^0 + \epsilon_{ij}^* \quad (4.38)$$

$$\sigma_{ij} = \sigma_{ij}^0 + \sigma_{ij}^* \quad (4.39)$$

express respectively the strain state and the stress state measured in the prestressed configuration V^* adopted as reference.

Hamilton's principle is written:

$$\delta \int_{t_1}^{t_2} (\mathcal{T} - \mathcal{V}) \, dt = 0$$

where the variation operates on the displacement from the initial state:

$$\delta u_i = \delta u_i^*$$

\mathcal{T} and \mathcal{V} are the kinetic and potential energies accumulated by the structure when passing from the initial to the deformed state:

$$\begin{aligned} \mathcal{T} &= \frac{1}{2} \int_{V^*} \rho^* \dot{u}_i \dot{u}_i \, dV \\ &= \frac{1}{2} \int_{V^*} \rho^* \dot{u}_i^* \dot{u}_i^* \, dV = \mathcal{T}^* \end{aligned} \quad (4.40)$$

where \mathcal{T}^* is the kinetic energy associated with displacement increments u_i^* . The potential energy is written as:

$$\mathcal{V} = \mathcal{V}_{int} + \mathcal{V}_{ext}$$

The internal energy can be expressed as:

$$\mathcal{V}_{int} = \frac{1}{2} \int_{V^*} C_{ijkl} (\epsilon_{ij}^0 + \epsilon_{ij}^*) (\epsilon_{kl}^0 + \epsilon_{kl}^*) \, dV$$

$$\begin{aligned}
&= \frac{1}{2} \int_{V^*} \left\{ C_{ijkl} \epsilon_{ij}^0 \epsilon_{kl}^0 + 2C_{ijkl} \epsilon_{ij}^0 \epsilon_{kl}^* + C_{ijkl} \epsilon_{ij}^* \epsilon_{kl}^* \right\} dV \\
&= \mathcal{V}_{int}^0 + \int_{V^*} \left\{ C_{ijkl} \epsilon_{ij}^0 \epsilon_{kl}^* + \frac{1}{2} C_{ijkl} \epsilon_{ij}^* \epsilon_{kl}^* \right\} dV
\end{aligned} \tag{4.41}$$

where \mathcal{V}_{int}^0 , the initial strain energy, is a constant. The latter thus makes no contribution and may be omitted from now on. By splitting the incremental deformation ϵ_{ij}^* into its linear and quadratic terms:

$$\begin{aligned}
\epsilon_{ij}^* &= \frac{1}{2} \left(\frac{\partial u_i^*}{\partial x_j} + \frac{\partial u_j^*}{\partial x_i} + \frac{\partial u_m^*}{\partial x_i} \frac{\partial u_m^*}{\partial x_j} \right) \\
&= \epsilon_{ij}^{*(1)} + \epsilon_{ij}^{*(2)}
\end{aligned} \tag{4.42}$$

the strain energy takes the form:

$$\begin{aligned}
\mathcal{V}_{int} &= \int_{V^*} \left\{ \sigma_{ij}^0 \epsilon_{ij}^{*(1)} + \sigma_{ij}^0 \epsilon_{ij}^{*(2)} \right\} dV \\
&\quad + \int_{V^*} C_{ijkl} \left\{ \frac{1}{2} \epsilon_{ij}^{*(1)} \epsilon_{kl}^{*(1)} + \epsilon_{ij}^{*(1)} \epsilon_{kl}^{*(2)} + \frac{1}{2} \epsilon_{ij}^{*(2)} \epsilon_{kl}^{*(2)} \right\} dV
\end{aligned}$$

We consider only the terms up to the second-order in the derivatives of u_i^* , in order to obtain linear equations of motion. Hence, dropping all higher terms yields:

$$\begin{aligned}
\mathcal{V}_{int} &= \int_{V^*} \left\{ \sigma_{ij}^0 \epsilon_{ij}^{*(1)} + \sigma_{ij}^0 \epsilon_{ij}^{*(2)} \right\} dV + \int_{V^*} C_{ijkl} \left\{ \frac{1}{2} \epsilon_{ij}^{*(1)} \epsilon_{kl}^{*(1)} \right\} dV \\
&= \int_{V^*} \left\{ \sigma_{ij}^0 \epsilon_{ij}^{*(1)} + \sigma_{ij}^0 \epsilon_{ij}^{*(2)} \right\} dV + \mathcal{V}_{int}^*
\end{aligned} \tag{4.43}$$

where \mathcal{V}_{int}^* is the strain energy of the linear strain increments $\epsilon_{ij}^{*(1)}$.

The potential energy of external forces can be expressed as:

$$\begin{aligned}
\mathcal{V}_{ext} &= - \int_{V^*} \left(\bar{X}_i^0 + \bar{X}_i^* \right) u_i dV - \int_{S_\sigma} \left(\bar{t}_i^0 + \bar{t}_i^* \right) u_i dS \\
&= \mathcal{V}_{ext}^0 + \mathcal{V}_{ext}^*
\end{aligned} \tag{4.44}$$

where \mathcal{V}_{ext}^0 is the potential of external forces creating the initial stresses and \mathcal{V}_{ext}^* is the potential of the additional external forces. According to the origin of the initial stresses, one may distinguish between two cases:

- The *externally prestressed* structures in which initial stresses result from external dead loads. In that case, the equilibrium of the prestressed structure under the action of the external loads \bar{X}_i^0 and \bar{t}_i^0 allows the virtual work principle to be expressed as:

$$\int_{V^*} \sigma_{ij}^0 \delta \epsilon_{ij}^{*(1)} dV + \delta \mathcal{V}_{ext}^0 = 0 \tag{4.45}$$

- The *internally prestressed* structures, in which the initial stress results from internal forces to the system, such as residual stresses arising from the forming or assembly process. Because these stresses are self-equilibrated, the virtual work principle takes the form:

$$\int_{V^*} \sigma_{ij}^0 \delta \epsilon_{ij}^{*(1)} dV = 0 \quad (4.46)$$

with $\mathcal{V}_{ext}^0 = 0$.

Collecting all these terms yields:

$$\mathcal{T} - \mathcal{V} = \mathcal{T}^* - \left\{ \mathcal{V}_{int}^* + \int_{V^*} \left(\sigma_{ij}^0 \epsilon_{ij}^{*(1)} + \sigma_{ij}^0 \epsilon_{ij}^{*(2)} \right) dV + \mathcal{V}_{ext}^0 + \mathcal{V}_{ext}^* \right\}$$

Because of the static equilibrium of the prestressing forces (Equation (4.45) or (4.46)), by introducing the concept of geometric strain energy due to initial stress:

$$\mathcal{V}_g = \int_{V^*} \sigma_{ij}^0 \epsilon_{ij}^{*(2)} dV \quad (4.47)$$

we obtain the Hamilton principle for a prestressed structure:

$$\boxed{\begin{aligned} \delta u_i^* \int_{t_1}^{t_2} (\mathcal{T}^* - \mathcal{V}_{int}^* - \mathcal{V}_g - \mathcal{V}_{ext}^*) dt &= 0 \\ \delta u_i^*(t_1) &= \delta u_i^*(t_2) = 0 \end{aligned}} \quad (4.48)$$

with

$$\mathcal{T}^* = \frac{1}{2} \int_{V^*} \rho^* \dot{u}_i^* \dot{u}_i^* dV \dots \dots \dots \text{the additional kinetic energy}$$

$$\mathcal{V}_{int}^* = \int_{V^*} C_{ijkl} \left\{ \frac{1}{2} \epsilon_{ij}^{*(1)} \epsilon_{kl}^{*(1)} \right\} dV \dots \dots \dots \text{the strain energy of incremental linear strains}$$

$$\mathcal{V}_g = \int_{V^*} \sigma_{ij}^0 \epsilon_{ij}^{*(2)} dV \dots \dots \dots \text{the geometric strain energy due to prestress}$$

$$\mathcal{V}_{ext} = - \int_{V^*} \bar{X}_i^* u_i^* dV - \int_{S_\sigma} \bar{t}_i^* u_i^* dS \dots \dots \dots \text{the potential of additional external loads}$$

This result shows that the additional displacement field u_i^* of a prestressed structure is obtained by a linear analysis from the prestressed state to the deformed state, with the geometric strain energy due to initial stress as an additional term.

The theory of the prestressed case forms the basis of structural stability analysis: the latter consists in computing the prestressing forces applied to the structure which render possible the existence of an equilibrium configuration distinct from the prestressed state $u_i^* = 0$, in static equilibrium under the only geometrically linear and nonlinear elastic forces. Hamilton's principle can then be reduced to the form

$$\boxed{\delta u_i^* (\mathcal{V}_{int}^* + \mathcal{V}_g) = 0} \quad (4.49)$$

As shown by Equation (4.48), prestressing modifies the vibration eigenfrequencies, and the limit case of a vanishing eigenfrequency corresponds to the limit of stability ($\mathcal{T}^* = 0$).

Let us finally mention that in the study of prestressed structures, the additional terms u_i^* , ϵ_{ij}^* , and σ_{ij}^* will be denoted u_i , ϵ_{ij} and σ_{ij} for simplicity's sake. One has, however, to keep in mind that these quantities refer to the prestressed configuration.

Example 4.3

In order to illustrate the concept of a prestressed structure, let us consider again the example of the cable with the central mass (Figure 4.2), and consider now that an initial stress of intensity N_0 is applied. Since only transverse motion is considered, and the axial deformation measured from the reference state:

$$\epsilon_x = \frac{1}{2} \left(\frac{\partial v}{\partial x} \right)^2 \quad (\text{E4.3.a})$$

contains only the quadratic term, there is no additional linear strain energy. The geometric strain energy may thus be written:

$$\mathcal{V}_g = \int_0^\ell N_0 \frac{1}{2} \left(\frac{\partial v}{\partial x} \right)^2 dx \quad (\text{E4.3.b})$$

Hamilton's principle thus takes the form:

$$\int_{t_1}^{t_2} \left\{ M \dot{v}_M \delta \dot{v}_M - \int_0^\ell N_0 \frac{\partial v}{\partial x} \delta \left(\frac{\partial v}{\partial x} \right) dx \right\} dt = 0$$

or

$$\int_{t_1}^{t_2} \left\{ M \dot{v}_M \delta \dot{v}_M - \int_0^\ell N_0 \frac{2v_M}{\ell} \frac{2}{\ell} \delta v_M dx \right\} dt = 0$$

The equation governing the free motion of mass M follows as:

$$M \ddot{v}_M + N_0 \frac{4v_M}{\ell} = 0$$

The restoring force is in this case proportional to the transverse displacement v_M as is shown by the free body diagram of Figure 4.10:

$$F = 2T_0 \sin \alpha$$

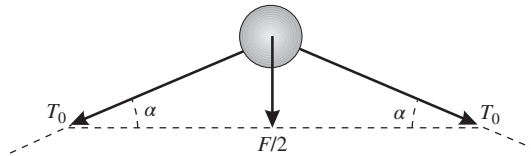


Figure 4.10 Cable with central mass particle: the prestressed case.

where the true force T_0 is computed from the Kirchhoff–Trefftz form N_0 as $T_0 = \frac{N_0}{\cos \alpha}$ so that:

$$F = 2N_0 \tan \alpha = N_0 \frac{4v_M}{\ell}$$

This shows that keeping only the terms quadratic in $\frac{\partial u_i}{\partial x_j}$ for the strain energy expression (4.43) is equivalent to neglecting the cable effect compared to the initial stress N_0 :

$$A\sigma_x \simeq A\sigma_x^0 = N_0$$

4.2 Free vibrations of linear continuous systems and response to external excitation

4.2.1 Eigenvalue problem

Let us consider the case of a linear system not subjected to any external force (Gérardin 1973). One may in this case assume harmonic motion:

$$u_i(x_j, t) = u_i(x_j) \cos \omega t \quad (4.50)$$

and the time interval $[t_1, t_2]$ may be chosen a priori in such a way that $\delta u_i(t_1) = \delta u_i(t_2) = 0$. For example,

$$[t_1, t_2] = \left[-\frac{\pi}{2\omega}, \frac{\pi}{2\omega} \right] \quad (4.51)$$

Owing to the linearity assumption, the kinetic energy (4.20) and the internal energy (4.22) are both quadratic in the displacements and may be reduced to the form:

$$\mathcal{T} = \mathcal{T}_{\max} \sin^2 \omega t \quad (4.52)$$

$$\mathcal{V} = \mathcal{V}_{\max} \cos^2 \omega t \quad (4.53)$$

with the kinetic energy and strain energy amplitudes:

$$\mathcal{T}_{\max} = \frac{1}{2} \omega^2 \int_{V_0} \rho_0 u_i u_i \, dV \quad (4.54)$$

$$\mathcal{V}_{\max} = \frac{1}{2} \int_{V_0} C_{ijkl} \epsilon_{ij} \epsilon_{kl} \, dV \quad (4.55)$$

The time integral of Hamilton's principle may be performed separately by taking account of:

$$\int_{-\frac{\pi}{2\omega}}^{\frac{\pi}{2\omega}} \cos^2 \omega t \, dt = \int_{-\frac{\pi}{2\omega}}^{\frac{\pi}{2\omega}} \sin^2 \omega t \, dt = \frac{\pi}{2\omega} \quad (4.56)$$

which makes it possible to rewrite (4.19) in the form of a variational problem operating only on the spatial variables:

$$\delta \mathcal{L}_g[u] = \delta \left[\frac{\omega^2}{2} \int_{V_0} \rho_0 u_i u_i \, dV - \frac{1}{2} \int_{V_0} C_{ijkl} \epsilon_{ij} \epsilon_{kl} \, dV \right] = 0 \quad (4.57)$$

Let us now define the following matrix quantities:

- the vectors \mathbf{u} , $\boldsymbol{\sigma}$ and $\boldsymbol{\varepsilon}$ collecting the displacement, stress and strain components:²

$$\mathbf{u} = [u_1 \ u_2 \ u_3]^T \quad (4.58)$$

$$\boldsymbol{\sigma} = [\sigma_{11} \ \sigma_{22} \ \sigma_{33} \ \sigma_{12} \ \sigma_{23} \ \sigma_{13}]^T \quad (4.59)$$

$$\boldsymbol{\varepsilon} = [\varepsilon_{11} \ \varepsilon_{22} \ \varepsilon_{33} \ \gamma_{12} \ \gamma_{23} \ \gamma_{13}]^T \quad (4.60)$$

with $\gamma_{ij} = 2\varepsilon_{ij}$,

- the spatial differentiation operator:

$$\mathbf{D}^T = \begin{bmatrix} \frac{\partial}{\partial x_1} & 0 & 0 & \frac{\partial}{\partial x_2} & 0 & \frac{\partial}{\partial x_3} \\ 0 & \frac{\partial}{\partial x_2} & 0 & \frac{\partial}{\partial x_1} & \frac{\partial}{\partial x_3} & 0 \\ 0 & 0 & \frac{\partial}{\partial x_3} & 0 & \frac{\partial}{\partial x_2} & \frac{\partial}{\partial x_1} \end{bmatrix} \quad (4.61)$$

- the associated matrix of the direction cosines of the outward normal:

$$\mathbf{N}^T = \begin{bmatrix} n_1 & 0 & 0 & n_2 & 0 & n_3 \\ 0 & n_2 & 0 & n_1 & n_3 & 0 \\ 0 & 0 & n_3 & 0 & n_2 & n_1 \end{bmatrix} \quad (4.62)$$

and the matrix of Hooke's law elastic coefficients \mathbf{H} such as:

$$\boldsymbol{\sigma} = \mathbf{H}\boldsymbol{\varepsilon} \quad (4.63)$$

The equations expressing local linear dynamic equilibrium may then be written in the matrix form:

$$\begin{cases} \mathbf{D}^T \boldsymbol{\sigma} + \omega^2 \rho_0 \mathbf{u} = \mathbf{0} & \text{in } V \\ \mathbf{N}^T \boldsymbol{\sigma} = \mathbf{0} & \text{on } S_\sigma \end{cases} \quad (4.64)$$

Similarly, the corresponding variational form can be expressed by:

$$\delta \left\{ \omega^2 \int_{V_0} \frac{1}{2} \rho_0 \mathbf{u}^T \mathbf{u} \, dV - \int_{V_0} \frac{1}{2} (\mathbf{D}\mathbf{u})^T \mathbf{H} (\mathbf{D}\mathbf{u}) \, dV \right\} = 0 \quad (4.65)$$

The homogeneous system of equations (4.64) and the associated variational form (4.65) define an eigenvalue problem of the *Sturm–Liouville* type. Its eigenvalues, in infinite number, are denoted:

$$\begin{cases} \mathbf{u}_{(1)}, \mathbf{u}_{(2)}, \mathbf{u}_{(3)}, \dots \\ 0 \leq \omega_1^2 \leq \omega_2^2 \leq \omega_3^2 \leq \dots \end{cases} \quad (4.66)$$

They verify individually the equations:

$$\begin{cases} \mathbf{D}^T \mathbf{H} \mathbf{D} \mathbf{u}_{(i)} + \omega_i^2 \rho_0 \mathbf{u}_{(i)} = \mathbf{0} & \text{in } V \\ \mathbf{N}^T \mathbf{H} \mathbf{D} \mathbf{u}_{(i)} = \mathbf{0} & \text{on } S_\sigma \end{cases} \quad i = 1, \dots, \infty \quad (4.67)$$

² Note that $\boldsymbol{\varepsilon}$ and $\boldsymbol{\sigma}$ as defined here are not the classical tensor forms. Because the stress and strain tensors are symmetric, we choose to represent their components in a vector form to simplify the presentation.

4.2.2 Orthogonality of eigensolutions

In order to prove the orthogonality properties of the eigensolutions, let us start from the equilibrium equations in the volume verified by eigenmode $\mathbf{u}_{(i)}$ and follow a reasoning similar to the proof of orthogonality for modes of discrete systems (Section 2.3.1). We multiply them by $\mathbf{u}_{(j)}$ and integrate over the volume to get:

$$\int_{V_0} \mathbf{u}_{(j)}^T \mathbf{D}^T \mathbf{H} \mathbf{D} \mathbf{u}_{(i)} dV + \int_{V_0} \omega_i^2 \rho_0 \mathbf{u}_{(j)}^T \mathbf{u}_{(i)} dV = 0 \quad (4.68)$$

The first term may be integrated by parts:

$$\int_{V_0} \mathbf{u}_{(j)}^T \mathbf{D}^T \mathbf{H} \mathbf{D} \mathbf{u}_{(i)} dV = \int_S \mathbf{u}_{(j)}^T \mathbf{N}^T \mathbf{H} \mathbf{D} \mathbf{u}_{(i)} dS - \int_{V_0} (\mathbf{D} \mathbf{u}_{(j)})^T \mathbf{H} (\mathbf{D} \mathbf{u}_{(i)}) dV \quad (4.69)$$

Owing to the compatibility of the displacement field and the surface equilibrium condition for eigenmode $\mathbf{u}_{(i)}$, which take the form:

$$\begin{aligned} \mathbf{u}_{(i)} &= \mathbf{0} && \text{on } S_u \\ \mathbf{N}^T \mathbf{H} \mathbf{D} \mathbf{u}_{(i)} &= \mathbf{0} && \text{on } S_\sigma \end{aligned}$$

Equation (4.68) reduces to:

$$\int_{V_0} \left[-(\mathbf{D} \mathbf{u}_{(j)})^T \mathbf{H} (\mathbf{D} \mathbf{u}_{(i)}) + \omega_i^2 \rho_0 \mathbf{u}_{(j)}^T \mathbf{u}_{(i)} \right] dV = 0 \quad (4.70)$$

By treating the equilibrium equation of eigenmode $\mathbf{u}_{(j)}$ in the same way and premultiplying it by eigenmode $\mathbf{u}_{(i)}$ we obtain:

$$\int_{V_0} \left[-(\mathbf{D} \mathbf{u}_{(i)})^T \mathbf{H} (\mathbf{D} \mathbf{u}_{(j)}) + \omega_j^2 \rho_0 \mathbf{u}_{(i)}^T \mathbf{u}_{(j)} \right] dV = 0 \quad (4.71)$$

Subtracting then (4.70) from (4.71) we get the result:

$$(\omega_j^2 - \omega_i^2) \int_{V_0} \rho_0 \mathbf{u}_{(j)}^T \mathbf{u}_{(i)} dV = 0$$

and if $\omega_i^2 \neq \omega_j^2$, supposing that the modal masses are normalized,

$$\boxed{\begin{aligned} \int_{V_0} \rho_0 \mathbf{u}_{(j)}^T \mathbf{u}_{(i)} dV &= \delta_{ij} \\ \int_{V_0} (\mathbf{D} \mathbf{u}_{(j)})^T \mathbf{H} (\mathbf{D} \mathbf{u}_{(i)}) dV &= \delta_{ij} \omega_i^2 \end{aligned}} \quad (4.72)$$

It can also be shown that the eigenmodes associated with a multiple eigenfrequency are linearly independent and thus that they can be chosen to be orthogonal. The orthonormality relationships (4.72) are thus valid in general.

4.2.3 Response to external excitation: mode superposition (homogeneous spatial boundary conditions)

As mentioned in the introduction, expressing the response to external excitation follows very much the same principles as in the discrete case. The set of eigenmodes provides a complete and orthogonal basis in terms of which the system response can be expanded. There are however two major differences: on the one hand, the eigenmodes are in infinite number, so that the computed response is always an approximation. If an exact static solution exists, it can be used to guarantee that the solution is exact at least in the static case, which can be guaranteed using the modal acceleration method. On the other hand, in many cases the excitation onto the system takes place through the boundary rather than inside the volume. The eigenmodes being computed with homogeneous boundary conditions, a particular solution (obtained under static conditions) has to be added to the expansion in order to transfer to the volume the excitation from the boundary.

For simplicity's sake, we will first consider the case where the excitation takes place inside the volume, and then, in Section 4.2.4, consider the more complex case of excitation through the boundary.

As is true for discrete systems (refer to Section 2.7), advantage can be taken of the eigenmode orthogonality property to reduce the equations of motion into a system of uncoupled normal equations. Indeed, since the eigenmodes form a complete set which allows expansion of the solution of problems with homogeneous boundary conditions, any displacement field of the continuous structure may be expressed in the form:

$$u(x_j, t) = \sum_{s=1}^{\infty} u_{(s)}(x_j) \eta_s(t) \quad (4.73)$$

where $\eta_s(t)$ are the normal coordinates associated with eigenmodes $u_{(s)}$. Owing to the boundary conditions verified by the eigenmodes, this general solution verifies the boundary conditions in space:

$$\begin{aligned} N^T H D u &= \bar{t} = 0 \quad \text{on } S_\sigma \\ u &= \bar{u} = 0 \quad \text{on } S_u \end{aligned} \quad (4.74)$$

with the matrix of external forces on the surface $\bar{t} = [\bar{t}_1 \ \bar{t}_2 \ \bar{t}_3]^T$. In matrix notation, the linear equilibrium equations take the form:

$$D^T H D u + \bar{X} - \rho \ddot{u} = 0 \quad \text{in } V \quad (4.75)$$

with the matrix of external forces in the volume $\bar{X} = [\bar{X}_1 \ \bar{X}_2 \ \bar{X}_3]^T$. Substitution in these equations of the expansion (4.73) yields:

$$\sum_{s=1}^{\infty} \eta_s D^T H D u_{(s)} + \bar{X} - \sum_{s=1}^{\infty} \rho \ddot{\eta}_s u_{(s)} = 0 \quad \text{in } V$$

After premultiplying the volume equilibrium equations by eigenmode $u_{(r)}^T$, integrating them over the volume V , and space-integrating by parts, one finds:

$$\begin{aligned} \sum_{s=1}^{\infty} \eta_s \int_S u_{(r)}^T N^T H D u_{(s)} dS - \sum_{s=1}^{\infty} \eta_s \int_V (D u_{(r)})^T H D u_{(s)} dV \\ + \int_V u_{(r)}^T \bar{X} dV - \sum_{s=1}^{\infty} \ddot{\eta}_s \int_V \rho u_{(r)}^T u_{(s)} dV = 0 \end{aligned}$$

Supposing that the modal masses are normalized, the use of the orthogonality relationships and of the boundary conditions (4.74) yields:

$$\omega_r^2 \eta_r + \ddot{\eta}_r = \phi_r \quad r = 1, \dots, \infty \quad (4.76)$$

where the ϕ_r are the participation factors of eigenmodes $\mathbf{u}_{(r)}$ to the excitation:

$$\phi_r = \int_V \mathbf{u}_{(r)}^T \bar{\mathbf{X}} \, dV \quad (4.77)$$

The relationships (4.76) are the *normal equations* and their solution can be written as (see Section 2.7.2, Equation (2.113)):

$$\eta_r(t) = \eta_r(0) \cos \omega_r t + \dot{\eta}_r(0) \frac{\sin \omega_r t}{\omega_r} + \frac{1}{\omega_r} \int_0^t \phi_r(\tau) \sin(\omega_r(t - \tau)) \, d\tau \quad (4.78)$$

with the initial conditions obtained from modal expansion of $\mathbf{u}(0)$ and $\dot{\mathbf{u}}(0)$ and using orthogonality:

$$\eta_r(0) = \int_V \rho \mathbf{u}_{(r)}^T \mathbf{u}(0) \, dV \quad \dot{\eta}_r(0) = \int_V \rho \mathbf{u}_{(r)}^T \dot{\mathbf{u}}(0) \, dV$$

Hence the general solution by mode superposition:

$$\begin{aligned} \mathbf{u}(x_j, t) = & \sum_{s=1}^{\infty} \mathbf{u}_{(s)} \cos \omega_s t \int_V \rho \mathbf{u}_{(s)}^T \mathbf{u}(0) \, dV + \sum_{s=1}^{\infty} \mathbf{u}_{(s)} \frac{\sin \omega_s t}{\omega_s} \int_V \rho \mathbf{u}_{(s)}^T \dot{\mathbf{u}}(0) \, dV \\ & + \sum_{s=1}^{\infty} \frac{\mathbf{u}_{(s)}}{\omega_s} \int_0^t \phi_s(\tau) \sin(\omega_s(t - \tau)) \, d\tau \end{aligned} \quad (4.79)$$

The mode displacement approximation corresponds to limiting the modal expansion (4.79) to k eigensolutions.

Static solution as a limit case

It is worthwhile considering the static problem associated to (4.75):

$$\mathbf{D}^T \mathbf{H} \mathbf{D} \mathbf{u}_{st} + \bar{\mathbf{X}} = \mathbf{0} \quad \text{in } V \quad (4.80)$$

with the boundary conditions (4.74). A useful form of the static response can be obtained from (4.79) by expressing it at $t = 0$ and observing that, the problem being stationary, $\mathbf{u}_{st} = \mathbf{u}(0)$. We thus get immediately the spectral identity:

$$\mathbf{u}_{st} = \sum_{s=1}^{\infty} \mathbf{u}_{(s)} \int_V \rho \mathbf{u}_{(s)}^T \mathbf{u}_{st} \, dV \quad (4.81)$$

A second form of spectral expansion of the static response can be obtained by developing it in series of eigenmodes:

$$\mathbf{u}_{st} = \sum_{s=1}^{\infty} \alpha_s \mathbf{u}_{(s)} \quad (4.82)$$

Substituting (4.82) into (4.80), multiplying by another mode $\mathbf{u}_{(s)}$, integrating over the volume and invoking orthogonality yields:

$$\mathbf{u}_{st} = \sum_{s=1}^{\infty} \frac{\mathbf{u}_{(s)}}{\omega_s^2} \int_V \mathbf{u}_{(s)}^T \bar{\mathbf{X}} dV \quad (4.83)$$

It is worthwhile noticing that Equation (4.83) generalizes to the continuous case the concept of flexibility introduced in (2.62) for discrete systems.

Mode acceleration method

The modal expansion being necessarily truncated for a continuous system, it always implies the notions of quasi-static and spectral convergence as presented for discrete systems (method of mode displacements, Section 2.8.1).

Likewise, the method of mode accelerations established in Section 2.8.2 for discrete systems can be extended to continuous systems. It could be done as before based the reasoning that the development of the inertia term is limited to the first k terms, but it can also be developed more directly in the following way.

Let us rewrite the solution (4.79) at a given time t by adding to it the identity (4.82) verified by the quasi-static³ solution $\mathbf{u}_{qs}(t)$. Limiting the modal expansion to the first k modes, it yields the following approximation:

$$\begin{aligned} \mathbf{u}^k(x_j, t) = & \sum_{s=1}^k \mathbf{u}_{(s)} \cos \omega_s t \int_V \rho \mathbf{u}_{(s)}^T \mathbf{u}(0) dV + \sum_{s=1}^k \mathbf{u}_{(s)} \frac{\sin \omega_s t}{\omega_s} \int_V \rho \mathbf{u}_{(s)}^T \dot{\mathbf{u}}(0) dV \\ & + \sum_{s=1}^k \frac{\mathbf{u}_{(s)}}{\omega_s} \int_0^t \phi_s(\tau) \sin(\omega_s(t - \tau)) d\tau + \mathbf{u}_{qs} - \sum_{s=1}^k \mathbf{u}_{(s)} \int_V \rho \mathbf{u}_{(s)}^T \mathbf{u}_{qs} dV \end{aligned} \quad (4.84)$$

Expressing (4.84) at $t = 0$ and recalling that $\mathbf{u}_{st} = \mathbf{u}(0)$ yields:

$$\begin{aligned} \mathbf{u}^k(x_j, 0) = & \sum_{s=1}^k \mathbf{u}_{(s)} \int_V \rho \mathbf{u}_{(s)}^T \mathbf{u}(0) dV + \mathbf{u}_{qs} - \sum_{s=1}^k \mathbf{u}_{(s)} \int_V \rho \mathbf{u}_{(s)}^T \mathbf{u}_{qs} dV \\ = & \mathbf{u}_{qs}(0) = \mathbf{u}_{st} \end{aligned} \quad (4.85)$$

which shows that *the approximation (4.84) obtained by adding the static solution deflated from the k eigenmodes already present in the expansion of the dynamic part of the solution is statically exact.*

³ We call a solution *quasi-static* if it corresponds to the response to a time-varying excitation obtained when disregarding the inertia forces. A quasi-static solution thus satisfies the expansion (4.83) at every time t .

4.2.4 Response to external excitation: mode superposition (nonhomogeneous spatial boundary conditions)

In order to separate the response to the spatial boundary conditions from the response to the body loads, let us invoke the superposition principle to express the complete solution in the form:

$$\mathbf{u}(x_j, t) = \mathbf{v}(x_j, t) + \mathbf{w}(x_j, t) \quad (4.86)$$

where $\mathbf{v}(x_j, t)$ is the response of the system to body loads and also includes the free response to initial conditions, while $\mathbf{w}(x_j, t)$ is the response to the nonhomogeneous boundary conditions on $S = S_\sigma \cup S_u$. \mathbf{v} and \mathbf{w} are thus the solutions of *Problem 1* and *Problem 2* as defined in Table 4.1.

The solution to *Problem 1* has already been obtained previously and is given by Equation (4.79) with \mathbf{v} instead of \mathbf{u} .

Let us then apply modal superposition to express the response to *Problem 2* in the form:

$$\mathbf{w}(x_j, t) = \mathbf{u}_{qs_{nh}}(x_j, t) + \sum_{s=1}^{\infty} \eta_s(t) \mathbf{u}_{(s)}(x_j) \quad (4.87)$$

where $\mathbf{u}_{qs_{nh}}$ is the quasi-static response solution of *Problem 3* in which inertia loads are absent. Thanks to the presence of the quasi-static solution in (4.87), this solution satisfies the nonhomogeneous boundary conditions of *Problem 2* on $S = S_\sigma \cup S_u$, the eigenmodes satisfying only homogeneous boundary conditions.

The initial conditions for $\mathbf{w}(t)$ then write:

$$\begin{aligned} \mathbf{w}(0) &= \mathbf{u}_{qs_{nh}}(0) + \sum_{s=1}^{\infty} \eta_s(0) \mathbf{u}_{(s)} = 0 \\ \dot{\mathbf{w}}(0) &= \dot{\mathbf{u}}_{qs_{nh}}(0) + \sum_{s=1}^{\infty} \dot{\eta}_s(0) \mathbf{u}_{(s)} = 0 \end{aligned} \quad (4.88)$$

where the initial displacements $\mathbf{u}_{qs_{nh}}(0)$ and velocities $\dot{\mathbf{u}}_{qs_{nh}}(0)$ associated to the quasi-static solution is obtained from solving *Problem 3* and its time derivative, driven by the surface loadings $\bar{\mathbf{t}}$ and $\bar{\mathbf{u}}$ and their derivatives at $t = 0$. Using the orthogonality relation of the modes (assuming as before that they are mass-normalized), one finds:

$$\begin{aligned} \eta_s(0) &= - \int_V \rho \mathbf{u}_{(s)}^T \mathbf{u}_{qs_{nh}}(0) dV \\ \dot{\eta}_s(0) &= - \int_V \rho \mathbf{u}_{(s)}^T \dot{\mathbf{u}}_{qs_{nh}}(0) dV \end{aligned} \quad (4.89)$$

Table 4.1 Splitting of the response of a system to nonhomogeneous spatial boundary conditions

	<i>Problem 1</i>	<i>Problem 2</i>	<i>Problem 3</i>
in V	$\mathbf{D}^T \mathbf{H} \mathbf{D} \mathbf{v} - \rho \ddot{\mathbf{v}} + \bar{\mathbf{X}} = \mathbf{0}$	$\mathbf{D}^T \mathbf{H} \mathbf{D} \mathbf{w} - \rho \ddot{\mathbf{w}} = \mathbf{0}$	$\mathbf{D}^T \mathbf{H} \mathbf{D} \mathbf{u}_{qs_{nh}} = \mathbf{0}$
on S_σ	$\mathbf{N}^T \mathbf{H} \mathbf{D} \mathbf{v} = \mathbf{0}$	$\mathbf{N}^T \mathbf{H} \mathbf{D} \mathbf{w} = \bar{\mathbf{t}}$	$\mathbf{N}^T \mathbf{H} \mathbf{D} \mathbf{u}_{qs_{nh}} = \bar{\mathbf{t}}$
on S_u	$\mathbf{v} = \mathbf{0}$	$\mathbf{w} = \bar{\mathbf{u}}$	$\mathbf{u}_{qs_{nh}} = \bar{\mathbf{u}}$
at $t = 0$	$\mathbf{v} = \mathbf{v}(0), \quad \dot{\mathbf{v}} = \dot{\mathbf{v}}(0)$	$\mathbf{w} = \mathbf{0}, \quad \dot{\mathbf{w}} = \mathbf{0}$	

Let us then substitute (4.87) in the volume equilibrium of *Problem 2*, premultiply by $\mathbf{u}_{(r)}^T$, and integrate by parts over domain V . Making use of the orthogonality relationships and of the boundary conditions verified by the eigenmodes, the governing equations for the normal coordinates are obtained:

$$\omega_r^2 \eta_r + \ddot{\eta}_r = - \int_V \rho \mathbf{u}_{(r)}^T \ddot{\mathbf{u}}_{qsh} dV \quad r = 1, \dots, \infty \quad (4.90)$$

They admit the solution (see (2.113)):

$$\eta_r(t) = \eta_r(0) \cos \omega_r t + \dot{\eta}_r(0) \frac{\sin \omega_r t}{\omega_r} - \frac{1}{\omega_r} \int_0^t \int_V \rho \mathbf{u}_{(r)}^T \ddot{\mathbf{u}}_{qsh}(\tau) dV \sin(\omega_r(t - \tau)) d\tau \quad (4.91)$$

So the solution to *Problem 2* is computed by substituting (4.91) in (4.87):

$$\begin{aligned} \mathbf{w}(x_j, t) = & \mathbf{u}_{qsh}(x_j, t) + \sum_{s=1}^{\infty} \mathbf{u}_{(s)} \left(\eta_s(0) \cos \omega_s t + \dot{\eta}_s(0) \frac{\sin \omega_s t}{\omega_s} \right) \\ & - \sum_{s=1}^{\infty} \frac{\mathbf{u}_{(s)}}{\omega_s} \int_0^t \int_V \rho \mathbf{u}_{(s)}^T \ddot{\mathbf{u}}_{qsh}(\tau) \sin(\omega_s(t - \tau)) dV d\tau \end{aligned} \quad (4.92)$$

Taking further into account (4.89), one obtains:

$$\begin{aligned} \mathbf{w}(x_j, t) = & \mathbf{u}_{qsh}(x_j, t) \\ & - \mathbf{u}_{(s)} \sum_{s=1}^{\infty} \left(\int_V \rho \mathbf{u}_{(s)}^T \mathbf{u}_{qsh}(0) dV \cos \omega_s t + \int_V \rho \mathbf{u}_{(s)}^T \dot{\mathbf{u}}_{qsh}(0) dV \frac{\sin \omega_s t}{\omega_s} \right) \\ & - \sum_{s=1}^{\infty} \frac{\mathbf{u}_{(s)}}{\omega_s} \int_0^t \int_V \rho \mathbf{u}_{(s)}^T \ddot{\mathbf{u}}_{qsh}(\tau) \sin(\omega_s(t - \tau)) dV d\tau \end{aligned} \quad (4.93)$$

Let us now perform a double integration by parts of the time integral of the last term in the right-hand side. Both terms depending on the initial conditions cancel, so that we get the solution to *Problem 2* in the form:

$$\begin{aligned} \mathbf{w}(x_j, t) = & \mathbf{u}_{qsh}(x_j, t) - \sum_{s=1}^{\infty} \mathbf{u}_{(s)} \int_V \rho \mathbf{u}_{(s)}^T \mathbf{u}_{qsh} dV \\ & + \sum_{s=1}^{\infty} \omega_s \mathbf{u}_{(s)} \int_0^t \int_V \rho \mathbf{u}_{(s)}^T \mathbf{u}_{qsh}(\tau) dV \sin(\omega_s(t - \tau)) d\tau \end{aligned} \quad (4.94)$$

which no longer implies the velocities and accelerations of the quasi-static field.

One could think that the first two terms on the right-hand side of (4.94) cancel out according to the spectral expansion of the quasi-static solution. Nevertheless since the eigenmodes $\mathbf{u}_{(s)}$ fulfill, by definition, homogeneous boundary conditions on S_u and S_σ it is not possible to write \mathbf{u}_{qsh} as a superposition of modes. So we introduce the function $\delta(S)$:

$$\delta(S) = \mathbf{u}_{qsh} - \sum_{s=1}^{\infty} \mathbf{u}_{(s)} \int_V \rho \mathbf{u}_{(s)}^T \mathbf{u}_{qsh} dV \quad (4.95)$$

allowing us to keep in mind the kinematic or equilibrium incompatibility between the quasi-static solution and its modal expansion on S . With this definition Equation (4.94) becomes:

$$\mathbf{w}(x_j, t) = \delta(S) + \sum_{s=1}^{\infty} \omega_s \mathbf{u}_{(s)} \int_0^t \int_V \rho \mathbf{u}_{(s)}^T \mathbf{u}_{qs_{nh}}(\tau) dV \sin(\omega_s(t - \tau)) d\tau \quad (4.96)$$

Finally, it is possible to transform the volume integral of the right-hand-side of Equations (4.94) or (4.96) into surface integrals involving the known boundary conditions. Let us multiply the equilibrium equation of *Problem 3* by the eigenmode $\mathbf{u}_{(s)}^T$, the equilibrium equation (4.67) for eigenmode s by $\mathbf{u}_{qs_{nh}}^T$, take the difference and integrate over the volume. We get the identity:

$$\int_V \mathbf{u}_{qs_{nh}}^T \mathbf{D}^T \mathbf{H} \mathbf{D} \mathbf{u}_{(s)} dV - \int_V \mathbf{u}_{(s)}^T \mathbf{D}^T \mathbf{H} \mathbf{D} \mathbf{u}_{qs_{nh}} dV + \omega_s^2 \int_V \rho \mathbf{u}_{qs_{nh}}^T \mathbf{u}_{(s)} dV = 0 \quad (4.97)$$

Integrating Equation (4.97) by parts over the volume yields:

$$\omega_s^2 \int_V \rho \mathbf{u}_{qs_{nh}}^T \mathbf{u}_{(s)} dV = \int_{S_\sigma} \mathbf{u}_{(s)}^T \bar{\mathbf{t}} dS + \int_{S_u} \mathbf{u}_{qs_{nh}}^T \mathbf{r}_{(s)} dS \quad (4.98)$$

with the definition of the modal reactions on S_u :

$$\mathbf{r}_{(s)} = -\mathbf{N}^T \mathbf{H} \mathbf{D} \mathbf{u}_{(s)} \quad (4.99)$$

The solution of *Problem 2* takes thus the final form:

$$\mathbf{w}(x_j, t) = \delta(S) + \sum_{s=1}^{\infty} \frac{\mathbf{u}_{(s)}}{\omega_s} \int_0^t \psi_s(\tau) \sin(\omega_s(t - \tau)) d\tau \quad (4.100)$$

where the modal participation factor to the loading can take two different forms:

$$\psi_s(t) = \omega_s^2 \int_V \rho \mathbf{u}_{qs_{nh}}^T \mathbf{u}_{(s)} dV \quad (4.101a)$$

$$= \int_{S_\sigma} \mathbf{u}_{(s)}^T \bar{\mathbf{t}}(t) dS + \int_{S_u} \bar{\mathbf{u}}(t)^T \mathbf{r}_{(s)} dS \quad (4.101b)$$

Using the form (4.101a) implies the availability of the quasi-static solution $\mathbf{u}_{qs_{nh}}$. In the form (4.101b), it represents the work produced by the boundary tractions $\bar{\mathbf{t}}$ along the eigenmode displacement $\mathbf{u}_{(s)}$ on S_u and the work produced by the eigenmode boundary reaction $\mathbf{r}_{(s)}$ along the imposed displacement $\bar{\mathbf{u}}$ on S_σ .

The solution to the general problem with nonhomogeneous boundary conditions and including also body loads is finally obtained by summing up the results (4.79) and (4.100):

$$\begin{aligned} \mathbf{u}(x_j, t) = & \sum_{s=1}^{\infty} \mathbf{u}_{(s)} \cos \omega_s t \int_V \rho \mathbf{u}_{(s)}^T \mathbf{u}(0) dV + \sum_{s=1}^{\infty} \mathbf{u}_{(s)} \frac{\sin \omega_s t}{\omega_s} \int_V \rho \mathbf{u}_{(s)}^T \dot{\mathbf{u}}(0) dV \\ & + \sum_{s=1}^{\infty} \frac{\mathbf{u}_{(s)}}{\omega_s} \int_0^t (\phi_s(\tau) + \psi_s(\tau)) \sin(\omega_s(t - \tau)) d\tau + \delta(S) \end{aligned} \quad (4.102)$$

expression in which $\phi_s(t)$ and $\psi_s(t)$ represent respectively the volume and surface loading distributions and $\delta(S)$, the singularity of the spectral expansion of $\mathbf{u}_{qs_{nh}}$ on the boundary.

The singular term $\delta(S)$ results from the fact that the surface tractions (including the boundary reactions on S_u) are assimilated to body forces of infinitely large amplitude but distributed on a zero thickness layer at the boundary of domain V .

The *mode displacement approximation*, which is obtained by limiting the expansion (4.102) to k eigensolutions and neglecting the contribution $\delta(S)$, is characterized by a slow convergence of the response to the exact solution. Indeed, taking into account only the eigenmodes in the solution expansion implies including the infinity of terms in the series to verify, at the limit, the nonhomogeneous kinematic or equilibrium conditions on the boundary.⁴

Static response as a limit case

Again, an expression of the static response can be obtained by expressing (4.102) at $t = 0$. We get:

$$\mathbf{u}_{st} = \sum_{s=1}^{\infty} \mathbf{u}_{(s)} \int_V \rho \mathbf{u}_{(s)}^T \mathbf{u}(0) dV + \delta(S) \quad (4.103)$$

with

$$\mathbf{u}(0) = \mathbf{u}_{st_h} + \mathbf{u}_{st_{nh}} \quad (4.104)$$

where \mathbf{u}_{st_h} designates the part of the static response due to body loads and homogeneous spatial boundary conditions, and $\mathbf{u}_{st_{nh}}$ the part due solely to the nonhomogeneous boundary conditions. Recalling the definition (4.95) of $\delta(S)$ and substituting also the spectral expansion (4.82), Equation (4.103) provides the expected result:

$$\begin{aligned} \mathbf{u}_{st} &= \sum_{s=1}^{\infty} \mathbf{u}_{(s)} \int_V \rho \mathbf{u}_{(s)}^T \mathbf{u}_{st_h} dV + \mathbf{u}_{st_{nh}} \\ &= \mathbf{u}_{st_h} + \mathbf{u}_{st_{nh}} = \mathbf{u}(0) \end{aligned} \quad (4.105)$$

It is worthwhile noticing from the result (4.105) that keeping the $\delta(S)$ term automatically guarantees the correctness of the static solution, even in case of truncation of the modal expansion of the solution.

Mode acceleration method

When the modal expansion is truncated, the $\delta(S)$ function which was representing the singularity of the solution on the boundary now becomes:

$$\delta(S) \simeq \mathbf{u}_{qs_{nh}} - \sum_{s=1}^k \mathbf{u}_{(s)} \int_V \rho \mathbf{u}_{(s)}^T \mathbf{u}_{qs_{nh}} dV \quad (4.106)$$

⁴ When the nonhomogeneity of the boundary conditions is only on S_σ , thus of equilibrium type, the effect of the discontinuity is less apparent since the displacement response would not be affected. The discontinuity appears when computing the stresses, their convergence being linked to the spatial derivatives of $\delta(S)$. This slow convergence of the solution expansion in computing the stresses when neglecting the $\delta(S)$ term will be illustrated in an example in Section 4.3.1.

The second term expresses the part of the spectral expansion already included in the dynamic part of the solution.

On the other hand, it has been shown that the correction to be added in the homogeneous case is (Equation (4.84)):

$$\mathbf{u}_{qs_h} - \sum_{s=1}^k \mathbf{u}_{(s)} \int_V \rho \mathbf{u}_{(s)}^T \mathbf{u}_{qs_h} dV \quad (4.107)$$

In all generality, the solution generated by the mode acceleration method in presence of body loads and with nonhomogeneous boundary conditions can thus be expressed in the form

$$\begin{aligned} \mathbf{u}(x_j, t) = & \sum_{s=1}^k \mathbf{u}_{(s)} \int_V \rho \mathbf{u}_{(s)}^T \left(\mathbf{u}(0) \cos \omega_s t + \dot{\mathbf{u}}(0) \frac{\sin \omega_s t}{\omega_s} \right) dV \\ & + \sum_{s=1}^k \frac{\mathbf{u}_{(s)}}{\omega_s} \int_0^t (\phi_s(\tau) + \psi_s(\tau)) \sin(\omega_s(t - \tau)) d\tau \\ & + \mathbf{u}_{qs} - \sum_{s=1}^k \mathbf{u}_{(s)} \int_V \rho \mathbf{u}_{(s)}^T \mathbf{u}_{qs} dV \end{aligned} \quad (4.108)$$

where the last two terms represent the static correction compensating for the missing modes in the modal expansion, calling $\mathbf{u}_{qs} = \mathbf{u}_{qs_h} + \mathbf{u}_{qs_{nh}}$ the total quasi-static solution.

4.2.5 Reciprocity principle for harmonic motion

The well-known *reciprocity principle*, also known as Betti-Maxwell reciprocity principle, can be extended to elastodynamics. In the context of harmonic motion, it can be established either for applied harmonic loads or imposed harmonic displacements, but in what follows we will address only the latter case.⁵

Let us consider the Dirichlet problem in harmonic regime:

$$\begin{cases} \mathbf{D}^T \mathbf{H} \mathbf{D} \mathbf{u} + \omega^2 \rho_0 \mathbf{u} = \mathbf{0} & \text{in } V \\ \mathbf{u} = \bar{\mathbf{u}} & \text{on } S_u \end{cases} \quad (4.109)$$

where \mathbf{u} is the amplitude of harmonic motion resulting from imposed harmonic displacement of amplitude $\bar{\mathbf{u}}$ on S_u .

Let us also define the virtual quasi-static problem with arbitrary boundary conditions $\bar{\mathbf{v}}$ that can be associated to it:

$$\begin{cases} \mathbf{D}^T \mathbf{H} \mathbf{D} \mathbf{v} = \mathbf{0} & \text{in } V \\ \mathbf{v} = \bar{\mathbf{v}} & \text{on } S_u \end{cases} \quad (4.110)$$

⁵ Formulating the reciprocity principle for the case of imposed harmonic loads on S_σ is equally easy as long as the continuum cannot undergo rigid body motion. The extension to a free-free continuum is possible but requires more complex handling since it implies the definition of self-equilibrated loads to get a solution to the associated quasi-static problem. Such concepts will be discussed only later in Chapter 6.

A reciprocity relationship can then be constructed between the solutions of Problems (4.109) and (4.110) in the following way.

Let us premultiply Equation (4.109) by \mathbf{v}^T , Equation (4.110) by \mathbf{u}^T and integrate the sum of these relations over the volume. We get:

$$\int_{V_0} (\mathbf{v}^T \mathbf{D}^T \mathbf{H} \mathbf{D} \mathbf{u} - \mathbf{u}^T \mathbf{D}^T \mathbf{H} \mathbf{D} \mathbf{v}) dV + \omega^2 \int_{V_0} \rho_0 \mathbf{v}^T \mathbf{u} dV = 0 \quad (4.111)$$

Integration by parts of the volume integral in (4.111) yields:

$$\int_S [\mathbf{v}^T (\mathbf{N}^T \mathbf{H} \mathbf{D} \mathbf{u}) - \mathbf{u}^T (\mathbf{N}^T \mathbf{H} \mathbf{D} \mathbf{v})] dS + \omega^2 \int_{V_0} \rho_0 \mathbf{v}^T \mathbf{u} dV = 0 \quad (4.112)$$

Let us define the surface tractions:

$$\mathbf{t}(\mathbf{u}) = \mathbf{N}^T \mathbf{H} \mathbf{D} \mathbf{u} \quad \mathbf{t}(\mathbf{v}) = \mathbf{N}^T \mathbf{H} \mathbf{D} \mathbf{v} \quad (4.113)$$

which correspond to reactions associated to the imposed surface displacements on S_u and are null on S_σ by definition of the Dirichlet problems (4.109) and (4.110). With these definitions and applying the boundary conditions, Equation (4.112) provides the reciprocity relationship

$$\int_{S_u} \bar{\mathbf{v}}^T \mathbf{t}(\mathbf{u}) dS = \int_{S_u} \bar{\mathbf{u}}^T \mathbf{t}(\mathbf{v}) dS - \omega^2 \int_{V_0} \rho_0 \mathbf{v}^T \mathbf{u} dV \quad (4.114)$$

Equation (4.114) can be further developed if we express \mathbf{u} as:

$$\mathbf{u} = \mathbf{u}_{qs} + \sum_{r=0}^{\infty} \alpha_r \mathbf{u}_{(r)} \quad (4.115)$$

where the eigensolutions $\mathbf{u}_{(r)}$ and the quasi-static solution \mathbf{u}_{qs} are those associated to (4.109), namely satisfying:

$$\begin{cases} \mathbf{D}^T \mathbf{H} \mathbf{D} \mathbf{u}_{(r)} + \omega_r^2 \rho_0 \mathbf{u}_{(r)} = \mathbf{0} & \text{in } V \\ \mathbf{u}_{(r)} = \mathbf{0} & \text{on } S_u \end{cases} \quad (4.116)$$

and

$$\begin{cases} \mathbf{D}^T \mathbf{H} \mathbf{D} \mathbf{u}_{qs} = \mathbf{0} & \text{in } V \\ \mathbf{u} = \bar{\mathbf{u}} & \text{on } S_u \end{cases} \quad (4.117)$$

Substituting (4.115) into Equation (4.109) we get:

$$\sum_{r=0}^{\infty} \alpha_r (\mathbf{D}^T \mathbf{H} \mathbf{D} \mathbf{u}_{(r)} + \omega^2 \rho_0 \mathbf{u}_{(r)}) + \omega^2 \rho_0 \mathbf{u}_{qs} = \mathbf{0} \quad (4.118)$$

and taking account of the orthogonality relationships between modes yields the expression of the coefficients:

$$\alpha_r(\omega^2) = \frac{\omega^2}{(\omega_r^2 - \omega^2) \mu_r} \int_{V_0} \rho_0 \mathbf{u}_{(r)}^T \mathbf{u}_{qs} dV = \frac{\omega^2 \beta_r}{\omega_r^2 - \omega^2} \quad (4.119)$$

with

$$\beta_r = \frac{1}{\mu_r} \int_{V_0} \rho_0 \mathbf{u}_{(r)}^T \mathbf{u}_{qs} dV \quad (4.120)$$

Finally, substituting the spectral development (4.115) with the coefficients (4.119) into (4.114) yields the relationship:

$$\begin{aligned} \int_{S_u} \bar{\mathbf{v}}^T \mathbf{t}(\mathbf{u}) \, dS &= \int_{S_u} \bar{\mathbf{u}}^T \mathbf{t}(\mathbf{v}) \, dS - \omega^2 \int_{V_0} \rho_0 \mathbf{v}^T \mathbf{u}_{qs} \, dV \\ &\quad - \sum_{r=0}^{\infty} \frac{\omega^4 \beta_r}{\omega_r^2 - \omega^2} \int_{V_0} \rho_0 \mathbf{v}^T \mathbf{u}_{(r)} \, dV \end{aligned} \quad (4.121)$$

The left-hand side of (4.121) expresses the virtual work of the reaction forces $\mathbf{t}(\mathbf{u})$ on the quasi-static displacement field \mathbf{v} .

The first term in the right-hand side is the quasi-static contribution to it. The second one represents a constant inertia contribution. The third one represents a dynamic contribution due to deformation of the continuum.

$\bar{\mathbf{v}}$ being arbitrary, Equation (4.121) can be rewritten in the more explicit form

$$\begin{aligned} \int_{S_u} \delta \bar{\mathbf{v}}^T \mathbf{t}(\mathbf{u}) \, dS &= \int_{S_u} \bar{\mathbf{u}}^T \mathbf{t}[\mathbf{v}(\delta \bar{\mathbf{v}})] \, dS - \omega^2 \int_{V_0} \rho_0 [\mathbf{v}(\delta \bar{\mathbf{v}})]^T \mathbf{u}_{qs} \, dV \\ &\quad - \sum_{r=0}^{\infty} \frac{\omega^4 \beta_r}{\omega_r^2 - \omega^2} \int_{V_0} \rho_0 [\mathbf{v}(\delta \bar{\mathbf{v}})]^T \mathbf{u}_{(r)} \, dV \end{aligned} \quad (4.122)$$

The virtual Equation (4.122) allows to compute the surface tractions $\mathbf{t}(\mathbf{u})$ generated in harmonic regime by an imposed harmonic displacement $\bar{\mathbf{u}}$ on the boundary. It forms the basis for the development of an *impedance relationship for a continuous elastic body* in the same way as we did for discrete systems. Its application is straightforward for 1-D systems where the boundary S_u generally reduces to local points. Its effective use for 2-D or 3-D continua depends on an assumption on the distribution of imposed displacements $\bar{\mathbf{u}}$ on the boundary (Rixen *et al.* 1996).

As it will be seen later on with examples, it immediately provides dynamic impedance expressions for one-dimensional systems provided that the quasi-static response \mathbf{u}_{qs} and the eigenmodes \mathbf{u}_r can be obtained.

4.3 One-dimensional continuous systems

Physical systems such as bars in extension, vibrating strings and beams in bending are included in the category of one-dimensional systems: the motion of the system is described by a displacement field function of the sole coordinate x . The displacement of the one-dimensional systems considered here is supposed to occur in a plane and is denoted:

$$u(x, t) \qquad v = 0 \qquad w(x, t)$$

for either longitudinal or transverse motion. In all cases, the equation of motion of such systems may be obtained through variation of a functional in Hamilton's principle as already presented in the three-dimensional case.⁶

⁶ It is also possible, rather than going back every time to the fundamental principle, to generalize the formulation of the Lagrange equations to continuous one-dimensional systems. See Section 4.5.1 in (Gérardin and Rixen 1997).

4.3.1 The bar in extension

Derivation of the equation of motion

Let us consider a bar of section $A(x)$ (Figure 4.11) for which displacements and stresses are supposed constant over the cross-section – a valid assumption for a system with slowly varying cross-section and loaded only in the axial direction.

An external load per unit length \bar{X} is applied to the bar along direction x , and either an axial load \bar{N} or a displacement \bar{u} is imposed at the ends, *defined positively in the x direction*.

In linear elasticity, the internal axial force $N(x)$ is expressed by:

$$N(x) = A(x)\sigma_x(x) = EA\epsilon_x \quad (4.123)$$

with, under the small displacement assumption,

$$\epsilon_x = \frac{\partial u}{\partial x} \quad (4.124)$$

Contrarily to the external load \bar{N} , the direction of the axial force $N(x)$ is determined according to the outer normal \mathbf{n} of the facet to which it applies.

The system energies are then given by:

$$\begin{aligned} \mathcal{V}_{int} &= \frac{1}{2} \int_0^\ell EA \left(\frac{\partial u}{\partial x} \right)^2 dx \\ \mathcal{T} &= \frac{1}{2} \int_0^\ell m \dot{u}^2 dx \end{aligned}$$

where $m = \rho A$ is the mass per unit length.

The potential energy of external forces is given by:

$$\mathcal{V}_{ext} = - \int_0^\ell \bar{X} u \, dx - \bar{N}(0)u(0) - \bar{N}(\ell)u(\ell)$$

Let us apply Hamilton's principle in the form (4.19)

$$\int_{t_1}^{t_2} \left\{ \int_0^\ell \left[m \dot{u} \delta \dot{u} - EA \frac{\partial u}{\partial x} \delta \left(\frac{\partial u}{\partial x} \right) + \bar{X} \delta u \right] dx + \bar{N}(0) \delta u(0) + \bar{N}(\ell) \delta u(\ell) \right\} dt = 0 \quad (4.125)$$

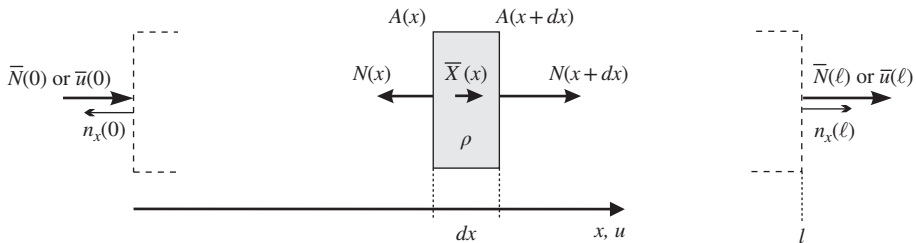


Figure 4.11 Bar element in extension.

Integrating by parts both in time and in space and recalling the fixed-end condition in time (4.18) yields:

$$\int_{t_1}^{t_2} \left\{ \int_0^\ell \left[-m\ddot{u} + \frac{\partial}{\partial x} \left(EA \frac{\partial u}{\partial x} \right) + \bar{X} \right] \delta u dx - \left[EA \frac{\partial u}{\partial x} \delta u \right]_0^\ell + \bar{N}(0) \delta u(0) + \bar{N}(\ell) \delta u(\ell) \right\} dt = 0 \quad (4.126)$$

Equation (4.126) vanishes provided that the following conditions are fulfilled:

$$\frac{\partial}{\partial x} \left(EA \frac{\partial u}{\partial x} \right) - m\ddot{u} + \bar{X} = 0 \quad \text{for } 0 < x < \ell \quad (4.127)$$

$$n_x EA \frac{\partial u}{\partial x} = \bar{N} \quad \text{or} \quad u = \bar{u} \quad \text{for } x = 0, \ell \quad (4.128)$$

n_x being the x component of the outer normal \mathbf{n} on the end sections of the bar (taking the values -1 at $x = 0$ and $+1$ at $x = \ell$).

It is easily verified from the free body diagram on Figure 4.11 that Equation (4.127) effectively expresses dynamic equilibrium of the bar element.

Vibration eigenmodes and frequencies of the uniform bar

In order to analyze the free vibrations of the bar in extension, the harmonic motion assumption $u(x, t) = u(x) \cos \omega t$ and the assumption of constant cross-section transform Equation (4.127) into:

$$EA \frac{d^2 u}{dx^2} + \omega^2 m u = 0 \quad (4.129)$$

which admits the general solution:

$$u(x) = a \sin \lambda \frac{x}{\ell} + b \cos \lambda \frac{x}{\ell} \quad (4.130)$$

with the nondimensional parameter:

$$\lambda^2 = \frac{\omega^2 m \ell^2}{EA} \quad (4.131)$$

For example, in the clamped–free case, the boundary conditions are:

$$(u)_{x=0} = 0 \quad \text{and} \quad \left(\frac{du}{dx} \right)_{x=\ell} = 0$$

and thus:

$$b = 0 \quad \text{and} \quad \cos \lambda = 0 \quad (4.132)$$

Equation (4.127) yields the characteristic roots:

$$\lambda_k = (2k - 1) \frac{\pi}{2} \quad k = 1, 2, \dots \quad (4.133)$$

and the eigenfrequencies ω_k are deduced from (4.131):

$$\omega_k = (2k-1) \frac{\pi}{2} \sqrt{\frac{EA}{m\ell^2}} \quad k = 1, 2, \dots \quad (4.134)$$

with the orthonormalized eigenshapes:

$$u_{(k)} = \sqrt{\frac{2}{m\ell}} \sin(2k-1) \frac{\pi x}{2\ell} \quad (4.135)$$

It is thus observed that the continuous character of the system yields an infinity of eigen-solutions. Table 4.2 provides the eigensolutions of the uniform bar under different possible homogeneous boundary conditions.

Table 4.2 Eigenfrequencies and orthonormalized eigenmodes of a uniform bar, $r = 1, \infty$

Boundary conditions	Eigenvalues ω_r^2	Eigenmodes $u_r(x)$
free-free	$\frac{EA}{m\ell^2} ((r-1)\pi)^2$	$\sqrt{\frac{2}{m\ell}} \cos \frac{(r-1)\pi x}{\ell}$
clamped-free	$\frac{EA}{m\ell^2} \left(\frac{(2r-1)\pi}{2} \right)^2$	$\sqrt{\frac{2}{m\ell}} \sin \frac{(2r-1)\pi x}{2\ell}$
clamped-clamped	$\frac{EA}{m\ell^2} (r\pi)^2$	$\sqrt{\frac{2}{m\ell}} \sin \frac{r\pi x}{\ell}$

Remark 4.1 The correspondence between discrete systems and continuous systems is easily illustrated in the simple case of the uniform bar. Let us consider the spring-mass system of Figure 4.12 as the discrete model with N degrees of freedom of the uniform clamped-free bar. Each mass M of the system obeys the free vibration equilibrium equation:

$$k(u_{j-1} - 2u_j + u_{j+1}) + \omega^2 M u_j = 0 \quad 0 < j < N \quad (4.136)$$

By giving to u_j the general solution form of repetitive systems (Biot and Lewis method (Von Karman and Biot 1940)):

$$u_j = a \sin(j\mu + \phi) \quad 0 \leq j \leq N \quad (4.137)$$

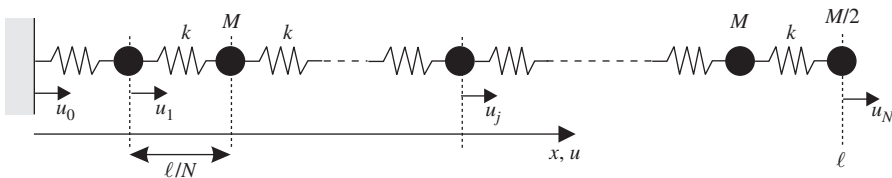


Figure 4.12 Discrete model of a bar in extension.

we obtain:

$$k [\sin((j-1)\mu + \phi) - 2 \sin(j\mu + \phi) + \sin((j+1)\mu + \phi)] + \omega^2 M \sin(j\mu + \phi) = 0 \quad (4.138)$$

or

$$2k [\sin(j\mu + \phi) \cos \mu - \sin(j\mu + \phi)] + \omega^2 M \sin(j\mu + \phi) = 0 \quad (4.139)$$

and thus, while $\sin(j\mu + \phi)$ does not vanish,

$$\omega^2 - \frac{2k}{M} (1 - \cos \mu) = 0$$

$$\omega = 2\sqrt{\frac{k}{M}} \sin \frac{\mu}{2} \quad (4.140)$$

The relation (4.140) links the frequency ω to the solution parameter μ . The parameters μ and ϕ are then determined by the boundary conditions expressing prescribed displacement and dynamic equilibrium of the end masses:

$$u_0 = 0 \quad (4.141)$$

$$k(u_{N-1} - u_N) + \omega^2 \frac{M}{2} u_N = 0 \quad (4.142)$$

The condition (4.141) at the clamped end determines the ϕ value which thus is:

$$\phi = 0 \quad (4.143)$$

Substituting next the general solution (4.137) into condition (4.142) at the free end, we obtain the characteristic equation governing μ :

$$k(\sin(N-1)\mu - \sin N\mu) + \omega^2 \frac{M}{2} \sin N\mu = 0$$

By developing the term $\sin(N-1)\mu$ and replacing ω^2 by its expression (4.140) we get:

$$\sin \mu \cos N\mu = 0 \quad (4.144)$$

The root $\sin \mu = 0$ is rejected since it generates the trivial solution $u_j = 0$. Thus we can write:

$$\mu = \frac{2r-1}{N} \frac{\pi}{2} \quad r = 1, 2, \dots \quad (4.145)$$

The eigenfrequencies and the associated modes of the discrete system are then given by:

$$\omega_r = 2\sqrt{\frac{k}{M}} \sin \left(\frac{2r-1}{4N} \pi \right) \quad (4.146)$$

$$u_{j(r)} = a \sin \left(j \frac{2r-1}{2N} \pi \right) \quad r = 1, 2, \dots, N \quad (4.147)$$

where r has an upper limit of N so that we need consider each possible positive value of ω_r only once.

As expected, only N different eigensolutions exist for the N -degree-of-freedom discrete system. In order to let this discrete system approach the continuous bar idealization, let us call x_j the mass positions:

$$x_j = j \frac{\ell}{N}$$

The mass per unit length and the extension stiffness can be expressed by:

$$m = \frac{M}{\ell/N} \quad \text{and} \quad EA = \frac{k\ell}{N}$$

When N tends to infinity, x_j becomes a continuous variable x , and by developing ω_r in series:

$$\omega_r = 2N \sqrt{\frac{EA}{m\ell^2}} \left[\frac{(2r-1)\pi}{4N} - \frac{1}{3!} \left(\frac{(2r-1)\pi}{4N} \right)^3 + \dots \right]$$

$$u_{(r)} = a \sin \left(\frac{Nx}{\ell} \frac{2r-1}{N} \frac{\pi}{2} \right)$$

By letting N tend to infinity we get:

$$\omega_r = (2r-1) \frac{\pi}{2} \sqrt{\frac{EA}{m\ell^2}} \quad (4.148)$$

$$u_{(r)}(x) = a \sin(2r-1) \frac{\pi x}{2\ell} \quad r = 1, 2, \dots, \infty \quad (4.149)$$

which correspond effectively to expressions (4.134) and (4.135).

Let us also note that result (4.146) provides a lower bound approximation to the eigenfrequencies, which can be explained by the fact that the mass distribution is approximated by a series of lumped masses.

Impedance matrix of the bar in extension

The impedance matrix characterizing the uniform bar in extension submitted to harmonic excitation at its extremities can easily be deduced from the general virtual work expression (4.122) established for a continuum in the following way.

The virtual quasi-static problem can be written as:

$$\begin{cases} EA \frac{d^2 v}{dx^2} = 0 & 0 < x < \ell \\ \bar{v}(0) = \delta \bar{v}_1, \quad \bar{v}(\ell) = \delta \bar{v}_2 \end{cases} \quad (4.150)$$

and the virtual displacement field v has thus for expression:

$$v(\delta \bar{v}) = \left(1 - \frac{x}{\ell} \right) \delta \bar{v}_1 + \frac{x}{\ell} \delta \bar{v}_2 \quad (4.151)$$

It generates the constant axial stress field:

$$EA \frac{dv}{dx} = \frac{EA}{\ell} (\delta \bar{v}_2 - \delta \bar{v}_1) \quad (4.152)$$

and the associated surface tractions (taking account of the outer normal to S_u) are:

$$\mathbf{t}(v)|_{S_u} = \frac{EA}{\ell} \begin{bmatrix} \delta \bar{v}_1 - \delta \bar{v}_2 \\ \delta \bar{v}_2 - \delta \bar{v}_1 \end{bmatrix} = \frac{EA}{\ell} \begin{bmatrix} 1 & -1 \\ -1 & 1 \end{bmatrix} \begin{bmatrix} \delta \bar{v}_1 \\ \delta \bar{v}_2 \end{bmatrix} = \mathbf{K} \delta \bar{\mathbf{v}} \quad (4.153)$$

with the stiffness matrix of the bar:

$$\mathbf{K} = \frac{EA}{\ell} \begin{bmatrix} 1 & -1 \\ -1 & 1 \end{bmatrix} \quad (4.154)$$

Collecting the imposed displacements into:

$$\mathbf{q} = \begin{bmatrix} \bar{u}_1 \\ \bar{u}_2 \end{bmatrix} \quad (4.155)$$

we can thus write the first term of the right-hand side of Equation (4.122) as:

$$\int_{S_u} \bar{\mathbf{u}}^T \mathbf{t} [\mathbf{v}(\delta \bar{\mathbf{v}})] dS = \delta \bar{\mathbf{v}}^T \mathbf{K} \mathbf{q} \quad (4.156)$$

On the other hand, the local values on the boundary of the unknown traction forces are defined as:

$$\mathbf{g} = \begin{bmatrix} g_1 \\ g_2 \end{bmatrix} \quad (4.157)$$

so that we can write the left-hand side of Equation (4.122) in the form:

$$\int_{S_u} \delta \bar{\mathbf{v}}^T \mathbf{t}(\mathbf{u}) dS = g_1 \delta \bar{v}_1 + g_2 \delta \bar{v}_2 = \delta \bar{\mathbf{v}}^T \mathbf{g} \quad (4.158)$$

The quasi-static solution is obtained by solving the same problem (4.150) with boundary conditions $[\bar{u}_1 \ \bar{u}_2]$. We thus get:

$$u_{qs}(x) = \left(1 - \frac{x}{\ell}\right) \bar{u}_1 + \frac{x}{\ell} \bar{u}_2 \quad (4.159)$$

Calculating the constant factor in the second term of the right-hand side of Equation (4.122) yields:

$$\int_{V_0} \rho_0 [\mathbf{v}(\delta \bar{\mathbf{v}})]^T \mathbf{u}_{qs} dV = \delta \bar{\mathbf{v}}^T \int_0^\ell m \begin{bmatrix} \left(1 - \frac{x}{\ell}\right)^2 & \left(1 - \frac{x}{\ell}\right) \frac{x}{\ell} \\ \left(1 - \frac{x}{\ell}\right) \frac{x}{\ell} & \left(\frac{x}{\ell}\right)^2 \end{bmatrix} dx \mathbf{q} = \delta \bar{\mathbf{v}}^T \mathbf{M} \mathbf{q} \quad (4.160)$$

with the mass matrix:

$$\mathbf{M} = \frac{m\ell}{6} \begin{bmatrix} 2 & 1 \\ 1 & 2 \end{bmatrix} \quad (4.161)$$

Let us finally compute the last term in Equation (4.122). The eigensolutions to be taken into the spectral expansion are the modes with fixed ends (Table 4.2). The following quantities have to be computed:

$$\begin{aligned} \int_0^\ell m \left(1 - \frac{x}{\ell}\right) \sin \frac{r\pi x}{\ell} dx &= \frac{m\ell(r\pi - \sin r\pi)}{(r\pi)^2} = \frac{m\ell}{r\pi} \\ \int_0^\ell m \frac{x}{\ell} \sin \frac{r\pi x}{\ell} dx &= \frac{m\ell(\sin r\pi - r\pi \cos r\pi)}{(r\pi)^2} = (-1)^{(r-1)} \frac{m\ell}{r\pi} \end{aligned} \quad (4.162)$$

Assuming the eigenmodes to be mass normalized, the coefficients β_r defined in (4.120) can be put in the form:

$$\beta_r = \frac{1}{\mu_r} \int_{V_0} \rho_0 \mathbf{u}_{(r)}^T \mathbf{u}_{qs} dV = \mathbf{a}_r^T \mathbf{q} \quad (4.163)$$

with the vectors:

$$\mathbf{a}_r = \frac{\sqrt{2m\ell}}{r\pi} \begin{bmatrix} 1 \\ (-1)^{(r-1)} \end{bmatrix} \quad (4.164)$$

One can likewise compute the integral:

$$\int_{V_0} \rho_0 [\mathbf{v}(\delta\bar{\mathbf{v}})]^T \mathbf{u}_{(r)} dV = \delta\bar{\mathbf{v}}^T \mathbf{a}_r \quad (4.165)$$

Finally, substituting (4.158), (4.156), (4.160), (4.164), (4.165) into (4.122) and considering that $\delta\bar{\mathbf{v}}$ is arbitrary yields the impedance relationship for the bar in extension:

$$\mathbf{g} = \mathbf{Z}(\omega^2) \mathbf{q} \quad (4.166)$$

with the impedance matrix:⁷

$$\mathbf{Z}(\omega^2) = \mathbf{K} - \omega^2 \mathbf{M} - \omega^4 \sum_{r=1}^{\infty} \frac{2m\ell}{(r\pi)^2(\omega_r^2 - \omega^2)} \begin{bmatrix} 1 & (-1)^{(r-1)} \\ (-1)^{(r-1)} & 1 \end{bmatrix} \quad (4.167)$$

Response of a bar excited by an end force

Let us consider a bar initially at rest (Figure 4.13) and subjected to a force $P(t)$ at its end at time $t = 0$ (Meirovitch 1967).

Supposing that the clamped–free bar has constant properties, the displacement $u(x, t)$ verifies the equation of motion:

$$EA \frac{\partial^2 u}{\partial x^2} - m\ddot{u} = 0 \quad (4.168)$$

and is subjected to the following end conditions:

– in time:

$$u(x, 0) = 0 \quad \dot{u}(x, 0) = 0 \quad 0 \leq x \leq \ell \quad (4.169)$$

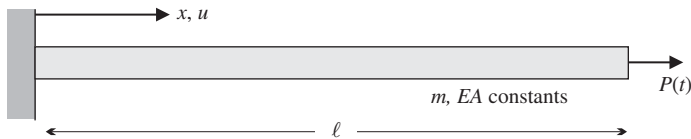


Figure 4.13 End excitation of a clamped–free bar.

⁷ The impedance matrix of the bar can also be built in transcendental form in terms of the eigenvalue parameter λ_r . Its Taylor expansion would reconstitute the result (4.167). The development of this alternate form is left as an exercise to the reader (Exercise 4.3).

– in space:

$$u(0, t) = 0 \quad EA \left(\frac{\partial u}{\partial x} \right)_{x=\ell} = P(t) \quad \forall t \quad (4.170)$$

The problem is characterized by a homogeneous differential equation of wave propagation type with nonhomogeneous boundary conditions. To solve it, we try the following two techniques:

- Mode superposition, leading to a solution in terms of standing waves.
- Laplace transform followed by a solution in terms of travelling waves.

Mode superposition, which is equivalent to a finite sine transform, reduces the equation of motion to a system of ordinary differential equations in time (normal equations). Conversely, the Laplace transform gives rise to an ordinary differential equation in terms of the only space variable.

Mode superposition solution

The spatial boundary conditions being nonhomogeneous, let us apply the modal expansion developed in Section 4.2.4, recognizing that in the present case no force in the volume is present. The system being excited through the nonhomogeneous boundary condition, its solution can be written as:

$$u(x, t) = u_{qs_{nh}}(x, t) + \sum_{s=1}^{\infty} \eta_s(t) u_{(s)}(x) \quad (4.171)$$

where $u_{(s)}$ are the normalized eigenmodes of the clamped–free beam (see Table 4.2) and where the quasi-static part $u_{qs_{nh}}$ is solution of (see *Problem 3* in Table 4.1):

$$\begin{cases} EA \frac{\partial^2 u_{qs_{nh}}}{\partial x^2} = 0 & \text{in } V \\ EA \frac{\partial u_{qs_{nh}}}{\partial x} = P(t) & \text{at } x = \ell \end{cases} \quad (4.172)$$

and verifies the kinematic condition $u_{qs_{nh}}(0, t) = 0$. We obtain:

$$u_{qs_{nh}} = \frac{P(t)}{EA} x \quad (4.173)$$

and the general form of the response is written:

$$u(x, t) = \frac{P(t)}{EA} x + \sum_{s=1}^{\infty} \eta_s(t) \sqrt{\frac{2}{m\ell}} \sin \left((2s-1) \frac{\pi x}{2\ell} \right) \quad (4.174)$$

In the particular case of a *step* loading:

$$P(t) = \begin{cases} 0 & t < 0 \\ p_0 & t \geq 0 \end{cases} \quad (4.175)$$

the static solution takes the form:

$$u_{qs_{nh}} = \frac{p_0}{EA} x \quad t \geq 0 \quad (4.176)$$

with

$$\dot{u}_{qs_{nh}}(x, t) = 0 \quad \text{and} \quad \ddot{u}_{qs_{nh}}(x, t) = 0$$

The modal amplitudes $\eta_s(t)$ in (4.174) can be computed by solving the normal equations as in (4.91). One can also directly write the final solution for the bar response by applying Equation (4.96) to obtain:

$$\begin{aligned} u(x, t) &= v(x, t) + w(x, t) = w(x, t) \\ &= \delta(S) + \sum_{s=1}^{\infty} \omega_s u_{(s)} \int_0^t \int_V \rho u_{(s)} \frac{p_0}{EA} x \, dV \sin(\omega_s(t - \tau)) \, d\tau \end{aligned} \quad (4.177)$$

where $v(x, t)$, the solution for the homogeneous problem (*problem I* in Table 4.1), is zero due to the zero initial conditions (4.169). Performing the integral over time in the last term and considering the definition (4.94) of $\delta(S)$, one obtains:

$$u(x, t) = \frac{p_0 x}{EA} - \sum_{s=1}^{\infty} \frac{2}{\ell} \sin \frac{(2s-1)\pi x}{2\ell} \cos \omega_s t \int_0^{\ell} \frac{p_0 x}{EA} \sin \frac{(2s-1)\pi x}{2\ell} dx \quad (4.178)$$

with

$$\omega_s = (2s-1) \frac{\pi c}{2\ell}$$

where $c = \sqrt{\frac{EA}{m}}$ denotes the wave propagation velocity in the bar. After some algebraic manipulation we get the results for the displacement and the axial force:

$$u(x, t) = \frac{p_0}{EA} x - \frac{8p_0 \ell}{\pi^2 EA} \sum_{s=1}^{\infty} \left\{ \frac{(-1)^{s-1}}{(2s-1)^2} \sin \frac{(2s-1)\pi x}{2\ell} \cos \frac{(2s-1)\pi ct}{2\ell} \right\} \quad (4.179)$$

and the normal force in the bar is obtained as:

$$\begin{aligned} N(x, t) &= EA \frac{\partial u}{\partial x} \\ &= p_0 \left\{ 1 - \frac{4}{\pi} \sum_{s=1}^{\infty} \left(\frac{(-1)^{s-1}}{(2s-1)} \cos \frac{(2s-1)\pi x}{2\ell} \cos \frac{(2s-1)\pi ct}{2\ell} \right) \right\} \end{aligned} \quad (4.180)$$

The response of the bar is thus composed of a quasi-steady part and a transient part expressed as a series of standing waves represented by the eigenmodes.

Let us show the problem of convergence that characterizes the mode superposition method when applied to systems with nonhomogeneous boundary conditions and not explicitly including the quasi-steady term. For the step load, that would correspond to setting $\delta(S) = 0$ in (4.177) which, after performing the time and space integration yields:⁸

$$u(x, t) = \frac{8p_0 \ell}{\pi^2 EA} \sum_{s=1}^{\infty} \left\{ \frac{(-1)^{s-1}}{(2s-1)^2} \sin \frac{(2s-1)\pi x}{2\ell} \left(1 - \cos \frac{(2s-1)\pi ct}{2\ell} \right) \right\} \quad (4.181)$$

⁸ This result can also be obtained by considering a mode superposition (4.100) for homogeneous boundary conditions, considering the applied end load as a concentrated volume load and taking as modal participation factor $\phi_s = u_{(s)}(\ell)p_0$.

The difference between (4.181) with (4.178) is the $\delta(S)$ term, which for the step load has for expression:

$$\delta(S_\sigma) = \frac{p_0 \ell}{EA} \left\{ \frac{x}{\ell} - \frac{8}{\pi^2} \sum_{s=1}^{\infty} \left(\frac{(-1)^{s-1}}{(2s-1)^2} \sin \frac{(2s-1)\pi x}{2\ell} \right) \right\} \quad (4.182)$$

The problem being inhomogeneous on S_σ , slower convergence is expected on the normal forces for which the correction term is:

$$EA \frac{d}{dx} \delta(S_\sigma) = p_0 \left\{ 1 - \frac{4}{\pi} \sum_{s=1}^{\infty} \left[\frac{(-1)^{s-1}}{(2s-1)} \cos \left((2s-1) \frac{\pi x}{2\ell} \right) \right] \right\} \quad (4.183)$$

Indeed Equation (4.181) shows that the displacement converges like s^{-2} while the axial force (4.180) will converge as s^{-1} . Both functions are displayed in nondimensional form on Figure 4.14. They show that the quasi-static correction will have little effect on the displacement response. Indeed if we consider the case where 10 modes are included in the series, $\max_x \left\{ \frac{EA}{p_0 \ell} \delta(S_\sigma) \right\} = 0.02$ but it has a drastic effect on the computation of the axial force since $\max_x \left\{ \frac{EA}{p_0} \frac{d}{dx} \delta(S_\sigma) \right\} = 1$ (at the loading point).

To further describe the effect of the static correction term $\delta(S_\sigma)$ let us consider the time response computed for the displacements and the normal forces (4.182) and (4.183). In Figure 4.15 the response is plotted when considering 10 modes in the series, with and without the static correction, for the locations $x/\ell = 1/3$ and $x/\ell = 0.9$. The effect of the static correction is significant for the normal force close to the end point where the load is applied. Clearly one recognizes the travelling wave nature of the response (see also next paragraph), but the solution obtained as combination of standing waves (eigenmodes) exhibits the well-known Gibbs phenomenon: the modal representation of the response along the bar is not well suited to represent the normal force, which is piecewise continuous in space and time due to the wave front created by the step load. Obviously for such problem a representation in terms of travelling wave would be more appropriate as explained next.

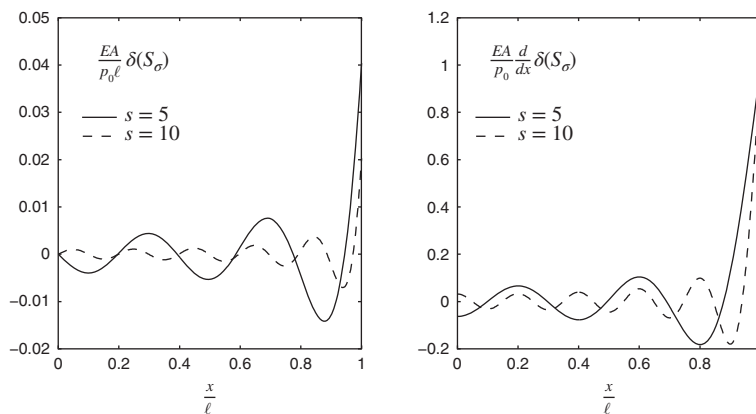


Figure 4.14 Discontinuity function $\delta(S_\sigma)$ (left) and its derivative (right) for the clamped–free bar submitted to end load (for a number of modes $s = 5$ and $s = 10$).

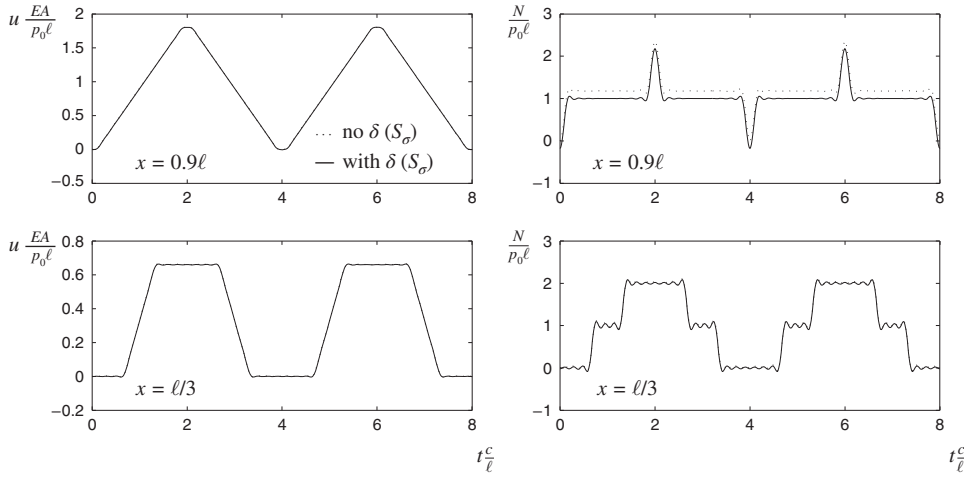


Figure 4.15 Time response of the clamped–free bar submitted to a load step at the free end: displacement (left) and axial force (right) at $x = 0.9\ell$ (top) and at $x = \ell/3$ (bottom). The solution is computed by mode superposition (10 modes) with (—) and without (···) static correction $\delta(S_\sigma)$.

Laplace transform solution and expansion in series of travelling waves

A different mathematical approach to the solution allows to put directly in evidence the travelling wave character of the response. To do so (Meirovitch 1967), in place of projecting the solution onto the eigenmode space, let us perform a Laplace transform:

$$\bar{u}(x, s) = \mathcal{L}[u] = \int_0^\infty u(x, t) e^{-st} dt \quad (4.184)$$

To compute the transformation, let us note on the one hand that:

$$\mathcal{L}\left[\frac{\partial^2 u}{\partial x^2}\right] = \frac{\partial^2}{\partial x^2} \mathcal{L}[u]$$

and on the other hand that:

$$\mathcal{L}[\ddot{u}] = s^2 \mathcal{L}[u] - su(x, 0) - \dot{u}(x, 0)$$

Hence, by taking account of the time boundary conditions, the equation of motion (4.168) is written:

$$\frac{\partial^2 \bar{u}}{\partial x^2} - \frac{s^2}{c^2} \bar{u} = 0 \quad (4.185)$$

with the boundary conditions in space:

$$\begin{aligned} \bar{u}(0, s) &= 0 \\ EA \left(\frac{\partial \bar{u}}{\partial x} \right)_{x=\ell} &= \bar{P}(s) \end{aligned} \quad (4.186)$$

The general solution to (4.184) is:

$$\bar{u}(x, s) = a_1 e^{\frac{sx}{c}} + a_2 e^{\frac{-sx}{c}} \quad (4.187)$$

and applying the boundary conditions (4.186) reduces the solution to the form:

$$\bar{u}(x, s) = \frac{c}{EA} \bar{f}(x, s) \bar{P}(s) \quad (4.188)$$

with the function:

$$\bar{f}(x, s) = \frac{e^{\frac{sx}{c}} - e^{\frac{-sx}{c}}}{s \left(e^{\frac{s\ell}{c}} + e^{\frac{-s\ell}{c}} \right)} \quad (4.189)$$

At this stage, it is easily verified that by rewriting \bar{f} in the form:

$$\bar{f}(x, s) = -\frac{i \sin \frac{isx}{c}}{s \cos \frac{is\ell}{c}} \quad (4.190)$$

where $i = \sqrt{-1}$, and then computing the inverse transform of (4.188), one obtains the solution in terms of standing waves (4.181).

However, the advantage of solving this problem by Laplace transform is in the possibility of constructing a different expression of the solution. To achieve this, let us put function $\bar{f}(x, s)$ into the form:

$$\begin{aligned} \bar{f}(x, s) &= \frac{1}{s} \frac{e^{\frac{sx}{c}} - e^{\frac{-sx}{c}}}{e^{\frac{s\ell}{c}} + e^{\frac{-s\ell}{c}}} = \frac{e^{\frac{-s\ell}{c}}}{s} \frac{e^{\frac{sx}{c}} - e^{\frac{-sx}{c}}}{1 + e^{\frac{-2s\ell}{c}}} \\ &= \frac{e^{\frac{-s\ell}{c}}}{s} \left(e^{\frac{sx}{c}} - e^{\frac{-sx}{c}} \right) \left(1 - e^{\frac{-2s\ell}{c}} + e^{\frac{-4s\ell}{c}} \dots \right) \end{aligned} \quad (4.191)$$

or

$$\bar{f}(x, s) = \frac{1}{s} \left(e^{\frac{-s(\ell-x)}{c}} - e^{\frac{-s(\ell+x)}{c}} - e^{\frac{-s(3\ell-x)}{c}} + e^{\frac{-s(3\ell+x)}{c}} + \dots \right) \quad (4.192)$$

The inverse transformation of (4.192) gives the result:

$$\begin{aligned} f(x, t) &= H \left(t - \frac{\ell-x}{c} \right) - H \left(t - \frac{\ell+x}{c} \right) \\ &\quad - H \left(t - \frac{3\ell-x}{c} \right) + H \left(t - \frac{3\ell+x}{c} \right) + \dots \end{aligned} \quad (4.193)$$

where H is the Heaviside step function such that:

$$H(t-d) = \begin{cases} 0 & t < d \\ 1 & t > d \end{cases}$$

It is then possible to compute the displacement $u(x, t)$ by taking the inverse Laplace transform of (4.188) using Duhamel's integral:

$$u(x, t) = \frac{c}{EA} \int_0^t P(\tau) f(x, t-\tau) d\tau$$

$$= \frac{c}{EA} \int_0^t P(\tau) \left[H\left(t - \frac{\ell-x}{c} - \tau\right) - H\left(t - \frac{\ell+x}{c} - \tau\right) - H\left(t - \frac{3\ell-x}{c} - \tau\right) + \dots \right] d\tau$$

Let us note next that:

$$\begin{aligned} - \text{ for } t < \frac{\ell-x}{c}, H\left(t - \frac{\ell-x}{c} - \tau\right) &= 0, \text{ when } \tau > 0 \\ - \text{ for } t > \frac{\ell-x}{c}, H\left(t - \frac{\ell-x}{c} - \tau\right) &= \begin{cases} 1 & \text{if } 0 < \tau < t - \frac{\ell-x}{c} \\ 0 & \text{if } t - \frac{\ell-x}{c} < \tau \end{cases} \end{aligned}$$

Hence the result:

$$\begin{aligned} u(x, t) = \frac{c}{EA} \left\{ H\left(t - \frac{\ell-x}{c}\right) \int_0^{t-\frac{\ell-x}{c}} P(\tau) d\tau \right. \\ \left. - H\left(t - \frac{\ell+x}{c}\right) \int_0^{t-\frac{\ell+x}{c}} P(\tau) d\tau \right. \\ \left. - H\left(t - \frac{3\ell-x}{c}\right) \int_0^{t-\frac{3\ell-x}{c}} P(\tau) d\tau \right. \\ \left. + H\left(t - \frac{3\ell+x}{c}\right) \int_0^{t-\frac{3\ell+x}{c}} P(\tau) d\tau + \dots \right\} \quad (4.194) \end{aligned}$$

In the case of a *step excitation* such as (4.175), the solution is written as:

$$\begin{aligned} u(x, t) = \frac{cp_0}{EA} \left\{ \left(t - \frac{\ell-x}{c}\right) H\left(t - \frac{\ell-x}{c}\right) \right. \\ \left. - \left(t - \frac{\ell+x}{c}\right) H\left(t - \frac{\ell+x}{c}\right) \right. \\ \left. - \left(t - \frac{3\ell-x}{c}\right) H\left(t - \frac{3\ell-x}{c}\right) \right. \\ \left. + \left(t - \frac{3\ell+x}{c}\right) H\left(t - \frac{3\ell+x}{c}\right) + \dots \right\} \quad (4.195) \end{aligned}$$

This relationship expresses the solution through superposition of travelling waves. The time instants $t = \frac{\ell-x}{c}, \frac{\ell+x}{c}, \frac{3\ell-x}{c}, \dots$ are the times at which the wave travels through point x . The first term in this expression represents a wave with a linearly increasing amplitude travelling in the negative x direction. The second term corresponds to a linearly decreasing wave travelling in the positive x direction, starting when the first wave has reached the boundary $x = 0$: it is a reflected wave on that fixed end. The terms of the series (4.195) are depicted in the diagrams of Figures 4.16 and 4.17, showing the phenomena of wave displacement, reflection and superposition.

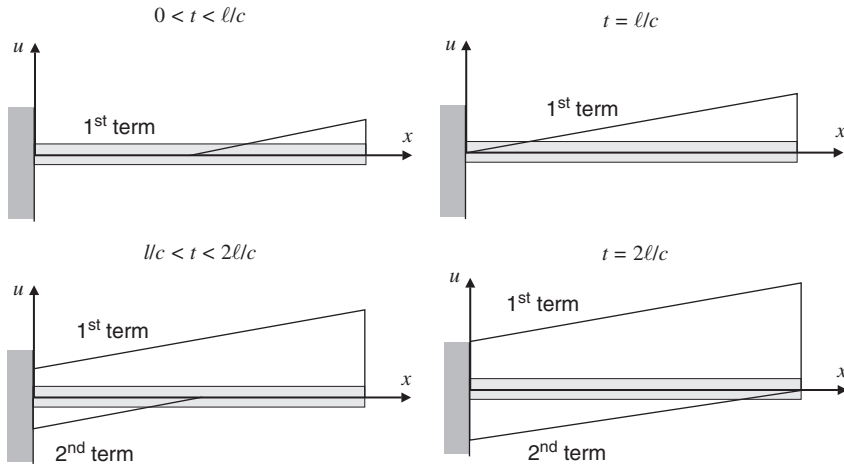


Figure 4.16 Response to a step load for a bar as a superposition of travelling waves, Equation (4.195).

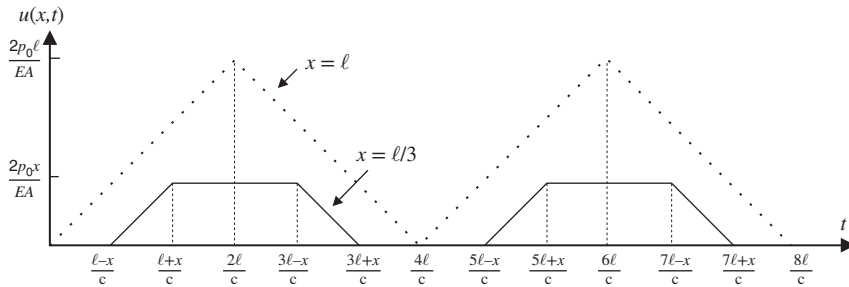


Figure 4.17 Response to a step load: axial displacement versus time.

It is also instructive to compute the axial force $N(x, t) = EA \frac{\partial u}{\partial x}$, namely:

$$N(x, t) = p_0 \left\{ H \left(t - \frac{\ell - x}{c} \right) + H \left(t - \frac{\ell + x}{c} \right) - H \left(t - \frac{3\ell - x}{c} \right) - H \left(t - \frac{3\ell + x}{c} \right) + \dots \right\} \quad (4.196)$$

The time evolution of the axial force is represented in Figure 4.18.

The results (4.195) and (4.196) are mathematically equivalent to (4.179) and (4.180). The former provide the standing wave representation of the solution while the latter correspond to the travelling wave form. Since the travelling wave representation obtained from the Laplace transform approach automatically includes the infinity of modes, the ripples inherent to modal truncation observed on Figure 4.15 have disappeared.

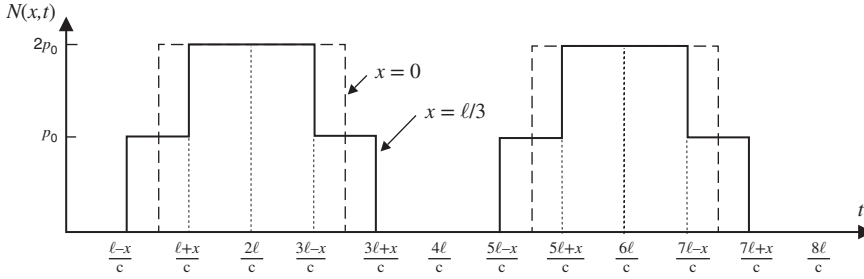


Figure 4.18 Response to a step load: axial force versus time.

4.3.2 Transverse vibrations of a taut string

Derivation of the equation of motion

A string is an idealized structure that has no flexural stiffness but undergoes transverse motion under the influence of an axial prestress N_0 . The string is a mono-dimensional system with coordinate x and we consider only its plane transverse motion (Figure 4.19). Thus we assume that the motion can be described solely by the transverse displacement $w(x)$ while disregarding the longitudinal motion. The strains are given by the general expression (4.6) and for the mono-dimensional taut string the only nonzero term is:

$$\epsilon_x = \frac{1}{2} \left(\frac{\partial w}{\partial x} \right)^2 \quad (4.197)$$

where w is the transverse displacement. The traction $N_0(x)$ is supposed to be dominant compared to the cable effect (see Examples 4.2 and 4.3). The problem will thus be studied according to the theory of prestressed structures, Equation (4.48). Since the strain results from the only quadratic term, the additional strain energy is zero and the geometric energy due to prestress is equal to

$$\mathcal{V}_g = \frac{1}{2} \int_0^\ell N_0 \left(\frac{\partial w}{\partial x} \right)^2 dx \quad (4.198)$$

The kinetic energy is computed by:

$$\mathcal{T} = \frac{1}{2} \int_0^\ell m \dot{w}^2 dx \quad (4.199)$$

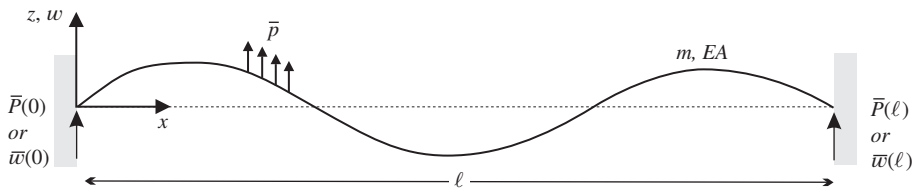


Figure 4.19 Transverse vibrations of a taut string.

The potential energy of external forces is given by:

$$\mathcal{V}_{ext} = - \int_0^\ell \bar{p}(x, t) w \, dx - \bar{P}(0) w(0) - \bar{P}(\ell) w(\ell) \quad (4.200)$$

where $\bar{p}(x, t)$ is the transverse load. Applying Hamilton's principle in the form (4.48) yields:

$$\int_{t_1}^{t_2} \left\{ \int_0^\ell \left[m \dot{w} \delta \dot{w} - N_0 \frac{\partial w}{\partial x} \delta \left(\frac{\partial w}{\partial x} \right) + \bar{p} \delta w \right] dx + \bar{P}(0) \delta w(0) + \bar{P}(\ell) \delta w(\ell) \right\} dt = 0 \quad (4.201)$$

and, after integration by parts in time and space, and taking into account the end conditions (4.18) for the time interval,

$$\begin{aligned} \int_{t_1}^{t_2} \left\{ \int_0^\ell \left[-m \ddot{w} \delta w + \frac{\partial}{\partial x} \left(N_0 \frac{\partial w}{\partial x} \right) \delta w + \bar{p} \delta w \right] dx \right. \\ \left. - \left[N_0 \frac{\partial w}{\partial x} \delta w \right]_0^\ell + \bar{P}(0) \delta w(0) + \bar{P}(\ell) \delta w(\ell) \right\} dt = 0 \end{aligned} \quad (4.202)$$

Hence, δw being arbitrary,

$$\frac{\partial}{\partial x} \left(N_0 \frac{\partial w}{\partial x} \right) - m \ddot{w} + \bar{p}(x, t) = 0 \quad (4.203)$$

with the associated boundary conditions:

$$\begin{aligned} N_0 \frac{\partial w}{\partial x} &= -\bar{P} \quad w = \bar{w} \quad \text{at } x = 0 \\ N_0 \frac{\partial w}{\partial x} &= \bar{P} \quad w = \bar{w} \quad \text{at } x = \ell \end{aligned} \quad (4.204)$$

It is easily verified on the free-body diagram of Figure 4.20 that the latter relationships express the transverse equilibrium of a taut string segment of infinitesimal length.

Free vibrations of a uniform taut string with fixed ends

Let us consider a uniform taut string with fixed ends and assume that the prestress and mass distribution are constant, namely:

$$N_0(x) = N_0 \quad \text{and} \quad m(x) = m$$

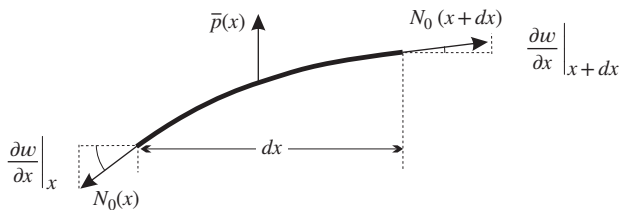


Figure 4.20 Equilibrium of a taut string segment.

The equation governing the free harmonic motion is written:

$$\boxed{\frac{d^2 w}{dx^2} + \frac{\omega^2 m}{N_0} w = 0} \quad (4.205)$$

It admits the same general solution as the bar in extension:

$$w(x) = a \sin \frac{\lambda x}{\ell} + b \cos \frac{\lambda x}{\ell} \quad (4.206)$$

with the eigenvalue:

$$\lambda^2 = \omega^2 \frac{m \ell^2}{N_0} \quad (4.207)$$

Because the string is attached at both ends, we find the eigenvalues:

$$\lambda_r = r\pi \quad r = 1, 2, \dots \quad (4.208)$$

to which the following natural frequencies and orthonormalized eigenshapes correspond:

$$\omega_r = r\pi \sqrt{\frac{N_0}{m \ell^2}} \quad w_r(x) = \sqrt{\frac{2}{m \ell}} \sin \frac{r\pi x}{\ell} \quad (4.209)$$

Wave propagation in the uniform taut string

When $\bar{p}(x, t) = 0$ and $N_0(x) = N_0$, Equation (4.203) governing the transverse motion becomes:

$$\boxed{\frac{\partial^2 w}{\partial x^2} - \frac{1}{c^2} \frac{\partial^2 w}{\partial t^2} = 0} \quad (4.210)$$

with the *phase speed*:

$$c = \sqrt{\frac{N_0}{m}} \quad (4.211)$$

Equation (4.210) describes a transverse wave with propagation velocity c since its general solution may be expressed in the form:

$$w(x, t) = F_1(x - ct) + F_2(x + ct) \quad (4.212)$$

where

$F_1(x - ct)$ is the displacement wave travelling in the positive x direction;
 $F_2(x + ct)$ is the backward wave.

The general solution is thus a superposition of displacement waves travelling in opposite directions, as already observed in the bar.

Response to initial conditions of a string of infinite length

Let us consider the problem of a uniform string of infinite length submitted to initial displacement and velocity fields:

$$\begin{cases} \frac{\partial^2 w}{\partial x^2} - \frac{1}{c^2} \frac{\partial^2 w}{\partial t^2} = 0 \\ w(x, 0) = W(x) \end{cases} \quad \begin{cases} -\infty < x < +\infty \\ \dot{w}(x, 0) = V(x) \end{cases} \quad (4.213)$$

The first equation expressing the dynamic equilibrium is automatically satisfied by the general form (4.212), and applying the initial condition yields:

$$F_1(x) + F_2(x) = W(x) \quad (4.214a)$$

$$-cF_1'(x) + cF_2'(x) = V(x) \quad (4.214b)$$

where F_1' and $F_2'(x)$ represent the derivative of F_1 and F_2 with respect to their variable $x - ct$ and $x + ct$ respectively. Let us integrate Equation (4.214b):

$$-cF_1(x) + cF_2(x) = \int_0^x V(\xi)d\xi + d \quad (4.215)$$

where d is an integration constant. Solving (4.214a) and (4.215) for F_1 and F_2 yields:

$$F_2(x) = \frac{1}{2} \left(W(x) + \frac{1}{c} \int_0^x V(\xi)d\xi + \frac{d}{c} \right)$$

$$F_1(x) = \frac{1}{2} \left(W(x) - \frac{1}{c} \int_0^x V(\xi)d\xi - \frac{d}{c} \right)$$

so that the general solution takes the form:

$$w(x, t) = \frac{1}{2} [W(x - ct) + W(x + ct)] + \int_{x-ct}^{x+ct} V(\xi)d\xi \quad (4.216)$$

In particular, the response to initial displacements consists of two identical signals of spatial shape $W(x)$ travelling at phase speed without dispersion into opposite directions:

$$w(x, t) = \frac{1}{2} [W(x - ct) + W(x + ct)] \quad (4.217)$$

Response to initial conditions of a string of finite length

Let us now consider the same problem for a string of finite length between fixed supports, with a initial displacement $W(x)$ and no initial velocity:

$$\left\{ \begin{array}{ll} \frac{\partial^2 w}{\partial x^2} - \frac{1}{c^2} \frac{\partial^2 w}{\partial t^2} = 0 & 0 < x < L \\ w(x, 0) = W(x) & \dot{w}(x, 0) = 0 \\ w(0, t) = w(L, t) = 0 \end{array} \right. \quad (4.218)$$

The general result (4.216) remains valid, but the boundary conditions in space imply that:

$$W(0) = W(L) = 0 \quad (4.219)$$

Taking the normal modes $w_{(r)}(x) = \sin \frac{r\pi x}{L}$ satisfying the same boundary conditions, $W(x)$ can be expanded in the form:

$$W(x) = \sum_{r=0}^{\infty} a_r w_{(r)}(x) \quad (4.220)$$

with the coefficients:

$$a_r = \frac{\int_0^L W(x)w_{(r)}(x)dx}{\int_0^L w_{(r)}^2(x)dx} \quad (4.221)$$

yielding for the string between fixed supports:

$$a_r = \frac{2}{L} \int_0^L W(x) \sin \frac{r\pi x}{L} dx \quad (4.222)$$

We get thus:

$$w(x, t) = \frac{1}{2} \sum_{r=1}^{\infty} a_r \left[\sin \frac{r\pi(x - ct)}{L} + \sin \frac{r\pi(x + ct)}{L} \right] \quad (4.223)$$

The solution takes thus the form of an infinite set of signals of sinusoidal shape *travelling in opposite directions at the same constant phase speed* c .

Equation (4.223) can also be transformed into:

$$w(x, t) = \sum_{r=1}^{\infty} a_r \sin \frac{r\pi x}{L} \cos \frac{r\pi ct}{L} \quad (4.224)$$

It shows that the travelling waves combine to generate standing waves which are the vibration modes of the string.

Let us finally note that it is customary to associate to Equation (4.224) the following quantities:

$$\begin{aligned} k_r &= \frac{r}{2L} && \text{the wave number of mode } r \\ \lambda_r &= \frac{1}{k_r} && \text{its wave length (i.e. spatial period)} \\ \omega_r &= \frac{r\pi c}{L} = 2\pi k_r c && \text{its natural frequency} \end{aligned}$$

Example 4.4

Let us consider the string with fixed ends submitted to the initial displacement field:

$$W(x) = \begin{cases} 0 & x < \frac{L-a}{2} \\ \frac{(2x-L+a)^2(2x-L-a)^2}{a^4} & \frac{L-a}{2} \leq x \leq \frac{L+a}{2} \\ 0 & x > \frac{L+a}{2} \end{cases}$$

The coefficients of the modal expansion (4.220) are obtained from (4.222) as:

$$a_r = \frac{128L^4}{a^4(r\pi)^5} \sin\left(\frac{r\pi}{2}\right) \left(12 \sin\left(\frac{r\pi a}{2L}\right) - 6 \frac{r\pi a}{L} \cos\left(\frac{r\pi a}{2L}\right) - \left(\frac{r\pi a}{L}\right)^2 \sin\left(\frac{r\pi a}{2L}\right) \right)$$

Figure 4.21 displays the response computed at different time instants with the following values: $L = 20$, $a = 2.93$, $c = 1$ and with 100 modes included in the modal expansion. It clearly

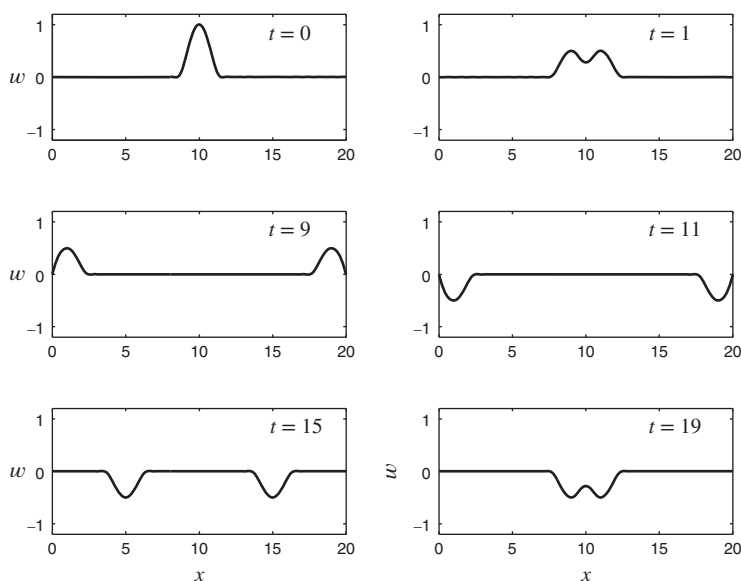


Figure 4.21 Response of string with fixed ends to initial displacement field $W(x)$.

shows the physical nature of the response: the initial shape splits into two equal waves travelling in opposite directions. They are reflected by the string boundaries at $t = 10$. There is no alteration of the initial shape $W(x)$ since all component waves travel at the same speed.

4.3.3 Transverse vibration of beams with no shear deflection

Euler-Bernoulli beam theory (also known as engineer's beam theory or *classical beam theory*) (Timoshenko 1937) is a simplification of the linear theory of elasticity which provides a simple means of calculating the load-carrying and deflection characteristics of beams by introducing the kinematic assumption that a cross-section plane does not deform and thus undergoes only rigid displacements and rotation. It provides an accurate solution for a large class of beam vibration and dynamics problems. In its early version, the rotatory inertia of cross-sections was also neglected. As will be seen in Section 4.3.5, the latter effect was introduced by Rayleigh (Lord Rayleigh 1894) in order to properly represent the phenomenon of longitudinal wave propagation in beams. When the rotatory inertia of cross-sections is included, the resulting beam model is generally referred to as *Rayleigh's beam model*.

Kinematic assumptions

Let us consider a beam of length ℓ , of mass density ρ_0 ($\simeq \rho$ in small deformations) and of cross-section area A . The axis system $Oxyz$ is such that Oz and Oy correspond to the principal

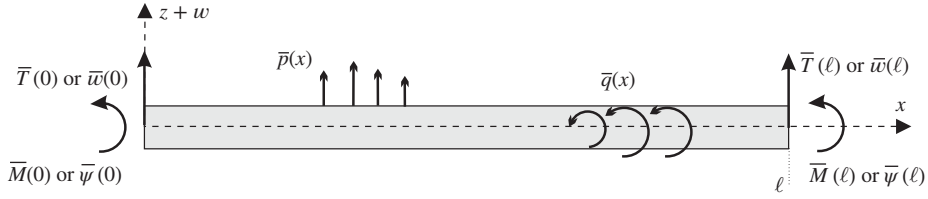


Figure 4.22 Definitions of loads and axis for transverse vibration of beams.

inertia axes. To analyze the transverse vibrations of the beam in bending, let us introduce the following kinematic assumptions:

1. The beam cross-section is not deformable;
2. The transverse displacement on it is uniform and, for simplicity's sake, is limited to the transverse displacement in the Oxz plane:⁹

$$w = w(x) \quad v = 0 \quad (4.225)$$

3. The axial displacement component results from the rotation of the cross-section. The rotation is such that the cross-sections remain orthogonal to the neutral axis:

$$u(x, z) = -z \frac{\partial w}{\partial x} \quad (4.226)$$

With the assumption of geometric linearity, we write the strain expressions:

$$\epsilon_x = \frac{\partial u}{\partial x} = -z \frac{\partial^2 w}{\partial x^2} \quad (4.227a)$$

$$\epsilon_z = \frac{\partial w}{\partial z} = 0 \quad (4.227b)$$

$$\epsilon_{xz} = \frac{1}{2} \left(\frac{\partial w}{\partial x} + \frac{\partial u}{\partial z} \right) = 0 \quad (4.227c)$$

Equation (4.227c) shows that assumption (4.226) is equivalent to neglecting the shear deformation of the material. This assumption, called the *Bernoulli* assumption, is illustrated by Figure 4.23.

Energy expressions and equation of motion of the beam with no prestress

Given (4.227a, 4.227c) the strain energy of the system is written:

$$\begin{aligned} \mathcal{V}_{int} &= \frac{1}{2} \int_A \int_0^\ell E z^2 \left(\frac{\partial^2 w}{\partial x^2} \right)^2 dx dA \\ &= \frac{1}{2} \int_0^\ell EI \left(\frac{\partial^2 w}{\partial x^2} \right)^2 dx \end{aligned} \quad (4.228)$$

⁹ If the neutral line of the beam is chosen as definition for the x axis, the transverse, mean longitudinal (axial) and torsional behaviours can be regarded as decoupled.

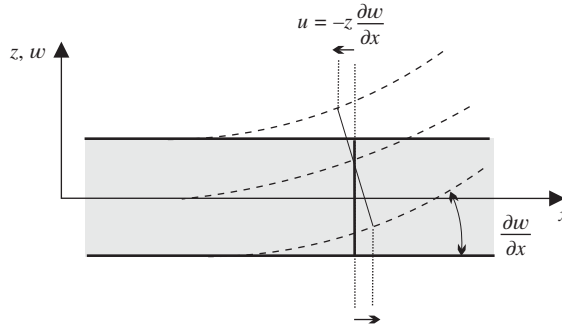


Figure 4.23 Bernoulli's kinematic assumption.

where

$I(x) = \int_A z^2 dA$ is the geometric moment of inertia of the cross-section

EI is the *bending stiffness* of the cross-section

$\frac{\partial^2 w}{\partial x^2}$ is the beam curvature

The kinetic energy is given by:

$$\begin{aligned}
 \mathcal{T} &= \frac{1}{2} \int_0^\ell \int_{A(x)} \rho (\dot{u}^2 + \dot{w}^2) dA dx \\
 &= \frac{1}{2} \int_0^\ell \int_{A(x)} \rho \left[z^2 \left(\frac{\partial \dot{w}}{\partial x} \right)^2 + \dot{w}^2 \right] dA dx \\
 &= \frac{1}{2} \int_0^\ell \rho I \left(\frac{\partial \dot{w}}{\partial x} \right)^2 dx + \frac{1}{2} \int_0^\ell \rho A \dot{w}^2 dx
 \end{aligned} \tag{4.229}$$

By defining next:

$m = A\rho$ the mass per unit of beam length

$r^2 = \frac{I}{A}$ where r is the gyration radius of the cross-section

we obtain the expression:

$$\mathcal{T} = \frac{1}{2} \int_0^\ell m \dot{w}^2 dx + \frac{1}{2} \int_0^\ell m r^2 \left(\frac{\partial \dot{w}}{\partial x} \right)^2 dx \tag{4.230}$$

The first term describes the kinetic energy for vertical translation, while the second is the rotational kinetic energy of the cross-sections.

In order to compute the potential energy of the external forces, we will suppose that the beam is subjected to a distributed vertical load $\bar{p}(x, t)$ and to distributed moments $\bar{q}(x, t)$ per unit length.¹⁰ At the beam ends, either the shear loads \bar{T} or the bending torques \bar{M} are applied or the

¹⁰ Concentrated loads may be considered as distributed loads with Dirac distribution function.

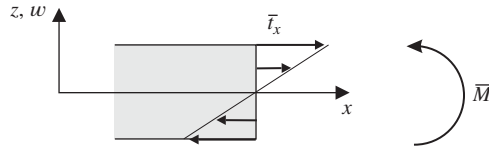


Figure 4.24 External bending torque as resultant of external surface tractions.

displacements \bar{w} or rotations $\bar{\psi}$ are imposed (Figure 4.22). We consider again that the external loads are dead loads, the case of displacement dependent loads being treated as explained earlier.

The externally applied moments \bar{M} originate from surface tractions \bar{t}_x and can be computed by expressing the associated potential (see Figure 4.24):

$$\begin{aligned}\mathcal{V}_{ext,M} &= - \int_A u \bar{t}_x dA \\ &= - \int_A \left(-z \frac{\partial w}{\partial x} \right) \bar{t}_x dA \\ &= -\bar{M} \frac{\partial w}{\partial x}\end{aligned}\quad (4.231)$$

and the total potential of external loads is written:

$$\begin{aligned}\mathcal{V}_{ext} &= - \int_0^\ell \bar{p} w dx - \int_0^\ell \bar{q} \frac{\partial w}{\partial x} dx - \bar{T}(0)w(0) - \bar{T}(\ell)w(\ell) \\ &\quad - \bar{M}(0) \left(\frac{\partial w}{\partial x} \right)_0 - \bar{M}(\ell) \left(\frac{\partial w}{\partial x} \right)_\ell\end{aligned}\quad (4.232)$$

Derivation of dynamic equilibrium equation from Hamilton's principle

Let us apply Hamilton's principle in the form (4.19):

$$\begin{aligned}\int_{t_1}^{t_2} \left\{ \int_0^\ell \left[m \dot{w} \delta \dot{w} + m r^2 \frac{\partial \dot{w}}{\partial x} \delta \left(\frac{\partial \dot{w}}{\partial x} \right) - EI \frac{\partial^2 w}{\partial x^2} \delta \left(\frac{\partial^2 w}{\partial x^2} \right) + \bar{p} \delta w + \bar{q} \delta \left(\frac{\partial w}{\partial x} \right) \right] dx \right. \\ \left. + \bar{T}(0) \delta w(0) + \bar{T}(\ell) \delta w(\ell) + \bar{M}(0) \left(\frac{\partial w}{\partial x} \right)_0 + \bar{M}(\ell) \left(\frac{\partial w}{\partial x} \right)_\ell \right\} dt = 0\end{aligned}\quad (4.233)$$

Integrating by parts both in time and in space and recalling the fixed-end condition in time (4.18) yields:

$$\begin{aligned}\int_{t_1}^{t_2} \left\{ \int_0^\ell \left[-m \ddot{w} + \frac{\partial}{\partial x} \left(m r^2 \frac{\partial \ddot{w}}{\partial x} \right) - \frac{\partial^2}{\partial x^2} \left(EI \frac{\partial^2 w}{\partial x^2} \right) + \bar{p} - \frac{\partial \bar{q}}{\partial x} \right] \delta w dx \right. \\ \left. + \left[\left\{ \frac{\partial}{\partial x} \left(EI \frac{\partial^2 w}{\partial x^2} \right) + \bar{q} - m r^2 \frac{\partial \ddot{w}}{\partial x} \right\} \delta w - EI \frac{\partial^2 w}{\partial x^2} \delta \left(\frac{\partial w}{\partial x} \right) \right]_0^\ell \right. \\ \left. + \bar{T}(0) \delta w(0) + \bar{T}(\ell) \delta w(\ell) + \bar{M}(0) \left(\frac{\partial w}{\partial x} \right)_0 + \bar{M}(\ell) \left(\frac{\partial w}{\partial x} \right)_\ell \right\} dt = 0\end{aligned}\quad (4.234)$$

we obtain the equation of motion:

$$m\ddot{w} - \frac{\partial}{\partial x} \left(mr^2 \frac{\partial \ddot{w}}{\partial x} \right) + \frac{\partial^2}{\partial x^2} \left(EI \frac{\partial^2 w}{\partial x^2} \right) = \bar{p} - \frac{\partial \bar{q}}{\partial x} \quad (4.235)$$

with the boundary conditions at $x = 0$ and at $x = \ell$ on rotation $\frac{\partial w}{\partial x}$ and transverse displacement w (taking also into account the direction cosine $n_x = \pm 1$ of the outward normal):

$$\begin{cases} \frac{\partial w}{\partial x} = \bar{\psi} & \text{or} & M = EI \frac{\partial^2 w}{\partial x^2} = n_x \bar{M} \\ w = \bar{w} & \text{or} & T = \left[mr^2 \frac{\partial \ddot{w}}{\partial x} - \frac{\partial}{\partial x} \left(EI \frac{\partial^2 w}{\partial x^2} \right) - \bar{q} \right] = n_x \bar{T} \end{cases} \quad (4.236)$$

where M and T are defined as the internal bending moment and shear force, respectively, as explained next.

Derivation of motion equation through expression of local equilibrium

Equation (4.235) is a linearized form of local equilibrium. This can be easily verified by introducing the bending and shear resultants $M(x)$ and $T(x)$ on the beam segment (Figure 4.25):

– Rotational equilibrium:

$$M(x) - M(x + dx) - T(x)dx + (\bar{p} - m\ddot{w})dx \frac{dx}{2} = \left(\bar{q} - mr^2 \frac{\partial \ddot{w}}{\partial x} \right) dx \quad (4.237)$$

and by making dx tend to 0,

$$T(x) = -\frac{\partial M}{\partial x} + mr^2 \frac{\partial \ddot{w}}{\partial x} - \bar{q} \quad (4.238)$$

– Translational equilibrium:

$$\begin{aligned} \bar{p} dx - T(x) + T(x + dx) &= m\ddot{w} dx \\ \bar{p} + \frac{\partial T}{\partial x} &= m\ddot{w} \end{aligned} \quad (4.239)$$

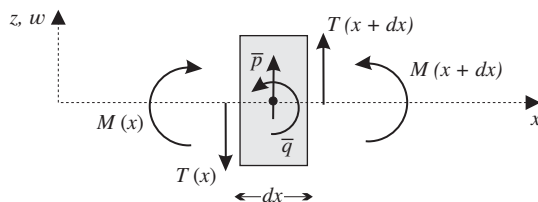


Figure 4.25 Equilibrium of a beam segment.

and by substituting (4.238) into (4.239):

$$\frac{\partial^2 M}{\partial x^2} - \frac{\partial}{\partial x} \left(mr^2 \frac{\partial \ddot{w}}{\partial x} \right) + m\ddot{w} = \bar{p} - \frac{\partial \bar{q}}{\partial x} \quad (4.240)$$

which is equivalent to Equation (4.235) if account is taken of the moment–curvature relationship:

$$M = EI \frac{\partial^2 w}{\partial x^2} \quad (4.241)$$

Equation (4.241) expresses the linear dependence between the internal bending moment M and the *beam curvature* with the bending stiffness EI as coefficient. It can be regarded as the constitutive equation for the beam undergoing pure bending.

Free vibration of the beam without shear deformation

The equation of free vibration of the beam is deduced from (4.235) by assuming harmonic motion $w(x, t) = w(x) \sin \omega t$:

$$\frac{d^2}{dx^2} \left(EI \frac{d^2 w}{dx^2} \right) - \omega^2 mw + \omega^2 \frac{d}{dx} \left(mr^2 \frac{dw}{dx} \right) = 0 \quad (4.242)$$

The kinematic assumption of no shear deformation remains valid provided that the ratio $\frac{l}{A} = r^2$ remains small. It is thus consistent in this case to neglect the rotatory inertia¹¹ of the cross-sections, so that the free vibration equation of the beam becomes:

$$\boxed{\frac{d^2}{dx^2} \left(EI \frac{d^2 w}{dx^2} \right) - \omega^2 mw = 0} \quad (4.243)$$

with the associated boundary conditions on rotation and displacement at $x = 0$ and $x = \ell$:

$$\begin{cases} w = 0 & \text{or} & T = \frac{d}{dx} \left(EI \frac{d^2 w}{dx^2} \right) = 0 \\ \frac{dw}{dx} = 0 & \text{or} & M = EI \frac{d^2 w}{dx^2} = 0 \end{cases} \quad (4.244)$$

Eigenmodes and frequencies of the uniform beam with no prestress

When the bending stiffness EI and the mass per unit length m remain constant over the beam length, the eigenvalue problem (4.235) becomes:

$$\frac{d^4 w}{dx^4} - \omega^2 \frac{m}{EI} w = 0 \quad (4.245)$$

It can be formulated in a nondimensional form by setting:

$$\xi = \frac{x}{\ell} \quad \text{and} \quad \eta = \frac{w}{\ell}$$

¹¹ However, as will be seen hereafter, the rotary inertia effect becomes important when considering wave propagation in the beam.

Equation (4.245) becomes:

$$\eta'''' - \mu^4 \eta = 0 \quad (4.246)$$

with the notation $(\)' = \frac{d}{d\xi}$ and by introducing the nondimensional eigenvalue:

$$\mu^4 = \omega^2 \frac{ml^4}{EI} \quad (4.247)$$

The general solution to (4.246) is of the form

$$\eta = e^{p\xi}$$

with the roots $p_{1,2} = \pm\mu$ and $p_{3,4} = \pm i\mu$. Hence the complete solution:

$$\eta = \alpha_1 e^{\mu\xi} + \alpha_2 e^{-\mu\xi} + \alpha_3 e^{i\mu\xi} + \alpha_4 e^{-i\mu\xi}$$

In general, it is preferable to make use of the *Duncan* functions:

$$\begin{aligned} s_1(\mu\xi) &= \sin(\mu\xi) + \sinh(\mu\xi) & c_1(\mu\xi) &= \cos(\mu\xi) + \cosh(\mu\xi) \\ s_2(\mu\xi) &= -\sin(\mu\xi) + \sinh(\mu\xi) & c_2(\mu\xi) &= -\cos(\mu\xi) + \cosh(\mu\xi) \end{aligned} \quad (4.248)$$

which have the interesting property of deriving from one another according to:

$$c_2(\mu\xi) = \frac{1}{\mu} s_2'(\mu\xi) = \frac{1}{\mu^2} c_1''(\mu\xi) = \frac{1}{\mu^3} s_1'''(\mu\xi)$$

The general solution is then rewritten in the form:

$$\eta = As_1(\mu\xi) + Bc_1(\mu\xi) + Cs_2(\mu\xi) + Dc_2(\mu\xi) \quad (4.249)$$

Example 4.5

Let us consider the clamped-free beam: the conditions at the clamped end:

$$\eta(0) = \eta'(0) = 0$$

yield

$$B = \mu \quad A = 0 \quad (E4.5.a)$$

while we have at the free end

$$\eta''(1) = \eta'''(1) = 0$$

giving:

$$\begin{aligned} \mu^2 [Cs_1(\mu) + Dc_1(\mu)] &= 0 \\ \mu^3 [Cc_1(\mu) + Ds_2(\mu)] &= 0 \end{aligned} \quad (E4.5.b)$$

The solution $\mu = 0$ would correspond to a rigid-body mode, which is physically impossible due to the boundary conditions. Hence the eigenvalue equation of transcendental form:

$$s_1(\mu)s_2(\mu) - c_1^2(\mu) = 0$$

which, in terms of trigonometric and hyperbolic functions, becomes:

$$\cosh \mu \cos \mu + 1 = 0 \quad (E4.5.c)$$

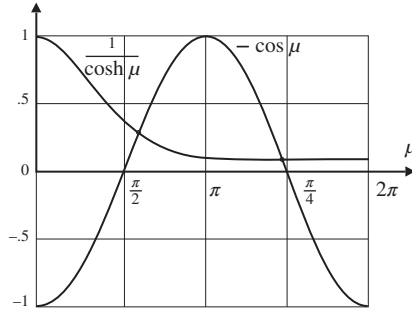


Figure 4.26 Iterative solution of the eigenvalue equation of a clamped–free beam.

Numerical solution

This problem can be solved iteratively when rewritten in the form:

$$-\cos \mu = \frac{1}{\cosh \mu}$$

It is then observed (Figure 4.5) that the roots μ_1, μ_2, \dots correspond to the crossing points of the curves:

$$f_1(\mu) = \frac{1}{\cosh \mu} \quad \text{and} \quad f_2(\mu) = -\cos \mu$$

Starting from an initial value $\mu_k^{(0)}$ that may be approximated by:

$$\mu_k^{(0)} \simeq (2k-1)\frac{\pi}{2} \quad (\text{E4.5.d})$$

the successive estimates $\mu_k^{(i)}$ given by the iterative process:

$$\mu_k^{(i+1)} = \cos^{-1} \left(\frac{-1}{\cosh(\mu_k^{(i)})} \right) \quad (\text{E4.5.e})$$

converge towards the exact value μ_k . For the fundamental eigenvalue we obtain:

$$\mu_1 = 1.8751 \quad \text{and} \quad \omega_1^2 = 12.36 \frac{EI}{m\ell^4}$$

Asymptotic solution

If only a good approximation to the eigenspectrum μ_k is required, it is possible to improve the zero-order approximation (E4.5.d) by a first-order correction when expressing the solutions of (E4.5.c) in the form:

$$\mu_k = (2k-1)\frac{\pi}{2} + \epsilon_k \quad k = 1, \dots, \infty$$

The correction ϵ_k is then computed in an asymptotic manner:

$$\cos \left[(2k-1)\frac{\pi}{2} + \epsilon_k \right] \cosh \left[(2k-1)\frac{\pi}{2} + \epsilon_k \right] + 1 = 0$$

Table 4.3 Vibration eigenfrequencies of a uniform beam under several boundary conditions

Boundary conditions	Eigenvalue μ_n			
	$n = 1$	$n = 2$	$n = 3$	$n > 3$
free–free	0	4.730	7.853	$(2n - 1)\frac{\pi}{2}$ (approx.)
free–guided	0	2.365	5.498	$(4n - 5)\frac{\pi}{2}$ (approx.)
free–pinned	0	3.927	7.069	$(4n - 3)\frac{\pi}{4}$ (approx.)
guided–guided	0	3.142	6.283	$(n - 1)\pi$ (exact)
guided–pinned	1.561	5.712	7.854	$(2n - 1)\frac{\pi}{2}$ (exact)
clamped–free	1.875	4.694	7.855	$(2n - 1)\frac{\pi}{2}$ (approx.)
bipinned	3.142	6.283	9.425	$n\pi$ (exact)
clamped–pinned	3.927	7.069	10.210	$(4n + 1)\frac{\pi}{4}$ (approx.)
clamped–guided	2.365	5.498	8.639	$(4n - 1)\frac{\pi}{4}$ (approx.)
biclampped	4.730	7.853	10.996	$(2n + 1)\frac{\pi}{2}$ (approx.)

$$\text{Circular frequency: } \omega_n = u_n^2 \sqrt{\frac{EI}{m\ell^4}}$$

By expanding this expression we obtain:

$$-\sin \epsilon_k \sin \left[(2k - 1)\frac{\pi}{2} \right] \left\{ \cosh \left[(2k - 1)\frac{\pi}{2} \right] \cosh \epsilon_k - \sinh \left[(2k - 1)\frac{\pi}{2} \right] \sinh \epsilon_k \right\} + 1 = 0$$

or, by making use of the approximations $\sinh \epsilon_k \simeq \sin \epsilon_k \simeq \epsilon_k$ and $\cosh \epsilon_k \simeq 1$ we obtain:

$$\epsilon_k = \frac{(-1)^{k-1}}{\cosh \left[(2k - 1)\frac{\pi}{2} \right]}$$

whence the asymptotic approximation:

$$\mu_k = (2k - 1)\frac{\pi}{2} + \frac{(-1)^{k-1}}{\cosh \left[(2k - 1)\frac{\pi}{2} \right]}$$

We obtain for the first eigenvalues the approximations:

$$\begin{array}{ll} \mu_1 \simeq 1.9693 & \mu_1 = 1.8751 \\ \mu_2 \simeq 4.6944 & \text{instead of } \mu_2 = 4.6941 \\ \mu_3 \simeq 7.8548 & \mu_3 = 7.8548 \end{array}$$

Whatever be the boundary conditions, all cases can be treated in the same way as is given above. The results obtained are displayed in the eigenfrequency Table 4.3.

Response to external excitation: mode superposition

Let us consider the case of a simply supported beam as depicted on Figure 4.27. It is suddenly subjected to the static load:

$$\bar{p}(x, t) = p_0 \frac{x}{\ell}$$

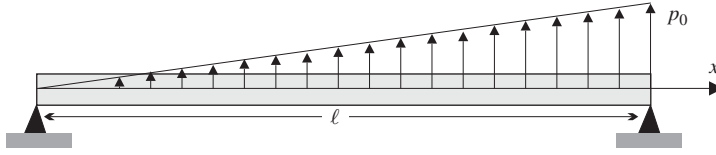


Figure 4.27 Excitation applied to a simply supported beam.

To determine the beam response versus time let us first compute the eigenmodes of the simply supported beam, verifying the eigenvalue equation with the homogeneous boundary conditions:

$$EI \frac{d^4 w}{dx^4} - \omega^2 m w = 0 \quad 0 < x < \ell$$

$$w = \frac{d^2 w}{dx^2} = 0 \quad \text{at } x = 0, \ell$$

It is easily verified that after normalization they can be expressed as:

$$w_{(n)}(x) = \sqrt{\frac{2}{m\ell}} \sin \frac{n\pi x}{\ell} \quad n = 1, 2, \dots$$

with the associated eigenvalues:

$$\omega_n^2 = (n\pi)^4 \frac{EI}{m\ell^4}$$

The participation factors (4.77) are expressed by:

$$\begin{aligned} \phi_n &= \int_0^\ell \sqrt{\frac{2}{m\ell}} \sin \frac{n\pi x}{\ell} p_0 \frac{x}{\ell} dx \\ &= -\sqrt{\frac{2}{m\ell}} p_0 \left\{ \left[\frac{\ell}{n\pi} \frac{x}{\ell} \cos \frac{n\pi x}{\ell} \right]_0^\ell - \int_0^\ell \frac{1}{n\pi} \cos \frac{n\pi x}{\ell} dx \right\} \\ &= -\sqrt{\frac{2}{m\ell}} p_0 \left[\frac{x}{n\pi} \cos \frac{n\pi x}{\ell} - \frac{\ell}{n^2 \pi^2} \sin \frac{n\pi x}{\ell} \right]_0^\ell \\ &= -\sqrt{\frac{2}{m\ell}} p_0 \frac{\ell}{n\pi} \cos n\pi \end{aligned}$$

hence

$$\phi_n = \sqrt{\frac{2}{m\ell}} \frac{p_0 \ell}{n\pi} (-1)^{n+1}$$

Thus the normal equation governing the time variation of the normal coordinates is:

$$\omega_n^2 \eta_n + \ddot{\eta}_n = \sqrt{\frac{2}{m\ell}} \frac{p_0 \ell}{n\pi} (-1)^{n+1}$$

Under the condition that the structure is at rest when the load is applied, the solution is:

$$\eta_n(t) = \frac{p_0 \ell}{n\pi} \sqrt{\frac{2}{m\ell}} \frac{(-1)^{n+1}}{\omega_n^2} (1 - \cos \omega_n t)$$

The beam response is then reconstructed through the modal superposition relationship (4.73):

$$w(x, t) = \sum_{s=1}^{\infty} \frac{2p_0(-1)^{s+1}}{s\pi m\omega_s^2} (1 - \cos \omega_s t) \sin \frac{s\pi x}{\ell} \quad (4.250)$$

The beam submitted to initial axial force

When an initial axial load N_0 is applied to a beam, the axial displacements result from the superposition of both the cross-sectional rotation effect according to Bernoulli's assumption and the initial displacement $u_0(x)$:

$$\begin{aligned} u(x, z) &= u_0(x) - z \frac{\partial w}{\partial x} \\ v &= 0 \\ w &= w(x) \end{aligned} \quad (4.251)$$

with

$$N_0(x) = AE\varepsilon_0(x) \quad (4.252)$$

Taking as reference the prestressed beam, the axial strain is written:

$$\varepsilon_x = \varepsilon_0 - z \frac{\partial^2 w}{\partial x^2} + \frac{1}{2} \left[\left(\frac{\partial u}{\partial x} \right)^2 + \left(\frac{\partial w}{\partial x} \right)^2 \right]$$

If one neglects $\left(\frac{\partial u}{\partial x} \right)^2$ compared to $\left(\frac{\partial w}{\partial x} \right)^2$ in the second-order term of the strain expression (large displacement approximation), the additional and geometric strain energies are expressed by:

$$\begin{aligned} \mathcal{V}_{int} &= \frac{1}{2} \int_0^\ell EI \left(\frac{\partial^2 w}{\partial x^2} \right)^2 dx \\ \mathcal{V}_g &= \frac{1}{2} \int_0^\ell N_0 \left(\frac{\partial w}{\partial x} \right)^2 dx \end{aligned} \quad (4.253)$$

Equilibrium equation for the beam with prestress

Hamilton's principle (4.48) for prestressed systems has to be applied in this case. It gives rise to an additional shear contribution in the equation of motion which thus becomes:

$$\frac{\partial^2}{\partial x^2} \left(EI \frac{\partial^2 w}{\partial x^2} \right) - \frac{\partial}{\partial x} \left(N_0 \frac{\partial w}{\partial x} \right) + m\ddot{w} - \frac{\partial}{\partial x} \left(mr^2 \frac{\partial \ddot{w}}{\partial x} \right) = \bar{p} - \frac{\partial \bar{q}}{\partial x} \quad (4.254)$$

The associated boundary conditions on displacement and rotation at $x = 0$ and $x = \ell$ are:

$$\begin{aligned} w &= \bar{w} & \text{or} & & mr^2 \frac{\partial \ddot{w}}{\partial x} - \frac{\partial}{\partial x} \left(EI \frac{\partial^2 w}{\partial x^2} \right) - q + N_0 \frac{\partial w}{\partial x} &= n_x \bar{T} \\ \frac{\partial w}{\partial x} &= \bar{\psi} & \text{or} & & EI \frac{\partial^2 w}{\partial x^2} &= n_x \bar{M} \end{aligned} \quad (4.255)$$

where, as before, $n_x = \pm 1$ is the outward normal of the surface at the extremities of the beam.

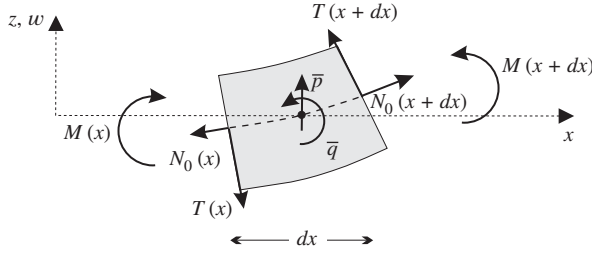


Figure 4.28 Beam segment under axial prestress.

As in the case of no prestress, it is easily verified that the relationships above express local equilibrium of an infinitesimal beam segment (Figure 4.28):

– Rotational equilibrium:

$$\begin{aligned} M(x) - M(x+dx) - \bar{q} dx - T(x)dx \\ + (\bar{p} - m\ddot{w})dx \frac{dx}{2} + N_0(x) \frac{1}{2} \frac{\partial w}{\partial x} dx^2 = -mr^2 \frac{\partial \ddot{w}}{\partial x} dx \end{aligned} \quad (4.256)$$

and when dx tends to zero,

$$T(x) = -\frac{\partial M}{\partial x} - \bar{q} + mr^2 \frac{\partial \ddot{w}}{\partial x} \quad (4.257)$$

– Vertical translational equilibrium:

$$\begin{aligned} -T(x) + T(x+dx) + \bar{p} dx - N_0(x) \frac{\partial w}{\partial x} \Big|_x + N_0(x+dx) \frac{\partial w}{\partial x} \Big|_{x+dx} = m\ddot{w} dx \\ \frac{\partial T}{\partial x} + \bar{p} + \frac{\partial}{\partial x} \left(N_0 \frac{\partial w}{\partial x} \right) = m\ddot{w} \end{aligned} \quad (4.258)$$

and owing to (4.257)

$$\frac{\partial M}{\partial x} - \frac{\partial}{\partial x} \left(N_0 \frac{\partial w}{\partial x} \right) + m\ddot{w} - \frac{\partial}{\partial x} \left(mr^2 \frac{\partial \ddot{w}}{\partial x} \right) = \bar{p} - \frac{\partial \bar{q}}{\partial x} \quad (4.259)$$

which is equivalent to (4.254) when substituting Equation (4.241).

As was explained for the nonprestressed beam, the rotatory inertia term may be neglected so that the *free vibration* equation of the prestressed beam is written:

$$\boxed{\frac{d^2}{dx^2} \left(EI \frac{d^2 w}{dx^2} \right) - \frac{d}{dx} \left(N_0 \frac{dw}{dx} \right) - \omega^2 mw = 0} \quad (4.260)$$

with the associated boundary conditions at $x = 0$ and $x = \ell$ on displacement and rotation:

$$\begin{aligned} w = 0 \quad \text{or} \quad \frac{d}{dx} \left(EI \frac{d^2 w}{dx^2} \right) - N_0 \frac{dw}{dx} = 0 \\ \frac{dw}{dx} = 0 \quad \text{or} \quad EI \frac{d^2 w}{dx^2} = 0 \end{aligned} \quad (4.261)$$

Eigenmodes and frequencies of a uniform simply supported prestressed beam

Considering the case of the uniform simply supported beam subjected to a constant axial prestress, the solution of the free vibration equation can be generally stated:

$$w(x) = a \sin \frac{n\pi x}{\ell} \quad n = 1, 2, \dots \quad (4.262)$$

This function verifies the boundary conditions, and by substitution into (4.260) one finds:

$$EI \left(\frac{n\pi}{\ell} \right)^4 + N_0 \left(\frac{n\pi}{\ell} \right)^2 - m\omega_n^2 = 0 \quad (4.263)$$

hence:

$$\begin{aligned} \omega_n^2 &= \left(\frac{n\pi}{\ell} \right)^4 \left[\frac{EI}{m} \left(1 + \frac{N_0 \ell^2}{n^2 \pi^2 EI} \right) \right] \\ &= \left(\frac{n\pi}{\ell} \right)^4 \left[\frac{EI}{m} \left(1 - \frac{N_0}{N_{cr,n}} \right) \right] \end{aligned} \quad (4.264)$$

by defining:

$$N_{cr,n} = -\frac{n^2 \pi^2 EI}{\ell^2} \quad (4.265)$$

to be the critical load such as when $N_0 = N_{cr,n}$, the eigenfrequencies ω_n become zero. In that case, the beam takes a nonzero but static deflected shape: it corresponds to global buckling of the beam, also called *Euler* buckling. Obviously, the buckling load, also called the stability limit, is the minimum of the $N_{cr,n}$:

$$N_{cr} = -\frac{\pi^2 EI}{\ell^2} = N_{cr,1} \quad (4.266)$$

In this manner it is shown that the first beam eigenfrequency vanishes for a compression force equal to the buckling load. This result was foreseeable since for the simply supported beam the first vibration mode has the same shape as the buckling mode.

Let us also note that eigenfrequencies are systematically lowered by a compression load and increased by a traction force. This observation is true for any straight beam regardless of its boundary conditions. Equation (4.264) shows that the eigenvalues decrease linearly with the axial load, the first one vanishing when the buckling load is reached. This result can be exploited to experimentally measure a buckling load through extrapolation without actually reaching the buckling load and destroying thus the specimen under testing.

Free vibration of a rotating beam

The rotating beam problem is a particular case of the prestressed beam, the practical importance of which is considerable especially in aeronautical engineering (for propeller, helicopter, turbine blades). Here we will limit ourselves to a very simplified analysis of the problem. Let us consider the system of Figure 4.29, made of a beam clamped at a distance e from the rotation axis Oz and rotating at constant speed Ω . To simplify the analysis, it is supposed that both the rotation speed Ω and the vibration frequencies are low enough to allow us to neglect the

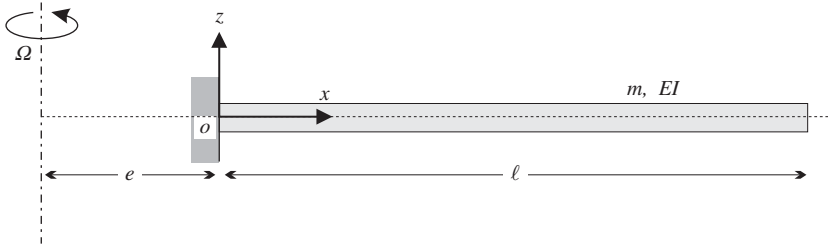


Figure 4.29 Vibrations of a rotating beam.

gyroscopic forces. Considering then the axial load on a cross-section arising from the centrifugal force of the bar segment between the section and the end, the axial prestress force N_0 is given by:

$$N_0(x) = \int_x^\ell m\Omega^2 (e + \xi + u) d\xi \quad (4.267)$$

or, to the first order and if m is constant,

$$\begin{aligned} N_0(x) &= \int_x^\ell m\Omega^2 (e + \xi) d\xi \\ &= m\Omega^2 \left[\frac{(\ell + e)^2}{2} - \frac{(x + e)^2}{2} \right] \end{aligned} \quad (4.268)$$

The free vibration Equation (4.260) then becomes:

$$\frac{d^2}{dx^2} \left(EI \frac{d^2 w}{dx^2} \right) - \frac{d}{dx} \left\{ m\Omega^2 \left[\frac{(\ell + e)^2}{2} - \frac{(x + e)^2}{2} \right] \frac{dw}{dx} \right\} - \omega^2 m w = 0 \quad (4.269)$$

with the associated boundary conditions at $x = 0$ and $x = \ell$:

$$\begin{aligned} w &= 0 & \text{or} & \quad \frac{d}{dx} \left(EI \frac{d^2 w}{dx^2} \right) - m\Omega^2 \left[\frac{(\ell + e)^2}{2} - \frac{(x + e)^2}{2} \right] \frac{dw}{dx} = 0 \\ \frac{dw}{dx} &= 0 & \text{or} & \quad EI \frac{d^2 w}{dx^2} = 0 \end{aligned} \quad (4.270)$$

Particular case: eigenfrequency of the hinged rigid blade

Let us now consider the case of a rigid blade hinged at a distance e from the rotation axis (Figure 4.30). The blade being rigid, the only admissible function $w(x)$ is:

$$w(x, t) = \alpha x \sin \omega t \quad (4.271)$$

where α , the rotation angle in the vertical plane about the hinge, is the only degree of freedom of the system. The energy expressions of the blade are given by:

$$\mathcal{V}_{int} = 0$$

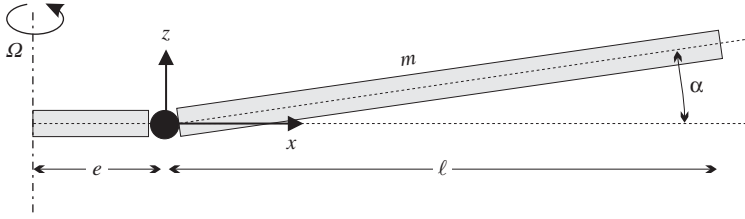


Figure 4.30 Free vibration of a hinged rigid blade.

$$\mathcal{V}_g = \frac{1}{2} \sin^2 \omega t \int_0^\ell N(x) \alpha^2 dx \quad (4.272)$$

$$\mathcal{T} = \frac{1}{2} \omega^2 \cos^2 \omega t \int_0^\ell m \alpha^2 x^2 dx$$

and the application of Hamilton's principle yields the relation:

$$\alpha \delta \alpha \int_0^\ell m \Omega^2 \left[\frac{(\ell + e)^2}{2} - \frac{(x + e)^2}{2} \right] dx - \alpha \delta \alpha \int_0^\ell \omega^2 m x^2 dx = 0 \quad (4.273)$$

Discarding the trivial solution $\alpha = 0$ and, since the variation $\delta \alpha$ is arbitrary, we obtain the vibration frequency:

$$\omega^2 = \Omega^2 \left[1 + \frac{3e}{2\ell} \right] \quad (4.274)$$

showing that, when the blade offset is zero, the vibration frequency coincides with the angular velocity.

4.3.4 Transverse vibration of beams including shear deflection

The Euler-Bernoulli beam model described in the previous section is conceptually simple and provides accurate results in most situations, but shows physical limitations due to the absence of shear deformation linked to the shear force. A more accurate beam model that takes also into account the shear deformation mechanism has been introduced by Timoshenko (Timoshenko 1921, 1922).

Kinematic assumptions

Let us consider again the beam of Figure 4.22 subjected to bending along one principal axis of inertia. Assumptions (1) and (2) of Section 4.3.3, Page 264 remain valid. On the other hand, the assumption that cross-sections remain orthogonal to the neutral axis is abandoned. The shear deflection of the cross-sections is taken into account by introducing a new variable ψ , the rotation of cross-sections (Figure 4.31). The displacements are then expressed by:

$$\begin{aligned} u(x, z) &= -z\psi(x) \\ v &= 0 \\ w &= w(x) \end{aligned} \quad (4.275)$$

where $\psi(x)$ is independent of w . The first-order approximations to the strains are:

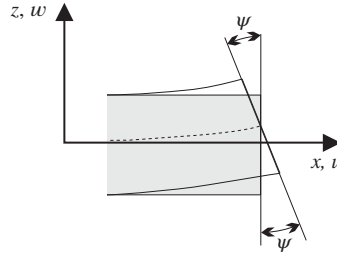


Figure 4.31 Rotation of cross-sections.

$$\begin{aligned}
 \epsilon_x &= \frac{\partial u}{\partial x} = -z \frac{\partial \psi}{\partial x} \\
 \epsilon_z &= 0 \\
 \gamma_{xz} &= 2\epsilon_{xz} \\
 &= \frac{\partial u}{\partial z} + \frac{\partial w}{\partial x} = -\psi + \frac{\partial w}{\partial x}
 \end{aligned} \tag{4.276}$$

the shear strain ϵ_{xz} being nonzero in general, according to the assumptions.

Energy expressions

The strain energy is equal to:

$$\mathcal{V}_{int} = \frac{1}{2} \int_0^\ell \left\{ \int_A E z^2 \left(\frac{\partial \psi}{\partial x} \right)^2 dA + \int_A \sigma_{xz} \left(-\psi + \frac{\partial w}{\partial x} \right) dA \right\} dx \tag{4.277}$$

In order to account for the fact that shear is distributed parabolically on a cross-section it is common to introduce a cross-sectional reduction factor k' in such a way that:

$$\int_A \sigma_{xz} dA = k' A G \gamma_{xz} \tag{4.278}$$

where A is the cross-sectional area and G is the shear modulus of the material. The factor $k'A$ is called *reduced section* and is computed from classical beam theory. For example, factor k' is equal to $5/6$ for a plain rectangular cross-section and $1/1.175$ for a plain circular cross-section. The strain energy is thus written as:

$$\mathcal{V}_{int} = \frac{1}{2} \int_0^\ell \left\{ EI \left(\frac{\partial \psi}{\partial x} \right)^2 + k' A G \left(-\psi + \frac{\partial w}{\partial x} \right)^2 \right\} dx \tag{4.279}$$

The kinetic energy is equal to:

$$\begin{aligned}
 \mathcal{T} &= \frac{1}{2} \int_0^\ell \int_A \rho (\dot{u}^2 + \dot{w}^2) dA dx \\
 &= \frac{1}{2} \int_0^\ell m r^2 \dot{\psi}^2 dx + \frac{1}{2} \int_0^\ell m \dot{w}^2 dx
 \end{aligned} \tag{4.280}$$

where m and r are respectively the mass per unit length and the radius of gyration as previously defined.

The expression of the applied bending torque \overline{M} results from the computation of potential of the surface tractions \bar{t}_x (Figure 4.24 and Equations (4.231)):

$$\mathcal{V}_{ext.M} = -\overline{M}\psi \quad (4.281)$$

and the total potential of external loads is written as:

$$\begin{aligned} \mathcal{V}_{ext} = & - \int_0^\ell (\bar{p}w + \bar{q}\psi) dx \\ & - \bar{T}(0)w(0) - \bar{T}(\ell)w(\ell) - \overline{M}(0)\psi(0) - \overline{M}(\ell)\psi(\ell) \end{aligned} \quad (4.282)$$

Derivation of motion equations from Hamilton's principle

Since both w and ψ are independent continuous variables, the application of Hamilton's principle in the form (4.48) yields:

$$\begin{aligned} \int_{t_1}^{t_2} \left\{ \int_0^\ell \left[mr^2 \dot{\psi} \delta \dot{\psi} + m \dot{w} \delta \dot{w} + \bar{p} \delta w + \bar{q} \delta \psi \right. \right. \\ \left. \left. - EI \frac{\partial \psi}{\partial x} \delta \left(\frac{\partial \psi}{\partial x} \right) - k' AG \left(\frac{\partial w}{\partial x} - \psi \right) \delta \left(\frac{\partial w}{\partial x} - \psi \right) \right] dx \right. \\ \left. + \bar{T}(0) \delta w(0) + \bar{T}(\ell) \delta w(\ell) + \overline{M}(0) \delta \psi(0) + \overline{M}(\ell) \delta \psi(\ell) \right\} dt = 0 \end{aligned} \quad (4.283)$$

Integrating by parts both in time and in space and recalling the fixed-end condition in time (4.18) yields:

$$\begin{aligned} \int_{t_1}^{t_2} \left\{ \int_0^\ell \left[-mr^2 \ddot{\psi} \delta \psi - m \ddot{w} \delta w + \bar{p} \delta w + \bar{q} \delta \psi \right. \right. \\ \left. \left. + \frac{\partial}{\partial x} \left(EI \frac{\partial \psi}{\partial x} \right) \delta \psi + k' AG \left(\frac{\partial w}{\partial x} - \psi \right) \delta \psi + \frac{\partial}{\partial x} \left[k' AG \left(\frac{\partial w}{\partial x} - \psi \right) \right] \delta w \right] dx \right. \\ \left. - \left[EI \frac{\partial \psi}{\partial x} \delta \psi + k' AG \left(\frac{\partial w}{\partial x} - \psi \right) \delta w \right]_0^\ell \right. \\ \left. + \bar{T}(0) \delta w(0) + \bar{T}(\ell) \delta w(\ell) + \overline{M}(0) \delta \psi(0) + \overline{M}(\ell) \delta \psi(\ell) \right\} dt = 0 \end{aligned} \quad (4.284)$$

The variations $\delta \psi$ and δw being arbitrary and independent, one gets the set of equations expressing dynamic equilibrium in translation and rotation:

$$\begin{aligned} \frac{\partial}{\partial x} \left[k'AG \left(\frac{\partial w}{\partial x} - \psi \right) \right] + \bar{p} &= m\ddot{w} \\ \frac{\partial}{\partial x} \left(EI \frac{\partial \psi}{\partial x} \right) + k'AG \left(\frac{\partial w}{\partial x} - \psi \right) + \bar{q} &= mr^2 \ddot{\psi} \end{aligned} \quad (4.285)$$

with the boundary conditions on the displacement and the rotation at $x = 0$ and $x = \ell$:

$$\begin{aligned} w &= \bar{w} & \text{or} & & k'AG \left(\frac{\partial w}{\partial x} - \psi \right) &= n_x \bar{T} \\ \psi &= \bar{\psi} & \text{or} & & EI \frac{\partial \psi}{\partial x} &= n_x \bar{M} \end{aligned} \quad (4.286)$$

taking into account the direction cosine $n_x = \pm 1$ of the outward normal.

Expression of the motion equations through local equilibrium

Once more, let us show that these equations represent, to the first order, the equilibrium of a beam element (Figure 4.32). To that purpose, let us introduce again the internal bending moment M and shear force T .

– Rotational equilibrium:

$$M(x) - M(x + dx) + mr^2 \ddot{\psi} dx + (\bar{p} - m\ddot{w})dx \frac{dx}{2} - T(x)dx - \bar{q} dx = 0 \quad (4.287)$$

and by making dx tend to zero

$$-\frac{\partial M}{\partial x} - T(x) + mr^2 \ddot{\psi} - \bar{q} = 0 \quad (4.288)$$

By noticing then that bending moment and the shear force can be computed through integration on the internal stresses on the cross-section:

$$M = - \int_A z \sigma_x dA = - \int_A z E \varepsilon_x dA = EI \frac{\partial \psi}{\partial x} \quad (4.289)$$

$$T = \int_A \sigma_{xz} dA = k'AG \gamma_{xz} = k'AG \left(\frac{\partial w}{\partial x} - \psi \right) \quad (4.290)$$

we find back the equation governing the rotation ψ .

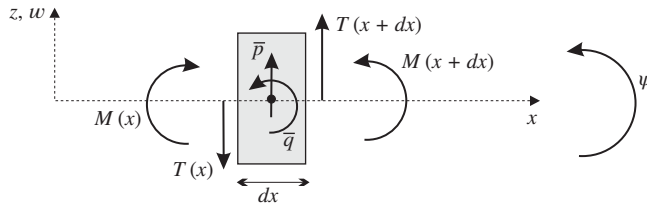


Figure 4.32 Local equilibrium of a beam element.

Equations (4.289) and (4.290) define the constitutive relationships for the beam with shear deformation:

$$\boxed{M = EI \frac{\partial \psi}{\partial x} \quad T = k'AG \left(\frac{\partial w}{\partial x} - \psi \right)} \quad (4.291)$$

They express that the internal bending moment is a linear function of the beam curvature $\frac{\partial \psi}{\partial x}$ with the bending stiffness EI as coefficient, while the internal shear force is proportional to the shear angle $\frac{\partial w}{\partial x} - \psi$ with $k'AG$ as shear stiffness. Contrarily to the Bernoulli model where the shear force is a force resultant without physical meaning, in Timoshenko's model the shear force results from a physical deformation mechanism allowed by the kinematical model.

– Vertical translational equilibrium:

$$\begin{aligned} -T(x) + T(x + dx) + \bar{p} \, dx &= m\ddot{w} \, dx \\ \frac{\partial T}{\partial x} + \bar{p} &= m\ddot{w} \end{aligned} \quad (4.292)$$

and owing to (4.289), the equation of motion governing the vertical displacement w is retrieved.

Timoshenko equation

The behaviour of the shear compliant beam is described by the set of equations of motion (4.296) coupling the rotation and displacement fields ψ and w . In the case of a uniform beam, however, it can be useful to eliminate ψ in order to obtain a single governing equation in w as originally proposed by Timoshenko (see for example Fung 1965).

Supposing, for simplicity's sake, that no external load is applied, the second equation in (4.296) is differentiated with respect to x and the first one rearranged to give:

$$\begin{aligned} \frac{\partial^3 \psi}{\partial x^3} + \frac{k'AG}{EI} \left(\frac{\partial^2 w}{\partial x^2} - \frac{\partial \psi}{\partial x} \right) &= \frac{mr^2}{EI} \frac{\partial^3 \psi}{\partial x \partial t^2} \\ \frac{\partial \psi}{\partial x} &= \frac{\partial^2 w}{\partial x^2} - \frac{m}{k'AG} \frac{\partial^2 w}{\partial t^2} \end{aligned} \quad (4.293)$$

Finally, using the second one to eliminate ψ from the first, we get the fourth-order equation in w known as *Timoshenko equation for lateral vibration of prismatic beams* (Fung 1965):

$$\frac{\partial^4 w}{\partial x^4} - \left(\frac{m}{k'AG} + \frac{mr^2}{EI} \right) \frac{\partial^4 w}{\partial x^2 \partial t^2} + \frac{m}{EI} \frac{\partial^2 w}{\partial t^2} + \frac{m}{k'AG} \frac{mr^2}{EI} \frac{\partial^4 w}{\partial t^4} = 0 \quad (4.294)$$

Free vibration equations

The free vibration equations are deduced from (4.285) by assuming harmonic motion:

$$\begin{aligned} \psi(x, t) &= \psi(x) \sin \omega t \\ w(x, t) &= w(x) \sin \omega t \end{aligned} \quad (4.295)$$

This yields:

$$\boxed{\begin{aligned} \frac{d}{dx} \left(EI \frac{d\psi}{dx} \right) + k'AG \left(\frac{dw}{dx} - \psi \right) + \omega^2 mr^2 \psi &= 0 \\ \frac{d}{dx} \left[k'AG \left(\frac{dw}{dx} - \psi \right) \right] + \omega^2 mw &= 0 \end{aligned}} \quad (4.296)$$

with the boundary conditions on the vertical displacement and on the rotation at $x = 0$ and $x = \ell$:

$$\begin{aligned} w = 0 & \quad \text{or} \quad k'AG \left(\psi - \frac{dw}{dx} \right) = 0 \\ \psi = 0 & \quad \text{or} \quad EI \frac{d\psi}{dx} = 0 \end{aligned} \quad (4.297)$$

For a beam of uniform characteristics, one can also consider Timoshenko's Equation (4.294), which for a free harmonic vibration is written as:

$$\boxed{\frac{d^4 w}{dx^4} + \omega^2 \left\{ \left(\frac{m}{k'AG} + \frac{mr^2}{EI} \right) \frac{d^2 w}{dx^2} - \frac{m}{EI} w \right\} + \omega^4 \frac{m^2 r^2}{k'AGEI} w = 0} \quad (4.298)$$

By combining Equations (4.296) for a uniform beam, we get the relationship between $\psi(x)$ and $w(x)$:

$$\psi = \frac{1}{k'AG - \omega^2 mr^2} \left\{ EI \frac{d^3 w}{dx^3} + \left(EI \frac{\omega^2 m}{k'AG} + k'AG \right) \frac{dw}{dx} \right\} \quad (4.299)$$

Using this result in the boundary condition (4.297) for w and recalling the second relation in (4.293) to substitute $d\psi/dx$ in the boundary condition for the rotation, the boundary conditions may be expressed in terms of $w(x)$:

$$\begin{aligned} w = 0 & \quad \text{or} \quad EI \frac{d^3 w}{dx^3} + \left(\frac{EI}{k'AG} + r^2 \right) \omega^2 m \frac{dw}{dx} = 0 \\ \psi = \text{Eq. (4.299)} = 0 & \quad \text{or} \quad \frac{dw}{dx} = \frac{d^2 w}{dx^2} + \frac{\omega^2 m}{k'AG} w = 0 \end{aligned} \quad (4.300)$$

Free vibrations of the uniform beam

In a general manner, for a uniform beam, the solution to Equation (4.298) may be expressed in the form (Warburton 1976):

$$w(x) = ae^{\frac{\lambda x}{\ell}} \quad (4.301)$$

We get:

$$\frac{\lambda^4}{\ell^4} + \frac{\omega^2}{\ell^2} \left(\frac{m}{k'AG} + \frac{mr^2}{EI} \right) \lambda^2 - \frac{m\omega^2}{EI} + \frac{m^2 r^2}{k'AGEI} \omega^4 = 0 \quad (4.302)$$

Defining next:

$$\begin{aligned} \tilde{\omega}^2 &= \omega^2 \frac{m\ell^4}{EI} && \text{the non dimensional eigenvalue} \\ \alpha^2 &= \frac{r^2}{\ell^2} && \text{the rotatory inertia parameter} \\ \eta^2 &= \frac{EI}{k'AG\ell^2} && \text{the shear parameter} \end{aligned} \quad (4.303)$$

yields the eigenvalue equation:

$$\lambda^4 + \tilde{\omega}^2 (\eta^2 + \alpha^2) \lambda^2 - \tilde{\omega}^2 + \tilde{\omega}^4 \eta^2 \alpha^2 = 0 \quad (4.304)$$

The roots of this quadratic equation in λ^2 are:

$$\lambda^2 = \frac{1}{2} \left[-\tilde{\omega}^2 (\eta^2 + \alpha^2) \pm \sqrt{\tilde{\omega}^4 (\eta^2 + \alpha^2)^2 - 4\tilde{\omega}^2 (\tilde{\omega}^2 \eta^2 \alpha^2 - 1)} \right]$$

hence:

$$\lambda^2 = \frac{1}{2} \left[-\tilde{\omega}^2 (\eta^2 + \alpha^2) \pm \sqrt{\tilde{\omega}^4 (\eta^2 - \alpha^2)^2 + 4\tilde{\omega}^2} \right] \quad (4.305)$$

The eigenvalue equation has one positive and one negative root under the condition:

$$\tilde{\omega}^4 (\eta^2 - \alpha^2)^2 + 4\tilde{\omega}^2 > \tilde{\omega}^4 (\eta^2 + \alpha^2)^2$$

or

$$\tilde{\omega}^2 \eta^2 \alpha^2 < 1 \quad (4.306)$$

It may thus be concluded that as long as the shear and rotatory inertia contributions remain small enough, the roots may be put in the form $\pm i\lambda_1, \pm\lambda_2$ and the general solution takes the form:

$$w(x) = a_1 \sin \frac{\lambda_1 x}{\ell} + a_2 \cos \frac{\lambda_1 x}{\ell} + a_3 \sinh \frac{\lambda_2 x}{\ell} + a_4 \cosh \frac{\lambda_2 x}{\ell} \quad (4.307)$$

The constants a_i as well as the characteristic equation then result from the application of the four boundary conditions of the beam.

The simply supported case

Let us analyze the case of the beam simply supported at both ends. The boundary conditions (4.300) are for that case:

$$w(0) = w(\ell) = 0 \quad (4.308)$$

and

$$\frac{d\psi}{dx} = \frac{d^2 w}{dx^2} + \omega^2 \frac{m}{k'AG} w = 0 \quad \text{at } x = 0, x = \ell \quad (4.309)$$

or, by combining both conditions,

$$\left(\frac{d^2 w}{dx^2} \right)_{x=0} = \left(\frac{d^2 w}{dx^2} \right)_{x=\ell} = 0 \quad (4.310)$$

From the conditions at $x = 0$ we deduce immediately that:

$$a_2 = a_4 = 0$$

while the conditions at $x = \ell$ yield:

$$\begin{aligned} a_1 \sin \lambda_1 + a_3 \sinh \lambda_2 &= 0 \\ -a_1 \lambda_1^2 \sin \lambda_1 + a_3 \lambda_2^2 \sinh \lambda_2 &= 0 \end{aligned}$$

The coefficients a_1 and a_3 are not identically zero, provided that the solution verifies the characteristic equation:

$$(\lambda_1^2 + \lambda_2^2) \sin \lambda_1 \sinh \lambda_2 = 0 \quad (4.311)$$

The trivial solution $\lambda_2 = 0, a_1 = 0$ being discarded, the characteristic equation may be put in the simple form:

$$\sin \lambda_1 = 0 \quad (4.312)$$

with $a_3 = 0$. Thus the roots are:

$$\lambda_1 = n\pi \quad n = 1, \dots \quad (4.313)$$

The associated eigenfrequencies are then computed from Equation (4.304) with $\lambda = \pm i\lambda_1$:

$$\tilde{\omega}_n^4 \eta^2 \alpha^2 - \tilde{\omega}_n^2 [(\eta^2 + \alpha^2)n^2 \pi^2 + 1] + n^4 \pi^4 = 0 \quad (4.314)$$

The solution reduces to that of Bernoulli–Euler beam theory when both η and α tend to zero, i.e. when both rotatory inertia and shear effects are neglected.

Example 4.6

In order to better apprehend the numerical importance of shear and rotatory inertia effects, let us compute the eigenspectrum of the uniform simply supported beam in the cases of plain rectangular and hollow circular cross-sections with Poisson coefficient $\nu = 0.3$.

i. Plain rectangular cross-section

Consider a rectangular cross-section of height h and width b . We have:

$$A = bh$$

$$I = \frac{bh^3}{12}$$

$$k' = \frac{5}{6}$$

According to the results obtained for a beam without shear deflection, the beam eigenfrequencies are given by:

$$\omega_{\alpha=0, \eta=0}^2 = n^4 \pi^4 \frac{EI}{m\ell^4} \quad (E4.6.a)$$

The nondimensional parameters take the values:

$$\alpha^2 = \frac{r^2}{\ell^2} = \frac{I}{A\ell^2} = \frac{h^2}{12\ell^2}$$

$$\eta^2 = \frac{EI}{k'AG\ell^2} = \frac{2(1+\nu)h^2}{12k'\ell^2} = 0.26 \frac{h^2}{\ell^2} \quad (E4.6.b)$$

Considering Equation (4.314),

when $\alpha = 0, \eta \neq 0$,

$$\omega_{\alpha=0, \eta \neq 0}^2 = \frac{1}{1 + 0.26n^2\pi^2 \frac{h^2}{\ell^2}} \quad \omega_{\alpha=0, \eta=0}^2 \quad (\text{E4.6.c})$$

when $\alpha \neq 0, \eta = 0$,

$$\omega_{\alpha \neq 0, \eta=0}^2 = \frac{1}{1 + \frac{n^2\pi^2}{12} \frac{h^2}{\ell^2}} \quad \omega_{\alpha=0, \eta=0}^2 \quad (\text{E4.6.d})$$

which shows that the shear deflection effect is more important than the rotatory inertia one and that both phenomena decrease the beam eigenfrequencies. The higher n and h/ℓ , the more the eigenfrequencies are affected.

ii. *Hollow circular cross-section*

Take now the case of a hollow circular cross-section of thickness e and mean radius R :

$$A \simeq 2\pi Re$$

$$I \simeq \pi R^3 e$$

$$k' = \frac{1}{2}$$

The nondimensional parameters then take the values:

$$\begin{aligned} \alpha^2 &= \frac{r^2}{\ell^2} = \frac{I}{A\ell^2} = \frac{R^2}{2\ell^2} \\ \eta^2 &= \frac{EI}{k'AG\ell^2} = \frac{2(1+\nu)R^2}{2k'\ell^2} = 2.6 \frac{R^2}{\ell^2} \end{aligned} \quad (\text{E4.6.e})$$

Considering again Equation (4.314),

when $\alpha = 0, \eta \neq 0$,

$$\omega_{\alpha=0, \eta \neq 0}^2 = \frac{1}{1 + 2.6n^2\pi^2 \frac{R^2}{\ell^2}} \quad \omega_{\alpha=0, \eta=0}^2 \quad (\text{E4.6.f})$$

when $\alpha \neq 0, \eta = 0$,

$$\omega_{\alpha \neq 0, \eta=0}^2 = \frac{1}{1 + \frac{n^2\pi^2}{2} \frac{R^2}{\ell^2}} \quad \omega_{\alpha=0, \eta=0}^2 \quad (\text{E4.6.g})$$

The rotatory inertia and shear deformation contributions are more important this time since, the cross-section being thin-walled, both the gyration radius and the shear stresses get larger. The conclusions are, however, the same as before – that is to say the eigenfrequencies are decreased by the shear effect and to a lesser degree by the rotatory inertia, and the higher n and R/ℓ , the more the eigenfrequencies are reduced by both phenomena.

4.3.5 Travelling waves in beams

Let us consider the same problem of response to initial deformation $W(x)$ as treated in Section 4.3.2 for the taut string. For sake of simplicity, let us consider the case of the simply supported beam since its eigenvalue problem always yields an analytical solution. As will be seen, the

different beam models considered before behave quite differently from one another as wave travelling guides. A more elaborate discussion of wave propagation in beams can be found in Fung (1965) and Sadd (2009).

Bernoulli-Euler beam model

For the Bernoulli-Euler beam model, the problem to be solved is:

$$\begin{cases} EI \frac{\partial^4 w}{\partial x^4} + m \frac{\partial^2 w}{\partial t^2} = 0 & 0 < x < \ell \\ w(x, t) = 0, \quad \frac{\partial^2 w}{\partial x^2} = 0 & \text{at } x = 0, \ell \\ w(x, 0) = W(x) \end{cases} \quad (4.315)$$

The response to initial conditions can be reconstructed through modal superposition as an infinite series of standing waves:

$$w(x, t) = \sum_{n=0}^{\infty} A_n \sin \frac{n\pi}{\ell} x \cos \omega_n t \quad (4.316)$$

with the coefficients A_n given by (4.222).

It is also possible to express it as an infinite series of travelling waves:

$$\begin{aligned} w(x, t) &= \frac{1}{2} \sum_{n=0}^{\infty} A_n \left[\sin \left(\frac{n\pi}{\ell} x - \omega_n t \right) + \sin \left(\frac{n\pi}{\ell} x + \omega_n t \right) \right] \\ &= \frac{1}{2} \sum_{n=0}^{\infty} A_n \left[\sin \left(\frac{2\pi}{\lambda_n} (x - c_n t) \right) + \sin \left(\frac{2\pi}{\lambda_n} (x + c_n t) \right) \right] \end{aligned} \quad (4.317)$$

with the wave length and phase speed of mode n :

$$\lambda_n = \frac{2\ell}{n} \quad (4.318)$$

$$c_n = \frac{\omega_n \lambda_n}{2\pi} = n\pi \sqrt{\frac{EI}{m\ell^2}} \quad (4.319)$$

Equation (4.317) shows that the response is now made of an infinity of waves travelling at different speeds c_n .

The result is displayed on Figure 4.33. Unlike in the taut string, the initial shape undergoes progressive alteration as it travels longitudinally since its component waves propagate at different speeds. This phenomenon is called *dispersion*.

The fact that the wave speed (4.319) is linearly increasing with the wave number n – and thus, tends to infinity as the wave length goes to zero – leads to a physical incoherence already pointed out by Lord Rayleigh (Lord Rayleigh 1894). It is due to the fact that at high frequency the vibration motion consists essentially into rotatory motion of the cross-sections a motion to which no inertia is attached in the Bernoulli-Euler model as described by Equations (4.315).

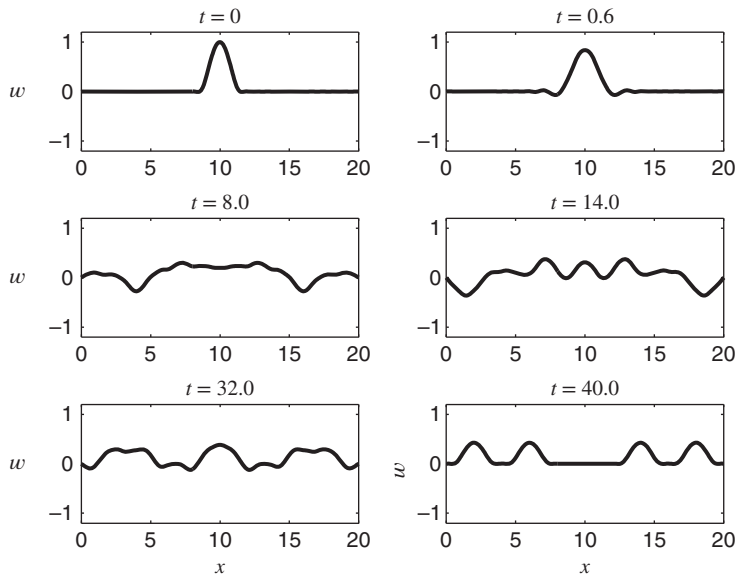


Figure 4.33 Response of simply-supported Euler-Bernoulli beam to initial displacement field illustrating the phenomenon of wave dispersion.

Rayleigh's beam model

This deficiency of Euler-Bernoulli's model can be removed by adopting Rayleigh's beam model that results from the introduction of the rotatory inertia mr^2 of the cross-section. The motion equation of Problem (4.315) is modified by considering the rotational inertia (Equation (4.235) written for a uniform beam and no external loads):

$$EI \frac{\partial^4 w}{\partial x^4} - mr^2 \frac{\partial^4 w}{\partial t^2 \partial x^2} + m \frac{\partial^2 w}{\partial t^2} = 0 \quad (4.320)$$

In the simply-supported case the mode shapes remain of the form:

$$w_n(x) = A_n \sin \frac{n\pi}{\ell} x \quad (4.321)$$

and, with the definition (4.303) of the rotatory inertia parameter α , the eigenvalue equation becomes:

$$\tilde{\omega}^2 (\alpha^2 n^2 \pi^2 + 1) - n^4 \pi^4 = 0 \quad (4.322)$$

The phase velocity becomes (recalling (4.318)):

$$c_n = \frac{\omega_n \lambda_n}{2\pi} = \frac{n\pi}{\sqrt{1 + \alpha^2 n^2 \pi^2}} \sqrt{\frac{EI}{m\ell^2}} \quad (4.323)$$

One verifies that if $\alpha = 0$ one retrieves the phase velocity (4.319) for the Bernoulli-Euler beam. When $\alpha \neq 0$ we observe that as the wave number increases, the phase speed now tends to the

finite value:

$$c_n = \frac{1}{\alpha} \sqrt{\frac{EI}{m\ell^2}} \quad n \rightarrow \infty$$

Recalling the definition (4.303) of α and since $m = \rho A$ it can be put in the final form:¹²

$$c_n = \sqrt{\frac{E}{\rho}} = c_L \quad n \rightarrow \infty \quad (4.324)$$

Timoshenko's beam model

Rayleigh's beam model still suffers from the fact that it only allows wave motion due to rotation of the cross-section thus propagated through axial deformation. This explained why its associated wave speed tends to the wave speed (4.324) characteristic of longitudinal motion.

The inability of Rayleigh's beam model to also propagate – as physically observed – transverse waves in the longitudinal direction results from the absence of shear deformation. Indeed in Rayleigh's model there is no deformation associated to the shear force: cross-sections are allowed to rotate but cannot undergo relative sliding motion.

Wave propagation in a simply-supported beam described by Timoshenko's model is governed by the system of equations and boundary conditions (Equation (4.285) written for a uniform beam and no loading):

$$\begin{cases} EI \frac{\partial^2 \psi}{\partial x^2} + k' AG \left(\frac{\partial w}{\partial x} - \psi \right) - mr^2 \frac{\partial^2 \psi}{\partial t^2} = 0 \\ k' AG \left(\frac{\partial^2 w}{\partial x^2} - \frac{\partial \psi}{\partial x} \right) - m \frac{\partial^2 w}{\partial t^2} = 0 \\ w(x, t) = \frac{\partial}{\partial x} \psi(x, t) = 0 \quad \text{at } x = 0, \ell \end{cases} \quad (4.325)$$

This model considers two independent fields, namely ψ the bending rotation and w the transverse displacement so that $\frac{\partial w}{\partial x} - \psi$ describes the shear deformation.

It has been demonstrated (Page 283) that the eigensolutions with simply-supported ends are of the form:

$$w_{(n)}(x) = a \sin \frac{n\pi x}{\ell} \quad \psi_{(n)}(x) = b \cos \frac{n\pi x}{\ell} \quad (4.326)$$

with the associated nondimensional eigenvalues $\tilde{\omega}^2 = \omega^2 \frac{EI}{m\ell^4}$ solution of:

$$\tilde{\omega}_n^4 \eta^2 \alpha^2 - \tilde{\omega}_n^2 [(\eta^2 + \alpha^2)n^2 \pi^2 + 1] + n^4 \pi^4 = 0 \quad (4.327)$$

Therefore for each eigenvalue n there are two roots $\tilde{\omega}^2$ solutions of (4.327):

$$\tilde{\omega}_n^2 = \frac{(\eta^2 + \alpha^2)n^2 \pi^2 + 1 \pm \sqrt{((\eta^2 + \alpha^2)n^2 \pi^2 + 1)^2 - 4\eta^2 \alpha^2 n^4 \pi^4}}{2\eta^2 \alpha^2} \quad (4.328)$$

¹² The result (4.324) corresponds to the longitudinal wave speed computed for a 3-D elastic medium (see Section 4.5.2) when neglecting the lateral contraction effect ($\nu = 0$).

For n sufficiently large, we can assume that $(\eta^2 + \alpha^2)n^2\pi^2 \gg 1$ so that the roots become:

$$\tilde{\omega}_n^2 = n^2\pi^2 \frac{\eta^2 + \alpha^2 \pm (\eta^2 - \alpha^2)}{2\eta^2\alpha^2} \quad (4.329)$$

and we thus get the eigenfrequencies:

$$\omega_{n,1} = \frac{n\pi}{\alpha} \sqrt{\frac{EI}{m\ell^4}} = \frac{n\pi}{\ell} \sqrt{\frac{E}{\rho}} \quad \omega_{n,2} = \frac{n\pi}{\eta} \sqrt{\frac{EI}{m\ell^4}} = \frac{n\pi}{\ell} \sqrt{\frac{k'G}{\rho}} \quad (4.330)$$

to which, owing to (4.319), correspond the phase velocities:

$$c_L = \sqrt{\frac{E}{\rho}} \quad \text{and} \quad c_T = \sqrt{\frac{k'G}{\rho}} \quad (4.331)$$

c_L is the same longitudinal phase speed as obtained with Rayleigh's model and corresponds to propagation of bending waves. The fact that bending waves propagate at longitudinal wave speed is explained by the fact that rotation of cross-sections is the result of longitudinal motion since $\psi(x) = z \frac{\partial u}{\partial x}$.

c_T is the transverse phase speed. It characterizes the propagation in the longitudinal direction x of a wave consisting of a motion in the transverse direction z . The mechanism of wave propagation in this case is shear, as confirmed by the dependence of the phase speed on shear modulus $k'G$.

The simultaneous existence of longitudinal and transverse wave propagation speeds in a 3-D homogeneous elastic medium will be demonstrated in Section 4.5.2.

Figure 4.34 displays the phase speed predictions obtained from the different beam models for a beam made of steel with thin-wall circular cross-section ($\alpha^2 = 0.005$, $\eta^2 = 0.26$). It shows that both Rayleigh and Euler models predict only a longitudinal phase speed. With the Bernoulli-Euler model it grows linearly with n , while it converges by increasing values to the longitudinal phase speed c_L for Rayleigh's model. Due to the independent assumptions for

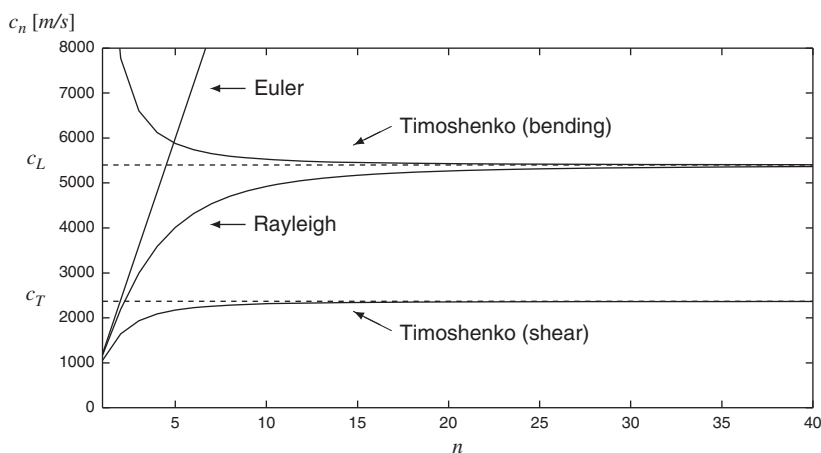


Figure 4.34 Comparison of phase speeds versus wave number for different beam models.

bending and shear deformations, Timoshenko's model is able to predict two different values corresponding to the propagation of bending and shear waves. Unlike with Rayleigh's model, the convergence of the bending wave speed towards c_L is by decreasing values. Note that c_L is not affected by the geometric properties of the beam, while c_T depends not only on material properties but also on the cross-sectional shear reduction factor k' .

4.4 Bending vibrations of thin plates

The objective of this section is to introduce the concept of thin plates in bending according to *Kirchhoff's* assumptions and to analyze their free vibration behaviour. Kirchhoff's plate model suffers in fact from the same limitations as the Euler-Bernoulli model in beam theory. Although it is sufficient to cover most of the situations encountered in engineering, it fails to represent properly the phenomenon of wave propagation in plates. Another drawback is the fact that, like in shear modelling, the concept of shear force lacks physical grounds since shear forces appear only as force resultants needed to express equilibrium but there is no deformation associated to it. As will be seen, this leads to cumbersome expression of the boundary conditions.

The plate model could be extended as was done in beam theory by allowing deformation of the material in shear, obeying then to *Reissner-Mindlin plate theory*. The reader is referred to Sander (1969) for a rigorous presentation of Reissner's plate theory (Reissner 1945) and its finite element implementation. Nowadays, most of the formulations proposed in finite element codes are rather based on Mindlin's plate theory (Mindlin 1951) which only differs from Reissner's by the hypothesis adopted regarding distribution of the normal stress through the thickness. A good presentation of Mindlin's model can be found in (Wikipedia n.d.).

The main motivation for presenting here Kirchhoff's plate model is that, contrarily to the Reissner-Mindlin model, it can provide analytical solutions for a few specific geometries and boundary conditions that allow getting some physical insight in plate vibration behaviour without having to resort to numerical simulation.

4.4.1 Kinematic assumptions

The kinematic assumptions adopted generalize to two dimensions those adopted for the beam with no shear deflection (Figure 4.35) (Sander 1969):

1. The plate is thin with thickness h and possesses a mean plane. The external layers of the plate are the planes $z = \pm \frac{1}{2}h$.
2. Only the transverse displacement w is considered.
3. The stress σ_z in the transverse direction is zero. Indeed, it must vanish on the external layers and, since the plate is thin, it is natural to assume that it vanishes for all z .
4. The cross-sections, initially normal to the mean plane, remain plane and orthogonal to it, implying that the transverse shear strain is neglected.
5. The displacements u and v in the Oxy plane result from two effects:
 - an initial displacement field, uniform over the thickness and resulting from a loading of the plate in its plane (extension or *membrane* behaviour);
 - the displacement field due to the rotation of the cross-section.

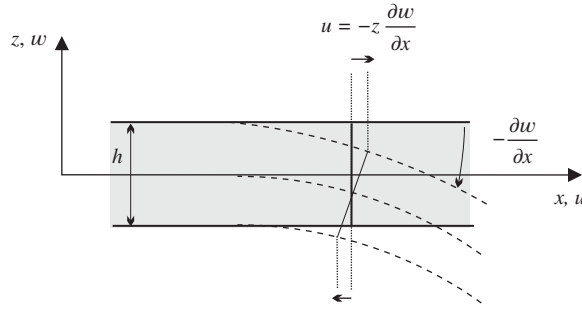


Figure 4.35 Kinematics of thin plate deformation.

These assumptions lead to the kinematic assumptions:

$$\begin{aligned}
 u &= u_0(x, y) - z \frac{\partial w}{\partial x} \\
 v &= v_0(x, y) - z \frac{\partial w}{\partial y} \\
 w &= w(x, y)
 \end{aligned} \tag{4.332}$$

where the displacements $u_0(x, y)$ and $v_0(x, y)$ result from an initial extension of the plate by a prestress loading in the mean plane and are regarded as *given*.

4.4.2 Strain expressions

Taking account of assumptions (4.332) – provided that the large rotation terms are kept in the Green strain expressions (4.3) (large displacements case) – the strains of the thin plate can be expressed by:

$$\begin{aligned}
 \epsilon_x &= \frac{\partial u}{\partial x} + \frac{1}{2} \left(\frac{\partial w}{\partial x} \right)^2 \\
 &= \frac{\partial u_0}{\partial x} - z \frac{\partial^2 w}{\partial x^2} + \frac{1}{2} \left(\frac{\partial w}{\partial x} \right)^2 \\
 \epsilon_y &= \frac{\partial v}{\partial y} + \frac{1}{2} \left(\frac{\partial w}{\partial y} \right)^2 \\
 &= \frac{\partial v_0}{\partial y} - z \frac{\partial^2 w}{\partial y^2} + \frac{1}{2} \left(\frac{\partial w}{\partial y} \right)^2 \\
 \epsilon_z &= \frac{\partial w}{\partial z} = 0 \\
 \gamma_{xy} &= 2\epsilon_{xy} = \left(\frac{\partial u}{\partial y} + \frac{\partial v}{\partial x} \right) + \frac{\partial w}{\partial x} \frac{\partial w}{\partial y}
 \end{aligned} \tag{4.333}$$

$$\begin{aligned}
&= \left(\frac{\partial u_0}{\partial y} + \frac{\partial v_0}{\partial x} \right) - 2z \frac{\partial w^2}{\partial x \partial y} + \frac{\partial w}{\partial x} \frac{\partial w}{\partial y} \\
\gamma_{xz} &= 2\epsilon_{xz} = \frac{\partial u}{\partial z} + \frac{\partial w}{\partial x} = 0 \\
\gamma_{yz} &= 2\epsilon_{yz} = \frac{\partial v}{\partial z} + \frac{\partial w}{\partial y} = 0
\end{aligned}$$

The nonzero components are collected in the strain column matrix:

$$\epsilon = \begin{bmatrix} \epsilon_x \\ \epsilon_y \\ \gamma_{xy} \end{bmatrix} \quad (4.334)$$

which can be decomposed in the form:

$$\epsilon = \epsilon^{(0)} + \epsilon^{(1)} + \epsilon^{(2)} \quad (4.335)$$

where $\epsilon^{(0)}$, $\epsilon^{(1)}$ and $\epsilon^{(2)}$ represent respectively the terms of degree 0, 1 and 2 in the displacement w :

$$\epsilon^{(0)} = \begin{bmatrix} \frac{\partial u_0}{\partial x} \\ \frac{\partial v_0}{\partial y} \\ \frac{\partial u_0}{\partial y} + \frac{\partial v_0}{\partial x} \end{bmatrix} \quad \epsilon^{(1)} = \begin{bmatrix} -z \frac{\partial^2 w}{\partial x^2} \\ -z \frac{\partial^2 w}{\partial y^2} \\ -2z \frac{\partial^2 w}{\partial x \partial y} \end{bmatrix} \quad \epsilon^{(2)} = \begin{bmatrix} \frac{1}{2} \left(\frac{\partial w}{\partial x} \right)^2 \\ \frac{1}{2} \left(\frac{\partial w}{\partial y} \right)^2 \\ \frac{\partial w}{\partial x} \frac{\partial w}{\partial y} \end{bmatrix} \quad (4.336)$$

It is important to notice that only part $\epsilon^{(1)}$ of the strains varies along the thickness, and it does so in a linear manner.

4.4.3 Stress–strain relationships

The stresses in the *linear and isotropic* material are computed from Hooke's law:

$$\begin{aligned}
\epsilon_x &= \frac{1}{E} [\sigma_x - \nu(\sigma_y + \sigma_z)] \\
\epsilon_y &= \frac{1}{E} [\sigma_y - \nu(\sigma_x + \sigma_z)] \\
\gamma_{xy} &= \frac{1}{G} \tau_{xy},
\end{aligned} \quad (4.337)$$

with the definition of the shear modulus:

$$G = \frac{E}{2(1 + \nu)} \quad (4.338)$$

It is assumed that the stress vanishes along the thickness:

$$\sigma_z = 0 \quad (4.339)$$

which leads to the stress–strain relationship:

$$\boldsymbol{\sigma} = \mathbf{H}\boldsymbol{\epsilon} \quad (4.340)$$

with the definition of the stress column matrix:

$$\boldsymbol{\sigma} = \begin{bmatrix} \sigma_x \\ \sigma_y \\ \tau_{xy} \end{bmatrix} \quad (4.341)$$

and the expression of the matrix of elastic coefficients:

$$\mathbf{H} = \frac{E}{1-\nu^2} \begin{bmatrix} 1 & \nu & 0 \\ \nu & 1 & 0 \\ 0 & 0 & \frac{1-\nu}{2} \end{bmatrix} \quad (4.342)$$

4.4.4 Definition of curvatures

The column matrix of curvatures is defined by:

$$\boldsymbol{\chi} = \begin{bmatrix} -\frac{\partial^2 w}{\partial x^2} \\ -\frac{\partial^2 w}{\partial y^2} \\ -2\frac{\partial^2 w}{\partial x \partial y} \end{bmatrix} \quad (4.343)$$

where the first two terms represent the principal curvatures of the plate in directions x and y , and the third one corresponds to the cross-curvature generated by plate torsion. The strains due to linear bending and the associated stresses are linked by:

$$\boldsymbol{\epsilon}^{(1)} = z\boldsymbol{\chi} \quad \text{and} \quad \boldsymbol{\sigma}^{(1)} = \mathbf{H}\boldsymbol{\epsilon}^{(1)} \quad (4.344)$$

4.4.5 Moment–curvature relationships

The bending moments per unit length in the plate (Figure 4.36) are computed by integration of the stresses over the thickness:

$$\begin{aligned} \mathbf{M} = \begin{bmatrix} M_x \\ M_y \\ M_{xy} \end{bmatrix} &= \int_{-\frac{h}{2}}^{\frac{h}{2}} z \boldsymbol{\sigma} dz \\ &= \int_{-\frac{h}{2}}^{\frac{h}{2}} z \mathbf{H} \boldsymbol{\epsilon} dz \end{aligned} \quad (4.345)$$

Because the antisymmetric terms of (4.336) are the only ones to contribute to the computation of moments, we may also write:

$$\begin{aligned} \mathbf{M} &= \int_{-\frac{h}{2}}^{\frac{h}{2}} z \boldsymbol{\sigma}^{(1)} dz \\ &= \int_{-\frac{h}{2}}^{\frac{h}{2}} z^2 \mathbf{H} \boldsymbol{\chi} dz \end{aligned} \quad (4.346)$$

and we obtain the expressions:

$$\begin{aligned} M_x &= -D \left[\frac{\partial^2 w}{\partial x^2} + \nu \frac{\partial^2 w}{\partial y^2} \right] \\ M_y &= -D \left[\frac{\partial^2 w}{\partial y^2} + \nu \frac{\partial^2 w}{\partial x^2} \right] \\ M_{xy} &= -D(1 - \nu) \frac{\partial^2 w}{\partial x \partial y} \end{aligned} \quad (4.347)$$

with the definition of the plate bending stiffness:

$$D = \frac{Eh^3}{12(1 - \nu^2)} \quad (4.348)$$

These expressions may be written in the matrix form:

$$\mathbf{M} = \mathbf{H}^* \boldsymbol{\chi} \quad (4.349)$$

with the matrix of elastic coefficients integrated over the thickness:

$$\mathbf{H}^* = \frac{Eh^3}{12(1 - \nu^2)} \begin{bmatrix} 1 & \nu & 0 \\ \nu & 1 & 0 \\ 0 & 0 & \frac{1-\nu}{2} \end{bmatrix} \quad (4.350)$$

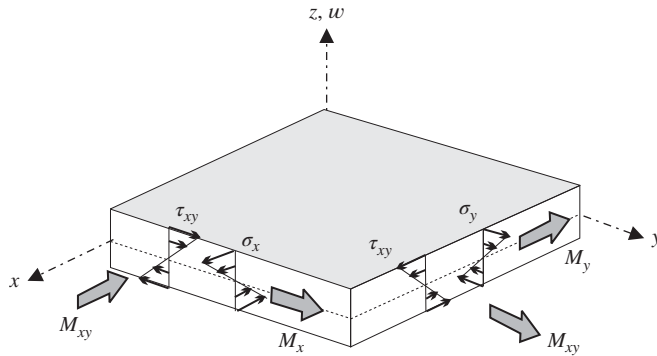


Figure 4.36 Bending moments in the plate.

4.4.6 Frame transformation for bending moments

Let us consider a plate of arbitrary external contour Γ , with $(\ell, m, 0)$ the direction cosines of the outward normal \vec{n} at a point of the contour (Figure 4.37). The moments on the plate boundary Γ are denoted M_n , M_s and M_{ns} where

M_n is the bending moment in plane Onz , oriented along the tangent to the contour;
 M_s is the bending moment in the perpendicular direction;
 M_{ns} is the twisting moment about the normal.

Equilibrium of the volume element on the plate boundary implies the frame transformations for the moments:

$$\begin{aligned} M_x &= \ell^2 M_n - 2\ell m M_{ns} + m^2 M_s \\ M_y &= \ell^2 M_s + 2\ell m M_{ns} + m^2 M_n \\ M_{xy} &= \ell m (M_n - M_s) + M_{ns} (\ell^2 - m^2) \end{aligned} \quad (4.351)$$

These relationships may be inverted in the form:

$$\begin{aligned} M_n &= \ell^2 M_x + 2\ell m M_{xy} + m^2 M_y \\ M_s &= \ell^2 M_y - 2\ell m M_{xy} + m^2 M_x \\ M_{ns} &= \ell m (M_y - M_x) + M_{xy} (\ell^2 - m^2) \end{aligned} \quad (4.352)$$

4.4.7 Computation of strain energy

The plate strain energy is computed by integrating the strain energy density over the volume:

$$\mathcal{V}_{int} = \frac{1}{2} \int_V \boldsymbol{\varepsilon}^T \mathbf{H} \boldsymbol{\varepsilon} dV \quad (4.353)$$

and it can be decomposed into its different terms of increasing order in w :

$$\mathcal{V}_{int} = \mathcal{V}_{int}^{(0)} + \mathcal{V}_{int}^{(1)} + \mathcal{V}_{int}^{(2)} + O(w^3) \quad (4.354)$$

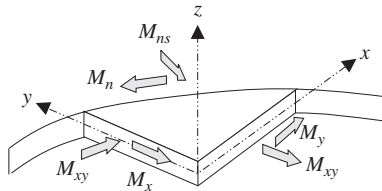


Figure 4.37 Frame transformation for bending moments.

with

- The strain energy resulting from initial extension of the plate:

$$\mathcal{V}_{int}^{(0)} = \frac{1}{2} \int_V \boldsymbol{\epsilon}^{(0)T} \mathbf{H} \boldsymbol{\epsilon}^{(0)} dV \quad (4.355)$$

If we impose the initial displacements (u_0, v_0) , we may write:

$$\mathcal{V}_{int}^{(0)} = \text{constant} \quad (4.356)$$

Thus this component has no contribution to the equation of motion.

- The first-order part of the strain energy:

$$\mathcal{V}_{int}^{(1)} = \int_{-\frac{h}{2}}^{\frac{h}{2}} z dz \int_S \boldsymbol{\chi}^T \mathbf{H} \boldsymbol{\epsilon}^{(0)} dS = 0 \quad (4.357)$$

This term will be omitted in the subsequent discussion since it plays a role only in the equilibrium expression of the plate under prestressing (see Equations (4.45) or (4.46)).

- The quadratic part of the strain energy:

$$\mathcal{V}_{int}^{(2)} = \frac{1}{2} \int_V \boldsymbol{\epsilon}^{(1)T} \mathbf{H} \boldsymbol{\epsilon}^{(1)} dV + \int_V \boldsymbol{\epsilon}^{(2)T} \mathbf{H} \boldsymbol{\epsilon}^{(0)} dV \quad (4.358)$$

By integration over the thickness this can be recast in the form:

$$\mathcal{V}_{int}^{(2)} = \frac{1}{2} \int_S \boldsymbol{\chi}^T \mathbf{H}^* \boldsymbol{\chi} dS + \int_S \mathbf{N}_0^T \boldsymbol{\epsilon}^{(2)} dS \quad (4.359)$$

where the first term is the bending strain energy of linear origin, and the second one represents the prestress effect. This is expressed in terms of the membrane initial stresses in the plate:

$$\begin{bmatrix} N_x \\ N_y \\ N_{xy} \end{bmatrix}_0 = \mathbf{N}_0 = \int_{-\frac{h}{2}}^{\frac{h}{2}} \mathbf{H} \boldsymbol{\epsilon}^{(0)} dz \quad (4.360)$$

According to their sign, it generates either stiffening or softening of the bending plate.

4.4.8 Expression of Hamilton's principle

In the absence of nonconservative forces applied to the system, Hamilton's principle is expressed by:

$$\delta \int_{t_1}^{t_2} (\mathcal{T} - \mathcal{V}) dt = 0 \quad (4.361)$$

The kinetic energy \mathcal{T} is computed through integration of the kinetic energy of the volume element:

$$\mathcal{T} = \frac{1}{2} \int_V \rho (\dot{u}^2 + \dot{v}^2 + \dot{w}^2) dV \quad (4.362)$$

or, in terms of the approximations (4.332):

$$\mathcal{T} = \frac{1}{2} \int_{-\frac{h}{2}}^{\frac{h}{2}} \int_S \rho \left\{ \dot{w}^2 + z^2 \left[\left(\frac{\partial \dot{w}}{\partial x} \right)^2 + \left(\frac{\partial \dot{w}}{\partial y} \right)^2 \right] \right\} dS dz \quad (4.363)$$

Integration may then be carried out over the thickness, and by defining:

- the mass per unit of surface:

$$m = \int_{-\frac{h}{2}}^{\frac{h}{2}} \rho dz \quad (4.364)$$

- the mass moment of inertia per unit of surface, expressed in terms of the gyration radius r of the cross-section:

$$mr^2 = \int_{-\frac{h}{2}}^{\frac{h}{2}} \rho z^2 dz \quad (4.365)$$

it yields the expression:

$$\mathcal{T} = \frac{1}{2} \int_S m \left\{ \dot{w}^2 + r^2 \left[\left(\frac{\partial \dot{w}}{\partial x} \right)^2 + \left(\frac{\partial \dot{w}}{\partial y} \right)^2 \right] \right\} dS \quad (4.366)$$

The first term of (4.366) represents the translation kinetic energy of the plate, while both remaining terms represent rotatory effects.

In the same manner as for the beam without shear deflection, the rotatory inertia terms are generally neglected, since they become significant only when the shear contribution is significant. In the context of thin plate theory it is thus customary to use the approximate expression:

$$\mathcal{T} \simeq \frac{1}{2} \int_S m \dot{w}^2 dS \quad (4.367)$$

The potential energy may be split into two parts:

$$\mathcal{V} = \mathcal{V}_{int} + \mathcal{V}_{ext} \quad (4.368)$$

the strain energy \mathcal{V}_{int} and the potential of external loads \mathcal{V}_{ext} .

First, concerning the strain energy, we will consider the case where the plate is not submitted to initial extension ($N_0 = 0$). The development of (4.359) then yields the expression:

$$\mathcal{V}_{int} = \frac{1}{2} \int_S D \left\{ \left(\frac{\partial^2 w}{\partial x^2} + \frac{\partial^2 w}{\partial y^2} \right)^2 - 2(1 - \nu) \left[\frac{\partial^2 w}{\partial x^2} \cdot \frac{\partial^2 w}{\partial y^2} - \left(\frac{\partial^2 w}{\partial x \partial y} \right)^2 \right] \right\} dS \quad (4.369)$$

The potential energy associated with the external distributed load $\bar{p}(x, y, t)$ takes the form:

$$\mathcal{V}_{ext} = - \int_S w \bar{p} dS \quad (4.370)$$

In order to present this simply, we will suppose that the plate is free of distributed moments and that it is not loaded on its boundary.

4.4.9 Plate equations of motion derived from Hamilton's principle

First, let us consider the variation of the strain energy term:

$$\begin{aligned}\delta\mathcal{V}_{int} = & \int_S D \left\{ \left[\left(\frac{\partial^2 w}{\partial x^2} + \frac{\partial^2 w}{\partial y^2} \right) - (1-\nu) \frac{\partial^2 w}{\partial y^2} \right] \delta \left(\frac{\partial^2 w}{\partial x^2} \right) \right. \\ & + \left[\left(\frac{\partial^2 w}{\partial x^2} + \frac{\partial^2 w}{\partial y^2} \right) - (1-\nu) \frac{\partial^2 w}{\partial x^2} \right] \delta \left(\frac{\partial^2 w}{\partial y^2} \right) \\ & \left. + 2(1-\nu) \frac{\partial^2 w}{\partial x \partial y} \delta \left(\frac{\partial^2 w}{\partial x \partial y} \right) \right\} dS\end{aligned}\quad (4.371)$$

and then integrate by parts the expression given above while taking account of the following equalities resulting from Green's theorem:

$$\begin{aligned}\int_S \frac{\partial u}{\partial x} v \, dS &= \int_\Gamma \ell uv \, d\Gamma - \int_S u \frac{\partial v}{\partial x} \, dS \\ \int_S \frac{\partial u}{\partial y} v \, dS &= \int_\Gamma muv \, d\Gamma - \int_S u \frac{\partial v}{\partial y} \, dS\end{aligned}\quad (4.372)$$

A first integration by parts yields the expression:

$$\begin{aligned}\delta\mathcal{V}_{int} = & \int_\Gamma \left\{ \left[\ell D \left(\frac{\partial^2 w}{\partial x^2} + \nu \frac{\partial^2 w}{\partial y^2} \right) + m(1-\nu) D \frac{\partial^2 w}{\partial x \partial y} \right] \delta \left(\frac{\partial w}{\partial x} \right) \right. \\ & + \left[m D \left(\frac{\partial^2 w}{\partial y^2} + \nu \frac{\partial^2 w}{\partial x^2} \right) + \ell(1-\nu) D \frac{\partial^2 w}{\partial x \partial y} \right] \delta \left(\frac{\partial w}{\partial y} \right) \Big\} d\Gamma \\ & - \int_S \left\{ \left[\frac{\partial}{\partial x} \left(D \left(\frac{\partial^2 w}{\partial x^2} + \nu \frac{\partial^2 w}{\partial y^2} \right) \right) + \frac{\partial}{\partial y} \left((1-\nu) D \frac{\partial^2 w}{\partial x \partial y} \right) \right] \delta \left(\frac{\partial w}{\partial x} \right) \right. \\ & \left. + \left[\frac{\partial}{\partial y} \left(D \left(\frac{\partial^2 w}{\partial y^2} + \nu \frac{\partial^2 w}{\partial x^2} \right) \right) + \frac{\partial}{\partial x} \left((1-\nu) D \frac{\partial^2 w}{\partial x \partial y} \right) \right] \delta \left(\frac{\partial w}{\partial y} \right) \right\} dS\end{aligned}\quad (4.373)$$

in which the first term expresses the virtual work of bending stresses (4.349) on the contour of the plate; it may also be expressed in terms of moments in the form:

$$\begin{aligned}\delta\mathcal{V}_{int} = & \int_\Gamma - \left[(\ell M_x + m M_{xy}) \delta \left(\frac{\partial w}{\partial x} \right) + (m M_y + \ell M_{xy}) \delta \left(\frac{\partial w}{\partial y} \right) \right] d\Gamma \\ & + \int_S \left\{ \left(\frac{\partial M_x}{\partial x} + \frac{\partial M_{xy}}{\partial y} \right) \delta \left(\frac{\partial w}{\partial x} \right) + \left(\frac{\partial M_{xy}}{\partial y} + \frac{\partial M_x}{\partial x} \right) \delta \left(\frac{\partial w}{\partial y} \right) \right\} dS\end{aligned}\quad (4.374)$$

By analogy with the beam, let us define the shear forces per unit length:

$$\begin{aligned}Q_x &= \frac{\partial M_x}{\partial x} + \frac{\partial M_{xy}}{\partial y} \\ Q_y &= \frac{\partial M_y}{\partial y} + \frac{\partial M_{xy}}{\partial x}\end{aligned}\quad (4.375)$$

in which case a second integration by parts yields the expression:

$$\begin{aligned} \delta \mathcal{V}_{int} = & \int_{\Gamma} \left\{ - \left[(\ell M_x + m M_{xy}) \delta \left(\frac{\partial w}{\partial x} \right) + (m M_y + \ell M_{xy}) \delta \left(\frac{\partial w}{\partial y} \right) \right] \right\} d\Gamma \\ & + \int_{\Gamma} \left\{ \ell \left(\frac{\partial M_x}{\partial x} + \frac{\partial M_{xy}}{\partial y} \right) + m \left(\frac{\partial M_x}{\partial y} + \frac{\partial M_{xy}}{\partial x} \right) \right\} \delta w d\Gamma \\ & - \int_S \left[\frac{\partial Q_x}{\partial x} + \frac{\partial Q_y}{\partial y} \right] \delta w dS \end{aligned} \quad (4.376)$$

Next, we write the first integral over the contour in terms of the derivatives of the plate deflection with respect to the current parameter s along the contour and its outward normal \vec{n} (Figure 4.38). We use the following differentiation formulas:

$$\begin{aligned} \frac{\partial}{\partial x} &= \ell \frac{\partial}{\partial n} - m \frac{\partial}{\partial s} \\ \frac{\partial}{\partial y} &= m \frac{\partial}{\partial n} + \ell \frac{\partial}{\partial s} \end{aligned} \quad (4.377)$$

By taking into account the moment transformation relationships (4.352), the contour term I_1 becomes:

$$\begin{aligned} I_1 &= \int_{\Gamma} \left\{ - [\ell^2 M_x + 2\ell m M_{xy} + m^2 M_y] \delta \left(\frac{\partial w}{\partial n} \right) \right. \\ &\quad \left. - [m\ell (M_y - M_x) + (\ell^2 - m^2) M_{xy}] \delta \left(\frac{\partial w}{\partial s} \right) \right\} d\Gamma \\ &= \int_{\Gamma} \left\{ -M_n \delta \left(\frac{\partial w}{\partial n} \right) - M_{ns} \delta \left(\frac{\partial w}{\partial s} \right) \right\} d\Gamma \end{aligned} \quad (4.378)$$

Finally, performing an integration by parts in terms of the current variable s along the contour yields the expression:

$$I_1 = \int_{\Gamma} \left[-M_n \delta \left(\frac{\partial w}{\partial n} \right) + \frac{\partial M_{ns}}{\partial s} \delta w \right] d\Gamma - [M_{ns} \delta w]_{\Gamma} \quad (4.379)$$

where the term $Z_n = [M_{ns} \delta w]_{\Gamma}$ expresses the variation of the twisting moment along the contour; it generates a nonzero contribution if the first derivative of the contour is discontinuous,

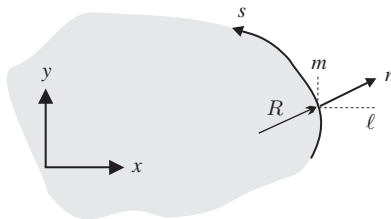


Figure 4.38 Curvilinear coordinates along contour Γ .

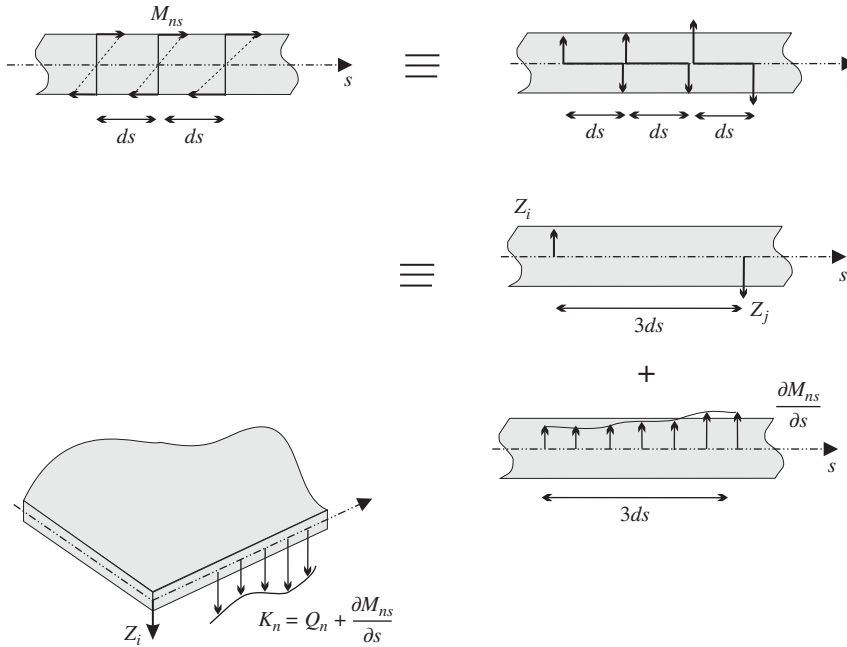


Figure 4.39 Physical meaning of the twisting moment contribution to the shear force at the plate edge.

and vanishes otherwise. Its physical origin is illustrated in Figure 4.39, and the resulting force is called *Kirchhoff's corner load*.

The second term on the contour:

$$I_2 = \int_{\Gamma} \left\{ \ell \left(\frac{\partial M_x}{\partial x} + \frac{\partial M_{xy}}{\partial y} \right) + m \left(\frac{\partial M_x}{\partial y} + \frac{\partial M_{xy}}{\partial x} \right) \right\} \delta w \, d\Gamma \quad (4.380)$$

may be transformed by using the differentiation formulas (4.377) and by noting also that the coordinates (n, s) form a curvilinear system; the direction cosines of the outward normal thus vary with the edge radius of curvature R according to the formulas:

$$\begin{aligned} \frac{\partial \ell}{\partial n} &= 0 & \frac{\partial \ell}{\partial s} &= -\frac{m}{R} \\ \frac{\partial m}{\partial n} &= 0 & \frac{\partial m}{\partial s} &= \frac{\ell}{R} \end{aligned} \quad (4.381)$$

After some algebra we get:

$$\begin{aligned} I_2 &= \int_{\Gamma} \left\{ \frac{\partial M_n}{\partial n} + \frac{\partial M_{ns}}{\partial s} + \frac{1}{R} (M_n - M_s) \right\} \delta w \, d\Gamma \\ &= \int_{\Gamma} \left\{ Q_n + \frac{1}{R} (M_n - M_s) \right\} \delta w \, d\Gamma \end{aligned} \quad (4.382)$$

For the variation of the strain energy the following final expression results:

$$\begin{aligned} \delta \mathcal{V}_{int} = & \int_{\Gamma} \left[-M_n \delta \left(\frac{\partial w}{\partial n} \right) + K_n \delta w \right] d\Gamma - [M_{ns} \delta w]_{\Gamma} \\ & - \int_S \left[\frac{\partial Q_x}{\partial x} + \frac{\partial Q_y}{\partial y} \right] \delta w dS \end{aligned} \quad (4.383)$$

where the term on the contour involves the so-called *Kirchhoff shear force*:

$$\begin{aligned} K_n &= Q_n + \frac{\partial M_{ns}}{\partial s} + \frac{1}{R} (M_n - M_s) \\ &= \frac{\partial M_n}{\partial n} + 2 \frac{\partial M_{ns}}{\partial s} + \frac{1}{R} (M_n - M_s) \end{aligned} \quad (4.384)$$

It is thus observed that added to the shear force Q_n are the distributed load $\partial M_{ns}/\partial s$ generated by the twisting moment and a term arising from the contour curvature. The physical meaning of the term generated by the twisting moment is shown by Figure 4.39.

In the case of a plate with uniform properties, the surface term is expressed very simply in terms of the vertical deflection:

$$\int_S \left[\frac{\partial Q_x}{\partial x} + \frac{\partial Q_y}{\partial y} \right] \delta w dS = - \int_S D \left[\frac{\partial^4 w}{\partial x^4} + \frac{\partial^4 w}{\partial y^4} + 2 \frac{\partial^4 w}{\partial x^2 \partial y^2} \right] \delta w dS$$

One proceeds with the variation of the kinetic energy:

$$\delta \int_{t_1}^{t_2} \mathcal{T} dt = \delta \int_{t_1}^{t_2} \int_S \frac{1}{2} m \dot{w}^2 dS dt = \int_{t_1}^{t_2} \int_S m \dot{w} \delta \dot{w} dS dt \quad (4.385)$$

and its integration by parts in time:

$$\delta \int_{t_1}^{t_2} \mathcal{T} dt = \left[\int_S m \dot{w} \delta w dS \right]_{t_1}^{t_2} - \int_{t_1}^{t_2} \int_S m \ddot{w} \delta w dS dt \quad (4.386)$$

The time-boundary term vanishes according to the application conditions of Hamilton's principle, giving the remaining term:

$$\delta \int_{t_1}^{t_2} \mathcal{T} dt = - \int_{t_1}^{t_2} \int_S m \ddot{w} \delta w dS dt \quad (4.387)$$

Finally, the variation of the external force potential energy yields:

$$\delta \mathcal{V}_{ext} = - \int_S \bar{p} \delta w dS \quad (4.388)$$

Gathering the terms (4.383), (4.387) and (4.388), the application of Hamilton's principle yields the variational expression:

$$\begin{aligned} \delta \int_{t_1}^{t_2} (\mathcal{T} - \mathcal{V}) dt = & \int_{t_1}^{t_2} \left\{ [M_{ns} \delta w]_{\Gamma} + \int_{\Gamma} \left[M_n \delta \left(\frac{\partial w}{\partial n} \right) - K_n \delta w \right] d\Gamma \right. \\ & \left. + \int_S \left[\frac{\partial Q_x}{\partial x} + \frac{\partial Q_y}{\partial y} - m \ddot{w} + \bar{p} \right] \delta w dS \right\} dt = 0 \end{aligned} \quad (4.389)$$

from which the plate equilibrium equations are deduced:

- at any point on the surface

$$\boxed{\frac{\partial Q_x}{\partial x} + \frac{\partial Q_y}{\partial y} - m\ddot{w} + \bar{p} = 0} \quad \text{on } S \quad (4.390)$$

- at any point on the regular part of the contour, according to whether it is free or fixed:
 - the condition on either the shear force or the vertical displacement:

$$K_n = 0 \quad \text{or} \quad w = 0 \quad \text{on } \Gamma \quad (4.391)$$

- the condition on either the normal bending moment or the normal slope:

$$M_n = 0 \quad \text{or} \quad \frac{\partial w}{\partial n} = 0 \quad \text{on } \Gamma \quad (4.392)$$

- at any angular point of the contour, in terms of either the Kirchhoff shear generated by the twisting moment discontinuity or the vertical displacement:

$$Z_n = M_{ns}^+ - M_{ns}^- = 0 \quad \text{or} \quad w = 0 \quad (4.393)$$

It is important to recall once more that the conditions of kinematic type ($w = 0$ and/or $\frac{\partial w}{\partial n}$ on part of the contour) are conditions which must be a priori verified by the comparison functions introduced in the variational principle operating on displacements. These are said to be *essential*. Conversely, the conditions describing the internal equilibrium of the plate are taken into account in a natural manner by the principle: they are said to be *natural*.

Let us observe that the translational equilibrium Equation (4.390) and the shear force definition (4.375) result from elementary equilibrium considerations (Figure 4.40). Indeed, vertical equilibrium of the plate element (dx, dy) yields the relation

$$dQ_x dy + dQ_y dx + (\bar{p} - m\ddot{w}) dx dy = 0$$

or

$$\frac{\partial Q_x}{\partial x} + \frac{\partial Q_y}{\partial y} - m\ddot{w} + \bar{p} = 0 \quad (4.394)$$

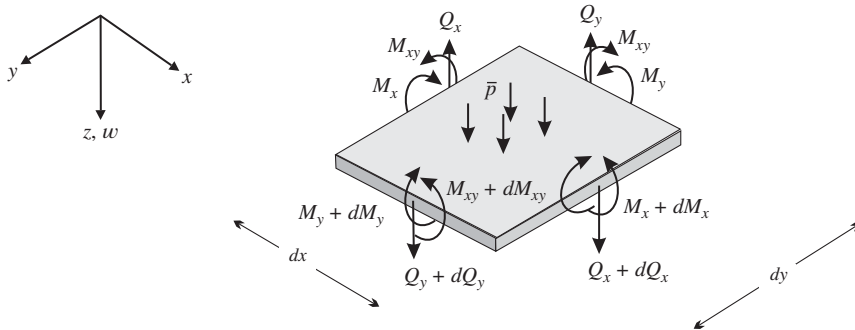


Figure 4.40 Equilibrium of the plate element.

while the shear force results from moment equilibrium of the plate element about O_x and O_y respectively. In a first-order approximation, we obtain:

– about O_y

$$dM_x dy + dM_{xy} dx - Q_x dx dy = 0$$

– about O_x

$$dM_y dx + dM_{xy} dy - Q_y dx dy = 0$$

giving the relationships:

$$\begin{aligned} Q_x &= \frac{\partial M_x}{\partial x} + \frac{\partial M_{xy}}{\partial y} \\ Q_y &= \frac{\partial M_y}{\partial y} + \frac{\partial M_{xy}}{\partial x} \end{aligned} \quad (4.395)$$

Substitution of (4.395) into (4.394) still allows us to rewrite vertical equilibrium in terms of the moments:

$$\boxed{\frac{\partial^2 M_x}{\partial x^2} + \frac{\partial^2 M_y}{\partial y^2} + 2 \frac{\partial^2 M_{xy}}{\partial y \partial x} + \bar{p} - m\ddot{w} = 0} \quad (4.396)$$

Finally, by returning to the moment–curvature relationships (4.347) and assuming uniform material properties, we obtain the partial differential equation governing the vertical plate deflection:

$$D \left(\frac{\partial^4 w}{\partial x^4} + \frac{\partial^4 w}{\partial y^4} + 2 \frac{\partial^4 w}{\partial x^2 \partial y^2} \right) + m\ddot{w} - \bar{p} = 0 \quad (4.397)$$

or, in terms of the Laplacian operator:

$$\Delta = \left(\frac{\partial^2}{\partial x^2} + \frac{\partial^2}{\partial y^2} \right) \quad (4.398)$$

the more compact expression:

$$\boxed{D \Delta \Delta w + m\ddot{w} - \bar{p} = 0} \quad (4.399)$$

4.4.10 Influence of in-plane initial stresses on plate vibration

In the case where initial extension resulting from in-plane stresses is taken into account, the strain energy $\mathcal{V}_{int}^{(2)}$ (4.359) may be decomposed into the linear part and the term of geometric origin:

$$\mathcal{V}_{int}^{(2)} = \mathcal{V}_{int}^{\ell} + \mathcal{V}_g \quad (4.400)$$

with

$$\mathcal{V}_{int}^\ell = \frac{1}{2} \int_S \chi^T \mathbf{H}^* \chi \, dS$$

$$\mathcal{V}_g = \frac{1}{2} \int_S \left\{ N_{x0} \left(\frac{\partial w}{\partial x} \right)^2 + N_{y0} \left(\frac{\partial w}{\partial y} \right)^2 + 2N_{xy0} \left(\frac{\partial w}{\partial x} \frac{\partial w}{\partial y} \right) \right\} dS \quad (4.401)$$

The geometric strain energy corresponds to definition (4.47), in which only the out-of-plane large rotation terms have been retained.

The variation of the linear term has been treated previously and yields Equation (4.383). Variation of the geometric strain energy yields:

$$\delta \mathcal{V}_g = \int_S \left\{ N_{x0} \frac{\partial w}{\partial x} \delta \left(\frac{\partial w}{\partial x} \right) + N_{y0} \frac{\partial w}{\partial y} \delta \left(\frac{\partial w}{\partial y} \right) + N_{xy0} \left[\frac{\partial w}{\partial x} \delta \left(\frac{\partial w}{\partial y} \right) + \frac{\partial w}{\partial y} \delta \left(\frac{\partial w}{\partial x} \right) \right] \right\} dS \quad (4.402)$$

and, by integrating by parts:

$$\delta \mathcal{V}_g = \int_\Gamma \left[\ell N_{x0} \frac{\partial w}{\partial x} + m N_{y0} \frac{\partial w}{\partial y} + m N_{xy0} \frac{\partial w}{\partial x} + \ell N_{xy0} \frac{\partial w}{\partial y} \right] \delta w \, d\Gamma$$

$$- \int_S \left\{ \frac{\partial}{\partial x} \left[N_{x0} \frac{\partial w}{\partial x} + N_{xy0} \frac{\partial w}{\partial y} \right] + \frac{\partial}{\partial y} \left[N_{y0} \frac{\partial w}{\partial y} + N_{xy0} \frac{\partial w}{\partial x} \right] \right\} \delta w \, dS \quad (4.403)$$

The term on the contour may still be modified by taking account of (4.377):

$$\delta \mathcal{V}_g = \int_\Gamma \left[N_{n0} \frac{\partial w}{\partial n} + N_{ns0} \frac{\partial w}{\partial s} \right] \delta w \, d\Gamma$$

$$- \int_S \left\{ \frac{\partial}{\partial x} \left[N_{x0} \frac{\partial w}{\partial x} + N_{xy0} \frac{\partial w}{\partial y} \right] + \frac{\partial}{\partial y} \left[N_{y0} \frac{\partial w}{\partial y} + N_{xy0} \frac{\partial w}{\partial x} \right] \right\} \delta w \, dS \quad (4.404)$$

with the definition of the in-plane stresses on the edge:

$$N_{n0} = \ell^2 N_{x0} + 2\ell m N_{xy0} + m^2 N_{y0}$$

$$N_{ns0} = \ell m (N_{y0} - N_{x0}) + (\ell^2 - m^2) N_{xy0} \quad (4.405)$$

The modified equilibrium equations result:

– on the surface

$$\boxed{\begin{aligned} & \frac{\partial}{\partial x} \left(Q_x + N_{x0} \frac{\partial w}{\partial x} + N_{xy0} \frac{\partial w}{\partial y} \right) \\ & + \frac{\partial}{\partial y} \left(Q_y + N_{y0} \frac{\partial w}{\partial y} + N_{xy0} \frac{\partial w}{\partial x} \right) - m\ddot{w} + \bar{p} = 0 \end{aligned}} \quad \text{on } S \quad (4.406)$$

- at any point of the regular contour portion, either in terms of the shear force or in terms of the vertical deflection:

$$K_n + N_{n0} \frac{\partial w}{\partial n} + N_{ns0} \frac{\partial w}{\partial s} = 0 \quad \text{or} \quad w = 0 \quad \text{on } \Gamma \quad (4.407)$$

according to whether the contour is free or fixed.

The conditions on the bending moment and on the corner force are not affected.

In the case of a plate with uniform properties, the surface equilibrium equation may still be expressed in terms of the vertical deflection:

$$D\Delta\Delta w - \left[N_{x0} \frac{\partial w}{\partial x} + N_{y0} \frac{\partial w}{\partial y} + 2N_{xy0} \frac{\partial^2 w}{\partial x \partial y} \right] + m\ddot{w} - \bar{p} = 0 \quad (4.408)$$

4.4.11 Free vibrations of the rectangular plate

The free vibration assumption (harmonic motion, zero external load \bar{p}) for the plate with no prestress and uniform properties yields the eigenvalue equation:

$$\Delta\Delta w - \frac{\omega^2 m}{D} w = 0 \quad (4.409)$$

To establish a general solution for this equation, let us define:

$$\beta^4 = \frac{\omega^2 m}{D} \quad (4.410)$$

Equation (4.409) may then be put in the form:

$$(\Delta + \beta^2)(\Delta - \beta^2)w = 0 \quad (4.411)$$

and the two functions w_1 and w_2 are defined:

$$(\Delta - \beta^2)w_1 = 0 \quad \text{and} \quad (\Delta + \beta^2)w_2 = 0 \quad (4.412)$$

It is then easily verified that the general solution to (4.411) may be written:

$$w = w_1 + w_2 \quad (4.413)$$

Indeed, by substitution of (4.413) into (4.411) we get:

$$(\Delta + \beta^2)(\Delta - \beta^2)(w_1 + w_2) = -2\beta^2(\Delta + \beta^2)w_2 = 0 \quad (4.414)$$

For the part w_1 , the general solution is of the exponential type:

$$w_1 = e^{\alpha x} e^{\gamma y} \quad \text{with} \quad \alpha^2 + \gamma^2 = \beta^2 \quad (4.415)$$

while the general solution of part w_2 takes the associated complex form:

$$w_2 = e^{i\alpha x} e^{i\gamma y} \quad \text{with} \quad \alpha^2 + \gamma^2 = \beta^2 \quad (4.416)$$

By taking account of the possible signs for the constants α and γ , we may express the complete solution in terms of hyperbolic and trigonometric functions:

$$\begin{aligned}
 w(x, y) = & A_1 \sin \alpha x \sin \gamma y + A_2 \cos \alpha x \sin \gamma y \\
 & + A_3 \sin \alpha x \cos \gamma y + A_4 \cos \alpha x \cos \gamma y \\
 & + A_5 \sinh \alpha x \sinh \gamma y + A_6 \cosh \alpha x \sinh \gamma y \\
 & + A_7 \sinh \alpha x \cosh \gamma y + A_8 \cosh \alpha x \cosh \gamma y
 \end{aligned} \tag{4.417}$$

The values of the constants A_i and parameters α and β depend on the application of the boundary conditions.

The simply supported plate

The only case of plate with rectangular geometry possessing an exact closed-form solution is the rectangular plate simply supported on its four edges (Figure 4.41).

Let a and b be the plate dimensions along x and y . The boundary conditions are given by:

$$\begin{aligned}
 w = 0 \quad \text{and} \quad M_x = 0 \quad \text{at} \quad x = 0 \quad \text{and} \quad x = a \\
 w = 0 \quad \text{and} \quad M_y = 0 \quad \text{at} \quad y = 0 \quad \text{and} \quad y = b
 \end{aligned} \tag{4.418}$$

Since the displacement is zero everywhere on the contour, by invoking the definition (4.347) of moments it is easily seen that the boundary conditions (4.418) may be put in the equivalent form:

$$\begin{aligned}
 w = 0 \quad \text{and} \quad \frac{\partial^2 w}{\partial x^2} = 0 \quad \text{at} \quad x = 0 \quad \text{and} \quad x = a \\
 w = 0 \quad \text{and} \quad \frac{\partial^2 w}{\partial y^2} = 0 \quad \text{at} \quad y = 0 \quad \text{and} \quad y = b
 \end{aligned} \tag{4.419}$$

Their application to the general solution (4.417) yields the effective solution:

$$w(x, y) = A \sin \alpha x \sin \gamma y$$

with the additional conditions:

$$\sin \alpha a = 0 \quad \text{and} \quad \sin \gamma b = 0 \tag{4.420}$$

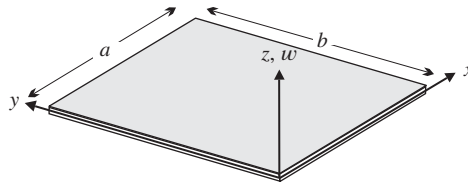


Figure 4.41 Simply supported rectangular plate.

The possible values of the constants are thus:

$$\alpha_r = \frac{r\pi}{a} \quad \text{and} \quad \gamma_n = \frac{n\pi}{b} \quad r, n = 1, 2, \dots, \infty \quad (4.421)$$

from which the eigenfrequencies of the simply supported plate result:

$$\omega_{rm} = \beta_{rm}^2 \sqrt{\frac{D}{m}} = \pi^2 \left[\left(\frac{r}{a} \right)^2 + \left(\frac{n}{b} \right)^2 \right] \sqrt{\frac{D}{m}} \quad (4.422)$$

and the corresponding eigenmodes:

$$w_{rm}(x, y) = \sin\left(\frac{r\pi x}{a}\right) \sin\left(\frac{n\pi y}{b}\right) \quad (4.423)$$

The values $(r - 1)$ and $(m - 1)$ determine the number of nodal lines of the eigenmode along y and x respectively. Figure 4.42 shows the first symmetric–symmetric mode (S–S), the first

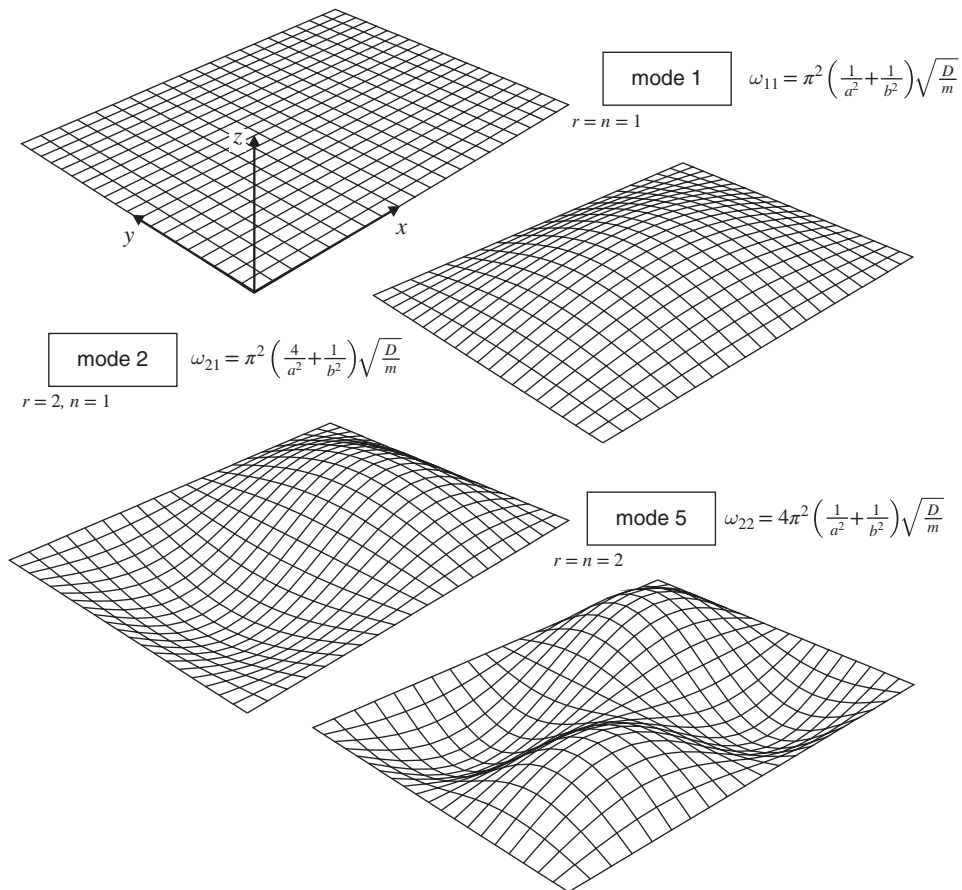


Figure 4.42 Eigenmodes of the simply supported rectangular plate, $b = \frac{3}{4}a$.

symmetric–antisymmetric mode (S–A) and the first antisymmetric–antisymmetric mode (A–A) modes for the simply supported rectangular plate.

4.4.12 Vibrations of circular plates

Vibration equation for circular plates

In order to establish the vibration equation for vibrating circular plates, let us restart from the corresponding equation in rectangular coordinates and transform it into polar coordinates:

$$x = r \cos \theta \quad \text{and} \quad y = r \sin \theta \quad (4.424)$$

The Jacobian matrix of the transformation is written:

$$\mathbf{J} = \begin{bmatrix} \frac{\partial x}{\partial r} & \frac{\partial x}{\partial \theta} \\ \frac{\partial y}{\partial r} & \frac{\partial y}{\partial \theta} \end{bmatrix} = \begin{bmatrix} \cos \theta & -r \sin \theta \\ \sin \theta & r \cos \theta \end{bmatrix} \quad (4.425)$$

and has as an inverse:

$$\mathbf{J}^{-1} = \begin{bmatrix} \cos \theta & \sin \theta \\ -\frac{1}{r} \sin \theta & \frac{1}{r} \cos \theta \end{bmatrix} \quad (4.426)$$

The first derivatives are thus transformed according to:

$$\begin{aligned} \frac{\partial}{\partial x} &= \cos \theta \frac{\partial}{\partial r} - \frac{1}{r} \sin \theta \frac{\partial}{\partial \theta} \\ \frac{\partial}{\partial y} &= \sin \theta \frac{\partial}{\partial r} + \frac{1}{r} \cos \theta \frac{\partial}{\partial \theta} \end{aligned} \quad (4.427)$$

and the expression of the Laplacian operator in polar coordinates is:

$$\Delta = \left(\frac{\partial^2}{\partial x^2} + \frac{\partial^2}{\partial y^2} \right) = \left(\frac{\partial^2}{\partial r^2} + \frac{1}{r} \frac{\partial}{\partial r} + \frac{1}{r^2} \frac{\partial^2}{\partial \theta^2} \right) \quad (4.428)$$

from which results the motion equation of circular plates with uniform properties in polar coordinates:

$$\left(\frac{\partial^2}{\partial r^2} + \frac{1}{r} \frac{\partial}{\partial r} + \frac{1}{r^2} \frac{\partial^2}{\partial \theta^2} \right)^2 w - \frac{\omega^2 m}{D} w = 0 \quad (4.429)$$

The corresponding boundary conditions are directly deduced from (4.391) and (4.392) with the observation that the curvilinear coordinates of plate contour become:

$$n = r \quad \text{and} \quad s = R\theta$$

where R is the plate external radius. The following conditions are obtained:

– on either shear force or vertical displacement on the edge:

$$\frac{\partial M_r}{\partial r} + \frac{2}{R} \frac{\partial M_{r\theta}}{\partial \theta} + \frac{1}{R} (M_r - M_\theta) = 0 \quad \text{or} \quad w = 0 \quad \text{at} \quad r = R \quad (4.430)$$

– on either normal moment or normal slope on the edge:

$$M_r = 0 \quad \text{or} \quad \frac{\partial w}{\partial r} = 0 \quad \text{at } r = R \quad (4.431)$$

Strain energy expression

The transformation (4.429) also allows expression of the plate strain energy (4.369) in polar coordinates:

$$\begin{aligned} \mathcal{V}_{int} = \frac{1}{2} \int_S D \left\{ \left(\frac{\partial^2 w}{\partial r^2} + \frac{1}{r} \frac{\partial w}{\partial r} + \frac{1}{r^2} \frac{\partial^2 w}{\partial \theta^2} \right)^2 \right. \\ \left. - 2(1 - \nu) \left[\frac{\partial^2 w}{\partial r^2} \left(\frac{1}{r} \frac{\partial w}{\partial r} + \frac{1}{r^2} \frac{\partial^2 w}{\partial \theta^2} \right) - \left(\frac{\partial}{\partial r} \left(\frac{1}{r} \frac{\partial w}{\partial \theta} \right) \right)^2 \right] \right\} r \, dr \, d\theta \end{aligned} \quad (4.432)$$

The case of the clamped circular plate

Let us consider the plate clamped on its perimeter and seek an exact closed-form solution. The following problem must be solved:

$$(\Delta^2 - \beta^4) w(r, \theta) = 0 \quad (4.433)$$

with

$$\beta^4 = \frac{\omega^2 m}{D} \quad (4.434)$$

and the boundary conditions on the external radius $r = a$:

$$w(a, \theta) = 0 \quad \text{and} \quad \left. \frac{\partial w}{\partial r} \right|_a = 0 \quad (4.435)$$

In a similar manner as for plates in Cartesian coordinates, the solution is split into two parts:

$$w = w_1 + w_2 \quad (4.436)$$

where w_1 and w_2 verify:

$$(\Delta + \beta^2) w_1 = 0 \quad \text{and} \quad (\Delta + (i\beta)^2) w_2 = 0 \quad (4.437)$$

First let us treat the part w_1 by separating it into a radial part and an angular one in the form:

$$w_1 = R(r)\Theta(\theta) \quad (4.438)$$

This yields the equation:

$$\left(\frac{\partial^2 R}{\partial r^2} + \frac{1}{r} \frac{\partial R}{\partial r} \right) \Theta + \frac{R}{r^2} \frac{\partial^2 \Theta}{\partial \theta^2} + \beta^2 R \Theta = 0 \quad (4.439)$$

which can be separated into equations governing the θ and r variables:

$$\begin{cases} \frac{\partial^2 \Theta}{\partial \theta^2} + k^2 \Theta = 0 \\ \frac{\partial^2 R}{\partial r^2} + \frac{1}{r} \frac{\partial R}{\partial r} + \left(\beta^2 - \frac{k^2}{r^2} \right) R = 0 \end{cases} \quad (4.440)$$

Periodicity of the angular part of the solution for one revolution implies an integer positive value for k , while the radial part obeys a Bessel equation and is thus expressed in terms of Bessel functions of the first and second kind:

$$\begin{aligned} \Theta_k(\theta) &= C_{1k} \sin k\theta + C_{2k} \cos k\theta \\ R_k(r) &= C_{3k} J_k(\beta r) + C_{4k} Y_k(\beta r) \end{aligned} \quad (4.441)$$

The first part of the general solution is thus:

$$w_1(r, \theta) = (A_{1k} J_k(\beta r) + A_{3k} Y_k(\beta r)) \sin k\theta + (A_{2k} J_k(\beta r) + A_{4k} Y_k(\beta r)) \cos k\theta \quad (4.442)$$

The second part of the solution involves the modified Bessel functions $I_k(x)$ and $K_k(x)$ which are linear combinations of $J_k(ix)$ and $Y_k(ix)$:

$$w_2(r, \theta) = (B_{1k} I_k(\beta r) + B_{3k} K_k(\beta r)) \sin k\theta + (B_{2k} I_k(\beta r) + B_{4k} K_k(\beta r)) \cos k\theta \quad (4.443)$$

The boundary conditions are then applied in the following manner:

- The solution must keep a finite value at the plate centre. Since the functions $Y_k(\beta r)$ and $K_k(\beta r)$ become singular at $r = 0$, the corresponding terms must be eliminated from both contributions (4.442) and (4.443) to the solution.
- The condition of zero displacement on the edge $w(a, \theta) = 0$ yields the equalities:

$$B_{1k} = -\frac{J_k(\beta a)}{I_k(\beta a)} A_{1k} \quad \text{and} \quad B_{2k} = -\frac{J_k(\beta a)}{I_k(\beta a)} A_{2k} \quad (4.444)$$

The solution thus takes the form:

$$w_k(r, \theta) = \left(J_k(\beta r) - \frac{J_k(\beta a)}{I_k(\beta a)} I_k(\beta r) \right) (A_{1k} \sin k\theta + A_{2k} \cos k\theta) \quad (4.445)$$

- The zero normal slope boundary condition on the perimeter generates the conditions:

$$\left[\frac{d}{dr} J_k(\beta r) - \frac{J_k(\beta a)}{I_k(\beta a)} \frac{d}{dr} I_k(\beta r) \right]_{r=a} = 0 \quad k = 0, 1, \dots \quad (4.446)$$

and thus the eigenvalue equation is:

$$I_k(\beta a) J_{k-1}(\beta a) - J_k(\beta a) I_{k-1}(\beta a) = 0 \quad (4.447)$$

It admits the solutions noted β_{kn} , $n = 1, 2, \dots$, from which the natural frequencies are deduced by (4.434):

$$\omega_{kn} = \beta_{kn}^2 \sqrt{\frac{D}{m}} \quad (4.448)$$

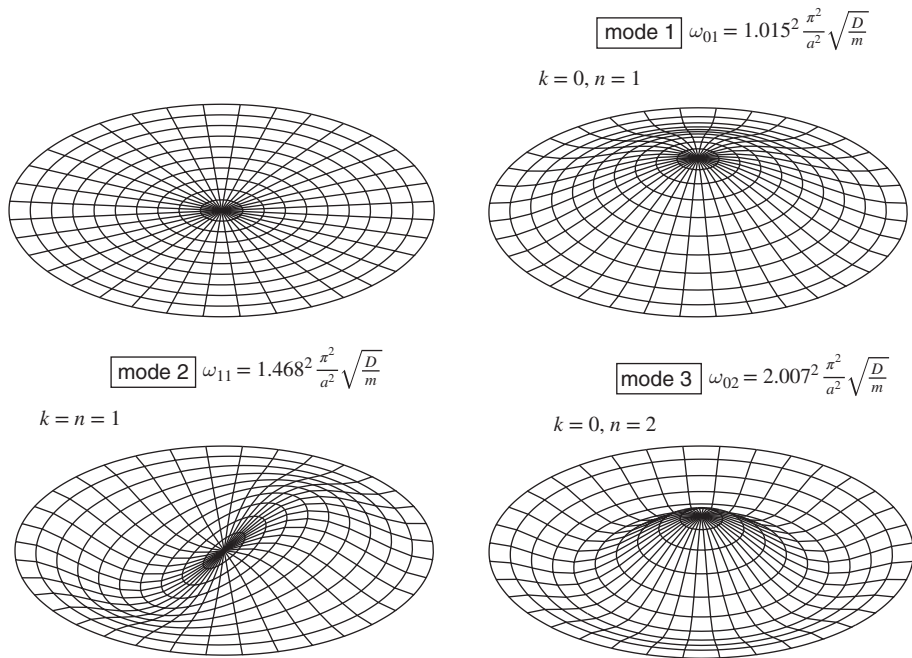


Figure 4.43 The first three eigenmodes of the clamped circular plate.

The eigenmodes are then of the form:

$$w_{kn}(r, \theta) = A_{kn} \left(I_k(\beta_{kn}a)J_k(\beta_{kn}r) - J_k(\beta_{kn}a)I_k(\beta_{kn}r) \right) \begin{cases} \cos k\theta \\ \sin k\theta \end{cases}$$

$$k = 0, 1, \dots$$

$$n = 1, 2, \dots$$
(4.449)

The first three eigenmodes of the circular plate clamped on its perimeter are represented by Figure 4.43.

A closed-form solution may be obtained in a similar manner for the circular plate simply supported on its perimeter.

4.4.13 An application of plate vibration: the ultrasonic wave motor

The ultrasonic wave motor (Daimler-Benz AG 1991, Hagedorn and Wallaschek 1990) is a technological application of plate vibration which is of interest in fields such as robotics and automotive engineering due to its small size and great simplicity.

In order to understand the operating principle for this motor, let us consider the free vibration of plates in the context of Kirchhoff assumptions. For axisymmetric boundary conditions, the

free vibration equation (4.429) of uniform circular and annular plates admits eigensolutions of the form:

$$w_{kn}(r, \theta) = A_{kn} R_{kn}(r) \begin{cases} \cos k\theta & k = 0, 1, \dots \\ \sin k\theta & n = 1, 2, \dots \end{cases} \quad (4.450)$$

where $R_{kn}(r)$ are Bessel functions. For a number of nodal diameters k different from zero, the cosine and sine modes w_c and w_s corresponding to the same eigenfrequency ω_{kn} of multiplicity 2 are linearly independent. Consider then the particular eigenmode formed by their combination:

$$\begin{aligned} w &= w_c + w_s \\ &= AR(r) \cos k\theta \cos \omega t + BR(r) \sin k\theta \sin(\omega t + \varphi) \end{aligned} \quad (4.451)$$

where A , B and φ are constants determined by the initial conditions. The combined eigenmode may still be put in the form:

$$\begin{aligned} w &= \frac{1}{2} R(r) [(A + B \cos \varphi) \cos(k\theta - \omega t) \\ &\quad + (A - B \cos \varphi) \cos(k\theta + \omega t) + 2B \sin \varphi \sin k\theta \cos \omega t] \end{aligned} \quad (4.452)$$

The first and second terms of this expression correspond respectively to a bending wave travelling in the positive and negative θ directions. The third term represents a standing wave. If it is supposed that the combined modes w_c and w_s are chosen so that $\varphi = 0$ and $A = B$, one finds:

$$w(r, \theta, t) = AR(r) \cos(k\theta - \omega t) \quad (4.453)$$

It may thus be concluded that the combination of two independent eigenmodes of a double eigenfrequency, if they are in phase and have the same amplitude, generates a travelling wave rotating with propagation velocity ω/k in the positive direction. The representation of such a wave at a given time is displayed by Figure 4.44 for an annular plate with $k = 10$.

This wave is used to induce the rotation of a rigid ring called the *rotor*, which is placed on top of the vibrating annular plate which plays the role of the *stator*. The rotor is not transported by the wave itself since, just like the water in a free surface wave, the stator material does not travel with the wave.

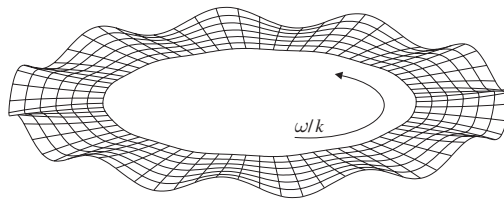


Figure 4.44 Transverse vibration wave in an annular plate.

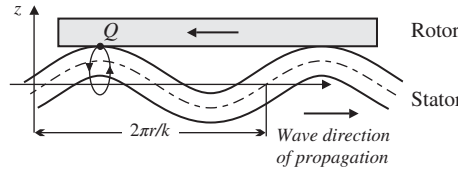


Figure 4.45 Driving of the rotor by the stator in an ultrasonic wave motor.

In order to better understand the driving mechanism, let us remember that the displacement w of Equation (4.453) describes the motion of the mean plane of the plate. Because the rotor is in contact with the external surface of the vibrating ring, let us compute both displacement and velocity at this point. Since, according to Kirchhoff's assumptions, the cross-sections remain orthogonal to the mean plane, the motion of a point Q located on the stator surface is described by:

$$[u_r, u_\theta, w]_Q = \left[\frac{-h}{2} \frac{\partial w}{\partial r}, \quad \frac{-h}{2r} \frac{\partial w}{\partial \theta}, \quad w \right] \quad (4.454)$$

By substituting in it the wave expression (4.453), the velocities can be computed:

$$[\dot{u}_r, \dot{u}_\theta, \dot{w}]_Q = -A\omega \left[\frac{-h}{2} \frac{\partial R}{\partial r} \sin(\omega t - k\theta), \right. \\ \left. \frac{hk}{2r} R \cos(\omega t - k\theta), \quad R \sin(\omega t - k\theta) \right] \quad (4.455)$$

Point Q describes an ellipse in the plane (θ, w) (Figure 4.45) in such a way that at a contact point between rotor and stator, $\cos(\omega t - k\theta) = 1$. The velocity field is then equal to:

$$\dot{u}_r = 0 \quad \dot{u}_\theta = -A\omega \frac{hk}{2r} R \quad \dot{w} = 0 \quad (4.456)$$

When no sliding occurs between the parts, the rotor angular velocity is given by:

$$\dot{\theta}_{rotor} = -A\omega \frac{hk}{2r} \frac{R(r)}{r} \quad (4.457)$$

It is observed that the rotor is driven in the direction opposite to the travelling wave. When a load is applied to the rotor, the stator transfers mechanical energy and must itself be excited to sustain the wave. The excitation is produced by piezoelectric elements covering the lower face of the stator. When these elements are polarized along the thickness, they contract and expand so as to induce a bending moment in the plate. In practice, the rotor has a complex shape and is notched in order to increase the distance between the mean plane and the plane of contact (Figure 4.46).

Expression (4.457) of the rotor angular velocity is valid only under zero slip. However, it is possible to observe that, w being small in practice, the rotor velocity is much lower than the wave propagation velocity and may be modulated by the wave amplitude A via the piezoelectric excitors.

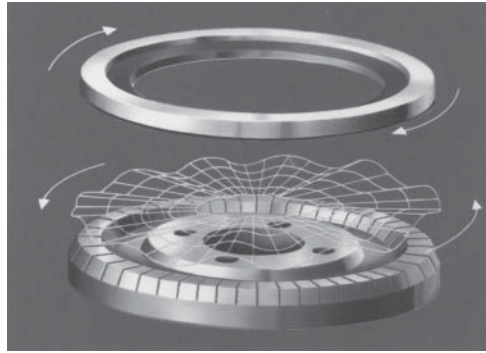


Figure 4.46 Rotor and stator of an ultrasonic wave motor. Source: Reproduced with permission from Daimler AG.

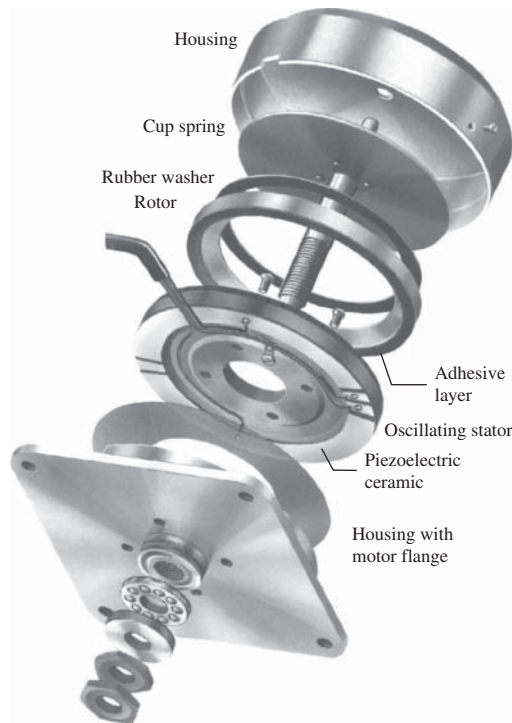


Figure 4.47 Example of an ultrasonic wave motor. Source: Reproduced with permission from Daimler AG.

An actual design of a complete ultrasonic wave motor is shown in Figure 4.47.

Further details on the theoretical analysis and technical realization for the motor may be found in the literature (Hagedorn and Wallaschek 1990). Let us here simply point out the main advantages of ultrasonic wave motors:

- Low angular velocity. This makes the use of reduction gears unnecessary for most practical applications. Indeed, let us consider the following example:

$$r = 45 \text{ mm} \quad \frac{h}{2r} = \frac{1}{10} \quad k = 11$$

$$\frac{\omega_{kn}}{2\pi} \simeq 40 \text{ kHz} \quad AR_{kn}(r) \simeq 1 \text{ } \mu\text{m}$$

The angular velocity is equal to:

$$\dot{\theta}_{rotor} \simeq \frac{-1}{40000} \omega_{kn} \simeq -60 \text{ rpm}$$

- Small dimensions compared to the large output torque: typically, 2 Nm for a volume of 200 cm³.
- At a constant excitation level, quasi-linear decrease of the angular velocity for increasing torque.
- High holding torque (typically 6 Nm).
- Fast response.
- High angular resolution.
- Low cost.

The main disadvantage of ultrasonic wave motors compared to classical electrical motors is that their global efficiency is of the order of 40%. This drawback is not, however, of primary importance for applications such as driving servomotors and auxiliary power units on automobiles.

Nowadays, the design of *mechatronic systems* such as piezoelectric devices is based on detailed numerical simulation that takes into account the strong coupling that develops between different interacting physical field. Including this strong interaction in the model is essential since the fundamental behaviour of those systems depends on it. For example, simulating the generation of mechanical motion in the ultrasonic (piezoelectric) motor is a multidisciplinary problem that requires accurate description of the elastic displacement, the electric fields and their physical cross-coupling.

The development of mechatronics as a new discipline (Preumont 2006) has motivated during the last two decades the development of a new generation of numerical software for engineering – generally based on the finite element method – that allows considering the same continuum as the material support for several physical fields (e.g. elastic, electric, magnetic, thermal) interacting with one another.

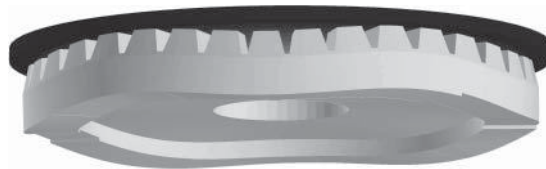


Figure 4.48 Numerical simulation of an ultrasonic motor: the rotor is mechanically driven through vibration of the rotor resulting from electrical excitation of the piezoelectric material. Source: Reproduced with permission from Open Engineering S.A.

The *Oofelie*® software (Klapka *et al.* 1998, Masson *et al.* 2007) is a good example of new generation finite element codes designed to solve this class of multiphysics problems. Figure 4.48 displays an instantaneous response of a piezoelectric motor modeled and simulated using *Oofelie*®. It clearly shows the mechanical interaction generated between stator and rotor of the piezoelectric motor due to appropriate vibration excitation of the piezoelectric rotor through the electrodes.

4.5 Wave propagation in a homogeneous elastic medium

The elastic continuum is a case of great interest in the study of undamped wave propagation. Our purpose here is not to discuss in depth the subject, but simply to introduce to the physical phenomenon of wave propagation in 3D media and show which main types of waves can be effectively observed. We will thus limit ourselves to the analysis of small amplitude free oscillations in infinite or semi-finite media (Fung 1965). Other related phenomena such as wave reflection, refraction and combination will not be considered here. For further reading and in-depth presentation of the topic, the reader is referred to excellent references such as (Kolsky 1953, Fung 1965 and Sadd 2009). Due to its fundamental importance for the field, the topic is also widely addressed in the literature on seismology.

4.5.1 The Navier equations in linear dynamic analysis

We have seen that when displacements and rotations are small, the expression of Green's strain tensor and the dynamic equilibrium equations may be restricted to the linear forms (4.6) and (4.36), and that for a linear elastic isotropic medium, stresses and strains are related by Hooke's law (4.14) or (4.16).

Combining Hooke's law in the form (4.16) and the expression (4.6) for linear strains, stresses can be related to displacements u_i by:

$$\sigma_{ij} = \lambda \left(\frac{\partial u_k}{\partial x_k} \right) \delta_{ij} + G \left(\frac{\partial u_i}{\partial x_j} + \frac{\partial u_j}{\partial x_i} \right)$$

and introducing the assumption of homogeneous medium (λ and G constants), the elastodynamic equilibrium equations (4.36) are written for the displacements as:

$$\lambda \frac{\partial}{\partial x_i} \left(\frac{\partial u_k}{\partial x_k} \right) \delta_{ij} + G \left(\frac{\partial^2 u_i}{\partial x_j \partial x_i} + \frac{\partial^2 u_j}{\partial x_i \partial x_i} \right) + \bar{X}_j - \rho \ddot{u}_j = 0 \quad j = 1, 2, 3$$

and thus:

$$(\lambda + G) \frac{\partial^2 u_i}{\partial x_j \partial x_i} + G \frac{\partial^2 u_j}{\partial x_i \partial x_i} + \bar{X}_j - \rho \ddot{u}_j = 0 \quad j = 1, 2, 3 \quad (4.458)$$

These three equilibrium equations governing the displacement field u_i , called *Navier's* equations, can also be written in the classical form:

$$G \nabla^2 u_j + (\lambda + G) \frac{\partial e}{\partial x_j} + \bar{X}_j = \rho \ddot{u}_j \quad j = 1, 2, 3 \quad (4.459)$$

where

∇^2 is the Laplacian operator,

$$e = \varepsilon_{11} + \varepsilon_{22} + \varepsilon_{33} = \frac{\partial u_1}{\partial x_1} + \frac{\partial u_2}{\partial x_2} + \frac{\partial u_3}{\partial x_3} \text{ is the divergence of the displacement field.}$$

e is also called *volumetric strain* since it expresses the local change of volume in the material (dilatation). The propagation of free waves in an isotropic continuum can be studied in all generality by assuming $\bar{X}_j = 0$ and solving the homogeneous equation:

$$G\nabla^2 u_j + (\lambda + G) \frac{\partial e}{\partial x_j} = \rho \ddot{u}_j \quad (4.460)$$

In this presentation, we will limit the discussion to the case where the displacement field remains invariant with respect to x_3 , meaning that we only consider waves propagating in the (x, y) plane. Therefore from here on we introduce the change of notations:

$$\begin{aligned} u_1(x_1, x_2, x_3, t) &\rightarrow u(x, y, t) \\ u_2(x_1, x_2, x_3, t) &\rightarrow v(x, y, t) \\ u_3(x_1, x_2, x_3, t) &\rightarrow w(x, y, t) \end{aligned} \quad (4.461)$$

Equation (4.460) yields the set of equations:

$$G \left(\frac{\partial^2}{\partial x^2} + \frac{\partial^2}{\partial y^2} \right) u + (\lambda + G) \left(\frac{\partial^2 u}{\partial x^2} + \frac{\partial^2 v}{\partial x \partial y} \right) - \rho \frac{\partial^2 u}{\partial t^2} = 0 \quad (4.462a)$$

$$G \left(\frac{\partial^2}{\partial x^2} + \frac{\partial^2}{\partial y^2} \right) v + (\lambda + G) \left(\frac{\partial^2 u}{\partial x \partial y} + \frac{\partial^2 v}{\partial x^2} \right) - \rho \frac{\partial^2 v}{\partial t^2} = 0 \quad (4.462b)$$

$$G \left(\frac{\partial^2}{\partial x^2} + \frac{\partial^2}{\partial y^2} \right) w - \rho \frac{\partial^2 w}{\partial t^2} = 0 \quad (4.462c)$$

It is observed that Equations (4.462a–4.462c) split in two groups. Equations (4.462a–4.462b) are coupled equations for u and v , second order in time and in space variables x and y . They will describe wave motion in the *propagation plane* (x, y) . Equation (4.462a) governs w and is not coupled to u or v . It is second order in time and in the space variables x and y in the direction orthogonal to w . It describes wave motion in the direction perpendicular to the propagation plane (x, y) .

In Section 4.5.2 we will first discuss two types of waves appearing in an unbounded medium: *longitudinal* and *transverse* waves. Such waves, also named P and S waves, are depicted in Figure 4.49.a–b showing the instantaneous deformed grid of a block of material inside an infinite homogeneous medium, assuming a wave propagation in the x direction.

Then in Section 4.5.3 special wave appearing at the surface of a half-space are outlined: *Rayleigh* and *Love* surface waves. Figure 4.49.c–d shows an instantaneous deformed state of a half-space (free surface $y = 0$) undergoing such waves propagating in the x direction.

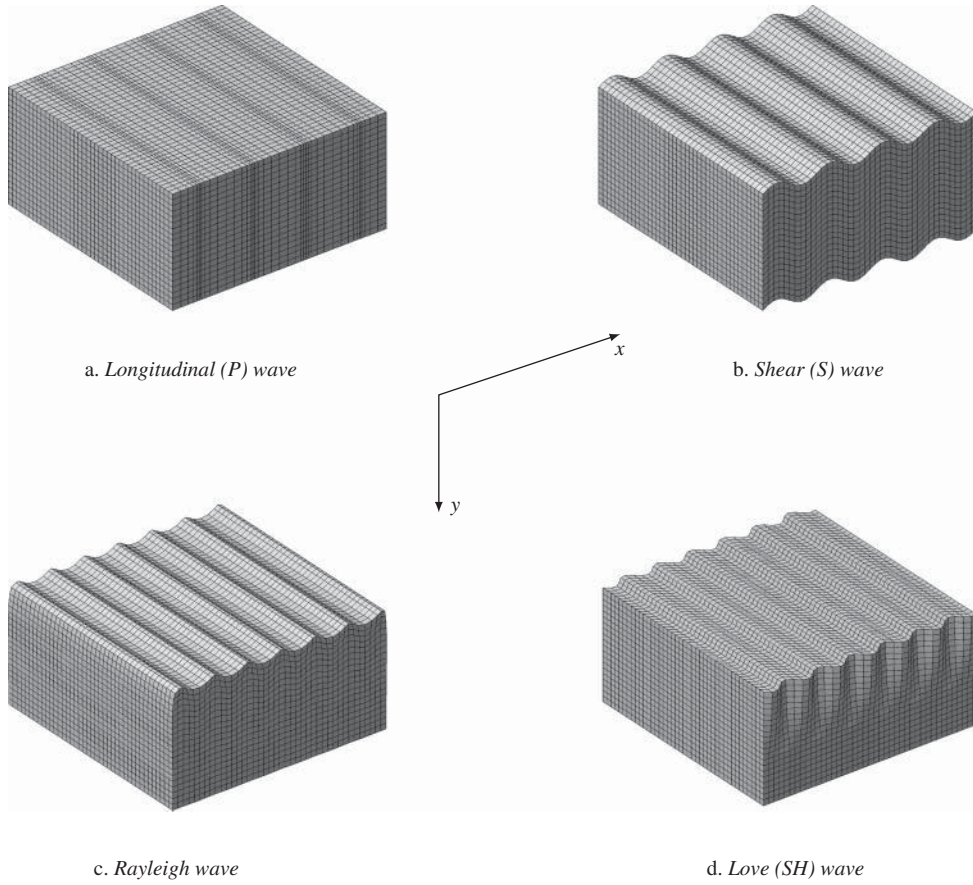


Figure 4.49 Fundamental deformation patterns generated by Longitudinal (P), Shear (S), Rayleigh and Love (SH) waves.

4.5.2 Plane elastic waves

Let us determine for example the existence of waves moving in the x direction and in such a way that the displacement field depends only on x and time t :

$$u(x, t) = u(x \pm ct) \quad v(x, t) = v(x \pm ct) \quad w(x, t) = w(x \pm ct) \quad (4.463)$$

where c is the propagation speed of the wave in the negative or positive x direction since for $x = \mp ct$ the displacements are invariant. The displacement field (4.463) represents a *plane wave*: indeed, at given time t , the displacement is identical at any point of the plane (y, z) perpendicular to the direction x of wave propagation. In this case only the strains ε_{xx} , ε_{xy} and ε_{xz} are nonzero and no deformations exist in plane (y, z) .

Substituting (4.463) into the set of Equations (4.462a–4.462c) provides the set of equations:

$$(\lambda + 2G) \frac{\partial^2 u}{\partial x^2} - c^2 \rho \frac{\partial^2 u}{\partial x^2} = 0 \quad (4.464a)$$

$$G \frac{\partial^2 v}{\partial x^2} - c^2 \rho \frac{\partial^2 v}{\partial x^2} = 0 \quad (4.464b)$$

$$G \frac{\partial^2 w}{\partial x^2} - c^2 \rho \frac{\partial^2 w}{\partial x^2} = 0 \quad (4.464c)$$

Equations (4.464a–4.464c) are uncoupled equations for the three components of the displacement field and show the existence of two fundamental solutions with different wave speeds.

Longitudinal waves

Longitudinal waves correspond to the case where the displacements are parallel to the direction of propagation (Figure 4.49.a). They result from the solution of (4.464a) and are thus characterized by the *transverse wave speed* c_L :

$$c_L = \sqrt{\frac{\lambda + 2G}{\rho}} = \sqrt{\frac{E(1 - \nu)}{(1 + \nu)(1 - 2\nu)\rho}} \quad (4.465)$$

Longitudinal waves were already observed in the bar in extension, with the difference that the lateral contraction effect was absent.

Transverse waves

When the displacements are orthogonal to the propagation direction, the wave is of the *transverse* type (Figure 4.49.b). They are solutions of Equation (4.464b) (or similarly, (4.464c)) and are characterized by the *transverse wave speed* c_T :

$$c_T = \sqrt{\frac{G}{\rho}} \quad (4.466)$$

The plane containing both the direction of propagation and the direction of displacement (e.g. the (x, y) plane when $w = 0$) is the *plane of polarization*.

Let us note that the ratio of the velocities c_L and c_T is a function of the Poisson ratio only:

$$c_T = c_L \sqrt{\frac{1 - 2\nu}{2(1 - \nu)}} \quad (4.467)$$

Figure 4.50 shows the dependence of the ratio c_T/c_L with respect to Poisson's ratio within the range $\nu \in [0, 0.5]$. The transverse wave speed c_T vanishes for an incompressible material, and comes close to $0.7 c_L$ when the lateral contraction effect disappears. It further increases for $\nu < 0$.¹³

¹³ There are some materials – called auxetic materials – that are characterized by a negative Poisson ratio. Most engineering materials, however, have a Poisson ratio close to 0.3.

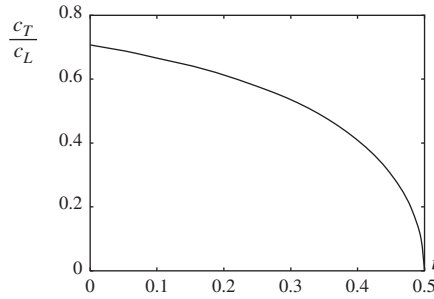


Figure 4.50 Variation of $\frac{c_T}{c_L}$ ratio with Poisson ratio ν .

It is worthwhile noticing that the wave propagation analysis performed before for the Timoshenko beam (Equation (4.331)) could predict the existence of both propagation speeds c_T and c_L , but with a different c_L due to the omission of the lateral contraction effect.

Both types of waves described above exist only in an infinite medium. In a finite medium, the plane waves are reflected or refracted in a manner analogous to acoustic or optical waves, with the difference that longitudinal waves are reflected or refracted while transforming themselves in a combination of transverse and longitudinal waves. The same statement holds for transverse waves. These properties can be studied by combining the simple cases just discussed in order to satisfy the boundary conditions encountered in practice.

4.5.3 Surface waves

When considering a semi-finite medium, it is possible to show the existence of waves of a special type which propagate on the boundary of the medium and take place essentially at a shallow depth. These waves are characterized by an amplitude which decreases exponentially with depth. They are similar to the waves appearing on the water surface when one throws a stone. These waves are called *surface waves* and correspond for example to the surface motion recorded by seismic instruments during earthquakes.

There are two main types of surface waves: *Rayleigh waves* and *Love waves* (Figure 4.49.c–d). The former are characterized by a wave motion (u, v) in the propagation plane (x, y) , while the latter occur when the wave motion $w(x, y)$ is orthogonal to the propagation plane.

Rayleigh surface waves (Rayleigh 1885)

Let us consider the simple case of the two-dimensional semi-finite medium represented by the half plane $y \geq 0$, the surface $y = 0$ being stress-free. Suppose the displacement field is represented by the real part of:

$$\begin{aligned} u &= A e^{-by} e^{ik(x-ct)} \\ v &= B e^{-by} e^{ik(x-ct)} \end{aligned} \quad (4.468)$$

where

A, B, \dots are complex constants,

b, \dots is a positive real number, wave amplitudes tending to zero while $y \rightarrow \infty$,

k, \dots is a real positive wave number such that $\omega = kc$.

By rewriting the Navier Equations (4.462a–4.462b) in the form:

$$c_T^2 \nabla^2 u + (c_L^2 - c_T^2) \left(\frac{\partial^2 u}{\partial x^2} + \frac{\partial^2 v}{\partial x \partial y} \right) - \frac{\partial^2 u}{\partial t^2} = 0 \quad (4.469a)$$

$$c_T^2 \nabla^2 v + (c_L^2 - c_T^2) \left(\frac{\partial^2 u}{\partial x \partial y} + \frac{\partial^2 v}{\partial x^2} \right) - \frac{\partial^2 v}{\partial t^2} = 0 \quad (4.469b)$$

and substituting the general expressions of the displacement field, the following homogeneous system of equations is obtained:

$$\begin{bmatrix} c_T^2 b^2 + (c^2 - c_L^2) k^2 & -ibk(c_L^2 - c_T^2) \\ -ibk(c_L^2 - c_T^2) & c_L^2 b^2 + (c^2 - c_T^2) k^2 \end{bmatrix} \begin{bmatrix} A \\ B \end{bmatrix} = 0 \quad (4.470)$$

The solution of (4.470) is not trivially zero provided that the determinant vanishes:

$$[c_L^2 b^2 - (c_L^2 - c^2) k^2] [c_T^2 b^2 - (c_T^2 - c^2) k^2] = 0 \quad (4.471)$$

Solving then (4.471) for b yields the following roots:

$$b_1 = k \sqrt{1 - \frac{c^2}{c_L^2}} \quad \text{and} \quad b_2 = k \sqrt{1 - \frac{c^2}{c_T^2}} \quad (4.472)$$

and the assumption that b is real results in $c < c_T < c_L$. The amplitude ratios corresponding to b_1 and b_2 are:

$$\left(\frac{B}{A} \right)_1 = -\frac{b_1}{ik} \quad \text{and} \quad \left(\frac{B}{A} \right)_2 = \frac{ik}{b_2} \quad (4.473)$$

The general solution (4.468) thus becomes:

$$\begin{aligned} u &= A_1 e^{-b_1 y} \exp[ik(x - ct)] + A_2 e^{-b_2 y} \exp[ik(x - ct)] \\ v &= -\frac{b_1}{ik} A_1 e^{-b_1 y} \exp[ik(x - ct)] + \frac{ik}{b_2} A_2 e^{-b_2 y} \exp[ik(x - ct)] \end{aligned} \quad (4.474)$$

The constants A_1, A_2 and the wave speed c are determined from the stress-free surface condition:

$$\sigma_{yy} = \sigma_{yx} = 0 \quad \text{at } y = 0 \quad (4.475)$$

By making use of Hooke's constitutive law and of the linear strain expression, the boundary conditions may still be put in the form:

$$\begin{aligned} \frac{\partial u}{\partial y} + \frac{\partial v}{\partial x} &= 0 \\ \lambda \left(\frac{\partial u}{\partial x} + \frac{\partial v}{\partial y} \right) + 2G \frac{\partial v}{\partial y} &= 0 \end{aligned} \quad \text{at } y = 0 \quad (4.476)$$

Let us next substitute in equations (4.476) the displacement expressions (4.474) and notice that:

$$G = \rho c_T^2 \quad \text{and} \quad \lambda = \rho (c_L^2 - 2c_T^2) \quad (4.477)$$

We obtain:

$$\begin{bmatrix} -2b_1 & -\left(b_2 + \frac{k^2}{b_2}\right) \\ (c_L^2 - 2c_T^2) - c_L^2 \frac{b_1^2}{k^2} & -2c_T^2 \end{bmatrix} \begin{bmatrix} A_1 \\ A_2 \end{bmatrix} = 0 \quad (4.478)$$

or, by taking into account the relationships (4.472),

$$\begin{bmatrix} 2\left(1 - \frac{c^2}{c_L^2}\right)^{\frac{1}{2}} & \left(2 - \frac{c^2}{c_T^2}\right)\left(1 - \frac{c^2}{c_T^2}\right)^{-\frac{1}{2}} \\ \left(2 - \frac{c^2}{c_T^2}\right) & -2 \end{bmatrix} \begin{bmatrix} A_1 \\ A_2 \end{bmatrix} = 0 \quad (4.479)$$

The constants A_1 and A_2 are not trivially zero if c verifies the characteristic equation:

$$\left(2 - \frac{c^2}{c_T^2}\right)^2 = 4\sqrt{1 - \frac{c^2}{c_L^2}}\sqrt{1 - \frac{c^2}{c_T^2}}$$

and after factorization of c^2/c_T^2 the *Rayleigh equation* is obtained:

$$\frac{c^2}{c_T^2} \left[\frac{c^6}{c_T^6} - 8\frac{c^4}{c_T^4} + c^2 \left(\frac{24}{c_T^2} - \frac{16}{c_L^2} \right) - 16 \left(1 - \frac{c_T^2}{c_L^2} \right) \right] = 0 \quad (4.480)$$

- If $c = 0$, u and v are not functions of time; the relationships (4.479) then give $A_1 = A_2 = 0$ and one finds $u = v = 0$, the trivial static solution.
- Since $c_T < c_L$ (Equation (4.467)), the second factor of (4.480) is negative for $c = 0$ and positive for $c = c_T$. A real root c between 0 and c_T thus always exists for equation (4.480), showing that surface waves having a velocity lower than c_T may appear.
- If $\nu = 1/4$, Equation (4.467) gives $c_L = \sqrt{3}c_T$ and $\lambda = G$. Equation (4.480) may then be written:

$$\frac{c^6}{c_T^6} - 8\frac{c^4}{c_T^4} + \frac{56}{3}\frac{c^2}{c_T^2} - \frac{32}{3} = 0 \quad (4.481)$$

It admits the three real roots:

$$\frac{c^2}{c_T^2} = 4, \quad 2 + \frac{2}{\sqrt{3}}, \quad 2 - \frac{2}{\sqrt{3}}$$

However, only in the case of the last root is it possible to verify the condition $c > c_T$ which is necessary for both b_1 and b_2 to be real. The first two roots are in practice parasitic roots introduced by the factorization in Equation (4.480). Thus, for a Rayleigh wave, one finds:

$$c_R = 0.9194 c_T \quad (4.482)$$

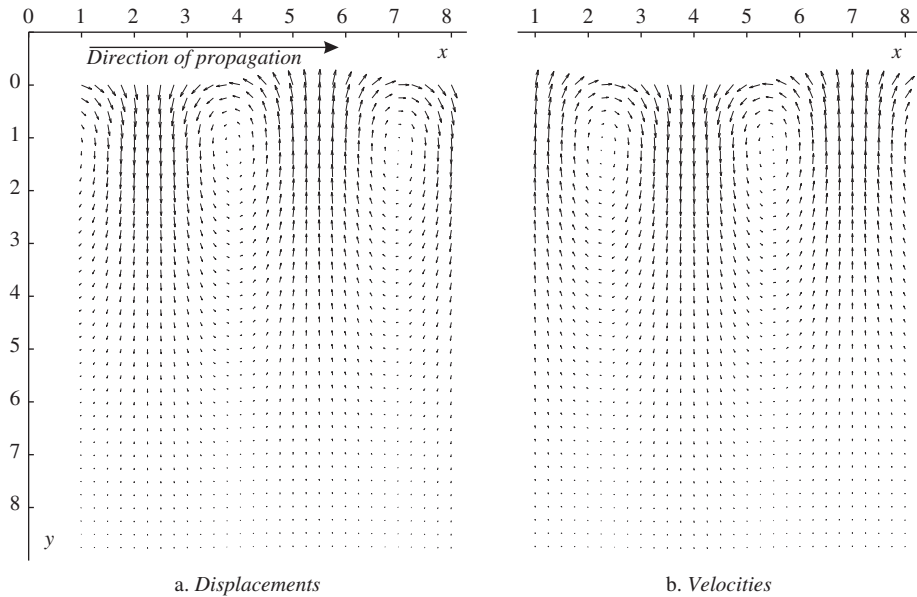


Figure 4.51 Spatial distribution of displacements and velocities generated by Rayleigh surface waves.

and substitution into (4.472) and (4.479) provides the displacements:

$$\begin{aligned} u &= A_1 \left[e^{-0.8475 ky} - 0.5773 e^{-0.3933 ky} \right] \cos(k(x - c_R t)) \\ v &= A_1 \left[-0.8475 e^{-0.8475 ky} + 1.4679 e^{-0.3933 ky} \right] \sin(k(x - c_R t)) \end{aligned} \quad (4.483)$$

The Rayleigh wave was illustrated in Figure 4.49.c. Figure 4.51 depicts the instantaneous displacements and velocities in the plane (x, y) as computed from (4.483). It shows that for the propagation of a Rayleigh wave the surface motion is backward elliptic, in contrast to the direct elliptic motion which characterizes the surface waves in a fluid. One notes also that the horizontal displacement u vanishes at a depth y equal to 0.192 times the wavelength $2\pi/k$, and then takes the opposite sign at higher depth.

Love waves (Love 1911)

All the wave motions described so far are restricted to the propagation plane. It is the case in particular for the Rayleigh surface waves presented above since, in the case considered, the Rayleigh waves are propagated along x on the surface $y = 0$, and the displacement w remains zero.

It can easily be shown that surface waves with displacement perpendicular to the propagation plane cannot exist in a homogeneous semi-infinite medium. Indeed they would obey to the motion equation (4.462c) under the boundary condition on the free surface:

$$\sigma_{yz} = \frac{\partial w}{\partial y} \quad \text{at } y = 0 \quad (4.484)$$

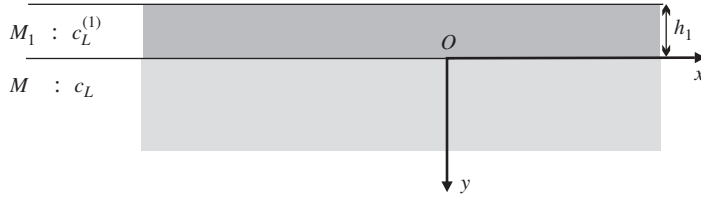


Figure 4.52 Love waves: two-layer homogeneous medium.

The general solution to the Navier equation (4.462c) with w tending to zero when y tends to infinity is:

$$w = A \exp \left\{ -ky \sqrt{1 - \left(\frac{c}{c_T} \right)^2} \right\} \exp(ik(x \pm ct)) \quad y \geq 0 \quad (4.485)$$

and applying the boundary condition (4.484) yields $A = 0$, cancelling thus completely the solution.

Surface waves with displacement perpendicular to the propagation plane and with amplitude similar to that of Rayleigh waves are nevertheless observed during earthquakes. Love (Love 1911) has shown that, in order to allow for their existence, it is sufficient to consider a homogeneous layer of material M_1 of thickness h_1 , superimposed on a semi-finite space of a different homogeneous material M .

Considering the axis system of Figure 4.52, the general solution (4.485) provides the expression of the displacement field for the forward wave

$$w = \begin{cases} A \exp \left[-ky \sqrt{1 - \frac{c^2}{c_T^2}} \right] e^{ik(x-ct)} & \text{in } M \\ \left(B \exp \left[-ky \sqrt{1 - \left(\frac{c}{c_T^{(1)}} \right)^2} \right] + B' \exp \left[ky \sqrt{1 - \left(\frac{c}{c_T^{(1)}} \right)^2} \right] \right) e^{ik(x-ct)} & \text{in } M_1 \end{cases} \quad (4.486)$$

The boundary conditions must express that w and σ_{yz} are continuous onto the surface $y = 0$ and that $\sigma_{yz} = 0$ at $y = -h_1$. These conditions yield:

$$A = B + B' \quad (4.487a)$$

$$GA \sqrt{1 - \frac{c^2}{c_T^2}} = G_1 (B - B') \sqrt{1 - \left(\frac{c}{c_T^{(1)}} \right)^2} \quad (4.487b)$$

$$B \exp \left[kh_1 \sqrt{1 - \left(\frac{c}{c_T^{(1)}} \right)^2} \right] = B' \exp \left[-kh_1 \sqrt{1 - \left(\frac{c}{c_T^{(1)}} \right)^2} \right] \quad (4.487c)$$

It is assumed – as verified a posteriori – that a solution exists under the condition that:

$$c_T^{(1)} \leq c \leq c_T \quad (4.488)$$

in which case the following real parameters can be defined:

$$\alpha = \sqrt{1 - \frac{c^2}{c_T^2}} \quad \beta = \sqrt{\left(\frac{c}{c_T^{(1)}}\right)^2 - 1} \quad (4.489)$$

so that Equations (4.487a–4.487c) become:

$$G(B + B')\alpha = iG_1 (B - B') \beta \quad (4.490a)$$

$$B \exp(kh_1\beta) = B' \exp(-ikh_1\alpha) \quad (4.490b)$$

B and B' can be eliminated by combining Equations (4.490a–4.490b) in the form:

$$\frac{B - B'}{B + B'} = -i \tan(kh_1\beta) = -i \frac{G \alpha}{G_1 \beta} \quad (4.491)$$

Returning to the definitions (4.489) yields:

$$G \sqrt{1 - \frac{c^2}{c_T^2}} - G_1 \tan \left[kh_1 \sqrt{\left(\frac{c}{c_T^{(1)}}\right)^2 - 1} \right] \sqrt{\left(\frac{c}{c_T^{(1)}}\right)^2 - 1} = 0 \quad (4.492)$$

which is the equation governing the propagation velocity c_{SH} of a surface wave with motion perpendicular to the propagation direction.

When $c_T^{(1)} < c_T$, Equation (4.492) provides a real value c_{SH} such as $c_T^{(1)} < c_{SH} < c_T$ since both terms are then real and have opposite signs.

The wave speed c_{SH} being known, the explicit form of the displacement field $w(x, y)$ is obtained after elimination of coefficients B and B' between Equations (4.487a) and (4.491). The final result is:

$$w(x, y) = \begin{cases} A e^{-\alpha y} e^{ik(x-ct)} & \text{in } M \\ A \frac{\cos[k(h_1 - y)\beta]}{\cos(kh_1\beta)} e^{ik(x-ct)} & \text{in } M_1 \end{cases} \quad (4.493)$$

with α and β given by (4.489).

These waves are called *Love waves*, and are particular type of horizontally polarized (*SH*) waves. They were illustrated in Figure 4.49.d showing that such waves are confined to the layer under the free surface. They can occur under the stated boundary conditions, provided that the shear velocity of the upper layer M_1 is less than that in the underlying medium M . Love waves of general shape may be derived by superimposing harmonic Love waves of type (4.493) with different values of k . The dependence of the wave number k introduces, like demonstrated for the beam in bending, a dispersion phenomenon that will not be considered here.

Example 4.7

In order to illustrate the physical concept of Love wave, let us compute the fundamental response ($k = 1$) for a composite structure made of a layer of wood (thickness: $h_1 = 0.6$) lying on steel. The materials have the following properties:

- Steel: $G = 8.0 \text{ E11 N/m}^2$, $\rho = 7.2 \text{ E03 kg/m}^3$, $c_T = 3350 \text{ m/s}$.
- Wood: $G_1 = 1.66 \text{ E08 N/m}^2$, $\rho_1 = 0.155 \text{ E03 kg/m}^3$, $c_T^{(1)} = 1034 \text{ m/s}$.

Equation (4.492) is solved by writing it in the form:

$$\beta \tan(ikh_1\beta) = \frac{G}{G_1} \alpha \quad (\text{E4.7.a})$$

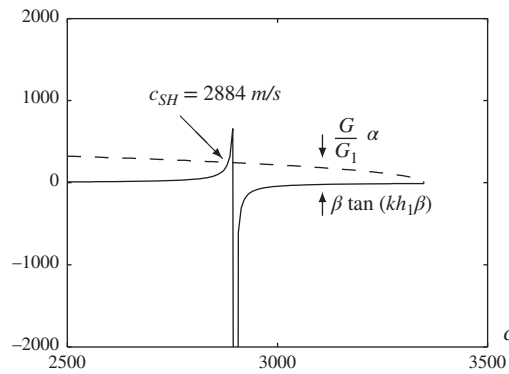


Figure 4.53 Determination of Love wave speed c_{SH} for a wood layer on steel.

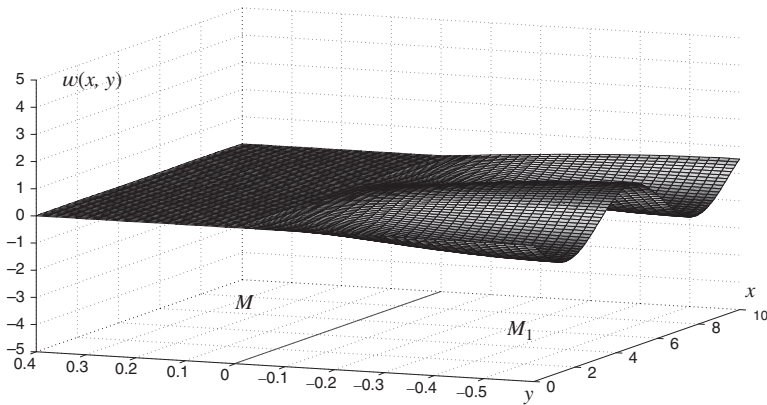


Figure 4.54 Love surface wave (SH): displacement field $w(x, y)$ in direction orthogonal to wave propagation.

and plotting both sides of Equation (E4.7.a) versus c as displayed on Figure 4.53. The intersection of both curves provides the wave speed $c_{SH} = 2884 \text{ m/s}$.

The displacement pattern for given t computed from Equation (4.493) is displayed on Figure 4.54. It has harmonic shape in the soft (M_1) region in both x and y directions, while it decays exponentially and is almost unnoticeable in the stiff underlayer. The maximum amplitude occurs on the free surface.

4.6 Solved exercises

Problem 4.1 Let us consider a uniform beam of length ℓ with stiffness and mass characteristics (EI , m) clamped at one end and with a mass M attached at the tip (Figure 4.55). You are asked:

1. to write down the equation for vibration motion of the system and the associated boundary conditions in nondimensional form.
2. to apply the boundary conditions to the general solution in order to get an equation governing the frequency parameter μ such that $\mu^4 = \frac{\omega^2 m \ell^4}{EI}$ as a function of the mass ratio $\alpha = \frac{M}{m\ell}$.
3. to verify the correctness of the result obtained when $\alpha \rightarrow 0$ and when $M \rightarrow \infty$.
4. to show how the roots (μ_s , $s = 1, \infty$) can be obtained graphically as functions of the α parameter.

Solution

1. In nondimensional form, the equation of motion and the associated boundary conditions take the form (see page 268)

$$\eta'''' - \mu^4 \eta = 0 \quad 0 < \xi < 1 \quad (\text{P4.1.a})$$

$$\eta(0) = 0 \quad \eta'(0) = 0 \quad (\text{P4.1.b})$$

$$\eta''(1) = 0 \quad \eta'''(1) = -\alpha \mu^4 \eta(1) \quad (\text{P4.1.c})$$

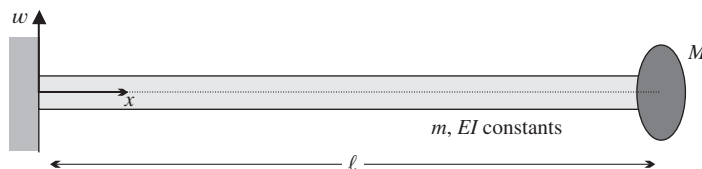


Figure 4.55 A clamped–free uniform beam with a mass at its end.

2. Expressing the solution in terms of Duncan functions (4.248) and applying the boundary conditions (P4.1.b) yields:

$$\eta(\mu\xi) = Cs_2(\mu\xi) + Dc_2(\mu\xi) \quad 0 < \xi < 1 \quad (\text{P4.1.d})$$

and applying next the boundary conditions (P4.1.c) provides the set of equations:

$$\mu^2 (Cs_1(\mu) + Dc_1(\mu)) = 0 \quad (\text{P4.1.e})$$

$$\mu^3 (Cc_1(\mu) + Ds_2(\mu)) = -\alpha\mu^4 (Cs_2(\mu) + Dc_2(\mu)) \quad (\text{P4.1.f})$$

to which corresponds the homogeneous system:

$$\begin{bmatrix} s_1(\mu) & c_1(\mu) \\ c_1(\mu) + \alpha\mu s_2(\mu) & s_2(\mu) + \alpha\mu c_2(\mu) \end{bmatrix} \begin{bmatrix} C \\ D \end{bmatrix} = 0 \quad (\text{P4.1.g})$$

The characteristic equation associated to (P4.1.g) can be put in the form:

$$\alpha\mu = \frac{s_1(\mu)s_2(\mu) - c_1^2(\mu)}{s_1(\mu)c_2(\mu) - c_1(\mu)s_2(\mu)} \quad (\text{P4.1.h})$$

or, in terms of trigonometric and hyperbolic functions:

$$\alpha = \frac{(1 + \cos \mu \cosh \mu)}{\mu(-\cosh \mu \sin \mu + \cos \mu \sinh \mu)} \quad (\text{P4.1.i})$$

3. The numerator of Equation (P4.1.i) corresponds to the eigenvalue Equation (E4.5.c) obtained for the clamped–free beam. Therefore when $\alpha = 0$ the solution obtained corresponds to the clamped–free configuration, which was to be expected. For large M , and thus infinite α , the solution is expected to correspond to the case of the clamped–pinned beam since the inertia of the tip mass becomes infinite and thus blocks the displacement. It can be verified that the numerator of Equation (P4.1.i) is nothing else than the eigenvalue equation for the clamped–pinned configuration.
4. The roots of Problem (P4.1.a) can be obtained for example by plotting the functions:

$$f_1(\mu) = \alpha\mu \quad \text{and} \quad f_2(\mu) = \frac{1 + \cos \mu \cosh \mu}{-\cosh \mu \sin \mu + \cos \mu \sinh \mu} \quad (\text{P4.1.j})$$

in which case the characteristic values μ_s are located at their intersection. Figure 4.56 shows the determination of the characteristic values μ_s for $\alpha = \frac{M}{m\ell} = 0.25$. The intersections of the curve $f_2(\mu)$ with the horizontal axis are the roots of the clamped–free beam while the asymptotes cross it at the roots of the clamped–pinned beam. The roots of the beam with tip mass are bracketed by them as physically expected.

4.7 Proposed exercises

Problem 4.2 Let us consider a uniform bar of length ℓ with stiffness and mass characteristics (EA, m) clamped at one end and with a mass M attached at the tip (similar to what was depicted for a beam in Figure 4.55). The size of the mass is assumed negligible compared to the length of the bar. You are asked:

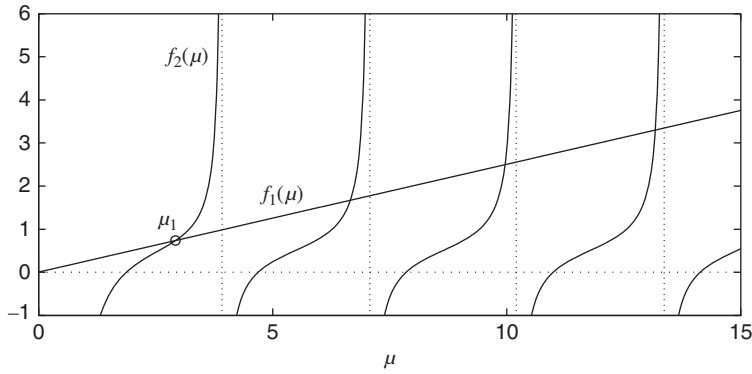


Figure 4.56 Graphical determination of the roots μ_s of a clamped-free beam with tip mass $\left(\frac{M}{m\ell} = 0.25\right)$.

1. to write down the equation for vibration motion of the system and the associated boundary conditions.
2. to apply the boundary conditions to the general solution in order to get an equation governing the frequency parameter $\lambda = \frac{\omega^2 m \ell^2}{EA}$ as a function of the mass ratio $\alpha = \frac{M}{m\ell}$.
3. to show how the eigenvalues (λ_s , $s = 1, \infty$) can be obtained graphically as functions of the α parameter.
4. to determine analytically the eigenvalues λ_s in the particular case $\alpha = 1$.
5. to observe the asymptotic behaviour of the solutions when $\alpha \rightarrow 0$ and when $M \rightarrow \infty$.

Problem 4.3 The impedance matrix of a continuous bar was found in (4.167) as an expansion in terms of its fixed-fixed eigenmodes. It is also possible to compute the impedance matrix directly by considering the dynamic equation:

$$EA \frac{d^2 u}{dx^2} + \omega^2 m u = 0 \quad (\text{P4.3.a})$$

describing the equilibrium in the bar for a harmonic motion, when no volume forces are present. This equation is identical to the free vibration equation (4.129), but now we consider nonhomogeneous boundary conditions in order to obtain the impedance matrix between the end displacements $\mathbf{q}^T = [u_1, u_2]$ and the end loads $\mathbf{p}^T = [N_1, N_2]$ in the form:

$$\mathbf{Z}(\lambda) \mathbf{q} = \mathbf{p} \quad (\text{P4.3.b})$$

where $\lambda = \frac{\omega^2 m \ell^2}{EA}$ is the nondimensional frequency parameter.

You are asked:

1. To obtain the exact impedance matrix of the bar by considering the general solution to the differential equation (P4.3.a) and apply the following steps:
 - specify the general solution by writing the undetermined constants in terms of the displacements (u_1, u_2) at the bar extremities $x = 0$ and $x = \ell$;

- express the applied axial forces (N_1 , N_2) at both ends of the bar (respecting the sign conventions of Figure 4.11);
 - write then the expression of (N_1 , N_2) in terms of (u_1 , u_2) in the matrix form (P4.3.b) to reveal the impedance matrix \mathbf{Z} .
2. To provide the physical interpretation of its individual elements.
 3. To show the link to the expansion (4.167) by:
 - assuming λ to be small and make a series expansion of $\mathbf{Z}(\lambda)$ up to second-order;
 - show that it gives rise to a linearized impedance relationship of the form

$$(\mathbf{K} - \omega^2 \mathbf{M})\mathbf{q} = \mathbf{p}$$

- observe that the stiffness and mass matrices are those given in (4.154) and (4.161).

Problem 4.4 The impedance matrix for the Euler-Bernoulli beam of length ℓ with uniform characteristics (EI , m) can be obtained from the application of the general formula (4.122) establishing a reciprocity relationship between imposed displacements on the boundary and the associated surface tractions. The procedure is the same as described in Section 4.3.1 (page 248) to determine the impedance matrix for the bar in extension. Following the same path, develop the explicit expression of the stiffness and mass matrices \mathbf{K} and \mathbf{M} .

1. The development supposes obtaining the solution of the associated quasi-static problem:

$$\begin{aligned} EI \frac{d^4 w}{dx^4} &= 0 & 0 < x < \ell \\ \bar{w}(0) &= \delta \bar{w}_1 & \bar{w}(\ell) &= \delta \bar{w}_2 \\ \bar{\psi}(0) &= \delta \bar{\psi}_1 & \bar{\psi}(\ell) &= \delta \bar{\psi}_2 \end{aligned} \quad (\text{P4.4.a})$$

Express the solution of (P4.4.a) in the form:

$$w(\delta \bar{w}) = P_1(x) \delta \bar{w}_1 + P_2(x) \delta \bar{\psi}_1 + P_3(x) \delta \bar{w}_2 + P_4(x) \delta \bar{\psi}_2 \quad (\text{P4.4.b})$$

where $P_i(x)$, $i = 1 \dots 4$ are interpolation polynomials. Develop their explicit expression.

2. Derive the expression obtained to compute the bending moment and shear force:

$$M(x) = EI \frac{d^2 w}{dx^2} \quad T(x) = -\frac{dM}{dx} \quad (\text{P4.4.c})$$

3. Deduce from Equation (P4.4.c) the expressions of the bending moments (M_1 , M_2) and shear forces (T_1 , T_2) (taking into account the orientation of the outward normal to the cross-section!). Deduce from the relationships so obtained the expression of the stiffness matrix \mathbf{K} linking the force resultants to (T_1 , M_1 , T_2 , M_2) to the imposed displacements ($\delta \bar{w}_1$, $\delta \bar{\psi}_1$, $\delta \bar{w}_2$, $\delta \bar{\psi}_2$).
4. Deduce the expression of the mass matrix \mathbf{M} from the evaluation of the term in ω^2 in the general expression (4.122).

Problem 4.5 Let us consider the case of a bar in extension clamped at one end and submitted in a stepwise manner to an imposed displacement u_0 at the other end.

$$\begin{aligned}
 EA \frac{\partial^2 u}{\partial x^2} - m\ddot{u} &= 0 & 0 \leq x \leq \ell \\
 u(x, 0) &= 0 & \dot{u}(x, 0) = 0 \\
 u(0, t) &= 0 & \forall t \\
 u(\ell, t) &= u_0 & t > 0
 \end{aligned}$$

This example is very similar to the case of a bar submitted to a tip load treated in Section 4.3.1, Figure 4.13, in the sense that the static response has a similar shape and the wave propagation of the initial disturbance will also be observed. However, due to the difference in boundary condition, a quite different type of solution will be obtained, also with different rate of convergence to it. The following steps are suggested to analyze the system behaviour:

1. Determine the eigensolutions of the free vibration problem with homogeneous boundary conditions and put them in orthonormal form.
2. Determine the quasi-static response of the system.
3. Deduce the response of the system from the general form given by Equation (4.102).
4. Assuming truncation of the modal expansion, plot the function $\delta(S_u)$ successively for 10, 20 and 50 modes.
5. Plot in a similar way its derivative $\delta_x(S_u)$ characterizing the convergence of the axial stress $N(x)$. Observe the behaviour of both functions at $x = \ell$. Explain it in relationship with their order of convergence with s .

Plot the displacement response $u(x)$ at $x = \frac{\ell}{2}$ and at $x = 0.95\ell$ obtained successively with the mode displacement and the mode acceleration methods, with increasing number of modes in the expansion (e.g. 10, 20 and 50 modes). Compare the quality of the solutions obtained. Explain.

Finally, plot the response $N(x)$ at $x = \frac{\ell}{2}$ and at $x = 0.95\ell$ obtained successively with the mode displacement and the mode acceleration methods, also with increasing number of modes in the expansion. Observe the extremely poor rate of convergence of the solution near the tip. Explain.

Problem 4.6 Let us consider a free-free uniform beam of length ℓ with stiffness and mass characteristics (EI , m). You are asked:

1. to write down the equation for vibration motion of the system and the associated boundary conditions.
2. to apply the boundary conditions to the general solution in order to get the transcendental equation governing the frequency parameter μ such that $\mu^4 = \frac{\omega^2 m \ell^4}{EI}$.
3. to demonstrate the existence of eigensolutions corresponding to rigid body motion and show how the nonzero roots (μ_s , $s = 1, \infty$) can be obtained graphically.

4. to setup an iteration procedure to compute a given root μ_s and determine their asymptotic behaviour of the roots as s increases.
5. starting from the asymptotic approximation obtained before, to compute the exact values (to 5 significant digits) of μ_1 and μ_2 . Determine the error characterizing the asymptotic solution.
6. to represent graphically the first two eigenmodes.

Problem 4.7 Let us consider a uniform beam, free-free, of length ℓ with stiffness and mass characteristics (EI, m) supported by a continuous elastic foundation of stiffness k per unit length (Figure 4.57.a). You are asked:

1. to write down the equation for vibration motion of the system and the associated boundary conditions.
2. to introduce the concept of foundation eigenfrequency $\omega_f = \sqrt{\frac{k}{m}}$ and give its physical meaning.
3. to define an appropriate nondimensional frequency parameter taking into account the foundation eigenfrequency.
4. to express the general solution and apply the boundary conditions.
5. to determine the eigensolutions and observe that the stiffness of the support modifies the system eigenspectrum, but not its eigenshapes.

Problem 4.8 Let us consider a uniform beam of length ℓ with stiffness and mass characteristics (EI, m) resting on elastic supports of stiffness k (Figure 4.57.b). The non-dimensional stiffness ratio between beam and support stiffness characteristics is defined as $\alpha = \frac{k\ell^3}{EI}$. You are asked:

1. to write down the equation for vibration motion of the system and the associated boundary conditions in nondimensional form.
2. to apply the boundary conditions to the general solution in order to get an equation governing the frequency parameter μ such that $\mu^4 = \frac{\omega^2 m \ell^4}{EI}$ as a function of the stiffness ratio α .
3. to verify the correctness of the result obtained when $\alpha \rightarrow 0$ and when $k \rightarrow \infty$.
4. to show how the roots $(\mu_s, s = 1, \infty)$ can be obtained graphically as functions of the α parameter.

Problem 4.9 Let us suppose that a bar is decomposed in slices as displayed on Figure 4.58, and consider a piece of length ℓ with uniform characteristics (EA, m) . In harmonic regime, a

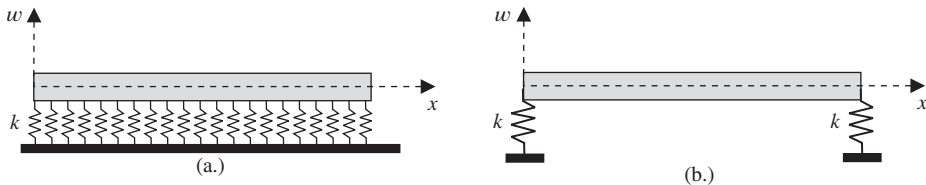


Figure 4.57 A beam on anelastic foundation (a.) and on elastic supports (b.).

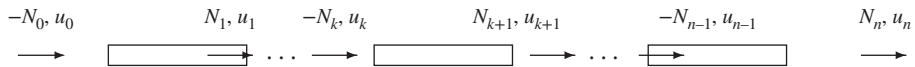


Figure 4.58 Transfer matrix representation of a bar.

transfer relationship of the form:

$$\begin{bmatrix} N_{k+1} \\ u_{k+1} \end{bmatrix} = \mathbf{T}(\lambda) \begin{bmatrix} N_k \\ u_k \end{bmatrix} \quad (\text{P4.9.a})$$

where \mathbf{T} is a 2×2 matrix that can be written along the same principles as presented for discrete systems in Exercise 2.7 of Chapter 2. The difference lies in the fact that here, the elements of matrix \mathbf{T} are determined from the closed form solution for the uniform bar, and are functions of the non-dimensional parameter $\lambda = \sqrt{\frac{\omega^2 m \ell^2}{EA}}$. You are asked:

1. To develop the explicit expression of the transfer matrix $\mathbf{T}(\lambda)$.
2. To deduce from its individual elements the eigenvalue equation of the bar under different boundary conditions.
3. to express the transfer matrix of a bar with a mass $M = \alpha m \ell$ attached at one end.
4. to deduce from it the eigenvalue equation for the bar clamped at one end and with a mass M at the other end.

References

- Daimler-Benz AG 1991 Travelling-wave motor – an electric drive system with future. Technical Report TE/P 6705.2104.02.0791.
- Debongnie J 1991 Consistence de l'étude linéarisée des structures précontraintes. Technical Report Report VF-72, University of Liège.
- Fung Y 1965 *Foundations of Solid Mechanics*. Prentice Hall, New Jersey.
- Géradin M and Rixen D 1997 *Mechanical Vibrations – Theory and Application to Structural Dynamics* second edn. John Wiley & Sons, Inc. New York.
- Géradin M 1973 *Analyse dynamique duale des structures par la méthode des éléments finis* PhD thesis University of Liège, Collection des Publications de la Faculté des Sciences Appliquées, no 36.
- Hagedorn P and Wallaschek J 1990 Travelling wave ultrasonic motors – part 1: Working principle and mathematical modelling of the stator. Technical report, TH Darmstadt.
- Klapka I, Cardona A and Géradin M 1998 An object-oriented implementation of the finite element method for coupled problems. *Revue européenne des éléments finis* 7(5), 469–504.
- Kolsky H 1953 *Stress Waves in Solids* 1953. Oxford University Press, Oxford.
- Lord Rayleigh BJWS 1894 *Theory of Sound, Vol. 1* 2nd edn. Macmillan and Co., London and New York (first edition in 1877).
- Love A 1911 *Some Problems of Geodynamics*. Cambridge University Press, Cambridge.
- Masson S, Le Traon O and Janiaud D 2007 Finite element analysis using Oofelie: Piezo-thermo-elastic simulations for vibrating inertial sensors *X Samtech Users Conference*.
- Meirovitch L 1967 *Analytical Methods in Vibrations*. The Macmillan Company, New York.
- Mindlin R 1951 Influence of rotary inertia and shear on flexural motions of isotropic, elastic plates. *Journal of Appl. Mech.* 18, 31–38.
- Preumont A 2006 *Mechatronics: Dynamics of Electromechanical and Piezoelectric Systems* vol. 136. Springer.
- Rayleigh L 1885 On waves propagated along the plane surface of an elastic solid. *Proceedings of the London Mathematical Society* s1-17(1), 4–11.

- Reissner E 1945 The effect of transverse shear deformation on the bending of elastic plates. *Journal of Applied Mechanics* **12**(2), 69–77.
- Rixen D, Thonon C and G  radin M 1996 Impedance and admittance of continuous systems and comparison between discrete and continuous models *ESA International Workshop on Advanced Mathematical Methods in the Dynamics of Flexible Bodies* ESTEC, Noordwijk.
- Sadd M 2009 *Wave motion and vibration of continuous media*. Department of Mechanical Engineering & Applied Mechanics, University of Rhode Island.
- Sander G 1969 Application de la m  thode des   l  ments finis    la flexion des plaques *Collection des Publications de la Facult   des Sciences Appliqu  es* number 15 Universit   de Li  ge.
- Timoshenko S 1937 *Vibration Problems in Engineering* 2nd. edn. D. Van Norstrand.
- Timoshenko SP 1921 On the correction factor for shear of the differential equation for transverse vibrations of bars of uniform cross-section. *Philosophical Magazine* **6**(41), 744–746.
- Timoshenko SP 1922 On the transverse vibrations of bars of uniform cross-section. *Philosophical Magazine* **6**(43), 125–131.
- Von Karman T and Biot MA 1940 *Mathematical Methods in Engineering*. McGraw-Hill Book Company, Inc., New York.
- Warburton G 1976 *The Dynamical Behaviour of Structures*. Pergamon Press, Oxford.
- Wikipedia n.d. Mindlin-Reissner plate theory Wikipedia, the free encyclopedia.

5

Approximation of Continuous Systems by Displacement Methods

Real engineering structures are made of components having continuously distributed mechanical properties. The dynamics of continuous systems was the subject of the previous chapter. It is sometimes useful and straightforward to idealize systems as discrete systems made of lumped masses and springs as presented on examples in Chapters 1 and 2, but such crude approximation is far from corresponding to the very reality of our environment.

On the other hand, the lesson that can be drawn from the introduction to continuous systems made in Chapter 4 is that closed-form solutions rarely exist. They are available in only a few cases, the limitations met arising essentially from the complexity of the system equations themselves, from the general shape of the domain for which they have to be solved, from the boundary conditions, from the inhomogeneity of the medium, from the load distribution, etc.

The purpose of this chapter is thus to show that it is possible to build approximate discrete models that allow to describe the behaviour of continuous systems with controllable accuracy.

The Rayleigh method (Lord Rayleigh 1894) which consists in approximating the fundamental eigenmode of a continuous system by one kinematically admissible function (i.e. satisfying the kinematical conditions of the problem) and to substitute it in a variational expression to get an approximation to the corresponding eigenvalue has been a giant step in the development of engineering tools. With Lord Rayleigh's method, the error characterizing the approximation to the fundamental eigenvalue is of an order of magnitude less than the error on the eigenshape, and the numerical value obtained is always an upper bound to the exact solution.

An equally important step was made by Ritz (1909) when he proposed to generalize Rayleigh's method by building the approximation to the continuous solution from a finite set of n selected kinematically admissible functions. The coefficients of the series expansion are then the discrete unknowns of the problem, which can be interpreted as generalized displacements. Applying the variational principle when the solution is expressed as a finite sum of functions leads to a $n \times n$ linear system of equations similar to the form governing lumped

models. The mass and stiffness matrices so obtained¹ are those associated to the unknown amplitudes of the chosen representative functions. The behaviour so computed corresponds to the best approximation to the solution of the continuous problem in the subspace spanned by the interpolation functions. With the Rayleigh–Ritz method, discretization methods were born.

The works of Lord Rayleigh and W. Ritz on variational methods together with B.G. Galerkin's weighted-residual approach (Galerkin 1915) form a consistent theoretical framework for the reduction of a continuous problem with an infinite number of degrees of freedom to a discrete one. However, in their original form they were all still lacking the flexibility needed to describe continuous systems with complex geometry and subject to arbitrary boundary conditions and loading distribution.

The Rayleigh–Ritz method has been largely used until 1960 for the development of approximation methods in structural dynamics. Aeroelasticity is probably the engineering discipline in which the method has found its widest field of application, as demonstrated by the classical works by R. Bisplinghoff and his co-workers (Bisplinghoff *et al.* 1955) and by Y.C. (Fung 1955).

It is generally agreed that the era of finite elements formally started with a lecture presented in 1941 by R. Courant in which he introduced the key concept of spatial discretization for the solution of the classical torsion problem (Courant 1943). Courant did not pursue his idea further, since computers were still largely unavailable for his research.

The real development of the finite element method was triggered ten years later both by the needs of the aerospace industry and by the concomitant progress in computer technology and matrix computation methods. In 1954, J.H. Argyris published his famous monograph on matrix structural analysis (Argyris *et al.* 1954). In 1956, R.W. Clough and his colleagues formulated the finite element method as a natural extension of matrix structural analysis (Turner *et al.* 1956).

The finite element method had its golden sixties, with in particular the publication of several seminal contributions into a single, now classical volume (Zienkiewicz and Holister 1965). Among others, the contribution therein by R. Clough was a mature presentation of the finite element method (Clough 1965). It is in the same collection of papers that B.M. Fraeijs de Veubeke laid the principles of dual analysis (based on the simultaneous use of the displacement and complementary energy variational principles) and introduced the concept of equilibrium models as an alternative to finite element models based on a kinematically admissible displacement interpolation (Fraeijs de Veubeke 1965).

It is impossible in the framework of this book devoted specifically to structural dynamics to be exhaustive in citing the numerous developments of the finite element method that took place since the early 1960s. The way was opened to the establishment of a new discipline now referred to as Computational Mechanics. The excellent book by O.C. Zienkiewicz

¹ In this chapter we will not discuss the discretization of damping effects. Often in practice the damping matrix is simply built as a combination of the mass and stiffness matrix as in (3.19). Such a damping model is often far from reality and, if possible, a damping matrix based on measured modal damping is to be preferred as explained in Section 3.1.3. More advanced techniques resorting to detailed description of the material (for instance as being visco-elastic) can be applied, but those issues are beyond the scope of the present text.

(Zienkiewicz 1977) and its later editions has largely contributed to establish the usefulness and popularity of the finite element method not only in different engineering disciplines, but also in other fields of science as well.

Nowadays the finite element method has become an essential tool in the field of structural engineering, and therefore has given rise to the development of a large number of general purpose commercial softwares distributed and used worldwide such as ABAQUS®, ADINA®, ANSYS®, COMSOL Multiphysics®, MSC NASTRAN® and NX NASTRAN®, SAMCEF®, ZEBULON® and others. A certain number of finite element toolboxes such as OOFELIE®, OPENSEES®, OpenFEM® and GetFEM++® are also available to develop tailored solutions using pre-defined finite element routines.

The goal of this chapter on approximation methods for continuous systems remains modest in comparison to the current stage of knowledge and practice. It consists simply in laying the fundamental concepts for obtaining discrete models of continuous systems in vibration and under dynamic loads.

In a first part, the principle of the Rayleigh–Ritz method is presented since it provides the theoretical framework on which the finite element relies. Some simple examples are presented to demonstrate the powerfulness of the method but also underline its limitations from a practical standpoint.

The second part is a short introduction to the finite element method. The principle of the method is described on the basis of the displacement variational principle, and the bar in extension and the beam without shear deformation are treated as examples. The assembly process of the finite element model is described to build the resulting discrete system of structural equations. The construction of finite element models for spatial trusses is also treated as an example. The few examples selected aim at demonstrating the versatility of the finite element method compared to the fundamental Rayleigh–Ritz approach.

Finally, the concept of equilibrium model (based on discretization of the complementary energy) is used at the end of the chapter to simplify the development of the stiffness matrix for a beam element with shear deformation.

For the reader interested in getting deeper knowledge of the method, there is a large collection of other excellent and/or classical textbooks devoted to the fundamentals of the finite element method, among which – without being exhaustive – (Strang and Fix 1973, Gallagher 1975, Oden and Reddy 1976, Hughes 1987, Batoz and Dhatt 1990, Dhatt and Batoz 1990, Crisfield 1991, Bathe 1996, Craveur 1996, Cook *et al.* 2007, Craveur and Jetteur 2010, Dhatt *et al.* 2012).

Definitions

The list below complements the general definitions given in the book introduction, but remains local to Chapter 5.

All quantities defined at the finite element level are denoted by subscript e (e.g. \mathbf{K}_e is the stiffness matrix of element e). When frame transformations are involved to describe two- or three-dimensional structures, subscripts eL and eS denote respectively the finite element matrices in local or structural axes.

$B(x_1, x_2, x_3, t)$	strain interpolation matrix (Rayleigh-Ritz method).
$F(x_1, x_2, x_3, t)$	displacement interpolation matrix (Rayleigh-Ritz method).
F_e	flexibility kernel matrix of element e .
$K^{(n)}$	stiffness matrix of Rayleigh-Ritz method with n interpolation functions.
L_e	localization operator of finite element e .
$M^{(n)}$	mass matrix of Rayleigh-Ritz method with n interpolation functions.
R_e	rotation matrix at a finite element node.
S_e	static connection matrix of element e .
T_e	rotation matrix of finite element e .
$f_j(x_1, x_2, x_3)$	j -th kinematically admissible displacement field (Rayleigh-Ritz method).
p_e, P	elementary and global generalized forces.
q_e, Q	elementary and global set of degrees of freedom.
$q_{(j),c}$	discrete form of eigenmode j (Rayleigh-Ritz method).
$u(x_1, x_2, x_3, t)$	3-dimensional displacement field.
$u_{(j),c}$	continuous form of eigenmode j computed by Rayleigh-Ritz method.
A	cross-section area of a beam or bar.
D	plate bending stiffness.
EI_y	beam bending stiffness about axis $O'y$.
EI_z	beam bending stiffness about axis $O'z$.
GJ_x	beam torsional stiffness about axis $O'x$.
L	total length of a bar or a beam.
$M(x)$	bending moment.
N_0	beam initial axial stress.
$OXYZ$	structural axis frame.
$O'xyz$	local frame to beam element.
$T(x)$	shear force.
(U_i, V_i, W_i)	displacements of element node i in structural axes.
\mathcal{V}_d	dislocation potential.
(X_i, Y_i, Z_i)	coordinates of element node i in structural axes.
$(\vec{e}_x, \vec{e}_y, \vec{e}_z)$	principal directions of beam element cross-section in structural axes.
$(\vec{e}_x, \vec{e}_y, \vec{e}_z)$	principal directions of beam element cross-section in local axes.
k'	cross-sectional reduction factor for shear in beam.
ℓ	length of a finite element.
m	mass per unit length in a beam or bar ($m = \rho A$).
\bar{p}	distributed transverse load applied on a beam.
r	transverse gyration radius of cross-section (bending).
r_t	gyration radius of cross-section about $O'x$ (torsion).
(u_i, v_i, w_i)	displacements of element node i in local axes.
$u(x)$	bar axial displacement.
$w(x)$	transverse displacement of beam in bending.
$w(x, y)$	transverse displacement of plate in bending.
(x_i, y_i, z_i)	coordinates of element node i in local axes.
Φ_e	shape function matrix of element e .
α_e	interpolation parameters.
$\phi_{(j),c}$	participation factor of eigenmode j to external load (Rayleigh-Ritz method).

$(\Psi_{Xi}, \Psi_{Yi}, \Psi_{Xi})$	rotations of element node i in structural axes.
α^2	non dimensional rotary inertia parameter.
β	shear angle.
κ	beam curvature.
η^2	non dimensional shear parameter.
λ_M, λ_T	Lagrange multipliers.
ϕ	non dimensional shear parameter in stiffness matrix.
$\phi_i(x)$	i -th shape function (bar, beam finite element).
$\phi(x)$	rotation of beam cross-section.
$(\psi_{xi}, \psi_{yi}, \psi_{zi})$	rotations of element node i in local axes.
$\sigma_{ij,cr}^0$	critical value of initial stress tensor (linear buckling).
$\omega_{j,c}^2$	approximation of j -th eigenvalue computed by Rayleigh-Ritz method.
$\omega_{j,cn}^2$	approximation of j -th eigenvalue computed by Rayleigh-Ritz method with n interpolation functions.
$\omega_{j,e}^2$	exact j -th eigenvalue of continuous system.

5.1 The Rayleigh–Ritz method

Among the problems of elastodynamics governed by a system of partial differential equations, some of which have been considered in the previous chapter, very few have a closed-form solution which simultaneously verifies the differential equations on the domain V and the boundary conditions on its external surface S .

The need to find an exact closed-form solution may be overcome through the application of the Rayleigh–Ritz method to a functional such as that of the displacement variational principle (4.19). What results is a substitution problem which possesses a finite number n degrees of freedom and is described by ordinary differential equations similar to those of discrete systems (Chapter 2). The Rayleigh–Ritz solution is seldom exact, but its quality improves with the number of degrees of freedom incorporated in its expression.

The method dates back to 1870 with the seminal work of Lord Rayleigh of vibration problems (Lord Rayleigh 1894): the displacement approximation was originally limited to one trial function (Rayleigh’s method). Ritz (1909) generalized the method by constructing an approximation of the displacement field in terms of several functions, each one associated with a different degree of freedom and satisfying the essential boundary conditions separately (i.e. boundary conditions of kinematic type).

5.1.1 Choice of approximation functions

The Rayleigh–Ritz method for a problem of elastodynamics described by Hamilton’s principle in the form (4.19) starts with the choice of approximation functions for the displacements. Each component u_i of the field $\mathbf{u}(x_1, x_2, x_3, t)$, $i = 1, 2, 3$, is described by a series whose characteristic term is a function $f_{ij}(x_1, x_2, x_3)$ multiplied by a time-dependent amplitude, denoted $q_j(t)$. The components q_j play the role of generalized coordinates. The Rayleigh–Ritz approximation is written in the form:

$$u_i(x_1, x_2, x_3, t) = \sum_{j=1}^n f_{ij}(x_1, x_2, x_3) q_j(t) \quad i = 1, 2, 3 \quad (5.1)$$

where each set of functions describing a particular displacement field:

$$\mathbf{f}_j(x_1, x_2, x_3) = \begin{bmatrix} f_{1j}(x_1, x_2, x_3) \\ f_{2j}(x_1, x_2, x_3) \\ f_{3j}(x_1, x_2, x_3) \end{bmatrix}$$

must be *kinematically admissible*,² which means that it must satisfy the internal compatibility conditions (C_0 continuity) and the essential boundary conditions. Conversely, they are not required to verify the natural conditions (namely, for the variational principle on displacements, the equilibrium conditions).

The resulting approximation may be put in the matrix form:

$$\mathbf{u}(x_1, x_2, x_3, t) = \sum_{j=1}^n \mathbf{f}_j(x_1, x_2, x_3) q_j(t) \quad (5.2)$$

and n , the number of terms to be included in the expansion in order to obtain the required accuracy, must be estimated first: the degrees of freedom of the approximation are the n amplitudes $q_j(t)$ that are determined via the variational procedure outlined below.

5.1.2 Discretization of the displacement variational principle

Let us express the approximation (5.2) in matrix form:

$$\mathbf{u}(x_1, x_2, x_3, t) = \mathbf{F}(x_1, x_2, x_3) \mathbf{q}(t) \quad (5.3)$$

where

$$\mathbf{q}(t) = [q_1 \quad \dots \quad q_n]^T \quad (5.4)$$

represents the vector of generalized coordinates, and matrix \mathbf{F} of dimension $3 \times n$ is the *displacement interpolation matrix*:

$$\mathbf{F}(x_1, x_2, x_3) = \begin{bmatrix} f_{11}(x_1, x_2, x_3) & \dots & f_{1n}(x_1, x_2, x_3) \\ f_{21}(x_1, x_2, x_3) & \dots & f_{2n}(x_1, x_2, x_3) \\ f_{31}(x_1, x_2, x_3) & \dots & f_{3n}(x_1, x_2, x_3) \end{bmatrix} \quad (5.5)$$

The strain components (4.60) are next evaluated by the relationship:

$$\begin{aligned} \boldsymbol{\varepsilon}(\mathbf{x}, t) &= \mathbf{D}\mathbf{F}(x_1, x_2, x_3) \mathbf{q}(t) \\ &= \mathbf{B}(x_1, x_2, x_3) \mathbf{q}(t) \end{aligned} \quad (5.6)$$

where matrix $\mathbf{B}(x_1, x_2, x_3)$ of dimension $6 \times n$ is the *strain interpolation matrix* computed from the displacement interpolation matrix through application of the differentiation operator 4.61:

$$\mathbf{B}(x_1, x_2, x_3) = \mathbf{D}\mathbf{F}(x_1, x_2, x_3) \quad (5.7)$$

² The simpler terminology 'admissible function' will also be used, since the methods of approximation in this chapter are based on kinematic assumption.

We then successively compute

- The kinetic energy, by substitution of (5.3) into (4.20):

$$\begin{aligned}\mathcal{T} &= \frac{1}{2} \int_V \rho \dot{\mathbf{q}}^T \mathbf{F}^T \mathbf{F} \dot{\mathbf{q}} dV \\ &= \frac{1}{2} \dot{\mathbf{q}}^T \mathbf{M} \dot{\mathbf{q}}\end{aligned}$$

with the mass matrix of the discrete system:

$$\mathbf{M} = \int_V \rho \mathbf{F}^T \mathbf{F} dV \quad (5.8)$$

It has dimension $n \times n$ and is necessarily symmetric and positive definite.

- The strain energy, through substitution of the discretized strain expression into (4.22):

$$\begin{aligned}\mathcal{V}_{int} &= \frac{1}{2} \int_V \boldsymbol{\varepsilon}^T \mathbf{H} \boldsymbol{\varepsilon} dV \\ &= \frac{1}{2} \int_V \mathbf{q}^T \mathbf{B}^T \mathbf{H} \mathbf{B} \mathbf{q} dV \\ &= \frac{1}{2} \mathbf{q}^T \mathbf{K} \mathbf{q}\end{aligned} \quad (5.9)$$

where \mathbf{H} is the Hooke matrix of elastic coefficients and \mathbf{K} is the stiffness matrix of the discretized system:

$$\mathbf{K} = \int_V \mathbf{B}^T \mathbf{H} \mathbf{B} dV \quad (5.10)$$

Like the mass matrix, it is necessarily symmetric and has dimension $n \times n$. It is, however, only positive semi-definite, the possible rigid-body modes denoted \mathbf{u} being solutions of

$$\mathbf{B} \mathbf{u} = \mathbf{0} \quad \text{or} \quad \mathbf{K} \mathbf{u} = \mathbf{0}$$

These are nonzero displacement modes producing no strain energy.

- The external potential energy which results from the substitution of (5.3) into 4.23:

$$\mathcal{V}_{ext} = - \int_{S_\sigma} (\mathbf{F} \mathbf{q})^T \bar{\mathbf{t}} dS - \int_V (\mathbf{F} \mathbf{q})^T \bar{\mathbf{X}} dV \quad (5.11)$$

or

$$\mathcal{V}_{ext} = -\mathbf{q}^T \mathbf{p} \quad (5.12)$$

with the external load vector

$$\mathbf{p}(t) = \int_{S_\sigma} \mathbf{F}^T \bar{\mathbf{t}} dS + \int_V \mathbf{F}^T \bar{\mathbf{X}} dV \quad (5.13)$$

By gathering all the terms, we obtain the expression of the discretized displacement variational principle:

$$\delta \int_{t_1}^{t_2} \left\{ \frac{1}{2} \dot{\mathbf{q}}^T \mathbf{M} \dot{\mathbf{q}} - \left(\frac{1}{2} \mathbf{q}^T \mathbf{K} \mathbf{q} - \mathbf{q}^T \mathbf{p} \right) \right\} dt = 0 \quad (5.14)$$

and if we next apply the virtual variation to the generalized coordinates \mathbf{q} we arrive at the equations of motion in the discrete form:

$$\boxed{\mathbf{K} \mathbf{q} + \mathbf{M} \dot{\mathbf{q}} = \mathbf{p}(t)} \quad (5.15)$$

5.1.3 Computation of eigensolutions by the Rayleigh–Ritz method

The free vibration and harmonic motion assumptions yield the expression of the discretized eigenvalue problem:

$$\mathbf{K} \mathbf{q} = \omega^2 \mathbf{M} \mathbf{q} \quad (5.16)$$

the solutions of which are approximations to the corresponding Sturm–Liouville problem (4.64) (Meirovitch 1967).

Let us denote $\omega_{i,c}^2$ the approximate eigenvalues computed by the Rayleigh–Ritz method, and $\omega_{i,e}^2$ the exact eigenvalues of the original continuous problem (4.67). The following result allows us to qualify the type of convergence obtained to the exact solution:

Each eigenvalue $\omega_{i,c}^2$ resulting from the discretization of the displacement variational principle by the Rayleigh–Ritz method is an upper bound to the corresponding exact eigenvalue $\omega_{i,e}^2$

$$\omega_{i,e}^2 \leq \omega_{i,c}^2 \quad i = 1, \dots, n \quad (5.17)$$

The proof holds as follows.

Let

$$\{f_1(\mathbf{x}), f_2(\mathbf{x}), \dots, f_n(\mathbf{x}), \dots\} \quad (5.18)$$

be a set of admissible displacement fields forming a complete set. The difference between the Rayleigh–Ritz approximation and the exact solution can be made arbitrarily small by increasing n , so that it may be concluded that the computed solution converges to the exact one as $n \rightarrow \infty$.

The selection of the first n solutions of the series has the effect of reducing the continuous system with an infinity of degrees of freedom to a discrete one possessing only n degrees of freedom. Discretization and truncation lead to omitting the higher terms in the set (5.18), which is equivalent to imposing on the infinite Rayleigh–Ritz development:

$$\mathbf{u}(\mathbf{x}) = \sum_{k=1}^{\infty} q_k \mathbf{f}_k(\mathbf{x}) \quad (5.19)$$

the constraints

$$q_{n+1} = q_{n+2} = \dots = 0 \quad (5.20)$$

Let us denote by $\mathbf{M}^{(n)}$ and $\mathbf{K}^{(n)}$ the mass and stiffness matrices constructed in terms of the n first terms of the series, and let $\omega_{j,cn}^2, j = 1, \dots, n$ be the corresponding eigenvalues, solutions of:

$$\mathbf{K}^{(n)} \mathbf{q} = \omega^2 \mathbf{M}^{(n)} \mathbf{q} \quad (5.21)$$

Then let $\mathbf{M}^{(n+1)}$ and $\mathbf{K}^{(n+1)}$ be the matrices obtained by adding the term $\mathbf{f}_{n+1}(\mathbf{x})$. They are deduced from $\mathbf{M}^{(n)}$ and $\mathbf{K}^{(n)}$ by adding to them one row and one column:

$$\mathbf{M}^{(n+1)} = \begin{bmatrix} \mathbf{M}^{(n)} & \mathbf{m}_{n,n+1} \\ \mathbf{m}_{n,n+1}^T & m_{n+1,n+1} \end{bmatrix} \quad \mathbf{K}^{(n+1)} = \begin{bmatrix} \mathbf{K}^{(n)} & \mathbf{k}_{n,n+1} \\ \mathbf{k}_{n,n+1}^T & k_{n+1,n+1} \end{bmatrix} \quad (5.22)$$

with the scalar quantities:

$$\begin{aligned} m_{j,n+1} &= \int_V \rho \mathbf{f}_{n+1}^T \mathbf{f}_j dV \\ \text{and} \quad j &= 1, \dots, n+1 \\ k_{j,n+1} &= \int_V (\mathbf{D}\mathbf{f}_{n+1})^T \mathbf{H}(\mathbf{D}\mathbf{f}_j) dV \end{aligned} \quad (5.23)$$

and the row matrices:

$$\begin{aligned} \mathbf{m}_{n,n+1}^T &= [m_{1,n+1} \dots m_{n,n+1}] \\ \mathbf{k}_{n,n+1}^T &= [k_{1,n+1} \dots k_{n,n+1}] \end{aligned} \quad (5.24)$$

Likewise, the eigenvalue problem (5.21) can be deduced from the problem of dimension $n+1$:

$$\mathbf{K}^{(n+1)} \mathbf{q} = \omega^2 \mathbf{M}^{(n+1)} \mathbf{q} \quad (5.25)$$

by adding the constraint $q_{n+1} = 0$.

Therefore, from the application of Rayleigh's theorem on constraints (refer to Section 2.10.6), it can be deduced that the eigenvalues of the problem of dimension n are bracketed by those of the problem of dimension $n+1$:

$$\omega_{1,cn+1}^2 \leq \omega_{1,cn}^2 \leq \omega_{2,cn+1}^2 \leq \omega_{2,cn}^2 \leq \dots$$

A recurrent procedure shows that the successive approximations provided by the Rayleigh–Ritz method for a given eigenvalue ω_j^2 obey the inequality:

$$\omega_{j,cn+1}^2 \leq \omega_{j,cn}^2 \leq \omega_{j,cn-1}^2 \leq \dots$$

which completes the proof.

Once the approximate solutions $\omega_{i,c}^2$ of eigenproblem (5.16) are known, the approximations $\mathbf{q}_{(i),c}$ to the associated eigenmodes verifying the relationship:

$$\mathbf{K}\mathbf{q}_{(i),c} - \omega_{i,c}^2 \mathbf{M}\mathbf{q}_{(i),c} = \mathbf{0} \quad (5.26)$$

are easily obtained. The approximate eigenmodes given by the Rayleigh–Ritz method are then written:

$$\mathbf{u}_{(i),c} = \mathbf{F}(x_1, x_2, x_3) \mathbf{q}_{(i),c} \quad (5.27)$$

Owing to Equation (5.26), the eigenvectors verify the orthogonality relationships established for discrete systems (Section 2.3). Assuming that the eigenvectors are normalized with respect to the mass matrix \mathbf{M} , we may write:

$$\begin{aligned} \mathbf{q}_{(i),c}^T \mathbf{M} \mathbf{q}_{(j),c} &= \delta_{ij} \\ \mathbf{q}_{(i),c}^T \mathbf{K} \mathbf{q}_{(j),c} &= \omega_{i,c}^2 \delta_{ij} \end{aligned} \quad (5.28)$$

Moreover, substituting for the matrices \mathbf{M} and \mathbf{K} their expressions (5.8) and (5.10) restores the orthonormality relationships verified by the approximated mode shapes:

$$\begin{aligned} \int_V \rho \mathbf{u}_{(i),c}^T \mathbf{u}_{(j),c} dV &= \delta_{ij} \\ \int_V (\mathbf{D} \mathbf{u}_{(i),c})^T \mathbf{H} (\mathbf{D} \mathbf{u}_{(j),c}) dV &= \omega_{i,c}^2 \delta_{ij} \end{aligned} \quad (5.29)$$

Remark 5.1 Note that the eigenmodes $\mathbf{u}_{(i),c}$ obtained from the discretization through (5.27) are not, in general, the exact eigenmodes of the continuous elastodynamic problem, even though they satisfy the orthogonality properties (5.29). Indeed the only eigenproblem satisfied by the discretized solution is (5.16). Considering the definitions of the mass and stiffness matrices (5.8) and (5.10) it can be rewritten as:

$$\int_V \mathbf{B}^T \mathbf{H} \mathbf{B} \mathbf{q}_{(i),c} dV - \omega_{i,c}^2 \int_V \rho \mathbf{F}^T \mathbf{F} \mathbf{q}_{(i),c} dV = 0 \quad (5.30)$$

or

$$\int_V (\mathbf{D} \mathbf{F})^T \mathbf{H} \mathbf{D} \mathbf{u}_{(i),c} dV - \omega_{i,c}^2 \int_V \rho \mathbf{F}^T \mathbf{u}_{(i),c} dV = 0 \quad (5.31)$$

Performing an integration by parts in space (Gauss' formula), one finds that the computed eigenvectors $\mathbf{u}_{(i),c}$ satisfy:

$$\int_{S_\sigma} \mathbf{F}^T \{ \mathbf{N}^T \mathbf{H} \mathbf{D} \mathbf{u}_{(i),c} \} dS - \int_V \mathbf{F}^T \{ \mathbf{D} \mathbf{H} \mathbf{D} \mathbf{u}_{(i),c} + \omega_{i,c}^2 \rho \mathbf{u}_{(i),c} \} dV = 0 \quad (5.32)$$

where \mathbf{N} contains the direction cosines of the outward normal to the free surface S_σ as defined in 4.62 and where we used the fact that on the fixed part S_u of the surface the solution is zero (the approximation functions verifying the essential boundary conditions).

It is now clear that the solution $\mathbf{u}_{(i),c}$ found through the discrete approximation satisfies the elastodynamic problem (4.67) only to such an extent that, if an error exists for the equilibrium in the volume and on S_σ , namely:

$$\begin{aligned} \mathbf{D} \mathbf{H} \mathbf{D} \mathbf{u}_{(i),c} + \omega_{i,c}^2 \rho \mathbf{u}_{(i),c} &= \boldsymbol{\epsilon}_V \\ \mathbf{N}^T \mathbf{H} \mathbf{D} \mathbf{u}_{(i),c} &= \boldsymbol{\epsilon}_{S_\sigma} \end{aligned}$$

then the residual forces ϵ_V and ϵ_{S_σ} must be such that they do not produce any work for the chosen approximation displacement functions. Another interpretation of (5.32) can be that the variational principal of displacement leads to finding a solution for which the equilibrium error vanishes in the space of the approximation functions.

5.1.4 Computation of the response to external loading by the Rayleigh–Ritz method

Since the eigenmodes computed by the Rayleigh–Ritz method verify the orthonormality relationships, the response to external loading may be constructed by modal superposition. It may then be written:

$$\mathbf{q}_c = \sum_{s=1}^n \eta_s(t) \mathbf{q}_{(s),c} \quad (5.33)$$

in which case, if the modal masses are normalized, the discretized Equations (5.15) are reduced to the uncoupled normal form (Section 2.7):

$$\ddot{\eta}_s + \omega_{s,c} \eta_s = \mathbf{q}_{(s),c}^T \mathbf{p} = \phi_{s,c} \quad (5.34)$$

Likewise, the continuous solution is reconstructed through superposition of the continuous mode shapes:

$$\mathbf{u}_c = \sum_{s=1}^n \eta_s(t) \mathbf{u}_{(s),c} \quad (5.35)$$

with the normal equations (Section 4.2.3):

$$\ddot{\eta}_s + \omega_{s,c} \eta_s = \int_S \mathbf{u}_{(s),c}^T \bar{\mathbf{t}} dS + \int_V \mathbf{u}_{(s),c}^T \bar{\mathbf{X}} dV = \phi_{s,c} \quad (5.36)$$

5.1.5 The case of prestressed structures

In the case of a structure subjected to an initial stress field σ_{ij}^0 , the following term must be added to the strain energy of the system (see Section 4.1.6):

$$\mathcal{V}_g = \int_V \sigma_{ij}^0 \epsilon_{ij}^{(2)} dV \quad (5.37)$$

where $\epsilon_{ij}^{(2)}$ represents the quadratic part of the strain tensor, using Einstein's notation:

$$\epsilon_{ij}^{(2)} = \frac{1}{2} \frac{\partial u_m}{\partial x_i} \frac{\partial u_m}{\partial x_j} \quad (5.38)$$

The substitution into (5.38) of the approximation (5.2) yields the relationship:

$$\epsilon_{ij}^{(2)} = \frac{1}{2} \frac{\partial f_{mk}}{\partial x_i} \frac{\partial f_{ml}}{\partial x_j} q_k q_l \quad k, l = 1, \dots, n$$

and the symmetric role played by the suffixes k and l results in the following approximation:

$$\mathcal{V}_g = \frac{1}{2} \mathbf{q}^T \mathbf{K}_g \mathbf{q} \quad (5.39)$$

with the *geometric stiffness matrix* components:

$$[K_g]_{kl} = \int_V \sigma_{ij}^0 \frac{\partial f_{mk}}{\partial x_i} \frac{\partial f_{ml}}{\partial x_j} dV \quad (5.40)$$

Since the geometric stiffness expression possesses the same form as the linear stiffness one, it is immediately obvious that the linear equations of motion are replaced in the prestressed case by:

$$\boxed{(K + K_g)q + M\ddot{q} = p(t)} \quad (5.41)$$

and the associated eigenvalue problem takes the form:

$$(K + K_g)q = \omega^2 Mq \quad (5.42)$$

A case of interest is the one in which the geometric stiffness is driven by a parameter λ (for example, angular velocity of a rotating system or axial load on a beam), in which case one may write:

$$\sigma_{ij}^0 = \lambda \sigma_{ij}^{0*}$$

and the geometric stiffness is itself proportional to this parameter:

$$K_g = \lambda K_g^*$$

The eigenvalues of the resulting problem:

$$(K + \lambda K_g^*)q = \omega^2 Mq \quad (5.43)$$

then become functions of λ .

When $\omega = 0$, we get an eigenproblem with eigenvalues λ_i corresponding to the critical loads:

$$(K + \lambda_i K_g^*)q_{(i)} = 0 \quad (5.44)$$

The eigenvalue λ_1 of the smallest module yields the prestress state:

$$\sigma_{ij,cr}^0 = \lambda_1 \sigma_{ij}^{0*}$$

in which the system buckles.

5.2 Applications of the Rayleigh–Ritz method to continuous systems

From the examples presented in the next sections it will immediately appear that a major drawback of the Rayleigh–Ritz method is its lack of generality. Indeed the choice of the interpolation functions (5.5) is fully dependent on the physical nature of the problem, its geometry and its kinematic boundary conditions.

Most of the time, the interpolation functions are chosen of polynomial form. For one-dimensional systems in particular, a complete set of n interpolation functions can be defined as:

$$f_k(x) = \sum_{j=0}^{k-1} a_{jk} \left(\frac{x}{\ell} \right)^j \quad k = 1 \dots n \quad (5.45)$$

They are thus defined in terms of $\frac{n(n+1)}{2}$ unknown coefficients a_{jk} which have to be either determined or chosen a priori in two steps as follows.

1. First, the boundary conditions of the problem have to be applied to each function (5.45) to render them kinematically admissible. Each kinematic boundary condition of the problem will thus eliminate n of them.
2. The choice of the remaining coefficients is left to the user. The easiest would consist to give them a fixed value (0 or 1). An alternative consists to impose orthogonality of the polynomials over the interval:

$$\int_0^\ell f_j(x)f_k(x)dx = 0 \quad j = 1 \dots k, k = 0 \dots n \quad (5.46)$$

Obviously, orthogonality has to be imposed after application of the boundary conditions. The advantage of imposing orthogonality can be two-fold:

- It can be shown that using orthogonal functions will improve the numerical conditioning of the resulting matrices, avoiding thus the numerical degeneracy of the solution when using a large number of interpolation polynomials.
- Orthogonality can be imposed with respect to the mass distribution, in which case the resulting mass matrix will be diagonal.

The choice of appropriate interpolation functions for 2- and 3-dimensional problems is significantly more complex. Depending on the geometry, separation of variables can be applied to obtain an appropriate interpolation space. For example:

- For 2-dimensional problem defined on a rectangular domain of dimension $a \times b$, the set of interpolation functions can be defined in the form:

$$f_{kl}(x, y) = P_k\left(\frac{x}{a}\right) P_l\left(\frac{y}{b}\right) \quad (5.47)$$

where the P_k are appropriate functions of one variable.

- For a 2-dimensional problem with circular symmetry defined in polar coordinates (r, θ) on a domain of dimension $[R_1, R_2] \times [0, 2\pi]$, the axisymmetry of the problem has to be taken into account in the definition of the interpolation functions. Therefore the set of interpolation functions has to be periodic in the θ direction. The most natural choice is:

$$f_{km}(r, \theta) = P_k(r)(A_{km} \cos m\theta + B_{km} \sin m\theta) \quad (5.48)$$

In conclusion, when applying the Rayleigh–Ritz method, the choice of the interpolation functions has to be made case by case, and the quality of the resulting numerical solution is strongly dependent on it.

5.2.1 The clamped–free uniform bar

Let us take again the example of the clamped–free bar (Section 4.3.1) and express the interpolation functions in the general form (5.45). Applying the boundary conditions yields:

$$a_{0k} = 0 \quad k = 1 \dots n \quad (5.49)$$

and we can arbitrarily set to 1 the coefficients of highest degree:

$$a_{k-1,k} = 1 \quad k = 2 \dots n \quad (5.50)$$

Setting then $k \leftarrow k - 1$ since the first interpolation function was identically zero, the resulting set of kinematically admissible interpolation functions is:

$$\begin{aligned} f_1(x) &= \frac{x}{\ell} \\ f_2(x) &= a_{12} \frac{x}{\ell} + \left(\frac{x}{\ell}\right)^2 \\ f_3(x) &= a_{13} \frac{x}{\ell} + a_{23} \left(\frac{x}{\ell}\right)^2 + \left(\frac{x}{\ell}\right)^3 \\ &\vdots \end{aligned} \quad (5.51)$$

The two options are:

1. Setting the remaining free coefficients to 0, in which case the set of admissible functions is in this case a sequence of monomials:

$$\{f_i(x)\} = \left\{ \frac{x}{\ell}, \quad \frac{x^2}{\ell^2}, \quad \frac{x^3}{\ell^3}, \quad \dots \right\} \quad (5.52)$$

2. Imposing orthogonality according to Equation (5.51), in which case the orthogonalized set of admissible functions is obtained as:

$$\{f_i(x)\} = \left\{ \frac{x}{\ell}, \quad -\frac{3}{4} \frac{x}{\ell} + \frac{x^2}{\ell^2}, \quad \frac{2}{5} \frac{x}{\ell} - \frac{4}{3} \frac{x^2}{\ell^2} + \frac{x^3}{\ell^3}, \quad \dots \right\} \quad (5.53)$$

The kinetic and strain energies of the system are approximated as:

$$\begin{aligned} \mathcal{T} &= \frac{1}{2} \int_0^\ell m \dot{u}^2 dx = \frac{1}{2} \sum_i \sum_j \dot{q}_i \dot{q}_j \int_0^\ell m f_i(x) f_j(x) dx \\ &= \frac{1}{2} \sum_i \sum_j m_{ij} \dot{q}_i \dot{q}_j \\ &= \frac{1}{2} \dot{\mathbf{q}}^T \mathbf{M} \dot{\mathbf{q}} \end{aligned} \quad (5.54a)$$

$$\begin{aligned} \mathcal{V} &= \frac{1}{2} \int_0^\ell EA \left(\frac{du}{dx} \right)^2 dx = \frac{1}{2} \sum_i \sum_j q_i q_j \int_0^\ell EA f'_i(x) f'_j(x) dx \\ &= \frac{1}{2} \sum_i \sum_j k_{ij} q_i q_j \\ &= \frac{1}{2} \mathbf{q}^T \mathbf{K} \mathbf{q} \end{aligned} \quad (5.54b)$$

with the stiffness and mass coefficients:

$$m_{ij} = \int_0^\ell m f_i(x) f_j(x) dx \quad k_{ij} = \int_0^\ell EA f'_i(x) f'_j(x) dx \quad (5.55)$$

Performing the integration for $n = 3$ provides the following expressions of the stiffness and mass matrices:

– with the sequence of monomials (5.52):

$$\mathbf{M} = m\ell \begin{bmatrix} \frac{1}{3} & \frac{1}{4} & \frac{1}{5} \\ \frac{1}{4} & \frac{1}{5} & \frac{1}{6} \\ \frac{1}{5} & \frac{1}{6} & \frac{1}{7} \end{bmatrix} \quad \mathbf{K} = \frac{EA}{\ell} \begin{bmatrix} 1 & 1 & 1 \\ 1 & \frac{4}{3} & \frac{3}{2} \\ 1 & \frac{3}{2} & \frac{9}{5} \end{bmatrix} \quad (5.56)$$

– with orthogonal polynomials (5.53):

$$\mathbf{M} = m\ell \begin{bmatrix} \frac{1}{3} & 0 & 0 \\ 0 & \frac{1}{80} & 0 \\ 0 & 0 & \frac{1}{1575} \end{bmatrix} \quad \mathbf{K} = \frac{EA}{\ell} \begin{bmatrix} 1 & \frac{1}{4} & \frac{1}{15} \\ \frac{1}{4} & \frac{19}{48} & \frac{13}{180} \\ \frac{1}{15} & \frac{13}{180} & \frac{43}{675} \end{bmatrix} \quad (5.57)$$

The numerical solutions of eigenvalue problem:

$$\mathbf{K}\mathbf{q} = \omega^2 \mathbf{M}\mathbf{q} \quad (5.58)$$

are obtained in terms of the nondimensional parameter:

$$\lambda = \frac{\omega^2 m \ell^2}{EA} \quad (5.59)$$

For example, using two interpolation functions of monomial type the numerical eigenvalues are solutions of the quadratic equation:

$$\begin{vmatrix} 1 - \frac{1}{3}\lambda & 1 - \frac{1}{4}\lambda \\ 1 - \frac{1}{4}\lambda & \frac{4}{3} - \frac{1}{5}\lambda \end{vmatrix} = 0 \quad (5.60)$$

or

$$3\lambda^2 - 104\lambda + 240 = 0 \quad (5.61)$$

One obtains the eigenvalues:

$$\omega_{1,c2}^2 = 2.49 \frac{EA}{m\ell^2} \quad \omega_{2,c2}^2 = 32.18 \frac{EA}{m\ell^2} \quad (5.62)$$

Of course, using the orthogonal interpolation functions would provide the same results.

The results (5.62) are compared in Table 5.2.1 to the analytical values obtained in Section 4.3.1. It is thus observed that using only two admissible functions is appropriate to approximate the first mode $u_{(1)} = a \sin \frac{\pi x}{2\ell}$ but does not allow correct representation of the second one. Adding the cubic admissible function gives the approximations also provided in Table (5.2.1).

It is worthwhile observing the monotonic convergence of the computed solutions from above towards the analytical eigenvalue as theoretically predicted in Section 5.1.3 (Equation (5.17)).

Table 5.1 Clamped free uniform bar: computation of eigenvalues by the Rayleigh–Ritz method

Mode i	2 functions $\omega_{i,c2}^2$	3 functions $\omega_{i,c3}^2$	Analytical ω_i^2
1	2.486	2.468	2.467
2	32.18	23.39	22.21
3	–	109.2	61.68

$$\lambda = \frac{\omega^2 m \ell^2}{EA}$$

5.2.2 The clamped–free uniform beam

As we did for the bar in extension, an approximate solution to the eigenvalue problem (4.243) can be constructed by superposition of admissible functions:

$$w(x) = \sum_{i=1}^n f_i(x) q_i$$

each function $f_i(x)$ verifying separately the kinematic boundary conditions of the problem, both on displacements and rotations.

The associated quadratic forms representing the kinetic and strain energies are constructed:

$$\begin{aligned} \mathcal{T}_{max} &= \frac{\omega^2}{2} \int_0^\ell m w^2 dx = \frac{\omega^2}{2} \sum_{i=1}^n \sum_{j=1}^n m_{ij} q_i q_j \\ \mathcal{V}_{max} &= \frac{1}{2} \int_0^\ell EI \left(\frac{d^2 w}{dx^2} \right)^2 dx = \frac{1}{2} \sum_{i=1}^n \sum_{j=1}^n k_{ij} q_i q_j \end{aligned}$$

with the mass and stiffness coefficients:

$$m_{ij} = \int_0^\ell m f_i(x) f_j(x) dx \quad k_{ij} = \int_0^\ell EI f_i''(x) f_j''(x) dx \quad (5.63)$$

The discretized equations are again expressed by Equation (5.58):

$$\mathbf{K} \mathbf{q} = \omega^2 \mathbf{M} \mathbf{q}$$

and the upper bound property of the exact eigenvalues remains verified by their solution.

As an example, let us compute an approximation to the eigenvalues of the uniform clamped–free beam by constructing an approximation to the deflection in terms of admissible functions, verifying thus the kinematic conditions:

$$f_i(0) = 0 \quad \text{and} \quad f_i'(0) = 0 \quad i = 1 \dots n$$

We choose in this case to construct the Rayleigh–Ritz approximation using the complete set of monomials from which the first two terms have been omitted since violating the boundary conditions:

$$\{f_i(x)\} = \left\{ \frac{x^2}{\ell^2}, \quad \frac{x^3}{\ell^3}, \quad \frac{x^4}{\ell^4}, \quad \dots \right\} \quad (5.64)$$

Computing the mass and stiffness coefficients for $n = 3$ provides the mass and stiffness matrices:

$$\mathbf{M} = m\ell \begin{bmatrix} \frac{1}{5} & \frac{1}{6} & \frac{1}{7} \\ \frac{1}{6} & \frac{1}{7} & \frac{1}{8} \\ \frac{1}{7} & \frac{1}{8} & \frac{1}{9} \end{bmatrix} \quad \mathbf{K} = \frac{EI}{\ell^3} \begin{bmatrix} 4 & 6 & 8 \\ 6 & 12 & 18 \\ 8 & 18 & \frac{144}{5} \end{bmatrix} \quad (5.65)$$

Setting $n = 2$ yields the quadratic eigenvalue problem:

$$\frac{EI}{\ell^3} \begin{bmatrix} 4 & 6 \\ 6 & 12 \end{bmatrix} \begin{bmatrix} q_1 \\ q_2 \end{bmatrix} - \omega^2 m\ell \begin{bmatrix} \frac{1}{5} & \frac{1}{6} \\ \frac{1}{6} & \frac{1}{7} \end{bmatrix} \begin{bmatrix} q_1 \\ q_2 \end{bmatrix} = 0 \quad (5.66)$$

By defining the nondimensional parameter:

$$\lambda = \frac{\omega^2 m\ell^4}{EI} \quad (5.67)$$

the eigenvalue Equation (5.66) becomes:

$$\lambda^2 - 1224\lambda + 15\,120 = 0$$

The eigenvalues thus obtained are:

$$\omega_{1,c2}^2 = 12.48 \frac{EI}{m\ell^4} \quad \omega_{2,c2}^2 = 1212 \frac{EI}{m\ell^4}$$

in place of the analytical values $12.36 \frac{EI}{m\ell^4}$ and $485.5 \frac{EI}{m\ell^4}$ deduced from Table 4.3.

Looking at the results given in Table 5.2, the same remarks can be made as for the bar:

- Limiting the monomial interpolation to the third degree allows accurate computation of only one eigenvalue. Adding the fourth-degree monomial term to the Rayleigh–Ritz approximation yields significantly more accurate results.
- Monotonic convergence by upper bounds towards the exact eigenvalues is obtained as theoretically predicted.

Table 5.2 Clamped free uniform beam: computation of eigenvalues by the Rayleigh–Ritz method

Mode i	2 functions $\omega_{i,c2}^2$	3 functions $\omega_{i,c3}^2$	Analytical ω_i^2
1	12.48	12.37	12.36
2	1212.0	494.3	485.5
3	–	13958.0	3807.0

$$\lambda = \frac{\omega^2 m\ell^4}{EI}$$

Example 5.1 Dynamic Response of an Aircraft Model

Let us consider the crude aircraft wing model of Figure 5.1. It consists of a uniform beam of span ℓ , distributed mass m_0 and bending stiffness EI . The fuselage is supposed to have a mass $M_1 = 2m_0\ell$ and both engines a mass $M_2 = m_0\ell$. The wing structure is suddenly submitted to a wind gust of uniform distribution over the span, with intensity:

$$p_{wg}(x, t) = \begin{cases} p_0 \sin(\omega_f t) & 0 < t < T_I \\ 0 & t \geq T_I \end{cases} \quad (\text{E5.1.a})$$

Both the structure and the loading being symmetric, the analysis can be limited to the symmetric modes. It is made using a set of three interpolation monomial functions $\{1, x^2, x^4\}$ that will be rendered orthogonal to the mass distribution.

The circular frequency ω_f of the excitation is taken equal to $\frac{1}{2}\omega_2$, ω_2 being the eigenfrequency of the first symmetrical eigenmode of the aircraft wing structure. The load applies during one-half period, i.e. $T_I = \frac{\pi}{\omega_f}$. The response is computed over the time interval $[0, 4T_I = 4\frac{2\pi}{\omega_2}]$. All results are presented in nondimensional form.

Modal analysis

The mass distribution over the wing structure can be written in terms of the Dirac function $\delta(x)$ in the form:

$$m(x) = m_0 + M_1 \delta(x) + M_2 \delta\left(x - \frac{\ell}{4}\right) + M_2 \delta\left(x + \frac{\ell}{4}\right) \quad (\text{E5.1.b})$$

Starting from the monomials $\{1, x^2, x^4\}$, a set of orthogonal functions is constructed by determining the unknown coefficients of the set:

$$\begin{aligned} f_1(x) &= 1 \\ f_2(x) &= a_{20} + x^2 \\ f_3(x) &= a_{30} + a_{32}x^2 + x^4 \end{aligned} \quad (\text{E5.1.c})$$

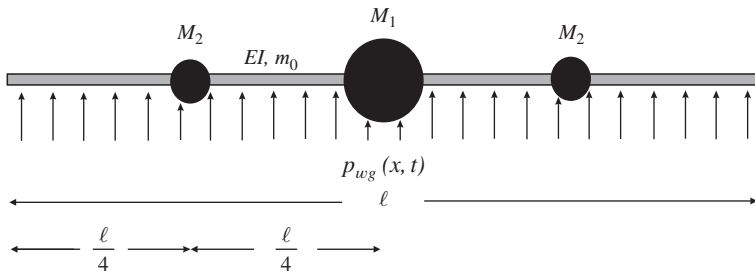


Figure 5.1 Crude model of an aircraft wing submitted to uniform wind gust: approximation by the Rayleigh–Ritz method.

Expressing the orthogonality with respect of the mass distribution:

$$m_{ij} = \int_{-\frac{\ell}{2}}^{\frac{\ell}{2}} m(x) f_i(x) f_j(x) dx = 0 \quad i \neq j \quad (\text{E5.1.d})$$

yields the following set of interpolation polynomials:

$$\begin{aligned} f_1(x) &= 1 \\ f_2(x) &= -\frac{1}{24} + x^2 \\ f_3(x) &= \frac{1989}{750400} - \frac{1209}{7504} x^2 + x^4 \end{aligned} \quad (\text{E5.1.e})$$

Owing to (E5.1.d) the mass matrix is diagonal. The remaining terms are:

$$m_{ii} = \int_{-\frac{\ell}{2}}^{\frac{\ell}{2}} m(x) f_i^2(x) dx \quad i = 1 \dots 3 \quad (\text{E5.1.f})$$

We get:

$$m_{11} = 5 m_0 \ell \quad m_{22} = \frac{67}{5760} m_0 \ell \quad m_{33} = \frac{605779}{7564032000} m_0 \ell$$

and thus:

$$\mathbf{M} = m_0 \ell \begin{bmatrix} 5. & 0 & 0 \\ 0 & 0.01163 & 0 \\ 0 & 0 & 8.0087 E - 5 \end{bmatrix} \quad (\text{E5.1.g})$$

The elements of the stiffness matrix are computed in a similar way:

$$k_{ij} = EI \int_{-\frac{\ell}{2}}^{\frac{\ell}{2}} f_i''(x) f_j''(x) dx \quad i, j = 1 \dots 3 \quad (\text{E5.1.h})$$

The nonzero coefficients are:

$$k_{22} = 4 \frac{EI}{\ell^3} \quad k_{23} = \frac{2543}{1876} \frac{EI}{\ell^3} \quad k_{33} = \frac{88644261}{70387520} \frac{EI}{\ell^3}$$

Hence the stiffness matrix:

$$\mathbf{K} = \frac{EI}{\ell^3} \begin{bmatrix} 0 & 0 & 0 \\ 0 & 4 & 1.3555 \\ 0 & 1.3555 & 1.2594 \end{bmatrix} \quad (\text{E5.1.i})$$

Solving the eigenproblem $\mathbf{KX} = \mathbf{MX}\Omega^2$ yields

– the matrix of eigenvalues:

$$\Omega^2 = \frac{EI}{m\ell^4} \begin{bmatrix} 0 & 0 & 0 \\ 0 & 216.69 & 0 \\ 0 & 0 & 15852 \end{bmatrix} \quad (\text{E5.1.j})$$

– the matrix of eigenmodes:

$$\mathbf{X} = \begin{bmatrix} 0.4472 & 0 & 0 \\ 0 & -9.2342 & 0.8363 \\ 0 & 10.0782 & 111.2874 \end{bmatrix} \quad (\text{E5.1.k})$$

Finally, performing the product:

$$\mathbf{U}(x) = [f_1(x) \ f_2(x) \ f_3(x)] \mathbf{X} \quad (\text{E5.1.l})$$

restores the approximation of the first 3 symmetric eigenmodes in analytical form:

$$\begin{aligned} w_{(1)}(x) &= 0.4472 \quad (\text{translation rigid body mode}) \\ w_{(2)}(x) &= 0.41147 - 10.8579 x^2 + 10.0782 x^4 \\ w_{(3)}(x) &= 0.26013 - 17.09367 x^2 + 111.287 x^4 \end{aligned} \quad (\text{E5.1.m})$$

They are displayed on Figure 5.2.

Dynamic response

The computation of the response to external excitation is done by solving Equation (5.15):

$$\mathbf{K}\mathbf{q} + \mathbf{M}\ddot{\mathbf{q}} = \mathbf{p}(t) \quad (\text{E5.1.n})$$

where the vector $\mathbf{q}(t)$ collects the amplitudes of the interpolation functions $\mathbf{F}(x)$ (Equation (5.3)).

In the present case, the load can be put in the form:

$$\mathbf{p}(t) = \mathbf{p}_0 \varphi(t) \quad (\text{E5.1.o})$$

with the participation factors of the interpolation functions to the loading:

$$p_{0,i} = \int_{-\frac{\ell}{2}}^{\frac{\ell}{2}} p_0 f_i(x) dx \quad i = 1, \dots, 3 \quad (\text{E5.1.p})$$

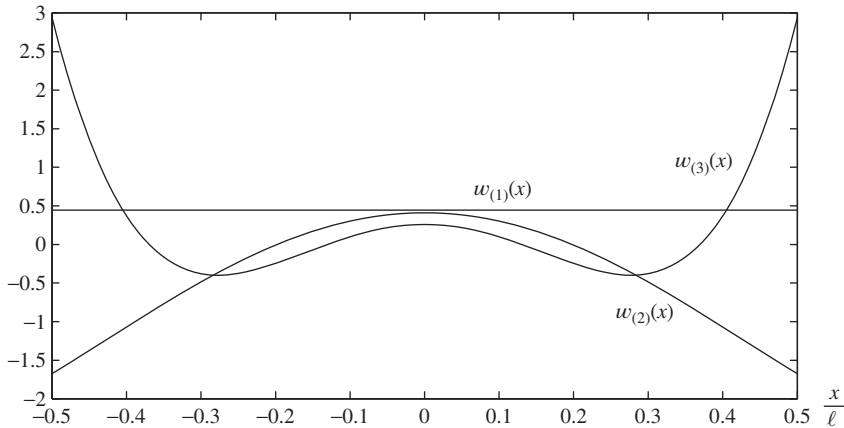


Figure 5.2 Aircraft model: first three eigenmodes computed by Rayleigh–Ritz method.

yielding thus:

$$\mathbf{p}_0^T = p_0 \begin{bmatrix} 1 & \frac{1}{24} & \frac{647}{375200} \end{bmatrix} \quad (\text{E5.1.q})$$

The eigenfrequency of the first symmetric elastic mode is obtained from $\omega_2 = \sqrt{216.69 \frac{EI}{m\ell^4}} = 14.72 \sqrt{\frac{EI}{m\ell^4}}$. The excitation frequency is thus $\omega_f = 7.36 \sqrt{\frac{EI}{m\ell^4}}$ and the period of load application $T_1 = \frac{\pi}{\omega_f} = 0.4268 \sqrt{\frac{m\ell^4}{EI}}$. The time interval of computation of the response is equal to $4T_1 = 8 \frac{\pi}{\omega_2} = 1.707 \sqrt{\frac{m\ell^4}{EI}}$. Expressed in terms of the nondimensional time $\tau = t \sqrt{\frac{EI}{m\ell^4}}$, the time-dependent part of the excitation has for expression:

$$\varphi(\tau) = \begin{cases} \sin(7.36 \tau) & 0 < \tau < 0.4268 \\ 0 & \tau \geq 0.4268 \end{cases} \quad (\text{E5.1.r})$$

The computation of the response could be obtained through integration of the normal equations and mode superposition. The choice has been made in this case to use the time-marching scheme suggested in Exercise 3.11 to directly time integrate the system (E5.1.n).

Once obtained the time evolution $\mathbf{q}(t)$, the bending displacement along the wing axis is computed as:

$$w(x, t) = \mathbf{F}(x)\mathbf{q}(t) \quad (\text{E5.1.s})$$

It has been evaluated versus time at locations $x = 0$ (mass M_1 of the fuselage), $x = \pm \frac{\ell}{4}$ (masses M_2 of the engines) and $x = \pm \frac{\ell}{2}$ (wing tips). Its time evolution is displayed on Figure 5.3. The results show that the rigid body motion of the aircraft (uniformly accelerated motion followed by motion at constant velocity) dominates the response since the main effect of the wind gust loading is to apply a vertical acceleration to the aircraft. The elastic deformation

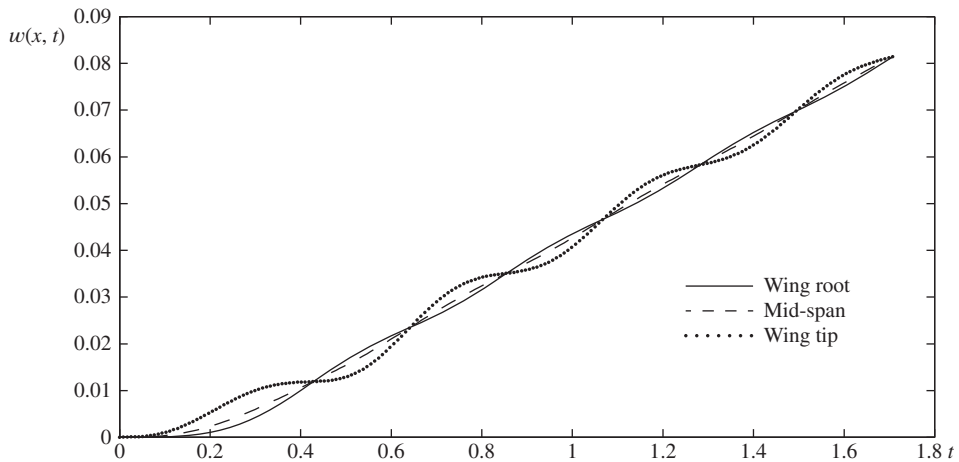


Figure 5.3 Aircraft model: total bending displacements versus time at wing root (—), engine level (---) and wing tip (...).

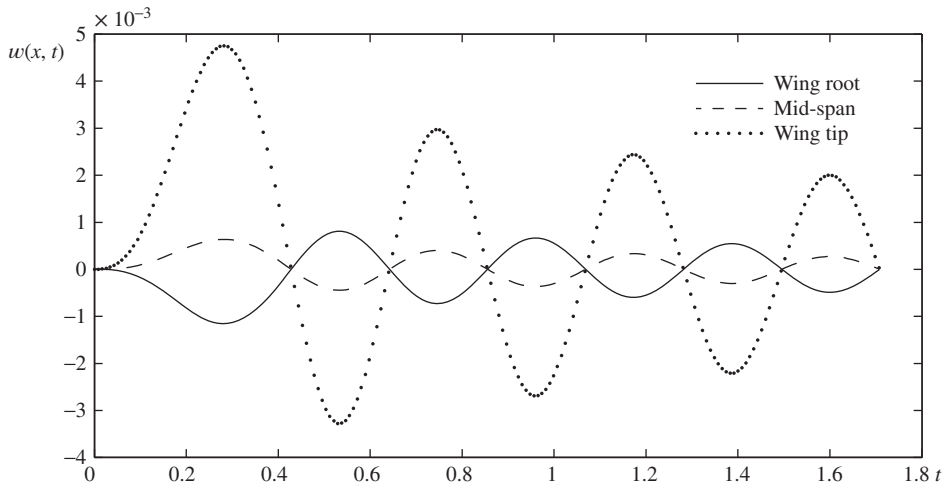


Figure 5.4 Aircraft wing model: elastic bending displacements versus time at wing root (—), engine level (---) and wing tip (...).

results essentially from excitation of the first elastic eigenmode. The intermediate masses (engines) being close to the node of the mode, their motion (dashed line) is almost not influenced by the elasticity of the structure. The elastic deformation is more perceptible at the fuselage (plain line) and very noticeable at the wing tips (dotted line).

This is confirmed by plotting the elastic part of the response (Figure 5.4), obtained simply by setting $f_1 = 0$ in the postprocessing of the displacements to remove the rigid body part. It clearly appears that the first elastic eigenmode dominates the response, which results from the facts that the static participation factor of the second elastic mode $w_{(3)}(x)$ is quite low and that the excitation frequency is well under the first elastic frequency ω_2 . The apparent damping in the elastic response is likely due to exchange of kinetic energy with the rigid body mode.

Finally, the model can also be used to predict the time evolution of the bending moment in the wing, computed as:

$$M(x, t) = EI \frac{d^2 F}{dx^2} q(t) \quad (\text{E5.1.t})$$

It has been evaluated at the same locations as the vertical displacements. Its time evolution is displayed in nondimensional form on Figure 5.5. However, this result is not quantitatively very correct – at least at the wing tip – since it is obtained from second differentiation of a rather crude displacement approximation. A more accurate result would require a higher number of interpolation functions. Still, it shows that the bending moment is the highest at the wing root (plain line), has lower intensity at mid-span (dashed line) and is the lowest at the wing tips (dotted line) where, according to the exact equilibrium boundary conditions, it should be zero (see discussion of the residual forces in Remark 5.1). This simple example is representative of the methodology that can be followed to develop simplified models in the early design stage of a project.

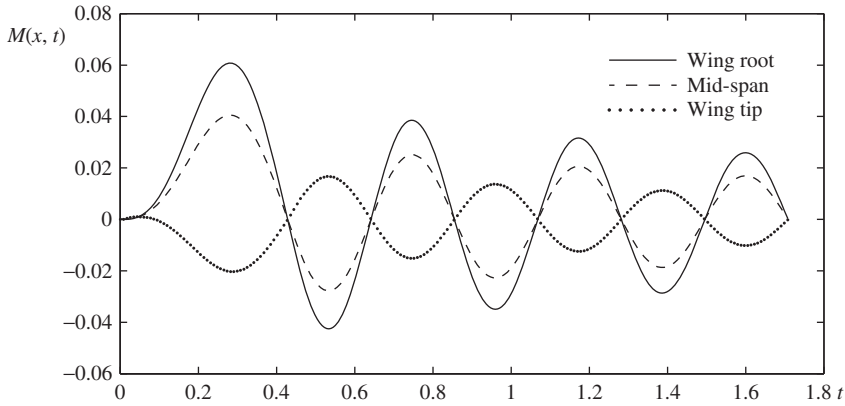


Figure 5.5 Aircraft wing model: bending moments versus time at wing root (—), engine level (---) and wing tip (...).

5.2.3 The uniform rectangular plate

For rectangular plates (Figure 5.6), an efficient choice of kinematically admissible functions consists in combining for each direction x and y the mode shapes of a beam verifying the same boundary conditions, since the latter have the interesting property of forming complete sets. This choice not only allows representation of the mode shapes of the plate in an appropriate manner but also generates significant simplifications in the evaluation of the stiffness and mass matrices, thanks to the orthogonality properties of mode shapes of a beam.

Let us construct the trial function:

$$w(x, y) = \sum_{k=1}^n \sum_{l=1}^m A_{kl} X_k(x) Y_l(y) \quad (5.68)$$

where A_{kl} are the generalized coordinates and $X_k(x)$, $Y_l(y)$ are the beam mode shapes verifying the boundary conditions at $x = 0, a$ and $y = 0, b$ respectively. These mode shapes have been obtained in Section 4.3.3 for uniform beams and they verify the fundamental property:

$$\frac{d^4 X_r}{dx^4} - \left(\frac{\mu_r^{(x)}}{a} \right)^4 X_r = 0 \quad \frac{d^4 Y_s}{dy^4} - \left(\frac{\mu_s^{(y)}}{b} \right)^4 Y_s = 0 \quad (5.69)$$

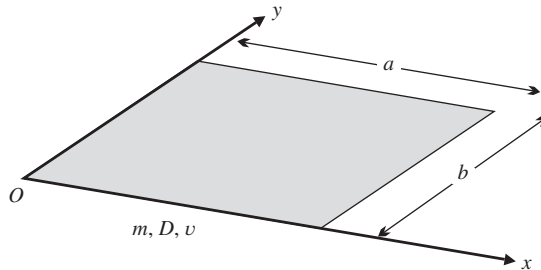


Figure 5.6 Rectangular plate.

where $\mu_r^{(x)}$ and $\mu_s^{(y)}$ are the nondimensional eigenfrequencies 4.247 of eigenshapes X_r and Y_s , the values of which are listed in Table 4.3. Let us suppose that the eigenmodes are normalized in such a way that the orthogonality relationships may be written:

$$\begin{aligned} \int_0^a X_r X_s dx &= a \delta_{rs} & \int_0^b Y_r Y_s dy &= b \delta_{rs} \\ \int_0^a \frac{d^2 X_r}{dx^2} \frac{d^2 X_s}{dx^2} dx &= \frac{\mu_r^{(x)^4}}{a^3} \delta_{rs} & \int_0^b \frac{d^2 Y_r}{dy^2} \frac{d^2 Y_s}{dy^2} dy &= \frac{\mu_r^{(y)^4}}{b^3} \delta_{rs} \end{aligned} \quad (5.70)$$

In order to compute the kinetic and strain energies 4.367 and 4.369 of the uniform plate:

$$\mathcal{T} = \frac{1}{2} m \omega^2 \int_0^a \int_0^b w^2 dx dy \quad (5.71a)$$

$$\begin{aligned} \mathcal{V}_{int} = \frac{D}{2} \int_0^a \int_0^b \left\{ \left(\frac{\partial^2 w}{\partial x^2} \right)^2 + \left(\frac{\partial^2 w}{\partial y^2} \right)^2 \right. \\ \left. + 2\nu \frac{\partial^2 w}{\partial x^2} \frac{\partial^2 w}{\partial y^2} + 2(1-\nu) \left(\frac{\partial^2 w}{\partial x \partial y} \right)^2 \right\} dx dy \end{aligned} \quad (5.71b)$$

let us set:

$$\begin{aligned} E_{rs} &= \int_0^a X_r \frac{d^2 X_s}{dx^2} dx & F_{rs} &= \int_0^b Y_r \frac{d^2 Y_s}{dy^2} dy \\ G_{rs} &= \int_0^a \frac{dX_r}{dx} \frac{dX_s}{dx} dx & H_{rs} &= \int_0^b \frac{dY_r}{dy} \frac{dY_s}{dy} dy \end{aligned} \quad (5.72)$$

Taking account of (5.70) and (5.72), the energies may then be expressed as:

$$\begin{aligned} \mathcal{T} &= \frac{1}{2} m a b \omega^2 \sum_{i=1}^n \sum_{j=1}^m \sum_{k=1}^n \sum_{l=1}^m A_{ij} A_{kl} \delta_{ik} \delta_{jl} \\ \mathcal{V}_{int} &= \frac{D}{2} \sum_{i=1}^n \sum_{j=1}^m \sum_{k=1}^n \sum_{l=1}^m \left\{ \left[\frac{b}{a^3} \mu_k^{(x)^4} + \frac{a}{b^3} \mu_l^{(y)^4} \right] \delta_{ik} \delta_{jl} \right. \\ &\quad \left. + \nu [E_{ik} F_{jl} + E_{kl} F_{ij}] \right. \\ &\quad \left. + 2(1-\nu) G_{ik} H_{jl} \right\} A_{ij} A_{kl} \\ &= \frac{D}{2} \sum_{i=1}^n \sum_{j=1}^m \sum_{k=1}^n \sum_{l=1}^m K_{ij,kl} A_{ij} A_{kl} \end{aligned} \quad (5.73)$$

where $K_{ij,kl}$ are the coefficients of the discretized stiffness matrix \mathbf{K} of size $nm \times nm$ which is symmetrical by construction. The eigenvalue equation is then written:

$$\mathbf{K} - \lambda \mathbf{I} = \mathbf{0} \quad (5.74)$$

with

$$\lambda = \omega^2 \frac{mab}{D} \quad (5.75)$$

The Rayleigh–Ritz method for plate bending can be used to compute systematically the vibration characteristics of plates whose geometry and boundary conditions do not allow an exact closed-form solution. A complete record of such results has been published in Blevins (1979).

Example 5.2 The Cantilever Plate

Let us consider the case of the rectangular plate clamped on one edge of length b parallel to the y axis (Figure 5.7) and with dimension ratio $a/b = 1.5$. Let us construct a two-degree-of-freedom trial function using the first mode of the cantilever beam in the x direction and the translation and rotation rigid-body modes of the free–free beam in direction y . Using the Duncan functions (4.248), the orthonormalized beam modes may be written:

$$\begin{aligned} X_1(x) &= \sqrt{\frac{1}{1.8556}} \left[s_2 \left(\mu_1^{(x)} \frac{x}{a} \right) - \frac{s_1(\mu_1^{(x)})}{c_1(\mu_1^{(x)})} c_2 \left(\mu_1^{(x)} \frac{x}{a} \right) \right] \\ Y_1(y) &= 1 \\ Y_2(y) &= \sqrt{12} \left(\frac{y}{b} - \frac{1}{2} \right) \end{aligned} \quad (\text{E5.2.a})$$

with $\mu_1^{(x)} = 1.8751$. The trial function is:

$$\begin{aligned} w(x, y) &= A_{11}X_1Y_1 + A_{12}X_1Y_2 \\ &= \sqrt{\frac{1}{1.8556}} \left[s_2 \left(\mu_1^{(x)} \frac{x}{a} \right) - \frac{s_1(\mu_1^{(x)})}{c_1(\mu_1^{(x)})} c_2 \left(\mu_1^{(x)} \frac{x}{a} \right) \right] \left[A_{11} + A_{12}\sqrt{12} \left(\frac{y}{b} - \frac{1}{2} \right) \right] \end{aligned} \quad (\text{E5.2.b})$$

Computing the integrals E_{rs} , F_{rs} , G_{rs} and H_{rs} then yields:

$$\begin{aligned} E_{11} &= \int_0^a X_1 \frac{d^2 X_1}{dx^2} dx = 0.2441 \frac{\mu_1^{(x)^2}}{a} & G_{11} &= \int_0^a \left(\frac{dX_1}{dx} \right)^2 dx = 1.322 \frac{\mu_1^{(x)^2}}{a} \\ F_{11} &= \int_0^b Y_1 \frac{d^2 Y_1}{dy^2} dy = 0 & H_{11} &= \int_0^b \frac{dY_1}{dy} \frac{dY_1}{dy} dy = 0 \\ F_{12} &= \int_0^b Y_1 \frac{d^2 Y_2}{dy^2} dy = 0 & H_{12} &= H_{21} = \int_0^b \frac{dY_1}{dy} \frac{dY_2}{dy} dy = 0 \\ F_{21} &= \int_0^b Y_2 \frac{d^2 Y_1}{dy^2} dy = 0 & H_{22} &= \int_0^b \frac{dY_2}{dy} \frac{dY_2}{dy} dy = \frac{12}{b} \\ F_{22} &= \int_0^b Y_2 \frac{d^2 Y_2}{dy^2} dy = 0 \end{aligned}$$

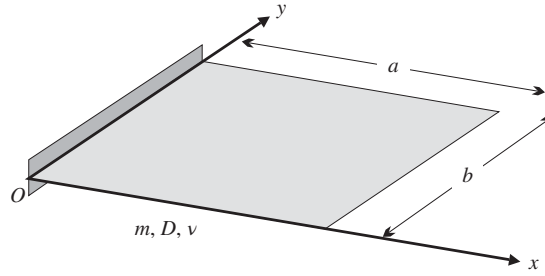


Figure 5.7 Cantilever rectangular plate.

The coefficients of the discretized stiffness matrix are written:

$$\begin{aligned}
 K_{11,11} &= \frac{b}{a^3} \mu_1^{(x)4} + 2\nu E_{11} F_{11} + 2(1-\nu) G_{11} H_{11} = \frac{b}{a^3} \mu_1^{(x)4} \\
 K_{11,12} &= K_{12,11} = \nu [E_{11} F_{12} + E_{11} F_{21}] + 2(1-\nu) G_{11} H_{12} = 0 \\
 K_{12,12} &= \frac{b}{a^3} \mu_1^{(x)4} + 2\nu E_{11} F_{22} + 2(1-\nu) G_{11} H_{22} \\
 &= \frac{b}{a^3} \mu_1^{(x)4} + 2(1-\nu) 1.322 \frac{12\mu_1^{(x)2}}{ab}
 \end{aligned} \tag{E5.2.c}$$

The resulting eigenvalue equation:

$$\begin{bmatrix} K_{11,11} & 0 \\ 0 & K_{12,12} \end{bmatrix} - \frac{mab}{D} \omega_c^2 \mathbf{I} = \mathbf{0}$$

admits the roots:

$$\begin{aligned}
 \omega_{1,c}^2 \frac{ma^3b}{D} &= \mu_1^{(x)4} \frac{b}{a} \\
 \omega_{2,c}^2 \frac{ma^3b}{D} &= \mu_1^{(x)4} \frac{b}{a} + 24(1-\nu) 1.322 \mu_1^{(x)2} \frac{a}{b}
 \end{aligned} \tag{E5.2.d}$$

For a dimension ratio $a/b = 1.5$ and a Poisson coefficient $\nu = 0.3$, we thus obtain:

$$\begin{aligned}
 \omega_{1,c}^2 \frac{ma^3b}{D} &= 8.242 \\
 \omega_{2,c}^2 \frac{ma^3b}{D} &= 125.4
 \end{aligned} \tag{E5.2.e}$$

Let us compute again the eigenfrequencies of the cantilever plate by including now in the trial function the first elastic mode in direction y:

$$Y_3(y) = \sqrt{\frac{1}{1.0359}} \left(s_1 \left(\mu_3^{(y)} \frac{y}{b} \right) - \frac{s_2(\mu_3^{(y)})}{c_2(\mu_3^{(y)})} c_1 \left(\mu_3^{(y)} \frac{y}{b} \right) \right) \tag{E5.2.f}$$

with $\mu_3^{(y)} = 4.730$. The three-degree-of-freedom trial function is:

$$w(x, y) = A_{11}X_1Y_1 + A_{12}X_1Y_2 + A_{13}X_1Y_3$$

$$= \left[s_2 \left(\mu_1^{(x)} \frac{x}{a} \right) - \frac{s_1(\mu_1^{(x)})}{c_1(\mu_1^{(x)})} c_2 \left(\mu_1^{(x)} \frac{x}{a} \right) \right] \times$$

$$\left[A_{11} + A_{12} \sqrt{12} \left(\frac{y}{b} - \frac{1}{2} \right) + A_{13} \sqrt{\frac{1}{1.0359}} \left(s_1 \left(\mu_3^{(y)} \frac{y}{b} \right) - \frac{s_2(\mu_3^{(y)})}{c_2(\mu_3^{(y)})} c_1 \left(\mu_3^{(y)} \frac{y}{b} \right) \right) \right]$$

(E5.2.g)

The additional coefficients to be computed are:

$$F_{13} = \int_0^b Y_1 \frac{d^2 Y_3}{dy^2} dy = -0.8309 \frac{\mu_3^{(y)^2}}{b} \quad H_{13} = H_{31} = \int_0^b \frac{dY_1}{dy} \frac{dY_3}{dy} dy$$

$$F_{31} = \int_0^b Y_3 \frac{d^2 Y_1}{dy^2} dy = 0 \quad = 0$$

$$F_{23} = \int_0^b Y_2 \frac{d^2 Y_3}{dy^2} dy = 0 H_{23} \quad = H_{32} = \int_0^b \frac{dY_2}{dy} \frac{dY_3}{dy} dy$$

$$F_{32} = \int_0^b Y_3 \frac{d^2 Y_2}{dy^2} dy = 0 \quad = 0$$

$$F_{33} = \int_0^b Y_3 \frac{d^2 Y_3}{dy^2} dy = -0.5499 \frac{\mu_3^{(y)^2}}{b} H_{33} \quad = \int_0^b \frac{dY_3}{dy} \frac{dY_3}{dy} dy = 2.2117 \frac{\mu_3^{(y)^2}}{b}$$

and the supplementary terms of \mathbf{K} are:

$$K_{11,13} = K_{13,11}$$

$$= \nu[E_{11}F_{13} + E_{11}F_{31}] + 2(1 - \nu)G_{11}H_{13} = \nu E_{11}F_{13}$$

$$K_{12,13} = K_{13,12}$$

$$= \nu[E_{11}F_{23} + E_{11}F_{32}] + 2(1 - \nu)G_{11}H_{23} = 0$$

$$K_{13,13} = \frac{b}{a^3} \mu_1^{(x)^4} + \frac{a}{b^3} \mu_3^{(y)^4} + 2\nu E_{11}F_{33} + 2(1 - \nu)G_{11}H_{33}$$

After simplification, for $a/b = 1.5$ and $\nu = 0.3$, the three-degree-of-freedom characteristic equation is written:

$$\begin{bmatrix} 8.2415 & 0 & -7.180 \\ 0 & 125.37 & 0 \\ -7.180 & 0 & 2171.1 \end{bmatrix} - \omega_c^2 \frac{ma^3b}{D} \mathbf{I} = \mathbf{0} \quad (\text{E5.2.h})$$

and admits the roots:

$$\omega_{1,c}^2 \frac{ma^3b}{D} = 8.218$$

$$\omega_{2,c}^2 \frac{ma^3b}{D} = 125.4$$

$$\omega_{3,c}^2 \frac{ma^3b}{D} = 2171$$

to be compared to the reference (converged) values given in Blevins (1979) and Barton (1951) obtained with higher number of modes.

$$\omega_1^2 \frac{ma^3b}{D} = 8.06$$

$$\omega_2^2 \frac{ma^3b}{D} = 90.95$$

$$\omega_3^2 \frac{ma^3b}{D} = 1935$$

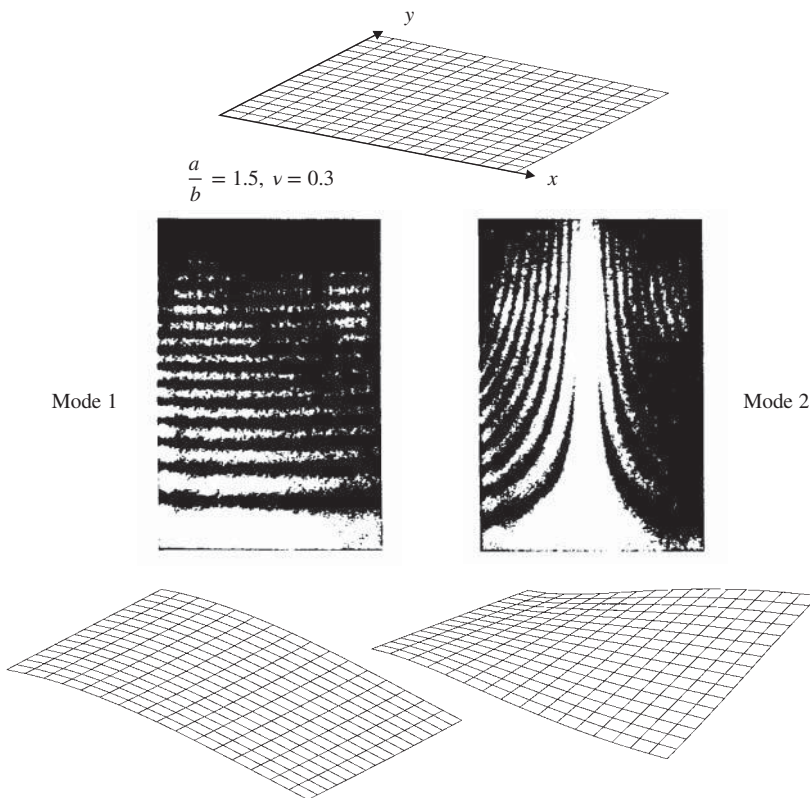


Figure 5.8 Cantilever plate eigenmodes: holographic visualization.

Let us note that there are two eigenfrequencies between ω_2 and ω_3 that have not been detected by the Rayleigh–Ritz method: they correspond to mode shapes with several antinodes along x , which may thus not be obtained using trial functions containing only the first beam bending mode. The first two computed vibration eigenmodes are represented by Figure 5.8. The figure also displays the same mode shapes obtained experimentally using holographic interferometry (1990).

The approximation function containing the first elastic beam mode allows for a better representation of the first symmetric mode of the plate, since its shape along y is not rectilinear due to the anticlastic effect generated by Poisson coupling. This effect is increased with lower dimension ratios a/b .

5.3 The finite element method

A complete volume should be dedicated to a systematic treatment of the *finite element method* (see e.g. Zienkiewicz and Taylor 1989, Hughes 1987). It is thus not our objective to make a comprehensive presentation of it here. Our purpose is simply to show its potential and mode of application in the context of elastodynamics: therefore this discussion will be limited to the cases of the bar element in extension, the beam element in bending and the combined bending, torsion and extension beam element.

The finite element method may be regarded as a particular application procedure of the Rayleigh–Ritz method. It consists of subdividing the deformable body or the structure into a finite number of elements (Figure 5.9) of simple geometry (line segment in the one-dimensional case, triangle or quadrangle in two dimensions, tetrahedron or hexahedron in three dimensions) with well-identified structural behaviour (bar, beam, membrane, plate, shell, 3-D solid, etc.).

The interpolation functions of the displacement field are chosen next in order to fulfill the following requirements:

1. Interpolation is performed in terms of *piecewise continuous* functions. Inside each element, the displacement field is represented by a superposition of a small number of functions which are chosen to be simple but representative of the element's structural behaviour in the global structure. They are generally of polynomial type.
2. These functions are also chosen in such a way that their intensity parameters, which are the *generalized coordinates* of the Rayleigh–Ritz method, are *local values of the displacement field* (see Figure 5.9) in the structure. In this way, the continuity of the global displacement field may be achieved at the structural level through simple identification of the parameters.

If both conditions are strictly satisfied, the approximation obtained is kinematically admissible in the sense of the Rayleigh–Ritz method: indeed, the displacement field is then differentiable over each element domain, and imposing equal values of the generalized coordinates at element interfaces allows us to keep the continuity of the displacement field at the global level.

A finite element respecting both conditions is said to be *kinematically admissible* and *co-deformable* or, simply speaking, *conforming*.

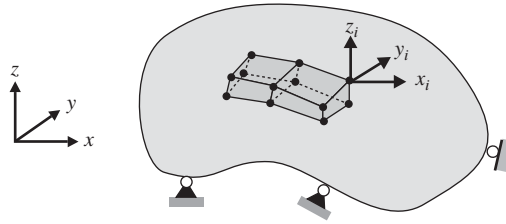


Figure 5.9 The finite element method.

5.3.1 The bar in extension

Generation of a bar element

Let us consider the case of a bar in extension possibly subjected to distributed loads $\bar{X}(t)$. The bar is first divided into N elements of length ℓ as sketched in Figure 5.10. We call P_1 and P_2 the loads at the ends of an element, representing the sum of applied external forces on the nodes and of inner normal forces originating from interaction with neighbouring elements. Next, the displacement field in the element is approximated by the linear interpolation:

$$u(x, t) = u_1(t)\phi_1(x) + u_2(t)\phi_2(x) \quad (5.76)$$

where

$u_1(t)$, $u_2(t)$ are the *connector* degrees of freedom, namely the axial displacements at both element ends, also called *nodes*.

$\phi_1(x)$, $\phi_2(x)$ are the *shape functions* of the element, chosen in such a way that:

$$u(0, t) = u_1(t) \quad u(\ell, t) = u_2(t)$$

If no internal parameter is introduced, they result from a linear interpolation:

$$\phi_1(x) = 1 - \frac{x}{\ell} \quad \phi_2(x) = \frac{x}{\ell} \quad (5.77)$$

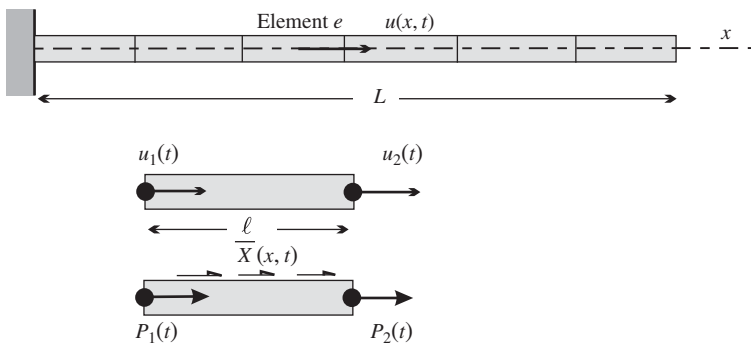


Figure 5.10 Bar in extension modelled by N finite elements.

Equation (5.76) may be put in matrix form:

$$u(x, t) = \Phi_e(x) \mathbf{q}_e(t) \quad x \in \text{element } e \quad (5.78)$$

where

$\Phi_e(x) = [\phi_1(x) \ \phi_2(x)]$ is the shape function matrix of element e
 $\mathbf{q}_e^T(t) = [u_1(t) \ u_2(t)]$ is the set of degrees of freedom of element e .

We may then compute successively:

- the element kinetic and strain energies as quadratic forms of the *mass and stiffness elementary matrices*:

$$\mathcal{T}_e = \frac{1}{2} \dot{\mathbf{q}}_e^T \mathbf{M}_e \dot{\mathbf{q}}_e \quad \text{and} \quad \mathcal{V}_{int,e} = \frac{1}{2} \mathbf{q}_e^T \mathbf{K}_e \mathbf{q}_e \quad (5.79)$$

given by

$$\begin{aligned} \mathbf{M}_e &= \int_0^\ell m \Phi_e^T \Phi_e \, dx \\ \mathbf{K}_e &= \int_0^\ell EA \frac{d\Phi_e^T}{dx} \frac{d\Phi_e}{dx} \, dx \end{aligned} \quad (5.80)$$

- the virtual work of external forces in the form:

$$\delta \mathcal{V}_{ext,e} = -\delta \mathbf{q}_e^T \mathbf{p}_e(t) \quad (5.81)$$

with the *generalized loads* $\mathbf{p}_e(t)$ conjugated to displacements $\mathbf{q}_e(t)$:

$$\mathbf{p}_e(t) = \int_0^\ell \Phi_e^T \bar{X}(x, t) \, dx + \begin{bmatrix} P_1(t) \\ P_2(t) \end{bmatrix} \quad (5.82)$$

The first term results from the discretization of the load per unit length and the second one contains the end loads of the element.

In particular, for the bar element of uniform characteristics modelled using linear interpolation functions, we obtain the *elementary stiffness and mass matrices*:

$$\mathbf{K}_e = \frac{EA}{\ell} \begin{bmatrix} 1 & -1 \\ -1 & 1 \end{bmatrix} \quad \mathbf{M}_e = m \frac{\ell}{6} \begin{bmatrix} 2 & 1 \\ 1 & 2 \end{bmatrix} \quad (5.83)$$

and the discretized force vector for the case of a uniform load \bar{X}_0 per unit length over the element:

$$\mathbf{p}_e = \frac{\bar{X}_0 \ell}{2} \begin{bmatrix} 1 \\ 1 \end{bmatrix} + \begin{bmatrix} P_1(t) \\ P_2(t) \end{bmatrix} \quad (5.84)$$

We verify that:

- the rigid body mode $\mathbf{u}_e^T = [1 \ 1]$ is such that $\mathbf{K}_e \mathbf{u}_e = 0$,
- the mass associated to the rigid body mode, obtained by projecting the mass matrix on it, yields the total mass of the element: $\mathbf{u}_e^T \mathbf{M}_e \mathbf{u}_e = m\ell$.

The mass matrix constructed in this way is said to be *consistent* in the sense that it is obtained from the same displacement approximation as the stiffness matrix. In particular it is observed that in the consistent mass matrix there are off-diagonal terms. This coupling of the nodal accelerations indicates that acceleration at one node induces inertia forces also for the other node, resulting from the fact that the nodes drive the amplitude of the motion in the entire element through the shape functions as indicated by (5.76).

By making use of results (5.79) and (5.80) the contribution of element e to Hamilton's principle may be expressed in the form:

$$\delta \int_{t_1}^{t_2} \left(\frac{1}{2} \dot{\mathbf{q}}_e^T \mathbf{M}_e \dot{\mathbf{q}}_e - \frac{1}{2} \mathbf{q}_e^T \mathbf{K}_e \mathbf{q}_e \right) dt + \delta \mathbf{q}_e^T \mathbf{p}_e = 0 \quad (5.85)$$

Remark 5.2 It should be noticed that the stiffness and mass matrices (5.83) of the bar element were in fact already obtained from the series expansion of the analytical expression of the impedance for the bar in extension (Chapter 4, pages 248–250). This result is not surprising since the quasi-static solution (4.159) from which the constant contributions to the impedance are computed and the assumed displacement field for the finite element discretization are the same.

Assembly process

In order to express dynamic equilibrium for the global system of Figure 5.10, let us construct the matrix of structural displacements \mathbf{q} collecting the $(N + 1)$ nodal displacements (Figure 5.11). The transpose of this matrix is:

$$\mathbf{q}^T = [u_0 \ u_1 \ u_2 \ u_3 \ \dots \ u_N] \quad (5.86)$$

such that the degrees of freedom of an element are retrieved as:

$$\mathbf{q}_e = \mathbf{L}_e \mathbf{q} \quad (5.87)$$

where the *localization operator* \mathbf{L}_e is a Boolean matrix, here with dimension $2 \times (N + 1)$. It contains only 1 and 0 terms and can be seen as a filter picking the nodal displacements \mathbf{q}_e of an element out of the global set of degrees of freedom \mathbf{q} . For instance, for elements 1 and 2 of

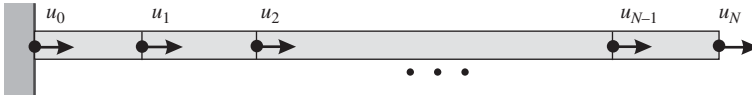


Figure 5.11 Nodal displacements of the system.

Figure 5.11,³

$$L_1 = \begin{bmatrix} 0 & 0 & 0 & 0 & \dots & 0 \\ 0 & 1 & 0 & 0 & \dots & 0 \end{bmatrix}$$

$$L_2 = \begin{bmatrix} 0 & 1 & 0 & 0 & \dots & 0 \\ 0 & 0 & 1 & 0 & \dots & 0 \end{bmatrix}$$

Relating all element nodal displacements to a unique global set through a localization operator ensures that the local piecewise continuous shape functions of the element is also continuous for the global structure and thus forms an approximation space that is kinematically admissible for any arbitrary variation $\delta \mathbf{q}$. In that sense the finite element approximation can be considered as a special case of the Rayleigh–Ritz method, each structural degree of freedom in \mathbf{q} governing a shape function in the element it is attached to.

By summing all the elements of the system, the structural variational equation becomes:

$$\delta \int_{t_1}^{t_2} \sum_{e=1}^N \left[\frac{1}{2} \dot{\mathbf{q}}_e^T \mathbf{M}_e \dot{\mathbf{q}}_e - \frac{1}{2} \mathbf{q}_e^T \mathbf{K}_e \mathbf{q}_e \right] dt + \int_{t_1}^{t_2} \sum_{e=1}^N \delta \mathbf{q}_e^T \mathbf{p}_e dt = 0 \quad (5.88)$$

and it may be expressed in terms of structural displacements through substitution of (5.87) into (5.88):

$$\delta \int_{t_1}^{t_2} \left\{ \frac{1}{2} \dot{\mathbf{q}}^T \left(\sum_{e=1}^N \mathbf{L}_e^T \mathbf{M}_e \mathbf{L}_e \right) \dot{\mathbf{q}} - \frac{1}{2} \mathbf{q}^T \left(\sum_{e=1}^N \mathbf{L}_e^T \mathbf{K}_e \mathbf{L}_e \right) \mathbf{q} \right\} dt + \int_{t_1}^{t_2} \delta \mathbf{q}^T \left(\sum_{e=1}^N \mathbf{L}_e^T \mathbf{p}_e \right) dt = 0 \quad (5.89)$$

We then define:

- the mass matrix of the assembled system, or *structural mass matrix*:

$$\mathbf{M} = \sum_{e=1}^N \mathbf{L}_e^T \mathbf{M}_e \mathbf{L}_e \quad (5.90)$$

- the *structural stiffness matrix*:

$$\mathbf{K} = \sum_{e=1}^N \mathbf{L}_e^T \mathbf{K}_e \mathbf{L}_e \quad (5.91)$$

- the *structural load vector*:

$$\mathbf{p} = \sum_{e=1}^N \mathbf{L}_e^T \mathbf{p}_e \quad (5.92)$$

³ With the notation adopted, the localization operators implicitly fix the degrees of freedom implied in the boundary conditions. The latter could also be kept in the assembly process and fixed later on.

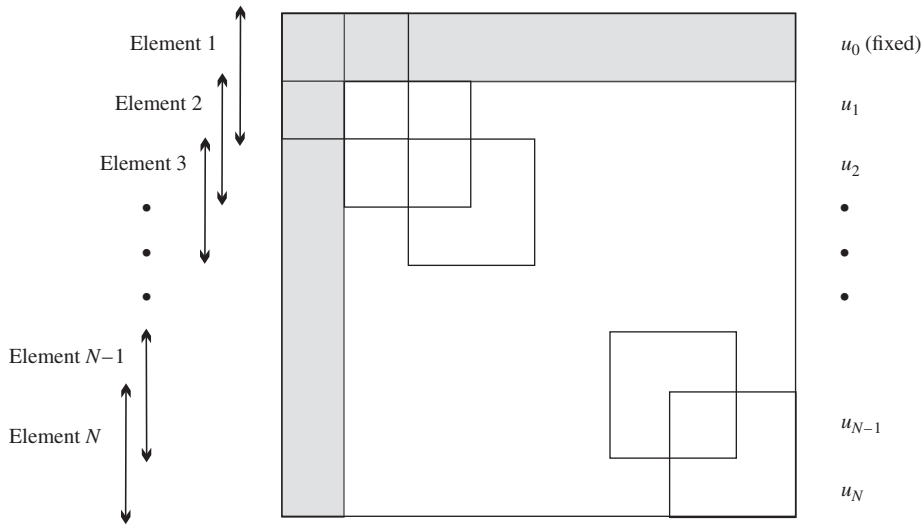


Figure 5.12 Assembly of structural matrices for the bar model.

It is important to note that expressions (5.90–5.92) simply correspond to a formal representation of the assembly operation. In practice, structural assembly may be performed much more simply by addressing correctly the matrices \mathbf{K}_e and \mathbf{M}_e in the structural matrices \mathbf{K} and \mathbf{M} (Figure 5.12).

The following observations can be made from the examination of Figure 5.12:

- The shaded zone corresponds to the clamped end of the bar and must therefore be wiped out. Removing the first column results from $u = 0$ whereas removing the first row means that the equilibrium equation associated to u_0 is not relevant when computing the motion of the system but can be used a posteriori to compute the reaction force associated to the essential boundary condition.
- The diagonal mass and stiffness terms add two by two on the diagonal of the structural matrix.
- Owing to the system topology (chain-type system or simply connected form) and the sequential numbering of the degrees of freedom, both \mathbf{K} and \mathbf{M} have tridiagonal form.

When all finite elements have the same length $\ell = \frac{L}{N}$, one obtains for the clamped–free bar:

$$\mathbf{K} = \frac{EA}{\ell} \begin{bmatrix} 2 & -1 & & & & \\ -1 & 2 & -1 & & & 0 \\ & -1 & 2 & \ddots & & \\ & & \ddots & \ddots & -1 & \\ 0 & & & -1 & 2 & -1 \\ & & & & -1 & 1 \end{bmatrix}$$

$$\mathbf{M} = m \frac{\ell}{6} \begin{bmatrix} 4 & 1 & & & \\ 1 & 4 & 1 & & \mathbf{0} \\ & 1 & 4 & \ddots & \\ & & \ddots & \ddots & 1 \\ \mathbf{0} & & & 1 & 4 & 1 \\ & & & & 1 & 2 \end{bmatrix} \quad (5.93)$$

For the structural load vector \mathbf{p} , the assembly operation (5.92) corresponds to the sum at each node of the contributions of the connecting elements. The internal forces between elements are eliminated by the assembly process (action-reaction): the forces applied externally are the only ones to remain in the structural load vector \mathbf{p} .

By taking the variation of the final discretized expression:

$$\delta \int_{t_1}^{t_2} \left(\frac{1}{2} \dot{\mathbf{q}}^T \mathbf{M} \dot{\mathbf{q}} - \frac{1}{2} \mathbf{q}^T \mathbf{K} \mathbf{q} \right) dt + \int_{t_1}^{t_2} \delta \mathbf{q}^T \mathbf{p} dt = 0$$

one obtains the discretized structural equations in the usual form:

$$\mathbf{K} \mathbf{q} + \mathbf{M} \ddot{\mathbf{q}} = \mathbf{p}(t) \quad (5.94)$$

Remark 5.3 *Worthwhile to be noticed is the double role played by the localization operator \mathbf{L}_e . On the one hand, Equation (5.87) expresses the fact that its kinematic role is to extract from the structural set \mathbf{q} the generalized displacements of the element \mathbf{q}_e . On the other hand, Equation (5.92) shows that the transposed operators \mathbf{L}_e^T play a static⁴ role as well since they allow to sum up the element forces \mathbf{p}_e to build the global force vector \mathbf{p} acting on the structure and cancel the contribution of the internal reaction forces. The operation \mathbf{L}_e^T can thus be interpreted as projecting the equation of motion of the individual elements into a space compatible with the constraints and thus plays the same role as $\frac{\partial U_{ik}}{\partial q_s}$ in the general virtual work principle 1.17.*

Remark 5.4 *The variational form (5.85) could not be directly exploited to compute the displacements \mathbf{q}_e of element e since the generalized loads \mathbf{p}_e contain the unknown reaction forces between element e and its neighbours. However, the equilibrium equation at element level that it provides:*

$$\mathbf{K}_e \mathbf{q}_e + \mathbf{M}_e \ddot{\mathbf{q}}_e = \mathbf{p}_e \quad (5.95)$$

can be used a posteriori: once the displacements and accelerations ($\mathbf{q}_e, \ddot{\mathbf{q}}_e$) have been determined from the solution of the global problem (5.94), the elementary nodal solutions extracted through (5.87) can be inserted in (5.95) to compute the forces \mathbf{p}_e acting on the element (including the internal forces) and the associated axial stress field.

⁴ Static in the sense that they allow expressing the contribution of element forces to global equilibrium, independently from the existence of inertia forces.

Closed form solution of the eigenvalue problem

Taking into account expressions (5.93) obtained for the matrices \mathbf{K} and \mathbf{M} , the dynamic equilibrium equation at node j is found to have the general form:

$$\frac{EA}{\ell}(-q_{j-1} + 2q_j - q_{j+1}) + m\frac{\ell}{6}(\ddot{u}_{j-1} + 4\ddot{u}_j + \ddot{u}_{j+1}) = p_j(t) \quad 0 < j < N \quad (5.96)$$

for the simple case of a uniform bar modelled by N elements of the same length. Its harmonic free vibration form is:

$$\frac{EA}{\ell}(q_{j-1} - 2q_j + q_{j+1}) + \omega^2 m\frac{\ell}{6}(q_{j-1} + 4q_j + q_{j+1}) = 0 \quad 0 < j < N \quad (5.97)$$

with, in the clamped-free case, the boundary conditions:

$$q_0 = 0 \quad (5.98)$$

$$\frac{EA}{\ell}(q_{N-1} - q_N) + \omega^2 m\frac{\ell}{6}(q_{N-1} + 2q_N) = 0 \quad (5.99)$$

Solving the system of Equations (5.97–5.99) proceeds in the same manner as in Section 4.3.1.

The substitution into (5.97) of a solution of the general form:

$$q_j = a \sin(j\mu + \phi) \quad 0 \leq j \leq N$$

yields the relationship:

$$\omega^2 = 6 \frac{EA}{m\ell^2} \frac{1 - \cos \mu}{2 + \cos \mu} \quad (5.100)$$

between the eigenvalue and the solution parameter μ . Applying the boundary condition (5.98) allows determination of the phase lag:

$$\phi = 0$$

while the substitution of the general solution form and the eigenvalue expression (5.100) into condition (5.99) yields the characteristic equation:

$$\sin(N-1)\mu - \sin N\mu + \frac{1 - \cos \mu}{2 + \cos \mu}(\sin(N-1)\mu + 2 \sin N\mu) = 0$$

and, after simplification,

$$\sin \mu \cos N\mu = 0$$

We obtain:

$$\mu = \frac{2r-1}{N} \frac{\pi}{2} \quad r = 1, 2, \dots$$

and the eigenfrequencies and associated mode shapes are given by:

$$\omega_r^2 = 6 \frac{EA}{m\ell^2} \frac{1 - \cos \left(\frac{2r-1}{N} \frac{\pi}{2} \right)}{2 + \cos \left(\frac{2r-1}{N} \frac{\pi}{2} \right)} \quad (5.101)$$

$$q_{j(r)} = a \sin \left(j \frac{2r-1}{N} \frac{\pi}{2} \right) \quad r, j = 1, \dots, N \quad (5.102)$$

The length of the clamped–free bar being L , the element length is $\ell = L/N$. By making a series expansion of:

$$\omega_r^2 = 6N^2 \frac{EA}{mL^2} \frac{1 - \cos\left(\frac{2r-1}{N} \frac{\pi}{2}\right)}{2 + \cos\left(\frac{2r-1}{N} \frac{\pi}{2}\right)}$$

one finds:

$$\omega_r^2 = \frac{EA}{mL^2} \left(\frac{(2r-1)\pi}{2} \right)^2 \left[1 + \frac{1}{12} \left(\frac{2r-1}{N} \frac{\pi}{2} \right)^2 + \dots \right]$$

or, for the corresponding frequency:

$$\omega_r = (2r-1) \frac{\pi}{2} \sqrt{\frac{EA}{mL^2}} \left[1 + \frac{1}{24} \left(\frac{2r-1}{N} \frac{\pi}{2} \right)^2 + \dots \right] \quad (5.103)$$

In this manner it has been verified that the solution (5.103) obtained by finite elements, as it results from an approximation of pure displacement type in the Rayleigh–Ritz sense, leads to an upper bound convergence to the exact eigenspectrum (4.134).

It is also worth noting that the solution developed in Section 4.3.1 may be interpreted as a finite element solution obtained with a lumped mass assumption: indeed, taking as elementary stiffness and mass matrices:

$$\mathbf{K}_e = \frac{EA}{\ell} \begin{bmatrix} 1 & -1 \\ -1 & 1 \end{bmatrix} \quad \mathbf{M}_e = m \frac{\ell}{2} \begin{bmatrix} 1 & 0 \\ 0 & 1 \end{bmatrix}$$

leads to the system of Equations (4.136) of Section 4.3.1 whose eigenfrequencies (Equation (4.146), page 247) are lower than the exact frequencies: in general mass lumping induces an overestimation of the inertia of the system.

This observation shows that using a *nonconsistent mass matrix* may lead to *the loss of the upper bound convergence property* of the computed eigenspectrum.

5.3.2 Truss frames

Let us consider the case of a structure made of bars, like the frame of Figure 5.13. The members are hinged at joints in such a way that they contribute to the global stiffness only through their extension stiffness. The structural mass and stiffness matrices are thus very easily constructed by using the bar element developed above, provided that *all elementary matrices describing individual members are expressed in a common axis system*.

Let us thus consider the case of an element making an angle α with the x axis (Figure 5.14). Passing from the local axial displacements u_i ($i = 1, 2$) to the structural displacements U_i, V_i is expressed by the transformation:

$$u_i = U_i \cos \alpha + V_i \sin \alpha \quad i = 1, 2 \quad (5.104)$$

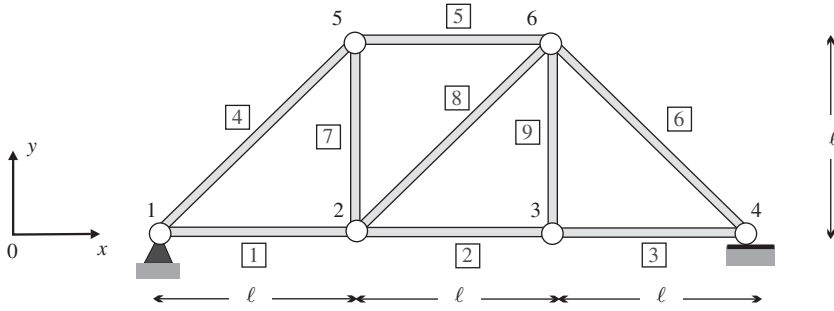


Figure 5.13 Truss frame structure.

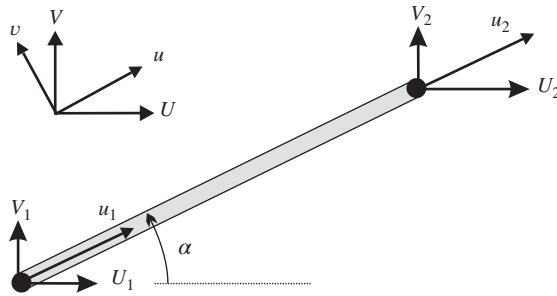


Figure 5.14 Bar element in arbitrary axes.

which gives rise to the matrix transformation:

$$\begin{bmatrix} u_1 \\ u_2 \end{bmatrix} = \begin{bmatrix} \cos \alpha & \sin \alpha & 0 & 0 \\ 0 & 0 & \cos \alpha & \sin \alpha \end{bmatrix} \begin{bmatrix} U_1 \\ V_1 \\ U_2 \\ V_2 \end{bmatrix} \quad (5.105)$$

or

$$\mathbf{q}_{eL} = \mathbf{R} \mathbf{q}_{eS} \quad (5.106)$$

where \mathbf{q}_{eL} and \mathbf{q}_{eS} represent respectively the element degrees of freedom in local and structural axes, and \mathbf{R} , the corresponding rotation operation.

Substituting (5.106) in the expression of the strain energy (5.79) of an element yields

$$\mathcal{V}_{int,e} = \frac{1}{2} \mathbf{q}_{eL}^T \mathbf{K}_{eL} \mathbf{q}_{eL} = \frac{1}{2} \mathbf{q}_{eS}^T \mathbf{K}_{eS} \mathbf{q}_{eS} \quad (5.107)$$

The transformation of the stiffness matrix is thus:

$$\mathbf{K}_{eS} = \mathbf{R}^T \mathbf{K}_{eL} \mathbf{R} \quad (5.108)$$

In order to compute the kinetic energy of a bar element in two-dimension, we have to observe that its expression (5.79) for the one-dimensional case must be modified since, unlike for the

strain energy, a transverse motion contributes to its kinetic energy:

$$\begin{aligned}\mathcal{T}_e &= \frac{1}{2} \int_0^\ell m(\dot{u}^2 + \dot{v}^2) dx \\ &= \frac{1}{2} \int_0^\ell m(\dot{U}^2 + \dot{V}^2) dx\end{aligned}\tag{5.109}$$

where we have used the fact that the norm of the velocity is independent of the axis system, resulting in the fact that the *elementary mass matrix is invariant under frame transformation*.

Explicitly, using the same linear shape functions for v and u as before, we obtain for the element of uniform properties:

$$\mathbf{K}_{eS} = \frac{EA}{\ell} \begin{bmatrix} \cos^2 \alpha & \cos \alpha \sin \alpha & \sin^2 \alpha & \text{Sym.} \\ \cos \alpha \sin \alpha & \cos^2 \alpha & \sin^2 \alpha & \\ \sin^2 \alpha & \sin \alpha \cos \alpha & \cos^2 \alpha & \\ \text{Sym.} & & & \end{bmatrix} \quad (5.110)$$

and

$$\mathbf{M}_{eS} = m \frac{\ell}{6} \begin{bmatrix} 2 & & & \text{Sym.} \\ 0 & 2 & & \\ 1 & 0 & 2 & \\ 0 & 1 & 0 & 2 \end{bmatrix} \quad (5.111)$$

The assembly process of the structural stiffness and mass matrices may then be organized as follows:

- (a) The structural degrees of freedom are identified (accounting for the boundary conditions) and are collected in the vector of structural displacements (see Figure 5.15)

$$\begin{aligned} \mathbf{q}^T &= [U_2 \quad V_2 \quad U_3 \quad V_3 \quad U_4 \quad U_5 \quad V_5 \quad U_6 \quad V_6] \\ &= [q_1 \quad q_2 \quad q_3 \quad q_4 \quad q_5 \quad q_6 \quad q_7 \quad q_8 \quad q_9] \end{aligned} \quad (5.112)$$

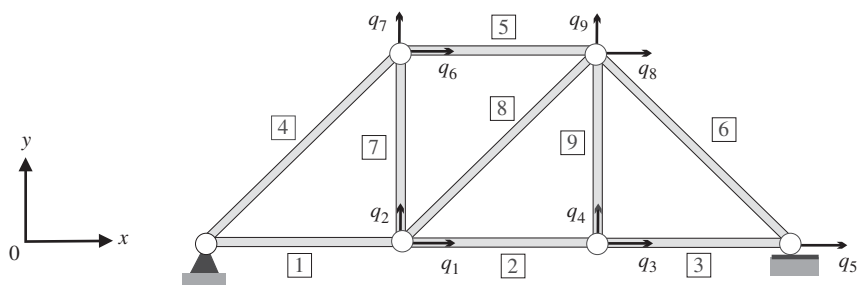


Figure 5.15 Truss frame degrees of freedom.

Table 5.3 Localization tables of the truss frame bar elements

Element	<i>local</i> table			
1	0	0	1	2
2	1	2	3	4
3	3	4	5	0
4	0	0	6	7
5	6	7	8	9
6	8	9	5	0
7	1	2	6	7
8	1	2	8	9
9	3	4	8	9

- (b) The *localization table* of each element is constructed by establishing the correspondence between elementary degrees of freedom and structural degrees of freedom:⁵

$$local(e,j) = \begin{cases} \text{position of degree of freedom} & q_{e,j} \\ \text{in structural vector} & \mathbf{q} \end{cases} \quad (5.113)$$

The same operation is done for each element while respecting the numbering of the degrees of freedom (Figure 5.15 and Table 5.3).

- (c) The elementary stiffness and mass matrices are constructed through application of (5.110) and (5.111). Owing to repetitions and symmetries, we have:
- for elements 1, 2, 3 and 5:

$$\mathbf{K}_{eS} = \frac{EA}{\ell} \begin{bmatrix} 1 & 0 & -1 & 0 \\ 0 & 0 & 0 & 0 \\ -1 & 0 & 1 & 0 \\ 0 & 0 & 0 & 0 \end{bmatrix} \quad \mathbf{M}_{eS} = m \frac{\ell}{6} \begin{bmatrix} 2 & 0 & 1 & 0 \\ 0 & 2 & 0 & 1 \\ 1 & 0 & 2 & 0 \\ 0 & 1 & 0 & 2 \end{bmatrix}$$

- for elements 7 and 9:

$$\mathbf{K}_{eS} = \frac{EA}{\ell} \begin{bmatrix} 0 & 0 & 0 & 0 \\ 0 & 1 & 0 & -1 \\ 0 & 0 & 0 & 0 \\ 0 & -1 & 0 & 1 \end{bmatrix} \quad \mathbf{M}_{eS} = m \frac{\ell}{6} \begin{bmatrix} 2 & 0 & 1 & 0 \\ 0 & 2 & 0 & 1 \\ 1 & 0 & 2 & 0 \\ 0 & 1 & 0 & 2 \end{bmatrix}$$

- for elements 4 and 8:

$$\mathbf{K}_{eS} = \frac{EA}{2\ell\sqrt{2}} \begin{bmatrix} 1 & 1 & -1 & -1 \\ 1 & 1 & -1 & -1 \\ -1 & -1 & 1 & 1 \\ -1 & -1 & 1 & 1 \end{bmatrix} \quad \mathbf{M}_{eS} = \frac{m\ell\sqrt{2}}{6} \begin{bmatrix} 2 & 0 & 1 & 0 \\ 0 & 2 & 0 & 1 \\ 1 & 0 & 2 & 0 \\ 0 & 1 & 0 & 2 \end{bmatrix}$$

⁵ In essence this table points to the nonzero terms in the localization operator \mathbf{L}_e defined earlier in (5.87) and is thus a more compact manner to describe the topology of the finite element model.

– for element 6:

$$K_{eS} = \frac{EA}{2\ell\sqrt{2}} \begin{bmatrix} 1 & -1 & -1 & 1 \\ -1 & 1 & 1 & -1 \\ -1 & 1 & 1 & -1 \\ 1 & -1 & -1 & 1 \end{bmatrix} \quad M_{eS} = \frac{m\ell\sqrt{2}}{6} \begin{bmatrix} 2 & 0 & 1 & 0 \\ 0 & 2 & 0 & 1 \\ 1 & 0 & 2 & 0 \\ 0 & 1 & 0 & 2 \end{bmatrix}$$

(d) The use of the localization operator obtained in step b allows assembly of the structural mass and stiffness matrices according to the following procedure (of C++ type):

```
Matrix K, M; int N;
for(int e=0; e<N ; ++e)           // loop over elements
{
    /* reading of localization vectors and elementary matrices */
    read_element(Matrix_el kel, Matrix_el mel, Vector locel);
    for( int i=0; i<4 ; ++i)       // loop over rows
    {
        for( int j=0; j<4 ; ++j)   // loop over columns
        {
            int ii = locel[i];      // localization of rows
            int jj = locel[j];      // localization of columns
            K[ii][jj] += kel[i][j]; // assembly of K
            M[ii][jj] += mel[i][j]; // assembly of M
        }
    }
}
```

As an exercise it can be verified that the following stiffness and mass matrices are obtained:

$$K_S = \frac{EA}{\ell} \begin{bmatrix} 2 + \frac{1}{2\sqrt{2}} & \frac{1}{2\sqrt{2}} & 1 + \frac{1}{2\sqrt{2}} & 0 & 2 & 0 & 0 & 0 & 0 & 0 & 0 & 0 & 0 & 0 & 0 & 0 \\ \frac{1}{2\sqrt{2}} & 1 + \frac{1}{2\sqrt{2}} & 0 & 0 & 0 & 0 & 0 & 0 & 0 & 0 & 0 & 0 & 0 & 0 & 0 & 0 \\ -1 & 0 & 2 & 0 & 0 & 0 & 0 & 0 & 0 & 0 & 0 & 0 & 0 & 0 & 0 & 0 \\ 0 & 0 & 0 & 1 & 0 & 0 & 0 & 0 & 0 & 0 & 0 & 0 & 0 & 0 & 0 & 0 \\ 0 & 0 & -1 & 0 & 1 + \frac{1}{2\sqrt{2}} & 0 & 0 & 0 & 0 & 0 & 0 & 0 & 0 & 0 & 0 & 0 \\ 0 & 0 & 0 & 0 & 0 & 1 + \frac{1}{2\sqrt{2}} & 0 & 0 & 0 & 0 & 0 & 0 & 0 & 0 & 0 & 0 \\ 0 & -1 & 0 & 0 & 0 & \frac{1}{2\sqrt{2}} & 1 + \frac{1}{2\sqrt{2}} & 0 & 0 & 0 & 0 & 0 & 0 & 0 & 0 & 0 \\ \frac{-1}{2\sqrt{2}} & \frac{-1}{2\sqrt{2}} & 0 & 0 & \frac{-1}{2\sqrt{2}} & -1 & 0 & 1 + \frac{1}{\sqrt{2}} & 0 & 0 & 0 & 0 & 0 & 0 & 0 & 0 \\ \frac{-1}{2\sqrt{2}} & \frac{-1}{2\sqrt{2}} & 0 & -1 & \frac{1}{2\sqrt{2}} & 0 & 0 & 0 & 1 + \frac{1}{\sqrt{2}} & 0 & 0 & 0 & 0 & 0 & 0 & 0 \\ \frac{1}{2\sqrt{2}} & \frac{1}{2\sqrt{2}} & 0 & 0 & \frac{1}{2\sqrt{2}} & 0 & 0 & 0 & 0 & 1 + \frac{1}{\sqrt{2}} & 0 & 0 & 0 & 0 & 0 & 0 \end{bmatrix}$$

$$M_S = \frac{m\ell}{6} \begin{bmatrix} 2(3 + \sqrt{2}) & 0 & 2(3 + \sqrt{2}) & 0 & 6 & 0 & 0 & 0 & 0 & 0 & 0 & 0 & 0 & 0 & 0 & 0 \\ 0 & 1 & 0 & 6 & 0 & 0 & 0 & 0 & 0 & 0 & 0 & 0 & 0 & 0 & 0 & 0 \\ 2(3 + \sqrt{2}) & 0 & 6 & 0 & 0 & 0 & 0 & 0 & 0 & 0 & 0 & 0 & 0 & 0 & 0 & 0 \\ 0 & 1 & 0 & 0 & 0 & 0 & 0 & 0 & 0 & 0 & 0 & 0 & 0 & 0 & 0 & 0 \\ 0 & 0 & 1 & 0 & 2(1 + \sqrt{2}) & 0 & 0 & 0 & 0 & 0 & 0 & 0 & 0 & 0 & 0 & 0 \\ 0 & 0 & 0 & 0 & 0 & 2(2 + \sqrt{2}) & 0 & 0 & 0 & 0 & 0 & 0 & 0 & 0 & 0 & 0 \\ 1 & 0 & 0 & 0 & 0 & 0 & 2(2 + \sqrt{2}) & 0 & 0 & 0 & 0 & 0 & 0 & 0 & 0 & 0 \\ 0 & 1 & 0 & 0 & 0 & 0 & 0 & 2(2 + \sqrt{2}) & 0 & 0 & 0 & 0 & 0 & 0 & 0 & 0 \\ \sqrt{2} & 0 & 1 & 0 & \sqrt{2} & 1 & 0 & 4(1 + \sqrt{2}) & 0 & 0 & 0 & 0 & 0 & 0 & 0 & 0 \\ 0 & \sqrt{2} & 0 & 1 & 0 & 0 & 1 & 0 & 4(1 + \sqrt{2}) & 0 & 0 & 0 & 0 & 0 & 0 & 0 \end{bmatrix}$$

Table 5.4 Eigenfrequencies of the truss frame structure by finite elements

r	$\frac{\omega_r}{2\pi} \sqrt{\frac{m\ell^2}{EA}}$
1	3.428×10^{-2}
2	5.810×10^{-2}
3	8.901×10^{-2}
4	12.15×10^{-2}
5	19.47×10^{-2}
6	23.42×10^{-2}
7	23.96×10^{-2}
8	24.67×10^{-2}
9	33.27×10^{-2}

(e) The solution of the resulting eigenvalue problem:

$$\mathbf{K}\mathbf{q} = \omega^2 \mathbf{M}\mathbf{q}$$

can only be performed numerically (see Chapter 6). It yields the nine eigenfrequencies given in Table 5.4. The first three eigenmodes are represented in Figure 5.16.

5.3.3 Beams in bending without shear deflection

Generation of a beam element (no prestress)

Consider the case of the beam in bending represented in Figure 5.17, possibly excited by a distributed load $\bar{p}(x, t)$.

Integration of the strain energy over the beam:

$$\mathcal{V}_{int} = \int_0^L EI \left(\frac{\partial^2 w}{\partial x^2} \right)^2 dx \quad (5.114)$$

implies that the function $w(x, t)$ and its first derivative are continuous (C_1 continuity). Therefore, to obtain a finite element approximation of pure displacement type in the Rayleigh–Ritz sense, the interpolation of the bending deflection must be at least cubic in order to maintain continuity of the deflection w and of the cross-section rotation (or slope) $\psi = \frac{\partial w}{\partial x}$ through nodal identification. The connectors of the element are the deflection and slope values at both ends (see Figure 5.18). In terms of the nondimensional variable $\xi = \frac{x}{\ell}$ over the element domain, the cubic approximation to the deflection may be written in the form:

$$\begin{aligned} w(\xi) &= w_1 \phi_1(\xi) + \psi_1 \phi_2(\xi) + w_2 \phi_3(\xi) + \psi_2 \phi_4(\xi) \\ &= \mathbf{\Phi}_e(\xi) \mathbf{q}_e(t) \end{aligned} \quad (5.115)$$

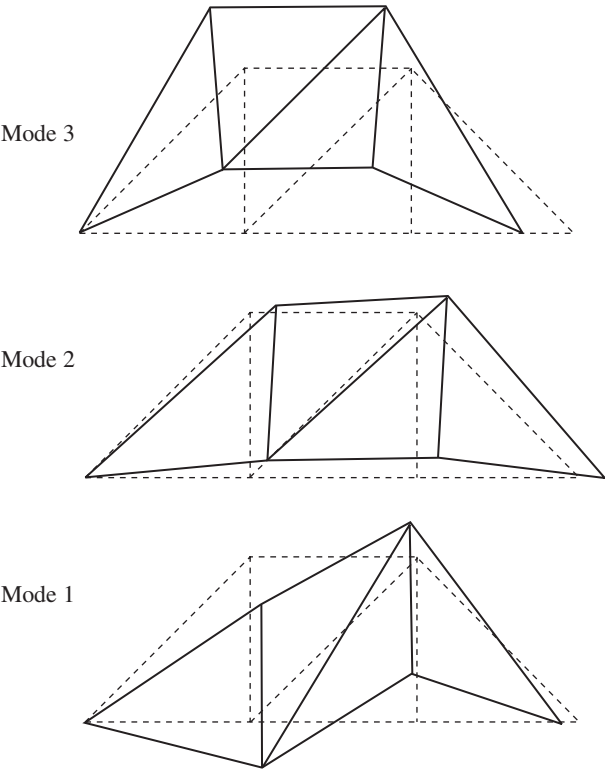


Figure 5.16 Eigenmodes of the truss frame structure.

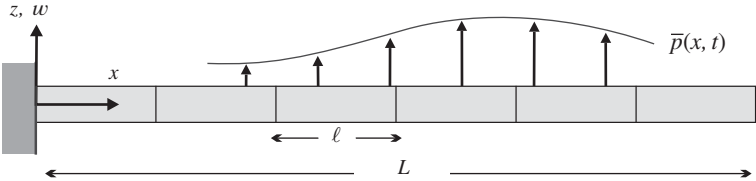


Figure 5.17 Beam in bending modelled by N finite elements.

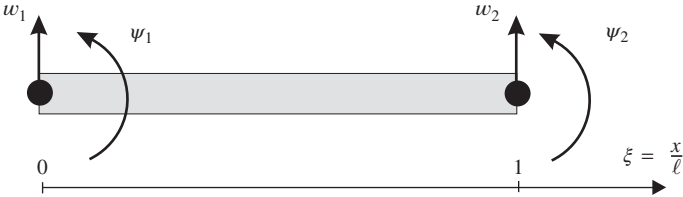


Figure 5.18 Connectors of the beam element in bending.

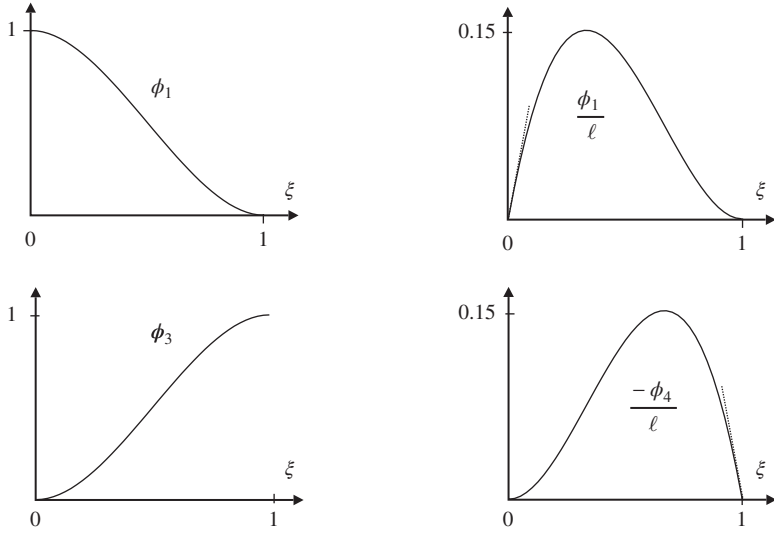


Figure 5.19 Shape functions: Hermitian polynomials of the third order.

where the shape functions $\phi_i(\xi)$, ($i = 1 \dots 4$) are the third-order *Hermitian polynomials*, matching the conditions (see Figure 5.19):

$$\begin{aligned}
 \phi_1(0) &= 1 & N'_1(0) &= 0 & \phi_1(1) &= N'_1(1) = 0 \\
 \phi_2(0) &= 0 & N'_2(0) &= \ell & \phi_2(1) &= N'_2(1) = 0 \\
 \phi_3(\xi) &= \phi_1(1 - \xi) \\
 \phi_4(\xi) &= -\phi_2(1 - \xi)
 \end{aligned} \tag{5.116}$$

Here we have used the notation N'_i for $\frac{dN_i}{d\xi}$. In this manner one obtains the matrix of shape functions:

$$\Phi_e^T(\xi) = \begin{bmatrix} 1 - 3\xi^2 + 2\xi^3 \\ \ell\xi(1 - \xi)^2 \\ \xi^2(3 - 2\xi) \\ \ell\xi^2(\xi - 1) \end{bmatrix} \tag{5.117}$$

associated with the element degrees of freedom:

$$\mathbf{q}_e^T = [w_1 \quad \psi_1 \quad w_2 \quad \psi_2] \tag{5.118}$$

Recalling the expressions (4.228) and (4.230) for the energy of a beam, one computes successively:

- the kinetic energy of the element (neglecting rotational energy as discussed for (4.243)):

$$\mathcal{T}_e = \frac{1}{2} \dot{\mathbf{q}}_e^T \mathbf{M}_e \dot{\mathbf{q}}_e \tag{5.119}$$

with the elementary mass matrix:

$$\mathbf{M}_e = \ell \int_0^1 m(\xi) \boldsymbol{\Phi}_e^T(\xi) \boldsymbol{\Phi}_e(\xi) d\xi \quad (5.120)$$

– the strain energy of the element:

$$\mathcal{V}_{int,e} = \frac{1}{2} \mathbf{q}_e^T \mathbf{K}_e \mathbf{q}_e \quad (5.121)$$

with the elementary stiffness matrix:

$$\mathbf{K}_e = \frac{1}{\ell^3} \int_0^1 EI(\xi) \left(\frac{d^2 \boldsymbol{\Phi}_e}{d\xi^2} \right)^T \left(\frac{d^2 \boldsymbol{\Phi}_e}{d\xi^2} \right) d\xi \quad (5.122)$$

– the virtual work of external loads:

$$\delta \mathcal{V}_{ext,e} = -\delta \mathbf{q}_e^T \mathbf{p}_e(t) \quad (5.123)$$

with the vector of external loads:

$$\mathbf{p}_e(t) = \ell \int_0^1 \boldsymbol{\Phi}_e^T(\xi) \bar{\mathbf{p}}(\xi, t) d\xi \quad (5.124)$$

Internal loads at the nodes of the elements are not included since they vanish during the assembly process as seen on page 379.

For an element of uniform characteristics excited by a constant distributed load $\bar{\mathbf{p}}_0$ we explicitly obtain:

$$\mathbf{K}_e = \frac{EI}{\ell^3} \begin{bmatrix} 12 & 6\ell & -12 & 6\ell \\ 6\ell & 4\ell^2 & -6\ell & 2\ell^2 \\ -12 & -6\ell & 12 & -6\ell \\ 6\ell & 2\ell^2 & -6\ell & 4\ell^2 \end{bmatrix} \quad (5.125)$$

$$\mathbf{M}_e = \frac{m\ell}{420} \begin{bmatrix} 156 & 22\ell & 54 & -13\ell^2 \\ 22\ell & 4\ell^2 & 13\ell & -3\ell^2 \\ 54 & 13\ell & 156 & -22\ell \\ -13\ell & -3\ell^2 & -22\ell & 4\ell^2 \end{bmatrix} \quad (5.126)$$

$$\mathbf{p}_e^T = \frac{\bar{\mathbf{p}}_0 \ell}{2} \begin{bmatrix} 1 & \frac{\ell}{6} & 1 & -\frac{\ell}{6} \end{bmatrix} \quad (5.127)$$

It is easily verified that the stiffness matrix has one translational rigid body mode:

$$\mathbf{u}_{(1)}^T = [1 \quad 0 \quad 1 \quad 0]$$

and one rotational rigid body mode (e.g. about the centre of mass):

$$\mathbf{u}_{(2)}^T = \left[1 \quad -\frac{\ell}{2} \quad 1 \quad \frac{\ell}{2} \right]$$

The quadratic forms $\mathbf{u}_{(1)}^T \mathbf{M} \mathbf{u}_{(1)}$ and $\mathbf{u}_{(2)}^T \mathbf{M} \mathbf{u}_{(2)}$ are then equal to the translation and rotatory inertias $m\ell$ and $\frac{m\ell^3}{12}$.

Remark 5.5 *In practice, the coefficients of Rayleigh–Ritz and finite element matrices are rarely integrated analytically as done in this chapter for simple structural components like bars and beams. They are rather computed through numerical quadrature. In one dimension, a quadrature formula to integrate function $f(\xi)$ over the interval $[-1, 1]$ is defined as*

$$\int_{-1}^1 f(\xi) d\xi = \sum_{l=1}^p f(\xi_l) W_l + R \simeq \sum_{l=1}^p g(\xi_l) \quad (5.128)$$

where p is the number of integration points, (ξ_l, W_l) are the coordinates of the integration points and their weight, and R is the remainder.

In one dimension, the Gauss quadrature formulas are optimal, accuracy of order $2p$ being achieved by p integration points. The first three Gauss integration rules are given in Table 5.5.

Table 5.5 Gaussian quadrature rules

p	ξ_l	W_l	R
1	0	2	$\frac{1}{3} \frac{d^2 f}{d\xi^2}(\bar{\xi})$
2	$-\frac{1}{\sqrt{3}}, \frac{1}{\sqrt{3}}$	1, 1	$\frac{1}{135} \frac{d^4 f}{d\xi^4}(\bar{\xi})$
3	$-\sqrt{\frac{3}{5}}, 0, \sqrt{\frac{3}{5}}$	$\frac{5}{9}, \frac{8}{9}, \frac{5}{9}$	$\frac{1}{15750} \frac{d^6 f}{d\xi^6}(\bar{\xi})$

$$\int_{-1}^1 f(\xi) d\xi = \sum_{l=1}^p f(\xi_l) W_l + R$$

The beam clamped at both ends

Because the number of degrees of freedom of a finite element model rapidly becomes too large to allow for explicit calculations, only a very limited number of examples can be treated if one does not make use of numerical solution methods. The beam clamped at both ends is one of the few cases well suited to calculation by hand: we will treat it successively with a two-element mesh and a three-element mesh to obtain quantitative information on the convergence of the method.

Two finite element model

After application of the boundary conditions, only two degrees of freedom are left in the model: displacement w_2 and slope ψ_2 at the centre of the beam (Figure 5.20). The localization vectors of these elements are:

$$\begin{aligned} \text{element 1:} & \quad [0 \quad 0 \quad 1 \quad 2] \\ \text{element 2:} & \quad [1 \quad 2 \quad 0 \quad 0] \end{aligned}$$

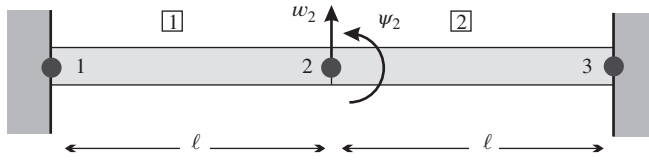


Figure 5.20 Modelling of the clamped–clamped beam using two finite elements.

giving the assembled mass and stiffness matrices:

$$\mathbf{K} = \frac{EI}{\ell^3} \begin{bmatrix} 24 & 0 \\ 0 & 8\ell^2 \end{bmatrix} \quad \mathbf{M} = \frac{m\ell}{420} \begin{bmatrix} 312 & 0 \\ 0 & 8\ell^2 \end{bmatrix} \quad (5.129)$$

It can be observed that, owing to symmetry, the eigensolutions contained in the model are directly uncoupled.

The solution of the eigenvalue problem yields:

$$\begin{aligned} \omega_1^2 &= 32.31 \frac{EI}{m\ell^4} & \omega_2^2 &= 420 \frac{EI}{m\ell^4} \\ \mathbf{q}_{(1)}^T &= [1 \quad 0] & \mathbf{q}_{(2)}^T &= [0 \quad 1] \end{aligned} \quad (5.130)$$

The first eigenmode is symmetric while the second one is antisymmetric. This approximate result may be compared to the exact closed-form solution (see Section 4.3.3) by making use of the total length $L = 2\ell$:

$$\begin{aligned} \omega_1^2 &= 516.92 \frac{EI}{mL^4} & \text{in place of } & 500.55 \frac{EI}{mL^4} \\ \omega_2^2 &= 6720.0 \frac{EI}{mL^4} & \text{in place of } & 3803.1 \frac{EI}{mL^4} \end{aligned} \quad (5.131)$$

It is thus observed that the two-element model restores with acceptable accuracy the first frequency, but that the approximation adopted is not able to represent the second eigenmode correctly.

Three finite element model

This time, four degrees of freedom are left in the structural model (Figure 5.21):

$$\mathbf{q}^T = [w_2 \quad \psi_2 \quad w_3 \quad \psi_3]$$

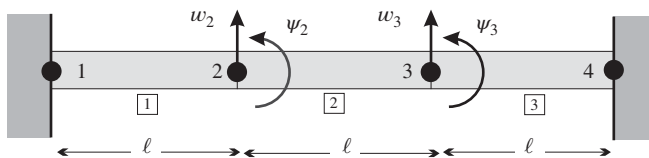


Figure 5.21 Modelling of the clamped–clamped beam using three finite elements.

and the three elements of the model have the localization vectors:

$$\begin{aligned}\text{element 1:} & \quad [0 \quad 0 \quad 1 \quad 2] \\ \text{element 2:} & \quad [1 \quad 2 \quad 3 \quad 4] \\ \text{element 3:} & \quad [3 \quad 4 \quad 0 \quad 0]\end{aligned}$$

giving the assembled stiffness and mass matrices:

$$\begin{aligned}\mathbf{K} &= \frac{EI}{\ell^3} \begin{bmatrix} 24 & 0 & -12 & 6\ell \\ 0 & 8\ell^2 & -6\ell & 2\ell^2 \\ -12 & -6\ell & 24 & 0 \\ 6\ell & 2\ell^2 & 0 & 8\ell^2 \end{bmatrix} \\ \mathbf{M} &= \frac{m\ell}{420} \begin{bmatrix} 312 & 0 & 54 & -13\ell \\ 0 & 8\ell^2 & 13\ell & -3\ell^2 \\ 54 & 13\ell & 312 & 0 \\ -13\ell & -3\ell^2 & 0 & 8\ell^2 \end{bmatrix}\end{aligned}\quad (5.132)$$

Although the resulting model has four degrees of freedom this time, it is still possible to compute its eigensolutions explicitly by taking advantage of symmetry of the system.

- *Symmetric modes*

The symmetric modes must satisfy the conditions:

$$w_3 = w_2 \quad \psi_3 = -\psi_2$$

and therefore by setting $\mathbf{y}^T = [w_2 \quad \psi_2]$ we can change the variables:

$$\mathbf{q} = \mathbf{C}\mathbf{y}$$

with the matrix of constraints:

$$\mathbf{C}^T = \begin{bmatrix} 1 & 0 & 1 & 0 \\ 0 & 1 & 0 & -1 \end{bmatrix}$$

We transform the eigenvalue problem into a problem of dimension 2×2 :

$$\mathbf{K}^*\mathbf{y} = \omega^2 \mathbf{M}^*\mathbf{y}$$

with $\mathbf{K}^* = \mathbf{C}^T \mathbf{K} \mathbf{C}$ and $\mathbf{M}^* = \mathbf{C}^T \mathbf{M} \mathbf{C}$. The reduced matrices are:

$$\mathbf{K}^* = \frac{EI}{\ell^3} \begin{bmatrix} 24 & -12\ell \\ -12\ell & 12\ell^2 \end{bmatrix} \quad \mathbf{M}^* = m \frac{\ell}{210} \begin{bmatrix} 366 & 13\ell \\ 13\ell & 11\ell^2 \end{bmatrix}\quad (5.133)$$

By setting $\lambda = \frac{\omega^2 m \ell^4}{210 EI}$ we then obtain the eigenvalue problem:

$$\begin{bmatrix} 24 - 366\lambda & -12\ell - 13\ell\lambda \\ -12\ell - 13\ell\lambda & 12\ell^2 - 11\ell^2\lambda \end{bmatrix} \begin{bmatrix} w_2 \\ \psi_2 \end{bmatrix} = \mathbf{0}$$

and its characteristic equation:

$$3857\lambda^2 - 4968\lambda + 144 = 0$$

The solutions are $\lambda = 0.02967$ and $\lambda = 1.2584$; they correspond to the first and third modes of the complete system, giving the approximate eigenvalues:

$$\omega_1^2 = 6.2305 \frac{EI}{m\ell^4} \quad \omega_3^2 = 264.26 \frac{EI}{m\ell^4}$$

or, in terms of the total beam length $L = 3\ell$:

$$\omega_1^2 = 504.67 \frac{EI}{mL^4} \quad \omega_3^2 = 21\,405 \frac{EI}{mL^4} \quad (5.134)$$

The associated eigenmodes are:

$$\begin{aligned} \mathbf{q}_{(1)}^T &= \begin{bmatrix} 1 & \frac{1.061}{\ell} & 1 & \frac{-1.061}{\ell} \end{bmatrix} \\ \mathbf{q}_{(3)}^T &= \begin{bmatrix} 1 & \frac{-15.39}{\ell} & 1 & \frac{15.39}{\ell} \end{bmatrix} \end{aligned} \quad (5.135)$$

- *Antisymmetric eigenmodes*

Similarly, the antisymmetric modes obey:

$$w_3 = -w_2 \quad \psi_3 = \psi_2$$

The matrix of constraints is thus:

$$\mathbf{C}^T = \begin{bmatrix} 1 & 0 & -1 & 0 \\ 0 & 1 & 0 & 1 \end{bmatrix}$$

and yields the reduced stiffness and mass matrices:

$$\mathbf{K}^* = \frac{EI}{\ell^3} \begin{bmatrix} 72 & 12\ell \\ 12\ell & 20\ell^2 \end{bmatrix} \quad \mathbf{M}^* = m \frac{\ell}{210} \begin{bmatrix} 258 & -13\ell \\ -13\ell & 5\ell^2 \end{bmatrix} \quad (5.136)$$

By setting also $\lambda = \frac{\omega^2 m \ell^4}{210EI}$, we obtain the eigenvalue problem:

$$\begin{bmatrix} 72 - 258\lambda & 12\ell + 13\ell\lambda \\ 12\ell + 13\ell\lambda & 20\ell^2 - 5\ell^2\lambda \end{bmatrix} \begin{bmatrix} w_2 \\ \psi_2 \end{bmatrix} = \mathbf{0}$$

and the characteristic equation:

$$1121\lambda^2 - 5832\lambda + 1296 = 0$$

with the roots $\lambda = 0.2326$ and $\lambda = 4.9699$, which correspond to eigenmodes 2 and 4 of the complete system. The eigenvalues are:

$$\omega_2^2 = 3\,956.9 \frac{EI}{mL^4} \quad \omega_4^2 = 84\,537 \frac{EI}{mL^4} \quad (5.137)$$

The eigenmode associated with eigenvalue ω_2^2 is:

$$\mathbf{q}_{(2)}^T = \begin{bmatrix} 1 & \frac{-0.798}{\ell} & -1 & \frac{-0.798}{\ell} \end{bmatrix} \quad (5.138)$$

Gathering the results, the numerical values are compared to the exact ones in Table 5.6. It can be observed that the number of nearly converged eigenvalues is equal to half the number of degrees of freedom in the model: it results from the aptitude of the model to represent the corresponding mode shape correctly. It can also be observed that all approximations obtained are

Table 5.6 Beam clamped at both ends: eigenvalues computed by finite elements

r	2 elements	3 elements	Exact
1	516.92	504.67	500.55
2	6 720.0	3 956.9	3 803.1
3	–	21 405.0	14 620.0
4	–	84 537.0	39 944.0

$$\omega_r^2 \frac{mL^4}{EI}$$

upper bounds to the exact ones, a property resulting from the conformity of the displacement field used to construct the finite element model.

Including the prestress effect

When an initial axial load N_0 is present in the beam a strain energy term of geometric origin needs to be considered, as found in (4.253):

$$\mathcal{V}_{g,e} = \frac{1}{2} \int_0^\ell N_0 \left(\frac{\partial w}{\partial x} \right)^2 dx$$

It will be computed for the representation of the solution through the shape functions. Noting that:

$$\frac{\partial w}{\partial x} = \frac{1}{\ell} \frac{d\Phi_e}{d\xi} \mathbf{q}_e, \quad (5.139)$$

it may be expressed in the quadratic form

$$\mathcal{V}_{g,e} = \frac{1}{2} \mathbf{q}_e^T \mathbf{K}_{g,e} \mathbf{q}_e \quad (5.140)$$

where $\mathbf{K}_{g,e}$ is the geometric stiffness matrix of the beam element

$$\mathbf{K}_{g,e} = \frac{1}{\ell} \int_0^1 N_0 \left(\frac{d\Phi_e}{d\xi} \right)^T \left(\frac{d\Phi_e}{d\xi} \right) d\xi \quad (5.141)$$

By noting that the shape function derivatives may be expressed as:

$$\left(\frac{d\Phi_e}{d\xi} \right)^T = \begin{bmatrix} 6\xi(\xi-1) \\ \ell(1-4\xi+3\xi^2) \\ 6\xi(1-\xi) \\ \ell(3\xi^2-2\xi) \end{bmatrix}$$

we obtain for a constant axial load N_0 :

$$\mathbf{K}_{g,e} = \frac{N_0}{30\ell} \begin{bmatrix} 36 & 3\ell & -36 & 3\ell \\ 3\ell & 4\ell^2 & -3\ell & -\ell^2 \\ -36 & -3\ell & 36 & -3\ell \\ 3\ell & -\ell^2 & -3\ell & 4\ell^2 \end{bmatrix} \quad (5.142)$$

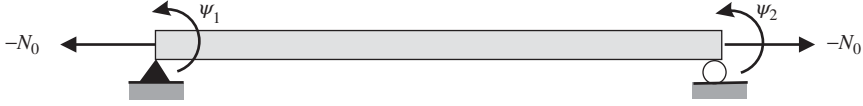


Figure 5.22 Modelling of the prestressed simply supported beam using one finite element.

Taking into account the prestress effect leads to the generalization of the discretized expression of Hamilton's principle in the form:

$$\delta \int_{t_1}^{t_2} \left(\frac{1}{2} \dot{\mathbf{q}}^T \mathbf{M} \dot{\mathbf{q}} - \frac{1}{2} \mathbf{q}^T (\mathbf{K} + \mathbf{K}_g) \mathbf{q} \right) dt = - \int_{t_1}^{t_2} \delta \mathbf{q}^T \mathbf{p} dt$$

which gives the discretized structural equations:

$$(\mathbf{K} + \mathbf{K}_g) \mathbf{q} + \mathbf{M} \ddot{\mathbf{q}} = \mathbf{p}(t) \quad (5.143)$$

in which the geometric stiffness contribution is simply added to the linear stiffness.

The prestressed simply supported beam

For comparison, let us consider again the case of the simply supported beam for which an exact solution exists in the prestressed case (Section 4.3.3). It is possible, in a first approximation, to model the system using a single finite element (Figure 5.22). The assembled structural matrices are:

$$\mathbf{K} = \frac{EI}{\ell} \begin{bmatrix} 4 & 2 \\ 2 & 4 \end{bmatrix} \quad \mathbf{M} = \frac{m\ell^3}{420} \begin{bmatrix} 4 & -3 \\ -3 & 4 \end{bmatrix} \quad \mathbf{K}_g = \frac{N_0\ell}{30} \begin{bmatrix} 4 & -1 \\ -1 & 4 \end{bmatrix} \quad (5.144)$$

and the eigenvalue problem is:

$$\begin{bmatrix} 4 \left(\frac{EI}{\ell} - \frac{\omega^2 m \ell^3}{420} + \frac{N_0 \ell}{30} \right) & \left(2 \frac{EI}{\ell} + \frac{3\omega^2 m \ell^3}{420} - \frac{N_0 \ell}{30} \right) \\ \left(2 \frac{EI}{\ell} + \frac{3\omega^2 m \ell^3}{420} - \frac{N_0 \ell}{30} \right) & 4 \left(\frac{EI}{\ell} - \frac{\omega^2 m \ell^3}{420} + \frac{N_0 \ell}{30} \right) \end{bmatrix} \begin{bmatrix} \psi_1 \\ \psi_2 \end{bmatrix} = \mathbf{0} \quad (5.145)$$

With the assumption of eigenmode symmetry ($\psi_2 = -\psi_1$), the approximate expression of the first eigenfrequency is directly obtained:

$$\omega_1^2 = 120 \frac{EI}{m\ell^4} \left[1 + \frac{N_0 \ell^2}{12EI} \right] \quad (5.146)$$

in place of the exact value:

$$\omega_1^2 = 97.41 \frac{EI}{m\ell^4} \left[1 + \frac{N_0 \ell^2}{9.87EI} \right]$$

Remark 5.6 The first eigenvalue becomes zero when the buckling load is reached. Since for conforming finite elements (and, more generally, the Rayleigh–Ritz method) eigenfrequencies are upper bounds to the physical model such an analysis results in overestimating the critical load. The results must thus be apprehended with care and convergence of the solution must be thoroughly checked.

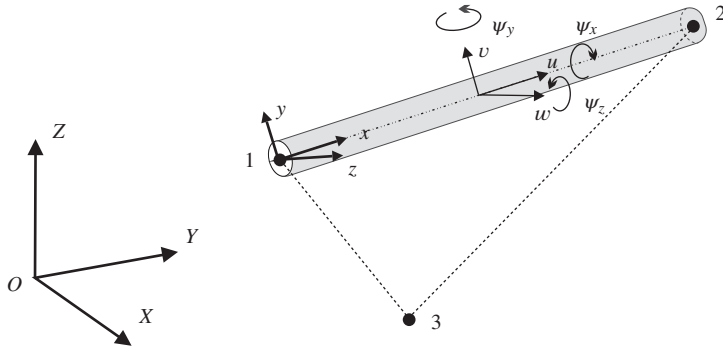


Figure 5.23 Three-dimensional beam element.

5.3.4 Three-dimensional beam element without shear deflection

Element generation

Real engineering construction are made of several beams assembled in a three-dimensional portal structure. To model such systems with finite elements, the beam behaviour has to be described with arbitrary orientation in space when it is subjected to combined loading (bending in two orthogonal directions, extension and torsion). Such general behaviour may be modelled as follows.

Let $OXYZ$ be a structural axis frame and $O'xyz$ be a local frame attached to the beam element (Figure 5.23). Let us make the following assumptions:

1. Axis $O'x$ is the beam neutral axis, chosen in such a way that a bending moment does not produce any axial deformation. Conversely, an axial load induces only axial deformation.
2. Axes $O'y$ and $O'z$ are the principal inertia axes for bending, defined in such a way that a bending moment about $O'y$ produces no bending about $O'z$, and conversely.

In the context of the kinematic Bernoulli assumptions for beams with no shear deflection, let us express the strain energy of the beam element (with no prestress) in the form:

$$\mathcal{V}_{int,e} = \frac{1}{2} \int_0^\ell \left[EI_z \left(\frac{\partial^2 v}{\partial x^2} \right)^2 + EI_y \left(\frac{\partial^2 w}{\partial x^2} \right)^2 + EA \left(\frac{\partial u}{\partial x} \right)^2 + GJ_x \left(\frac{\partial \psi_x}{\partial x} \right)^2 \right] dx \quad (5.147)$$

where

- The first term represents the bending energy in plane $O'xy$. It is computed in terms of the displacement field $v(x)$ and of the bending stiffness about the local axis $O'z$:

$$EI_z = \int_A E(y, z) y^2 dA$$

- The second term represents the bending energy in plane $O'xz$. It is computed in terms of the displacement field $w(x)$ and of the bending stiffness about the local axis $O'y$:

$$EI_y = \int_A E(y, z) z^2 dA$$

- The third term represents the extension energy of the beam. It is computed in terms of the axial displacement $u(x)$ and of the axial stiffness:

$$EA = \int_A E(y, z) dA$$

- The fourth term represents the torsional deformation energy of the beam. It is computed in terms of the local rotation ψ_x and the torsional stiffness GJ_x , the latter being evaluated following the classical techniques used in strength of materials with the assumption of free cross-sectional warping.

The elementary stiffness matrix is computed in terms of the element degrees of freedom expressed in local axes:

$$\mathbf{q}_{eL}^T = [u_1 \quad v_1 \quad w_1 \quad \psi_{x_1} \quad \psi_{y_1} \quad \psi_{z_1} \quad u_2 \quad v_2 \quad w_2 \quad \psi_{x_2} \quad \psi_{y_2} \quad \psi_{z_2}] \quad (5.148)$$

noting that the rotations ψ_y and ψ_z are linked to deflections by:

$$\psi_z = \frac{\partial v}{\partial x} \quad \psi_y = -\frac{\partial w}{\partial x} \quad (5.149)$$

For the torsion term, we assume linear variation of the torsion angle: it thus takes the same form as the extension term.

Considering the strain energy (5.147) and using the shape functions introduced in Section 5.3.1 for the axial and torsional behaviour and those discussed in Section 5.3.3 for the bending behaviour, the discretized strain energy of the beam element may be expressed in the form:

$$\mathcal{V}_{int,e} = \frac{1}{2} \mathbf{q}_{eL}^T \mathbf{K}_{eL} \mathbf{q}_{eL} \quad (5.150)$$

where the elementary stiffness matrix in local axes is given by

$$\mathbf{K}_{eL} = \begin{bmatrix} \frac{EA}{\ell} & 0 & 0 & 0 & 0 & 0 & -\frac{EA}{\ell} & 0 & 0 & 0 & 0 & 0 \\ 0 & \frac{12EI_z}{\ell^3} & 0 & 0 & 0 & 0 & 0 & \frac{12EI_z}{\ell^3} & 0 & 0 & 0 & 0 \\ 0 & 0 & \frac{12EI_y}{\ell^3} & 0 & 0 & 0 & 0 & 0 & \frac{12EI_y}{\ell^3} & 0 & 0 & 0 \\ 0 & 0 & 0 & \frac{GJ_x}{\ell} & 0 & 0 & 0 & 0 & 0 & \frac{GJ_x}{\ell} & 0 & 0 \\ 0 & 0 & -\frac{6EI_y}{\ell^2} & 0 & \frac{4EI_y}{\ell} & 0 & 0 & 0 & 0 & 0 & \frac{4EI_y}{\ell} & 0 \\ 0 & \frac{6EI_z}{\ell^2} & 0 & 0 & 0 & \frac{4EI_z}{\ell} & 0 & 0 & 0 & 0 & 0 & \frac{4EI_z}{\ell} \\ -\frac{EA}{\ell} & 0 & 0 & 0 & 0 & 0 & \frac{EA}{\ell} & 0 & 0 & 0 & 0 & 0 \\ 0 & -\frac{12EI_z}{\ell^3} & 0 & 0 & 0 & -\frac{6EI_z}{\ell^2} & 0 & \frac{12EI_z}{\ell^3} & 0 & 0 & 0 & 0 \\ 0 & 0 & -\frac{12EI_y}{\ell^3} & 0 & \frac{6EI_y}{\ell^2} & 0 & 0 & 0 & \frac{12EI_y}{\ell^3} & 0 & 0 & 0 \\ 0 & 0 & 0 & -\frac{GJ_x}{\ell} & 0 & 0 & 0 & 0 & 0 & \frac{GJ_x}{\ell} & 0 & 0 \\ 0 & 0 & -\frac{6EI_y}{\ell^2} & 0 & \frac{2EI_y}{\ell} & 0 & 0 & 0 & \frac{6EI_y}{\ell^2} & 0 & 0 & \frac{4EI_y}{\ell} \\ 0 & \frac{6EI_z}{\ell^2} & 0 & 0 & 0 & \frac{2EI_z}{\ell} & 0 & -\frac{6EI_z}{\ell^2} & 0 & 0 & 0 & \frac{4EI_z}{\ell} \end{bmatrix} \quad \text{Sym.} \quad (5.151)$$

2. Directions \vec{e}_y and \vec{e}_z corresponding to the principal axes of the cross-section are constructed from the knowledge of a third point $P_3 = (X_3, Y_3, Z_3)$ contained in the plane Oxz . Noting:

$$\vec{d}_i = [X_i - X_1 \quad Y_i - Y_1 \quad Z_i - Z_1]$$

direction \vec{e}_y is obtained from the vector operation:

$$\vec{e}_y = \frac{\vec{d}_3 \times \vec{d}_2}{\|\vec{d}_3 \times \vec{d}_2\|} \quad (5.156)$$

3. Direction \vec{e}_z results from the cross product:

$$\vec{e}_z = \vec{e}_x \times \vec{e}_y \quad (5.157)$$

4. The rotation operator \mathbf{R}_e describing the frame transformation:

$$\begin{bmatrix} x_i \\ y_i \\ z_i \end{bmatrix} = \mathbf{R}_e \begin{bmatrix} X_i \\ Y_i \\ Z_i \end{bmatrix} \quad i = 1, 2 \quad (5.158)$$

is next constructed in terms of dot products of the base vectors:

$$\mathbf{R}_e = \begin{bmatrix} \vec{e}_X \cdot \vec{e}_x & \vec{e}_Y \cdot \vec{e}_x & \vec{e}_Z \cdot \vec{e}_x \\ \vec{e}_X \cdot \vec{e}_y & \vec{e}_Y \cdot \vec{e}_y & \vec{e}_Z \cdot \vec{e}_y \\ \vec{e}_X \cdot \vec{e}_z & \vec{e}_Y \cdot \vec{e}_z & \vec{e}_Z \cdot \vec{e}_z \end{bmatrix} \quad (5.159)$$

5. Displacements and rotations in local and in structural axes are linked respectively by:

$$\begin{bmatrix} u_i \\ v_i \\ w_i \end{bmatrix} = \mathbf{R}_e \begin{bmatrix} U_i \\ V_i \\ W_i \end{bmatrix} \quad \begin{bmatrix} \psi_{xi} \\ \psi_{yi} \\ \psi_{zi} \end{bmatrix} = \mathbf{R}_e \begin{bmatrix} \psi_{Xi} \\ \psi_{Yi} \\ \psi_{Zi} \end{bmatrix} \quad i = 1, 2 \quad (5.160)$$

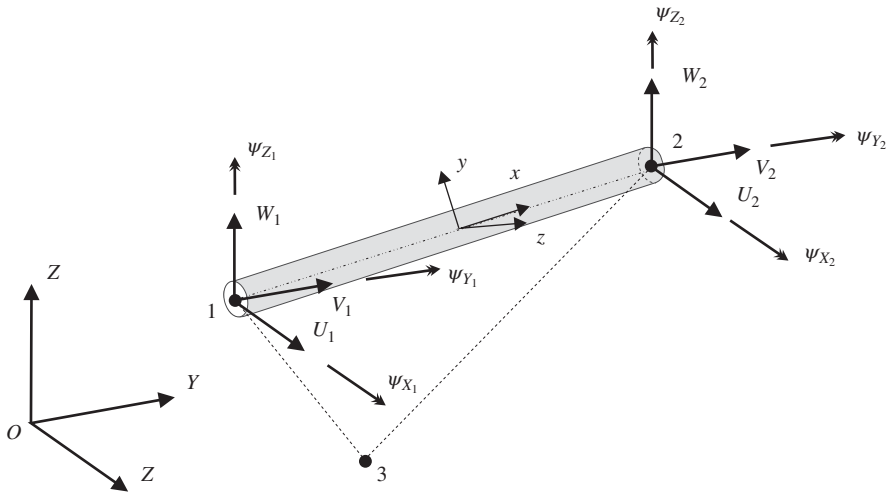


Figure 5.24 Three-dimensional beam element in arbitrary axes.

from which we deduce the transformation to structural degrees of freedom for the element:

$$\mathbf{q}_{eS}^T = [U_1 \quad V_1 \quad W_1 \quad \psi_{X_1} \quad \psi_{Y_1} \quad \psi_{Z_1} \quad U_2 \quad V_2 \quad W_2 \quad \psi_{X_2} \quad \psi_{Y_2} \quad \psi_{Z_2}]$$

$$\mathbf{q}_{eL} = \mathbf{T}_e \mathbf{q}_{eS} \quad (5.161)$$

with:

$$\mathbf{T}_e = \begin{bmatrix} \mathbf{R}_e & 0 & 0 & 0 \\ 0 & \mathbf{R}_e & 0 & 0 \\ 0 & 0 & \mathbf{R}_e & 0 \\ 0 & 0 & 0 & \mathbf{R}_e \end{bmatrix} \quad (5.162)$$

The resulting stiffness and mass matrices of the element expressed in structural axes are:

$$\mathbf{K}_{eS} = \mathbf{T}_e^T \mathbf{K}_{eL} \mathbf{T}_e \quad \mathbf{M}_{eS} = \mathbf{T}_e^T \mathbf{M}_{eL} \mathbf{T}_e \quad (5.163)$$

Example 5.3

Let us consider the three-dimensional portal frame of Figure 5.25, composed of beams with the following characteristics:

– Properties of vertical beams:

$$\begin{aligned} A &= 5.14 \cdot 10^{-3} \text{ m}^2 & J_x &= 1.73 \cdot 10^{-7} \text{ m}^4 \\ I_y &= 6.90 \cdot 10^{-6} \text{ m}^4 & I_z &= 8.49 \cdot 10^{-5} \text{ m}^4 \end{aligned}$$

– Properties of horizontal beams:

$$\begin{aligned} A &= 5.68 \cdot 10^{-3} \text{ m}^2 & J_x &= 1.76 \cdot 10^{-7} \text{ m}^4 \\ I_y &= 1.20 \cdot 10^{-4} \text{ m}^4 & I_z &= 7.30 \cdot 10^{-6} \text{ m}^4 \end{aligned}$$

The material is steel:

$$E = 2.1 \cdot 10^{11} \text{ N/m}^2 \quad \nu = 0.3 \quad \rho = 7.8 \cdot 10^3 \text{ kg/m}^3$$

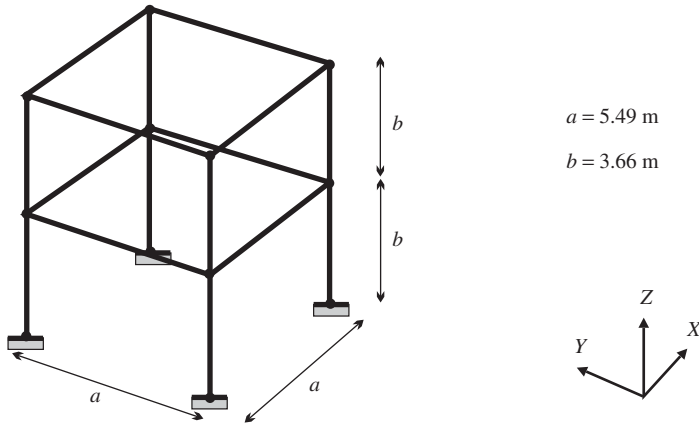


Figure 5.25 Three-dimensional portal frame.

The column bases are clamped to the ground and the local axes are defined as follows:

- Vertical beams:

$$\vec{e}_x = \vec{e}_Z \quad \vec{e}_y = \vec{e}_X \quad \vec{e}_z = \vec{e}_Y$$

- Horizontal beams parallel to OX:

$$\vec{e}_x = \vec{e}_X \quad \vec{e}_y = \vec{e}_Y \quad \vec{e}_z = \vec{e}_Z$$

- Horizontal beams parallel to OY:

$$\vec{e}_x = \vec{e}_Y \quad \vec{e}_y = -\vec{e}_X \quad \vec{e}_z = \vec{e}_Z$$

Let us model the structure with 16 3-D beam elements of the type developed above. Each mesh intersection being a node, the model has 12 nodes and 72 degrees of freedom, 24 of them being fixed. This example is representative of the preliminary design models that are often used in Civil Engineering to assess the overall dynamic properties of a building under project.

The eigenfrequencies and mode shapes are then computed numerically (Samcef 1992) and the results are presented on Figure 5.26.

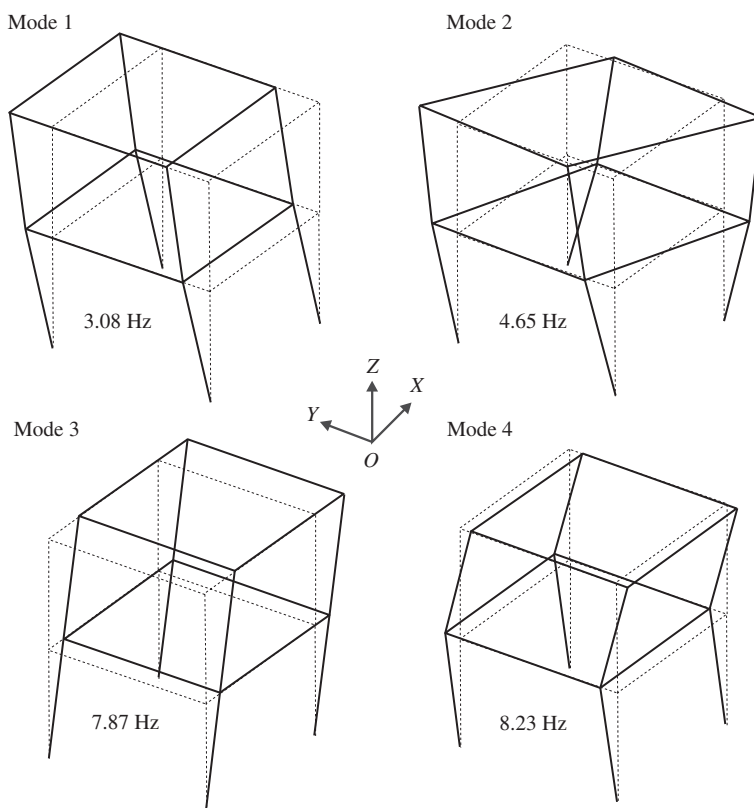


Figure 5.26 Mode shapes and eigenfrequencies of the portal frame.

It is observed that modes 1 and 3 are the first bending modes in the planes OYZ and OXZ respectively. Mode 2 is the first torsion mode, and mode 4 is the second bending mode in plane OY Z. The mode shapes being drawn without considering the nodal rotations but adopting a simple linear interpolation of the displacements between nodes, the C_1 continuity of the bending deflection is lost in the graphical representation.

5.3.5 Beams in bending with shear deformation

Preliminary remarks

It has been shown in Section 4.3.4 that, when taking into account the shear deformation, the rotation of cross-sections ψ and the beam deflection w become two independent fields. Therefore in the displacement approach, the most natural solution would be to adopt a linear interpolation for both fields in the form:

$$w(x) = w_1(1 - \frac{x}{\ell}) + w_2 \frac{x}{\ell} \quad \psi(x) = \psi_1(1 - \frac{x}{\ell}) + \psi_2 \frac{x}{\ell} \quad (5.164)$$

so that continuity of both deflection and slope are insured, and compute the shear strain as:

$$\beta = \gamma_{xz} = \frac{\partial w}{\partial x} - \psi \quad (5.165)$$

However the quality of such interpolation is poor, since it leads to a constant interpolation of the slope $\frac{\partial w}{\partial x}$ over the element. Moreover, locking will appear in the integration of the shear strain energy due to the fact that the shear strain (5.165) is computed from the difference of two fields with different polynomial orders (Hughes 1987).

The possible solutions to increase the quality of the beam model with shear are:

- to increase the degree of the polynomial interpolation by adding internal degrees of freedom;
- to start from the linear interpolation (5.164) and improve the resulting model through artificial manipulations such as reduced integration or residual flexibility correction (see for example (Géradin and Cardona 2001, Hughes 1987);
- to depart from the pure displacement approach in order to build a more efficient finite model. As it will be seen hereafter, starting from force and moment fields that satisfy a priori equilibrium in a beam element allows building a model with a statically exact stiffness matrix (Dhatt and Batoz 1990). In which case, the model has to be complemented with a mass matrix which is not consistent in the variational sense.

This last approach, which provides an example of *statically admissible* elements, will be described in the remainder of the section.

Variational expression for static response under end loads

Let us restrict the variational description to the case of static response under concentrated end loads. By referring to Section 4.3.4 we get:

$$\delta(\mathcal{V}_{int} + \mathcal{V}_{ext}) = 0 \quad (5.166)$$

with the following expressions of strain and external potential energies

$$\mathcal{V}_{int} = \frac{1}{2} \int_0^\ell \left\{ EI \left(\frac{\partial \psi}{\partial x} \right)^2 + k' AG \left(-\psi + \frac{\partial w}{\partial x} \right)^2 \right\} dx \quad (5.167)$$

$$\mathcal{V}_{ext} = -\bar{T}(0)w(0) - \bar{T}(\ell)w(\ell) - \bar{M}(0)\psi(0) - \bar{M}(\ell)\psi(\ell) \quad (5.168)$$

In order to weaken the kinematic conditions (5.165–5.170) let us enforce them explicitly using Lagrangian multipliers λ_M and λ_T by introducing the dislocation potential:

$$\mathcal{V}_d = \int_0^\ell \left\{ \lambda_M \left(\frac{\partial \psi}{\partial x} - \kappa \right) + \lambda_T \left(\frac{\partial w}{\partial x} - \psi - \beta \right) \right\} dx \quad (5.169)$$

where β (Equation (5.165) and

$$\kappa = \frac{\partial \psi}{\partial x} \quad (5.170)$$

are new variables having respectively the meanings of shear angle and curvature. We get the extended variational expression:

$$\delta(\mathcal{V}_{int} + \mathcal{V}_{ext} + \mathcal{V}_d) = 0 \quad (5.171)$$

where (5.167) now reads:

$$\mathcal{V}_{int} = \frac{1}{2} \int_0^\ell \{ EI \kappa^2 + k' AG \beta^2 \} dx \quad (5.172)$$

Performing the variation on κ and β in (5.171) yields the constitutive equations of the beam in the form:

$$\begin{aligned} \delta \kappa : \quad & \lambda_M - EI \kappa = 0 \\ \delta \beta : \quad & \lambda_T - k' AG \beta = 0 \end{aligned} \quad (5.173)$$

while the variation on the displacement fields ψ and w provides the equilibrium equation expressed in terms of the Lagrange multipliers λ_M and λ_T :

$$\begin{aligned} \delta \psi : \quad & \frac{\partial \lambda_M}{\partial x} + \lambda_T = 0 \\ \delta w : \quad & \frac{\partial \lambda_T}{\partial x} = 0 \end{aligned} \quad (5.174)$$

The constitutive Equations (5.173) indicate that the multipliers have the physical meaning of bending moment and shear force:

$$\lambda_M = M \quad \lambda_T = T \quad (5.175)$$

so that the dislocation potential (5.169) can be rewritten as:

$$\mathcal{V}_d = \int_0^\ell \left\{ M \left(\frac{\partial \psi}{\partial x} - \kappa \right) + T \left(\frac{\partial w}{\partial x} - \psi - \beta \right) \right\} dx \quad (5.176)$$

and the equilibrium equations (5.174) are the classical local static equilibrium equations of a beam (see Equations (4.288) and (4.292), assuming no distributed load and no inertia effects).

Let us introduce next the *complementary strain energy* for the beam according to the general definition (4.11):

$$\begin{aligned}\mathcal{V}_{int}^* &= \int_0^\ell \{M\kappa + T\beta\} dx - \mathcal{V}_{int} \\ &= \int_0^\ell \left\{ M\kappa + T\beta - \frac{1}{2}EI\kappa^2 - k'AG\beta^2 \right\} dx \\ &= \frac{1}{2} \int_0^\ell \left\{ \frac{M^2}{EI} + \frac{T^2}{k'AG} \right\} dx\end{aligned}\quad (5.177)$$

Owing to (5.177) the dislocation potential (5.176) can be put in the form:

$$\begin{aligned}\mathcal{V}_d &= \int_0^\ell \left\{ M \frac{\partial \psi}{\partial x} + T \left(\frac{\partial w}{\partial x} - \psi \right) \right\} dx - (\mathcal{V}_{int} + \mathcal{V}_{int}^*) \\ &= [M\psi + Tw]_0^\ell - \int_0^\ell \left(\frac{\partial M}{\partial x} \psi + \frac{\partial T}{\partial x} w + T\psi \right) dx - \mathcal{V}_{int} - \mathcal{V}_{int}^*\end{aligned}\quad (5.178)$$

so that the variational Equation (5.171) becomes:

$$\delta \left\{ -\mathcal{V}_{int}^* + \mathcal{V}_{ext} + [M\psi + Tw]_0^\ell - \int_0^\ell \left(\left(\frac{\partial M}{\partial x} + T \right) \psi + \frac{\partial T}{\partial x} w \right) dx \right\} = 0 \quad (5.179)$$

The combination of the second and third terms of (5.179) yields:

$$\begin{aligned}\mathcal{V}_{ext} + [M\psi + Tw]_0^\ell &= -(\bar{T}_0 + T_0)w_0 - (\bar{M}_0 + M_0)\psi_0 \\ &\quad - (\bar{T}_\ell + T_\ell)w_\ell - (\bar{M}_\ell + M_\ell)\psi_\ell\end{aligned}\quad (5.180)$$

Either the shear force and/or moment at the boundaries are imposed, in which case the corresponding terms in parenthesis at the right of (5.180) are zero at equilibrium (see (4.286)), or the boundary forces and/or moments are not imposed but the displacements and rotations are prescribed, in which case the previous result leads to:

$$\mathcal{V}_{ext} + [M\psi + Tw]_0^\ell = -T_0\bar{w}_0 - M_0\bar{\psi}_0 + T_\ell\bar{w}_\ell + M_\ell\bar{\psi}_\ell = -\mathcal{V}_{ext}^* \quad (5.181)$$

The last integral in (5.179) vanishes provided that the stress field is in static equilibrium:

$$\frac{\partial M}{\partial x} + T = 0 \quad \frac{\partial T}{\partial x} = 0 \quad (5.182)$$

Finally, the *complementary energy variational principle* for static behaviour of the beam with shear deformation takes the form:

$$\delta \left\{ -\frac{1}{2} \int_0^\ell \left(\frac{M^2}{EI} + \frac{T^2}{k'AG} \right) dx - T_0\bar{w}_0 - M_0\bar{\psi}_0 + T_\ell\bar{w}_\ell + M_\ell\bar{\psi}_\ell \right\} = 0 \quad (5.183)$$

or

$$\delta(\mathcal{V}_{int}^* + \mathcal{V}_{ext}^*) = 0 \quad (5.184)$$

its independent variables being the variables of stress type (M , T) which a priori verify the essential conditions, namely Equations (5.182) and the boundary conditions:

$$\begin{aligned} \bar{T}_0 + T &= 0 & \bar{M}_0 + M &= 0 & \text{at } x &= 0 \\ \bar{T}_\ell - T &= 0 & \bar{M}_\ell - M &= 0 & \text{at } x &= \ell \end{aligned} \quad (5.185)$$

in case external forces or moments are imposed at the boundaries.

Finite element discretization

The finite element discretization is achieved by constructing a polynomial interpolation of the stress field that a priori verifies the equilibrium conditions (5.182). Assuming a linear interpolation of the moment field we thus get:

$$M = \alpha_0 + \alpha_1 \frac{x}{\ell} \quad T = -\frac{\alpha_1}{\ell} \quad (5.186)$$

The discretized form of the complementary energy can be expressed in the form (setting the origin of the axis in the middle of the beam to simplify the computation):

$$\mathcal{V}_{int,e}^* = \frac{1}{2} \int_{-\ell/2}^{\ell/2} \left(\frac{M^2}{EI} + \frac{T^2}{k'AG} \right) dx = \frac{1}{2} \alpha_e^T F_e \alpha_e \quad (5.187)$$

with the stress parameters $\alpha_e^T = [\alpha_0 \ \alpha_1]$ and the flexibility kernel:

$$F_e = \frac{\ell}{EI} \begin{bmatrix} 1 & 0 \\ 0 & \frac{1}{12} + \frac{EI}{k'AG\ell^2} \end{bmatrix} \quad (5.188)$$

By introducing the linear interpolation of the moment into the boundary conditions similar to (5.185) but now expressed at $x = -1/2\ell, x = 1/2\ell$, we deduce the local values of the moments and shear forces on the element as displayed on Figure 5.27:

$$\begin{bmatrix} T_1 \\ M_1 \\ T_2 \\ M_2 \end{bmatrix} = \begin{bmatrix} 0 & \frac{1}{\ell} \\ -1 & \frac{1}{2} \\ 0 & -\frac{1}{\ell} \\ 1 & \frac{1}{2} \end{bmatrix} \begin{bmatrix} \alpha_0 \\ \alpha_1 \end{bmatrix}$$

$$p_e = S_e \alpha_e \quad (5.189)$$

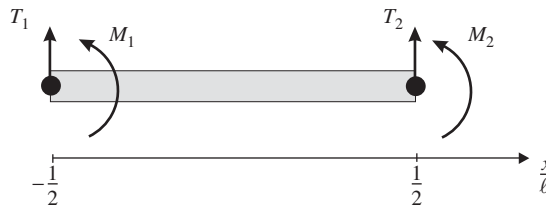


Figure 5.27 Force connectors of the beam element in bending.

with the static connection matrix of the element:

$$\mathbf{S}_e = \begin{bmatrix} 0 & \frac{1}{\ell} \\ -1 & \frac{1}{2} \\ 0 & -\frac{1}{\ell} \\ 1 & \frac{1}{2} \end{bmatrix} \quad (5.190)$$

The discretized form of Equation (5.183) becomes:

$$\delta \left\{ \frac{1}{2} \alpha_e^T \mathbf{F}_e \alpha_e - \mathbf{p}_e^T \mathbf{q}_e \right\} = 0 \quad (5.191)$$

where \mathbf{q}_e is the vector of generalized displacements conjugated to the stress resultants \mathbf{p}_e . Substituting the static relationship (5.189) into (5.191) and performing the variation on α_e yields the system equation:

$$\mathbf{F}_e \alpha_e = \mathbf{S}_e^T \mathbf{q}_e \quad (5.192)$$

Finally, inverting the flexibility kernel and premultiplying by the static connection matrix yields the stiffness relationship:

$$\begin{aligned} \mathbf{p}_e &= \mathbf{S}_e \mathbf{F}_e^{-1} \mathbf{S}_e^T \mathbf{q}_e \\ &= \mathbf{K}_e \mathbf{q}_e \end{aligned} \quad (5.193)$$

The explicit expression of the stiffness matrix can be obtained through substitution of Equations (5.188, 5.190) into (5.193). After simplification we get:

$$\mathbf{K}_e = \frac{\text{EI}}{\ell^3(\phi + 1)} \begin{bmatrix} 12 & 6\ell & -12 & 6\ell \\ 6\ell & (4 + \phi)\ell^2 & -6\ell & (2 - \phi)\ell^2 \\ -12 & -6\ell & 12 & -6\ell \\ 6\ell & (2 - \phi)\ell^2 & -6\ell & (4 + \phi)\ell^2 \end{bmatrix} \quad (5.194)$$

with the definition of the shear parameter:

$$\phi = \frac{12\text{EI}}{k'AG\ell^2} = 12\eta \quad (5.195)$$

Interestingly, when $\phi \rightarrow 0$, the expression (5.194) of the stiffness matrix converges to that obtained for the slender beam (Equation (5.126)).

Getting a consistent expression of the mass matrix is not straightforward. The only way to build a mass matrix in line with the statically admissible approach would be to increase the interpolation degree of the moment and shear force fields (5.186) in order to take into account nonzero force distribution on the element (Gérardin 1970). There are however alternatives to build a mass matrix approximation which is not consistent with the assumed stress distribution.

- A simple expression of the mass matrix can be obtained from the linear interpolation (5.164) of the displacement field using the generalized displacements of the equilibrium model. The beam kinetic energy may be expressed as:

$$\mathcal{T}_e = \frac{1}{2} \int_0^\ell m r^2 \dot{\psi}^2 dx + \frac{1}{2} \int_0^\ell m \dot{w}^2 dx \quad (5.196)$$

r being the gyration radius of the cross-section about the transverse axis. Substitution of (5.164) into (5.196) provides the very simple, explicit expression of the mass matrix:

$$\mathbf{M}_e = \frac{m\ell}{6} \begin{bmatrix} 2 & 0 & 1 & 0 \\ 0 & 2r^2 & 0 & r^2 \\ 1 & 0 & 2 & 0 \\ 0 & r^2 & 0 & 2r^2 \end{bmatrix} \quad (5.197)$$

It provides exact representation of the kinetic inertia generated by rigid body motion of the element but does not include the higher-order inertia effects linked to deformation.

- An alternative consists to adopt the mass matrix obtained with the shape functions of the beam model without shear deformation, neglecting in this way the effect of shear deformation on the distribution of inertia forces.⁶ Expressing the kinetic energy (5.196) with the shape functions (5.117) yields the expression of the mass matrix split into translation and rotatory inertia contributions:

$$\mathbf{M}_e = \mathbf{M}_{trans} + \mathbf{M}_{rot} \quad (5.198)$$

with

$$\begin{aligned} \mathbf{M}_{trans} &= \frac{m\ell}{420} \begin{bmatrix} 156 & 22\ell & 54 & -13\ell \\ 22\ell & 4\ell^2 & 13\ell & -3\ell^2 \\ 54 & 13\ell & 156 & -22\ell \\ -13\ell & -3\ell^2 & -22\ell & 4\ell^2 \end{bmatrix} \\ \mathbf{M}_{rot} &= \frac{mr^2}{30\ell} \begin{bmatrix} 36 & 3\ell & -36 & 3\ell \\ 3\ell & 4\ell^2 & -3\ell & -\ell^2 \\ -36 & -3\ell & 36 & -3\ell \\ 3\ell & -\ell^2 & -3\ell & 4\ell^2 \end{bmatrix} \end{aligned} \quad (5.199)$$

Example 5.4

Let us consider the case of a cantilever beam with circular hollow cross-section. It is characterized by an aspect ratio defined as $\frac{R}{\ell}$ where R is the radius of the cross-section. The wall thickness e is supposed small, so that the nondimensional parameters α^2 and η^2 (Equation (4.303)) take the values (Equation (E4.6.e))

$$\alpha^2 = \frac{r^2}{\ell^2} = \frac{R^2}{2\ell^2} \quad \eta^2 = \frac{EI}{k'AG\ell^2} = 2.6 \frac{R^2}{\ell^2} \quad (E5.4.a)$$

and thus

$$\phi = 12 \frac{EI}{k'AG\ell^2} = 12\eta^2 = 31.2 \frac{R^2}{\ell^2} \quad (E5.4.b)$$

⁶ A negligible effect since the eigensolutions are characterized by low sensitivity to errors on distribution of inertia forces.

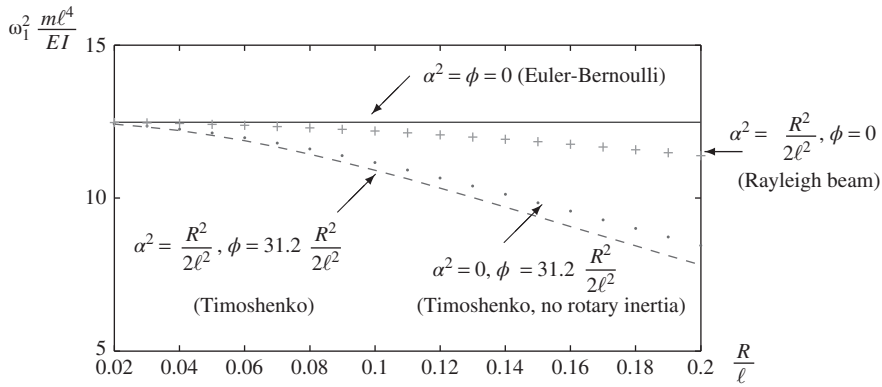


Figure 5.28 First eigenvalue of clamped beam with circular hollow cross-section: influence of shear flexibility (ϕ parameter) and rotatory inertia (α^2 parameter) with varying aspect ratio $\frac{R}{\ell}$ of the cross-section.

The stiffness and mass matrices obtained using a single element (with the mass matrix according to (5.198)) are:

$$\mathbf{K} = \frac{EI}{\ell^3(\phi + 1)} \begin{bmatrix} 12 & -6\ell \\ -6\ell & (4 + \phi)\ell^2 \end{bmatrix}$$

$$\mathbf{M} = \frac{m\ell}{420} \begin{bmatrix} 156 + 504\alpha^2 & -(22 + 42\alpha^2)\ell \\ -(22 + 42\alpha^2)\ell & (4 + 56\alpha^2)\ell^2 \end{bmatrix} \quad (\text{E5.4.c})$$

The resulting eigenvalue equation $\det(\mathbf{K} - \omega^2 \mathbf{M}) = 0$ is quadratic in the frequency parameter $\mu = \frac{\omega^2 EI}{m\ell^4}$.

Figure 5.28 shows the evolution of the first eigenvalue versus the aspect ratio $\frac{R}{\ell}$. In order to quantify the relative effects of rotatory inertia and shear flexibility, four cases have been considered:

1. $\alpha = \phi = 0$ (classical Euler-Bernoulli beam model).
2. $\alpha^2 = \frac{R^2}{2\ell^2}, \phi = 0$ (Rayleigh beam model).
3. $\alpha = 0, \phi = 31.2 \frac{R^2}{2\ell^2}$ (Timoshenko beam model without rotatory inertia).
4. $\alpha^2 = \frac{R^2}{2\ell^2}, \phi = 31.2 \frac{R^2}{2\ell^2}$ (Timoshenko beam model without rotatory inertia).

It confirms the fact that both effects become significant for high cross-section aspect ratio (reduction of the first eigenvalue by about 30% for $\frac{R}{\ell}$, but also that the shear flexibility effect is dominant.

5.4 Exercises

Even with the simple structural models proposed in this chapter, it is not easy to devise a large variety of exercises that can easily be solved analytically. Therefore the solution of some of the problems proposed hereafter is greatly facilitated by the use of symbolic computation and/or of a numerical toolbox.

5.4.1 Solved exercises

Problem 5.1 Let us consider an idealized model of a tree as described in Figure 5.29.a. It is assumed that the tree can be considered as a beam prestressed by its own weight and that its cross-section varies linearly from bottom to top so that its diameter is given by:

$$d = d_{bot} \left(1 - \frac{x}{H} \right) \quad (\text{P5.1.a})$$

and we assume that:

$$d_{bot} = H/150 \quad (\text{P5.1.b})$$

The tree's volumic mass is taken as $\rho = 800 \text{ kg/m}^3$ (roughly corresponding to an oak tree) and its Young modulus is $E = 11.5 \cdot 10^9 \text{ N/m}^2$. To account for the weight of the branches, we will assume a factor 1.5 on the volumic mass so that the effective density is $\rho_e = 1.5\rho$.

The tree's behaviour will be approximated using a Rayleigh–Ritz method with a transverse displacement assumed of the form:

$$v(x) = \mathbf{F}\mathbf{q} = \begin{bmatrix} (3\xi^2 - 2\xi^3) & (H\xi^3 - H\xi^2) \end{bmatrix} \begin{bmatrix} v_t \\ \psi_t \end{bmatrix} \quad \text{where} \quad \xi = x/H, \quad (\text{P5.1.c})$$

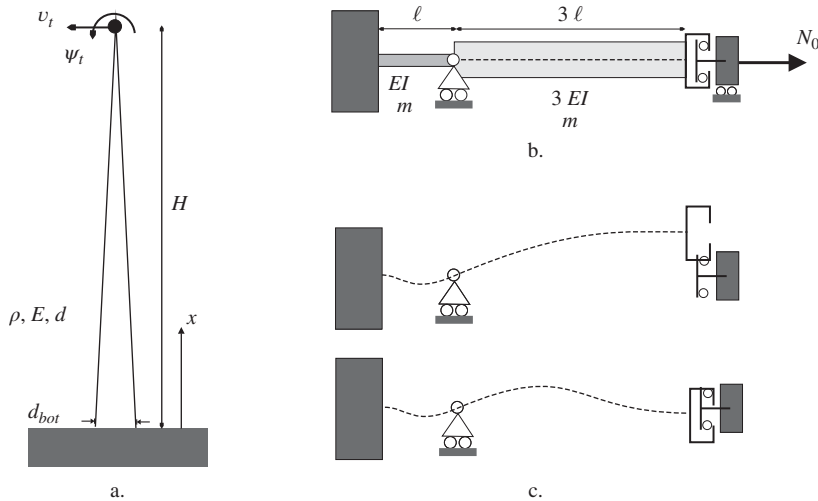


Figure 5.29 Solved problems: (a) a simplified model of a tree, (b) a beam assembly under prestress.

where the approximation functions are shape functions of the beam element, so that the parameters v_t and ψ_t are respectively the transverse displacement and the rotation at the tip of the tree.

You are asked to perform a stability and vibration analysis according to the following steps:

1. Compute the stiffness and mass matrices of the model.
2. Find the prestress load in the tree as a function of x . Then compute the geometric stiffness matrix of the model.
3. Compute the maximum height of the tree before it buckles under its own weight. Determine what would be the maximum height for a pine tree having a density $\rho = 550 \text{ Kg/m}^3$ and a Young's modulus $E = 10.5 \cdot 10^9 \text{ N/m}^2$ (assuming as before that $\rho_e = 1.5\rho$).
4. Compute the first vibration frequency (in Hz) and eigenmode of the oak tree when gravity prestress is neglected and the height is equal to 50 m.
5. Compute the first eigenfrequency (in Hz) and eigenmode when the stiffness effect of prestress is included and when the height is equal to 50m.

Solution

The stiffness matrix of the tree is obtained from the discretization of the strain energy and is written as:

$$\mathbf{K} = \frac{1}{H^3} \int_0^1 EI(\xi) \frac{\partial^2 \mathbf{F}(\xi)^T}{\partial \xi^2} \frac{\partial^2 \mathbf{F}(\xi)}{\partial \xi^2} d\xi$$

where

$$I(\xi) = \frac{\pi}{64} d(\xi)^4 = \frac{\pi}{64} d_{bot}^4 (1 - \xi)^4$$

and where, for the chosen shape function (P5.1.c),

$$\frac{\partial^2 \mathbf{F}(\xi)}{\partial \xi^2} = \begin{bmatrix} (6 - 12\xi) & (6H\xi - 2H) \end{bmatrix}$$

After integration one finds (possibly using a symbolic computation toolbox):

$$\mathbf{K} = \frac{\pi E d_{bot}^4}{1120 H^3} \begin{bmatrix} 66 & -19H \\ -19H & 6H^2 \end{bmatrix} \quad (\text{P5.1.d})$$

The mass matrix is obtained from:

$$\mathbf{M} = \int_0^1 m(\xi) \mathbf{F}(\xi)^T \mathbf{F}(\xi) H d\xi$$

where $m(\xi)$ is the mass per unit length:

$$m(\xi) = \rho_e A(\xi) = \rho_e \pi \frac{d(\xi)^2}{4} = \rho_e \frac{\pi}{4} d_{bot}^2 (1 - \xi)^2$$

Integration results in:

$$\mathbf{M} = \rho_e \frac{\pi}{4} \frac{H d_{bot}^2}{2520} \begin{bmatrix} 76 & -17H \\ -17H & 4H^2 \end{bmatrix} \quad (\text{P5.1.e})$$

The axial prestress in the tree is obtained by considering the weight acting at a position x due to the tree segment above x and is written as:

$$N_0(x) = - \int_x^H g \rho_e \frac{\pi d^2(\zeta)}{4} H d\zeta = -g \rho_e \frac{\pi}{12} H d_{bot}^2 (1 - \xi)^3$$

and the geometric stiffness matrix is:

$$\mathbf{K}_g = \frac{1}{H} \int_0^1 N_0(\xi) \frac{\partial \mathbf{F}(\xi)^T}{\partial \xi} \frac{\partial \mathbf{F}(\xi)}{\partial \xi} d\xi$$

where

$$\frac{\partial \mathbf{F}}{\partial \xi} = \begin{bmatrix} (6\xi - 6\xi^2) & (3H\xi^2 - 2H\xi) \end{bmatrix}$$

Integration results in

$$\mathbf{K}_g = -g \rho_e \frac{\pi}{12} \frac{d_{bot}^2}{840} \begin{bmatrix} 180 & -42H \\ -42H & 11H^2 \end{bmatrix} \quad (\text{P5.1.f})$$

The tree becomes unstable when a nonzero solution exist for:

$$(\mathbf{K} + \mathbf{K}_g) \mathbf{q} = \mathbf{0}$$

thus when

$$\det(\mathbf{K} + \mathbf{K}_g) = 0$$

Hence

$$\det \left(\begin{bmatrix} 66 & -19H \\ -19H & 6H^2 \end{bmatrix} - \frac{g \rho_e}{9E} \frac{H^3}{d_{bot}^2} \begin{bmatrix} 180 & -42H \\ -42H & 11H^2 \end{bmatrix} \right) = 0$$

so that for $d_{bot} = \frac{H}{150}$ we get after simplification the eigenvalue problem:

$$\det \left(\begin{bmatrix} 66 & -19 \\ -19 & 6 \end{bmatrix} - \lambda \begin{bmatrix} 180 & -42 \\ -42 & 11 \end{bmatrix} \right) = 0$$

with

$$\lambda = 2500 \frac{\rho_e H}{E}$$

Solving this eigenvalue equation for λ , one finds:

$$\lambda_1 = 0.2136 \quad \text{and thus} \quad H_{crit} = 0.2136 \frac{E}{2500 \rho_e}$$

For an oak tree where $\rho_e = 1200 \text{ kg/m}^3$, $E = 11.5 \cdot 10^9 \text{ N/m}^2$ and $g = 9.81 \text{ m/s}^2$, one finds:

$$H_{crit,oak} = 83.46 \text{ m}$$

For a pine tree where $\rho_e = 825 \text{ kg/m}^3$, $E = 10.5 \cdot 10^9 \text{ N/m}^2$, one finds:

$$H_{crit,pine} = 110.84 \text{ m}$$

The eigenfrequencies in the absence of prestress are found by solving:

$$(\mathbf{K} - \omega^2 \mathbf{M})\mathbf{q} = \mathbf{0}$$

For an oak tree, when $H = 50$, one finds:

$$\omega_{1,oak}^2 = 0.8125 \quad (\text{rad/s})^2$$

hence a first frequency of 0.1435 Hz. The associated eigenmode is:

$$\begin{bmatrix} 1 \\ 0.0515 \end{bmatrix}$$

When the prestress is taken into account, the eigenvalue problem to consider is:

$$(\mathbf{K} + \mathbf{K}_g - \omega^2 \mathbf{M})\mathbf{q} = \mathbf{0}$$

For an oak tree, when $H = 50$, one finds:

$$\omega_{1,oak}^2 = 0.3288 \quad (\text{rad/s})^2$$

hence a first frequency of 0.09126 Hz. The associated eigenmode has very similar shape:

$$\begin{bmatrix} 1 \\ 0.0534 \end{bmatrix}$$

Problem 5.2 Let us consider the beam assembly depicted in 5.29.b. The assembly is pre-stressed by an axial force N_0 and is simply supported at the junction between the left slender beam and the right thick beam. The left end is clamped whereas the right one is attached to a massless slider blocking the end-rotation.

The system is modelled with 2 beam elements, one at each side of the support. You are asked to do the following:

- To compute the stiffness (geometric and elastic) and the mass matrices of the system.
- Taking $EI = 1$ and $\ell = 1$, to estimate the critical load of the construction.
- Assuming further that $m = 420/9$ and $N_0 = -1$, to compute the eigenfrequencies and eigenmodes and to depict the overall shape of the vibration modes.

Solution

There are 2 degrees of freedom for the system: the rotation ψ at the interface of the beams (ψ_2 of left beam, equal to ψ_1 of right beam) and the transverse displacement v at the right end (v_2 of the right beam). Considering the general forms (5.125) and (5.126) the contribution of left beam to the system matrices are:

$$\mathbf{K}_S^{\text{left}} = \frac{EI}{\ell^3} \begin{bmatrix} 4\ell^2 & 0 \\ 0 & 0 \end{bmatrix} \quad \mathbf{K}_{g,S}^{\text{left}} = \frac{N_0}{30\ell} \begin{bmatrix} 4\ell^2 & 0 \\ 0 & 0 \end{bmatrix} \quad \mathbf{M}_S^{\text{left}} = \frac{m\ell}{420} \begin{bmatrix} 4\ell^2 & 0 \\ 0 & 0 \end{bmatrix}$$

For the right beam,

$$\mathbf{K}_S^{right} = \frac{EI}{3\ell^3} \begin{bmatrix} 12\ell^2 & -6\ell \\ -6\ell & 4 \end{bmatrix} \quad \mathbf{K}_{g,S}^{right} = \frac{N_0}{10\ell} \begin{bmatrix} 4\ell^2 & -\ell \\ -\ell & 4 \end{bmatrix}$$

$$\mathbf{M}_S^{right} = \frac{m\ell}{140} \begin{bmatrix} 36\ell^2 & 39\ell \\ 39\ell & 156 \end{bmatrix}$$

Hence the total matrices are:

$$\mathbf{K}_S = \frac{EI}{3\ell^3} \begin{bmatrix} 24\ell^2 & -6\ell \\ -6\ell & 4 \end{bmatrix} \quad \mathbf{K}_{g,S} = \frac{N_0}{30\ell} \begin{bmatrix} 16\ell^2 & -3\ell \\ -3\ell & 12 \end{bmatrix} \quad (\text{P5.2.a})$$

$$\mathbf{M}_S = \frac{m\ell}{420} \begin{bmatrix} 112\ell^2 & 117\ell \\ 117\ell & 468 \end{bmatrix} \quad (\text{P5.2.b})$$

Taking now $EI = 1$, $\ell = 1$ and solving the eigenvalue problem:

$$(\mathbf{K}_S + \mathbf{K}_{g,S})\mathbf{x} = \mathbf{0}$$

for N_0 one finds:

$$N_0 = -2.17 \quad \text{and} \quad N_0 = -15.1$$

the critical buckling load being $N_0 = -2.17$.

Assuming further that $m = 420/9$ and setting $N_0 = -1$, the solution of

$$(\mathbf{K}_S + \mathbf{K}_{g,S}) - \omega^2 \mathbf{M}_S \mathbf{x} = \mathbf{0}$$

yields, for mode 1:

$$\omega_1^2 = 7.537 \cdot 10^{-3} \quad \begin{bmatrix} v \\ \psi \end{bmatrix}_1 = \begin{bmatrix} 1 \\ 3.69 \end{bmatrix}$$

and for mode 2:

$$\omega_2^2 = 0.9326 \quad \begin{bmatrix} v \\ \psi \end{bmatrix}_2 = \begin{bmatrix} 1 \\ -0.295 \end{bmatrix}$$

The modes are sketched in 5.29.c.

Problem 5.3 It is at first sight surprising, but also noteworthy to observe that the finite element model of the Euler-Bernoulli beam can be obtained through series expansion of its exact impedance matrix $\mathbf{Z}(\omega^2)$.

To do so:

- Develop the exact expression of the impedance matrix $\mathbf{Z}(\omega^2)$ for a Euler-Bernoulli beam element.
- Show that the elements of the stiffness and mass matrices (5.125) and (5.126) can be computed as

$$k_{ij} = \lim_{\omega^2 \rightarrow 0} z_{ij}(\omega^2) \quad m_{ij} = \lim_{\omega^2 \rightarrow 0} \frac{z_{ij}(\omega^2) - k_{ij}}{\omega^2} \quad (\text{P5.3.a})$$

Justify the result obtained.

Solution

The displacement field solution of the homogeneous equilibrium equation (4.245) can be expanded in terms of Duncan's functions (4.248) as:

$$w(x) = a_1 s_1 \left(\frac{\mu x}{\ell} \right) + a_2 c_1 \left(\frac{\mu x}{\ell} \right) + a_3 s_2 \left(\frac{\mu x}{\ell} \right) + a_4 c_2 \left(\frac{\mu x}{\ell} \right) \quad (\text{P5.3.b})$$

Let us express the relationship between the vector of local displacements and rotations:

$$\mathbf{q}^T = [w_1 \quad \psi_1 \quad w_2 \quad \psi_2] \quad (\text{P5.3.c})$$

in terms of the unknown parameters (a_i , $i = 1 \dots 4$) as:

$$\mathbf{a} = \mathbf{C} \mathbf{q} \quad (\text{P5.3.d})$$

where \mathbf{C} is the displacement connection matrix. Its inverse \mathbf{C}^{-1} is computed from (P5.3.b) and has for explicit expression

$$\mathbf{C}^{-1} = \begin{bmatrix} 0 & 2 & 0 & 0 \\ \frac{2\mu}{\ell} & 0 & 0 & 0 \\ s_1(\mu) & c_1(\mu) & s_2(\mu) & c_2(\mu) \\ \frac{\mu c_1(\mu)}{\ell} & \frac{\mu s_2(\mu)}{\ell} & \frac{\mu c_2(\mu)}{\ell} & \frac{\mu s_1(\mu)}{\ell} \end{bmatrix} \quad (\text{P5.3.e})$$

Performing the inversion and simplifying the notation by writing $s_1 \leftarrow s_1(\mu)$ and so forth provides the result:

$$\mathbf{C} = \frac{1}{2} \begin{bmatrix} 0 & \frac{\ell}{\mu} & 0 & 0 \\ 1 & 0 & 0 & 0 \\ \frac{c_2 s_2 - c_1 s_1}{c_2^2 - s_2 s_1} & \frac{(c_1 c_2 - s_1^2) \ell}{(c_2^2 - s_2 s_1) \mu} & \frac{-s_1}{c_2^2 - s_2 s_1} & \frac{c_2 \ell}{(c_2^2 - s_2 s_1) \mu} \\ \frac{s_2^2 - c_1 c_2}{c_2^2 - s_2 s_1} & \frac{(c_1 s_2 - s_1 c_2) \ell}{(c_2^2 - s_2 s_1) \mu} & \frac{c_2}{c_2^2 - s_2 s_1} & \frac{-s_2 \ell}{(c_2^2 - s_2 s_1) \mu} \end{bmatrix} \quad (\text{P5.3.f})$$

Likewise, let us compute the shear forces and moments at the beam ends:

$$\mathbf{p}^T = [T_1 \quad M_1 \quad T_2 \quad M_2] \quad (\text{P5.3.g})$$

and express them in terms of the interpolation parameters \mathbf{a} in the form:

$$\mathbf{p} = \mathbf{S} \mathbf{a} \quad (\text{P5.3.h})$$

By making use of the beam equations:

$$M = EI \frac{d^2 w}{dx^2} \quad T + \frac{dM}{dx} = 0 \quad (\text{P5.3.i})$$

and taking account of the sign convention of Figure 5.27 we get the expression of the 'static' connection matrix:

$$S = \frac{EI\mu^2}{\ell^2} \begin{bmatrix} 0 & 0 & \frac{2\mu}{\ell} & 0 \\ 0 & 0 & 0 & -2 \\ -\frac{c_2\mu}{\ell} & -\frac{s_1\mu}{\ell} & -\frac{c_1\mu}{\ell} & -\frac{s_2\mu}{\ell} \\ s_2 & c_2 & s_1 & c_1 \end{bmatrix} \quad (\text{P5.3.j})$$

The impedance matrix Z is then obtained from the multiplication:

$$Z = SC \quad (\text{P5.3.k})$$

Taking into account the following identities verified by the Duncan functions:

$$c_1 c_2 = \frac{1}{2}(s_1^2 + s_2^2) \quad s_1 s_2 = \frac{1}{2}(c_1^2 + c_2^2) - 2 \quad (\text{P5.3.l})$$

we get after simplification:

$$Z = \frac{EI\mu^3}{\ell^3(c_2^2 - s_1 s_2)} \begin{bmatrix} c_1 s_1 - c_2 s_2 & (c_1 c_2 - s_2^2) \frac{\ell}{\mu} & -2s_1 & 2c_2 \frac{\ell}{\mu} \\ (c_1 c_2 - s_2^2) \frac{\ell}{\mu} & (s_1 c_2 - c_1 s_2) \frac{\ell^2}{\mu^2} & -2c_2 \frac{\ell}{\mu} & 2s_2 \frac{\ell^2}{\mu^2} \\ -2s_1 & -2c_2 \frac{\ell}{\mu} & c_1 s_1 - c_2 s_2 & (s_2^2 - c_1 c_2) \frac{\ell}{\mu} \\ 2c_2 \frac{\ell}{\mu} & 2s_2 \frac{\ell^2}{\mu^2} & (s_2^2 - c_1 c_2) \frac{\ell}{\mu} & (s_1 c_2 - c_1 s_2) \frac{\ell^2}{\mu^2} \end{bmatrix} \quad (\text{P5.3.m})$$

or, in terms of trigonometric and hyperbolic functions:

$$Z = \frac{EI\mu^3}{\ell^3(1 - \cos \mu \cosh \mu)} \times \begin{bmatrix} \cos \mu \sinh \mu + \sin \mu \cosh \mu & \frac{\ell}{\mu} \sin \mu \sinh \mu & -(\sin \mu + \sinh \mu) & \frac{\ell}{\mu} (\cosh \mu - \cos \mu) \\ \frac{\ell}{\mu} \sin \mu \sinh \mu & \frac{\ell^2}{\mu^2} (\cosh \mu \sin \mu - \sinh \mu \cos \mu) & \frac{\ell}{\mu} (\cos \mu - \cosh \mu) & \frac{\ell^2}{\mu^2} (\sinh \mu - \sin \mu) \\ -(\sin \mu + \sinh \mu) & \frac{\ell}{\mu} (\cos \mu - \cosh \mu) & \cos \mu \sinh \mu + \sin \mu \cosh \mu & \frac{-\ell}{\mu} \sinh \mu \sin \mu \\ \frac{\ell}{\mu} (\cosh \mu - \cos \mu) & \frac{(\sinh \mu - \sin \mu) \ell^2}{\mu^2} & \frac{-\ell}{\mu} \sinh \mu \sin \mu & \frac{\ell^2}{\mu^2} (\cos \mu \sinh \mu - \sin \mu \cosh \mu) \end{bmatrix} \quad (\text{P5.3.n})$$

The stiffness and mass coefficients are then computed from a Taylor expansion of the coefficients $z_{ij}(\mu)$. We get for the upper part:

$$\begin{aligned}
 z_{11}(\mu) = z_{33}(\mu) &= \frac{EI}{\ell^3} \frac{(\cos \mu \sinh \mu + \sin \mu \cosh \mu) \mu^3}{1 - \cos \mu \cosh \mu} = \frac{EI}{\ell^3} \left(12 - \frac{13}{35} \mu^4 + O(\mu^8) \right) \\
 z_{22}(\mu) = z_{44}(\mu) &= \frac{EI}{\ell^3} \frac{(\cosh \mu \sin \mu - \cos \mu \sinh \mu) \mu}{1 - \cos \mu \cosh \mu} = \frac{EI}{\ell^3} \left(4 - \frac{1}{105} \mu^4 + O(\mu^8) \right) \\
 z_{12}(\mu) = -z_{34}(\mu) &= \frac{EI}{\ell^3} \frac{\mu^2 \sinh \mu \sin \mu}{1 - \cos \mu \cosh \mu} = \frac{EI}{\ell^3} \left(6 - \frac{11}{210} \mu^4 + O(\mu^8) \right) \\
 z_{13}(\mu) &= -\frac{EI}{\ell^3} \frac{\mu^3 (\sinh \mu + \sin \mu)}{1 - \cos \mu \cosh \mu} = \frac{EI}{\ell^3} \left(-12 - \frac{9}{70} \mu^4 + O(\mu^8) \right) \\
 z_{14}(\mu) = -z_{23}(\mu) &= \frac{EI}{\ell^3} \frac{\mu^2 (\cosh \mu - \cos \mu)}{1 - \cos \mu \cosh \mu} = \frac{EI}{\ell^3} \left(6 + \frac{13}{420} \mu^4 + O(\mu^8) \right) \\
 z_{24}(\mu) &= -\frac{EI}{\ell^3} \frac{\mu (\sinh \mu - \sin \mu)}{1 - \cos \mu \cosh \mu} = \frac{EI}{\ell^3} \left(2 + \frac{1}{140} \mu^4 + O(\mu^8) \right)
 \end{aligned} \tag{P5.3.o}$$

The stiffness coefficients are immediately obtained from Equations (P5.3.o) as:

$$k_{ij} = z_{ij}(0) \tag{P5.3.p}$$

and it can be verified that the resulting matrix \mathbf{K} coincides with (5.125). Likewise, the mass coefficients are computed as:

$$m_{ij} = \left(\frac{z_{ij}(\mu) - z_{ij}(0)}{\omega^2} \right)_{\mu=0} = \frac{m\ell^4}{EI} \left(\frac{z_{ij}(\mu) - z_{ij}(0)}{\mu^4} \right)_{\mu=0} \tag{P5.3.q}$$

and they provide the same mass matrix (5.126) as the finite element discretization.

This equivalence results from the fact that the cubic shape functions adopted for the finite element discretization allow representing the exact solution of the homogeneous static problem.⁷

5.4.2 Selected exercises

Problem 5.4 Let us consider the system made of two beams of length ℓ , clamped at both sides (Figure 5.30.a). The left beam has a bending stiffness of $2EI$ and a distributed mass m per unit length. The right beam has a bending stiffness of EI , a negligible distributed mass but a concentrated mass M in its middle.

Using two beam finite elements of length ℓ , you are asked:

- To write the stiffness and mass matrix of the system. This requires in particular to construct the mass matrix of the right beam for the point mass located in its middle.
- To compute the eigenmodes and eigenfrequencies of the model when $M = (32/105) m\ell$ and draw the mode shapes.

⁷ The same reasoning could be followed to get the stiffness matrix (5.194) of the beam with shear deformation.

- To compute the response amplitude of the system when a unit transverse harmonic force is applied on mass M with a forcing frequency equal to $\omega_1/2$.
- To compare the forced vibration deformation of the system obtained previously with the static response to a unit transverse force on M .

Problem 5.5 Let us consider the system of Figure 5.30.b made of two beams of length ℓ , clamped on both sides. The left beam has a bending stiffness of $2EI$ and a distributed mass m per unit length. The right beam has a bending stiffness of EI and a negligible distributed mass. Two concentrated masses M are rigidly attached to the mid-point of the system, with a vertical offset $\ell/2$. The mass of the rigid link is neglected.

Using two beam finite elements of length ℓ , you are asked

- to write the stiffness and mass matrix of the system;
- to compute the eigenmodes and eigenfrequencies of the model when $M = (16/105) m\ell$ and to draw the mode shapes;
- to compute the response amplitude of the system when a unit transverse harmonic force is applied on mass M with a forcing frequency equal to $\omega_1/2$;
- to compute the response amplitude of the system when a harmonic torque is generated with a forcing frequency equal to $\omega_1/2$ by applying unit loads parallel to the beam on masses M .

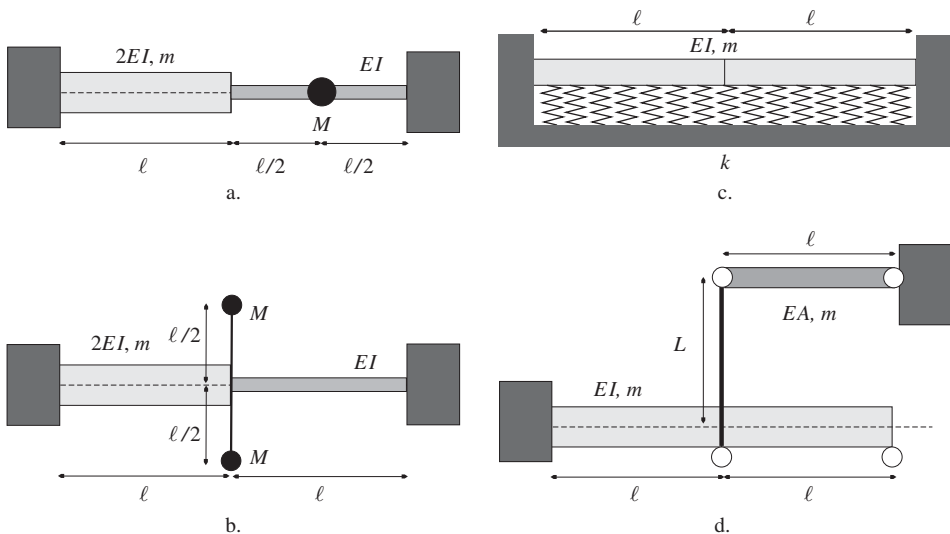


Figure 5.30 Unsolved finite element problems.

Problem 5.6 Consider the model of a clamped-clamped beam as described in Figure 5.30.c. The beam is supported on the ground with a soil stiffness represented by a distributed translational spring of stiffness k per unit length (hence the vertical force created by the soil is equal to $df = k w(x) dx$).

Perform the following computations:

- Build the mass and stiffness matrix of a two-finite element model for the transverse motion.

- Compute the eigenfrequencies and eigenmodes of the model when $k = EI/4\ell^4$.
- Plot the eigenmodes of the system and compare them to the eigenmodes of the unsupported clamped-clamped beam.

Problem 5.7 Let us consider the assembly of a beam and a bar as depicted in Figure 5.30.d. The beam is clamped to its left and hinged in its middle and at its right end. The bar is hinged at its ends and connected to the middle of the beam through a rigid and massless link.

You are asked:

- to build the mass and stiffness matrices considering two elements of length ℓ for the beam and one element for the bar;
- to compute the eigenfrequencies and eigenmodes of the system when $A = \frac{I}{\ell^2}$ and $L = \frac{\ell}{4}$ and to depict the mode shapes;
- to compute the amplitude of the forced response when the system is excited by a unit moment at the right end of the beam (assuming again $A = \frac{I}{\ell^2}$ and $L = \frac{\ell}{4}$).

Problem 5.8 Let us consider again the system made of a rotating hinged blade with eccentricity e from the rotation axis flapping in the vertical direction (Figure 4.30), taking now into account the bending deformation of the blade. It is assumed that both bending stiffness EI and mass distribution m are constant over the blade length ℓ .

For sake of simplicity, the system is modelled using a single beam finite element. Its stiffness and mass matrices being directly available, only the geometric stiffness matrix resulting from the centrifugal force needs to be computed (remember that the geometric stiffness matrix (5.142) is for a constant axial prestress and cannot be used for the present case).

In order to get insight in the vibration behaviour of the system, the dynamic equilibrium problem will be put in nondimensional form. Therefore a dimensionless displacement vector \tilde{q} is defined for the finite element by the transformation:

$$\mathbf{q} = \begin{bmatrix} \ell & 0 & 0 & 0 \\ 0 & 1 & 0 & 0 \\ 0 & 0 & \ell & 0 \\ 0 & 0 & 0 & 1 \end{bmatrix} \tilde{\mathbf{q}}$$

The stiffness and mass matrices can then be expressed as:

$$\mathbf{K} = \frac{EI}{\ell^2} \tilde{\mathbf{K}} \quad \text{and} \quad \mathbf{M} = m\ell^2 \tilde{\mathbf{M}}$$

with nondimensional matrices $\tilde{\mathbf{K}}$ and $\tilde{\mathbf{M}}$.

You are asked to:

- to demonstrate that the geometric stiffness matrix of the system can be put likewise in the non-dimensional form:

$$\mathbf{K}_g = m\Omega^2 \ell^2 \tilde{\mathbf{K}}_g$$

where $\tilde{\mathbf{K}}_g$ is a nondimensional matrix function only of the *eccentricity ratio*:

$$\eta = \frac{e}{\ell}$$

- to demonstrate that the eigenvalue problem admits the nondimensional form:

$$(\tilde{\mathbf{K}} + \tilde{\Omega}^2 \tilde{\mathbf{K}}_g - \tilde{\omega}^2 \tilde{\mathbf{M}}) \tilde{\mathbf{q}} = 0 \quad (\text{P5.8.a})$$

where $\tilde{\Omega}$ and $\tilde{\omega}$ are respectively the nondimensional rotating velocity and frequency defined by:

$$\tilde{\Omega}^2 = \frac{\Omega^2 m \ell^4}{EI} \quad \text{and} \quad \tilde{\omega}^2 = \frac{\omega^2 m \ell^4}{EI}$$

- to write a routine to numerically compute (using Gauss quadrature) the matrix $\tilde{\mathbf{K}}_g$ assuming that the beam element is hinged at its left-end with eccentricity e from the rotation axis (note: determine first the minimum number of Gauss points needed to perform exactly the numerical integration);
- to develop a small computer program to compute the eigenvalues $\tilde{\omega}_i^2$ of Equation (P5.8.a) versus the rotation speed parameter $\tilde{\Omega}^2$ for a specified value of eccentricity ratio η over a range $\tilde{\Omega}^2 \in [0, \tilde{\Omega}_{\max}^2]$;
- to plot the first two eigenvalues $\tilde{\omega}_1^2$ and $\tilde{\omega}_2^2$ over the rotation speed range $\tilde{\Omega}^2 \in [0, 10]$ for the eccentricity ratios $\eta = 0, 0.05, 0.1, 0.15$;
- to comment the results obtained.

Problem 5.9 let us consider the same aircraft structural model as addressed in Example 5.1, but now submitted to a wind gust generating an anti-symmetric load distribution over the wing as displayed on Figure 5.31. The dynamic response of the structure has thus to be developed in terms of the anti-symmetric modes of the structure. The antisymmetric load distribution takes the form:

$$p_{wg}(x, t) = \begin{cases} \frac{2p_0 x}{\ell} \sin(\omega_f t) & t < T_I \\ 0 & t \geq T_I \end{cases} \quad (\text{P5.9.a})$$

where the load application time interval T_I corresponds to one-half period of the first antisymmetric mode.

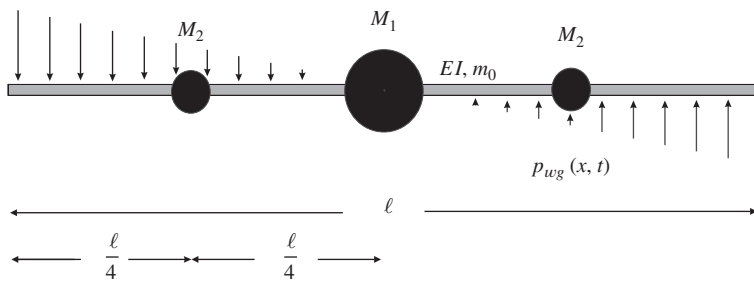


Figure 5.31 Crude model of an aircraft wing submitted to antisymmetric wind gust: approximation by the Rayleigh–Ritz method.

You are asked:

- to build a set of three \mathbf{M} -orthogonal antisymmetric interpolation functions allowing to describe the anti-symmetric displacement field of the structure;

- to express the stiffness and mass matrices of the Rayleigh–Ritz discretized system;
- to compute the eigenvalues and mode shapes of the system and interpret their physical meaning.
- to compare the magnitude of the eigenvalues obtained to those of the symmetric eigenmodes found in (E5.1.j);
- to visualize the antisymmetric mode shapes;
- to compute the spatial participation factors of the interpolation functions to the loading;
- to express the bending displacement along the wing axis through modal superposition;
- to plot the bending displacements versus time at $x = \pm \frac{\ell}{4}$ and $x = \pm \frac{\ell}{2}$ over the time interval $[0, 4T_I]$;
- to plot the rigid body rotation of the structure over the same time interval;
- to plot the elastic part of the bending displacements versus time at $x = \pm \frac{\ell}{4}$ and $x = \pm \frac{\ell}{2}$ over the same time interval;
- to compute and display the bending moments versus time at the same points over the same time interval, and compare their magnitude to the symmetric loading case.

Problem 5.10 The vibration analysis of circular Kirchhoff plates can easily be performed using polar coordinates and assuming periodic variation of the solution in the azimuthal direction:

$$w(r, \theta) = R(r)(A \cos k\theta + B \sin k\theta) \quad (\text{P5.10.a})$$

With the the Rayleigh–Ritz method, the displacement field $R(r)$ in the radial direction can be best approximated using beam eigenmodes with same kinematic boundary conditions. The strain and kinetic energies of the plate are then computed from (4.432) and (4.367).

The case to be considered is the *simply supported* circular plate on its external contour. You are asked:

1. to determine which beam eigenfunctions should be taken in the case $k = 0$ to match the kinematic boundary conditions of the simply supported circular plate;
2. to approximate the fundamental eigenvalue of the plate by the *Rayleigh* (i.e. using one interpolation function) method, and to compare in magnitude the result obtained to the fundamental eigenvalue of the clamped circular plate;
3. to compute the first two axisymmetric eigensolutions ($k = 0$) by the Rayleigh–Ritz method using two interpolation functions; to display the eigenmodes; to observe to which extent the accuracy on the first eigenvalue has been improved;
4. to determine which beam eigenfunctions should be taken in the case $k = 1$ to match the kinematic boundary conditions;
5. Likewise, to compute the first antisymmetric eigensolution ($k = 1$);
6. to determine the multiplicity of the eigenvalue and interpret the physical nature of the corresponding eigenmodes at the light of the degeneracy theorem on multiple eigenvalues (Section 2.3.2).

Note: in the present case the surface integrals involved in the computation of the strain and kinetic energies of the plate can be obtained in closed form (in which case it is advised to use symbolic computation), but it is far more efficient to compute them through numerical quadrature.

Problem 5.11 Let us consider a circular Kirchhoff plate undergoing axisymmetric vibration ($k = 0$). Determining its vibration modes becomes a two-dimensional problem which can be addressed by constructing an axisymmetric finite element model kinematically similar to the beam element, using thus shape functions similar to (5.117) to interpolate the plate deflection in the radial direction. The strain and kinetic energies are computed from (4.432) and (4.367).

You are asked:

- to observe that, contrarily to the beam element, the axisymmetric plate finite element model is built for a specified interval $[r_1, r_2]$ and therefore is not translatable in the radial direction;
- to observe the singularity of the strain energy at $r = 0$;
- to approximate the strain and kinetic energies of a finite element on the interval $[0, R]$ using a two-point Gauss quadrature rule and deduce its stiffness and mass matrices;
- to apply the appropriate boundary conditions to compute the eigensolutions of the simply supported plate using a single finite element;
- to compare the results obtained to those of Problem 5.10.

Problem 5.12 In Section 5.3.1 (Page 411), a closed form solution has been developed for the eigensolutions of the clamped-free bar in extension. The mode shapes and eigenvalues are given by Equations (5.101–5.102). The elastic deformation under a given eigenmode generates a dynamic axial stress distribution that can be computed as:

$$N(x) = \frac{du}{dx} \quad (\text{P5.12.a})$$

you are asked:

- to determine the type of spatial variation obtained for the strain in a bar from the finite element discretization;
- to compute the closed form expression of the axial stress vector obtained for eigenmode r of the clamped-free;
- to display its spatial shape for modes 1 and 2 using a finite element model of five elements.

Problem 5.13 Computing the dynamic stresses in a structure modelled by finite elements implies the a priori computation of a stress matrix T_e such that:

$$\sigma_e = T_e q_e \quad (\text{P5.13.a})$$

Generally, the stress vector σ_e collects average values of the characteristic stresses in the element. You are asked:

- to compute the stress matrix of a beam element providing the *average* values of the bending moment and shear force in the element;
- to compute and display the bending moment and shear force diagrams for the modes of the clamped-clamped beam of Figure 5.21 modelled with three finite elements.

Problem 5.14 The aircraft model of Figure 5.1 already considered in Example 5.1 (symmetric case) and in Problem 5.9 (antisymmetric case) can easily be treated using a simple finite element model. However, the resulting number of degrees of freedom for the model would

not allow to perform the analysis by hand. The problem will thus be solved numerically by developing an appropriate piece of software (using any numerical toolbox). The steps of the analysis will be as follows:

1. Assume in all generality that the loading on an element connecting nodes i and $i + 1$ is of the form:

$$p(x, t) = \left(p_i \left(1 - \frac{x}{\ell} \right) + p_{i+1} \frac{x}{\ell} \right) \phi(t) \quad (\text{P5.14.a})$$

and deduce from Equation (P5.14.a) the discretized load vector $\mathbf{p}_e(t)$.

2. Develop functions or procedures to generate the matrices (stiffness and mass matrices, load vector, stress matrix) describing a single element e .
3. Perform the assembly of the structural model following the assembly procedure described in Section 5.3.1, page 412.
4. Solve the eigenvalue problem using the eigensolution method provided by the numerical toolbox (e.g. 'eig(K,M)' function).
5. Compare the solutions obtained to those of Example 5.1 (symmetric case) and in Problem 5.9 (antisymmetric case).
6. Apply the modal superposition method to compute the dynamic response under symmetric loading (Figure 5.1). Compare the global and elastic displacements versus time obtained with the results of the solution developed in Example 5.1.
7. Repeat the same dynamic response analysis under antisymmetric loading (Figure 5.31).

Note: All results can be obtained in nondimensional form by assuming that the beam characteristics (bending stiffness EI , mass per unit length m , wing half-span ℓ and load intensity p_0 have unit value).

References

- Argyris J *et al.* 1954 Energy theorems and structural analysis: A generalized discourse with applications on energy principles of structural analysis including the effects of temperature and non-linear stress-strain relations. *Aircraft Engineering and Aerospace Technology* **26**(11), 383–394.
- Barton M 1951 Vibration of rectangular and skew cantilever plates. *ASME Jnl. Appl. Mech.* pp. 129–134.
- Bathe K 1996 *Finite Element Procedures in Engineering Analysis*. Prentice Hall, Englewood Cliffs NJ.
- Batoz J and Dhatt G 1990 *Modélisation des structures par éléments finis* vol. 1, 2 and 3. Presses Université Laval.
- Bisplinghoff RL, Ashley H and Halfman R 1955 *Aeroelasticity*. Addison-Wesley, Cambridge, Mass.
- Blevins R 1979 *Formulas for Natural Frequency and Mode Shape*. Van Nostrand Reinhold.
- Clough RW 1965 The finite element method in structural mechanics. *Stress Analysis* pp. 85–119.
- Cook RD, Malkus DS, Plesha ME and Witt RJ 2007 *Concepts and Applications of Finite Element Analysis* 4th edn. John Wiley & Sons, Inc. New York.
- Courant R 1943 Variational methods for the solution of problems of equilibrium and vibrations. *Bull. Amer. Math. Soc* **49**(1), 23.
- Craveur JC 1996 *Modélisation des structures, calcul par éléments finis*. Masson, Paris.
- Craveur JC and Jetteur P 2010 *Introduction à la mécanique non linéaire*. Dunod, Paris.
- Crisfield MA 1991 *Nonlinear Finite Element Analysis of Solids and Structures. Volume 1: Essentials*. John Wiley & Sons, Inc. New York.
- Dhatt G and Batoz JL 1990 *Modélisation des structures par éléments finis: poutres et plaques* vol. 2. Hermes.
- Dhatt G, Touzot G *et al.* 2012 *Finite Element Method*. John Wiley & Sons, Inc. New York.
- (ed. Zienkiewicz OC and Holister GS) 1965 *Stress Analysis: Recent Developments in Numerical and Experimental Methods*. John Wiley & Sons, Inc. New York.

- Fraeijns de Veubeke B 1965 Displacement and equilibrium models in the finite element method In *Stress Analysis: Recent Developments in Numerical and Experimental Methods* (ed. Zienkiewicz OC and Holister GS) John Wiley & Sons, Inc. New York, pp. 145–197.
- Fung Y 1955 *An Introduction to the Theory of Aeroelasticity*. John Wiley & Sons, Ltd, Chichester.
- Galerkin BG 1915 Series solution of some problems of elastic equilibrium of rods and plates. *Vestn. Inzh. Tekh* **19**, 897–908.
- Gallagher RH 1975 *Finite Element Analysis: fundamentals* Civil Engineering and Engineering Mechanics Series. Prentice-Hall, Englewood Cliffs.
- Gérardin M. 1970 Computational efficiency of equilibrium models in eigenvalue analysis *Proceedings of the IUTAM Colloquium on High Speed Computing of Elastic Structures*, Liège.
- Gérardin M and Cardona A 2001 *Flexible Multibody Dynamics: The Finite Element Method Approach*. John Wiley & Sons, Ltd, Chichester.
- Hughes TJR 1987 *The Finite Element Method – Linear Static and Dynamic Finite Element Analysis*. Prentice Hall Inc., New Jersey.
- Lord Rayleigh BJWS 1894 *Theory of Sound, Vol. 1* 2nd edn. Macmillan and Co., London and New York (first edition in 1877).
- Meirovitch L 1967 *Analytical Methods in Vibrations*. The Macmillan Company, New York.
- Oden J and Reddy J 1976 *An Introduction to the Mathematical Theory of Finite Elements*. John Wiley & Sons, Inc. New York.
- Renotte E 1990 Visualisation de modes normaux de vibration par interférométrie holographique. Student final project, University of Liège, Belgium.
- Ritz W 1909 Über eine neue Methode zur Lösung gewisser Variationsprobleme der Mathematischen Physik. *Journal für die Reine und Angewandte Mathematik* **135**, 1–61.
- Samcef. 1992 *Samcef manual: Asef–Stabi–Dynam–Repdyn (M4)* Samtech SA Liège, Belgium.
- Strang G and Fix GJ 1973 *An Analysis of the Finite Element Method*. Prentice-Hall, Englewood Cliffs.
- Turner M, Clough RW, Martin HC and Topp L 1956 Stiffness and deflection analysis of complex structures. *J. Aero Space Sci* **23**, 805–823.
- Zienkiewicz O 1977 *Finite Element Method*. (Published 1967 as *Finite Element Method in Structural and Continuum Mechanics*; published 1971 as *Finite Element Method in Engineering Science*). McGraw Hill.
- Zienkiewicz O and Taylor R 1989 *The Finite Element Method* 4th edn. McGraw-Hill. 2 volumes.

6

Solution Methods for the Eigenvalue Problem

Fifty years ago, an entire chapter devoted specifically to the numerical solution of the eigenvalue problem in a book devoted to mechanical vibration would not exist, or would be reduced to its simplest expression. For a long time, computing the Rayleigh quotient using a supposedly good approximation of the first eigenmode was common practice. Eventually, a method based on the development of the characteristic equation of the eigenvalue problem was used to get the first two or three eigensolutions.

A significant breakthrough has been the development of the power algorithm since the latter allows us to compute the first eigensolution of an eigenvalue problem regardless of its size. According to the engineering community the method was proposed and first published in Mises and Pollaczek-Geiringer (1929), but mathematicians object that the principle of the power algorithm has been introduced earlier by (Muntz 1913). Although the application of the method to vibration problems of aeronautical engineering was already advised in Frazer *et al.* (1938), the full potential of the method could not be exploited by hand computing.

During the period 1950–1960, tremendous progress was achieved with the fundamental work of several numerical analysts. The Jacobi method for real symmetric matrices (Jacobi 1846) was rediscovered and improved (e.g. Forsythe and Henrici 1960). The concept of the reduction to tridiagonal form of a symmetric matrix was introduced by Givens (1953) in order to avoid the iterative character of the Jacobi method. The same algorithm was proposed in a different but more efficient form in Householder (1958). More general transformation methods such as the LR (Rutishauser 1958) and QR (Francis 1961, 1962) were also proposed to treat the unsymmetric eigenvalue problem.

Following a different path, Lanczos (1950) investigated the concept of Krylov's sequence (Krylov 1931). He has shown that orthogonalization of the Krylov vectors can be achieved through an orthogonalization scheme similar to the conjugate gradient method (Hestenes and Stiefel 1952) applicable to the solution of symmetric static problems, and that the resulting sequence of transformations generates a reduced eigenvalue problem of tridiagonal form that spans the lower eigenspectrum of the initial eigenvalue problem. The concept was also generalized by Arnoldi (1951) to unsymmetric problems.

The concept of subspace iteration starts in 1957 with H. Bauer's work (Bauer 1957) under the name of *Treppen* (stairs) iteration with orthogonalization.

In 1965 appears the seminal reference book (Wilkinson 1965) which sums up all the progress accomplished regarding the solution of the algebraic problem. It still remains a bible for numerical analysts specializing in the solution of the algebraic eigenvalue problem.

Until the late 60s the structural engineering community was generally considering the solution of a static problem of type $\mathbf{K}\mathbf{q} = \mathbf{p}$ and the solution of an eigenvalue problem $\mathbf{K}\mathbf{x} = \omega^2\mathbf{M}\mathbf{x}$ as two completely different problems. There was very little interaction inside engineering offices between specialists of static analysis and structural dynamics.

The situation changed drastically during the 1960–1970 period with the appearance of new concepts, namely:

- *Dynamic reduction.* It is during the 1960–1970 period that computer technology started its exponential development, but the main bottleneck then faced by structural dynamicists was the *number of degrees of freedom barrier*.¹ The first implementations of the finite element method could already take into account the model topology to generate sparse stiffness matrices. It was immediately observed that the sparse character of the stiffness matrix could be exploited in developing specific solution methods such as the frontal method (Irons 1970) to take into account only the active profile and develop out-of-core solution procedures. On the other hand, it became also clear that, while it is important to generate sufficiently detailed finite element models to get accurate representation of internal stresses, using a large set of degrees of freedom to model the inertia load distribution is superfluous. The concept of *dynamic reduction* which consists in partitioning the system degrees of freedom and transferring in a static manner the inertial load distribution on a reduced set of degrees of freedom was thus introduced. The principle of static condensation for dynamic problems was published simultaneously but independently by Irons (1965) and Guyan (1965). It was rapidly extended to *dynamic substructuring*, a technique which consists in enriching the reduced set of degrees of freedom with amplitudes of some free vibration modes (Craig and Bampton 1968). Originally, dynamic reduction was viewed as a *degrees-of-freedom economizer*, but revealed itself later on a very useful concept for other purposes. For example, despite the fact that the number of degrees of freedom barrier was rapidly raised, dynamic reduction is still widely used today in the context of large projects involving exchange of large-size dynamic models between teams and/or softwares.
- *Inverse iteration.* The other significant step made during the 1960–1970 period has been to recognize that the problems of static solution and eigenvalue analysis should not be dissociated as done before. As the size of the eigenvalue problem increases, efficiency of its numerical solution can only be achieved following a two-step strategy based on the inverse power iteration scheme. The first step consists in computing the successive iterates of the power method as a sequence of static problems to build up a *subspace spanning the fundamental eigensolutions* of the original problem. The second step then consists in solving the so-called *eigenvalue interaction problem* whose solutions approximate those of the lower frequency solutions of the original problem. All variants of the *Lanczos algorithm* and of

¹ For example, a machine such as the IBM 7040 available for scientific computing in 1968 was equipped with a memory of 16K words of 36 bits and the technology of virtual memory did not exist, which limited de facto the size of the front of equations to less than 180 degrees of freedom. Out-of-core implementation of the static problem could already be developed using magnetic tapes as sequential auxiliary memory.

the *subspace iteration method* (Bathe and Wilson 1972) which are nowadays considered as standard eigensolvers for finite element analysis fall into this category.

As a result, it turns out that the efficiency of eigensolution extraction algorithms for the generalized problem $\mathbf{K}\mathbf{x} = \omega^2\mathbf{M}\mathbf{x}$ is largely dependent on that of the linear solver used to solve the sequence of static problems needed to construct the subspace in which the solution will be sought for. This explains why a significant part of the material that follows is devoted to the description of efficient linear solvers.

The progress achieved in the last two decades lies essentially in the optimization and efficient computer implementation of nowadays well-known algorithms. Considerable progress has been achieved on topics such as robust improvement of the eigenvalue extraction process, implementation of storage schemes for minimization of computational cost, development of powerful substructuring methods, implementation of efficient parallel computing strategies, etc. Extracting today the first hundred eigensolutions of a problem with from 10^6 to 10^7 degrees of freedom requires probably less effort to a structural analyst disposing of appropriate software and hardware resources than to his elder to extract the first ten eigensolutions from a system with 150 unknowns 50 years ago.

Let us underline the fact that the main objective of this chapter is not to present all the latest developments. Doing so would render the material presented obsolete almost immediately. The purpose is rather to focus on the principle of the methods, to understand their fundamental behaviour and to identify their possible strengths and drawbacks. The matrix methods for solving the generalized eigenvalue problem of structural dynamics described in this chapter are in fact relevant to the more general discipline referred to as *matrix structural analysis*. A very interesting description of the milestones jumped over to lead to the current stage of knowledge and capability in matrix structural analysis can be found in Felippa (2001).

Finally, two important related topics are developed at the end of the chapter.

- *Error analysis*. Since all eigenvalue extraction methods are approximate, it is important to dispose of methods that allow us to characterize a posteriori the *computational error* affecting the obtained eigensolutions. Error bound algorithms are thus presented to bracket the computed eigenvalues between upper and lower bounds.
- *Eigensolution sensitivity*. It is often important to determine in which manner the eigensolutions of a physical system will be affected by a stiffness or mass change. Therefore the methodology to compute the derivatives of eigensolutions with respect to design parameters (e.g. material properties, geometric parameters, lumped masses and/or stiffnesses) is briefly presented.

Definitions

The list below complements the general definitions given in the book introduction, but remains local to Chapter 6.

- superscript denoting a truncated set of eigensolutions (modal synthesis).
- ~ superscript denoting quantities of a condensed system (matrices, eigenvalues, eigenmodes).
- + superscript denoting quantities of a condensed system (matrices, eigenvalues, eigenmodes).

B	subscript referring to boundary dof (modal synthesis).
C	subscript referring to condensed dof (Guyan-Irons method).
I	subscript referring to internal dof (modal synthesis).
R	subscript referring to retained dof (Guyan-Irons method).
\mathbb{E}_k^p	approximation of subspace \mathbb{E}^p at iteration k .
C	Choleski's lower triangular factor of a positive definite matrix (e.g. mass matrix).
D	dynamical matrix.
D_k	deflated dynamical matrix.
E	residual error matrix (Lanczos method).
$K_{,p}$	sensitivity of stiffness matrix on parameter p .
\tilde{K}_k	reduced stiffness matrix at iteration k (subspace iteration).
$M_{,p}$	sensitivity of mass matrix on parameter p .
\tilde{M}_k	reduced mass matrix at iteration k (subspace iteration).
P_k	M-orthogonal projection operator.
P_U	projection operator filtering the rigid body modes U .
Q_r	Hermitian operator (Householder's method).
R	rotation operator (Jacobi method).
S	symmetric iteration matrix.
S_k	transformed symmetric iteration matrix at step k .
T	iteration matrix of Arnoldi and Lanczos methods.
U	matrix of the rigid body modes.
V_k	matrix of eigenmodes of iteration problem at iteration k .
X^p	matrix of first p eigenmodes.
X_k^p	matrix of first p eigenmodes at iteration k .
Z_k	matrix spanning eigenmode subspace \mathbb{E}^p at iteration k .
Z_k^*	orthogonalized directions of matrix Z_k .
$p_{(r)}$	inertia load distribution of eigenmode $x_{(r)}$.
r	residual error vector.
u_r	unitary vector to build Hermitian operator Q_r .
$v_{(s)}$	eigenmode s of interaction problem.
$x_{(s),k}$	approximation of eigenmode $x_{(s)}$ at iteration k .
$y_{(r)}$	eigenmode r of symmetric iteration matrix S .
y_p	inertia load distribution of iterate z_p .
z_p	iteration vector at iteration p (power iteration method).
N_{it}	number of iterations to convergence (power iteration).
$P(\lambda)$	characteristic polynomial of a matrix.
$Q(S)$	sum of the squared non diagonal terms of matrix S .
a_{ip}	upper triangle coefficients of interaction matrix (Arnoldi method).
m	number of nullspace vectors, or of rigid body modes, or. size of reduction basis.
\tilde{Q}^2	eigenvalues of interaction problem.
$\Delta(\lambda)$	determinant of characteristic polynomial.
α_k	diagonal coefficients of Lanczos' interaction matrix.
γ_k	lower-diagonal coefficients of interaction matrix (Arnoldi and Lanczos methods).
ϵ	user defined tolerance or infinitesimal quantity.

λ	eigenvalue $\frac{1}{\omega^2}$ of dynamic matrix D .
$\lambda_{i(c)}$	computed eigenvalue.
λ_{k_p}	approximation to eigenvalue λ_k at iteration p .
μ	shift for the eigenvalue problem.
ρ_{2p}	Rayleigh quotient associated to iteration vector z_p .
ρ_{2p+1}	Schwarz quotient formed with iteration vectors z_p and z_{p+1} .
σ	error measure coefficient for eigenvalues.
θ	rotation angle (Jacobi method).

Independent matrix notations are used in Section 6.6 to describe the solution of an arbitrary linear system $Ax = b$.

A	$n \times n$ arbitrary matrix.
A^+	generalized inverse of A .
B	matrix of linear constraints.
C	$n \times n$ positive definite lower triangular matrix.
D	$n \times n$ diagonal matrix.
L	$n \times n$ lower triangular matrix with unit diagonal.
P	permutation operator.
N	null space of A (dimension $n \times m$).
U	$n \times n$ upper triangular matrix.
W	$(n - m) \times m$ matrix (computation of nullspace).
h	right-hand side of linear constraints.
b	right-hand side vector.
n_r	nullspace vector for a general matrix A .
x	vector of unknowns.
m	dimension of nullspace.
n	matrix dimension.

6.1 General considerations

We have seen that the problem of determining the natural vibration frequencies and the associated mode shapes of a mechanical system in discrete form always leads to solving the eigenproblem of the homogeneous linear system:

$$Kx = \omega^2 Mx \quad (6.1)$$

where the mass and stiffness matrices are nearly always symmetric and positive definite. However, they become semi-positive definite when:

- all the degrees of freedom are not mass-supplied,
- the system contains rigid-body modes.

The situation often occurs in which constraints are imposed between degrees of freedom by the Lagrange multiplier method. In that case, the problem remains semi-positive definite in the subspace of the solutions fulfilling the constraining conditions.

It is supposed that the eigensolutions of an n -degree-of-freedom system are numbered in the following order:

$$\begin{cases} 0 \leq \omega_1^2 \leq \omega_2^2 \leq \dots \leq \omega_n^2 \\ \mathbf{x}_{(1)}, \mathbf{x}_{(2)}, \dots, \mathbf{x}_{(n)} \end{cases} \quad (6.2)$$

6.1.1 Classification of solution methods

The different methods that can be used to solve the eigenproblem (6.1) belong to one of the following categories:

- Methods based on the development of the *characteristic equation* of the eigenvalue problem, namely $\det(\mathbf{K} - \omega^2 \mathbf{M}) = 0$.
- Methods based on the *calculation of the determinant* $d(\omega^2) = \det(\mathbf{K} - \omega^2 \mathbf{M})$ for sequences of estimates ω^2 .
- Methods based on the application of *successive transformations* which reduce the initial problem either to the diagonal or to the tridiagonal form.
- Iteration methods on the *eigenvectors*.
- Iteration methods on the *eigenvalues*.
- *Staged methods* based on the preliminary construction of a subspace containing an approximation to the solutions which are to be found. This subspace itself can be generated either by iteration on the eigenvectors, by a condensation or by substructuring techniques. The final problem then consists of solving an *interaction problem* in the constructed subspace.

6.1.2 Criteria for selecting the solution method

The choice of an appropriate method (Géradin 1978) for the computation of eigenvectors of Equation (6.1) depends on a number of criteria, the most important of which are now discussed.

Number of degrees of freedom in the system

We can define in a fairly heuristic way different classes of problems according to their number of degrees of freedom n :

- Class I: $0 \leq n \leq 10$
- Class II: $10 \leq n \leq 1\,000$
- Class III: $1\,000 \leq n \leq 10\,000$
- Class IV: $10\,000 \leq n \leq 1\,000\,000$
- Class V: $n > 1\,000\,000$

For problems belonging to class I, we can directly develop the characteristic equation by semi-analytical methods.

Problems of class II can always be solved in the central memory of standard computers and therefore are well adapted to the use of standard methods well known in numerical analysis (Jacobi's method, power algorithm with deflation, and Givens–Householder's method).

The problems of class III can also be solved in central memory on condition that full benefit is taken from the band character of the \mathbf{K} and \mathbf{M} matrices resulting from the finite element method. Methods based on the reduction concept can also be applied to these problems.

Due to the high complexity of real systems and because of the accuracy required for their analysis, most eigenvalue problems formulated by finite elements belong to class IV. The most effective solution method then consists of transforming the eigenvalue problem into a sequence of static equations having the form $\mathbf{K}\mathbf{x} = \mathbf{p}$. Methods derived from the power algorithm such as the inverse iteration method (with or without spectral shifting), the subspace method and Lanczos' method are all based on this principle. For these methods, a static solution algorithm is used which takes maximum advantage of the very sparse topology of the \mathbf{K} matrix (e.g. frontal method, 'skyline' method and sparse solvers). The mass matrix \mathbf{M} is then implied only in matrix-times-vector operations.

Nowadays, engineers often have to face problems belonging to class V: in this case, the same base methods as for class IV are applied but their implementation on supercomputers must be optimized according to numerous aspects. These include:

- efficient handling of inputs and outputs,
- taking account of vectorization,
- exploitation of parallel computing.

Obviously, due to the increasing computer power and memory capacity of modern computers, the numbers of degrees of freedom defining the different categories in the discussion above change over time. But the effective handling of large structural problems is and will remain for a long time a very important research field.

Number of required eigenvalues

This number can vary considerably depending on the application field and the type of analysis performed on the model. For all vibration problems in mechanics the lowest frequencies of the spectrum are usually the most interesting ones. On the other hand, for problems in acoustics, one may be mainly interested in determining the eigenspectrum in the mid or high frequency range.

In most cases, we should evaluate not more than about 30 eigensolutions. However, we may have to carry the spectrum calculation further for high modal density structures, or when the excitation frequency for modal expansion methods is fairly high.

Required frequency spectrum

This criterion has already been mentioned in the previous paragraph. In most cases, the different methods which are used lead naturally to calculation of the eigenvalues in the

increasing modulus order. However, some methods (e.g. the spectral shifting) make it possible to have direct access to a given range of the spectrum without having to calculate the lowest frequencies.

Preservation of the sparse character of the K and M matrices

This criterion has to be taken into account when we examine problems of class III or higher. We will briefly discuss the storage methods of K and M and the solution methods which make use of the particular topology of the matrices.

Ability to separate close eigenvalues

From a numerical point of view the problem related to the presence of almost identical eigenvalues is critical; it very often occurs when dealing with structures which have numerous symmetries or which result from the repetition of the same basic component (for instance spatial trusses and turbine disks). Consequently, it is essential that the applied methods allow computation of close eigenvalues.

Rate of convergence

The rapid convergence of a solution method is important to limit the computational burden (i.e. computational effort per iteration times the number of iterations needed) and to avoid accumulation of numerical errors. This criterion is closely linked to the previous one, since the convergence of eigensolution extraction methods depends essentially on the existence of close eigenvalues.

Computational cost

The computational cost of a given calculation can be broken down into the following factors:

- CPU cost,
- cost of input–output operations,
- congestion of the computer memory,
- complexity and difficulty of bringing the algorithm into operation.

Computational effectiveness is also a matter of programmers' know-how, and thus the computational cost of a given algorithm can vary significantly depending on its implementation.

Automatic extraction of the rigid-body modes

Since structures frequently have rigid-body modes (analysis of remote components, rotating shafts, flying aircraft, satellites, etc.), it is important that the algorithm automatically detects their presence. They then appear to be associated with a zero frequency, or multiple zero frequencies in the case of several distinct rigid-body modes.

The automatic determination of rigid-body eigenvectors also makes it possible to spot potential mechanisms.

Handling of coupled problems

Some interaction problems, such as the ones involving fluid–structure coupling (e.g. sloshing of liquid in a tank, loudspeaker oscillations, and vibration of an immersed structure), may lead to eigenvalue problems of type (6.1), but with \mathbf{K} and \mathbf{M} matrices of very particular topologies. The handling of problems of this sort has implications both for the choice of the algorithm and for its application.

Use within the substructuring context

The substructuring concept is frequently used in the dynamic analysis of structures. Substructuring consists in sectioning the structure to be studied and in working out separately the modal analysis of each of the substructures. Decomposing the problem may be useful either to make the analysis easier or to share the responsibilities for its achievement. The modal analysis of the whole structure is then performed by assembling the results obtained for each substructure.

The use of substructuring has implications for the solution method to be used, especially concerning:

- the topology of the matrices resulting from the reduction of each substructure,
- the choice of the modes selected for each part.

6.1.3 Accuracy of eigensolutions and stopping criteria

Since eigenvalues are related to the roots of the characteristic polynomial of the eigenproblem, closed-form solutions can only be found in simple cases such as when the system is described by two or three degrees of freedom. It is readily understood that, for most practical cases, eigensolutions can be found only through successive approximation methods such as described later in this chapter. In other words: eigensolvers are iterative in nature. This raises the issue of defining a measure for the accuracy of the solution and of devising a stopping criterion once the accuracy has reached a user-defined tolerance. An eigensolution being defined as an eigenvector-eigenvalue pair that satisfies the eigenproblem (6.1), several stopping criteria can be devised:

- *Controlling the stabilization of the approximation to the eigenfrequency.* A stopping criterion can be defined based on the eigenfrequency estimates ω_{s_k} obtained at iteration k :

$$\max_s \left| \frac{\omega_{s_k} - \omega_{s_{k-1}}}{\omega_{s_k}} \right| < \epsilon \quad (6.3)$$

where ϵ is a user-defined tolerance. Note that this criterion is monitoring the relative change in eigenfrequency estimates, but does not provide an estimation of the error on the eigenfrequency itself. In particular, when the convergence of the algorithm is slow, this stopping criterion alone does not guarantee a good accuracy of the computed eigenvalues.

- *Computing error bounds on the eigenvalues.* Upper and lower bounds can be computed for the eigenvalues (see Chapter 6.10). For low tolerance (say $\epsilon = 10^{-3}$ or smaller), these bounds are usually sharp enough to define a practical stopping criterion. Note however that

computing the bounds requires additional operations, but at a computational cost usually small compared to that of an iteration of the eigensolver.

- *Controlling the stabilization of the approximation to the eigenvectors.* One can also decide to stop the iterations when the changes in the normalized iterates is under a user-defined tolerance. Monitoring the individual components of the eigenvectors, one sets:

$$\max_{s,j} \left| \frac{[\mathbf{x}_{(s)k} - \mathbf{x}_{(s)k-1}]_j}{[\mathbf{x}_{(s)k}]_j} \right| < \epsilon \quad (6.4)$$

Alternatively one can monitor the L^2 norm of the eigenvectors as in:

$$\max_s \frac{\|\mathbf{x}_{(s)k} - \mathbf{x}_{(s)k-1}\|}{\|\mathbf{x}_{(s)k}\|} < \epsilon \quad (6.5)$$

However in cases where the degrees of freedom are not of the same nature (e.g. displacement and rotations in beam elements) this norm is not a proper engineering measure and one should consider energy norms such as the K -norm:

$$\max_s \frac{\|\mathbf{x}_{(s)k} - \mathbf{x}_{(s)k-1}\|_K}{\|\mathbf{x}_{(s)k}\|_K} < \epsilon \quad (6.6)$$

where $\|\mathbf{x}\|_K$ is defined as $\sqrt{\mathbf{x}^T \mathbf{K} \mathbf{x}}$. Obviously a similar criterion can be devised using an M -norm. Similarly to what was discussed for the monitoring of the stabilization of the eigenfrequency, monitoring the changes in the eigenmodes might not be a good indicator of the accuracy of the eigenmodes in case of slow convergence of the iterations. Also note that monitoring the eigenvectors is obviously closely related to the monitoring of the eigenvalues since they are related through the Rayleigh quotient as explained in Section 2.10.1.

- *Controlling the residual on the eigenproblem.* The original eigenvalue problem (6.1) for which a solution is sought can be interpreted as a force equilibrium between the elastic forces $\mathbf{K}\mathbf{x}$ and the inertia forces $-\omega^2 \mathbf{M}\mathbf{x}$ when the system vibrates freely according to mode \mathbf{x} . Hence a natural stopping criterion consists in checking the force error related to the equilibrium of the estimate k :

$$\max_s \frac{\|\mathbf{K}\mathbf{x}_{(s)k} - \omega_{s_k}^2 \mathbf{M}\mathbf{x}_{(s)k}\|}{\|\mathbf{K}\mathbf{x}_{(s)k}\|} < \epsilon \quad (6.7)$$

Alternatively, premultiplying the eigenvalue problem (6.1) by the static flexibility \mathbf{K}^{-1} (assuming the stiffness matrix to be regular),

$$\max_s \frac{\|\mathbf{x}_{(s)k} - \omega_{s_k}^2 \mathbf{K}^{-1} \mathbf{M}\mathbf{x}_{(s)k}\|}{\|\mathbf{x}_{(s)k}\|} < \epsilon \quad (6.8)$$

This criterion is associated to the dynamical matrix (6.9) introduced in Section 6.2. Once more one has to be aware that when the equilibrium equations are of different nature (e.g. moment and force equilibrium in beam elements), using a L^2 norm in (6.7), (6.8) is not sound from an engineering point of view and energy norms should be used.

The criterion (or combination of criteria) that should be considered is dependent on what the eigensolutions will be used for. In many commercial codes, convergence is monitored through an estimate of the eigenvalue error in order to guarantee a certain accuracy on the eigenfrequencies ω_s .

6.2 Dynamical and symmetric iteration matrices

The dynamical matrix concept allows the initial eigenvalue problem (6.1) to be reduced to the standard form in which eigenvalues of any matrix having positive eigenvalues are computed.

Let us suppose that the system we are dealing with has no rigid-body modes. As long as the stiffness matrix \mathbf{K} is nonsingular the eigenvalue problem can be written as:

$$\mathbf{D}\mathbf{x} = \lambda\mathbf{x} \quad (6.9)$$

on condition that we construct:

$$\mathbf{D} = \mathbf{K}^{-1}\mathbf{M} \quad (6.10)$$

and that we associate its characteristic eigenvalues with the eigenfrequencies of the system by:

$$\lambda_r = \frac{1}{\omega_r^2}$$

Matrix \mathbf{D} defined by (6.10) is called the *dynamical matrix* of the system² and was introduced in (Frazer *et al.* 1938). It can be interpreted as the operator providing the static response resulting from the application of the inertial loading generated by an arbitrary displacement distribution. We will see later in this chapter that the dynamical matrix \mathbf{D} plays a central role in all algorithms based on power iteration to compute eigensolutions and it is therefore also called the *iteration matrix*.

The eigenvalues of (6.9) are set in the following order:

$$\lambda_1 \geq \lambda_2 \geq \dots \geq \lambda_n \quad (6.11)$$

Because the eigenproblem (6.9) is nonsymmetric, the associated problem:

$$\mathbf{D}^T \mathbf{p} = \lambda \mathbf{p} \quad (6.12)$$

may be considered. It is readily seen that its eigenvalues are identical to those of the original problem. However, its eigenvectors have the meaning of inertia force distribution corresponding to the eigenvectors of the initial system:

$$\mathbf{p}_{(r)} = \mathbf{M}\mathbf{x}_{(r)} \quad (6.13)$$

As a matter of fact, the bi-orthogonality relationship between the eigensolutions of (6.9) and those of (6.12) expresses orthogonality between the distinct eigenvectors:

$$\mathbf{p}_{(r)}^T \mathbf{x}_{(s)} = \mathbf{x}_{(r)}^T \mathbf{M}\mathbf{x}_{(s)} = \mu_r \delta_{rs} \quad (6.14)$$

² In the former edition it was referred to as the dynamic flexibility matrix. However, such appellation is somewhat misleading since matrix \mathbf{D} has not the physical meaning of flexibility, and should not be confused with the admittance matrix – sometimes also called also dynamic flexibility matrix – defined in Section 2.6.1.

It is worthwhile to note that from a numerical point of view the explicit construction of the dynamical matrix is not an advantageous operation, since:

- the cost of operation (6.10) is of the order of $O(n^3)$;
- the matrix \mathbf{D} is nonsymmetric and generally full, therefore requiring lots of memory space for storage.

A *symmetric iteration matrix* can be constructed by making use of the symmetry of matrices \mathbf{K} and \mathbf{M} according to the following technique.

Because the mass matrix is by definition positive definite, it can be factorized into a product of a lower triangular matrix \mathbf{C} and its transposed counterpart:

$$\mathbf{M} = \mathbf{C}\mathbf{C}^T \quad (6.15)$$

This factorization is obtained using the *Choleski* triangularization algorithm (see Section 6.6.1, page 447). By substitution of (6.15), the homogeneous linear system (6.9) can be written as:

$$\mathbf{K}^{-1}\mathbf{C}\mathbf{C}^T\mathbf{x} = \lambda\mathbf{x} \quad (6.16)$$

Multiplying (6.16) by \mathbf{C}^T and introducing the change of variables:

$$\mathbf{y} = \mathbf{C}^T\mathbf{x} \quad (6.17)$$

the eigenvalue problem takes the modified form:

$$\mathbf{S}\mathbf{y} = \lambda\mathbf{y} \quad (6.18)$$

with the symmetrized dynamical matrix:

$$\mathbf{S} = \mathbf{C}^T\mathbf{K}^{-1}\mathbf{C} \quad (6.19)$$

The orthogonality relationships between eigenvectors $\mathbf{y}_{(i)}$ are changed into those corresponding to a system of unit mass matrix:

$$\mathbf{y}_{(r)}^T\mathbf{y}_{(s)} = 0 \quad \mathbf{y}_{(r)}^T\mathbf{S}\mathbf{y}_{(s)} = 0 \quad r \neq s \quad (6.20)$$

Once the eigenvectors and eigenvalues of (6.18) are known, the solution of the linear system (6.17) for the restitution of the eigenvectors in the initial coordinates \mathbf{x} requires a simple backward substitution, owing to the upper triangular form of \mathbf{C}^T .

6.3 Computing the determinant: Sturm sequences

Sturm's sequences method can be applied to tridiagonal matrices arising either from a chain-type topology (see the bar in extension example, page 370) or from Householder's reduction (Section 6.4.2).

Let us write the tridiagonal matrix as follows:

$$\begin{bmatrix} c_1 & b_1 & & & 0 \\ b_1 & c_2 & \ddots & & \\ & \ddots & \ddots & \ddots & \\ 0 & & \ddots & b_{n-1} & c_n \end{bmatrix} \quad (6.21)$$

Let $P_r(\lambda)$ be the characteristic polynomial of the r -dimensional diagonal submatrix:

$$\begin{bmatrix} c_1 - \lambda & b_1 & & 0 \\ b_1 & c_2 - \lambda & \ddots & \\ 0 & & \ddots & b_{r-1} \\ & & & c_r - \lambda \end{bmatrix} \quad (6.22)$$

To evaluate $P_{r+1}(\lambda)$, the minor determinant rule gives the recurrence relation:

$$P_{r+1}(\lambda) = (c_{r+1} - \lambda)P_r(\lambda) - b_r^2 P_{r-1}(\lambda) \quad (6.23)$$

with

$$P_0(\lambda) = 1 \quad \text{and} \quad P_1(\lambda) = c_1 - \lambda \quad (6.24)$$

This recursive sequence is known as *Sturm's sequence* and is a very efficient way to compute the determinant of a tridiagonal matrix. From (6.23) and (6.24), it is obvious that:

$$P_r(\lambda) > 0 \quad \text{as} \quad \lambda \rightarrow -\infty \quad (6.25)$$

The properties of the Sturm sequences are based on the following important result:

$$\text{If } P_r(\lambda) = 0, \text{ then } P_{r+1}(\lambda)P_{r-1}(\lambda) < 0 \quad (6.26)$$

The proof holds by multiplying (6.23) by $P_{r-1}(\lambda)$:

$$P_{r+1}(\lambda)P_{r-1}(\lambda) = -b_r^2 P_r^2(\lambda) < 0$$

From (6.26) we deduce the first property (Figure 6.1):

The roots of $P_{r+1}(\lambda)$ bracket those of $P_r(\lambda)$

Let us illustrate this first property by considering the successive characteristic polynomials in the case of $n = 3$. Let us write their roots (Figure 6.1):

$$\begin{array}{ll} \text{for } P_1(\lambda) & v_1 \\ \text{for } P_2(\lambda) & \mu_1, \mu_2 \\ \text{for } P_3(\lambda) & \lambda_1, \lambda_2, \lambda_3 \end{array}$$

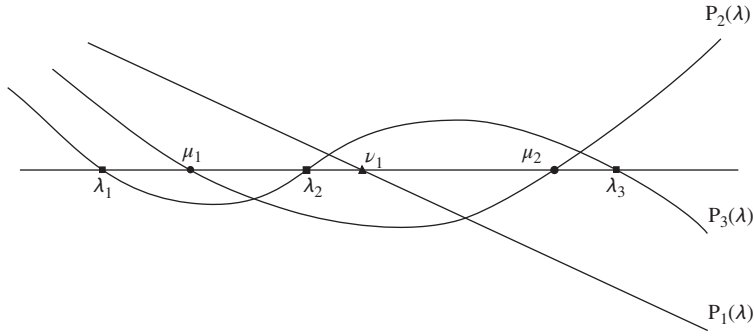


Figure 6.1 Sturm sequences.

For $P_2(\lambda)$, we have $P_2(\pm\infty) = +\infty$ and $P_2(\nu_1)P_0(\nu_1) = P_2(\nu_1) < 0$. Hence, the roots of $P_2(\lambda)$ certainly bracket the characteristic value ν_1 of P_1 , as shown in Figure 6.1. For $P_3(\lambda)$, we also have $P_3(-\infty) = +\infty$, $P_3(+\infty) = -\infty$ and

$$P_3(\mu_1)P_1(\mu_1) = -b_2^2 P_1^2(\mu_1) \quad \text{hence } P_3(\mu_1) < 0$$

$$P_3(\mu_2)P_1(\mu_2) = -b_2^2 P_1^2(\mu_2) \quad \text{hence } P_3(\mu_2) > 0$$

Therefore, we can state that the roots of $P_3(\lambda)$ bracket those of $P_2(\lambda)$, and so on.

Remark 6.1 Strictly speaking, the bracketing takes place only if $b_r \neq 0$, in which case there are no multiple frequencies. Indeed, let μ simultaneously be a root of $P_{r+1}(\lambda)$ and of $P_r(\lambda)$. If $b_r \neq 0$, owing to (6.23), μ would also be a root of $P_{r-1}(\lambda)$. And so on, with $P_0(\mu) = 0$, which is contradictory to (6.24). Hence, if a symmetric matrix has a root of multiplicity k , the corresponding tridiagonal matrix contains $(k - 1)$ zeros under and above the diagonal line. However, the presence of $b_r = 0$ terms does not necessarily imply the existence of multiple roots.

Remark 6.2 It should be observed that the characteristic polynomial $P_r(\lambda)$ can be looked at as the eigenvalue equation associated with an n -degree-of-freedom chain-type structure having its $n - r$ last degrees of freedom fixed. The roots of $P_{r+1}(\lambda)$ are the eigenfrequencies of the latter when there is one less fixed degree of freedom. Hence, the bracketing property of Sturm sequences is a particular case of Rayleigh's theorem on constraints (2.241).

Let us call $a(\lambda)$ the number of sign correspondences in the sequence of characteristic polynomials:

$$\{1, P_1(\lambda), P_2(\lambda), \dots, P_n(\lambda)\}$$

with the convention that if $P_i(\lambda) = 0$, $\text{sign}(P_i(\lambda)) = -\text{sign}(P_{i-1}(\lambda))$. The second property of the Sturm sequences can be expressed as follows:

The number of sign correspondences $a(\lambda)$ is equal to the number of roots of $P_n(\lambda)$ which are strictly higher than λ .

We can easily exhibit this property for the case $n = 3$ by considering Figure 6.1 and setting up the following table:

	$[-\infty, \lambda_1[$	$[\lambda_1, \mu_1[$	$[\mu_1, \lambda_2[$	$[\lambda_2, \nu_1[$	$[\nu_1, \mu_2[$	$[\mu_2, \lambda_3[$	$[\lambda_3, \infty[$
$P_0(\lambda)$	+	+	+	+	+	+	+
$P_1(\lambda)$	+	+	+	+	−	−	−
$P_2(\lambda)$	+	+	−	−	−	+	+
$P_3(\lambda)$	+	−	−	+	+	+	−
$a(\lambda)$	3	2	2	1	1	1	0

Interesting use can be made of the second property by computing the eigenvalues of the tridiagonal matrix (6.21) using a bisection method.

Assuming the eigenvalues are numbered in the decreasing order of their modulus, let us consider the problem of extracting the k th eigenvalue of the tridiagonal matrix. Let α_0 and β_0 be two numbers for which:

$$\beta_0 > \alpha_0 \quad a(\alpha_0) \geq k \quad a(\beta_0) < k \quad (6.27)$$

From this, we deduce that $\lambda_k \in]\alpha_0, \beta_0]$ and we can locate λ_k in an interval $[\alpha_p, \beta_p]$ of width $(\beta_0 - \alpha_0)2^{-p}$ through p iterations by the following algorithm:

1. calculation of the middle point of the interval:

$$\gamma_r = \frac{1}{2}(\alpha_{r-1} + \beta_{r-1})$$

2. construction of the sequence:

$$\{P_0(\gamma_r), P_1(\gamma_r), \dots, P_n(\gamma_r)\}$$

which gives $a(\gamma_r)$;

3. definition of a new interval so that $\lambda_k \in]\alpha_r, \beta_r]$:

- if $a(\gamma_r) \geq k$, we take $\alpha_r = \gamma_r$ and $\beta_r = \beta_{r-1}$
- if $a(\gamma_r) < k$, we take $\alpha_r = \alpha_{r-1}$ and $\beta_r = \gamma_r$.

Various procedures for selecting a starting interval $[\alpha_0, \beta_0]$ to verify (6.27) can be used. For instance, it can be constructed by Gerschgorin's standard method (Wilkinson 1965).

Let us note that the sign correspondence property described above is also true for nontridiagonal matrices. The sign correspondence property forms the basis of the method proposed in (Wittrick and Williams 1971) classically used to solve nonstandard eigenvalue problems of the general form $A(\lambda)x = 0$ arising typically from transcendental formulation of the dynamic stiffness $Z(\omega^2)$ (see Problems 4.3 and 5.3, pages 329 and 403).

Finally let us note that the second property of Sturm's sequences is often used also to verify that no eigenfrequency was forgotten when extracting the eigensolutions with one of the iterative methods outlined later.

6.4 Matrix transformation methods

6.4.1 Reduction to a diagonal form: Jacobi's method

Jacobi's method (Jacobi 1846) yields simultaneously all the eigenvalues of a symmetric matrix (Schwarz *et al.* 1973). Therefore, using it to compute vibration eigenfrequencies of a mechanical system requires the preliminary construction of the symmetric dynamic flexibility matrix (6.19) of the system.

Although it is over a hundred years old, Jacobi's method is still frequently used: indeed, it is characterized by an exceptional stability and a very great simplicity. It can be applied without restriction to any symmetric matrix, whether its eigenvalues are positive, negative or null.

Algorithm

Jacobi's algorithm consists of progressively reducing the initial symmetric matrix to diagonal form by an infinite sequence of orthogonal transformations. To achieve this, we construct a series of matrices verifying the recurrence relationship:

$$\mathbf{S}^{(k+1)} = \mathbf{R}_k^T \mathbf{S}^{(k)} \mathbf{R}_k \quad \text{where} \quad \mathbf{R}_k^T \mathbf{R}_k = \mathbf{I} \quad (6.28)$$

The spectrum of eigenvalues is invariant with respect to the transformation since

$$\begin{aligned} \det(\mathbf{S}^{(k+1)} - \lambda \mathbf{I}) &= \det(\mathbf{R}_k^T \mathbf{S}^{(k)} \mathbf{R}_k - \lambda \mathbf{I}) \\ &= \det(\mathbf{R}_k^T \mathbf{S}^{(k)} \mathbf{R}_k - \lambda \mathbf{R}_k^T \mathbf{R}_k) \\ &= \det(\mathbf{R}_k) \det(\mathbf{S}^{(k)} - \lambda \mathbf{I}) \det(\mathbf{R}_k) = \det(\mathbf{S}^{(k)} - \lambda \mathbf{I}) \end{aligned}$$

The number of orthogonal transformations needed to achieve the diagonal form is infinite, since a polynomial equation cannot generally be solved by a finite number of iterations. In practice, however, the process can be stopped when the nondiagonal terms tend towards zero with the required accuracy.

For simplicity's sake, let us omit the k index and call \mathbf{S}' the transformed matrix $\mathbf{S}^{(k+1)}$. Let s_{pq} be the nondiagonal element of \mathbf{S} which has the largest modulus. We construct the transformation matrix \mathbf{R} in such a manner that:

- the nondiagonal element is nullified by the transformation,
- \mathbf{R} is an orthogonal matrix ($\mathbf{R}^T \mathbf{R} = \mathbf{I}$),
- \mathbf{S}' is different from \mathbf{S} only by the rows and columns p and q .

As a consequence, the \mathbf{R} matrix has to be:

$$\mathbf{R} = \mathbf{I} + (\cos \theta - 1)(\mathbf{e}_p \mathbf{e}_p^T + \mathbf{e}_q \mathbf{e}_q^T) + \sin \theta (\mathbf{e}_p \mathbf{e}_q^T - \mathbf{e}_q \mathbf{e}_p^T) \quad (6.29)$$

where \mathbf{e}_j is the unit vector in the j direction, so that:

$$\begin{aligned} \mathbf{R} \mathbf{e}_j &= \mathbf{e}_j \quad j \neq p, q \\ \mathbf{R} \mathbf{e}_p &= \cos \theta \mathbf{e}_p - \sin \theta \mathbf{e}_q \\ \mathbf{R} \mathbf{e}_q &= \sin \theta \mathbf{e}_p + \cos \theta \mathbf{e}_q \end{aligned}$$

– if we then take:

$$t = \begin{cases} \frac{1}{\alpha + \operatorname{sign}(\alpha) \sqrt{\alpha^2 + 1}} & \text{if } \alpha \neq 0 \\ 1 & \text{if } \alpha = 0 \end{cases}$$

we finally calculate:

$$\cos \theta = \frac{1}{\sqrt{1 + t^2}}$$

$$\sin \theta = t \cos \theta$$

Hence, we have $\cos \theta \geq \frac{1}{\sqrt{2}}$, $|t| \leq 1$, $\sin \theta \leq \frac{1}{\sqrt{2}}$ and the variation interval of θ is:

$$-\frac{\pi}{4} \leq \theta \leq \frac{\pi}{4}$$

Convergence of the method

Jacobi's method has an essentially iterative character, since an element brought to zero by a rotation can generally be made non-null by a further transformation.

The convergence of the method results from the fact that the plane rotations cause a systematic decrease of the sum of the squared nondiagonal terms. Let us define:

$$Q(S) = \sum_{i=1}^n \sum_{\substack{j=1 \\ j \neq i}}^n (s_{ij})^2 \quad (6.31)$$

After rotation we have:

$$Q(S') = \sum_{\substack{i=1 \\ i \neq p,q}}^n \sum_{\substack{j=1 \\ j \neq p,q \\ j \neq i}}^n s_{ij}'^2 + \sum_{\substack{i=1 \\ i \neq p,q}}^n (s_{ip}'^2 + s_{iq}'^2) + \sum_{\substack{j=1 \\ j \neq p,q}}^n (s_{pj}'^2 + s_{qj}'^2) + 2s_{pq}'^2$$

It is easily deduced from relationships (6.30) that the following dimensions are invariant:

$$s_{ij}'^2 = s_{ij}^2$$

$$s_{ip}'^2 + s_{iq}'^2 = s_{ip}^2 + s_{iq}^2$$

$$s_{pj}'^2 + s_{qj}'^2 = s_{pj}^2 + s_{qj}^2$$

If we also take into account the fact that $s_{pq}' = 0$, we obtain the relationship:

$$Q(S') = Q(S) - 2s_{pq}^2$$

showing that the sum of the squared nondiagonal terms is systematically decreased by the successive rotations, implying the convergence of the method.

Supposing that the element of largest modulus has been brought to zero, then:

$$Q(S) \leq \frac{n(n-1)}{2} [Q(S) - Q(S')]$$

or

$$Q(S') \leq \left(1 - \frac{2}{n(n-1)}\right) Q(S)$$

Consequently, the repeated application of the algorithm yields the following inequality:

$$Q(S^{(k)}) \leq \left(1 - \frac{2}{n(n-1)}\right)^k Q(S^{(0)})$$

In particular, if we want to achieve a convergence of t significant figures:

$$\frac{Q(S^{(k)})}{Q(S^{(0)})} < 10^{-t}$$

we have:

$$\left(1 - \frac{2}{n(n-1)}\right)^k < 10^{-t}$$

that is to say, a number of iterations running to:

$$k \simeq \frac{n^2}{2} t$$

Hence, the number of Jacobi iterations to be performed is proportional to the number of required significant figures, but increases in proportion to the square of the matrix dimension n .

On account of this property, the method cannot be applied to large matrices ($n > 50$). Therefore, despite its simplicity and very great stability, it is used in structural analysis only after the initial eigenvalue problem has first been projected onto a sufficiently small subspace.

Variants of the method

If we apply Jacobi's method in its genuine form, we notice that the highest cost of an iteration lies in the process of searching for the largest diagonal element, not in the rotation operation itself.

Hence the interest of Jacobi's cyclic method which consists of successively applying the rotation operator to all nondiagonal elements whatever their size: a cycle of the method corresponds to a scanning of the entire matrix.

The disadvantage of the cyclic method is that during a cycle we may be led to perform a large number of rotations on zero or almost-zero terms. Thus the method can be improved if we apply the rotation to a given element only if the modulus of the element is greater than a prescribed threshold: this is called *Jacobi's threshold cyclic method*. In practice, the threshold is refined as the number of cycles increases: it can be defined as:

$$\left(\frac{s_{ij}^2}{s_{ii}s_{jj}}\right)^{1/2} < 10^{-2m}$$

where m is the number of cycles.

6.4.2 Reduction to a tridiagonal form: Householder's method

Householder's method (Householder 1958; Schwarz *et al.* 1973) is a successive transformation method for reducing the initial matrix to a tridiagonal form in $(n - 2)$ steps. Unlike Jacobi's method, it implies a finite number of transformations.

The eigenvalues of the resulting tridiagonal can be computed either by the bisection method using the properties of Sturm sequences (Section 6.3) or by the *QR algorithm*. Once the eigenfrequencies are found, the associated eigenvectors are obtained by computing the nullspace of $(\mathbf{K} - \omega^2 \mathbf{M})$ as explained in Section 6.6.2.

Because of their low cost, tridiagonalization methods are widely used for solving moderate-size problems; however, they are not suitable for problems of larger size.

Reduction to the tridiagonal form

We aim at constructing successive orthogonal transformation matrices $\mathbf{Q}_1, \mathbf{Q}_2, \dots, \mathbf{Q}_r$ so that the matrix resulting from the r th transformation expressed by:

$$\mathbf{S}_r = \mathbf{Q}_r \mathbf{Q}_{r-1} \dots \mathbf{Q}_1 \mathbf{S} \mathbf{Q}_1^T \dots \mathbf{Q}_{r-1}^T \mathbf{Q}_r^T$$

takes the form:

$$\mathbf{S}_r = \left[\begin{array}{cccccccc} * & * & & & & & & \\ * & * & * & & & & & \\ & * & * & \ddots & & & & \mathbf{0} \\ & & \ddots & \ddots & * & & & \\ & & & * & * & * & * & * \\ & & & & * & * & * & * \\ \mathbf{0} & & & & * & * & * & * \\ & & & & * & * & * & * \end{array} \right] \left. \vphantom{\begin{array}{c} * \\ * \\ * \\ * \\ * \\ * \\ * \\ * \end{array}} \right\} r \text{ rows}$$

$\underbrace{\hspace{10em}}_{r \text{ columns}}$

To do so, we consider elementary Hermitian transformations such as:

$$\mathbf{Q}_r = \mathbf{I}_r - 2\mathbf{u}_r \mathbf{u}_r^T \quad \mathbf{u}_r^T \mathbf{u}_r = 1 \quad (6.32)$$

By definition, these are orthogonal and symmetric, and they can be geometrically interpreted as a reflection with respect to the hyperplane orthogonal to \mathbf{u}_r and passing through the origin.

These transformations are constructed so as to leave the $(r - 1)$ first rows and columns of \mathbf{S}_{r-1} unchanged and to set to zero the nontridiagonal terms of line and column number r ; this condition is fulfilled by equating to zero the first r terms of \mathbf{u}_r . In this way, we come to the tridiagonal form in $(n - 2)$ transformations.

Let us show how to construct \mathbf{Q}_1 . The other matrices are successively obtained through the same algorithm applied to the not yet reduced submatrix.

Let \mathbf{u}_1 be of the following form:

$$\mathbf{u}_1^T = [0 \quad * \quad * \quad * \quad \dots \quad *] \quad (6.33)$$

By premultiplication of S by (6.32) it is possible, by an appropriate choice of the nonzero terms of \mathbf{u}_1 , to transform it into:

$$(\mathbf{I} - 2\mathbf{u}_1\mathbf{u}_1^T)S = \begin{bmatrix} * & * & * & \dots & * \\ * & * & * & \dots & \vdots \\ 0 & * & * & \dots & * \\ \vdots & \vdots & \vdots & \ddots & \vdots \\ 0 & * & * & \dots & * \end{bmatrix}$$

with the first row of the resulting matrix remaining identical to that of S . Since the first column is also not affected by the post-multiplication, we may write:

$$S_1 = (\mathbf{I} - 2\mathbf{u}_1\mathbf{u}_1^T)S(\mathbf{I} - 2\mathbf{u}_1\mathbf{u}_1^T) = \begin{bmatrix} * & * & 0 & \dots & 0 \\ * & * & * & \dots & * \\ 0 & * & * & \dots & \vdots \\ \vdots & \vdots & \vdots & \ddots & \vdots \\ 0 & * & * & \dots & * \end{bmatrix}$$

Hence, the problem consists of finding \mathbf{u} such that:

$$(\mathbf{I} - 2\mathbf{u}_1\mathbf{u}_1^T)\mathbf{s} = \mathbf{c} \quad (6.34)$$

with $\mathbf{u}_1^T\mathbf{u}_1 = 1$, $\mathbf{u}_1 = (0 \quad * \quad * \quad * \quad \dots \quad *)$, $\mathbf{c}^T = (* \quad * \quad 0 \quad \dots \quad 0)$ and \mathbf{s} being the first column of S . We then construct the \mathbf{u}_1 vector by making use of the following lemma.

Lemma

Let \mathbf{x} and \mathbf{y} verify $\mathbf{x} \neq \mathbf{y}$ and

$$\|\mathbf{x}\| = \|\mathbf{y}\| \quad (6.35)$$

Then, there exists a vector \mathbf{u} so that:

$$(\mathbf{I} - 2\mathbf{u}\mathbf{u}^T)\mathbf{x} = \mathbf{y} \quad (6.36)$$

and the latter has the following expression:

$$\mathbf{u} = \frac{\mathbf{x} - \mathbf{y}}{\|\mathbf{x} - \mathbf{y}\|} \quad (6.37)$$

By substituting (6.37) into (6.36), and taking into account (6.35),

$$\begin{aligned} \left(\mathbf{I} - 2 \frac{(\mathbf{x} - \mathbf{y})(\mathbf{x} - \mathbf{y})^T}{(\mathbf{x} - \mathbf{y})^T(\mathbf{x} - \mathbf{y})} \right) \mathbf{x} &= \mathbf{x} - \frac{2(\mathbf{x}^T\mathbf{x} - \mathbf{y}^T\mathbf{x})}{2(\mathbf{x}^T\mathbf{x} - \mathbf{y}^T\mathbf{x})}(\mathbf{x} - \mathbf{y}) \\ &= \mathbf{y} \end{aligned}$$

and the uniqueness of the solution results from the fact that:

$$(I - 2\mathbf{v}\mathbf{v}^T)\mathbf{x} = (I - 2\mathbf{u}\mathbf{u}^T)\mathbf{x}$$

implies $\mathbf{v}(\mathbf{v}^T\mathbf{x}) = \mathbf{u}(\mathbf{u}^T\mathbf{x})$ and thus $\mathbf{u} = \pm\mathbf{v}$. Let us apply (6.36–6.37) to the transformation (6.34) and let us write that \mathbf{c} has the following form:

$$\mathbf{c}^T = [s_{11}, \pm r, 0, \dots, 0] \quad \text{with} \quad \|\mathbf{c}\| = \|\mathbf{s}\|$$

We then obtain:

$$r^2 = \|\mathbf{s}\|^2 - s_{11}^2 = \sum_{j=2}^n s_{j1}^2$$

and the expression of the transformation vector:

$$\mathbf{u}_1^T = \frac{\mathbf{s} - \mathbf{c}}{\|\mathbf{s} - \mathbf{c}\|} = \frac{1}{\|\mathbf{s} - \mathbf{c}\|} [0, s_{21} \mp r, s_{31}, \dots, s_{n1}] \quad (6.38)$$

The resulting matrix \mathbf{S}_1 takes the form:

$$\mathbf{S}_1 = \begin{bmatrix} s_{11} & \pm r & 0 & \dots & 0 \\ \pm r & * & * & \dots & * \\ 0 & * & * & \dots & * \\ \vdots & \vdots & \vdots & \ddots & \vdots \\ 0 & * & * & \dots & * \end{bmatrix}$$

To complete the tridiagonal form, we note that the same transformation can be applied to the subdiagonal matrix of dimension $(n-1)$ without altering the first row and column of \mathbf{S}_1 . In the same way we recursively perform $(n-2)$ transformations with the following vectors:

$$\mathbf{u}_r = \left(\underbrace{0 \ 0 \ 0 \ \dots \ 0}_{r \text{ zeros}} \underbrace{* \ * \ * \ * \ * \ \dots \ *}_{n-r \text{ nonzero terms}} \right)$$

to obtain the tridiagonal matrix \mathbf{S}_{n-2} .

6.5 Iteration on eigenvectors: the power algorithm

The power algorithm (see for instance G  rardin 1973, Wilkinson 1965) is the basis of all methods using iteration on eigenvectors. Its fundamental properties, that render it very attractive in principle, are the following:

- it makes it possible to limit the solving of the eigenvalue problem to the number of required solutions,
- the convergence rate towards a given solution is independent of the matrix size, which potentially makes it the ideal method for very large systems.

However, in its fundamental form as described in this section, it has two important drawbacks:

- It requires the explicit construction of the dynamical matrix (6.10) or (6.19).
- Its convergence properties deteriorate exponentially with the difference between two or several close eigenvalues.
- It is not directly applicable in the presence of rigid body modes.

Some remedies can be used:

- On one hand, the inverse iteration concept makes it possible to avoid the explicit construction of an iteration matrix: the method then implies disposing of appropriate solvers for the efficient solution of a sequence of static problems.
- On the other hand, convergence in the presence of close eigenvalues can be improved considerably in two different ways:
 - Performing inverse iteration together with spectral shifting allows to increase considerably the convergence by enlarging the relative distance between neighbouring eigenvalues.
 - Subspace construction methods aim at computing a subspace spanning the eigensolutions rather than directly computing them. The size of the eigenproblem to be solved is then considerably reduced, so that its solution becomes fast and accurate. *Subspace iteration* and the *Lanczos algorithm* are the most widely used methods falling into that category.

However, the very kernel of inverse iteration and subspace iteration methods consists in solving a relatively large sequence of linear problems. Therefore, before presenting these important developments of the power iteration algorithm, the entire Section 6.6 will be devoted to the efficient solution of linear problems. The present section concentrates on the basic features of the algorithm.

6.5.1 Computing the fundamental eigensolution

A solution by iteration of the standard problem $D\mathbf{x} = \lambda\mathbf{x}$ is obtained by forming the successive \mathbf{z}_p of an arbitrary starting vector \mathbf{z}_0 by the relation:

$$\boxed{\mathbf{z}_{p+1} = D\mathbf{z}_p} \quad (6.39)$$

In order to understand why this very simple procedure converges to an eigenvector, let us view the starting vector in its normal modes expansion form:

$$\mathbf{z}_0 = \sum_{i=1}^n \alpha_i \mathbf{x}_{(i)} \quad (6.40)$$

the modes $\mathbf{x}_{(i)}$ being ordered in such a way that the associated eigenvalues are set in decreasing order:

$$\lambda_1 \geq \lambda_2 \geq \dots \geq \lambda_n \quad (6.41)$$

Obviously the modal coordinates α_i in (6.40) are not known and depend on the choice of the arbitrary starting vector. After p successive applications of the algorithm (6.39) to the starting

vector (6.40) the modal expansion of the iterate becomes:

$$\mathbf{z}_p = \mathbf{D}^p \mathbf{z}_0 = \lambda_1^p \left(\alpha_1 \mathbf{x}_{(1)} + \sum_{i=2}^n \alpha_i \left(\frac{\lambda_i}{\lambda_1} \right)^p \mathbf{x}_{(i)} \right) \quad (6.42)$$

In view of the order selected in (6.41) for the characteristic values sequence, and disregarding for now the case of multiple eigenvalues, the quotients (λ_i/λ_1) remain less than 1 and their powers $(\lambda_i/\lambda_1)^p$ tend towards zero when p is sufficiently large. Thus, for $p \rightarrow \infty$,

$$\mathbf{z}_p \rightarrow \lambda_1^p \alpha_1 \mathbf{x}_{(1)} \quad (6.43)$$

and

$$\mathbf{z}_{p+1} \rightarrow \lambda_1^{p+1} \alpha_1 \mathbf{x}_{(1)} \quad (6.44)$$

So, if $\alpha_1 \neq 0$ and if $\lambda_1 \neq 0$, the iterates converge to *the first eigenmode* and the ratio of corresponding nonzero components of two successive iteration vectors tends towards the largest eigenvalue λ_1 . In the fortuitous case of α_1 being null, the starting vector has no first mode component and, in theory, the iterates will converge to the next eigenmode. In practice, however, due to buildup of round-off errors in the numerical computation of the iterates, a small component of $\mathbf{x}_{(1)}$ will appear and the iterates will still converge to the fundamental solution, but slowly.

From a practical point of view, in order to avoid an excessive increase or decrease of the components of two successive iteration vectors because of the factor λ_1^p in (6.42), the iterates will be normalized and the power algorithm will be:

$$\begin{cases} \mathbf{z}_{p+1}^* = \mathbf{D} \mathbf{z}_p \\ \mathbf{z}_{p+1} = \frac{\mathbf{z}_{p+1}^*}{\|\mathbf{z}_{p+1}^*\|} \end{cases} \quad (6.45)$$

The convergence process of the power iteration method is graphically illustrated for the case of $n = 2$ in Figure 6.2. This figure clearly illustrates that the recursive application of matrix \mathbf{D} to a vector amplifies its fundamental modal component more than the other ones so that after several iterations the fundamental mode ‘sticks out’.

The case in which the $m < n$ first characteristic values λ_i are equal (e.g. due to physical symmetry of a structure) does not present any difficulty. Indeed, the algorithm then converges towards their common value λ_1 , and the associated characteristic vector is any linear combination of the m modes $\mathbf{x}_{(i)}$.

On the contrary, the fact that the m first eigenvalues of the algorithm would be close to one another considerably hinders the convergence of the algorithm.

Stopping the iteration process

To obtain an estimate of the eigenvalue corresponding to the approximate eigenvector at iteration $p + 1$, Equations (6.43,6.44) suggest to consider the ratio between a component j of successive iterates, namely:

$$\lambda_{1p} = \frac{z_{p+1,j}^*}{z_{p,j}} \quad (6.46)$$

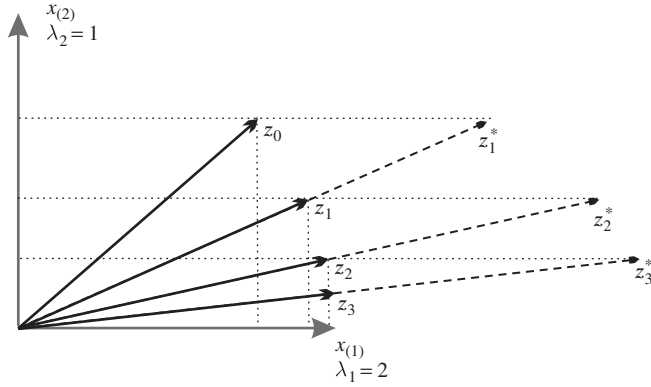


Figure 6.2 Convergence of the power method for $n = 2$ when $\lambda_1 = 2$ and $\lambda_2 = 1$.

which in practice will be computed only for the component j of largest modulus. Alternatively an eigenvalue estimate can be found by forming either the Rayleigh quotient of the original eigenvalue problem (6.1) or a similar quotient with the dynamical matrix (6.9):

$$\lambda_{1_p} = \frac{\mathbf{z}_p^T \mathbf{M} \mathbf{z}_p}{\mathbf{z}_p^T \mathbf{K} \mathbf{z}_p} \quad \text{or} \quad \lambda_{1_p} = \frac{\mathbf{z}_p^T \mathbf{D} \mathbf{z}_p}{\mathbf{z}_p^T \mathbf{z}_p} = \mathbf{z}_p^T \mathbf{z}_{p+1}^* \quad (6.47)$$

Once the iterations have been stopped according to one of the stopping criteria discussed in Section 6.1.3 the approximate eigensolution is obtained as:

$$\begin{cases} \lambda_1 \simeq \lambda_{1_p} \\ \mathbf{x}_{(1)} \simeq \mathbf{z}_{p+1} \end{cases}$$

Algorithm convergence analysis

Since characteristic vectors are defined with any scaling factor, two nonnormalized successive iteration vectors can be expressed by:

$$\begin{aligned} \mathbf{z}_p &= \lambda_1^p \mathbf{x}_{(1)} + \lambda_2^p \mathbf{x}_{(2)} + \dots \\ \mathbf{z}_{p+1} &= \lambda_1^{p+1} \mathbf{x}_{(1)} + \lambda_2^{p+1} \mathbf{x}_{(2)} + \dots \end{aligned} \quad (6.48)$$

Assuming that convergence is monitored on the estimation (6.46) of the eigenvalue, we can write:

$$\frac{z_{p+1,j}}{z_{p,j}} = \frac{\lambda_1(x_{(1),j} + r^{p+1}x_{(2),j} + \dots)}{(x_{(1),j} + r^p x_{(2),j} + \dots)} \quad (6.49)$$

where r is the ratio:

$$r = \frac{\lambda_2}{\lambda_1} \quad (6.50)$$

If we define:

$$a_j = \frac{x_{(2),j}}{x_{(1),j}}$$

and if we assume that $|\lambda_2| < |\lambda_1|$, we obtain at iteration p the p th estimate of the eigenvalue:

$$\lambda_{1p} = \frac{z_{p+1,j}}{z_{p,j}} = \frac{\lambda_1(1 + a_j r^{p+1} + \dots)}{(1 + a_j r^p + \dots)} \simeq \lambda_1(1 + a_j r^p(r-1)) \quad (6.51)$$

for a large enough p .

Thus, we can calculate the number N_{it} of iterations after which the eigenvalue is stabilized with t significant figures, by solving the following inequality:

$$\left| \frac{\lambda_{1(N_{it}+1)} - \lambda_{1(N_{it})}}{\lambda_{1(N_{it})}} \right| \leq 10^{-t}, \quad \text{hence} \quad a_j r^{N_{it}} \simeq 10^{-t}$$

From this we can deduce the approximate rule that enables us to evaluate the number of necessary iterations:

$$N_{it} \simeq \frac{t}{\log \left(\frac{\lambda_1}{\lambda_2} \right)} \quad (6.52)$$

This shows that the power algorithm convergence depends solely on the ratio of the two largest eigenvalues of the matrix: it remains independent of its size n .

Figure 6.3 illustrates the validity of relation (6.52) for computing the largest eigenvalue of several matrices of dimension 100. Each time, a column of the matrix has been taken as starting

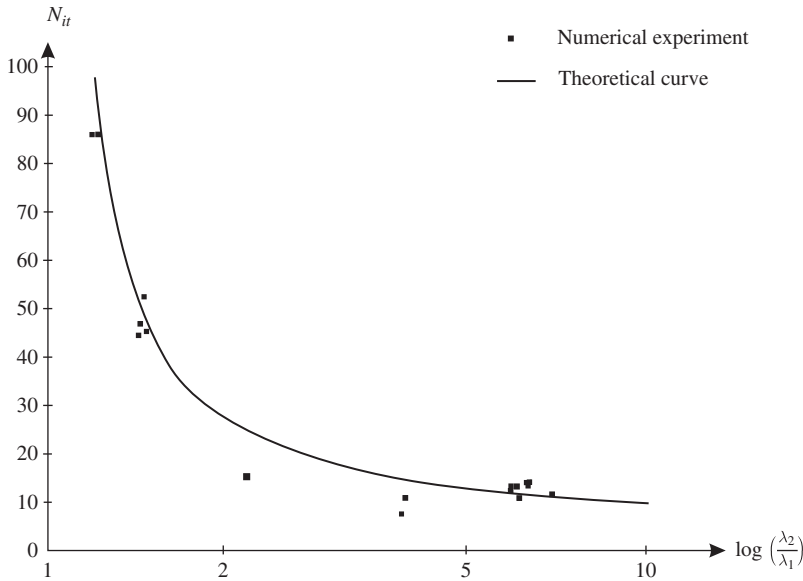


Figure 6.3 Convergence of the power method: $n = 100$, $t = 8$.

vector. This diagram confirms the theoretical result and shows that one cannot hope to use the power algorithm to separate eigenvalues the ratio of which is smaller than roughly 1.1.

6.5.2 Determining higher modes: orthogonal deflation

The fundamental eigenvector $\mathbf{x}_{(1)}$ having been determined, we can form the orthogonal projection operator:

$$\mathbf{P}_1 = \mathbf{I} - \frac{\mathbf{x}_{(1)}\mathbf{x}_{(1)}^T \mathbf{M}}{\mathbf{x}_{(1)}^T \mathbf{M} \mathbf{x}_{(1)}}$$

in such a way that its application to any vector projects the latter orthogonally to $\mathbf{x}_{(1)}$. If the eigenmodes are orthonormalized with respect to \mathbf{M} , we get the simplified expression:

$$\mathbf{P}_1 = \mathbf{I} - \mathbf{x}_{(1)}\mathbf{x}_{(1)}^T \mathbf{M} \quad (6.53)$$

Indeed, we can verify that for any vector \mathbf{z} :

$$\mathbf{x}_{(1)}^T \mathbf{M} (\mathbf{P}_1 \mathbf{z}) = \mathbf{x}_{(1)}^T \mathbf{M} \mathbf{z} - \mathbf{x}_{(1)}^T \mathbf{M} \mathbf{x}_{(1)} \mathbf{x}_{(1)}^T \mathbf{M} \mathbf{z} = 0$$

In theory, it would be sufficient to construct a starting vector:

$$\mathbf{z}_0^* = \mathbf{P}_1 \mathbf{z}_0 = \sum_{i=2}^n \alpha_i \mathbf{x}_{(i)}$$

which has the property of containing no component of the $\mathbf{x}_{(1)}$ mode. The iterative scheme (6.39) would give the eigensolution $(\lambda_2, \mathbf{x}_{(2)})$. In practice, however, the eigenvector $\mathbf{x}_{(1)}$ will progressively reappear in the successive iteration vectors because of the buildup of numerical errors. This unwanted reappearance of the first mode can be cured if, at each iteration, we project the resulting iterate so that it is orthogonal to the eigenmode $\mathbf{x}_{(1)}$:

$$\begin{cases} \mathbf{z}_p^* &= \mathbf{P}_1 \mathbf{z}_p \\ \mathbf{z}_{p+1} &= \mathbf{D} \mathbf{z}_p^* \end{cases} \quad (6.54)$$

The iterative scheme (6.54) is equivalent to replacing the dynamical matrix $\mathbf{D} = \mathbf{K}^{-1} \mathbf{M}$ by either one of the matrices $\mathbf{P}_1 \mathbf{D}$ or $\mathbf{D} \mathbf{P}_1$ obtained through application of the projection operator either in pre- or post-multiplication.

These matrices have the same eigenvalues as \mathbf{D} , except λ_1 which is shifted to the origin. Indeed, the deflated matrix:

$$\mathbf{D}_1 = \mathbf{P}_1 \mathbf{D} = \mathbf{D} \mathbf{P}_1 = \mathbf{D} - \lambda_1 \mathbf{x}_{(1)} \mathbf{x}_{(1)}^T \mathbf{M} \quad (6.55)$$

multiplied by any eigenvector $\mathbf{x}_{(i)}$ yields:

$$\begin{aligned} \mathbf{D}_1 \mathbf{x}_{(i)} &= \lambda_i \mathbf{x}_{(i)} & i \neq 1 \\ \mathbf{D}_1 \mathbf{x}_{(1)} &= 0 \end{aligned}$$

$\mathbf{x}_{(1)}$ thus remains an eigenvector of \mathbf{D}_1 , with the associated eigenvalue replaced by zero. The largest nonzero eigenvalue of \mathbf{D}_1 is now λ_2 , corresponding to the unchanged eigenvector $\mathbf{x}_{(2)}$. The power method applied to \mathbf{D}_1 will consequently lead to convergence towards λ_2 and $\mathbf{x}_{(2)}$.

The projection process (6.55), proposed by *Hotelling*, is called the *orthogonal deflation method* since it forces the iterates to live in a ‘deflated’ space of dimension $n - 1$, the direction $\mathbf{x}_{(1)}$ being excluded from the original space.

The process can be generalized for the extraction of further higher modes. Indeed, assuming again the modes to be mass-normalized, the operators:

$$\mathbf{P}_j = \mathbf{I} - \mathbf{x}_{(j)} \mathbf{x}_{(j)}^T \mathbf{M} \quad j = 1, \dots, n \quad (6.56)$$

have, as a consequence of the orthonormality relationships, the following property:

$$\mathbf{P}_j \mathbf{x}_{(i)} = \mathbf{x}_{(i)} (1 - \delta_{ij})$$

It is seen that they commute with each other:

$$\mathbf{P}_j \mathbf{P}_i = \mathbf{P}_i \mathbf{P}_j \quad (6.57)$$

and that, as shown by (6.55) in the particular case of $j = 1$, they commute with \mathbf{D} :

$$\mathbf{P}_j \mathbf{D} = \mathbf{D} \mathbf{P}_j \quad (6.58)$$

Let us note that applying multiple projectors $\mathbf{P}_1 \mathbf{P}_2 \dots \mathbf{P}_k$ can be efficiently performed by observing that:

$$\mathbf{P}_1 \mathbf{P}_2 \dots \mathbf{P}_k = \mathbf{I} - \sum_{j=1}^k \mathbf{x}_{(j)} \mathbf{x}_{(j)}^T \mathbf{M} \quad (6.59)$$

$$= \mathbf{I} - \mathbf{X} \mathbf{X}^T \mathbf{M} = \mathbf{P}_{12 \dots k} \quad (6.60)$$

where we assume that \mathbf{X} contains in its columns all the modes up to number k .

Applying to the initial matrix the operator $\mathbf{P}_1 \mathbf{P}_2 \dots \mathbf{P}_k$ gives the deflated dynamical matrix:

$$\mathbf{D}_k = \mathbf{D} - \sum_{i=1}^k \lambda_i \mathbf{x}_{(i)} \mathbf{x}_{(i)}^T \mathbf{M} \quad (6.61)$$

It is readily verified that this leads to convergence towards mode $\mathbf{x}_{(k+1)}$. The deflated matrices satisfy the recurrence relation:

$$\mathbf{D}_k = \mathbf{D}_{k-1} - \lambda_k \mathbf{x}_{(k)} \mathbf{x}_{(k)}^T \mathbf{M} \quad (6.62)$$

Finally, since any vector \mathbf{z} vanishes when transformed by the operator $\mathbf{P}_1 \mathbf{P}_2 \dots \mathbf{P}_N$, we deduce that the same is true for matrix \mathbf{D} :

$$\mathbf{D} \mathbf{P}_1 \mathbf{P}_2 \dots \mathbf{P}_N = \mathbf{D} - \sum_{k=1}^N \lambda_k \mathbf{x}_{(k)} \mathbf{x}_{(k)}^T \mathbf{M} = \mathbf{0} \quad (6.63)$$

This relation reveals the spectral expansion of the dynamical matrix \mathbf{D} (see also Section 2.4). Deflation thus consists of subtracting from \mathbf{D} the different components of its spectral expansion.

Since deflation is performed with the previously computed eigenmodes and since those eigenmodes always entail a certain error (depending on the convergence tolerance), the deflated subspace in which the subsequent modes are computed suffers from the previous inaccuracies. The accumulation of errors in the successive deflation process is one of the drawbacks of the method. The deterioration of the higher eigensolutions obtained through iteration and deflation can be measured in several ways:

- The simplest test consists in checking the conservation of the trace by calculating the ratio:

$$\eta = \frac{\text{trace}(\mathbf{D}_k) + \sum_{i=1}^k \lambda_{i(c)} - \text{trace}(\mathbf{D})}{\text{trace}(\mathbf{D})}$$

where $\lambda_{i(c)}$ stands for the calculated eigenvalues. It should not vary if there are no approximation errors, since the trace of a matrix is equal to the sum of its eigenvalues.

- After obtaining the eigenvector $\mathbf{x}_{(i)}$, we can also form its first iterate vector with respect to the nondeflated matrix, and calculate the difference vector between the latter and the former. This check is in fact similar to controlling the residual of the eigenvalue problem as described by Equation (6.7).
- Finally, we can apply algorithms for evaluating error bounds to the calculated eigenvalues (see Section 6.10).

6.5.3 Inverse iteration form of the power method

If one applies the power iteration (6.39) to find eigenmodes of a dynamic system, it is not desirable to construct the dynamical matrix $\mathbf{D} = \mathbf{K}^{-1}\mathbf{M}$ explicitly since it is fully populated and it requires performing a forward-backward substitution for each column of matrix \mathbf{M} . So in practice it is much more efficient to compute an iterate from:

$$\mathbf{z}_{p+1}^* = \mathbf{D}\mathbf{z}_p = \mathbf{K}^{-1}(\mathbf{M}\mathbf{z}_p)$$

so that the power method can be recast in the mathematically equivalent form:

$$\left\{ \begin{array}{l} \mathbf{y}_p = \mathbf{M}\mathbf{z}_p \\ \text{Solve } \mathbf{K}\mathbf{z}_{p+1}^* = \mathbf{y}_p \\ \mathbf{z}_{p+1} = \frac{\mathbf{z}_{p+1}^*}{\|\mathbf{z}_{p+1}^*\|} \end{array} \right. \quad \begin{array}{l} (6.64a) \\ (6.64b) \\ (6.64c) \end{array}$$

In this form, the power algorithm is called the *inverse iteration method*. It does not require building the dynamical matrix explicitly but involves solving the static problem (6.64b). As will be shown in Section 6.6, this implies factorizing the matrix \mathbf{K} once at the beginning of the iteration, and then performing one forward-backward substitution per iteration.

Performing the matrix product (6.64a) does not require assembly of the mass matrix: in the finite element method context, for instance, it can be done by summing up the contributions of the elementary mass matrices.

It is interesting to note that the static problem (6.64b) corresponds to finding a response of the system under load distribution equal to the inertia forces associated to the previous iterate. So one can also interpret the inverse iteration method as some kind of fixed point iteration on the original eigenvalue equation:

$$\mathbf{K}\mathbf{x} = \omega^2\mathbf{M}\mathbf{x}$$

The computational efficiency of the power method put in inverse iteration form depends largely on the efficiency of the solution step (6.64b) since, for systems with large number of degrees of freedom, most of the computer time will be spent in solving (6.64b). This is true for all eigenvalue extraction methods based on inverse iteration (e.g. the subspace iteration and Lanczos methods described in Section 6.8). Therefore, before describing them, let us briefly recall in Section 6.6 how to solve a system of linear equations. Emphasis will be put on the solution of symmetrical systems (indeed the system matrix in (6.64b) is symmetric), on their possible singularity due to the existence of rigid body modes, and on their efficient solution when applied to large sparse systems as generally arising in structural mechanics.

6.6 Solution methods for a linear set of equations

In this chapter we shortly review methods related to the solution of a system of equations such as encountered in static problems arising from finite element models. We have seen in Section 6.5.3 that solving a static-like problem is the most computationally expensive part of the inverse iteration algorithm for computing eigensolutions. Such static-like problems also arise in other eigensolvers commonly used in engineering (as explained in further sections of this chapter) as well as in time-stepping algorithms to compute the transient dynamic response of systems (Chapter 7). Here we will discuss the often used direct solvers and will assume a general system of equations of the form:

$$\mathbf{A}\mathbf{x} = \mathbf{b} \quad (6.65)$$

where \mathbf{A} is square. The case of rectangular matrices will not be treated since of no interest in the present context.

Iterative solution techniques, such as the Conjugate Gradient method (Golub and Van Loan 1989, Hestenes and Stiefel 1952), will not be discussed here: even though iterative solvers are sometimes applied in engineering mechanics, explaining their principle and all the accessories necessary to make them efficient is beyond the scope of the present book. For the reader interested in the topic, description of a semi-iterative algorithm (The Finite Element Tearing and Interconnecting method) often used as parallel solver for mechanical problems can be found in Farhat and Roux (1991), Rixen (2002).

When dealing with the solution of the eigenvalue problem (6.1) using the inverse iteration scheme (6.64a–6.64c), \mathbf{A} can be the stiffness matrix \mathbf{K} or, more generally, a matrix of the form $(\mathbf{K} - \mu\mathbf{M})$ resulting from spectral shift (see Section 6.7.2).

In the more general context of structural dynamics, it can also be:

- the dynamic stiffness matrix $(\mathbf{K} - \omega^2\mathbf{M})$ in forced harmonic analysis;
- the time-stepping matrix for time integration in transient analysis (see Section 7.2.1).

In this section general notations will be used that do not necessarily follow the main nomenclature of the book or of this chapter, but since they are used only in this local context this should not lead to any confusion.

6.6.1 Nonsingular linear systems

In this section, we consider a linear system of the general form (6.65) where \mathbf{A} is a nonsingular square matrix, so that a unique solution exists for \mathbf{x} . The case where \mathbf{A} is square but singular will be discussed in Section 6.6.2.

Nonsymmetric systems: the LU factorization

The most natural method that comes to mind for solving a system as in (6.65) consists in recasting the first equation as:

$$x_1 = \frac{1}{a_{11}}(b_1 - a_{12}x_2 - \dots - a_{1n}x_n) \quad (6.66)$$

so that x_1 can be eliminated from all subsequent equations by substitution of (6.66). Repeating the process for x_2 in the second equation and so on leads to a sequence of transformed equations, the last of which yields x_n . Substituting back the value of x_n into the transformed equation $n - 1$ then yields x_{n-1} and substituting further into the transformed equations yields x_{n-2}, \dots, x_1 recursively.

This procedure can also be understood as building linear combinations of the original equations so as to bring matrix \mathbf{A} to an upper triangle form \mathbf{U} . Assuming that x_1, \dots, x_{k-1} have already been eliminated, the operator of the transformed system is as in Figure 6.4. Step k then consists in transforming equations $k + 1, \dots, n$ by adding a linear combination of equation k so as to zero the coefficients of x_k . Hence, if \mathbf{U} and $\tilde{\mathbf{b}}$ are initially set to \mathbf{A} and \mathbf{b} respectively, every row i below k becomes:

step k

$$u_{ij} \leftarrow u_{ij} - l_{ik}u_{kj} \quad i, j = k + 1, \dots, n \quad (6.67a)$$

$$\tilde{b}_i \leftarrow \tilde{b}_i - l_{ik}\tilde{b}_k \quad (6.67b)$$

$$\text{where} \quad l_{ik} = \frac{u_{ik}}{u_{kk}} \quad (6.67c)$$

in order to zero u_{ik} , $i = k + 1, \dots, n$. After $n - 1$ steps, \mathbf{U} is an upper triangular matrix.

The solution is then found by *backward substitution* first for x_n , then for x_{n-1} and so on:

$$x_i = \frac{1}{u_{ii}} \left(\tilde{b}_i - \sum_{j=i+1}^n u_{ij}x_j \right) \quad i = n, n - 1, \dots, 1 \quad (6.68)$$

The algorithm is known as *Gauss elimination* and can be viewed as transforming \mathbf{A} into a product of a lower triangular matrix \mathbf{L} and an upper triangular matrix \mathbf{U} , i.e.

$$\mathbf{A} = \mathbf{LU} \quad (6.69)$$

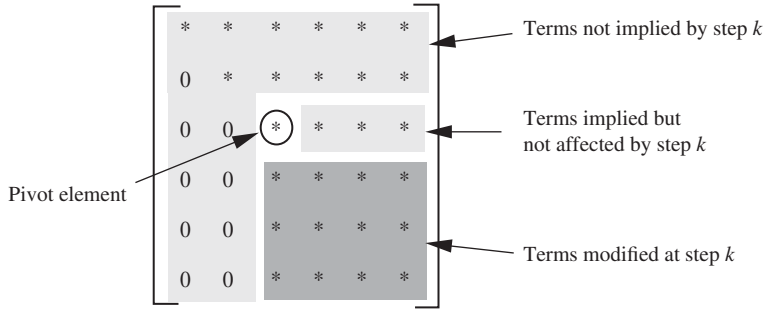


Figure 6.4 Gauss elimination: transforming A into an upper triangular form U .

where L is the lower triangular matrix of coefficients l_{ik} as defined by Equation (6.67a). It obviously has *unit diagonal*.

The direct solution procedure can thus be summarized as follows:

- Factorize $A = LU$ according to Equations (6.67a–6.67c), so that the system is written as

$$LUx = L\tilde{b} = b \quad \text{where we define} \quad \tilde{b} = Ux \quad (6.70a)$$

- Solve successively the triangular systems:

$$L\tilde{b} = b \quad (6.70b)$$

$$Ux = \tilde{b} \quad (6.70c)$$

Solving Equation (6.70b) corresponds to transforming the right-hand side as in (6.67b) and is called *forward substitution* whereas solving (6.70c) is a *backward substitution* as defined by (6.68). The factorization of the matrix requires $2n^3/3$ operations, while the forward and backward substitutions involve $O(n^2)$ operations each. If the system must be solved for multiple right-hand sides, the factorization needs to be performed only once, and one forward and backward substitution must be performed for every right-hand side.

Example 6.1

$$\begin{aligned}
 A = \begin{bmatrix} 1 & 2 & 3 \\ 1 & 1 & 2 \\ 1 & 0 & -1 \end{bmatrix} &\xrightarrow{k=1} \underbrace{\begin{bmatrix} 1 & 2 & 3 \\ 1 & 1 & 2 \\ 1 & 0 & -1 \end{bmatrix}}_{l_{i1}} \xrightarrow{k=2} \underbrace{\begin{bmatrix} 1 & 2 & 3 \\ 0 & -1 & -1 \\ 0 & 0 & -2 \end{bmatrix}}_{l_{i2}} \Rightarrow LU = \begin{bmatrix} 1 & 0 & 0 \\ 1 & 1 & 0 \\ 1 & 2 & 1 \end{bmatrix} \begin{bmatrix} 1 & 2 & 3 \\ 0 & -1 & -1 \\ 0 & 0 & -2 \end{bmatrix}
 \end{aligned}$$

Remark 6.3 At step k of the elimination, the diagonal element u_{kk} is called a pivot (Figure 6.4) and must be nonzero in (6.67c). In order to have a nonzero pivot and to ensure numerical stability of the elimination, it is required to apply permutations on the rows and columns $k + 1$ to n (i.e. changing the order of the equations and unknowns) in order to bring on the diagonal k the element of highest modulus of the sub-matrix yet to be triangularized. This procedure is called pivoting. The factorization is then expressed as:

$$\mathbf{P}_1 \mathbf{A} \mathbf{P}_2 = \mathbf{L} \mathbf{U} \quad (6.71)$$

where \mathbf{P}_1 and \mathbf{P}_2 are permutation operators related to the pivoting of the rows and columns respectively. If only the rows are re-ordered, the procedure is known as partial pivoting. Since permutation matrices are identity matrices with re-ordered rows,

$$\det(\mathbf{A}) = \pm \det(\mathbf{P}_1 \mathbf{A} \mathbf{P}_2) = \pm \det(\mathbf{L}) \det(\mathbf{U}) = \pm \det(\mathbf{U}) = \pm \prod_{k=1}^n u_{kk} \quad (6.72)$$

Therefore one is guaranteed to find a nonzero pivot if pivoting is applied and if \mathbf{A} is nonsingular.

Remark 6.4 In order to minimize memory requirements, the initial matrix \mathbf{A} is usually overwritten by the coefficients of \mathbf{U} and \mathbf{L} , being understood that the unit diagonal of \mathbf{L} need not be stored.

Remark 6.5 Solving a problem using factorization techniques is mathematically equivalent to computing $\mathbf{x} = \mathbf{A}^{-1} \mathbf{b}$, but it is numerically very different from the procedure that would consist in computing the inverse \mathbf{A}^{-1} and performing the multiplication $\mathbf{A}^{-1} \mathbf{b}$. Indeed, computing the inverse can be seen as solving a linear system for every column of \mathbf{A}^{-1} such that $\mathbf{A} \mathbf{A}^{-1} = \mathbf{I}$. It is thus much more expensive than just solving one linear system. Moreover, computing the inverse and then performing the multiplication results in more numerical errors and thus yields a less accurate result.

Symmetric systems: \mathbf{LDL}^T and Cholesky factorization

When the system matrix is symmetric, its reduction to a triangular form can be organized so as to require only half the number of operations of the \mathbf{LU} factorization. Let us take the \mathbf{LU} factorization and introduce a diagonal matrix \mathbf{D} containing the diagonal values of \mathbf{U} such that:

$$\mathbf{A} = \mathbf{L} \mathbf{D} \tilde{\mathbf{U}}$$

where $\tilde{\mathbf{U}}$ is a kind of scaled \mathbf{U} . Since \mathbf{A} is symmetric, one must have that $\tilde{\mathbf{U}} = \mathbf{L}^T$, which shows that \mathbf{A} can be factorized into the symmetric form:

$$\mathbf{A} = \mathbf{L} \mathbf{D} \mathbf{L}^T$$

or

$$\begin{bmatrix} a_{11} & a_{21} & a_{31} & \cdots \\ a_{21} & a_{22} & a_{32} & \\ a_{31} & a_{32} & a_{33} & \\ \vdots & & & \ddots \end{bmatrix} = \begin{bmatrix} 1 & & & \\ l_{21} & 1 & & \\ l_{31} & l_{32} & 1 & \\ \vdots & & & \ddots \end{bmatrix} \begin{bmatrix} d_{11} & d_{11}l_{21} & d_{11}l_{31} & \cdots \\ & d_{22} & d_{22}l_{32} & \\ & & d_{33} & \\ \mathbf{0} & & & \ddots \end{bmatrix} \quad (6.73)$$

where \mathbf{L} is a lower triangular matrix with unit diagonal and \mathbf{D} is diagonal. Comparing (6.73) to the LU factorization, the upper triangular matrix \mathbf{U} is expressed as $\mathbf{D}\mathbf{L}^T$ in the symmetric case. The solution \mathbf{x} of system (6.65) is then found as for the LU factorization, i.e. by forward and backward substitution similar to (6.70b) and (6.70c).

At step k of the LDL^T factorization (6.73), the first $k-1$ rows of \mathbf{L} and \mathbf{D} are known. The coefficients of \mathbf{L} on row k are recursively computed by successively identifying $a_{k1}, a_{k2}, \dots, a_{kk-1}$ to the right-hand side in (6.73), and d_{kk} is then found by identifying the diagonal a_{kk} , i.e.

step k :

$$a_{kj} = d_{jj}l_{kj} + \sum_{s=1}^{j-1} l_{ks}d_{ss}l_{js} \quad j = 1, \dots, k-1$$

$$\Rightarrow l_{kj} = \frac{1}{d_{jj}} \left(a_{kj} - \sum_{s=1}^{j-1} l_{ks}d_{ss}l_{js} \right) \quad (6.74a)$$

$$a_{kk} = d_{kk} + \sum_{s=1}^{k-1} d_{ss}l_{ks}^2$$

$$\Rightarrow d_{kk} = a_{kk} - \sum_{s=1}^{k-1} d_{ss}l_{ks}^2 \quad (6.74b)$$

In order to reduce the number of multiplications, we can write (6.74a–6.74b) in terms of the temporary variables $\tilde{l}_{kj} = d_{jj}l_{kj}$, namely:

$$\tilde{l}_{kj} = a_{kj} - \sum_{s=1}^{j-1} \tilde{l}_{ks}l_{js} \quad j = 1, \dots, k-1 \quad (6.75a)$$

$$d_{kk} = a_{kk} - \sum_{s=1}^{k-1} \tilde{l}_{ks}l_{ks} \quad (6.75b)$$

One can therefore determine first \tilde{l}_{kj} and, after step k , determine l_{kj} by:

$$l_{kj} = \frac{\tilde{l}_{kj}}{d_{jj}} \quad j = 1, \dots, k-1 \quad (6.76)$$

In this form the LDL^T factorization uses approximatively half the number of operations of the LU factorization, that is $n^3/3$ operations.

Remark 6.6 As for the LU factorization, the elimination process can break down if d_{kk} becomes zero: to avoid this and to ensure numerical stability, pivoting should be applied. For the matrix to remain symmetric after pivoting, the same permutation must be applied to the row and to the columns of \mathbf{A} . The pivoting strategy for symmetric matrices therefore consists in interchanging at step k row and column k with the row and column of index higher than k and which diagonal term has the highest modulus. The factorization is thus now expressed as:

$$\mathbf{P}_1 \mathbf{A} \mathbf{P}_1^T = \mathbf{L} \mathbf{U} \quad (6.77)$$

and we get in this case:

$$\det(\mathbf{A}) = \det(\mathbf{P}_1 \mathbf{A} \mathbf{P}_1^T) = \det(\mathbf{L}) \det(\mathbf{D}) \det(\mathbf{L}) = \det(\mathbf{D}) = \prod_{k=1}^n d_{kk} \quad (6.78)$$

since the change of sign in (6.72) was coming from nonsymmetric pivoting.

Remark 6.7 In case matrix \mathbf{A} is positive definite, all diagonal submatrices are also positive definite and thus the diagonal terms d_{kk} are strictly positive. Symmetric positive definite systems are very common in structural mechanics since they typically derive from quadratic energy functions which are positive and symmetric due to the very underlying physical principles. In that case, the factorization of \mathbf{A} can also be expressed as:

$$\mathbf{A} = \mathbf{L} \mathbf{D} \mathbf{L}^T = \mathbf{L} \mathbf{D}^{\frac{1}{2}} \mathbf{D}^{\frac{1}{2}} \mathbf{L}^T = \mathbf{C} \mathbf{C}^T \quad (6.79)$$

which is known as the Cholesky factorization. The Cholesky algorithm is similar to the \mathbf{LDL}^T factorization and requires the same number of operations, but it involves computing square roots of the pivots. Note that when \mathbf{A} is positive definite, all pivots are guaranteed to be strictly positive, so that in that particular case pivoting is no longer compulsory.

Remark 6.8 In practice, only half of \mathbf{A} is stored (e.g. its lower triangular part) and \mathbf{A} can be overwritten by \mathbf{L} and the diagonal of \mathbf{D} (or by \mathbf{C} for the Cholesky algorithm), so that solving the system barely requires any additional memory.

Sparse matrices

Since discretization methods such as the Rayleigh–Ritz or the boundary element methods use functions defined over the entire computational domain to approximate the solution, they usually lead to small but full (or dense) matrices. When performing detailed analyses, the more versatile finite element or finite volume methods based on the definition of a fine discretization mesh are however preferred. The latter may generate a very large number of unknowns, but the shape or flux functions being local, the connectivity between unknowns is limited to neighbouring nodes so that the system matrix has sparse topology. Special storage and solution techniques must then be applied in order to take advantage of sparsity.

To avoid storing the zeros of a sparse matrix, one can store the index $[i, j]$ of its nonzero entries together with their values. This is the basic principle of sparse storage schemes. Special variants of the factorization algorithms sometimes called *sparse solvers* have been developed where the fill-in terms are identified at for-hand by analysis of the graph of the matrix so that computations are performed only on nonzero terms. Unfortunately, when a sparse matrix is factorized (see Section 6.6.1), many zero entries become nonzeros (called *fill-ins*) so that the initial graph of the matrix is modified.

Renumbering schemes are usually applied to the system of equations, i.e. permutation of rows (re-ordering of the equations) and/or columns (re-numbering of the unknowns) is performed in order to concentrate the nonzero terms along the diagonal of the matrix (see Figure 6.5). Since the factorization of the matrix corresponds to building linear combinations with previous rows, no fill-in will occur above the first nonzero entry in a column so that the sparsity of the re-numbered matrix will not be significantly altered during factorization.

When re-numbering a symmetric matrix, the same permutation is applied to rows and columns in order to preserve symmetry. The two most commonly used re-numbering schemes in the context of finite element analysis are:

- the *Reverse Cuthill-McKee* (RCM) method (George and Liu 1981), an improved version of the original Cuthill-McKee algorithm (Cuthill and McKee 1969) based on the minimization of the topological distance between degrees of freedom in the graph of the mesh connectivity;
- *Sloan's* algorithm (Sloan and Randolph 1983) based on a heuristics to regroup degrees of freedom that are neighbours in the finite element mesh.

The nonzero entries of the re-numbered matrix being close to the diagonal, one can store all the entries between the skyline and the diagonal. This leads to the *skyline storage* technique as illustrated in Figure 6.5 for a symmetric matrix: the elements of the columns between the skyline and the diagonal are stored in the one-dimensional array \mathbf{a} while pointers for the position of the diagonal terms in \mathbf{a} are stored separately in \mathbf{j}_{diagA} . Obviously, the skyline of the matrix remains unchanged when factorization is applied without pivoting. Calling b the maximum height of a column under the skyline of a symmetric matrix (commonly called the *bandwidth*), the number of operations required for its factorization is $O(nb^2)$.

Static condensation and the frontal method

Elimination algorithms can be re-arranged in several different ways. In particular, re-writing the system (6.65) in the block partitioned form:

$$\begin{bmatrix} A_{11} & A_{12} \\ A_{21} & A_{22} \end{bmatrix} \begin{bmatrix} x_1 \\ x_2 \end{bmatrix} = \begin{bmatrix} b_1 \\ b_2 \end{bmatrix} \quad (6.80)$$

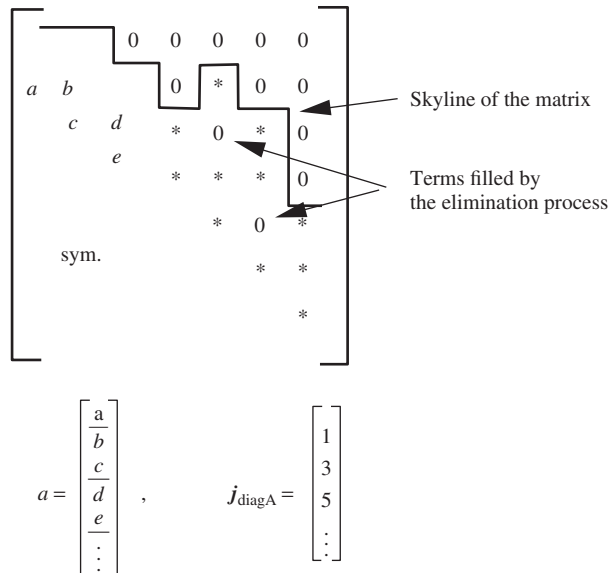


Figure 6.5 Skyline storage of a symmetric matrix.

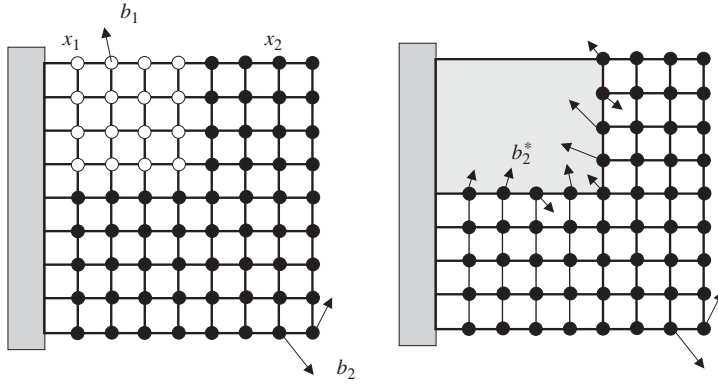


Figure 6.6 Schematic representation of static condensation.

one can use the first set of equations to eliminate the set of unknowns x_1 in a way similar to (6.66), i.e.

$$x_1 = A_{11}^{-1}(b_1 - A_{12}x_2) \quad (6.81)$$

where A_{11} is assumed to be nonsingular. Substituting (6.81) into the partitioned form (6.80) yields the *block triangular form*:

$$\begin{bmatrix} A_{11} & A_{12} \\ \mathbf{0} & A_{22} - A_{21}A_{11}^{-1}A_{12} \end{bmatrix} \begin{bmatrix} x_1 \\ x_2 \end{bmatrix} = \begin{bmatrix} b_1 \\ b_2 - A_{21}A_{11}^{-1}b_1 \end{bmatrix} \quad (6.82)$$

or

$$\begin{bmatrix} A_{11} & A_{12} \\ \mathbf{0} & A_{22}^* \end{bmatrix} \begin{bmatrix} x_1 \\ x_2 \end{bmatrix} = \begin{bmatrix} b_1 \\ b_2^* \end{bmatrix} \quad (6.83)$$

This last equation should be compared to U in Figure 6.4. The lower diagonal block $A_{22}^* = A_{22} - A_{21}A_{11}^{-1}A_{12}$ is the matrix A when the unknowns x_1 have been condensed out. Hence, one can now solve for x_2 in:

$$A_{22}^*x_2 = b_2^* \quad (6.84)$$

and then recover x_1 by (6.81).

If A is a stiffness matrix, A_{22}^* represents the stiffness operator coupling the variables x_2 when x_1 are left free. This is illustrated in Figure 6.6. The condensed part can be seen as a macro (or super) element. To mathematicians, A_{22}^* is known as the *Schur complement* of A for x_2 .

The blocks $A_{11}^{-1}A_{12}$ and $A_{11}^{-1}b_1$ in (6.82) can be computed by factorizing A_{11} and performing forward and backward substitutions for A_{12} and b_1 . The factorization of A is then completed by factorizing A_{22}^* . There are several advantages in using this block factorization approach:

- Applying this idea successively to several blocks, one can devise the *block LU* factorization which involves mainly matrix-matrix operations and thereby renders the factorization more efficient on vector and parallel computers. The block *LU* allows also to organize the swapping on disk when the RAM memory is not large enough to hold all the matrices during factorization.

- When analysis is required for several variants of a same structure where only a subpart is modified, the factorization of the common part needs to be done only once. Hence, computing time can be improved for re-analysis.
- In static analysis, using static condensation of subparts is an exact procedure. In dynamic analysis, as will be seen later, it leads to an interesting approximate reduction technique.

The frontal method

The concept of static condensation leads to a very efficient and often used way to organize the factorization of structural matrices arising in finite element analysis: the *frontal method* (Irons 1970). In that procedure, the order of the elimination of the degrees of freedom in the factorization is obtained automatically as follows.

At the start, a corner element is considered as *active* and all degrees of freedom that are inside the active part are eliminated. Then neighbouring elements are added to the active set and the procedure is repeated (see Figure 6.7). Hence, at every step, one computes the reduced matrix on the *active front*.

The frontal method can thus be seen as a static reduction technique and is often used because the global assembled matrix needs not be assembled, the elements being assembled only once they become active in the algorithm. Only the active front is present in memory (i.e. the condensed matrix on the front and the newly activated element matrices). The memory required is

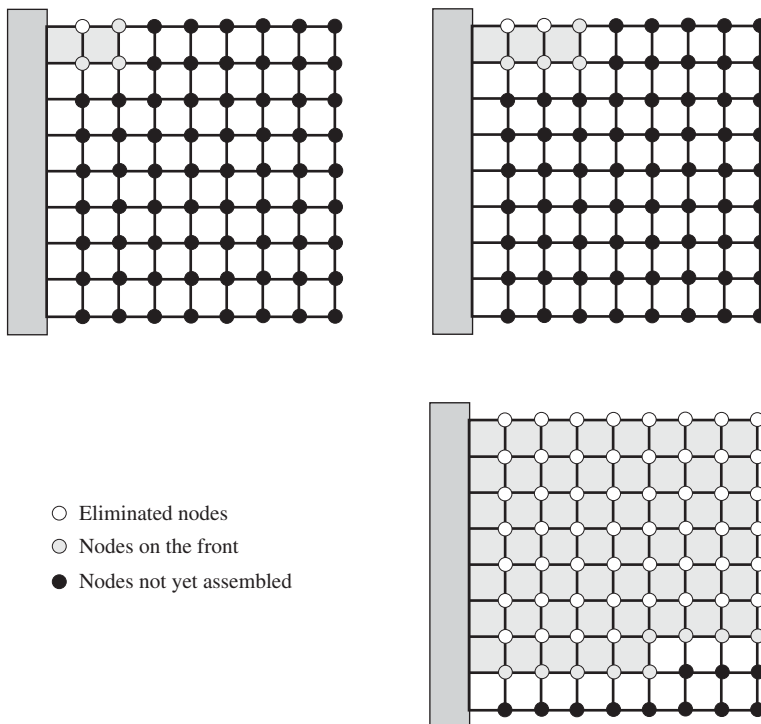


Figure 6.7 The frontal method.

thus low. Also, in this scheme, no specific numbering is required since the order of elimination is defined by the element topology.

6.6.2 Singular systems: nullspace, solutions and generalized inverse

Singular operators are not rare in structural analysis. For instance, the stiffness matrix of a structure having rigid body modes is singular, namely there exists displacement modes creating no deformation energy (e.g. translations and rotations of an aircraft in flight or a satellite in orbit). We will first define in Section 6.6.3 the nullspace of a singular matrix and in Section 6.6.4 we discuss the conditions under which a solution exists for a singular system. The concept of generalized inverse is then introduced in Section 6.6.5.

Here, we consider the case of a square symmetric matrix \mathbf{A} of dimension $n \times n$. Further discussions on the general singular matrices can be found for instance in Ben-Israel and Greville (1974) and Farhat and Rixen (2002).

6.6.3 Singular matrix and nullspace

The set of all m independent solutions \mathbf{n}_s of:

$$\mathbf{A}\mathbf{n}_s = \mathbf{0} \quad s = 1, \dots, m \quad (6.85)$$

forms the *nullspace* of \mathbf{A} . For a stiffness matrix, \mathbf{n}_s represent the rigid body modes $\mathbf{u}_{(s)}$ if not enough boundary conditions exist to restrain the structure. Note that any linear combination of \mathbf{n}_s satisfies (6.85).

If m nullspace vectors \mathbf{n}_s exist for \mathbf{A} of dimension $n \times n$, (6.85) indicates that only $n - m$ columns and rows are linearly independent.

Let us assume without loss of generality but only to simplify the notations that the system can be partitioned as:

$$\begin{bmatrix} \mathbf{A}_{11} & \mathbf{A}_{12} \\ \mathbf{A}_{21} & \mathbf{A}_{22} \end{bmatrix} \begin{bmatrix} \mathbf{x}_1 \\ \mathbf{x}_2 \end{bmatrix} = \begin{bmatrix} \mathbf{b}_1 \\ \mathbf{b}_2 \end{bmatrix} \quad (6.86)$$

where \mathbf{A}_{11} is a nonsingular square matrix of dimension equal to the rank of \mathbf{A} , i.e. \mathbf{A}_{11} is the largest nonsingular submatrix of \mathbf{A} . Since the m columns labelled 2 in (6.86) are linearly dependent on the $n - m$ first ones, there exists a matrix \mathbf{W} of dimension $(n - m) \times m$ such that:

$$\begin{bmatrix} \mathbf{A}_{12} \\ \mathbf{A}_{22} \end{bmatrix} = \begin{bmatrix} \mathbf{A}_{11} \\ \mathbf{A}_{21} \end{bmatrix} \mathbf{W} \quad (6.87)$$

The first set of equations in (6.87) allows determining the coefficients of the linear combination and yields:

$$\mathbf{W} = \mathbf{A}_{11}^{-1} \mathbf{A}_{12} \quad (6.88)$$

Substituting in the second set of equations in (6.87),

$$\mathbf{A}_{22} - \mathbf{A}_{21} \mathbf{A}_{11}^{-1} \mathbf{A}_{12} = \mathbf{0} \quad (6.89)$$

The left-hand side of the expression above is the system operator when \mathbf{x}_1 has been eliminated from the equations as indicated by (6.82). Hence every type of Gauss elimination (\mathbf{LU} , \mathbf{LDL}^T

or Cholesky factorization) would break down after $n - m$ steps since the lower diagonal block of dimension $m \times m$ is then zero. This is in fact an indication that the inverse of \mathbf{A} does not exist. If \mathbf{A} is a stiffness matrix, $\mathbf{A}_{22} - \mathbf{A}_{21}\mathbf{A}_{11}^{-1}\mathbf{A}_{12}$ is the condensed stiffness and the structure can not be properly fixed if the degrees of freedom \mathbf{x}_2 are not restrained. In other words, \mathbf{x}_2 defines a set of fixations that renders the structure *statically determined*. From (6.87) we can write:

$$\begin{bmatrix} \mathbf{A}_{11} & \mathbf{A}_{12} \\ \mathbf{A}_{21} & \mathbf{A}_{22} \end{bmatrix} \begin{bmatrix} -\mathbf{W} \\ \mathbf{I}_{m \times m} \end{bmatrix} = \mathbf{0} \quad (6.90)$$

where $\mathbf{I}_{m \times m}$ is the identity matrix of dimension m . Hence, the nullspace of \mathbf{A} can be represented by:

$$\mathbf{N} = [\mathbf{n}_1 \cdots \mathbf{n}_m] = \begin{bmatrix} -\mathbf{A}_{11}^{-1}\mathbf{A}_{12} \\ \mathbf{I}_{m \times m} \end{bmatrix} \quad (6.91)$$

6.6.4 Solution of singular systems

If the matrix operator of a system is square but singular, the inverse of \mathbf{A} cannot be defined. Nevertheless solutions to the system may exist. Indeed, let us assume that \mathbf{b}_1 and \mathbf{b}_2 exhibit the same linear dependency as the rows and columns of \mathbf{A} , namely according to (6.87),

$$\mathbf{b}_2 = \mathbf{W}^T \mathbf{b}_1 \quad (6.92)$$

The set of equations associated with the linearly dependent rows $[\mathbf{A}_{21} \ \mathbf{A}_{22}]$ are then redundant and the system $\mathbf{A}\mathbf{x} = \mathbf{b}$ contains only $n - m$ independent equations for which an infinite number of solutions exist. If (6.92) does not hold, then no solution can exist.

Taking account of (6.91), (6.92) is equivalent to $\mathbf{N}^T \mathbf{b} = \mathbf{0}$. Thus, it can be stated that:

A solution to the system $\mathbf{A}\mathbf{x} = \mathbf{b}$ exists

if and only if

\mathbf{b} is orthogonal to the null space of \mathbf{A} , \mathbf{A} being symmetric

If \mathbf{A} is a stiffness matrix, this shows that a static solution exists if and only if the applied forces are self-equilibrated with respect to the rigid body modes. If we define the *image* (or *range*) of \mathbf{A} as the space spanned by $\mathbf{A}\mathbf{y}$ for any vector \mathbf{y} , it can be equivalently stated that:

A solution to the system $\mathbf{A}\mathbf{x} = \mathbf{b}$ exists

if and only if

\mathbf{b} belongs to the image of \mathbf{A}

Indeed, by definition, if \mathbf{b} belongs to the image of \mathbf{A} , there exists \mathbf{y} such that:

$$\mathbf{A}\mathbf{x} = \mathbf{b} = \mathbf{A}\mathbf{y} \quad (6.93)$$

and \mathbf{y} is obviously a solution for \mathbf{x} .

Besides, if a solution \mathbf{x} exists while there exists a nullspace \mathbf{N} , this solution is clearly not unique since:

$$\mathbf{A}(\mathbf{x} + \sum_{s=1}^m \alpha_s \mathbf{n}_s) = \mathbf{A}\mathbf{x} = \mathbf{b} \quad (6.94)$$

for any linear combination α_s of the nullspace vectors. Hence the component of the solution lying in the nullspace is undetermined. In the context of structural mechanics, this means that if the forces are self-equilibrated, a static solution exists but the rigid body displacements are arbitrary.

Example 6.2

Let us consider a single uniform beam element as depicted in Figure 6.8. The element matrices for this beam were derived in Section 5.3.3. The stiffness matrix is

$$\mathbf{K}_e = \frac{EI}{\ell^3} \begin{bmatrix} 12 & 6\ell & -12 & 6\ell \\ 6\ell & 4\ell^2 & -6\ell & 2\ell^2 \\ -12 & -6\ell & 12 & -6\ell \\ 6\ell & 2\ell^2 & -6\ell & 4\ell^2 \end{bmatrix}$$

The null space is defined by two rigid body modes,³ for instance:

$$\mathbf{u}_{beam,trans}^T = [1 \quad 0 \quad 1 \quad 0] \quad \text{and} \quad \mathbf{u}_{beam,rot}^T = \left[-\frac{\ell}{2} \quad 1 \quad \frac{\ell}{2} \quad 1\right]$$

Hence no static solution exists for the applied force:

$$\mathbf{f}^T = [1 \quad 0 \quad -1 \quad 0]$$

since it does not satisfy the rotation self-equilibrium ($\mathbf{u}_{beam,rot}^T \mathbf{f} \neq 0$), but there exists a static solution (actually an infinity of solutions) for the load:

$$\mathbf{f}^T = [1 \quad 0 \quad -1 \quad \ell]$$

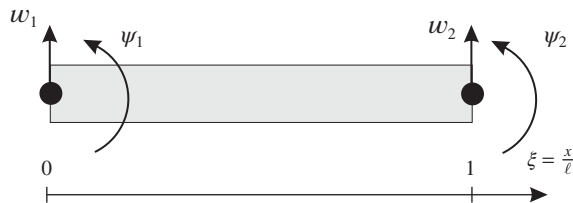


Figure 6.8 A free–free beam element.

³ The notation \mathbf{u} is used here to denote the columns of the nullspace of the stiffness matrix since they are the rigid body modes of the structure.

6.6.5 A family of generalized inverses

Since, under the conditions described above, solutions \mathbf{x} exist for singular systems, we can define an operator \mathbf{A}^+ , called *generalized inverse* or *pseudo-inverse* such that a solution \mathbf{x} is expressed as:

$$\mathbf{x} = \mathbf{A}^+ \mathbf{b} \quad (6.95)$$

Substituting the solution (6.95) in the system Equation (6.65), we obtain:

$$\mathbf{A}\mathbf{A}^+ \mathbf{b} = \mathbf{b}$$

This relation does not hold for all \mathbf{b} because, as seen earlier, a solution exists only if \mathbf{b} is in the image of \mathbf{A} , and thus:

$$\mathbf{A}\mathbf{A}^+ \mathbf{A} \mathbf{y} = \mathbf{A} \mathbf{y}$$

which now holds for any \mathbf{y} . Hence, the generalized inverse \mathbf{A}^+ of \mathbf{A} can also be defined as an operator satisfying:

$$\mathbf{A}\mathbf{A}^+ \mathbf{A} = \mathbf{A} \quad (6.96)$$

which stipulates that the image of \mathbf{A} is unchanged by the operator $\mathbf{A}\mathbf{A}^+$. For singular matrices, $\mathbf{A}\mathbf{A}^+$ is not the identity but has the same effect as an identity matrix when applied to the image of \mathbf{A} . Obviously, if \mathbf{A} is nonsingular, $\mathbf{A}^+ = \mathbf{A}^{-1}$.

Let us point out that unless \mathbf{A} is nonsingular, the generalized inverse satisfying (6.96) is not unique. Indeed, calling \mathbf{N} the nullspace of \mathbf{A} as defined in Section 6.6.3, and calling \mathbf{A}^+ a generalized inverse satisfying (6.96), then:

$$\tilde{\mathbf{A}}^+ = \mathbf{A}^+ + \mathbf{B}\mathbf{N}^T + \mathbf{N}\mathbf{V} \quad (6.97)$$

also satisfies (6.96) for any \mathbf{B} and \mathbf{V} . Equation (6.97) thus defines a family of generalized inverses. The solution obtained with $\tilde{\mathbf{A}}^+$ in (6.97) is:

$$\mathbf{x} = \mathbf{A}^+ \mathbf{b} + \mathbf{B}\mathbf{N}^T(\mathbf{A}\mathbf{y}) + \mathbf{N}\mathbf{V}\mathbf{b} = \mathbf{A}^+ \mathbf{b} + \mathbf{N}\mathbf{V}\mathbf{b} \quad (6.98)$$

which differs from the solution $\mathbf{A}^+ \mathbf{b}$ only by its rigid body mode content.

Example 6.3

Let us show that, using the block notation introduced in (6.86), the matrix \mathbf{A}^+ defined by:

$$\mathbf{A}^+ = \begin{bmatrix} \mathbf{A}_{11}^{-1} & \mathbf{0} \\ \mathbf{0} & \mathbf{0} \end{bmatrix} \quad (\text{E6.3.a})$$

is a generalized inverse, \mathbf{A}_{11} being as before a square submatrix of maximum range, i.e. \mathbf{A}_{11} is formed by any $n - m$ linearly independent columns and rows of \mathbf{A} .

To show that $\mathbf{A}^{[11]+}$ is a generalized inverse, we prove that it satisfies (6.96) as follows:

$$\begin{aligned} \mathbf{A}\mathbf{A}^+ \mathbf{A} &= \begin{bmatrix} \mathbf{A}_{11} & \mathbf{A}_{12} \\ \mathbf{A}_{21} & \mathbf{A}_{22} \end{bmatrix} \begin{bmatrix} \mathbf{A}_{11}^{-1} & \mathbf{0} \\ \mathbf{0} & \mathbf{0} \end{bmatrix} \begin{bmatrix} \mathbf{A}_{11} & \mathbf{A}_{12} \\ \mathbf{A}_{21} & \mathbf{A}_{22} \end{bmatrix} \\ &= \begin{bmatrix} \mathbf{A}_{11} & \mathbf{A}_{12} \\ \mathbf{A}_{21} & \mathbf{A}_{21}\mathbf{A}_{11}^{-1}\mathbf{A}_{12} \end{bmatrix} \end{aligned} \quad (\text{E6.3.b})$$

and recalling from (6.89) that $A_{21}A_{11}^{-1}A_{12}$ is equal to A_{22} concludes the proof. Another proof (left to the reader) can be constructed by showing that A^+b is a solution of $Ax = b$ when $N^Tb = 0$.

As will be discussed next, this particular form of generalized inverse is of particular importance since it results automatically from the factorization of a full-rank submatrix of A .

6.6.6 Solution by generalized inverses and finding the nullspace N

Factorization of a singular matrix: constructing a generalized inverse

If a solution exists, it can be computed using the generalized inverse A^+ defined in Example 6.3 so that:

$$\begin{bmatrix} x_1 \\ x_2 \end{bmatrix} = \begin{bmatrix} A_{11}^{-1} & 0 \\ 0 & 0 \end{bmatrix} \begin{bmatrix} b_1 \\ b_2 \end{bmatrix} \quad (6.99)$$

namely by solving the system $Ax = b$ for a maximum set of independent variables and equations, i.e. $x_1 = A_{11}^{-1}b_1$, and setting to zero the remaining unknowns x_2 .

When a factorization technique is used, it corresponds to advancing the elimination process as long as nonzero pivots exist. When factorizing a nondefinite system, pivoting must then be used and the factorization is stopped when the remaining submatrix is zero. For semi-definite matrices, pivoting is not required since zero pivots appear only when the row of the pivot is a linear combination of all preceding rows. In that case, when a zero pivot is found at step k , the corresponding unknown x_k is flagged as being part of x_2 and the factorization is continued by skipping step k .

In structural mechanics, setting to zero the degrees of freedom x_2 corresponds to adding *fictitious links* to the system to render it statically determined. Since the forces applied must be self-equilibrated for a static solution to exist if the structure is floating, applying temporary constraints for the system to be exactly statically determined does not affect the solution as far as deformations are concerned, but simply sets the rigid body displacement of the solution.

Computing the null space

Let us recall from equation (6.91) that the nullspace of A can be computed as:

$$N = \begin{bmatrix} -A_{11}^{-1}A_{12} \\ I \end{bmatrix} \quad (6.100)$$

When a factorization technique is applied, only the nonsingular matrix A_{11} is factored as explained above. Hence the rigid body modes can be found by applying a forward and backward substitution to the submatrix A_{12} . When A is a stiffness matrix, (6.100) indicates that the rigid body modes are found by solving the system for x_1 when setting to 1 a degree of freedom x_2 , the other x_2 being set to zero.

Since, in order to minimize memory usage, the matrix A is overwritten by its factored form, A_{12} does no longer exist after the factorization. Nevertheless, from the factorization methods described in Sections 6.6.1 and 6.6.1, it is understood that when a null pivot is found at step k , column k stores a column of A_{12} transformed by a forward substitution. Hence computing $A_{11}^{-1}A_{12}$ simply requires to perform a backward substitution on the columns of the null pivots.

When the nullspace of a matrix is computed as a by-product of its factorization, the threshold used to detect null pivots plays an essential role in finding the nullspace of a matrix. Since the threshold to detect correctly the null pivots strongly depends on the conditioning of the matrix and on the machine precision, the automatic detection and computation of the nullspace as described above might yield a wrong nullspace. To circumvent this delicate problem in structural mechanics, some methods first detect rigid body modes by geometric inspection and use that information to build the nullspace during the factorization in a more robust way (Brzobohatý *et al.* 2011, Farhat and G radin 1998, Papadrakakis and Fragakis 2001).

Example 6.4

Let us consider again the single element free-free beam of Example 6.2. Let us compute its rigid body modes as a by-product of the factorization and find a static solution for the force distribution:

$$\mathbf{f}^T = [1 \ 0 \ -1 \ \ell]$$

The LU factorization for the beam element stiffness successively yields:

$$\begin{aligned} \frac{EI}{\ell^3} \begin{bmatrix} 12 & 6\ell & -12 & 6\ell \\ 6\ell & 4\ell^2 & -6\ell & 2\ell^2 \\ -12 & -6\ell & 12 & -6\ell \\ 6\ell & 2\ell^2 & -6\ell & 4\ell^2 \end{bmatrix} \begin{bmatrix} w_1 \\ \psi_1 \\ w_2 \\ \psi_2 \end{bmatrix} &= \begin{bmatrix} 1 \\ 0 \\ -1 \\ \ell \end{bmatrix} \\ \frac{EI}{\ell^3} \begin{bmatrix} 12 & 6\ell & -12 & 6\ell \\ 0 & 1\ell^2 & 0 & -1\ell^2 \\ 0 & 0 & 0 & 0 \\ 0 & -1\ell^2 & 0 & 1\ell^2 \end{bmatrix} \begin{bmatrix} w_1 \\ \psi_1 \\ w_2 \\ \psi_2 \end{bmatrix} &= \begin{bmatrix} 1 \\ -\ell/2 \\ 0 \\ \ell/2 \end{bmatrix} \\ \frac{EI}{\ell^3} \begin{bmatrix} 12 & 6\ell & -12 & 6\ell \\ 0 & 1\ell^2 & 0 & -1\ell^2 \\ 0 & 0 & 0 & 0 \\ 0 & 0 & 0 & 0 \end{bmatrix} \begin{bmatrix} w_1 \\ \psi_1 \\ w_2 \\ \psi_2 \end{bmatrix} &= \begin{bmatrix} 1 \\ -\ell/2 \\ 0 \\ 0 \end{bmatrix} \end{aligned} \quad (\text{E6.4.a})$$

The first rigid body mode is then obtained by setting $w_2 = 1$ and $\psi_2 = 0$ and by solving:

$$\frac{EI}{\ell^3} \begin{bmatrix} 12 & 6\ell & -12 & 6\ell \\ 0 & 1\ell^2 & 0 & -1\ell^2 \end{bmatrix} \begin{bmatrix} w_1 \\ \psi_1 \\ 1 \\ 0 \end{bmatrix} = \mathbf{0}$$

which yields:

$$\mathbf{u}_{trans}^T = [1 \ 0 \ 1 \ 0]$$

The second rigid mode is found by setting $w_2 = 0$ and $\psi_2 = 1$ and solving:

$$\frac{EI}{\ell^3} \begin{bmatrix} 12 & 6\ell & -12 & 6\ell \\ 0 & 1\ell^2 & 0 & -1\ell^2 \end{bmatrix} \begin{bmatrix} w_1 \\ \psi_1 \\ 0 \\ 1 \end{bmatrix} = \mathbf{0}$$

which yields:

$$\mathbf{u}_{rot}^T = [-\ell \quad 1 \quad 0 \quad 1]$$

We then verify that a static solution exists for \mathbf{f} since $\mathbf{u}_{trans}^T \mathbf{f} = 0$ and $\mathbf{u}_{rot}^T \mathbf{f} = 0$. This is also directly seen from the fact that the last two lines of the right hand side in (E6.4.a) are null. The solution is found by setting $w_2 = 0$ and $\psi_2 = 0$ and solving:

$$\frac{EI}{\ell^3} \begin{bmatrix} 12 & 6\ell \\ 0 & 1\ell^2 \end{bmatrix} \begin{bmatrix} w_1 \\ \psi_1 \end{bmatrix} = \begin{bmatrix} 1 \\ -\ell/2 \end{bmatrix} \rightarrow \mathbf{x}^T = \frac{\ell^3}{EI} \begin{bmatrix} \frac{1}{3} & \frac{-1}{2\ell} & 0 & 0 \end{bmatrix}$$

6.6.7 Taking into account linear constraints

In some cases, static or dynamic problems are subjected to linear constraints expressed in the form:

$$\mathbf{B}\mathbf{q} - \mathbf{h} = \mathbf{0} \quad (6.101)$$

where \mathbf{B} is a rectangular matrix of dimension $p \times n$ and \mathbf{h} a vector of constants.

The linear constrained problem:

$$\mathbf{K}\mathbf{q} = \mathbf{g} \quad \text{submitted to} \quad \mathbf{B}\mathbf{q} - \mathbf{h} = \mathbf{0}$$

can easily be handled by the method of Lagrange multipliers developed in Section 1.6. It is solution of a quadratic stationarity problem in which the constraints are introduced by a dislocation potential (Equation (1.83)):

$$\delta_{\mathbf{q}, \lambda} \left\{ \frac{1}{2} \mathbf{q}^T \mathbf{K} \mathbf{q} - \mathbf{q}^T \mathbf{g} + \lambda^T (\mathbf{B}\mathbf{q} - \mathbf{h}) \right\} = 0 \quad (6.102)$$

where λ is a vector containing the Lagrange multipliers associated with the constraints. The resulting matrix equation is:

$$\begin{bmatrix} \mathbf{K} & \mathbf{B}^T \\ \mathbf{B} & \mathbf{0} \end{bmatrix} \begin{bmatrix} \mathbf{q} \\ \lambda \end{bmatrix} = \begin{bmatrix} \mathbf{g} \\ \mathbf{h} \end{bmatrix} \quad (6.103)$$

It involves an extended stiffness matrix which is still symmetric, but no longer positive definite.

Gauss elimination may be applied to a system of type (6.103) provided that it is implemented with a maximum pivot strategy so as to avoid pivoting on zero diagonal terms before their disappearance through fill-in. Each linear constraint gives finally rise to a negative pivot, but the positive definite character of the extended strain energy:

$$\frac{1}{2} \mathbf{q}^T \mathbf{K} \mathbf{q} + \lambda^T (\mathbf{B}\mathbf{q} - \mathbf{h}) \geq 0 \quad (6.104)$$

is still preserved for any vector \mathbf{q} that a priori fulfills the constraining conditions.

The use of Lagrange multipliers to solve linear constrained systems is particularly useful for the static solution of mechanical systems with rigid body modes since it allows to enforce orthogonality between the loading and the rigid body motion (see Problems 6.6 and 6.7).

6.7 Practical aspects of inverse iteration methods

The inverse iteration concept has already been introduced in Section 6.5.3 in order to remove the main limitation of the power algorithm, i.e. the need to form explicitly matrix $\mathbf{K}^{-1}\mathbf{M}$. It is described by Equations (6.64a–6.64c). Those basic iteration steps are at the heart of several eigensolvers as will be seen later in this chapter. Its effective implementation requires solving the linear system (6.64b), a matter that has been discussed in Section 6.6.

When applying inverse iteration methods, also known as Krylov methods in the mathematical community, one is confronted with three important issues:

1. Structures exhibiting rigid body and/or kinematic modes need appropriate treatment. These modes are collected in matrix \mathbf{U} and can be interpreted as eigenmodes with zero eigenvalue. They form in fact the nullspace of the stiffness matrix. As shown in Section 6.6.3, they can be obtained as a by-product of the factorization of the stiffness matrix \mathbf{K} . A straightforward modification of the inverse iteration scheme based on the use of the deflation and projection operator introduced in Section 6.7.1 will allow us to always converge towards the vibration modes, the latter lying in the image of \mathbf{K} .
2. By essence inverse iteration methods converge to the eigensolutions of the lower frequency spectrum. To target eigensolutions in the vicinity of a specific frequency, spectral shifting can be applied as explained in Section 6.7.2. As will be seen, such a procedure can also be used to improve the converge rate of inverse iterations, which is strongly affected by the presence of close eigenvalues (as seen for the inverse iteration in Section 6.5).
3. The convergence rate of the power iteration scheme drops exponentially (see Figure 6.3) when close eigenvalues occur. It can be significantly improved by the frequency shifting technique described in Section 6.7.2 which provides a trick to modify the spacing between eigenvalues. However, a more efficient remedy to convergence deficiency due to eigenvalue spacing is provided by methods such as subspace iteration or the Lanczos method since they postpone the problem of separating close eigenvalues to the solution of an interaction eigenvalue problem, the latter being then much smaller and thus solvable by a method of successive transformations.

6.7.1 Inverse iteration in presence of rigid body modes

In case the structure exhibits rigid body modes (or mechanisms), the stiffness matrix \mathbf{K} is singular and there exist m independent solutions $\mathbf{u}_{(i)}$ satisfying:

$$\mathbf{K}\mathbf{u}_{(i)} = \mathbf{0} \quad i = 1, \dots, m$$

The solutions $\mathbf{u}_{(i)}$ can be considered as vibration modes associated to null eigenfrequencies (see Section 2.2.2). According to Equation (6.91), they form the nullspace \mathbf{U} of matrix⁴ \mathbf{K} and can be found as by-product of its factorization:

$$\mathbf{U} = [\mathbf{u}_{(1)} \cdots \mathbf{u}_{(m)}] = \begin{bmatrix} -(\mathbf{K}_{11}^{-1}\mathbf{K}_{12}) \\ \mathbf{I}_{m \times m} \end{bmatrix} \quad (6.105)$$

⁴ The notation \mathbf{U} is used here to denote the nullspace of the stiffness matrix since it consists of the rigid body modes $\mathbf{u}_{(i)}$ of the structure.

In the presence of rigid body modes solving the static problem of the inverse iteration requires special care. As seen in Section 6.6.4 a solution exists only if the right-hand side of the static equation (6.64b) is self-equilibrated, namely if $U^T M z_p = \mathbf{0}$. Let us therefore define the projector:

$$P_U = I - U(U^T M U)^{-1} U^T M$$

Assuming subsequently that the rigid body modes forming U are mass-orthonormalized, we can also write:

$$P_U = I - U U^T M \quad (6.106)$$

If we thus replace iterate z_p by $P_U z_p$ we guarantee that:

$$U^T M P_U z_p = \mathbf{0}$$

the projector P_U removing any component of z_p that is not M -orthogonal. The inverse iteration must then be written as:

$$\left\{ \begin{array}{l} y_p = M z_p \\ \text{Solve } K z_{p+1}^* = y_p \\ z_{p+1} = P_U \frac{z_{p+1}^*}{\|z_{p+1}^*\|} \end{array} \right. \quad \begin{array}{l} (6.107a) \\ (6.107b) \\ (6.107c) \end{array}$$

Solving the singular static problem (6.107b) requires applying special factorization techniques implying a generalized inverse K^+ , as explained in Section 6.6.6. The algorithm (6.107a–6.107c) can then be interpreted as inverse iterations using the specific generalized inverse $K^\dagger = P_U K^+ P_U$, which is unique (according to (6.97)). It is the flexibility matrix in the space of the elastic modes, namely the inverse having as spectral expansion:

$$K^\dagger = \sum_{s=1}^{n-m} \frac{\mathbf{x}_{(s)} \mathbf{x}_{(s)}^T}{\omega_s^2 \mu_s} \quad (6.108)$$

The similarity between (6.106) and (6.60) suggests that the projection step can also be interpreted as an *orthogonal deflation with respect to the space of the rigid body modes*, exactly like deflation with respect to earlier extracted elastic modes. Hence the projector P_U is ensuring simultaneously that the iterates are computed in the subspace orthogonal to the rigid-body modes (the subspace of elastic modes) and that the static problem is well-posed.

Example 6.5

Let us consider again the free-free beam of Example 6.2. Its rigid-body modes were obtained as a by-product of factorization of the stiffness matrix and are collected in:

$$U = [\mathbf{u}_{trans} \quad \mathbf{u}_{rot}] = \begin{bmatrix} 1 & -\ell \\ 0 & 1 \\ 1 & 0 \\ 0 & 1 \end{bmatrix}$$

The first rigid mode has a unit amplitude. For this reason its generalized mass is the total mass of the beam:

$$\mu_1 = \mathbf{u}_{trans}^T \mathbf{M} \mathbf{u}_{trans} = m\ell$$

It is normalized in the form:

$$\mathbf{u}_{(1)}^T = \frac{1}{\sqrt{\mu_1}} \mathbf{u}_{trans}^T = \frac{1}{\sqrt{m\ell}} \begin{bmatrix} 1 & 0 & 1 & 0 \end{bmatrix}$$

The rigid mode \mathbf{u}_{rot} is a combination of translation and of rotation around the centre of mass. We first perform its orthogonalization to the first mode:

$$\mathbf{u}'_{(2)} = \mathbf{u}_{rot} - \alpha \mathbf{u}_{(1)}$$

so that $\mathbf{u}'_{(2)T} \mathbf{M} \mathbf{u}_{(1)} = 0$. We obtain:

$$\alpha = \mathbf{u}_{rot}^T \mathbf{M} \mathbf{u}_{(1)} = -\frac{\ell}{2} \sqrt{m\ell}$$

We thus obtain the orthogonal mode:

$$\mathbf{u}'_{(2)} = \begin{bmatrix} -\frac{\ell}{2} & 1 & \frac{\ell}{2} & 1 \end{bmatrix}$$

which effectively corresponds to a rotation around the centre of mass.

We then calculate its generalized mass:

$$\mu_2 = \mathbf{u}'_{(2)T} \mathbf{M} \mathbf{u}'_{(2)} = \frac{m\ell^3}{12}$$

which is the moment of inertia around the center of mass of the element. After orthonormalization, the second mode may be written as:

$$\mathbf{u}_{(2)}^T = \sqrt{\frac{12}{m\ell^3}} \begin{bmatrix} -\frac{\ell}{2} & 1 & \frac{\ell}{2} & 1 \end{bmatrix}$$

After the rigid modes have been orthonormalized, the filtering operator can be constructed in the form:

$$\mathbf{P}_U = \mathbf{I} - \mathbf{u}_{(1)} \mathbf{u}_{(1)}^T \mathbf{M} - \mathbf{u}_{(2)} \mathbf{u}_{(2)}^T \mathbf{M}$$

All calculations done, we obtain the explicit expression the filtering operator:

$$\mathbf{P}_U = \begin{bmatrix} -\frac{1}{10} & -\frac{2\ell}{15} & \frac{1}{10} & \frac{\ell}{30} \\ \frac{6}{5\ell} & \frac{11}{10} & -\frac{6}{5\ell} & \frac{1}{10} \\ \frac{1}{10} & -\frac{\ell}{30} & -\frac{1}{10} & \frac{2\ell}{15} \\ \frac{6}{5\ell} & \frac{1}{10} & -\frac{6}{5\ell} & \frac{11}{10} \end{bmatrix}$$

which has the expected properties $\mathbf{P}_U \mathbf{u}_{(1)} = \mathbf{P}_U \mathbf{u}_{(2)} = \mathbf{0}$.

6.7.2 Spectral shifting

Let us write the eigenvalue problem in the equivalent form:

$$(\mathbf{K} - \mu\mathbf{M})\mathbf{x} = (\omega^2 - \mu)\mathbf{M}\mathbf{x}$$

and define:

$$\mathbf{K}_{shift} = \mathbf{K} - \mu\mathbf{M} \quad (6.109)$$

$$\omega_{shift}^2 = \omega^2 - \mu \quad (6.110)$$

respectively the shifted stiffness matrix and eigenvalue. The eigenproblem can then be written:

$$\mathbf{K}_{shift}\mathbf{x} = \omega_{shift}^2\mathbf{M}\mathbf{x} \quad (6.111)$$

where the spectrum of ω_{shift}^2 is related to the original spectrum through a shifting of μ (Figure 6.9).

Applying the inverse iteration scheme (6.64a–6.64c) on the shifted problem results in (dropping the scaling step for simplicity):

$$\begin{cases} \mathbf{y}_p &= \mathbf{M}\mathbf{z}_p \\ (\mathbf{K} - \mu\mathbf{M})\mathbf{z}_{p+1} &= \mathbf{y}_p \end{cases}$$

and involves, at each iteration, a linear solution with matrix $(\mathbf{K} - \mu\mathbf{M})$.

Following the same reasoning as in Section 6.5.1 but now for the shifted problem (6.111), it is obvious that the inverse iteration will converge towards the eigenmode $\mathbf{x}_{(r)}$ of eigenvalue ω_r^2 which verifies:

$$|\omega_r^2 - \mu| = \min_j \{ |\omega_j^2 - \mu| \}$$

Obviously, the convergence becomes better as μ is chosen closer to ω_r^2 since the ratio between the first and the second eigenfrequencies increases.

Spectral shifting is commonly applied mainly for three purposes:

- In case the stiffness is singular (presence of rigid body modes) one can avoid solving a singular system in the inverse iteration as explained in Section 6.7.1 by applying a negative shift $\mu < 0$. Indeed in that case the shifted matrix $\mathbf{K} - \mu\mathbf{M}$ becomes regular. Let us note however that this might negatively affect the converge of the power iteration due to the fact that the ratio between consecutive eigenvalues might be unfavourably modified. In addition, the rigid body modes need in this case to be computed as eigensolutions whereas in fact they can be obtained at nearly no cost as explained in Section 6.6.6.

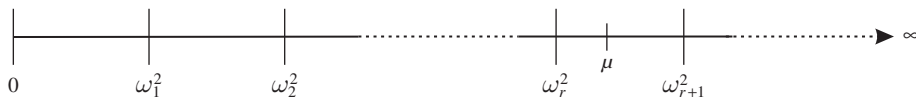


Figure 6.9 Spectral shifting.

- Applying a positive shift μ forces the power iteration and deflation to find the eigensolutions having eigenvalues ω_r in the vicinity of μ . This is very handy in case one is interested in a specific spectral band (for instance in case the loading acting on the system is known to excite only a limited frequency band). Hence one can find the relevant modes without having to compute all the lower modes that are not of interest.
- Spectral shifting may also be integrated within the iteration process to accelerate convergence towards a given eigenvalue ω_r^2 . In this case, the Rayleigh quotient allows one to calculate at each step the best estimate of the eigenvalue in order to adjust the shifting value. Moreover, the number of negative elements obtained in the pivot sequence on the Gauss elimination of $(\mathbf{K} - \mu\mathbf{M})$ gives an indication on the position of the solution in the eigenspectrum. In this form, however, the algorithm has the disadvantage of requiring a new triangularization each time the iteration matrix changes, which increases its cost.

6.8 Subspace construction methods

As seen in Section 6.7, the inverse iteration scheme combined with a deflation process is a very interesting concept allowing to compute a given number of eigensolutions. However this basic method has still major drawbacks that render its applicability to practical problems rather limited. It is thus essential to further improve the method so that it can handle close eigenvalues and provide several eigensolutions with high accuracy and maximum efficiency.

To achieve this goal, we first observe that when applying the inverse iteration method to find a k th eigensolution by deflation, the eigensolutions are searched for one after the other. As a consequence,

- the iteration process starts from scratch for every eigensolution, namely all the information produced while iterating to find the previous solutions is thrown away;
- every eigensolution converges without knowledge of higher eigensolutions and therefore the convergence rate is poor for close eigenvalues.

Subspace iteration and the *Lanczos algorithm* provide two different approaches to improve or maximize the use of the information generated from the iteration process.

6.8.1 The subspace iteration method

The idea behind the subspace iteration method is to perform inverse iterations *simultaneously* on several vectors.

Algorithm

The principle of subspace iteration (Bathe 1971) consists of generating a sequence of matrices $\mathbf{Z}_0, \dots, \mathbf{Z}_k$ of dimension $(n \times p)$, their columns being basis vectors that span successive subspaces $\mathbb{E}_0^p, \mathbb{E}_1^p, \dots, \mathbb{E}_k^p$ of dimension p . The aim is to let those subspaces converge towards subspace $\mathbb{E}_\infty^p = \mathbb{E}^p$ spanning the first p eigenmodes contained in \mathbf{X}^p . This is schematically illustrated in Figure 6.10.

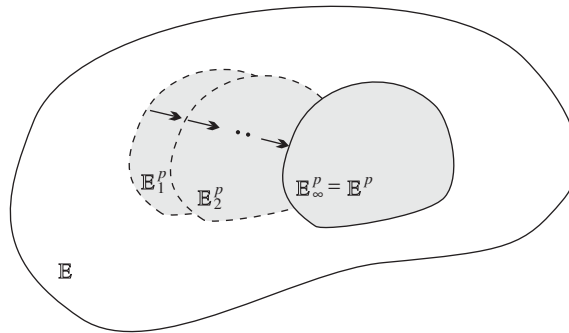


Figure 6.10 Schematic description of the subspace iteration concept.

Recalling that the inverse iteration has as fundamental property to orient the iterates in the direction of the lowest modes, the successive spaces are obtained by applying to each vector in \mathbf{Z}_k an inverse iteration step. The kernel of the method is thus described by:

$$\begin{cases} \mathbf{Y}_k &= \mathbf{M}\mathbf{Z}_k \\ \mathbf{K}\mathbf{Z}_{k+1} &= \mathbf{Y}_k \end{cases} \quad (6.112)$$

which can be interpreted as an inverse iteration by blocks, namely on all directions in \mathbf{Z}_k simultaneously. Algorithm (6.112) would let every column of \mathbf{Z}_k converge individually towards the first eigenmode, which would be useless. If we want the space described by \mathbf{Z}_k to represent a set of lower eigenmodes, we have to enforce that the columns of \mathbf{Z}_k remain linearly independent.

A first idea could be to apply a Gram-Schmidt orthonormalization to ensure that the second column in \mathbf{Z}_k is \mathbf{M} -orthogonal to the first, the third orthogonal to the first two and so on. In that case the first column would converge to the first mode, the second to the second mode and so on. In fact this would be very similar to the deflated power iteration of the previous section, except that iterations would be done simultaneously and deflation would be performed not with the converged modes but with their current estimates. But in essence we would not improve on the basic power iteration method.

A much better idea is as follows: instead of taking the first column of \mathbf{Z}_k as an approximate for the first mode, let us try to search for its best approximation using *all* the vectors in the subspace represented by \mathbf{Z}_k . Similarly, for any higher mode let us try to find a best approximate in the entire subspace. Mathematically speaking, let us write the approximation:

$$\mathbf{x}_{(s)} \simeq \mathbf{x}_{(s),k} = \mathbf{Z}_k \mathbf{v}_{(s),k} \quad (6.113)$$

where $\mathbf{v}_{(s),k}$ can be seen as the coordinates of the approximation $\mathbf{x}_{(s),k}$ of mode s in the subspace described by \mathbf{Z}_k . Substituting this approximation in the original eigenvalue problem (6.1) and projecting the eigenvalue problem on the subspace, i.e. pre-multiplying it by \mathbf{Z}_k^T and adopting matrix notation one finds the reduced eigenvalue problem:⁵

$$\tilde{\mathbf{K}}_k \mathbf{V}_k = \tilde{\mathbf{M}}_k \mathbf{V}_k \tilde{\mathbf{Q}}^2 \quad (6.114)$$

⁵ Note that this process corresponds to a reduction process of the problem in the subspace of \mathbf{Z}_k , as explained in Section 6.9.

with

$$\tilde{\mathbf{K}}_k = \mathbf{Z}_k^T \mathbf{K} \mathbf{Z}_k \quad \text{and} \quad \tilde{\mathbf{M}}_k = \mathbf{Z}_k^T \mathbf{M} \mathbf{Z}_k \quad (6.115)$$

This eigenvalue problem (6.114) is of dimension $p \times p$, thus, in practice, very small compared to the original problem. It is determining the best combination of the vectors in \mathbf{Z}_k to approximate the eigenmodes $\mathbf{x}_{(s)}$. It expresses the interaction between the eigenvalue problem and the subspace \mathbf{Z}_k and is thus also called the *interaction problem*. The eigenvalues $\tilde{\omega}_s^2$ found from the interaction problem (6.114) can be considered as the best approximations to ω_s^2 and the corresponding eigenmodes in the physical domain are retrieved by substituting the subspace eigenvectors $\mathbf{v}_{(s),k}$ in (6.113).

Remember that we were not just looking for an approximation of the eigensolution in the subspace, but we started the discussion by mentioning the need to ensure that the directions stored in \mathbf{Z}_k are kept independent in order to avoid that they all become parallel to the first eigenmode, yielding a degenerated subspace. This issue can now be solved in an elegant way by noting that the interaction problem is a (reduced) symmetric eigenproblem so that the eigenvectors $\mathbf{v}_{(s),k}$ satisfy $\tilde{\mathbf{M}}$ - and $\tilde{\mathbf{K}}$ -orthogonality, namely (assuming the eigenvectors to be mass normalized):

$$\begin{aligned} \mathbf{V}_k^T \tilde{\mathbf{K}} \mathbf{V}_k &= \mathbf{X}_k^{pT} \mathbf{K} \mathbf{X}_k^p = \tilde{\mathbf{Q}}^2 \\ \mathbf{V}_k^T \tilde{\mathbf{M}} \mathbf{V}_k &= \mathbf{X}_k^{pT} \mathbf{M} \mathbf{X}_k^p = \mathbf{I} \end{aligned}$$

indicating also, by definition of the reduced matrices, that the mode approximations satisfy \mathbf{M} - and \mathbf{K} -orthogonality.⁶ Hence the approximation $\mathbf{X}_k^p = \mathbf{Z}_k \mathbf{V}_k$ of the eigenmode subspace \mathbf{X}^p can be taken as a proper basis to guarantee that the process will not degenerate.

In the practical description of the algorithm distinction has to be made between matrix \mathbf{Z}_k after and before projection. With the notation \mathbf{Z}_{k+1}^* to denote the result of power iteration before projection, the subspace iteration method can now be summarized by the following basic steps:

$$\left\{ \begin{array}{ll} \mathbf{Y}_k = \mathbf{M} \mathbf{Z}_k & (6.116a) \\ \text{Solve } \mathbf{K} \mathbf{Z}_{k+1}^* = \mathbf{Y}_k & (6.116b) \\ \text{Build } \tilde{\mathbf{K}}_{k+1} = \mathbf{Z}_{k+1}^{*T} \mathbf{K} \mathbf{Z}_{k+1}^* \quad \text{and} \quad \tilde{\mathbf{M}}_{k+1} = \mathbf{Z}_{k+1}^{*T} \mathbf{M} \mathbf{Z}_{k+1}^* & (6.116c) \\ \text{Solve (eigenproblem) } \tilde{\mathbf{K}}_{k+1} \mathbf{V}_{k+1} = \tilde{\mathbf{M}}_{k+1} \mathbf{V}_{k+1} \tilde{\mathbf{Q}}^2 & (6.116d) \\ \mathbf{Z}_{k+1} = \mathbf{X}_{k+1}^p = \mathbf{Z}_{k+1}^* \mathbf{V}_{k+1} & (6.116e) \end{array} \right.$$

Algorithm convergence properties

Let us summarize the significant convergence properties of the subspace method (details of the analysis can be found for instance in Bathe (1977)). It can be shown that:

1. The subspaces $\mathbb{E}_k^p \subset \mathbb{E}$ built on the p columns of the successive iterates \mathbf{Z}_k converge towards subspace \mathbb{E}^p corresponding to the columns of \mathbf{X}^p . In other words, referring to (6.116e), the

⁶ The fact that the vectors $\mathbf{x}_{(s),k}$ satisfy exactly both the \mathbf{M} - and \mathbf{K} -orthogonality does not imply that they are the exact modes. Indeed they do not necessarily satisfy the original eigenvalue problem but only satisfy the reduced eigenvalue problem (6.114).

vectors $\mathbf{x}_{(s),k+1}$ converge to the lowest modes of the free vibration problem, provided that \mathbf{Z}_0 is not orthogonal to any of them.

2. The convergence rate towards each of the modes $\mathbf{x}_{(j)}$ is of the order of $O(r_j^k)$, with the ratio:

$$r_j = \frac{\omega_j^2}{\omega_{p+1}^2} \quad (6.117)$$

measuring the difference between the eigenvalue of concern and the eigenvalue which is immediately exterior to the subspace we are seeking. This property of the algorithm is essential because it shows that global convergence towards subspace $\mathbb{E}^p \in \mathbb{E}$ containing an eigensolution $\mathbf{x}_{(j)}$ ($j \leq p$) depends entirely on the ratio of the associated eigenvalue to that of mode number $p + 1$. This is a significant improvement compared to the convergence obtained with the inverse iteration and deflation scheme. It means that, in the case of close eigenvalues inside the subspace, the total convergence of the algorithm is in no way affected, the problem of separating them being postponed to the level of the interaction analysis.

Accelerating the convergence rate: buffer vectors

Because the convergence of the method is driven by the ratio $\left(\frac{\omega_j}{\omega_{p+1}}\right)^2$, it is advantageous to augment iteration matrix \mathbf{Z}_0 by a certain number t of *buffer vectors*, the only aim of which is to increase the rate of convergence towards the last required eigenvalue ω_p^2 . Indeed, the convergence rate for calculating the latter becomes $O\left(\frac{\omega_p}{\omega_{p+t+1}}\right)^2$ instead of $O\left(\frac{\omega_p}{\omega_{p+1}}\right)^2$. The dilemma now resides in choosing a number of buffer vectors which is sufficient to improve the algorithm convergence without significantly increasing the number of operations per iteration. A total number of iteration vectors of $\min\{2p, p + 8\}$ is commonly adopted (Bathe and Wilson 1973).

Limiting the cost per iteration

Let us observe that the cost of a subspace iteration resides in the inverse iteration step (6.116b) and in the interaction problem (6.116c–6.116d). The inverse iteration step is the heart of the algorithm and can be made efficient using fast solvers for the static problem. The interaction problem requires building the reduced matrices $\tilde{\mathbf{K}}_{k+1}$ and $\tilde{\mathbf{M}}_{k+1}$, then solving the reduced eigenvalue problem. To perform this interaction analysis, we have to use a method for solving the eigenvalue problem which allows access to all solutions with a satisfactory resolution. For example, we can use Jacobi's method. However, the most appropriate algorithm is without any doubt the successive transformation algorithm *LR* of Rutishauser (Schwarz *et al.* 1973) or its *QR* variant (Francis 1961, 1962).

Let us remind that the interaction problem has two purposes: first it allows finding the best approximates of the eigensolution in the latest subspace, secondly it builds an orthonormal basis for the subspace so that the successive subspaces do not degenerate by letting all the vectors in \mathbf{Z}_k converge to the lowest mode. For the first iterations of the algorithm, we know that the subspace is not yet well converged to the desired space of the lowest eigenmodes and

thus one can decide to skip searching for the best eigensolution in the subspace and just update the subspace by an inverse iteration step. However, if the interaction problem is not performed, the columns of \mathbf{Z}_k could become, after a few iterations, comparable up to the digital round-off error of the computer, leading to the degeneracy of the subspace. Hence, in case no interaction problem is solved, one will ensure that the directions in the subspace remain well independent by performing a simple Gram-Schmidt orthonormalization on the columns of \mathbf{Z}_k . An efficient way to perform such an orthonormalization can be implemented as follows:

1. from a matrix \mathbf{Z}_k^* with nonorthogonal columns, construct:

$$\mathbf{S}_k = \mathbf{Z}_k^{*T} \mathbf{Z}_k^* \quad (6.118)$$

2. perform a Choleski decomposition (see Section 6.6.1):

$$\mathbf{S}_k = \mathbf{C}\mathbf{C}^T \quad (6.119)$$

where \mathbf{C} is a lower triangular matrix;

3. construct the new orthogonal directions \mathbf{Z}_k by solving the systems:

$$\mathbf{C}\mathbf{Z}_k^T = \mathbf{Z}_k^{*T} \quad (6.120)$$

Indeed, we verify that $\mathbf{Z}_k^T \mathbf{Z}_k = \mathbf{C}^{-1} \mathbf{Z}_k^{*T} \mathbf{Z}_k^* \mathbf{C}^{-T} = \mathbf{I}$.

Such an orthonormalization will require significantly less operations than the interaction problem since it mainly involves the construction of matrix \mathbf{S}_k and its triangularization. However, it gives no indication about the algorithm convergence for the eigenvalues. Consequently, one must proceed by solving the interaction problem whenever it is necessary to test convergence. The frequency at which an interaction analysis should be carried out generally depends on the algorithm convergence: it is higher as the convergence speeds up. The subspace algorithm including the Gram-Schmidt process is best summarized by the flowchart of Figure 6.11.

6.8.2 The Lanczos method

The subspace iteration method is very often used in finite element analysis because it allows one to extract the eigensolutions of very large systems with a robustness that other methods cannot offer. Its convergence rate is quite high. However, it requires a great deal of memory space and its computational cost is higher than that of the Lanczos method introduced hereafter and first published in 1950 (Lanczos 1950).

The principle of the *Lanczos* method consists in generating from a single starting vector a growing subspace that will approximate the space spanning the system fundamental eigensolutions. The approximation space will be built recursively by inverse iteration on one starting vector \mathbf{z}_0 . From the latter we construct the *Krylov sequence*:

$$\left\{ \mathbf{z}_0, \mathbf{K}^{-1}\mathbf{M}\mathbf{z}_0, (\mathbf{K}^{-1}\mathbf{M})^2\mathbf{z}_0, \dots \right\} \quad (6.121)$$

the terms of which are made orthogonal to each other by a construction process of conjugate directions as explained later. The eigensolutions of the problem will be searched in this growing subspace. As will be seen, finding approximate eigensolutions in the Krylov subspace (i.e. solving the so-called *interaction problem*) can be done very efficiently.

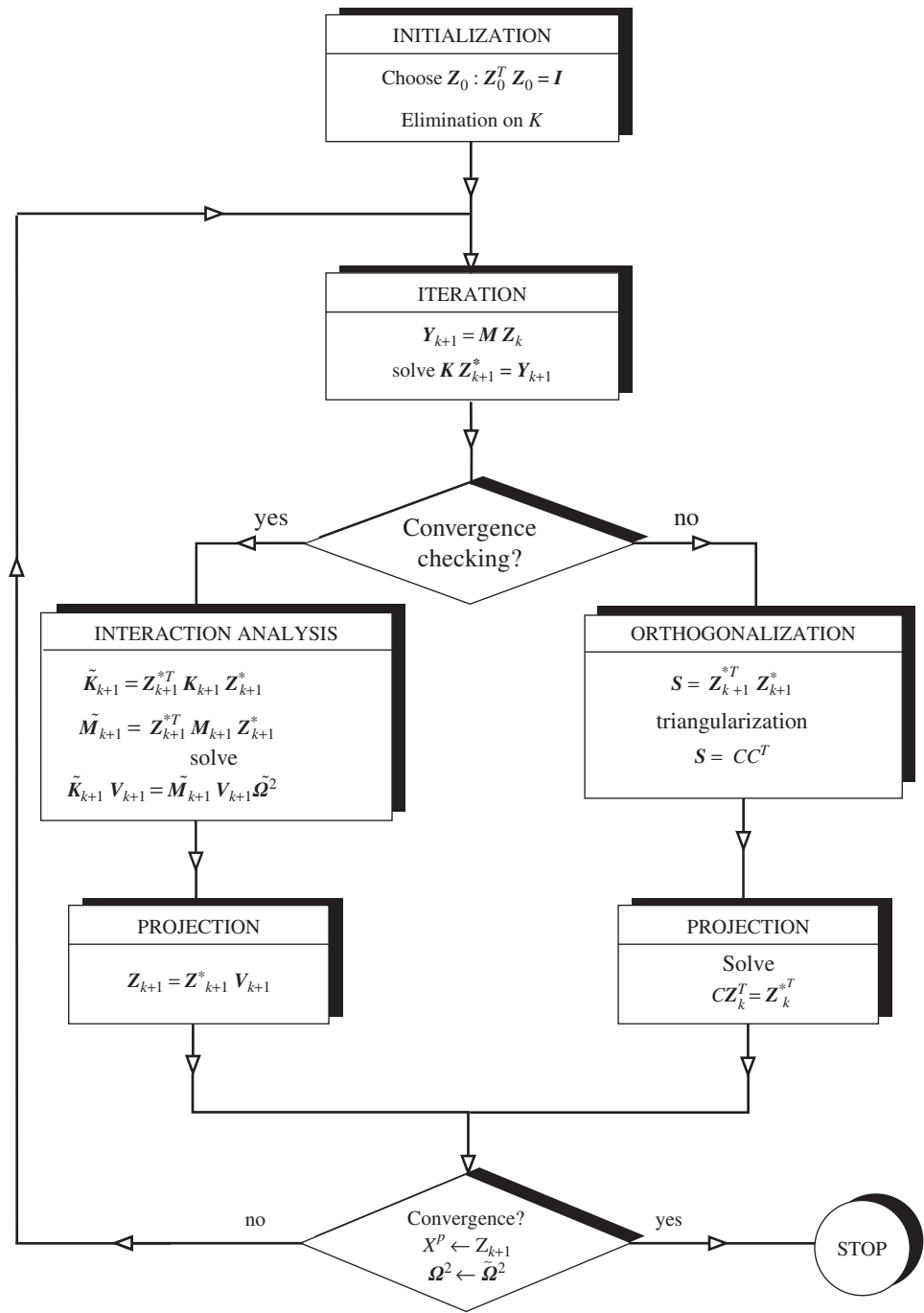


Figure 6.11 The subspace iteration algorithm.

In fact the Lanczos algorithm can be seen as a method that, conceptually speaking, fits between the basic inverse iteration and the subspace method: like in the inverse iteration method one applies the operator $\mathbf{K}^{-1}\mathbf{M}$ recursively on a direction but now one keeps all directions computed during the iterations and one looks for estimates of the eigenmodes in the so-generated subspace. Compared to the subspace algorithm, the Lanczos method is similar in that it looks for the eigensolutions in a subspace, but it is different in that the subspace is generated from a single starting vector and growing recursively. It is also noteworthy to observe that in the inverse iteration and subspace methods one discards at every step the information generated at all previous iterations, whereas in the Lanczos method previously generated information is recycled since all iterates are used to find the best approximation in a growing subspace. This is the fundamental reason why the Lanczos method is the optimum approach and is therefore often used in practice.

The Lanczos method can be seen as a particular case of the more general Arnoldi algorithm (Arnoldi 1951) and the latter will thus be outlined first.

First step to the Lanczos method

Let us call \mathbf{z}_0 a starting vector. Observe that we use the notation \mathbf{z} instead of \mathbf{x} since, similarly to the subspace method, the vectors generated during the Krylov sequence (6.121) will form a subspace in which the eigensolutions will be looked for, but are not the eigenmodes themselves.

We impose that all vectors generated in the Krylov sequence are mass-normalized, hence:

$$\mathbf{z}_0 \leftarrow \mathbf{z}_0 / \sqrt{\mathbf{z}_0^T \mathbf{M} \mathbf{z}_0}$$

Now let us compute the next vector of the Krylov basis as:

$$\bar{\mathbf{z}}_1 = \mathbf{K}^{-1} \mathbf{M} \mathbf{z}_0$$

which in practice is computed by applying the two operations of the inverse iteration (6.64a–6.64b). Now we \mathbf{M} -orthogonalize $\bar{\mathbf{z}}_1$ with respect to \mathbf{z}_0 to make sure that the process does not degenerate, knowing that otherwise the iterates will end up being aligned with the first mode (see the power iteration):

$$\mathbf{z}_1 = \bar{\mathbf{z}}_1 - a_{00} \mathbf{z}_0 \quad \text{with} \quad a_{00} = \mathbf{z}_0^T \mathbf{M} \bar{\mathbf{z}}_1$$

and we ensure that this new vector is mass-normalized by writing:

$$\mathbf{z}_1 \leftarrow \mathbf{z}_1 / \gamma_1 \quad \text{with} \quad \gamma_1 = \sqrt{\mathbf{z}_1^T \mathbf{M} \mathbf{z}_1}$$

This procedure can be continued recursively as summarized in the following steps:

$$\bar{\mathbf{z}}_{p+1} = \mathbf{K}^{-1} \mathbf{M} \mathbf{z}_p \quad (6.122a)$$

$$\mathbf{z}_{p+1} = \bar{\mathbf{z}}_{p+1} - \sum_{i=0}^p a_{ip} \mathbf{z}_i \quad \text{with} \quad a_{ip} = \mathbf{z}_i^T \mathbf{M} \bar{\mathbf{z}}_{p+1} \quad (6.122b)$$

$$\mathbf{z}_{p+1} \leftarrow \mathbf{z}_{p+1} / \gamma_{p+1} \quad \text{with} \quad \gamma_{p+1} = \sqrt{\mathbf{z}_{p+1}^T \mathbf{M} \mathbf{z}_{p+1}} \quad (6.122c)$$

where the second step renders the new iterate \mathbf{M} -orthogonal to all previous iterates. The vectors \mathbf{z}_p generated by the algorithm (6.122a–6.122c) are not exactly the same as the Krylov vectors

in (6.121) since they undergo a normalization and orthogonalization process. Nevertheless since (6.122b) merely involves linear combinations of vectors, the vectors \mathbf{z}_p span exactly the same space as (6.121).

From the reasoning behind the power iteration algorithm we understand that the space spanned by the directions \mathbf{z}_p will represent the space of the modes of lowest frequencies, although the \mathbf{z}_p themselves are not the eigenmodes. Then looking for the modes in that subspace will yield good approximations of the first eigenmodes: that will be the *interaction problem*. Before building the interaction problem let us first note that the sequence (6.122a–6.122b) generates vectors that by construction satisfy:

$$\gamma_{p+1}\mathbf{z}_{p+1} = \mathbf{K}^{-1}\mathbf{M}\mathbf{z}_p - \sum_{i=0}^p a_{ip}\mathbf{z}_i \quad (6.123)$$

or

$$\mathbf{K}^{-1}\mathbf{M}\mathbf{z}_p = \gamma_{p+1}\mathbf{z}_{p+1} + \sum_{i=0}^p a_{ip}\mathbf{z}_i \quad (6.124)$$

which in matrix form can be written as:

$$\boxed{\mathbf{K}^{-1}\mathbf{M}\mathbf{Z} = \mathbf{Z}\mathbf{T} + \mathbf{E}} \quad (6.125)$$

where

$$\begin{aligned} \mathbf{Z} &= [\mathbf{z}_0 \quad \mathbf{z}_1 \quad \mathbf{z}_2 \quad \cdots \quad \mathbf{z}_p] \\ \mathbf{T} &= \begin{bmatrix} a_{00} & a_{01} & a_{02} & a_{03} & \cdots & a_{0p} \\ \gamma_1 & a_{11} & a_{12} & a_{13} & \cdots & a_{1p} \\ 0 & \gamma_2 & a_{22} & a_{23} & \cdots & a_{2p} \\ 0 & 0 & \gamma_3 & a_{33} & \cdots & a_{3p} \\ \vdots & & & \ddots & \ddots & \vdots \\ 0 & & \cdots & 0 & \gamma_p & a_{pp} \end{bmatrix} \\ \mathbf{E} &= [\mathbf{0} \quad \cdots \quad \mathbf{0} \quad \gamma_{p+1}\mathbf{z}_{p+1}] \end{aligned} \quad (6.126)$$

The orthogonality of the iterates can be written as:

$$\mathbf{Z}^T\mathbf{M}\mathbf{Z} = \mathbf{I} \quad \mathbf{Z}^T\mathbf{M}\mathbf{E} = \mathbf{0} \quad (6.127)$$

Note the special topology of the matrix \mathbf{T} (known as *upper Hessenberg matrix*).

To formulate the interaction problem, we use \mathbf{Z} as a subspace in which we want to find an approximation of the eigenmodes, namely:

$$\boxed{\mathbf{x}_{(s)} \simeq \mathbf{Z}\mathbf{y}_{(s)}} \quad (6.128)$$

$\mathbf{y}_{(s)}$ being the coordinates of the mode approximations in the Krylov subspace. In order to exploit the property (6.125) the original eigenvalue problem (6.1) is rewritten as:

$$(\mathbf{I} - \omega_s^2 \mathbf{K}^{-1}\mathbf{M})\mathbf{x}_{(s)} = \mathbf{0}$$

and after substitution of the approximation (6.128):

$$(\mathbf{I} - \omega_s^2 \mathbf{K}^{-1}\mathbf{M})\mathbf{Z}\mathbf{y}_{(s)} = \mathbf{0} + \mathbf{r} \quad (6.129)$$

where \mathbf{r} is a residue indicating that since in general the modes $\mathbf{x}_{(s)}$ cannot be represented exactly in the subspace \mathbf{Z} , there will always be an error in the free vibration equation, whatever the choice of $\mathbf{y}_{(s)}$. But we will look for a solution $\mathbf{y}_{(s)}$ that ensures at least that the residue \mathbf{r} is zero in the subspace of \mathbf{MZ} , namely we want:⁷

$$\mathbf{Z}^T \mathbf{M} \mathbf{r} = \mathbf{0}$$

Thus the eigenvalue problem (6.129) in the subspace \mathbf{Z} is written as:

$$\mathbf{Z}^T \mathbf{M} (\mathbf{I} - \omega_s^2 \mathbf{K}^{-1} \mathbf{M}) \mathbf{Z} \mathbf{y}_{(s)} = \mathbf{0} \quad (6.130)$$

which is the interaction problem describing how to find the approximate eigenmodes in the Krylov subspace. Recalling now the fundamental properties (6.125, 6.127) of the iterates \mathbf{z}_p , this interaction problem can be written as:

$$\left(\frac{1}{\omega_s^2} \mathbf{I} - \mathbf{T} \right) \mathbf{y}_{(s)} = \mathbf{0} \quad (6.131)$$

This form of the interaction problem indicates that in the subspace \mathbf{Z} the approximate modes can be found by computing the eigensolutions of \mathbf{T} , then computing the approximate eigenmodes by substituting $\mathbf{y}_{(s)}$ in (6.128). Solving the eigenproblem (6.131) is cheap since \mathbf{T} is of dimension p , and because efficient eigensolvers like the QR algorithm exist for upper Hessenberg matrices.

The algorithm derived so far is not yet the Lanczos algorithm, but is inspired from an algorithm known as the *Arnoldi iteration* (Arnoldi 1951). The differences with the original Arnoldi algorithm are that here, the method is particularized to the symmetric eigenvalue problem and orthogonality of the iteration vecotors is expressed in the \mathbf{M} metrics. One major issue in this algorithm is the required memory space in order to store all the Krylov vectors. Hence, for very large problems, the iterations have sometimes to be restarted using the most relevant results obtained so far (see Lehoucq and Sorensen (1996), Sorensen (1992) for a description of the *Implicitly Restarted Arnoldi iteration*).

The algorithm outlined above does not exploit the symmetry property of the system matrices. In what follows we will use symmetry to reduce the number of operations involved in the iterations, which will result in the Lanczos algorithm.

The Lanczos algorithm

The previous algorithm can be improved by using the two following properties resulting from the symmetry of the eigenvalue problem:

- *Recursive orthogonality*: Let us rewrite the orthogonalization coefficients a_{ip} in (6.122b) as:

$$\begin{aligned} a_{ip} &= \mathbf{z}_i^T \mathbf{M} \bar{\mathbf{z}}_{p+1} \quad i = 0, \dots, p \\ &= \mathbf{z}_i^T \mathbf{M} (\mathbf{K}^{-1} \mathbf{M} \mathbf{z}_p) \\ &= (\mathbf{z}_i^T \mathbf{M} \mathbf{K}^{-1}) \mathbf{M} \mathbf{z}_p = (\mathbf{K}^{-1} \mathbf{M} \mathbf{z}_i)^T \mathbf{M} \mathbf{z}_p \end{aligned}$$

⁷ We will do something very similar in the reduction methods outlined in Section 6.9.

where we made use of the symmetry of \mathbf{K} and \mathbf{M} . Using the fact that \mathbf{z}_i were also obtained with the recurrence formula (6.124) we can write:

$$a_{ip} = \left(\gamma_{i+1} \mathbf{z}_{i+1} + \sum_{j=0}^i a_{ji} \mathbf{z}_j \right)^T \mathbf{M} \mathbf{z}_p \quad i = 0, \dots, p \quad (6.132)$$

and finally, due to the \mathbf{M} -orthogonality of the iterates, we conclude that:

$$a_{ip} = 0 \quad \text{if} \quad i < p - 1 \quad (6.133)$$

This means that a new iterate $\bar{\mathbf{z}}_{p+1}$ needs to be \mathbf{M} -orthogonalized only with the direction \mathbf{z}_p and \mathbf{z}_{p-1} , the \mathbf{M} -orthogonality with respect to all the earlier directions being automatically satisfied recursively.

- *Symmetry of \mathbf{T}* : Writing the relation (6.132) for $i = p - 1$ one finds:

$$a_{p-1,p} = \left(\gamma_p \mathbf{z}_p + \sum_{j=0}^{p-1} a_{ji} \mathbf{z}_j \right)^T \mathbf{M} \mathbf{z}_p$$

which, owing to the orthonormality of the iterates, lets us conclude that:

$$a_{p-1,p} = \gamma_p \quad (6.134)$$

These properties allow, at least in theory, reducing the computational cost significantly since they indicate that the matrix \mathbf{T} is in fact a symmetric tri-diagonal, often written as:⁸

$$\mathbf{T} = \begin{bmatrix} \alpha_0 & \gamma_1 & & & \mathbf{0} \\ \gamma_1 & \alpha_1 & \gamma_2 & & \\ & \ddots & \ddots & \ddots & \\ & & \ddots & \ddots & \gamma_p \\ \mathbf{0} & & & \gamma_p & \alpha_p \end{bmatrix} \quad (6.135)$$

where

$$\begin{aligned} \alpha_k &= a_{kk} = \mathbf{z}_k^T \mathbf{M} \bar{\mathbf{z}}_{k+1} = \mathbf{z}_k^T \mathbf{M} \mathbf{K}^{-1} \mathbf{M} \mathbf{z}_k \\ \gamma_k &= a_{k-1,k} = \mathbf{z}_{k-1}^T \mathbf{M} \bar{\mathbf{z}}_{k+1} = \mathbf{z}_{k-1}^T \mathbf{M} \mathbf{K}^{-1} \mathbf{M} \mathbf{z}_k \end{aligned}$$

However in practice, as a consequence of the finite precision in numerical computation, the recursive orthogonality will be lost after a few iterations. This will result in the appearance of spurious solutions and a loss of accuracy even for a small number of desired eigenvalues. Hence, in practice, full orthogonalization is performed as in (6.122b) to avoid the breakdown of the process due to the loss of orthogonality between the directions \mathbf{z}_i . Note that including the off-diagonal terms in the \mathbf{T} matrix for the interaction problem does not bring any improvement

⁸ Another way to show that \mathbf{T} is tridiagonal and thus to derive relations (6.133, 6.134) is as follows: taking the fundamental relation (6.125) of the Arnoldi vectors and premultiplying by $\mathbf{Z}^T \mathbf{M}$ one finds:

$$\mathbf{Z}^T \mathbf{M} \mathbf{K}^{-1} \mathbf{M} \mathbf{Z} = \mathbf{Z}^T \mathbf{M} \mathbf{Z} \mathbf{T} + \mathbf{Z}^T \mathbf{M} \mathbf{E} = \mathbf{T}$$

Observing now that the left-hand side is symmetric one can conclude that \mathbf{T} , of general expression (6.126), is symmetric and thus tri-diagonal.

since those coefficients are theoretically zero. The fact that they have to be computed in a full re-orthogonalization process is only to cure the loss of orthogonality incurred by the finite precision of the computation, but does not need to be reflected in the matrix T . Therefore, the matrix T is often taken as tri-diagonal.

Lanczos in practice

The Lanczos algorithm outlined above can be organized as described in Algorithm 1.

Algorithm 1 The Lanczos algorithm to compute eigensolutions of symmetric systems

Given n_{eig} (desired number of eigensolutions)

Given ϵ_{eig} (error tolerance) and n_{iter}^{max} (max. number of iterations)

-Initialize-

Factorize K

$p = 0, \omega_{s,old}^2 = 0, \text{error}_{eig} = 1$

Construct an initial z_0

$m_0 = Mz_0, \gamma = \sqrt{z_0^T m_0}, z_0 = z_0/\gamma, m_0 = m_0/\gamma_0$

-Iterate-

while $\text{error}_{eig} > \epsilon_{eig}$ **AND** $p < n_{iter}^{max}$ **do**

if $p > 0$ **then**

$T(p, p+1) = \gamma, T(p+1, p) = \gamma$

end if

 Solve $Kz_{p+1} = m_p$

-Orthogonalization-

for $i = 0 : p$ **do**

$a = m_i^T z_{p+1}, z_{p+1} = z_{p+1} - az_i$

if $i = p$ **then**

$T(p+1, p+1) = a$

end if

end for

$m_{p+1} = Mz_{p+1}, \gamma = \sqrt{z_{p+1}^T m_{p+1}}, z_{p+1} = z_{p+1}/\gamma, m_{p+1} = m_{p+1}/\gamma$

-Interaction problem-

if $p > n_{eig}$ **then**

 Find $y_{(s)}$ and $1/\omega_s^2$ the eigensolutions of $T, s = 1 \dots n_{eig}$

$\text{error}_{eig} = \max \left| \frac{\omega_s^2 - \omega_{s,old}^2}{\omega_s^2} \right|$

$\omega_{s,old}^2 = \omega_s^2$

end if

$p = p + 1$

end while

$x_{(s)} = Zy_{(s)}$

Note in Algorithm 1 the use of the intermediate vectors \mathbf{m}_i which minimizes the number of multiplications by the mass matrix. The convergence in this algorithm is checked on the relative error of the eigenvalues. Another approach to check convergence would consist in checking the error in the eigenvalue problem, namely:

$$\|(\mathbf{I} - \omega_s^2 \mathbf{K}^{-1} \mathbf{M})\mathbf{x}_{(s)}\| / \|\mathbf{x}_{(s)}\| < \epsilon_{\text{eig}}$$

This error can be computed efficiently if we observe that, using the relation (6.125),

$$\begin{aligned} (\mathbf{I} - \omega_s^2 \mathbf{K}^{-1} \mathbf{M})\mathbf{x}_{(s)} &= (\mathbf{I} - \omega_s^2 \mathbf{K}^{-1} \mathbf{M})\mathbf{Z}\mathbf{y}_{(s)} \\ &= \mathbf{Z}(\mathbf{I} - \omega_s^2 \mathbf{T})\mathbf{y}_{(s)} - \omega_s^2 \mathbf{E}\mathbf{y}_{(s)} = -\omega_s^2 \mathbf{E}\mathbf{y}_{(s)} \end{aligned}$$

and given the form of \mathbf{E} (see (6.126)), the error is found as:

$$\mathbf{r} = (\mathbf{I} - \omega_s^2 \mathbf{K}^{-1} \mathbf{M})\mathbf{x}_{(s)} = -\gamma_{p+1} \omega_s^2 \mathbf{z}_{p+1} y_{(s),p+1} \quad (6.136)$$

where $y_{(s),p+1}$ is component $p + 1$ of $\mathbf{y}_{(s)}$.

The Lanczos method for eigenvalue extraction is extremely powerful; it makes it possible to treat very large systems, but its implementation is delicate and its use requires some precaution. We will neither analyze in detail the difficulties of the Lanczos method, nor discuss the remedies to overcome them. Let us simply note the following important points:

- *Identical eigenvalues*: Theoretically, multiple eigenvectors cannot be extracted using the Lanczos method. Indeed, the starting vector contains only a linear combination of those multiple modes, and this combination remains unchanged in the course of iterations. In practice, due to the progressive loss of orthogonality caused by round-off errors, multiple solutions will reappear progressively. However, if one restarts the algorithm with other starting vectors, it is then easier to guarantee effective computation of all the eigenvectors associated with a multiple eigenvalue.
- *Skipping of solutions*: Skipping of solutions occurs in two cases:
 - the structure has multiple frequency solutions (see previous item),
 - the structure is such that there exists a complete uncoupling between certain deformation modes (e.g. pure bending, pure extension).

The solutions found by the Lanczos algorithm then depend on the choice of the starting vector. A restart procedure of the algorithm with a different starting vector can overcome this shortcoming. Using a block version of the algorithm is another often used remedy for this problem.

In practice, experience shows that the Lanczos method requires two to four inverse iterations per converged eigenvalue, which is a small computing effort compared to that required by the subspace method. Just as in the power method, this number remains independent of the problem size. It is also not very strongly affected by the closeness of the eigenvalues.

Nowadays, the Lanczos algorithm is used in most finite element analysis codes. Several variants of this algorithm have been devised in order to improve its numerical stability and its computational efficiency. The most noticeable ones are:

- The preconditioned Lanczos method where approximations of the inverse the operator is used in order to improve the conditioning of the problem and speed-up the convergence.

- The block Lanczos method where the Krylov sequence is built for a set of vectors at a time, starting with a initial set \mathbf{Z}_0 . This method shows improved robustness in the presence of multiple eigenvalues and optimizes the use of the processor architecture.
- The Implicit Restarted Arnoldi/Lanczos iteration (Sorensen 1992, 1996) can be applied on very large problems by avoiding having to store all the iterates.

Finally let us mention that several variants of the Lanczos method use spectral shifting in the iterations (similar to the shifting of the Power Iteration in Section 6.7.2) in order to accelerate the convergence.

Computing performance of the Lanczos method

Due to its high computing performance, the Lanczos algorithm is widely used for eigenvalue extraction in the context of large engineering projects requiring detailed structural dynamic analysis. Most of the commercial finite element softwares propose it as standard eigenvalue solver (Komzsik 2003) and integrate the so-called BCSLIB-EXT⁹ implementation based on the work by (Grimes *et al.* 1994). It combines a multi-frontal linear solver based on the concept of supernodes (Liu 1992) with a Block-Lanczos method with shift as eigenvalue extraction algorithm.

Figure 6.12 displays one eigenmode of a stator section of a civil aircraft turbofan engine computed in free-free condition. The meshing has been made with 3-D solid elements using the SAMCEF[®] finite element software, leading to a finite element model of more than twelve millions degrees of freedom. We concentrate here exclusively on the features of the resulting system of equations, which are representative of the order of magnitude and complexity of the eigenvalue problems solved today on a nearly day-to-day basis in engineering offices. Its main characteristics are:

- number of degrees of freedom: $N_{dof} = 1.22 \cdot 10^7$;
- number of nonzero off-diagonal terms in the lower triangles of \mathbf{K} and \mathbf{M} : $NNZ_K = NNZ_M = 3.21 \cdot 10^8$;
- number of nonzero off-diagonal terms in the lower triangular matrix \mathbf{C} after Choleski factorization: $NNZ_L = 5.53 \cdot 10^9$.

It is worthwhile observing at this stage the very high initial sparsity of \mathbf{K} , since the ratio of nonzero terms is initially $4.32 \cdot 10^{-6}$. This ratio becomes $7.43 \cdot 10^{-5}$ after factorization, which means that, despite of near-optimal renumbering, the number of nonzero terms is multiplied by 17.2 through fill-in. Matrix \mathbf{C} has an average bandwidth of 453, but this figure does not reflect the fact the the active front of equations can become much higher during factorization due to the axisymmetric topology of the component. A maximum size of 15165 is reported for the front of equations in the analysis data, which means that the (fully populated) front matrix has a number of nonzero terms up to $1.15 \cdot 10^8$.

⁹ Mathematical software library for solving large linear algebra problems developed by Boeing Research and Technology.

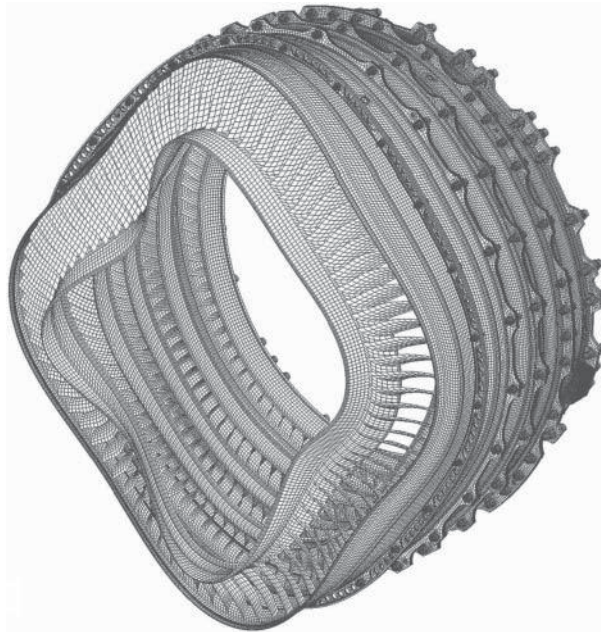


Figure 6.12 Vibration mode of stator section of civil aircraft turbofan engine. Source: Reproduced with permission from Techspace Aero-SAFRAN Group.

The computational costs to generate the finite element model and renumber the equations are not reported, but they remain extremely small compared to the cost of the numerical solution.

In what follows, the performance of the eigenvalue extraction algorithm is assessed exclusively in terms of the number of floating point operations (FLOP) to provide computing cost measures independent of machine performance and other parameters.

With the only knowledge of the number of degrees of freedom and of nonzero terms in \mathbf{K} it is not possible to calculate an estimate of the factorization cost since it depends on its specific topology. For the example under consideration, the factorization cost is provided by a virtual solution preceding the numerical one. It is reported to be $P_{fact} = 8.99 \cdot 10^{12}$ FLOP in the analysis data issued by the software.

After factorization, the basic operations are:

- a linear solution (one forward and one backward substitution), the cost of which can be estimated by considering that, per nonzero term, one addition and one multiplication are performed, leading to an estimated cost $\simeq 4 * NNZ_L = 2.2 \cdot 10^{10}$ FLOP. The effective cost mentioned in the analysis data is very close: $P_{solve} = 2.13 \cdot 10^{10}$ FLOP. The relative cost of one linear solution compared to factorization is thus $P_{solve}/P_{fact} = 2.37 \cdot 10^{-3}$.
- the matrix \times vector product, the real cost of which can be computed as $P_{mult} = N_{dof} + 4 * NNZ_M = 1.30 \cdot 10^9$ FLOP. The relative cost of one matrix \times vector product compared to factorization is thus $P_{mult}/P_{fact} = 1.44 \cdot 10^{-4}$.

The following information is also reported in the analysis data:

- number of eigenvalues extracted: 91;
- number of factorizations (resulting from two different shifts): 2;
- number of iteration vectors in a block: 8;
- number of Lanczos steps: 36;
- number of block solves: 45;
- number of matrix multiplications: 1892.

Taking into account the number of iteration vectors in a block, it is remarkable to observe that the total number of Lanczos iterations is equal to 288, corresponding thus to an average number of iterations per extracted eigenvalue equal to 3.16, thus in the range reported before. This shows that the average number of iteration per converged eigenvalue remains independent not only of the system size, but also of the spread of its eigenspectrum.

The total number of linear solutions reported (360) and matrix multiplications (1892) is however significantly higher than the minimum (288) strictly required by the Lanczos iterations, which can probably be explained by the computational effort spent in additional operations such as algorithm startup, reorthogonalization, error analysis and recuperation of eigenvectors.

The second important observation is to compare the total numbers of operations required by factorizations, linear solutions and matrix-vector multiplications. The corresponding numbers and ratios are given in Table 6.1. More than 60% of the computational effort is devoted to factorization, the rest being spent in linear solutions and matrix-vector products. The remainder computational costs linked to eigenvalue extraction (e.g. solution of the interaction problem) are not included but remain negligible compared to those of the three fundamental operations.

However, the ratios given in Table 6.1 cannot be directly extrapolated to computational times. Indeed the latter are strongly influenced by the computational rates that can be obtained for each type of operation. The computational rates are themselves strongly dependent on the size of the system, the type of machine used and its number of processors or the software implementation of the fundamental matrix operations. Much higher computational rates (typically 2 or 3 times higher) can generally be achieved in factorizations than in linear solutions and matrix \times vector multiplications. Such a computation lasts in the order of six hours of elapsed time on current machines (one CPU).

Table 6.1 Computational costs of representative Lanczos run ($1.22 \cdot 10^7$ dofs, 91 eigenvalues extracted)

Operation type	FLOP	Ratio to total
Factorization	$1.80 \cdot 10^{13}$	0.62
Linear solve	$8.44 \cdot 10^{12}$	0.29
Matrix-vector product	$2.45 \cdot 10^{12}$	0.08
Total	$2.89 \cdot 10^{13}$	

The merit of this crude performance analysis on a representative engineering example is to at least demonstrate that adequate implementation of the Lanczos algorithm leads, for problems of very large size, to computational costs resulting mainly from matrix factorization. The cost of Lanczos remains therefore of the same order of magnitude as for a linear static solution.

6.9 Dynamic reduction and substructuring

The so-called reduction and substructuring methods (Fraeijs de Veubeke *et al.* 1972) are very frequently used in dynamic analysis, essentially for the two following reasons:

- Because we are, in most cases, only interested in lower frequency eigensolutions it may prove to be advantageous to reduce from the start the eigenvalue problem to a smaller dimension. In this case a genuine reduction is performed, the reduction method being seen as a *dof economizer*.
- In the context of large projects, the analysis is frequently subdivided into several parts (in some cases, it is performed by distinct teams). A separate model is constructed for each part of the system and will later be used to reconstruct the model of the whole system. In an aircraft model, for instance, wings, engine nacelles and landing-gear are generally studied by different groups. Therefore, lines or interconnecting surfaces have to be defined carefully so as to ensure the compatibility of the different parts of the model. That is what we call *substructuring*.

The general principle of a method for reducing the size of an eigenvalue problem:

$$\mathbf{K}\mathbf{x} = \omega^2 \mathbf{M}\mathbf{x} \quad (6.137)$$

consists of building a subspace \mathbf{R} ($\dim(\mathbf{R}) = n \times m$, $m < n$) in such a way that the solution of (6.137) can be approximated in the form:

$$\mathbf{x} \simeq \mathbf{R}\tilde{\mathbf{x}} \quad (6.138)$$

If we return to the variational problem from which (6.137) originates:

$$\delta \left(\frac{1}{2} \mathbf{x}^T \mathbf{K} \mathbf{x} - \frac{\omega^2}{2} \mathbf{x}^T \mathbf{M} \mathbf{x} \right) = 0$$

we can deduce the reduced problem:

$$\delta \left(\frac{1}{2} \tilde{\mathbf{x}}^T \tilde{\mathbf{K}} \tilde{\mathbf{x}} - \frac{\omega^2}{2} \tilde{\mathbf{x}}^T \tilde{\mathbf{M}} \tilde{\mathbf{x}} \right) = 0$$

that is to say:

$$\tilde{\mathbf{K}} \tilde{\mathbf{x}} = \tilde{\omega}^2 \tilde{\mathbf{M}} \tilde{\mathbf{x}} \quad (6.139)$$

with the reduced stiffness and mass matrices:

$$\tilde{\mathbf{K}} = \mathbf{R}^T \mathbf{K} \mathbf{R} \quad \text{and} \quad \tilde{\mathbf{M}} = \mathbf{R}^T \mathbf{M} \mathbf{R} \quad (6.140)$$

and where $\tilde{\omega}^2$ denotes the eigenvalues of the reduced eigenproblem. The better the subspace spanning the columns of matrix \mathbf{R} represents the fundamental modes, the closer are the solutions $\{\tilde{\omega}_r^2, \mathbf{R}\tilde{\mathbf{x}}_r\}$ obtained from (6.139) to the eigensolutions of the initial problem.

Remark 6.9 *A reduction scheme that can be described by Equations (6.140) is said consistent, meaning that the same reduction transformation applies to the stiffness and mass matrices. Such transformation can be regarded as a set of constraints applied to the original eigenvalue problem. Therefore a direct consequence of Rayleigh's theorem on constraints is that the eigenvalues of the reduced eigenvalue problem (6.139) are upper bounds to those of the original one.*

The principle of reduction can of course be extended to the more general problem of dynamic equilibrium:

$$\mathbf{K}\mathbf{q} + \mathbf{M}\ddot{\mathbf{q}} = \mathbf{p}(t) \quad (6.141)$$

Substituting into (6.141) the reduction assumption:

$$\mathbf{q}(t) = \mathbf{R}\tilde{\mathbf{q}}(t) \quad (6.142)$$

yields

$$\mathbf{K}\mathbf{R}\tilde{\mathbf{q}} + \mathbf{M}\mathbf{R}\ddot{\tilde{\mathbf{q}}} = \mathbf{p}(t) + \mathbf{r} \quad (6.143)$$

\mathbf{r} being the force residue associated to the approximation.

Looking for a solution for which the residue is null in the reduction space (i.e. $\mathbf{R}^T\mathbf{r} = 0$) yields the reduced dynamic equilibrium equation:

$$\tilde{\mathbf{K}}\tilde{\mathbf{q}} + \tilde{\mathbf{M}}\ddot{\tilde{\mathbf{q}}} = \tilde{\mathbf{p}}(t) \quad (6.144)$$

with the reduced dynamic load:

$$\tilde{\mathbf{p}}(t) = \mathbf{R}^T\mathbf{p}(t) \quad (6.145)$$

Equation (6.144) is a generalization of Equation (6.139) to the transient case. The way to obtain it has provided another interpretation of the reduction concept which consists to cancel the residue of the equilibrium equation in the subspace defined by the reduction matrix \mathbf{R} .

The various substructuring and condensation methods differ from each other only by the choice of the reduction matrix \mathbf{R} . Although there is a broad literature on the subject proposing different choices of reduction bases (of which an excellent synthesis can be found in Craig and Kurdila (2006)), the presentation hereafter will be limited to the following reduction choices:

- the Guyan-Irons reduction algorithm (Guyan 1965, Irons 1965) based on static condensation of unwanted degrees of freedom, which can be seen both as a degree of freedom economizer and as a substructuring method;
- the Craig-Bampton method (Craig and Bampton 1968), also commonly referred to as the *component modes method* (or *modal synthesis*), which is mainly used as a dynamic substructuring method;
- the McNeal *hybrid synthesis method* (MacNeal 1971), which departs from the general reduction scheme (6.140) and is thus not consistent;

- the Rubin method (Rubin 1975), which results from a modification of the McNeal hybrid synthesis method to render it consistent with the reduction scheme 6.140.

The presentation of the different methods is limited to the reduction of the eigenvalue problem, the extension to transient dynamics being trivial. Reducing the damping contribution can be handled in a similar way but the topic is beyond the present text.

6.9.1 Static condensation (Guyan–Irons reduction)

The algorithm

Let us consider the matrix equation (6.137) that governs the system eigenmodes and eigenfrequencies. To reduce the size of matrices \mathbf{K} and \mathbf{M} , one can choose to eliminate a subset of degrees of freedom. The remaining and condensed coordinates are written respectively \mathbf{x}_R and \mathbf{x}_C . The equation can thus be partitioned as follows:

$$\begin{bmatrix} \mathbf{K}_{RR} & \mathbf{K}_{RC} \\ \mathbf{K}_{CR} & \mathbf{K}_{CC} \end{bmatrix} \begin{bmatrix} \mathbf{x}_R \\ \mathbf{x}_C \end{bmatrix} = \omega^2 \begin{bmatrix} \mathbf{M}_{RR} & \mathbf{M}_{RC} \\ \mathbf{M}_{CR} & \mathbf{M}_{CC} \end{bmatrix} \begin{bmatrix} \mathbf{x}_R \\ \mathbf{x}_C \end{bmatrix}$$

or

$$\mathbf{K}_{RR}\mathbf{x}_R + \mathbf{K}_{RC}\mathbf{x}_C = \omega^2(\mathbf{M}_{RR}\mathbf{x}_R + \mathbf{M}_{RC}\mathbf{x}_C) \quad (6.146a)$$

$$\mathbf{K}_{CR}\mathbf{x}_R + \mathbf{K}_{CC}\mathbf{x}_C = \omega^2(\mathbf{M}_{CR}\mathbf{x}_R + \mathbf{M}_{CC}\mathbf{x}_C) \quad (6.146b)$$

An approximation can be found by separating the condensed coordinates \mathbf{x}_C into a static and a dynamic contribution:¹⁰

$$\mathbf{x}_C = \mathbf{x}_S + \mathbf{x}_D \quad (6.147)$$

with the ‘static’ part deduced from:

$$\mathbf{x}_S = -\mathbf{K}_{CC}^{-1}\mathbf{K}_{CR}\mathbf{x}_R \quad (6.148)$$

This is obtained by neglecting the inertia forces in (6.146b). Substituting (6.147) and (6.148) in (6.146b), we see that the ‘dynamic’ part satisfies:

$$(\mathbf{K}_{CC} - \omega^2\mathbf{M}_{CC})\mathbf{x}_D = \omega^2\tilde{\mathbf{M}}_{CR}\mathbf{x}_R \quad (6.149)$$

with

$$\tilde{\mathbf{M}}_{CR} = \mathbf{M}_{CR} - \mathbf{M}_{CC}\mathbf{K}_{CC}^{-1}\mathbf{K}_{CR} \quad (6.150)$$

¹⁰ One could eliminate the condensed coordinates from these equations by solving (6.146b) for \mathbf{x}_C and substituting in (6.146a), similarly to what we did in the development of the mechanical impedance (Section 2.9.3). However this would lead to an intricate eigenvalue problem nonlinear in ω^2 and would not result in an approximation nor in a simplification of the problem.

The static condensation algorithm consists then in neglecting \mathbf{x}_D so that the condensed degrees of freedom are directly related to the retained ones by (6.148) and the approximation is written as:

$$\mathbf{x} \simeq \begin{bmatrix} \mathbf{I} \\ -\mathbf{K}_{CC}^{-1}\mathbf{K}_{CR} \end{bmatrix} \mathbf{x}_R = \mathbf{R}\mathbf{x}_R \quad (6.151)$$

Column j of the reduction matrix \mathbf{R} corresponds to the static deformation of the structure when the j th retained degree of freedom is set to one, the others being set to zero.

The reduced matrices are computed as:

$$\tilde{\mathbf{K}} = \mathbf{R}^T \mathbf{K} \mathbf{R} = \mathbf{K}_{RR} - \mathbf{K}_{RC} \mathbf{K}_{CC}^{-1} \mathbf{K}_{CR} \quad (6.152)$$

$$\begin{aligned} \tilde{\mathbf{M}} = \mathbf{R}^T \mathbf{M} \mathbf{R} = & \mathbf{M}_{RR} - \mathbf{M}_{RC} \mathbf{K}_{CC}^{-1} \mathbf{K}_{CR} - \mathbf{K}_{RC} \mathbf{K}_{CC}^{-1} \mathbf{M}_{CR} \\ & + \mathbf{K}_{RC} \mathbf{K}_{CC}^{-1} \mathbf{M}_{CC} \mathbf{K}_{CC}^{-1} \mathbf{K}_{CR} \end{aligned} \quad (6.153)$$

The eigenvalue problem is then reduced to:

$$(\tilde{\mathbf{K}} - \tilde{\omega}^2 \tilde{\mathbf{M}}) \mathbf{x}_R = \mathbf{0} \quad (6.154)$$

An example of static condensation is presented on page 494.

Remark 6.10 *It is noteworthy observing that the mass of the condensed degrees of freedom is not disregarded but redistributed on the remaining degrees of freedom according to the motion described by the static modes. It is thus consistent with the reduction of the stiffness matrix.*

First-order correction

The validity of the condensation algorithm depends on the extent to which correction \mathbf{x}_D is negligible (Carnoy and G  radin 1983, G  radin 1971). So let us consider the homogeneous problem associated with (6.149) for the dynamic part of the condensed degrees of freedom:

$$(\mathbf{K}_{CC} - \omega_c^2 \mathbf{M}_{CC}) \mathbf{x}_C = \mathbf{0} \quad (6.155)$$

which we deduce from the initial problem (6.137) by setting the constraints $\mathbf{x}_R = \mathbf{0}$. Let:

$$0 \leq \omega_{c1}^2 \leq \omega_{c2}^2 \leq \dots \leq \omega_{cm}^2 \quad (6.156)$$

be its eigenvalues, and

$$\mathbf{x}_{C(1)}, \mathbf{x}_{C(2)}, \dots, \mathbf{x}_{C(m)} \quad (6.157)$$

the corresponding eigenvectors, with the orthogonality relationships:

$$\mathbf{x}_{C(i)}^T \mathbf{M}_{CC} \mathbf{x}_{C(j)} = \delta_{ij} \quad (6.158)$$

Let us remember that, according to Equation (2.55), the identity matrix of dimension $(m \times m)$ has as its spectral expansion:

$$\mathbf{I} = \sum_{i=1}^m \mathbf{x}_{C(i)} \mathbf{x}_{C(i)}^T \mathbf{M}_{CC} \quad (6.159)$$

From this, we can deduce the following interesting relations:

$$\omega^2 \mathbf{K}_{CC}^{-1} \mathbf{M}_{CC} = \sum_{i=1}^m \frac{\omega^2}{\omega_{Ci}^2} \mathbf{x}_{C(i)} \mathbf{x}_{C(i)}^T \mathbf{M}_{CC} \quad (6.160)$$

$$\mathbf{K}_{RC} = \sum_{i=1}^m (\mathbf{K}_{RC} \mathbf{x}_{C(i)}) (\mathbf{M}_{CC} \mathbf{x}_{C(i)})^T \quad (6.161)$$

$$\omega^2 \mathbf{M}_{RC} = \sum_{i=1}^m \frac{\omega^2}{\omega_{Ci}^2} (\mathbf{M}_{RC} \mathbf{x}_{C(i)}) (\mathbf{K}_{CC} \mathbf{x}_{C(i)})^T, \quad (6.162)$$

which enable us to show that the validity field of the condensation algorithm is:

$$\frac{\omega^2}{\omega_{C1}^2} = \epsilon \ll 1 \quad (6.163)$$

where ϵ is the error measure that is admitted on the lowest eigenfrequencies and eigenmodes of the spectrum.

Indeed, let us rewrite the nonreduced dynamic equations (6.146a, 6.146b) by expressing the condensed coordinates in their static and dynamic contributions \mathbf{x}_R and \mathbf{x}_D as given by (6.147, 6.148). One finds:

$$\begin{aligned} (\tilde{\mathbf{K}} - \omega^2 \tilde{\mathbf{M}}) \mathbf{x}_R &= (\omega^2 \mathbf{M}_{RC} - \mathbf{K}_{RC}) \mathbf{x}_D + \omega^2 \mathbf{K}_{RC} \mathbf{K}_{CC}^{-1} \tilde{\mathbf{M}}_{CR} \mathbf{x}_R \\ (\mathbf{I} - \omega^2 \mathbf{K}_{CC}^{-1} \mathbf{M}_{CC}) \mathbf{x}_D &= \omega^2 \mathbf{K}_{CC}^{-1} \tilde{\mathbf{M}}_{CR} \mathbf{x}_R \end{aligned} \quad (6.164)$$

where the second relation was already found in (6.149). Equations (6.160) and (6.161) show that:

$$\omega^2 \mathbf{K}_{CC}^{-1} \mathbf{M}_{CC} \quad \text{is of } O(\epsilon) \text{ with respect to } \mathbf{I} \quad (6.165)$$

Making the assumption that \mathbf{K}_{RC} is of the same order of magnitude as \mathbf{K}_{RR} and \mathbf{K}_{CC} , and assuming also that \mathbf{M}_{RC} is of the same order of magnitude as \mathbf{M}_{CC} and \mathbf{M}_{RR} , the equalities (6.161) and (6.162) imply that:

$$\omega^2 \mathbf{M}_{RC} \quad \text{is of } O(\epsilon) \text{ with respect to } \mathbf{K}_{RC} \quad (6.166)$$

Using the two relations above, the definition (6.150) shows that $\omega^2 \tilde{\mathbf{M}}_{RC}$ is of $O(\epsilon)$ with respect to \mathbf{K}_{RC} . Further assuming that $\mathbf{K}_{CC}^{-1} \mathbf{K}_{RC}$ is of the same order as \mathbf{I} , we state that:

$$\omega^2 \mathbf{K}_{CC}^{-1} \tilde{\mathbf{M}}_{CR} \quad \text{is of } O(\epsilon) \text{ with respect to } \mathbf{I} \quad (6.167)$$

Thus, we can develop the eigenfrequency and the eigenmode into a sequence of terms of orders of magnitude ϵ and ϵ^2 respectively:

$$\omega^2 = \tilde{\omega}^2 + \Delta \omega^2 + \Delta^2 \omega^2 \quad (6.168)$$

$$\mathbf{x}_R = \tilde{\mathbf{x}}_R + \Delta \mathbf{x}_R + \Delta^2 \mathbf{x}_R \quad (6.169)$$

$$\mathbf{x}_D = \tilde{\mathbf{x}}_D + \Delta \mathbf{x}_D + \Delta^2 \mathbf{x}_D \quad (6.170)$$

and introduce these approximations into (6.164). We obtain successively:

- At order 0:

$$\begin{aligned}\tilde{\mathbf{x}}_D &= 0 \\ (\tilde{\mathbf{K}} - \tilde{\omega}^2 \tilde{\mathbf{M}}) \tilde{\mathbf{x}}_R &= 0\end{aligned}\quad (6.171)$$

showing that the solution obtained by static condensation is accurate at order 0.

- At order 1:

$$\begin{aligned}\Delta \mathbf{x}_D &= \tilde{\omega}^2 \mathbf{K}_{CC}^{-1} \tilde{\mathbf{M}}_{CR} \tilde{\mathbf{x}}_R \\ \Delta \omega^2 &= 0 \\ \Delta \mathbf{x}_R &= 0\end{aligned}\quad (6.172)$$

a result that we could expect from the stationary value property of the Rayleigh quotient calculated from the solution at order zero (see Section 2.10.2). Only the displacements are affected at order 1.

- At order 2:

$$\begin{aligned}\Delta^2 \mathbf{x}_D &= \tilde{\omega}^2 \mathbf{K}_{CC}^{-1} \mathbf{M}_{CC} \Delta \mathbf{x}_D \\ \Delta^2 \omega^2 &= - \frac{\Delta \mathbf{x}_D^T \mathbf{K}_{CC} \Delta \mathbf{x}_D}{\tilde{\mathbf{x}}_R^T \tilde{\mathbf{M}} \tilde{\mathbf{x}}_R}\end{aligned}\quad (6.173)$$

$\Delta^2 \mathbf{x}_R$ being the solution of:

$$(\tilde{\mathbf{K}} - \tilde{\omega}^2 \tilde{\mathbf{M}}) \Delta^2 \mathbf{x}_R = \tilde{\omega}^2 \tilde{\mathbf{M}}_{RC} \Delta \mathbf{x}_D + \Delta^2 \omega^2 \tilde{\mathbf{M}} \tilde{\mathbf{x}}_R \quad (6.174)$$

An important consequence of the analysis at order 2 is that the exact eigenvalue can be expressed by the development:

$$\omega^2 = \tilde{\omega}^2 - \frac{\Delta \mathbf{x}_D^T \mathbf{K}_{CC} \Delta \mathbf{x}_D}{\tilde{\mathbf{x}}_R^T \tilde{\mathbf{M}} \tilde{\mathbf{x}}_R} + O(\epsilon^3)$$

which shows that condensation always leads to an excess approximation to the eigenvalue spectrum as predicted from the Rayleigh theorem on constraints (see also Remark 6.9).

6.9.2 Craig and Bampton's substructuring method

While The Guyan-Irons method can be regarded mainly as a degree of freedom economizer where the remaining and condensed degrees of freedom are spread over the entire model (also called master and slave degrees of freedom), the following methods are substructuring techniques where parts of the model are reduced on common interfaces before assembly.

It is also worthwhile noticing that the principle of the component modes method was in fact indirectly introduced in Chapter 2, Section 2.9.3 when discussing the concept of mechanical impedance. It was then shown that the latter admits a spectral expansion in terms of:

- the static modes resulting from imposed unit displacements on the boundary degrees of freedom (Figure 6.13a),
- the internal vibration modes of the subsystem clamped on the boundary (Figure 6.13b).

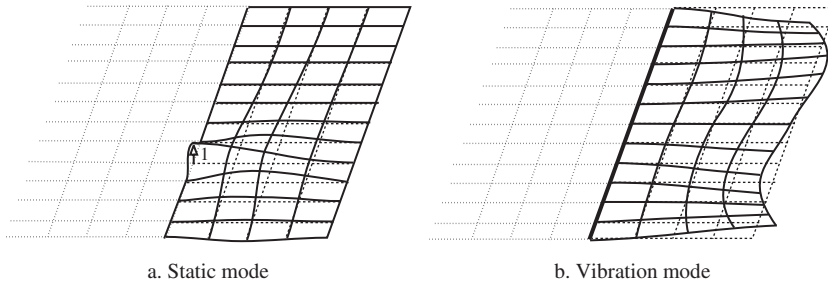


Figure 6.13 Static modes and internal vibration modes of a substructure.

Collecting these modes into the reduction matrix (6.141) corresponds to the choice made by Craig and Bampton (1968) to develop their component modes method.

Instead of being condensed as was done in the impedance analysis (in order to make a number of poles appear, equal to the number of internal modes), the internal vibration modes contribute explicitly to the reduced model and appear in association with internal variables.

Thus, let us write:

$$\begin{aligned} \mathbf{x}_B & \quad \text{the boundary degrees of freedom} \\ \mathbf{x}_I & \quad \text{the subsystem internal degrees of freedom} \end{aligned}$$

In frequency analysis the subsystem contribution to the complete system may be partitioned in the form:

$$\begin{bmatrix} \mathbf{K}_{BB} & \mathbf{K}_{BI} \\ \mathbf{K}_{IB} & \mathbf{K}_{II} \end{bmatrix} \begin{bmatrix} \mathbf{x}_B \\ \mathbf{x}_I \end{bmatrix} - \omega^2 \begin{bmatrix} \mathbf{M}_{BB} & \mathbf{M}_{BI} \\ \mathbf{M}_{IB} & \mathbf{M}_{II} \end{bmatrix} \begin{bmatrix} \mathbf{x}_B \\ \mathbf{x}_I \end{bmatrix} = \begin{bmatrix} \mathbf{p}_B \\ \mathbf{0} \end{bmatrix} \quad (6.175)$$

the only force amplitudes on the model being the reaction forces \mathbf{p}_B with the other parts of the system. Extension to the transient case is obvious.

If there were no inertia forces, the internal degrees of freedom could be calculated by static condensation:

$$\mathbf{x}_I = -\mathbf{K}_{II}^{-1} \mathbf{K}_{IB} \mathbf{x}_B$$

whence the matrix of the static modes on the boundary:

$$\mathbf{R}_B = \begin{bmatrix} \mathbf{I} \\ -\mathbf{K}_{II}^{-1} \mathbf{K}_{IB} \end{bmatrix} \quad (6.176)$$

which describes a subspace of n_B independent solutions, n_B being the number of boundary degrees of freedom. It is the same reduction matrix as in the Guyan-Irons method, except that the remaining degrees of freedom are now interface ones.

We can complete the representation of the solution space if we construct the $n_I = n - n_B$ independent modes obtained by solving the vibration problem of the substructure fixed on its boundary:

$$\mathbf{K}_{II} \mathbf{x}_I = \omega_I^2 \mathbf{M}_{II} \mathbf{x}_I \quad (6.177)$$

These fixed interface modes are stored in the columns of matrix \mathbf{X}_I so that:

$$\begin{aligned}\mathbf{X}_I^T \mathbf{K}_{II} \mathbf{X}_I &= \text{diag}(\omega_{I1}^2 \quad \dots \quad \omega_{In_I}^2) = \mathbf{\Omega}_I^2 \\ \mathbf{X}_I^T \mathbf{M}_{II} \mathbf{X}_I &= \mathbf{I}\end{aligned}\quad (6.178)$$

They allow us to construct the second part of the reduction matrix:

$$\mathbf{R}_I = \begin{bmatrix} \mathbf{0} \\ \mathbf{X}_I \end{bmatrix} \quad (6.179)$$

and the relation:

$$\mathbf{x} = \begin{bmatrix} \mathbf{I} & \mathbf{0} \\ -\mathbf{K}_{II}^{-1} \mathbf{K}_{IB} & \mathbf{X}_I \end{bmatrix} \begin{bmatrix} \mathbf{x}_B \\ \boldsymbol{\eta} \end{bmatrix} \quad (6.180)$$

represents a usual basis transformation applied to the initial degrees of freedom. The coordinates $\boldsymbol{\eta}$ are the *intensity parameters* of the substructure internal vibration modes; their number is equal to the dimension of \mathbf{x}_I .

We then have to reduce the initial model. To do so, we keep in \mathbf{R}_I only a certain number $m < n_I$ of the internal vibration modes:

$$\bar{\mathbf{X}}_I = [\mathbf{x}_{I(1)} \quad \dots \quad \mathbf{x}_{I(m)}] \quad (6.181)$$

On the other hand, all the static modes on the boundary have to be preserved so as to ensure deformation compatibility at the interfaces: \mathbf{x}_B will serve as connectors for the substructures.

This yields the final reduction matrix:

$$\mathbf{R} = \begin{bmatrix} \mathbf{I} & \mathbf{0} \\ -\mathbf{K}_{II}^{-1} \mathbf{K}_{IB} & \bar{\mathbf{X}}_I \end{bmatrix} \quad (6.182)$$

of dimension $n \times (n_B + m)$. Working the reduced stiffness and mass matrices explicitly gives:

$$\tilde{\mathbf{K}} = \begin{bmatrix} \tilde{\mathbf{K}}_{BB} & \mathbf{0} \\ \mathbf{0} & \bar{\mathbf{\Omega}}_I^2 \end{bmatrix} \quad \text{and} \quad \tilde{\mathbf{M}} = \begin{bmatrix} \tilde{\mathbf{M}}_{BB} & \tilde{\mathbf{M}}_B \\ \tilde{\mathbf{M}}_B^T & \mathbf{I} \end{bmatrix} \quad (6.183)$$

with the fully populated submatrices:

$$\begin{aligned}\tilde{\mathbf{K}}_{BB} &= \mathbf{K}_{BB} - \mathbf{K}_{BI} \mathbf{K}_{II}^{-1} \mathbf{K}_{IB} \\ \tilde{\mathbf{M}}_{BB} &= \mathbf{M}_{BB} - \mathbf{M}_{BI} \mathbf{K}_{II}^{-1} \mathbf{K}_{IB} - \mathbf{K}_{BI} \mathbf{K}_{II}^{-1} \mathbf{M}_{IB} + \mathbf{K}_{BI} \mathbf{K}_{II}^{-1} \mathbf{M}_{II} \mathbf{K}_{II}^{-1} \mathbf{K}_{IB} \\ \tilde{\mathbf{M}}_B &= \bar{\mathbf{X}}_I^T (\mathbf{M}_{IB} - \mathbf{M}_{II} \mathbf{K}_{II}^{-1} \mathbf{K}_{IB}) = \tilde{\mathbf{M}}_B^T\end{aligned}\quad (6.184)$$

The reduced matrices (6.183) form the reduced representation of the substructure. In the finite element context, they constitute a so-called *superelement*, which may be used again and assembled with the rest of the structure like an ordinary finite element.

The modal expansion of the impedance of a substructure (Section 2.9.3) has shown that the internal vibration modes can be selected according to the intensity of the associated boundary reactions $(\mathbf{K}_{BI} - \omega_{I(r)}^2 \mathbf{M}_{BI}) \mathbf{x}_{I(r)} \simeq \mathbf{K}_{BI} \mathbf{x}_{I(r)}$. The choice of the vibration modes to be included in the reduced basis can also be made based on the following criteria:

- A criterion often used in engineering practice consists in keeping all the internal modes having a frequency 1.8 times the maximum frequency of interest for the total model.
- A more refined procedure consists in selecting the modes according to their effective modal masses (see Section 2.9.5).
- The choice can also be based on the computation of error estimators (Craig and Chang 1977, Jakobsson and Larson 2011).

When the physical domain is split in a high number of substructures, the number of interface degrees of freedom may become so large that also those ones have to be reduced. In which case, one of the methods is to project the interface degrees of freedom on modes obtained from the Guyan-Irons reduction (Craig and Chang 1977).

Component mode synthesis is also now being used in a purely numerical context. A sparse eigenvalue algorithm, referred to as *algebraic multi-level substructuring* (AMLS), has been developed which exploits the concept of component mode synthesis to split the original eigenvalue problem into smaller ones according to a multi-frontal scheme, each subproblem being then reduced by the Craig-Bampton method (Bennighof and Lehoucq 2004, Gao *et al.* 2008). The method is approximate, but can provide significant speedup and further extends the size limit of the problems that can be addressed. It is now being implemented in several commercial finite element softwares and tends to be preferred to the Lanczos method for the eigenvalue solution of very large finite element models.

6.9.3 McNeal's hybrid synthesis method

It has already been shown in the context of the mode acceleration method (Section 2.8.3) that a model reduction can be made on selected coordinates corresponding the loaded degrees of freedom. Assuming that the latter are the boundary degrees of freedom (the only loads being the reaction forces on the boundary for the free vibration problem), Equation (2.173b) can be rewritten in the harmonic case as:

$$\mathbf{x}_B = \mathbf{F}'_{BB} \mathbf{p}_B + \bar{\mathbf{X}}_B \bar{\boldsymbol{\eta}} \quad (6.185)$$

where \mathbf{F}'_{BB} , \mathbf{p}_B and $\bar{\mathbf{X}}_B$ and are respectively the residual flexibility matrix, the loads and the reduced set of free-free modes on the boundary.

Equation (6.185) cannot conveniently be used as such to build a reduction relationship of type (6.138) since the type of variables in the right-hand side is mixed: the first term has force amplitudes as unknowns, while the mode amplitudes are kinematic variables. It can however be solved with respect the force amplitudes:

$$\mathbf{p}_B = [\mathbf{F}'_{BB}]^{-1} (\mathbf{x}_B - \bar{\mathbf{X}}_B \bar{\boldsymbol{\eta}}) \quad (6.186)$$

and combined with the normal equations governing the intensities of the retained modes as done in Section 2.8.3. This yielded the reduced system (Equation (2.142)):

$$\begin{bmatrix} [\mathbf{F}'_{BB}]^{-1} & -[\mathbf{F}'_{BB}]^{-1} \bar{\mathbf{X}}_B \\ -\bar{\mathbf{X}}_B^T [\mathbf{F}'_{BB}]^{-1} & \bar{\boldsymbol{\mu}} \bar{\boldsymbol{\Omega}}^2 + \bar{\mathbf{X}}_B^T [\mathbf{F}'_{BB}]^{-1} \end{bmatrix} \begin{bmatrix} \mathbf{x}_B \\ \bar{\boldsymbol{\eta}} \end{bmatrix} - \omega^2 \begin{bmatrix} \mathbf{0} & \mathbf{0} \\ \mathbf{0} & \bar{\boldsymbol{\mu}} \end{bmatrix} \begin{bmatrix} \mathbf{x}_B \\ \bar{\boldsymbol{\eta}} \end{bmatrix} = \begin{bmatrix} \mathbf{p}_B \\ \mathbf{0} \end{bmatrix} \quad (6.187)$$

Equation (6.187) corresponds to the McNeal reduction model. Two important observations should be made about it:

1. McNeal's hybrid synthesis appears to be a substructuring method dual to the Craig-Bampton method since the modes involved in the reduction are:
 - the free-free vibration modes of the substructure,
 - the residual flexibility modes that correspond to application of unit loads on the boundary.
2. The mass matrix in Equation (6.187) is not consistent but remarkably simple since it consists of the diagonal matrix of generalized masses for the retained modes. However, this is at the same time a defect of McNeal's model since the mass that should be carried by the residual flexibility modes is neglected. There is thus a mass deficiency that may become significant if only a few normal modes are retained.

6.9.4 Rubin's substructuring method

Rubin (Rubin 1975) has improved the previous method by observing that the reduced stiffness matrix of McNeal's model:

$$\tilde{\mathbf{K}} = \begin{bmatrix} [\mathbf{F}'_{BB}]^{-1} & -[\mathbf{F}'_{BB}]^{-1}\bar{\mathbf{X}}_B \\ -\bar{\mathbf{X}}_B^T[\mathbf{F}'_{BB}]^{-1} & \bar{\mu}\bar{\boldsymbol{\Omega}}^2 + \bar{\mathbf{X}}_B^T[\mathbf{F}'_{BB}]^{-1}\bar{\mathbf{X}}_B \end{bmatrix} \quad (6.188)$$

can in fact be put in the general form:

$$\tilde{\mathbf{K}} = \mathbf{R}^T \mathbf{K} \mathbf{R} \quad (6.189)$$

the reduction matrix being such that:

$$\begin{bmatrix} \mathbf{x}_B \\ \mathbf{x}_I \end{bmatrix} \simeq \mathbf{R} \begin{bmatrix} \mathbf{x}_B \\ \bar{\boldsymbol{\eta}} \end{bmatrix} \quad (6.190)$$

The first row of Equation (6.190) results from the trivial identity $\mathbf{x}_B = \mathbf{x}_B$. The second one results from the substitution of (6.186) into the expression of internal degrees of freedom (2.137a):

$$\mathbf{x}_I \simeq \mathbf{F}'_{IB}\mathbf{p}_B + \bar{\mathbf{X}}_I\bar{\boldsymbol{\eta}} \quad (6.191)$$

We thus get the reduction matrix:

$$\mathbf{R} = \begin{bmatrix} \mathbf{I} & \mathbf{0} \\ \mathbf{F}'_{IB}[\mathbf{F}'_{BB}]^{-1} & \bar{\mathbf{X}}_I - \mathbf{F}'_{IB}[\mathbf{F}'_{BB}]^{-1}\bar{\mathbf{X}}_B \end{bmatrix} \quad (6.192)$$

It is easily verified that the transformation (6.189) restitutes the stiffness matrix (6.188).

Rubin's method consists in using the reduced mass matrix:

$$\tilde{\mathbf{M}} = \mathbf{R}^T \mathbf{M} \mathbf{R} \quad (6.193)$$

which is now the result of a consistent approximation and therefore does not suffer from mass deficiency as McNeal's method. The price to pay for using a consistent mass approximation is that the reduced mass matrix (6.193) is fully populated.

6.10 Error bounds to eigenvalues

Since approximation methods of the eigenvalue problem based on modal reduction yield necessarily to an error in the determination of eigenvalues and eigenvectors, it is important to

dispose of methods allowing quantifying at least the error on the computed eigenspectrum. In what follows a methodology is described, which consists of bracketing the exact eigenvalues of the system between upper and lower bounds.

While upper bounds are immediately obtained from the approximation to the eigenmodes using the fundamental property of the Rayleigh quotient (Section 2.10.1), it is not straightforward to get corresponding lower bounds too and thus quantify the error characterizing the computed eigenvalues.

The results presented in the next sections are based on classical work by (Kato 1949, Temple 1952) using the concept of Krylov's sequence. Excellent review on this topic can be found in (Fox *et al.* 1967, Kestens 1956). Practical application of bound algorithms for error estimation in the numerical solution of large eigenvalue problems using dynamic reduction techniques can be found in Carnoy and G  radin (1983), Fraeijs de Veubeke *et al.* (1972), G  radin (1971, 1973). More recent work on error estimation specifically for the Craig-Bampton substructuring method can be found in Jakobsson and Larson (2011).

6.10.1 Rayleigh and Schwarz quotients

For a given mode estimate (as produced typically by inverse iteration, by subspace or Lanczos iteration and by modal reduction) the best estimate of the associated eigenfrequency is provided by the associated Rayleigh quotient (see Section 2.10.1 where it was shown that for an error of the order ϵ on the mode, the Rayleigh quotient has an error of the order of ϵ^2). It is also worthwhile recalling that the eigenvalues resulting from the interaction problem of the subspace and Lanczos methods are in fact Rayleigh quotients as well.

Let us consider the successive iterates \mathbf{z}_p of a starting vector \mathbf{z}_0 forming the Krylov sequence (6.121). The Rayleigh quotient at iteration p is defined as:

$$\rho_{2p} = \frac{\mathbf{z}_p^T \mathbf{K} \mathbf{z}_p}{\mathbf{z}_p^T \mathbf{M} \mathbf{z}_p} > 0 \quad (6.194)$$

Since the Krylov sequence generated by inverse iteration converges to an eigenvector in a monotonic way (to the first eigenmode when performing the basic power iteration), one can easily understand that the corresponding Rayleigh quotient converges monotonically. One can thus use the Rayleigh quotient as an upper bound to the exact eigenfrequency. This will be proven more thoroughly here below.

Let us consider \mathbf{z}_p to be an approximation to an eigenmode and let us view it in terms of its (unknown) modal components:

$$\mathbf{z}_p = \sum_{s=1}^n a_s \mathbf{x}_{(s)} = \mathbf{X} \mathbf{a} \quad (6.195)$$

In this section we assume in all generality that the eigenmodes are mass-normalized. The associated Rayleigh quotient can be written as:

$$\rho_{2p} = \frac{\mathbf{a}^T \mathbf{X}^T \mathbf{K} \mathbf{X} \mathbf{a}}{\mathbf{a}^T \mathbf{X}^T \mathbf{M} \mathbf{X} \mathbf{a}} = \frac{\mathbf{a}^T \boldsymbol{\Omega}^2 \mathbf{a}}{\mathbf{a}^T \mathbf{a}} = \frac{\sum_s a_s^2 \omega_s^2}{\sum_s a_s^2} \geq \omega_1^2 \quad (6.196)$$

In case the iterates are aiming at approximating the k th eigensolution, assuming that a deflation process (see Section 6.5.2) is used so that $a_s = 0$ for $s < k$, one obtains:

$$\rho_{2p} \geq \omega_k^2 \quad (6.197)$$

Let us call z_{p+1} the next iterate defined by:

$$z_{p+1} = K^{-1} M z_p \quad (6.198)$$

Using the fundamental property of eigenmodes $KX = MX\Omega^2$, its spectral expansion is obtained from (6.195) in the form:

$$z_{p+1} = \sum_{s=1}^n \frac{1}{\omega_s^2} a_s x_{(s)} = X\Omega^{-2}a \quad (6.199)$$

Computing now the Rayleigh quotient of this new iterate yields:

$$\rho_{2p+2} = \frac{z_{p+1}^T K z_{p+1}}{z_{p+1}^T M z_{p+1}} = \frac{z_p^T M K^{-1} M z_p}{z_p^T M K^{-1} M K^{-1} M z_p} = \frac{a^T \Omega^{-2} a}{a^T \Omega^{-4} a} \quad (6.200)$$

Let us then make use of the *Cauchy-Schwarz inequality* stating that:

$$(v^T w)^2 \leq (v^T v)(w^T w) \quad \forall (v, w) \quad (6.201)$$

and apply it twice by setting successively:

$$\begin{cases} v & \leftarrow a \\ w & \leftarrow \Omega^{-2}a \end{cases} \quad \text{and} \quad \begin{cases} v & \leftarrow \Omega a \\ w & \leftarrow \Omega^{-1}a \end{cases}$$

we get the inequalities:

$$(a^T \Omega^{-2} a)^2 \leq (a^T a)(a^T \Omega^{-4} a) \quad (6.202a)$$

$$(a^T a)^2 \leq (a^T \Omega^2 a)(a^T \Omega^{-2} a) \quad (6.202b)$$

(6.202a–6.202b) can be combined to provide the double inequality:

$$\frac{a^T \Omega^{-2} a}{a^T \Omega^{-4} a} \leq \frac{a^T a}{a^T \Omega^{-2} a} \leq \frac{a^T \Omega^2 a}{a^T a} \quad (6.203)$$

Owing to Equations (6.196, 6.200) it can be rewritten as:

$$\rho_{2p+2} \leq \frac{a^T a}{a^T \Omega^{-2} a} \leq \rho_{2p} \quad (6.204)$$

The result (6.204) clearly shows that the Rayleigh quotient is monotonically decreasing in the iterations. It also provides an intermediate estimate of the eigenfrequency in the form:

$$\rho_{2p+1} = \frac{a^T a}{a^T \Omega^{-2} a} = \frac{z_p^T M z_p}{z_p^T M z_{p+1}} = \frac{z_p^T K z_{p+1}}{z_p^T M z_{p+1}} \quad (6.205)$$

The intermediate quotient ρ_{2p+1} is called the *Schwarz quotient*. Expliciting the result (6.204) provides the well-known Schwarz inequality verified by two successive iterates:

$$\frac{z_{p+1}^T K z_{p+1}}{z_{p+1}^T M z_{p+1}} \leq \frac{z_p^T K z_{p+1}}{z_p^T M z_{p+1}} \leq \frac{z_p^T K z_p}{z_p^T M z_p} \quad (6.206)$$

according to which the interlaced sequences of the Rayleigh and Schwarz quotients result in a monotonic convergence towards the fundamental eigenvalue of the system:

$$\boxed{\rho_{2p} \geq \rho_{2p+1} \geq \rho_{2p+2}} \quad (6.207)$$

It shows that the Rayleigh and Schwarz quotients necessarily give an upper bound approximation to the fundamental frequency so that they cannot be used directly to measure the error on the latter.

The following section shows that some algorithms may exploit Inequality (6.207) to obtain upper and lower bounds to the calculated eigenvalues. This enables us to measure the error on a given eigenvalue ω_s^2 by bracketing it.

6.10.2 Eigenvalue bracketing

Algorithms for eigenvalue bracketing can be developed based on the sign properties of the following expression $A(\alpha, \beta)$ computed in terms of two successive quotients of the Schwarz sequence (6.207):

$$A(\alpha, \beta) = \rho_k \rho_{k+1} - (\alpha + \beta) \rho_{k+1} + \alpha \beta \quad \alpha, \beta \text{ positive constants} \quad (6.208)$$

Owing to Equations (6.196, 6.197, 6.205) one can write two successive quotients of the Schwarz sequence in the form:

$$\left\{ \begin{array}{l} \text{for even } k : \quad \rho_k = \frac{a^T \Omega^2 a}{a^T a}, \quad \rho_{k+1} = \frac{a^T a}{a^T \Omega^{-2} a} \\ \text{for odd } k : \quad \rho_k = \frac{a^T a}{a^T \Omega^{-2} a}, \quad \rho_{k+1} = \frac{a^T \Omega^{-2} a}{a^T \Omega^{-4} a} \end{array} \right. \quad (6.209)$$

and by setting:

$$\left\{ \begin{array}{l} \text{for even } k : \quad b = \Omega^{-1} a \\ \text{for odd } k : \quad b = \Omega^{-2} a \end{array} \right. \quad (6.210)$$

one easily verifies that $A(\alpha, \beta)$ defined by (6.208) takes the general expression:

$$\begin{aligned} A(\alpha, \beta) &= \rho_k \rho_{k+1} - (\alpha + \beta) \rho_{k+1} + \alpha \beta \\ &= \frac{b^T (\Omega^2 - \alpha I) (\Omega^2 - \beta I) b}{b^T b} \quad \forall k \end{aligned} \quad (6.211)$$

in terms of which bound algorithms can be developed.

Krylov–Bogoliubov bounds

Let us start from (6.211) and set $\alpha = \beta$. We get:

$$\begin{aligned} \rho_k \rho_{k+1} - 2\alpha \rho_{k+1} + \alpha^2 &= \frac{\mathbf{b}^T (\mathbf{\Omega}^2 - \alpha \mathbf{I})(\mathbf{\Omega}^2 - \alpha \mathbf{I}) \mathbf{b}}{\mathbf{b}^T \mathbf{b}} \quad \forall k \\ &\geq \min_s (\omega_s^2 - \alpha)^2 \end{aligned} \quad (6.212)$$

Let us now consider the nearest eigenvalue ω_j^2 to α . To get the closest inequality, we take $\alpha = \rho_{k+1}$, which gives the minimal value of the left-hand side. The following inequality is obtained:

$$\rho_{k+1}(\rho_k - \rho_{k+1}) \geq (\omega_j^2 - \rho_{k+1})^2 \quad (6.213)$$

from which we deduce the Krylov–Bogoliubov bounds:

$$\rho_{k+1} - \sqrt{\rho_{k+1}(\rho_k - \rho_{k+1})} \leq \omega_j^2 \leq \rho_{k+1} + \sqrt{\rho_{k+1}(\rho_k - \rho_{k+1})} \quad (6.214)$$

In particular, let \mathbf{z}_0 be a reasonable approximation of a computed mode $\mathbf{x}_{(i)}$ (for instance by modal reduction) and $\mathbf{z}_1 = \mathbf{K}^{-1} \mathbf{M} \mathbf{z}_0$ its first iterate. The associated Schwarz and Rayleigh quotients are:

$$\rho_0 = \frac{\mathbf{z}_0^T \mathbf{K} \mathbf{z}_0}{\mathbf{z}_0^T \mathbf{M} \mathbf{z}_0} \quad \text{and} \quad \rho_1 = \frac{\mathbf{z}_0^T \mathbf{M} \mathbf{z}_0}{\mathbf{z}_0^T \mathbf{M} \mathbf{z}_1} \quad (6.215)$$

From these we can define the error measure coefficient:

$$\sigma^2 = \frac{\rho_0}{\rho_1} - 1 \geq 0 \quad (6.216)$$

and put relation (6.214) for the upper and lower bounds to eigenvalue ω_j^2 in the following form:

$$\rho_0 \frac{1 - \sigma}{1 + \sigma^2} \leq \omega_j^2 \leq \rho_0 \frac{1 + \sigma}{1 + \sigma^2} \quad (6.217)$$

In practice, ρ_0 being already an upper bound to ω_j^2 , Equation (6.217) is used only to provide the lower bound, so that the bracketing algorithm becomes:

$$\rho_0 \frac{1 - \sigma}{1 + \sigma^2} \leq \omega_j^2 \leq \rho_0 \quad (6.218)$$

Relation (6.218) provides a first algorithm for bracketing any eigenvalue ω_j^2 . However, it generally gives a poor approximation due to the fact that σ results from the computation of a square root (Equation (6.216)). We can improve it afterwards by using another bound algorithm described below.

6.10.3 Temple–Kato bounds

Let us suppose that α and β are contained in the interval between any two successive eigenvalues:

$$\omega_i^2 \leq \alpha < \beta \leq \omega_{i+1}^2 \quad (6.219)$$

In that case Equation (6.208) verifies for any k the property:

$$A(\alpha, \beta) = \rho_k \rho_{k+1} - (\alpha + \beta) \rho_{k+1} + \alpha \beta > 0 \quad (6.220)$$

since all the terms of its modal expansion resulting from (6.211):

$$A(\alpha, \beta) = \frac{1}{\mathbf{b}^T \mathbf{b}} \left\{ \sum_{s=1}^n b_s^2 (\omega_s^2 - \alpha)(\omega_s^2 - \beta) \right\} \quad (6.221)$$

remain positive under Condition (6.219).

Let us rewrite Inequality (6.220) in terms of the quotients obtained from the successive approximations z_0 and z_1 to a computed mode $\mathbf{x}_{(i)}$:

$$A(\alpha, \beta) = \rho_0 \rho_1 - (\alpha + \beta) \rho_1 + \alpha \beta > 0 \quad (6.222)$$

Making use of the error measure coefficient (6.216) allowing to write:

$$\rho_1 = \frac{\rho_0}{1 + \sigma^2} \quad (6.223)$$

we get:

$$A(\alpha, \beta) = \frac{\rho_0^2}{1 + \sigma^2} - (\alpha + \beta) \frac{\rho_0}{1 + \sigma^2} + \alpha \beta > 0$$

or

$$A(\alpha, \beta) = \rho_0^2 - (\alpha + \beta) \rho_0 + \alpha \beta (1 + \sigma^2) > 0 \quad (6.224)$$

Result (6.224) is known as Kato's inequality (Kato 1949, Temple 1952).

As we are interested in getting a lower bound estimate to eigenvalue ω_j , let us agree to take $\alpha = \omega_j^2$ and β so that:

$$\omega_j^2 \leq \rho_0 < \beta \leq \omega_{j+1}^2 \quad (6.225)$$

From (6.224) we get the inequality

$$\rho_0^2 - (\omega_j^2 + \beta) \rho_0 + \omega_j^2 \beta (1 + \sigma^2) > 0 \quad (6.226)$$

providing thus the lower bound to ω_j^2

$$\omega_j^2 > \rho_0 \frac{\beta - \rho_0}{\beta(1 + \sigma^2) - \rho_0} \quad (6.227)$$

which is obtained from the knowledge not only of the corresponding Rayleigh quotient and of the error coefficient (6.216), but also of a lower bound β to the next eigenvalue in the eigenspectrum. Whether formula (6.227) is applicable or not depends thus on the possibility to obtain a sufficiently good lower bound β to ω_{j+1}^2 so as to fulfill the condition (6.225).

A suitable β can generally be obtained by applying first the Krylov–Bogoliubov algorithm (Equation (6.218)) to ω_{j+1}^2 .

Since Inequality (6.227) depend now on σ^2 rather than on its square root, it yields a much closer lower bound than (6.218) as soon as ρ_0 and β are sufficiently separated from each other, in other words as soon as the eigenvalue spectrum is sufficiently spread around ω_j^2 .

Example 6.6

To illustrate the procedure to compute lower bounds to eigenfrequencies and thereby to characterize an approximate eigenvalue solution, let us consider the example of a beam clamped at both ends. A finite element model made of three elements is used to calculate its eigenmodes and eigenfrequencies. This example has been considered earlier in Chapter 5, Figure 5.21, and is depicted again here in Figure 6.14 where the fixed nodes are left out of the numbering.

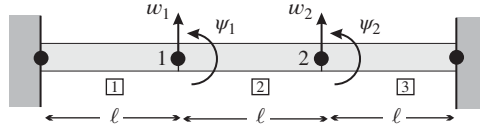


Figure 6.14 Model of a clamped–clamped beam.

In terms of the structural degrees of freedom:

$$\mathbf{q}^T = [w_1 \ w_2 \ \psi_1 \ \psi_2] \quad (\text{E6.6.a})$$

we obtain after reordering the structural stiffness and mass matrices:

$$\mathbf{K} = \frac{EI}{\ell^3} \begin{bmatrix} 24 & -12 & 0 & 6\ell \\ -12 & 24 & -6\ell & 0 \\ 0 & -6\ell & 8\ell^2 & 2\ell^2 \\ 6\ell & 0 & 2\ell^2 & 8\ell^2 \end{bmatrix} \quad \text{and} \quad \mathbf{M} = \frac{m\ell}{420} \begin{bmatrix} 312 & 54 & 0 & -13\ell \\ 54 & 312 & 13\ell & 0 \\ 0 & 13\ell & 8\ell^2 & -3\ell^2 \\ -13\ell & 0 & -3\ell^2 & 8\ell^2 \end{bmatrix}$$

Model condensation

In order to calculate the eigenvalues by hand, one may decide to condense the rotational degrees of freedom following Guyan & Irons' method, which leads to:

$$\mathbf{q}_R^T = [w_1 \ w_2] \quad \mathbf{q}_C^T = [\psi_1 \ \psi_2]$$

Then we successively calculate:

$$\begin{aligned} \mathbf{K}_{CC} &= \frac{EI}{\ell} \begin{bmatrix} 8 & 2 \\ 2 & 8 \end{bmatrix} & \mathbf{K}_{CC}^{-1} &= \frac{\ell}{30EI} \begin{bmatrix} 4 & -1 \\ -1 & 4 \end{bmatrix} \\ \mathbf{K}_{CR} &= \frac{EI}{\ell^2} \begin{bmatrix} 0 & -6 \\ 6 & 0 \end{bmatrix} & -\mathbf{K}_{CC}^{-1}\mathbf{K}_{CR} &= \frac{1}{5\ell} \begin{bmatrix} 1 & 4 \\ -4 & -1 \end{bmatrix} \end{aligned}$$

from which we deduce:

– the reduction matrix:

$$\mathbf{R} = \begin{bmatrix} \mathbf{I} \\ -\mathbf{K}_{CC}^{-1}\mathbf{K}_{CR} \end{bmatrix} = \begin{bmatrix} 1 & 0 \\ 0 & 1 \\ \frac{1}{5\ell} & \frac{4}{5\ell} \\ \frac{-4}{5\ell} & \frac{-1}{5\ell} \\ \frac{1}{5\ell} & \frac{1}{5\ell} \end{bmatrix}$$

– the reduced stiffness matrix:

$$\tilde{\mathbf{K}} = \mathbf{K}_{RR} - \mathbf{K}_{RC}\mathbf{K}_{CC}^{-1}\mathbf{K}_{CR} = \frac{6EI}{5\ell^3} \begin{bmatrix} 16 & -11 \\ -11 & 16 \end{bmatrix}$$

– the reduced mass matrix:

$$\tilde{\mathbf{M}} = \mathbf{R}^T\mathbf{M}\mathbf{R} = \ell \frac{m}{2100} \begin{bmatrix} 1696 & 319 \\ 319 & 1696 \end{bmatrix}$$

Solution of the reduced problem

If we write:

$$\lambda = \frac{\tilde{\omega}^2 m \ell^4}{2520EI}$$

the reduced eigenvalue problem is expressed by:

$$\begin{vmatrix} 16 - 1696\lambda & -11 - 319\lambda \\ -11 - 319\lambda & 16 - 1696\lambda \end{vmatrix} = 0$$

We thus obtain, calling $L = 3\ell$ the total length,

$$\tilde{\boldsymbol{\Omega}}^2 = \begin{bmatrix} \tilde{\omega}_1^2 & 0 \\ 0 & \tilde{\omega}_2^2 \end{bmatrix} = \frac{EI}{m\ell^4} \begin{bmatrix} 6.253 & 0 \\ 0 & 49.412 \end{bmatrix} = \frac{EI}{mL^4} \begin{bmatrix} 506.5 & 0 \\ 0 & 4002 \end{bmatrix} \quad (\text{E6.6.b})$$

Table 6.2 compares these results with the eigenfrequencies of the unreduced system given in Table 5.6. The analytical values result from the closed-form solution of the continuous system as listed in Table 4.3. We thus observe that for the same final number of degrees of freedom, Guyan-Irons reduction of the three-element model provides significantly better results than the two-element model.

Table 6.2 Beam clamped at both ends: comparison of condensed and noncondensed models

r	2 elements 2 d.o.f.	3 elements 2 d.o.f.	3 elements 4 d.o.f.	analytical
1	516.9	506.5	504.7	500.6
2	6720	4002	3957	3803

$$\omega_r^2 \sqrt{\frac{mL^4}{EI}}$$

Expression of the eigenmodes and of the Rayleigh quotients

Since the structure is symmetric, the eigenmodes of the reduced system may be found by a simple inspection. They are collected in matrix $\tilde{\mathbf{X}}_R$:

$$\tilde{\mathbf{X}}_R = [\tilde{\mathbf{x}}_{R(1)} \quad \tilde{\mathbf{x}}_{R(2)}] = \begin{bmatrix} 1 & 1 \\ 1 & -1 \end{bmatrix}$$

They may be restored to their complete form by the following relation:

$$\tilde{\mathbf{x}}_{(r)} = \mathbf{R}\tilde{\mathbf{x}}_{R(r)} \quad r = 1, 2$$

that is to say:

$$\tilde{\mathbf{X}} = [\tilde{\mathbf{x}}_{(1)} \quad \tilde{\mathbf{x}}_{(2)}] = \begin{bmatrix} 1 & 1 \\ 1 & -1 \\ \frac{1}{\ell} & -\frac{3}{5\ell} \\ -\frac{1}{\ell} & -\frac{3}{5\ell} \end{bmatrix}$$

Obviously the associated Rayleigh quotients are the eigenvalues E6.6.b. Those quotients will be taken as initial estimates ρ_0 for the eigenvalues:

$$\begin{bmatrix} \rho_{0,1} \\ \rho_{0,2} \end{bmatrix} = \frac{EI}{m\ell^4} \begin{bmatrix} 6.253 \\ 49.412 \end{bmatrix} \quad (\text{E6.6.c})$$

Calculation of the first iterates

Taking as the starting matrix the solution obtained by static condensation:

$$\mathbf{Z}_0 = \tilde{\mathbf{X}}$$

we define its first iterate by the relation:

$$\mathbf{K}\mathbf{Z}_1 = \mathbf{M}\mathbf{Z}_0$$

the right-hand side of which may be assimilated to a set of static load distributions. Let us write:

$$\mathbf{G} = \mathbf{M}\mathbf{Z}_0$$

and partition the system into retained and condensed coordinates:

$$\begin{bmatrix} \mathbf{K}_{RR} & \mathbf{K}_{RC} \\ \mathbf{K}_{CR} & \mathbf{K}_{CC} \end{bmatrix} \begin{bmatrix} \mathbf{Z}_{1R} \\ \mathbf{Z}_{1C} \end{bmatrix} = \begin{bmatrix} \mathbf{G}_R \\ \mathbf{G}_C \end{bmatrix}$$

This linear system can be solved by the a block elimination (equivalent to a static condensation of \mathbf{q}_C , see Section 6.6.1, page 450):

– calculation of the equivalent reduced load:

$$\tilde{\mathbf{G}}_R = \mathbf{G}_R - \mathbf{K}_{RC}\mathbf{K}_{CC}^{-1}\mathbf{G}_C$$

– solution of the reduced system:

$$\tilde{\mathbf{K}}\mathbf{Z}_{1R} = \tilde{\mathbf{G}}_R$$

– *restitution of the condensed displacements:*

$$\mathbf{Z}_{1C} = \mathbf{K}_{CC}^{-1}[\mathbf{G}_C - \mathbf{K}_{CR}\mathbf{G}_R]$$

We successively get:

$$\begin{aligned}\mathbf{G} &= \mathbf{M}\mathbf{Z}_0 = \frac{m\ell}{420} \begin{bmatrix} 379 & 379 & 24\ell & -24\ell \\ 265.8 & -265.8 & -16\ell & -16\ell \end{bmatrix}^T \\ \tilde{\mathbf{G}}_R &= \frac{m\ell}{420} \begin{bmatrix} 403 & 275.5 \\ 403 & -275.4 \end{bmatrix} \\ \mathbf{Z}_{1R} &= \frac{m\ell^4}{EI} \begin{bmatrix} 0.1599 & 0.0202 \\ 0.1599 & -0.0202 \end{bmatrix} = \frac{m\ell^4}{EI} \begin{bmatrix} 1 & 1 \\ 1 & -1 \end{bmatrix} \begin{bmatrix} 6.253 & 0 \\ 0 & 49.412 \end{bmatrix}^{-1} \\ &= \begin{bmatrix} 1 & 1 \\ 1 & -1 \end{bmatrix} \tilde{\mathbf{Q}}^{-2}\end{aligned}$$

which shows that the retained components have same contribution to iterates 0 and 1 since they differ only by a factor equal to the inverse of the corresponding eigenvalue.¹¹ We then calculate:

$$\mathbf{Z}_{1C} = \mathbf{K}_{CC}^{-1}(\mathbf{G}_C - \mathbf{K}_{CR}\mathbf{Z}_{1R}) = \frac{m\ell^3}{EI} \begin{bmatrix} 0.1694 & -0.0160 \\ -0.1694 & -0.0160 \end{bmatrix}$$

and hence:

$$\mathbf{Z}_1 = \frac{m\ell^3}{EI} \begin{bmatrix} 0.1599 & 0.0202 \\ 0.1599 & -0.0202 \\ 0.1694 & -0.0160 \\ -0.1694 & -0.0160 \end{bmatrix} \quad (\text{E6.6.d})$$

Calculation of the Schwarz quotients

The Schwarz quotients of the first order can be calculated by the formula:

$$\rho_1 = \frac{\mathbf{z}_0^T \mathbf{M} \mathbf{z}_0}{\mathbf{z}_0^T \mathbf{M} \mathbf{z}_1}$$

for each eigenvalue of the system, \mathbf{z} being the associate column in \mathbf{Z} . We find:

$$\begin{bmatrix} \rho_{1,1} \\ \rho_{1,2} \end{bmatrix} = \frac{EI}{m\ell^4} \begin{bmatrix} \frac{\mathbf{z}_{0,1}^T \mathbf{M} \mathbf{z}_{0,1}}{\mathbf{z}_{0,1}^T \mathbf{M} \mathbf{z}_{1,1}} \\ \frac{\mathbf{z}_{0,2}^T \mathbf{M} \mathbf{z}_{0,2}}{\mathbf{z}_{0,2}^T \mathbf{M} \mathbf{z}_{1,2}} \end{bmatrix} = \frac{EI}{m\ell^4} \begin{bmatrix} 1.9190 \\ 0.3080 \\ 1.3114 \\ 0.0268 \end{bmatrix} = \frac{EI}{m\ell^4} \begin{bmatrix} 6.2310 \\ 48.8772 \end{bmatrix} \quad (\text{E6.6.e})$$

¹¹ The fact that the retained coordinates have in this case equal contributions in iterates 0 and 1 results from the fact that iterate 0 was obtained by static condensation of the initial eigenvalue problem. The demonstration of it is proposed as exercise (Problem (6.8)).

Table 6.3 Beam clamped at both ends (three finite elements): computation of upper and lower bounds

r	upper bound $\tilde{\omega}_r^2$	lower bound Krylov–Bogoliubov	lower bound Temple–Kato	exact ω_r^2
1	506.5	474.7	504.4	504.7
2	4002	3545	–	3957

$$\omega_r^2 \sqrt{\frac{mL^4}{EI}}$$

The error measure coefficients have the following expressions:

$$\begin{bmatrix} \sigma_1^2 \\ \sigma_2^2 \end{bmatrix} = \begin{bmatrix} \frac{\rho_{0,1}}{\rho_{1,1}} - 1 \\ \frac{\rho_{0,2}}{\rho_{1,2}} - 1 \end{bmatrix} = \begin{bmatrix} 3.547 \\ 10.94 \end{bmatrix} \times 10^{-3} \quad (\text{E6.6.f})$$

The successive estimates ρ_0 and ρ_1 given by (E6.6.c, E6.6.e) together with the error measure coefficients (E6.6.f) are first used to compute lower bounds to the eigenfrequencies according to Krylov–Bogoliubov formula (Equation (6.218)):

$$\omega_{1,KB}^2 = \rho_{0,1} \frac{1 - \sigma_1}{1 + \sigma_1^2} = 5.860 \frac{EI}{m\ell^4} = 474.7 \frac{EI}{mL^4} \leq \omega_1^2 \quad (\text{E6.6.g})$$

$$\omega_{2,KB}^2 = \rho_{0,2} \frac{1 - \sigma_2}{1 + \sigma_2^2} = 43.766 \frac{EI}{m\ell^4} = 3545.0 \frac{EI}{mL^4} \leq \omega_2^2 \quad (\text{E6.6.h})$$

In particular the lower bound (E6.6.h) obtained to ω_2^2 is used to compute a better lower bound to ω_1^2 according to Temple–Kato formula (Equation (6.227)). Setting $\beta = \omega_{2,KB}^2$ and verifying that it then verifies $\rho_{0,1} < \beta$, conditions (6.225) are verified. We can thus apply formula (6.227) yielding the lower bound:

$$\omega_{1,TK}^2 = \rho_{0,1} \frac{\beta - \rho_{0,1}}{\beta(1 + \sigma_1^2) - \rho_{0,1}} = 6.227 \frac{EI}{m\ell^4} = 504.4 \frac{EI}{mL^4} < \omega_1^2 \quad (\text{E6.6.i})$$

The results are summarized in Table 6.3, the last column showing the exact solution of the 4×4 (unreduced) eigenvalue problem. One observes that the second algorithm provides a very good bracketing of the first frequency, as expected.

6.11 Sensitivity of eigensolutions, model updating and dynamic optimization

Nowadays, thanks to the efficiency of simulation techniques and to the computing power available, numerical simulation tends to replace expensive experimental validation of designs.

In practice, many assumptions are implicitly or explicitly made while setting up the model (e.g. screwed connections, boundary conditions, mass distribution, material properties). On the other hand, the real product or prototype might not have been produced exactly according to the blue prints due to manufacturing constraints, tolerances ...

Hence, in order to verify the accuracy of the model on which the design evaluation is based, one needs at some stage of the modelling to compare simulated results to experimental measurements. The model parameters (e.g. spring and connector stiffness, concentrated masses, elasticity coefficients of materials, dimensions) are then tuned in order to have a good agreement between measured and simulated results. Such a procedure is called *Model Updating*. For many applications where the dynamics of the system is critical (e.g. tooling machines, vehicle design, aeronautics and aerospace), one usually wants to ensure that the model can represent the free vibration of the structure with a high fidelity in terms of eigenshapes, eigenfrequencies and damping. Typically, for critical applications such as launchers or aircrafts the eigenfrequencies should be represented by the model with a relative error of less than 2 or 3 % in the operational frequency range.

The Model Updating procedure in structural dynamics is schematically described in Figure 6.15. We should not forget that the simulated results contain numerical errors due to discretization (in space and/or time), to approximate solution techniques and to round-off errors during computation. Also the experimental measurements are polluted by noise, sampling, sensor accuracy, signal analysis and numerical algorithms used for instance to identify the free vibration modes.

Measurement points in the experiment and degrees of freedom in the model do not necessarily have the same location/direction. There are usually many more degrees of freedom than measurement points.¹² Hence an important issue in model updating is to handle the so-called spatial incompatibility and to properly map numerical dofs and measured points. One way to build a correspondence between model degrees of freedom and measurement points is to evaluate the simulated results in the model for the location/directions of the measurement points (e.g. by using the finite element shape functions): this is known as *observation* or *projection*. Another approach consists in using the test measurements to estimate the system response in the entire structure: such techniques are called *expansion*. Specific methods for these steps can for instance be found in Friswell and Mottershead (1995).

The next issue to be handled is then to decide which measured mode/frequency corresponds to which eigensolution of the numerical model. For the complex structures usually encountered in practice, this is far from obvious and specific indicators such as the Modal Assurance Criterion (MAC) are used to estimate the matching between measured and simulated eigenmodes (Allemang and Brown 1982). The MAC between two modes (for instance a measured and a computed one, $\mathbf{x}_{(s),meas}$ and $\mathbf{x}_{(r),comp}$) indicates how well those modes match. Its simplest definition is:

$$MAC(\mathbf{x}_{(s),meas}, \mathbf{x}_{(r),comp}) = \frac{(\mathbf{x}_{(s),meas}^T \mathbf{x}_{(r),comp})^2}{\|\mathbf{x}_{(s),meas}\|^2 \|\mathbf{x}_{(r),comp}\|^2} \quad (6.228)$$

which is equal to 1 when the modes exactly match.

Finally one needs to decide how to modify the model parameters in order to get a model with improved fidelity. Here an objective function (or cost function) has to be defined in order

¹² Note that this tends to be no longer true when novel measuring techniques such as laser vibrometer scanning or holographic interferometry are used since the latter can handle many measurement points.

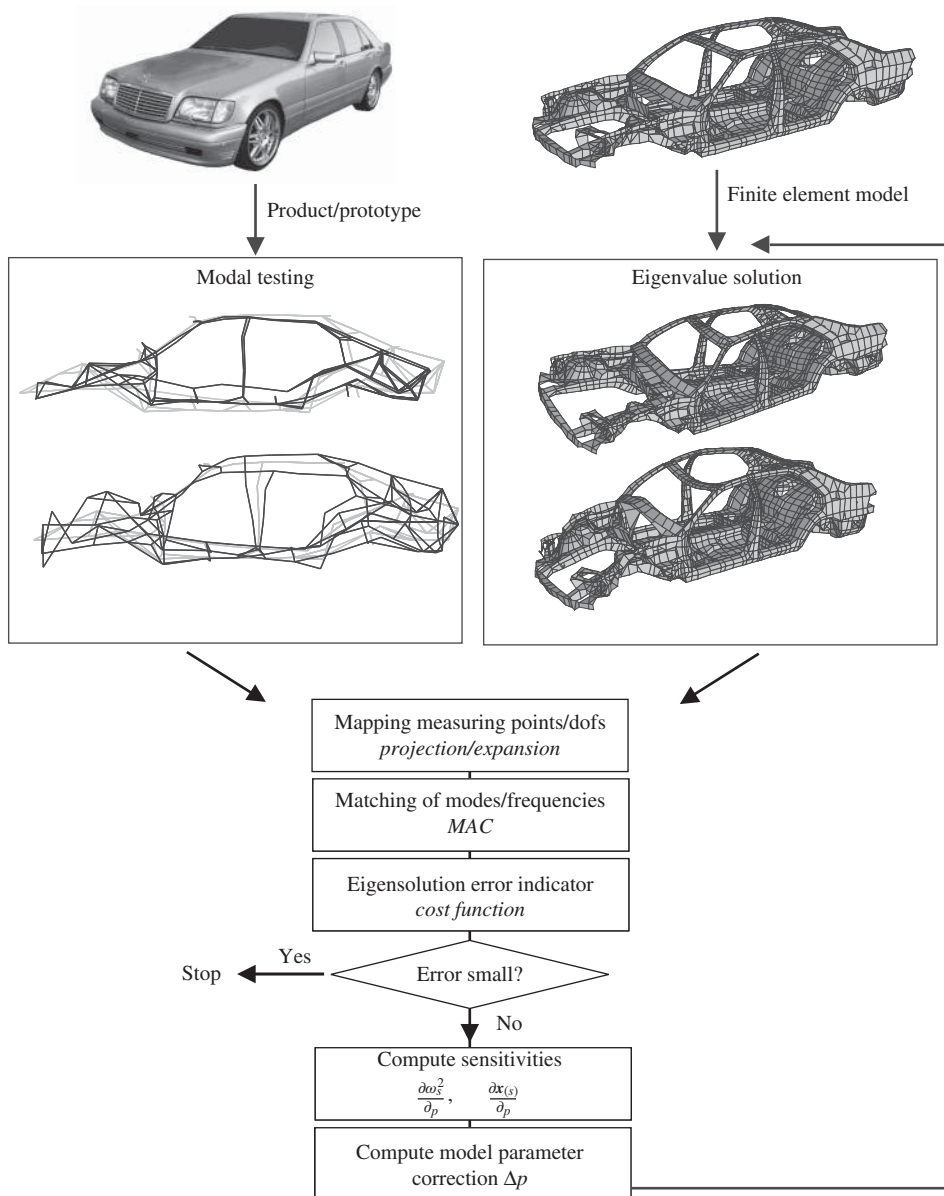


Figure 6.15 Modal Updating procedure.

to quantify the quality of the model. The cost function is usually a combination of scalar error indicators on the eigenmodes and eigenfrequencies, with weights depending on the confidence one has in the respective measured properties. Then, the parameters of the model can be updated based on the sensitivity of the model eigensolutions to these parameters.

Remark 6.11 *Since model matrices (mass and stiffness) can be nonlinear functions of updating parameters (e.g. bending stiffness depends nonlinearly on thickness) and because eigensolutions are nonlinear functions of model parameters, an optimum in terms of model fidelity can be obtained only iteratively. This is described in Figure 6.15. Hence a full modal analysis must be performed at every updating step and Modal Updating thus requires tremendous computing resources.*

Remark 6.12 *The updating procedure can efficiently improve the model only if*

- *the measurements have been performed at locations where the modal displacements are not small (observability),*
- *the applied load excites the relevant modes (controllability),*
- *the chosen updating design parameters allow to improve the model (visibility).*

Choosing the right experimental test configuration and parametric model is a major challenge.

Remark 6.13 *Modal Updating procedures are sometimes applied to damage detection: if one has a good model for a nominal system, modal updating can, at least in theory, locate defaults in structures.*

Remark 6.14 *When performing dynamic optimization, namely when one tries to find design properties that fulfill specific design requirements and dynamic response properties, a procedure very similar to the model updating one is applied. The only difference is then that the objective is no longer to minimize the difference between measured and simulated results, but for instance to minimize the weight, stresses or displacements under specific constraints for the eigenfrequencies. Knowing the sensitivity of the model eigensolutions to design parameters is also crucial in this kind of optimization.*

As can be seen, model updating of dynamic systems is an important and exciting field which combines many issues. In what follows we will only briefly describe how the sensitivity of the eigensolutions of the model can be evaluated.

6.11.1 Sensitivity of the structural model to physical parameters

The aim of sensitivity analysis is to obtain some quantitative information about the sensitivity of structural eigenfrequencies and eigenmodes to variations of physical parameters.

Let us suppose that the dynamic model is obtained by finite element discretization so that the assembly procedure of the stiffness and mass matrices can be written:

$$K = \sum_{e \in \text{model}} L_e^T K_e L_e \quad \text{and} \quad M = \sum_{e \in \text{model}} L_e^T M_e L_e \quad (6.229)$$

L_e being the Boolean localization operator of element e in the global set of degrees of freedom (see Section 5.3.1). Let us next suppose that we are interested in the sensitivity with respect to one physical/design parameter denoted by p and that element matrices are thus function of that parameter:

$$K_e = K_e(p) \quad M_e = M_e(p) \quad (6.230)$$

Let us adopt for the corresponding derivatives the notation:

$$\mathbf{K}_{e,p} = \frac{\partial \mathbf{K}_e}{\partial p} \quad \mathbf{M}_{e,p} = \frac{\partial \mathbf{M}_e}{\partial p} \quad (6.231)$$

The matrices (6.231) are elementary sensitivity matrices (null if the element does not depend on the parameter p). If one assembles those elementary sensitivity matrices, one obtains the global sensitivity matrices:

$$\mathbf{K}_{,p} = \frac{\partial \mathbf{K}}{\partial p} = \sum_{e \in \text{model}} \mathbf{L}_e^T \mathbf{K}_{e,p} \mathbf{L}_e \quad \mathbf{M}_{,p} = \frac{\partial \mathbf{M}}{\partial p} = \sum_{e \in \text{model}} \mathbf{L}_e^T \mathbf{M}_{e,p} \mathbf{L}_e \quad (6.232)$$

6.11.2 Sensitivity of eigenfrequencies

When the model parameters are perturbed, the eigensolutions will change in a way such that the equation for the eigensolution ($\omega_s^2, \mathbf{x}_{(s)}$):

$$(\mathbf{K} - \omega_s^2 \mathbf{M}) \mathbf{x}_{(s)} = \mathbf{0} \quad (6.233)$$

remains satisfied. Hence the sensitivity of the eigensolution can be obtained by deriving (6.233) with respect to parameter p :

$$\left(\frac{\partial \mathbf{K}}{\partial p} - \omega_s^2 \frac{\partial \mathbf{M}}{\partial p} \right) \mathbf{x}_{(s)} - \frac{\partial \omega_s^2}{\partial p} \mathbf{M} \mathbf{x}_{(s)} + (\mathbf{K} - \omega_s^2 \mathbf{M}) \frac{\partial \mathbf{x}_{(s)}}{\partial p} = \mathbf{0} \quad (6.234)$$

Let us project this relation on $\mathbf{x}_{(s)}$. Taking account of (6.233) and using definitions (6.232) yields:

$$\frac{\partial \omega_s^2}{\partial p} = \frac{\mathbf{x}_{(s)}^T (\mathbf{K}_{,p} - \omega_s^2 \mathbf{M}_{,p}) \mathbf{x}_{(s)}}{\mu_s} \quad (6.235)$$

This result shows three things:

- The derivative of a given eigenvalue with respect to the parameter can be obtained in terms of the corresponding elementary sensitivity matrices since the products $\mathbf{K}_{,p} \mathbf{x}_{(s)}$ and $\mathbf{M}_{,p} \mathbf{x}_{(s)}$ can be performed element-wise (see (6.232)).
- The derivative of an eigenvalue depends on the corresponding eigensolution only.
- An increase of stiffness increases frequency, whereas an increase of mass reduces it.

Because the elementary sensitivity matrices can be constructed from the finite element formulation (or using software for automatic differentiation of subroutines), the calculation of eigenvalue sensitivities by relation (6.235) requires only a very small computational effort in the finite element calculation context.

6.11.3 Sensitivity of free vibration modes

To obtain the eigenmode sensitivity, one first computes the eigenvalue sensitivity $\frac{\partial \omega_s^2}{\partial p}$ from

(6.235) and then solves (6.234) for $\frac{\partial \mathbf{x}_{(s)}}{\partial p}$:

$$(\mathbf{K} - \omega_s^2 \mathbf{M}) \frac{\partial \mathbf{x}_{(s)}}{\partial p} = \left(-\mathbf{K}_{,p} + \omega_s^2 \mathbf{M}_{,p} + \frac{\partial \omega_s^2}{\partial p} \mathbf{M} \right) \mathbf{x}_{(s)} \quad (6.236)$$

Let us observe that in (6.236) $(\mathbf{K} - \omega_s^2 \mathbf{M})$ is singular according to the definition (6.233), and $\mathbf{x}_{(s)}$ is its nullspace. Nevertheless, since $\frac{\partial \omega_s^2}{\partial p}$ is solution of (6.235), the right hand side of (6.236) is orthogonal to the nullspace $\mathbf{x}_{(s)}$ and a solution thus exists. Let us call:

$$\frac{\partial \mathbf{x}_{(s)}^\circ}{\partial p} = (\mathbf{K} - \omega_s^2 \mathbf{M})^+ \left(-\mathbf{K}_{,p} + \omega_s^2 \mathbf{M}_{,p} + \frac{\partial \omega_s^2}{\partial p} \mathbf{M} \right) \mathbf{x}_{(s)} \quad (6.237)$$

a particular solution of (6.236), $(\mathbf{K} - \omega_s^2 \mathbf{M})^+$ being a generalized inverse (see Section 6.6.6). Then the general solution for the eigenvector sensitivity Equation (6.236) is given by:

$$\frac{\partial \mathbf{x}_{(s)}}{\partial p} = \frac{\partial \mathbf{x}_{(s)}^\circ}{\partial p} + \mathbf{x}_{(s)} \alpha \quad (6.238)$$

where the amplitude α is undetermined. One way to fix it and thus define a unique eigenvector sensitivity consists in requiring that the eigenmodes change with the design parameter in such a way that their modal mass μ_s remains constant, that is:

$$\mathbf{x}_{(s)}(p)^T \mathbf{M} \mathbf{x}_{(s)}(p) = \mu_s \quad \text{constant} \quad (6.239)$$

Deriving the above relation with respect to the design parameter p ,

$$\mathbf{x}_{(s)}^T \mathbf{M} \frac{\partial \mathbf{x}_{(s)}}{\partial p} = -\frac{1}{2} \mathbf{x}_{(s)}^T \mathbf{M}_{,p} \mathbf{x}_{(s)} \quad (6.240)$$

Substituting the general solution (6.238) into 6.240 one obtains:

$$\alpha = -\frac{1}{\mu_s} \left(\frac{1}{2} \mathbf{x}_{(s)}^T \mathbf{M}_{,p} \mathbf{x}_{(s)} + \mathbf{x}_{(s)}^T \mathbf{M} \frac{\partial \mathbf{x}_{(s)}^\circ}{\partial p} \right)$$

and thus:

$$\frac{\partial \mathbf{x}_{(s)}}{\partial p} = \left(\mathbf{I} - \frac{1}{\mu_s} \mathbf{x}_{(s)} \mathbf{x}_{(s)}^T \mathbf{M} \right) \frac{\partial \mathbf{x}_{(s)}^\circ}{\partial p} - \frac{1}{2\mu_s} \mathbf{x}_{(s)} \mathbf{x}_{(s)}^T \mathbf{M}_{,p} \mathbf{x}_{(s)} \quad (6.241)$$

Computing a pseudo-inverse to $\mathbf{K} - \omega_s^2 \mathbf{M}$ can be avoided by using the Lagrange multiplier method to remove the singularity of system (6.236) through imposition of the constraint (6.240). A constrained linear problem is then solved in the form (Nelson 1976):

$$\begin{bmatrix} \mathbf{K} - \omega_s^2 \mathbf{M} & \mathbf{M} \mathbf{x}_{(s)} \\ \mathbf{x}_{(s)}^T \mathbf{M} & 0 \end{bmatrix} \begin{bmatrix} \frac{\partial \mathbf{x}_{(s)}}{\partial p} \\ \lambda \end{bmatrix} = \begin{bmatrix} \left(-\mathbf{K}_{,p} + \omega_s^2 \mathbf{M}_{,p} + \frac{\partial \omega_s^2}{\partial p} \mathbf{M} \right) \mathbf{x}_{(s)} \\ -\frac{1}{2} \mathbf{x}_{(s)}^T \mathbf{M}_{,p} \mathbf{x}_{(s)} \end{bmatrix} \quad (6.242)$$

Unfortunately, the extended system matrix in (6.242) has not the same sparsity as the dynamic stiffness kernel.

6.11.4 Modal representation of eigenmode sensitivity

To find a particular solution (6.237) to the eigenmode sensitivity equation (6.236), one can either use special factorization techniques for singular matrices (see Section 6.6.2) or use a mode superposition representation:

$$\frac{\partial \mathbf{x}_{(s)}^\circ}{\partial p} = \sum_{r \neq s} \gamma_r \mathbf{x}_{(r)} \quad (6.243)$$

Note that the eigenmode \mathbf{x}_s for which the sensitivity is computed is not part of the combination since its amplitude is undefined (see discussion here above). Substituting this relation into expression (6.236) and making use of the orthogonality relations, we obtain the following coefficients:

$$\gamma_r = \frac{\mathbf{x}_{(r)}^T (\mathbf{K}_{,p} - \omega_s^2 \mathbf{M}_{,p}) \mathbf{x}_{(s)}}{(\omega_s^2 - \omega_r^2) \mu_r} \quad (6.244)$$

This result shows two things:

- Unlike eigenvalue sensitivities, calculating an eigenmode sensitivity implies knowledge of all the other eigensolutions.
- The sensitivity of mode $\mathbf{x}_{(s)}$ strongly depends on other modes having similar eigenfrequencies, that is when $\omega_r^2 \simeq \omega_s^2$.

Because one seldom possesses the complete modal basis, it is generally preferred to compute the eigenmode sensitivities directly as described in Section 6.11.3. Approximate eigenmode sensitivities can also be computed using a reduced basis representation.

Finally, let us note that a special procedure has to be implemented for multiple frequencies (Ojalvo 1988).

6.12 Exercises

6.12.1 Solved exercises

Problem 6.1 Let us consider the system of equations:

$$\begin{bmatrix} \mathbf{K} & \mathbf{L}_r^T \\ \mathbf{L}_r & \mathbf{0} \end{bmatrix} \begin{bmatrix} \mathbf{q} \\ \lambda \end{bmatrix} = \begin{bmatrix} \mathbf{p} \\ \mathbf{0} \end{bmatrix} \quad (\text{P6.1.a})$$

where \mathbf{K} is a stiffness matrix from a structural system with global set of degrees of freedom:

$$\mathbf{q} = \mathbf{q}_i \cup \mathbf{q}_r \quad (\text{P6.1.b})$$

\mathbf{q}_r and \mathbf{q}_i being respectively internal and restrained degrees of freedom and λ being a set of Lagrange multipliers. The former are extracted from the global set \mathbf{q} by the Boolean operations involving the matrices \mathbf{L}_i and \mathbf{L}_r :

$$\mathbf{q}_i = \mathbf{L}_i \mathbf{q} \quad \mathbf{q}_r = \mathbf{L}_r \mathbf{q} \quad (\text{P6.1.c})$$

Show that solving the system (P6.1.a) is equivalent to solving the internal system $\mathbf{K}_{ii}\mathbf{q}_i = \mathbf{p}_i$ and that the λ provide the reactions on the restrained degrees of freedom.

Solution

Let us note first that owing to (P6.1.b) the Boolean matrices \mathbf{L}_i and \mathbf{L}_r are such that:

$$\mathbf{q} = \mathbf{L}_i^T \mathbf{q}_i + \mathbf{L}_r^T \mathbf{q}_r \quad (\text{P6.1.d})$$

$$\mathbf{L}_r \mathbf{L}_r^T = \mathbf{I}_r \text{ and } \mathbf{L}_i \mathbf{L}_r^T = \mathbf{0} \quad (\text{P6.1.e})$$

The second Equation (P6.1.a) expresses the fact the \mathbf{q}_r are fixed since:

$$\mathbf{L}_r \mathbf{q} = \mathbf{q}_r = \mathbf{0} \quad (\text{P6.1.f})$$

while the first equation can be rewritten as:

$$\mathbf{K}\mathbf{q} = \mathbf{K}\mathbf{L}_i^T \mathbf{q}_i = \mathbf{p} - \mathbf{L}_r^T \lambda \quad (\text{P6.1.g})$$

Multiplying then Equation (P6.1.g) by \mathbf{L}_i and \mathbf{L}_r successively yields:

$$\mathbf{L}_i \mathbf{K} \mathbf{L}_i^T \mathbf{q}_i = \mathbf{L}_i \mathbf{p} \text{ or } \mathbf{K}_{ii} \mathbf{q}_i = \mathbf{p}_i \quad (\text{P6.1.h})$$

and

$$\mathbf{L}_r \mathbf{K} \mathbf{L}_i^T \mathbf{q}_i = \mathbf{L}_r \mathbf{p} - \mathbf{L}_r \mathbf{L}_r^T \lambda \quad (\text{P6.1.i})$$

Hence the expression of the multipliers:

$$\lambda = \mathbf{p}_r - \mathbf{K}_{ri} \mathbf{q}_i \quad (\text{P6.1.j})$$

6.12.2 Selected exercises

Problem 6.2 The two-degrees-of-freedom vibrating system of Figure 3.1 has for stiffness and mass matrices

$$\mathbf{K} = \begin{bmatrix} 4 & -2 \\ -2 & 6 \end{bmatrix} \quad \mathbf{M} = \begin{bmatrix} 5 & 0 \\ 0 & 10 \end{bmatrix} \quad (\text{P6.2.a})$$

You are asked:

- to construct for the system a symmetric iteration matrix \mathbf{S} .
- to put it in diagonal form through single Jacobi rotation transformation: $\mathbf{V} = \mathbf{R}^T \mathbf{S} \mathbf{R}$.
- to deduce the eigenfrequencies and compute the eigenmodes (validate the results with those of Example 3.1).

Problem 6.3 let is consider again the undamped two-degrees-of-freedom vibrating system defined by the stiffness and mass matrices (P6.2.a). You are asked:

- to construct the iteration matrix $\mathbf{D} = \mathbf{K}^{-1} \mathbf{M}$ of the system.
- starting from the initial vector $\mathbf{z}_0^T = [1 \ 0]$, to perform five power iterations according to the iteration scheme (6.45).
- to display on a two-dimensional plot the successive iterates \mathbf{z}_p obtained.

- to observe the convergence of the successive approximations obtained to the first eigenvalue $\lambda_1 = \omega_1^{-2}$.
- assuming that the exact eigenvalues λ_1 and λ_2 are known from Exercise 6.2, verify how well the prediction (6.52) of the number of iterations needed to stabilize t significant figures is verified.

Problem 6.4 The stiffness matrix of a clamped-free bar discretized with N elements is a $N \times N$ tridiagonal matrix of the form:

$$\mathbf{K} = k \begin{bmatrix} 2 & -1 & 0 & \dots & \dots & 0 \\ -1 & 2 & -1 & \ddots & \ddots & \vdots \\ 0 & -1 & 2 & -1 & \ddots & \vdots \\ \vdots & \ddots & \ddots & \ddots & \ddots & 0 \\ \vdots & \ddots & \ddots & \ddots & 2 & -1 \\ 0 & \dots & \dots & 0 & -1 & 1 \end{bmatrix} \quad (\text{P6.4.a})$$

You are asked:

- to perform the LU decomposition of \mathbf{K} for $N = 5$.
- to deduce from the result obtained the LU decomposition for any N .
- to verify that $\mathbf{U} = \mathbf{DL}^T$ with \mathbf{D} diagonal.
- Using the previous results, to solve the system $\mathbf{K}\mathbf{q} = \mathbf{p}$ with $\mathbf{p}^T = [0 \ 0 \ 1 \ 0 \ 0]$ and to justify the physical meaning of the obtained solution.

Problem 6.5 Consider a free-free beam element as depicted in Figure 6.8. Similar to what was done in Example 6.4 we want to factorize the stiffness matrix and compute the rigid body modes. However now we assume that the beam element is prestressed by a force N_0 so that the total stiffness matrix includes, in addition to the elastic part, also a geometric contribution (see page 376). For this case you are asked:

- To factorize the matrix of the prestressed free-free beam element.
- To compute the rigid body modes.
- To discuss why one of the rigid body modes existing in the absence of prestress is no longer present.

Problem 6.6 Let us consider the static problem:

$$\mathbf{K}\mathbf{q} = \mathbf{p} \quad (\text{P6.6.a})$$

with \mathbf{K} singular. It has been demonstrated in Section 6.6.4 that a solution to it exists if and only if the load vector \mathbf{p} is orthogonal to the rigid body modes \mathbf{U} :

$$\mathbf{U}^T \mathbf{p} = 0 \quad (\text{P6.6.b})$$

Demonstrate that starting from an arbitrary load vector \mathbf{p} , solving the extended system:

$$\begin{bmatrix} \mathbf{K} & \mathbf{MU} \\ \mathbf{U}^T \mathbf{M} & \mathbf{0} \end{bmatrix} \begin{bmatrix} \mathbf{q} \\ \lambda \end{bmatrix} = \begin{bmatrix} \mathbf{p} \\ \mathbf{0} \end{bmatrix} \quad (\text{P6.6.c})$$

where λ is a Lagrange multiplier generates de facto a load vector \mathbf{p}' verifying Equation (P6.6.b) and that the resulting displacement vector \mathbf{q} is \mathbf{M} -orthogonal to the rigid body modes.

Problem 6.7 An alternative method to solve the singular linear system (P6.6.a) under conditions (P6.6.b), called inertia relief method, consists in selecting a set \mathbf{q}_r of m degrees of freedom so as to block the m rigid-body modes of the system. They are extracted from the global set by the Boolean operation \mathbf{L}_r :

$$\mathbf{q}_r = \mathbf{L}_r \mathbf{q} \quad (\text{P6.7.a})$$

An extended system with $m + 1$ right-hand sides is then formed¹³ in which the inertia loads of the rigid body modes are transferred to the right-hand side:

$$\begin{bmatrix} \mathbf{K} & \mathbf{L}_r^T \\ \mathbf{L}_r & \mathbf{0} \end{bmatrix} \begin{bmatrix} \mathbf{q} & \mathbf{Q} \\ \lambda & \mathbf{A} \end{bmatrix} = \begin{bmatrix} \mathbf{p} & \mathbf{MU} \\ \mathbf{0} & \mathbf{0} \end{bmatrix} \quad (\text{P6.7.b})$$

The $n \times m$ matrix \mathbf{Q} is the static response to the additional load cases, and \mathbf{A} is a diagonal matrix of m associated multipliers.

You are asked:

- To interpret the fact that the corresponding solutions $[\mathbf{q} \ \mathbf{Q}]$ are such that $\mathbf{L}_r[\mathbf{q} \ \mathbf{Q}] = \mathbf{0}$.
- To demonstrate that matrix $\mathbf{U}_R = \mathbf{L}_R \mathbf{U}$ is square and nonsingular.
- To expand the equilibrium equation by expressing the solution of (P6.7.b) to a linear combination of the load vectors:

$$\mathbf{p}' = \mathbf{p} + \mathbf{MU} \mathbf{a} \quad (\text{P6.7.c})$$

in terms of the individual solutions to (P6.7.b) as:

$$\begin{bmatrix} \mathbf{q}' \\ \lambda' \end{bmatrix} = \begin{bmatrix} \mathbf{q} \\ \lambda \end{bmatrix} + \begin{bmatrix} \mathbf{Q} \\ \mathbf{A} \end{bmatrix} \mathbf{a} \quad (\text{P6.7.d})$$

- To make use of the rigid body modes to eliminate from it the stiffness contribution and get the relationship linking the external load distribution (P6.7.c) to the Lagrange multipliers λ and \mathbf{A} .
- To express which condition ought to be verified by the Lagrange multipliers in order to get a load distribution (P6.7.c) orthogonal to the rigid body modes and determine the corresponding set of coefficients \mathbf{a} .
- At the light of the result obtained, to deduce the physical meaning of the multipliers.

Problem 6.8 Let us consider a vibrating system with all distinct eigenvalues, and construct the $n \times n$ square matrix $\mathbf{Z} = [\mathbf{z}_0 \ \mathbf{z}_2 \ \dots \ \mathbf{z}_{n-1}]$ collecting the successive iterates of the Krylov sequence $\mathbf{z}_{p+1} = \mathbf{K}^{-1} \mathbf{M} \mathbf{z}_p$ ($p = 0 \ \dots \ n - 1$). Prove that \mathbf{Z} is nonsingular provided that the coefficients of the spectral expansion of the starting vector \mathbf{z}_0 are all nonzero.

Problem 6.9 In Example 6.6 it has been observed experimentally that the zero-order approximation \mathbf{Z}_0 to the eigenmodes and its first iterate \mathbf{Z}_1 obtained from inverse iteration are such that:

$$\mathbf{Z}_{1R} = \tilde{\mathbf{Q}}^{-2} \mathbf{Z}_{0R} \quad (\text{P6.9.a})$$

¹³ The inertia relief technique is nothing else than a specific implementation of the method of fictitious links mentioned Page 457. Its advantage over the method described in Problem (6.6) lies in the fact that building up the extended stiffness matrix (Equation (P6.7.b)) is much simpler, since consisting simply in the addition of a few terms of unit value. In the method of Problem (6.6) full rows and columns were added.

which means the first inverse iteration:

$$\mathbf{K}\mathbf{Z}_1 = \mathbf{M}\mathbf{Z}_0 \quad (\text{P6.9.b})$$

does not affect the eigenmode components corresponding to the retained coordinates.

Demonstrate that property (P6.9.a) is specific to static condensation and results from the fact that the zero-order approximation \mathbf{Z}_0 obeys to:

$$\mathbf{Z}_0 = \mathbf{R}\mathbf{X}_R \quad (\text{P6.9.c})$$

with the reduction matrix:

$$\mathbf{R} = \begin{bmatrix} \mathbf{I} \\ -\mathbf{K}_{CC}^{-1}\mathbf{K}_{CR} \end{bmatrix} \quad (\text{P6.9.d})$$

and with \mathbf{X}_R solution of:

$$\tilde{\mathbf{K}}\mathbf{X}_R = \tilde{\Omega}^2\tilde{\mathbf{M}}\mathbf{X}_R \quad (\text{P6.9.e})$$

References

- Allemang RJ and Brown DL 1982 A correlation coefficient for modal vector analysis *Proceedings of the 1st International Modal Analysis Conference*, vol. 1, pp. 110–116–SEM, Orlando.
- Arnoldi WE 1951 The principle of minimized iterations in the solution of the matrix eigenvalue problem. *Quart. Appl. Math* **9**(1), 17–29.
- Bathe K 1971 Solution methods for large generalized eigenvalue problems in structural engineering. Technical Report UC SESM 71-20, Structural Engineering Laboratory, University of California, Berkeley.
- Bathe K 1977 Convergence of subspace iteration In *Formulations and Numerical Algorithms in Finite Element Analysis* (ed. K.J. Bathe JO and Wunderlich W) MIT Press, Cambridge, MA pp. 575–598.
- Bathe KJ and Wilson EL 1972 Large eigenvalue problems in dynamic analysis. *Journal of the Engineering Mechanics Division* **98**(6), 1471–1485.
- Bathe KJ and Wilson EL 1973 Solution methods for eigenvalue problems in structural mechanics. *International Journal for Numerical Methods in Engineering* **6**(2), 213–226.
- Bauer FL 1957 Das Verfahren der Treppeniteration und verwandte Verfahren zur Lösung algebraischer Eigenwertprobleme. *Zeitschrift für angewandte Mathematik und Physik ZAMP* **8**(3), 214–235.
- Ben-Israel A and Greville T 1974 *Generalized Inverse: Theory and Applications*. John Wiley & Sons, Inc., New York.
- Bennighof JK and Lehoucq RB 2004 An automated multilevel substructuring method for eigenspace computation in linear elastodynamics. *SIAM Journal on Scientific Computing* **25**(6), 2084–2106.
- Brzobohatý T, Dostál Z, Kozubek T, Kovár P and Markopoulos A 2011 Cholesky–SVD decomposition with fixing nodes to stable computation of a generalized inverse of the stiffness matrix of a floating structure. *Int. Journal for Numerical Methods in Engineering* **88**(5), 493–509.
- Carnoy, E. and Géraudin, M. 1983 On the practical use of the Lanczos algorithm in finite element applications to vibration and bifurcation problems In *Matrix Pencils* (ed. Kågström B and Ruhe A) vol. 973 of *Lecture Notes in Mathematics* Springer Berlin / Heidelberg pp. 156–176.
- Craig R and Bampton M 1968 Coupling of substructures for dynamic analysis. *AIAA Jnl.* **6**(7), 1313–1319.
- Craig R and Chang C 1977 Substructure coupling for dynamic analysis and testing. Technical Report CR-2781, NASA.
- Craig R and Kurdila A 2006 *Fundamentals of Structural Dynamics*. John Wiley & Sons, Inc. New York.
- Cuthill E and McKee J 1969 Reducing the bandwidth of sparse symmetric matrices *Proceedings of the 1969 24th national conference*, pp. 157–172 ACM.
- Farhat C and Géraudin M 1998 On the general solution by a direct method of a large-scale singular system of linear equations: Application to the analysis of floating structures. *International Journal for Numerical Methods in Engineering* **41**(4), 675–696.
- Farhat C and Rixen D 2002 Linear algebra. In *Encyclopedia of Vibration* Academic Press, pp. 710–720.
- Farhat C and Roux FX 1991 A method of finite tearing and interconnecting and its parallel solution algorithm. *International Journal for Numerical Methods in Engineering* **32**(6), 1205–1227.

- Felippa CA 2001 A historical outline of matrix structural analysis: a play in three acts. *Computers & Structures* **79**(14), 1313–1324.
- Forsythe GE and Henrici P 1960 The cyclic Jacobi method for computing the principal values of a complex matrix. *Transactions of the American Mathematical Society* **94**(1), 1–23.
- Fox L, Henrici P and Moler C 1967 Approximations and bounds for eigenvalues of elliptic operators. *SIAM Journal on Numerical Analysis* **4**(1), 89–102.
- Fraeijs de Veubeke B, G rardin M and Huck A 1972 *Structural Dynamics*. number 126 in *CISM Lecture Notes (Udine, Italy)*. Springer.
- Francis JGF 1961 The QR transformation: a unitary analogue to the LR transformation – Part 1. *The Computer Journal* **4**(3), 265–271.
- Francis JGF 1962 The QR transformation – Part 2. *The Computer Journal* **4**(4), 332–345.
- Frazer R, Duncan W and Collar A 1938 *Elementary Matrices*. Cambridge University Press.
- Friswell M and Mottershead JE 1995 *Finite Element Model Updating in Structural Dynamics* vol. 38. Springer.
- Gao W, Li XS, Yang C and Bai Z 2008 An implementation and evaluation of the AMLS method for sparse eigenvalue problems. *ACM Transactions on Mathematical Software (TOMS)* **34**(4), 20.
- George A and Liu JW 1981 *Computer Solution of Large Sparse Positive Definite Systems*. Prentice Hall.
- G rardin M 1971 Error bounds for eigenvalue analysis by elimination of variables. *Jnl. Sound & Vibration* **19**(2), 111–132.
- G rardin M 1973 *Analyse dynamique duale des structures par la m thode des  l ments finis* PhD thesis University of Li ge, Collection des Publications de la Facult  des Sciences Appliqu es, no 36.
- G rardin M 1978 Une  tude comparative des m thodes num riques en analyse dynamique des structures *Association Technique Maritime et A ronautique*.
- Givens W 1953 A method of computing eigenvalues and eigenvectors suggested by classical results on symmetric matrices. *Nat. Bur. Standards Appl. Math. Ser* **29**, 117–122.
- Golub GH and Van Loan CF 1989 *Matrix Computations*. John Hopkins University Press.
- Grimes RG, Lewis JG and Simon HD 1994 A shifted block Lanczos algorithm for solving sparse symmetric generalized eigenproblems. *SIAM J. Matrix Anal. Appl.* **15**(1), 228–272.
- Guyan R 1965 Reduction of stiffness and mass matrices. *AIAA Jnl.* **3**(2), 380.
- Hestenes MR and Stiefel E 1952 Methods of conjugate gradients for solving linear systems. *Journal of Research of the National Bureau of Standards*, **49**(6), 409–436.
- Householder AS 1958 Unitary triangularization of a nonsymmetric matrix. *Journal of the ACM (JACM)* **5**(4), 339–342.
- Irons B 1965 Structural eigenvalue problems: elimination of unwanted variables. *AIAA Jnl.* **5**, 961–962.
- Irons B 1970 A frontal solution for finite element analysis. *Int. Jnl. Num. Meth. Eng.* **2**, 5–32.
- Jacobi C 1846  ber ein leichtes Verfahren die in der Theorie der S cularst r ungen vorkommenden Gleichungen numerisch aufzul sen. *Journal f r die reine und angewandte Mathematik* **30**, 51–94.
- Jakobsson H and Larson MG 2011 A posteriori error analysis of component mode synthesis for the elliptic eigenvalue problem. *Comput. Methods Appl. Mech. Engrg.* (200), 2840–2847.
- Kato T 1949 On the upper and lower bounds of eigenvalues. *J. Phys. Soc. Japan* **4**, 334–339.
- Kestens J 1956 Le probl me aux valeurs propres normales et bornes sup rieures et inf rieures par la m thode des it rations. *M moires de l'Acad mie Royale de Belgique, Classe des Sciences*.
- Komzsik L 2003 *The Lanczos method: Evolution and application*. SIAM.
- Krylov A 1931 On the numerical solution of equations whose solution determine the frequency of small vibrations of material systems. *Izv. Akad. Nauk. SSSR Otd Mat. Estest* **1**, 491–539.
- Lanczos C 1950 An iteration method for the solution of the eigenvalue problem of linear differential and integral operators. *Journal of Research of the National Bureau of Standards* **45**, 255–282.
- Lehoucq RB and Sorensen DC 1996 Deflation techniques for an implicitly restarted Arnoldi iteration. *SIAM J. Matrix Analysis and Applications* **17**(4), 789–821.
- Liu JW 1992 The multifrontal method for sparse matrix solution: Theory and practice. *SIAM review* **34**(1), 82–109.
- MacNeal RH 1971 A hybrid method of component mode synthesis. *Computers and Structures* **1**(4), 581–601.
- Mises RV and Pollaczek-Geiringer H 1929 Praktische Verfahren der Gleichungsl sung. *ZAMM – Journal of Applied Mathematics and Mechanics / Zeitschrift f r Angewandte Mathematik und Mechanik* **9**(1), 58–77.
- Muntz C 1913 Solution directe de l' quation s culaire et de quelques probl mes analogues. *Comptes Rendus de l'Acad mie des Sciences* **156**, 43–46.
- Nelson RB 1976 Simplified calculation of eigenvector derivatives. *AIAA Journal* **14**(9), 1201–1205.

- Ojalvo I 1988 Efficient computation of modal sensitivities for systems with repeated frequencies. *AIAA Journal* **26**(3), 361–366.
- Papadrakakis M and Fragakis Y 2001 An integrated geometric-algebraic method for solving semi-definite problems in structural mechanics. *Computer Methods in Applied Mechanics and Engineering* **190**(49–50), 6513–6532.
- Rixen D 2002 *Encyclopedia of Vibration* Academic Press. Chapter Parallel Computation, pp. 990–1001.
- Rubin S 1975 Improved component-mode representation for structural dynamic analysis. *AIAA journal* **13**(8), 995–1006.
- Rutishauser H 1958 Solution of eigenvalue problems with the LR-transformation. *Nat. Bur. Standards Appl. Math. Ser* **49**, 47–81.
- Schwarz H, Rutishauser H and Stiefel E 1973 *Numerical Analysis of Symmetric Matrices*. Prentice Hall, Englewood Cliffs NJ.
- Sloan S and Randolph MF 1983 Automatic element reordering for finite element analysis with frontal solution schemes. *International Journal for Numerical Methods in Engineering* **19**(8), 1153–1181.
- Sorensen DC 1992 Implicit application of polynomial filters in a k-step Arnoldi method. *SIAM J. Matrix Analysis and Applications* **13**, 357–385.
- Sorensen DC 1996 Implicitly restarted Arnoldi / Lanczos methods for large scale eigenvalue calculations. Technical Report NASA Contractor Report 198342, ICASE Report No. 96-40, Institute for Computer Applications in Science and Engineering NASA Langley Research Center, Hampton, VA 23681-0001.
- Temple G 1952 The accuracy of Rayleigh's method of calculating the natural frequencies of vibrating systems. *Proceedings of the Royal Society of London. Series A. Mathematical and Physical Sciences* **211**(1105), 204–224.
- Wilkinson J 1965 *The Algebraic Eigenvalue Problem*. Clarendon Press, Oxford.
- Wittrick W and Williams F 1971 A general algorithm for computing natural frequencies of elastic structures. *Quart. Journ. Mech. and Applied Math.* **XXIV**, 263–284.

7

Direct Time-Integration Methods

To solve the structural dynamic equations of motion under arbitrary excitation

$$\begin{cases} K\mathbf{q} + C\dot{\mathbf{q}} + M\ddot{\mathbf{q}} = \mathbf{p}(t) \\ \mathbf{q}_0, \dot{\mathbf{q}}_0 \text{ given} \end{cases} \quad (7.1)$$

we can consider two approaches, namely modal superposition techniques and direct time-integration methods.

Modal expansion techniques have been presented in Sections 2.7.2–2.8.2 for the discrete case and in Section 4.2.1 for continuous systems. They are based on results from linear modal analysis, and consist in expressing the dynamic response in an eigenmode series expansion. The effectiveness of the modal superposition method is remarkable as long as fundamental modes predominate in the response.

In the opposite case, where the frequency spectrum requires the inclusion of a high number of modes so as to ensure good quasi-static and spectral convergence, modal expansion techniques should be replaced by direct integration methods since the latter make it possible to account for high frequency components in a straightforward manner. However, direct time integration of the equations of motion is not to be used as a black box. Indeed, the parameters of the method (time step and other free parameters) are to be adjusted correctly according to the accuracy and the stability required and in order to control numerical damping.

A major reason for the huge effort devoted to time integration methods over the years is that, contrarily to superposition methods, direct time-integration is not limited to the linear case but can easily be extended to nonlinear systems as described in Section 7.6. Direct integration becomes thus an essential tool in the context of nonlinear structural dynamics.

Direct integration is based upon finite time differences. It acts as numerical filtering on the solution and time-step selection is a critical issue of the method. Its value is not only dependent on the frequency spectrum of the excitation, but also on discretization in space, since it has to be consistent with wave propagation speed within the model (Courant's condition).

Direct integration formulas can be developed in different ways. Numerical analysts have concentrated their effort on the development of integration formulas applicable to systems of first-order differential equations in the general form

$$\dot{\mathbf{y}} = \mathbf{f}(\mathbf{y}, t) \quad (7.2)$$

An important class of general methods applicable to Equation (7.2) are the linear multistep methods. They are also applicable to the equations of structural dynamics in the form (7.1) provided that the latter are recast in first-order state-space form. Their principle and properties will be briefly described in Section 7.1. However, they suffer from two disadvantages: they do not take full advantage of the specific form of the system equations (7.1) to be solved, and depending on their order of accuracy they may require keeping the system solution on a relatively large number of time steps.

A major breakthrough in the field of structural dynamics has been the introduction by N. M. Newmark (Newmark 1959) of a *one-step integration formula directly applicable to second-order systems*. Newmark's method was immediately considered as a standard numerical tool in the community of structural dynamics. The powerfulness of it lies in the availability of two free parameters to adjust the numerical properties of the method. With appropriate choice of the free parameters, the method has the remarkable property of *unconditional stability*, which means that its stability is not affected by a change in time step size, the latter having then effect only on the accuracy of the solution. Much effort has been devoted to the analysis of the stability domain and accuracy properties of Newmark's method in the limited context of structural dynamics, and it led to important later developments in order to further increase its stability and accuracy. The standard Newmark algorithm is presented in Section 7.2, and its further developments based on equilibrium averaging are introduced in Section (7.3).

In its most common form, Newmark's method is *implicit* in the sense that the computation of displacements and velocities at a given time step implies the knowledge of accelerations at the same time. Keeping the implicit character of the method has the advantage that the method can be maintained unconditionally stable when applied to problems of structural dynamics. When the system remains linear, the implicit character of the method implies that an iteration matrix has to be constructed to compute the current solution. The iteration matrix is a linear combination of stiffness, mass and damping matrices that depends on time step size and parameters of the method. The system being linear, getting the solution simply results from the solution of a linear system in terms of the iteration matrix. When the system is nonlinear however, the situation becomes more complicated since getting the current solution implies iterating until equilibrium is achieved.

A specific choice of the parameters renders Newmark's method *explicit*, in which case it degenerates into the so-called *central-difference algorithm*. The method being explicit means that the current displacements can now be computed without a priori knowledge of accelerations at the current time step. New accelerations can thus be computed solving a linear system with the mass matrix \mathbf{M} as system matrix. And, most importantly, it does not require iteration on equilibrium to time integrate a system involving nonlinearities. The price to pay for this computational simplicity – exploited in practice in all the so-called explicit finite element codes – is that the central-difference is only conditionally stable, the step size limit for stability being easily determined from the Courant condition. The central-difference method is most appropriate for the solution of problems with response of high frequency content as generated by shocks, impacts or explosions. Its practical implementation is briefly described in Section 7.5.

A huge amount of literature has been produced on direct integration in structural dynamics. The list of references provided in this chapter is thus far from being exhaustive.

Definitions

The list below complements the general definitions given in the book introduction, but remains local to Chapter 7.

A	evolution matrix of first-order system.
J	Jordan canonical form of a matrix.
P	eigenmode matrix of amplification matrix T .
T	amplification matrix.
X	matrix of eigenmodes of undamped system.
Y	eigenmodes of evolution matrix A .
e	diagonal matrix of damping coefficients ε_r .
$p_{(r)}$	r -th eigenmode of amplification matrix T .
$q_{n+1}^*, \dot{q}_{n+1}^*$	predictors for displacements and velocities at t_{n+1} .
$u(t)$	state vector of first-order system.
u_n	state vector at time t_n .
I_i	i -th invariant of amplification matrix T .
h	time step size.
Λ	matrix of eigenvalues of amplification matrix T .
α	damping parameter (Newmark and HHT methods).
α_f, α_m	equilibrium averaging parameters.
α_j, β_j	coefficients of linear multistep formula.
β, γ	free parameters of Newmark's integration formula.
$\varepsilon, \bar{\varepsilon}$	exact and numerically computed critical damping ratios.
ε_r	critical damping ratio of mode r .
η, η_r	normal coordinate (of mode r).
λ	solution amplification factor.
λ_r	eigenvalues of amplification matrix T .
ν_r	eigenvalues of evolution matrix A .
$\omega_{cr}, \omega_{bif}$	critical and bifurcation frequencies of time integration formula.
$\omega, \bar{\omega}$	exact and numerical frequencies of undamped oscillator.
$\omega_d, \bar{\omega}_d$	exact and numerical damped frequencies.
ωh	frequency parameter (also noted ξ).
ρ_∞	asymptotic value of spectral radius.
$\rho(T)$	spectral radius of amplification matrix T .

7.1 Linear multistep integration methods

In a general way, direct *multistep integration methods* for first-order differential systems in the form (7.2) can be stated as:

$$y_{n+1} = \sum_{j=1}^m \alpha_j y_{n+1-j} - h \sum_{j=0}^m \beta_j \dot{y}_{n+1-j} \quad (7.3)$$

where $h = t_{n+1} - t_n$ is the time step and where y_{n+1} is the solution to (7.2) at time t_{n+1} calculated from the solutions at the m preceding times, from their derivatives and from the derivative of y_{n+1} itself.

For $\beta_0 \neq 0$, the integration scheme (7.3) is said to be *implicit*, since the solution at time t_{n+1} is a function of its own time derivative. Therefore, the integration relationships have to be recast before they can be solved. The solution method becomes iterative in the nonlinear case.

For $\beta_0 = 0$, y_{n+1} can be deduced directly from the results at the previous time steps: the method is then said to be *explicit*.

Furthermore, when α_j and β_j are zero for $j > 1$, relationship (7.3) corresponds to a *one-step method*, the system at time t_{n+1} being a function solely of its previous state at time t_n .

A quite general and rigorous description of multistep formulas can be found in the excellent book by Gear (Gear 1971). The following presentation is limited to an elementary presentation aiming at introducing some aspects of their use in structural dynamics.

7.1.1 Development of linear multistep integration formulas

One possible way to build linear multistep integration formulas is to perform an interpolation of the solution to the first-order differential equation (7.2) using Lagrange polynomials.

Let us interpolate the solution $y(t)$ to (7.2) at $m + 1$ equidistant points $0, h, 2h, \dots, mh$:

$$y_0, y_1, \dots, y_{m-1}, y_m \quad (7.4)$$

Lagrange interpolation polynomials can be built recursively as follows:

$$p_0(t) = y_0 \quad (7.5a)$$

$$p_1(t) = p_0(t) + c_1 t \quad (7.5b)$$

$$p_2(t) = p_1(t) + c_2 t(t - h) \quad (7.5c)$$

$$\vdots$$

$$p_m(t) = p_{m-1}(t) + c_m t(t - h) \dots (t - (m - 1)h) \quad (7.5d)$$

The correction added to polynomial $p_{r-1}(t)$ is such that $p_{r-1}(t)$ and $p_r(t)$ interpolate the same r points. The c_r coefficients are set so that:

$$p_r(rh) = y_r \quad r = 0, \dots, m \quad (7.6)$$

We thus obtain:

$$c_1 = \frac{1}{h}(p_1(h) - p_0(h)) = \frac{1}{h}(y_1 - y_0) \quad (7.7a)$$

$$c_2 = \frac{1}{2h^2}(p_2(2h) - p_1(2h)) = \frac{1}{2h^2}(y_2 - 2y_1 + y_0) \quad (7.7b)$$

$$\vdots$$

$$c_m = \frac{1}{m!h^m}(p_m(mh) - p_{m-1}(mh)) = \frac{1}{m!h^m}(y_m - p_{m-1}(mh)) \quad (7.7c)$$

Let us now consider the next approximation $p_{m+1}(t)$ to $y(t)$ and take its $(m + 1)$ -th derivative. We get the constant result over the time interval:

$$\frac{d^{m+1}}{dt^{m+1}} p_{m+1}(t) = p_{m+1}^{(m+1)}(t) = (m + 1)! c_{m+1}$$

It allows us to write $p_{m+1}(t)$ in the form:

$$\begin{aligned} p_{m+1}(t) &= p_m(t) + c_{m+1}t(t-h) \dots (t-mh) \\ &= p_m(t) + \frac{t(t-h) \dots (t-mh)}{(m+1)!} p_{m+1}^{(m+1)} \end{aligned}$$

Assuming that $p_{m+1}(t)$ corresponds to the solution $y(t)$ and that its $(m+1)$ -th derivative takes the same value as the $(m+1)$ -th derivative of $y(t)$ at some point of the interpolation interval, we can write intuitively a well known result from numerical analysis:

$$y(t) = p_m(t) + \frac{t(t-h) \dots (t-mh)}{(m+1)!} y^{(m+1)}(\tau) \text{ for some } \tau \in [0, mh] \quad (7.8)$$

7.1.2 One-step methods

The simplest formulas that can be derived from (7.8) are first-order one-step methods. To advance the solution from a time-step n to $n+1$ we make use of the general theory here above where t is replaced by \bar{t} , the time counted from t_n , and where y_0, y_1 are replaced by y_n, y_{n+1} respectively.

Let us develop according to Equations (7.5c) and (7.7a) the second-degree polynomial $p_2(t)$ computed from two successive time steps (c_2 being not explicitly given because it will not be needed):

$$p_2(\bar{t}) = y_n + (y_{n+1} - y_n) \frac{\bar{t}}{h} + c_2(\bar{t} - h)\bar{t} \quad (7.9)$$

(7.8) allows building the approximation to the solution on the time interval $[t_n, t_{n+2}]$:

$$y(\bar{t}) = p_2(\bar{t}) + \frac{\bar{t}(\bar{t}-h)(\bar{t}-2h)}{3!} y^{(3)}(\tau) \quad \tau \in [0, 2h] \quad (7.10)$$

and we can compute the approximation to its derivative:

$$\begin{aligned} \dot{y}(\bar{t}) &= \dot{p}_2(\bar{t}) + \frac{1}{3!} \frac{d}{d\bar{t}} (\bar{t}(\bar{t}-h)(\bar{t}-2h)) y^{(3)}(\tau) \\ &= \frac{y_{n+1} - y_n}{h} + c_2(2\bar{t} - h) + \frac{1}{3!} (3\bar{t}^2 - 6\bar{t}h + 2h^2) y^{(3)}(\tau) \end{aligned} \quad (7.11)$$

Equation (7.11) can be used in different ways.

- An *explicit one-step formula* can be obtained by computing $\dot{y}(t)$ at $t = t_n$ ($\bar{t} = 0$). The result is a first-order accurate approximation known as *Euler's backward formula*:

$$\begin{aligned} \dot{y}_n &= \frac{y_{n+1} - y_n}{h} - c_2h + \frac{2h^2}{3!} y^{(3)}(\tau) \\ &= \frac{y_{n+1} - y_n}{h} + O(h) \end{aligned} \quad (7.12)$$

It corresponds to the general scheme (7.3) with coefficients $\alpha_1 = 1$, $\beta_0 = 0$, $\beta_1 = -1$.

- A fully *implicit one-step formula* can be obtained by computing $\dot{y}(t)$ at $t = t_{n+1}$ ($\bar{t} = h$). The result is also a first-order accurate approximation known as *Euler's forward formula*:

$$\begin{aligned}\dot{y}_{n+1} &= \frac{y_{n+1} - y_n}{h} + c_2 h - \frac{h^2}{3!} y^{(3)}(\tau) \\ &= \frac{y_{n+1} - y_n}{h} + O(h)\end{aligned}\quad (7.13)$$

It corresponds to the general scheme (7.3) with coefficients $\alpha_1 = 0$, $\beta_0 = -1$, $\beta_1 = 0$.

- A second-order approximation can be obtained by taking the average of approximations (7.12) and (7.13), in which case the terms in c_2 cancel so that the result is a *second-order accurate implicit formula* known as the *trapezoidal rule*:

$$\begin{aligned}\frac{\dot{y}_n + \dot{y}_{n+1}}{2} &= \frac{y_{n+1} - y_n}{h} + \frac{h^2}{12} y^{(3)}(\tau) \\ &= \frac{y_{n+1} - y_n}{h} + O(h^2)\end{aligned}\quad (7.14)$$

It corresponds to the general scheme (7.3) with coefficients $\alpha_1 = 1$, $\beta_0 = \beta_1 = -\frac{1}{2}$.

7.1.3 Two-step second-order methods

The most widely used two-step method used in structural dynamics is the so-called *central-difference formula*, which applies to second-order differential equations of type:

$$\ddot{y} = f(y, t)$$

The central-difference formula can be obtained as follows.

Calling \bar{t} the time counted from t_{n-1} and taking for y_0, y_1, y_2 in the general theory the successive steps y_{n-1}, y_n, y_{n+1} , the second-degree polynomial $p_2(t)$ is obtained from Equations (7.5c) as:

$$p_2(\bar{t}) = y_{n-1} + c_1 \bar{t} + c_2 (\bar{t} - h) \bar{t} \quad (7.15)$$

where c_1 and c_2 are given by (7.7a) and (7.7b):

$$c_1 = \frac{1}{h}(y_n - y_{n-1}) \quad c_2 = \frac{1}{2h^2}(y_{n+1} - 2y_n + y_{n-1}) \quad (7.16)$$

Again (7.8) allows building the approximate solution:

$$y(\bar{t}) = p_2(\bar{t}) + \frac{\bar{t}(\bar{t} - h)(\bar{t} - 2h)}{3!} y^{(3)}(\tau) \quad \tau \in [0, 2h] \quad (7.17)$$

and the integration scheme is then found through double differentiation of (7.17):

$$\dot{y}(\bar{t}) = c_1 + c_2(2\bar{t} - h) + \frac{1}{3!}(3\bar{t}^2 - 6\bar{t}h + 2h^2)y^{(3)}(\tau) \quad (7.18)$$

$$\begin{aligned}\ddot{y}(\bar{t}) &= 2c_2 + (\bar{t} - h)y^{(3)}(\tau) \\ &= \frac{y_{n+1} - 2y_n + y_{n-1}}{h^2} + (\bar{t} - h)y^{(3)}(\tau) \quad \bar{t} \in [0, 2h]\end{aligned}\quad (7.19)$$

When computing (7.19) at the middle of the interval the first-order approximation of the local error cancels, so that we get the well known *central-difference formula* providing a *second-order accurate explicit* approximation for accelerations:

$$\ddot{y}_n = \frac{y_{n+1} - 2y_n + y_{n-1}}{h^2} + O(h^2) \quad (7.20)$$

Equation (7.20) is the time integration formula implemented in all *finite element explicit codes*. Section 7.5 will be devoted to its effective implementation.

7.1.4 Several-step methods

Different formulas with two steps and more have been proposed in the past in the context of structural dynamics. They are seldom implemented and used in general purpose finite element codes, with the exception of the central difference formula (7.20) which has the remarkable property of being second-order accurate despite its explicit character.

The reader interested in a more detailed description and discussion of multi-step methods in the context of structural dynamics will find it in (Gérardin 1974) and (Hughes 1983).

Let us simply mention for historical reasons the pioneering work from (Houbolt 1950) in the context of research on aeroelasticity. The three-step implicit method that he proposed was at the time a significant step forward in the development of numerical methods for solving transient problems in structural dynamics. The development and analysis of Houbolt's algorithm will be left as an exercise (Problem 7.2).

Worthwhile mentioning also is Park's method (Park 1975), a second-order accurate three-step algorithm which retains good accuracy in the low frequencies while providing strong dissipative characteristics in the high frequencies.

7.1.5 Numerical observation of stability and accuracy properties of simple time integration formulas

To get a good understanding of accuracy and stability concepts linked to direct time-integration, let us consider the undamped one-degree-of-freedom oscillator submitted to an initial displacement:

$$\begin{cases} \ddot{\eta} + \omega^2 \eta = 0 \\ \eta(0) = 1, \dot{\eta}(0) = 0 \end{cases} \quad \text{with } \omega = \pi \text{ rad/s} \quad (7.21)$$

Its exact solution is $\eta(t) = \cos \omega t$.

Let us put Equation (7.21) for the single-degree-of-freedom oscillator in the form of a first-order system in the state space $\mathbf{u}^T = [\dot{\eta} \quad \eta]$:

$$\dot{\mathbf{u}} = \mathbf{A}\mathbf{u} \quad (7.22)$$

with the initial condition:

$$\mathbf{u}^T(0) = [0 \quad 1] \quad (7.23)$$

The evolution matrix A of the system can be expressed by:

$$A = \begin{bmatrix} 0 & -\omega^2 \\ 1 & 0 \end{bmatrix} \quad (7.24)$$

Let us apply to (7.22) the three one-step integration formulas developed before:

(i) *Euler forward formula* (explicit, Equation (7.12)):

$$\mathbf{u}_{n+1} = \mathbf{u}_n + h\dot{\mathbf{u}}_n \quad (7.25)$$

(ii) *Euler backward formula* (implicit, Equation (7.13)):

$$\mathbf{u}_{n+1} = \mathbf{u}_n + h\dot{\mathbf{u}}_{n+1} \quad (7.26)$$

(iii) *Trapezoidal rule* (implicit, Equation (7.14)):

$$\mathbf{u}_{n+1} = \mathbf{u}_n + \frac{h}{2} (\dot{\mathbf{u}}_n + \dot{\mathbf{u}}_{n+1}) \quad (7.27)$$

A qualitative interpretation of the type of time evolution induced by all three integration schemes is sketched on Figure 7.1. Euler's forward scheme (Figure 7.1.c) overestimates accelerations and velocities, and thus displacements, while the contrary effect happens with Euler's backwards scheme (Figure 7.1.b). Thanks to averaging, the trapezoidal rule (Figure 7.1.a) produces correct estimates of accelerations and velocities, and therefore the computed displacements tend to follow the exact curve.

By substituting the integration relations in the canonical state-space equation of motion (7.22), we find a linear system of equations which is solved for \mathbf{u}_{n+1} at time t_{n+1} .

The numerical solutions, computed for a time interval $T = 3$, using a time step $h = T/32$, are plotted on Figure 7.2 together with the exact solution.

These curves illustrate the following phenomena:

- Euler's forward scheme induces a noticeable period increase and the amplitude of the response is increasing with time, which can be interpreted as negative numerical damping. It lacks thus accuracy as predicted (only first-order accurate) and, what's more, it is unstable.
- Euler's backward integration method leads to the same period increase as the forward formula, but the response amplitude is now decreasing with time, which can be interpreted as positive numerical damping. The response is thus numerically stable, but still characterised by low accuracy.
- The numerical solution computed by the trapezoidal rule is the most accurate one in the sense that there is no error on the amplitude of the response, whereas the motion period is lightly overestimated.

7.1.6 Stability analysis of multistep methods

The stability behaviour of multistep integration methods when applied to a system of linear differential equations in the form (7.22) is established by analyzing their characteristic equation as follows (Gérardin 1974).

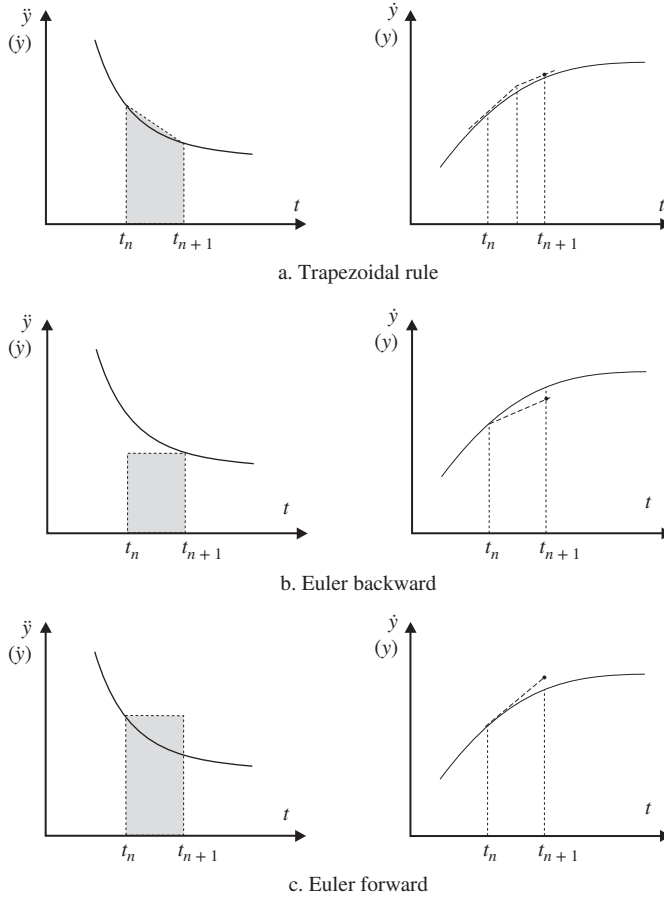


Figure 7.1 Basic time-integration formulas.

Going back to the general multistep scheme (7.3), let us apply it to the homogeneous form (7.22):

$$\sum_{j=0}^m [\alpha_j I - h\beta_j A] u_{n+1-j} = 0 \quad (7.28)$$

with $\alpha_0 = -1$.

Let us call ν_r the eigenvalues of A , and Y the matrix of the associated eigenvectors. The characteristic equation corresponding to (7.28) is found by taking as general solution the expression:

$$u_n = \lambda^n Y a \quad (7.29)$$

where λ is a complex number called the solution *amplification factor*. Let us substitute (7.29) into (7.28):

$$\lambda^{n-m+1} \sum_{j=0}^m [\alpha_j I - h\beta_j A] \lambda^{m-j} Y a = 0$$

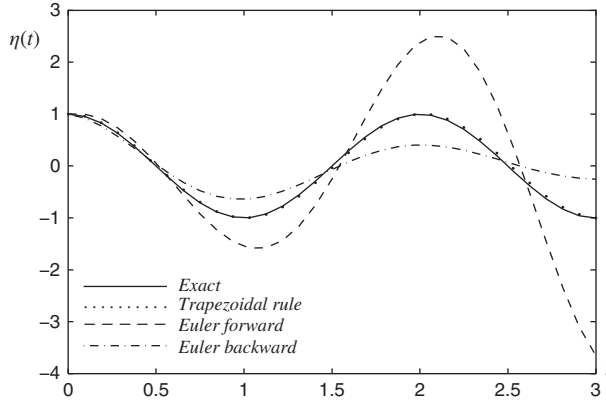


Figure 7.2 Exact and numerical solutions of the one-degree-of-freedom undamped oscillator.

Making use of the relation $\mathbf{Y}^{-1}\mathbf{A}\mathbf{Y} = \text{diag}(\nu_r)$ and discarding the trivial solution $\lambda = 0$ yields:

$$\sum_{j=0}^m [\alpha_j - h\beta_j \text{diag}(\nu_r)] \lambda^{m-j} \mathbf{a} = \mathbf{0}$$

whence, this relation holding for any coordinates \mathbf{a} ,

$$\sum_{j=0}^m [\alpha_j - h\beta_j \nu_r] \lambda^{m-j} = 0 \quad r = 1, 2 \quad (7.30)$$

This is the characteristic equation for the amplification factor λ .

The general form (7.29) of the solution shows that the numerical response obtained by the integration formula (7.21) remains bounded if $|\lambda^k| < 1$, $k = 1, \dots, m$. In the particular case $|\lambda| = 1$, the solution amplitude is neither divergent nor damped. Hence, the stability limit is a circle of unit radius ($\lambda = e^{i\theta}$, $0 \leq \theta \leq 2\pi$). In the complex plane of νh , the stability limit is given by the relationship:

$$\nu h = \frac{\sum_{j=0}^m \alpha_j e^{i(m-j)\theta}}{\sum_{j=0}^m \beta_j e^{i(m-j)\theta}} \quad (7.31)$$

Let us now study the stability of the basic one-step formulas ($m = 1$) which have been applied to the one-degree-of-freedom oscillator:

- (i) Euler forward (explicit): substituting $\alpha_1 = 1$, $\beta_0 = 0$, $\beta_1 = -1$ into (7.31) and reminding that by definition $\alpha_0 = -1$, one finds:

$$\nu h = e^{i\theta} - 1$$

The stability boundary is a circle of unit radius and of centre $\nu h = -1$. The solution is unstable in the entire νh space except inside the circle (Figure 7.3).

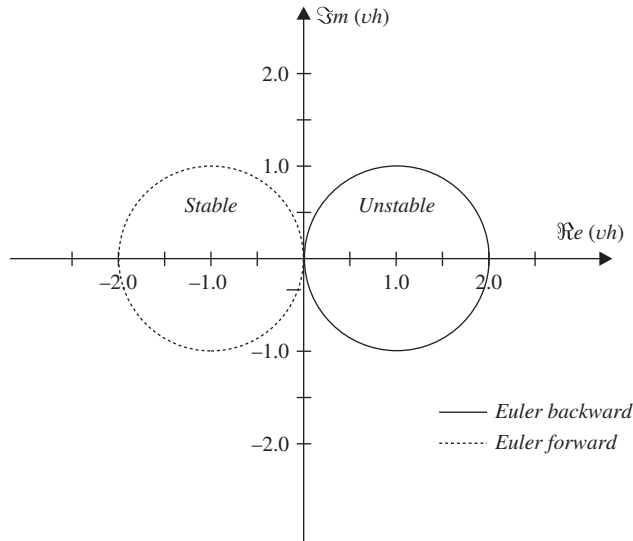


Figure 7.3 Stability limits for Euler implicit and explicit methods.

- (ii) Euler backward (implicit): with the set of values $\alpha_1 = 1$, $\beta_0 = -1$, $\beta_1 = 0$ we get:

$$vh = 1 - e^{-i\theta}$$

The stability boundary is a circle of unit radius centred at $vh = 1$. The solution is stable everywhere except inside the circle (Figure 7.3).

- (iii) Trapezoidal rule (implicit): the set of values $\alpha_1 = 1$, $\beta_0 = -\frac{1}{2}$, $\beta_1 = -\frac{1}{2}$ yields:

$$vh = \frac{2i \sin \frac{\theta}{2}}{\cos \frac{\theta}{2}}$$

The stability boundary is the imaginary axis and the numerical solution is stable in the entire left-hand plane.

Note that for the single-degree-of-freedom oscillator, the eigenvalues are $v = \pm i\omega_0$. The roots vh are thus located in the stable region of the Euler backward formula, in the unstable region of the Euler forward formula, and on the stability boundary of the trapezoidal rule. This explains why the amplitude of the trapezoidal rule solution is preserved, and why one observes a decay for the Euler backward scheme and an amplification for the forward scheme.

Most of the implicit methods that are commonly used (trapezoidal rule, Newmark, etc.) are stable for the entire left-hand complex plane. This property is referred to as *A-stability* by mathematicians (Gear 1971) and as unconditional stability in structural mechanics. On the other hand, all the existing explicit formulas are stable only inside a subdomain of the left-hand plane.

From a computational point of view, the price paid for the unconditional stability of implicit schemes is the necessity to solve simultaneous systems of equations at each time step, whereas

the limited stability of explicit formulas is compensated by their computational simplicity, since they involve only vector calculations when associated with diagonal mass matrices.

Stability of integration methods will be discussed again in more depth and in a different way for Newmark's method, using the concept of *amplification matrix*.

7.2 One-step formulas for second-order systems: Newmark's family

7.2.1 The Newmark method

In 1959 N.M. Newmark (Newmark 1959) proposed a single-step integration formula directly applicable to the time integration of the second-order differential equations of structural dynamics in the form (7.1). The method, which turned out to be a major step in the field and underwent significant further developments, can be stated as follows.

The state vector of the system at a time $t_{n+1} = t_n + h$ is deduced from the already known state vector at time t_n , through a Taylor series expansion of the displacements and velocities:

$$f(t_n + h) = f(t_n) + hf'(t_n) + \frac{h^2}{2}f''(t_n) + \dots + \frac{h^s}{s!}f^{(s)}(t_n) + R_s \quad (7.32)$$

where R_s is the remainder of the development to the order s :

$$R_s = \frac{1}{s!} \int_{t_n}^{t_n+h} f^{(s+1)}(\tau) [t_n + h - \tau]^s d\tau \quad (7.33)$$

Relation (7.32) allows us to compute the velocities and displacements of a system at time t_{n+1} :

$$\begin{aligned} \dot{q}_{n+1} &= \dot{q}_n + \int_{t_n}^{t_{n+1}} \ddot{q}(\tau) d\tau \\ q_{n+1} &= q_n + h\dot{q}_n + \int_{t_n}^{t_{n+1}} (t_{n+1} - \tau) \ddot{q}(\tau) d\tau \end{aligned} \quad (7.34)$$

The approximation then consists of evaluating in (7.33) the integral terms of the acceleration by numerical quadrature. Therefore, let us express $\ddot{q}(\tau)$ in the time interval $[t_n, t_{n+1}]$ as a function of \ddot{q}_n and \ddot{q}_{n+1} at the interval limits:

$$\begin{aligned} \ddot{q}_n &= \ddot{q}(\tau) + q^{(3)}(\tau) (t_n - \tau) + q^{(4)}(\tau) \frac{(t_n - \tau)^2}{2} + \dots \\ \ddot{q}_{n+1} &= \ddot{q}(\tau) + q^{(3)}(\tau) (t_{n+1} - \tau) + q^{(4)}(\tau) \frac{(t_{n+1} - \tau)^2}{2} + \dots \end{aligned} \quad (7.35)$$

By multiplying Equations (7.35) by $(1 - \gamma)$ and by γ , we obtain:

$$\ddot{q}(\tau) = (1 - \gamma)\ddot{q}_n + \gamma\ddot{q}_{n+1} + q^{(3)}(\tau) [\tau - h\gamma - t_n] + O(h^2 q^{(4)}) \quad (7.36)$$

Likewise, multiplying (7.35) by $(1 - 2\beta)$ and by 2β yields:

$$\ddot{q}(\tau) = (1 - 2\beta)\ddot{q}_n + 2\beta\ddot{q}_{n+1} + q^{(3)}(\tau) [\tau - 2h\beta - t_n] + O(h^2 q^{(4)}) \quad (7.37)$$

Hence, by substituting (7.36) and (7.37) in the integral terms of (7.34), we obtain the quadrature formulas:

$$\begin{aligned} \int_{t_n}^{t_{n+1}} \ddot{\mathbf{q}}(\tau) d\tau &= (1 - \gamma)h\dot{\mathbf{q}}_n + \gamma h\dot{\mathbf{q}}_{n+1} + \mathbf{r}_n \\ \int_{t_n}^{t_{n+1}} (t_{n+1} - \tau) \ddot{\mathbf{q}}(\tau) d\tau &= \left(\frac{1}{2} - \beta\right) h^2 \ddot{\mathbf{q}}_n + \beta h^2 \ddot{\mathbf{q}}_{n+1} + \mathbf{r}'_n \end{aligned} \quad (7.38)$$

and the corresponding error measures:

$$\begin{aligned} \mathbf{r}_n &= \left(\gamma - \frac{1}{2}\right) h^2 \mathbf{q}^{(3)}(\tilde{\tau}) + O(h^3 \mathbf{q}^{(4)}) \\ \mathbf{r}'_n &= \left(\beta - \frac{1}{6}\right) h^3 \mathbf{q}^{(3)}(\tilde{\tau}) + O(h^4 \mathbf{q}^{(4)}) \end{aligned} \quad t_n < \tilde{\tau} < t_{n+1} \quad (7.39)$$

The constants γ and β are parameters associated with the quadrature scheme. Choosing

$$\gamma = \frac{1}{2} \quad \beta = \frac{1}{6}$$

leads to *linear interpolation of accelerations* $\ddot{\mathbf{q}}(\tau) = \ddot{\mathbf{q}}_n + (\tau - t_n) \frac{\ddot{\mathbf{q}}_{n+1} - \ddot{\mathbf{q}}_n}{h}$ in the time interval $[t_n, t_{n+1}]$. In the same way,

$$\gamma = \frac{1}{2} \quad \beta = \frac{1}{4}$$

corresponds to considering the *acceleration* average value $\ddot{\mathbf{q}}(\tau) = \frac{\ddot{\mathbf{q}}_n + \ddot{\mathbf{q}}_{n+1}}{2}$ over the time interval.

By substituting relationship (7.38) in (7.34), we get the following approximation formulas for the Newmark method:

$$\begin{aligned} \dot{\mathbf{q}}_{n+1} &= \dot{\mathbf{q}}_n + (1 - \gamma)h\ddot{\mathbf{q}}_n + \gamma h\ddot{\mathbf{q}}_{n+1} \\ \mathbf{q}_{n+1} &= \mathbf{q}_n + h\dot{\mathbf{q}}_n + h^2 \left(\frac{1}{2} - \beta\right) \ddot{\mathbf{q}}_n + h^2 \beta \ddot{\mathbf{q}}_{n+1} \end{aligned} \quad (7.40)$$

Let us then assume that the equations of dynamics (7.1) are linear, i.e. that matrices \mathbf{M} , \mathbf{C} and \mathbf{K} are independent of \mathbf{q} , and let us introduce the numerical scheme (7.40) in the equations of motion at time t_{n+1} so as to compute the acceleration $\ddot{\mathbf{q}}_{n+1}$:

$$\begin{aligned} [\mathbf{M} + \gamma h \mathbf{C} + \beta h^2 \mathbf{K}] \ddot{\mathbf{q}}_{n+1} &= \mathbf{p}_{n+1} - \mathbf{C} [\dot{\mathbf{q}}_n + (1 - \gamma)h\ddot{\mathbf{q}}_n] \\ &\quad - \mathbf{K} \left[\mathbf{q}_n + h\dot{\mathbf{q}}_n + \left(\frac{1}{2} - \beta\right) h^2 \ddot{\mathbf{q}}_n \right] \end{aligned} \quad (7.41)$$

The linear system of equations (7.41) is associated with the iteration matrix:

$$[\mathbf{M} + \gamma h \mathbf{C} + \beta h^2 \mathbf{K}]$$

which is symmetric and positive definite owing to the properties of \mathbf{M} , \mathbf{C} and \mathbf{K} . Proceeding with a constant time step, the matrix can be factorized once for all. We then calculate the velocities and displacements $\dot{\mathbf{q}}_{n+1}$ and \mathbf{q}_{n+1} according to (7.40).

The Newmark method for implicit time-integration of the structural dynamics equations (7.1) is summarized by a flowchart in Figure 7.4.

For efficiency the algorithm is organized in such a way that the predictors:

$$\begin{aligned}\dot{q}_{n+1}^* &= \dot{q}_n + (1 - \gamma)h\ddot{q}_n \\ q_{n+1}^* &= q_n + h\dot{q}_n + h^2 \left(\frac{1}{2} - \beta \right) \ddot{q}_n\end{aligned}\quad (7.42)$$

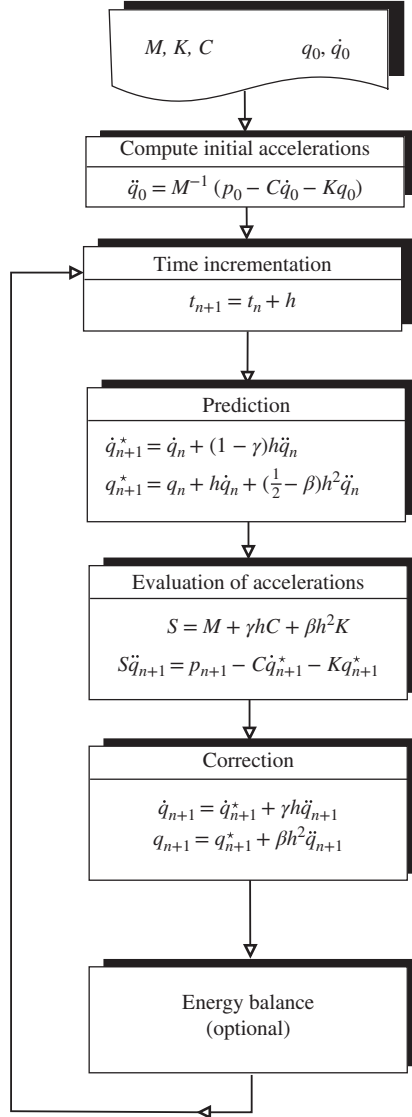


Figure 7.4 Flowchart of the Newmark integration scheme for linear systems.

needed for the updates (7.40) and for the right hand side of (7.41) are computed only once. They represent the solution at time t_{n+1} obtained as an extrapolation of the solution at time t_n when \ddot{q}_{n+1} is set to zero.

Remark 7.1 *Violating the condition of dynamic equilibrium would generate in the first phase of the response oscillations which are not representative of true system behaviour. Initial accelerations have thus to be computed from the initial conditions in the form:*

$$\ddot{q}_0 = M^{-1} (p_0 - Kq_0 - C\dot{q}_0) \quad (7.43)$$

Remark 7.2 *The accuracy of the numerical response can be estimated by evaluating the variation of the energies (Hughes 1987), as suggested in the flowchart of Figure 7.4 and explained in Section 7.4.1.*

7.2.2 Consistency of Newmark's method

The space vector $u_n^T = [\dot{q}_n^T \ q_n^T]$ completely describes the state of a system at time t_n . Indeed, the corresponding accelerations can be deduced by making use of the dynamic equilibrium Equations (7.1). The consistency of the integration method given by (7.40) is based on the comparison of vector u_n at two successive instants.

An integration scheme is said to be *consistent* if:

$$\lim_{h \rightarrow 0} \frac{u_{n+1} - u_n}{h} = \dot{u}(t_n) \quad (7.44)$$

This condition is fulfilled by the Newmark integration operator, since relation (7.40), together with (7.36), yields:

$$\begin{aligned} \lim_{h \rightarrow 0} \frac{u_{n+1} - u_n}{h} &= \lim_{h \rightarrow 0} \begin{bmatrix} (1 - \gamma)\ddot{q}_n + \gamma\ddot{q}_{n+1} \\ \dot{q}_n + \left(\frac{1}{2} - \beta\right)h\ddot{q}_n + \beta h\ddot{q}_{n+1} \end{bmatrix} \\ &= \lim_{\substack{h \rightarrow 0 \\ \tau \rightarrow t_n}} \begin{bmatrix} \ddot{q}(\tau) - q^{(3)}(\tau) [\tau - h\gamma - t_n] + O(h^2 q^{(4)}) \\ \dot{q}_n + \left(\frac{1}{2} - \beta\right)h\ddot{q}_n + \beta h\ddot{q}_{n+1} \end{bmatrix} = \begin{bmatrix} \ddot{q}_n \\ \dot{q}_n \end{bmatrix} \end{aligned}$$

The consistency condition is a necessary condition for convergence, i.e. for ensuring the convergence of the numerical solution towards the exact solution as the time step h tends to zero.

7.2.3 First-order form of Newmark's operator – amplification matrix

The Newmark operator given by relationships (7.40) can easily be recasted in first-order matrix form. To this purpose, let us write down the equations of motion at times t_n and t_{n+1} :

$$\begin{aligned} M\ddot{q}_n &= -C\dot{q}_n - Kq_n + p_n \\ M\ddot{q}_{n+1} &= -C\dot{q}_{n+1} - Kq_{n+1} + p_{n+1} \end{aligned} \quad (7.45)$$

By premultiplying relations (7.40) by \mathbf{M} and taking account of (7.45), we get the recurrence relationships:

$$\begin{aligned}\mathbf{M}\dot{\mathbf{q}}_{n+1} &= \mathbf{M}\dot{\mathbf{q}}_n + h(1 - \gamma) [-\mathbf{C}\dot{\mathbf{q}}_n - \mathbf{K}\mathbf{q}_n + \mathbf{p}_n] \\ &\quad + \gamma h [-\mathbf{C}\dot{\mathbf{q}}_{n+1} - \mathbf{K}\mathbf{q}_{n+1} + \mathbf{p}_{n+1}] \\ \mathbf{M}\mathbf{q}_{n+1} &= \mathbf{M}\mathbf{q}_n + h\mathbf{M}\dot{\mathbf{q}}_n + \left(\frac{1}{2} - \beta\right) h^2 [-\mathbf{C}\dot{\mathbf{q}}_n - \mathbf{K}\mathbf{q}_n + \mathbf{p}_n] \\ &\quad + \beta h^2 [-\mathbf{C}\dot{\mathbf{q}}_{n+1} - \mathbf{K}\mathbf{q}_{n+1} + \mathbf{p}_{n+1}]\end{aligned}\quad (7.46)$$

In order to get better understanding of the interaction between the time integration operator and the spectral content of the dynamic system (7.1), let us make the hypothesis of diagonal damping and expand the successive solutions in terms of eigenmodes of the undamped system

$$\mathbf{q}_n = \mathbf{X}\boldsymbol{\eta}_n$$

where $\boldsymbol{\eta}_n$ stands for the vector of normal coordinates $\eta_s(t)$ at time t_n . After premultiplication by \mathbf{X}^T Equations (7.46) become:

$$\begin{aligned}(\mathbf{I} + 2\gamma h\mathbf{e}\boldsymbol{\Omega})\dot{\boldsymbol{\eta}}_{n+1} + \gamma h\boldsymbol{\Omega}^2\boldsymbol{\eta}_{n+1} &= [\mathbf{I} - 2(1 - \gamma)h\mathbf{e}\boldsymbol{\Omega}]\dot{\boldsymbol{\eta}}_n - (1 - \gamma)h\boldsymbol{\Omega}^2\boldsymbol{\eta}_n \\ &\quad + (1 - \gamma)h\boldsymbol{\phi}_n + \gamma h\boldsymbol{\phi}_{n+1} \\ 2\beta h^2\mathbf{e}\boldsymbol{\Omega}\dot{\boldsymbol{\eta}}_{n+1} + (\mathbf{I} + \beta h^2\boldsymbol{\Omega}^2)\boldsymbol{\eta}_{n+1} &= \left[h\mathbf{I} - 2\left(\frac{1}{2} - \beta\right)h^2\mathbf{e}\boldsymbol{\Omega}\right]\dot{\boldsymbol{\eta}}_n \\ &\quad + \left[\mathbf{I} - \left(\frac{1}{2} - \beta\right)h^2\boldsymbol{\Omega}^2\right]\boldsymbol{\eta}_n \\ &\quad + \left(\frac{1}{2} - \beta\right)h^2\boldsymbol{\phi}_n + \beta h^2\boldsymbol{\phi}_{n+1}\end{aligned}\quad (7.47)$$

with the following definitions:

$$\boldsymbol{\Omega} = \text{diag}(\omega_i) \quad \boldsymbol{\mu} = \text{diag}(\mu_i) \quad \mathbf{e} = \text{diag}(\varepsilon_i) \quad \boldsymbol{\phi} = \boldsymbol{\mu}^{-1}\mathbf{X}^T\mathbf{p}$$

They can be put in the form of a first-order recurrence relationship:

$$\mathbf{u}_{n+1} = \mathbf{T}(h)\mathbf{u}_n + \mathbf{b}_{n+1}(h) \quad (7.48)$$

where

$$\mathbf{T}(h) = \mathbf{H}_1^{-1}\mathbf{H}_0 \quad \mathbf{u}_n = \begin{bmatrix} \dot{\boldsymbol{\eta}}_n \\ \boldsymbol{\eta}_n \end{bmatrix} \quad (7.49)$$

$$\mathbf{H}_1 = \begin{bmatrix} \mathbf{I} + 2\gamma h\mathbf{e}\boldsymbol{\Omega} & \gamma h\boldsymbol{\Omega}^2 \\ 2\beta h^2\mathbf{e}\boldsymbol{\Omega} & \mathbf{I} + \beta h^2\boldsymbol{\Omega}^2 \end{bmatrix} \quad (7.50)$$

$$\mathbf{H}_0 = \begin{bmatrix} \mathbf{I} - 2(1 - \gamma)h\mathbf{e}\boldsymbol{\Omega} & -(1 - \gamma)h\boldsymbol{\Omega}^2 \\ h\mathbf{I} - (1 - 2\beta)h^2\mathbf{e}\boldsymbol{\Omega} & \mathbf{I} - \left(\frac{1}{2} - \beta\right)h^2\boldsymbol{\Omega}^2 \end{bmatrix} \quad (7.51)$$

$$\mathbf{b}_{n+1} = \mathbf{H}_1^{-1} \begin{bmatrix} (1 - \gamma)h\boldsymbol{\phi}_n + \gamma h\boldsymbol{\phi}_{n+1} \\ \left(\frac{1}{2} - \beta\right)h^2\boldsymbol{\phi}_n + \beta h^2\boldsymbol{\phi}_{n+1} \end{bmatrix} \quad (7.52)$$

Matrix $\mathbf{T}(h)$ of dimension $2N \times 2N$, where N is the number of degrees of freedom, is called the *amplification matrix* associated with the integration operator, expressed here in terms of the normal coordinates. Therefore it is made of diagonal blocks of dimension N .

It plays a fundamental role in the stability analysis of the algorithm. Its behaviour can be characterized by considering the 2×2 block of the amplification matrix acting on one single normal coordinate η_s . Its expression can be developed from (7.49):

$$\mathbf{T} = \begin{bmatrix} t_{11} & t_{12} \\ t_{21} & t_{22} \end{bmatrix} \quad (7.53)$$

with the coefficients:

$$\begin{aligned} D &= \det(\mathbf{H}_1) = 1 + 2\varepsilon\gamma\omega h + \beta\omega^2 h^2 \\ t_{11} &= \frac{1}{D} \left[1 + 2(\gamma - 1)\varepsilon\omega h + (\beta - \gamma)\omega^2 h^2 + (\gamma - 2\beta)\varepsilon\omega^3 h^3 \right] \\ t_{22} &= \frac{1}{D} \left[1 + 2\gamma\varepsilon\omega h + \left(\beta - \frac{1}{2} \right) \omega^2 h^2 + (2\beta - \gamma)\varepsilon^2\omega^3 h^3 \right] \\ t_{12} &= \frac{1}{D} \left[-\omega^2 h + \left(\frac{\gamma}{2} - \beta \right) \omega^4 h^3 \right] \\ t_{21} &= \frac{1}{D} \left[h + (2\gamma - 1)\varepsilon\omega h^2 + 2(2\beta - \gamma)\varepsilon^2\omega^2 h^3 \right] \end{aligned} \quad (7.54)$$

For the purpose of stability analysis we will also need in the future the expression of the invariants:

$$I_1 = \frac{1}{2} \text{tr}(\mathbf{T}) = 1 - \frac{1}{D} \left[\varepsilon\omega h + \frac{1}{2} \left(\frac{1}{2} + \gamma \right) \omega^2 h^2 \right] \quad (7.55a)$$

$$I_2 = \det(\mathbf{T}) = 1 - \frac{1}{D} \left[2\varepsilon\omega h + \left(\gamma - \frac{1}{2} \right) \omega^2 h^2 \right] \quad (7.55b)$$

and make use of its norm and spectral radius as defined in the next paragraph.

7.2.4 Matrix norm and spectral radius

Determining the stability domain of an integration method from the analysis of its amplification matrix is based on the concepts of matrix norm and spectral properties. Therefore these concepts are recalled before proceeding to the stability analysis.

The norm to an arbitrary $(n \times n)$ matrix \mathbf{A} is defined as:

$$\|\mathbf{A}\| = \max_x \frac{\|\mathbf{A}\mathbf{x}\|}{\|\mathbf{x}\|} \quad (7.56)$$

and appears thus to be dependent on the vector norm adopted. When using the quadratic vector norm (or vector 2-norm) $\|\mathbf{x}\| = (\mathbf{x}^T \mathbf{x})^{\frac{1}{2}}$, the matrix norm (7.56) becomes:

$$\|\mathbf{A}\| = \max_x \frac{(\mathbf{x}^T \mathbf{A}^T \mathbf{A} \mathbf{x})^{\frac{1}{2}}}{(\mathbf{x}^T \mathbf{x})^{\frac{1}{2}}} \quad (7.57)$$

The matrix 2-norm (7.57) is often referred to as the *matrix spectral norm*. It is nothing else than the Rayleigh quotient associated to the symmetric, positive semi-definite matrix $\mathbf{A}^T \mathbf{A}$. It is thus such that:

$$\|\mathbf{A}\| \leq \sigma_1^2 \quad (7.58)$$

σ_1^2 being the largest eigenvalue of matrix $\mathbf{A}^T \mathbf{A}$. As direct consequence of Equation (7.56), the following inequality holds:

$$\|\mathbf{A}\mathbf{x}\| \leq \|\mathbf{A}\| \|\mathbf{x}\| \quad (7.59)$$

Let us next consider the associated eigenvalue problem $\mathbf{A}\mathbf{x} = \lambda\mathbf{x}$. Computing its vector norm yields:

$$\|\mathbf{A}\mathbf{x}\| = |\lambda| \|\mathbf{x}\| \leq \|\mathbf{A}\| \|\mathbf{x}\|$$

and thus, all eigenvalues of \mathbf{A} matrix verify the inequality:

$$|\lambda_i| \leq \|\mathbf{A}\| \quad (7.60)$$

The matrix norm of a matrix product $\mathbf{A}\mathbf{B}$ can be computed as:

$$\|\mathbf{A}\mathbf{B}\| = \max_x \frac{\|\mathbf{A}\mathbf{B}\mathbf{x}\|}{\|\mathbf{x}\|} \leq \|\mathbf{A}\| \max_x \frac{\|\mathbf{B}\mathbf{x}\|}{\|\mathbf{x}\|} \quad (7.61)$$

and thus

$$\|\mathbf{A}\mathbf{B}\| \leq \|\mathbf{A}\| \|\mathbf{B}\| \quad (7.62)$$

Finally, it is convenient to define the *spectral radius* of matrix \mathbf{A} as:

$$\rho(\mathbf{A}) = \max_i |\lambda_i| \quad (7.63)$$

According to (7.60) the following inequality holds:

$$\rho(\mathbf{A}) \leq \|\mathbf{A}\| \quad (7.64)$$

7.2.5 Stability of an integration method – spectral stability

An integration scheme:

$$\mathbf{u}_{n+1} = \mathbf{T}\mathbf{u}_n + \mathbf{b}_{n+1}$$

is said to be stable (Gérardin 1974) if there exists an integration step $h_0 > 0$ so that for any $h \in [0, h_0]$, a finite variation of the state vector at time t_n induces only a nonincreasing variation of the state vector \mathbf{u}_{n+j} calculated at a subsequent instant t_{n+j} .

Let us consider an initial disturbance:

$$\delta \mathbf{u}_0 = \mathbf{u}'_0 - \mathbf{u}_0$$

The nonperturbed solution is successively given by:

$$\mathbf{u}_{n+1} = \mathbf{T}\mathbf{u}_n + \mathbf{b}_{n+1}$$

$$\begin{aligned}
&= T^2 \mathbf{u}_{n-1} + T \mathbf{b}_n + \mathbf{b}_{n+1} \\
&\vdots \\
&= T^{n+1} \mathbf{u}_0 + \sum_{j=0}^{n+1} T^{n-j+1} \mathbf{b}_j
\end{aligned}$$

On the other hand, the perturbed solution verifies:

$$\mathbf{u}'_{n+1} = T^{n+1} \mathbf{u}'_0 + \sum_{j=0}^{n+1} T^{n-j+1} \mathbf{b}_j$$

whence, by subtracting the relations above, the effect of the initial disturbance at the instant t_{n+1} is:

$$\delta \mathbf{u}_{n+1} = T^{n+1} \delta \mathbf{u}_0 \quad (7.65)$$

Its amplitude growth is thus governed by the following inequality:

$$\|\delta \mathbf{u}_n\| \leq \|T^n\| \|\mathbf{u}_0\| \quad (7.66)$$

and remains thus limited provided that:

$$\|T^n\| \leq c \quad \forall n \quad (7.67)$$

It can be shown that Inequality (7.67) is satisfied if:

- (i) $\rho(T) \leq 1$.
- (ii) *Eigenvalues of T with multiplicity $r > 1$ are strictly less than 1 in modulus.*

In which case, matrix T is said to be *spectrally stable* (Hughes 1983). The proof holds by considering two cases.

Case 1: T has linearly independent eigenvectors. Let us collect into (\mathbf{A}, \mathbf{P}) the eigensolutions of:

$$T\mathbf{p} = \lambda\mathbf{p}$$

allowing it to be written as

$$T\mathbf{P} = \mathbf{P}\mathbf{A} \quad \rightarrow \quad T^n = \mathbf{P}\mathbf{A}^n\mathbf{P}^{-1} \quad (7.68)$$

Taking the norm of (7.68) results in:

$$\|T^n\| = \|\mathbf{P}\mathbf{A}^n\mathbf{P}^{-1}\| \leq \|\mathbf{P}\| \|\mathbf{A}^n\| \|\mathbf{P}^{-1}\| = \|\mathbf{A}^n\| \quad (7.69)$$

\mathbf{A}^n being of the form:

$$\mathbf{A}^n = \text{diag}(\lambda_1^n \dots \lambda_{2N}^n)$$

it is clear that:

$$\text{if} \quad \rho(T) = \max_i |\lambda_i| \leq 1 \quad \text{then} \quad \|T^n\| = \|\mathbf{A}^n\| \leq c \quad (7.70)$$

Case 2: T has linearly dependent eigenvectors. It is no longer possible to make the spectral decomposition of T in the form (7.68), but the Jordan canonical form has to be used instead:

$$T^n = QJ^nQ^{-1} \quad (7.71)$$

where Q is a unitary matrix and J is a block diagonal matrix of the form:

$$J = \begin{bmatrix} J_1 & & \\ & \ddots & \\ & & J_n \end{bmatrix}$$

with

$$J_i = \lambda_i \quad \text{for a linearly independent eigensolution,} \quad (7.72a)$$

$$J_i = \begin{bmatrix} \lambda_i & 1 & & \\ & \ddots & \ddots & \\ & & \ddots & 1 \\ & & & \lambda_i \end{bmatrix} \quad \text{for a set of } r \text{ linearly dependent eigensolutions} \quad (7.72b)$$

associated to a r -multiple eigenvalue λ_i

Taking the norm of (7.71) yields:

$$\|T^n\| = \|J^n\|$$

It is easily verified that the contribution of each Jordan submatrix (7.72b) into J^n takes the form:

$$J_i^n = \begin{bmatrix} \lambda_i^n & n\lambda_i^{n-1} & & \\ & \ddots & \ddots & \\ & & \ddots & n\lambda_i^{n-1} \\ & & & \lambda_i^n \end{bmatrix} \quad (7.73)$$

Therefore if all multiple eigenvalues are such that $|\lambda_i| < 1$, $\|J_i^n\| \rightarrow 0$ and consequently the condition:

$$\|T^n\| = \|J^n\| < c \quad \forall n \quad (7.74)$$

is verified. Conversely, if there is one r -multiple eigenvalue such that $|\lambda_i| = 1$, Equation (7.73) shows that $\|J_i^n\|$ and thus $\|J^n\|$ will grow linearly with n so that condition (7.74) is no longer fulfilled.

7.2.6 Spectral stability of the Newmark method

The stability characteristics of the Newmark method can be determined by examining the spectral properties of its amplification matrix for a 1-DOF system. In the present case T is a (2×2) matrix, so that a particularly simple and elegant analysis can be performed (Hughes 1983).

The eigenvalues of T are solutions of the characteristic equation:

$$\det(T - \lambda I) = \lambda^2 - 2I_1\lambda + I_2 = 0 \quad (7.75)$$

where I_1 and I_2 are the two invariants of T given by Equations (7.55a–7.55b).

The roots are:

$$\lambda = I_1 \pm (I_1^2 - I_2)^{\frac{1}{2}} \quad (7.76)$$

From (7.76) we see that:

- if $I_1^2 < I_2$ the roots are complex conjugate;
- if $I_1^2 = I_2$ the roots are real and identical;
- if $I_1^2 > I_2$ the roots are real and distinct.

The requirements of spectral stability may be viewed as restricting the allowable values of (I_1, I_2) in $(I_1 - I_2)$ space, the boundary of the stability region being the points verifying the condition $\rho(\mathbf{T}) = 1$. It can be determined by setting $\lambda = e^{i\theta}$ into (7.75). We get:

$$\begin{aligned} e^{2i\theta} - 2I_1 e^{i\theta} + I_2 &= \\ [2 \cos \theta (\cos \theta - I_1) + I_2 - 1] + i[2 \sin \theta (\cos \theta - I_1)] &= 0 \end{aligned} \quad (7.77)$$

Setting to zero the real and imaginary parts in (7.77):

$$[2 \cos \theta (\cos \theta - I_1) + I_2 - 1] = 0 \quad (7.78a)$$

$$[2 \sin \theta (\cos \theta - I_1)] = 0 \quad (7.78b)$$

provides the locus of $\rho(\mathbf{T}) = 1$ by considering three cases:

$$\theta = 0 \quad \rightarrow \quad 1 - 2I_1 + I_2 = 0 \quad (7.79a)$$

$$\theta = \pi \quad \rightarrow \quad 1 + 2I_1 + I_2 = 0 \quad (7.79b)$$

$$\cos \theta = I_1 \quad \rightarrow \quad I_2 = 1 \quad (7.79c)$$

Equations (7.79a–7.79c) describe in (I_1, I_2) space three straight lines forming a triangular region (see Figure 7.5) such that $\rho(\mathbf{T}) = 1$ on its boundary. It is straightforward to show that $\rho(\mathbf{T}) < 1$ inside it. Indeed for the origin $I_1 = I_2 = 0$ lying inside the triangular domain, $\rho(\mathbf{T}) = 0$. Therefore, $\rho(\mathbf{T})$ being a continuous function of I_1 and I_2 and nowhere equal to 1 inside the domain, it can be concluded that $\rho(\mathbf{T}) < 1$ everywhere throughout the interior.

The triangular stability region defined by Equations (7.79a–7.79c) can be better described by the following two sets of conditions:

$$-(I_2 + 1)/2 \leq I_1 \leq (I_2 + 1)/2 \quad -1 \leq I_2 < 1 \quad (7.80a)$$

$$-1 < I_1 < 1 \quad I_2 = 1 \quad (7.80b)$$

Further we see from (7.77) that the parabola $I_2 = I_1^2$ (Figure 7.5) determines the locus of points giving rise to double roots. The roots are complex conjugate when $I_2 > I_1^2$, thus inside the parabola. They become real outside, i.e. when $I_2 < I_1^2$. It intersects the boundary of the stability zone at points $(I_1, I_2) = (\pm 1, 1)$. These two points located on the stability boundary $\rho(\mathbf{T}) = 1$ give rise to a double root of modulus equal to 1. They can thus generate a weak instability as deduced from Equation (7.73) and have to be excluded from the stability region. *Hence, the stability region is the closed triangle minus the two points $(I_1, I_2) = (\pm 1, 1)$.*

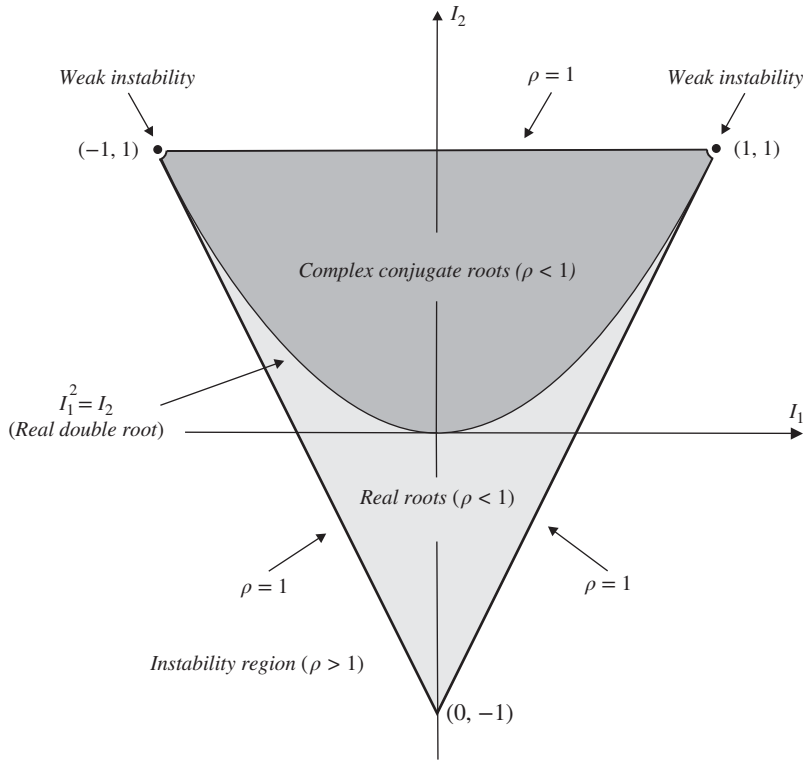


Figure 7.5 Stability of Newmark's method in the (I_1, I_2) plane.

Making use of the explicit expressions (7.55a–7.55b) of the invariants, the stability conditions (7.80a–7.80b) can be developed in the form:

$$1 - I_2 \geq 0 \quad \rightarrow \quad 2\epsilon\omega h + \left(\gamma - \frac{1}{2}\right)\omega^2 h^2 \geq 0 \quad (7.81a)$$

$$1 + I_2 \geq 0 \quad \rightarrow \quad 2 + 4\left(\gamma - \frac{1}{2}\right)\epsilon\omega h + \left(\gamma - \frac{1}{2} + 2\beta\right)\omega^2 h^2 \geq 0 \quad (7.81b)$$

$$(1 + I_2)/2 - I_1 \geq 0 \quad \rightarrow \quad \omega^2 h^2 \geq 0 \quad (7.81c)$$

$$(1 + I_2)/2 + I_1 \geq 0 \quad \rightarrow \quad (2\beta - \gamma)\omega^2 h^2 + 4\left(\gamma - \frac{1}{2}\right)\epsilon\omega h + 2 \geq 0 \quad (7.81d)$$

Two cases may thus be considered:

1. The numerical solution is *unconditionally stable* if:

$$2\beta \geq \gamma \geq \frac{1}{2} \quad (7.82)$$

2. The numerical solution is *conditionally stable* if:

$$\gamma \geq \frac{1}{2}, \quad 0 \leq \beta < \frac{\gamma}{2} \quad (7.83a)$$

$$\omega < \omega_{cr} \quad (7.83b)$$

with the critical frequency ω_{cr} necessary to satisfy (7.81d):

$$\omega_{cr}h = \frac{\left(\gamma - \frac{1}{2}\right)\varepsilon + \sqrt{\frac{\gamma}{2} - \beta + \left(\gamma - \frac{1}{2}\right)^2\varepsilon^2}}{\frac{\gamma}{2} - \beta} \quad (7.83c)$$

In particular, in the absence of physical damping or when $\gamma = \frac{1}{2}$, the critical frequency is given by the simpler formula:

$$\omega_{cr}h = \frac{1}{\sqrt{\frac{\gamma}{2} - \beta}} \quad (7.83d)$$

7.2.7 Oscillatory behaviour of the Newmark response

Equations (7.82) and (7.83a–7.83d) guarantee the stability of the response generated by the Newmark algorithm, but not the fact that it is physically correct.

The exact response of a single degree-of-freedom system being oscillatory, it must be verified that the integration will preserve the physical nature of the response. Therefore the parameters of the integration operator must be chosen so as to remain inside the subregion of the (I_1, I_2) plane delimited by the parabola $I_2 = I_1^2$.

Recalling the explicit expressions (7.55a–7.55b) of I_1 and I_2 we get thus the condition

$$I_1^2 - I_2 = \frac{\omega^2 h^2}{16D^2} \left[((1 + 2\gamma)^2 - 16\beta) \omega^2 h^2 + 8\varepsilon(1 - 2\gamma)\omega h + 16(\varepsilon^2 - 1) \right] < 0 \quad (7.84)$$

It proceeds immediately from (7.84) that:

- The method is unconditionally stable and the roots are complex conjugate over the whole frequency range if

$$0 \leq \varepsilon < 1, \quad \gamma \geq \frac{1}{2}, \quad \beta \geq \frac{1}{4}(1 + 2\gamma)^2 \quad (7.85)$$

- The method is unconditionally stable if

$$0 \leq \varepsilon < 1, \quad \gamma \geq \frac{1}{2}, \quad \frac{1}{4}\left(\gamma + \frac{1}{2}\right)^2 > \beta \geq \frac{\gamma}{2} \quad (7.86)$$

and generates an oscillatory response provided that the frequency remains under a bifurcation threshold

$$\omega h < (\omega h)_{bif} = \frac{\frac{1}{2}\varepsilon\left(\gamma - \frac{1}{2}\right) + \left[\frac{1}{4}\left(\frac{1}{2} + \gamma\right)^2 - \beta + \varepsilon^2\left(\beta - \frac{1}{2}\gamma\right)\right]^{\frac{1}{2}}}{\frac{1}{4}\left(\frac{1}{2} + \gamma\right)^2 - \beta} \quad (7.87)$$

In the absence of physical damping ($\varepsilon = 0$), the bifurcation threshold obeys the simpler formula

$$(\omega h)_{bif} = \left(\frac{1}{4}\left(\gamma + \frac{1}{2}\right)^2 - \beta\right)^{-\frac{1}{2}}$$

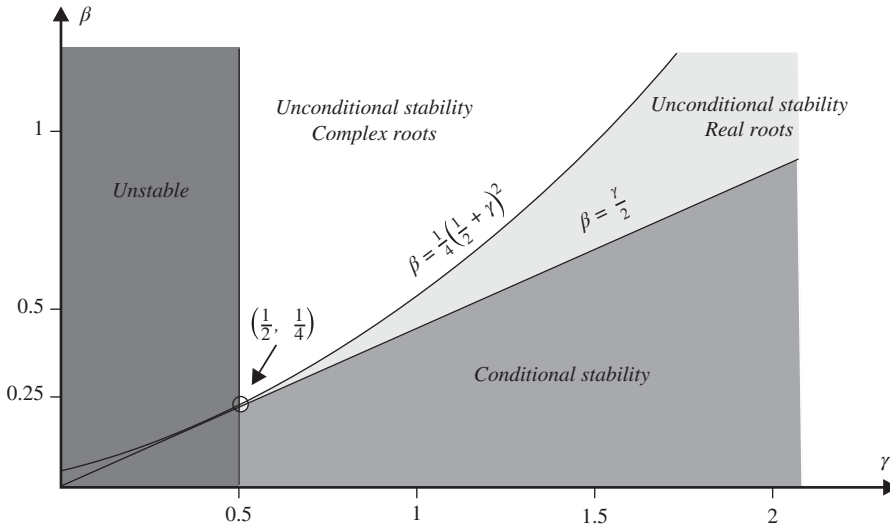


Figure 7.6 Description of Newmark's method in the (β, γ) plane.

For frequencies above this bifurcation limit the roots are real and the numerical solution is nonoscillatory.

The different regions in the (γ, β) plane are displayed on Figure 7.6.

Let us finally note that, *in the case of oscillatory response*,¹ the asymptotic behaviour of Newmark's algorithm as $\omega h \rightarrow \infty$ can be obtained from Equations (7.76) and (7.55b) in a straightforward manner. Indeed for complex roots we get

$$|\lambda| = I_2$$

and thus

$$\rho_\infty = \lim_{\omega h \rightarrow \infty} = I_2 = 1 - \frac{2\gamma - 1}{2\beta} \quad (7.88)$$

showing, in particular, that the spectral radius is equal to 1 when $\gamma = \frac{1}{2}$.

Example 7.1

Let us consider the case of Newmark's method applied to an undamped 1-DOF system ($\epsilon = 0$) with $\gamma = 0.7$. According to Equations (7.85–7.87), it generates an unconditionally stable response if $\beta \geq \frac{1}{2}\gamma = 0.35$, and the response remains oscillatory over the whole frequency range if $\beta \geq \frac{1}{4}\left(\gamma + \frac{1}{2}\right)^2 = 0.36$. Figure 7.7 displays the curves of $\rho(\mathbf{T})$ versus ωh for $\beta = 0.35$ and 0.36.

¹ When the roots become real, the eigenvalue of larger module has to be computed from (7.76) instead.

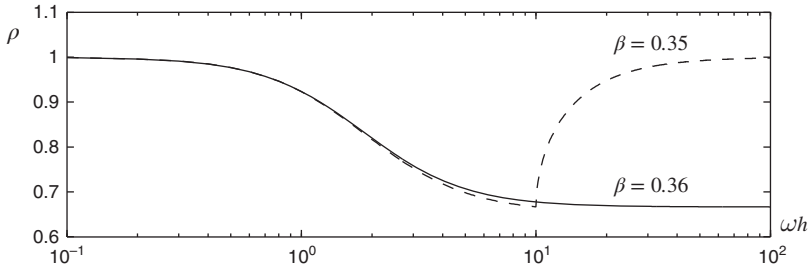


Figure 7.7 Spectral radius of Newmark's method ($\gamma = 0.7$): occurrence of real roots for $\frac{1}{4}\left(\gamma + \frac{1}{2}\right)^2 > \beta \geq \frac{1}{2}\gamma$.

- For $\beta = 0.36$, the spectral radius is a monotonous function of ωh and tends to the asymptotic value $\rho_\infty = 0.667$. The latter can be computed from Equation (7.88).
- For $\beta = 0.35$, the spectral radius decreases up to the bifurcation value $(\omega h)_{bif} = \left(\frac{1}{4}\left(\gamma + \frac{1}{2}\right)^2 - \beta\right)^{-\frac{1}{2}} = 10$. Beyond this value the roots become real, and one of them tends to unity so that $\rho_\infty = 1$.

7.2.8 Measures of accuracy: numerical dissipation and dispersion

In order to characterize the accuracy properties of the Newmark method, let us compare the exact solution of the damped 1-DOF oscillator under initial conditions

$$\begin{cases} \omega^2 \eta + 2\varepsilon \omega \dot{\eta} + \ddot{\eta} = 0 \\ \eta(0) = \eta_0, \quad \dot{\eta}(0) = \dot{\eta}_0 \end{cases} \quad (7.89)$$

to the numerical solution generated by the algorithm. Solving (7.89), the former is found to be

$$\eta(t) = e^{-\varepsilon \omega t} \left(\eta_0 \cos \omega_d t + \frac{\dot{\eta}_0 + \varepsilon \omega \eta_0}{\omega_d} \sin \omega_d t \right) \quad \text{with} \quad \omega_d = \sqrt{1 - \varepsilon^2} \omega \quad (7.90)$$

ω_d being the physically damped eigenfrequency.

Owing to (7.48) the numerical solution can be expressed in the form

$$\mathbf{u}_n = \mathbf{T} \mathbf{u}_{n-1} \quad \text{with} \quad \mathbf{u}_0 = \begin{bmatrix} \dot{\eta}_0 \\ \eta_0 \end{bmatrix} \quad (7.91)$$

Equations (7.91) can be developed as

$$\dot{\eta}_n = t_{11} \dot{\eta}_{n-1} + t_{12} \eta_{n-1} \quad (7.92a)$$

$$\eta_n = t_{21} \dot{\eta}_{n-1} + t_{22} \eta_{n-1} \quad (7.92b)$$

and we have also

$$\eta_{n+1} = t_{21} \dot{\eta}_n + t_{22} \eta_n \quad (7.92c)$$

so that elimination of $\dot{\eta}_n$ and $\dot{\eta}_{n-1}$ between (7.92a–7.92c) provides the difference equation involving the invariants of \mathbf{T}

$$\eta_{n+1} - 2I_1\eta_n + I_2\eta_{n-1} = 0 \quad (7.93)$$

Substituting into (7.93) a solution of the form

$$\eta_n = c\lambda^n$$

yields the eigenvalue equation

$$\lambda^{n-1}(\lambda^2 - 2I_1\lambda + I_2) = 0 \quad (7.94)$$

Discarding the solution $\lambda = 0$ we get Equation (7.75). The general solution to (7.93) is thus

$$\eta_n = c_1\lambda_1^n + c_2\lambda_2^n \quad (7.95)$$

where (λ_1, λ_2) are the eigenvalues of \mathbf{T} and c_1 and c_2 are constants depending on the initial conditions.

The exact solution of (7.89) being oscillatory, let us assume that the integration parameters (β, γ) and that the time step size h have been selected so that the roots of \mathbf{T} are complex conjugate

$$\lambda_{1,2} = I_1 \pm i\sqrt{I_2 - I_1^2} \quad (I_2 - I_1^2 > 0) \quad (7.96)$$

By analogy with the exact response (7.90) of a damped 1-DOF oscillator, they can be put in the form

$$\lambda_{1,2} = e^{-\bar{\varepsilon}\bar{\omega}h}(\cos \bar{\omega}_d h + i \sin \bar{\omega}_d h) \quad (7.97)$$

where $\bar{\omega}$, $\bar{\varepsilon}$ and $\bar{\omega}_d$ are the numerical counterparts of the physical parameters ω , ε and ω_d characterizing the 1-DOF damped oscillator. In particular, $\bar{\varepsilon}$ is called the *numerical damping ratio*. The frequencies $\bar{\omega}_d$ and $\bar{\omega}$ are linked together by

$$\bar{\omega}_d = \bar{\omega}\sqrt{1 - \bar{\varepsilon}^2} \quad (7.98)$$

The numerical damping will affect the amplitude of the system response. The change in frequency is of secondary importance when considering the 1-DOF system, but in a multi-degree of freedom system it will generate dispersion in the response since each spectral component will be affected differently by the time integrator.

Equating the modulus and phase of the roots given in Equations (7.96) and (7.97) we get

$$\bar{\varepsilon}\bar{\omega}h = -\frac{1}{2}\log(I_2) \quad (7.99a)$$

$$\bar{\omega}_d h = \arctan\left(\sqrt{\frac{I_2}{I_1^2} - 1}\right) \quad (7.99b)$$

The accuracy of the numerical integration can be measured by the numerical damping ratio $\bar{\varepsilon}$ and the periodicity error

$$\frac{\Delta T}{T} = \frac{\bar{T}}{T} - 1 = \frac{\omega}{\bar{\omega}} - 1 \quad (7.100)$$

Note that the periodicity error is measured based on the undamped period in order to clearly separate it from the amplitude error (numerical damping). Closed form expressions for (7.99a) and (7.100) are not available, but they can be approximated through series expansion in ωh . The following results are obtained for the undamped system²

$$\bar{\varepsilon} = \frac{1}{2} \left(\gamma - \frac{1}{2} \right) \omega h - \frac{1}{2} \left[\left(\beta + \frac{\gamma}{2} - \frac{1}{4} \right) \left(\gamma - \frac{1}{2} \right) \right] \omega^3 h^3 + O(\omega^5 h^5) \quad (7.101a)$$

$$\frac{\Delta T}{T} = \frac{1}{2} \left(\beta + \frac{11}{48} + \frac{\gamma}{4}(\gamma - 3) \right) \omega^2 h^2 + O(\omega^4 h^4) \quad (7.101b)$$

The numerical damping generated by the Newmark algorithm grows linearly with ωh , showing thus that the algorithm has only first-order accuracy. It is generally controlled in practice by a single parameter α that guarantees a stable, numerically damped harmonic solution

$$0 \leq \alpha < 1 \quad \gamma = \frac{1}{2} + \alpha \quad \beta = \frac{(1 + \alpha)^2}{4} \quad (7.102)$$

in which case the accuracy measures (7.101a–7.101b) become

$$\bar{\varepsilon} \simeq \frac{\alpha}{2} \omega h \quad (7.103a)$$

$$\frac{\Delta T}{T} \simeq \left(\frac{1}{12} + \frac{\alpha^2}{4} \right) \omega^2 h^2 \quad (7.103b)$$

In the presence of physical damping, the results (7.103a–7.103b) are no longer valid. When taking into account a physical damping ratio, they are modified as follows:

$$\bar{\varepsilon} \simeq \varepsilon + \frac{\alpha}{2} \omega h \quad (7.104a)$$

$$\frac{\Delta T}{T} \simeq \frac{3}{2} \left(\frac{1}{2} - \gamma \right) \varepsilon \omega h + \left(\frac{1}{12} + \frac{\alpha^2}{4} \right) \omega^2 h^2 \quad (7.104b)$$

They show that numerical and physical damping simply add together, while there is an increase of the periodicity error proportional to the product of physical and numerical damping ratios, which can be regarded as a second-order effect.

The properties of the algorithm from the Newmark family applied to an undamped oscillator are summarized in Table 7.1. The values provided for the numerical damping ratio and the periodicity error are those given by Equations (7.101a) and (7.101b).

The following conclusions may be drawn:

- The purely explicit scheme is not used in practice, since it is in any case unstable.
- The Fox and Goodwin algorithm does not generate damping and leads to a periodicity error of fourth order, but is conditionally stable.
- The average constant acceleration algorithm is the best unconditionally stable scheme since it does not generate numerical damping and is characterized by a periodicity error of second order.

² The results (7.101a) and (7.104b) were obtained through symbolic computation.

Table 7.1 Integration schemes of the Newmark family ($\varepsilon = 0$)

Algorithm	γ	β	Stability limit ωh	Numerical damping ratio $\bar{\varepsilon}$	Periodicity error $\frac{\Delta T}{T}$
<i>Purely explicit</i>	0	0	0	$\frac{-\omega h}{4}$	–
<i>Central difference</i>	$\frac{1}{2}$	0	2	0	$\frac{-\omega^2 h^2}{24}$
<i>Fox & Goodwin</i>	$\frac{1}{2}$	$\frac{1}{12}$	2.45	0	$O(\omega^4 h^4)$
<i>Linear acceleration</i>	$\frac{1}{2}$	$\frac{1}{6}$	3.46	0	$\frac{\omega^2 h^2}{24}$
<i>Average constant acceleration</i>	$\frac{1}{2}$	$\frac{1}{4}$	∞	0	$\frac{\omega^2 h^2}{12}$
<i>Average constant acceleration (with damping)</i>	$\frac{1}{2} + \alpha$	$\frac{(1 + \alpha)^2}{4}$	∞	$\frac{\alpha}{2} \omega h$	$\left(\frac{1}{12} + \frac{\alpha^2}{4} \right) \omega^2 h^2$

- The average constant acceleration scheme modified to introduce numerical damping is characterized by a numerical damping ratio growing linearly with ωh . It is interesting to note that the first-order error that results from taking $\gamma \neq \frac{1}{2}$ manifests itself in the form of excessive numerical dissipation, but not in period discrepancy since the latter remains of second-order for $\alpha \neq 0$.

Table 7.1 provides also important information concerning the choice of the integration time step depending on the method.

For example, when making use of the central difference scheme, the time step must satisfy the condition

$$h \leq \frac{2}{\omega_{\max}} \quad (7.105)$$

ω_{\max} being the highest frequency included in the model eigenspectrum (also called the critical frequency ω_{cr}). In practice an upper bound of the maximum frequency is often obtained by computing the highest frequency of all isolated element, typically considering the smallest element. Indeed, the nonzero frequencies of an isolated element will always be higher than the corresponding frequencies of the element when assembled (as explained by Rayleigh's theorem on constraints, Section 2.10.6).

For the average constant acceleration method, the time step may be given any value as far as the stability is concerned. In practice, however, it has to be adapted with reference to the

periodicity error. Assuming that the frequency content of the response to be represented with periodicity error

$$\frac{\Delta T}{T} \leq \epsilon_{pe} \quad (7.106)$$

is $[0, \omega_{max}]$, h should be chosen so as to match the condition

$$h \leq \frac{\sqrt{12\epsilon_{pe}}}{\omega_{max}} \simeq \frac{3.5(\epsilon_{pe})^{\frac{1}{2}}}{\omega_{max}} \quad (7.107)$$

7.3 Equilibrium averaging methods

The main conclusion of the preceding section is that Newmark's algorithm appears to be a simple and efficient time integration method as long as one can avoid introducing numerical dissipation. If it is not the case, the method is no longer second-order accurate as shown from the expression (7.101a) of the numerical damping ratio. In (Hilber *et al.* 1977) an elegant way has been proposed to introduce damping in the Newmark method without degrading the order of accuracy. It consists of keeping the Newmark formulas (7.40), whereas the time-discrete equilibrium equations are modified by averaging the internal (i.e. elastic and damping) forces and the external forces between both time instants. With the notation

$$\mathbf{f}(\mathbf{q}, \dot{\mathbf{q}}) = \mathbf{K}\mathbf{q} + \mathbf{C}\dot{\mathbf{q}}$$

to describe the system internal forces, the system equations then take the more general form

$$\mathbf{M}\ddot{\mathbf{q}}_{n+1} + (1 - \alpha)\mathbf{f}(\mathbf{q}_{n+1}, \dot{\mathbf{q}}_{n+1}) + \alpha\mathbf{f}(\mathbf{q}_n, \dot{\mathbf{q}}_n) = (1 - \alpha)\mathbf{g}(\mathbf{q}_{n+1}, t) + \alpha\mathbf{g}(\mathbf{q}_n, t) \quad (7.108)$$

still applicable to nonlinear systems. The integration scheme obtained in this way is referred to as the HHT (Hilber-Hughes-Taylor) or α -method (Hughes 1983).

Later on, the α -method concept has been further developed in Chung and Hulbert (1993) by introducing also in the equilibrium equation similar averaging on inertia forces, but with a distinct averaging parameter. Equation (7.108) then becomes

$$\begin{aligned} (1 - \alpha_m)\mathbf{M}\ddot{\mathbf{q}}_{n+1} + \alpha_m\mathbf{M}\ddot{\mathbf{q}}_n + (1 - \alpha_f)\mathbf{f}(\mathbf{q}_{n+1}, \dot{\mathbf{q}}_{n+1}) + \alpha_f\mathbf{f}(\mathbf{q}_n, \dot{\mathbf{q}}_n) \\ = (1 - \alpha_f)\mathbf{g}(\mathbf{q}_{n+1}, t) + \alpha_f\mathbf{g}(\mathbf{q}_n, t) \end{aligned} \quad (7.109)$$

where α_f and α_m are two averaging parameters affecting respectively the inertia and internal/external forces.

Clearly,

- if $\alpha_m = \alpha_f = 0$, the integration method reduces to Newmark's scheme;
- if $\alpha_m = 0$, $\alpha_f = \alpha$, the integration method corresponds to the HHT scheme;
- if α_m and $\alpha_f \neq 0$, the integration method corresponds to the Generalized- α method proposed by (Chung and Hulbert 1993).

The HHT method being a particular case of the Generalized- α method, the latter will be developed first. The properties of the HHT method will be directly obtained through reduction of the number of parameters of the Generalized- α method.

7.3.1 Amplification matrix

Similarly to the Newmark algorithm, the numerical solution given by the Generalized- α scheme can be stated in the recurrent form

$$\mathbf{u}_{n+1} = \mathbf{T}(h)\mathbf{u}_n + \mathbf{b}_{n+1}(h) \quad (7.110)$$

where

- $\mathbf{u}_n^T = [\mathbf{q}_n^T \quad h\dot{\mathbf{q}}_n^T \quad h^2 \ddot{\mathbf{q}}_n^T] \dots$ is now a $(3N \times 1)$ vector describing the state of the system at time t_n ;
 $\mathbf{T}(h) \dots$ is the system amplification matrix, now of dimension $(3N \times 3N)$;
 $\mathbf{b}(h) \dots$ is the $(3N \times 1)$ external load vector. Its expression is not given since it will not be needed.

For a one-degree-of-freedom system, it can be expressed in terms of the damping ratio ε and the frequency parameter ξ defined as

$$\xi = \omega h \quad (7.111)$$

in the form

$$\mathbf{T}(h) = \mathbf{H}_1^{-1} \mathbf{H}_0 \quad \text{with} \quad \mathbf{u}_n = \begin{bmatrix} \eta_n \\ h\dot{\eta}_n \\ h^2\ddot{\eta}_n \end{bmatrix} \quad (7.112)$$

and

$$\mathbf{H}_1 = \begin{bmatrix} 1 & 0 & -\beta \\ 0 & 1 & -\gamma \\ \xi^2(1-\alpha_f) & 2\varepsilon\xi(1-\alpha_f) & 1-\alpha_m \end{bmatrix} \quad \mathbf{H}_0 = \begin{bmatrix} 1 & 1 & \frac{1}{2}-\beta \\ 0 & 1 & 1-\gamma \\ -\xi^2\alpha_f & -2\varepsilon\xi\alpha_f & -\alpha_m \end{bmatrix} \quad (7.113)$$

The first two lines of this system correspond to the Newmark formula whereas the third is related to the averaged equilibrium (7.109). The closed-form expression of the amplification matrix can be worked out³

$$\mathbf{T} = \frac{1}{D} \begin{bmatrix} 1 - \alpha_m + 2\gamma\varepsilon\xi(1 - \alpha_f) & 1 - \alpha_m + 2\gamma\varepsilon\xi(1 - \alpha_f) & \frac{1}{2}(1 - 2\beta - \alpha_m) + \varepsilon\xi(1 - \alpha_f)(\gamma - 2\beta) \\ -\xi^2\beta\alpha_f & -2\xi\varepsilon\beta & \\ -\xi^2\gamma & 1 - \alpha_m - 2\gamma\varepsilon\xi\alpha_f + \xi^2(1 - \alpha_f)(\beta - \gamma) & 1 - \alpha_m - \gamma + \xi^2(1 - \alpha_f)\left(\beta - \frac{1}{2}\gamma\right) \\ -\xi^2 & -\xi^2(1 - \alpha_f) - 2\varepsilon\xi & \xi^2(1 - \alpha_f)\left(\beta - \frac{1}{2}\right) - \alpha_m + \varepsilon\xi(1 - \alpha_f)(2\gamma - 1) \end{bmatrix} \quad (7.114)$$

where

$$D = \det(\mathbf{H}_1) = 1 - \alpha_m + 2\gamma\varepsilon\xi(1 - \alpha_f) + \xi^2\beta(1 - \alpha_f) \quad (7.115)$$

³ Symbolic computation has been used to work out the expressions obtained in this section.

7.3.2 Finite difference form of the time-marching formula

Let us consider the time integration of a system in free motion. Owing to (7.110) its solution obeys to the recursion formula

$$\mathbf{u}_{n+1} = \mathbf{T}\mathbf{u}_n \quad (7.116)$$

Let us start from an arbitrary initial solution \mathbf{u}_0 and calculate 3 successive solutions $\mathbf{u}_1, \mathbf{u}_2, \mathbf{u}_3$. We have thus

$$\mathbf{u}_0 = \mathbf{T}^i \mathbf{u}_0 \quad i = 0 \dots 3 \quad (7.117)$$

In general, $\mathbf{u}_0, \mathbf{u}_1, \mathbf{u}_2$ will be linearly independent, so that they can be combined with \mathbf{u}_3 into an homogeneous linear equation

$$c_0 \mathbf{u}_0 + c_1 \mathbf{u}_1 + c_2 \mathbf{u}_2 - \mathbf{u}_3 = 0 \quad (7.118)$$

Supposing that \mathbf{T} is not defective, its eigensolutions can be noted $(\lambda_r, \mathbf{p}_{(r)}), r = 1 \dots 3$.

Let us express the starting vector \mathbf{u}_0 as a linear combination of the eigenmodes. We can thus write

$$\mathbf{u}_n = a_1 \lambda_1^n \mathbf{p}_{(1)} + a_2 \lambda_2^n \mathbf{p}_{(2)} + a_3 \lambda_3^n \mathbf{p}_{(3)} \quad n = 0 \dots 3 \quad (7.119)$$

where the a_r are arbitrary nonzero coefficients.

Combining (7.118) and (7.119) we thus get

$$\sum_{r=1}^3 (c_0 + c_1 \lambda_r + c_2 \lambda_r^2 - \lambda_r^3) a_r \mathbf{p}_{(r)} = 0 \quad (7.120)$$

Since \mathbf{u}_0 and thus the a_r are arbitrary, (7.120) will vanish under the conditions that

$$c_0 + c_1 \lambda_r + c_2 \lambda_r^2 - \lambda_r^3 = 0 \quad r = 1 \dots 3 \quad (7.121)$$

which means that (c_0, c_1, c_2) are the coefficients of the characteristic equation of \mathbf{T}

$$c_0 + c_1 \lambda + c_2 \lambda^2 - \lambda^3 = \det(\mathbf{T} - \lambda \mathbf{I}) = 0 \quad (7.122)$$

The development of the latter is generally written in the form

$$\lambda^3 - I_1 \lambda^2 + I_2 \lambda - I_3 = 0 \quad (7.123)$$

where the coefficients I_1, I_2, I_3 are the 3 invariants of matrix \mathbf{T} . We deduce the meaning of the coefficients of (7.122)

$$c_2 = I_1 = \text{trace } \mathbf{T} \quad (7.124)$$

$$c_1 = I_2 = \text{sum of the principal minors of } (\mathbf{T}) \quad (7.125)$$

$$c_0 = I_3 = \det(\mathbf{T}) \quad (7.126)$$

The recurrence form of the integration formula results from (7.118)

$$\mathbf{u}_n = I_1 \mathbf{u}_{n-1} - I_2 \mathbf{u}_{n-2} + I_3 \mathbf{u}_{n-3} \quad (7.127)$$

Equation (7.127) governs equally the evolution of all three components of \mathbf{u} . Thus, for a single DOF system, the numerical approximation $\bar{\eta}$ to the normal coordinate $\eta(t)$ is solution of

$$\bar{\eta}_n = I_1 \bar{\eta}_{n-1} - I_2 \bar{\eta}_{n-2} + I_3 \bar{\eta}_{n-3} \quad (7.128)$$

7.3.3 Accuracy analysis of equilibrium averaging methods

Equation (7.128) represents a discretized form of equilibrium obtained in the form of difference equation over four successive steps. The numerical solution that it generates should thus be compared to the exact solution (7.90) of the original Equation (7.89).

Let us suppose that we express the latter at the same time steps

$$\begin{aligned}\eta_{n-k} &= \eta(t_{n-k}) \\ &= e^{-\varepsilon\omega_d t_{n-k}} \left(\eta_0 \cos \omega_d t_{n-k} + \frac{\dot{\eta}_0 + \varepsilon\omega\eta_0}{\omega_d} \sin \omega_d t_{n-k} \right) \quad k = 0 \dots 3\end{aligned}\quad (7.129)$$

If the numerical integration scheme were free from errors the solution (7.129) would satisfy the recurrence relation (7.128). Therefore substituting the numerical solution $\bar{\eta}$ in (7.128) by the exact one results in an error measure expressed as

$$e(\eta) = \eta_n - I_1\eta_{n-1} + I_2\eta_{n-2} - I_3\eta_{n-3} \quad (7.130)$$

However, the derivation of Newmark's formulas from (7.34) tells us that in order to verify the consistency of the method, the discretization error has in fact to be measured on accelerations. The consistency of the integration method is thus measured by considering the recurrence relation verified by the numerical solution for accelerations, namely the third set in (7.127) pertaining to $h^2\ddot{\eta}_n$. Substituting $\ddot{\eta}_n$ by the exact solution $\ddot{\eta}_n$ yields the error measure

$$e(\ddot{\eta}) = \frac{1}{\omega^2 h^2} (\eta_n - I_1\eta_{n-1} + I_2\eta_{n-2} - I_3\eta_{n-3}) \quad (7.131)$$

The explicit expression of the invariants I_1, I_2, I_3 is

$$I_1 = \frac{1}{D} \left(2 - 3\alpha_m + 2\varepsilon (\gamma (2 - 3\alpha_f) - 1 + \alpha_f) \xi + \left(\beta(2 - 3\alpha_f) - (1 - \alpha_f)(\gamma + \frac{1}{2}) \right) \xi^2 \right) \quad (7.132a)$$

$$I_2 = \frac{1}{D} \left(1 - 3\alpha_m + 2\varepsilon (\gamma(1 - 3\alpha_f) - 1 + 2\alpha_f) \xi + \left(\beta + \frac{1}{2} - \gamma + \alpha_f(2\gamma - 3\beta) \right) \xi^2 \right) \quad (7.132b)$$

$$I_3 = \frac{1}{D} \left(-\alpha_m + 2\varepsilon\alpha_f(1 - \gamma)\xi + \alpha_f \left(\gamma - \frac{1}{2} - \beta \right) \xi^2 \right) \quad (7.132c)$$

Substituting (7.129) and (7.132a–7.132c) into (7.131) provides a quite complex expression of $e(\ddot{\eta})$. However, its Taylor expansion in ωh yields the remarkably simple result

$$e(\ddot{\eta}) = \frac{2\varepsilon}{1 - \alpha_m} \left(\frac{1}{2} - \gamma + \alpha_f - \alpha_m \right) \omega^2 h^2 + O(\omega^3 h^3) \quad (7.133)$$

which shows that

the Generalized- α method will be second-order accurate provided that we take

$$\gamma = \frac{1}{2} + \alpha_f - \alpha_m \quad (7.134)$$

7.3.4 Stability domain of equilibrium averaging methods

Determining the stability domain of equilibrium averaging methods method cannot be performed analytically by examining the roots of the characteristic equation (7.123) since their closed-form expression is not available. The Routh-Hurwitz criterion has to be used instead (Hughes 1983), the latter allowing us to determine under which conditions the real part of the roots remains negative.

Since the limit of stability domain in the λ plane is the circle $|\lambda| = 1$, one makes use of the transformation

$$\lambda = \frac{1 + \zeta}{1 - \zeta} \quad \text{such that} \quad |\lambda| \leq 1 \quad \leftrightarrow \quad \Re(\zeta) \leq 0 \quad (7.135)$$

The characteristic equation (7.123) is transformed into

$$p_0 \zeta^3 + p_1 \zeta^2 + p_2 \zeta + p_3 = 0 \quad (7.136)$$

Routh-Hurwitz's criterion states that a necessary and sufficient condition for the roots of Equation (7.136) to lie in the $\Re(\zeta) \leq 0$ plane (and thus, for the λ to lie within the $|\lambda| = 1$ circle) is

$$p_0 = 1 - I_1 + I_2 - I_3 \geq 0 \quad (7.137a)$$

$$p_1 = 3 - I_1 - I_2 + 3I_3 \geq 0 \quad (7.137b)$$

$$p_2 = 3 + I_1 - I_2 - 3I_3 \geq 0 \quad (7.137c)$$

$$p_3 = 1 + I_1 + I_2 + I_3 \geq 0 \quad (7.137d)$$

$$\frac{1}{8}(p_1 p_2 - p_0 p_3) = 1 - I_2 + I_3(I_1 - I_3) \geq 0 \quad (7.137e)$$

Through substitution into (7.137a–7.137e) of Equations (7.132a–7.132c) the following non-trivial stability conditions are obtained:

$$\gamma - \frac{1}{2} \geq 0 \quad (7.138a)$$

$$\gamma - \frac{1}{2} - \alpha_f + \alpha_m \geq 0 \quad (7.138b)$$

$$\beta \geq \left(\gamma - \frac{1}{2}\right) \alpha_f + \frac{1}{4} \quad (7.138c)$$

$$\frac{1}{2} \geq \alpha_f \geq \alpha_m \geq 0 \quad (7.138d)$$

The stability limit provided by (7.138b) corresponds also to the value of γ obtained from (7.134) for second-order accuracy. However, respecting the stability conditions does not guarantee the fact that the physical nature of the solution will be preserved. In order to verify that the method will generate for $\varepsilon < 1$ an oscillatory solution within the stability domain, the asymptotic behaviour of the eigenvalues must also be examined.

7.3.5 Oscillatory behaviour of the solution

Let us look at the asymptotic behaviour of the solution by examining the eigenspectrum of the amplification matrix at infinite frequency. For $\omega h \rightarrow \infty$ we get

$$\mathbf{T}_\infty = \begin{bmatrix} \frac{-\alpha_f}{1-\alpha_f} & 0 & 0 \\ \frac{-\gamma}{\beta(1-\alpha_f)} & \frac{\beta-\gamma}{\beta} & \frac{-\gamma+2\beta}{2\beta} \\ \frac{-1}{\beta(1-\alpha_f)} & -\frac{1}{\beta} & \frac{-1+2\beta}{2\beta} \end{bmatrix} \quad (7.139)$$

and its eigenvalues are

$$\lambda_1 = \frac{-\alpha_f}{1-\alpha_f}, \quad \lambda_{2,3} = \frac{1+2\gamma-4\beta \pm \sqrt{(1+2\gamma)^2 - 16\beta}}{4\beta} \quad (7.140)$$

λ_1 is the parasitic value. It remains real negative and its absolute value smaller than 1 for $0 \leq \alpha_f < \frac{1}{2}$. The pair of eigenvalues (λ_2, λ_3) is complex for $\beta > \frac{1}{4}(\gamma + \frac{1}{2})^2$. When $\beta = \frac{1}{4}(\gamma + \frac{1}{2})^2$, the matrix \mathbf{T}_∞ becomes defective since to the double eigenvalue is associated a single eigenvector

$$\lambda_{2,3} = \frac{2\gamma-3}{2\gamma+1} \quad \mathbf{p}_{(2)} = \mathbf{p}_{(3)} = \left[0 \quad \frac{1}{2} \left(\gamma + \frac{1}{2} \right) \quad 1 \right]^T \quad (7.141)$$

In that case, the matrix being defective, stability requires that the multiple eigenvalues have a modulus strictly lower than 1 (see discussion in Section 7.2.5). Further, if we adopt for γ the value (7.134) giving second-order accuracy, one gets for $\omega h \rightarrow \infty$ the eigenvalues

$$\lambda_1 = \frac{-\alpha_f}{1-\alpha_f} \quad \lambda_{2,3} = \frac{\alpha_f - \alpha_m - 1}{\alpha_f - \alpha_m + 1} \quad (7.142)$$

which are all strictly lower than 1 owing to the stability condition (7.138d). To summarize, with the combined set of values

$$\gamma = \frac{1}{2} + \alpha_f - \alpha_m \quad \beta = \frac{1}{4}(1 + \alpha_f - \alpha_m)^2 \quad (7.143)$$

the resulting time integration algorithm

- has second-order accuracy,
- is unconditionally stable and generates numerical damping of intensity controlled by the two averaging parameters α_f and α_m ,
- has for spectral radius at infinity

$$\rho_\infty = \max_{\alpha_f, \alpha_m} \left(\frac{\alpha_f}{1-\alpha_f}, \frac{1-\alpha_f+\alpha_m}{1+\alpha_f-\alpha_m} \right) \quad (7.144)$$

7.3.6 Particular forms of equilibrium averaging

Different algorithms with specific accuracy and stability properties can be obtained, depending on the choice of the parameters. Four different choices are discussed below, namely

- the Newmark method,
- the Hilber-Hughes-Taylor α -method (HHT),
- the Generalized- α method,
- the Mid-point rule.

Newmark's method

The Newmark method can be considered as a specific implementation of the algorithm in which the second-order accuracy condition (7.134) is not verified. It is thus obtained with the specific choice of parameters

$$\left. \begin{aligned} \gamma &= \frac{1}{2} + \alpha, & \alpha_f = \alpha_m = 0 \\ \beta &= \frac{1}{4}(1 + \alpha)^2 \end{aligned} \right\} \quad \text{with } \alpha \geq 0 \quad (7.145)$$

Its asymptotic behaviour as $\omega h \rightarrow \infty$ can be deduced from (7.141)

$$1 \geq \rho_\infty = \frac{|1 - \alpha|}{1 + \alpha} \quad (7.146)$$

The algorithm remains second-order accurate when $\alpha = 0$ since condition (7.134) remains then verified. Its numerical properties for $\alpha \neq 0$ and no physical damping ($\varepsilon = 0$) will be used as a reference to show the benefit of adopting other sets of parameters. Its spectral radius, numerical damping ratio and periodicity error versus frequency parameter are displayed on Figures 7.8–7.10. To the value $\alpha = 0.0526$ adopted to generate the figures corresponds a asymptotic spectral radius $\rho_\infty = 0.9$.

Note that the spectral radius plot covers the frequency range $\omega h \in [0, 100]$ while the numerical damping ratio and periodicity error curves have been limited to $\omega h \in [0, 5]$. The reason for it is that for a frequency parameter ωh bigger than π , one gets the ratio $\frac{h}{T} = \frac{\omega h}{2\pi} > \frac{1}{2}$, which means that the algorithm is no longer able to sample the oscillation correctly. At $\omega h = \pi$ a periodicity error of about 40% is effectively observed. It is negative, since the filtering by the time integration induces a frequency reduction.

It is also important recalling that the periodicity error as displayed on Figure 7.10 is measured on the numerical undamped frequency, which means that it does not take into account the period increase generated by numerical damping (factor $(1/\sqrt{1 - \bar{\varepsilon}^2})$). Second-order accuracy is obtained on the undamped frequency since the curve exhibits zero slope at $\omega h = 0$.

Hilber-Hughes-Taylor α -method (HHT)

The HHT method (Hilber *et al.* 1977) respects the second-order accuracy condition (7.134) but makes use of only one of the parameters of the general method. It is obtained by setting

$$\left. \begin{aligned} \alpha_f &= \alpha, & \gamma &= \frac{1}{2} + \alpha \\ \beta &= \frac{1}{4}(1 + \alpha)^2 \end{aligned} \right\} \quad \text{with } \frac{1}{3} > \alpha \geq 0 \quad (7.147)$$

The upper limit to α results from the fact that $|\lambda_1|$ (Equation (7.142)) should not exceed $|\lambda_{2,3}|$ (Hilber *et al.* 1977) since that would increase the spectral radius. The asymptotic spectral radius is thus constrained between the following limits

$$1 \geq \rho_\infty = \frac{1 - \alpha}{1 + \alpha} \geq \frac{1}{2} \quad (7.148)$$

The spectral radius, numerical damping ratio and periodicity error versus frequency parameter obtained for the same value $\alpha = 0.0526$ (with $\varepsilon = 0$) are displayed on the same Figures 7.8–7.10. The asymptotic spectral radius is the same as with Newmark's method, as could be predicted from Equation (7.144). There is however significant improvement in the intermediate frequency range:

- For a same value of ρ_∞ , the decrease of the spectral radius versus ωh is significantly delayed, providing thus a wider frequency range with small to negligible dissipation.
- This is confirmed by the evolution of the numerical damping ratio curve with zero slope in the low frequency range, due to the second-order accuracy of the algorithm.
- The periodicity error on the undamped eigenfrequency is the same as with Newmark's method.

Generalized- α method

The Generalized- α method (Chung and Hulbert 1993), like HHT, respects the second-order accuracy condition (7.134) but makes use of both parameters α_f and α_m to introduce different

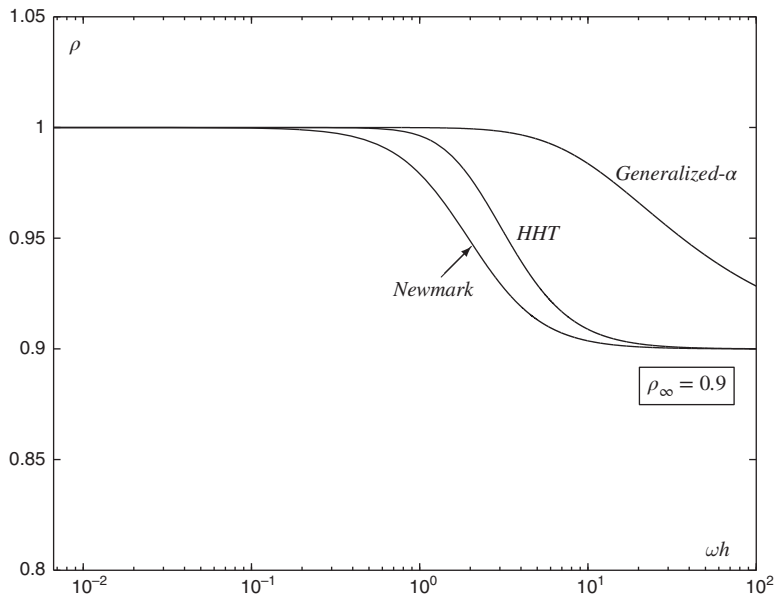


Figure 7.8 Spectral radius for Newmark, HHT and Generalized- α methods ($\rho_\infty = 0.9$).

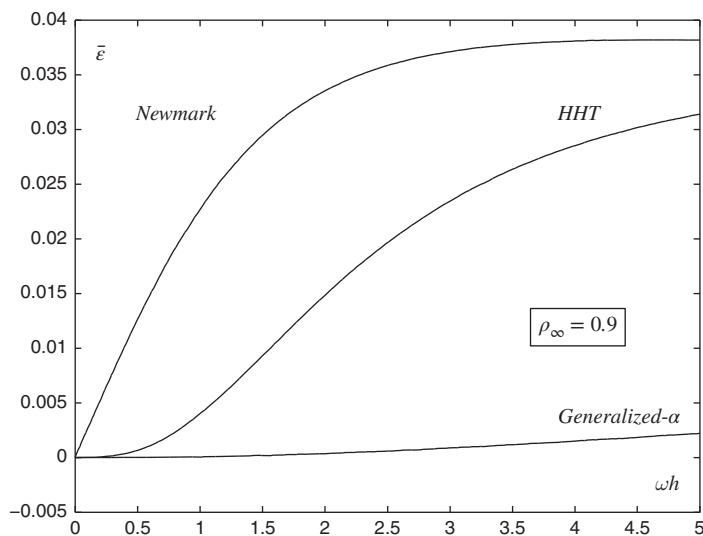


Figure 7.9 Numerical damping ratio for Newmark, HHT and Generalized- α methods ($\rho_\infty = 0.9$).

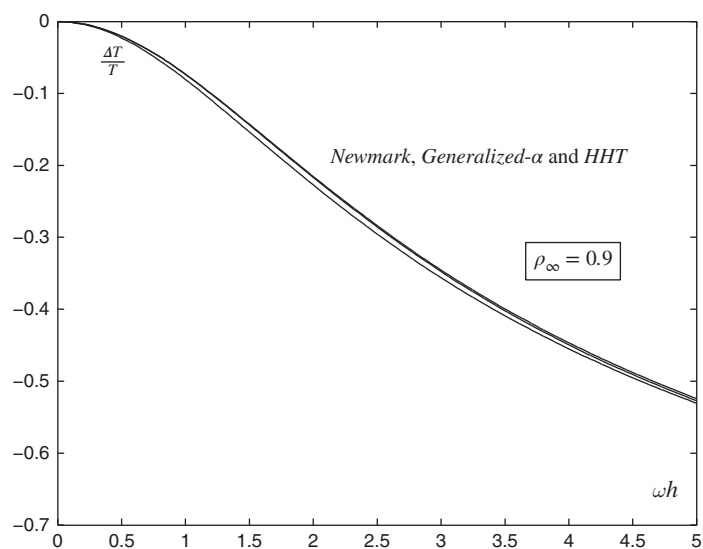


Figure 7.10 Periodicity error for Newmark, HHT and Generalized- α methods ($\rho_\infty = 0.9$).

averaging on internal/external forces and on inertia forces. It is thus described by

$$\left. \begin{aligned} \gamma &= \frac{1}{2} + \alpha_f - \alpha_m \\ \beta &= \frac{1}{4}(1 + \alpha_f - \alpha_m)^2 \end{aligned} \right\} \quad \text{with} \quad 0 \leq \alpha_m \leq \alpha_f \leq \frac{1}{2} \quad (7.149)$$

They can be chosen according to Equation (7.144) to impose a prescribed asymptotic radius

$$\alpha_m = \frac{2\rho_\infty - 1}{\rho_\infty + 1} \quad \alpha_f = \frac{\rho_\infty}{\rho_\infty + 1} \quad \text{with} \quad 0 \leq \rho_\infty \leq 1 \quad (7.150)$$

It provides thus maximum flexibility in controlling the amount of dissipation introduced in the high frequency range. Its numerical performance versus frequency parameter is compared to Newmark and HHT methods on the same Figures 7.8–7.10, where the parameters have been chosen according to (7.150) and taking the same limit $\rho_\infty = 0.9$ as for the other methods. It is observed that:

- For a same value of ρ_∞ , the decrease of the spectral radius versus ωh is further delayed, providing thus an even wider frequency range with small to negligible dissipation than HHT.
- The numerical damping ratio remains extremely small in the low frequency range even by comparison with HHT.
- The periodicity error on the undamped eigenfrequency remains the same as with Newmark's method.

As a conclusion, one may state that the HHT and Generalized- α schemes are excellent choices when requiring an unconditionally stable implicit algorithm that introduces high numerical damping in the high frequency range while nearly preserving the maximum accuracy attribute of the average constant acceleration method for the low frequency band.

The two methods – with still a preference for Generalized- α – are recommended both for nonlinear systems and for systems having constrained degrees of freedom (e.g. multibody systems) since the latter introduce double frequencies at infinity which may generate weak instability in the solution (Cardona and G  rardin 1989).

Remark 7.3 *Equilibrium averaging is not the only possible way to introduce the Generalized- α method. In (Arnold and Br  ils 2007) a different implementation of the method is presented which does not rely on a weighted formulation of the residual equation. In the variant proposed, dynamic equilibrium is still enforced exactly at every time step, but a vector \mathbf{a} of pseudo-accelerations is introduced by the recurrence relation*

$$(1 - \alpha_m)\mathbf{a}_{n+1} + \alpha_m\mathbf{a}_n = (1 - \alpha_f)\ddot{\mathbf{q}}_{n+1} + \alpha_f\ddot{\mathbf{q}}_n \quad \mathbf{a}_0 = \ddot{\mathbf{q}}_0 \quad (7.151)$$

\mathbf{a} is thus an auxiliary variable which is not equal to the true accelerations $\ddot{\mathbf{q}}$. The Generalized- α scheme is obtained by using \mathbf{a} in the Newmark integration formulas (7.40) modified in the form

$$\begin{aligned} \dot{\mathbf{q}}_{n+1} &= \dot{\mathbf{q}}_n + (1 - \gamma)h\mathbf{a}_n + \gamma h\mathbf{a}_{n+1} \\ \mathbf{q}_{n+1} &= \mathbf{q}_n + h\dot{\mathbf{q}}_n + h^2\left(\frac{1}{2} - \beta\right)\mathbf{a}_n + h^2\beta\mathbf{a}_{n+1} \end{aligned} \quad (7.152)$$

The new accelerations $\ddot{\mathbf{q}}_{n+1}$ result then from the solution of the dynamic equilibrium equation at t_{n+1} .

The method has three major advantages (Arnold and Br  ils 2007):

- the accelerations are computed with second-order accuracy;

- the consistency of the algorithm is not affected if the mass matrix is not constant;
- the algorithm is closer to the physics of the problem, which also simplifies theoretical investigations.

For nonlinear systems, the implementation proposed in Arnold and Brüls (2007) is more appropriate than equilibrium averaging while it is easily verified that for a linear system, both implementations are equivalent.

Mid-Point rule

Another integration method of interest is obtained with the specific choice of parameters

$$\alpha_f = \alpha_m = \frac{1}{2} \quad \text{and thus} \quad \gamma = \frac{1}{2}, \quad \beta = \frac{1}{4} \quad (7.153)$$

It has obviously the same stability and accuracy properties as Newmark's method without damping, which can also be verified by computing the eigenvalues of the amplification matrix

$$\lambda_1 = -1, \quad \lambda_{2,3} = \frac{\pm i\omega h - (\omega^2 h^2 - 4)}{\omega^2 h^2 + 4} \rightarrow |\lambda_i| = 1, \quad i = 1 \dots 3 \quad (7.154)$$

the only difference being the presence of the spurious root $\lambda_1 = -1$.

The interesting aspect of the method is that it uses the equilibrium equation at half-interval, which can be written in the form

$$\mathbf{M}\ddot{\mathbf{q}}_{n+\frac{1}{2}} + \mathbf{C}\dot{\mathbf{q}}_{n+\frac{1}{2}} + \mathbf{K}\mathbf{q}_{n+\frac{1}{2}} = \mathbf{p}_{n+\frac{1}{2}} \quad (7.155)$$

where we defined the unknowns at mid-interval. Accounting for Newmark's formulas (7.40) they can be written as

$$\ddot{\mathbf{q}}_{n+\frac{1}{2}} = \frac{1}{2}(\ddot{\mathbf{q}}_n + \ddot{\mathbf{q}}_{n+1}) \quad (7.156a)$$

$$\dot{\mathbf{q}}_{n+\frac{1}{2}} = \frac{1}{2}(\dot{\mathbf{q}}_n + \dot{\mathbf{q}}_{n+1}) = \dot{\mathbf{q}}_n + \frac{h}{2}\ddot{\mathbf{q}}_{n+\frac{1}{2}} \quad (7.156b)$$

$$\mathbf{q}_{n+\frac{1}{2}} = \frac{1}{2}(\mathbf{q}_n + \mathbf{q}_{n+1}) = \mathbf{q}_n + \frac{h}{2}\dot{\mathbf{q}}_{n+\frac{1}{2}} \quad (7.156c)$$

which is convenient for computer implementation. It is interesting to note that those definitions, according to (7.156b, 7.156c), can also be interpreted as

$$\ddot{\mathbf{q}}_{n+\frac{1}{2}} = \frac{\dot{\mathbf{q}}_{n+1} - \dot{\mathbf{q}}_n}{h} \quad (7.157a)$$

$$\dot{\mathbf{q}}_{n+\frac{1}{2}} = \frac{\mathbf{q}_{n+1} - \mathbf{q}_n}{h} \quad (7.157b)$$

When applied to linear problems, the mid-point rule generates exactly the same solution as Newmark with zero damping. It has however at least two main characteristics that make it attractive:

- the fact of expressing equilibrium at mid-interval is generally beneficial to improve the convergence of the iteration process when solving nonlinear dynamic problems;
- it provides a natural approach to generate energy conserving solutions (see for example Cardona and Géradin (1989), Lens *et al.* (2004)).

7.4 Energy conservation

The stability properties of the Newmark algorithm, for average constant acceleration ($\beta = \frac{1}{4}$, $\gamma = \frac{1}{2}$), can be linked to the concept of energy conservation: indeed, we will show that unconditional stability of the algorithm and absence of amplitude errors lead to the conservation of the total energy of the system during the computation of its motion. The proof will be established for the mid-point rule outlined in Section 7.3.6, but it could be equally done using Newmark's method in its standard form, i.e. with equilibrium expressed at time t_{n+1} as it was done in G  rardin and Rixen (1997).

As already mentioned in Chapter 1, Equation (1.58), any dynamic system with scleronomic constraints satisfies the power balance

$$\frac{d}{dt} (\mathcal{T} + \mathcal{V}) = -mD + \sum_{s=1}^N Q_s \dot{q}_s \quad (7.158)$$

where N is the number of degrees of freedom of the system. In the case of linear systems driven by Equations (7.1), the potential and kinetic energies are quadratic functions:

$$\mathcal{T} = \frac{1}{2} \dot{\mathbf{q}}^T \mathbf{M} \dot{\mathbf{q}} \quad \text{and} \quad \mathcal{V} = \frac{1}{2} \mathbf{q}^T \mathbf{K} \mathbf{q} \quad (7.159)$$

The dissipation function for linear viscous damping is also quadratic in terms of velocities ($m = 2$)

$$D = \frac{1}{2} \dot{\mathbf{q}}^T \mathbf{C} \dot{\mathbf{q}} \quad (7.160)$$

The external force component of the power balance can be expressed by

$$\sum_{s=1}^N Q_s \dot{q}_s = \dot{\mathbf{q}}^T \mathbf{p} \quad (7.161)$$

so that by integrating (7.158) over a time step $[t_n, t_{n+1}]$, we can write

$$[\mathcal{T} + \mathcal{V}]_{t_n}^{t_{n+1}} = \int_{t_n}^{t_{n+1}} (-\dot{\mathbf{q}}^T \mathbf{C} \dot{\mathbf{q}} + \dot{\mathbf{q}}^T \mathbf{p}) dt \quad (7.162)$$

Let us then calculate the kinetic and potential energy variations by

$$\mathcal{T}_{n+1} - \mathcal{T}_n = \frac{1}{2} (\dot{\mathbf{q}}_{n+1} - \dot{\mathbf{q}}_n)^T \mathbf{M} (\dot{\mathbf{q}}_{n+1} + \dot{\mathbf{q}}_n) \quad (7.163a)$$

$$\mathcal{V}_{n+1} - \mathcal{V}_n = \frac{1}{2} (\mathbf{q}_{n+1} - \mathbf{q}_n)^T \mathbf{K} (\mathbf{q}_{n+1} + \mathbf{q}_n) \quad (7.163b)$$

Assuming that the time integration is carried out by the mid-point rule as defined in Equations (7.156a–7.156c) and considering also (7.157a–7.157b) leading to

$$\dot{\mathbf{q}}_n + \dot{\mathbf{q}}_{n+1} = 2\dot{\mathbf{q}}_{n+\frac{1}{2}} = \frac{2}{h} (\mathbf{q}_{n+1} - \mathbf{q}_n) \quad (7.164a)$$

$$\dot{\mathbf{q}}_{n+1} - \dot{\mathbf{q}}_n = h\ddot{\mathbf{q}}_{n+\frac{1}{2}} \quad (7.164b)$$

we can rewrite the variation of kinetic and potential energies as

$$\mathcal{T}_{n+1} - \mathcal{T}_n = (\mathbf{q}_{n+1} - \mathbf{q}_n)^T \mathbf{M} \dot{\mathbf{q}}_{n+\frac{1}{2}} \quad (7.165a)$$

$$\mathcal{V}_{n+1} - \mathcal{V}_n = (\mathbf{q}_{n+1} - \mathbf{q}_n)^T \mathbf{K} \mathbf{q}_{n+\frac{1}{2}} \quad (7.165b)$$

Thus the total energy variation is given by

$$[\mathcal{T} + \mathcal{V}]_{t_n}^{t_{n+1}} = (\mathbf{q}_{n+1} - \mathbf{q}_n)^T [\mathbf{K} \mathbf{q} + \mathbf{M} \dot{\mathbf{q}}]_{n+\frac{1}{2}} \quad (7.166)$$

and taking account of the dynamic equilibrium Equation (7.155) yields

$$[\mathcal{T} + \mathcal{V}]_{t_n}^{t_{n+1}} = (\mathbf{q}_{n+1} - \mathbf{q}_n)^T [\mathbf{p} - \mathbf{C} \dot{\mathbf{q}}]_{n+\frac{1}{2}} \quad (7.167)$$

which, owing to (7.164a), can be rewritten as

$$[\mathcal{T} + \mathcal{V}]_{t_n}^{t_{n+1}} = (\mathbf{q}_{n+1} - \mathbf{q}_n)^T \mathbf{p}_{n+\frac{1}{2}} - h \dot{\mathbf{q}}_{n+\frac{1}{2}}^T \mathbf{C} \dot{\mathbf{q}}_{n+\frac{1}{2}} \quad (7.168)$$

Hence, we can make the following observations:

- When applied to a linear conservative system (i.e. $\mathbf{C} = \mathbf{0}$ and $\mathbf{p} = \mathbf{0}$), the mid-point rule (equivalent to Newmark's algorithm with parameters $\beta = \frac{1}{4}$ and $\gamma = \frac{1}{2}$) preserves the total energy.
- For nonconservative systems, both right-hand components of the power balance Equation (7.168) result from the numerical quadrature relationships consistent with the mid-point rule

$$\int_{t_n}^{t_{n+1}} \dot{\mathbf{q}}^T \mathbf{p} \, dt \simeq (\mathbf{q}_{n+1} - \mathbf{q}_n)^T \mathbf{p}_{n+\frac{1}{2}} \quad (7.169a)$$

$$\int_{t_n}^{t_{n+1}} \dot{\mathbf{q}}^T \mathbf{C} \dot{\mathbf{q}} \, dt \simeq h \dot{\mathbf{q}}_{n+\frac{1}{2}}^T \mathbf{C} \dot{\mathbf{q}}_{n+\frac{1}{2}} \quad (7.169b)$$

showing that the total energy variation is equal to the work of external and internal nonconservative forces over one time step.

The property of energy conservation, valid for any time step, implies that the amplitude of the system displacements and velocities do not increase: it thus gives yet another proof of the unconditional stability of the algorithm.

When applying Newmark's method with $\gamma \geq \frac{1}{2}$ and $\beta \geq \frac{1}{4} \left(\gamma + \frac{1}{2} \right)^2$, it can be shown in a general manner that the total energy balance over one time step is negative, which is a result of the numerical damping brought in by the integration algorithm (Hughes 1987). Conversely, for β and γ within the instability domain of the algorithm, the energy balance is found to be positive.

Computing an energy balance is most useful in the context of solving nonlinear problems: it then gives a measure of the stability of the method in the presence of nonlinearities.

7.4.1 Application: the clamped–free bar excited by an end force

Let us consider once more the clamped–free bar subjected to a step load on its free end (Section 4.3.1) for which a closed-form solution was found (Equation 4.181).

For a model made of N finite elements of equal length $\ell = \frac{L}{N}$, the mass and stiffness matrices are given by (5.93). The nondimensional properties of the bar and of its model are given in Figure 7.11, the element length ℓ being taken as reference length.

An upper bound to the frequencies can be found by noticing that the eigenfrequency of an isolated element with consistent mass matrix is given by:

$$\frac{EA}{\ell} \begin{bmatrix} 1 & -1 \\ -1 & 1 \end{bmatrix} \begin{bmatrix} q_1 \\ q_2 \end{bmatrix} = \omega^2 \frac{m\ell}{6} \begin{bmatrix} 2 & 1 \\ 1 & 2 \end{bmatrix} \begin{bmatrix} q_1 \\ q_2 \end{bmatrix}$$

whose unique nonzero solution yields $\omega_{cr} = 2\sqrt{3}$.

Hence for the central difference algorithm, the stability condition $\omega h \leq 2$ (see Table 7.1) requires that $h \leq 1/\sqrt{3}$.

The transient response of the bar to a step load on its end has been computed by the Newmark algorithm according to the flowchart in Figure 7.4 with the same time step $h = 3$ (i.e. more than five times the critical value for the central difference scheme):

- without numerical damping: $\beta = \frac{1}{4}$, $\gamma = \frac{1}{2}$;
- with small numerical damping: $\gamma = \frac{1}{2} + \alpha$, $\beta = \frac{1}{4} \left(\gamma + \frac{1}{2} \right)^2$ with $\alpha = 0.05$, yielding to an asymptotic spectral radius $\rho_\infty = 0.905$.

The resulting curves of Figure 7.29 respectively display the displacements at nodes 1, 10 and 20, the velocities at nodes 10 and 20, the axial stress N in elements 1 and 20, and finally the energy loss of the computation.

We can make the following observations:

- Due to discretization, the longitudinal wave is strongly scattered, so that the response curve is fairly different from the exact solution curve (see Section 4.3.1). This effect is mostly noticeable near the built-in end. This difference arises from the poor convergence of the solution with the number of eigenmodes included in the model, when the load is applied on the boundary of the model.
- Displacement and stress response curves clearly show that their maximum is always equal to about twice the static value:

$$q_{max} \simeq 2 \frac{x}{L} \quad \text{and} \quad N_{max} \simeq 2F$$

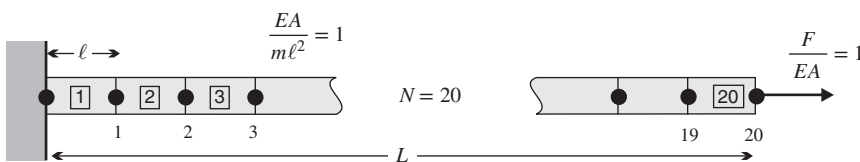


Figure 7.11 A clamped–free bar excited by a step end load (finite element discretization).

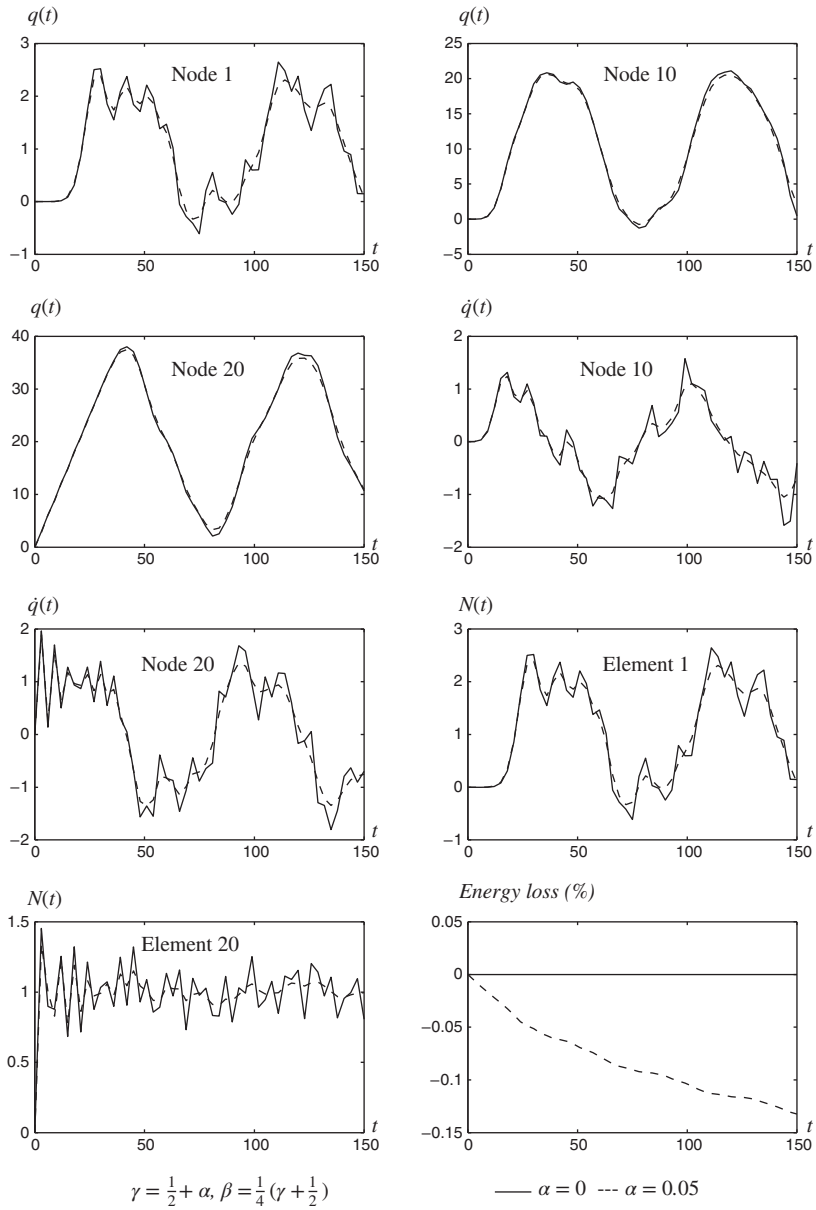


Figure 7.12 Newmark method: transient response of a clamped–free bar, step size $h = 3.0$.

- The small numerical damping ($\alpha = 0.05$) introduced in the second analysis slightly alters the displacement response, whereas it significantly affects the velocities and the stress results.
- The energy balance is strictly zero in the absence of numerical damping ($\gamma = \frac{1}{2}, \beta = \frac{1}{4}$). In the case when $\alpha = 0.05$, its evolution shows that after two computed periods, about 15% of the energy put into the system by the excitation has been dissipated.

The same transient response is then computed using also the Hilber-Hughes-Taylor and the Generalized- α algorithms on a twice longer time interval with numerical damping parameters corresponding to $\rho_\infty = 0.905$. Comparing the solution to the previous results, we observe that the energy loss during the time interval induced by the HHT and Generalized- α methods is significantly smaller, as shown by Figure 7.13. It is already about three times smaller with the HHT algorithm, and about ten times smaller with Generalized- α using the same step size and imposing the same asymptotic spectral radius.

In order to better visualize the effect of the different integration schemes, the same problem (with the same total length L) has been recomputed for 80 elements. Details of the response are shown in Figure 7.14 where a zoom on the displacement versus time at mid-length is presented, showing that all displacement responses are quite close. One can however notice the higher decrease of the response amplitude using Newmark's method with damping.

Figure 7.15 shows a zoom on the velocity at the tip of the bar for the first part of the response. It indicates a significantly larger discrepancy between the velocity responses generated by the different algorithms. Newmark without damping and Generalized- α are very close, while Newmark with damping tends to smooth rather heavily the velocity response.

Let us notice, however, that a stable response is not necessarily an accurate response. In particular, the oscillations observed on the velocities in Figure 7.15 are not physical but are in fact linked to sampling by the algorithm. To be convinced of it, the same velocity response has been computed with time step 20 times smaller ($h = 0.15$), which allows us to capture the high frequency content of the model. Figures 7.16 and 7.17 show the velocity curve obtained with

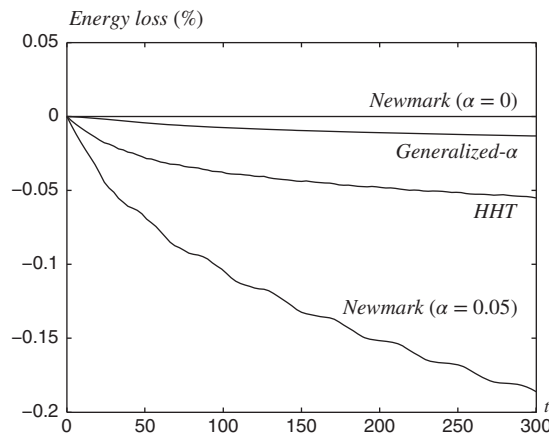


Figure 7.13 Energy losses induced by Newmark, HHT and Generalized- α methods with same asymptotic radius $\rho_\infty = 0.905$, step size $h = 3.0$.

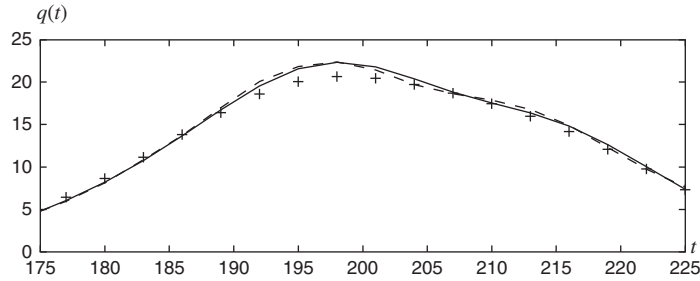


Figure 7.14 Zoom on displacement ($t \in [175, 225]$) at mid-length by Newmark (+), HHT (—) and Generalized- α (---) methods with same asymptotic radius $\rho_\infty = 0.905$, step size $h = 3.0$.

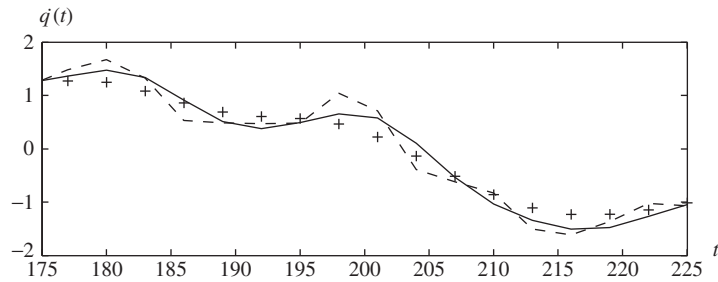


Figure 7.15 Zoom on velocity ($t \in [175, 225]$) at the tip computed by Newmark (+), HHT (—) and Generalized- α (---) methods with same asymptotic radius $\rho_\infty = 0.905$, step size $h = 3.0$.

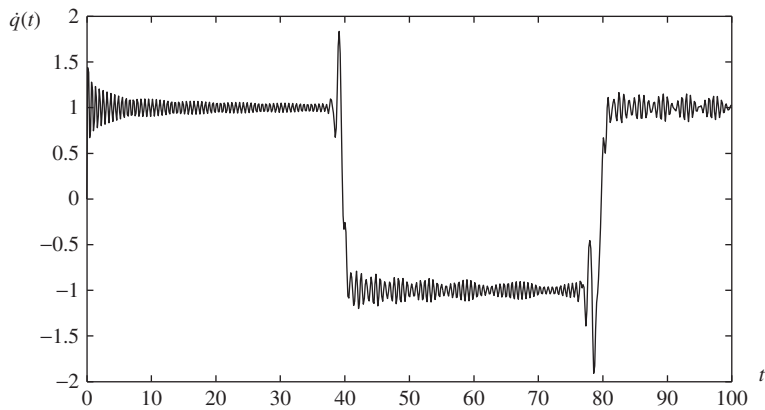


Figure 7.16 Zoom on velocity ($t \in [0, 100]$) at the tip computed by Generalized- α method with time step $h = 0.15$.

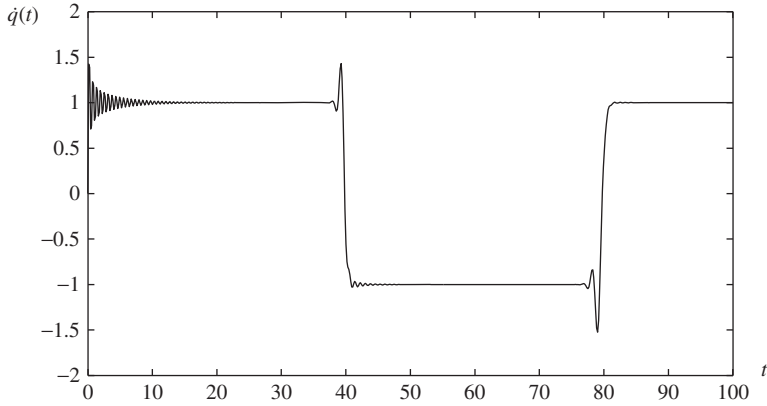


Figure 7.17 Zoom on velocity ($t \in [0, 100]$) at the tip computed by HHT method with time step $h = 0.15$.

Generalized- α and HHT methods on the same time interval. The ripples at low frequency have disappeared, and the velocity curve now exhibits the wave propagation nature of the solution. We thus conclude that the response with large time steps was stable and provides correct order of magnitude and fundamental frequency of the solution, but its accuracy is strongly affected by a too low time sampling.

7.5 Explicit time integration using the central difference algorithm

7.5.1 Algorithm in terms of velocities

Let h_{n+1} be the time step between t_n and t_{n+1} :

$$h_{n+1} = t_{n+1} - t_n \quad (7.170)$$

It is readily seen that the central difference algorithm, i.e. Newmark's scheme with $\gamma = \frac{1}{2}$ and $\beta = 0$,

$$\dot{q}_{n+1} = \dot{q}_n + \frac{h_{n+1}}{2} (\ddot{q}_n + \ddot{q}_{n+1}) \quad (7.171)$$

$$q_{n+1} = q_n + h_{n+1} \dot{q}_n + \frac{h_{n+1}^2}{2} \ddot{q}_n \quad (7.172)$$

can be put in an equivalent three-step form. We only need to express the displacement relationship (7.172) at the preceding time step:

$$q_n = q_{n-1} + h_n \dot{q}_{n-1} + \frac{h_n^2}{2} \ddot{q}_{n-1}$$

By dividing (7.172) by h_{n+1} and the latter relation by h_n , and then subtracting them, we obtain:

$$\frac{q_{n+1} - q_n}{h_{n+1}} - \frac{q_n - q_{n-1}}{h_n} = \dot{q}_n - \dot{q}_{n-1} + \frac{1}{2} (h_{n+1} \ddot{q}_n - h_n \ddot{q}_{n-1})$$

Furthermore, taking account of the velocity relationships (7.171) at the previous time step:

$$\dot{\mathbf{q}}_n = \dot{\mathbf{q}}_{n-1} + \frac{h_n}{2} (\ddot{\mathbf{q}}_n + \ddot{\mathbf{q}}_{n-1})$$

we get:

$$\ddot{\mathbf{q}}_n = \frac{h_n (\mathbf{q}_{n+1} - \mathbf{q}_n) - h_{n+1} (\mathbf{q}_n - \mathbf{q}_{n-1})}{h_{n+\frac{1}{2}} h_n h_{n+1}} \quad (7.173)$$

where

$$h_{n+\frac{1}{2}} = \frac{h_n + h_{n+1}}{2}$$

Equation (7.173) allows us to express the acceleration in terms of displacements at three successive instants, without explicit velocity evaluation.

For a constant time step h , Equation (7.173) reduces to the well-known classic expression:

$$\ddot{\mathbf{q}}_n = \frac{\mathbf{q}_{n+1} - 2\mathbf{q}_n + \mathbf{q}_{n-1}}{h^2} \quad (7.174)$$

However, from the algorithmic point of view, it is more efficient to take the velocity at half-time intervals as an intermediate variable:

$$\dot{\mathbf{q}}_{n+\frac{1}{2}} = \dot{\mathbf{q}}(t_{n+\frac{1}{2}}) = \frac{1}{h_{n+1}} (\mathbf{q}_{n+1} - \mathbf{q}_n) \quad (7.175)$$

in which case the interpolation formula (7.173) becomes:

$$\ddot{\mathbf{q}}_n = \frac{1}{h_{n+\frac{1}{2}}} (\dot{\mathbf{q}}_{n+\frac{1}{2}} - \dot{\mathbf{q}}_{n-\frac{1}{2}}) \quad (7.176)$$

The corresponding algorithm flowchart for the undamped linear case is given in Figure 7.18.

Note the following items:

- Solving the linear system of equations arising from the computation of accelerations becomes trivial when lumped mass matrices are used.
- In the presence of damping forces the computation becomes more expensive since, even when a lumped mass matrix is used, a system needs to be solved (as can be seen from the general time-stepping form (7.41) with $\gamma = 0.5$, $\beta = 0$). This arises from the fact that the central difference scheme is explicit in the displacements, yet implicit in velocities (Newmark's formulas (7.40)). However, in many engineering problems, the damping forces are small and can be included in the integration scheme of Figure 7.18 by performing fixed-point iterations at each time step, i.e. by considering it as an external force first computed with the velocities of the previous time step and then updated with the new acceleration in further iterations, convergence being achieved rapidly if the damping is small.
- Extending the method to nonlinear systems is straightforward since nonlinear forces may be computed explicitly (see Section 7.6.1).

As already mentioned in 7.2.8 (see Table 7.1), the central difference algorithm is equivalent to the Newmark method when $\gamma = \frac{1}{2}$, $\beta = 0$, and its stability boundary in the frequency domain

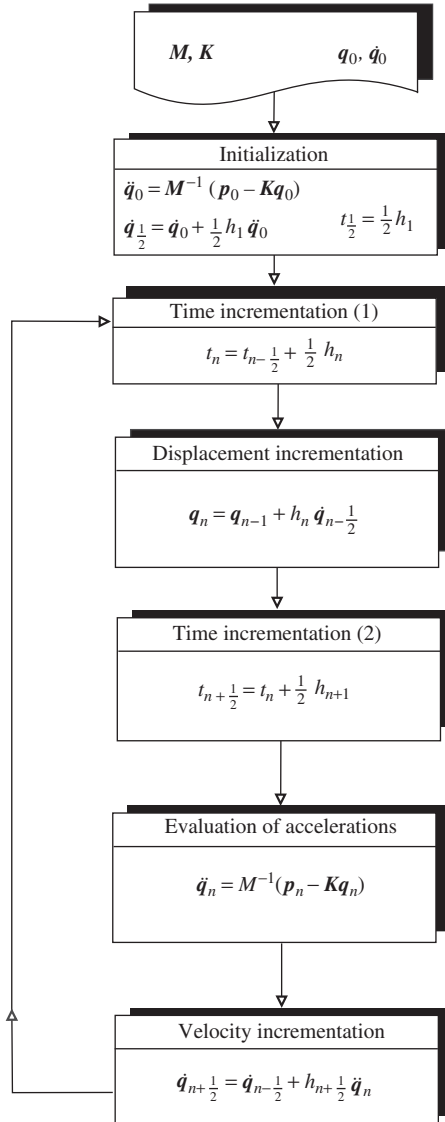


Figure 7.18 Flowchart of the central difference algorithm.

is such that $\omega_{cr}h \leq 2$ where ω_{cr} is the highest frequency contained in the model. This stability condition for the central difference scheme is known as the *Courant condition*. In finite element computations, ω_{cr} is taken as the highest of the eigenfrequencies of the individual elements since it can be shown that it corresponds to an upper bound to the eigenfrequencies of the complete model.

7.5.2 Application example: the clamped–free bar excited by an end load

Let us again consider the example of Sections 4.3.1 and 7.4.1 dealing with a clamped–free bar of unit nondimensional characteristics (Figure 7.11) and subjected stepwise to an end load. The numerical model is made out of $N = 20$ elements of equal length $\ell = \frac{L}{N}$, and this time it will be built using lumped mass matrices. Hence,

$$\mathbf{K} = \frac{EA}{\ell} \begin{bmatrix} 2 & -1 & & & & \\ -1 & 2 & -1 & & & \\ & -1 & 2 & \ddots & & \\ & & \ddots & \ddots & -1 & \\ & \mathbf{0} & & -1 & 2 & -1 \\ & & & & -1 & 1 \end{bmatrix} \quad \mathbf{M} = \frac{m\ell}{2} \begin{bmatrix} 2 & & & & & \\ & 2 & & & & \\ & & 2 & & & \\ & & & \ddots & & \\ & \mathbf{0} & & & 2 & \\ & & & & & 1 \end{bmatrix}$$

The system response to a step load on the bar end is now computed using the central difference algorithm as described above. The critical time step is obtained by considering the highest frequency of the finite element problem. It can be found if we go back to the analytical solution (4.146), Section 4.3.1, of the discretized system:

$$\omega_r = 2\sqrt{\frac{k}{M}} \sin\left(\frac{2r-1}{4N}\pi\right) \quad r = 1, 2, \dots, N \quad (7.177)$$

Substituting in the latter relation $k = EA/\ell$ and $M = m\ell$, we find for $N = 20$ that $\omega_{\max} = \omega_{cr} = 1.99846$ and thus a critical time step of:

$$h_{cr} = 1.00077$$

Three different time-step values have been used:

- $h = 1$, which is only slightly smaller than the critical time step. This time step is related to the upper bound of the maximum frequency obtained by considering an isolated element. Indeed, $\omega_{upper} = 2$ is the frequency deduced from the eigenfrequency equation:

$$\frac{EA}{\ell} \begin{bmatrix} 1 & -1 \\ -1 & 1 \end{bmatrix} \begin{bmatrix} q_1 \\ q_2 \end{bmatrix} = \omega^2 \frac{m\ell}{2} \begin{bmatrix} 1 & 0 \\ 0 & 1 \end{bmatrix} \begin{bmatrix} q_1 \\ q_2 \end{bmatrix}$$

where $\frac{EA}{m\ell^2} = 1$. Note that the upper bound would also be found from (7.177) if N tends to infinity. Remembering that the eigenfrequency of an element is $2\sqrt{3}$ for a consistent mass matrix (Section 7.4.1), one observes once more that using a diagonal mass matrix lowers the eigenspectrum (see Section 5.3.1).

- $h = 0.707$ which is well inside the stability domain of the time-integration method.
- $h = 1.0012$, slightly beyond the stability limit.

Let us analyze the displacement response curves at nodes 1, 10 and 20, the velocity curves at node 10 and the axial stress curves in elements 1 and 20. From Figures 7.19 and 7.20, we can make the following observations:

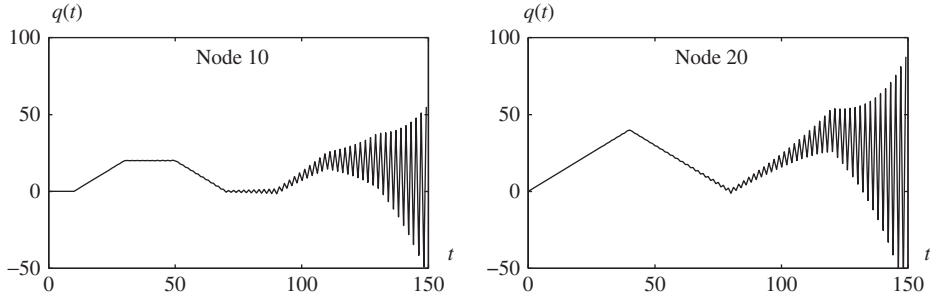


Figure 7.20 The central difference method: transient response of a clamped–free bar, time step $h = 1.0012$ higher than the stability limit.

would remain stable but small ripples would also be seen. Hence the time step $h = 1$ is special as will be discussed in the next section.

- For $h = 1.0012$, the unstable behaviour of the numerical solution is clearly apparent in Figure 7.20.

7.5.3 Restitution of the exact solution by the central difference method

The preceding example showed that the central difference algorithm possesses the remarkable property of restoring the exact solution when the so-called *Courant condition* equality $\omega_{upper}h = 2$ is fulfilled, ω_{upper} being the upper bound of the model eigenfrequency spectrum.

This numerical behaviour can be explained by comparing the exact solution of the free vibration of a bar to the analytical expression of the numerical solution for the discretized free vibration equation of motion developed with respect to time and space.

To find the analytical expression of the numerical solution computed by the central difference scheme, let us call $q_{j,n}$ the displacement $q(x, t)$ at $x = x_j$ on the model at time $t = t_n$. Except for the boundary conditions, the degree of freedom $q_{j,n}$ is driven by the following equation discretized with respect to time by the central difference formula:

$$\frac{EA}{\ell} (-q_{j-1,n} + 2q_{j,n} - q_{j+1,n}) + \frac{m\ell}{h^2} (q_{j,n+1} - 2q_{j,n} + q_{j,n-1}) = 0 \quad (7.178)$$

Let us take as solution the general expression for chain-type systems:

$$q_{j,n} = \sin(j\mu + \phi) [a \cos n\theta + b \sin n\theta] \quad (7.179)$$

where the term $\sin(j\mu + \phi)$ represents the space component of the solution and $a \cos n\theta + b \sin n\theta$ is the time function. Comparing this expression to the exact harmonic solution for the free vibration of the relevant continuous system, we deduce that $n\theta = \bar{\omega}t = n\bar{\omega}h$, yielding:

$$\bar{\omega} = \frac{\theta}{h} \quad (7.180)$$

which can be looked at as the numerical frequency resulting from the time integration of the lumped finite element model by the central-difference scheme.

By introducing the general form (7.179) into the discretized equation of motion (7.178) and denoting $\lambda^2 = \frac{m\ell^2}{EAh^2}$ we obtain:

$$2 \left[(1 - \cos \mu) - \lambda^2 (1 - \cos \theta) \right] q_{j,n} = 0$$

Thus we find the relationship between the time parameter θ and the space parameter μ to be

$$1 - \cos \mu = \lambda^2 (1 - \cos \theta) \quad (7.181)$$

The parameter μ can be determined by making use of the homogeneous boundary condition in space (see Section 4.3.1). We find:

$$\mu_r = \frac{2r-1}{N} \frac{\pi}{2} \quad r = 1, 2, \dots \quad (7.182)$$

The corresponding value of the time parameter θ is then deduced from (7.181):

$$1 - \cos \mu_r = \lambda^2 (1 - \cos \theta_r)$$

and, in the case $\lambda^2 = 1$ corresponding to the fulfillment of Courant's condition,

$$\theta_r = \mu_r$$

Since the time step h is then equal to:

$$h = \sqrt{\frac{m\ell^2}{EA}} \quad (7.183)$$

the numerical frequencies resulting from time integration of the lumped model are:

$$\bar{\omega}_r = \frac{\theta_r}{h} = \frac{2r-1}{N} \frac{\pi}{2} \sqrt{\frac{EA}{m\ell^2}} \quad r = 1 \dots N$$

and in terms of the total length $L = N\ell$,

$$\bar{\omega}_r = (2r-1) \frac{\pi}{2} \sqrt{\frac{EA}{mL^2}} \quad (7.184)$$

In this case, *the numerical frequency $\bar{\omega}_r$ resulting from the time integration of the lumped finite element model by the central-difference scheme coincides with the r^{th} eigenfrequency of the continuous system.* It shows that, for an appropriate time step, the algorithm has the capacity of restoring the exact physical behaviour of the system. This property explains the numerical results of the Section 7.5.2.

It is worthwhile to observe that the time step (7.183) is the time required for a longitudinal wave to travel through an element of length ℓ , since its propagation speed is:

$$c = \sqrt{\frac{EA}{m}}$$

Hence, the Courant condition states no information should travel through more than one element during the time interval h .

Another way to understand this result is to say that the errors arising from the integration scheme, from the finite element discretization and from the mass lumping exactly cancel in the case of the bar model composed of equal finite elements. Indeed, the numerical frequency associated with the eigenfrequency r of the finite element model can be computed directly from the invariants (7.55a) and (7.55b) of the amplification matrix for the r -th normal equation. Setting $\gamma = \frac{1}{2}$, $\beta = 0$ and $\varepsilon = 0$, we get:

$$D = 1 \quad I_1 = 1 - \frac{1}{2}\omega_r^2 h^2 \quad I_2 = 1$$

and Equations (7.99a–7.99b) yield thus the results:

$$\bar{\varepsilon}_r = 0 \quad \text{and} \quad \tan(h\bar{\omega}_r) = \frac{\omega_r h \sqrt{1 - \frac{\omega_r^2 h^2}{4}}}{1 - \frac{\omega_r^2 h^2}{2}} \quad (7.185)$$

Considering expression (7.177) of the eigenfrequencies of the lumped finite model and calling $\omega_{r,ex}$ the exact eigenfrequency (7.184) of the continuous bar model, we can write:

$$\omega_r = 2 \sin(\omega_{r,ex}/2) \quad (7.186)$$

where we assume for simplicity that $\frac{EA}{m\ell^2} = 1$ so that the critical time step is equal to 1. Substituting in (7.185) and setting $h = 1$ yields:

$$\bar{\omega}_r = \arctan\left(\frac{2 \sin \frac{\omega_{r,ex}}{2} \cos \frac{\omega_{r,ex}}{2}}{1 - 2 \sin^2 \frac{\omega_{r,ex}}{2}}\right) = \omega_{r,ex} \quad (7.187)$$

This shows that for all eigenfrequencies, the overestimation of the eigenspectrum due to the integration scheme and the underestimation due to the discretization and lumping of the model compensate one another. For this reason and because the explicit scheme propagates information only from one node to another during a time step, the numerical solution corresponds to the exact response for a bar model made of elements of equal length and for a lumped mass when h is taken as the Courant limit. Such behaviour is lost when using a consistent mass model which has for effect to generate wave dispersion. In general, however, for practical models (multidimensional, unequal elements, etc.), the numerical response will not be exact when one applies the central difference scheme with lumped mass for such a time step. However, it still seems appropriate to combine lumped mass and central difference time integration because the integration algorithm as outlined in Figure 7.18 then becomes trivial.

Therefore, in impact analysis where wave propagation phenomena appear to be significant, it is common practice to use the explicit central difference algorithm together with a lumped mass matrix, and to choose h to verify the Courant condition. However, the main drawback is that h happens to be so small that the number of steps to compute is huge and, although performing one explicit integration step is inexpensive, the actual computing time may become prohibitive.

Finally, let us note that this integration technique is also commonly applied to nonlinear systems because, in addition to the advantages described above, it only implies explicit calculation of nonlinear forces and therefore is straightforward to implement. One should, however, be aware of the fact that the stability condition of the integration scheme relates to the linear

case and that, strictly speaking, Courant's condition is no longer relevant. For this reason its use should be considered with care, especially when significant nonlinear effects appear between two time steps.

7.6 The nonlinear case

This presentation outlines basic notions for solving nonlinear dynamic equations, without discussing in detail the actual nature of the nonlinearities, which can be either of geometric or of material origin.

Let us consider the case in which the equations which drive the transient response of the structure behaving in a nonlinear manner can be stated in the general form (Gérardin *et al.* 1987):

$$\begin{cases} M\ddot{q} + f(q, \dot{q}) = p(q, t) \\ q_0, \dot{q}_0 \quad \text{given} \end{cases} \quad (7.188)$$

It is assumed that the inertia coefficients do not depend on the configuration. This assumption implies that the reference state is fixed and that the motion is described in terms of Cartesian coordinates.

The expression $f(q, \dot{q})$ represents the internal forces of the structure. Generally speaking, it is a function of displacements and velocities. It includes both the elastic forces and the internal dissipation forces. Its calculation is performed at the element level by integrating over the volume the stresses $\sigma(\epsilon, \dot{\epsilon})$, which are nonlinear functions of the strains ϵ and of the strain rates $\dot{\epsilon}$:

$$f_e(q, \dot{q}) = \int_V B_e^T \sigma(\epsilon, \dot{\epsilon}) dV \quad (7.189)$$

If the system remains linear from a geometric point of view, B_e is the element strain matrix (5.7) which relates the local strains to the nodal displacements. In the geometrically non-linear case, B_e expresses the relationship between increments of the latter two quantities. The expression $p(q, t)$ is the external force term. In the general case, it may be a function of the system displacements.

As for the linear case, integrating the transient response requires a preliminary estimate of the solution behaviour for the equations of motion (7.188). The oscillatory part of the solution may continually change, depending on the loading and/or on the nonlinearities. Whenever the response is driven by high frequency terms, the problem is of the wave propagation type, whereas in the case of lower frequencies being dominant it belongs to classical dynamics of structures.

The problem type dictates whether it is best to resort to an explicit or to an implicit integration scheme.

7.6.1 The explicit case

When making use of an explicit integration algorithm, the nonlinearities of the system do not by themselves increase the difficulty of the integration compared to the linear case. Indeed, the dynamic equilibrium equations can be put in the form:

$$\ddot{q} = M^{-1} (p(q, t) - f(q, \dot{q})) \quad (7.190)$$

showing that, by explicitly predicting the displacements and the velocities, one can use the equilibrium equations to compute the accelerations without iterating on the system non-linearity. Hence, the explicit integration scheme in Figure 7.18 remains valid for non-linear problems. The only alteration to be made – even for the linear case – is to provide an explicit prediction of velocities when the internal forces actually depend on strain velocities (viscous damping, viscoplastic material, etc.).

A large amount of literature exists on the development of explicit finite element codes based on the central difference formula and its application to a class of nonlinear problems referred to as *fast dynamics*.

In particular, a full description of the implementation of the explicit central difference method for the analysis of structures undergoing impact loading and large deformation is presented in (Belytschko and Hughes 1983).

Worthwhile also mentioning is the comprehensive set of notes (Casadei 2010) covering not only the principles method, but also its implementation and application to nonlinear problems of fluid–structure interaction.

7.6.2 The implicit case

When one is applying an implicit integration scheme, the displacements, velocities and accelerations involved in the equilibrium Equations (7.188) can no longer be considered to be independent, since they are linked to one another by the integration operator. Let us rewrite the equilibrium equations as a relationship in terms of the displacements $\mathbf{q}(t)$:

$$\mathbf{r}(\mathbf{q}) = \mathbf{M}\ddot{\mathbf{q}}(t) + \mathbf{f}(\mathbf{q}, \dot{\mathbf{q}}) - \mathbf{p}(\mathbf{q}, t) = \mathbf{0} \quad (7.191)$$

where \mathbf{r} is the residual vector. Newmark's time-integration relationships may be inverted in the following way:

$$\begin{aligned} \ddot{\mathbf{q}}_{n+1} &= \frac{1}{\beta h^2}(\mathbf{q}_{n+1} - \mathbf{q}_{n+1}^*) \\ \dot{\mathbf{q}}_{n+1} &= \dot{\mathbf{q}}_{n+1}^* + \frac{\gamma}{\beta h}(\mathbf{q}_{n+1} - \mathbf{q}_{n+1}^*) \end{aligned} \quad (7.192)$$

where the predictors are deduced from (7.40) by setting $\ddot{\mathbf{q}}_{n+1} = \mathbf{0}$:

$$\begin{aligned} \dot{\mathbf{q}}_{n+1}^* &= \dot{\mathbf{q}}_n + (1 - \gamma)h\ddot{\mathbf{q}}_n \\ \mathbf{q}_{n+1}^* &= \mathbf{q}_n + h\dot{\mathbf{q}}_n + \left(\frac{1}{2} - \beta\right)h^2\ddot{\mathbf{q}}_n \end{aligned} \quad (7.193)$$

By substituting (7.192) into (7.191), the residual equation is expressed in terms of \mathbf{q}_{n+1} only:

$$\mathbf{r}(\mathbf{q}_{n+1}) = \mathbf{0} \quad (7.194)$$

Most of the methods for solving a set of nonlinear equations like (7.194) make use of linearization techniques.

Let us denote \mathbf{q}_{n+1}^k an approximate value of \mathbf{q}_{n+1} resulting from iteration k . In the neighbourhood of this value the residual equation can be replaced with enough accuracy by the linear expression:

$$\mathbf{r}_L(\mathbf{q}_{n+1}^{k+1}) = \mathbf{r}(\mathbf{q}_{n+1}^k) + \mathbf{S}(\mathbf{q}_{n+1}^k)(\mathbf{q}_{n+1}^{k+1} - \mathbf{q}_{n+1}^k) \quad (7.195)$$

in terms of the Jacobian (also called iteration) matrix:

$$S(q_{n+1}^k) = \left[\frac{\partial r}{\partial q} \right]_{q_{n+1}^k} \quad (7.196)$$

Its expression is:

$$S(q) = \frac{\partial f}{\partial q} + \frac{\partial f}{\partial \dot{q}} \frac{\partial \dot{q}}{\partial q} + M \frac{\partial \ddot{q}}{\partial q} - \frac{\partial p}{\partial q} \quad (7.197)$$

and its different components have the following meanings:

$\frac{\partial f}{\partial q}$ is the variation of the internal forces with respect to displacements
and thus represents the tangent stiffness matrix K^t

$\frac{\partial f}{\partial \dot{q}}$ is the variation of the internal forces with respect to velocities and
thus represents the tangent damping matrix C^t

$\frac{\partial p}{\partial q}$ describes the dependence of external loads on the displacements
of the system.

Unlike the first two terms, the last one is generally nonsymmetric and is very often omitted so as to preserve the symmetry of the iteration matrix. By making use of the definitions above and noticing that the integration relationships (7.192) yield:

$$\frac{\partial \ddot{q}}{\partial q} = \frac{1}{\beta h^2} I \quad \text{and} \quad \frac{\partial \dot{q}}{\partial q} = \frac{\gamma}{\beta h} I$$

the iteration matrix is finally given by:

$$S(q) = K^t + \frac{\gamma}{\beta h} C^t + \frac{1}{\beta h^2} M \quad (7.198)$$

The nonlinear system (7.194) is then solved in an iterative manner by means of the Newton-Raphson method. At iteration k of the time step $n+1$, the displacement, velocity and acceleration approximations $(q_{n+1}^k, \dot{q}_{n+1}^k, \ddot{q}_{n+1}^k)$ are corrected and become $(q_{n+1}^k + \Delta q^k, \dot{q}_{n+1}^k + \Delta \dot{q}^k, \ddot{q}_{n+1}^k + \Delta \ddot{q}^k)$.

The displacement corrections are computed by solving the linearized equations:

$$S \Delta q^k = -r(q_{n+1}^k) \quad (7.199)$$

Then the velocity and acceleration corrections are found by writing the integration relationships (7.192) as:

$$\begin{aligned} \Delta \ddot{q}^k &= \frac{1}{\beta h^2} \Delta q^k \\ \Delta \dot{q}^k &= \frac{\gamma}{\beta h} \Delta q^k \end{aligned} \quad (7.200)$$

These relationships lead to the time integration scheme given by the flowchart in Figure 7.21. It contains within the time loop an iteration loop on the equilibrium: the latter is stopped when

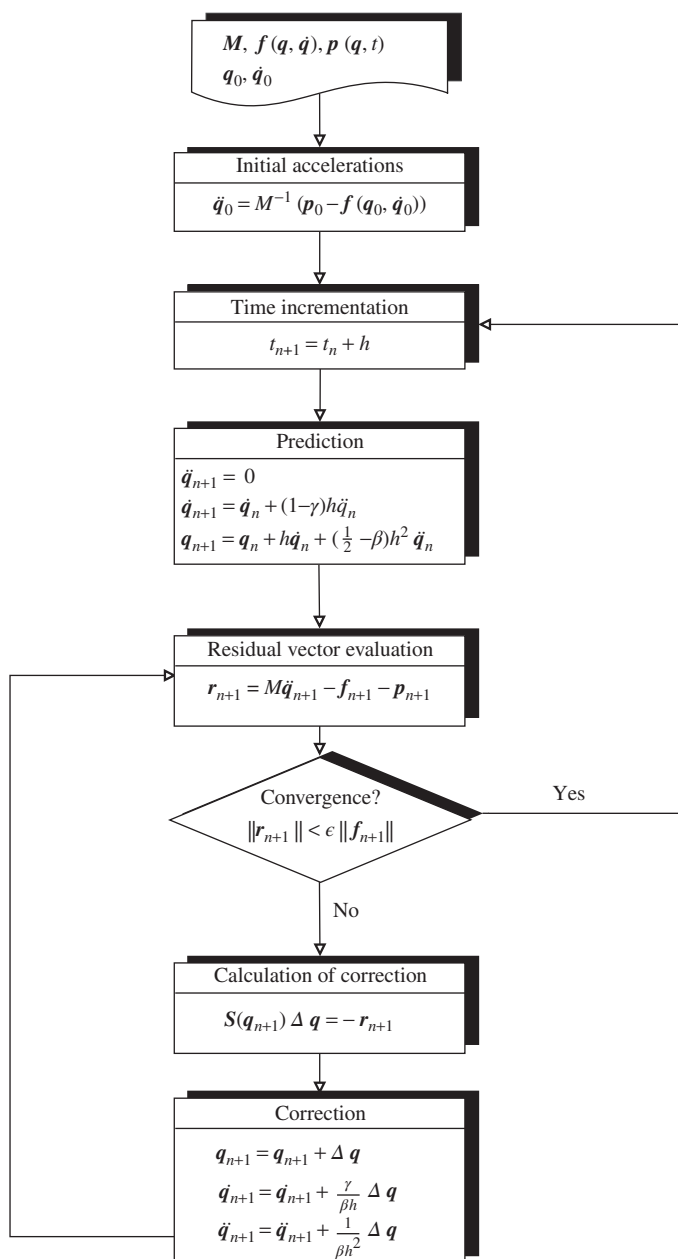


Figure 7.21 Flowchart of the Newmark integration scheme for a nonlinear system.

the residual value of the equilibrium equations has dropped below an accuracy threshold:

$$\|\mathbf{r}(\mathbf{q}_{n+1}^k)\| < \epsilon \|\mathbf{f}\|$$

where $\|\mathbf{f}\|$ is a measure of the forces within the system.

The computational procedure as described by Figure 7.21 gives rise to the following comments:

1. At each time step, the iteration has to be started from a prediction of the displacements, velocities and accelerations. Experience has shown expression (7.193), corresponding to $\ddot{\mathbf{q}}_{n+1}^* = \mathbf{0}$, to be a starting prediction that leads to a fairly stable iteration procedure.
2. Because the Newton-Raphson method is affected by a convergence radius in the vicinity of the solution, convergence of the iteration procedure is ensured only near the solution of (7.194). Hence in the nonlinear case, the time step not only drives the accuracy of the integration but also governs the stability of the iteration process. Thus, choosing an adequate time step is a critical issue. Techniques have been developed to automatically determine a suitable value according to the response characteristics (Cassano and Cardona 1991).
3. The set of linear equations for the calculation of the correction terms implies computing the Jacobian matrix (7.198). Since it varies according to the state of the system, the Jacobian matrix must be recomputed at every iteration. The setup and the solving of the system (7.199) contributes greatly to the computing cost. Therefore, lots of variants of the method exist in order to use only an approximation of the Jacobian matrix and thereby to reduce the cost of an iteration.

Example 7.2 The elastic pendulum

Let us consider the elastic pendulum as shown in Figure 7.22. It has two degrees of freedom: taking the absolute coordinates (x, y) as generalized coordinates, its kinetic and potential energies are:

$$\begin{aligned}\mathcal{T} &= \frac{1}{2}m(\dot{x}^2 + \dot{y}^2) \\ \mathcal{V} &= -mgx + \frac{1}{2}k(\ell - \ell_0)^2\end{aligned}$$

where ℓ_0 is the length of the unstretched pendulum and $\ell = \sqrt{x^2 + y^2}$ its instantaneous length.

Working out the equations of motion, we get:

$$m\ddot{x} + k(\ell - \ell_0)\frac{x}{\ell} - mg = 0 \quad m\ddot{y} + k(\ell - \ell_0)\frac{y}{\ell} = 0$$

These equations are highly nonlinear due to the expression of the pendulum length. The tangent stiffness matrix is given by:

$$\mathbf{K}^t = \begin{bmatrix} k\left(1 - \frac{\ell_0}{\ell} + \frac{\ell_0 x^2}{\ell^3}\right) & k\frac{\ell_0 xy}{\ell^3} \\ k\frac{\ell_0 xy}{\ell^3} & k\left(1 - \frac{\ell_0}{\ell} + \frac{\ell_0 y^2}{\ell^3}\right) \end{bmatrix}$$

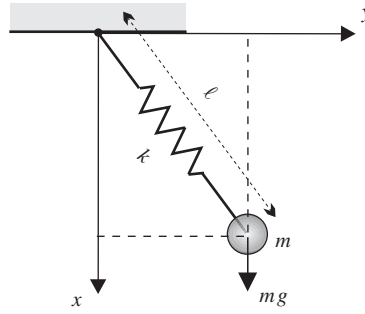


Figure 7.22 The elastic pendulum.

The response of the system has been computed applying the Newmark method ($\gamma = \frac{1}{2}$, $\beta = \frac{1}{4}$) and the numerical values are:

$$m = 1 \text{ kg} \quad k = 30 \text{ N/m}, \quad g = 10 \text{ m/s}^2, \quad \ell_0 = 1 \text{ m}$$

$$h = 3 \times 10^{-2} \text{ s} \quad \text{iteration threshold of } \|\mathbf{r}\| : mg \times 10^{-5},$$

$$\text{Initial state} \quad \begin{cases} x(0) = 0, & y(0) = 1.5 \text{ m} \\ \dot{x}(0) = \dot{y}(0) = 0 \end{cases}$$

The number of iterations on the equilibrium never exceeds 3 for the fairly small time step chosen in the example.

Figures 7.23–7.26 successively display:

- the displacement response $x(t)$ and $y(t)$ between $t = 0$ s and $t = 20$ s
- the corresponding velocities $\dot{x}(t)$ and $\dot{y}(t)$

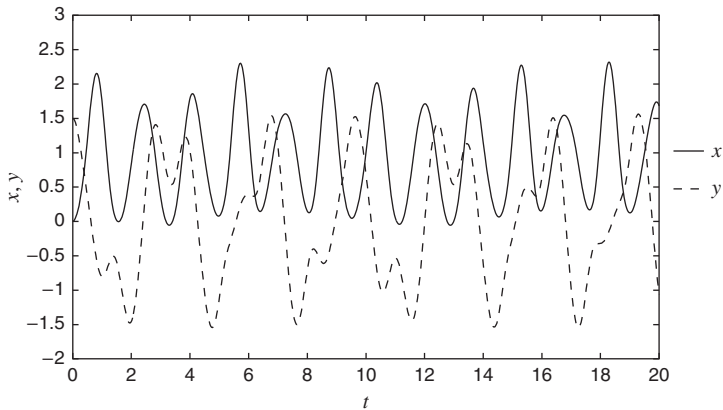


Figure 7.23 The elastic pendulum: x, y displacement response.

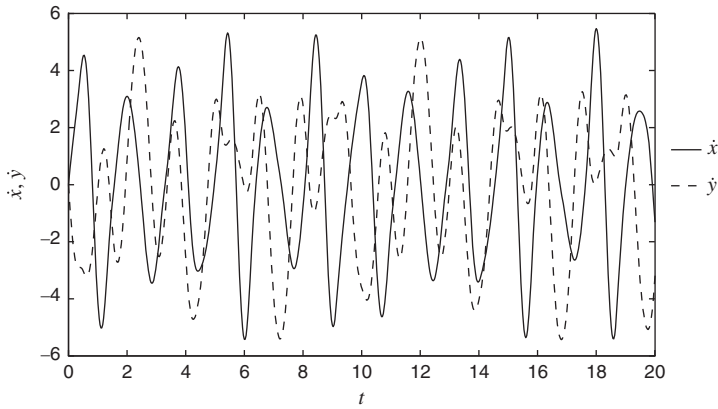


Figure 7.24 The elastic pendulum: velocities \dot{x} , \dot{y} .

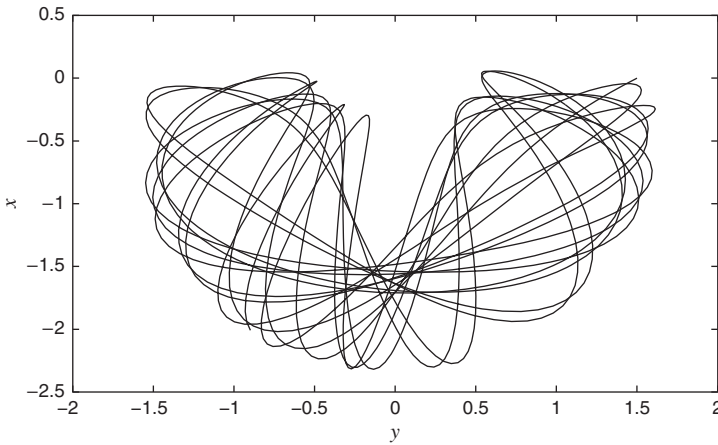


Figure 7.25 The elastic pendulum: trajectory of the pendulum.

- the pendulum trajectory in the plane (x, y)
- the phase space diagram (x, \dot{x}) and (y, \dot{y}) for the time interval $t = 0$ s to $t = 60$ s.

Let us finally notice that the motion of the system remains within the limits $[-1.5, 1.5]$ in the y direction and the maximum value of x is 2.35, which corresponds to the bounds of the pendulum under the combined effect of gravity and of the initial conditions.

The figures clearly point out the nearly periodic behaviour of the system even though it is highly nonlinear. The phase-space diagram of the y coordinate reveals two attraction zones centred on the extremum position of the unstretched pendulum.

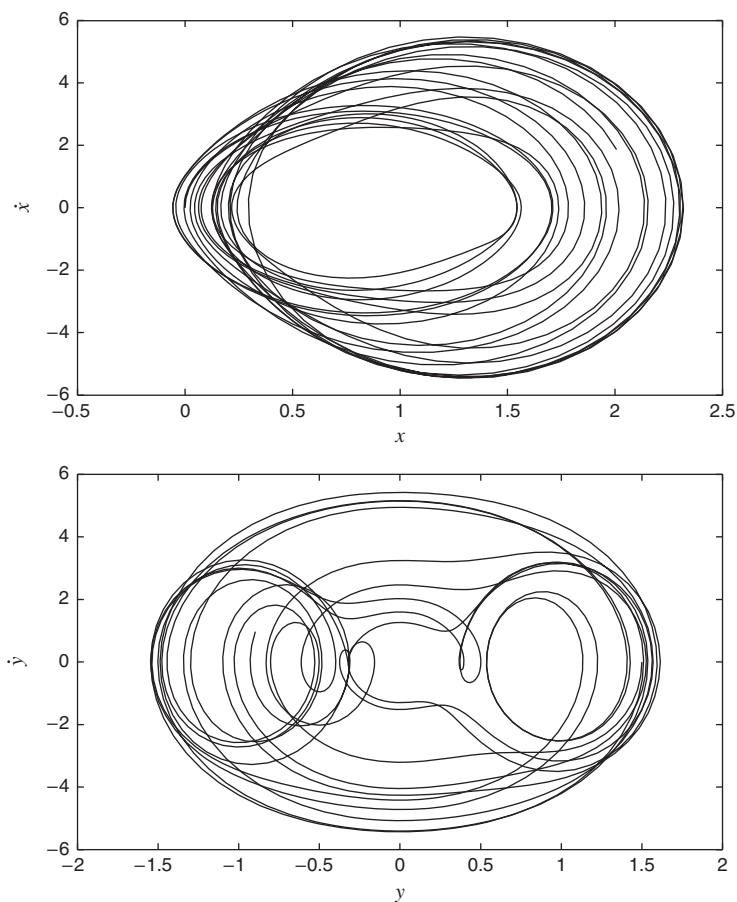


Figure 7.26 The elastic pendulum: phase-space diagrams.

7.6.3 Time step size control

Implicit case

Any time implicit integration algorithm such as Newmark and HHT requires the user to choose a time increment for the integration of the time equations. Adopting a priori a fixed time step size might raise some difficulties.

- if the time step is too large, some higher frequencies contribution of the response might be filtered out thus missing some important details. Moreover, the accuracy of the integration will be degraded and even lead, in some nonlinear cases, to instability of Newmark's scheme.
- if the time step is too small, the computational cost will increase with a waste of CPU resources, leading sometimes to unacceptable solution time.

- Changes of system physical behaviour over the time interval (e.g. load discontinuity, change of material properties due to material nonlinearity) might require local adaptation of time step size in order to maintain constant accuracy during the time integration process and successfully pass discontinuities in the time response.

In addition, an appropriate algorithm for time step size control might help the user to automatically select a suitable step size for a specific problem.

A time step adjustment during the numerical integration in time is generally based on some measure of the integration error brought in by the integration scheme. Recalling the remainder of the displacement approximation (7.39), the error made in a time step can be written as:

$$r = \left(\beta - \frac{1}{6} \right) h^3 \left| \frac{d\ddot{q}}{dt} \right| \quad (7.201)$$

and thus depends on a measure of the variation of acceleration within the time step. This quantity is not calculated (the time integration considering only up to the second order derivative of the solution) but it can be approximated. For example, if the finite difference scheme is used:

$$\frac{d\ddot{q}}{dt} = \frac{\ddot{q}(t+h) - \ddot{q}(t)}{h} \quad (7.202)$$

We are then able to give an estimation of the integration error:

$$r = \left(\beta - \frac{1}{6} \right) h^2 |\ddot{q}(t+h) - \ddot{q}(t)| = \left(\beta - \frac{1}{6} \right) h^2 \Delta \ddot{q} \quad (7.203)$$

The error is thus proportional to the square of the time step and to the jump of the acceleration over the time step. It has to be noted that this estimate is based on the approximation of the derivative of the acceleration with simple finite difference. The time step needs to be already small enough for this to be valid.

The time step h can then be adjusted during the time integration in order not to exceed a prescribed tolerance ϵ . It should be noted that for linear systems the time step adjustment strategy should keep the time step fixed for relatively long periods in order to avoid to re-compute and re-factorize the iteration matrix S too often and also to meet the stability criteria of the chosen integration scheme. For further details about automatic time step selection in the implicit case, see for instance (Géradin and Cardona 2001).

Explicit case

As shown earlier, the stable time step for the explicit scheme is very small and it is related to the time required for an elastic wave to cross an element. This feature makes this integration scheme suitable for high-frequency dynamic problems, such as impact and wave propagation. However, explicit codes are successfully used also for other applications, as for instance metal forming and spring-back calculations (spring back is the elastic recovery of a metal sheet that is plastically deformed during manufacturing, e.g. car body parts). These applications are characterized by slow dynamics and almost negligible inertial effects. However, the fact that no system of equations needs to be solved makes the explicit scheme an appealing alternative. The time step can be effectively increased (and therefore the computational cost

drops) through artificial mass scaling of the system. Recalling that the elastic wave speed c is proportional to:

$$c \propto \sqrt{\frac{E}{\rho}}$$

where E is the elastic modulus and ρ is the material density, the wave speed can be reduced (and thus the critical time step be increased) by scaling the density. This can be done selectively just on the critical elements. It should be noted that an increase of the density by a factor α results in an increase of the critical time step of a factor of only $\sqrt{\alpha}$. The solution should be checked after mass scaling in order to assure that the inertial effects are kept small.

7.7 Exercises

Problem 7.1 The application of the the trapezoidal rule in the form (7.27) to the single-degree-of-freedom undamped oscillator equation put in the state space form (7.22):

$$\dot{\mathbf{u}} = \mathbf{A}\mathbf{u}$$

allows us to describe the time integration process in the recurrence form:

$$\mathbf{u}_{n+1} = \mathbf{T}\mathbf{u}_n$$

where \mathbf{T} is the amplification matrix.

- Express matrix \mathbf{T} in terms of the system matrix \mathbf{A} and time step size h .
- Develop its closed form expression by making use of the explicit expression (7.24) for \mathbf{A} . Determine on which nondimensional parameter it depends.
- Compute its determinant, and relate the result obtained to the stability behaviour of the trapezoidal rule as displayed on Figure 7.2.
- Compute its eigenvalues, and relate the result obtained to the time shape of the response as displayed on Figure 7.2. Predict how the numerical response will deteriorate when increasing the time step size h .

Problem 7.2 The first time integration method that has been developed in the context of structural dynamics has been Houbolt's method. It is a 3-step backward implicit scheme for second-order differential equations:

$$\dot{\mathbf{y}} = \mathbf{f}(\mathbf{y}, \dot{\mathbf{y}}, t)$$

It is based on Lagrange interpolation of the response, taking thus the form:

$$\begin{aligned} h\dot{\mathbf{y}}_{n+1} &= \alpha_0 \mathbf{y}_{n+1} + \sum_{j=1}^3 \alpha_j \mathbf{y}_{n+1-j} \\ h\dot{\mathbf{y}}_{n+1} &= \gamma_0 \mathbf{y}_{n+1} + \sum_{j=1}^3 \gamma_j \mathbf{y}_{n+1-j} \end{aligned} \tag{P7.2.a}$$

You are asked:

- To determine the coefficients $(\alpha_i, \gamma_i, i = 0 \dots 3)$ through Lagrange interpolation of the solution and differentiation of the resulting polynomial $p_3(t)$.

- To express the difference equation obtained from the application of the scheme (P7.2.a) to the single DOF oscillator (7.89).
- Assuming that the solution is amplified in the form:

$$\eta_{n+1} = \lambda \eta_n$$

allows us to put the time-marching scheme so obtained in the form:

$$\mathbf{u}_{n+1} = \mathbf{T} \mathbf{u}_n \quad (\text{P7.2.b})$$

where \mathbf{u}_n is defined as the (3×1) state vector:

$$\mathbf{u}_n^T = [\eta_n \quad \eta_{n-1} \quad \eta_{n-2}] \quad (\text{P7.2.c})$$

Develop the explicit form of amplification matrix \mathbf{T} in terms of the parameters $(\omega h, \epsilon)$ and of the coefficients (α_i, γ_i) of the integration scheme (hint: make use of the trivial identity $\eta_n = \eta_n$).

- To compute numerically and plot the spectral radius of Houbolt's method versus ωh . Observe its asymptotic behaviour. Compare it to the spectral radius of the Generalized- α method for $\rho_\infty = 0.9$.
- To compute and plot the numerical damping ratio and the periodicity error. Perform again the same comparison with the Generalized- α method.
- To write down the computational flow to implement Houbolt's applied to the system of dynamic equations (7.1). Observe that the scheme is not self-starting since \mathbf{q}_{-1} and \mathbf{q}_{-2} are unknown. Try to develop a starting procedure to take into account the nonhomogeneous initial conditions.

Problem 7.3 Assuming that the response of the undamped 1-DOF oscillator under nonhomogeneous initial conditions is numerically integrated using Newmark's formula $(\gamma = \frac{1}{2}, \beta = \frac{1}{4})$, the difference equation:

$$x_{n+2} - 2I_1 x_{n+1} + I_2 x_n = 0 \quad (\text{P7.3.a})$$

allows us to compute the numerical response.

In order to assess the accuracy of the integration method, the *local truncation error* $e(\omega h)$ can be computed by plugging the exact solution into the difference equation:

$$x_{n+2, \text{ exact}} - 2I_1 x_{n+1, \text{ exact}} + I_2 x_{n, \text{ exact}} = e(\omega h) \quad (\text{P7.3.b})$$

- Develop the local truncation error through series expansion in ωh of Equation (P7.3.b) and observe its order of accuracy.
- Discuss the result obtained.

Problem 7.4 The mid-point rule introduced at page 549 is often adopted as integration method for nonlinear systems. Let us consider the particular case of a system with nonlinear, displacement-dependent restoring forces:

$$M\ddot{\mathbf{q}} + \mathbf{f}(\mathbf{q}) = \mathbf{p}(t)$$

as in Example 7.2. The purpose of the exercise is to lay out a time integration procedure based on the mid-point rule and apply it to the example. In order to do so:

- Define the acceleration at mid-interval as:

$$\ddot{\mathbf{q}}_{n+\frac{1}{2}} = \frac{1}{2} (\ddot{\mathbf{q}}_n + \ddot{\mathbf{q}}_{n+1})$$

and write the corresponding expression of velocities and displacements $\dot{\mathbf{q}}_{n+\frac{1}{2}}$ and $\mathbf{q}_{n+\frac{1}{2}}$.

- In order to develop the Newton-Raphson iteration procedure, express the relationship between increments:

$$\Delta \mathbf{q}_{n+\frac{1}{2}}, \quad \Delta \dot{\mathbf{q}}_{n+\frac{1}{2}} \quad \text{and} \quad \Delta \ddot{\mathbf{q}}_{n+\frac{1}{2}}$$

- Express the residual equation corresponding the dynamic equilibrium at mid-point.
- Define an iteration matrix such that:

$$S \Delta \mathbf{q}_{n+\frac{1}{2}}^k = -\mathbf{r}(\mathbf{q}_{n+\frac{1}{2}}^k) + O(\Delta^2)$$

- Establish a flowchart for the time integration procedure.
- Include in the flow a step corresponding to verification of energy conservation.
- Apply the resulting procedure to the system of Example 7.2 and implement it in a computer program.
- Run the computer code with the same data as those of Example 7.2. Observe the rate of convergence of the iteration procedure and check your results.
- Observe the energy balance over the period of integration.

References

- Arnold M and Brüls O 2007 Convergence of the generalized- α scheme for constrained mechanical systems. *Multibody System Dynamics* **18**(2), 185–202.
- Belytschko T and Hughes TJR 1983 *Computational Methods for Transient Analysis*. North-Holland.
- Cardona A and Géradin M 1989 Time integration of the equations of motion in mechanism analysis. *Computers and Structures* **33**(3), 801–820.
- Casadei F 2010 Numerical simulation of fast transient dynamic phenomena in fluid-structure systems. Proceedings of a course given at Universitat Politècnica de Catalunya, Barcelona, JRC.
- Cassano A and Cardona A 1991 A comparison between three variable-step algorithms for the integration of the equations of motion in structural dynamics. *Computational Mechanics*, **11**, 223–233.
- Chung J and Hulbert G 1993 A time integration algorithm for structural dynamics with improved numerical dissipation: the generalized- α method. *Journal of Applied Mechanics* **60**(2), 371–375.
- Gear C 1971 *Numerical Initial Value Problems in Ordinary Differential Equations*. Prentice Hall, Englewood Cliffs, NJ.
- Géradin M and Cardona A 2001 *Flexible Mutibody Dynamics: The Finite Element Method Approach*. John Wiley & Sons, Ltd, Chichester.
- Géradin M and Rixen D 1997 *Mechanical Vibrations—Theory and Application to Structural Dynamics* second edn. John Wiley & Sons, Inc. New York.
- Géradin M, Hogge M and Robert G 1987 Integration of linear and nonlinear dynamic problems In *Finite Element Handbook* (ed. Pilkey W) McGraw-Hill, Part 4, 1.4.
- Géradin M 1974 A classification and discussion of integration operators for transient structural response *AIAA 12th Aerospace Sciences Meeting*. Paper 74–105.
- Hilber HM, Hughes TJ and Taylor RL 1977 Improved numerical dissipation for time integration algorithms in structural dynamics. *Earthquake Engineering & Structural Dynamics* **5**(3), 283–292.
- Houbolt JC 1950 A recurrence matrix solution for the dynamic response of elastic aircraft. *Journal of the Aeronautical Sciences (Institute of the Aeronautical Sciences)* **17**, 540–550.
- Hughes TJR 1983 Analysis of transient algorithms with particular reference to stability behavior. *Computational methods for transient analysis (A 84-29160 12-64)*. Amsterdam, North-Holland, 1983, pp. 67–155.

- Hughes TJR 1987 *The Finite Element Method—Linear Static and Dynamic Finite Element Analysis*. Prentice Hall Inc., New Jersey.
- Lens EV, Cardona A and G  radin M 2004 Energy preserving time integration for constrained multibody systems. *Multibody System Dynamics* **11**(1), 41–61.
- Newmark N 1959 A method of computation for structural dynamics. *Journal of the Engineering Mechanics Division of ASCE* (85 (EM3)), 67–94. Proc. Paper 2094.
- Park KC 1975 An improved stiffly stable method for direct integration of nonlinear structural dynamics. *Journal of Applied Mechanics*, **42**(2), 464–470.

Author Index

- Abramowitz M., 32
Allemang R.J., 499
Argyris J.H., 7, 336
Arnold M., 548, 549
Arnoldi W.E., 415, 470, 472
Ashley H., 8, 336
- Bai Z., 487
Bampton M.C.C., 416, 480, 485
Barton M.V., 362
Bathe K.J., 8, 337, 417, 464, 466, 467
Batoz J.L., 8, 337, 392
Bauchau O.A., 8
Bauer F.L., 416
Belytschko T., 9, 565
Ben-Israel A., 453
Bennighof J.K., 487
Berthier P., 7
Biezeno C., 7
Biot M.A., 246
Bisplinghoff R.L., 8, 336
Blevins R.D., 359, 362
Brandt A., 8, 180
Brincker R., 9, 199
Brown D.L., 182, 499
Brüls O., 548, 549
Brzobohatý T., 458
- Cardona A., 8, 13, 44, 392, 548, 549, 567, 572
Carnoy E., 482, 489
Casadei F., 565
Cassano A., 567
Caughey T.K., 157
Chang C.J., 487
Chung J., 539, 546
Clough R.W., 7, 336
Collar A.R., 415, 425
Cook R., 337
Cooley J.W., 188
Courant R., 40, 42, 116, 117, 336
Craig R.R., 7, 416, 480, 485, 487
Crandall S.H., 7
Craveur J.C., 8, 337
Crede C.E., 7
Crisfield M.A., 337
Cuthill E., 450
- Dat R., 196
Debongnie J.F., 227
Del Pedro M., 7
den Hartog J.P., 7
Der Hagopian J., 7, 9
Dhatt G., 8, 337, 392
Dostál Z., 458

- Dowell E.H., 8
Duncan W.J., 415, 425
- Ewins D.J., 9, 180, 181
- Fahy F.J., 8
Farhat C., 444, 453, 458
Felippa C.A., 417
Ferraris G., 9
Fix G.J., 337
Formenti D.L., 190, 193
Försching H.W., 8
Forsythe G.E., 415
Fox L., 489
Fox R.L., 537, 538
Fracijs de Veubeke B.M., 7, 8, 116, 154,
166, 171–172, 336, 479, 489
Fragakis Y., 458
Francis J.G.F., 415, 467
Frazer R.A., 415, 425
Friswell M.I., 9, 499
Fung Y.C., 8, 220, 223, 281, 286, 316,
336
- Galerkin B.G., 336
Gallagher R.H., 337
Gao W., 487
Gardonio P., 8
Garvey S.D., 9
Gear C.W., 9, 514, 521
Genta G., 7, 9
George A., 450
Géradin M., 7, 8, 13, 44, 158, 212, 231, 243,
392, 396, 420, 436, 458, 482, 489,
517, 518, 528, 548–550, 564, 572
Givens W., 415
Goldstein H., 8, 13
Golub G.H., 9, 444
Grammel R., 7
Greville T.N.E., 453
Grimes R.G., 476
Guillaume P., 193
Guyan R.J., 416, 480
- Hagedorn P., 7, 311, 314
Halfman R.L., 8, 336
- Hamilton W.R., 23
Harris C.M., 7
Henrici P., 415, 489
Hestenes M.R., 415, 444
Heylen W., 9, 180
Hilber H.M., 539, 545, 546
Hilbert D., 40, 42, 54, 116, 117
Hogge M., 564
Holister G.S., 336
Holzer H., 143
Houbolt J.C., 517
Householder A.S., 9, 415, 434
Huck A., 7, 116, 154, 479, 482
Hughes T.J.R., 8, 9, 337, 362, 392,
517, 525, 529, 530, 539, 543,
551, 565
Hulbert G.M., 539, 546
Hurty W.C., 7
Hussey M., 7
- Imbert J.F., 8, 109
Irons B.M., 416, 452, 480
- Jacobi C.G.J., 415, 430
Jakobsson H., 487, 489
Janiaud D., 315
Jetteur P., 337
- Kane T.R., 14
Kardestuncer H., 8
Kato T., 489, 493
Kestens J., 489
Klapka I., 315
Kolsky H., 316
Komszik L., 9, 476
Kovàr P., 458
Kozubek T., 458
Krylov A.N., 415
Kurdila A.J., 7, 480
- Lagrange J.L., 25
Lalanne M., 7, 9
Lammens S., 9, 180
Lancaster P., 177
Lanczos C., 8, 44, 415, 468
Larson M.G., 487, 489

- Le Traon O., 315
Lee A.W., 9
Lehoucq R.B., 472, 487
Lens E.V., 549
Levinson D.A., 14
Lewis J.G., 476
Li X.S., 487
Liu J.W.H., 450, 476
Love A., 323–327
Luré L., 13
- MacNeal R.H., 100, 480
Magnus K., 7
Maia N.M.M., 180
Malkus D., 337
Marin F., 196
Mark W.D., 7
Markopoulos A., 458
Martin H.C., 336
Masson S., 315
Mazet R., 7
McConnell K.G., 9, 180
McKee J., 450
Mead D.J., 149
Meirovitch L., 7, 8, 13, 112, 143, 250, 254, 342
Mergeay M., 182
Mindlin R.D., 290
Mlejnek H.P., 7
Moler C., 489
Mook D.T., 7
Morand H.J.P., 8
Mottershead J.E., 499
Müller P.C., 7
Muntz C.L., 415
Myklestad N.O., 143
- Nayfeh A.H., 7
Nelson R.B., 503
Newmark N.M., 512, 522
Norrie D.H., 8
- Oden J.T., 337
Ohayon R., 8
Ojalvo I.U., 504
- Pahud P., 7
Papadrakakis M., 458
Park K.C., 517
Peeters P., 193
Penny J.E.T., 9
Penzien J., 7
Pfeiffer F., 8
Plesha M., 337
Preumont A., 7, 9, 109, 315
- Randolph M.F., 450
Rao S.S., 7
Rayleigh J.W.S., 1, 97, 112, 152, 156, 263, 286, 320–323, 335, 339
Reddy J.N., 337
Reissner E., 290
Renotte E., 362
Richardson M.H., 190, 193
Ritz W., 336, 339
Rixen D., 158, 212, 243, 444, 453, 550
Robert G., 575
Rocard Y., 7
Roseau M., 7
Roux F.X., 444
Rubin S., 481, 488
Rubinstein M.F., 7
Rutishauser H., 415
- Sadd M.H., 286, 316
Sander G., 290
Sas P., 9
Schiehlen W.O., 7
Schwarz H.R., 430, 434, 467
Shabana A.A., 8
Silva J.M.M., 9
Simon H.D., 509
Sloan S.W., 450
Soize C., 8
Sorensen D.C., 472, 476
Stegun I., 32
Stiefel E., 415, 444
Strang G., 337
- Taylor R.L., 362
Temple G., 489, 493
Thonon C., 334

Timoshenko S.P., 263, 277,
281
Tong K., 7
Topp L.J., 413
Touzot G., 8
Tukey J.W., 188
Turner M.J., 336

Van der Auweraer H., 209
Van Loan C.F., 9, 444, 450
Vanlanduit S., 209
Varoto P.S., 9, 180
Verboven P., 209
Von Karman T., 246
von Mises R., 415

Wallaschek J., 311, 314
Warburton G.B., 282
Wazwaz A.M., 94
Whittaker E.T., 8, 13
Wilkinson J.H., 9, 416, 429, 436
Williams F., 429
Wilson E.L., 417, 467
Witt R., 337
Wittrick W., 429

Yang C., 487

Zaveri K., 9, 169
Zienkiewicz O.C., 8, 336, 337, 362
Zimmerman R.D., 182

Subject Index

- acceleration
 - average value, 523
 - centripete, 38
 - Coriolis, 38
 - global, 108
 - linear interpolation, 523
 - relative, 38
 - support, differential, 102
- accuracy
 - direct integration, 511, 517
- additional mass, 101, 110
- admissible function, 340
- aerodynamic drag, 35
- aeroelasticity, 336
- aircraft model
 - dynamic response, 352
- AMLS, 487
- amplification matrix, 527, 540
 - characteristic equation, 530
 - complex conjugate roots, 531
 - Generalized- α method, 540
 - HHT method, 540
 - real roots, 531
- analytical dynamics, 13
- antiresonance, 86, 87
- appropriate excitation, 195
- appropriation, 164
 - force, 169
- approximation, 339
 - degrees of freedom, 340
 - displacement, 339
 - function, 340
 - kinematic, 339
 - matrix form, 340
- Arnoldi
 - algorithm, 470
 - interaction problem, 471
 - re-orthogonalization, 470
- assembly, 337, 368, 373, 375
- axes
 - local, 372, 386, 388
 - structural, 372, 386, 388
- backward substitution, 446, 451
- bandwidth, 450
- bar in extension, 243, 244, 337
 - clamped-free, 245, 347, 552
 - clamped-free, uniform, 347, 370
 - eigenmodes, 370
 - eigenvalues, 246, 349, 370
- discrete model, 246
- end force excitation, 250
- finite element, 364
- impedance matrix, 366
- response to a step load, 252, 256
- shape functions, 364
- transient response, 552, 559
- wave propagation, 256
- beam, 243
 - axial stiffness, 387

- beam (*continued*)
 - bending moment, 356
 - bending stiffness, 386
 - bi-clamped, uniform, 271, 380, 494
 - clamped–free, uniform, 269, 271, 350, 351
 - clamped–guided, uniform, 271
 - clamped–pinned, uniform, 271
 - combined excitation, 386
 - critical load, 385
 - curvature, 393
 - eigenfrequency, 268, 271
 - Euler-Bernoulli, 263, 398
 - finite element
 - with shear deformation, 392
 - without shear deformation, 376
 - free vibration, 281
 - free–free, uniform, 271, 458
 - free–guided, uniform, 271
 - free–pinned, uniform, 271
 - guided–guided, uniform, 271
 - guided–pinned, uniform, 271
 - kinematic assumptions, 263
 - load vector, 379
 - mass matrix, 379, 388
 - neutral axis, 386
 - prestress, 273, 384
 - principal inertia axes, 386
 - Rayleigh model, 263, 398
 - rigid body mode, 269, 379
 - rotating, 275
 - rotatory inertia, 379, 398
 - shape functions, 378
 - shear deflection, 277
 - shear parameter, 396
 - simply supported, uniform, 271, 283
 - prestress, 275, 385
 - response, 271
 - stiffness matrix, 379, 387
 - Timoshenko, 277, 398
 - torsional stiffness, 387
 - translation inertia, 379
 - transverse vibration, 263
 - with shear deformation, 337, 392
 - constitutive equations, 393
 - equilibrium equations, 393
 - mass matrix, 397
 - without shear deflection, 263,
 - without shear deformation, 337, 376
- bellmouth, 196
- bending
 - torque, 265
- bending moment, 265, 268, 356
 - plate, frame transformation, 295
- bending stiffness, 265, 268
- Bernoulli's kinematic assumption, 263, 273, 386
- Bessel function, 310, 312
- Betti-Maxwell
 - reciprocity principle, 212, 241
- bi-orthogonality, 425
- Biot-Lewis method, 246
- blade, rigid hinged, 276
- boundary
 - load, 239
 - reaction, 106
- boundary condition
 - essential, 221, 223, 302, 340
 - homogeneous spatial, 234
 - internal compatibility, 223, 340
 - kinematic, 212, 340
 - natural, 221, 223, 302, 340
 - nonhomogeneous spatial, 237
 - spatial, 212
 - uncertainty, 199
- buckling
 - critical load, 275, 346
 - mode, 275
- buffer vector, 467
- cable, 230
 - effect, 226, 258
 - transverse motion, 225
- Cauchy-Schwarz inequality, 490
- causality, 93
- central difference, 517
 - closed-form solution, 560, 561
 - critical time step, 552
 - flowchart, 558
 - formulation, velocities, 556, 557
 - impact, 563

- integration scheme, 512, 552, 556
- stability condition, 538, 552, 558
- three-step form, 556
- change of momentum, 43
- characteristic phase lag, 170, 171
- Choleski factorization, 447, 454
- Choleski triangularization, 426
- coefficient
 - damping, 155, 158
 - elasticity, 341
 - inertia, 62, 88
 - modal damping, 156, 158
 - stiffness, 61
 - stiffness, effective, 64
- complementary energy
 - discretization, 337, 395
 - strain, 394
 - variational principle, 336
- component mode, 107, 480, 484
- configuration
 - deformed, 214
 - equilibrium, 59, 61, 63, 66
 - initial stress, 227
 - instantaneous, 18
 - neutrally stable equilibrium, 82
 - reference, 18, 214
 - stable equilibrium, 65, 68, 77, 82
 - undeformed, 214
 - unstable equilibrium, 65
- conjugate directions, 468
- conjugate eigensolutions, 176
- conjugate gradient method, 415
- consistency
 - integration scheme, 525
 - Newmark method, 525
- constraint, 114, 115, 117, 119, 419, 459, 548
 - holonomic, 36
 - kinematic, 17, 18, 36
 - linear, 114, 459
 - non holonomic, 19
 - rheonomic, 18, 36, 66
 - scleronomic, 18, 36, 550
 - temporary, 457
- continuous
 - medium, 211
 - system, 211
 - approximation, 335
 - motion equation, 221
- convergence
 - global, 97
 - integration scheme, 525
 - quasi-static, 96, 97, 236, 511
 - spectral, 96, 511
- convolution product, 92, 93, 97, 130
- coordinate
 - condensed, 481
 - generalized, 340
 - normal, 78, 82, 238
 - remaining, 481
 - transformation, 388
- Coriolis
 - force, 29
- coupling
 - damping, 153, 155
 - elastic, 79
 - gyroscopic, 119
 - inertial, 79
- Courant
 - condition, 511, 513, 552, 558, 560
 - principle, 116
- Craig-Bampton method, 480, 484
- critical
 - frequency, 538
- critical load, 275, 346
- cross-section
 - gyration radius, 388
 - hollow circular, 285
 - plain rectangular, 284
 - rotation, 392
- curvature, 393
- curvature radius
 - thin plate, 300
- d'Alembert, 14
- damping, 91, 152
 - Caughey, 158
 - coefficient, 152, 156
 - equivalent viscous, 162
 - hysteretic, 160, 162
 - light, 153, 154, 160, 178, 179
 - loss factor, 162

- damping (*continued*)
 - modal, 153, 155, 156, 160, 168
 - numerical, 511, 518, 539, 551
 - proportional, 156
 - Rayleigh, 156
 - structural, 162, 212
 - viscous, 35, 149, 152, 160, 174
- deflation, 421, 441
 - rigid body modes, 461
- deformation
 - incremental, 228
- degeneracy theorem, 72–74, 125, 173
- degrees of freedom, 14, 20
 - boundary, 484
 - condensed, 481
 - internal, 105, 484
 - remaining, 481
- density
 - complementary energy, 220
 - strain energy, 219, 224
- design parameters, 498
- differential equation
 - first-order, 511
 - second-order, 512
- dilatation, 317
- direct integration, 95, 153, 511
 - accuracy, 511, 517
 - explicit, 514, 556, 564
 - implicit, 514, 523, 565
 - nonlinear case, 564
 - operator, 511
 - stability, 511, 517, 518, 520, 528
- discontinuity
 - velocity, 39, 42
- discrete model, 211
- discretization, 340
 - complementary energy, 337
 - displacement principle, 340
 - error, 499
 - in time, 511
 - method, 336
 - residual forces, 345
 - spatial, 336, 511
- discretized eigenvalue problem, 342
- dislocation potential, 393
- displacement
 - field, 214, 340
 - C_0 continuity, 340
 - admissible, 342
 - generalized, 20
 - imposed, 214
 - interpolation matrix, 340
 - large, 217, 218
 - local, 372
 - model, 336
 - relative, 102, 108
 - rigid, 108
 - small, 223, 224
 - structural, 372
 - variational principle, 213, 335, 336, 339, 342
 - discretized expression, 342
 - virtual, 21
- dissipation, 32, 153
 - function, 35, 36, 152, 550
 - light, 153, 155
- dof economizer, 479
- dry friction, 35
- du Bois-Reymond theorem, 40–42
- dual analysis, 336
- Duhamel integral, 93, 130
- Duncan function, 269, 359
- dynamic amplification, 85
- dynamic equilibrium, 14, 480
 - reduced, 480
 - residue, 480
 - surface, 223
 - volume, 223
- dynamic reduction, 416, 479
- dynamic substructuring, 416
- dynamical matrix, 425
 - deflation, 441
- earthquake, 320
- effect
 - anticlastic, 363
 - cable, 230
 - nonlinear, 223, 224, 227
 - rotatory inertia, 284
 - shear, 284
- effective modal mass, 101

- eigenfrequency
 - damped, 178
- eigenmode
 - sensitivity, 502
- eigensolutions, 233
- eigenvalue
 - bracketing, 491, 492
 - characterization, 111
 - close, 422, 437, 460
 - error bound, 417, 424, 443
 - Krylov–Bogoliubov, 492
 - Temple–Kato, 492
 - lower bound, 492, 493
 - multiple, 428, 529
 - multiplicity, 74
 - sensitivity, 502
 - upper bound, 116, 342, 350, 370, 371, 383, 480, 484, 489, 492, 493
 - zero, 75, 460
- eigenvalue problem, 74, 231, 269, 415, 419
 - associated variational form, 232
 - calculation of the determinant, 420
 - characteristic equation, 420
 - clamped bar, 370
 - closed form solution, 370
 - discretized, 342
 - interaction problem, 416, 420, 471, 474
 - iteration method
 - on eigenvalues, 420
 - on eigenvectors, 420, 436
 - nonsymmetric, 425
 - numerical solution, 419
 - method selection, 420
 - projection, 465
 - reduced, 479, 482
 - residual, 424, 443
 - rotating system, 124
 - staged methods, 420
 - static condensation, 420, 480, 481
 - substructuring, 420, 479
 - successive transformations, 420
 - symmetric, 124, 426
 - tridiagonal, 429
- eigenvector
 - linearly independent, 73
 - normalization, 344
- Einstein convention, 215, 221
- elastic pendulum, 568
- elastodynamics, 211, 339, 363
- element sensitivity, 502
- elliptic integral, 32
- energy
 - balance, 525, 550
 - complementary, 220
 - conservation, 29, 550
 - dissipated per cycle, 172
 - external potential, 221
 - geometric strain, 229, 345
 - initial strain, 228
 - integral, 30
 - internal, 33, 219
 - kinetic, 24, 27, 30, 60, 62, 221
 - level, 30
 - potential, 30, 36, 60, 221
 - effective, 64
 - strain, 214, 219, 221
- energy conservation
 - mid-point rule, 549
- equation
 - canonical, 178
 - discretized displacement, 342
 - Lagrange, 23, 25
 - linearized equilibrium, 566
 - normal, 78, 92, 152, 156, 235
 - of motion, discretized, 342
 - of virtual work, 23
 - partial differential, 339
 - power balance, 551
 - residual equilibrium, 565
 - uncoupled, 78
 - wave, 254
- equilibrium
 - iteration, 566
 - neutrally stable, 66, 69, 70
 - position, 30
 - stable, 59, 62, 67
- equilibrium averaging method, 539
 - accuracy analysis, 542
 - amplification matrix, 540
 - consistency, 542
 - finite-difference form, 541
 - particular forms, 544

- equilibrium averaging method (*continued*)
 - stability analysis, 543
- equilibrium model, 336
- Euler
 - backward formula, 515
 - backward integration, 518, 521
 - critical load, 275
 - forward formula, 516
 - forward integration, 518, 520
 - theorem, 28
- Euler-Bernoulli
 - beam, 263
- Eulerian description, 214
- excitation
 - appropriate, 164, 165, 170
 - arbitrary, 174
 - combined, 386
 - external, 129, 234
 - harmonic, 90, 160, 171, 179
 - simultaneous, 169
 - support, differential, 110
- expansion, 499
 - modal, 76
 - spectral, 76, 84, 160
- experimentation, 152, 170
- explicit
 - integration scheme, 514, 556, 564
 - method, 512
- explosion, 512
- external potential energy
 - discretization, 341
- factorization, 446, 451
 - block LU, 451
 - Choleski, 447
 - LDL^T, 447
 - LU, 445
 - singular matrix, 457
- fictitious link, 457
- fill-in, 449
- finite element, 363
 - assembly, 337, 366, 375
 - bar in extension, 363, 364
 - beam in bending, 363, 376, 392
 - beam, prestress, 384
 - beam, three-dimensional, 386
 - Boolean matrix, 367
 - changing axes, 388
 - co-deformable, 363
 - commercial software, 337
 - conforming, 363
 - connector, 364
 - degrees of freedom, 363
 - equilibrium, 336
 - generalized load, 365
 - geometric stiffness matrix, 384
 - geometry, 363
 - kinematically admissible, 336, 363
 - lumped mass, 371
 - mass matrix, 365
 - method, 336
 - node, 364
 - shape functions, 363
 - statically admissible, 392
 - stiffness matrix, 365
- first iterate, 492
- first-order error, 112
- flexibility matrix
 - spectral expansion, 461
- fluid–structure interaction, 423
- force
 - appropriation method, 91
 - body, 214, 221
 - centrifugal, 38, 64, 119, 276
 - conservative, 35, 221
 - damping, 166
 - dissipative, 34, 35, 165
 - elastic, 33, 166
 - excitation, 166
 - external, 17, 35, 36, 231
 - generalized, 23, 27, 33
 - generalized, conservative, 32
 - generalized, external, 32
 - generalized, internal, 32
 - gyroscopic, 36, 38, 275
 - impulse, 41
 - inertia, 27, 36, 166, 425
 - generalized, 27
 - internal, 35
 - nonlinear, 564
 - linking, 17, 33

- nonconservative, 36
- prestressing, 229
- reaction, 17, 368, 369
- relative inertia, 38
- restoring, 64
- self-equilibrated, 455, 457
- form
 - positive definite, 68
 - quadratic, 61, 68, 71
- forward substitution, 446, 451
- Fourier transform, 180
 - discrete, 187
 - fast, 188
 - inverse, 180
- free vibrations, 77
- frequency, 69
 - antiresonance, 85–87
 - critical, 538
 - cut-off, 559
 - excitation, 84, 90
 - lower bound approximation, 248
 - multiple, 72, 73, 233, 312
 - numerical, 561
 - prestressed system, 346
 - resonance, 85–87
 - rotating beam, 275
 - upper bound, 552, 559
- frontal method, 416, 421, 450, 452
- function
 - admissible, 340
 - dissipation, 550
 - kinematically admissible, 335, 340
 - shape, 365
 - transfer, 170
- Galerkin
 - weighted-residual method, 336
- Gauss
 - elimination, 445, 451, 454, 464
 - maximum pivot strategy, 459
 - integration by parts, 222
 - quadrature, 380
- Gear, 521
- general comparison principle, 114
- generalized
 - coordinate, 363
 - force, 21
 - mass, 71, 169
 - stiffness, 71
- generalized inverse, 453, 456, 457
 - family, 456
- Generalized- α method, 546–554
 - second-order accuracy, 546
 - spectral radius, 546
 - unconditional stability, 548
- geometric stiffness matrix, 345
- Gerschgorin standard method, 429
- Gibbs phenomenon, 253
- Givens–Householder method, 421
- Gram–Schmidt orthogonalization, 75
- Gram–Schmidt orthonormalization, 465
- Green, 214, 215
 - strain tensor, 223
 - theorem, 298
- Guyan–Irons
 - reduction algorithm, 480, 481
- gyration radius, 265
- gyroscopic
 - coupling, 37, 65, 119
 - force, 29
 - generalized force, 36
- Hamilton principle, 14, 23, 24, 39, 41, 112, 213, 214, 231, 339, 366
- harmonic
 - excitation, 90, 179
 - forced response, 90, 106, 179
 - motion, 69
 - regime, 83
- Hermitian polynomials, 378
- Hermitian transformation, 434
- Hessian, 113
- HHT method, 545, 554
 - amplification matrix, 540
 - second-order accuracy, 545
 - spectral radius, 545
 - unconditional stability, 548
- holographic interferometry, 363
- holonomic, 18, 20
- homogeneous
 - elastic medium, 316

- homogeneous (*continued*)
 - function, 28, 35
 - system, 67, 153, 175, 176
- Hooke
 - law, 220
 - matrix, 341
- Hotelling orthogonal deflation, 441
- Householder tridiagonal form, 426, 434
- hybrid synthesis, 480, 487
- hyperelastic material, 219
- identification, 174
 - modal, 180
- impact, 512
- implicit
 - integration scheme, 514, 523, 565
- implicit method, 512
- impulse response, 129
- impulsive loading, 39, 41–43
 - Lagrange equation, 43
- inertia
 - apparent, 88
 - equivalent, 88
 - rotation, 397
 - translation, 397
- inertia force, 24
 - classification, 27
 - complementary, 29
 - relative, 28
 - transport, 28
- influence coefficient
 - dynamic, 84, 160, 179
 - principal, 85–87, 160
 - static, 84, 160
- initial condition, 78, 82, 93, 94, 128
 - disturbance, 528
 - nonhomogeneous, 77
- initial stress, 227
- instability, 65
- integration method
 - free parameter, 512
- integration scheme
 - average acceleration, 538, 539
 - central difference, 538, 552, 556
 - characteristic equation, 518
 - consistency, 525
 - Euler backward, 518, 521
 - Euler forward, 518, 520, 521
 - HHT, 539
 - implicit, 514
 - linear acceleration, 538
 - modified average acceleration, 538
 - Newmark, 522
 - predictor, 524
 - purely explicit, 538
 - trapezoidal rule, 518, 521
 - unconditionally stable, 521, 548
- interaction problem, 416, 420, 466, 468, 471, 474
- interpolation function
 - circular symmetry, 347
 - polynomial, 346
 - rectangular domain, 347, 357
- inverse iteration, 416, 421, 422, 437, 463, 468
 - by blocks, 465
 - practical aspects, 460
 - spectral shifting, 463
 - with rigid body modes, 460
- iteration
 - inverse, 416
 - matrix, 523, 566
- Jacobi method, 415, 421, 430
 - convergence, 432
 - cyclic, 433
 - threshold, 433
 - diagonalization, 421, 430
- Jordan canonical form, 530
- Kato inequality, 493
- kinematic
 - boundary condition, 340
 - constraint, 20
- kinematically admissible
 - displacement interpolation, 336
 - function, 335
- kinetic energy, 27
 - amplitude, 231
 - cross-section rotation, 265
 - discretization, 341

- linearization, 61
- mutual, 27, 65
- relative, 27, 65
- rotational, 388
- translational, 388
- transport, 27, 36, 59
- vertical translation, 265
- Kirchhoff
 - assumptions, 290
 - corner load, 300
 - shear load, 300, 302
- Kirchhoff–Trefftz
 - stress tensor, 220, 223, 226
- Kronecker symbol, 71
- Krylov
 - method, 415, 460
 - sequence, 415, 468, 470, 489
 - subspace, 471
- Krylov–Bogoliubov bounds, 492, 493
- Lagrange
 - action, 221
 - equation, 13, 23, 25, 28, 36, 59, 62
 - impulse equation, 43
 - multiplier, 393, 419, 459
- Lagrangian description, 214
- Lamé constants, 220
- Lanczos method, 421, 437, 460, 468, 472
 - algorithm, 416, 472
 - algorithm restarting, 475
 - by blocks, 476
 - computing performance, 476
 - interaction problem, 474
 - numerical instability, 475
 - preconditioned, 475
 - re-orthogonalization, 474
 - spectral shifting, 476
 - spurious solutions, 474
- Laplace transform, 92, 130
- Laplacian operator, 303, 308, 317
- large displacement, 291
- large rotation, 291
- LDL^T factorization, 447
- least-squares complex exponential, 182, 184
- Legendre transformation, 220
- linear
 - combination, 73
 - constraint, 459
 - independence, 73, 74
 - multistep method, 512
 - system
 - nonsingular, 445
 - nonsymmetric, 445
 - singular, 453
 - solution, 444
 - symmetric, 447
- linearity
 - excitation, 94
 - geometric, 216, 223, 224, 564
- linearization, 64, 565
- load
 - axial prestress, 276
 - corner, 300
- localization
 - operator, 367, 374
 - table, 374
- locking
 - in shear, 392
- Love wave, 320, 323
- LR algorithm, 415, 467
- LU factorization, 445
- lumped mass matrix, 248, 557
- mass matrix
 - lumped, 371
 - nonconsistent, 371
 - reduced, 488
- material
 - hyperelastic, 219
 - isotropic, 220
 - linear, 220
- matrix
 - admittance, 84
 - amplification, 527, 540
 - assembled mass, 375
 - assembled stiffness, 375
 - band, 421
 - bandwidth, 450
 - Boolean, 367
 - boundary static modes, 485
 - consistent mass, 366, 552, 559

matrix (*continued*)

- damping, 37, 152, 158, 160, 178
- degrees of freedom, 365
- direction cosines, 232
- displacement interpolation, 340
- dynamic influence, 86, 87, 106
- dynamic influence coefficients, 84
- dynamic stiffness, 429, 444
- dynamical, 425
 - deflated, 442
- effective stiffness, 37
- elastic mode, 82
- element mass, 371
- element sensitivity, 502
- element stiffness, 365, 371
- factorization, 446, 451
- filtering, rigid mode, 462
- generalized inverse, 453, 456
- generalized, influence coefficients, 462
- geometric stiffness, 345, 384
- gyroscopic coupling, 37
- Hooke matrix, 341
- image, 454, 456
- impedance, 105, 429
- iteration, 566
 - deflated, 442
 - nonsymmetric, 425
 - symmetric, 426, 430
- Jacobian, 566
- Jordan canonical form, 530
- localization, 367
- lower triangular, 426, 445
- lumped mass, 371, 522, 557
- mass, 37, 62, 77, 341
- modal damping, 156
- modified stiffness, 119
- nonsingular stiffness, 77
- norm, 527
- nullspace, 453, 454
- permutation, 447
- positive definite, 61, 62
- pseudo-inverse, 456
- range, 454
- reduced impedance, 105, 106
- reduced mass, 118, 479, 486
- reduced stiffness, 118, 479, 486
- reduction, 486
- residual flexibility, 487
- rigid mode, 82
- second derivative, 113
- semi-definite, 457
- semi-positive definite, 419
- sensitivity, 502
- singular, 457
- skyline, 449
- sparse, 421, 449
- static connection, 396
- stiffness, 61, 66, 77, 341
- strain, 340, 564
- structural displacements, 367
- structural mass, 367, 375
- structural stiffness, 367, 375
- symmetric, 61
 - Choleski factorization, 447
- tangent damping, 566
- tangent stiffness, 566, 568
- time-stepping, 444
- trace, 443
- tridiagonal, 426, 427, 434, 473
- unit, 76
- upper Hessenberg, 471
- upper triangular, 426, 445
- matrix structural analysis, 336
- McNeal method, 480, 487
- mechanical impedance, 105, 484
- mechanism, 67
- medium
 - homogeneous, 323
 - infinite, 316, 319
 - linear elastic isotropic, 316
 - semi-finite, 316, 320, 323
- method
 - approximation
 - displacements, 339
 - stresses, 395
 - Biot-Lewis, 246
 - bisection, 429
 - central-difference, 512
 - component modes, 480, 484
 - condensation, 480
 - diagonalization, 430
 - discretization, 336, 339

- equilibrium averaging, 539
- explicit, 514
- fictitious link, 457
- finite element, 336, 363
- frontal, 450, 452
- Generalized- α , 539, 546
- Givens–Householder, 421
- hybrid synthesis, 480, 487
- implicit, 514
- inverse iteration, 421, 422, 437, 443, 463
- Jacobi, 421
- Lanczos, 421, 437, 460, 468
- linear multistep, 512
- matrix transformation, 430
- modal synthesis, 480, 484
- mode acceleration, 97, 153, 236
- mode displacement, 97, 153, 236
- multistep, 513, 519
- Newmark, 512, 522
- Newton–Raphson, 566, 568
- one-step, 512, 514, 520, 522
- power algorithm, 421, 436
- Rayleigh, 335
- Rayleigh–Ritz, 336, 339
- reduction, 107, 421
- Sturm sequences, 426, 434
- subspace iteration, 417, 421, 437, 460
- substructuring, 480
- tridiagonalization, 434
- weighted-residuals, 336
- mid-point rule, 549, 550
 - energy conservation, 549
 - second-order accuracy, 549
 - spectral radius, 549
- minimax principle, 118
- minimum
 - absolute, 115
 - Rayleigh quotient, 116, 118
- modal
 - acceleration, 97, 153
 - analysis
 - experimental, 180, 196
 - operational, 199
 - damping, 156
 - damping ratio, 156
 - displacements, 153
 - mass, 233
 - participation factor, 77, 92, 235, 239
 - superposition, 97, 153, 235, 237, 251, 271, 345, 511
 - synthesis, 480, 484
- Modal Assurance Criterion, 499
- mode
 - acceleration method, 97, 153
 - antisymmetric, 383
 - complex, 68, 177
 - displacement method, 96, 153
 - distinct eigenfrequencies, 70
 - eigenmode, 68–70
 - elastic, 70, 75, 82
 - excitation, 165
 - internal, 484
 - kinematic, 422, 460
 - normal excitation, 90
 - normal response, 171, 173
 - normal vibration, 67
 - orthonormalized, 78
 - residual flexibility, 488
 - rigid body, 67, 69, 70, 75, 82, 84, 87, 341, 422, 453, 460
 - static, 102
 - superposition, 76
 - symmetric, 352, 382
- model updating, 498
- momentum, 41
- monomial series, 348, 350
- monotonicity principle, 114
- motion
 - backward elliptic, 323
 - differential, 101
 - direct elliptic, 323
 - global, 64, 101
 - harmonic, 160, 231, 342
 - overall, 70
 - relative, 66
 - rigid, 101
 - steady, 66
 - support, 110
 - synchronous, 155
 - transport, 64, 83

- motion equation
 - continuous system, 221
- multiplicity
 - degree, 73
 - eigenvalue, 74, 125
- Navier equations, 316, 321
- Newmark method, 512, 522, 523, 545
 - accuracy, 536
 - amplification matrix, 527
 - amplitude error, 538
 - average acceleration, 523
 - consistency, 525
 - displacement prediction, 565, 568
 - energy conservation, 551
 - family, 538
 - flowchart, 524
 - nonlinear, 567
 - free parameters, 523
 - frequency dispersion, 535
 - nonlinear case, 566
 - numerical damping ratio, 537, 538
 - numerical dissipation, 535
 - parameter summary, 538
 - periodicity error, 536, 538
 - properties, 538
 - quadrature error, 523
 - second-order accuracy, 545
 - spectral radius, 545
 - spectral stability, 530
 - stability analysis, 527
 - stability limit, 538
 - unconditional stability, 548, 550, 551
 - velocity prediction, 565, 568
- Newton–Raphson
 - convergence radius, 568
 - iteration strategy, 568
 - method, 566, 568
- non linearity
 - geometric, 223, 224
- nonholonomic, 19, 20
- nonlinear behaviour, 169, 198, 564
- normal equation, 345
 - initial condition, 92
 - integration, 92
- normal mode excitation, 90
- normalization, 233
- nullspace, 453, 457
 - automatic computation, 458
- numerical conditioning, 111
- numerical damping, 511, 551
- numerical damping ratio
 - Newmark method, 537
- numerical filtering, 511
- numerical solution instability, 518, 521
- Nyquist
 - diagram, 160–162
 - plane, 160
- observation, 499
- operator
 - direct integration, 511
 - explicit, 514, 556, 564
 - filtering, rigid mode, 462
 - implicit, 514, 523, 565
 - localization, 374
 - projection, 115
 - rotation, 372, 388
 - spatial differentiation, 232
- optimization, 498
- orthogonal
 - basis, 73
 - deflation, 441
 - polynomials, 347
 - projection, 441
 - rigid body modes, 461
 - transformation, 430, 431
- orthogonal polynomials, 348, 353
- orthogonality, 70, 78, 91, 92, 173, 176, 211
 - eigensolutions, 233
 - recursive, 472
 - relation, 71, 91, 127, 344, 357, 426
 - rotating system, 127
- orthonormalization
 - Gram-Schmidt, 465
- oscillations, 31
- oscillator
 - n -degree-of-freedom, 70
 - one-degree-of-freedom, 517
- outward normal, 214

- parameter, 20
- participation factor, 235
- particle, 14
- pendulum, 62
 - double, 22
 - elastic, 568
 - simple, 21, 25, 26
- period, 31
- periodicity error, 518
 - Newmark method, 536
- permutation matrix, 447
- phase lag, 165
- phase quadrature, 164–166
 - criterion, 164, 166
- phase space, 30, 570
- physical damping ratio, 537
- physical parameters, 498
- Piola–Kirchhoff
 - stress tensor, 220
- pivot, 447
- pivoting, 447, 457, 464
 - partial, 447
- plate
 - rectangular, uniform, 357
- Poisson ratio, 220, 319
- polarization plane, 319
- portal frame, 390
- position
 - equilibrium, 30, 59
 - neutrally stable equilibrium, 66
- potential
 - dislocation, 393
 - external forces, 35
 - modified, 36, 59
 - total, 36
- potential energy
 - linearization, 61
- power
 - active, 168
 - complex, 168
 - dissipated, 35
 - evaluation, 36
 - instantaneous, 29
 - reactive, 168
 - stationary reactive, 166
- power method, 415, 460
 - algorithm, 421, 437
 - convergence, 436, 439, 463
 - equal eigenvalues, 438
 - fundamental mode, 437
 - higher modes, 441
 - inverse iteration form, 443
 - orthogonal deflation, 441
 - stopping criteria, 439
- prestress, 227, 345
 - external, 228
 - geometric energy, 258
 - internal, 229
- principle
 - best approximation, 112
 - Courant, 118
 - displacement variational, 221
 - general comparison, 114, 115
 - Hamilton, 14, 23, 24, 39, 112, 213, 229, 339, 340
 - continuous system, 221, 223
 - minimax, 116, 118
 - monotonicity, 114, 115, 118
 - Rayleigh, 112
 - variational, 13
 - virtual work, 14, 17, 23
- problem
 - eigenvalue, 74
 - spatial variational, 231
 - Sturm–Liouville, 232
- projection, 499
 - operator, 115
- propagation
 - wave, 316
- propagation, wave
 - direction, 319
- pseudo-acceleration, 548
- pseudo-inverse, 456
- pseudo-resonance, 89
- QR algorithm, 415, 434, 467
- rational fraction polynomial, 190
- Rayleigh, 97
 - beam, 263
 - beam model, 398
 - constraint, 117

- Rayleigh (*continued*)
 - damping, 156
 - equation, 322
 - principle, 112
 - quotient, 71, 112–115, 117, 176, 415, 439, 464, 484, 489, 492
 - theorem on constraints, 117, 343, 428, 480, 484
 - wave, 320
- Rayleigh method, 335
- Rayleigh–Ritz
 - approximation, 340
 - convergence, 342
 - eigensolutions, 342
 - eigenvalues, 343
 - eigenvectors, 343
 - method, 336, 342, 345, 347, 363
 - interpolation functions, 346
 - numerical conditioning, 347
- reaction, 17, 103, 105
- reactive power, 170
 - stationary, criterion, 164, 166, 168
- reciprocity
 - Betti-Maxwell principle, 212, 241
- recurrence, 113, 115
 - relation, 93, 526, 540
- reduced integration, 392
- reduction
 - dynamic, 479
 - method, 421
- relation
 - moment–curvature relationship, 268, 293
 - orthogonality, 70, 173, 176
 - stress–strain, 219, 292
- renumbering scheme, 449
- residual equilibrium
 - convergence test, 566
 - linearization, 565
- residual flexibility correction, 392
- residual flexibility matrix, 487
- residual flexibility mode, 488
- residual vector, 565
- residues, 181
- resonance, 86, 87, 89, 90
- response
 - external excitation, 91, 234, 237, 345
 - forced harmonic, 83, 105, 106, 160, 164
 - harmonic, 89, 105
 - impulse, 92, 93
 - quasi-static, 102
 - step, 92
 - time integration, 511
 - transient, 91, 96, 511
- rheonomic, 18
- rigid body mode, 67, 422, 453, 460
 - deflation, 461
 - orthogonalization, 462
 - orthonormalized, 461
 - rotation, 462
 - translation, 462
- rolling condition, 19
- rotation
 - large, 218
 - small, 223, 224
- rotatory inertia
 - cross-section, 268, 274
- rotor, 38
- Rubin method, 488
- SAMCEF, 2, 198, 337, 391, 413, 476
- Schur complement, 451
- Schwarz
 - inequality, 491
 - quotient, 491, 492
- scleronomic, 18, 29, 550
- second-order error, 112, 113
- sensitivity
 - eigenmode, 502, 503
 - modal representation, 504
 - eigensolution, 417, 498
 - eigenvalue, 502
 - multiple eigenvalues, 504
- shape function, 364
 - bar in extension, 364
 - beam, 378
- shear
 - angle, 393
 - deformation, 220, 392
 - load, 265

- locking, 392
- modulus, 220, 278
- parameter, 396
- reduced section, 278
- strain, 278, 392
- strain energy, 392
- shock, 41, 512
- singular system
 - solution, 454
- skyline
 - algorithm, 421
 - storage, 449
- solver
 - backward substitution, 445
 - forward substitution, 446
- sparse matrix, 449
 - fill-in, 449
 - renumbering scheme, 449
 - storage scheme, 449
- sparse solver, 449
- spatial discretization, 336, 511
- spectral expansion, 84
- spectral radius, 527
 - asymptotic, 554
- spectral shifting, 421, 422, 437, 460, 463
- spectral stability, 529
- stability, 64, 65
 - boundary, 518, 520
 - direct integration, 511, 517, 518, 528
 - equilibrium, 60
 - solution, 177
 - structure, 229
 - time solution, 68
 - type A, 521
 - unconditional, 521, 548
- standing wave, 212
- state space, 128, 174
- state vector, 175, 513, 525
- static condensation, 102, 450, 480, 481, 485
 - first-order correction, 482
- static problem
 - singular, 461
- stationary power criterion, 166
- stationary value
 - Rayleigh quotient, 112, 113, 484
- stiffness
 - complex, 162
- stiffness matrix
 - generalized inverse, 461
 - image, 460
 - nullspace, 455, 460
 - reduced, 488
 - statically exact, 392
- stopping criteria, 423
- strain
 - axial, 216, 217
 - complementary energy, 394
 - compute, 214
 - Green, 220
 - Green's measure, 214
 - infinitesimal, 216, 218
 - interpolation matrix, 340
 - large, 216
 - state, 220
 - tensor, 220
 - volumetric, 317
- strain energy, 214, 220
 - additional, 230, 273
 - amplitude, 231
 - geometric, 273
- stress
 - initial, 227, 229, 345, 346
 - interpolation, 395
 - residual, 229
 - state, 220
- structure
 - externally prestressed, 228
 - internally prestressed, 229
 - prestressed, 229, 345
 - statically determined, 454, 457
 - truss frame, 371
 - unrestrained, 453
- Sturm sequences, 426, 427, 434
 - bracketing property, 427
 - sign correspondences, 428
- Sturm–Liouville problem, 232, 342
- subspace, 73, 118
 - construction, 464
 - eigenmodes, 466

- subspace (*continued*)
 - elastic modes, 461
 - rigid body modes, 461
- subspace iteration, 416, 421, 460, 464
 - buffer vector, 467
 - convergence, 466
 - convergence acceleration, 467
 - convergence control, 467
 - method, 437, 466
- substitution
 - backward, 446, 451
 - forward, 446, 451
- substructure, 485
- substructuring, 417, 423, 479
 - algebraic multi-level, 487
- subsystem
 - clamped, 105
 - eigenmode, 107
- superelement, 451, 486
- superposition
 - eigenmode, 77
- surface portion, 214
- surface traction, 221
- symmetry
 - simplification, 382
 - skew, 29
- system
 - n -degree-of-freedom, 59, 151
 - associated conservative, 152, 154, 155, 160, 165, 196
 - associated homogeneous linear, 90
 - chain topology, 368
 - clamped, 102
 - conservative, 60, 82
 - conservative rotating, 119, 130
 - continuous, 13, 211, 231, 339, 347
 - one-dimensional, 211
 - damped, 151, 174
 - discrete, 13, 211, 246, 339
 - first-order, 128, 130, 517
 - gyroscopic, 119, 129
 - homogeneous, 67
 - linear, 419
 - lightly damped, 160, 179
 - linear
 - homogeneous, 426
 - nonlinear, 548, 564
 - of particles, 17, 42
 - one-dimensional continuous, 243
 - prestressed, 229
 - repetitive, 246
 - rotating, 64, 66, 346
 - rotation, 65
 - stability, 38
 - stable, 30, 78
 - statically underdeterminate, 67
 - symmetric, 124
- taut string
 - eigenfrequency, 260
 - free vibration, uniform, 259
 - transverse vibration, 243, 258
 - wave equation, 260
- Taylor
 - error, 522
 - expansion, 61, 522
 - formula, 522
- Temple–Kato bounds, 492
- tensor
 - strain, 215
 - stress, 220
- thin plate
 - bending stiffness, 294
 - bending vibration, 290
 - boundary, 295
 - circular, application, 311
 - circular, clamped, 309
 - circular, eigensolutions, 310
 - circular, eigenvalue problem, 309
 - circular, free vibrations, 308
 - circular, strain energy, 309
 - curvature, 293
 - elasticity coefficients, 293, 294
 - equation of motion, 298
 - equilibrium equation, 302, 304
 - geometric energy, 304
 - Hamilton principle, 296
 - initial extension, 303
 - kinematic assumptions, 290
 - kinetic energy, 358
 - Kirchhoff shear force, 300, 302
 - moment–curvature relationship, 293

- normal bending moment, 302
- normal slope, 302
- prestress, 291, 296, 303
- rectangular, clamped–free, 359
- rectangular, eigenfrequencies, 307
- rectangular, eigenmodes, 307
- rectangular, free vibrations, 305
- rectangular, simply supported, 306
- rectangular, uniform, 357
- rotation equilibrium, 303
- rotational kinetic energy, 297
- shear load, 298
- strain, 291
- strain energy, 295, 297, 303, 358
- stress–strain relationship, 292
- translation kinetic energy, 297
- twisting moment, 301
- vertical equilibrium, 302
- time discretization, 511
- time integration, 92, 511
 - energy loss, 554
 - equilibrium averaging, 512, 539
 - error
 - amplitude, 538
 - periodicity, 518
 - explicit method, 512
 - free parameter, 512
 - Generalized- α method, 539
 - HHT method, 539
 - implicit method, 512
 - multistep method, 512
 - Newmark method, 522
 - nonlinear system, 539, 548, 557, 564
 - one-step formula, 512
 - second-order accuracy, 539
 - unconditional stability, 512
- time step, 511
 - maximum size, 538
- Timoshenko
 - beam, 277, 398
- trajectory, 14, 24, 31
- transformation
 - Hermitian, 434
 - Laplace, 254, 255
 - orthogonal, 430, 431
 - sinus, 251
- transient response
 - bar in extension, 559
- trapezoidal rule
 - integration formula, 518, 521
- travelling wave, 212
- triangularization algorithm, 426
- truncation, 96, 236
- truss frame, 371
- ultrasonic wave motor, 311
 - piezoelectric excitation, 313
 - rotor, 312
 - stator, 312
- unconditional stability, 512
- uncoupling, 82
- variation operator, 14
- variational
 - approach, 112
 - eigenvalue analysis, 113
 - equation, 39
 - method, 111
- variational principle, 213
 - complementary energy, 336
 - on displacements, 335
- velocity
 - angular, 346
 - discontinuity, 39
 - half-time interval, 557
 - virtual, 40
- vibrations
 - n -degree-of-freedom, 83, 92
 - damped system, 151, 153, 154
 - distinct, 70
 - forced, 83
 - free, 62, 67, 342
 - linear, 59
 - testing, 156, 164
 - undamped, 59
- virtual displacement, 14, 18
- virtual work, 14, 21, 23, 33, 36
 - elastic forces, 71
 - external forces, 365
 - inertia forces, 70

- viscous
 - damper, 36
 - damping, 35
- volumetric dilatation, 220
- wave
 - acoustic, 320
 - backward, 260, 312
 - direct, 260, 312
 - dispersion, 286, 552
 - displacement direction, 323
 - length, 323
 - longitudinal, 317, 319, 552, 563
 - Love, 317, 320, 323, 325
 - optical, 320
 - plane, 319
 - plane elastic, 318
 - propagation, 212, 316
 - direction, 325
 - speed, 511
 - velocity, 255, 319, 325
 - Rayleigh, 317, 320
 - reflection, 316, 320
 - refraction, 316, 320
 - scattering, 552
 - standing, 212, 252, 253, 255, 312
 - surface, 320
 - transverse, 317, 319
 - travelling, 212, 253, 256, 262, 312
- weighted-residual method, 336
- Young's modulus, 220

WILEY END USER LICENSE AGREEMENT

Go to www.wiley.com/go/eula to access Wiley's ebook EULA.